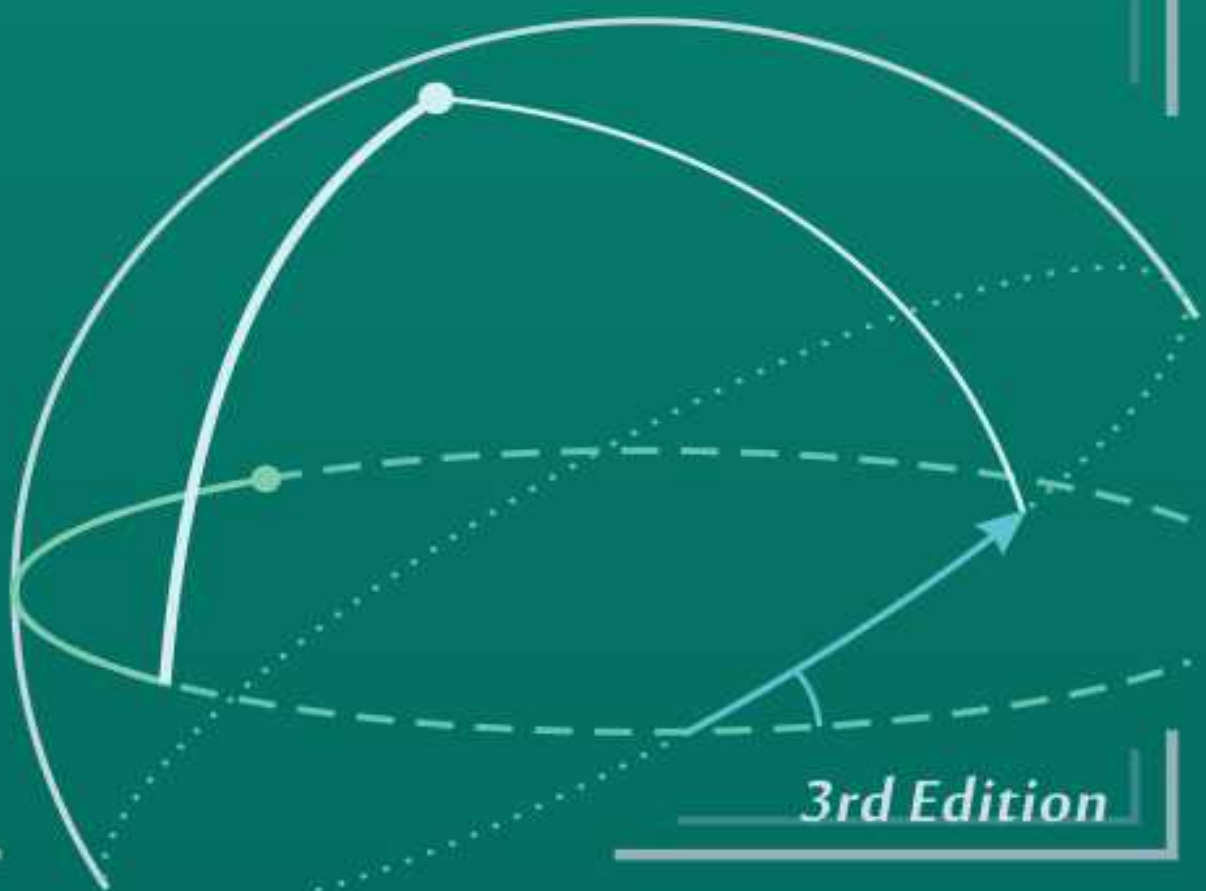
EXPLANATORY SUPPLEMENT to the ASTRONOMICAL ALMANAC

Edited by

Sean E. Urban and P. Kenneth Seidelmann



3rd Edition

Explanatory Supplement to the Astronomical Almanac

THIRD EDITION

Edited by

Sean E. Urban
US Naval Observatory

P. Kenneth Seidelmann
University of Virginia

Foreword by Roger Sinnott



UNIVERSITY SCIENCE BOOKS
Mill Valley, California

Explanatory Supplement
to the Astronomical Almanac

Explanatory Supplement to the Astronomical Almanac

THIRD EDITION

Sean E. Urban
US Naval Observatory

P. Kenneth Seidelmann
University of Virginia

Foreword by Roger Sinnott



UNIVERSITY SCIENCE BOOKS
Mill Valley, California

University Science Books
www.uscibooks.com

Production Manager: *Paul C. Anagnostopoulos, Windfall Software*
Text Design: *Paul C. Anagnostopoulos*
Illustrator: *Laurel Muller*
Compositor: *Windfall Software*
Cover Design: *Genette Itoko McGrew*
Printer & Binder: *Edwards Brothers, Inc.*

This book was set in Times Roman and Myriad Pro and composed with ZzTEX, a macro package for Donald Knuth's TEX typesetting system.

This book is printed on acid-free paper. ♾

The appearance of non-US government website addresses does not constitute endorsement by the United States Department of Defense (DoD), the United States Department of the Navy, or the U.S. Naval Observatory of those websites, or the information, products or services contained therein. The above-mentioned parties do not exercise any editorial control over the information you may find at these locations nor do they accept responsibility for loss or damage arising from the use of the information on these site.

ISBN: 978-1-891389-85-6

Library of Congress Cataloging-in-Publication Data

Explanatory supplement to the Astronomical almanac. — 3rd ed. / edited by Sean Urban, P. Kenneth Seidelmann.
p. cm.
Includes bibliographical references and index.
ISBN 978-1-891389-85-6 (alk. paper)
1. Nautical almanacs. I. Urban, Sean E. II. Seidelmann, P. Kenneth. III. Astronomical almanac for the year 2013 Supplement.
QB8.U6E95 2013
528–dc23 2012012745

Printed in the United States of America
10 9 8 7 6 5 4 3 2 1

	Foreword	xxvii
	Preface	xxxi
	Contributing Authors	xxxiii
1	Introduction to Positional Astronomy	1
2	Relativity for Astrometry, Celestial Mechanics and Metrology	45
3	Time	75
4	The Fundamental Celestial Reference System	105
5	Terrestrial Coordinates and the Rotation of the Earth	123
6	Precession, Nutation, Polar Motion, and Earth Rotation	199
7	Positions	249
8	Orbital Ephemerides of the Sun, Moon, and Planets	305
9	Planetary Satellites and Rings	347
10	Physical Ephemerides of Solar System Bodies	399
11	Eclipses of the Sun and Moon	453
12	Astronomical Phenomena	505
13	Stars and Stellar Systems	529
14	Computational Techniques	555
15	Calendars	585
A	Bases and Constants	625
B	Acronyms	627
C	Glossary	633
	Index	661

Foreword xxvii
Preface xxxi
Contributing Authors xxxiii

1 Introduction to Positional Astronomy 1

1.1 Introduction 1
1.1.1 Purpose 1
1.1.2 Introduction to The Astronomical Almanac *1*
1.1.3 The Astronomical Almanac *and* The Explanatory Supplement *3*
1.1.4 Conceptual Changes since the Last Edition 3
1.1.5 Implementation of the Changes 7
1.1.6 Deletions from This Edition and The Astronomical Almanac *9*

1.2 Timescales and Calendars 9
1.2.1 Atomic Timescales 9
1.2.2 Dynamical Time 10
1.2.3 Timescales Based on Earth's Rotation 11
1.2.4 Coordinated Universal Time (UTC) 13
1.2.5 Enumeration of Dates 14

1.3 Celestial and Terrestrial Coordinates 15
1.3.1 Coordinate Systems and Frames 15
1.3.2 Celestial Coordinate Systems 18
1.3.3 Terrestrial Coordinate Systems 20
1.3.4 The Rotation of the Earth 24
1.3.5 Connections between Terrestrial and Celestial Coordinates 25
1.3.6 Effects of the Position and Motion of the Object and Observer 27

1.4 Orbital Motion 29
1.4.1 Motion in Two-Body Systems 29
1.4.2 Ephemerides 33
1.4.3 Perturbations by and on Extended Bodies 35

1.5 Solar System 36
1.5.1 Sun 36
1.5.2 Planets 37
1.5.3 Satellites 37
1.5.4 Other Bodies 38
1.5.5 Planetary Coordinates 38

1.6 Astronomical Phenomena 38
1.6.1 Rising, Setting, and Twilight 39
1.6.2 Meridian Transit 39
1.6.3 Conjunction, Opposition, and Elongation 40
1.6.4 Eclipses, Occultations, and Transits 40
1.6.5 Satellite Phenomena 41
1.6.6 Physical Observations of the Sun, Moon, and Planets 42
References 43

2 Relativity for Astrometry, Celestial Mechanics and Metrology 45
2.1 Introduction 45
2.2 Newtonian Formalism 46
2.3 Special Relativity and the Metric Tensor 48
2.4 Einstein's Theory of Gravity 50
2.5 The Problem of Observables 52
2.5.1 The Ranging Observable 52
2.5.2 The Spectroscopic Observable 52
2.5.3 Astrometric Observables 54
2.6 The Post-Newtonian Framework 55
2.6.1 Coordinate Timescales and Proper Time 56
2.6.2 The Barycentric Celestial Reference System 56
2.6.3 BCRS versus ICRS 59
2.6.4 The Geocentric Celestial Reference System 59
2.6.5 Coordinate Transformations 62
2.6.6 Relativistic Potential Coefficients 62
2.7 Applications 63
2.7.1 Other Versions of the Geocentric Celestial Reference System 63
2.7.2 Rotating Reference Systems 64
2.7.3 The Einstein-Infeld-Hoffmann Equations of Motion 64
2.7.4 Equations of Motion in the GCRS 66
2.7.5 Astrometry 66
2.7.6 VLBI Observations 68
2.8 Relativistic Timescales, their Definitions and Units 68
2.8.1 Practical Transformations of Timescales 68
2.8.2 Scaled Coordinate Timescales 69
2.8.3 Units of Timescales 70
References 71

3 Time 75
3.1 Introduction 75
3.1.1 Absolute (or Newtonian) Time 75
3.1.2 Proper Time 75
3.1.3 Coordinate Time 76
3.2 Time and the Earth's Rotation 76
3.2.1 Sidereal Time 77
3.2.2 UT1 80

3.3 Dynamical Time 81
3.3.1 Ephemeris Time 82
3.3.2 TDT/TDB 83
3.4 Atomic Time 83
3.4.1 International Atomic Time, TAI 84
3.4.2 Terrestrial Time, TT 84
3.5 Civil Time 85
3.5.1 Coordinated Universal Time, UTC 85
3.5.2 Time Zones 86
3.6 Barycentric and Geocentric Coordinate Time 88
3.6.1 Barycentric Coordinate Time, TCB and Barycentric Ephemeris Time, T_{eph} 88
3.6.2 Geocentric Coordinate Time, TCG 89
3.7 Julian Date 91
3.8 Summary of Useful Relationships 92
3.9 Timekeeping 93
3.9.1 Devices 93
3.9.2 International Agencies 95
3.10 Time Dissemination 96
3.10.1 High-Frequency Radio Time Signals 97
3.10.2 Low-Frequency Radio Time Signals 97
3.10.3 LORAN-C 97
3.10.4 Global Positioning System (GPS) 98
3.10.5 GLONASS 98
3.10.6 GALILEO 98
3.10.7 Two-Way Satellite Time Transfer (TWSTT) 99
3.10.8 Time Transfer by Internet 99
3.11 Relativistic Effects 99
3.11.1 Clock Transport from a Rotating Reference Frame 99
3.11.2 Non-rotating Local Inertial Reference Frame 100
3.11.3 Electromagnetic Signal Transfer from a Rotating Reference Frame 101
3.11.4 Electromagnetic Signal Transfer from a Non-rotating, Local Inertial Frame 101
References 101

4 The Fundamental Celestial Reference System 105
4.1 Summary 105
4.2 The ICRS, the ICRF, and the HCRF 105
4.3 Background: Reference Systems and Reference Frames 108
4.4 The Effect of Catalog Errors on Reference Frames 109
4.5 Late 20th Century Developments 111
4.6 ICRS Implementation 112
4.6.1 The Defining Extragalactic Frame 112
4.6.2 The Frame at Optical Wavelengths 113
4.6.3 Standard Algorithms 114

4.6.4 Relationship to Other Systems 114
4.6.5 Data in the ICRS 115
4.7 Formulae 117
References 118

5 Terrestrial Coordinates and the Rotation of the Earth 123
5.1 Introduction 123
5.2 Terrestrial Reference Systems 124
5.2.1 Reference Systems and Reference Frame Concepts 124
5.2.2 The Figure of the Earth and Geodetic Reference Surfaces 127
5.2.3 Geodetic Datums 128
5.2.4 Geocentric, Geodetic, and Astronomical Coordinates 131
5.2.5 Local Coordinate Systems 134
5.3 Gravity, Tides, and Motions of the Crust 148
5.3.1 Modeling the Earth's Gravity Field 149
5.3.2 Representation of the Earth's Gravity Field 150
5.3.3 Solid Earth Tides 153
5.3.4 Ocean Tide Model 158
5.3.5 Site Displacement Due to Ocean and Atmospheric Loading 162
5.3.6 Plate Motions 169
5.3.7 Tidal Effects in UT1 170
5.3.8 Tidal Effects in Polar Motion 171
5.4 Monitoring the Orientation of the Earth 175
5.4.1 Very Long Baseline Interferometry 176
5.4.2 Global Navigation Satellite System 177
5.4.3 Laser Ranging 179
5.4.4 Doppler Orbitography and Radiopositioning Integrated by Satellite (DORIS) 181
5.4.5 Historical Methods 181
5.4.6 Alternative Techniques 183
5.4.7 International Services 184
References 187

6 Precession, Nutation, Polar Motion, and Earth Rotation 199
6.1 Introduction 199
6.2 The Celestial Reference System (CRS) and the Terrestrial Reference System (TRS) 200
6.2.1 Reference Systems in The Astronomical Almanac *202*
6.2.2 The Conventional International Origin and the International Terrestrial Reference Frame (ITRF) 203
6.2.3 The Celestial Intermediate Reference System and the Celestial Intermediate Pole (CIP) 204
6.2.4 The Equinoxes 206
6.3 The Equation of the Equinoxes, $E_e(T)$ 207

6.4 The Equation of the Origins, $E_o(T)$ 208
6.5 The J2000.0 to ICRS Frame Bias Matrix 208
6.6 Precession and Nutation 209
6.6.1 The IAU 2000 Precession-Nutation Theory and IAU 2006/2000A 209
6.6.2 Precession 211
6.6.3 Nutation 223
6.7 The Celestial Intermediate Origin (CIO) 227
6.8 Time and Earth Orientation 229
6.8.1 Apparent Solar Time, Mean Solar Time, and the Equation of Time 230
6.8.2 Greenwich Mean Time 231
6.8.3 Universal Time (UT) 232
6.8.4 Earth Rotation Angle (ERA or θ) 233
6.8.5 Sidereal Time 234
6.8.6 Conversions between Universal Time and Sidereal Time 235
6.8.7 Conversion of Local Apparent Sidereal Time to UT1 237
6.8.8 Local Time and Hour Angle 238
6.9 The Terrestrial Intermediate Origin (TIO) 239
6.9.1 The Ephemeris Meridian 239
6.9.2 Polar Motion 240
References 244

7 Positions 249

Introduction 249
7.1 Summary of Systems, Places, and Coordinates 250
7.1.1 Reference Systems 251
7.1.2 Places 252
7.1.3 Coordinates 253
7.1.4 Summary of Notations 257
7.2 Components Used in the Reduction of Positions 258
7.2.1 Space Motion 258
7.2.2 Parallax 261
7.2.3 Aberration 263
7.2.4 Gravitational Light-Deflection 270
7.2.5 Celestial "Of Date" Positions 272
7.2.6 Terrestrial "Of Date" Positions 275
7.2.7 Refraction 277
7.3 Reduction of Positions from the BCRS to the GCRS 281
7.3.1 Proper Place 281
7.3.2 Local Place 281
7.3.3 Astrometric Place 281
7.3.4 Differential Astrometry 283
7.4 Algorithms for the Reductions of Positions 283
7.4.1 Apparent and Intermediate Place Algorithm for Planets 283
7.4.2 Apparent and Intermediate Place Algorithm for Stars 290

7.4.3 Topocentric Place Algorithm 293
7.4.4 Summary of the Algorithms 297
7.4.5 Approximate Algorithms 298
References 301
Further Reading 303

8 Orbital Ephemerides of the Sun, Moon, and Planets 305
8.1 Fundamental Ephemerides 305
8.2 Previous Ephemerides Used in *The Astronomical Almanac* 306
8.2.1 Ephemerides Prior to 1984 306
8.2.2 Ephemerides from 1984 through 2002 307
8.2.3 Ephemerides Starting in 2003 307
8.3 Equations of Motion 307
8.3.1 Point-Mass Interactions 308
8.3.2 Solar System Barycenter 309
8.3.3 Figure Effects 309
8.3.4 Lunar Gravity Coefficients 310
8.3.5 Lunar Physical Libration: Coordinates 311
8.3.6 Physical Libration Differential Equations 311
8.3.7 The Moment of Inertia Tensor 312
8.3.8 Time Derivative of the Inertia Tensor 312
8.3.9 Principal Moments 313
8.3.10 Figure–Point Mass Torques upon the Moon 313
8.3.11 Figure–Figure Torque upon the Moon 313
8.3.12 Acceleration of the Moon from Earth Tides 314
8.4 The Numerical Integration of DE405/LE405 315
8.4.1 Estimated Integration Error 315
8.4.2 Adopted Constants 315
8.5 Observational Data Fit by the Planetary and Lunar Ephemerides 316
8.5.1 Optical Data 316
8.5.2 Meridian Transits 316
8.5.3 Photographic and CCD Astrometry 317
8.5.4 Occultation Timings 317
8.5.5 Astrolabe 317
8.5.6 Radiometric Emission Measurements 317
8.5.7 Ranging Data 317
8.5.8 Orbiter Range Points 320
8.5.9 Lander Range Data 320
8.5.10 VLBI Data 320
8.5.11 Lunar Laser Range Data 320
8.6 The Orientation of DE405/LE405 321
8.6.1 Adjustment of DE405 onto the ICRF Reference Frame 321
8.7 Various Formulae Used in the Reduction of the Observational Data 321
8.7.1 Phase Corrections 322
8.7.2 Corrections to Precession and Equinox Drift 322
8.7.3 Computation of Ranges 322

8.7.4 Antenna Location 323
8.7.5 Time Delay for Relativity 323
8.7.6 Time Delay for the Solar Corona 323
8.7.7 Time Delay for the Troposphere 324
8.7.8 Modeling the Surface of Mercury 324
8.7.9 Modeling the Surface of Venus 324
8.7.10 Modeling the Surface of Mars—Closure Points 325
8.7.11 Viking Lander Computations 325
8.8 Initial Conditions and Constants of DE405/LE405 325
8.8.1 Asteroids 332
8.9 Positional Errors of the Planetary and Lunar Ephemerides 332
8.9.1 Inner Four Planets: Ephemerides from Ranging and VLBI 332
8.9.2 Uncertainties from Asteroid Perturbations 333
8.9.3 Outer Planets: Reliance on the Classical Optical Observations 333
8.9.4 Planetary Positional Errors in the Almanacs, 1984–2002 333
8.9.5 Planetary Position Uncertainties in 2003 333
8.10 Keplerian Elements for Approximate Positions of the Major Planets 338
8.10.1 Formulae for Using the Keplerian Elements 339
8.10.2 Solution of Kepler's Equation, $M = E - e \sin E$ 340
8.10.3 Approximate Accuracies of the Keplerian Formulae 341
8.11 The Availability of Ephemerides 341
References 342

9 Planetary Satellites and Rings 347
9.1 Introduction 347
9.2 Orbital Elements and Perturbations 347
9.2.1 Orbital Elements 347
9.2.2 Secular Perturbations of the Orbit 349
9.2.3 Perturbations due to Commensurabilities 351
9.2.4 Long-Period Perturbations by Other Satellites 352
9.3 Planetocentric Rectangular Coordinates 353
9.4 Traditional Method 356
9.4.1 The Apparent Orbit 356
9.4.2 Calculating Tabulated Values 360
9.5 Modern Method 361
9.5.1 The Apparent Orbit 361
9.5.2 Calculating Tabulated Values 363
9.6 Satellite Data in *The Astronomical Almanac* and Notation 365
9.6.1 Presented Data 365
9.6.2 Notation 365
9.7 The Satellites of Mars 367
9.8 The Satellites of Jupiter 369
9.8.1 The Galilean Satellites 369
9.8.2 Jupiter's Fifth Satellite, Amalthea 373
9.8.3 Jupiter's Sixth through Thirteenth Satellites 375

9.9 The Rings and Satellites of Saturn 376
9.9.1 The Rings of Saturn 376
9.9.2 The Satellites of Saturn 378
9.10 The Rings and Satellites of Uranus 388
9.11 The Satellites of Neptune 393
9.11.1 Triton 393
9.11.2 Nereid 394
9.12 The Satellites of Pluto 396
References 397

10 Physical Ephemerides of Solar System Bodies 399
10.1 Introduction 399
10.2 Rotational Elements and Cartographic Coordinates 399
10.2.1 Planetocentric and Planetographic Coordinate Systems 401
10.2.2 Coordinate Systems of Small Bodies 406
10.3 Phases and Magnitudes 410
10.3.1 Absolute and Apparent Magnitudes 410
10.3.2 Surface Brightness 412
10.4 The Apparent Disk of a Solar System Body 415
10.4.1 Sub-Earth Points and Sub-Solar Points 417
10.4.2 The Greatest Defect of Illumination 422
10.4.3 The Apparent Magnitudes of the Minor Planets 422
10.5 Physical Ephemeris of the Sun 426
10.6 Physical Ephemeris of the Moon 427
10.6.1 Calculating Librations 429
10.7 Physical Ephemerides of the Planets 434
10.7.1 Mercury 435
10.7.2 Venus 435
10.7.3 Mars 436
10.7.4 Jupiter 436
10.7.5 Saturn 436
10.7.6 Uranus 437
10.7.7 Neptune 437
10.8 Physical Ephemerides of the Dwarf Planets 437
10.9 Physical Ephemerides of the Satellites 438
10.9.1 Satellites of Mars 438
10.9.2 Satellites of Jupiter 439
10.9.3 Satellites of Saturn 441
10.9.4 Satellites of Uranus 441
10.9.5 Satellites of Neptune 443
10.9.6 Satellites of Pluto 447
References 447

11 Eclipses of the Sun and Moon 453

11.1 Introduction 453
11.1.1 Eclipse Data Available from the Nautical Almanac Offices 454
11.1.2 Corrections to the Ephemerides 456

11.2 The Occurrence of Lunar and Solar Eclipses 457
11.2.1 Overview 457
11.2.2 Geocentric Least Angular Separation 457
11.2.3 Occurrence of Lunar Eclipses 459
11.2.4 Occurrence of Solar Eclipses 461

11.3 Solar Eclipses 464
11.3.1 Fundamental Equations: Introduction 464
11.3.2 Besselian Elements 464
11.3.3 Coordinates of the Observer 470
11.3.4 Conditional and Variational Equations 474
11.3.5 Calculation of General Solar Eclipse Phenomena 477
11.3.6 Local Circumstances 487

11.4 Lunar Eclipses 491
11.4.1 Introduction 491
11.4.2 Computations 492

11.5 Eclipses Online 495
11.5.1 Solar Eclipses 495
11.5.2 Lunar Eclipses 497

11.6 Transits 499

References 502

Further Reading 502

12 Astronomical Phenomena 505

12.1 General Aspects of the Night Sky 505

12.2 Configurations of the Sun, Moon, and Planets 506
12.2.1 Interesting Phenomena of the Sun, Earth, and Moon 506
12.2.2 Geocentric Phenomena 508
12.2.3 Heliocentric Phenomena 511

12.3 Risings, Settings, and Twilight 511
12.3.1 Sunrise, Sunset, and Twilight 512
12.3.2 Moonrise and Moonset 514
12.3.3 Formulae Associated with Rising and Setting 515
12.3.4 Illumination 518

12.4 Occultations 521
12.4.1 Occultations of Stars 521
12.4.2 Occultations of Planets 524

12.5 Pole Star Tables 525
12.5.1 Derivation of the Pole Star Coefficients 527

References 528

13 Stars and Stellar Systems 529

13.1 Introduction 529
13.1.1 Data Presentation 529
13.1.2 Sources of Data 530
13.1.3 Sources of Position 530

13.2 Stellar Data 531
13.2.1 Bright Stars 531
13.2.2 Double Stars 532
13.2.3 Photometric Standards 534
13.2.4 Radial Velocity Standards 536
13.2.5 Variable Stars 537
13.2.6 Exoplanets and Host Stars 538
13.2.7 Pulsars 539

13.3 Clusters and Galaxies 539
13.3.1 Open Star Clusters 539
13.3.2 Globular Star Clusters 541
13.3.3 Bright Galaxies 542
13.3.4 Quasi-Stellar Objects 544

13.4 Wavelength Specific Sources 545
13.4.1 Radio-Source Positional Calibrators 545
13.4.2 Radio-Flux Calibrators 546
13.4.3 X-Ray and Gamma Ray Sources 547

References 548

14 Computational Techniques 555

14.1 Introduction to Computing Techniques 555

14.2 Interpolation and Subtabulation 559
14.2.1 Introduction and Notation 559
14.2.2 Interpolation Formulae 560
14.2.3 Inverse Interpolation 561
14.2.4 Polynomial Representations 561
14.2.5 Chebyshev Polynomials 562

14.3 Plane and Spherical Trigonometry 563

14.4 Matrix and Vector Techniques 565
14.4.1 Matrix Multiplication 565
14.4.2 Rotation of Axes Using Matrices 565
14.4.3 Spherical Coordinates Using Vectors 567
14.4.4 Specific Coordinate Transformations 569

14.5 Numerical Calculus 572
14.5.1 Numerical Differentiation 572
14.5.2 Numerical Integration 574

14.6 Statistics 578
14.6.1 Accumulation of Error 578
14.6.2 The Method of Least-Squares 579

References 583

15 Calendars 585

15.1 Introduction 585
15.1.1 Overview 585
15.1.2 Uses of Calendars 586
15.1.3 Astronomical Bases of Calendars 586
15.1.4 Astronomical, Observational and Arithmetic Calendars 587
15.1.5 Visibility of the Crescent Moon 588
15.1.6 Non-astronomical Cycles and the Week 588
15.1.7 Historical Eras and Chronology 589
15.1.8 The Christian Era 589
15.1.9 Dates 591
15.1.10 Julian Day Numbers and Julian Dates 591
15.1.11 Luni-solar Calendars 592
15.1.12 Accuracy of Calendars 593

15.2 The Ancient Egyptian Calendar 593
15.2.1 History of the Egyptian Calendars 593
15.2.2 Rules of the Egyptian Calendar 594

15.3 The Roman and Julian Calendars 594
15.3.1 Introduction 594
15.3.2 Divisions of the Roman Months 595
15.3.3 Caesar's Reform 595
15.3.4 The Julian Calendar in Medieval Europe 597
15.3.5 Rules for the Julian Calendar 597

15.4 The Gregorian Calendar 598
15.4.1 History of the Gregorian Reform 598
15.4.2 Rules for the Civil Use of the Gregorian Calendar 599
15.4.3 Rules for the Ecclesiastical Calendar 599
15.4.4 Calculation of the Date of Easter Sunday 600

15.5 The Jewish Calendar 601
15.5.1 History of the Jewish Calendar 601
15.5.2 Rules for the Modern Jewish Calendar 602
15.5.3 Rules for Postponement (Dehiyyot) 603
15.5.4 Determining Tishri 1 604
15.5.5 Determining the Length of the Year 605
15.5.6 Terminology of the Jewish Calendar 606

15.6 The Islamic Calendar 606
15.6.1 Introduction 606
15.6.2 History of the Islamic Calendar 607
15.6.3 Rules for the Arithmetic Islamic Calendar 607

15.7 The Indian Calendars 608
15.7.1 History of Indian Calendars 608
15.7.2 The Traditional Indian Solar Calendar 609
15.7.3 The Traditional Indian Luni-solar Calendar 609
15.7.4 Rules of the Reformed Saka Calendar 610

15.8 The Chinese Calendar 610
15.8.1 History of the Chinese Calendar 610
15.8.2 Sexagenary Cycle 612

15.8.3 Major and Minor Terms 612
15.8.4 Rules for the Modern Chinese Calendar 613
15.8.5 Finding the First Day of a Chinese Year 614
15.8.6 Finding the First Day of Each Month in a Chinese Year 615
15.9 The French Republican Calendar 616
15.10 The Bahá'i Calendar 616
15.11 Calendar Conversion Algorithms 617
15.11.1 Introduction 617
15.11.2 Calculating the Day of the Week 618
15.11.3 Interconverting Dates and Julian Day Numbers 618
15.11.4 Converting Dates in the Jewish Calendar 619
15.11.5 Calculating the Date of Easter 621
15.12 Calendar Conversion Programs 621
References 622

A Bases and Constants 625
A.1 Bases 625
A.2 Astronomical Constants 625
A.2.1 CODATA 626
A.2.2 Future of the Astronomical Unit 626
References 626

B Acronyms 627

C Glossary 633

Index 661

List of Figures

1.1 Calculation of sidereal time 12
1.2 Variation in the equation of time through the year 13
1.3 Representation of the vector **r** in rectangular coordinates 17
1.4 Equatorial and ecliptic reference planes 19
1.5 Geocentric and geodetic coordinates 21
1.6 Relation between geographic latitude and the altitude of the celestial pole 24
1.7 Parallax of an object 27
1.8 Geometric properties of conic sections 31
1.9 Angular orbital elements 32
2.1 Schematic of a ranging observable 53
2.2 Schematic of a spectroscopic observable 53
2.3 Schematic of an astrometric observable 55
3.1 World time zone map 88
3.2 Relationship among timescales 90
3.3 Interrelationship of timescales 93
4.1 Schematic of the celestial coordinates of a catalog object 108
4.2 Errors in proper motion resulting from the random errors in the measurement of position at various epochs 111
5.1 The Earth's surface and reference surfaces 128
5.2 Geocentric (ϕ') and geodetic (ϕ) latitude 130
5.3 Astronomical latitude and longitude 130
5.4 Deflection of the vertical on a unit sphere 133
5.5 Geocentric Cartesian coordinates and geographical coordinates 133
5.6 Horizon system altitude and azimuth 135
5.7 UTM and UPS grid zone designations 138
6.1 Relationship between origins of right ascension 202
6.2 Motions on the sky of the ecliptic pole, the Earth's mean pole and the CIP 210
6.3 General precession connects the mean equinox of epoch to the mean equinox of date 213
6.4 Precession angles connect the mean pole of epoch to the mean pole of date 214
6.5 The difference between Lieske et al. (1977) and the Newcomb (1895) definitions of the general precession 215
6.6 The Lieske et al. (1977) precession angles 217

6.7 The nutations in longitude and latitude relate the mean pole of date to the CIP via the ecliptic pole of date 225

6.8 Schematic representation of the relationships between the different fiducial meridians encountered in the celestial and terrestrial coordinate systems 240

6.9 Motion of the pole with respect to the *Conventional International Origin* from 1973.0 through 2009.5 241

6.10 Polar motion in x, y from 1973.0 through 2009.5 242

7.1 Relationships of origins 254

7.2 Light-time displacement 264

7.3 Stellar aberration 265

7.4 Gravitational light-deflection 271

7.5 Light from the planets and stars deflected by the Sun 273

8.1 Differences in right ascension, declination and distance between DE200−DE409 334

8.6 Differences in right ascension, declination and distance between DE200−DE409 335

8.11 Differences in right ascension, declination and distance between DE405−DE409 336

8.16 Differences in right ascension, declination and distance between DE405−DE409 337

9.1 The orbital elements used to describe the orbital plane relative to a reference plane 348

9.2 An equivalent form of the orbital elements 348

9.3 The Laplacian plane 350

9.4 The satellite orbit referred to an intermediate plane 355

9.5 Coordinates of the satellite relative to the planet 355

9.6 Planetocentric celestial sphere 357

9.7 Spherical triangle used to compute U, B, and P 358

9.8 Spherical triangle used to compute σ and $p - P$ 358

9.9 Apparent orbit of a satellite as projected on the geocentric sphere 359

9.10 Apparent orbit of the satellite projected on to the tangent plane, and the coordinate system used 362

9.11 Reference system for Phobos and Deimos 368

9.12 Reference system for Amalthea and Thebe 374

9.13 Reference plane for Mimas, Enceladus, Tethys, and Dione 379

9.14 Reference system for Rhea, Titan, Hyperion, Iapetus, and Phoebe 383

9.15 Angles needed to evaluate solar perturbations on Titan 383

9.16 Reference system for the Uranian satellites 392

9.17 Reference system for Triton 394

9.18 Reference system for Nereid 395

10.1 The position of the north pole and prime meridian of a solar system body in Earth equatorial coordinates 400

10.2 Planetocentric and planetographic coordinates systems 403

10.3 The basic vectors and angle of illumination, i, in the Earth–Sun–planet plane 411

10.4 The geometric appearance of the apparent polar radius, b' 416

10.5 The disk of a planet as seen from an observer on the Earth 418

10.6 Planetocentric unit vectors and angles 420

10.7 Lunar angles given in the JPL ephemerides vs. the traditional angles 430

10.8 The angles of the lunar orbit used in the determination of the apparent librations of the Moon 432
11.1 Geometric construct for determining whether an eclipse will occur 458
11.2 Geometric parameters of the Earth's penumbral shadow 460
11.3 Geometric parameters of the Earth's umbral shadow 460
11.4 Limiting conditions for lunar eclipses 461
11.5 Geometric parameters for a partial solar eclipse when Moon is externally tangent 462
11.6 Geometric parameters for a partial solar eclipse when Moon is internally tangent 463
11.7 Transformation of geocentric equatorial coordinates to the fundamental plane 465
11.8 Components of shadow cones in the Besselian fundamental reference system 467
11.9 Relationships among angular semidiameter, apparent semidiameter, and parallax 468
11.10 Vertex angle of the penumbra 469
11.11 Vertex angle of the umbra 469
11.12 Angular quantities in the geocentric equatorial plane 470
11.13 Relationship between rectangular and polar reference systems 478
11.14 Definition of auxiliary quantity ψ 484
11.15 Visualization of the magnitude of a solar eclipse 489
11.16 Visualization of the obscuration of a solar eclipse 490
11.17 Total solar eclipse diagram from *Eclipses Online* 496
11.18 Total lunar eclipse diagram from *Eclipses Online* 498
11.19 Transits across the Sun 501
12.1 The analemmic curve 514
12.2 The horizon at rising or setting 517
12.3 Ground illumination from various sources 519
12.4 Fundamental plane showing path of occultation 524
12.5 PZS triangle for Polaris 525
12.6 Polaris north polar distance 2096–2105 527
14.1 Spherical triangle 556
14.2 The first few Chebyshev polynomials of the first kind 563
14.3 Arc of circle 565
14.4 Triangle on unit sphere 568

List of Tables

1.1 Variations in the Earth's rate of rotation 25

3.1 TAI − UTC (ΔAT) 87

3.2 Low-frequency radio time signals 97

5.1 Earth ellipsoids 143

5.2 Historical geodetic datums 144

5.3 Suggested truncation levels for use of EGM2008 at different orbits 151

5.4 Low-degree coefficients of the conventional geopotential model. 152

5.5 Solid tide corrections when $k_2 = 0.30$ 154

5.6 Ocean tide coefficients from the Schwiderski model 160

5.7 Displacement due to ocean loading 164

5.8 Cartesian rotation vector for each plate using absolute plate model NNR-NUVEL-1A (no net rotation) 170

5.9 Zonal tide terms with periods up to 35 days 172

5.10 Zonal tide terms with periods greater than 35 days 173

5.11 Ocean tidal variations in polar motion and polar motion excitation 174

5.12 Estimated accuracies of EOP techniques 175

6.1 Coefficients of the series for the equation of the equinoxes, E_e, larger than 0.5 μas 207

6.2 Coefficients describing the position of the ecliptic of date with respect to the ecliptic of J2000.0 213

6.3 IAU recommended coefficients describing the position of the ecliptic of date with respect to the ecliptic of J2000.0 216

6.4 Lieske et al. (1977) coefficients describing the position of the ecliptic of date with respect to the ecliptic of J2000.0 (obsolete) 216

6.5 Precession angles with respect to the mean equator and equinox of B1950.0 at 1984 Jan. $1^d\ 0^h$ for various precession theories 222

6.6 Critical arguments for the IAU 2000A nutation 227

7.1 Summary of reference systems 250

7.2 Summary of places 250

7.3 Coefficients (nma/c) for the planets 267

7.4 Apparent deflection angles 272

8.1 Observational data fit by DE405 318

8.2 Initial conditions at JED (T_{eph}) 2440400.5 (June 28, 1969) 326

8.3 J2000.0 angular coordinates of the lunar physical librations 326

8.4 Dynamical constants used in the integration of DE405/LE405 327
8.5 Auxiliary constants used in the observational reductions for DE405/LE405 329
8.6 The 297 non-Big 3 individual asteroids used in the integration of DE405 330
8.7 Keplerian elements and their rates, with respect to the mean ecliptic and equinox of J2000.0, valid for the time-interval A.D. 1800–A.D. 2050 338
8.8 Keplerian elements and their rates, with respect to the mean ecliptic and equinox of J2000.0, valid for the time-interval 3000 B.C.–A.D. 3000 339
8.9 Additional terms for the computation of M for Jupiter through Pluto 339
8.10 Approximate errors in right ascension, α, declination, δ, and distance, ρ, from the Keplerian formulation of § 8.10.3 341
9.1 Principal commensurabilities among satellites 353
9.2 Summary of satellite positional data in *The Astronomical Almanac* 366
9.3 The starting planetocentric coordinates and velocities of some Jovian satellites 376
10.1 The positions of the poles and prime meridians of the planets and Pluto 402
10.2 The equatorial radii and flattenings of the planets and Pluto 403
10.3 The radii of planetary satellites 404
10.4 The radii and effective radius of selected asteroids and comets 408
10.5 The diameters of the asteroids 408
10.6 The visual magnitudes and phase coefficients for the planets, Pluto, and the Galilean satellites of Jupiter 413
10.7 The visual magnitudes and Johnson colors of the satellites 413
10.8 The H and G parameters for the minor planets 424
10.9 The rotation parameters for Mars' satellites 439
10.10 The rotation parameters for Jupiter's satellites 440
10.11 Standard cartographic longitudes for Jupiter's satellites 441
10.12 Rotation parameters for Saturn's satellites 442
10.13 Standard cartographic longitudes for Saturn's satellites 443
10.14 Rotation parameters for Uranus' satellites 444
10.15 Rotation parameters for Neptune's satellites 446
10.16 Rotation parameters for Pluto's satellite, I Charon 447
11.1 Selected USNO eclipse circulars 455
11.2 Sequences and conditions for contact times 494
11.3 Transits of Mercury for 112 years 500
12.1 Time of commencement of the seasons during the 21st century 507
12.2 Geocentric phenomena for which $f(t) = 0$ 509
12.3 Geocentric phenomena for which $f'(t) = 0$ 510
12.4 Visibility criteria for geocentric phenomena 510
12.5 Synodic periods of selected solar system objects 510
12.6 Long-period cycles of Mercury, Venus, and Mars 511
12.7 Heliocentric phenomena 511
12.8 Coefficients for calculating ground illumination 519
14.1 Precision of angle and number of decimals for trigonometric functions 557

14.2 The method of inverse use 558
14.3 Range of precision of the inverse determination of an angle 558
14.4 Differences in tabular arguments 560
14.5 Formulae for plane and spherical triangles 564
14.6 Derivatives to an order of 10 575
14.7 Accumulation of error in arithmetical operations 579
15.1 Approximate lengths of the astronomical cycles 587
15.2 Some eras 590
15.3 Months in the ancient Egyptian calendar 594
15.4 Roman dating in the Julian calendar 596
15.5 Months and days therein of the Julian and Gregorian calendars 597
15.6 Number of days in the six categories of the Jewish year 603
15.7 Months and days therein of the Jewish calendar 603
15.8 Periods corresponding to different numbers of lunations 605
15.9 Months and days therein of the formal Islamic calendar 607
15.10 Months of the Indian solar calendar 609
15.11 Months in the Indian luni-solar calendar 610
15.12 Celestial Stems and the Earthly Branches of the sexagenary cycle 612
15.13 Chinese solar terms 613
15.14 Selected arithmetic calendars, with parameters for algorithms 617
15.15 Number of days in the Jewish calendar that precede the first day of the month for a year 618

Foreword

From ancient times, astronomers have crafted almanacs and star lists. Mariners once needed them to steer their ships at sea, and farmers to plant crops. Rulers have used them to schedule holy days and holidays alike. And astronomers themselves have always relied on such works for feedback about their understanding of the universe. (Do follow-up observations match predictions? Is anything amiss with established theories?)

To the majority of almanac users it makes little difference how the calculations are done, so long as they can be trusted. But to the last category of user—astronomers—the underlying basis is just as important as any ephemeris. They need to know exactly where the numbers came from, and how the calculations might be carried forward into the future. Responsible parties, in their rush to issue timely tabular data or for other reasons, have not always met this last need adequately.

To take one early example, Alexandrian astronomer Claudius Ptolemy might have been a little clearer about the positions of 1,028 stars in his *Almagest*. Exactly how he updated an earlier star catalog for precession, or revised it using his own observations, are questions that still vex historians of astronomy two millennia later.

In fact, a detailed explanatory supplement is a fairly new feature in the long saga of astronomical tables. During the 1930s the British *Nautical Almanac* began providing more detailed information about the derivation and use of its tabular data, only to see the page count swell and make the annual volumes unwieldy. Plans to migrate explanatory material to a separate companion book, initially delayed by World War II, were further postponed by the decision to distinguish between Universal Time and Ephemeris Time. Not until 1961 did the first *Explanatory Supplement* appear on the scene. Jointly produced and applying to the astronomical almanacs of both the United Kingdom and the United States, it was the direct ancestor of the present volume.

That first *Explanatory Supplement* reflected a tranquil time when planetary motions and the celestial reference frame seemed mostly under control. Newtonian mechanics was still state of the art, apart from minor relativistic or empirical corrections for certain fast-moving bodies. Analytical theories worked out decades earlier by Simon Newcomb for the inner planets and Ernest W. Brown for the Moon continued to reign. The physical ephemerides of a few planets and their satellites were still tied to values derived in the 19th century. Many pages in the back of the book listed constants connected with the planets' masses, motions, and physical characteristics that were intended to serve for years to come.

The philosophy of those years was *leave well enough alone*. So long as the astronomical almanacs provided enough accuracy for all civil and navigational purposes (which they

did), it was perfectly all right—even desirable—to let the predictions drift from reality by tiny amounts that only astronomers with delicate equipment might detect. The 1961 work explained the situation in a classic pronouncement:

> Most non-astronomers, and even many astronomers not working in the dynamics of the solar system, expect to find in a national ephemeris a list of constants the values of which, if they are not absolutely accurate, are at least as up to date as possible. The importance of self-consistency in the system is little appreciated, and the even greater importance of perpetuating a value that is known to be incorrect is admitted but seldom. The guardians of the system are accused of inaction and negligence, and even prejudice, by those who for one reason or another wish to introduce a new value for some constant.

That approach, admirable in its day, helped in the way orbits and constants were eventually improved. To work on a particular body, an astronomer could simply look up its ephemeris in a long run of almanacs, compare that against an equally long run of observations, and solve for corrections to form an improved theory. Calculating positions anew would have made the task formidable. It's been said that a skilled astronomer needed six hours of pencil-and-paper work with Brown's 1919 *Tables of the Motion of the Moon* to calculate a single, highly accurate position.

But the widespread use of computers has changed all that. Today it is easier to program an old theory, run off "calculated" values, and compare them on the fly with the "observed" ones. There is no longer a need to resist updating constants and planetary theories every few years. Starting with the 1984 almanacs and documented in the much revamped *Explanatory Supplement* of 1992, tweaks to the traditional ephemerides became more frequent.

The 2012 *Explanatory Supplement* goes a big step further. Readers may be surprised to see no master list of constants, past or present, in the back of this book. As Appendix A explains, such constants are being refined so often that it makes better sense to state them in the yearly almanacs to which they apply and on appropriate websites. By focusing instead on procedures and minimizing numerical specifics, the printed *Explanatory Supplement* can retain its authority and usefulness longer.

Several other realities made this third edition necessary. Notice the up-front treatment of relativity (Chapter 2). Those who doubt the impact of relativistic effects on daily life need look no further than the GPS devices in their cars. Similarly, to reduce the stellar data from the European Space Agency's Hipparcos mission, astronomers had to take into account the bending of starlight by the Sun's gravity at elongations up to 90° and beyond. Since 1992 we've also seen the wholesale replacement of the celestial reference frame, an outcome from the linking of Hipparcos's optical stellar positions with those from radio interferometry.

But the book isn't entirely about rigorous measurements and procedures. Along with specialists, a far broader audience will welcome the handy shortcuts, sprinkled throughout, when simple approximations are okay for things like atmospheric refraction, precession, and the equation of time. Historians will want to bookmark the thorough treatise on calendars (Chapter 15). Turning to the carefully honed glossary in the back, readers will find a better guide to common astronomical terms than any of the world's great dictionaries.

In recent years, with solar-system exploration and breakthroughs in cosmology in the limelight, the general public and even some scientists probably came to regard astrometry as an unglamorous backwater, a field of quaint techniques, echoing a sailor with a sextant. The

stunning success of Hipparcos helped jar things back into perspective, and future astrometric missions like Gaia will drive the point home. Careful measurements have always been the key to mastery of planetary and stellar dynamics and the cosmic distance scale. The material detailed in this book is the very bedrock underlying much else that we know about our own solar system and beyond.

Roger W. Sinnott
Senior Contributing Editor, *Sky & Telescope*

Preface

The primary goal of *The Explanatory Supplement to the Astronomical Almanac* is to offer explanatory material, supplemental information, and detailed descriptions of the computational models and algorithms used to produce *The Astronomical Almanac*. A secondary goal is to provide complementary information that does not change annually, such as conceptual explanations, data, and bibliographic references. To fulfill these goals, this book covers many aspects of modern positional astronomy; it is written at a scientifically technical—but non-expert—level. We hope it provides a useful reference for a full range of users including astronomers, engineers, navigators, surveyors, space scientists, educators, historians as well as the general public.

The genesis of this work actually took place over 100 years ago, beginning with the "Astronomical Papers of the American Ephemeris and Nautical Almanac" series. The material was compiled in one publication, now commonly known as "The Explanatory Supplement." The first edition, titled *Explanatory Supplement to the Astronomical Ephemeris and The American Ephemeris and Nautical Almanac*, was prepared jointly by the US Naval Observatory (USNO) Nautical Almanac Office (US NAO) and Her Majesty's Nautical Almanac Office (HMNAO); it was published by Her Majesty's Stationery Office (London) in 1961 and reprinted in 1974. The second edition, titled *Explanatory Supplement to the Astronomical Almanac*, was prepared by USNO staff, HMNAO staff, and a few non-government subject-matter experts; it was published in 1992 by University Science Books. This book is the third in the series. It is essentially a complete revision of the 1992 edition. Each chapter was updated; several of them completely re-written. Along with subjects covered in the previous two editions, it also contains descriptions of the major advancements in positional astronomy over the last 20 years.

Since the previous edition, several changes have taken place in positional astronomy. The International Celestial Reference System, new precession and nutation models, and a new positional paradigm no longer using the ecliptic and equinox have all come into existence. Thus, the staffs of HMNAO and US NAO decided it is time for a new edition.

The intention of the book is to explain the information in *The Astronomical Almanac*, not to form a complete discourse on astronomy. Because *The Astronomical Almanac* prints primarily positional data, this book goes into great detail on techniques to get astronomical positions. The book, however, is not a basic textbook on spherical, dynamical, or positional astronomy. We hope it supplements such textbooks because it contains detailed explanations and current methods of application.

Although most of the authors are from either the USNO or HMNAO, some other subject-matter experts were asked to write about their area of expertise. They included Michael Soffel, Sergei Klioner, Bernard Guinot, Brent Archinal, James Slater, Nikolaos Pavlis, E. Myles Standish, James Williams, James Rhode, Andrew Sinclair, Raynor Duncombe, and Edward Richards. We are indebted to each of them for their contributions. The glossary has been evolving for years and the entire staffs of the USNO Astronomical Applications Department and HMNAO have contributed; Dennis McCarthy, Sergei Klioner, and Sergei Kopekin helped as well. We thank the management team of the UK Hydrographic Office for supporting the contributions of the HMNAO staff, without which this book would have been impossible. Finally, we acknowledge the support given over the years by the management team at USNO, specifically John Bangert, Head of the Astronomical Applications Department; Kenneth Johnston, Scientific Director of the USNO, and the various superintendents that have led USNO while this work was being compiled.

Sean E. Urban
Chief, Nautical Almanac Office
US Naval Observatory

P. Kenneth Seidelmann
Department of Astronomy
University of Virginia

Brent A. Archinal
US Geological Survey. Chapter 5.

John A. Bangert
US Naval Observatory. Chapter 11.

Steven A. Bell
Her Majesty's Nautical Almanac Office. Chapter 11, Chapter 12.

Raynor L. Duncombe
University of Texas at Austin. Chapter 14.

Alan Fiala
US Naval Observatory (retired, deceased). Chapter 11.

Barnard Guinot
Observatoire de Paris (retired). Chapter 3.

James L. Hilton
US Naval Observatory. Chapter 6, Chapter 10.

Catherine Hohenkerk
Her Majesty's Nautical Almanac Office. Chapter 7, Chapter 12.

George H. Kaplan
US Naval Observatory (retired). Chapter 4, appendixes.

Sergei Klioner
Lohrmann Observatory, Technical University, Dresden, Germany. Chapter 2.

Dennis D. McCarthy
US Naval Observatory. Chapter 3, Chapter 6.

Nikolaos K. Pavlis
National Geospatial-Intelligence Agency. Chapter 5.

E. G. Richards
The University of London. Chapter 15.

James R. Rohde
National Geodetic Survey. Chapter 9.

P. Kenneth Seidelmann
University of Virginia. Chapter 1, appendixes.

James A. Slater
National Geospatial-Intelligence Agency (retired). Chapter 5.

Michael Hermann Soffel
Lohrmann Observatory, Technical University, Dresden, Germany. Chapter 2.

E. Myles Standish
Jet Propulsion Laboratory/California Institute of Technology (retired). Chapter 8.

Beth E. Stetzler
US Naval Observatory. Chapter 5.

Susan G. Stewart
US Naval Observatory. Chapter 13.

Mark T. Stollberg
US Naval Observatory. Chapter 9.

Sean E. Urban
US Naval Observatory. Preface, appendixes.

James G. Williams
Jet Propulsion Laboratory/California Institute of Technology (retired). Chapter 8.

Bernard Yallop
Her Majesty's Nautical Almanac Office (retired). Chapter 12.

Explanatory Supplement
to the Astronomical Almanac

CHAPTER 1

Introduction to Positional Astronomy

P. KENNETH SEIDELMANN

1.1 Introduction

1.1.1 Purpose

The Astronomical Almanac gives data on the positions and, where appropriate, orientations of the Sun, Moon, planets, satellites, and stars during the course of a year. These data depend upon the fundamental concepts of spherical and dynamical astronomy. Spherical astronomy provides the tools, algorithms, and theories to determine the varying directions of celestial objects; dynamical astronomy provides the tools, algorithms, and theories to predict their motions. Together, they determine the positional astronomy that underlies the data presented in *The Astronomical Almanac* and this volume. *The Explanatory Supplement* provides the theoretical background and expanded explanations concerning the material tabulated annually in *The Astronomical Almanac*, as well as other publication such at *The Nautical Almanac* and *The Air Almanac*. To aid the user of these books, this chapter introduces the concepts, terminology, and notation of spherical and dynamical astronomy, and also introduces the changes to *The Astronomical Almanac* since the 1992 edition of the *Explanatory Supplement* (Seidelmann 1992). Rigorous definitions, formulae, and explanations appear in later chapters of this book. The glossary gives concise definitions of words particular to spherical and dynamical astronomy. A summary list of the many acronyms used in the book is provided. The reference data are presented in a summary of tables or websites for the convenience of the reader.

1.1.2 Introduction to *The Astronomical Almanac*

The precise measurement of positions of the Sun, Moon, planets, and stars were necessary for the development of mechanics as well as solar system dynamics. The great world system of Ptolemy (c. A.D. 140) depended upon the stellar catalog of Hipparchus (c. 150 B.C.). Nicholas Copernicus (A.D. 1473–1543) depended upon Ptolemy's catalogs. Similarly, Johannus Kepler (A.D. 1571–1630) needed the stellar catalogs by Tycho Brahe (A.D. 1546–1601) to develop his famous three laws, and Brahe started with the positions of Hipparchus. The great synthesis of mechanics created by Isaac Newton (A.D. 1643–1727), combined with Kepler's Laws, the further developments by Carl Friedrich Gauss (1777–1855), Pierre-Simon LaPlace (1749–1827), Simon Newcomb (1835–1909) and many others, all standing on the works of these early scientists, led to the entire fields of celestial mechanics and solar system dynamics, upon which the computations of modern spacecraft orbits and celestial positions depend so

heavily. Their great chain of knowledge and dreams led to the sophisticated sciences of today. *The Astronomical Almanac*, drawing from the works of these great scientists, provides a yearly synthesis of the celestial kinematics and dynamics needed for today's precise astronomy and related sciences.

The Astronomical Almanac is a joint publication of the United States Nautical Almanac Office (USNAO) and Her Majesty's Nautical Almanac Office (HMNAO). First published in 1767 as *The Astronomical Ephemeris and Nautical Almanac* by the UK, they continued to publish it as *The Astronomical Ephemeris* until 1981. The U.S. began publishing the *American Ephemeris and Nautical Almanac* in 1852 for the year 1855. In 1912 the U.S. and UK began their long and successful collaboration to share production of the data. In 1981 the two countries combined the two books into one edition—*The Astronomical Almanac*. *The Nautical Almanac* became a separate publication in the UK and U.S. in 1915 and 1916, respectively. This collaboration between the two offices preceded the formation of the International Astronomical Union (IAU), which was established in 1921 to encourage communication, cooperation, and standards in astronomy.

The almanac offices of France, Germany, and Russia, in addition to the U.S. and UK, first met in 1896 to discuss cooperation and began sharing the work between them to avoid duplication of effort and minimize overall costs. This led eventually to many countries using *The Astronomical Almanac* and to sharing of data for other publications between the offices.

The Astronomical Almanac serves a diverse group of users: astronomers, other scientists, lawyers, surveyors, navigators, the military, government agencies, historians, teachers, the general public, calendar makers, and many others around the world. The book is highly leveraged; i.e., one book may serve a wide audience through a central resource such as a library or observatory. It is a worldwide standard for its data.

The Astronomical Almanac presents a variety of data, each data type appropriate to the celestial object. Most of the data are positional; i.e., coordinates of the various objects. Also included are photometric and rotational data, timescales, astronomical standards, and observatory information. The selected catalog data list the positions for the mid-year of publication. Sun and most planet coordinates are with respect to the mean equator and ecliptic of date. The astrometric coordinates (α, δ) for Pluto and the minor planets use the mean equator and equinox of J2000.0. Rectangular coordinates and osculating elements are also given. Some data (Sun, Moon, major planets, planetary satellites) list apparent places (α, δ) as tabulated ephemerides; i.e., the apparent place versus time—usually for each day of the year at 0^h TT. In many cases additional data (e.g., physical properties) accompany each entry.

The Astronomical Almanac follows a specific structure. The book has several independent sections, each section addressing a different scientific area. Traditionally either the U.S. or UK has technical responsibility for an entire section. The almanac offices provide the information in the book's first section—Phenomena—a year earlier than the rest as a booklet, *Astronomical Phenomena*.

The book contains some useful, often-overlooked sections. The Notes and References Section at the back provides an overview and description of the theories and data. Errata appear in the next edition. Some information appears regularly and changes only when warranted; e.g., the section that lists the coordinates of observatories around the world.

Observatories can request addition to this list by writing to the almanac offices. The section on Tables and Data lists the astronomical constants used by the almanac offices to produce the data as well as other useful information.

Each country provides its data which are collected at the USNAO. Although the book is a joint publication of the UK Hydrographic Office (UKHO) in the UK and the U.S. Government Printing Office (GPO), it is printed solely at GPO; it is available for sale both at UKHO, GPO and other booksellers. The GPO provides copies to Depository Libraries around the United States. The data from the U.S. are in the public domain; the data from HMNAO are under copyright. The Preface of each edition contains details regarding the copyright information.

1.1.3 *The Astronomical Almanac* and *The Explanatory Supplement*

As a guide to the various chapters in this book, use the sections in *The Astronomical Almanac* itself as a guide.

Phenomena. See Chapters 11, 12, and 15 for information on this section.

Time Scales and Coordinate Systems. See Chapter 3 for information on time. See Chapters 4, 5, 6, and 7 for information on reference systems and positional astronomy.

Sun. See Chapters 8 and 10 for information on this section.

Moon. See Chapters 8 and 10 for information on this section.

Major Planets. See Chapters 8 and 10 for information on this section.

Satellites of the Planets. See Chapter 9 for information on this section.

Minor Planets and Comets. See Chapter 10 for information on this section.

Stars and Stellar Systems. See Chapter 13 for information on this section.

Tables and Data. See Chapters 1, 6, and Appendix A for information on this section.

Notes and References. This book gives the details upon which the section is based.

1.1.4 Conceptual Changes since the Last Edition

There have been a number of major changes since the 1992 edition of *The Explanatory Supplement*. The *International Celestial Reference System* (ICRS) has replaced the FK5 reference system. New precession and nutation theories have been adopted. New timescales and coordinate transformations have been introduced. Earth Orientation methods have been improved.

Increases in accuracy, and the theories required by the increased accuracies, have driven most of these changes. For example, Very Long Baseline Interferometers (VLBI) have achieved sub-milliarcsecond accuracies for observations of extragalactic radio sources. These observations have been used to define a conceptually new reference system. Space astrometry led to milliarcsecond (mas) optical observations of stars brighter than ninth magnitude by the Hipparcos satellite. The Hipparcos and Tycho-2 Catalogues contain positions, proper motions, and parallaxes of mas or tens of mas accuracy. The Global Positioning System

(GPS) provides accurate and continuous time transfers. Geodetic observations are used to determine sub-milliarcsecond and sub-daily nutation, polar motion, and Earth rotation on a continuous basis. At these accuracy levels, the definitions of the reference systems and the methods of reduction and analysis require the theory of relativity.

The new, space-fixed, barycentric astronomical reference system is based on the availability of VLBI observations of distant, extragalactic, radio sources. Thus, the FK5 reference frame, based on bright, moving, nearby stars, and a dynamical frame determined from solar system motions, specifically the celestial equator and the equinox, determined from the ecliptic, has been replaced. The new frame was defined to be close to the previous reference frame specified by the FK5 at J2000.0, within the errors of that frame. The x-axis of the ICRS points as closely as possible to the dynamical mean equinox of J2000.0. The new reference system, called the *International Celestial Reference System* (ICRS), is defined by a series of International Astronomical Union (IAU) resolutions passed in 1991, 1997, 2000, 2003 and 2006 (URL[4]).

In order to define rigorously the ICRS in relativistic terms, the IAU introduced two systems: one at the barycenter of the solar system, the *Barycentric Celestial Reference System* (BCRS), and one at the geocenter of the Earth, the *Geocentric Celestial Reference System* (GCRS). Both have post-Newtonian metric tensors with a generalized Lorentz transformation between them that contains the acceleration of the geocenter and the gravitational potential. Unless specifically noted otherwise, the BCRS is assumed to be orientated according to the ICRS axes. The BCRS and GCRS have no kinematical rotation between them, but they have different time coordinates, specifically *Barycentric Coordinate Time* (TCB) and *Geocentric Coordinate Time* (TCG), respectively.

The *International Celestial Reference Frame* (ICRF) is defined by about 300 primary radio sources, which give the frame an accuracy of about 20 microarcseconds. The ICRF is the realization of the ICRS by radio sources. The second realization of the ICRF was adopted by the IAU in 2009 (IERS 2009). The coordinate axes of the ICRF are fixed and not a function of time to the accuracy of the system of VLBI observations. The ICRS does not depend on either the pole of rotation of the Earth or the pole of the ecliptic, which are now subjects of observation.

The VLBI observations that are used to determine the ICRF are generally made from the Earth, so they are with respect to the GCRS. Since the GCRS is in motion around the barycenter, but has fixed directions with respect to the extragalactic sources, there is a Coriolis-like effect from the relativistic theory of the *Lorentz transformation*, if referred to the BCRS. This transformation is the *geodesic precession and nutation*, which is included in the IAU-sanctioned precession and nutation models (see § 6.6).

The realization of the ICRS in optical wavelengths comes from those stars in the Hipparcos Catalogue without problem flags. This catalog's axes have an uncertainty with respect to the ICRS of 0.25 mas/yr in rotation and 0.60 mas in the position of the origin at the epoch 1991.25 (Kovalevsky et al. 1997). The ICRS axes are valid for all dates; to determine astrometric positions on the ICRS for specific dates, the star positions only have to be corrected for their proper motions. This is different than using dynamical axes (such as those of the FK series) where rotations due to the moving equator and equinox needed to be applied in addition to the proper motions.

While the celestial reference frame (ICRF) is a space-fixed frame, the Earth still has many variable motions that are observed accurately by VLBI, GPS, radar, and satellite and lunar laser ranging. There is still the need for a moving reference frame of date, which is based on the true Earth equator of date. The moving reference frame tied to a dynamical reference frame defined by the solar system is still in use, and appropriate data are provided on that system. It is discussed later in this section.

However, the moving reference frame does not have to be tied to a dynamical reference frame. The IAU established a new moving reference frame of date defined by a kinematic system based on the motions of the observing platform, the Earth, rather than a dynamical system based on solar system motions. Both systems are expected to be used and data provided for an extended period of time.

Although the definition of this new moving reference frame is arbitrary, continuation of past methods is clearly desirable where possible. To accomplish this, the IAU introduced new concepts and definitions including a new combined precession-nutation model (with precession corrections and geodesic precession and nutation) called IAU 2000A (IAU 2001, res. B1.6; URL[4]). The nutation portion of this model, called *IAU 2000A nutation* in this publication, was considered finalized, but the precession model in IAU 2000A was understood to be an interim one; it was later revised (see the next paragraph). There are two versions of nutation: IAU 2000A is accurate to 0.1 mas while IAU 2000B is accurate to 1 mas. In the models there are no terms with periods shorter than two days. All periodic terms less than two days are included in polar motion. Geodesic precession and nutation, which is a very different effect than the regular precession and nutation, is included in the new models. Free core nutation is not included in the models.

In 2006 a new precession theory was adopted (IAU 2008, res. B1; URL[4]), replacing the interim one in IAU 2000A. This precession theory is based on Capitaine, Wallace, and Chapront (2003) and is called *IAU 2006 precession* in this publication. This precession theory should be used with IAU 2000A nutation for best accuracies. The new precession theory provides accurate means of determining mean and true positions in the *equinox-based* system; the combination of IAU 2006 precession with IAU 2000A nutation is referred to as *IAU 2006/2000A* in this book.

In 2006 the IAU passed a resolution that recommended that the terms *luni-solar precession* and *planetary precession* be replaced by *precession of the equator* and *precession of the ecliptic*, respectively (Hilton et al. 2006; IAU 2008, res. B1; URL[4]). That resolution also recommended that the ecliptic pole be defined by the mean orbital angular momentum vector of the Earth-Moon barycenter in the BCRS. This means that the *rotating* ecliptic, which follows the geometrical path of the Earth-Moon barycenter and has been historically used since Newcomb, is being replaced by the *inertial* ecliptic, which follows the Earth-Moon barycentric orbital angular-momentum vector in the BCRS.

The IAU defined a new *Celestial Intermediate Pole* (CIP), replacing the Celestial Ephemeris Pole (CEP). It is determined by the IAU 2000A nutation and IAU 2006 precession model. The CIP is the pole of the intermediate equator of date. The IAU introduced the word "intermediate" for the reference frame between the celestial and terrestrial reference frames.

Since the ICRS is independent of the moving equinox, there is no need for the orientation of the x-axis, or departure point, of the moving reference frame of date to be tied to the

equinox. After considering a number of possible choices for a departure point, the *Celestial Intermediate Origin* (CIO), was chosen as an alternative to the equinox. This has some significant advantages:

1. It avoids the confusion between the catalog equinox and dynamical equinox, which itself has several possible definitions.
2. The CIO is defined such that its motion on the fixed sphere has no motion along the equator. This means that the instantaneous movement of the CIO is always at right-angles to the instantaneous equator. The CIO has been called the non-rotating origin in previous papers (Guinot 1979).
3. The angle, called the Earth Rotation Angle, measured along the equator between the CIO and the Terrestrial Intermediate Origin (TIO), in the International Terrestrial Reference Frame (ITRF), is such that it yields UT1 through a strictly linear relation. The time derivative of UT1 is proportional to the instantaneous angular velocity of the Earth.

The location of the CIO on the equator is defined by an integral that involves the path of the precessing-nutating pole since the reference epoch (Capitaine et al 1986). This can be computed from the IAU 2000A nutation and IAU 2006 precession models and from observations. The position of the CIO has a zig-zag secular motion across the ICRF over long periods of time (tens of thousands of years). The small motion of the CIO is due to the choice of the constant of integration and the x-axis of the ICRF being near the equinox of J2000.0. The small motion of the CIO is based on the true motion of the CIP. The hour angle of the CIO is the *Earth Rotation Angle*, which is equivalent to sidereal time.

The Earth Rotation Angle is the replacement for the Greenwich Apparent Sidereal Time (GAST). The origin of the GAST is the equinox, which has components of motion along the equator; these are due to the motion of the equator and ecliptic with respect to each other. Thus, the relationship between GAST and UT1 includes terms due to precession and nutation. The Earth Rotation Angle, and its relation to UT1, does not depend on combinations of precession and nutation.

The *International Terrestrial Reference System* (ITRS) is defined by the International Union of Geodesy and Geophysics (IUGG 1992) and represented by the *International Terrestrial Reference Frame* (ITRF), which is a catalog of positions and velocities of point marks on the Earth. The longitude origin in the ITRF is the *Terrestrial Intermediate Origin* (TIO).

A precession-nutation model, $PN(t)$ transforms the space-fixed ICRF to a reference frame of date, the *Celestial Intermediate Frame* (CIF). The transformation from the CIF to the ITRF involves the matrices for Earth rotation, $R(t)$, and polar motion, $W(t)$. Thus, the transformation from ITRF to ICRF, which may all be considered part of the Earth orientation computation, is accomplished by the expression:

$$\text{ICRF} = PN(t) \times R(t) \times W(t) \times \text{ITRF}. \tag{1.1}$$

Based on the ICRF definition of a fixed reference frame and its realizations, there are currently two different moving reference systems of date available for use. Both use the new precession and nutation models and the latest values of all constants. One reference system uses the equinox-based moving reference frame, and the other uses the new system with the

CIO for the origin of the moving system. The reference system with the precession, nutation, and constants as introduced in 1984 and the equinox-based moving reference frame is no longer recommended for use.

The two systems are referred to as *equinox-based* or *CIO-based*. Right ascensions may be measured from either the equinox or the CIO in the moving frames, and also given in the ICRF in the fixed frame. The terms *equinox right ascension* and *CIO right ascension*, respectively, can be used. CIO right ascensions and declinations are also called true, or intermediate, positions. The *equation of the origins* is the distance between the CIO and the equinox along the intermediate equator; it represents the CIO right ascension of the equinox, or equivalently, the difference between the Earth Rotation Angle and Greenwich Apparent Sidereal Time (ERA-GAST).

Each of the origins of reference frames has its own specific timescale as required by the theory of relativity. Thus, there are Barycentric Coordinate Time (TCB) and Geocentric Coordinate Time (TCG), for coordinate times for those origins, and *Terrestrial Time* (TT) as a proper time on the geoid. (The acronyms are appropriate for the French versions of the names of the timescales.) These timescales are defined by specified gravitational potentials, by the rate of the SI second at the origins, and by Lorentz transformations between them. Thus, there are scaling factors between the different timescales resulting in different relative rates and corresponding differences in their units of length. The JPL Development Ephemerides rescales its barycentric ephemeris time such that it has the same rate as Terrestrial Time. This timescale is called T_{eph}, functionally equivalent to Barycentric Dynamical Time (TDB), which is now defined as a fixed linear function of TCB.

With the availability of new and more accurate observations, the planetary and lunar ephemeredes have improved. Thus, the DE405/LE405 ephemerides have replaced the DE200/LE200 ephemerides. The former were introduced in the 2003 volume replacing DE200/LE200, which were introduced in the 1984 volume and discussed in the previous edition of *The Explanatory Supplement*.

Many of the quantities discussed here are tabulated in the Time-Scales and Coordinate Systems section of *The Astronomical Almanac*. Also in that section, beginning with the 2006 edition, are practical discussions on relationships between different timescales, coordinate systems, and the reduction of coordinates using the traditional and new methodologies. More information about the new reference systems and their implementation can be found in Kaplan (2005), Seidelmann and Kovalevsky (2002), Kovalevsky and Seidelmann (2004), IERS Conventions (2003), and IAU Transactions (1992, 1999, 2001, and 2006).

1.1.5 Implementation of the Changes

The details of the conceptual changes introduced in § 1.1.4 are discussed more thoroughly in this volume. Chapter 2 discusses the general relativistic concepts used for these space-time metrics, the specific space-time metrics for three reference systems: the *Barycentric Reference System* (BCRS), the *Geocentric Reference System* (GCRS), and the *International Celestial Reference System (ICRS)*, and the relativistic concepts needed for time, positional astronomy, celestial mechanics, and metrology. Chapter 3 discusses the timescales appropriate for the various systems and further details on the Earth Rotation Angle. The ICRS and ICRF are presented in Chapter 4. Chapter 5 discusses the ITRS. The new precession

and nutation models sanctioned by the IAU, specifically IAU 2000A nutation (IAU 2001, res. B1.6; URL[4]) and IAU 2006 precession (IAU 2008, res. B1; URL[4]), are given in detail in Chapter 6. These replace the Lieske (1979) theory of precession and the IAU (1980) Theory of Nutation. In addition, the Earth Rotation Angle, θ, as a linear function of Universal Time, the Celestial Intermediate Pole (CIP), and Earth orientation parameters are specified in Chapter 6. The application of all the changes to determine positions in the different reference frames is explained in Chapter 7. Chapter 8 details the new bases for the planetary and lunar ephemerides. The chapters following Chapter 8 have been revised with improvements in knowledge and values in revised explanations.

The USNAO and HMNAO use astronomical software packages NOVAS and SOFA to perform many of the required astronomical calculations. These software packages are independent and conceptually different, yet based on the same models. They are used to provide independent checks on the computations. Resulting computations typically are in agreement at the microarcsecond level. NOVAS is available at URL[2], and the SOFA routines are located at URL[3].

In 1994 the IAU decided to follow the model used by the Committee on Data for Science and Technology (CODATA) and publish tri-annual updates to the IAU (1976) Astronomical Constants. Rather than establish occasional new lists, the IAU, IERS, and IUGG Working Groups produce Best Estimates Lists. *The Astronomical Almanac* now draws its constants from several sources: the latest *Best Estimates List of Astronomical Constants*, *IERS Conventions*, the *Report of the IAU Working Group on Cartographic Coordinates and Rotational Elements*, and the Jet Propulsion Laboratory Planetary Ephemeris. Each edition provides the constants used in the Tables and Data section. Similarly, it is now necessary for scientists to document the values or sources of constants that they have used.

The IAU recommended that the International Earth Rotation and Reference Systems Service (IERS) introduce the new CIO-based reference system on January 1, 2003, and to continue to provide data on the equator-ecliptic system. The IERS has done this. The concepts are sufficiently distinct from the current usage that they cannot substitute directly into existing equations. The form and meaning of the equations change. As of the 2003 edition, *The Astronomical Almanac* uses the DE405/LE405 JPL Planetary Ephemeris. Much of the stellar data now rely on the Hipparcos catalog for their positions. The nutation and precession models from the IAU 2000A theory (as modified by the IERS) appeared in the 2006 edition of *The Astronomical Almanac*. In the 2009 edition, this was changed to the IAU 2000A nutation (IAU 2001, res. B1.6; URL[4]) and IAU 2006 precession (IAU 2008, res. B1; URL[4]). See § 6.6 for details on which implementations are used in the book. The book plans no changes to the equator-ecliptic coordinate system it uses at this time. The majority of data presented rely on a mean equator. Conversion algorithms and tables for determining values in both the *equinox-based* and *CIO-based* systems are given in Section B of *The Astronomical Almanac*.

1.1.5.1 *The Astronomical Almanac Online*

Since the 1992 edition of *The Explanatory Supplement* (Seidelmann 1992), the internet has become a valuable tool in data dissemination. In 2000, HMNAO and USNO launched *The Astronomical Almanac Online*, currently found at URL[1]. This complementary website does not try to duplicate what is in the printed volume; instead it presents data best suited for a computer. Examples are animations of eclipses and visibility maps of lunar occultations.

In some cases, data in the printed volumes can be tailored to users needs using searchable databases; several of the Stars and Stellar Systems tables and the Observatory data have search engines associated with them. The website contains some data no longer found in the printed volume (see § 1.1.6). Although every effort is made to keep the book as error-free as possible, some errors are found. *The Astronomical Almanac Online* provides a tool to give users up-to-date information on any errata brought to the attention of the offices. Updates and expansion of the site occur regularly; as web-based tools continue to evolve, so will the site.

1.1.6 Deletions from This Edition and *The Astronomical Almanac*

The introduction of new concepts and new information has also led to the deletion of some material from this volume and from *The Astronomical Almanac*. In addition, the availability of websites provides a convenient means of providing data for computer application, rather on a printed page. Certain data deleted from the printed edition now appear on a complementary website provided by USNO and HMNAO at http://asa.usno.navy.mil or http://asa.hmnao.com. These include osculating elements referred to equator and equinox of date, the Johnson UBVRI standard stars, and the lunar polynomials. The ICRS has replaced the FK5 and its predecessors, so details of the FK5 have been minimized. The new methods of data reduction and the general use of computers have eliminated the use of Besselian Day Numbers. Greenwich Mean Time is the legal time in England; it is no longer used as a scientific or international timescale or included in the volumes. The ephemeris system DE200/LE200 has been replaced by DE405/LE405 based on more recent observations. The 1976 IAU system of constants is no longer used. There is not an internationally accepted new system of constants; rather there are a number of separate sources of constants. As a result, this volume and *The Astronomical Almanac* use constants from various sources, and the values are tabulated with their sources.

1.2 Timescales and Calendars

1.2.1 Atomic Timescales

1.2.1.1 International Atomic Time

For scientific, practical, and legal purposes, the standard unit for the measurement of intervals of time is the SI second, which is defined by the adoption of a fixed value for the frequency of a particular transition of cesium atoms. Time can be measured in this unit by the use of time standards based on processes of physics. Cesium frequency standards, Cesium fountains, hydrogen masers, ion storage devices, and other such devices are able to count seconds and subdivide them very precisely. Thus, such a device can provide a timescale whose accuracy is dependent on the precision of the measurement and the stability of the device. Such a timescale provides a measure of time for identifying the instants at which events occur; the interval of time between two events can be calculated as the differences between the times of the events. The results of the intercomparison of about 200 frequency standards located around the world are combined to form a standard timescale that can be used for identifying uniquely the instants of time at which events occur on the Earth. This standard timescale is known as *International Atomic Time* (TAI). It is the basis for all timescales in general use.

It is distributed by many different means, including radio time signals; navigation systems, such as the Global Positioning System; communication satellites; and precise time standards.

1.2.1.2 Relativistic Effects

In high-precision timekeeping, and for some purposes in solar system dynamics and astrometry, it is necessary to take into account the effects of special and general relativity and to recognize, for example, that the rate of an atomic clock depends on the gravitational potential in which it is placed, and that the rate will appear to depend on its motion relative to another clock with which it is compared. In particular, one should recognize that the independent variable, or timescale, of the equations of motion of the bodies of the solar system (or of a subset of them) depends upon the coordinate system to which the equations refer. The relationship between any such timescale and TAI, which is appropriate for use at sea level on the surface of the Earth, may be specified by an appropriate formula containing periodic terms and an arbitrary linear term. Starting in 1984 *The Astronomical Almanac* introduced Terrestrial Dynamical Time (TDT) as the timescale for the geocentric ephemerides (giving, for example, apparent positions with respect to the center of the Earth), whereas Barycentric Dynamical Time (TDB) was used as the timescale for the ephemerides that refer to the center of the solar system. TDT differs from TAI by a constant offset, which was chosen arbitrarily to give continuity with Ephemeris Time (see § 1.2.2), whereas TDB and TDT differ by small periodic terms that depend on the form of the relativistic theory being used.

1.2.2 Dynamical Time

The equations of motion of the bodies of the solar system involve time as the independent variable. Until 1960, mean solar time was used, but when it was recognized that the rotation of the Earth was irregular, a new timescale was introduced that corresponded to the independent variable. This was called ephemeris time (ET) and was based on the motion of the Sun. Later, when it was necessary to distinguish between relativistic effects—which cause differences between timescales for the center of the Earth and the center of the solar system—the dynamical time arguments, Terrestrial Dynamical Time, and Barycentric Dynamical Time, were introduced in 1984. TDT was defined in a way that maintains continuity with ET. Since ET was not specified as either TDT or TDB, either can be considered to be the extension of ET. Since TDT (now Terrestrial Time) is defined in terms of the SI second, which can be determined only back to 1956, the determination of dynamical time prior to 1956 must be based on comparison of observations and theories of the motions of the Sun, Moon, and planets. This is a Revised Ephemeris Time.

In 1991 the International Astronomical Union (IAU) adopted resolutions introducing new timescales which all have units of measurement consistent with the SI second (URL[4]). Terrestrial Time (TT) has a unit of measurement of the SI second on the geoid, and can be considered a continuation of TDT. TT is an idealized time. Geocentric Coordinate Time (TCG) and Barycentric Coordinate Time (TCB) are coordinate times for coordinate systems that have their origins at the center of mass of the Earth and of the solar system, respectively. Their units of measurement are chosen to be consistent with the SI second. Because of relativistic transformations, these timescales will exhibit secular variations with respect to Terrestrial Time. For example, TCB will differ in rate by approximately 49 seconds per

century. A timescale T_{eph} is used as the timescale of the JPL ephemerides. T_{eph} is developed from a form of TCB and is rescaled to have a rate similar to TT. In 2006 the IAU redefined TDB to be a fixed linear function of TCB such that effectively TDB is equivalent to T_{eph} and TDB has the same rate as TT. TDB can be used as the time argument of ephemerides and in almanacs.

1.2.3 Timescales Based on Earth's Rotation

As the Earth rotates about its axis, it also moves in its orbit around the Sun. Thus, while the Earth rotates once with respect to a fixed star, the Earth moves in its orbit so that additional rotation is necessary with respect to the Sun to bring the fixed star back to the meridian. The rotation of the Earth with respect to the equinox is called *sidereal time*. The Earth's rotation with respect to the Sun is the basis of *Universal Time* (UT), also called solar time. Since the rotation of the Earth is subject to irregular forces, sidereal time and Universal Time are irregular with respect to atomic time. Sidereal time is the hour angle of the equinox and is subject to the motion (due to precession and nutation) of the equinox itself. Otherwise, it is a direct measure of the diurnal rotation of the Earth. Sidereal time reflects the actual rotation of the Earth and can be determined by observations of stars, artificial satellites, extragalactic radio sources, and data from Global Positioning System satellites. On the other hand, the apparent diurnal motion of the Sun involves both the non-uniform diurnal rotation of the Earth and the motion of the Earth in its orbit around the Sun. In practice, Universal Time, specifically UT1, is directly related to sidereal time by means of a numerical formula. For each local meridian there is a corresponding *local sidereal time*. The measure of the rotation of the Earth with respect to the true equinox is called *apparent sidereal time*. The measure with respect to the mean equinox of date is referred to as *mean sidereal time*. Apparent sidereal time minus mean sidereal time is called the *equation of the equinoxes*.

In 2000 the IAU redefined UT1 to be a linear function of the Earth Rotation Angle (ERA), which is the geocentric angle between the CIO, which has no instantaneous rotation, and the TIO, which rotates with the Earth. So, the ERA is a direct measure of the Earth's rotational motion. Sidereal time, Earth Rotation Angle, and UT1 are mathematically linked and affected by variations in the Earth's rate of rotation (length of day), which are unpredictable and must be determined for observations.

1.2.3.1 Sidereal Time

The local hour angle of the equinox has a special significance since it serves to specify the orientation of the celestial (equatorial) coordinate system with respect to the local terrestrial coordinate system in which the hour angle is measured. The local hour angle of the equinox is known as the local sidereal time (LST) and it increases by 24^h in a sidereal day. The fundamental relation for some celestial object X is

$$\text{local hour angle of } X = \text{local sidereal time} - \text{right ascension of } X. \tag{1.2}$$

This may be written in the abbreviated form

$$\text{LHA } X = \text{LST} - \text{RA } X. \tag{1.3}$$

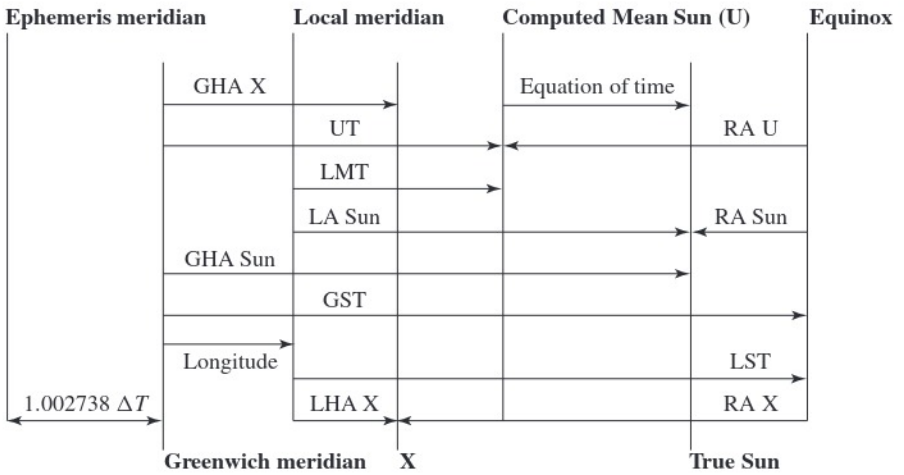


Figure 1.1 Calculation of sidereal time

The value of the local sidereal time is equal to the right ascension of the local meridian, and so may be determined by observing the meridian transits of stars of known right ascensions, the positions of radio sources using Very Long Baseline Interferometry, the motion of GPS satellites in their orbits, or the distance from a location on Earth to a retroreflector on the Moon by Lunar Laser Ranging. Local sidereal time can be calculated from the sidereal time on the prime meridian (Greenwich) when the difference in geographic longitude is known (see Fig. 1.1); thus

$$\text{local sidereal time} = \text{Greenwich sidereal time} + \text{east longitude}. \tag{1.4}$$

1.2.3.2 Solar and Universal Time

The general form of the relationship between solar time and Universal Time may be derived by substituting the Sun for X in Eq. 1.3. The local hour angle of the Sun is, by definition, 12 hours less than local apparent solar time (LAT) and so

$$\text{LAT} = \text{LST} - \text{RA Sun} - 12^{\text{h}}. \tag{1.5}$$

The right ascension of the Sun does not vary uniformly with time nor does the Sun move on the equator, but it is possible to introduce the concept of a point U that moves around the celestial equator at a uniform rate. Hence, Universal Time is defined in terms of Greenwich Sidereal Time (GST) by an expression of the form

$$\text{UT} = \text{GST} - \text{RA } U - 12^{\text{h}} \tag{1.6}$$

where the coefficients in the expression for RA U are chosen so that UT may for most purposes be regarded as mean solar time on the Greenwich meridian.

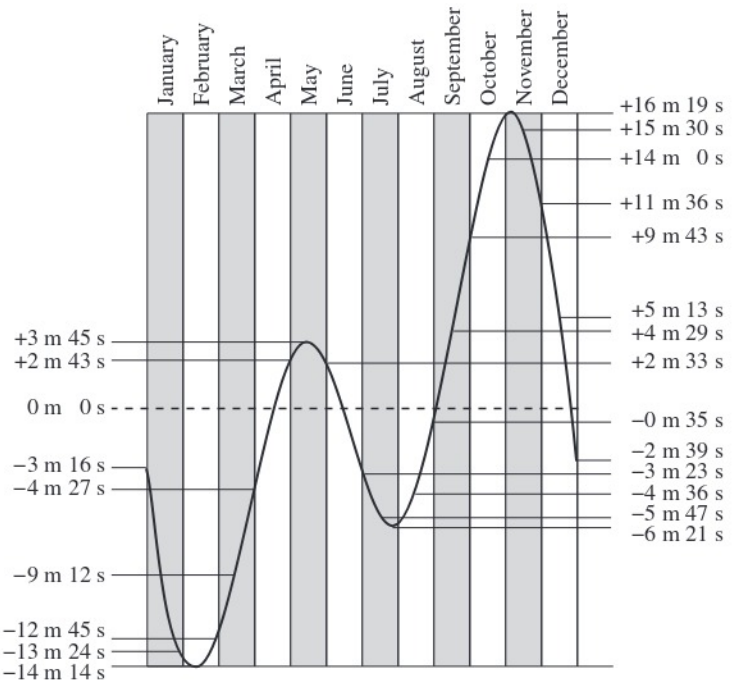


Figure 1.2 Variation in the equation of time through the year

1.2.3.3 Equation of Time

The difference between local mean time (LMT) and local apparent solar time is known as the *equation of time*, and the relationship is now expressed in the form

$$\text{LAT} = \text{LHA Sun} + 12^{\text{h}} = \text{LMT} + \text{equation of time} \tag{1.7}$$

although the equation of time used to be regarded as the correction to be applied to apparent time to obtain mean time. The principal contributions to the equation of time arise from the eccentricity of the Earth's orbit around the Sun (which causes a non-uniformity in the apparent motion of the Sun around the ecliptic) and the inclination of the plane of the ecliptic to the plane of the equator. The equation of time varies through the year in a smoothly periodic manner by up to 16 minutes, as shown in Fig. 1.2.

1.2.4 Coordinated Universal Time (UTC)

Although TAI provides a continuous, uniform, and precise timescale for scientific reference purposes, it is not convenient for general use. In everyday life it is more convenient to use a system of timescales that correspond to the alternation of day and night, apply over fairly wide areas, and can be easily related to each other and to TAI. In these timescales, the numerical expression, or measure, of the time of an event is given in the conventional form of years, months, days, hours, minutes, seconds, and decimals of seconds—i.e., as a calendar date and time of day. The standard time on the prime meridian is known as Coordinated Universal

Time (UTC). UTC is an atomic timescale that is kept in close agreement with Universal Time (UT), which is a measure of the rotation of the Earth on its axis. The rate of rotation of the Earth is not uniform (with respect to atomic time), and the difference between TAI and UT is increasing irregularly by about 1 second every 18 months. The difference between UTC and TAI is always an integral number of seconds. UTC is maintained in close agreement, to better than one second, with UT by introducing extra seconds, known as *leap seconds*, to UTC, usually at the end of the last day of June or December. The Earth is divided into standard-time zones in which the time kept is that of a standard meridian (multiples of 15° longitude). Thus, the local noon at any place in the zone is near twelve noon of the standard time. These standard times usually differ from UTC by integral numbers of hours. In summer, the time may be advanced by an hour to increase the hours of daylight in the evening.

1.2.4.1 Greenwich Mean Time (GMT)

In the past, the term "Greenwich Mean Time" (GMT) has been used for UTC and UT1. It remains the basis of the civil time for the United Kingdom and, as such, is related to UTC. However, in navigation terminology, GMT means Universal Time. For precise purposes it is recommended that the term "GMT" not be used, since it is ambiguous.

Prior to 1925, GMT was measured for astronomical purposes from noon to noon, so that the date would not change in the middle of a night for an observer in Europe. In 1925 that practice was discontinued, and GMT was then measured from midnight to midnight. Thus, care must be taken in using time references before 1925. The term "Greenwich Civil Time" was used for a while for time measured from midnight.

1.2.5 Enumeration of Dates

1.2.5.1 Civil Calendars

The alternation of day and night is a clear physical phenomenon that is repetitive and countable; so the solar day is the basic unit of all calendars. Some calendars use the lunar month and/or solar year for longer units, but these periods are neither fixed nor made up of integral numbers of days. Moreover, the length of the lunar month is not a simple rational fraction of the solar year. However, the cycle of weeks, each of seven named days, is very widely used, and it continues independently of the enumeration of days in the calendar.

The Gregorian calendar is now commonly used throughout most countries of the world for the identification of solar days. It was derived from the Julian calendar, so named because its system of months was introduced by Julius Caesar. The system for the enumeration of years in the Julian calendar was introduced only gradually after A.D. 500; the extension of the system to earlier years is known as the Julian proleptic calendar. The change from the Julian calendar to the Gregorian calendar took place in most countries in western Europe (and in their colonies) between 1583 and 1753. However, many other countries did not change systems until much later, and at times both systems were used concurrently. One must be very careful when using astronomical data published at times and in places where the calendrical system in use may be in doubt. Many other calendars have been used, and may still be used for some purposes, in other countries. Such calendars often depend on various astronomical phenomena and cycles, but are now primarily of religious significance.

A particular instant of time may be identified precisely by giving the calendar date (assumed to be Gregorian unless otherwise specified) and the time of day in a specified time system.

1.2.5.2 Julian Date

For many astronomical purposes it is more convenient to use a continuous count of days that is known as the Julian day number. The day number is extended by the addition of the time of day, expressed as a decimal fraction of day, to give the Julian date (JD). It is important to note, however, that the integral values of the Julian date refer to the instants of Greenwich mean noon (since the system was introduced when the astronomical day began at noon rather than at midnight); correspondingly, the Julian date for 0^h UT always ends in ".5." This, and the fact that current Julian dates require seven digits to express their integral parts, make the Julian date system inconvenient for some purposes. The value of JD minus 2400000.5 is sometimes used for current dates; it is known as the modified Julian date (MJD). The Julian date system may be used with TAI, TT, TCB, or UTC, so when the difference is significant, the particular timescale should be indicated.

1.2.5.3 Besselian and Julian Years

For some astronomical purposes, such as the specification of the epoch of a celestial coordinate system, it is convenient to measure time in years and to identify an instant of time by giving the year and the decimal fraction of the year to a few places. Such a system was introduced by Bessel and is still in use, but it has two disadvantages. First, the length of the year varies slowly, and second, the instants at the beginning of the years (.0) do not correspond to Julian dates, which are convenient for use in dynamical astronomy. The Besselian system has been replaced by a new system in which 100 years is exactly 36525 days (or 1 Julian century) and in which 1900.0 corresponds exactly to the epoch 1900 January 0.5, from which the time interval was reckoned in the principal theories of the motions of the Sun, Moon, and planets. The old and new systems are distinguished when necessary by the use of the prefix letters "B" and "J." The standard epoch that is now recommended for use for new star catalogs and theories of motion is

$$\text{J2000.0} = \text{2000 January 1.5} = \text{JD 2451545.0 TT}. \tag{1.8}$$

1.3 Celestial and Terrestrial Coordinates

1.3.1 Coordinate Systems and Frames

In astronomy, it is necessary and convenient to represent the position of an object, such as a star or a planet, in several different coordinate systems according to the context in which the position is to be used. Each coordinate system corresponds to a particular way of expressing the position of a point with respect to a coordinate frame, such as a set of rectangular axes. Often the coordinate frames with respect to which observations are made differ from the coordinate frames that are convenient for the comparison of observational data with theory. In general, each position is represented by a set of three coordinates that specify the position of the object with respect to a particular coordinate frame. In many cases, the distance of the

object is not known; so two coordinates are sufficient to represent the direction to the object, although three direction cosines may be used.

In general, an object is moving with respect to the coordinate frame, and the coordinate frame is moving and rotating in "space." Therefore, it is necessary to specify the time to which the three spatial coordinates refer and the time for which the coordinate frame is defined. These two times may be the same but are often different. Times may be expressed in terms of different timescales. Both spatial coordinates and times may be expressed in a variety of units. As a further complication, positions may be of several kinds, according to whether allowances have been made for aberration, diurnal rotation, refraction, and other factors that affect the direction in which an object is observed. Ephemerides and catalogs that represent high-precision positions and properties of astronomical objects at given times must always be accompanied by a precise statement that specifies all of these various factors, if the numbers are to be used properly to their full precision.

A coordinate frame is usually represented by three mutually perpendicular (rectangular) axes, and is defined by specifying its origin, a fundamental reference plane (the xy-plane), a direction in that plane (the x-axis), and the positive (or north) side of the plane. Other fundamental planes or directions may be used; for example, the direction of the z-axis (i.e., the normal to, or *pole* of, the xy-plane) may be specified, or the x-axis may be specified as the line of intersection, or *node*, of two reference planes.

The vector $\mathbf{r}$ from the origin to the object may be represented by rectangular coordinates (x, y, z); that is, by the projections of the distance r on the three axes. It can also be represented by spherical coordinates, in which direction is usually specified by the longitudinal angle (λ) in the xy-reference plane and the latitudinal angle (β) from the reference plane (see Fig. 1.3). Less frequently the polar angle ($90° - \beta$), or complement of the latitudinal angle, is used; the prefix "co" may be added to the name in such cases. The longitudinal and latitudinal angles are given different names and symbols in different coordinate frames. If the longitudinal angle is measured in the negative (or left-handed) sense with respect to the z-axis, the prefix "co" may be used to indicate the complement to 360°.

The geometric transformations of coordinates between different coordinate systems, and the allowances for physical effects, may be carried out using the techniques of spherical trigonometry or those of vector and matrix algebra. Generally, matrices would be the preferred method, but some transformations are easier to explain using spherical trigonometry. The concept of the celestial sphere will be used for purposes of explanation, with the arcs on the sphere representing angles between directions. The center of the sphere can be located in many different places, but in most cases the sphere will be used to illustrate a particular reference frame with a specific origin. It must be remembered that when an object represented on the sphere is changing radial distances from the center, these changes must be incorporated into the mathematics of the computation.

1.3.1.1 Coordinate Designations

Many different coordinate systems are used to specify the positions of celestial objects. Each system depends on the choice of coordinate frame and on the way of specifying coordinates with respect to the frame. The term "celestial coordinate frame" is used here for a coordinate frame that does not rotate with the Earth (or other planet), so that the coordinates of stars, for

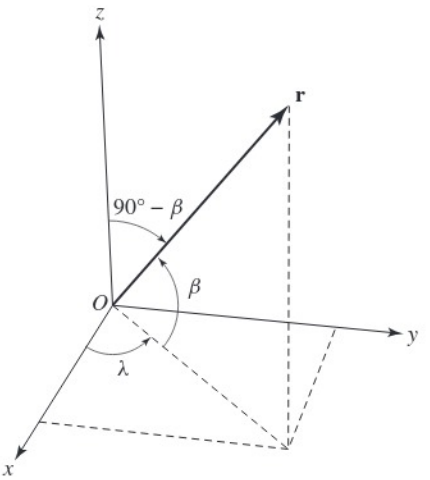


Figure 1.3 Representation of the vector **r** in rectangular coordinates

example, change only slowly with time. (Frames that rotate with the Earth are discussed in § 1.3.3.)

The designations used to indicate the principal origins of celestial coordinate frames are as follows:

1. topocentric: viewed or measured from the surface of the Earth.
2. geocentric: viewed or measured from the center of the Earth.
3. selenocentric: viewed or measured from the center of the Moon.
4. planetocentric: viewed or measured from the center of a planet (with corresponding designations for individual planets).
5. heliocentric: viewed or measured from the center of the Sun.
6. barycentric: viewed or measured from the center of the mass of the solar system (or of the Sun and a specified subset of planets).

The heliocenter and the barycenter are not coincident. The heliocenter has a small orbit about the solar system barycenter. The resulting positional error does not exceed 0.1 mas in the worst case. The principal celestial reference planes through the appropriate origins are as follows:

1. astronomical horizon: the plane that is normal to the local vertical (or apparent direction of gravity) and passes through the observer.
2. local meridian: the plane that contains the local vertical and the direction of the axis of rotation of the Earth.
3. celestial equator: the plane that is normal to the axis of rotation of the Earth and passes through the Earth's center.

4. ecliptic: the mean plane (i.e., ignoring periodic perturbations) of the orbit of the Earth-Moon barycenter around the solar system barycenter.
5. planet's meridian: a plane that contains the axis of rotation of the planet and passes through the observer.
6. planet's equator: the plane that is normal to the axis of rotation of the planet and passes through the planet's center.
7. orbital plane: the plane of the orbit of a body around another (e.g., of a planet around the Sun or barycenter).
8. invariable plane or Laplacian plane: the plane that is normal to the axis of angular momentum of a system and passes through its center.
9. galactic equator: the mean plane of the Milky Way normal to the North Galactic Pole—which is in the constellation Coma at α (1950) $= 12^{\mathrm{h}}49^{\mathrm{m}}$, δ (1950) $= 27^{\circ}\ 27\overset{\prime}{.}4$—and passes through the Galactic Center—which is in the constellation Sagitarius at ICRS (J2000) $\alpha = 17^{\mathrm{h}}45^{\mathrm{m}}.6$, $\delta = -26\overset{\circ}{.}56$.

1.3.2 Celestial Coordinate Systems

1.3.2.1 Equatorial and Ecliptic Frames

The line of intersection of the mean plane of the equator and the ecliptic defines the direction of the vernal equinox (Υ) and the autumnal equinox, as per the northern hemisphere. Using the vernal equinox as the origin, the right ascension (α) is measured in the plane of the equator and ecliptic longitude (λ) is measured in the plane of the ecliptic (see Fig. 1.4). Right ascension, like hour angle, is usually expressed in time measure from 0^{h} to 24^{h}, and both right ascension and longitude are measured in the positive (or right-handed) sense. The complement of right ascension with respect to 24^{h} is known as sidereal hour angle (SHA); in navigational publications it is usually expressed in degrees. Declination is measured from the equatorial plane, positive to the north, from 0° to 90°. Ecliptic latitude is measured from the ecliptic plane, positive to the north, from 0° to 90°.

The equinox is at the ascending node of the ecliptic on the equator; this is the direction at which the Sun, in its annual apparent path around the Earth, crosses the equator from south to north. By definition, it is the time that the apparent ecliptic longitude of the Sun is 0 degrees. It is also referred to as *the first point of Aries*, and it is the vernal (spring) equinox for the Northern Hemisphere. (See Fig. 1.4.) The inclination of the plane of the ecliptic to the plane of the equator is known as the *obliquity of the ecliptic*, ϵ.

The equator and ecliptic are moving because of the effects of perturbing forces on the rotation and motion of the Earth. Hence, the equinox and obliquity change as a function of time; so these celestial coordinate frames must be carefully defined in such a way that they can be related to a standard frame fixed in space.

The International Celestial Reference System (ICRS) was introduced by the IAU in 1998. It is a fixed reference system that does not move with time. It is realized by positions of well observed extragalactic sources that are sufficiently distant so they should have no apparent motions; these sources form the International Celestial Reference Frame (ICRF). The ICRF sources are bright in radio wavelengths but very faint optically, therefore a high-quality subset of the optically bright Hipparcos star catalog is used as a realization of the ICRF at optical

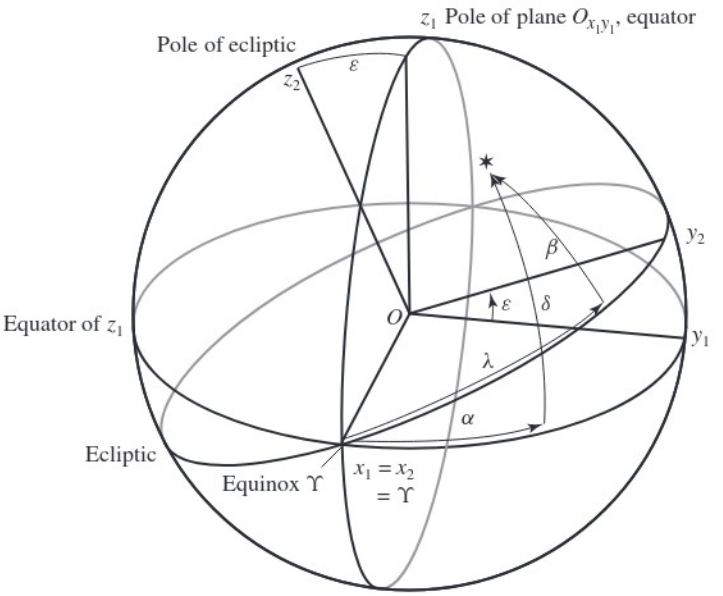


Figure 1.4 Equatorial and ecliptic reference planes

wavelengths. The stars in the Hipparcos catalog are moving due to their proper motions, so positions must be corrected for those motions to specific dates. Since the Earth's equatorial plane is in motion, observations made with respect to the moving reference frame of the Earth must be properly transformed to the ICRF.

1.3.2.2 Precession and Nutation

The celestial pole, which is in the direction of the axis of rotation of the Earth, is not fixed in space, but changes because of gravitational forces, mainly from the Moon and Sun, that act on the non-spherical distribution of matter within the Earth. The quasi-conical motion of the mean celestial pole around the pole of the ecliptic is known as *precession of the equator*, formerly luni-solar precession. The much smaller motion of the actual, or true, celestial pole around the mean pole is known as *nutation*. The period of the precessional motion is about 26,000 years; the principal period of the nutation is 18.6 years. The motions of the celestial pole are accompanied by corresponding motions of the celestial equator and of the equinox.

The motion of the equinox due to precession gives rise to an almost steady increase in the ecliptic longitudes of all stars at the rate of about $50''$ per year, but the ecliptic latitudes are hardly affected. The corresponding changes in right ascensions and declinations depend on the position of the stars in the sky. The nutational motion has an amplitude of about $9''$; it is usually represented as the sum of two components, one in longitude and one in obliquity. There is also a small rotation of the plane of the ecliptic that gives a precession of the equinox of about $12''$ per century and a decrease of the obliquity of the ecliptic of about $47''$ per century; this is known as *precession of the ecliptic*, formerly planetary precession, since it is due to the effects of planetary perturbations on the motions of the Earth and Moon. These motions of the equatorial and ecliptic coordinate frames can be modeled; however, some parameters have

to be determined from observations, since, for example, the internal structure of the Earth is not known well enough. A statement of the celestial coordinates of a star or other celestial object must always specify precisely the coordinate frame to which they refer. It must also be recognized that the coordinates that represent the position (direction) of a celestial object depend on the position and motion of the observer as well as on the origin and orientation of the coordinate frame to which they are referred.

1.3.3 Terrestrial Coordinate Systems

For astronomical purposes it is necessary to specify the position of an observer, or other object, at or near the surface of the Earth in a geocentric coordinate frame that rotates with the Earth and that may be related to the geocentric celestial frame used for specifying the positions of the "fixed" stars. It is also necessary to set up topocentric coordinate frames that may be regarded as fixed with respect to the surface of the Earth and that may be used in the measurement of the positions of celestial objects. The direction of the axis of rotation of the Earth provides an observable reference axis for both geocentric and topocentric frames, and the direction of the vertical (or apparent direction of gravity) provides an additional observable reference axis for topocentric frames.

1.3.3.1 Horizon Reference

The lines of intersection of the plane of the meridian with the planes of the horizon and equator define the directions from which *azimuth* (A) and *local hour angle* (h) are measured. Azimuth is measured in the plane of the horizon from the north, increasing in positive value toward the east. Local hour angle is measured in units of time: 1 hour for each 15° positive to the west with respect to the local meridian.

The latitudinal angles with respect to the horizon and equator are known as *altitude* (a) and *declination* (δ). Altitude is measured positively toward the zenith; in astronomy the zenith distance ($z = 90° - a$) is more generally used. Declination (δ) is measured from the equator, positive toward the north pole of rotation. The zenith distance of the North Pole, which is the same as the co-declination of the local vertical (or zenith), is equal to the geographic co-latitude of the point of observation. This relationship is the basis of the astronomical methods for the determination of geographic latitude.

1.3.3.2 Shape of the Earth

For some astronomical purposes the Earth may be regarded as a sphere, but often one must treat the Earth as an oblate ellipsoid of revolution, or spheroid, and may need to take into account other departures from sphericity. In particular, the height above mean sea level of a point on the Earth is measured from an irregular surface that is known as the geoid (see § 1.3.3.6). Such heights satisfy the condition that water flows downhill under gravity. There are several systems of terrestrial coordinates; so any set of precise coordinates should be accompanied by a precise description of their basis.

The oblateness of the Earth is a consequence of the rotation of the Earth—the axis of rotation coincides on average with the axis of principal moment of inertia, which is usually referred to as the *axis of figure*. The axis of rotation and the axis of figure do not coincide exactly, but the axis of rotation moves slowly in the Earth around the axis of figure in a quasi-periodic motion with a maximum amplitude of about 0.″3 (or about 9 m on the surface of the

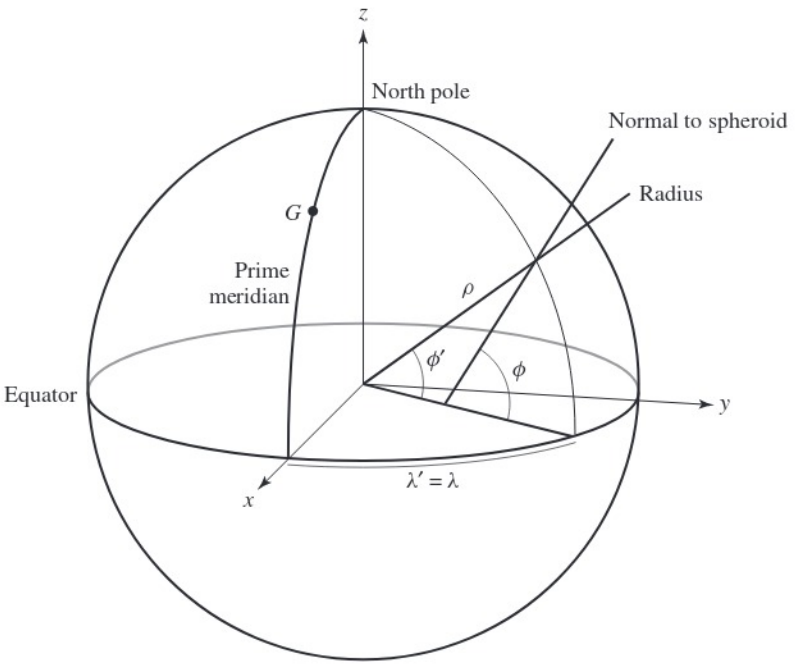


Figure 1.5 Geocentric and geodetic coordinates

Earth). This is referred to as *polar motion*. An arbitrary division between nutation and polar motion has been introduced such that all periodic motions with periods less than two days are considered polar motion. The equator of the Earth passes through the center of mass of the Earth.

1.3.3.3 Geocentric Coordinates

Geocentric coordinates are coordinates that refer to a coordinate frame whose origin is at the center of mass of the Earth and whose fundamental planes are the equator and an (arbitrary) prime meridian through *Greenwich* (see Fig. 1.5). This frame defines a system of rectangular coordinates (x, y, z) or of spherical coordinates, (longitude $[\lambda']$, latitude $[\phi']$, and radial distance $[\rho]$). Longitude is measured positively to the east and usually designated from $\pm 180°$. Longitude may be expressed in time units from 0^h to 24^h for some applications. Latitude is measured from the equator $(0°)$ to $\pm 90°$, positively to the north.

The Earth is not a rigid body, but is subject to secular and periodic changes in shape and in the distribution of mass. The crust of the Earth may be considered to consist of plates that move slowly over the mantle and that are subject to deformation. In these circumstances, the coordinate frame is realized by the adoption of values for the positions and motions of a set of primary reference points on the surface of the Earth. These values are chosen in an endeavor to satisfy certain conditions; for example, so that the prime meridian nominally passes through Greenwich and so that there is no net rotation of the primary points with respect to the frame. In practice, different techniques of observation and analysis give rise to reference frames

that differ from each other, and from the standard frame, in origin, orientation, and scale. The International Union of Geodesy and Geophysics (IUGG) has adopted the International Terrestrial Reference Frame (ITRF) with a Terrestrial Intermediate Origin (TIO) to specify coordinates on the Earth (see Chapter 5).

1.3.3.4 Geodetic Coordinates

Geodetic coordinates (longitude, latitude, and height) refer to an adopted spheroid whose equatorial radius and flattening (or equivalent parameter) must be specified. Geodetic longitude (λ) is defined in the same way as geocentric longitude (λ'), and these two coordinates are equal to each other apart from any error in the adopted origin of geodetic longitude. Geodetic latitude (ϕ) is equal to the inclination to the equatorial plane of the normal to the spheroid (see Fig. 1.5). Geodetic latitude may differ from geocentric latitude (ϕ') by up to $10'$ in mid-latitudes. Geodetic height (h) is the distance above the spheroid measured along the normal to the spheroid (see § 5.2).

Geodetic coordinates may be formally referred to an internationally adopted spheroid whose origin and fundamental planes are those specified for geocentric coordinates. Generally, however, they are referred to a spheroid that has been fit to the geoid over a particular region. The center of such a spheroid may differ significantly from the center of mass of the Earth, and the fundamental planes may not be parallel to those of the international spheroid. The orientation of the reference frame of a regional spheroid is specified by the adopted coordinates of the origin point, which is usually a geodetic reference station near the center of the region concerned. Geodetic coordinates may also be referred to globally defined spheroids whose origins and fundamental planes may be found to differ from the ideal specification. Usually the term "datum" is used in geodesy for regional or global reference frames such as the ones given in § 5.2.3 for the international spheroid and also for certain global and regional spheroids. In certain cases up-to-date values of these parameters are given in *The Astronomical Almanac*.

1.3.3.5 Geographic Coordinates

The term *geographic coordinates* is used for terrestrial longitude and latitude when these are determined by astronomical observations with respect to the celestial pole and the local meridian through the local vertical; and for height above the geoid, commonly referred to as height above mean sea level. The terms *astronomical coordinates* and *terrestrial coordinates* are also used for such coordinates.

The geographic longitude of a point may be defined as the angle between the plane of the astronomical meridian through the point and the plane of the prime meridian through Greenwich. The astronomical meridian is the plane that contains the direction of the local vertical and the direction of the line through the point that is parallel to the axis of rotation of the Earth. The local vertical is affected by local gravity anomalies and by the varying gravity fields of the Sun, Moon, and oceans. Therefore, the astronomical meridian is not precisely the same as the geodetic meridian that passes through the point and the actual axis of figure through the center of the Earth. Consequently, the geographic and geodetic longitudes of a point differ slightly. Geographic longitude is equal to the difference between (observed) local sidereal time and Greenwich Sidereal Time at any instant.

Geographic latitude is also defined in terms of the local vertical and the axis of rotation, and so is not equal to the geodetic latitude. The inclination of the local vertical to the normal to the reference spheroid is known as the *deflection of the vertical*. The corresponding difference between the geographic and geodetic coordinates may be as much as $1'$ (that is up to 4^s in time-measure). The motion of the axis of rotation within the Earth causes the values of geographic longitude and latitude to vary by up to about $0.''3$ over a period of a few years. The daily tidal variations in the direction of the vertical may reach about $0.''01$.

1.3.3.6 Height and Geoid

The height (or altitude) of a point on (or near) the surface of the Earth depends on the reference surface to which it is referred. Geodetic heights are measured with respect to a specified geodetic datum (or reference spheroid), but the more commonly used geographic heights are measured with respect to a surface that is known as the geoid. The geoid is a particular equipotential surface in the gravity field of the Earth and is commonly referred to as the mean sea level surface. The geoid is an irregular surface that may lie above or below the international-reference spheroid by as much as 100 m; this difference is known as the *undulation of the geoid* and should be taken into account in the precise derivation of geocentric coordinates when the height above mean sea level is given. For very precise studies, it is also necessary to take into account the variations in height due to Earth tides and ocean loading (see § 5.3.3 and § 5.3.5).

1.3.3.7 Topocentric Coordinate Systems

There are two main topocentric coordinate frames. One is based on the direction of the local vertical, which defines the plane of the astronomical horizon; the other is based on the direction of the Earth's axis of rotation, which defines the plane of the celestial equator. The local meridian, which contains the direction of the local vertical and the direction of the axis of rotation, is common to both frames.

The angular coordinates in the topocentric coordinate frame of the horizon and local meridian are known as azimuth and altitude. Azimuth (A) is measured from $0°$ to $360°$ from north in the direction of east; that is, in the left-handed sense with respect to the direction of the zenith. (In some circumstances azimuth may be measured from the south, and so the convention that is used should be stated to avoid ambiguity.) Altitude (a) is measured positively from the horizon toward the zenith; however, in astronomy, the zenith distance ($z = 90° - a$) is more commonly used. Both the altitude and the azimuth of any celestial object change rapidly as the Earth rotates, and therefore, for many purposes it is more convenient to use the topocentric frame of the celestial equator and the local meridian. The direction of the north celestial pole is parallel to the Earth's axis of rotation, and the altitude of the pole is equal to the geographic latitude of the point of observation. This is illustrated in Fig. 1.6, which shows the Earth as a sphere.

In this topocentric equatorial frame, the angular coordinates are known as local hour angle (LHA, or h) and declination (δ). LHA is measured from $0°$ to $360°$, or from 0^h to 24^h, from south in the direction of west (i.e., in the left-handed sense with respect to the direction of the north celestial pole), and the LHA of a celestial object increases by about $15°$, or 1^h, for every hour of time. Declination is measured from the equator to the celestial pole, positive toward the north. Co-declination, measured from the pole toward the equator, is sometimes

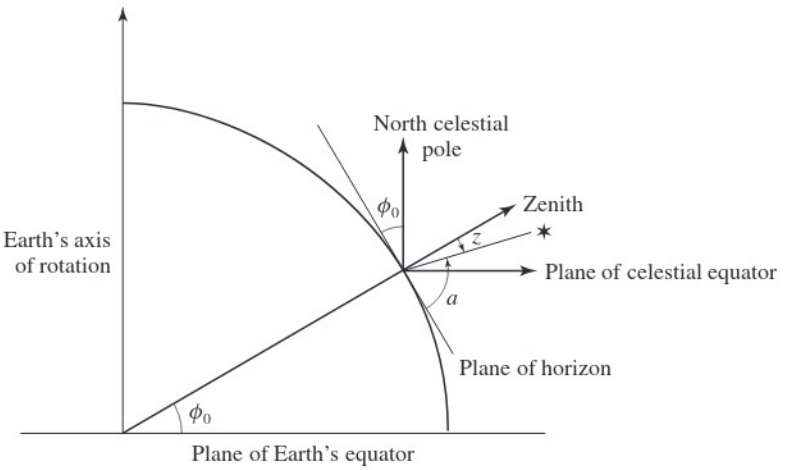


Figure 1.6 Relation between geographic latitude and the altitude of the celestial pole

used instead of declination. The declination of a celestial object is not changed by the diurnal rotation of the Earth.

1.3.4 The Rotation of the Earth

The connection between a local coordinate frame (defined with respect to the Earth at the point of observation) and a celestial coordinate frame is complicated by three aspects of the rotation of the Earth: the precession and nutation of the axis of rotation (§ 1.3.2.2), the motion of the pole of rotation within the Earth (§ 1.3.4.1), and the variability of the rate of rotation (§ 1.3.4.2).

1.3.4.1 Polar Motion

Measurements of the zenith distances of the celestial pole of rotation at different places and times show that the Earth's axis of rotation is not fixed within the Earth, but moves around the axis of maximum moment of inertia. This phenomenon is known as *polar motion*. Since it cannot be predicted accurately in advance, the position of the pole is determined from regular observations as an international service. In a celestial coordinate system, the axis of maximum moment of inertia moves around the axis of rotation in a complex motion in which an annual component and a 14-month (Chandler) component create beats. The amplitude of the quasi-circular motion varies between $0''.05$ and $0''.25$ in a six-year cycle, an area about the size of a baseball field.

1.3.4.2 Length of Day

The variations in the Earth's rate of rotation are, at present, unpredictable and are due to several different causes. There is a long-term slowing down of the rate of rotation that appears to be due largely to the effect of *tidal friction*. There are irregular changes with characteristic periods of a few years that appear to be due to an interchange of angular momentum between the mantle and the core of the Earth. There are also seasonal and short-period irregular changes

Table 1.1 Variations in the Earth's rate of rotation

Characteristics Time	Change in Length of Day	Difference in time	Difference in Orientation
a few days	0.1 ms	1 ms	0.″01
100 days	1 ms	0.2 s	3″
a few years	3 ms	10 s	3′

that appear to be due largely to exchanges of angular momentum between the solid Earth and the atmosphere. The total effect on the orientation of the Earth in space is determined from observations by an international monitoring service that provides future predictions based on the observations.

These variations are usually represented by the corresponding changes in the length of the day (with respect to a day of 86400 SI seconds) and by the accumulated difference between UT and TAI (or ET before 1955). The latter difference in time may be expressed as a corresponding difference in angular orientation of the Earth. Table 1.1 shows the orders of magnitude of the different variations.

The accumulated effect of the changes in the rate of rotation can be seen most clearly in the geographic longitudes and times at which certain phenomena, such as eclipses of the Sun, were observed in early history. The accumulated effect of the changes in the rate of rotation has amounted to two hours over the last two thousand years. This was a source of much confusion when the rotation of the Earth provided the standard timescale for all purposes. It is now recognized that sidereal time and Universal Time are best regarded as measures of angles that serve to specify the orientation of terrestrial coordinate systems with respect to celestial coordinate systems. They must be determined from observations, although man-made clocks can be used for interpolation and extrapolation.

1.3.5 Connections between Terrestrial and Celestial Coordinates

In studies of the distribution and motion of celestial bodies it is necessary to have procedures for the transformation, or reduction, of "observed" topocentric coordinates, which are referred to a terrestrial frame that rotates with the Earth, to (or from) "reduced" barycentric coordinates, which are referred to a celestial frame that is fixed in space. The generally adopted traditional procedure uses an intermediate system of geocentric coordinates, which are referred to a celestial equatorial frame of date that is defined by the current directions of the Earth's axis of rotation and of the equinox. The principal stages of the full reduction are as follows:

Stage 1. Rotation of the terrestrial frame from the horizon to the equator and from the local meridian to the prime meridian.

Stage 2. Translation of the origin of the terrestrial frame from the observer to the geocenter—a change from UTC to TT may be required.

Stage 3. Rotation of the terrestrial frame for polar motion; i.e., from the conventional pole to the true celestial pole (or celestial intermediate pole).

Stage 4. Rotation of the terrestrial frame around the true pole from the Greenwich meridian to the celestial frame whose prime meridian passes through the true equinox. (The angle of rotation varies rapidly as the Earth rotates, and is known as the Greenwich Apparent Sidereal Time. Alternately, this is the rotation through the Earth Rotation Angle from the TIO to the CIO.)

Stage 5. Rotation of the celestial frame for nutation from the true pole and true equinox to the mean pole and mean equinox of date.

Stage 6. Rotation of the celestial frame for precession from the geocentric mean equator and equinox of date to barycentric ICRF of J2000.0. A change from TT to TCB may be required.

Stage 1 requires a knowledge of the geographic longitude, latitude, and height of the place of observation. If appropriate, the effect of the tides on the deflection of the vertical and on the height may have to be taken into account. Correction for refraction is also required.

Stage 2 requires a knowledge of the geodetic longitude, latitude, and height for reducing the coordinates of very close objects. For distant objects, such as stars, the translations of the origin may be treated as small rotations corresponding to small parallactic shifts in direction. Correction for aberration may be required.

The standard values of the coordinates of the pole that are required in Stage 3 are published in arrears; "quick-look" and predicted values are also made available. Indicative values are tabulated at a wide interval in *The Astronomical Almanac* (p. K10).

For Stage 4, the required value of the Greenwich Sidereal Angle at the time of observation may be calculated in three steps from the UTC of the instant of observation. The first step is to apply the difference between UT and UTC values to the value of UTC. Standard values are published in arrears, but a quick-look or predicted value may be of sufficient accuracy. The value of UT is then used to compute the values of the Greenwich Mean Sidereal Time, or Earth Rotation Angle, from a polynomial expression. Finally, the equation of the equinoxes is applied to give the Greenwich Apparent Sidereal Time, which is converted to angular measure to give the required Greenwich Sidereal Angle.

The values of the nutation in longitude and obliquity that are required in Stage 5 may be computed from harmonic series that are based on an adopted theory of nutation. In some circumstances it may be appropriate to apply further small corrections obtained from the analysis of recent VLBI observations.

The values of the precession that are required in Stage 6 may be computed from adopted expressions for the angular quantities concerned. Stages 5 and 6 may be combined in a single rotation matrix; daily values of the matrix are published in *The Astronomical Almanac* in Section B.

The rectangular coordinates of the geocenter with respect to the barycenter may be obtained from published ephemerides, such as that printed in Section B of *The Astronomical Almanac*, which gives daily values of both position and velocity.

With the CIO-based moving reference system, the following changes would take place in the above stages:

- In stage 4, rotation would be from the Terrestrial Intermediate Origin (TIO) to the Celestial Intermediate Origin (CIO).

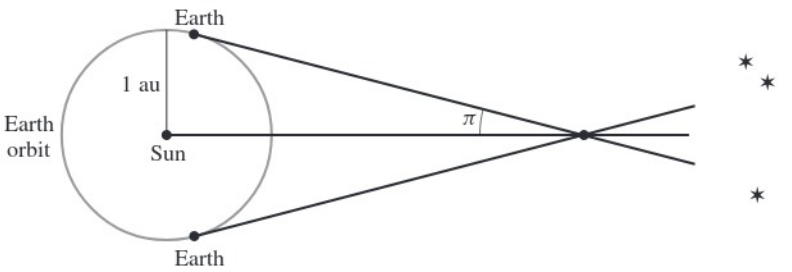


Figure 1.7 Parallax of an object

- Stages 5, 6, and 7 would be combined with the transformation of the precession-nutation model, which includes precession, nutation, geodesic precession and nutation, and translation from geocentric to barycentric origins—the change from TT to TCB would still be required.
- Stages 3 through 7 can be accomplished by the matrix equation

$$\text{ICRF} = PN(t) \times R(t) \times W(t) \times \text{ITRF} \tag{1.9}$$

where $PN(t)$ is the precession-nutation model, $R(t)$ is the Earth rotation matrix, and $W(t)$ is the polar motion matrix.

1.3.6 Effects of the Position and Motion of the Object and Observer

1.3.6.1 Parallax

The direction in which an object is seen depends on the position of the observer as well as on the position of the object. The change in the direction of a celestial object caused by a change in the position of the observer is known as a *parallactic shift*. The amount of change in direction corresponding to a standard linear change in the position of the observer, across the line of sight, is known as the *parallax of the object*—it is an inverse measure of the distance of the object from the observer (see Fig. 1.7). For objects within the solar system the standard linear change is the equatorial radius of the Earth. For the stars and other such distant objects, however, the standard linear change is the *astronomical unit of distance* (au) or, in effect, the mean radius of the Earth's orbit around the Sun. The basis of the parallax can be deduced immediately from knowledge of the type of object. The parallax of an object in the solar system is usually referred to as a *horizontal parallax*, since the actual parallactic shift takes this value when the object is seen on the horizon (from a point on the Earth's equator). The parallax of a star is often referred to as an *annual parallax*, since the parallactic shift varies with a period of one year. By analogy, a horizontal parallax may be referred to as a *diurnal parallax*; the oblateness of the Earth must be taken into account in the precise computation of the parallactic shift of the Moon.

Distances within the solar system are conveniently and precisely expressed in astronomical units and may be expressed in meters using a conversion factor based on radar measurements to planets. Prior to 1960, this conversion factor was based on determinations

of the solar parallax, i.e., of the equatorial horizontal parallax of the Sun when at a distance of 1 au.

The catalog positions of stars and other objects outside the solar system are usually referred to the barycenter of the solar system. The correction for annual parallax may be applied with sufficient accuracy for many purposes by assuming that the orbit of the Earth is circular. For full precision, however, it is usual to express the correction in terms of the barycentric rectangular coordinates of the Earth that are tabulated in *The Astronomical Almanac*. These coordinates are also used to reduce the times of observation of such phenomena as pulsar emissions to a common origin at the barycenter of the solar system.

1.3.6.2 Proper Motion and Radial Velocity

The motion of an object outside the solar system is usually expressed in terms of its proper motion and radial velocity. Proper motion is expressed in terms of the secular rates of change in the right ascension and declination with respect to a standard coordinate frame. It is necessary to know the distance (or parallax) of the object before the motion transverse to the line of sight can be expressed in linear measure. Radial velocity is the name given to the motion of the object along the line of sight and is derived from observations of the Doppler shift in the radiation from the object. It is usually expressed in km/s. An observational value must be corrected for the rotational motion of the point of observation and the orbital motion of the Earth around the barycenter. When the parallax is known, the proper motion and radial velocity can be combined to form a space-motion vector that represents the motion of the object with respect to the standard reference frame. This space-motion vector should be used when computing apparent positions for any date and transforming positions from one standard epoch to another.

1.3.6.3 Aberration

Because the velocity of light is finite, the direction in which a moving celestial object is seen by a moving observer (its apparent position) is not the same as the direction of the straight line between the observer and the object (its geometric position) at the same instant. This displacement of the apparent position from the geometric position may be attributed in part to the motion of the object and in part to the orbital and rotational motion of the observer, both of these motions being referred to a standard coordinate frame. The former part, which is independent of the motion of the observer, is referred to as the *light-time displacement*; the latter part, which is independent of the motion or distance of the object, is referred to as *stellar aberration*. (For stars the correction for light-time is ignored.) The sum of the two parts is called *planetary aberration* because it is applicable to planets and other members of the solar system. The term *aberration* is used in this supplement to include the effects of the motions of both object and observer, but it is sometimes used elsewhere for the effect due to the motion of the observer alone. For precise astrometry, stellar aberration must be calculated from the formulae of the special theory of relativity, but for most classical purposes the theory depending on only the first power in v/c, where v is the velocity of the observer and c is the velocity of light, is sufficient. In the past, secular aberration, due to the linear and rotational motion of the entire solar system in the galaxy, has been ignored. For accuracies of microarcseconds, these effects must be included in observation reduction procedures.

The motion of an observer on the Earth is the resultant of the Earth's diurnal rotation and the Earth's annual orbital motion around the barycenter of the solar system. Stellar aberration

is therefore regarded as the sum of diurnal aberration and annual aberration, for which the maximum effects are about $0.''3$ and $20''$, respectively.

Annual aberration affects all objects in the same part of the sky in a similar way, and so, in observations of star fields, it does not obscure the much smaller effect of annual parallax, which noticeably affects the apparent positions of the nearby stars.

In determining precisely the differences between the celestial coordinates of a solar system object and a fixed star, it is necessary to take into account the differential aberration between the object and the star. In constructing an ephemeris of a moving object that is to be compared directly with the catalog positions of stars at some epoch, it is necessary to take into account the correction for light-time but not stellar aberration; such an ephemeris is known as an *astrometric ephemeris*. An ephemeris in which aberration is fully taken into account along with precession, nutation, and light-bending is known as an *apparent ephemeris*.

1.3.6.4 Deflection of Light

In precise computations it is necessary to take into account the effect of the gravitational field of the Sun (or other massive object) on the velocity of propagation of light. The effect causes a bending of the path, so that the apparent angular distance from the Sun is greater, and an increase in the travel time, so that pulsed radiation is retarded. This effect resembles refraction in the Earth's atmosphere, although the latter effect is usually much greater.

1.3.6.5 Refraction

Refraction in the Earth's atmosphere affects most directional observations. It depends largely on the altitude of the object above the horizon, and its precise value depends on the atmospheric conditions at the time. Since the effect depends on the position of the object with respect to the observer, it cannot be included in ephemerides. Nominal allowances are made for refraction in the computations of the times of rising and setting phenomena, for which the effects of refraction are greatest. Refraction increases the apparent altitude of a celestial body and increases the travel times of laser pulses. Most analytical theories and tables of refraction assume that the surfaces of equal refractive index in the atmosphere are concentric and that it is sufficient to know the pressure, temperature, and relative humidity at the point of observation. Significant variation from such models can occur so that the angular refraction may not be exactly zero in the zenith. Measurements of azimuth may also be affected by refraction in the horizontal plane.

The refraction of radio waves depends largely on the properties of the ionosphere and is much more variable than refraction for light waves. Multiple-frequency measurements may be used to determine the refraction correction for radio waves.

1.4 Orbital Motion

1.4.1 Motion in Two-Body Systems

1.4.1.1 Laws of Motion

Over a short period of time the motion of a planet around the Sun, or of a satellite around a planet, can usually be treated as if the two objects are isolated in space and moving around each other in accordance with Newton's laws of motion and gravitation (i.e., Keplerian or two-body motion). The smaller, or secondary, body moves around the larger, or primary, body in an orbit that lies in a plane passing through the primary. The orbit is in the shape of

an ellipse with the primary at a focus. Correspondingly, the larger body moves in a smaller orbit around the center of mass of the pair. The orbits of the major planets and most satellites are almost circular, whereas the orbit of Comet Halley, for example, is extremely elongated. The shape of an ellipse is usually characterized by its eccentricity, e. A circle is a limiting case as e approaches zero, and e tends to unity with increasing elongation. Comets may also move in parabolic ($e = 1$) or hyperbolic ($e > 1$) orbits. The geometric properties of these conic sections are summarized in Fig. 1.8.

Kepler discovered the elliptical character of the orbit of Mars, and found that the speed of motion of Mars was such that the line joining Mars to the Sun swept out equal areas in equal times. He also found that the squares of the periods of revolution (P) of the planets are proportional to the cubes of the lengths of their semimajor axes (a). Newton was the first to demonstrate that these properties were consistent with the existence of a gravitational force of attraction between the Sun and the planet. This attraction varies inversely as the square of the distance (r) between the two bodies and directly as the product of their masses (M and m). Newton defined the mass of a body as a measure of the amount of matter in the body, and the momentum of a body as the product of its mass and its velocity. His second law of motion states that the rate of change of momentum of a body is proportional to the force acting on it and is in the same direction.

If the Sun and a planet are regarded as forming an isolated system, then the system's center of mass can be regarded as being at rest or moving at a uniform velocity in space. This point can be treated as the origin of a set of nonrotating coordinate axes, which are then used to form an inertial coordinate frame to which Newton's laws of motion and gravitation apply. One can then write the equations of motion of the Sun and of the planet with respect to the frame. The equation for the motion of the planet relative to the Sun (i.e., treating the Sun as the origin of a coordinate frame whose axes remain parallel to those of the inertial frame) may then be derived; it takes the simple form

$$\ddot{\mathbf{r}} = -\frac{G(M+m)\mathbf{r}}{r^3} \tag{1.10}$$

where $\mathbf{r}$ and $\ddot{\mathbf{r}}$ are the position and acceleration of the planet with respect to the Sun expressed as vectors, with Newton's dot notation to denote differentiation with respect to time, and where G is the constant of gravitation. If the vector $\mathbf{r}$ has components x, y, z with respect to the coordinate axes, then Eq. 1.10 is equivalent to three separate equations of the form

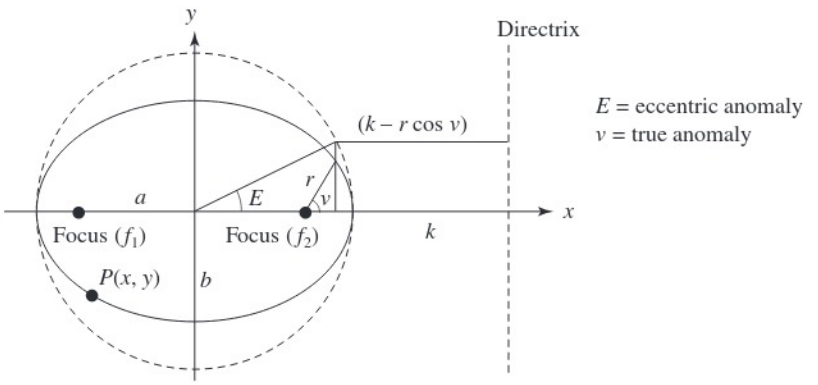
$$\ddot{x} = -\frac{G(M+m)x}{r^3}. \tag{1.11}$$

Many of the basic properties of motion in an ellipse may be derived by considering the case when the orbit lies in the xy-plane and expressing x and y in polar coordinates r and θ. The principal results are given in Fig. 1.8a.

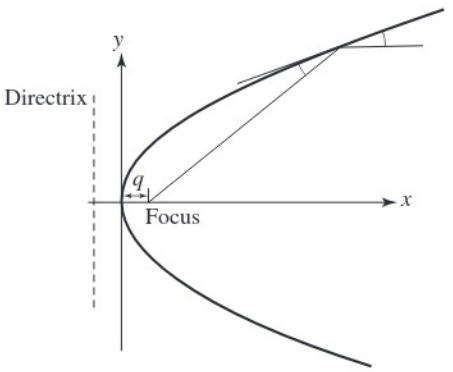
It is convenient to use an astronomical system of units in which the unit of mass is equal to the mass of the Sun, and the unit of time is one day. When this is done, Eq. 1.10 is written as

$$\ddot{\mathbf{r}} = -\frac{k^2(1+m)\mathbf{r}}{r^3} \tag{1.12}$$

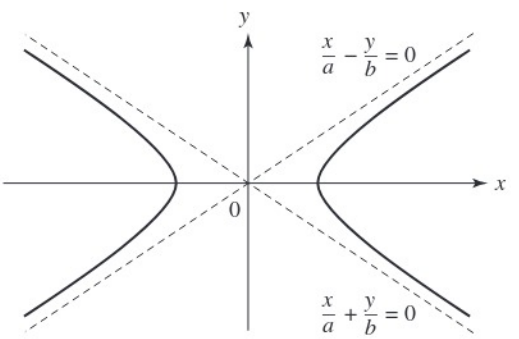
where k is known as the Gaussian constant of gravitation. It is now the practice to treat the value of k as a fixed constant that serves to define the astronomical unit of length (au), which



(a) Ellipse $(0 \le e < 1)$: $\frac{x^2}{a^2} + \frac{y^2}{b^2} = 1$



(b) Parabola $(e = 1)$: $y^2 = 4qx$



(c) Hyperbola $(e > 1)$: $\frac{x^2}{a^2} - \frac{y^2}{b^2} = 1$

Figure 1.8 Geometric properties of conic sections

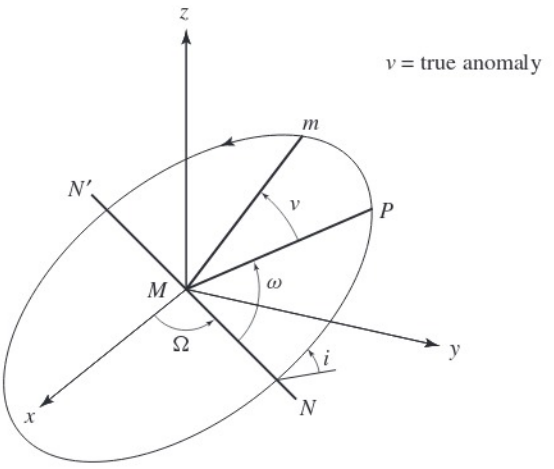


Figure 1.9 Angular orbital elements

is slightly less than the semimajor axis of the orbit of the Earth around the Sun (see Chapter 8). However, it is expected that at the 2012 IAU General Assembly, a resolution will pass that will make the au a fixed constant; the au then will be used to define k (see Appendix A).

1.4.1.2 Orbital Parameters

Positions of a body moving in an elliptical orbit can be computed from a set of six orbital parameters (or elements) that specify the size, shape, and orientation of the orbit in space and the position of the body at a particular instant in time known as the epoch. Commonly used parameters are:

a. the semimajor axis of the ellipse;
e. the eccentricity of the ellipse;
i. the inclination of the orbital plane to the reference plane;
Ω. the longitude of the node (N) of the orbital plane on the reference plane;
ω. the argument of the pericenter (P) (angle from N to P);
T. the epoch at which the body is at the pericenter.

The longitude of the pericenter, ϖ, which is the sum of Ω and ω, may be used instead of ω. And the value of the mean anomaly, M, or mean longitude ($L = \varpi + M$) at an arbitrary epoch may be used instead of T. The reference plane is usually the ecliptic, and the epoch for which the reference plane is specified must be stated. These angular parameters are shown in Fig. 1.9. The mean daily motion of a planet (n) in its orbit may be determined from

$$n = \frac{2\pi}{P} = \frac{k\sqrt{1+m}}{a^{3/2}} \tag{1.13}$$

where P is the period in mean solar days and n is in radians per day.

The elements may be given as mean elements where the values are a type of average value over some period of time. The elements may be given as osculating elements, which are the instantaneous values of the elements, or the elements for the elliptical motion that the body would follow if perturbing effects were removed. Since the solar system bodies are in well-behaved orbits, this set of elements may be used. In cases where the eccentricity or inclination may be zero, a universal set of parameters should be used instead.

The orbital parameters can be used to compute the velocity as well as the position of the body in its orbit. Conversely, if the position and velocity of a body are known at a given instant, it is possible to calculate the parameters of the elliptical orbit. When a new minor planet is discovered, each observation gives two coordinates (usually, right ascension and declination). At least three observations, preferably more, are required to determine the parameters of an elliptical orbit that would pass through the observed positions. Gauss' and Laplace's methods can be used for this procedure (Herget 1948; Danby 1988).

1.4.2 Ephemerides

1.4.2.1 Types of Perturbations

It is only for applications where reduced accuracy is required that two-body motion is adequate for the representation of the motion of a planet or satellite. For other applications a number of perturbation effects must be included:

(a) The attractions of other planets or satellites must be included in all cases.

(b) The non-sphericity of the distribution of mass in a primary body must be included in calculating the motions of satellites.

(c) The tidal forces that arise when the bodies cannot be treated simply as point-sources must be included in the motions of satellites.

(d) The non-gravitational forces, or reactive forces, must be included when computing the orbit of a comet.

(e) The effect of atmospheric drag and solar wind must be included in the computation of orbits of artificial satellites.

(f) Radiation pressure must be included in the motion of artificial satellites and in the motion of particles in the rings around planets.

1.4.2.2 Ephemerides Computations

For precise calculations of the motion of the planets and the Moon, the equations of motion must include the relativistic terms. This is normally done using the parameterized post-Newtonian (PPN) version of the equations. The independent variable, time, in the PPN equation for the solar system is the Barycentric Coordinate Time (TCB). When converting the barycentric positions of the planets to geocentric positions, one must convert the time according to the relativistic metric used in the computation. Similarly, the optical observations being compared to the ephemerides must be corrected for gravitational light bending, and radar observations must be corrected for the appropriate time delay involved. With the exception of the Moon, the natural satellite ephemerides do not require the inclusion of relativistic effects to the accuracies currently being used. Observations must be corrected for many non-relativistic effects, such as refraction and aberration.

The perturbation effects may be computed either by numerical integration of the motion of the body or by the use of a general theory that provides an expression for the motion of the body as a function of time. Currently, it is not possible to achieve the accuracy of observations by means of a general-theory approach for the motion of the planets and the Moon. On the other hand, for rapidly moving satellites, such as the Galilean satellites, it is not possible to numerically integrate those bodies over an extended period of time and retain the necessary accuracy required for observations.

1.4.2.3 Numerical Integration

Numerical integration is the most accurate method of calculating the motion of bodies in the solar system, particularly the Moon and planets. There are many methods of numerical integration. Textbooks on celestial mechanics describe such methods. Usually, Cowell's method is used with an equation that includes the PPN relativistic formulation. The initial conditions for the numerical integration are adjusted to fit available observational data, and a second numerical integration is performed based on that correction. This process is repeated until the numerical integration represents the observational data to the required accuracy.

1.4.2.4 Analytical Theories

As an alternative to numerical integration, an analytical theory, usually in the form of a Fourier series or Chebyshev series, can be developed to represent the motion of the bodies. Historically, this was the method of computation for the planets and the Moon, and the technique is represented by Newcomb's theories of the Sun, Mercury, and Venus; Hill's theory of Jupiter and Saturn; and Brown's lunar theory. Today this method is used only for planetary satellites, where sufficient accuracy can be achieved by this method. These theories permit determination of the positions of the bodies for any time within the period of validity for the theory. Theories of the planets and the Moon have been developed by Bretagnon, Simon, Chapront, and Chapront-Touze, but they do not achieve the accuracies of numerical integration.

1.4.2.5 Observational Data

The computation of accurate ephemerides of the Sun, Moon, and planets depends upon the availability of accurate observations of their positions at precisely known times. Optical observations of the Sun, Moon, and planets have been made with the unaided eye in the pretelescope era, with transit and meridian circles and telescopes, using visual and electronic detectors, such as charge coupled devices (CCD). Observations of Mercury, Venus, and Mars can be made by radar ranging. Observations of the Moon have been made using laser ranging since 1969. Planetary radar ranging, Very Long Baseline Interferometer (VLBI), and Lunar Laser Ranging provide much more precise measurements than transit-circle observations. Radio observations of spacecraft on a planet, in orbit around a planet, or encountering a planet also provide very precise positional data. There are no observing programs obtaining precise visual measurements of the large planets at this time.

Observations of the satellites can be made by photographic or CCD techniques, and by recording the times of mutual phenomena (eclipses, transits, or occultations) of these bodies. Hipparcos made some observations of the brighter satellites. Accurate observational data go back to only about 1830; so computations of the motions of bodies in our solar system are limited by the 180 years of observational history. Observational accuracies have been continually improved over the period.

1.4.2.6 Differential Corrections

The process of correcting a numerical integration or an analytical theory to give a better fit to the observational data is referred to as the *differential correction process*. In this process, an equation of condition can be written for each observation. This equation provides the relationship between corrections to the initial adopted conditions of the motion and the difference between the computed and observed position of the body. These equations of condition are combined into normal equations, which are then solved to determine the improved initial conditions for the motions. This process is described in textbooks on celestial mechanics.

1.4.2.7 Representative Ephemerides

It is often advantageous to compute the positions of the bodies from formulae rather than to read ephemerides that were based on either numerical integrations or analytical theories. A representative ephemeris can be prepared by evaluating a limited expression that represents the motion of the body to a specified level of accuracy over a limited time period. These expressions, which are usually power series or Chebyshev polynomials, provide the most efficient means of generating the ephemerides with computers. (See Chapter 8 concerning modern ephemerides.)

1.4.3 Perturbations by and on Extended Bodies

1.4.3.1 Gravity Field of Extended Bodies

Newton's law of gravitation formally applies to idealized point masses, but it can be shown that the gravitational force due to a spherically symmetric body is the same as if all the mass were concentrated at the center. In practice, astronomical bodies are rarely spherically symmetric, and most are rotating at such a rate as to cause the bodies to be clearly oblate. In addition, surfaces of equal density are not spherical, and the gravitational attraction on an external point mass is not normally in the radial direction. Other departures from purely radial variation in density occur; so the external gravity field of an extended body, such as a planet, is represented by a spherical harmonic series. The coefficients of such a series may be determined by analyzing the departures of the motion of a satellite from a fixed ellipse. The effects are most noticeable for close satellites, and the effects of the higher-order terms decrease very rapidly with distance. The most noticeable effect is that of the second-order zonal harmonic, J_2, which causes the pole of a satellite orbit to precess around the polar axis of the planet, though the inclination to the equator remains unaltered. The direction of the pericenter also precesses around the orbit.

The equations of motion of a satellite may be referred to a coordinate system that is fixed relative to the planet, if the appropriate Coriolis terms are included to take account of the rotation of the planet. The expression for the potential function may also be modified in a similar way—the arbitrary constant in the potential function is usually chosen so that the surface of zero potential corresponds to mean sea level (or the geoid) in the case of the Earth. This is the surface from which height is measured for mapping purposes.

1.4.3.2 Forces on Extended Bodies

The gravitational forces on an extended body may be resolved into a force and a couple. The force acts through the center of mass and causes an acceleration of the body in its orbit. The

couple changes the rotational motion of the body. A simple example is that of a two-body system, such as the Sun and a planet, in which one body is an oblate spheroid that is rotating about its principal axis. The torque, which may be considered to act on the equatorial bulge, has a gyroscopic effect and causes the principal axis to precess around the normal to the orbit plane at a constant inclination. In more complex systems, a nutational motion is superimposed on the main precessional motion, and an irregular body may "tumble" as it moves around its orbit.

The forces on an extended body will also cause a tidal distortion even if it is a solid, but slightly elastic, body. The effect is similar to that of the ocean tides on the Earth. For a simple model there are two *high tides* and two *low tides* that remain stationary with respect to the attracting body. The line of the high tides is slightly displaced from the line joining the centers of the two bodies. This causes a net torque that tends to change the rate of rotation of the body. On the other hand, the existence of the tidal distortion changes the attraction on the other body and gives a small component at right angles to the line of centers, thus causing the orbit to expand or contract, depending on the circumstances. This effect is referred to as *tidal friction*.

The principal elastic properties of a spherical body may be represented in terms of parameters known as *Love numbers*. Resonance effects may occur if the tidal forces contain a periodic component that matches one of the natural frequencies of vibration of the body. The dissipation of the tidal energy may be large enough to heat the body significantly; this is believed to be the case for Io of the Galilean satellites of Jupiter.

The forces that give rise to the nutation of the rotation and the tidal distortion of the shape of a body are essentially the same, although in the past they have often been expressed in different forms and with different notations. These forces can be derived from a potential function that allows the various periodic terms in the nutation and in the tides to be identified and computed. The accurate computation of the Earth's nutation requires the adoption of a model of its elastic properties and also of the viscous properties and shape of the fluid core.

1.5 Solar System

The solar system bodies, their positions, motions, dynamics, physical characteristics, and coordinates compose a major part of the contents of *The Astronomical Almanac*. Even so, all the detailed information about all the bodies in the solar system cannot fit into the book. Likewise this volume cannot provide all that information. This section will provide a summary of the solar system in preparation for more details to follow in the chapters.

1.5.1 Sun

The primary body of the solar system is the Sun, a single star located in a spiral arm of our galaxy, which we call the Milky Way. The Sun is moving around the center of the galaxy and the galaxy is moving in the universe. These motions have small effects, called secular aberration, on observations. The Sun is also rotating, as detected by observations of the motions of sunspots, so a physical ephemeris of the Sun is tabulated. Due to the planets moving around the Sun, the center of the Sun, the heliocenter, moves around the barycenter of the solar system, so there is an apparent motion of the Sun. This effect, if viewed from 100 parsecs away, is about 100 microarcseconds. The search for extra-solar planets looks for this same motion in other stars.

1.5.2 Planets

The Sun is surrounded by planets, mostly in orbital planes close to a plane defined by the orbit of the Earth-Moon barycenter, the ecliptic. The planets can be classified into groups. In 2006 the IAU passed a resolution dividing the solar system bodies into planets, dwarf planets, and small solar system bodies (URL[4]). This reduced the number of planets to eight, made Pluto, Ceres, and unspecified other bodies dwarf planets, and removed the distinction between comets and minor planets. This resolution was and continues to be controversial. Independent of how they are classified, the solar system is made up of the terrestrial planets, (Mercury, Venus, Earth and Mars) the giant gaseous planets, (Jupiter, Saturn, Uranus, and Neptune) Pluto and the Kuiper belt objects, dwarf and minor planets, satellites orbiting around all types of planets, comets and various small matter. The planets tend to have equatorial planes close to the ecliptic plane, except for Uranus, whose rotational pole is nearly 90 degrees from its orbital pole, and Pluto, whose orbit is inclined about 17 degrees from the ecliptic plane.

There are thousands of minor planets (asteroids), many are in the main belt between Mars and Jupiter, more are being discovered in the Kuiper belt beyond Neptune, and others are located throughout the solar system. Attention is increasing on the minor planets in orbits inside Mars; some of these cross the Earth's orbit and can approach the Earth; these are called Near Earth Asteroids (NEA). Due to the variations in the composition of minor planets—some are solid irregularly shaped bodies, some seem to be collections of two or more individual pieces gravitationally bound—it may be unclear whether a piece is a satellite or part of the primary minor planet.

The planets have satellites in motion around them, the terrestrial planets have only a few satellites while the giant planets each have large numbers of satellites. Even the minor planets have satellites in some cases. In addition, the giant planets each have ring systems around them.

The solid planets and satellites are marked by craters and surface features, which are used to specify surface coordinate systems. The gaseous bodies have assigned coordinate systems based on determinations of the poles and rotation rates of the bodies. The gaseous bodies have changing features on the visible appearances of the bodies.

1.5.3 Satellites

The Earth has one satellite, the Moon, whose rotation rate is in resonance with its orbital motion so that approximately the same side of the Moon always faces the Earth. The Moon is the source of phenomena, rises and sets, phases, tides, and eclipses, and calendar quantities, such as months and lunar cycles. It is about the same apparent size as the Sun, so it is a dominant feature in the sky, and its illumination is an important consideration for astronomical observing.

Mars has two small, solid, rapidly moving satellites. Pluto has at least four satellites; one (Charon) is relatively large and close, and in a resonant relation. The other known satellites are more distant and fainter. The giant gaseous planets each have many satellites, which are characterized as large, close satellites; small inner satellites; distant regular satellites; and distant irregular satellites. The regular satellites move in direct motion, the same as the planets, the irregular satellites revolve in the opposite direction of the planet's revolution and rotation. These irregular satellites are thought to have been captured rather than formed in those orbits. Exceptions to the pattern are Triton, the large inner satellite of Neptune, with

retrograde motion, and co-orbiting satellites of Saturn, where satellites are at the libration points or are interacting in a single orbit. In addition, satellites are being discovered around minor planets.

1.5.4 Other Bodies

There are also comets and small matter. The distinction between a comet and a minor planet has been based on the appearance of the body when it was discovered. If there was a tail or a fuzzy appearance, it was called a comet. Some bodies have lost their tails, and others on better observation have been found to have a fuzzy appearance, but their designations are generally not changed. Comets, whose orbits have been determined, are periodic comets and their reappearances are somewhat predictable. New comets are discovered as they make their first appearance in the inner solar system. Due to outgassing of comets, which appears as tails, the motions of comets are subject to non-gravitational forces. These forces must be determined from observations, and result in deviations from the motions calculated by methods of celestial mechanics. There is a cloud of comets far out beyond Neptune in Oort's cloud. Some of these comets come closer into the solar system, some becoming part of the Kuiper belt, still beyond Neptune. Others progress in still closer and can develop orbits that come close to the Sun, or can be associated with the giant planets, due to the gravitational influences of those planets. They become periodic comets.

There is smaller material in the solar system, some of which is located in rings about the giant planets, the most obvious being around Saturn. There are rings of different numbers and types around Jupiter, Uranus and Neptune. In addition, there is material that is observed when it enters the Earth's atmosphere as meteors and as zodiacal light and gegenschein.

1.5.5 Planetary Coordinates

The positions of the bodies are given in the International Celestial Reference System (ICRS). The coordinates on the surfaces, or apparent surfaces, of the bodies are specified in two different manners. Both systems are based on the axis of rotation, but differ in their definitions of latitude, longitude, and range. Planetocentric coordinates are used for general purposes and are based on a right-handed system of axes with its origin at the center of mass of the object. Planetographic coordinates are used for cartographic purposes and depend on the adoption of a reference surface, usually a spheroid that approximates an equipotential surface of the object. *The Astronomical Almanac* updates these values based on the triennial report of the IAU/IAG Working Group on Cartographic Coordinates and Rotational Elements.

1.6 Astronomical Phenomena

The various motions involved in the solar system, including the rotation of the Earth, the orbital motion of the Earth and planets, and the motion of the Moon around the Earth, cause a number of important and interesting astronomical phenomena. Some of these phenomena are events that can be timed exactly, some are matters of arbitrary definitions, and others are not subject to either exact timing or exact definitions.

1.6.1 Rising, Setting, and Twilight

The rising and setting times of an object are given with respect to sea level, a clear horizon, and refraction based on normal meteorological conditions. Rising and setting times are strictly local phenomena depending upon the longitude, latitude, and height of the place on the Earth's surface. For the Sun and Moon, the times of rising and setting refer to the instants when the upper limb of the body appears on the apparent horizon.

The actual times of rising and setting may differ considerably from the tabulated values, especially near extreme conditions when the rising/setting body's altitude is changing very slowly. Thus, the computation of the time of moonrise and moonset or sunrise and sunset for very northern or southern latitudes can be subject to large uncertainties. In addition, the illumination at the beginning or the end of twilight can vary greatly because of meteorological conditions and the physical surroundings. Although accuracies below a second can be computed for ideal conditions, precise times have little practical significance, which is why *The Astronomical Almanac's* values for rise, set, and twilight are printed to the nearest minute.

1.6.1.1 Times of Sunrise and Sunset

The calculated times of sunrise and sunset are based on the Sun having a geocentric zenith distance of 90° 50′ (34′ is allowed for horizontal refraction using a standard atmospheric model, and 16′ for the semidiameter). Corrections are necessary if the meteorological conditions differ significantly from the standard model or to allow for the height of the observer or the elevation of the actual horizon. The times of rising and setting and associated phenomena change rapidly from day to day in polar regions or may not occur for long periods. When the Sun is continuously very near the horizon, actual accurate times are difficult to predict.

1.6.1.2 Twilight Conditions

Twilight is caused when sunlight is scattered by the upper layers of the Earth's atmosphere. Twilight takes place before sunrise or after sunset. There are three distinct types of twilight. *Civil twilight* ends in the evening or begins in the morning when the center of the Sun reaches a zenith distance of 96°. *Nautical twilight* ends or begins when the Sun reaches a zenith distance of 102°. *Astronomical twilight* ends or begins when the Sun reaches a zenith distance of 108°. In good weather conditions and in the absence of other illumination, the indirect illumination of the Sun at the beginning or end of civil twilight allows the brightest stars to be visible and the sea horizon to be clearly defined. For the beginning or end of nautical twilight, the sea horizon is generally not visible, and it is too dark for observations of altitudes with reference to the horizon. At the beginning or end of astronomical twilight, the indirect illumination from the Sun is less than the contribution from starlight and is of the same order as that from the aurora, airglow, zodiacal light, and the gegenschein. In all cases the actual brightness of the sky depends on direction as well as meteorological conditions.

1.6.2 Meridian Transit

Once each day at a given location the Earth's rotation causes a celestial body to cross the meridian plane defined by the north and south poles and the zenith. When this happens, the object will have its maximum altitude with respect to the horizon. Generally, observations with a telescope are best made when the object has an hour angle of less than two hours.

For objects near the pole that can be observed as circumpolar objects from a given location, there can be a second meridian transit when the object is below the pole (lower transit). Observations when the object is above the pole are called upper transit. These two observations permit an independent determination of the location of the pole.

1.6.3 Conjunction, Opposition, and Elongation

The times of conjunction and opposition of the planets are those at which the difference between the apparent geocentric ecliptic longitudes of the planet and the Sun are 0° and 180°, respectively. Conjunctions for the outer planets take place when the planets are in the direction of the Sun from the Earth. Oppositions occur when the planets are in the opposite direction from the Sun with respect to the Earth. For Mercury and Venus, superior conjunctions take place when the planets are more distant from the Earth than the Sun, and inferior conjunctions occur when the planets are closer to the Earth than the Sun.

If heliocentric geometric longitudes are used in place of geocentric ecliptic longitudes, a small correction must be applied to correct for the effect of light-time. This correction can be a maximum of 10 minutes for the conjunctions of Venus and Mars. Due to the eccentricities and inclinations of the orbits and the effect of perturbations, the times for these phenomena may be different from those at which the geocentric distance is a minimum at inferior conjunction of Mercury or Venus or opposition of a superior planet, or at which the distance is a maximum at superior conjunction of Mercury or Venus or conjunction of a superior planet.

The elongation (E) of a planet, measured eastward or westward from the Sun, is calculated as the angle formed by the planet, the Earth, and the Sun. The elongations are measured from 0° to 180° east or west of the Sun and are tabulated to the nearest degree. Because of the inclination of the planetary orbits, the elongations do not necessarily pass through 0° or 180° as they change from east to west or west to east.

1.6.4 Eclipses, Occultations, and Transits

An *eclipse* takes place when one body passes into the shadow of another body. An *occultation* takes place when a larger body passes in front of a smaller body so that it cannot be seen by the observer. A *solar eclipse* takes place when the Moon blocks the light of the Sun as seen by an observer on Earth and so is really an occultation. A *transit* takes place when a smaller body passes in front of a larger body, e.g., when a satellite passes in front of a planet or when a planet passes in front of the Sun. A *shadow transit* takes place when the shadow of a smaller body passes in front of a larger body. This can occur when the shadows of satellites pass in front of planets. These shadows cast by the Galilean satellites, whose times are tabulated in *The Astronomical Almanac*, are easily visible on Jupiter.

1.6.4.1 Transits

Transits of Mercury and Venus across the Sun's disk can occur only when both the Earth and the planet are simultaneously very close to the same node of the planet's orbit on the ecliptic. Because of the near constancy of the longitude of the nodes and perihelia of the planets, the Earth will be near the nodes on about the same dates each year, and the planets will be at the same point in their orbits when they pass through the ecliptic. For the eccentric orbit of Mercury, this means that the conditions and limits at the November transits are very different from those at the May transits. During the twentieth century there were fourteen transits of

Mercury—ten in November and four in May, including grazing transits in 1937 May and 1999 November. In the twenty-first century there will be fourteen transits—five in May and nine in November (Meeus 1989). The transits of Venus are quite rare. Generally there are two transits of Venus within an eight-year period and then a gap of over 100 years until the next pair of transits. Transits of Venus in the twenty-first century are on 2004 June 8 and 2012 June 6. *The Astronomical Almanac* devotes special pages to transits for the years that they occur.

1.6.4.2 Solar Eclipses

Eclipses of the Sun or Moon occur when the centers of the Sun, Earth, and Moon are nearly in a straight line. This condition can be fulfilled only when conjunction or opposition occurs in the vicinity of a node of the lunar orbit on the ecliptic. A total solar eclipse takes place when the disk of the Moon appears to completely cover the disk of the Sun. Alternatively, an annular solar eclipse takes place when the apparent disk of the Moon is smaller than the apparent disk of the Sun, so that the light of the Sun is not completely blocked. A partial eclipse of the Sun takes place when the location on the Earth is not in the path of the umbral shadow cast by the Moon. The exterior tangents to the surfaces of the Sun and Moon form the umbral shadow cone. The interior tangents form the penumbral cone. The common axis of the cones is the axis of the shadow. The actual size of the shadow will be rather small, leading to a narrow path and a short duration for an eclipse. The path of the shadow on the surface of the Earth can be rather complicated, due to the orbital motions of the Earth and Moon, and the rotation of the Earth. Seven minutes of total solar eclipse is a rather long period for totality. The actual length of time and width of the path varies for solar eclipses. Solar eclipses come in certain patterns that repeat after a long interval called a Saros. A Saros is approximately 223 lunations, which is approximately 19 passages of the Sun through a node or approximately 6585 1/3 days (see Chapter 11). Maps and circumstances for solar eclipses are presented each year in *The Astronomical Almanac*.

1.6.4.3 Lunar Eclipses

A lunar eclipse takes place when the Moon passes through the shadow of the Earth. In this case, the times and circumstances are the same for all parts of the Earth from which the Moon is visible. There are three types of lunar eclipses: A *penumbral eclipse* takes place when the Moon enters only the penumbra of the Earth. A *partial eclipse* occurs when the Moon enters the umbra without being entirely immersed in it. A *total eclipse* takes place when the Moon is entirely immersed within the umbra. Visibility diagrams and timing data are presented in *The Astronomical Almanac* for each lunar eclipse.

1.6.5 Satellite Phenomena

The Galilean satellites of Jupiter undergo the phenomena of eclipses, occultations, transits, and shadow transits. The times for beginning or ending of these phenomena (i.e., the disappearance and reappearance for eclipses and occultations, and the ingress and egress for transits and shadow transits) are given in *The Astronomical Almanac*. When Jupiter is in opposition, the shadow may be hidden by the disk and no eclipse can be observed. In effect the satellite is occulted by the planet before it goes into eclipse. In general, eclipses may be observed on the western side of Jupiter before opposition and on the eastern side after opposition. Because of the finite disks of the satellites, the phenomena do not take place instantaneously. The times

given refer to the centers of the disks. At certain times similar phenomena can take place for Saturn satellites. Predictions of these phenomena are made in special publications. Times of geocentric conjunctions and elongations for selected satellites are given in *The Astronomical Almanac*.

1.6.6 Physical Observations of the Sun, Moon, and Planets

In addition to needing information about the positions of the bodies and the phenomena due to the relative positions of the bodies, one also needs information about the physical appearance of the bodies. A physical ephemeris gives information about the orientation, illumination, and appearance of the body; it also provides data that can be used in determining the cartographic coordinates of points on the surface. For each body, it is necessary to adopt a set of rotational elements and other parameters that specify the shape of the surface and identify the position of the prime meridian. For the planets and satellites the north pole is the pole that lies above the invariable plane of the solar system, and rotation can be either direct or retrograde. For the Sun, and for planets and satellites whose solid surfaces cannot be seen, it is necessary to adopt conventional values of the rotational elements. It also may be convenient to adopt different values of the rate of rotation for certain bands of latitude. The position of the prime meridian is fixed by adopting a value for the longitude of the central meridian (which passes through the pole of rotation and the apparent center of the disk) at some suitable arbitrary epoch. For a body with a solid surface, the prime meridian is usually defined with respect to a clear, sharp, surface feature. The appropriate ephemeris data are tabulated for the Sun, Moon, and planets in *The Astronomical Almanac*. The basic values for the Sun, Moon, planets, and satellites are given in their respective sections.

The fraction of the area of the apparent disk of the Moon or planet that is illuminated by the Sun is called the *phase*. It depends on the planetocentric elongation of the Earth from the Sun, which is called the *phase angle*. Neglecting the oblateness of the body, the apparent disk is circular, and the *terminator* is the orthogonal projection, onto a plane perpendicular to the line of sight, of the great circle that bounds the illuminated hemisphere of the body. The terminator is therefore, in general, an ellipse, reducing to a straight line at a phase angle of 90° and becoming a circle at a phase angle of 0° or 180°.

The elements of the rotational motion are the period of rotation, the position of the axis of rotation in space (represented either by the coordinates of the point on the celestial sphere toward which the axis is directed; i.e., the pole of the rotation, or by the inclination and node of the equator on an adopted reference plane), and the planetographic longitude of the central point of the apparent disk at an adopted epoch. This longitude defines the central meridian on the disk.

In general, the apparent positions of points on the disk are represented most conveniently by the apparent distance and position angle relative to the central point of the disk. Position angles are ordinarily measured from the north point of the disk toward the east. The central point of the apparent disk is the sub-terrestrial point on the surface. Its position on the geocentric celestial sphere is diametrically opposite the apparent position of the Earth on the planetocentric celestial sphere. The north point of the disk is on the apparent northern limb at its intersection with the celestial meridian that passes through the north celestial pole and the center of the disk. The vertex of the disk is on the apparent upper limb at its intersection with the vertical circle that passes through the zenith and the center of the disk.

Two types of coordinate systems are used for physical observations. Planetocentric coordinates are for general use where the z-axis is the mean axis of rotation, the x-axis is the intersection of the planetary equator (normal to the z-axis through the center of mass) and an arbitrary prime meridian, and the y-axis completes a right-hand coordinate system. Longitude of a point is measured positive to the east from the ephemeris position of the prime meridian as defined by rotational elements. Latitude of a point is the angle between the planetary equator and a line to the center of mass. The radial distance is measured from the center of mass to the surface point.

Planetographic coordinates are used for cartographic purposes and are dependent on an equipotential surface or an adopted ellipsoid as a reference surface. Longitude of a point is measured in the direction opposite to the rotation (positive to the west for direct rotation) from the cartographic position of the prime meridian defined by a clearly observable surface feature. Latitude of a point is the angle between the planetary equator (normal to the z-axis and through the center of mass) and the normal to the reference surface at the point. The height of a point is specified as the distance above a point with the same longitude and latitude on the reference surface.

For minor planets and comets, there is substantial indirect evidence for large precession of the rotational poles, which can cause the rotational pole to move back and forth between north and south. Therefore, for minor planets and comets, the pole is selected that follows the right-hand rule and that pole is designated as the *positive* pole. To be consistent with this definition, increasing longitudes should always follow the right-hand rule.

REFERENCES

1. The Astronomical Almanac Online:
http://asa.usno.navy.mil or http://asa.hmnao.com.

2. Naval Observatory Vector Astrometry Software (NOVAS):
http://www.usno.navy.mil/USNO/astronomical-applications/software-products/novas/.

3. IAU Standards of Fundamental Astronomy (SOFA) Software Collection:
http://www.iausofa.org/.

4. IAU Resolutions Adopted by the General Assemblies:
http://www.iau.org/administration/resolutions/general_assemblies/.

Brouwer, D. and G. M. Clemence (1961). *Methods of Celestial Mechanics*. New York and London: Academic Press.

Capitaine, N., B. Guinot, and J. Souchay (1986). A non-rotating origin on the instantaneous equator - Definition, properties and use. *Celestial Mechanics 39*(3), 283–307.

Capitaine, N., P. T. Wallace, and J. Chapront (2003). Expressions for the IAU 2000 precession quantities. *Astronomy and Astrophysics 412*, 567.

Danby, J. M. A. (1962 and 1988). *Fundamentals of Celestial Mechanics*. Richmond, VA: Willmann-Bell, Inc.

Guinot, B. (1979). Basic problems in the kinematics of the rotation of the Earth. In D. D. McCarthy and J. D. H. Pilkington (Eds.), *Time and the Earth's Rotation, IAU Symp 82*, pp. 7. D. Reidel Publ Co.

Hagihara, Y. (1970a). *Celestial Mechanics Volumes I and II*. Cambridge, MA and London, England: MIT Press.

Hagihara, Y. (1970b). *Celestial Mechanics Volumes III, IV, and V*. Tokyo: Japan Society for the Promotion of Science, Kojimachi, Cheyoda-ku.

Herget, P. (1948). *Computation of Orbits*. Willmann-Bell, Inc., Richmond, VA: Published privately by the author.

Hilton, J. L., N. Capitaine, J. Chapront, et al. (2006). Report of the Interrnational Astronomical Union Division I Working Group on Precession and the Ecliptic. *Celestial Mechanics and Dynamical Astronomy 94*, 351–367.

IAU (1992). In J. Bergeron (Ed.), *Transactions of the International Astronomical Union*, Volume XXI B, Dordrecht, pp. 41. Kluwer. Proc. 21st General Assembly, Beunos Aires, 1991.

IAU (1999). In J. Andersen (Ed.), *Transactions of the International Astronomical Union*, Volume XXIII B, Dordrecht, pp. 40. Kluwer. Proc. 23rd General Assembly, Kyoto, 1997.

IAU (2001). In H. Rickman (Ed.), *Transactions of the International Astronomical Union*, Volume XXIV B, San Francisco. Astronomical Society of the Pacific. Proc. 24th General Assembly, Manchester, 2000.

IAU (2007). In O. Engvold (Ed.), *Transactions of the International Astronomical Union*, Volume XXV B, San Francisco. Astronomical Society of the Pacific. Proc. 25th General Assembly, Sydney, 2003.

IAU (2008). In K. A. van der Hucht (Ed.), *Transactions of the International Astronomical Union*, Volume XXVI B, Cambridge. Cambridge University Press. Proc. 26th General Assembly, Prague, 2006.

IERS (2004). Conventions (2003). Technical Note 32, International Earth Rotation Service, Frankfurt am Main. Verlag des Bundsesants fur Kartographie und Geodesie, D. D. McCarthy and G. Petit (Eds.).

IERS (2009). The Second Realization of the International Celestial Reference Frame By Very Long Baseline Interferometry. Technical Note 35, International Earth Rotation Service, Frankfurt am Main. Verlag des Bundsesants fur Kartographie und Geodesie, A. Fey and D. Gordon (Eds.).

IUGG (1994). *Bulletin Geodesique 66*, 128–129.

Kaplan, G. H. (2005). The IAU Resolutions on Astronomical Reference Systems, Time Scales, and Earth Rotation Models. Circular 179, U.S. Naval Observatory, Washington, DC.

Kovalevsky, J., L. Lindegren, M. A. C. Perryman, et al. (1997). The HIPPARCOS catalogue as a realisation of the extragalactic reference system. *Astronomy and Astrophysics 323*, 620–633.

Kovalevsky, J. and P. K. Seidelmann (2004). *Fundamentals of Astrometry*. Cambridge: Cambridge University Press.

Meeus, J. (1989). *Transits*. Richmond, VA.: Willman-Bell, Inc.

Mueller, I. I. (1969). *Spherical and Practical Astronomy as Applied to Geodesy*. New York: Ungar.

Nautical Almanac Offices of UK and USA (1961). *Explanatory Supplement to The Astronomical Ephemeris and The American Ephemeris and Nautical Almanac*. London: Her Majesty's Stationery Office.

Seidelmann, P. K. (Ed.) (1992). *Explanatory Supplement to The Astronomical Almanac*. Mill Valley, CA: University Science Books.

Seidelmann, P. K. and J. Kovalevsky (2002). Application of the new concepts and definitions (ICRS, CIP, and CEO) in fundamental astronomy. *Astronomy and Astrophysics 392*, 341–351.

Woolard, E. W. and G. M. Clemence (1966). *Spherical Astronomy*. New York and London: Academic Press.

CHAPTER 2

Relativity for Astrometry, Celestial Mechanics and Metrology

M. SOFFEL & S. KLIONER

2.1 Introduction

Most high precision astronomical techniques have passed the threshold where a Newtonian formulation is no longer sufficient and Einstein's theory of gravity (General Relativity Theory, GRT) has to be employed as the basis.

This point is especially obvious in the field of astrometry. It is well known that the gravitational light-deflection at the limb of the Sun amounts to $1.''75$ and decreases as $1/r$ with increasing impact parameter r of a light ray to the solar center. Thus, for light rays incident at about 90° from the Sun, the angle of light-deflection still amounts to 4 milliarcseconds (mas). To describe the accuracy of astrometric measurements it is useful to make use of the parameter γ of the parametrized post-Newtonian (PPN) formalism. In the PPN formalism, the angle of light-deflection is proportional to $(\gamma + 1)/2$, so that astrometric measurements can be used for a precise determination of the parameter γ. An advanced processing of VLBI data provided the estimates $\gamma = 0.9996 \pm 0.0017$ (Lebach et al. 1995) and $\gamma = 0.99994 \pm 0.00031$ (Eubanks et al. 1997). Current accuracy of modern optical astrometry, as represented by the Hipparcos catalog, is about 1 mas, which gave a determination of γ at the level of 0.997 ± 0.003 (Froeschlé, Mignard, and Arenou 1997). Finally, in 2003 the accuracy for γ was improved by the CASSINI Doppler experiment (Bertotti, Iess, and Tortora 2003) which gave $\gamma = 1 + (-2.1 \pm 2.3) \times 10^{-5}$. Future astrometric missions such as GAIA will push the accuracy even below this limit. The accuracy of such future missions will be at the level of a few microarcseconds (μas), where the light-deflection caused by the oblateness of the Jupiter or the post-post Newtonian light-deflection near the limb of the Sun will become measurable.

Relativity crucially enters the problem of time measurement, time dissemination, and timescales. The main reason for that is the improvement of frequency oscillators (atomic clocks) and the fact that relativistic effects are most pronounced in the time domain. Cesium fountain clocks achieve stabilities of better than one part in 10^{15} when averaged over a day. Meanwhile, optical clocks with frequencies approaching 10^{15} Hz are stable to almost one part in 10^{15} simply by averaging over a few seconds. Such stable clocks allow highly accurate use of various space techniques like Very Long Baseline Interferometry (VLBI), GPS, Satellite Laser Ranging (SLR) or Lunar Laser Ranging (LLR). The precision of these techniques is so high that relativity has to be taken into account to fully exploit their observational potential (Müller, Soffel, and Klioner 2008). Note, that relativistic effects produced by the gravity field of the Earth itself are of order

$U_E/c^2 \simeq 7 \times 10^{-10}$ in the vicinity of its surface. At present several clock experiments in terrestrial orbit are planned, such as the Atomic Clock Ensemble in Space project (ACES, Lemonde et al. 2001) that requires a detailed account of many subtle relativistic effects.

Finally we would like to mention the problem of geodesic precession-nutation (a relativistic effect that is discussed in more detail below, e.g., Misner, Thorne, and Wheeler 1973; Soffel 1989) and the description of Earth's rotation in a suitably chosen Geocentric Celestial Reference System (GCRS). Geodesic precession amounts to $1.''9$ per century and geodesic nutation is dominated by an annual term with amplitude 0.15 mas. Since the GCRS is chosen to be kinematically non-rotating, geodesic precession-nutation should be contained in the model describing the relation between the GCRS and the International Terrestrial Reference System (ITRS). According to the International Astronomical Union (IAU) 2000 Resolution B1.6 this relativistic precession-nutation is indeed contained in the present IAU precession-nutation model (IAU 2001; URL[2]).

These examples show clearly that high-precision modern astronomical observations can no longer be described by Newtonian theory, but require Einstein's theory of gravity.

2.2 Newtonian Formalism

A remarkable feature of Newton's theory of gravity is the absolute character of space and time. Space is Euclidean while the time measured by an observer flows independently of the observer's position, velocity or acceleration, or from the matter and physical fields. In Newton's theory there exist Cartesian inertial coordinate systems $(t, \mathbf{x})$ that cover the entire Newtonian universe in which dynamical equations of motion show no inertial forces. Such inertial systems are related by Galilean transformations. Such inertial coordinates in Newton's theory are unique up to the choice of origin, scales, the orientation of spatial axes, and a constant velocity of origin. If the origin of an inertial system Σ_m with coordinates $(T, \mathbf{X})$ moves with constant velocity $\mathbf{v}$ with respect to the inertial system Σ_r with coordinates $(t, \mathbf{x})$, then in the simplest case of parallel spatial axes we have

$$T = t, \qquad \mathbf{X} = \mathbf{x} - \mathbf{v}t. \tag{2.1}$$

In astronomy such inertial systems play a fundamental role for many purposes. With the origin in the barycenter of the solar system one introduces a (Newtonian) Barycentric Celestial Reference System (BCRS) with coordinates $(t, \mathbf{x})$. The transformation (Eq. 2.1) with $\mathbf{x}_E(t)$ replacing $\mathbf{v}t$ defines the (Newtonian) Geocentric Celestial Reference System (GCRS) with coordinates $(T, \mathbf{X})$. This geocentric celestial system might be called quasi-inertial, since the spatial axes are non-rotating in the Newtonian absolute sense whereas the geocenter is accelerated.

The barycentric celestial system is used for solar system ephemerides, for concepts such as an ecliptic, for interplanetary spacecraft navigation, etc. The positions of remote astronomical objects such as distant stars or quasars can be defined in that system. The barycentric celestial system presents the fundamental astrometric system, where concepts such as stellar position, radial velocity, or proper motion can be defined. On the other hand the GCRS is employed

for the description of physical processes in the vicinity of the Earth, for satellite theory, the dynamics of the Earth including Earth's rotation, etc. It is also used for the introduction of concepts like equator and the International Terrestrial Reference System (ITRS).

In Newton's theory inertial coordinates are physically preferred in the sense that they have direct physical meaning and observables can be derived from them directly. Consider a light ray with parametrization in BCRS coordinates

$$\mathbf{x}_\gamma(t) = \mathbf{x}_0 + c\mathbf{n}(t - t_0) \tag{2.2}$$

and a second one given by $\mathbf{x}'_\gamma(t) = \mathbf{x}'_0 + c\mathbf{n}'(t - t_0)$. If the observer is at rest with respect to the BCRS, the observed angle φ between the two incident light rays is given by $\cos\varphi = \mathbf{n}\cdot\mathbf{n}'$, where the dot indicates the usual Euclidean scalar product. Next we consider the same situation but the observer moving with velocity $\mathbf{v}$ in the BCRS. For each of the two incident light rays we can associate a Euclidean unit vector of the form $\mathbf{m} = \alpha(\mathbf{n} - \boldsymbol{\beta})$ with $\boldsymbol{\beta} = \mathbf{v}/c$. The normalization constant α to first order in β is given by $\alpha \simeq 1 + \mathbf{n}\cdot\boldsymbol{\beta}$. From these quantities one derives the observed angle φ between the two rays according to

$$\cos\varphi = \mathbf{m}\cdot\mathbf{m}' = \mathbf{n}\cdot\mathbf{n}' + (\mathbf{n}\cdot\mathbf{n}' - 1)((\mathbf{n} + \mathbf{n}')\cdot\boldsymbol{\beta}) + \mathcal{O}(\beta^2) \tag{2.3}$$

including first-order aberration terms.

In Newton's theory of gravity the gravitational interaction is described by one single scalar potential $U(t, \mathbf{x})$, the Newtonian gravitational potential, that in any inertial reference system satisfies the Poisson equation

$$\Delta U = -4\pi G\rho. \tag{2.4}$$

Here, G is the gravitational constant and ρ is the matter density that acts as a gravitational source. In the BCRS we usually assume the Newtonian potential to vanish at spatial infinity, so that the desired solution of Eq. 2.4 takes the form

$$U(t, \mathbf{x}) = G\int d^3x' \frac{\rho(t, \mathbf{x}')}{|\mathbf{x} - \mathbf{x}'|}. \tag{2.5}$$

Note that the Poisson equation (Eq. 2.4) is linear, i.e., in the gravitational N-body problem U is given by a sum over the individual bodies A of the form

$$U = \sum_A U_A \tag{2.6}$$

where U_A is given by Eq. 2.5 with the integral taken over body A only. Usually in astronomy the explicit expression of the gravitational potential in terms of the matter density, however, is not needed. In astronomy one is usually not interested in the gravitational field inside of the astronomical bodies. In the outer vicinity of some astronomical body, A, the gravitational potential U_A will admit a convergent power series expansion in terms of the inverse distance to the body's center by means of suitable mass multipole moments (potential coefficients). The usual Newtonian multipole expansion of the Earth in the GCRS reads

$$U_E(T, \mathbf{X}) = \frac{GM_E}{R}\left[1 + \sum_{l=2}^{\infty}\sum_{m=0}^{l}\left(\frac{R_E}{R}\right)^l P_{lm}(\cos\theta)(C_{lm}\cos m\phi + S_{lm}\sin m\phi)\right]. \tag{2.7}$$

Here, M_E is the Newtonian mass of the Earth, R_E some suitably chosen Earth's radius and (R, θ, ϕ) are the usual polar coordinates of $\mathbf{X}$. Expression 2.7 assumes that the origin of the GCRS coincides with the Earth's center of mass, so that the mass dipole moments (the $l = 1$ terms in the spherical harmonics expansion) vanish.

In the gravitational N-body problem the BCRS acceleration $\mathbf{a}_A$ of body A is determined by the external gravitational potential

$$U_{\text{ext}}(t, \mathbf{x}) = \sum_{B \neq A} U_B(t, \mathbf{x}). \tag{2.8}$$

If the gravitational field of body A can be neglected or if A is spherically symmetric (a mass monopole), then

$$\mathbf{a}_A = \nabla U_{\text{ext}}. \tag{2.9}$$

For a system of mass monopoles we then have

$$\mathbf{a}_A = -\sum_{B \neq A} \frac{GM_B}{r_{AB}^2} \mathbf{n}_{AB} \tag{2.10}$$

where $r_{AB} \equiv |\mathbf{x}_A(t) - \mathbf{x}_B(t)|$ and $\mathbf{n}_{AB} = [\mathbf{x}_A(t) - \mathbf{x}_B(t)]/r_{AB}$.

Because of the weak equivalence principle (all uncharged test bodies in some external gravitational field fall at the same rate) in the GCRS, the external gravitational potential $\mathcal{U}_{\text{ext}}$ differs from the barycentric U_{ext}:

$$\mathcal{U}_{\text{ext}} = \mathcal{U}_{\text{tidal}} + \mathcal{U}_{\text{iner}}. \tag{2.11}$$

Here the Newtonian tidal potential $\mathcal{U}_{\text{tidal}}$ is given by

$$\mathcal{U}_{\text{tidal}}(\mathbf{X}) = U_{\text{ext}}(\mathbf{x}_E + \mathbf{X}) - U_{\text{ext}}(\mathbf{x}_E) - \mathbf{X} \cdot \nabla U_{\text{ext}}(\mathbf{x}_E). \tag{2.12}$$

The inertial potential $\mathcal{U}_{\text{iner}}$ results from the coupling of the Earth's higher mass multipole moments to the external potential and vanishes for a purely spherical Earth. Mathematically it is given by

$$\mathcal{U}_{\text{iner}} = (\nabla U_{\text{ext}} - \mathbf{a}_E) \cdot \mathbf{X}. \tag{2.13}$$

2.3 Special Relativity and the Metric Tensor

Special relativity theory (SRT) is based upon certain principles. The *principle of the constancy of the velocity of light* says that the velocity of light in vacuum is independent of the motion of the source and of frequency, intensity and polarization (note that this has nothing to do with the motion of the observer relative to some "medium" in which electromagnetic waves propagate).

No signal can propagate in the vacuum faster than light; massless particles move with the speed of light c; massive particles always have a speed less than c.

If the unit of length is defined (as in the old days) by some meter stick or as the 1 650 763, 73 multiple of the wavelength of the orange line ($5d_5 \rightarrow 2p_{10}$) of ^{86}Kr, then the numerical value for c can be measured. It then turns out that it does not depend upon the

speed of the observer and the direction in space (the result of the famous Michelson and Morley experiment). As is well known, this result was historically the starting point for the development of the SRT. Taking this result for granted during the 17th conference on measures and weights in 1983, a new definition of the meter was given:

> *The meter is the length of the path traveled by light in vacuum during a time interval of* 1/299 792 458 *of a second.*

This new definition of the meter has important consequences: i) the numerical value for c can no longer be measured and ii) the Michelson-Morley (and related) experiments have to be interpreted in a different manner (e.g., the length of a meter stick in some inertial frame does not depend upon its orientation in space).

We now come to the next important principle of SRT, *Einstein's relativity principle*: with respect to all (non-gravitational) laws of physics two inertial frames $\Sigma_r[x^\mu = (ct, \mathbf{x})]$ and $\Sigma_m[X^\alpha = (cT, \mathbf{X})]$ are completely indistinguishable. This implies that by means of physical experiments it is impossible to tell in which inertial system one is located.

These principles imply that in each inertial frame with Cartesian coordinates $(t, \mathbf{x})$ the electromagnetic wave equation takes the form

$$\left(-\frac{1}{c^2}\frac{\partial^2}{\partial t^2} + \Delta\right) u = 0 \tag{2.14}$$

if u is the wave amplitude and c is the same for each inertial frame. Especially for the propagation of a spherical wave originating from the origin of an inertial frame we can write $(\Delta\mathbf{x})^2 = c^2(\Delta t)^2$. Because of this we can introduce a spacetime metric $g_{\mu\nu}$ with

$$ds^2 = g_{\mu\nu}\, dx^\mu dx^\nu \tag{2.15}$$

(according to Einstein's summation convention over equal indices a summation is automatically carried out) such that in each inertial Cartesian (or pseudo-Cartesian) coordinate system $x^\mu = (c\,t, x, y, z)$ (note that we are now including a factor of c in the definition of $x^0 = c\,t$; then all four coordinates have the same dimension of a length)

$$g_{\mu\nu} = \eta_{\mu\nu} \equiv \mathrm{diag}(-1, +1, +1, +1) \tag{2.16}$$

or, equivalently,

$$g_{00} = -1\,,\; g_{0i} = 0\,,\; g_{ij} = \delta_{ij}\,.$$

Equation 2.15 together with 2.16 gives

$$ds^2 = -c^2dt^2 + d\mathbf{x}^2. \tag{2.17}$$

Hence, we have introduced a spacetime metric that has the first important property: light rays are geodesic curves with $ds^2 = 0$. In the absence of gravity they are straight lines with

$$ds^2 = 0 = -c^2dt^2 + d\mathbf{x}^2. \tag{2.18}$$

In SRT the metric tensor in every inertial system is given by Eq. 2.16. This invariance determines the relation between the corresponding coordinates. If the origin of an inertial system Σ_m with coordinates $(cT, \mathbf{X})$ moves with constant velocity $\mathbf{v}$ with respect to the inertial system Σ_r with coordinates $(ct, \mathbf{x})$, then for the case of parallel spatial axes the Lorentz transformation reads:

$$T = \Gamma \left(t - \frac{\mathbf{v} \cdot \mathbf{x}}{c^2} \right), \qquad \mathbf{X} = \mathbf{x} - \Gamma \, \mathbf{v} t + \frac{(\Gamma - 1)}{v^2} (\mathbf{v} \cdot \mathbf{x}) \mathbf{v} \,, \tag{2.19}$$

where

$$\Gamma \equiv \left(1 - \frac{\mathbf{v} \cdot \mathbf{v}}{c^2} \right)^{-1/2} . \tag{2.20}$$

Note, that even in the absence of gravitational fields and the acceleration of the geocenter because of Special Relativity, the BCRS and the GCRS coordinates would be related by a Lorentz transformation, a 4-dimensional spacetime transformation that generalizes the Galilean transformation of Eq. 2.1.

Proper time τ of an observer is the time measured by an (ideal) clock moving together with that observer. If in some inertial system a clock is at rest ($d\mathbf{x} = 0$), the time indicated by this clock coincides with the coordinate time t. If the clock is moving with respect to the inertial system, this will no longer be the case. Each observable has, mathematically speaking, to be a scalar, because the clock and the observer do not care what coordinates someone is using to describe the situation. In the general case, proper time, τ, as indicated by some clock is directly related with the spacetime metric according to

$$ds^2 = -c^2 d\tau^2 \tag{2.21}$$

where ds is taken along the clock's worldline. This constitutes the second important property of the spacetime metric.

Finally, we would like to note that not only the observed proper time, but also any other kind of observable, mathematically has to be presented by some coordinate-independent, scalar quantity. We will come back to this point below.

2.4 Einstein's Theory of Gravity

The equivalence principle presents one of the cornerstones of Einstein's theory of gravity. Einstein's equivalence principle says (Weinberg 1972, Section 3.1) that at every spacetime point in an arbitrary gravitational field it is possible to choose a "locally inertial coordinate system" such that, within a sufficient small spacetime region of the point in question, the laws of nature take the same form as in inertial reference frames of Special Relativity.

This form of the equivalence principle has the consequence that gravity can be described by a metric theory (Will 1993), i.e., by at least a $g_{\mu\nu}$-field and possibly by "other gravitational fields." At each point in spacetime there exists a bundle of local freely falling systems (Einstein elevators) in which the spacetime metric $g_{\mu\nu}$ reduces to the flat spacetime metric $\eta_{\mu\nu}$. The world lines of test bodies with vanishing own gravitational fields are geodesics of $g_{\mu\nu}$. This follows from the fact that these world lines are straight lines in the local freely falling system, i.e., geodesics with respect to the flat spacetime metric. Hence, they must be

geodesics with respect to the spacetime metric $g_{\mu\nu}$. This is the third important property of the metric.

Einstein's theory is the simplest of all metric theories of gravity. In Einstein's theory there are no other gravitational fields, but only one spacetime metric that also describes the gravitational interaction and satisfies Einstein's field equations

$$E_{\mu\nu}(g, \partial g, \partial^2 g) = \kappa\, T_{\mu\nu}. \tag{2.22}$$

The left-hand side of Eq. 2.22, the Einstein tensor, contains $g_{\mu\nu}$ and its first and second partial derivatives with respect to the spacetime coordinates. On the right-hand side the energy-momentum tensor, $T_{\mu\nu}$, describes the field-generating sources; it generalizes the density ρ of the Poisson equation (Eq. 2.4). In relativity, energy, density, pressure, and stresses all act as sources of the gravitational field. The energy-momentum tensor contains the Newtonian matter density, ρ, in its time-time component

$$T_{00} = \rho c^2 + \dots . \tag{2.23}$$

The corresponding field equation to lowest order in $1/c$ reads

$$\Delta g_{00} = -\kappa\, T_{00} = -\kappa\, \rho c^2. \tag{2.24}$$

If we write

$$g_{00} = -1 + \frac{2U}{c^2} + \mathcal{O}(c^{-3}) \tag{2.25}$$

the potential U satisfies the Poisson equation (2.4) and the coupling constant $\kappa = 8\pi G/c^4$. In this way we see how gravity enters the spacetime metric: in our coordinate system the Newtonian potential is contained in the $1/c^2$ term of g_{00}.

Einstein's equations form a complicated set of ten partial differential equations of second order. Because both sides of the Einstein field equations have zero divergence (due to the conservation of energy and momentum), these ten equations are not independent, only six of them are independent (because of four additional relations). Hence, the equations determine only six out of ten degrees of freedom of the metric tensor $g_{\mu\nu}$. Four degrees of freedom for the metric tensor remain, expressing the freedom in the choice of the four spacetime coordinates. Of course the field equations cannot tell what coordinates should be used; instead the coordinates can be fixed by four (more or less) arbitrary conditions for the metric tensor. This is the coordinate or *gauge* freedom of the theory. This gauge freedom is one of the most important differences to the classical Newtonian theory of gravity. Physically preferred coordinates usually do not exist and observables have to be constructed as scalar quantities.

However, the situation is simpler for isolated systems with an asymptotically flat spacetime. E.g., the solar system might be idealized in this manner: we forget about distant masses (distant depends upon the problem; for pulsar timing now the masses of our galaxy have to be taken into account) and think of the solar system as being isolated. Then, far from the solar system the gravitational fields will become weaker, with increasing distance spacetime asymptotically will approach the flat spacetime from SRT in this idealized picture. In the asymptotic region preferred (inertial and e.g., Cartesian) coordinates exist such that there $g_{\mu\nu} \to \eta_{\mu\nu}$. If, however, we get closer to the gravitating masses, preferred coordinates cease to exist; i.e., many different coordinates have equal rights.

One might deal with that gauge problem in different ways. One way to avoid confusion is to define certain relevant reference systems, such as the BCRS and the GCRS, by completely specifying their metric tensors as was done by the IAU 2000 Resolution B1.3 (IAU 2001; URL[2]). Note that even for that case the observables have to be constructed as coordinate-independent quantities.

2.5 The Problem of Observables

Usually coordinates in Einstein's theory of gravity have no direct physical meaning. To relate the theory with measured quantities (observables) one has to proceed as follows. First one chooses a coordinate system (reference system) that covers the spacetime region of interest. All relevant elements of the system such as extended bodies, light rays, physical fields, etc., have to be described in this coordinate picture. The coordinate dynamics of the system follows from fundamental laws of physics such as Einstein's field equations. In such a coordinate picture light rays and observers are described by means of curves or world lines. The astronomical observables have to be constructed as coordinate-independent quantities. Usually the coordinate picture contains a lot of parameters such as initial positions of astronomical bodies, their masses, etc., that can be fitted to observations by means of least-squares methods.

2.5.1 The Ranging Observable

Let us consider a typical astronomical measurement in the solar system: lunar laser ranging (LLR). Here laser pulses are emitted from LLR stations on the Earth to retro-reflectors on the lunar surface. Typically a single photon per several pulses finds its way back into the receiving telescope of the station and one measures the total travel time of a pulse from the station to the Moon and back. This situation is depicted in Fig. 2.1. In the right part of the figure we see the world line of the clock with the two events E: emission of the pulse and R: reception of the pulse. The observed time interval between E and R is given by

$$\Delta\tau = \int_E^R d\tau \tag{2.26}$$

where

$$d\tau^2 = -\frac{1}{c^2} ds^2.$$

In practice this indicated time interval $\Delta\tau$ can be related with a corresponding interval of some other timescale. The same sort of observable is used in SLR and radio ranging.

2.5.2 The Spectroscopic Observable

We now consider the following problem: one observer emits some monochromatic electromagnetic wave of frequency f_E. Another observer receives this signal and measures the frequency f_R and we ask about the relation between the two frequencies. If we concentrate upon one single light ray propagating from the emitter to the receiver, the situation is shown in Fig. 2.2. Here γ_E is the world line of the emitter, γ_R that of the receiver, γ_L that of the light ray. We consider tangent vectors to these three world lines. A tangent vector u^μ

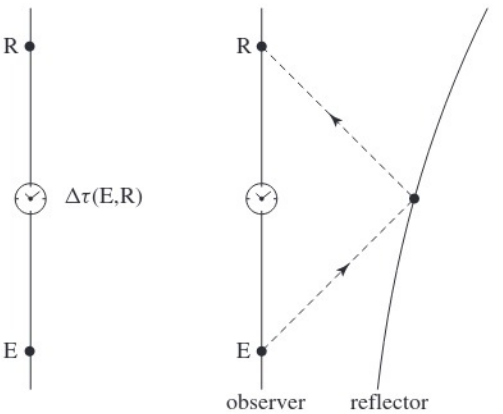


Figure 2.1 Left: The ranging observable is a propagation time interval between emission and reception of some electromagnetic pulse. In Lunar Laser Ranging it is a laser pulse that travels from some LLR station on the Earth to some retro-reflector on the lunar surface and back to the ground station. Right: the observable is the proper time interval that has elapsed between the instant of emission and the instant of reception of an electromagnetic pulse.

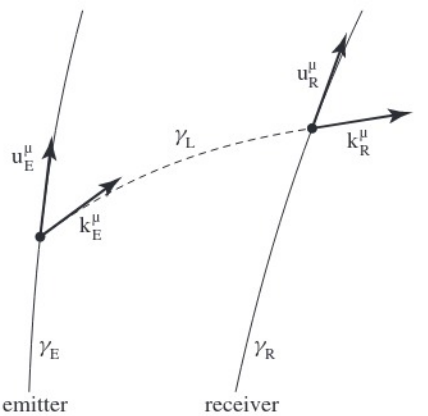


Figure 2.2 The spectroscopic observable is the frequency ratio f_R/f_E. Some observer (emitter) emits some electromagnetic signal of frequency f_E. This signal is observed by another observer (receiver) who measures the frequency f_R (see text).

to the world line of the emitter or observer is called 4-velocity and given by $u^\mu = dx^\mu/d\tau$, if τ indicates proper time along the corresponding world line. The 4-velocity is, obviously, normalized according to

$$g_{\mu\nu}u^\mu u^\nu = -c^2. \tag{2.27}$$

A tangent vector to a light ray will be denoted by k^μ. If λ is a suitable curve parameter $k^\mu = dx^\mu/d\lambda$. Because of the first metric property

$$g_{\mu\nu}k^\mu k^\nu = 0 \tag{2.28}$$

and, therefore, light rays are called *null geodesics* (geodesics of zero length). Let u^μ_E be the 4-velocity of the emitter at the point of emission, and u^μ_R be that of the receiver at the point of reception. Let k^μ be the tangent vector onto γ_L, then the frequency ratio is given by

$$\frac{f_R}{f_E} = \frac{(g_{\mu\nu}k^\mu u^\nu)_R}{(g_{\mu\nu}k^\mu u^\nu)_E}. \tag{2.29}$$

If in the absence of gravitational fields we consider the receiver at rest at the point of reception and the emitter moving with coordinate velocity $\mathbf{v}$ at the point of emission, then

$$f_R = f_E\,\frac{\sqrt{1-\boldsymbol{\beta}^2}}{1-\boldsymbol{\beta}\cdot\mathbf{n}} \tag{2.30}$$

where $\mathbf{n}$ is the direction of light propagation, so that $k^\mu \propto (1, \mathbf{n})$. This is the well-known formula for the Doppler effect in Special Relativity.

2.5.3 Astrometric Observables

In astrometry one principle observable is the observed angle between two incident light rays. This situation is depicted in Fig. 2.3. Here $\gamma_{\rm obs}$ is the world line of the observer, γ_* and γ'_* are two light rays from two different astronomical sources that are simultaneously observed by the observer in some event O. Let u^μ be the 4-velocity of the observer in O, k^μ and k'^μ be the wave vectors of the two incident light rays. Then

$$P^\mu_{\ \nu} \equiv \delta^\mu_{\ \nu} + \frac{1}{c^2}u^\mu u_\nu \tag{2.31}$$

is a projection tensor that projects vectors into their components perpendicular to u^μ, i.e.,

$$P^\mu_{\ \nu}\,u^\nu = u^\mu + \frac{1}{c^2}u^\mu u_\nu u^\nu = 0 \tag{2.32}$$

in virtue of the normalization condition Eq. 2.27. In a certain sense u^μ points into the time-direction of the observer and the projection operator points into the space "experienced" by the observer. Now k^μ is a vector obeying Eq. 2.28, but

$$\bar{k}^\mu = P^\mu_{\ \nu}k^\nu \tag{2.33}$$

is a vector of non-vanishing length. The observed angle φ between two incident light rays γ_* and γ'_* is generally given by

$$\cos\varphi = \frac{g_{\mu\nu}\bar{k}^\mu\bar{k}'^\nu}{|\bar{k}^\mu|\,|\bar{k}'^\mu|} \tag{2.34}$$

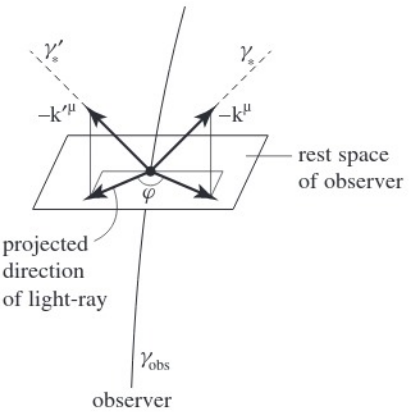


Figure 2.3 The astrometric observable: the observed angle φ between two incident light rays γ_* and γ'_* as seen by an observer moving along the world line γ_{obs}

where $\mid A^{\mu} \mid = (g_{\mu\nu} A^{\mu} A^{\nu})^{\frac{1}{2}}$. In the absence of gravity fields from this we get

$$\cos\varphi = \frac{\mathbf{n}\cdot\mathbf{n}' - 1 + \Gamma^2(1-\boldsymbol{\beta}\cdot\mathbf{n})(1-\boldsymbol{\beta}\cdot\mathbf{n}')}{\Gamma^2(1-\boldsymbol{\beta}\cdot\mathbf{n})(1-\boldsymbol{\beta}\cdot\mathbf{n}')} \tag{2.35}$$

where $\boldsymbol{\beta} = \mathbf{v}/c$. This is the aberration formula of Special Relativity. A Taylor expansion in terms of c^{-1} yields

$$\begin{aligned}\cos\varphi = \mathbf{n}\cdot\mathbf{n}' + (\mathbf{n}\cdot\mathbf{n}' - 1)\Big[&(\mathbf{n}+\mathbf{n}')\cdot\boldsymbol{\beta} + (\mathbf{n}\cdot\boldsymbol{\beta})^2 \\ &+ (\mathbf{n}'\cdot\boldsymbol{\beta})^2 + (\mathbf{n}\cdot\boldsymbol{\beta})(\mathbf{n}'\cdot\boldsymbol{\beta}) - \boldsymbol{\beta}^2\Big] + \mathcal{O}(c^{-3})\end{aligned} \tag{2.36}$$

generalizing Eq. 2.3.

In future high-precision astrometric missions different observables might play a role, e.g., the observed angles between incident light rays and certain reference directions in a spacecraft. In that case these reference directions have to be introduced explicitly into the theory. If one of such reference directions is represented by a reference vector e^{μ}, the corresponding directional cosine can be obtained from

$$\cos\theta = \frac{g_{\mu\nu}\bar{k}^{\mu}e^{\nu}}{|\bar{k}^{\mu}|\ |e^{\nu}|}. \tag{2.37}$$

2.6 The Post-Newtonian Framework[1]

The full Einstein equations form a complicated set of non-linear equations. Many exact solutions of Einstein's equations are in fact known, but most of them apply only to the vacuum case for highly symmetric situations. Apart from the well-known Schwarzschild solution (the spherically symmetric vacuum solution) most known exact solutions have little

1. Parts of this Section are close to the text of Soffel et al. 2003.

or nothing to do with reality. For that reason for applications in the solar system the so-called post-Newtonian approximation to Einstein's theory is used. The idea of the post-Newtonian theory is to employ the fact that in the solar system velocities of astrophysical bodies are small and gravitational fields are weak. The post-Newtonian theory is a *slow motion, weak field approximation*. The post-Newtonian approximation to Einstein's theory is determined with respect to equations of motion. One starts with Newtonian equations of motion for the massive bodies in our solar system and approximates terms in Einstein's theory such that next higher order terms in $1/c$ are considered explicitly.

2.6.1 Coordinate Timescales and Proper Time

We have already made it clear that in Einstein's theory of gravity one has first to choose a coordinate system or reference system to create a coordinate picture of the system of interest. For the construction of a barycentric ephemeris the Barycentric Celestial Reference System (BCRS) with coordinate $x^\mu = (ct, \mathbf{x})$ is a necessary starting point. One component of such a reference system is a time coordinate that defines a timescale that attributes a value of time for any event covered by the underlying coordinate system. For the BCRS the timescale is $t = \text{TCB}$ (Barycentric Coordinate Time). Since the BCRS covers at least the solar system, any event in the solar system is associated with a TCB value. Another basic reference system of importance is the GCRS (Geocentric Celestial Reference System) whose time coordinate is TCG (Geocentric Coordinate Time). Although the GCRS is physically adequate for the physical phenomena in a vicinity of the Earth (say, within the geostationary orbit), the GCRS also covers the whole solar system. Therefore, any event in the solar system can be alternatively labelled by TCG and the spatial coordinates of the GCRS. From these two basic timescales, TCB and TCG, additional ones have been introduced for practical reasons: TDB, TT and TAI; these will be discussed below.

The relation between a reference system and the real world is established via observational data. For the problem of timescales the readings of certain atomic clocks, defining TAI (International Atomic Time), are employed. Mathematically, a reference system is defined by the form of the corresponding metric tensor. The readings of an idealized atomic clock can be derived from Eq. 2.21 by means of the metric tensor. Hence, whereas 'proper times' refer to the indication of certain individual clocks, coordinate times represent mathematical models and refer to any event covered by the reference system. They present a necessary basis for the coordinate picture of an astronomical system.

Moreover, coordinate times present the crucial tool for the synchronization of clocks at different locations. Note, that the concept of simultaneity is an indispensable part of any clock comparison algorithm. The coordinate simultaneity is the only logical possibility of saving the concept of simultaneity in General Relativity (Klioner 1992; Wolf and Petit 1995): two events are called simultaneous if and only if the corresponding coordinate times have the same value for both of them.

2.6.2 The Barycentric Celestial Reference System

IAU 2000 Resolution B1.3 (IAU 2001; URL[2]) concerns the definition of Barycentric Celestial Reference System (BCRS) and the Geocentric Celestial Reference System (GCRS). The BCRS is defined with coordinates $(ct, x^i) = x^\mu$ where $t = \text{TCB}$ (Barycentric Coordinate Time). The BCRS is a particular version of the barycentric reference system of the solar

system. The Resolution recommends to write the metric tensor of the BCRS in the form

$$\begin{aligned} g_{00} &= -1 + \frac{2w}{c^2} - \frac{2w^2}{c^4} + \mathcal{O}(c^{-5}) \\ g_{0i} &= -\frac{4}{c^3} w^i + \mathcal{O}(c^{-5}) \\ g_{ij} &= \delta_{ij} \left(1 + \frac{2}{c^2} w\right) + \mathcal{O}(c^{-4}). \end{aligned} \tag{2.38}$$

A comparison reveals that this form of the metric presents an extension of the flat metric from SRT, Eq. 2.16, and of the 'Newtonian limit' Eq. 2.25 for g_{00}. Whereas the 'Newtonian limit' of the metric contains only the Newtonian potential, U, the new one contains a scalar potential, w, and a vector potential, w^i.

Actually the equations for g_{00} and g_{0i} from Eq. 2.38 without the order symbols $\mathcal{O}(c^{-5})$ are always correct and can be simply considered as definitions of w and w^i in terms of g_{00} and g_{0i}. To specify the post-Newtonian metric we have added order symbols in Eq. 2.38. E.g., for g_{00} the order symbol indicates that terms of order c^{-5} will systematically be neglected. With these forms for g_{00} and g_{0i} one finds that spatially isotropic coordinates x^i exist such that g_{ij} from Eq. 2.38 with the potential w from g_{00} solves Einstein's field equations to the first post-Newtonian order. Note that the form of Eq. 2.38 implies that the barycentric spatial coordinates x^i satisfy the harmonic gauge condition (see e.g., Brumberg and Kopeikin 1989; Damour, Soffel, and Xu 1991). At this point, because of the freedom in the time coordinate, many different 'time gauge conditions' are still possible. IAU 2000 Resolution B1.3 proceeds by recommending a specific kind of space and time *harmonic gauge* (IAU 2001; URL[2]). Tremendous work on General Relativity has been done with the harmonic gauge that was found to be a useful and simplifying gauge for many kinds of applications. The harmonic gauge condition (e.g., Weinberg 1972; Fock 1959)

$$g^{\mu\nu}\Gamma^{\lambda}_{\mu\nu} = 0 \tag{2.39}$$

where $\Gamma^{\lambda}_{\mu\nu}$ are the Christoffel symbols of the metric tensor, is not restricted to some post-Newtonian approximation, but can be defined in Einstein's theory of gravity without any approximations. With the harmonic gauge condition the post-Newtonian Einstein field equations take the form

$$\left(-\frac{1}{c^2}\frac{\partial^2}{\partial t^2} + \Delta\right) w = -4\pi G\sigma + \mathcal{O}(c^{-4}) \tag{2.40}$$

$$\Delta w^i = -4\pi G\sigma^i + \mathcal{O}(c^{-2}). \tag{2.41}$$

Here σ and σ^i are the gravitational mass and mass current density related to the *energy-momentum tensor* $T^{\mu\nu}$ by

$$\sigma = \frac{1}{c^2}\left(T^{00} + T^{ss}\right), \quad \sigma^i = \frac{1}{c}\,T^{0i}. \tag{2.42}$$

In practice, however, the energy-momentum tensor will usually not appear explicitly. This is because the gravitational potentials w and w^i from Eqs. 2.40–2.41 are completely determined by σ and σ^i which can be considered as primary quantities. If we deal with problems where

gravitational fields play a role only *outside* of astronomical bodies and admit a useful convergent expansion in terms of multipole moments (potential coefficients), only corresponding integral characteristics of the bodies like masses, quadrupole moments, etc., show up explicitly, which are defined in terms of σ and σ^i and whose numerical values will be fixed by observations. Because of Eq. 2.41, w^i is sometimes called the gravitomagnetic potential, since it results from mass currents (moving or rotating masses) just as the electromagnetic vector potential results from electric currents in Maxwell's theory of electromagnetism.

Equation 2.40 generalizes the Poisson equation (Eq. 2.4), and, hence, the scalar potential w presents a relativistic generalization of the Newtonian potential U. Because of problems related with homogeneous solutions and boundary conditions mathematically, it is clear that these differential equations do not fix the harmonic solutions uniquely. Assuming spacetime to be asymptotically flat (no gravitational fields far from the system), i.e.,

$$\lim_{\substack{r\to\infty \\ t=\text{const}}} g_{\mu\nu} = \eta_{\mu\nu} \tag{2.43}$$

the solution reads

$$w(t, \mathbf{x}) = G \int d^3x' \, \frac{\sigma(t, \mathbf{x}')}{|\mathbf{x} - \mathbf{x}'|} + \frac{1}{2c^2} G \frac{\partial^2}{\partial t^2} \int d^3x' \, \sigma(t, \mathbf{x}')|\mathbf{x} - \mathbf{x}'| \tag{2.44}$$

$$w^i(t, \mathbf{x}) = G \int d^3x' \frac{\sigma^i(t, \mathbf{x}')}{|\mathbf{x} - \mathbf{x}'|}. \tag{2.45}$$

Comparing our form of the metric tensor with other forms that can be found in the literature (e.g., Will 1993), one might get the erroneous impression that something is missing in Eq. 2.38 and Eqs. 2.44–2.45, which is not the case. If matter is described by some fluid model, then formally (w, w^i) might be split into the various pieces resulting from kinetic energy, gravitational potential energy, specific internal energy density, pressure, etc., and the equivalence of our form of the metric tensor, e.g., with that given in Will (1993) can be shown (Soffel et al. 2003).

The point, however, is that a split of (σ, σ^i) of our metric potentials (w, w^i), or of the metric tensor itself into various pieces is usually unnecessary. If only gravitational fields outside the relevant bodies play a role (as is typically the case in celestial mechanics and astrometry), it is advantageous to keep such pieces together, since it will be the sum that determines the observables. One might argue U is the 'Newtonian potential' and the rest can be identified as 'relativistic corrections'. This way of thinking, however, can be very misleading and presents a source of errors. As has been shown in the literature (e.g., Damour, Soffel, and Xu 1991, 1993), suitably defined potential coefficients based upon w (not U) and w^i can be introduced that can be determined from satellite data. From a more theoretical point of view the introduction of (w, w^i) has the advantage that the field equations 2.40–2.41 are formally *linear*, although the corresponding metric is not (because of the w^2-term). We used the word 'formally' since σ depends upon w implicitly. This linearity implies that for an ensemble of N-bodies

$$w(t, \mathbf{x}) = \sum_{A=1}^{N} w_A(t, \mathbf{x}), \qquad w^i(t, \mathbf{x}) = \sum_{A=1}^{N} w^i_A(t, \mathbf{x}) \tag{2.46}$$

where the index A indicates the contribution related with body A where the integrals have to be taken over body A only. This linearity, however, does not imply that body-body interaction

terms have been neglected. If written explicitly, w_A will in general contain contributions from bodies $B \neq A$.

2.6.3 BCRS versus ICRS

BCRS is a dynamical concept. The statement "we use BCRS" in General Relativity is analogous to the statement "we use barycentric inertial coordinates" in Newtonian physics. The mathematical language and physical content of General Relativity make it indispensable to fully fix the metric tensor of the BCRS to make the choice of coordinates unique. On the basis of the metric tensor of the BCRS, one derives the dynamical equations of motion of celestial bodies and light rays, and finally constructs relativistic models of observable quantities.

ICRS is a kinematical concept. From the physical point of view the idea of the ICRS is the cosmological assumption that distant quasars do not rotate with respect to asymptotically flat reference systems like BCRS (or with respect to inertial coordinates in the Newtonian framework). In principle such an assumption could and should be checked by testing if the motion of solar system bodies is compatible with the equations of motion, with no Coriolis and centrifugal forces. Up to now no contradictions have been noticed here.

The BCRS as defined by the IAU 2000 Resolution has no specific orientation. IAU 2006 Resolution 2 completes the definition of the BCRS by adding that unless otherwise stated, the BCRS is assumed to be oriented according to the ICRS axes (IAU 2007; URL[2]). One can say that the BCRS provides a way to prolong coordinate lines of the ICRS from distance quasars to any point of the solar system.

2.6.4 The Geocentric Celestial Reference System

IAU 2000 Resolution B1.3 continues to define the GCRS which represents a particular version of the local geocentric reference system for the Earth. The coordinates (T, X^a) of the GCRS have two remarkable properties:

(a) The gravitational field of external bodies is represented only in the form of tidal terms, that are at least quadratic in the spatial coordinates and coincides with the Newtonian tidal potential in the Newtonian limit.

(b) The internal gravitational field of the central body coincides with the gravitational field of the corresponding isolated source provided that the tidal field of external masses is neglected.

The fact that these two properties can be satisfied simultaneously is a direct consequence of the so-called *Strong Equivalence Principle* that is satisfied in General Relativity (but not necessarily in alternative theories of gravity).

Spatial coordinates X^a of the GCRS are kinematically non-rotating with respect to the barycentric ones (see e.g., Brumberg and Kopeikin 1989; Klioner and Soffel 1998). The geocentric coordinates are denoted by $(T, \mathbf{X})$, where $T = \mathrm{TCG}$. In the relation between x^i and X^a from IAU 2000 Resolution B1.3 let us replace the unit matrix δ_{ai} by a general rotation matrix R_{ai}

$$X^a = R_{ai}\left[r_E^i + \frac{1}{c^2}(\ldots)\right] + \mathcal{O}(c^{-4})$$

where $\mathbf{r}_E = \mathbf{x} - \mathbf{x}_E$. If the two sets of spatial coordinates are aligned for all times, i.e., if $R_{ai} = \delta_{ai}$ as is the case for the GCRS spatial coordinates, then X^a is defined to be kinematically non-rotating with respect to the barycentric spatial coordinates x^i. The metric tensor of the GCRS in the same form as the barycentric one, but with potentials $W(T, \mathbf{X})$ and $W^a(T, \mathbf{X})$:

$$\begin{aligned} G_{00} &= -1 + \frac{2W}{c^2} - \frac{2W^2}{c^4} + \mathcal{O}(c^{-5}) \\ G_{0a} &= -\frac{4}{c^3} W^a + \mathcal{O}(c^{-5}) \\ G_{ab} &= \delta_{ab} \left(1 + \frac{2}{c^2} W \right) + \mathcal{O}(c^{-4}) \end{aligned} \tag{2.47}$$

and the geocentric field equations formally look the same as the barycentric ones (Eqs. 2.40–2.41), but with all variables referred to the GCRS. Again one decisive advantage of this form of the GCRS is the formal linearity of the field equations. This linearity admits a unique split of the geocentric metric into a part coming from the Earth itself and a remaining part resulting from inertial and tidal forces. Therefore, the potentials W and W^a can be split according to

$$\begin{aligned} W(T, \mathbf{X}) &= W_E(T, \mathbf{X}) + W_{\text{ext}}(T, \mathbf{X}) \\ W^a(T, \mathbf{X}) &= W^a_E(T, \mathbf{X}) + W^a_{\text{ext}}(T, \mathbf{X}). \end{aligned} \tag{2.48}$$

The Earth's potentials W_E and W^a_E are defined in the same way as w_E and w^a_E, (i.e., Eqs. 2.44–2.45 with integrals taken over the volume of the whole Earth) but with quantities calculated in the GCRS. Outside the Earth the potentials (W, W^a) admit a power series expansion in terms of $R \equiv |\mathbf{X}|$ and all negative powers of R are contained in W_E and W^a_E. For that reason the Earth's potentials admit multipole expansions that look very similar to the Newtonian ones.

It is useful to split the external potentials W_{ext} and W^a_{ext} further. They can be written in the form

$$W_{\text{ext}} = W_{\text{tidal}} + W_{\text{iner}}, \qquad W^a_{\text{ext}} = W^a_{\text{tidal}} + W^a_{\text{iner}} \tag{2.49}$$

where the tidal terms are at least quadratic in X^a and the inertial contributions W_{iner} and W^a_{iner} are just linear in X^a. Explicitly,

$$\begin{aligned} W_{\text{iner}} &= Q_a \, X^a \\ W^a_{\text{iner}} &= -\frac{1}{4} \, c^2 \, \epsilon_{abc} \Omega^b_{\text{iner}} \, X^c. \end{aligned} \tag{2.50}$$

Mathematically the Q_a term is related with the 4-acceleration of the geocenter in the external gravitational field, a quantity that vanishes for a purely spherical and non-rotating Earth (for a mass monopole, more precisely) that moves along a geodesic in the external gravitational field. The Q_a term therefore results from the coupling of higher order multipole moments of the Earth to the external tidal gravitational fields (to the external curvature tensor of spacetime in mathematical language). Further details on the definition of Q_a and its properties can be found in Soffel et al. (2003). Here we note that for the GCRS $|Q_a| < 4 \times 10^{-11}$ m/s^{-2}.

The term $W^a_{\rm iner}$ describes a relativistic Coriolis force due to the rotation of the GCRS with respect to a dynamically non-rotating geocentric reference system. Such a rotation has several components, the dominant of which is called geodesic precession

$$\mathbf{\Omega}_{\rm iner} \simeq \mathbf{\Omega}_{\rm GP} \tag{2.51}$$

with

$$\mathbf{\Omega}_{\rm GP} = -\frac{3}{2c^2}\,\mathbf{v}_E \times \nabla w_{\rm ext}(\mathbf{x}_E) \tag{2.52}$$

where

$$w_{\rm ext}(t, \mathbf{x}) = \sum_{A \neq E} w_A(t, \mathbf{x}). \tag{2.53}$$

The order of magnitude is given by $|\mathbf{\Omega}_{\rm GP}| \sim 3 \times 10^{-15}\ {\rm s}^{-1} \sim 2''$/century.

The definition of the GCRS implies that the spatial GCRS coordinates $\mathbf{X}$ are kinematically non-rotating with respect to the BCRS ones, $\mathbf{x}$ (as indicated by the δ_{ai}-term in Resolution B1.3). Because of geodesic precession, locally inertial coordinates precess with respect to the GCRS by an amount of $|\mathbf{\Omega}_{\rm iner}| = 1.''9198$/century (Brumberg, Bretagnon, and Francou 1992). Let us forget about the mass of the Earth and imagine a torque free gyroscope at the geocenter, moving along the actual trajectory of the geocenter. It will precess by this amount in our GCRS. Since the GCRS does not present a locally inertial reference system, Coriolis forces caused by geodesic precession-nutation appear in every GCRS dynamical equation of motion, e.g., of Earth's satellites. As recommended by the IERS (2004) these additional forces should be taken into account. Moreover, geodesic precession-nutation has to be considered in the precession-nutation model formulated in the GCRS. As long as observations of Earth's orientation parameters are referred to the GCRS they will contain geodesic precession-nutation automatically. Because of the eccentricity of the Earth orbit the leading term in $\mathbf{\Omega}_{\rm iner}$ has an annual and a semi-annual part that leads to geodesic nutation in longitude with

$$\Delta\psi_{\rm GP} = 0.153 \sin l' + 0.002 \sin 2l' \tag{2.54}$$

where the amplitudes are in mas and l' is the mean anomaly of the Earth-Moon barycenter (Fukushima 1991; Brumberg et al. 1992; Bois and Vokrouhlický 1995).

$W_{\rm tidal}$ is a generalization of the Newtonian tidal potential $\mathcal{U}_{\rm tidal}$ of Eq. 2.12. Full post-Newtonian expressions for $W_{\rm tidal}$ and $W^a_{\rm tidal}$ can be found in Damour, Soffel, and Xu (1992). There $W_{\rm ext}$ is denoted by $\overline{W}$ and a tidal expansion in powers of local spatial coordinates by means of suitably defined tidal moments is given in Eq. 4.15 of Damour, Soffel, and Xu (1992). Expressions for $W_{\rm tidal}$ and $W^a_{\rm tidal}$ in closed form are given in Klioner and Voinov (1993) (see also Klioner and Soffel 2000).

Finally, the local gravitational potentials W_E and W^a_E of the Earth are related to the barycentric gravitational potentials w_E and w^i_E by ($\delta^a_i = \delta^i_a = \delta_{ai}$)

$$\begin{aligned} w_E(t, \mathbf{x}) &= W_E(T, \mathbf{X}) \left(1 + \frac{2}{c^2}\, v_E^2\right) + \frac{4}{c^2}\, \delta_{ia} v^i_E\, W^a_E(T, \mathbf{X}) + \mathcal{O}(c^{-4}) \\ w^i_E(t, \mathbf{x}) &= \delta^i_a\, W^a_E(T, \mathbf{X}) + v^i_E\, W_E(T, \mathbf{X}) + \mathcal{O}(c^{-2}). \end{aligned} \tag{2.55}$$

The relations between the geocentric gravitational potentials W and W^a, and the barycentric ones w and w^i follow from the coordinate transformations between the BCRS and GCRS discussed below.

2.6.5 Coordinate Transformations

The metric tensors of the BCRS and GCRS allow one to derive the rules for the transformations between the BCRS coordinates, x^μ, and the GCRS ones, X^α. It is obvious that these transformations can be written in two equivalent forms: i) as $x^\mu(T, X^a)$ or ii) as $X^\alpha(t, x^i)$. Both forms can be found in the literature. It should be pointed out that the transformation from one version to the other is not so trivial, because of the barycentric coordinate position of the geocenter that appears in the first form as a function of Geocentric Coordinate Time (TCG) and as a function of Barycentric Coordinate Time (TCB) in the second one. Here $T = \mathrm{TCG}$ and X^a are presented as functions of $t = \mathrm{TCB}$ and x^i. The explicit form of this transformation can be found in Soffel et al. (2003) and in Resolution B1.3 itself (URL[2]). For the time transformation one finds

$$T = t - \frac{1}{c^2}[A(t) + v_E^i r_E^i] + \mathcal{O}(c^{-4}) \tag{2.56}$$

where $(\mathbf{r}_E = \mathbf{x} - \mathbf{x}_E)$

$$\frac{d}{dt}A(t) = \frac{1}{2}v_E^2 + w_{\mathrm{ext}}(\mathbf{x_E}). \tag{2.57}$$

Here x_E^i and v_E^i are the barycentric position and velocity vectors of the Earth, and the external potential, w_{ext}, is given by Eq. 2.53.

2.6.6 Relativistic Potential Coefficients

For many problems it is advantageous to present the local gravitational potentials of the Earth as multipole series that usually converge everywhere outside the Earth. To this end one has to introduce a certain set of multipole moments or *potential coefficients* for the Earth. A certain set of potential coefficients, called Blanchet-Damour (BD) moments (Blanchet and Damour 1989; Damour, Soffel, and Xu 1991) defined to first post-Newtonian order has especially attractive features. Moreover, by using such Blanchet-Damour moments we get a very simple form of the multipole expansion of the post-Newtonian potentials. Basically two sets of BD moments occur in the formalism: mass multipole moments and spin multipole moments. Theoretically these moments can be derived from the distribution of mass and matter currents inside the body (Blanchet and Damour 1989; Damour, Soffel, and Xu 1991), but for an observer they simply present parameters which can be directly estimated from observations.

In Soffel et al. (2003) it is shown that the metric potential $W_E(T, \mathbf{X})$ outside the Earth can be written as

$$W_E(T, \mathbf{X}) = \frac{GM_E}{R}\left[1 + \sum_{l=2}^{\infty}\sum_{m=0}^{l}\left(\frac{R_E}{R}\right)^l P_{lm}(\cos\theta)(C_{lm}\cos m\phi + S_{lm}\sin m\phi)\right]. \tag{2.58}$$

Here, M_E is the mass of the Earth, defined to post-Newtonian order, R_E some suitably chosen Earth's radius and (C_{lm}, S_{lm}) are the post-Newtonian Blanchet-Damour potential coefficients of the Earth. The $l = 1$ term is missing in Eq. (2.58) because the origin of the GCRS is assumed to coincide with the Earth's center of mass. To derive this relation certain approximations related with the shape of the Earth have been made that are explained in Soffel et al. (2003), but, nevertheless, it is valid to post-Newtonian accuracy. Note that formally this expression for W_E in Eq. 2.58 agrees with that for the Newtonian potential of the Earth in Eq. 2.7, showing the great simplicity of the formalism in virtue of the way of writing the metric tensor and of using the Blanchet-Damour multipole moments. In Soffel et al. (2003) it was also demonstrated that the gravitomagnetic vector potential resulting from the motion of the various material elements of the Earth in the GCRS can be written in the form

$$W_E^a(T, \mathbf{X}) = -\frac{G}{2}\frac{(\mathbf{X} \times \mathbf{S}_E)^a}{R^3} \tag{2.59}$$

where $\mathbf{S}_E$ is the total angular momentum vector of the Earth, that here is needed only to Newtonian accuracy. Higher order spin moments of the Earth have been neglected in this expression that can be found in many standard textbooks on GRT (Weinberg 1972; Will 1993). W_E^a is usually related with Lense-Thirring effects resulting from the Earth's rotational motion.

2.7 Applications

2.7.1 Other Versions of the Geocentric Celestial Reference System

The technique developed to construct the GCRS can be directly applied for other purposes if other bodies are taken as central bodies instead of the Earth.

If the whole solar system is considered as such a central body and if the gravitational field of other bodies in the Galaxy are taken into account, the technique used in the GCRS allows one to construct a reference system for the whole solar system (a version of the BCRS) with external gravitational fields explicitly taken into account. As was discussed above, in this case the external gravitational fields due to the Galaxy are tidal fields. One can estimate the magnitude of accelerations and other effects due to these tidal forces and find them to be negligible for the current level of accuracy. It is, therefore, one more argument for the BCRS in the form discussed above.

A GCRS-like reference system can be constructed not only for the Earth, but for any other body of the solar system. Such a reference system for the Moon is used to model the rotational motion of the Moon as well as to model the LLR data. One can expect that GCRS-like reference systems for Mars and Mercury will be used soon to study the rotational motion and physics of these planets. Also for other bodies such reference systems will be of importance. For example, the gravitational fields of all bodies are defined by Eq. 2.58 defined in the corresponding reference system.

Finally, considering an observer as the central body for a GCRS-like reference system one immediately gets a reference system which can be directly used for modelling of any sort of observables as seen by the observer or to study the local physical phenomena in the immediate vicinity of that observer (e.g., attitude of a spacecraft). Usually, one can neglect

the mass of the observer and this simplifies the formulae for the GCRS-like metric tensor since the internal potentials (denoted by W_E and W_E^a in the GCRS) vanish. On the other side the inertial potentials (Eq. 2.50) may become much larger than for the GCRS. For example, for an observer on the surface of the Earth one has $|Q_a| \approx 9.81\,\mathrm{m/s^2}$. At the origin of the GCRS-like reference system of an observer, its coordinate time coincides with the proper time of that observer. Moreover, the coordinate basis of the GCRS-like system at its origin represents a kinematically non-rotating tetrad. The latter is the standard tool to convert coordinate-dependent quantities into coordinate-independent observables in General Relativity; see Klioner (2004) for a detailed discussion.

Let us also note that the BCRS and GCRS are given by the IAU Resolutions in the framework of General Relativity. Variants of these reference systems in the framework of the PPN formalism are discussed in Will (1993); Klioner and Soffel (2000); Klioner (2004); Kopeikin and Vlasov (2004).

2.7.2 Rotating Reference Systems

Another important variant of a GCRS-like reference system is a local reference system rotating with respect to the corresponding celestial (i.e., non-rotating) reference system. Such a rotating reference system with coordinates $(\overline{T}, \overline{X}^a)$ is defined from the GCRS-like (kinematically non-rotating) reference system by the following transformations:

$$\begin{aligned} \overline{T} &= T \\ \overline{X}^b &= P^{ab}(T)\, X^b \end{aligned} \tag{2.60}$$

where $P^{ab}(T)$ is an arbitrary time-dependent orthogonal matrix. Matrix P^{ab} defines a rotation of spatial coordinates $\overline{X}^a$ with respect to the kinematically non-rotating coordinates X^a. Such rotating reference systems can be used to separate the dynamics of the central body into a *rotation* and a *deformation*. Thus, for the Earth the rotating coordinates of this kind provide a relativistic model for ITRS/ITRF. The matrix in this case represents the rotation between GCRS and ITRS and describes precession, nutation, and polar motion. The same sort of coordinates can be used for other planets and for, e.g., spacecrafts. In all cases the matrices P represent a relativistically meaningful way to describe the attitude of the central body with respect to the kinematically non-rotating GCRS-like coordinates.

2.7.3 The Einstein-Infeld-Hoffmann Equations of Motion

In the gravitational N-body problem the potential coefficients of a body A are defined in its corresponding local reference system (analogous to the GCRS for the Earth). For many applications it is sufficient to keep only the mass monopoles of the solar system bodies. If we go into the local system of body A with coordinates $X_A^\alpha = (cT_A, \mathbf{X}_A)$,

$$W_A = \frac{GM_A}{R}, \qquad W_A^a = 0 \tag{2.61}$$

where $R = |\mathbf{X}_A|$. Note that this expression for W_A looks perfectly Newtonian though M_A is defined to post-Newtonian order.

From the transformation rules for the metric potentials of Eq. 2.55, and formula 2.46, one derives the metric in the barycentric coordinate system in the form of Eq. 2.38 with

$$w = \sum_A \frac{GM_A}{r_A} - \frac{1}{c^2}\sum_A \Delta_A(t, \mathbf{x}) \tag{2.62}$$

with ($\mathbf{r}_{BA} = \mathbf{x}_B - \mathbf{x}_A$ and $\mathbf{a}_A = d\mathbf{v}_A/dt$)

$$\begin{aligned}\Delta_A(t, \mathbf{x}) &= \frac{GM_A}{r_A}\left(-\frac{3}{2}v_A^2 + \sum_{B\neq A}\frac{GM_B}{r_{BA}}\right) - \frac{1}{2}GM_A\, r_{A,tt} \\ &= \frac{GM_A}{r_A}\left[-2v_A^2 + \sum_{B\neq A}\frac{GM_B}{r_{BA}} + \frac{1}{2}\left(\frac{(r_A^k v_A^k)^2}{r_A^2} + r_A^k a_A^k\right)\right].\end{aligned} \tag{2.63}$$

Furthermore, in our approximation

$$w^i(t, \mathbf{x}) = \sum_A \frac{GM_A}{r_A} v_A^i. \tag{2.64}$$

Note the remarkable fact that the post-Newtonian BCRS mass monopole metric with potentials given in Eqs. 2.62 and 2.64 has been derived from the GM_A/R potentials in the local system of body A by means of the transformation rules of Eq. 2.55.

From this metric the well-known Einstein-Infeld-Hoffmann equations of motion can be derived. In Damour, Soffel, and Xu (1991) it is shown that to post-Newtonian order every spherically symmetric body A follows a geodesic in the external metric given by w_{ext} and w^i_{ext} described by formula 2.46 where the potentials due to body A are excluded from the sums. These geodesic equations, the Einstein-Infeld-Hoffmann (EIH) equations, finally read:

$$\begin{aligned}\ddot{\mathbf{x}}_A = &-\sum_{B\neq A}\frac{GM_B}{r_{AB}^2}\mathbf{n}_{AB}\left[1 + \frac{1}{c^2}\left(\mathbf{v}_A^2 + 2\mathbf{v}_B^2 - 4\mathbf{v}_A\cdot\mathbf{v}_B - \frac{3}{2}(\mathbf{n}_{AB}\cdot\mathbf{v}_B)^2\right)\right. \\ &\left. -4\sum_{C\neq A}\frac{GM_C}{c^2 r_{AC}} - \sum_{C\neq B}\frac{GM_C}{c^2 r_{BC}}\left[1 + \frac{1}{2}\frac{r_{AB}}{r_{BC}}\mathbf{n}_{AB}\cdot\mathbf{n}_{CB}\right]\right] \\ &-\frac{7}{2}\sum_{B\neq A}\sum_{C\neq B}\mathbf{n}_{BC}\frac{G^2 M_B M_C}{c^2 r_{AB} r_{BC}^2} \\ &+\sum_{B\neq A}(\mathbf{v}_A - \mathbf{v}_B)\frac{GM_B}{c^2 r_{AB}^2}(4\mathbf{n}_{AB}\cdot\mathbf{v}_A - 3\mathbf{n}_{AB}\cdot\mathbf{v}_B).\end{aligned} \tag{2.65}$$

These EIH equations of motion are used to model the motion of our solar system and to form the basis of modern solar system ephemerides. They are also used for high-accuracy calculations of asteroid orbits.

2.7.4 Equations of Motion in the GCRS

The motion of artificial satellites is usually described in the GCRS with TCG or terrestrial time TT (see below) as the timescale. In the GCRS the equation of motion of a satellite is given by the geodesic equation in the GCRS metric, Eq. 2.47. The dominant relativistic acceleration results from the mass of the Earth. For this post-Newtonian Schwarzschild acceleration one considers

$$W_E(T, \mathbf{X}) = \frac{GM_E}{R}.$$

Without external contributions to the metric tensor (tidal and inertial terms) the geodesic equation takes the form

$$\frac{d^2X^a}{dT^2} = -\frac{GM_E X^a}{R^3} + \frac{GM_E}{c^2R^3}\left[\left(4\frac{GM_E}{R} - \mathbf{V}^2\right)X^a + 4(\mathbf{X}\cdot\mathbf{V})V^a\right] \qquad (2.66)$$

where $\mathbf{X}$ and $\mathbf{V}$ are the satellite position and velocity in GCRS coordinates. Other effects that should be taken into account in practical calculations are geodesic and Lense-Thirring precessions. The corresponding terms can be easily derived from the second equation in Eqs. 2.50 and 2.59, respectively. Detailed theoretical discussions of the equations of motion of Earth's satellites in the GCRS can be found in Damour, Soffel, and Xu (1994); Brumberg (1991); Klioner and Soffel (2000). Section 10.2 of IERS (2004) contains a practical approximation to these equations.

2.7.5 Astrometry

As indicated above the relativistic description of astrometric measurements proceeds in two steps: first one formulates a coordinate picture of the astrometric situation including the light source, the observer, and the light rays that propagate through the cosmos under the influence of various gravitational fields. In a second step the observables have to be calculated as explained in § 2.5. If the solar system is considered to be isolated, one forgets about the large-scale structure of the universe which for cosmological questions clearly is not justified. For cosmological problems one might use some metric averaged over a large cosmological volume so that it becomes homogeneous and isotropic like the Friedman-Robertson-Walker metric (e.g., Weinberg 1972) on large scales. However, the matching of such a cosmological metric to our BCRS metric still presents serious difficulties and this work is still in progress (Klioner and Soffel 2005).

For an isolated gravitational N-body system, the formulation of relativistic astrometry has evolved to μas precision. We will only consider the simplest case here.

As we have seen earlier light rays are null geodesics, i.e., curves $x^\mu(\lambda)$ satisfying the geodesic equation and the condition

$$g_{\mu\nu}\frac{dx^\mu}{d\lambda}\frac{dx^\nu}{d\lambda} = 0.$$

If the metric tensor $g_{\mu\nu}$ is fully specified, these equations can be solved for a mathematical description of light rays in the form $\mathbf{x}_\gamma(t)$ where coordinate time t serves as curve parameter. In the first post-Newtonian approximation one usually writes

$$\mathbf{x}_\gamma(t) = \mathbf{x}_N + \Delta\mathbf{x}_\gamma$$
$$\mathbf{x}_N = \mathbf{x}_0 + \boldsymbol{\sigma}\, c(t - t_0). \tag{2.67}$$

Here, $\mathbf{x}_N$ represents the unperturbed (*Newtonian*) trajectory of the light ray. We now consider the gravitational potential w to be generated by some 'roughly spherical' matter distribution. I.e., outside the matter we consider only the mass monopole M situated at the origin of our coordinates and write $w = GM/r$, where $r = |\mathbf{x}|$. Then to first post-Newtonian order the light ray equations are solved by

$$\Delta\mathbf{x}_\gamma(t) = -2m\left[\boldsymbol{\sigma}\ln\left(\frac{x_N + \mathbf{x}_N\cdot\boldsymbol{\sigma}}{x_0 + \mathbf{x}_0\cdot\boldsymbol{\sigma}}\right) + \frac{\mathbf{d}}{d^2}[r_N - r_0 + c(t - t_0)]\right] \tag{2.68}$$

where $x_N = |\mathbf{x}_N|$, $x_0 = |\mathbf{x}_0|$,

$$m \equiv \frac{GM}{c^2}$$

and $\mathbf{d}$ is the vector joining the center of the gravitating body and the point of closest approach of the unperturbed ray (Will 1993), and $d = |\mathbf{d}|$. The logarithmic term is in the direction of the unperturbed light ray; it describes the so-called gravitational time delay. Finally the last part, proportionally to $\mathbf{d}$, describes the gravitational light-deflection.

Let $\mathbf{n}$ be the unit coordinate direction of light propagation at the point of observation: $\mathbf{n} = \dot{\mathbf{x}}_\gamma/|\dot{\mathbf{x}}_\gamma|$. Then at the position $\mathbf{x}_{\rm obs}$ of observation one has (Klioner 2003):

$$\mathbf{n} = \boldsymbol{\sigma} - 2\,m\,\frac{\mathbf{d}}{d^2}\left(1 + \boldsymbol{\sigma}\cdot\frac{\mathbf{x}_{\rm obs}}{|\mathbf{x}_{\rm obs}|}\right). \tag{2.69}$$

These formulae give the main relativistic effect of light-deflection. The gravitational light-deflection due to the Sun amounts to $1''.75$ for a grazing ray, and attains 4 mas if the angular distance between the source and the Sun is 90°. The deflection due to Jupiter can be as large as 16 mas. Other effects include the influence of the quadrupole gravitational fields of giant planets (up to 240 μas) and higher-order Schwarzschild effects (up to about 16 μas). Furthermore, it is important to know that the motion of the deflecting body in the BCRS must also be taken into account, and that the position of the gravitating body should be calculated at the retarded moment t^* defined as

$$t^* = t_{\rm obs} - \frac{1}{c}\,|\mathbf{x}_\gamma(t_{\rm obs}) - \mathbf{x}_A(t^*)| \tag{2.70}$$

where $\mathbf{x}_A(t)$ is the BCRS position of the gravitating body as a function of time t (Kopeikin and Schäfer 1999). For a more exhaustive discussion of relativistic astrometry the reader is referred to Klioner (2003).

Currently in *The Astronomical Almanac*, geocentric positions (apparent places) are computed using deflection of light from the mass of the Sun, Jupiter, and Saturn. If the observer is not at the geocenter (e.g., for topocentric positions which may be available via *The Astronomical Almanac Online*), light-deflection due to the Earth is also included.

Let us consider a light ray propagating from point $\mathbf{x}_0$ to point $\mathbf{x}_1$. In the presence of a gravitational field the travel time $t_1 - t_0$ between these two points is slightly larger than the distance $R = |\mathbf{x}_1 - \mathbf{x}_0|$ divided by c. In the spherically symmetric gravitational field of a mass monopole one has

$$c\,(t_1 - t_0) = R + 2m\,\ln\frac{x_1 + x_0 + R}{x_1 + x_0 - R}. \tag{2.71}$$

This additional retardation in light propagation is called the Shapiro delay and can amount to 240 microseconds for observations of Venus in superior conjunction with the Sun.

2.7.6 VLBI Observations

The model of VLBI observations is one of the most complicated relativistic models. This model naturally combines quantities and parameters defined in the BCRS and the GCRS. The positions of observing stations and the corresponding baseline vectors are defined in the GCRS. Also in the GCRS one describes the rotational motion of the Earth. The coordinate transformation between BCRS and GCRS, as well the BCRS position of the geocenter, are then used to calculate the positions of observing station in the BCRS. The positions of the quasars are defined in the BCRS. Considering the light propagation between a given quasar and two observing stations, one calculates the difference in propagation time between these two light rays in coordinate time TCB. Then the derived coordinate time difference can be converted in any other coordinate time (e.g., TT). The details of the derivation of this model are rather complicated. A detailed practical summary is given in Section 11.1 of IERS (2004).

2.8 Relativistic Timescales, their Definitions and Units

2.8.1 Practical Transformations of Timescales

So far we have extensively discussed Geocentric Coordinate Time (TCG) and Barycentric Coordinate Time (TCB) as timescales of the GCRS and the BCRS, respectively. To sufficient accuracy the relation between these two timescales is given in IAU 2000 Resolution B1.5 (IAU 2001; URL[2]). This Resolution contains a slightly simplified version of the coordinate transformations between TCG and TCB that are given in Resolution B1.3. The transformation between TCG and TCB evaluated at the geocenter can be calculated by a numerical integration of the corresponding equations using a solar system ephemeris.

The relation between proper time τ of some observer with coordinates $\mathbf{x}_{\rm obs}(t)$ and $t = \mathrm{TCB}$ may be written in the form (Soffel et al. 2003)

$$\begin{aligned}\frac{d\tau}{d\mathrm{TCB}} &= 1 - \frac{1}{c^2}\left(w_0 + w_L + \frac{v^2}{2}\right)\\ &\quad + \frac{1}{c^4}\left(-\frac{1}{8}v^4 - \frac{3}{2}v^2 w_0 + 4v^i w^i + \frac{1}{2}w_0^2 + \Delta\right)\end{aligned} \tag{2.72}$$

where v^i is the BCRS coordinate velocity of the observer,

$$w_0 = \sum_A \frac{GM_A}{|\mathbf{x}_{\rm obs} - \mathbf{x}_A|} \tag{2.73}$$

w_L contains contributions from higher potential coefficients, and $\Delta \equiv \sum_A \Delta_A$ with Δ_A being given by Eq. 2.63. The uncertainty of relations in Resolution B1.5 and Eq. 2.72 is less than 5×10^{-18} in rate.

For some clock in the vicinity of the Earth the relation between its proper time τ and TCG can be obtained from Eq. 2.21 and the GCRS metric Eq. 2.47. At the indicated level of accuracy the contributions from W^2, W^a, and W_{iner} can be neglected (Soffel et al. 2003).

2.8.2 Scaled Coordinate Timescales

Resolutions IAU 1991 A4 and IAU 2000 B1.3 have defined TCB and TCG as the time coordinates of the BCRS and GCRS, respectively, and IAU Resolution B3 (Note 6) has encouraged the use of TCB for solar system ephemerides. From the considerations of practical convenience one often uses two additional timescales, TT and TDB. The reasons for and the mathematical details of the relativistic scaling of BCRS and GCRS, and in particular their coordinate times, are summarized, e.g., by Klioner (2008). TT and TDB are conventional linear functions of TCG and TCB, respectively. The definition of TT is given by IAU 2000 Resolution B1.9 and IAU 1991 Resolution A4 as

$$\mathrm{TT} = F_G\,\mathrm{TCG} \tag{2.74}$$

where $F_G = 1 - L_G$, and $L_G = 6.969290134 \times 10^{-10}$ is a defining constant. TDB is defined in IAU 2006 Resolution 3 by its conventional relation to TCB:

$$\mathrm{TDB} = F_B\,\mathrm{TCB} + \mathrm{TDB}_0 \tag{2.75}$$

where $F_B = 1 - L_B$, and $L_B = 1.550519768 \times 10^{-8}$ and $\mathrm{TDB}_0 = -6.55 \times 10^{-5}$ s are defining constants. In Eqs. 2.74 and 2.75 TT, TCG, TCB and TDB should be expressed by the corresponding Julian dates reckoned from $\mathrm{T}_0 = 2443144.500372$ that stands for the event 1977 January 1 00h 00m 00s TAI at the geocenter. Many of the defining constants, including L_B and L_G, are given annually in Section K (Tables and Data) of *The Astronomical Almanac*.

The slopes F_G and F_B of both linear functions have the same purpose: both TT and TDB should show no linear drift with respect to proper times of observers situated on the rotating geoid. Since this requirement depends on our model of the solar system (i.e., on a planetary ephemeris and on a number of astronomical and geodesic constants), it cannot be satisfied exactly. Therefore, some conventional constants have been chosen in the definitions of TT and TDB so that the requirement is satisfied approximately, but with an accuracy totally sufficient for practical purposes. Similarly, the constant TDB_0 was chosen merely to keep TDB − TT approximately centered on zero.

International Atomic Time (TAI) is a physical realization of TT with a shift of −32.184 s for historical reasons. Therefore, TAI is a realization of coordinate time "TT−32.184 s". The difference between TAI and an ideal realization of "TT−32.184 s" is only due to imperfections of the participating clocks and the clock synchronization procedures.

Finally, the timescale T_{eph} has been introduced by Standish (1998) to mean the time coordinate used in Jet Propulsion Laboratory's DE/LE ephemerides (for more, see Chapter 8 of this publication). Although T_{eph} is defined as a linear function of TCB, with the slope depending on the ephemeris, in practice T_{eph} was defined by a fixed relation to TT (by the formulae of Moyer (1981) or Fairhead and Bretagnon (1990)). For practical purposes TDB,

as defined by Eq. 2.75 for the JPL ephemeris DE405, agrees with T_{eph}. In the near future each new solar system ephemeris will include the TDB − TT transformation at the geocenter, thus becoming 4-dimensional as it is naturally required by the theory of relativity (Fienga et al. 2009).

2.8.3 Units of Timescales

There has been a long debate of the question of time units. The basic unit is the SI second:

> *the second is the duration of* 9 192 631 770 *periods of the radiation corresponding to the transition between the two hyperfine levels of the ground state of the cesium atom.*

This definition contains no indication of any specific location, gravitational potential, or state of motion of the observer realizing the SI second. Thus, this definition is merely a recipe for how some observer can realize the SI second. The SI second is the natural unit for proper time. Via the theoretical relation between proper time of some (idealized) clock and the coordinates of a reference system, the unit for proper time (the SI second) is naturally induced as a canonical unit for any other timescale, as long as there is a direct relation to proper time and no explicit rescaling of units.

From the metrological point of view, the theoretical relations between proper time and the coordinate times are relations between quantities and are independent of the choice of units. The same is true for the theoretical relations between different coordinate timescales themselves. This means that basically any units can be used to convert these quantities into numerical values. The SI second is the canonical unit for proper time of some observer. If a theoretical formula relating the proper time and a coordinate time is used to compute the values of the corresponding coordinate time starting from the values of proper time in SI seconds, the resulting values of coordinate time will also be expressed in terms of SI seconds.

If one consider the timescales TT and TDB, two standpoints might be taken. One possible standpoint is that using TT and TDB is nothing but a rescaling of the TCG or TCB time unit, respectively. However, this standpoint easily leads to confusions and possible mistakes. For example, in this case one cannot consider TAI and TT as expressed in the seconds of SI. For these reasons it is logical to avoid notations such as "TDB units" ("TDB seconds/meters"), "TT units" ("TT seconds/meters"), and avoid contrasting these terms with "SI units" ("SI seconds/meters"). It is straightforward to interpret TT and TDB as being evolved from a coordinate transformation of TCG and TCB, respectively. In this way, the SI second is the only unit for any timescale. If TT or TDB are used as basic timescales in dynamical equations, then either the conversion parameters F_G and F_B have to be included in the equations of motion explicitly, or TT-compatible and TDB-compatible values for dimensional quantities (e.g., mass parameters $\mu = GM$ of celestial bodies) have to be considered. In general, all quantities intended for use with timescale xxx should be called xxx-compatible (xxx being TT, TDB, TCG or TCB). Moreover, numerical values of all such quantities (called xxx-compatible values) should be considered to be expressed in the usual units of the SI. More details on this subject and formal nomenclature can be found in Klioner (2008) and Klioner et al. (2009).

REFERENCES

1. The Astronomical Almanac Online:
http://asa.usno.navy.mil or http://asa.hmnao.com.

2. IAU Resolutions Adopted by the General Assemblies:
http://www.iau.org/administration/resolutions/general_assemblies/.

Bertotti, B., L. Iess, and P. Tortora (2003). A test of general relativity using radio links with the Cassini spacecraft. *Nature 425*, 374–376.

Blanchet, L. and T. Damour (1989). Post-Newtonian generation of gravitational waves. *Annales de L'Institut Henri Poincare Section Physique Theorique 50*, 377–408.

Bois, E. and D. Vokrouhlický (1995). Relativistic spin effects in the Earth-Moon system. *Astronomy and Astrophysics 300*, 559.

Brumberg, V. A. (1991). *Essential Relativistic Celestial Mechanics*. Bristol: A. Hilder.

Brumberg, V. A., P. Bretagnon, and G. Francou (1992). Analytical algorithms of relativistic reduction of astronomical observations. In N. Capitaine (Ed.), *Les Journées 1991*, pp. 141–148. Paris: Observatoire de Paris.

Brumberg, V. A. and S. M. Kopeikin (1989). Relativistic Theory of Celestial Reference Frames. In J. Kovalevsky et al. (Eds.), *Reference Frames*, pp. 115. Dordrecht, Holland: Kluwer.

Damour, T., M. Soffel, and C. Xu (1991). General-relativistic celestial mechanics. I. Method and definition of reference systems. *Physcial Review D 43*(10), 3273–3307.

Damour, T., M. Soffel, and C. Xu (1992). General-relativistic celestial mechanics. II. Translational equations of motion. *Physcial Review D 45*(4), 1017–1044.

Damour, T., M. Soffel, and C. Xu (1993). General-relativistic celestial mechanics. III. Rotational equations of motion. *Physcial Review D 47*(8), 3124–3135.

Damour, T., M. Soffel, and C. Xu (1994). General-relativistic celestial mechanics. IV. Theory of satellite motion. *Physcial Review D 49*(2), 618–635.

Eubanks, T. M., D. N. Matsakis, J. O. Martin, B. A. Archinal, D. D. McCarthy, S. A. Klioner, S. Shapiro, and I. I. Shapiro (1997). Advances in Solar System Tests of Gravity. *APS Meeting Abstracts*, K11.05.

Fairhead, L. and P. Bretagnon (1990). An analytical formula for the time transformation TB-TT. *Astronomy and Astrophysics 229*, 240–247.

Fienga, A., J. Laskar, T. Morley, H. Manche, P. Kuchynka, C. Le Poncin-Lafitte, F. Budnik, M. Gastineau, and L. Somenzi (2009). INPOP08, a 4-D planetary ephemeris: From asteroid and time-scale computations to ESA Mars Express and Venus Express contributions. *Astronomy and Astrophysics 507*, 1675–1686.

Fock, V. A. (1959). *The Theory of Space, Time and Gravitation*. Oxford: Pergamon. Translated into English from *Teoriya prostranstva vremeni i tyagoteniya*, 1955, Fizmazgiz, Moscow.

Froeschlé, M., F. Mignard, and F. Arenou (1997). Determination of the PPN Parameter γ with the Hipparcos Data. In *Proceedings of the ESA Symposium "Hipparcos - Venice 97", 13-16 May 1997, Venice, Italy*, Volume SP-402, pp. 49. ESA.

Fukushima, T. (1991). Geodesic nutation. *Astronomy and Astrophysics 244*, L11.

IAU (2001). In H. Rickman (Ed.), *Transactions of the International Astronomical Union*, Volume XXIV B, San Francisco. Astronomical Society of the Pacific. Proc. 24th General Assembly, Manchester, 2000.

IAU (2007). In O. Engvold (Ed.), *Transactions of the International Astronomical Union*, Volume XXV B, San Francisco. Astronomical Society of the Pacific. Proc. 25th General Assembly, Sydney, 2003.

IERS (2004). Conventions (2003). Technical Note 32, International Earth Rotation Service, Frankfurt am Main. Verlag des Bundsesamts für Kartographie und Geodäsie, D. D. McCarthy and G. Petit (Eds.).

Klioner, S., N. Capitaine, W. Folkner, B. Guinot, T. Y. Huang, S. Kopeikin, G. Petit, E. Pitjeva, P. K. Seidelmann, and M. Soffel (2009). Units of Relativistic Time Scales and Associated Quantities. In S. Kioner, P. K. Seidelmann, and M. Soffel (Eds.), *Proceedings of IAU Symposium 261. Relativity in Fundamental Astronomy: Dynamics, Reference Frames, and Data Analysis*, pp. 79. Cambridge University Press.

Klioner, S. A. (1992). The problem of clock synchronization - A relativistic approach. *Celestial Mechanics and Dynamical Astronomy 53*, 81–109.

Klioner, S. A. (2003). A Practical Relativistic Model for Microarcsecond Astrometry in Space. *Astronomical Journal 125*, 1580–1597.

Klioner, S. A. (2004). Physically adequate proper reference system of a test observer and relativistic description of the GAIA attitude. *Physcial Review D 69*(12), 124001.

Klioner, S. A. (2008). Relativistic scaling of astronomical quantities and the system of astronomical units. *Astronomy and Astrophysics 478*(3), 951–958.

Klioner, S. A. and M. Soffel (1998). Nonrotating astronomical relativistic reference frames. *Astronomy and Astrophysics 334*, 1123–1135.

Klioner, S. A. and M. Soffel (2000). Relativistic celestial mechanics with PPN parameters. *Physcial Review D 62*(2), ID 024019.

Klioner, S. A. and M. Soffel (2005). Refining the Relativistic Model for Gaia: Cosmological Effects in the BCRS. In C. Turon, K. S. O'Flaherty, and M. A. C. Perryman (Eds.), *The Three-Dimensional Universe with Gaia: Proceedings of the GAIA meeting 4-7 October 2004, Paris*, Volume SP-576, pp. 305. ESA.

Klioner, S. A. and A. V. Voinov (1993). Relativistic theory of astronomical reference systems in closed form. *Physcial Review D 48*, 1451–1461.

Kopeikin, S. M. and G. Schäfer (1999). Lorentz covariant theory of light propagation in gravitational fields of arbitrary-moving bodies. *Physcial Review D 60*(12), 124002.

Kopeikin, S. M. and I. Vlasov (2004). Parametrized post-Newtonian theory of reference frames, multipolar expansions and equations of motion in the N-body problem. *Physics Reports 400*(4-6), 209–318.

Lebach, D. E., B. E. Corey, S. I. I., M. I. Ratner, J. C. Webber, A. E. E. Rogers, J. L. Davis, and T. A. Herring (1995). Measurement of the Solar Gravitational Deflection of Radio Waves Using Very-Long-Baseline Interferometry. *Physical Review Letters 75*(8), 1439–1442.

Lemonde, P., P. Laurent, G. Santarelli, M. Abgrall, Y. Sortais, S. Bize, C. Nicolas, S. Zhang, A. Clairon, N. Dimarcq, P. Petit, A. G. Mann, A. N. Luiten, S. Chang, and C. Salomon (2001). Cold-Atom Clocks on Earth and in Space. In A. N. Luiten (Ed.), *Frequency Measurement and Control*, pp. 131–153. Springer.

Misner, C., K. Thorne, and J. A. Wheeler (1973). *Gravitation*. San Francisco: Freeman.

Moyer, T. D. (1981). Transformation from Proper Time on Earth to Coordinate Time in Solar System Barycentric Space-Time Frame of Reference, Parts I and II. *Celestial Mechanics and Dynamical Astronomy 23*(1), 33 & 68.

Müller, J., M. Soffel, and S. A. Klioner (2008). Geodesy and relativity. *Journal of Geodesy 82*, 133–145.

Soffel, M. (1989). *Relativity in Astrometry, Celestial Mechanics and Geodesy*. Berlin: Springer.

Soffel, M., S. A. Klioner, G. Petit, P. Wolf, S. M. Kopeikin, P. Bretagnon, V. A. Brumberg, N. Capitaine, T. Damour, T. Fukushima, B. Guinot, T. Huang, L. Lindegren, C. Ma, K. Nordtvedt, J. C. Ries, P. K. Seidelmann, D. Vokrouhlický, C. M. Will, and C. Xu (2003). The IAU 2000 Resolutions for Astrometry, Celestial Mechanics, and Metrology in the Relativistic Framework: Explanatory Supplement. *Astronomical Journal 126*, 2687–2706.

Standish, M. (1998). Time scales in the JPL and CfA ephemerides. *Astronomy and Astrophysics 336*, 381–384.

Weinberg, S. (1972). *Gravitation and Cosmology: Principles and Applications of the General Theory of Relativity*. New York: J. Wiley & Sons.

Will, C. M. (1993). *Theory and Experiment in Gravitational Physics*. Cambridge: Cambridge University Press.

Wolf, P. and G. Petit (1995). Relativistic theory for clock syntonization and the realization of geocentric coordinate times. *Astronomy and Astrophysics 304*, 653–661.

CHAPTER 3

Time

D. McCARTHY & B. GUINOT

3.1 Introduction

Measurement of time requires knowledge of an observable, repeatable phenomenon and a conventional reference by which the changes in the repeatable phenomenon can be described. The rotation of the Earth, for example, has been used throughout history as a convenient measure of time where the repeatable phenomenon is the daily repetition of sunrise or sunset. A number of conventional dating and timing systems have been used to distinguish epochs depending on cultural preferences.

Common civil or technical timescales in modern times have made use of three types of repeatable phenomena. These are (1) the Earth's rotation, (2) the revolution of the Earth around the Sun, and (3) atomic energy level transitions. Each of these processes has provided a variety of timescales that have been used to meet particular user applications. The conventional units of time (i.e., days, hours, minutes, seconds) are defined in each of these systems, but because the underlying phenomena are not equivalent, each of these units is of different length. The length of the second currently accepted as the international standard in the International System of Units (SI) is defined as the duration of 9 192 631 770 periods of the radiation corresponding to the transition between the two hyperfine levels of the ground state of the caesium 133 atom, and is referred to as the SI second (BIPM 2006). Units of time in this chapter correspond to the SI definition of the second unless otherwise stated. The historical development of time keeping is outlined in *Explanatory Supplement to the Astronomical Almanac* (1992). More information on Time is given in McCarthy and Seidelmann (2009).

3.1.1 Absolute (or Newtonian) Time

Absolute time is conceptually a unique uniform time valid for the whole universe to be used in the expression of the laws of physics and in particular of Newtonian mechanics. The increasing accuracy of measurements led progressively, during the 20th century, to the adoption of Special Relativity and General Relativity, and to the introduction of the notions of *proper time* and *coordinate time* (see § 3.1.2 and § 3.1.3). The relativistic theories are applied in such a way that the Newtonian theory remains a good approximation, but Newtonian time is not used in *The Astronomical Almanac*.

3.1.2 Proper Time

In the theory of General Relativity, proper time is the time measured along the trajectory of an observer in space-time (*world line*). Proper time is invariant in any coordinate change. In

practice, it is measured by a physical clock accompanying the observer. This clock should be insensitive to environmental conditions, including gravity or other types of acceleration. These conditions are fulfilled to a high level of accuracy by atomic clocks. The use of proper time keeps the laws of local physics and the physical constants involved invariant. Proper time, which may also be called *clock time* or *process time* (although this terminology is not used in *The Astronomical Almanac*), cannot be used for modeling phenomena in extended domains such as those encountered in astronomy. In these domains the time dimension is described by *coordinate time*.

3.1.3 Coordinate Time

In the context of General Relativity, a four-dimensional space-time reference system is described by four coordinates among which three are the spatial coordinates and the other is $x_0 = ct$, where c is the velocity of light in vacuum and t is the *coordinate time* in this reference system. Coordinate time provides an unambiguous way of dating events in a specified reference system. It is the time basis (or coordinate) to be used in the theory of motion referred to this system. The relation of the proper time of an observer to the coordinate time is provided by a *metric*, which takes into account the observer's motion in space-time and the surrounding masses and energy.

3.2 Time and the Earth's Rotation

The rotation of the Earth has long served as the basis for timekeeping. Practical measurement of time using the Earth's rotation depends on determining the relationship between a reference direction defined in a rotating terrestrial reference system with respect to a reference direction defined in the celestial reference system.

The transformation from the terrestrial reference system (TRS) to the celestial reference system (CRS) at epoch t can be written as

$$[\text{CRS}] = \mathbf{Q}(t)\ \mathbf{R}(t)\ \mathbf{W}(t)\ [\text{TRS}] \tag{3.1}$$

where $\mathbf{Q}(t)$, $\mathbf{R}(t)$, and $\mathbf{W}(t)$ are the transformation matrices arising from the motion of the celestial pole in the celestial system, the rotation of the Earth, and the motion of the pole in the terrestrial system, respectively.

Two equivalent procedures were provided in IERS (1996) to transform from the TRS to the CRS. The equinox-based procedure, described as option 1, makes use of the equinox to realize the intermediate reference frame of epoch t. Greenwich Sidereal Time (GST) is used in the transformation matrix $\mathbf{R}(t)$ and the classical precession and nutation parameters in the transformation matrix $\mathbf{Q}(t)$. The second procedure, described as option 2, makes use of the *Earth Rotation Angle* (θ) between the non-rotating origins (Guinot 1979; Capitaine 2000) defining the Celestial Intermediate Origin (CIO) and the Terrestrial Intermediate Origin (TIO) to realize the intermediate reference frame of epoch t. In this procedure the transformation matrix $\mathbf{R}(t)$ is

$$\mathbf{R}(t) = \mathbf{R_3}(-\theta) \tag{3.2}$$

where $\mathbf{R_3}$ represents a rotation about the z-axis.

Only the second procedure complies with Resolution B1.8, adopted by the XXIVth General Assembly of the International Astronomical Union (IAU 2001; URL[6]), which recommends the use of the *non-rotating origin* both in the CRS and the TRS as well as the position of the Celestial Intermediate Pole (CIP) in the CRS and in the TRS (IERS 2004). In practice, both methods will give equal results. The CIO-based method was implemented in *The Astronomical Almanac* beginning with the 2006 edition.

The Earth's rotation can be described either with respect to the Sun or with respect to a reference frame defined by directions to celestial objects. The two are not equivalent since the orbital motion of the Earth causes the apparent direction to the Sun to move with respect to the celestial reference frame. Time reckoned with respect to the Sun is now designated by a set of timescales and called Universal Time. Time reckoned with respect to the celestial reference frame attached to the equinox is called sidereal time. Because the Earth's rotational speed is not constant, the units of timescales based on the Earth's rotation vary with time.

There are three general kinds of variation in the Earth's rotation (Nelson et al. 2001). These are (1) a steady deceleration, (2) random fluctuations, and (3) periodic changes. Analyses of solar eclipses (Stephenson and Morrison 1984, 1995) show that the long-term average rate of increase in the length of the day is about 1.7 ms per century. Energy dissipation by tidal friction corresponds to a rate of increase in the length of day of 2.3 ms per century. To account for the observed deceleration, there must also be a component in the opposite direction acting to decrease the length of day by about 0.6 ms per century, which is possibly associated with changes in the figure of the Earth caused by post-glacial rebound (Yoder et al. 1983) or with deep ocean dissipation (Egbert and Ray 2000).

In addition to this steady decrease in the rotational velocity, the Earth's rotation is subject to apparently random changes (Jones 1949; Brouwer 1952). These were first observed directly using atomic clocks in the mid-1950s (Essen et al. 1958). They generate fluctuations in time of a few seconds over periods of a few decades. These changes are probably due to the interaction of the core and mantle of the Earth. There are also periodic seasonal variations caused principally by meteorological effects and periodic variations caused by luni-solar tides. The seasonal variation in the length of the day is of the order of 0.5 ms (Munk and MacDonald 1975; Lambeck 1980).

3.2.1 Sidereal Time

Until the introduction of the CIO-based system (IAU 2001) by the IAU in 2000, sidereal time was primarily used to compute hour angles. Now hour angles can be obtained by use of the Earth Rotation Angle θ, as shown in § 3.2.1.3. Sidereal Time has been defined previously in the *Explanatory Supplement* (1992), p. 3 in the equinox-based system as "the hour angle of the catalog equinox." On p. 48 it is defined:

> "In general terms, sidereal time is the hour angle of the vernal equinox, which is also known as the first point of Aries."

It goes on to distinguish

> "The sidereal time measured by the hour angle of the true equinox—i.e., the intersection of the true equator of date with the ecliptic of date—is *apparent sidereal time*."

and

> "The time measured by the diurnal motion of the mean equinox of date, which is affected by only the secular inequalities due to the precession of the axis, is *mean sidereal time*. Apparent sidereal time minus mean sidereal time is the equation of the equinoxes."

Despite possible confusion about "catalog" versus "vernal equinox" these definitions represent the traditionally accepted definitions of sidereal time.

The sidereal day is the time interval between successive transits of the equinox implicitly defined by the conventionally adopted precession-nutation model; it is approximately equal to 86 164.0905 SI seconds. It represents the Earth's rotation with respect to the Celestial Intermediate Reference System, i.e., the geocentric reference system related to the Geocentric Celestial Reference System by a time-dependent rotation taking precession-nutation into account. Because of precession, the sidereal day is not equivalent to the period of rotation of the Earth in inertial space. It is about 0.0084s shorter than the actual rotation period, which is approximately 86 164.0989 mean solar seconds.

3.2.1.1 Calculating Sidereal Time with IAU 2000A Nutation and IAU 2006 Precession

The relationship between Greenwich Sidereal Time (GST) and the Earth Rotation Angle (θ) is described in IERS (2004). The term *Greenwich Sidereal Time* refers to the sidereal time measured at those locations with terrestrial longitude of 0°. These locations may be considered to be on the *Greenwich meridian* but this term is loosely defined. The numerical expression consistent with the IAU 2000A nutation (IAU 2001, res. B1.6; URL[6]) and IAU 2006 precession models (IAU 2008, res. B1; URL[6]) was obtained following a procedure ensuring consistency at the microarcsecond level with the previous expression as well as continuity in UT1 at the date of change on 1 January 2003 (Capitaine, Wallace, and McCarthy 2003). The numerical expression for Greenwich Sidereal Time can be split into two components.

The first component is the Earth Rotation Angle defined by its relationship to UT1 = UTC + (UT1 − UTC),

$$\theta(t_U) = 2\pi\,(0.779\,057\,273\,2640 + 1.002\,737\,811\,911\,354\,48\,t_U) \tag{3.3}$$

where t_U is the Julian UT1 date−2451545.0. The second component is the equation of the origins, E_0, which equals the accumulated precession-nutation of the equinox in right ascension. It is made up of two subcomponents: a portion, E_{prec}, representing the accumulated precession, and the equation of the equinoxes, $E_e(t)$, representing the accumulated nutation. Thus, $E_0(t) = E_{\text{prec}}(t) - E_e(t)$. The precession portion is given in units of arcseconds by

$$\begin{aligned} E_{\text{prec}}(t) = {} & -0.''0145\,06 - 4612.''156\,534\,t - 1.''391\,5817\,t^2 \\ & + 0.''000\,000\,44\,t^3 + 0.''000\,029\,956\,t^4 \end{aligned} \tag{3.4}$$

where t is measured in the terrestrial timescale (TT; see § 3.4.2), in Julian centuries of 36525 days, from JD 245 1545.0 at 12h TT. The equation of the equinoxes, in arcseconds, is given by

$$\begin{aligned} E_e(t) = \Delta\psi \cos\varepsilon_A \\ &+ 0.002\,640\,96 \sin(\Omega) \\ &+ 0.000\,063\,52 \sin(2\Omega) \\ &+ 0.000\,011\,75 \sin(2F - 2D + 3\Omega) \\ &+ 0.000\,011\,21 \sin(2F - 2D + \Omega) \\ &- 0.000\,004\,55 \sin(2F - 2D + 2\Omega) \\ &+ 0.000\,002\,02 \sin(2F + 3\Omega) \\ &+ 0.000\,001\,98 \sin(2F + \Omega) \\ &- 0.000\,001\,72 \sin(3\Omega) \\ &- 0.000\,000\,87\, t \sin(\Omega) \end{aligned} \tag{3.5}$$

where $\Delta\psi$ is the nutation in longitude, ε_A is the obliquity referred to the ecliptic of date, F, D, and Ω are fundamental luni-solar arguments. Greenwich Sidereal Time is then given by

$$\mathrm{GST}(t_U, t) = \theta(t_U) - E_0(t). \tag{3.6}$$

This is often referred to as Greenwich Apparent Sidereal Time (GAST). Greenwich Mean Sidereal Time (GMST), then, is given by

$$\mathrm{GMST}(t_U, t) = \theta(t_U) - E_{\mathrm{prec}}(t). \tag{3.7}$$

So that

$$\mathrm{GST}(t_U, t) = \mathrm{GMST}(t_U) + E_e(t). \tag{3.8}$$

Daily tabulations of Greenwich mean and apparent sidereal time, nutation in longitude, and obliquity referred to the ecliptic are provided in *The Astronomical Almanac*; also included are examples of computing local sidereal time. The expressions for GST and GMST distinguish between θ, expressed as a function of Universal Time, and the accumulated precession-nutation in right ascension, which is expressed as a function of Terrestrial Time (TT) (see § 3.4.2). The expression for Greenwich Mean Sidereal Time (GMST) of Aoki et al. (1982) that was adopted previously used only Universal Time (UT1), giving rise to an additional difference dGMST of (TT−UT1) multiplied by the speed of precession in right ascension. If TT−TAI = 32.184 s (see § 3.4.2), this is given by:

$$d\mathrm{GMST} = 47\mu\mathrm{as} + 1.5\mu\mathrm{as}\ (\mathrm{TAI} - \mathrm{UT1}) \tag{3.9}$$

where TAI−UT1 is in seconds.

A convenient expression for GMST in time units is given by

$$\begin{aligned} \mathrm{GMST}(t_U, t) = 86\,400\mathrm{s}\ (0.779\,057\,273\,2640 + 1.002\,737\,811\,911\,354\,48\ t_U) \\ &+ 0.000\,967\,07\mathrm{s} + 307.477\,102\,27\mathrm{s}\ t + 0.092\,772\,113\mathrm{s}\ t^2 \\ &- 0.000\,000\,029\mathrm{s}\ t^3 - 0.000\,001\,997\mathrm{s}\ t^4. \end{aligned} \tag{3.10}$$

To enumerate successive sidereal days, the concepts of Greenwich sidereal date and Greenwich sidereal day number have sometimes been used. The Greenwich sidereal date is defined as the interval in sidereal days elapsed on the Greenwich meridian since the beginning of the sidereal day that was in progress at Julian Date 0.0 (See § 3.7 for a discussion of Julian

Date). The integral part of the Greenwich sidereal date is the Greenwich sidereal day number, which is tabulated daily in *The Astronomical Almanac*.

3.2.1.2 Calculating Hour Angles in the Equinox-based System

In the equinox-based system, sidereal time is used to calculate hour angle using the relations:

$$\text{local mean sidereal time} = \text{GMST} + \text{east longitude} \tag{3.11}$$

$$\text{local apparent sidereal time} = \text{local mean sidereal time} + \text{eq. of equinoxes} \tag{3.12}$$

$$= \text{GAST} + \text{east longitude} \tag{3.13}$$

$$\text{local hour angle} = \text{local apparent sidereal time} - \text{apparent right ascension} \tag{3.14}$$

(See § 7.1.3 for a discussion of apparent right ascension).

3.2.1.3 Calculating Hour Angles in the CIO-based System

In the CIO-based system, using the linear expression for Earth Rotation Angle $\theta(t_U)$ (see Eq. 3.3) the calculation of hour angles is simpler than using sidereal time.

$$\text{local hour angle} = \text{Earth Rotation Angle} - \text{intermediate right ascension} + \text{east longitude, or} \tag{3.15}$$

$$\text{local hour angle} = \text{GAST} + \text{equation of the origins} - \text{intermediate right ascension} + \text{east longitude,} \tag{3.16}$$

where the intermediate right ascension is computed using the IAU 2000 recommendations. Calculating hour angles using either the equinox-based system or the CIO-based system will provide identical results. Note that the Earth Rotation Angle is (nearly) the Greenwich Hour Angle of the right ascension origin of the International Celestial Reference System, a convenience for mental arithmetic.

3.2.2 UT1

UT1 is a measure of the Earth's rotation angle expressed in time units and treated conventionally as an astronomical timescale defined by the rotation of the Earth with respect to the Sun. In practice, Universal Time was defined until 1 January 2003 by means of conventional formulae defining sidereal time. Resolution B1.8 adopted by the XXIVth General Assembly of the International Astronomical Union (IAU 2001; URL[6]) recommended the use of the *non-rotating origin* (Guinot 1979) both in the Geocentric Celestial Reference System (GCRS) and the International Terrestrial Reference System (ITRS). These origins are designated as the Celestial Intermediate Origin (CIO) and the Terrestrial Intermediate Origin (TIO) in these systems, respectively. The *Earth Rotation Angle* is defined as the angle measured along the equator of the Celestial Intermediate Pole between the CIO and the TIO. This resolution also recommended that UT1 be linearly proportional to the Earth Rotation Angle, and that the transformation between the ITRS and GCRS be specified using the Earth Rotation Angle.

The Earth Rotation Angle, θ, is linked to UT1 by the conventional relationship as given by Capitaine (2000) (Eq. 3.3). This definition of UT1 based on the CIO is insensitive at the microarcsecond level to the precession-nutation model and to the observed celestial pole offsets. UT1 is observed using Very Long Baseline Interferometry (VLBI) measurements of

selected radio point sources, mostly quasars and interpolated by tracking of GPS satellites. Strictly speaking, because of the motion of satellite orbital nodes in space, VLBI provides the only rigorous determination of UT1.

The ratio of mean sidereal time to UT1 is

$$r' = 1.002\,737\,379\,093\,507\,95 + 5.9006 \times 10^{-11} t - 5.9 \times 10^{-15} t^2. \tag{3.17}$$

The ratio of UT1 to mean sidereal time is

$$1/r' = 0.997\,269\,566\,329\,084 - 5.8684 \times 10^{-11} t + 5.9 \times 10^{-15} t^2. \tag{3.18}$$

In both Eqs. 3.17 and 3.18, t represents the number of Julian centuries elapsed since J2000.0.

UT1 is considered to be nominally equivalent to mean solar time reckoned from midnight on the meridian of Greenwich. The mean solar day is the time interval between successive transits of a conventionally defined direction in the celestial reference system. The mean solar second, is 1/86 400 of a mean solar day (Kovalevsky 1965; McCarthy 1991). Before the adoption of the Aoki et al. (1982) expression for sidereal time as a function of solar time, this conventional point was called the fictitious mean Sun, which was Simon Newcomb's expression for a fictitious point whose motion in the celestial reference system corresponds to the average motion of the Sun in the sky. Apparent solar time, the time determined by using a sundial or by measuring the altitude of the Sun, is defined by the motion of the observed Sun. However, the day measured by the time interval between successive passes of the actual Sun over the local meridian varies because the Earth's axis is tilted in space and because the Earth's orbit is not circular. The difference between mean and apparent solar time is called the equation of time. The maximum amount by which apparent noon precedes mean noon is about 16.5 minutes around 3 November, while the maximum amount by which mean noon precedes apparent noon is about 14.5 minutes around 12 February (Nelson et al. 2001).

UT0, a designation no longer in common use, is UT1 corrupted by the effect of the motion of the pole of the Earth's rotational axis with respect to the terrestrial reference frame. The difference between the two is of the order of a few tens of milliseconds (Guinot 1989).

UT2 is a timescale, rarely used in practice, resulting from a conventional correction to UT1 accounting for the seasonal variation in the Earth's rotation. The correction accounts for the fact that the Earth rotates slower by about 30 ms in May and faster by a similar amount in November. The difference between UT2 and UT1 is a conventional expression given in McCarthy (1991).

$$\mathrm{UT2} = \mathrm{UT1} + 0.022\mathrm{s} \sin 2\pi t_B - 0.012\mathrm{s} \cos 2\pi t_B - 0.006\mathrm{s} \sin 4\pi t_B + 0.007\mathrm{s} \cos 4\pi t_B \tag{3.19}$$

where t_B is the fraction of the Besselian year and given by

$$t_B = \mathrm{mod}\left[2000 + \frac{(\text{Julian Date} - 2\,451\,544.533)}{365.2422}, 1\right]. \tag{3.20}$$

3.3 Dynamical Time

A timescale based on the dynamics of the motions of solar system bodies was originally conceived as an answer to the need for a more uniform, astronomically-based timescale.

Ephemeris Time, which came into use in the 1950s, was based on ephemerides that assumed Newtonian mechanics. Since that time, a series of dynamical timescales have been developed to account for evolving developments in modeling the effects of general relativity. In current practice, dynamical timescales are used to provide the independent variable of the equations of motion of the bodies in the solar system.

3.3.1 Ephemeris Time

Ephemeris Time (ET) refers to the timescale suggested by G. M. Clemence (1948). He proposed a timescale based on the period of the revolution of the Earth around the Sun, as represented by Newcomb's *Tables of the Sun* published in 1895. ET is defined practically through the use of Newcomb's formula for the geometric mean longitude of the Sun (Newcomb 1895):

$$L = 279^\circ\ 41'\ 48.''04 + 129\ 602\ 768.''13\ T + 1.''089\ T^2 \tag{3.21}$$

where T is the time reckoned in Julian centuries of 36 525 days since January 0, 1900, 12h UT. The IAU adopted this proposal in 1952 at its 8th General Assembly in Rome (IAU 1954).

Newcomb's formula implies that, if we use the motion of the Sun at $T = 0$, that is $\delta L/\delta T = 1\,296\,027.''6813$ per year, we would expect the year to contain

$$365.25 \text{ days} \times 86\,400 \text{ s/day} \times (360 \times 60 \times 60''/\text{rev.})/(\delta L/\delta T) = 31\,556\,925.9747 \text{ s}.$$

The 10th General Conference on Weights and Measures (CGPM) in 1954, therefore, proposed the definition of the second, "The second is the fraction 1/31 556 925.975 of the length of the tropical year for 1900.0." Consequently the International Committee for Weights and Measures (CIPM) in 1956, defined the second of ephemeris time to be "the fraction 1/31 556 925.9747 of the tropical year for 1900 January 0 at 12 hours ephemeris time." This definition was ratified by the 11th CGPM in 1960 (BIPM 1956; BIPM 2006, p. 148). In 1958, the International Astronomical Union General Assembly defined the epoch of ET by (IAU 1960): "Ephemeris Time (ET), or Temps des Ephémérides (TE), is reckoned from the instant, near the beginning of the calendar year A.D. 1900, when the geometric mean longitude of the Sun was 279° 41′ 48.″04, at which instant the measure of Ephemeris Time was 1900 January 0^{d} 12^{h} precisely."

As Newcomb's formula (Eq. 3.21) was mostly based on observations made during the 19th century and referred to mean solar time, the duration of the ephemeris second represents approximately the mean duration of the second of mean solar time during this century.

Although ET was defined using Newcomb's expression, it was realized using observations of the position of the Moon with respect to the celestial reference frame. These observed lunar positions were used together with conventional lunar ephemerides to derive estimates of ET. This led to a set of realizations of ET based on the actual ephemeris used that were denoted ET0, ET1 and ET2 (Guinot 1989).

ET was determined in practice using the expression

$$\mathrm{ET} = \mathrm{UT1} + \Delta T \tag{3.22}$$

where ΔT was determined from astronomical observations.

Although astronomical ephemerides adopted ET as the independent variable, it was inconvenient to obtain accurate real-time estimates of ET, and it did not include relativistic effects, nor did it distinguish between proper and coordinate time.

3.3.2 TDT/TDB

The 16th IAU General Assembly in 1976 defined time-like arguments, consistent with the general theory of relativity, that distinguish coordinate systems with origins at the center of the Earth and the center of the solar system (IAU 1977). The recommendations for the definition of dynamical time adopted at the IAU General Assembly of 1976 were:

(a) At the instant 1977 January $01^{d}\ 00^{h}\ 00^{m}\ 00^{s}$ TAI, the value of the new timescale for apparent geocentric ephemerides will be 1977 January $1^{d}.000\ 3725$ ($1^{d}\ 00^{h}\ 00^{m}\ 32^{s}.184$) exactly.

(b) The unit of this timescale will be a day of 86 400 SI seconds at mean sea level.

(c) The timescales for equations of motion referred to the barycenter of the solar system will be such that there will be only periodic variations between these timescales and those of the apparent geocentric ephemerides.

These were given the names Terrestrial Dynamical Time (TDT) and Barycentric Dynamical Time (TDB), respectively, in 1979 (IAU 1980).

The epoch of TDT is referred to International Atomic Time (TAI) on 1 January 1977 0^{h}, as shown in (a) above (see § 3.4 for a discussion of TAI). Its basic unit is the SI second, and it maintains continuity with ET. The reason for the selection of the epoch in January 1977 is that at this time, a rate correction of -10×10^{-13} was applied to TAI to bring the unit of TAI more closely into accord with the SI second (IAU 1977, p. 66; Seidelmann 1992, p. 85). For years prior to 1955, when atomic time was not available, TDT must be extrapolated backward, using dynamical theory fit to observations.

During the 1980s, the definition of TDB was found to be ambiguous. In particular, the form of the relativistic metric was not made explicit. This led to improvements in 1991, 2000, and 2006 (see § 3.6). T_{eph} (see § 3.6.1) is now essentially equivalent to TDB.

3.4 Atomic Time

In 1955, L. Essen and J. V. L. Parry of the National Physical Laboratory (NPL) calibrated the resonance frequency of the laboratory's caesium standard with respect to the UT2 second of that epoch (Essen and Parry 1955). Together with Wm. Markowitz and R. G. Hall at the U. S. Naval Observatory (USNO), they later calibrated the frequency in terms of the ET second using observations made with the USNO dual-rate Moon camera over the period 1955.50 to 1958.25. The measured caesium frequency was 9 192 631 770 Hz with an uncertainty of ±20 Hz, mostly due to the measurement of ET (Markowitz et al. 1958).

In 1967 the 13th CGPM adopted the atomic second as the unit of time in the International System of Units. It was defined as "the duration of 9 192 631 770 periods of the radiation corresponding to the transition between the two hyperfine levels of the ground state of the

Caesium 133 atom" (BIPM 1967; Terrien 1968; BIPM 2006, pp. 112–113). The second of atomic time, therefore, is in principle equivalent to the second of Ephemeris Time, and, therefore, approximately equivalent to the mean value of the second of UT1 in the 19th century.

3.4.1 International Atomic Time, TAI

Around 1960, some organizations, including the USNO and the Bureau International de l'Heure (BIH), began to use atomic timescales based on the caesium frequency of 9 192 631 770 Hz. By convention, these scales were set in agreement with UT2 on 1 January 1958, 0^h UT2. In 1970 the Comité Consultatif pour la Définition de la Seconde (CCDS) of the CIPM recommended the adoption of International Atomic Time (TAI) stating,

> "International Atomic Time (TAI) is the time reference coordinate established by the Bureau International de l'Heure on the basis of the readings of atomic clocks operating in various establishments in accordance with the definition of the second, the unit of time of the International System of Units." (BIPM 1970b; Terrien 1971; BIPM 2006, p. 155).

Also in 1970 the CCDS recognized that TAI would be in approximate agreement with UT2 on 1 January 1958, 0^h UT2 (BIPM 1970a). The 14th CGPM approved the establishment of TAI in 1971. In 1980 the definition of TAI was refined by the statement, "TAI is a coordinate timescale defined in a geocentric reference frame with the SI second as realized on the rotating geoid as the scale unit." (BIPM 1980; Giacomo 1981; BIPM 2006, p. 155). This requires that relativistic corrections for the primary laboratory realizations of the SI second be used in the calibration of TAI to compensate for the frequency shifts between their individual locations and a point fixed on the surface of the rotating geoid. In 1988 the Bureau International des Poids et Mesures (BIPM) assumed responsibility for maintaining TAI.

TAI is realized in practice in two steps. First an intermediate timescale, called Échelle Atomique Libre (EAL) is formed by combining data from all available high-precision atomic standards maintained at national timing laboratories around the world. The data from the individual clocks are combined using an algorithm that minimizes the effect of adding and dropping clocks and that weights clocks appropriately. After analysis of EAL, corrections are applied using data from primary laboratory standards to provide a unit of time as close as possible to the definition of the SI second. This adjusted timescale is published as TAI. Since TAI is only realized through the published corrections to each contributing timescale, it is a paper timescale; that is, there is no clock keeping TAI.

3.4.2 Terrestrial Time, TT

In 1991 the IAU renamed TDT as Terrestrial Time (TT). IAU Resolution B1.9 (IAU 2000; URL[6]) re-defined Terrestrial Time (Petit 2000). A practical realization of TT (IAU 1977, p. 65; Seidelmann 1992, p. 48; Guinot 1995) is

$$\mathrm{TT} = \mathrm{TAI} + 32.184\ \mathrm{s}. \tag{3.23}$$

The constant offset represents the difference between ET and UT1 at the defining epoch of TAI on 1 January 1958. TT is to be used as the time reference for apparent geocentric

ephemerides. Any difference between TAI and TT—except for the 32.184 second offset—is a consequence of the physical defects of atomic time standards, and has probably remained within the approximate limits of $\pm 20\mu$s. It will increase at a slower rate in the future as time standards improve. In most cases, and particularly for the publication of ephemerides, this deviation is negligible.

The unit of measurement of TT was initially defined as the SI second on the geoid. In 2000 the IAU redefined the unit of TT by adoption of a conventional relationship with the Geocentric Coordinate Time TCG (see § 3.6.2). Multiples, such as the TT day of 86 400 TT seconds and the TT Julian Century of 36525 TT days are used. The reference to TT is indicated whenever ambiguity might arise. Corresponding time intervals of TAI are in agreement with the TT intervals within uncertainties of the primary atomic standards. It has been suggested that realizations of TT be designated by TT(xxx), where xxx is an identifier, for example Eq. 3.23 might be written TT(TAI) = TAI + 32.184 s. The BIPM has also issued timescales TT(BIPMxx), where 19xx or 20xx is the year of computation.

3.5 Civil Time

For civil applications time is regulated by civil authorities within each country and is sometimes related to local mean solar time. The International Meridian Conference formally recommended the Greenwich meridian as a worldwide standard reference for time in 1884. (Smith 1976; Howse 1997). In modern times civil timescales are generally related to Coordinated Universal Time (UTC), either officially or in practice.

3.5.1 Coordinated Universal Time, UTC

Beginning in 1960 the UK and U.S. began to coordinate their time and frequency transmissions. Gradually other countries joined this system, which began to be coordinated by the Bureau International de l'Heure (BIH) in 1961. In 1965, the BIH related UTC to its atomic timescale A3 (which eventually became the basis for TAI) by a mathematical relationship (Bureau International de l'Heure 1965). This led to the link between TAI and UTC (Nelson et al. 2001). The name "Coordinated Universal Time (UTC)" was approved by a resolution of IAU Commissions 4 and 31 at the 13th General Assembly in 1967 (IAU 1968; URL[6]).

Details of the UTC system were formalized by the International Radio Consultative Committee (CCIR) Study Group 7 in 1962 and were formally adopted by the CCIR in Recommendation 374 of 1963 (International Radio Consultative Committee 1963). Offsets in the atomic frequency to match the rotational speed of the Earth were announced each year by the BIH, and steps of 100 ms were inserted as needed on dates determined by the BIH, to maintain time signals to within less than 0.1s of UT2. As UTC included rate offsets, the broadcast time signals indicated neither the SI second nor the mean solar second, but rather variable intervals designed to stay in step with UT2, from which the SI second could be obtained by applying known corrections. This process caused inconvenience by requiring frequent adjustments in complex electronic instrumentation resulting in a revised definition of UTC.

The current UTC system is defined by the Radiocommunications Section of the International Telecommunications Union (ITU-R) (formerly CCIR) Recommendation ITU-R TF.460-5: "UTC is the timescale maintained by the BIPM, with assistance from the IERS, which forms the basis of a coordinated dissemination of standard frequencies and time signals. It corresponds exactly in rate with TAI but differs from it by an integral number of seconds. The UTC scale is adjusted by the insertion or deletion of seconds (positive or negative leap seconds) to ensure approximate agreement with UT1." (ITU-R 1998). Seconds of UTC are thus exactly equal to the seconds of TAI and disseminate the SI second of proper time on the geoid. Step adjustments are now made in order to ensure that $|\mathrm{UT1} - \mathrm{UTC}| < 0.9\mathrm{s}$. The preferred times to make the adjustment are at the end of the last minute of June 30 or December 31. Leap second adjustments may also be made in the last minute of March 31 or September 30 as a secondary choice, and, if necessary, adjustments can be made during the last minute of the last day of any month in the year. A history of rate offsets and step adjustments in UTC is given in Table 3.1 and at URL[1].

The terms "mean solar time," "Greenwich Mean Time," or "GMT" are generally considered as being equivalent to UTC. The 15th CGPM in 1975 adopted the following resolution (Terrien 1975; BIPM 2006, p. 157):

> "The 15th Conférence Générale des Poids et Mesures,
>
> **considering** that the system called "Coordinated Universal Time" (UTC) is widely used, that it is broadcast in most radio transmissions of time signals, that this wide diffusion makes available to the users not only frequency standards but also International Atomic Time and an approximation to Universal Time (or, if one prefers, mean solar time),
>
> **notes** that this Coordinated Universal Time provides the basis of civil time, the use of which is legal in most countries,
>
> **judges** that this usage can be strongly endorsed."

The continued use of leap second adjustments is under discussion. In January 2012, the ITU-R decided to postpone a decision regarding eliminating the leap second until at least 2015 so additional investigations into the pros and cons can be made.

3.5.2 Time Zones

Time zones were first proposed in 1870 by Charles F. Dowd (Dowd 1930) to regulate time for railroads in the United States. A worldwide system of standard time zones is based on 15° (i.e., one hour) increments in longitude. These standard time zones are identified with letter designations, in addition to appropriate names. Thus the standard time zone for 0° is labeled Z. The standard time zone for 15° east longitude is labeled A, etc. (see Fig. 3.1).

Each country determines the time zone or zones for itself, and some have adopted a zone on a fraction of an hour. Many also adopt daylight saving time, sometimes called summer time or advanced time, which is generally one hour in advance of the standard time normally kept in that zone. The dates for changing to and from daylight saving time vary among the countries; a few retain advanced time all year.

Table 3.1 TAI − UTC (ΔAT)

From	To	TAI − UTC
1961 Jan. 1	1961 Aug. 1	1.422818s + (MJD − 37300) × 0.001296s
Aug. 1	1962 Jan. 1	1.372818s + (MJD − 37300) × 0.001296s
1962 Jan. 1	1963 Nov. 1	1.845858s + (MJD − 37665) × 0.0011232s
1963 Nov. 1	1964 Jan. 1	1.945858s + (MJD − 37665) × 0.0011232s
1964 Jan. 1	April 1	3.240130s + (MJD − 38761) × 0.001296s
April 1	Sept. 1	3.340130s + (MJD − 38761) × 0.001296s
Sept. 1	1965 Jan. 1	3.440130s + (MJD − 38761) × 0.001296s
1965 Jan. 1	Mar. 1	3.540130s + (MJD − 38761) × 0.001296s
Mar. 1	Jul. 1	3.640130s + (MJD − 38761) × 0.001296s
Jul. 1	Sept. 1	3.740130s + (MJD − 38761) × 0.001296s
Sept. 1	1966 Jan. 1	3.840130s + (MJD − 38761) × 0.001296s
1966 Jan. 1	1968 Feb. 1	4.313170s + (MJD − 39126) × 0.002592s
1968 Feb. 1	1972 Jan. 1	4.213170s + (MJD − 39126) × 0.002592s
1972 Jan. 1	Jul. 1	10s
Jul. 1	1973 Jan. 1	11s
1973 Jan. 1	1974 Jan. 1	12s
1974 Jan. 1	1975 Jan. 1	13s
1975 Jan. 1	1976 Jan. 1	14s
1976 Jan. 1	1977 Jan. 1	15s
1977 Jan. 1	1978 Jan. 1	16s
1978 Jan. 1	1979 Jan. 1	17s
1979 Jan. 1	1980 Jan. 1	18s
1980 Jan. 1	1981 Jul. 1	19s
1981 Jul. 1	1982 Jul. 1	20s
1982 Jul. 1	1983 Jul. 1	21s
1983 Jul. 1	1985 Jul. 1	22s
1985 Jul. 1	1988 Jan. 1	23s
1988 Jan. 1	1990 Jan. 1	24s
1990 Jan. 1	1991 Jan. 1	25s
1991 Jan. 1	1992 Jul. 1	26s
1992 Jul. 1	1993 Jul. 1	27s
1993 Jul. 1	1994 Jul. 1	28s
1994 Jul. 1	1996 Jan. 1	29s
1996 Jan. 1	1997 Jul. 1	30s
1997 Jul. 1	1999 Jan. 1	31s
1999 Jan. 1	2006 Jan. 1	32s
2006 Jan. 1	2009 Jan. 1	33s
2009 Jan. 1	2012 Jul. 1	34s
2012 Jul. 1		35s

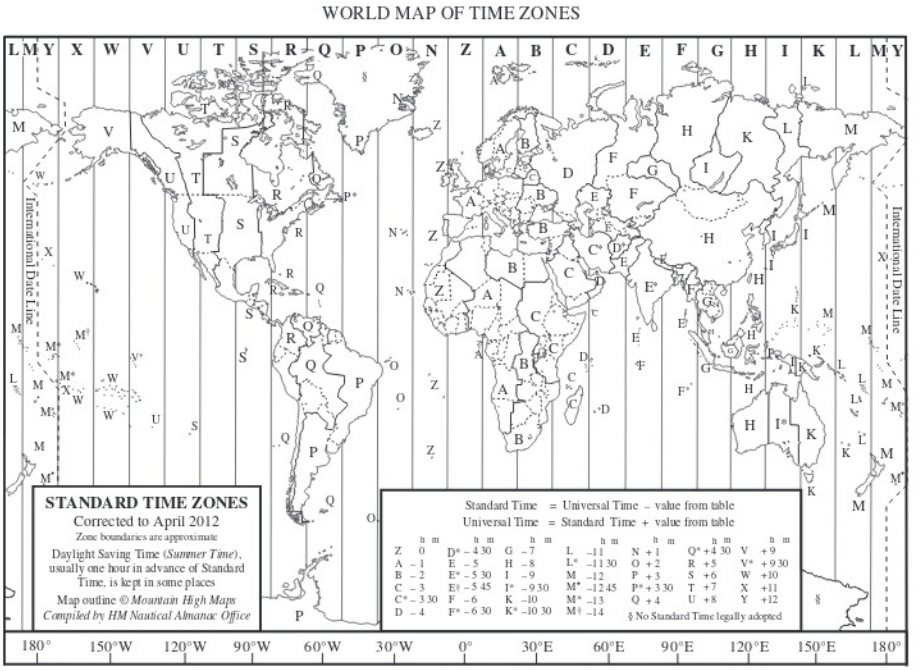


Figure 3.1 World time zone map

3.6 Barycentric and Geocentric Coordinate Time

The XXIst IAU General Assembly in 1991 adopted nine recommendations in resolution A4 dealing with the celestial and terrestrial reference systems and the space-time metrics (IAU 1992; URL[6]; Guinot 1995). The simplest form of these metrics, which does not introduce scaling factors, defines Barycentric Coordinate Time (TCB) and Geocentric Coordinate Time (TCG) (Seidelmann and Fukushima 1992). These coordinate times differ in mean rate between themselves and also with TDB and TT. They are related by four-dimensional space-time coordinate transformations (IAU 1992; Guinot 1995; IERS 1996). These definitions were further made more precise by resolutions adopted at the XXIVth IAU General Assembly held in Manchester in 2000 (IAU 2001; URL[6]; IERS 2004). At the same General Assembly, TT was redefined by a linear conventional relation with TCG, its unit being very close to the proper second on the rotating geoid (see § 3.6.2).

The origins of coordinate times have been arbitrarily set so that these times all coincide with the Terrestrial Time (TT) at the geocenter of 1977 January 1 $0^h\ 0^m\ 0^s$ TAI. When realizations of TCB and TCG are needed, these realizations should be designated by expressions such as TCB (xxx) where xxx indicates the source of the realized timescale (e.g., TAI) and the theory used for transformation into TCB or TCG.

3.6.1 Barycentric Coordinate Time, TCB and Barycentric Ephemeris Time, T_{eph}

Recommendation 5 of IAU Commissions 4, 8, and 31 (IAU 1977), completed by Recommendation 5 of IAU Commissions 4, 19, and 31 (IAU 1980), stated that Terrestrial

Dynamical Time (TDT) and Barycentric Dynamical Time (TDB) should differ only by periodic variations (Kaplan 1981). Therefore TDB and TCB differ in rate. The relationship between these timescales in seconds is now defined by an IAU recommendation (IAU 2008) to be

$$\mathrm{TDB} = \mathrm{TCB} - \mathrm{L_B} \times (\mathrm{JD_{TCB}} - 2\,443\,144.500\,3725) \times 86\,400\mathrm{s} + \mathrm{TDB_0} \qquad (3.24)$$

where $\mathrm{TDB_0} = -6.55 \times 10^{-5}$s and the value of L_B is defined to be $1.550\,519\,768 \times 10^{-8}$.

Barycentric Ephemeris Time ($\mathrm{T_{eph}}$) is a coordinate time related to TCB by an offset and a scale factor. Ephemerides based upon the coordinate time $\mathrm{T_{eph}}$ are automatically adjusted in the creation process so that the rate of $\mathrm{T_{eph}}$ has no overall difference from the rate of Terrestrial Time (TT) (see Standish 1998), therefore also no overall difference from the rate of Barycentric Dynamical Time (TDB). For this reason space coordinates obtained from the ephemerides are consistent with TDB.

3.6.2 Geocentric Coordinate Time, TCG

The relation TCB − TCG involves a full four-dimensional transformation

$$\mathrm{TCB} - \mathrm{TCG} = c^{-2} \left[\int_{t_0}^{t} \left(\frac{\mathbf{v_e}^2}{2} + U_{ext}(\mathbf{x_e}) \right) dt + \mathbf{v_e} \cdot (\mathbf{x} - \mathbf{x_e}) \right] + O(c^{-4}) \qquad (3.25)$$

where $\mathbf{x_e}$ and $\mathbf{v_e}$ denote the barycentric position and velocity of the Earth's center of mass, and $\mathbf{x}$ is the barycentric position of the observer. The external potential U_{ext} is the Newtonian potential of all solar system bodies apart from the Earth and is evaluated at the geocenter. In the integral, $t = \mathrm{TCB}$ and t_0 is chosen to agree with the epoch of Terrestrial Time (TT). As an approximation to TCB − TCG in seconds one might use

$$\mathrm{TCB} - \mathrm{TCG} = \frac{\mathrm{L_C} \times (\mathrm{TT} - \mathrm{TT_0}) + \mathrm{P(TT)} - \mathrm{P(TT_0)}}{1 - \mathrm{L_B}} + \mathrm{c}^{-2} \mathbf{v_e} \cdot (\mathbf{x} - \mathbf{x_e}). \qquad (3.26)$$

The value of $\mathrm{L_B}$ is $1.550\,519\,768 \times 10^{-8}$; the current estimate of the value of $\mathrm{L_C}$ is $1.480\,826\,867\,41 \times 10^{-8}$ ($\pm 2 \times 10^{-17}$) (IERS 2010). $\mathrm{TT_0}$ corresponds to JD 2 443 144.5 TAI (1977 January 1, 0^{h}). Periodic terms denoted by P(TT) have a maximum amplitude of around 1.7 ms and can be evaluated by the "FB" analytical model (Fairhead and Bretagnon 1990; Bretagnon 2001). Alternately, $\mathrm{P(TT)} - \mathrm{P(TT_0)}$ may be provided by a numerical time ephemeris such as TE405 (Irwin and Fukushima 1999), which provides values with an accuracy of ±0.1 ns from 1600 to 2200. A series, HF2002, providing the value of $\mathrm{L_C(TT - TT_0)} + \mathrm{P(TT)} - \mathrm{P(TT_0)}$ as a function of TT over the years 1600–2200 has been fit (Harada and Fukushima 2003) to TE405. This fit differs from TE405 by less than 3 ns over the years 1600–2200 with an rms error of ±0.5 ns. The last term of Eq. 3.26 is diurnal at the surface of the Earth, with an amplitude smaller than 2.1 μs.

Terrestrial Time differs from TCG by a scaling factor, and the difference can be approximated by

$$\mathrm{TCG} - \mathrm{TT} = \mathrm{L_G} \times (\mathrm{MJD(TAI)} - 43\,144.0) \times 86\,400\ \mathrm{s}. \tag{3.27}$$

The value of $\mathrm{L_G}$ providing continuity with TT in which the scale unit agrees with the SI second on the geoid is $6.969\,290\,134 \times 10^{-10}$ (IERS 2010). Figure 3.2 shows the relationship among these time scales.

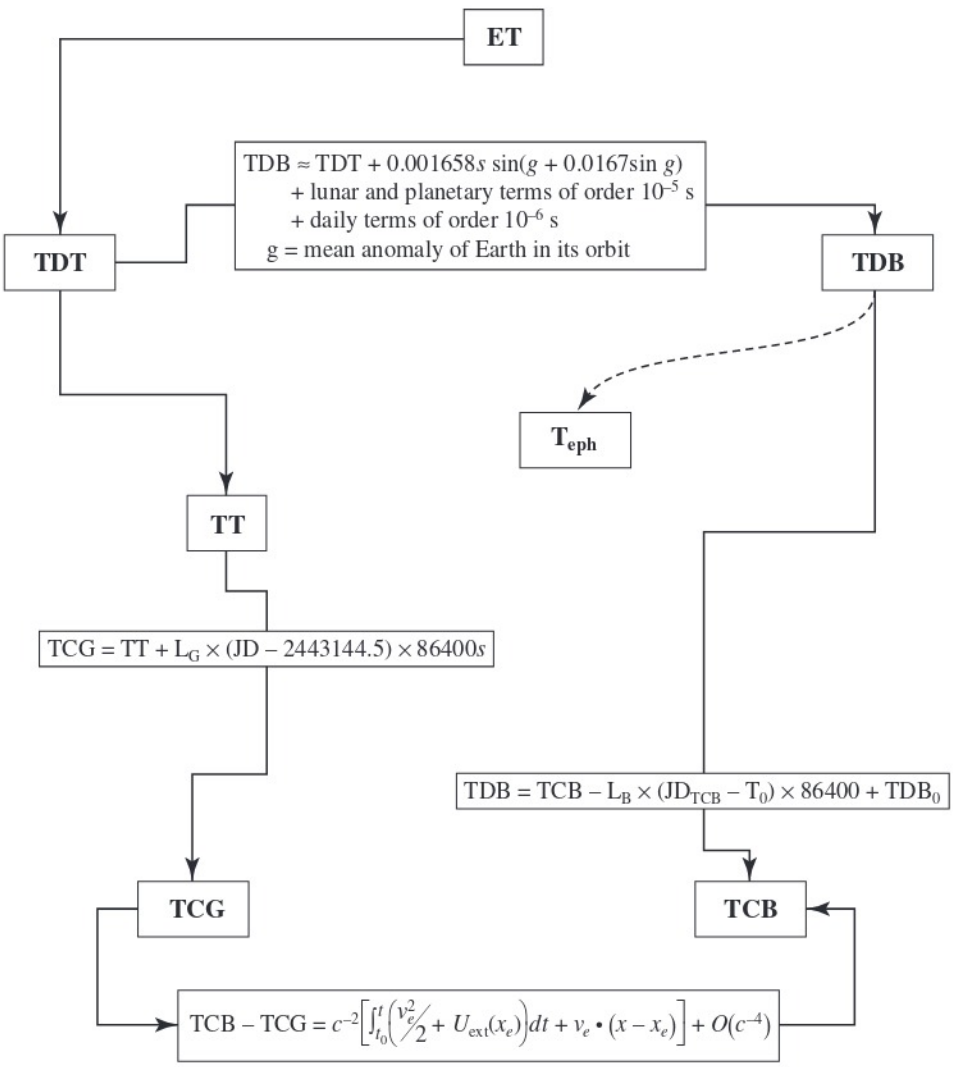


Figure 3.2 Relationship among timescales

3.7 Julian Date

Julian days are used for continuous counts of days. Joseph Justus Scaliger in 1583 began the process that led to the Julian day number count when he attempted to clarify the confusing calendars in use during the Middle Ages. Scaliger used three cycles of importance in early Christian calendars:

- The Julian calendar in use until the Gregorian calendar reform of 1582, where the normal year had 365 days, and a leap year of 366 days occurred every fourth year without exception.
- The *Golden Number* cycle associated with Meton who flourished in Athens in the fifth century B.C., equated 19 years with 235 months.
- A tax cycle or *indiction* of 15 years was used in legal and financial organization of the Roman Empire under Constantine and later emperors.

Scaliger reasoned that any year could be characterized by its position (S) within a 28-year solar cycle, its position (G) within the 19-year cycle of Golden Numbers, and its position (I) within the Roman tax cycle. Because 15, 19 and 28 have no common factors a particular combination of S, G, and I would repeat after $28 \times 19 \times 15 = 7980$ years. This period Scaliger called a Julian period, not in honor of his father as is frequently asserted, but because of the involvement of the Julian Calendar. Knowing that the year 1 B.C. was characterized by S=1, G=1, I=3, Scaliger computed that the combination of S=1, G=1, I=1 occurred for 4713 B.C.. This provided him with the starting year from which to begin a continuous counting of years (McCarthy 1998).

A further development took place in 1948, when the Time Department of the Royal Greenwich Observatory began the use of continuous day numbers in order to reduce the confusion of dates associated with data reported to them for international time comparisons. Humphrey Smith, Secretary of IAU Commission 31 (Time), introduced this concept for discussion at the General Assembly of the IAU in 1955, and there the decision was taken to create a Modified Julian Date (MJD) by dropping the first two digits of the Julian day number as being, for most purposes, superfluous, and by making the correction of 0.5 days to bring the beginning of the day into agreement with Universal Time. At the 1973 General Assembly of the IAU, in recognition of the fact that a dating system in which the day began at midnight was useful for monitoring time signals and that such a system had been in use for some time, a resolution was passed recommending the use of MJD as the equivalent of JD−2400000.5. The Bureau International de l'Heure began to use MJD in its monthly circulars in October 1973 and in its Annual Report for 1973.

The IAU General Assembly held in Kyoto in 1997 accepted the following definitions. The Julian day number (JDN) is the number assigned to a day in a continuous count of days beginning with the Julian day number 0 assigned to the day starting at Greenwich mean noon on 1 January 4713 B.C. in the Julian calendar extrapolated backwards (*proleptic*). The

Julian Date begins at $12^h\ 0^m\ 0^s$, and the calendar date 2000 January 1, $12^h\ 0^m\ 0^s$ (exactly) is equivalent to the Julian Date 2 451 545.0 (exactly). Finally, the Modified Julian Date (MJD) is defined as JD−2 400 000.5. The timescale should be specified when precision matters, e.g., MJD 47479.25 TAI.

3.8 Summary of Useful Relationships

Figure 3.3 shows graphically the current array of timescales. Useful expressions for relating timescales are given below. The numbers in brackets refer to the number of the expression in the text above. For an epoch expressed in UTC (the numbers between square brackets in the expressions below refer to the equations in the text):

$$\begin{aligned}
\mathrm{UT1} &= \mathrm{UTC} + (\mathrm{UT1} - \mathrm{UTC}) && \mathrm{UT1} - \mathrm{UTC}\ \text{available from IERS}\\
\mathrm{TAI} &= \mathrm{UTC} + \Delta\mathrm{AT} && [\text{Table 3.1}]\\
\mathrm{TT} \equiv \mathrm{TDT} &\approx \mathrm{TAI} + 32.184\mathrm{s} && [\text{Eq. 3.23}]\\
\mathrm{ET} &= \mathrm{UT1} + \Delta T && [\text{Eq. 3.22}]\\
&\quad \Delta T\ \text{obtained from ephemerides, or currently}\\
&\quad \Delta T = \mathrm{TT} - \mathrm{UT1} = 32.184\mathrm{s} + \Delta\mathrm{AT} - (\mathrm{UT1} - \mathrm{UTC})\\
\mathrm{GMST}(t_U, t) &= \theta(t_U) - E_{\mathrm{prec}}(t) && [\text{Eq. 3.7}]\\
t &= (\mathrm{TT} - 2\,451\,545.0\ \mathrm{TT})\ \text{in days}/36525\\
\theta(t_U) &= 2\pi(0.779\,057\,273\,2640 + 1.002\,737\,811\,911\,354\,48\, t_U) && [\text{Eq. 3.3}]\\
t_U &= \text{Julian UT1 date} - 2\,451\,545.0\\
E_{\mathrm{prec}}(t) &= -0.''014\,506 - 4612.''156\,533\,53\, t - 1.''391\,581\,65\, t^2\\
&\quad +0.''000\,000\,44\, t^3 + 0.''000\,029\,956\, t^4 && [\text{Eq. 3.4}]\\
\mathrm{TCG} - \mathrm{TT} &= \mathrm{L_G} \times (\mathrm{MJD(TAI)} - 43\,144.0) \times 86\,400\mathrm{s} && [\text{Eq. 3.27}]\\
\mathrm{L_G} &= 6.969\,290\,134 \times 10^{-10}\\
\mathrm{TCB} &= \mathrm{TCG} + \tfrac{\mathrm{L_C} \times (\mathrm{TT} - \mathrm{TT_0}) + \mathrm{P(TT)} - \mathrm{P(TT_0)}}{1 - \mathrm{L_B}} + \mathrm{c}^{-2}\mathbf{v_e} \cdot (\mathbf{x} - \mathbf{x_e}) && [\text{Eq. 3.26}]\\
\mathrm{L_C} &= 1.480\,826\,8674 \times 10^{-8}\\
\mathrm{L_B} &= 1.550\,519\,7678 \times 10^{-8}\\
\mathrm{TDB} &= \mathrm{TCB} - \mathrm{L_B} \times (\mathrm{JD_{TCB}} - 2\,443\,144.500\,3725) \times 86\,400\mathrm{s} + \mathrm{TDB_0} && [\text{Eq. 3.24}]\\
\mathrm{TDB_0} &= -6.55 \times 10^{-5}\mathrm{s}\\
\mathrm{T_{eph}} &\cong \mathrm{TDB}.
\end{aligned}$$

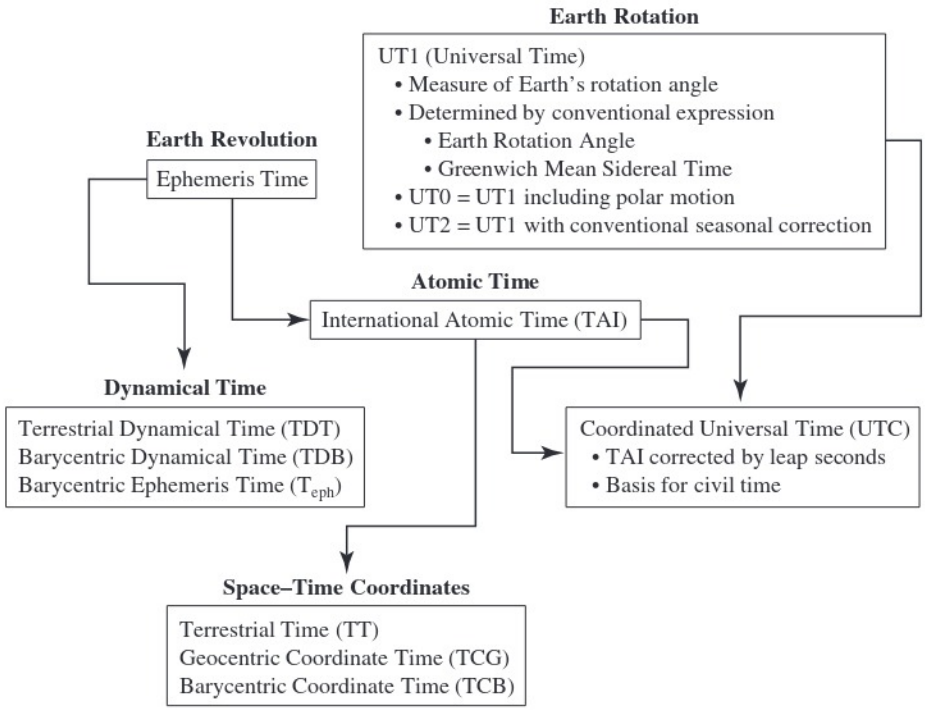


Figure 3.3 Interrelationship of timescales

3.9 Timekeeping

The currently adopted standard for timekeeping is a hyperfine transition of the caesium -133 atom (F=3, $m_F = 0$ to F=4, $m_F = 0$), which is defined to be 9 192 631 770 Hz in a magnetic field of **H**=0 (see § 3.4). This standard provides the SI (International System of Units) second realized in TAI, and consequently in UTC.

3.9.1 Devices

A comprehensive review of modern timekeeping devices can be found in Quinn (2005), and Audoin and Guinot (2001) provides details on atomic clocks.

3.9.1.1 Quartz-crystal Oscillators

Although quartz-crystal oscillators do not provide a frequency based on the caesium atom, they do have a critical role in timekeeping. They are frequently used as the sources of stable frequencies in many electronic systems, including atomic clocks. They make use of the piezoelectric property of a quartz crystal. The crystal has a natural frequency of vibration that depends on its size and shape. When it distorts, a difference of electric potential is produced between two of its faces. If it is placed in an oscillating electric circuit having nearly the same frequency as the crystal, it is caused to vibrate at its natural frequency, and the frequency of the

entire circuit becomes the same as the natural frequency of the crystal. The actual oscillation frequency depends not only on the quartz crystal, but also on the oscillator circuit. Accuracy depends on the precision of the cut, the degree of contamination of the quartz, and stability of the resonator environment.

Quartz-crystal oscillators can be free-running or locked to an external reference signal (e.g., caesium, hydrogen, or GPS) with time constants ranging from milliseconds to days. The performance characteristics may range from 10^{-4} to 10^{-13} (when locked to an external reference) in frequency stability per day.

3.9.1.2 Atomic Beam Standards (Caesium)

The first caesium beam standard contributing to a national timescale was constructed by Essen and Parry in 1955 (Essen and Parry 1955; Ramsey 2005), and caesium atoms continue to provide the definition of the second. The length of the second defined by caesium atoms is provided by the frequency of an energy level transition produced by the magnetic interaction of the unpaired electron with the nucleus. The ground state is split into two separate states called hyperfine levels. The energy splitting of these two levels is defined in frequency units as 9 192 631 770 Hz, which, in turn, defines the second. In atomic beam frequency standards, a beam of atoms, produced by an oven, transits a microwave cavity and interacts with a microwave field. Energy-level transitions are excited, and changes in the population of the atoms in the two different levels are measured to provide the proper frequency.

Laboratory caesium-beam frequency standards currently realize the second with an accuracy of about a few parts in 10^{16}/day. As of 2012, operating laboratory instruments are located in France, Germany, Italy, Japan, Korea, and the United States. Commercially available frequency standards are less accurate (5×10^{-13}), but may provide stability equal to laboratory standards up to about one year. The stability of high-performance clocks is 1×10^{-14} for time intervals of five days.

3.9.1.3 Hydrogen Masers

Hydrogen masers are used where the highest stability is needed for integration times from ten seconds to ten days. This stability can reach about 1×10^{-15} for integration times of 1000 to 10000 seconds. The frequency of the atomic level transition in the case of the hydrogen atom is the transition F=1, m_F=0 to F=0, m_F=0, and is f_h=1 420 405 751.768 Hz. Hydrogen atoms are passed through a magnetic field, and those in the F=1, m_F=1, 0 state are introduced into a specially coated storage bulb. The coating provides a surface with minimal interaction with the atoms. The bulb, placed in a low magnetic field at room temperature, is in a cavity resonator that is tuned to the frequency corresponding to the transition. The atoms in the F=1, m_F=0 state then transition to the F=0, m_F=0 state.

Some hydrogen masers with automatic cavity tuning in controlled environments may have long-term stability of the same order as the best caesium standards. Vessot (2005) provides a review of hydrogen maser principles and capabilities.

3.9.1.4 Vapor Cell Clocks (Rubidium, Caesium)

A vapor cell clock uses atoms confined in vapor cell(s) that are excited by light from either a lamp or laser. The excited atoms decay to two ground state energy levels with equal probability. A microwave signal is injected into the vapor cell to induce atoms to change in

the ground state energy level. As the atoms change their state in response to the microwaves, the light absorption in the cell is changed and is monitored on a photodiode. A quartz crystal that provides the frequency of the microwave signal is tuned to provide the least absorption and this provides the reference frequency for the clock.

Vapor cell clocks are most often built using rubidium atoms with a microwave interrogation frequency of 6.8 GHz. The rubidium clock is an appropriate device when a relatively low-cost clock is needed that has stability better than a quartz-crystal clock. The rubidium clock can reach a stability of 1×10^{-13} per day under the best conditions.

3.9.1.5 Trapped Ion Frequency Standards

In trapped-ion devices radio-frequency fields are used to suspend ions and thus prevent their contact with any containment device. Absorption of injected microwave energy is sensed by the amount of fluorescence of the ions and variations in the fluorescence are used to tune the input microwave frequency. Mercury and Ytterbium ions have been used in such devices. Frequency stability better than 1×10^{-15} can be achieved.

3.9.1.6 Atomic Fountain Standards

The principle of atomic fountain standards is to increase the duration of the interaction of atoms with a microwave field by allowing them to move in a fountain-like manner. This permits greater precision in the determination of the microwave frequency and results in an improved clock. Atoms are placed in a vacuum chamber, and laser beams are used to slow the movement of the atoms to extremely low temperatures of roughly 1 microkelvin. The lasers are controlled in such a way as to throw the ball of cooled atoms up through a microwave cavity periodically by a distance of the order of a meter. Gravity returns the atoms, and their atomic state is determined after they have passed through the cavity for a second time. The frequency of the microwaves through which the atoms pass is varied until the maximum number of atoms is found to be in the proper state. This frequency can then be used to drive a clock.

Caesium atomic fountains are being built in many national standards laboratories with several (France, Germany, Japan, and the United States) reporting routinely to the BIPM. Reported accuracies are as low as 2×10^{-16}.

3.9.2 International Agencies

Following the international convention for the definition of UTC as outlined in § 3.5.1, two international agencies are involved in formulating the international standard for time. The International Earth Rotation and Reference Systems Service (IERS) provides the astronomical information regarding the Earth's rotation angle and makes decisions on the insertion of leap seconds. The Bureau International des Poids et Mesures (BIPM) uses data provided by the world's timing laboratories to provide a uniform atomic timescale (TAI).

3.9.2.1 IERS

One of the responsibilities of the IERS is to decide when UTC is to be adjusted to keep it within 0.9 seconds of UT1. The IERS was formed in 1987 by the International Astronomical Union (IAU) and the International Union of Geodesy and Geophysics (IUGG). At that time it was

known as the International Earth Rotation Service. In 2003 it was renamed the International Earth Rotation and Reference Systems Service.

The organization provides a number of services including the International Celestial Reference Frame, International Terrestrial Reference Frame, IERS Conventions, Earth orientation data, as well as leap second announcements. It is made up of a variety of national and academic organizations. Its Central Bureau, which is responsible for the general management and communications, is located at the Bundesamt für Kartographie und Geodäsie in Frankfurt, Germany. A summary of the IERS organization, products and services can be found on its web site at URL[1].

3.9.2.2 BIPM

The Bureau International des Poids et Mesures (BIPM) was established in the Convention of the Metre to provide the standards for a system of measurements traceable to the International System of Units (SI). The Convention of the Metre is an international treaty with 51 member states. Under the terms of this treaty the BIPM maintains its headquarters near Paris, France. The Time Section computes TAI using the data from about 300 atomic clocks that are contributed by national metrology institutions and observatories around the world. The length of the second of TAI is kept as close as possible to the SI second through the use of caesium primary frequency standards. As outlined in § 3.5.1, UTC is derived from TAI. The BIPM does not maintain a physical standard clock. The timescales are made available monthly through the BIPM Circular T, which provides contributors with the tabular values of the time differences between the contributing clocks and the computed standard. A summary of the work of the BIPM can be found on their website at URL[2].

3.9.2.3 National Time Laboratories

Users of precise time are able to access UTC through their national time laboratories. These are institutions that report their clock data to the BIPM and, in return, receive information from the BIPM detailing the relationship of their clocks to the international time standard. There are approximately sixty institutions recognized by the BIPM as national time laboratories that serve as providers of local standards of time.

3.10 Time Dissemination

Accurate time may be obtained through a variety of means appropriate for the accuracy required. The International Telecommunications Union—Radio-communications Section (ITU-R) provides a handbook *Selection and Use of Precise Frequency and Time Systems* (1997) (see URL[3]) that contains information on modern time dissemination systems.

Systems that provide precise time can either make use of one-way or two-way methods. In the former it is necessary to estimate the delay in the propagation of the time signal. Errors due to the modeling of these estimates can range from a few nanoseconds to more than a few milliseconds depending on the method used. Two-way techniques use the nearly simultaneous exchange of time signals along the same path. In this case the propagation delay is practically eliminated in the data processing. When time transfer is required with accuracy better than $\pm 1\mu$s, relativistic effects should be considered.

3.10.1 High-Frequency Radio Time Signals

Radio time signals continue to be a simple means of distributing time. The transmitted time is generally UTC, with a code or voice transmission of DUT1, so that an estimate of UT1 accurate to the nearest tenth of a second can be obtained using the relation UT1 = UTC + DUT1. Some countries provide standard-frequency transmissions continuously. The common frequencies are 2.5, 5, 10, 15, 20, and 25 MHz. Some also have transmissions at other frequencies at specific times.

The accuracy of a few milliseconds is limited by unmodeled variations in the travel time of the radio signals, particularly at higher frequencies. The received signal may contain a combination of signals that have traveled to the receiver on different paths, and reception conditions are likely to vary considerably, particularly with a daily period. A comprehensive listing of stations and codes that are broadcast is available in National Geospatial-Intelligence Agency Publication 117, *Radio Navigational Aids*, 2005, which is available online at URL[4].

3.10.2 Low-Frequency Radio Time Signals

Low-frequency (long-wave) signals are commonly used in modern time dissemination, because they possess a number of advantages over high-frequency signals. They are not affected as seriously by ground features or buildings. They can cover large areas and pass though many types of building walls. The stability of the timing signal is affected by variations in the ionosphere, and the accuracy is of the order of tens of microseconds.

Various countries provide long-wave radio transmitters that broadcast a time code signal in the 40–80 kHz range. Some commonly used stations are shown in Table 3.2.

3.10.3 LORAN-C

The LORAN-C navigation system has also been used as a means of time transfer. This system relies on synchronized broadcasts of signals from a number of stations, separated by distances of kilometers to determine the location of the receiver. The stations emit coded signals with 100 kHz bursts with varying strengths. Specially designed timing receivers are used to track the third sub-pulse of the received bursts. Each LORAN-C station has caesium standards that are used to synchronize the signals and these are related to national standards.

Table 3.2 Low-frequency radio time signals

Station Call Name	Frequency	Power	Location
JJY	40 KHz	50 KW	Fukushima Prefecture, Japan
	60 Khz	50 KW	Saga Prefecture, Japan
DCF	77.5 KHz	50 KW	Mainflingen, Germany
MSF	60 KHz	25 KW	Rugby, United Kingdom
WWVB	60 KHz	50 KW	Fort Collins, Colorado, USA
RTZ	50 KHz	10 KW	Irkutsk, Russia
HBG	75 KHz	20 KW	Prangins, Switzerland

Coverage is highly variable, depending on radiated power and the surface conductivity along the path between transmitter and receiver. The accuracy can be of the order of 50 ns to 300 ns. The limiting source of error is modeling the variations in path delay due mainly to weather-related events.

Enhancements to the Loran system, termed "e-LORAN," are being implemented in some countries so that broadcasting stations, each having three caesium standards, will be provided with improved transmitters and measurement systems. Stations are synchronized using Global Positioning System signals and will provide a new ninth pulse in the broadcast signal that can be used for precise timing. A broadcast message provides information on leap seconds, differential corrections, and station identification. In the best cases it is expected that accuracies of the order of tens of nanoseconds will be possible depending on the distances from the transmitters. It is worth noting that the United States and Canada have phased out the use of LORAN.

3.10.4 Global Positioning System (GPS)

One of the most common means to obtain accurate timing information is through the Global Positioning System (GPS). Although the system is designed primarily for navigation, it is also an important source of precise time. The current GPS constellation consists of 32 satellites, each carrying multiple caesium and/or rubidium atomic clocks. The accuracy of timing data obtained directly by means of a GPS receiver depends on the quality of the receiver. Accuracy on the order of tens of nanoseconds is possible. It is possible to improve this accuracy by using more sophisticated techniques such as is done when timing laboratories compare clocks by using a common satellite clock as a means of comparison. It is also possible to monitor the carrier wave as well as the code to obtain very precise time comparisons.

GPS provides accurate UTC, but the system makes use of an internal timescale called GPS System Time, or sometimes GPS Time. GPS Time is maintained close to UTC or TAI modulo one second, the offset being less than one microsecond and generally of the order of tens of nanoseconds. The clocks of the GPS system located in monitoring sites and in the satellites are used to realize this internal scale. Leap seconds are not inserted in this timescale, and its starting epoch is midnight of 5/6 January 1980, so that TAI is ahead of GPS Time by 19s, a nearly constant value. User receivers, however, generally provide UTC, making use of information that the satellites broadcast containing the time offset between UTC and GPS Time.

3.10.5 GLONASS

The Russian Global Navigation Satellite System (GLONASS) provides services similar to GPS. However, it uses Moscow Time (UTC $+ 3^{h}$) as its time reference instead of an internal timescale. Thus, this system is directly affected by leap second insertions. General information is provided online at URL[5].

3.10.6 GALILEO

The European system of satellite positioning (GALILEO), which should be operational in ~2015, will provide time information similar to that of GPS.

3.10.7 Two-Way Satellite Time Transfer (TWSTT)

For the most accurate time transfer applications, the two-way satellite time transfer (TWSTT) technique may be used. This technique makes use of geostationary communications satellites to transmit simultaneously spread-spectrum timing codes between two users desiring to compare their clocks. Accuracy at the sub-nanosecond level has been achieved. The process takes advantage of the fact that the most significant propagation errors cancel. Asymmetric delays in the communication satellite can be a source of error and relativistic corrections should be applied to achieve the highest precision.

3.10.8 Time Transfer by Internet

Servers on the Internet which are connected directly to precise reference clocks can also be used to provide accurate time. Network Time Protocol (NTP), the most commonly used time protocol, provides the best performance. User software runs continuously as a background task that automatically updates the computer clock using servers at many different locations around the world.

3.11 Relativistic Effects

In General Relativity there is no unique definition of clock synchronization and comparison. The convention in use for time keeping is that two distant clocks are synchronized in a specified coordinate system, when their readings remain equal at common dates in the coordinate time t of this system. This is known as *coordinate synchronization*. *Coordinate clock comparison* is defined as the difference of clock readings at the same date in t. In applications on the Earth or near the Earth, for example up to the orbit of geostationary satellites, two coordinate systems are used, both being geocentric: one rotating with the Earth, the International Terrestrial Reference System (ITRS), the other, Geocentric Celestial Reference System (GCRS), non-rotating. The non-rotating system is that defined by the IAU in 1991 and improved in 2000. The rotating system is obtained from the latter by a change of space coordinates which does not modify the coordinate time. Therefore, the use of these two systems leads to the same results and one can select freely the one which is the more convenient for the application at hand. The use of either TT or TCG also leads to the same results if properly handled. In this text the formulae assume that TT (practically realized by $\mathrm{TT} = \mathrm{TAI} + 32.184\mathrm{s}$) is the coordinate time t.

When comparing the readings of distant clocks and their frequencies, the definition of coordinate synchronization and comparison requires the evaluation of the accumulated coordinate time during a transfer of time, either by the physical transportation of a clock or the transmission of a signal. A key quantity for clock A generating proper time τ_A is the ratio $d\tau_A/dt$, which is, in general, variable along the world line of the clock. Discussions of relativistic time comparisons appear in the *Explanatory Supplement* (Seidelmann 1992) and in Guinot (1997).

3.11.1 Clock Transport from a Rotating Reference Frame

When time is transferred from point P to point Q by means of a portable clock, it is convenient to use the rotating reference frame and to consider the potential $W(\mathbf{r})$, which includes the

potential of the Earth's rotational motion. The coordinate time accumulated during transport is

$$\Delta t = \int_P^Q \left[1 - \frac{\Delta W(\mathbf{r})}{c^2} + \frac{v^2}{2c^2}\right] d\tau + \frac{2\omega}{c^2} A_{\mathrm{E}} \tag{3.28}$$

where c is the speed of light, ω is the angular velocity of the Earth's rotation, v is the velocity of the clock with respect to the ground, $\mathbf{r}$ is a vector from the center of the Earth to the clock, which is moving from P to Q, A_{E} is the equatorial projection of the area swept out during the time transfer by the vector $\mathbf{r}$ as its terminus moves from P to Q, $\Delta W(\mathbf{r})$ is the potential difference between the location of the clock at $\mathbf{r}$ and the geoid as viewed from an Earth-fixed coordinate system with the convention that $\Delta W(\mathbf{r})$ is positive when the clock is above the geoid, and $d\tau$ is the increment of proper time accumulated on the portable clock. The increment of proper time is the time accumulated on the portable time standard as measured in the rest frame of the clock, i.e., the reference frame traveling with the clock. A_{E} is measured in an Earth-fixed coordinate system. As the area A_{E} is swept out, it is taken as positive when the projection of the clock's path on the equatorial plane is eastward. At the height h of the clock above the geoid of 20 km, the approximation of $\Delta W(\mathbf{r})$ by gh, where g is the total acceleration due to gravity (including the rotational acceleration of the Earth) evaluated at the geoid, leads to an error which may reach about 1×10^{-14} in relative frequency. For a better approximation, the potential difference $\Delta W(\mathbf{r})$ can be calculated to greater accuracy by

$$\begin{aligned}\Delta W(\mathbf{r}) = & -GM\left(\frac{1}{r} - \frac{1}{a_e}\right) - \frac{1}{2}\omega^2(r^2 \sin^2\theta - a_e^2) \\ & + \frac{J_2 G M_e}{2a_e}\left[1 + \left(\frac{a_3}{r}\right)^3 [3\cos^2\theta - 1]\right].\end{aligned} \tag{3.29}$$

In this equation a_e is the equatorial radius of the Earth, r is the magnitude of the vector $\mathbf{r}$, θ is the co-latitude, GM_e is the product of the Earth's mass and the gravitation constant, and J_2 is the quadrupole moment coefficient of the Earth ($J_2 = +1.083 \times 10^{-3}$). See also Klioner (1997) for an evaluation of $\Delta W(\mathbf{r})/c^2$ as a function of the altitude.

3.11.2 Non-rotating Local Inertial Reference Frame

When time is transferred from point P to Q by means of a clock, the coordinate time elapsed during the motion of the clock is

$$\Delta t = \int_P^Q \left[1 - \frac{V(\mathbf{r}) - U_g}{c^2} + \frac{v^2}{2c^2}\right] d\tau. \tag{3.30}$$

Here $V(\mathbf{r})$ is the potential at the location of the clock and v is the velocity of the clock, both as viewed—in contrast to the expression for clock transport in a rotating reference frame given in Eq. 3.28—from a geocentric non-rotating reference frame. U_g is the potential at the geoid, including the effect of the potential of the Earth's rotational motion. Note that $V(\mathbf{r})$ does not include the effect of the Earth's rotation and should include the tide generating potential of external bodies. This equation also applies to clocks in geostationary orbits, but should not be used beyond a distance of about 50 000 km from the center of the Earth.

3.11.3 Electromagnetic Signal Transfer from a Rotating Reference Frame

From the viewpoint of a geocentric, Earth-fixed, rotating frame, the coordinate time elapsed between emission and reception of an electromagnetic signal in vacuum is

$$\Delta t = \frac{1}{c}\int_P^Q \left[1 - \frac{\Delta V(\mathbf{r})}{c^2}\right] d\sigma + \frac{2\omega}{c^2} A_{\mathrm{E}} \tag{3.31}$$

where $d\sigma$ is the increment of standard length, or proper length, along the transmission path, and $\Delta V(\mathbf{r})$ is the potential at the point $\mathbf{r}$ on the transmission pass less the potential at the geoid, as viewed from an Earth-fixed coordinate system. A_E is the area circumscribed by the equatorial projection of the triangle whose vertices are at the center of the Earth, at the point of transmission of the signal P, and at the point of reception of the signal Q. The area A_E is positive when the signal path has an eastward component.

The second term amounts to about a nanosecond for a round-trip trajectory from the Earth to a geostationary satellite. In the third term, $2\omega/c^2 = 1.6227 \times 10^{-6}$ ns km^{-2}; this term can contribute hundreds of nanoseconds for practical values of A_E. The increment of proper length $d\sigma$ can be taken as the length measured using standard rigid rods at rest in the rotating system. This is equivalent to measurement of length by taking $c/2$ times the time (normalized to vacuum) of a two-way electromagnetic signal sent from P to Q along its transmission path.

3.11.4 Electromagnetic Signal Transfer from a Non-rotating, Local Inertial Frame

From the viewpoint of a geocentric non-rotating, local inertial frame, the coordinate time elapsed between emission and reception of an electromagnetic signal is

$$\Delta t = \frac{1}{c}\int_P^Q \left[1 - \frac{V(\mathbf{r}) - U_g}{c^2}\right] d\sigma \tag{3.32}$$

where $V(\mathbf{r})$ and U_g are defined as above, and $d\sigma$ is the increment of standard length, or proper length, along the transmission path.

REFERENCES

1. International Earth Rotation and Reference System Service: http://www.iers.org.
2. Bureau International des Poids et Mesures: http://www.bipm.fr.
3. International Telecommunications Union: http://www.itu.int/publications.
4. National Geospatial-Intelligence Agency Publications: http://msi.nga.mil/MSISiteContent/StaticFiles/NAV_PUBS/RNA/Pub117bk.pdf.
5. Global Navigation Satellite System: http://www.glonass-center.ru.
6. IAU Resolutions Adopted by the General Assemblies: http://www.iau.org/administration/resolutions/general_assemblies/.

Aoki, S., B. Guinot, G. H. Kaplan, H. Kinoshita, D. D. McCarthy, and P. K. Seidelmann (1982). The New Definition of Universal Time. *Astronomy and Astrophysics 105*, 359–361.

Audoin, C. and B. Guinot (2001). *The Measurement of Time*. Cambridge: Cambridge University Press.

BIPM (1956). *Proc.-Verb. Com. Int. Poids et Mesures*, Volume 25. BIPM.

BIPM (1967). *Proc.-Verb. Com. Int. Poids et Mesures*, Volume 35. BIPM.

BIPM (1970a). *Com. Cons. Déf. Seconde*, Volume 5. BIPM. reprinted in Time and Frequency: Theory and Fundamentals, Natl. Bur. Stand. (U.S.) Monograph 140 (Edited by B. E. Blair), Washington, D.C., U.S. Govt. Printing Office, 1974, 19-22.

BIPM (1970b). *Proc.-Verb. Com. Int. Poids et Mesures*, Volume 38. BIPM.

BIPM (1980). *Com. Cons. Déf. Seconde*, Volume 9. BIPM.

BIPM (2006). *The International System of Units (SI)* (8th ed.). BIPM and Online.

Bretagnon (2001). Private Communication.

Brouwer, D. (1952). A Study of the changes in the rate of rotation of the Earth. *Astronomical Journal 57*, 125–146.

Bureau International de l'Heure (1965). *Bulletin Horaire*, Volume 7. Bureau International de l'Heure.

Capitaine, N. (2000). Definition of the Celestial Ephemeris Pole and the Celestial Ephemeris Origin. In K. J. Johnston, D. D. McCarthy, B. J. Luzum, and G. H. Kaplan (Eds.), *Towards Models and Constants for Sub-Microarcsecond Astrometry*, pp. 153–163. U.S. Naval Observatory.

Capitaine, N., P. T. Wallace, and D. D. McCarthy (2003). Expressions for the Earth Rotation Angle and Sidereal Time consistent with the IAU 2000A precession-nutation model. *Astronomy and Astrophysics 406*, 1135–1149.

Clemence, G. M. (1948). On the system of astronomical constants. *Astronomical Journal 53*, 169–179.

Dowd, C. F. (1930). *A Narrative of His Services in Originating and Promoting the System of Standard Time*. New York: Knickerbocker Press. Edited by C. N. Dowd.

Egbert, G. D. and R. D. Ray (2000). Significant dissipation of tidal energy in the deep ocean inferred from satellite altimeter data. *Nature 405*, 775–778.

Essen, L. and J. V. L. Parry (1955). An Atomic Standard of Frequency and Time Interval: A Caesium Resonator. *Nature 176*, 280–282.

Essen, L., J. V. L. Parry, W. Markowitz, and R. G. Hall (1958). Variation in the Speed of Rotation of the Earth since June 1955. *Nature 181*, 1054.

Fairhead, L. and P. Bretagnon (1990). An Analytic Formula for the Time Transformation TB-TT. *Astronomy and Astrophysics 229*, 240–247.

Giacomo, P. (1981). News from the BIPM. *Metrologia 17*, 70.

Guinot, B. (1979). Basic Problems in the Kinematics of the Rotation of the Earth. In D. D. McCarthy and J. D. Pilkington (Eds.), *Time and the Earth's Rotation*, pp. 7–18. D. Reidel Publishing Company.

Guinot, B. (1989). General Principles of the Measure of Time: Astronomical Time. In J. Kovalevsky (Ed.), *Reference Frames for Astronomy and Geophysics*. Kluwer.

Guinot, B. (1995). Scales of Time. *Metrologia 31*, 431–440.

Guinot, B. (1997). International Report: Application of general relativity to metrology. *Metrologia 34*, 261–290.

Harada, W. and T. Fukushima (2003). Harmonic Decomposition of Time Ephemeris TE405. *Astronomical Journal 126*, 2557–2561.

Howse, D. (1997). *Greenwich Time and the Longitude*. London: Philip Wilson. pp. 65-78, 125-143.

IAU (1954). In P. T. Oosterhoff (Ed.), *Transactions of the International Astronomical Union*, Volume VIII, New York, pp. 66. Cambridge University Press. Proc. 8th General Assembly, Rome, 1952.

IAU (1960). In D. H. Sadler (Ed.), *Transactions of the International Astronomical Union*, Volume X, New York, pp. 72. Cambridge University Press. Proc. 10th General Assembly, Moscow, 1958.

IAU (1968). In L. Perek (Ed.), *Transactions of the International Astronomical Union*, Volume XIII B, Dordrecht, pp. 181. Reidel. Proc. 13th General Assembly, Prague, 1967.

IAU (1977). In E. A. Muller and A. Jappel (Eds.), *Transactions of the International Astronomical Union*, Volume XVI B, Dordrecht, pp. 60. Reidel. Proc. 16th General Assembly, Grenoble, 1977.

IAU (1980). In P. A. Wayman (Ed.), *Transactions of the International Astronomical Union*, Volume XVII B, Dordrecht, pp. 71. Reidel. Proc. 17th General Assembly, Grenoble, 1979.

IAU (1992). In J. Bergeron (Ed.), *Transactions of the International Astronomical Union*, Volume XXI B, Dordrecht, pp. 41–52. Reidel. Proc. 21th General Assembly, Beunos Aires, 1991.

IAU (2001). In H. Rickman (Ed.), *Transactions of the International Astronomical Union*, Volume XXIV B, Provo. Astronomical Society of the Pacific. Proc. 24th General Assembly, Manchester, 2000.

IAU (2008). In K. A. van der Hucht (Ed.), *Transactions of the International Astronomical Union*, Volume XXVI B, Cambridge. Cambridge University Press. Proc. 26th General Assembly, Prague, 2006.

IERS (1996). Conventions (1996). Technical Note 21, International Earth Rotation Service, Paris. Observatoire de Paris, D. D. McCarthy (Ed.).

IERS (2004). Conventions (2003). Technical Note 32, International Earth Rotation Service, Frankfurt am Main. Verlag des Bundsesants fur Kartographie und Geodesie, D. D. McCarthy and G. Petit (Eds.).

IERS (2010). Conventions (2010). Technical Note 36, International Earth Rotation and Reference Systems Service, Frankfurt am Main. Verlag des Bundsesamts für Kartographie und Geodäsie, G. Petit and B. Luzum (Eds.).

International Radio Consultative Committee (1963). Recommendation 374, Standard-Frequency and Time-Signal Emissions. In *Documents of the Xth Plenary Assembly Geneva, Switzerland*, Volume III, pp. 193. Geneva: International Telecommunication Union.

Irwin, A. W. and T. Fukushima (1999). A Numerical Time Ephemeris of the Earth. *Astronomy and Astrophysics 348*, 642–652.

ITU-R (1998). ITU-R Recommendations:Time Signals and Frequency Standards Emissions. Geneva. p. 15.

Jones, H. S. (1949). The Determination of Precise Time, 16th Arthur Lecture, 14 April 1949. In *Ann. Report Smithsonian Institution*, pp. 189–202.

Kaplan, G. (1981). The IAU Resolutions on Astronomical Constants, Time Scale and the Fundamental Reference Frame. Circular 163, US Naval Observatory, Washington, DC.

Klioner, S. (1992). The Problem of Clock Synchronization: A Relativistic Approach. *Celestial Mechanics and Dynamical Astronomy 53*, 81–109.

Kovalevsky, J. (1965). Astronomical Time. *Metrologia 1*, 169–180.

Lambeck, K. (1980). *The Earth's Variable Rotation*. Cambridge: Cambridge University Press.

Markowitz, W., R. G. Hall, L. Essen, and J. V. L. Parry (1958). Frequency of Cesium in Terms of Ephemeris Time. *Physical Review Letters 1*, 105–107.

McCarthy, D. D. (1991). Astronomical Time. *Proceedings of the IEEE 79*, 915–920.

McCarthy, D. D. (1998). The Julian and Modified Julian Dates. *Journal for the History of Astronomy 29*, 327–330.

McCarthy, D. D. and P. K. Seidelmann (2009). *Time—from Earth Rotation to Atomic Physics*. Weinheim, Germany: Wiley–VCH.

Munk, W. H. and G. J. F. MacDonald (1975). *The Rotation of the Earth*. Cambridge: Cambridge University Press. pp. 77-78.

Nelson, R. A., D. D. McCarthy, S. Malys, J. Levine, B. Guinot, H. F. Fliegel, R. L. Beard, and T. R. Bartholomew (2001). The leap second: its history and possible future. *Metrologia 38*, 509–529.

Newcomb, S. (1895). Tables of the Sun. *Astronomical Papers Prepared for the Use of the American Ephemeris and Nautical Almanac VI, Part I*, 9. U.S. Govt. Printing Office, Washington, D.C.

Petit, G. (2000). Report of the BIPM/IAU Joint Committee on relativity for space-time reference systems and metrology. In K. J. Johnston, D. D. McCarthy, B. J. Luzum, and G. H. Kaplan (Eds.), *Proceedings of IAU Colloquium 180*, Washington, D.C., pp. 275–282. US Naval Observatory.

Quinn, T., (Ed.) (2005). Special Issue: Fifty Years of Atomic Time-Keeping: 1955 to 2005. *Metrologia 42*(3).

Ramsey, N. F. (2005). History of early atomic clocks. *Metrologia 42*(3). Quinn, T. (Ed.).

Seidelmann, P. K. (Ed.) (1992). *Explanatory Supplement to The Astronomical Almanac*. Mill Valley, CA: University Science Books.

Seidelmann, P. K. and T. Fukushima (1992). Why New Time Scales. *Astronomy and Astrophysics 265*, 833–838.

Smith, H. M. (1976). Greenwich Time and the Prime Meridian. *Vistas in Astronomy 20*, 219–229.

Standish, E. M. (1998). Time Scales in the JPL and CfA Ephemerides. *Astronomy and Astrophysics 336*, 381–384.

Stephenson, F. R. and L. V. Morrison (1984). Long-term changes in the rotation of the Earth: 700 B.C. to A.D. 1980. *Philos. Trans. R. Soc. London A313*, 47–70.

Stephenson, F. R. and L. V. Morrison (1995). Long-Term Fluctuations in the Earth's Rotation: 700 BC to AD 1990. *Philos. Trans. R. Soc. London A351*, 165–202.

Terrien, J. (1968). News from the International Bureau of Weights and Measures. *Metrologia 4*, 43.

Terrien, J. (1971). News from the International Bureau of Weights and Measures. *Metrologia 7*, 43.

Terrien, J. (1975). News from the International Bureau of Weights and Measures. *Metrologia 11*, 180.

Vessot, R. F. C. (2005). The atomic hydrogen maser oscillator. *Metrologia 42*(3). Quinn, T. (Ed.).

Yoder, C. F., J. G. Williams, J. O. Dickey, B. E. Schutz, R. J. Eanes, and B. D. Tapley (1983). Secular variation of Earth's gravitational harmonic J_2 coefficient from Lageos and non-tidal acceleration of Earth rotation. *Nature 303*, 757–762.

CHAPTER 4

The Fundamental Celestial Reference System

GEORGE H. KAPLAN

4.1 Summary

Reference data for positional astronomy, such as the data in astrometric star catalogs or barycentric planetary ephemerides, are now specified within the International Celestial Reference System (ICRS). The ICRS is a coordinate system whose origin is at the solar system barycenter and whose axis directions are effectively defined by the adopted coordinates of an ensemble of extragalactic radio sources determined by long-baseline radio interferometry. These radio sources (quasars and active galactic nuclei) are assumed to have no observable intrinsic angular motions. Thus, the ICRS is a "space-fixed" system (more precisely, a kinematically non-rotating system) without an associated epoch. However, the ICRS closely matches the conventional dynamical system defined by the Earth's mean equator and equinox of J2000.0; the alignment difference is at the 0.02 arcsecond level, negligible for many applications. The ICRS replaced the FK5 as the IAU-recommended fundamental astronomical reference system in 1998.

Strictly speaking, the ICRS is somewhat of an abstraction, a set of coordinate directions that perfectly satisfies a list of criteria. The list of radio source positions that define it for practical purposes is called the International Celestial Reference Frame (ICRF), now in its second generation. In the terminology that is now commonly used, a *reference system* like the ICRS is "realized" by a *reference frame* like the ICRF, and there can be more than one such realization. In the case of the ICRS, there is, in fact, a lower-accuracy realization for work at optical wavelengths, called the Hipparcos Celestial Reference Frame (HCRF). The HCRF is composed of the positions and proper motions of the astrometrically well-behaved stars in the Hipparcos Catalogue.

Astrometric data referred to the ICRS are becoming more common, with new catalogs now available in the optical, infrared, and radio.

The ICRS defines the spatial orientation of the Barycentric Celestial Reference System, which incorporates the relativistic metric specified in IAU resolution B1.3 of 2000 for solar system barycentric coordinate systems.

4.2 The ICRS, the ICRF, and the HCRF

The fundamental celestial reference system for astronomical applications is now the International Celestial Reference System (ICRS), as provided in IAU resolution B2 of 1997 (IAU 1999; URL[4]). The ICRS is a coordinate system with its origin at the solar system barycenter and axis directions that are fixed with respect to distant objects in the universe; it is to be

used to express the fundamental positions and motions of stars, planets, and other celestial objects. Unlike geocentric or topocentric systems that are used for expressing the apparent directions of celestial objects for observational purposes (see Chapter 7), the ICRS is a system in which the equations of motion of these objects are relatively simple (it is close to being a locally inertial system), and is, therefore, suitable for basic reference data, such as star catalogs or barycentric planetary ephemerides derived from numerical integration. The ICRS has replaced the previous FK5 system but is consistent with it to within the FK5's errors.

The specifications for what became the ICRS were established by IAU working groups in the late 1980s and early 1990s, and most particularly in IAU resolution A2 of 1991 (Recommendations VI and VII) (IAU 1992; URL[4]). These specifications can be summarized as follows:

- Origin at solar system barycenter
- Defining objects are unresolved, stationary, and stable extragalactic radio sources (i.e., with minimal structural variations), including a large proportion with "well identified optical counterparts"
- Positions of defining objects determined by long baseline radio interferometry
- Direction of axes are fixed in space—do not rotate with respect to defining objects
- To be "as near as possible" to system defined by the Earth mean equator and equinox of J2000.0 and to the FK5
- Independent of time and specific realizations (if the objects that define it eventually are changed)

The relativistic basis of the ICRS is that of the Barycentric Celestial Reference System (BCRS) as defined by IAU resolution B1.3 of 2000 (IAU 2001; URL[4]), which is described in Chapter 2 of this book. Strictly speaking, according to IAU resolution 2 (recommendation 2) of 2006 (IAU 2008), the ICRS is the spatial orientation of the BCRS, and as such its axes are *kinematically non-rotating* (see § 2.6.3). Because the ICRS and BCRS are so closely linked, the two terms are often used interchangeably. The two terms refer to different aspects of the fundamental barycentric reference system and are not, therefore, independent. A simple way of understanding the connection is that BCRS vectors are expressed with respect to the ICRS spatial axes and ICRS data are based on the BCRS metric.

To establish the ICRS as a practical system, in 1997 the IAU specified a set of distant benchmark objects, observable at radio wavelengths, whose adopted coordinates effectively define the directions of the ICRS axes. This first "realization" of the ICRS, called the International Celestial Reference Frame (ICRF or, now, ICRF1), is a set of high accuracy positions of extragalactic radio sources measured by Very Long Baseline Interferometry (VLBI) (Ma and Feissel 1997; Ma et al. 1998). In 2009, the IAU replaced the original list of sources and coordinates with a revised and enlarged list (Ma et al. 2009), referred to as ICRF2. The ICRS is realized at optical wavelengths—but at lower accuracy—by the Hipparcos Celestial Reference Frame (HCRF), consisting of the *Hipparcos Catalogue* (ESA 1997) of star positions and motions, with certain exclusions (IAU 2001, res. B1.2). The areal density of the two ICRS realizations is quite different: the ICRF2 consists of about 3400 radio sources, while the HCRF contains about 100,000 stars. The coordinates of the ICRF radio

sources and HCRF stars are given relative to the ICRS origin at the solar system barycenter, and a number of transformations are required to obtain the coordinates that would be observed from a given location on or near the Earth at a specific date and time; see Chapter 7. [1]

Although the directions of the ICRS coordinate axes are not defined by the kinematics of the Earth, the ICRS axes (as implemented by the ICRF1, ICRF2, and HCRF) closely approximate the axes that would be defined by the mean Earth equator and equinox of J2000.0 (to within about 0.02 arcsecond), if the latter is considered to be a barycentric system. Because the ICRS axes are meant to be "space fixed", i.e., kinematically non-rotating, there is no date associated with the ICRS. Furthermore, since the defining radio sources are assumed to be so distant that their angular motions, seen from Earth, are negligible, there is no epoch associated with the ICRF. It is technically incorrect, then, to say that the ICRS is a "J2000.0 system", even though for many current data sources, the directions in space defined by the equator and equinox of J2000.0 and the ICRS axes are the same to within the uncertainties of the data.

The IAU Working Group on Nomenclature for Fundamental Astronomy (URL[1]), which worked from 2003 to 2006, recommended the following definitions for the ICRS and ICRF:

International Celestial Reference System (ICRS): The idealized barycentric coordinate system to which celestial positions are referred. It is kinematically non-rotating with respect to the ensemble of distant extragalactic objects. It has no intrinsic orientation, but was aligned close to the mean equator and dynamical equinox of J2000.0 for continuity with previous fundamental reference systems. Its orientation is independent of epoch, ecliptic or equator and is realized by a list of adopted coordinates of extragalactic sources.

International Celestial Reference Frame (ICRF): A set of extragalactic objects whose adopted positions and uncertainties realize the ICRS axes and give the uncertainties of the axes. It is also the name of the radio catalog whose 212 defining sources are currently the most accurate realization of the ICRS. Note that the orientation of the ICRF catalog was carried over from earlier IERS radio catalogs and was within the errors of the standard stellar and dynamic frames at the time of adoption. Successive revisions of the ICRF are intended to minimize rotation from its original orientation. Other realizations of the ICRS have specific names (e.g., Hipparcos Celestial Reference Frame).

As previously noted, the ICRF has been superseded by the ICRF2; there are now 295 defining sources.

The Astronomical Almanac lists the coordinates of the defining radio sources for the ICRF2 in Section H. By definition, then, these coordinates are expressed in the ICRS. The barycentric position and velocity vectors of the Earth given in Section B and the Earth-Sun vectors given in Section C are also in the ICRS. Most quantities in *The Astronomical Almanac* are geocentric and are given with respect to an equator-of-date system (see § 4.3), but the fundamental data from which those tabulations are computed are inherently ICRS.

1. Observations taken from or near the Earth are expressed in the Geocentric Celestial Reference System (GCRS). The GCRS is described in Chapter 2, as is the transformation between the BCRS and GCRS. The standard algorithms for computing geocentric "apparent places" of stars or planets, described in Chapter 7, incorporate the BCRS-to-GCRS transformation.

The ICRS, with its origin at the solar system barycenter and "space fixed" axis directions, is meant to represent the most appropriate coordinate system currently available for expressing reference data on the positions and motions of celestial objects.

4.3 Background: Reference Systems and Reference Frames

The terminology that has become standard over the past decade or so distinguishes between a *reference system* and a *reference frame*. A reference system is the complete specification of how a celestial coordinate system is to be formed. Both the origin and the orientation of the fundamental planes (or axes) are defined. A reference system also incorporates a specification of the fundamental models needed to construct the system; that is, the basis for the algorithms used to transform between observable quantities and reference data in the system. A reference frame, on the other hand, consists of a set of identifiable fiducial points on the sky along with their coordinates, which serves as the practical realization of a reference system.

For example, the fundamental plane of an astronomical reference system has conventionally been the extension of the Earth's equatorial plane, at some date, to infinity. *Declination* is the angular distance north or south of this plane, and *right ascension* is the angular distance measured eastward along the equator from some defined reference point (see Fig. 4.1). This reference point, the right ascension origin, has traditionally been the *equinox*: the point at which the Sun, in its yearly circuit of the celestial sphere, crosses the equatorial plane moving from south to north. The Sun's apparent yearly motion lies in the *ecliptic*, the plane of the Earth's orbit. The equinox, therefore, is a direction in space along the nodal line defined by the intersection of the ecliptic and equatorial planes; equivalently, on the celestial sphere, the equinox is at one of the two intersections of the great circles representing these planes. Because both of these planes are moving, the coordinate systems that they define must have a date associated with them; such a reference system must therefore be specified as "the equator and equinox of (some date)".

Of course, such a reference system is an idealization, because the theories of motion of the Earth that define how the two planes move are imperfect. In fact, the very definitions of these planes are problematic for high precision work. Even if the fundamental planes of a reference system are defined without any connection to the motions of the Earth, there is no way magically to paint them on the celestial sphere at any particular time. Therefore, in practice, we use a specific reference frame—a set of fiducial objects with assigned coordinates—as the practical representation of an astronomical reference system. The scheme is completely analogous to how terrestrial reference systems are established using survey control stations (geodetic reference points) on the Earth's surface.

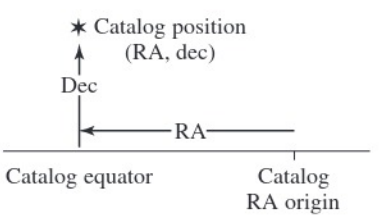


Figure 4.1 Celestial coordinates of objects in a catalog are expressed with respect to the catalog equator and right ascension origin, which generally are close approximations to the mean Earth equator and equinox at some date (e.g., J2000.0). Conversely, the tabulated coordinates of all the objects in a catalog define, in an average sense, the location of the catalog equator and equinox on the sky.

Most commonly, a reference frame consists of a catalog of precise positions (and motions, if measurable) of stars or extragalactic objects, as seen from the solar system barycenter at a specific epoch. That epoch is now usually "J2000.0", which is 12^h TT (or TDB) on 1 January 2000. Each object's instantaneous position, expressed as right ascension and declination, indicates the object's angular distance from the catalog's equator and origin of right ascension. (A catalog's right ascension origin was formerly referred to as the *catalog equinox*, a now-obsolete term.) Therefore, any two such objects in the catalog—if they are not coincident or antipodal—uniquely orient a spherical coordinate system on the sky—a reference frame.

To be useful, a reference frame must be implemented at the time of actual observations, and this requires the computation of the apparent coordinates of the catalog objects at arbitrary dates and times. Astrometric star catalogs list *proper motions*, which are the projection of each star's space motion onto the celestial sphere, expressed as an angular rate in right ascension and declination per unit time (usually now milliarcseconds/year). For stars or other galactic objects, the proper motions allow the reference frame to be established at epochs other than that of the positions listed in the catalog.

The positions of solar system objects can also be used to define a reference frame. For each solar system body involved, an *ephemeris* (plural *ephemerides*) is used, which is simply a table of the celestial coordinates of the body as a function of time (or an algorithm that yields such a table). A reference frame defined by the ephemerides of one or more solar system bodies is called a *dynamical reference frame*. Because the ephemerides used incorporate the motion of the Earth as well as that of the other solar system bodies, dynamical reference frames embody in a very fundamental way the moving equator and ecliptic, hence the equinox. They have, therefore, been used to correct the orientation of star catalog reference frames (the star positions were systematically adjusted) on the basis of simultaneous observations of stars and planets. In a sense, the solar system is used as a gyrocompass. However, dynamical reference frames are not very practical for establishing a coordinate system for day-to-day astronomical observations, because the sky density of solar system objects is low, many are resolved, and they tend to be clustered near the ecliptic plane.

Descriptions of reference frames and reference systems often refer to three coordinate axes, which are simply the set of right-handed cartesian axes that correspond to the usual celestial spherical coordinate system. The xy-plane is the equator, the z-axis points toward the north celestial pole, and the x-axis points toward the origin of right ascension. Although in principle this allows us to specify the position of any celestial object in rectangular coordinates, the distance scale (based on stellar parallaxes) is not established to high precision beyond the solar system. What a reference system actually defines is the way in which the two conventional astronomical *angular* coordinates, right ascension and declination, relate to real observable points in the sky.

4.4 The Effect of Catalog Errors on Reference Frames

A modern astrometric catalog contains data on a large number of objects (N), so the coordinate system it defines is vastly overdetermined. The quality of the reference frame provided by a catalog depends on the extent to which the coordinates of all possible pairs of objects ($\approx N^2/2$) serve to define the identical equator and right ascension origin, within the expected random errors. Of course, in practice, the catalog's equator and right ascension origin

are effectively defined by averages over the objects that are used for a specific application. Therefore, random errors in the coordinates of the selected objects limit the accuracy with which the reference frame approximates the intended reference system for the particular application; generally, the accuracy will be proportional to the square root of the number of objects used.

However, the positions listed in catalogs also may contain systematic errors, which are errors in the coordinates that are similar for objects that are in the same area of the sky, or are of the same magnitude (flux) or color (spectral index). Systematic errors in position mean that the reference frame is warped, or is effectively different for different classes of objects. Systematic errors do not obey square-root-of-n statistics, and may be unrecognized, so they tend to be more pernicious in effect than random errors. Obviously, minimizing systematic errors, when a catalog is constructed, is at least as important as minimizing the random errors, although much more difficult.

Typical applications of reference frames involve sets of astronomical observations taken at various dates. To establish a reference frame based on stars or other galactic objects at the dates of the observations, the proper motions in the catalog must be used to update the positions. The accuracy of the proper motions in the catalog largely determines how well the reference frame can be established for dates that are many years beyond (or prior to) the catalog's epoch. Because the tabulated proper motions are never perfect, any celestial reference frame based on galactic objects deteriorates with time. Just as for the positions, errors in proper motion can be both random and systematic.

Random errors in proper motion will naturally result from the random errors in the measurements of an object's positions at various epochs (see Fig. 4.2), but they can also result from an incomplete model of the object's motion. Many stars are components of binary or multiple systems. Ideally, the catalog's proper motion should reflect the linear space motion of the center of mass of the system, and the orbit of the star about that center of mass would then have to be taken into account as part of the computation of the star's position for any arbitrary date. Alternatively, stars may be listed with second- or higher-order terms in their motion (as in the Hipparcos Catalogue). However, in practice, a relatively small number of binary systems have well determined orbits, or are even recognized as such. The orbital motion of many stars is unknown and contaminates their measured proper motion (see Makarov and Kaplan (2005) and references therein). This is especially true of catalogs based on a relatively short time span of observations, where the slight curvature of the star's path may be less than the observational uncertainty. Undersampling of short-period binary orbits has a similar effect. A related problem arises from measurements of the positions of the blended images of binaries that are unresolved to the instrument(s) used in a catalog's construction. However, such binaries may be resolved with other instruments, or the blended image may appear displaced at other wavelength bands if the two stars are of different colors. For the individual stars involved, such modeling or observational problems would be considered systematic errors, although the net effect of many such errors on the reference frame as a whole would be random.

Additionally, there may be systematic errors in a catalog's proper motions. If the causes of the systematic errors in position are time-dependent, then the proper motions will also be corrupted. Systematic errors in the proper motions can produce time-dependent warpings and spurious rotations of the frame. Therefore, the accuracy and consistency of the proper motions are critical to the overall quality, utility, and longevity of reference frames defined by stars.

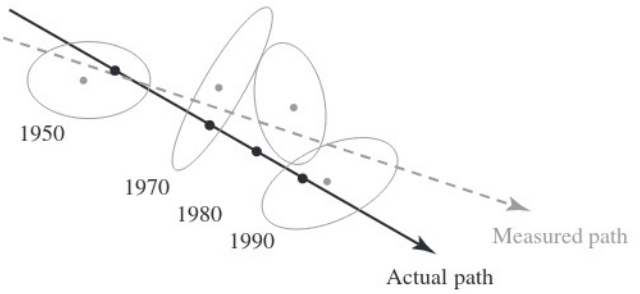


Figure 4.2 The true path of a star (black line), with its positions at several epochs marked. The measured positions of the star (gray points) on the same dates are also shown, with their error ellipses. The catalog proper motion of the star (which determines its computed path across the sky) derived from these measurements is in error; therefore, the predicted positions of the star will deteriorate in accuracy with time. Since all the stars in a catalog share this problem to some extent, the reference frame that the catalog defines slowly degrades. If the proper motion errors have systematic trends across the sky, the catalog's reference frame may develop warps or exhibit a small, spurious net rotation.

Even reference frames defined by extragalactic objects, which are usually considered to have zero proper motion (i.e., unmeasurably small), may deteriorate because many of these objects show small apparent motions at radio wavelengths that are artifacts of their emission mechanisms. Furthermore, if an object is even partially resolved, observations at wavelengths other than that used in the construction of the catalog may show an image center displaced from the catalog's position, arising from a color or spectral index gradient across the image. The variable radio flux and image structure of these objects may mean that some of them eventually must be replaced as reference frame benchmarks.

4.5 Late 20th Century Developments

The establishment of celestial reference systems is coordinated by the IAU. The previous astronomical reference system was based on the equator and equinox of J2000.0 determined from observations of planetary motions, together with the IAU (1976) System of Astronomical Constants and related algorithms (Kaplan 1982). The reference frame that embodied this system for practical purposes was the Fifth Fundamental Catalogue (FK5). The FK5 is a catalog of 1535 bright stars (to magnitude 7.5), supplemented by a fainter extension of 3117 additional stars (to magnitude 9.5), compiled at the Astronomische Rechen-Institut in Heidelberg and the U.S. Naval Observatory in Washington, DC (Fricke et al. 1988; Fricke et al. 1991). The FK5 was the successor to the FK3 and FK4 catalogs, all of which were based on meridian observations taken in the visual band—many such observations were, in fact, taken by eye. The formal uncertainties in the star positions of the FK5 at the time of its publication in 1988 were about 30–40 milliarcseconds over most of the sky, but the errors are considerably worse when systematic trends are taken into account.

Beginning in the 1970s, the most precise wide-angle astrometry was conducted, not in the optical regime, but at radio wavelengths, involving the techniques of Very Long Baseline Interferometry (VLBI) and pulsar timing. Uncertainties of radio source positions listed in all-sky VLBI catalogs are now typically less than one milliarcsecond, and often a factor of ten better. Furthermore, because these radio sources are very distant extragalactic objects (mostly optically faint quasars) that are not expected to show measurable intrinsic motion, a reference frame defined by VLBI positions should be "more inertial" (less subject to spurious rotation) than a reference frame defined by galactic objects, such as stars or pulsars. The origin of right ascension in VLBI catalogs is somewhat arbitrary, because VLBI has little sensitivity to the ecliptic plane and the location of the equinox is not easily determined. The VLBI origin of right ascension has effectively been carried over from one catalog to the next; it was originally based on the right ascension of the source 3C 273B based on lunar occultations.

Because of the accuracy and stability of radio reference frames, since the mid 1980s, astronomical measurements of the Earth's rotation—from which universal time (UT1) is determined—have depended heavily on VLBI, with classical methods based on star transits being phased out. Hence, the situation evolved to where the definition of the fundamental astronomical reference frame (the FK5) became irrelevant to some of the most precise and important astrometric measurements. VLBI revealed, in addition, that the models of the Earth's precession and nutation that were part of the old system were inadequate for modern astrometric precision. In particular, the "constant of precession"—a measurement of the long-term rate of change of the orientation of the Earth's axis in space—had been overestimated by about 0.3 arcsecond/century. Moreover, the success of the European Space Agency's Hipparcos astrometric satellite, launched in 1989, promised to provide a new, very accurate set of star coordinates in the optical regime.

Thus, beginning in 1988, a number of IAU working groups began considering the requirements for a new fundamental astronomical reference system (Lieske and Abalakin 1990; Hughes, Smith, and Kaplan 1991). The resulting series of IAU resolutions, passed in 1991, 1994, 1997, and 2000 (IAU 1992, 1996, 1999, 2001; URL[4]), effectively form the specifications for the ICRS. The axes of the ICRS are defined by the adopted positions of a specific set of extragalactic objects, which are assumed to have no measurable proper motions. The ICRS axes are consistent, to about 0.02 arcsecond, with the equator and equinox of J2000.0 defined by the dynamics of the Earth. However, the ICRS axes are meant to be regarded as fixed directions in space that have an existence independent of the dynamics of the Earth or the particular set of objects used to define them at any given time.

Feissel and Mignard (1998) have written a concise review of the ICRS adoption and its implications. Seidelmann and Kovalevsky (2002) published a broader review of the ICRS and the new IAU Earth orientation models.

The promotion, maintenance, extension, and use of the ICRS are the responsibilities of IAU Division I (Fundamental Astronomy).

4.6 ICRS Implementation

4.6.1 The Defining Extragalactic Frame

The International Celestial Reference Frame (ICRF or ICRF1) is a catalog of positions of 608 extragalactic radio sources observed with VLBI, all strong (> 0.1 Jy) at S and X bands

(wavelengths 13 and 3.6 cm) (Ma and Feissel 1997; Ma et al. 1998; URL[2]). The catalog was adopted by the IAU in 1997 as the primary realization of the ICRS. Most of the sources in the catalog have faint optical counterparts (typically $m_V \gg 18$) and the majority are quasars. Of these objects, 212 are *defining sources* that establish the orientation of the ICRS axes, with origin at the solar system barycenter. Typical position uncertainties for the defining sources are of order 0.5 milliarcsecond; the orientation of the axes is defined from the ensemble to an accuracy of about 0.02 milliarcsecond. As described in § 4.6.4, these axes correspond closely to what would conventionally be described as "the mean equator and equinox of J2000.0".

The International Earth Rotation and Reference Systems Service (IERS) monitors the radio sources involved in the ICRF. This monitoring is necessary because, at some level, most of the sources are variable in both flux and structure and the centers of emission can display spurious motions, which may not be linear or constant (see discussion in Ma et al. (1998), Section 8). As a result of additional observations and analysis, ICRF Extensions 1 and 2 were developed (Fey et al. 2004); the positions of the non-defining sources were improved and new sources were added. The positions of the 212 defining sources were left unchanged.

By 2006, it was recognized that a major update of the ICRF was needed to maintain the accuracy and fixed orientation of the overall frame, and an IAU working group was established to update the list of sources and coordinates. The working group presented a revised and extended list of sources and coordinates. The new list was adopted by the IAU in 2009 as the "Second Realization of the International Celestial Reference Frame," or ICRF2 (Ma et al. 2009; URL[2]) superseding the original in defining the spatial orientation of the ICRS at S and X bands. The ICRF2 has 295 defining sources, chosen from a solution for the positions of 3414 sources. Only 97 of the defining sources are also defining sources in ICRF1, reflecting the results of the ongoing analysis of source stability and the working group's goal of mitigating source position variations. The positional uncertainties have been reduced considerably and the new list is more evenly distributed across the sky, especially in the south. Typical ICRF2 defining source position errors, all things considered, are not expected to exceed 0.1 milliarcseconds; the "noise floor" is 0.040 milliarcseconds. The overall orientation of the axes is estimated to be stable within 0.010 milliarcseconds and is consistent with that of ICRF1.

4.6.2 The Frame at Optical Wavelengths

The ICRS is realized at optical wavelengths by a subset of the Hipparcos Catalogue of 118,218 stars, some as faint as visual magnitude 12 (ESA 1997). Only stars with uncomplicated and well-determined proper motions (e.g., no known binaries) are used for the ICRS realization. This subset, referred to as the Hipparcos Celestial Reference Frame (HCRF), comprises 85% of the stars in the Hipparcos Catalogue.[2] Hipparcos star coordinates and proper motions are given within the ICRS coordinate system, but are listed for epoch J1991.25. (That is, the catalog effectively represents a snapshot of the positions and motions of the stars taken on 2 April 1991, a date that is near the mean epoch of the Hipparcos observations.) At the catalog epoch, Hipparcos uncertainties for stars brighter than 9th magnitude have median values somewhat better than 1 milliarcsecond in position and 1 milliarcsecond/year in proper

2. The HCRF excludes the stars in the Hipparcos Catalogue with astrometric solutions flagged C, G, O, V, or X.

motion (ESA 1997; Mignard 1997). The overall alignment to the ICRF at that epoch is estimated to be within 0.6 milliarcsecond, with any spurious rotations or distortions less than 0.25 milliarcsecond/year. Projected to epoch 2010, typical position errors for the brighter Hipparcos stars are approximately 20 milliarcseconds.

A major reanalysis of the original Hipparcos observations (van Leeuwen 2007a; van Leeuwen 2007b) has resulted in a new Hipparcos Catalogue with substantially improved astrometric data. However, the IAU has not taken any action that officially replaces the original Hipparcos Catalogue as the basis for the HCRF.

Extensions of the ICRS to fainter magnitudes are described in § 4.6.5.

4.6.3 Standard Algorithms

Chapters 2, 3, 6, and 7 of this book describe algorithms appropriate for use of data referred to the ICRS. The IAU has provided specific guidance in two areas: the relativistic bases for the reference systems (including timescales) and the models for the orientation of the Earth.

The 2000 IAU resolutions provide the relativistic metric tensors for the Barycentric Celestial Reference System (BCRS) and the Geocentric Celestial Reference System (GCRS), as well as expressions for the transformation between the two systems; see Chapter 2 and IAU (2001). These resolutions also define the coordinate times of these systems and the relation connecting them; see Chapter 3. IAU resolution 2 of 2006 (IAU 2008) provides that the orientation of the BCRS axes be understood to be that of the ICRS/ICRF (now ICRF2).

In 2000 and 2006, the IAU also adopted new models for the computation of the Earth's instantaneous orientation, which affect the analysis of VLBI observations that are used to define and maintain the ICRS, as well as the calculation of various observable quantities from ICRS-compatible reference data. The new models include what is now referred to as the *IAU 2006/2000A precession-nutation model*, a new definition of the celestial pole, and two new reference points in the equatorial plane for measuring the rotational angle of the Earth around its instantaneous axis. These algorithms are described in Chapter 6 of this book and in the IERS Conventions (IERS 2010). A detailed explanation of the resolutions and their implementation is also found in Kaplan (2005).

The new Earth orientation models are, of course, relevant only to fundamental observations made from the surface of the Earth. Astrometric observations taken from space platforms, or those that are differential in nature (based on reference objects all located within a small field), do not use these models. However, there are other effects that must be taken into account in analyzing astrometric observations—e.g., proper motion, parallax, aberration, and gravitational light-bending—and algorithms for these may be found in Chapter 7 of this book and in Volumes 1 and 3 of the Hipparcos Catalogue documentation (ESA 1997). For analysis of very high accuracy observations from space, see the development by Klioner (2003).

4.6.4 Relationship to Other Systems

The orientation of the ICRS axes is consistent with the equator and equinox of J2000.0 represented by the FK5, within the errors of the latter. See Feissel and Mignard (1998) for a short discussion. Systematically, the FK5 equator is tilted by 22 milliarcseconds and its origin of right ascension is offset by 23 milliarcseconds with respect to the ICRS. But the

uncertainties of the FK5 equator and right ascension system with respect to the dynamical equator and equinox of J2000.0 are 50 and 80 milliarcseconds, respectively. Because, at J2000.0, the errors of the FK5 are significantly worse than those of Hipparcos, the ICRS (as realized by the HCRF) can be considered to be a refinement of the FK5 system (ESA 1997) at (or near) that epoch. For a more complete discussion of FK5 errors, see Mignard and Frœschlé (2000).

The ICRS can also be considered to be a good approximation (at least as good as the FK5) to the conventionally defined dynamical equator and equinox of J2000.0 (Feissel and Mignard 1998), if the latter system is considered to be barycentric. This follows from the IAU resolution passed in 1991 (IAU (1992), described in § 4.2) that provided the original specifications for the new fundamental astronomical reference system based on extragalactic objects—what became the ICRS. In fact, the equator is well determined fundamentally from the VLBI observations that are the basis for the ICRS, and the ICRS pole is within 20 milliarcseconds of the dynamical pole.[3] The zero point of VLBI-derived right ascensions is arbitrary, but traditionally has been set by assigning to the right ascension of source 3C 273B a value derived from lunar occultation timings—the Moon's ephemeris thus providing an indirect link to the dynamical equinox.[4] The ICRS origin of right ascension was made to be consistent with that in a group of VLBI catalogs previously used by the IERS, each of which had been individually aligned to the lunar occultation right ascension of 3C 273B. The difference between the ICRS origin of right ascension and the dynamical equinox has been independently measured by two groups that used different definitions of the equinox, but in both cases the difference found was less than 0.1 arcsecond.

Because of its consistency with previous reference systems, implementation of the ICRS will be transparent to any applications with accuracy requirements of no better than 0.1 arcseconds near epoch J2000.0. That is, for applications with modest accuracy requirements, the distinctions between the ICRS, FK5, and dynamical equator and equinox of J2000.0 are not significant.

4.6.5 Data in the ICRS

Although the ICRF2 and HCRF are its basic radio and optical realizations, the ICRS is gradually being extended to fainter magnitudes and other wavelengths. Thus, an increasing amount of fundamental astronomical data is being brought within the system. A number of projects for the densification of the ICRS have been completed or are in progress.

As described above, the ICRF2 consists of the adopted positions of 3414 extragalactic radio sources, less than a tenth of which are defining sources. Because all of the observational data were part of a common catalog solution, the adopted coordinates of all the sources are

3. The reason that the ICRS pole is not perfectly aligned with the dynamical pole is complex. The ICRF was created from almost 20 years of VLBI observations from which a grand solution was made for the directions to the extragalactic radio sources and the changing position of the celestial pole. A specific decision made in that analysis resulted in an offset of the ICRF (hence ICRS) pole at J2000.0. With respect to the ICRS X and Y axes, the dynamical mean pole of J2000.0 has coordinates on the unit sphere, in milliarcseconds, of approximately $(-16.6, -6.8)$.

4. The original right ascension value, with respect to the equinox of 1950.0, was given by Hazard et al. (1971); the equivalent value in the J2000.0 system was first computed by Kaplan et al. (1982).

in the ICRS. The non-defining sources tend to have positional uncertainties that are larger than those of the defining sources. Many of the non-defining sources are part of the VLBA Calibrator Survey (described below) and have a very limited observational base—1966 of them were observed in only one session. Thus their long-term stability has not been evaluated.

The VLBA Calibrator Survey is a list of radio sources, with positions in the ICRS, to be used as calibrators for the Very Long Baseline Array and the Very Large Array. The original list was prepared by Beasley et al. (2002); the list has been extended several times and the current version is known as VCS6 (Petrov et al. 2008). The ICRS is also being established at higher radio frequencies (8, 24, 32, and 43 GHz); see, e.g., Jacobs et al. (2005); Jacobs and Sovers (2008); Fey et al. (2009).

In the optical regime, the Tycho-2 Catalogue (Høg et al. 2000) (which supersedes the original Tycho Catalogue and the ACT Reference Catalog) combines a re-analysis of the Hipparcos star mapper observations with data from 144 ground-based star catalogs. The ground-based catalogs include the Astrographic Catalogue (AC), a large photographic project carried out near the beginning of the 20th century, involving 20 observatories worldwide. Tycho-2 contains 2,539,913 stars, to about magnitude 12, and combines the accuracy of the recent Hipparcos position measurements with proper motions derived from a time baseline of almost a century. Proper motion uncertainties are 1–3 milliarcseconds/year. The epoch J2000.0 Tycho-2 positions of stars brighter than 9th magnitude are typically in error by 20 milliarcseconds. However, the positional accuracy degrades quite rapidly for magnitudes fainter than 9, so that 12th magnitude stars generally have a median J2000.0 position error exceeding 100 milliarcseconds.

Also in the optical band, the U.S. Naval Observatory CCD Astrograph Catalog (UCAC) provides ICRS-compatible positions and proper motions for 100 million stars over the entire sky as faint as red magnitude 16. See Zacharias et al. (2010) for information on the third release of UCAC data; the fourth and final version is anticipated in 2012. The accuracy of the UCAC4 coordinates near epoch 2000 is estimated to be in the 15–100 milliarcsecond range, depending on magnitude. Proper motion errors are about 1–3 milliarcseconds/year for stars to 12th magnitude, and up to 10 milliarcseconds/year for fainter stars to 16th magnitude. Observations have begun for a successor catalog, URAT, which will go deeper, to red magnitude 17.5, and will be tied directly to the ICRF2 using the optical counterparts of some of the radio sources defining that frame.

The Large Quasar Reference Frame (LQRF) (Andrei et al. 2009) is another representation of the ICRS at faint optical magnitudes. It contains the coordinates of 100,165 quasars, well distributed around the sky, accurate to about 100 milliarcseconds.

The ICRS has been extended to the near infrared through the Two Micron All Sky Survey (2MASS) (Cutri et al. 2003; Zacharias et al. 2005). This ground-based program provides positions for 471 million point sources, most of which are stars, observed in the J, H, and K_s infrared bands. 2MASS is a single epoch survey without proper motions; positions are listed for J2000.0, which is within the 4-year span of observations. Astrometric accuracy is around 80 milliarcseconds in the K_s magnitude range 9–14, with larger errors at both brighter and fainter magnitudes.

The Jet Propulsion Laboratory DE405/LE405 planetary and lunar ephemerides (usually just referred to as DE405) (Standish 1998) have been aligned to the ICRS. These ephemerides

provide the positions and velocities of the planets, Pluto, and the Moon with respect to the solar system barycenter, in rectangular coordinates. The data are represented in Chebyshev series form, and Fortran subroutines are provided to read and evaluate the series for any date and time. DE405 spans the years 1600 to 2200; a long version, DE406, spans the years −3000 to +3000 with lower precision. See Chapter 8 for further details. More recent ephemerides from JPL, such as DE421, are also aligned to the ICRS, as are fundamental planetary ephemerides from the Institute of Applied Astronomy (IAA) in Russia and Institut de Mécanique Céleste et de Calcul des Éphémérides (IMCCE) in France. For a review and comparison of the JPL, IAA, and IMCCE ephemerides, see the papers from Session 2 of the Journées 2010 conference proceedings (URL[5]).

As previously noted, the barycentric data tabulated in *The Astronomical Almanac* are in the ICRS; this began with the 2003 edition. Planetary and lunar ephemerides are derived from DE405/LE405. *The Astronomical Almanac* for 2006 is the first edition fully to support the new ICRS-related algorithms, including the new IAU Earth rotation models. Geocentric coordinates are given, therefore, with respect to the GCRS.

4.7 Formulae

A matrix $\mathbf{B}$ is required to convert ICRS data to the dynamical mean equator and equinox of J2000.0 (the "J2000.0 system"), the latter considered for this purpose to be a barycentric system. The same matrix is used in the geocentric transformations described in Chapter 6 to adjust vectors in the GCRS (the "geocentric ICRS") so that they can be operated on by the conventional precession and nutation matrices. The matrix $\mathbf{B}$ is called the *frame bias matrix*, and it corresponds to a fixed set of very small rotations. In the barycentric case it is used as follows:

$$\mathbf{r}_{\text{mean(2000)}} = \mathbf{B}\mathbf{r}_{\text{ICRS}} \tag{4.1}$$

where $\mathbf{r}_{\text{ICRS}}$ is a vector with respect to the ICRS and $\mathbf{r}_{\text{mean(2000)}}$ is a vector with respect to the dynamical mean equator and equinox of J2000.0. Both of the $\mathbf{r}$'s are column vectors and, if they represent a direction on the sky, are of the general form

$$\mathbf{r} = \begin{bmatrix} \cos\delta\ \cos\alpha \\ \cos\delta\ \sin\alpha \\ \sin\delta \end{bmatrix} \tag{4.2}$$

where α is the right ascension and δ is the declination, with respect to the ICRS, or the dynamical system of J2000.0, as appropriate.

In the geocentric case, $\mathbf{r}_{\text{ICRS}}$ is replaced by $\mathbf{r}_{\text{GCRS}}$ and $\mathbf{r}_{\text{mean(2000)}}$ is then a geocentric vector. This transformation must be carried out, for example, before precession is applied to GCRS vectors, since the precession algorithm assumes a dynamically-based coordinate system. That is, the above transformation is a necessary step in obtaining coordinates with respect to the mean equator and equinox of date, if one starts with ICRS reference data. See Chapter 6 for more information.

The matrix **B** is, to first order,

$$\mathbf{B} = \begin{bmatrix} 1 & d\alpha_0 & -\xi_0 \\ -d\alpha_0 & 1 & -\eta_0 \\ \xi_0 & \eta_0 & 1 \end{bmatrix} \tag{4.3}$$

where, in milliarcseconds, $d\alpha_0 = -14.6$, $\xi_0 = -16.6170$, and $\eta_0 = -6.8192$; convert to radians by dividing by 206 264 806.247. The values of the three small angular offsets are taken from the IERS Conventions (IERS 2010). They can be considered adopted values; previous investigations of the dynamical-ICRS relationship obtained results that differ at the milliarcsecond level or more, depending on the technique and assumptions. See the discussion in Hilton and Hohenkerk (2004). The angles ξ_0 and η_0 are the ICRS pole offsets, and $d\alpha_0$ is the offset in the ICRS right ascension origin with respect to the dynamical equinox of J2000.0, as measured in an inertial (non-rotating) system.

The above matrix can also be used to transform vectors from the ICRS to the FK5 system at J2000.0. Simply substitute $d\alpha_0 = -22.9$, $\xi_0 = 9.1$, and $\eta_0 = -19.9$ (milliarcseconds). However, there is also a time-dependent rotation of the FK5 with respect to the ICRS (i.e., a slow spin), reflecting the non-inertial nature of the FK5 proper motions; see Mignard and Frœschlé (2000).

Although the above matrix is adequate for most applications, a more precise result can be obtained by using the second-order version:

$$\mathbf{B} = \begin{bmatrix} 1 - \frac{1}{2}(d\alpha_0^2 + \xi_0^2) & d\alpha_0 & -\xi_0 \\ -d\alpha_0 - \eta_0\xi_0 & 1 - \frac{1}{2}(d\alpha_0^2 + \eta_0^2) & -\eta_0 \\ \xi_0 - \eta_0 d\alpha_0 & \eta_0 + \xi_0 d\alpha_0 & 1 - \frac{1}{2}(\eta_0^2 + \xi_0^2) \end{bmatrix}. \tag{4.4}$$

The above matrix, from Slabinski (2005), is an excellent approximation to the set of rotations $\mathbf{R}_1(-\eta_0)\mathbf{R}_2(\xi_0)\mathbf{R}_3(d\alpha_0)$, where $\mathbf{R}_1$, $\mathbf{R}_2$, and $\mathbf{R}_3$ are standard rotations about the x, y, and z axes, respectively. See Chapter 14 for a discussion on rotational matrices.

REFERENCES

1. IAU Working Group on Nomenclature:
http://syrte.obspm.fr/iauWGnfa/.

2. ICRF source coordinates:
http://hpiers.obspm.fr/icrs-pc/.

3. IERS Conventions (2010):
http://tai.bipm.org/iers/conv2010/conv2010.html.

4. IAU Resolutions Adopted by the General Assemblies:
http://www.iau.org/administration/resolutions/general_assemblies/.

5. Proceedings of Journees 2010 conference:
http://syrte.obspm.fr/jsr/journees2010/index.php?page=proceedings.

Andrei, A. H., J. Souchay, N. Zacharias, R. L. Smart, R. Vieira Martins, D. N. da Silva Neto, J. I. B. Camargo, M. Assafin, C. Barache, S. Bouquillon, J. L. Penna, and F. Taris (2009). The large quasar reference frame (LQRF). An optical representation of the ICRS. *Astronomy and Astrophysics 505*, 385–404.

Beasley, A. J., D. Gordon, A. B. Peck, L. Petrov, D. S. MacMillan, E. B. Fomalont, and C. Ma (2002). The VLBA Calibrator Survey—VCS1. *Astrophysical Journal Supplement 141*, 13–21.

Cutri, R. M., M. F. Skrutskie, S. Van Dyk, C. A. Beichman, J. M. Carpenter, T. Chester, L. Cambresy, T. Evans, J. Fowler, J. Gizis, E. Howard, J. Huchra, T. Jarrett, E. L. Kopan, J. D. Kirkpatrick, R. M. Light, K. A. Marsh, H. McCallon, S. Schneider, R. Stiening, M. Sykes, M. Weinberg, W. A. Wheaton, S. Wheelock, and N. Zacharias (2003). *2MASS All-Sky Catalog of Point Sources*. Pasadena: IPAC/California Institute of Technology.

ESA (1997). *The Hipparcos and Tycho Catalogues*. Noordwijk, Netherlands: European Space Agency. SP-1200 (17 volumes).

Feissel, M. and F. Mignard (1998). The Adoption of ICRS on 1 January 1998: Meaning and Consequences. *Astronomy and Astrophysics 331*, L33–L36.

Fey, A. L., D. Boboltz, P. Charlot, E. Fomalont, G. Lanyi, C. Jacobs, and K-Q VLBI Survey Collaboration (2009). Extending the ICRF to Higher Radio Frequencies. In *American Astronomical Society Meeting Abstracts*, Volume 214, p. 676.

Fey, A. L., C. Ma, E. F. Arias, P. Charlot, M. Feissel-Vernier, A. M. Gontier, C. S. Jacobs, J. Li, and D. S. MacMillan (2004). The Second Extension of the International Celestial Reference Frame: ICRF-EXT.1. *Astronomical Journal 127*, 3587–3608.

Fricke, W., H. Schwan, T. Corbin, U. Bastian, R. Bien, C. Cole, E. Jackson, R. Järling, H. Jahreiß, T. Lederle, and S. Röser (1991). *Fifth Fundamental Catalogue (FK5), Part II, The FK5 Extension—New Fundamental Stars*. Heidelberg: Astronomisches Rechen-Institut. Veröffentlichungen #33.

Fricke, W., H. Schwan, T. Lederle, U. Bastian, R. Bien, G. Burkhardt, B. du Mont, R. Hering, R. Järling, H. Jahreiß, R. S., H. M. Schwerdtfeger, and H. G. Walter (1988). *Fifth Fundamental Catalogue (FK5), Part I, The Basic Fundamental Stars*. Heidelberg: Astronomisches Rechen-Institut. Veröffentlichungen #32.

Hazard, C., J. Sutton, A. N. Argue, C. M. Kenworthy, L. V. Morrison, and C. A. Murray (1971). 3C 273B-Coincidence of radio and optical positions. *Nature Physical Science 233*, 89.

Hilton, J. L. and C. A. Hohenkerk (2004). Rotation Matrix from the Mean Dynamical Equator and Equinox at J2000.0 to the ICRS. *Astronomy and Astrophysics 413*, 765–770.

Høg, E., C. Fabricius, V. V. Makarov, S. Urban, T. Corbin, G. Wycoff, U. Bastian, P. Schwekendiek, and A. Wicenec (2000). The Tycho-2 Catalog of the 2.5 Million Brightest Stars. *Astronomy and Astrophysics 355*, L27–L30.

Hohenkerk, C. Y., B. D. Yallop, C. A. Smith, and A. T. Sinclair (1992). Celestial Reference Systems. In P. K. Seidelmann (Ed.), *Explanatory Supplement to The Astronomical Almanac*, Chapter 3. Mill Valley, CA: University Science Books.

Hughes, J. A., C. A. Smith, and G. H. Kaplan (Eds.) (1991). *IAU Colloq. 127, Reference Systems*. Washington, D.C.: U.S. Naval Observatory.

IAU (1992). In J. Bergeron (Ed.), *Transactions of the International Astronomical Union*, Volume XXI B, Dordrecht, pp. 30–78. Kluwer. Proc. 21st General Assembly, Buenos Aires, 1991.

IAU (1996). In I. Appenzeller (Ed.), *Transactions of the International Astronomical Union*, Volume XXII B, Dordrecht, pp. 24–60. Kluwer. Proc. 22nd General Assembly, The Hague, 1994.

IAU (1999). In J. Andersen (Ed.), *Transactions of the International Astronomical Union*, Volume XXIII B, Dordrecht, pp. 31–51. Kluwer. Proc. 23rd General Assembly, Kyoto, 1997.

IAU (2001). In H. Rickman (Ed.), *Transactions of the International Astronomical Union*, Volume XXIV B, San Francisco, pp. 34–59. Astronomical Society of the Pacific. Proc. 24th General Assembly, Manchester, 2000.

IAU (2008). In K. A. van der Hucht (Ed.), *Transactions of the International Astronomical Union*, Volume XXVI B, Cambridge, pp. 34–47. Cambridge University Press. Proc. 26th General Assembly, Prague, 2006.

IERS (2010). Conventions (2010). Technical Note 36, International Earth Rotation Service, Frankfurt am Main. Verlag des Bundsesants fur Kartographie und Geodesie, G. Petit and B. Luzum (Eds.). Available at URL[3].

Jacobs, C. S., G. E. Lanyi, C. J. Naudet, O. J. Sovers, L. D. Zhang, P. Charlot, D. Gordon, and C. Ma (2005). Extending the ICRF to Higher Radio Frequencies: Initial Global Astrometric Results. In R. Gaume, D. D. McCarthy, and J. Souchay (Eds.), *IAU XXV Joint Discussion 16, The International Celestial Reference System: Maintenance and Future Realizations*, Washington, D.C., pp. 36–43. U.S. Naval Observatory.

Jacobs, C. S. and O. J. Sovers (2008). Extending the ICRF to Higher Radio Frequencies: Global Astrometric Results at 32/8 GHz. In A. Finkelstein and D. Behrend (Eds.), Measuring the Future, *Proceedings of the Fifth IVS General Meeting*, St. Petersburg, pp. 284–288. Nauka.

Johnston, K. J., D. D. McCarthy, B. J. Luzum, and G. H. Kaplan (Eds.) (2000). *IAU Colloq. 180, Towards Models and Constants for Sub-Microarcsecond Astrometry*. Washington, D.C.: U.S. Naval Observatory.

Kaplan, G. H. (1982). The IAU Resolutions on Astronomical Constants, Time Scales, and the Fundamental Reference Frame. Circular 163, U.S. Naval Observatory, Washington, DC.

Kaplan, G. H. (2005). The IAU Resolutions on Astronomical Reference Systems, Time Scales, and Earth Rotation Models. Circular 179, U.S. Naval Observatory, Washington, DC.

Kaplan, G. H., J. A. Hughes, P. K. Seidelmann, C. A. Smith, and B. D. Yallop (1989). Mean and Apparent Place Computations in the New IAU System. III. Apparent, Topocentric, and Astrometric Places of Planets and Stars. *Astronomical Journal 97*, 1197–1210.

Kaplan, G. H., F. J. Josties, P. E. Angerhofer, K. J. Johnston, and J. H. Spencer (1982). Precise radio source positions from interferometric observations. *Astronomical Journal 87*, 570–576.

Klioner, S. A. (2003). A Practical Relativistic Model for Microarcsecond Astrometry in Space. *Astronomical Journal 125*, 1580–1597.

Lieske, J. H. and V. K. Abalakin (Eds.) (1990). *IAU Symp. 141, Inertial Coordinate System on the Sky*. Dordrecht: Kluwer.

Ma, C., E. F. Arias, G. Bianco, D. A. Boboltz, S. L. Bolotin, P. Charlot, G. Engelhardt, A. L. Fey, R. A. Gaume, A.-M. Gontier, R. Heinkelmann, C. S. Jacobs, S. Kurdubov, S. B. Lambert, Z. M. Malkin, A. Nothnagel, L. Petrov, E. Skurikhina, J. R. Sokolova, J. Souchay, O. J. Sovers, V. Tesmer, O. A. Titov, G. Wang, V. E. Zharov, C. Barache, S. Boeckmann, A. Collioud, J. M. Gipson, D. Gordon, S. O. Lytvyn, D. S. MacMillan, and R. Ojha (2009). The Second Realization of the International Celestial Reference Frame by Very Long Baseline Interferometry. Technical Note 35, International Earth Rotation Service, Frankfurt am Main. Verlag des Bundsesamts fur Kartographie und Geodasie, A. Fey and D. Gordon (Eds.).

Ma, C., E. F. Arias, T. M. Eubanks, A. L. Fey, A.-M. Gontier, C. S. Jacobs, O. J. Sovers, B. A. Archinal, and P. Charlot (1998). The International Celestial Reference Frame as Realized by Very Long Baseline Interferometry. *Astronomical Journal 116*, 516–546.

Ma, C. and M. Feissel (1997). Definition and Realization of the International Celestial Reference System by VLBI Astrometry of Extragalactic Objects. Technical Note 23, International Earth Rotation Service, Paris: Obs. Paris.

Makarov, V. V. and G. H. Kaplan (2005). Statistical Constraints for Astrometric Binaries with Nonlinear Motion. *Astronomical Journal 129*, 2420–2427.

Mignard, F. (1997). Astrometric Properties of the Hipparcos Catalogue. In B. Battrick (Ed.), *Proceedings of the ESA Symposium 'Hipparcos—Venice '97*, Noordwijk, The Netherlands, pp. 5–10. ESA. SP-402.

Mignard, F. and M. Frœschlé (2000). Global and Local Bias in the FK5 from the Hipparcos Data. *Astronomy and Astrophysics 354*, 732–739.

Petrov, L., Y. Y. Kovalev, E. B. Fomalont, and D. Gordon (2008). The Sixth VLBA Calibrator Survey: VCS6. *Astronomical Journal 136*, 580–585.

Seidelmann, P. K. (Ed.) (1992). *Explanatory Supplement to The Astronomical Almanac*. Mill Valley, CA: University Science Books.

Seidelmann, P. K. and J. Kovalevsky (2002). Application of the New Concepts and Definitions (ICRS, CIP and CEO) in Fundamental Astronomy. *Astronomy and Astrophysics 392*, 341–351.

Slabinski, V. (2005). Private communications.

Standish, E. M. (1998). JPL Planetary and Lunar Ephemerides, DE405/LE405. IOM 312.F-98-048, Jet Propulsion Laboratory.

van Leeuwen, F. (Ed.) (2007a). *Hipparcos, the New Reduction of the Raw Data*, Volume 350 of *Astrophysics and Space Science Library*.

van Leeuwen, F. (2007b). Validation of the new Hipparcos reduction. *Astronomy and Astrophysics 474*, 653–664.

Zacharias, N., C. Finch, T. Girard, N. Hambly, G. Wycoff, M. I. Zacharias, D. Castillo, T. Corbin, M. DiVittorio, S. Dutta, R. Gaume, S. Gauss, M. Germain, D. Hall, W. Hartkopf, D. Hsu, E. Holdenried, V. Makarov, M. Martinez, B. Mason, D. Monet, T. Rafferty, A. Rhodes, T. Siemers, D. Smith, T. Tilleman, S. Urban, G. Wieder, L. Winter, and A. Young (2010). The Third US Naval Observatory CCD Astrograph Catalog (UCAC3). *Astronomical Journal 139*, 2184–2199.

Zacharias, N., H. L. McCallon, E. Kopan, and R. M. Cutri (2005). Extending the ICRF into the infrared: 2MASS-UCAC astrometry. *Highlights of Astronomy 13*, 603–604.

CHAPTER 5

Terrestrial Coordinates and the Rotation of the Earth

BRENT ARCHINAL, BETH STETZLER,
JAMES SLATER, & NIKOLAOS PAVLIS

5.1 Introduction

The task of establishing or defining the terrestrial coordinates of a point is inextricably linked to establishing the rotation of the Earth over time. The definition of any terrestrial reference system (TRS) is given by establishing a celestial reference coordinate system (CRS) and a suitable transformation between them. This transformation is what is generally called *Earth orientation* (or *Earth rotation*), including the various changes in the orientation of the Earth's axis in space and internally, and the rotation (and rotational variations) about that axis. (This latter rotation is also often defined as *Earth rotation*—both uses of this term will be made here with the meaning being given from context.) One could connect the celestial and terrestrial coordinate system at any given instant using three Eulerian angles, and then form a time series of such angles to define Earth orientation. However, for historical reasons (mostly in order to associate the motions of the Earth with physical processes and to allow for successive approximations of the motion), in practice these angles are expressed in terms of precession, nutation, polar motion, and rotation about the Earth's axis; see Chapter 6 for details on these topics.

Before we proceed into any explanation of terrestrial coordinates, it is also necessary to distinguish between a (celestial or terrestrial) *reference system* and a *reference frame*. A reference system is the conceptual definition of an "ideal" coordinate system, based on some abstract principle(s). For example, an ideal terrestrial system would be one in which the Earth's crust shows only deformation with no rotations or translations. A *conventional reference system* is one where the model used to define coordinates is given in detail; that is, specific model choices have been made. The realization of a reference system, using actual observations, adopted station coordinates, etc., provides a *reference frame* (Kovalevsky and Mueller 1981; Mueller 1988; Kovalevsky, Mueller, and Kalaczek 1989).

This chapter will begin with a discussion on the concept of terrestrial reference systems and frames and give some detail on the current standard system (ITRS) and some widely used frames (ITRF, WGS 84). Various coordinate systems for measuring longitude and latitude are introduced. Also included is information on the actual transformation of coordinates from one frame to another. This will be followed by information, mostly extracted from the *IERS Conventions (2010)* (IERS 2010), regarding the Earth's gravity field (to a limited extent), tides, and plate tectonics. Methods for monitoring the Earth's rotation (past, present, and future) are described and information on the IERS and the data it produces is provided.

An overview of Earth rotation and its causes in general has not been given because space is lacking for such a complete treatment, and the ample coverage from this viewpoint by

Teisseyre (1989), Moritz and Mueller (1987), Lambeck (1980), and Munk and MacDonald (1960). The motion of the Earth's celestial pole due to precession and nutation is covered in Chapter 6. [Readers seeking more detailed information on the subjects of gravity, geodesy, geodetic astronomy, and terrestrial reference systems should consult standard texts such as Mueller and Rockie (1966), Heiskanen and Moritz (1967), Mueller (1969), Bomford (1971), Moritz (1980), Moritz and Mueller (1987), Kovalevsky, Mueller, and Kolaczek (1989), Torge (2001), and McCarthy and Seidelmann (2009).]

5.2 Terrestrial Reference Systems

5.2.1 Reference Systems and Reference Frame Concepts

Locating a point on or near the Earth's surface requires the definition of a reference system that enables a set of coordinates to be unambiguously associated with or assigned to the point. It also provides a consistent means for identifying the location of one point with respect to another. To do this, the concept of a *terrestrial reference system* is introduced. Such a system is generally defined by three orthogonal Cartesian coordinate axes (x, y, z) fixed to the Earth's crust, the location of the origin, a specified orientation in space, and a set of mathematical and physical models, constants, conventions, and parameters. A *geocentric terrestrial reference system* is one in which the origin coincides with the geocenter—the center of mass of the solid Earth, oceans and atmosphere—and in which the coordinate axes rotate with the Earth. This has been adopted by the international scientific community as the standard conceptual definition of a global geodetic reference system. The z-axis is oriented along the rotation axis of the Earth, the x- and y-axes are in the equatorial plane, the x-axis intersects the equator at the point where a *reference* (or *zero*) *meridian* crosses it, and the y-axis is perpendicular to the x- and z-axes to complete a right-handed system. A standard set of procedures and models (conventions), prescribed by the International Earth Rotation and Reference Systems Service (IERS), formally relates this Earth-centered Earth-fixed reference system to the Celestial Reference System (see Chapter 4). The geocentric terrestrial reference system with these adopted conventions is designated as the *International Terrestrial Reference System* (ITRS) (IERS 2004).

The practical realization of a terrestrial reference system is accomplished by establishing a set of reference points on the topographic surface of the Earth and determining their 3-dimensional Cartesian coordinates and velocities from actual observations, currently done by using space geodetic techniques and applying the reference system conventions. These physical points and the underlying conventions then define the *geocentric terrestrial reference frame*. The more accurately the reference point positions can be determined, the better the reference frame can be realized.

Two of the most widely used geocentric terrestrial reference frames, the International Terrestrial Reference Frame (ITRF) and the World Geodetic System (WGS), are described in more detail below. In addition, South America and Europe have implemented regional realizations of the ITRS—Sistema de Referencia Geocentrico para Las Américas (SIRGAS) (Hoyer et al. 1998; URL[1]) and the European Terrestrial Reference Frame (ETRF), (URL[2]) respectively. By adopting the IERS Conventions and incorporating ITRF reference points (stations) into the individual reference frame realizations, WGS, SIRGAS and ETRF (and

others) attempt to constrain their frames to have the same origin, orientation and scale as the ITRF.

5.2.1.1 The International Terrestrial Reference System

The International Terrestrial Reference System (ITRS) specifies a set of physical constants, conventions and models to be used for estimating the coordinates of points with respect to the Earth. The ITRS is defined to be geocentric with its orientation traceable to that of the Bureau International de l'Heure (BIH) Terrestrial System at 1984.0; its standard unit of length is the meter (SI), and its time evolution is constrained to a condition of no-net-rotation with regard to horizontal plate tectonic motions over the Earth as a whole (IERS 2004, p. 25).

The physical realization (or materialization) of the ITRS is the International Terrestrial Reference Frame (ITRF), defined by the 3-dimensional coordinates and linear velocities of a global network of ground stations (on the Earth's crust) at a specific epoch in time. These coordinates and velocities are derived from observations collected at the stations using four space-based techniques: Very Long Baseline Interferometry (VLBI), satellite laser ranging (SLR), the Global Positioning System (GPS), and Doppler Orbitography and Radiopositioning Integrated by Satellite (DORIS). The origin, coordinate system orientation and the scale are implicitly defined by the Cartesian coordinates and velocities of the stations, and the solutions conform to the ITRS and IERS conventions and standards. This represents the fundamental scientific standard reference frame (Boucher and Altamimi 1996).

The ITRS is a direct continuation of the BIH Terrestrial System (BTS), first established in 1985 and continued through 1987. The BTS had in turn evolved from the BIH 1968 System, which was established in 1969 by the BIH on the basis of a comparison of data collected by the BIH and the International Polar Motion Service (IPMS) during the mid-1960s. However, it should be emphasized that this was *not* a complete terrestrial reference system; it was a reference system for orientation only, being based on the observed astronomical coordinates of the involved observing stations. The comparison of the BIH collected data with the IPMS data allowed the BIH 1968 System to be referenced to the IPMS reference pole. This pole is the Conventional International Origin[1] which was the approximate average position of the true celestial pole of the Earth from 1900.0 to 1905.0, but was actually defined by the adopted latitudes of five International Latitude Service (ILS) stations. (For further information on the history of the terrestrial reference frame prior to 1988, see IERS (1989), or the BIH Annual Reports for the appropriate year(s), or see Mueller (1969) for further information on these systems for the pre-1969 period.)

The IERS Reference Pole (IRP) and Reference Meridian are consistent with the corresponding directions in the BIH Terrestrial System (BTS) within $\pm 0.''005$. The BIH reference pole was adjusted to the Conventional International Origin in 1967. It was then kept stable independently until 1987. Re-reduction of the available data (BIH 1989, p. A-3) tied the BTS (and therefore the IRP) with the Conventional International Origin to $\pm 0.''03$.

As noted in the 2010 update to the IERS conventions (IERS 2010, chapter 4), there have been 12 versions of the ITRF released since 1988. ITRF2005 used, for the first time as input,

1. The conventional international origin is *not* the same as the celestial intermediate origin, although both can be denoted by CIO. To avoid confusion, the use of CIO in this book is reserved only for the celestial intermediate origin.

time series of station positions and Earth orientation parameter values from each of the space geodesy techniques. The most recent realization of the ITRF was computed by the IERS in 2008 with an epoch of 2005.0 (Altamimi, Collilieux and Métivier 2011). This solution used the same procedure as ITRF2005, incorporating observations from VLBI (29 years), SLR (26 years), DORIS (16 years) and GPS (12.5 years). ITRF2008 is constituted by 934 stations at 580 sites, with 105 of those sites supporting two or more of the four space geodesy techniques. Transformation parameters computed from ITRF2008 to ITRF2005 show no rotational differences, about a 5 mm difference in the location of the origins, and 0.94 parts per billion scale difference (IERS 2010, Table 4.1).

5.2.1.2 The World Geodetic System 1984

The terrestrial reference system used by the U.S. Department of Defense is the World Geodetic System 1984 (WGS 84) (NIMA 1997). It is also the standard reference system for the Global Positioning System (GPS). WGS 84 actually constitutes a coherent set of global models and definitions that include the WGS 84 terrestrial reference frame, a prescribed set of constants, models and conventions that are largely adopted from the IERS Standards (IERS 2004; IERS 1996), an Earth Gravitational Model (currently EGM2008), and a World Magnetic Model (currently WMM 2010). For more details on EGM2008, see Pavlis et al. (2012) and URL[4], and for more details on WMM 2010, see URL[5], URL[6], and Maus (2010). The Defense Mapping Agency was responsible for the initial development and maintenance of the World Geodetic System, and this responsibility passed to its successor agencies, the National Imagery and Mapping Agency (NIMA) and the National Geospatial-Intelligence Agency (NGA). The World Geodetic System geocentric terrestrial reference frame was first developed in 1960 with subsequent updates in 1966 (WGS 66), 1972 (WGS 72), and 1984 (WGS 84). The original WGS 84 reference frame was realized from a set of Transit satellite (Doppler) station coordinates and aligned as closely as possible with the origin, scale and orientation of the BIH Terrestrial System. Transit-realized WGS 84 coordinates were derived for the Department of Defense GPS monitor stations and were used until 1994. Refinements were made to the WGS 84 reference frame in 1994, 1996, and 2002 and the reference frames are respectively designated as WGS 84 (G730), WGS 84 (G873) and WGS 84 (G1150). The 'G' indicates that the reference frame is derived from GPS observations and the number is the GPS Week Number that the reference frame became operationally effective for GPS orbit production by NGA and the Air Force's GPS Operations.

The WGS 84 reference frame is defined by a global network of GPS stations whose coordinates are closely aligned to the ITRF. This has been done by constraining the coordinate solutions to the ITRF through the incorporation of up to several dozen independent GPS reference stations with well-defined ITRF positions and velocities in these solutions. Each realization of the WGS 84 reference frame has improved the reference frame accuracy relative to the ITRF. WGS 84 (G1150) was aligned to ITRF2000 to approximately 1 cm in each coordinate (Malys and Slater 1994; Slater and Malys 1998; Merrigan et al. 2002). Another realignment of the WGS 84 reference frame to ITRF2008 is expected in the 2011–2012 time frame, as well as adoption of relevant parts of the *IERS Conventions (2010)* (IERS 2010) into the updated WGS 84 reference system.

Since the GPS reference orbits computed by the Air Force are in the WGS 84 reference frame, the broadcast satellite navigation message orbits generated from these are also

referenced to WGS 84. Therefore, any position coordinates derived directly from the GPS broadcast orbits will also be in the WGS 84 reference frame. Due to the few centimeter alignment of the WGS 84 reference frame with the ITRF, for most practical applications, WGS 84 and ITRF are considered equivalent, and no transformation is required between the reference frames.

5.2.2 The Figure of the Earth and Geodetic Reference Surfaces

Note that, up to this point, there has been no explicit need to introduce a conceptual model for the Earth's surface; however, most positioning and navigation applications need to convert Cartesian coordinates to more meaningful coordinates that refer to some representation of the surface from a local, regional or global perspective. From a purely geometric perspective, the best fitting figure of the Earth is a *rotational ellipsoid* since its shape can conform to the flattening of the Earth at the poles and it is relatively simple mathematically. (A more complicated surface, such as a triaxial ellipsoid, will not greatly improve the representation, but will greatly complicate the mathematics involved in using it.) Latitude and longitude can be defined as horizontal coordinates with respect to the ellipsoid surface, and heights can be referenced to the ellipsoid as well. Conventionally, the longitude line passing through Greenwich, England was chosen as the zero longitude and the equator defined zero latitude.

Prior to the era of satellite geodesy, individual countries or geographic regions would adopt reference ellipsoids that seemed to best fit the country or region, but as a result, these ellipsoids were frequently not geocentric and not necessarily aligned with the Earth's rotation axis and equator. For global applications and especially satellite operations, reference ellipsoids are defined to be geocentric and their semimajor and semiminor axes aligned with the axes of a geocentric terrestrial reference frame. Coordinates such as those derived from Global Positioning System observations can be readily converted from Cartesian x, y, z to latitude, longitude and height above the ellipsoid or the reverse (see § 5.2.4). The choice of a reference ellipsoid is inherent in the definitions of geodetic datums (see § 5.2.5.3) and map projections (see § 5.2.5.2) which will be discussed later in this chapter.

Although mathematically pleasing, the abstract nature of the ellipsoid makes it less than optimal for visualizing terrain or the sea surface, and it cannot be used to determine the direction that water will flow. A reference surface that is better suited for these purposes is one defined by a level surface of equal gravity potential, also called a *geopotential surface* or *geop*. Note that gravity potential here includes the centrifugal potential and the gravitational potential. There are an infinite number of geopotential surfaces that theoretically can be defined; however, the one that "best fits" the mean sea level is chosen as the standard geopotential reference surface. This particular level surface is called the *geoid*. Conceptually, the geoid can be thought of as an imaginary "surface coinciding with the mean sea-level in the oceans, and lying under the land at the level to which the sea would reach if admitted by small frictionless channels" (Bomford 1971). Various other definitions are given in Heiskanen and Moritz (1967, pp. 48–50); Moritz (1980, p. 6); and Torge (1980, pp. 2–3). Elevation can then be expressed as height above mean sea level or height with respect to the geoid, where mean sea level and the geoid define zero elevation. At any point on the Earth, the gravity vector will be perpendicular to the level surface (geop) that passes through that point. Frequently, instruments or sensors operating on the topographic surface of the Earth need

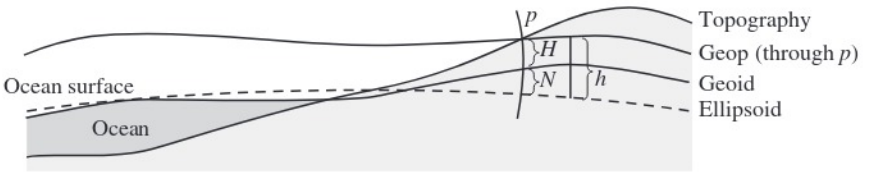


Figure 5.1 The Earth's surface and reference surfaces

to be aligned with the local vertical, in effect the local gravity vector, and accomplish this through the use of plumb bobs, bubble levels and pools of mercury. The geopotential surface is also a critical construct in hydrology, since water bodies conform to a level surface and water flows "downhill" from higher potential to lower potential. It is important to realize that the geoid surface is irregular and determined by the distribution of the local underlying mass. In practice, gravity potential must be derived from actual aerial and terrestrial gravity measurements, and satellite orbital data. On the other hand, the mean sea surface is derived from global satellite altimetry measurements of the sea surface and local coastal tide gauge observations.

The relationships among the three reference surfaces—the topography, ellipsoid and geopotential—are illustrated in Fig. 5.1. The observer is at point p on the surface of the Earth (topography). A reference ellipsoid lies below the topography. A geop passes through p, but the geoid itself lies close to the reference ellipsoid. Note that although the geop and geoid surfaces are not the same as that of the topography, there are some similarities since the mass of the topography influences the local gravity. Also shown in the figure are the geoid undulation (N), which is the height separation between the geoid and the ellipsoid, the ellipsoidal height (h), which is the height of p above the ellipsoid, and the mean sea level height or orthometric height (H), which is the height of p above the geoid. These are related as:

$$N \approx h - H. \tag{5.1}$$

This relationship is approximate since H is actually measured along the curved vertical or plumb line through p, whereas h and N are measured along a straight line through p perpendicular to the ellipsoid. For the best current reference ellipsoid and global geoid models, the separation between them does not exceed 100 m.

5.2.3 Geodetic Datums

The set of parameters that defines the relationship between a specific reference ellipsoid and a terrestrial reference system is called a *geodetic datum*. A global geodetic datum is one in which the reference ellipsoid is the "best fit" for the Earth as whole, its origin is geocentric, and its major and minor axes are coincident with the coordinate axes of the adopted terrestrial reference system. A local geodetic datum, on the other hand, is one in which the reference ellipsoid is frequently not geocentric and its surface is a best fit only to the local or regional area for which it is intended to be used. The axes of the local reference ellipsoid also may not be aligned with the coordinate axes of a geocentric terrestrial reference system. For mapping

and surveying applications, especially prior to satellite technology, datums were traditionally defined as either *horizontal datums* or *vertical datums*. The horizontal datum provides a means of identifying latitude and longitude of a point on the surface of the reference ellipsoid, while the height of the point is separately determined with respect to local mean sea level or a geoid model (the vertical datum).

A local horizontal datum is defined by the size and shape of the reference ellipsoid and by the positioning of the ellipsoid relative to the figure of the Earth (represented by the geoid). The ellipsoid's size and shape are specified by two parameters, generally its *semimajor axis* (a) and *flattening* (f) (the relative difference in length of the semimajor and *semiminor* axes). An initial point (origin) is chosen near the surface of the ellipsoid (specified by its astronomical latitude and longitude, (Φ, Λ)), and the *deflection of the vertical* and geoid undulation (N) determined at the chosen origin along with an azimuth (α) from the origin to another point. See § 5.2.5.3 and Figs. 5.2 and 5.3. The ellipsoid is chosen so as to represent the geoid as well as possible over the area of interest (a region or the entire Earth). The position of the ellipsoid with respect to the geoid is given by the deflection of the vertical (the angle between the local vertical gravity direction and the ellipsoidal normal) and the geoid undulation. Historically, local datums were usually established in support of large triangulation networks. The origin was chosen to be at the center of the network in order to minimize errors in measurements relative to the origin as one moved outward in the network. In order to simplify the datum definition, the deflection of the vertical and geoid undulation were frequently chosen to be zero at the origin, in effect forcing the ellipsoid and geoid to be coincident at that point. By imposing the condition that the vertical axis of the reference ellipsoid be parallel with the Earth's rotation axis, the deflection of the vertical and geoid undulation can then be related to the offset between the center of the ellipsoid and the geocenter. This is equivalent to a translational shift in x, y and z between a coordinate system whose origin is at the geocenter and a coordinate system whose origin is at the center of the local datum's ellipsoid. Specific datums and datum conversions are discussed in § 5.2.5.3 and § 5.2.5.4.

Many maps are still based on local datums. In these cases the reference ellipsoid is used only as a horizontal (2-dimensional) datum, whose origin and orientation are defined by six topocentric parameters. North American Datum 1927 (NAD 27) is one example. Its origin is a survey point in Kansas. North American Datum 1983 (NAD 83) replaced NAD 27 as the official horizontal datum for the U.S. in 1989 (NOAA 1989). It was derived from Doppler satellite observations as a geocentric global datum. NAD 83 removed significant local distortions in NAD 27 and replaced the Clarke 1866 reference ellipsoid with the Geodetic Reference System 1980 (GRS 80) ellipsoid. However, it still retained some biases in the origin and orientation and was used primarily as a horizontal datum. Beginning in 1994, to meet the growing demands and capabilities of geodetic surveying with GPS, the National Geodetic Survey organized a network of continuously operating reference stations that were positioned using GPS and tied to the ITRF. Additional stations have been added to the network over time and new 3-dimensional coordinates have been computed, tying these stations to the latest realizations of the ITRF (Snay and Soler 2000).

A vertical datum is the reference surface for orthometric heights. Vertical datums are traditionally defined as Mean Sea Level (MSL) or averaged tidal observations based on low or high water (for example, Mean Lower Low Water). Many national and regional vertical

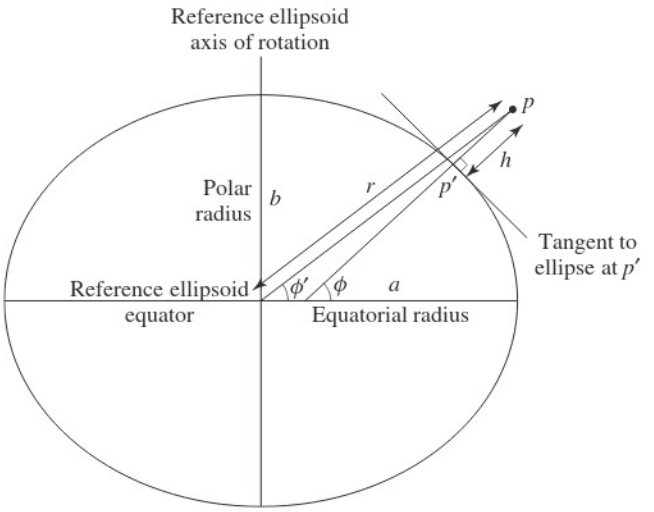


Figure 5.2 Geocentric (ϕ') and geodetic (ϕ) latitude

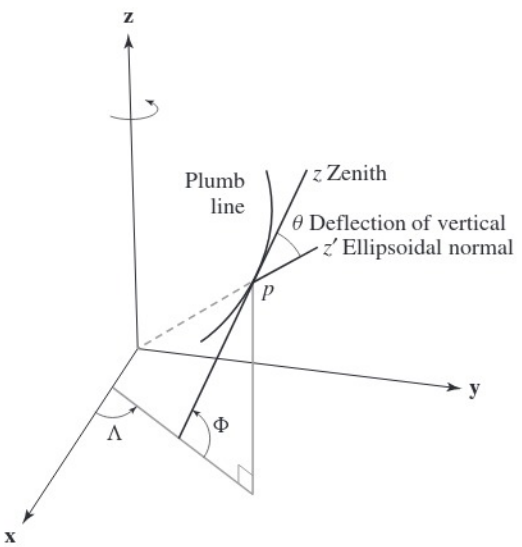


Figure 5.3 Astronomical latitude and longitude

datums are tied to a local mean sea level, which may differ significantly (decimeters) from global mean sea level due to local effects such as river run off and extremes in coastal tidal effects. Thus, such national and regional vertical datums around the world will differ from one another significantly when considered on a global basis. North American Vertical Datum 1988 (NAVD 88) applied this concept by adopting the single tide gauge elevation at Point Rimouski, Quebec, Canada as the continental elevation reference point and essentially references all

other elevations in the U.S. to this. NAVD 88 was designated the official vertical datum of the U.S. in 1993. By contrast, the U.S. National Vertical Datum 1929 (NGVD 29) was fixed to a set of reference tide gauges, without correction for local variations in the sea state, as a method of defining the vertical reference.

From a global perspective, the best fitting approximation of the mean sea surface is the geopotential surface represented by the global geoid. Due to effects such as atmospheric pressure, temperature, prevailing winds and currents, and salinity variations, the mean sea level will depart from the geoid by a meter or more. Thus, the geoid can be considered as a surrogate for mean sea level, but not equal to mean sea level, which is an important distinction. Once defined, the geoid becomes the zero-elevation surface to which orthometric heights can be referenced worldwide. The best model currently is the WGS 84 EGM2008 geoid, which is accurate to better than 15 cm (RMS error) over areas where high accuracy gravity data were available for inclusion in the model (Pavlis et al. 2012; URL[4]).

The pervasiveness of global navigation satellite systems has shifted the traditional concept of separate horizontal and vertical datums to one of 3-dimensional global datums. Satellite positioning enables one to obtain a 3-dimensional position in Cartesian (x, y, z) coordinates, or latitude, longitude and height, with respect to a global geocentric datum and its reference ellipsoid anywhere in the world. A geoid model can then be used to convert ellipsoidal heights to orthometric heights if needed. For such a global geodetic datum, the reference ellipsoid is defined to be an equipotential surface, with its angular velocity equal to that of the Earth, and an associated gravitational constant GM. Four fundamental parameters must be chosen as defining constants for an equipotential ellipsoid. The semimajor axis (a), *inverse flattening* ($1/f$), GM, and the angular velocity are one possible set, but other related groups of independent parameters also may be used. In the case of the International Terrestrial Reference System, the GRS 80 ellipsoid is specified as the reference ellipsoid (Moritz 1992). Instead of specifying f, it uses as a fundamental constant J_2, the coefficient in the spherical harmonic representation of the gravitational potential that is related to the dynamical form of the Earth (Stacey and Davis 2008, pp. 81–89). The WGS 84 reference ellipsoid is essentially the same as GRS 80, with the same values for a, GM and the angular velocity, but it specifies a value for f, not J_2. The result is a difference of 0.1 mm in the derived value of the semiminor axis b in the two ellipsoids, so for all practical purposes the ellipsoids are identical (NIMA 1997, p. 3-2)). For more information on datums and map projections see, for example, Iliffe and Lott (2008).

5.2.4 Geocentric, Geodetic, and Astronomical Coordinates

Various coordinate systems exist for measuring longitude and latitude. *Geocentric* coordinates are determined from the center of the Earth; *geodetic* coordinates are determined relative to a reference ellipsoid; and *astronomical* coordinates are determined relative to the observer's local vertical. See, for example, Misra and Enge (2001, chapter 3), Seeber (2003, chapter 2) and Torge (2001). Figure 5.2 illustrates the difference between geocentric and geodetic latitude, once again for a point p on the Earth's surface. The *geocentric latitude* ϕ' is measured in the meridian plane, and is the angle between the ellipsoid's equatorial plane and the line from p to the center of the ellipsoid. The *geodetic latitude* ϕ is the angle between the ellip-

soid's equatorial plane and the normal from p to the ellipsoid (at point p'); a and b are the semimajor and semiminor axes of the ellipsoid, respectively; f, the flattening, or $1/f$, the inverse flattening, is often used, with

$$f = \frac{a-b}{a}. \tag{5.2}$$

The *geocentric longitude* (λ) is measured in the equatorial plane, and is defined by the angle between the reference meridian and the meridian of point p (and p'), measured eastward around the Earth from 0° to 360° (IAU 1983, p. 47). The *geodetic longitude* will be the same as the geocentric longitude if the reference ellipsoid has been chosen with the same axes, reference meridian and center as the Earth—this is assumed to be the case in further discussion here. The astronomical coordinates of point p are determined relative to the local vertical (plumb line) direction (or *zenith*) at point p (see Fig. 5.3, where z indicates the direction of the zenith and z' the direction of the ellipsoidal normal). A vertical (or plumb) line passing through p will intersect the Earth's equatorial plane with the angle Φ, the *astronomical latitude* of p. *Astronomical longitude* Λ is the angle between the reference meridian plane and the plane including the local vertical through p, measured along the equator. Note that the local vertical does not necessarily pass through the Earth's axis.

The angle between the local vertical direction and ellipsoidal normal through p is known as the *deflection of the vertical* θ. The deflection of the vertical is often broken into two orthogonal components, ξ and η, (see Fig. 5.4, where z indicates the direction of the zenith, and z' the direction of the ellipsoidal normal), with ξ in the meridional direction, and η in the orthogonal *prime vertical* direction. Relations between the geodetic and astronomical longitude and latitude and these components of the deflection of the vertical are

$$\sin\phi = \cos\eta \sin(\Phi - \xi) \tag{5.3}$$

$$\sin\eta = \cos\phi \sin(\Lambda - \lambda). \tag{5.4}$$

Using small-angle formulae ($\sin\alpha \simeq \alpha$, $\cos\alpha \simeq 1$) these can also be given as

$$\xi = \Phi - \phi \tag{5.5}$$

$$\eta = (\Lambda - \lambda)\cos\phi. \tag{5.6}$$

The deflection of the vertical at a point on the Earth can be determined with high accuracy from stellar observations using a specially designed vertical telescope to obtain the astronomical position (Φ, Λ) and GPS satellite observations to obtain the geodetic position (ϕ, λ) at the same point, and then combining them in the equations above (Hirt 2001).

The height or radial component of point p is expressed in different ways depending upon the coordinate system being used. As discussed in § 5.2.2, for geodetic coordinates, the ellipsoidal height (h) is the height component, while in other cases, height above mean sea level or the geoid (H) is appropriate, especially when the coordinates are related to the leveling of an instrument with respect to local gravity. In a *geocentric Cartesian coordinate* system, the geocentric radius r is used to define the radial position of a point using the algebraic relationship $r = \sqrt{x^2 + y^2 + z^2}$. r is also the radial component for a *geocentric geographical coordinate* system (ϕ', λ, r), where ϕ' is the angle between the x-y plane and

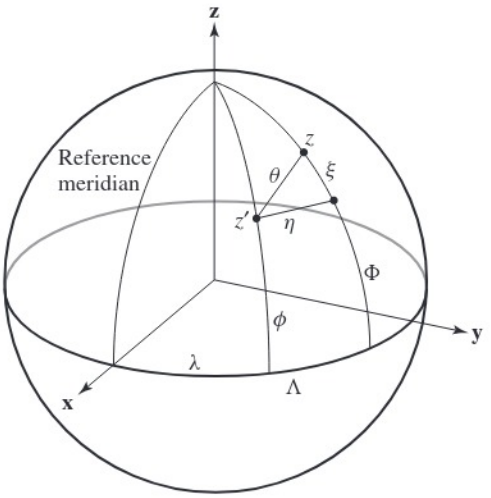


Figure 5.4 Deflection of the vertical on a unit sphere

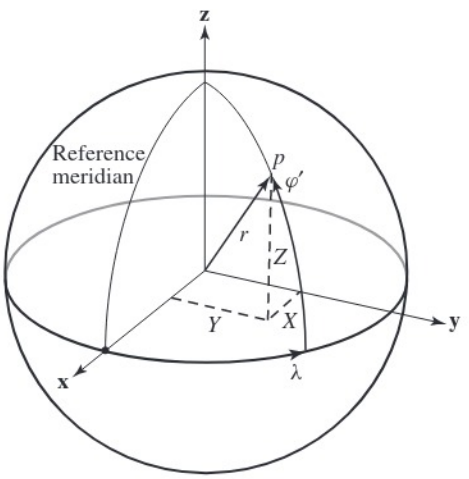


Figure 5.5 Geocentric Cartesian coordinates and geographical coordinates

the radial vector to point p, and λ is the angle in the x-y plane measured from the x-axis to the projection of p on the x-y plane; see Fig. 5.5. Conversion from (geocentric) geographical coordinates to (geocentric) Cartesian coordinates is given by

$$\begin{bmatrix} X \\ Y \\ Z \end{bmatrix}_p = r \begin{bmatrix} \cos\phi' \cos\lambda \\ \cos\phi' \sin\lambda \\ \sin\phi' \end{bmatrix}. \tag{5.7}$$

Conversion from (geocentric) geodetic to (geocentric) Cartesian coordinates is given by

$$\begin{bmatrix} X \\ Y \\ Z \end{bmatrix}_p = \begin{bmatrix} (N_\phi + h)\cos\phi\cos\lambda \\ (N_\phi + h)\cos\phi\sin\lambda \\ ((1-e^2)N_\phi + h)\sin\phi \end{bmatrix} \tag{5.8}$$

where e is the *eccentricity* of the ellipsoid

$$e = \frac{\sqrt{a^2 - b^2}}{a} = \sqrt{2f - f^2} \tag{5.9}$$

and N_ϕ is the ellipsoidal *radius of curvature in the prime vertical*, and is given by

$$N_\phi = \frac{a}{\sqrt{1 - e^2\sin^2\phi}}. \tag{5.10}$$

Conversion from (geocentric) Cartesian to (geocentric) geographical coordinates is given by

$$\begin{bmatrix} \phi' \\ \lambda \\ r \end{bmatrix}_p = \begin{bmatrix} \tan^{-1}\frac{Z}{\sqrt{X^2+Y^2}} \\ \tan^{-1}\frac{Y}{X} \\ \sqrt{X^2+Y^2+Z^2} \end{bmatrix}. \tag{5.11}$$

Note that $\phi' = \sin^{-1} Z/\sqrt{X^2+Y^2+Z^2}$ may also be used to determine ϕ', and that these functions are evaluated such that $-90° \le \phi$ (or ϕ') $\le +90°$, and $0° \le \lambda < 360°$.

Conversion from geocentric Cartesian to geodetic coordinates is not as simple a matter, however. The geodetic longitude λ can be determined by inverting the relationships in Eq. 5.8: $Y/X = \tan\lambda$ or $\lambda = \tan^{-1}(Y/X)$. Determining ϕ and h are a much more difficult problem. Two general approaches have been used—(a) iterative and non-iterative approximation methods, and (b) closed-form solutions. Most of the proposed methods are of the first type and include Bowring (1976), Lin and Wang (1995), Fukishima (1999, 2006), Pollard (2002), Turner (2009) and Feltens (2008, 2009). Borkowski (1989) derived an exact solution, but it has some singularities and special conditions. Much of the work on this problem has been devoted to finding faster algorithms and better approximation techniques to solve the problem.

5.2.5 Local Coordinate Systems

Many possibilities exist for establishing local coordinate systems, either systems designed for a specific observer or systems designed to cover a given local area. Most systems specific to an observer are *horizon* (or altitude and azimuth) coordinate systems and a "standard" one is described below. Coordinate systems designed to cover a localized area are usually based on a *map projection* coordinate system, such that the coordinates of a point relative to the reference ellipsoid are projected onto a plane upon which computations can be done with relative simplicity (as opposed to working on the ellipsoid itself). A few of the most commonly used systems—Universal Transverse Mercator, Lambert conformal conic and (U.S.) state plane coordinates—are described below.

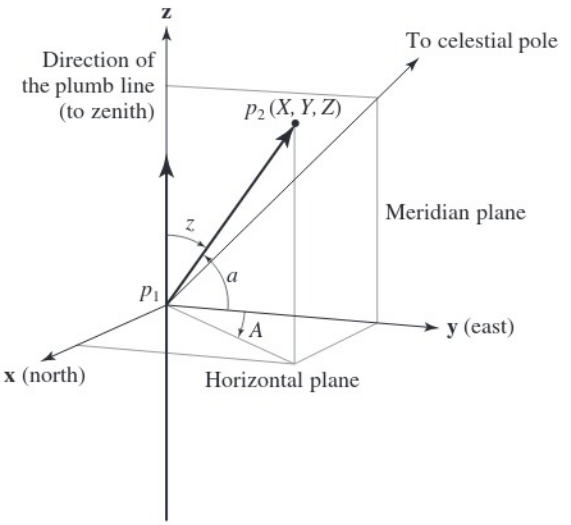


Figure 5.6 Horizon system altitude and azimuth

5.2.5.1 Horizon System

Depending on the author, slight variations exist in the definition of any local horizon coordinate system. However, a more or less "standard" system is described as follows.

First, any such system must have at least two reference planes. The primary reference plane here is the *local horizon*, and the secondary is the *local meridian* (see Fig. 5.6). The horizon is the plane perpendicular to the observer's local vertical, while the meridian is the plane perpendicular to the horizon that passes through the north and south celestial poles, the observer and the zenith. The direction of any point p_2 (from the observer at p_1) in this system is then given by its altitude and azimuth. If we imagine a plane passing through p_2 and the zenith z, the angle between the horizon and the point p_2 in this plane is the altitude a (also sometimes known as the *elevation angle*). The angle between the meridian and this plane measured clockwise from north, as viewed from above, is the azimuth A. (Some users in the past, particularly for geodetic purposes, have defined azimuth as being measured clockwise from south. This practice is no longer much in use but users of old observations should be aware of it.) The altitude is defined from $-90°$ to $+90°$ (negative if the object is below the horizon and positive if above), and the azimuth is measured from $0°$ to $360°$. Instead of this spherical coordinate system, a left-handed three-dimensional Cartesian coordinate system is also used, with the z-axis positive up, the x-axis positive north, and the y-axis positive east (through $90°$ azimuth).

A further variation of this system is to use the zenith distance z instead of the altitude. The *zenith distance* is simply the complement of the altitude, i.e., the angular distance of p_2 from the zenith z. It has the advantage of always being positive, with values from $0°$ to $180°$. It is computed from altitude as

$$z = 90° - a \tag{5.12}$$

where the z and a are in degrees.

5.2.5.2 Grid Coordinate Systems

For computational convenience and for ease of use in local and regional areas, it is common to represent sections of the curved surface of the Earth with a plane. Various systems have been devised to do this, all based on given transformation equations from the sphere or ellipsoid to the plane. These transformations are, in fact, map projections, in many cases the same as those used for mapping large regional areas or the entire Earth. *Conformal* projections are commonly used because they preserve the true shapes of small areas; relative angles (directions) about any point are approximately correct; and the local scale in all directions about any given point is constant. In these projections, the meridians and parallels of latitude intersect at right angles.

The coordinate systems based on such map projections are usually termed *grid coordinate systems*. The most widely used are the Universal Transverse Mercator (UTM), Universal Polar Stereographic (UPS), and Lambert conformal conic (LCC) projections. In the United States, the state plane coordinate systems are based on UTM or LCC projections (Burkholder 2008, chapter 10) while the U.S. National Grid (USNG) System (FGDC 2001) is based on UTM and the Military Grid Reference System (see Universal Transverse Mercator grid section below). Obviously many other systems exist for various countries and areas, but the basic principles (and many times the projection formulae, with the exception of constants) are the same.

For any grid coordinate system, several fundamental transformations and quantities are of importance. The fundamental transformations are the direct conversion from geodetic coordinates (ϕ, λ) to grid coordinates (X, Y), and the inverse transformation from grid coordinates to geodetic coordinates. Other quantities of interest include: (a) the convergence of the meridians, i.e., the angle between grid north and true north on the grid (γ); (b) the angle on the grid between the *geodesic* (the shortest path connecting two points on the surface of the reference ellipsoid) and the straight line between them (known in some of the references as "t–T"); (c) the scale at a given point (k); and (d) the scale factor along a line. Equations for the transformations and scale are given below (based on Snyder (1983)); equations for the other quantities are available from the other references, particularly Thomas (1952). The specific coordinates of a point on the grid are determined by the choice of the reference ellipsoid (in effect, the geodetic datum) to which latitude and longitude are referred and whose parameters are used in the map projection equations, as shown below. Software for coordinate conversions of UTM and USNG grid coordinates is available from the U.S. National Geodetic Survey (URL[7], URL[8]). UTM, UPS and LCC are also discussed in Parker and Bartholomew (1989) and ISO (2009).

Fundamental quantities and expressions used in the transformation equations are summarized as follows:

ϕ = geodetic latitude of point;

λ = geodetic longitude of point;

ϕ_0 = latitude of the origin;

λ_0 = longitude of the origin (and the central meridian for the UTM grid);

$\Delta\lambda$ = difference of longitude from the central meridian ($\Delta\lambda = \lambda - \lambda_0$)(in radians);

a = semimajor axis of the ellipsoid;

b = semiminor axis of the ellipsoid;

e = eccentricity of the ellipsoid ($e^2 = \dfrac{a^2 - b^2}{a^2}$);

e' = second eccentricity of the ellipsoid ($e'^2 = \dfrac{a^2 - b^2}{b^2}$).

The equations that are given below for the Transverse Mercator, Polar Stereographic, and Lambert Conformal Conic projections can be used with many other grid systems with just a change of the appropriate constants.

Universal Transverse Mercator grid. The Universal Transverse Mercator (UTM) grid coordinate system divides the world into sixty 6°-wide zones of longitude, with zone 1 going from −180° to −174° longitude, zone 2 from −174° to −168° longitude, etc. Latitude bands are designated with letters at 8° intervals from 80°S to 72°N and one 12° interval from 72–84°N (DMA 1990). The grid zone designations are shown in Fig. 5.7 and were devised by the U.S. Army in 1947 as a way to systematically represent smaller geographic areas on large scale maps. This *Military Grid Reference System* or MGRS (DMA 1990), originally designed for artillery operations, has become a standard for commercial applications and was adopted in the U.S. as the U.S. National Grid (FGDC 2001). It essentially divides each 6x8 degree zone into 100,000-meter squares, which are each given a two-letter designation. Within each of these squares the coordinates of a point can be specified in terms of Easting (X) and Northing (Y) *grid coordinates*, in units of meters, with precisions of 10,000 meters to 1 meter depending on the application.

In the UTM grid system (DMA 1989), the central meridian is the central meridian of each zone, with a scale factor of $k_0 = 0.9996$. This results in a maximum scale error of 1/1000 anywhere in a zone, or 1/2500 for points on the central meridian or above 45° or below −45° latitude. (Of course, as with all grid systems, there is no scale error if the appropriate corrections for scale are made.) In each zone, the central meridian is defined as the Easting (X) coordinate origin with a value of X = 500 000 meters (called the *false Easting*). The Northing (Y) origin for all zones is the equator at which *false Northings* are defined as Y = 0 meters for northern hemisphere zones and Y=10 000 000 meters for southern hemisphere zones. This scheme avoids the need for negative coordinate values. UTM grid coordinates always increase from south to north and west to east within a zone.

For UTM, starting with our previously given expressions, we continue by computing S_ϕ, the length of the meridional arc, the true meridional distance on the ellipsoid from the equator to latitude ϕ:

$$\begin{aligned} S_\phi = a[&(1 - e^2/4 - 3e^4/64 - 5e^6/256 - \cdots)\phi \\ &- (3e^2/8 + 3e^4/32 + 45e^6/1024 + \cdots)\sin 2\phi \\ &+ (15e^4/256 + 45e^6/1024 + \cdots)\sin 4\phi \\ &- (35e^6/3072 + \cdots)\sin 6\phi + \cdots] \end{aligned} \tag{5.13}$$

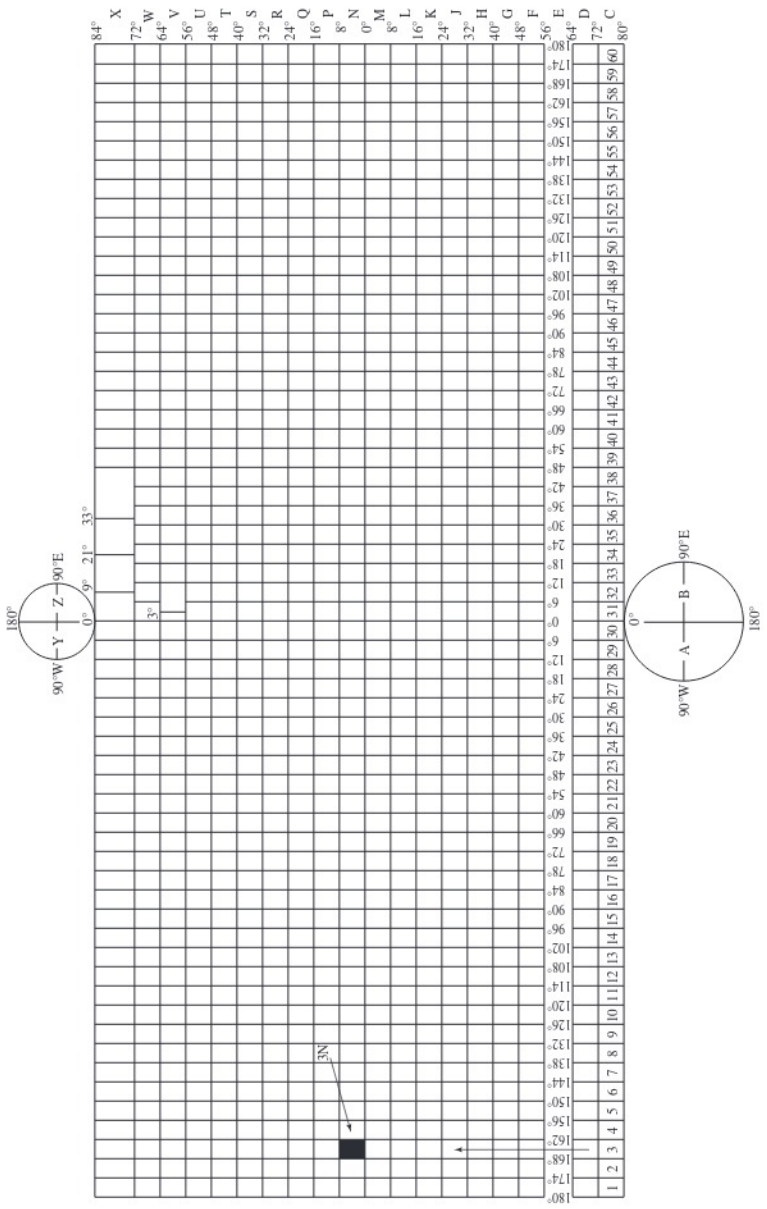


Figure 5.7 UTM and UPS grid zone designations

where ϕ is in radians. Also needed are other auxiliary quantities:

$$T = \tan^2 \phi \tag{5.14}$$

$$C = e'^2 \cos^2 \phi \tag{5.15}$$

$$A = \Delta\lambda \cos \phi. \tag{5.16}$$

We also compute S_{ϕ_0} as given by S computed at the latitude ϕ_0 at the origin of the X and Y coordinates. Then the direct transformation from (ϕ, λ) to (X, Y) is given by

$$X = k_0 N_\phi [A + (1 - T + C)A^3/6 + (5 - 18T + T^2 + 72C - 58e'^2)A^5/120] \tag{5.17}$$

$$Y = k_0 \{S_\phi - S_{\phi_0} + N_\phi \tan\phi [A^2/2 + (5 - T + 9C + 4C^2)A^4/24 + (61 - 58T + T^2 + 600C - 330e'^2)A^6/720]\}. \tag{5.18}$$

The actual UTM coordinates are obtained by adding the appropriate false Easting and false Northing values to these X and Y coordinates. The scale factor at any given point is given by

$$k = k_0 \left[1 + (1 + C)\frac{A^2}{2} + (5 - 4T + 42C + 13C^2 - 28e'^2)\frac{A^4}{24} + (61 - 148T + 16T^2)\frac{A^6}{720}\right]. \tag{5.19}$$

The inverse formulae, for converting (X, Y) to (ϕ, λ) are

$$\phi = \phi_1 - (N_{\phi_1} \tan\phi_1 / R_1)[D^2/2 - (5 + 3T_1 + 10C_1 - 4C_1^2 - 9e'^2)D^4/24 + (61 + 90T_1 + 298C_1 + 45T_1^2 - 252e'^2 - 3C_1^2)D^6/720] \tag{5.20}$$

$$\lambda = \lambda_0 + [D - (1 + 2T_1 + C_1)D^3/6 + (5 - 2C_1 + 28T_1 - 3C_1^2 + 8e'^2 + 24T_1^2)D^5/120]/\cos\phi_1 \tag{5.21}$$

where ϕ_1 is the *footpoint latitude* or the latitude at the central meridian which has the same Y coordinate as that of the point (ϕ, λ). It is given by

$$\phi_1 = \mu + (3e_1/2 - 27e_1^3/32 + \cdots)\sin 2\mu + (21e_1^2/16 - 55e_1^4/32 - \cdots)\sin 4\mu + (151e_1^3/96 + \cdots)\sin 6\mu + \cdots \tag{5.22}$$

where

$$e_1 = \frac{1 - \sqrt{1 - e^2}}{1 + \sqrt{1 - e^2}} \tag{5.23}$$

$$\mu = S/[a(1 - e^2/4 - 3e^4/64 - 5e^6/256 - \cdots)] \tag{5.24}$$

$$S = S_{\phi_0} + Y/k_0. \tag{5.25}$$

For the other terms, in addition to needing C, T, and N_ϕ for the footpoint latitude ϕ_1 we also have

$$R_1 = a(1 - e^2)/(1 - e^2 \sin^2\phi_1)^{3/2} \tag{5.26}$$

$$D = X/(N_{\phi_1} k_0). \tag{5.27}$$

R_1 is the ellipsoidal radius of curvature in the meridian.

Universal Polar Stereographic grid. The Universal Polar Stereographic Grid System (UPS) consists of two polar stereographic projections, one for the north polar region and one for the south polar region (DMA 1989). The north region covers all areas north of 84°

latitude, and the south region all areas south of $-80°$ latitude. The grid scheme is defined by the MGRS. A single letter is used to designate the eastern or western half of each region in the grid, instead of the zone numbers used for the UTM grid. Two-letter identifiers are used again to represent 100,000-meter squares in each region (DMA 1990). The scale factor at the origin (the poles) is $k_0 = 0.994$. In both regions, a 2,000,000-meter X-coordinate line coincides with the $0°$ and $180°$ meridians. The pole will have coordinates of $X = 2,\,000,\,000$ meters, and $Y = 2,\,000,\,000$ meters.

For UPS coordinates, the direct equations are

$$X = 2\,000\,000 + \rho \sin \Delta\lambda \tag{5.28}$$

$$Y_{\text{north}} = 2\,000\,000 - \rho \cos \Delta\lambda \tag{5.29}$$

$$Y_{\text{south}} = 2\,000\,000 + \rho \cos \Delta\lambda. \tag{5.30}$$

The first Y is for the north zone, the second for the south zone. The auxiliary quantities are obtained from

$$\rho = \frac{2ak_0 t}{\sqrt{(1+e)^{1+e}(1-e)^{1-e}}} \tag{5.31}$$

$$t = \tan\left(\frac{\pi}{4} - \frac{|\phi|}{2}\right)\left[\frac{1 + e\sin|\phi|}{1 - e\sin|\phi|}\right]^{e/2} \tag{5.32}$$

$$\text{for } 0 \le \phi < \frac{\pi}{2} \quad \text{north zone}$$

$$\text{and } -\frac{\pi}{2} < \phi \le 0 \quad \text{south zone.}$$

We also have for the scale

$$k = \frac{\rho}{am} \tag{5.33}$$

where

$$m = \frac{\cos\phi}{\sqrt{1 - e^2\sin^2\phi}}. \tag{5.34}$$

The inverse solution for ϕ and λ for the north zone is given by

$$\phi = \frac{\pi}{2} - 2\arctan\left\{t\left[\frac{1 - e\sin\phi}{1 + e\sin\phi}\right]^{e/2}\right\} \tag{5.35}$$

$$\lambda = \lambda_0 + \arctan\frac{X}{-Y} \tag{5.36}$$

where ϕ is solved iteratively using as the starting value

$$\phi = \frac{\pi}{2} - 2\arctan t. \tag{5.37}$$

The inverse solutions for the south zone are the same as the north zone, but the signs of ϕ, λ, λ_0, X, and Y are reversed. For additional details, see Snyder (1983, pp. 160–164), ISO (2009, pp. 77–80), and DMA (1989).

Lambert conformal conic grid. The equations for the Lambert conformal conic (LCC) projection are taken from Snyder (1983, pp. 107–109); see also ISO (2009, pp. 74–76). Define

$\phi_0 =$ latitude of the origin;

$\phi_1, \phi_2 =$ latitude of the standard parallels for the Lambert conformal conic grid.

The direct equations are

$$X = \rho \sin\theta \tag{5.38}$$

$$Y = \rho_0 - \rho\cos\theta \tag{5.39}$$

$$k = \frac{\rho_0 n}{am} \tag{5.40}$$

where

$$\rho = aFt^n \tag{5.41}$$

$$\theta = n(\lambda - \lambda_0) \tag{5.42}$$

$$\rho_0 = aFt_0^n \tag{5.43}$$

$$n = \frac{\ln m_1 - \ln m_2}{\ln t_1 - \ln t_2} \tag{5.44}$$

$$m = \frac{\cos\phi}{\sqrt{1 - e^2\sin^2\phi}} \tag{5.45}$$

$$t = \tan\left(\frac{\pi}{4} - \frac{\phi}{2}\right)\left[\frac{(1 + e\sin\phi)}{(1 - e\sin\phi)}\right]^{e/2} \tag{5.46}$$

$$F = \frac{m_1}{nt_1^n} \tag{5.47}$$

with the same subscripts 1, 2, or none applied to m and ϕ in the equation for m, and the subscripts 0, 1, 2, or none applied to t and ϕ in the equation for t. n, F, and ρ_0 need be computed only once per zone. Note that published (in some cases officially adopted) tables may give (negligible) differences, as the tables were computed with simpler, less-precise formulae (Snyder 1983, p. 108).

The inverse formulae are

$$\phi = \frac{\pi}{2} - 2\arctan\left\{t\left[\frac{1 - e\sin\phi)}{1 + e\sin\phi)}\right]^{e/2}\right\} \tag{5.48}$$

where

$$t = \left(\frac{\rho}{aF}\right)^{1/n} \tag{5.49}$$

$$\rho = \pm\sqrt{X^2 + (\rho_0 - Y)^2} \tag{5.50}$$

and

$$\lambda = \frac{\theta}{n} + \lambda_0 \tag{5.51}$$

where

$$\theta = \arctan\frac{X}{\rho_0 - Y}. \tag{5.52}$$

The sign of ρ is taken from n. If n is negative, the signs of X, Y, and ρ_0 in the equation for θ must be reversed, and the quadrant of θ determined accordingly. Also note that the equation for ϕ requires iteration on ϕ, as in the UPS case, and will converge rapidly with the same initial assumption

$$\phi = \frac{\pi}{2} - 2 \arctan t. \tag{5.53}$$

State plane coordinates. In the United States, a state plane coordinate system has been established so that each state has its own grid coordinate system. These systems were originally designed by the U.S. Geological Survey in the 1930s and 1940s, and have since been legally adopted by the state legislatures of most states. States or areas of states with a mostly north–south orientation are represented in a transverse Mercator map projection, whereas states or areas with a predominantly east-west orientation use a Lambert conformal conic projection. (An exception is the oblique transverse Mercator projection used for part of Alaska.) There are 136 separate zones covering all of the 50 states. (The U.S. Virgin Islands, American Samoa, and other territories all also have their own projections, some of which are *not* conformal). Snyder (1983, pp. 58–62, Table 8) lists all the zones, by projection and state, with the central meridian, its scale error for the Lambert conformal conic zones, and the standard parallels and origin for the transverse Mercator zones. The coordinates of the origins are also given in a footnote to that table. Unlike UTM grid zones, state plane coordinate grid zones are very irregular and are defined by county, state and international boundaries. Software to convert state plane coordinates to or from geographic coordinates (latitude, longitude) is available from the National Geodetic Survey (URL[8]). Note that *U.S. survey feet* (1 U.S. survey foot = 1200/3937 m) are used rather than international feet (1 International foot = 0.3048 m = 0.999 993 U.S. survey feet exactly). In addition, state plane coordinates derived from NAD 83 are given in meters, while state plane coordinates derived from NAD 27 are given in U.S. survey feet. These systems were originally established under the assumption that any calculations done assuming plane coordinates would not have errors worse than 1 in 10,000. Their definition in many states is also legally tied to NAD 27 or NAD 83, and land parcels may be defined or even *must* be defined in terms of state plane coordinates. Many governmental and commercial organizations currently use state plane coordinates heavily. [For more information on state plane coordinates and projections, see Stem (1989), Mitchell and Simmons (1945), and Snyder (1983, pp. 56–63). General surveying texts, such as Moffit and Bouchard (1975) and Burkholder (2008), also contain information on state plane coordinates.]

The equations for the transverse Mercator and Lambert conformal conic projections have already been given above. The only changes for their application with state plane coordinates will be for constants such as the central meridian (λ_0), the scale factor on the central meridian (k_0), and the grid coordinates of the origin.

5.2.5.3 Specific Ellipsoids, Datums, and Reference Systems

Table 5.1 lists various ellipsoids that have been used as the basis of geodetic datums and reference systems. Note that as previously mentioned, only a and $1/f$ are necessary for the definition of an ellipsoid. Table 5.2 lists geodetic datums (also giving the origin station if any and its latitude and longitude) and notes that are associated with specific terrestrial reference

Table 5.1 Earth ellipsoids

Ellipsoid (Name and Year Computed)	Semimajor Axis (a) (Meters)	Inverse Flattening ($1/f$)
Airy 1830	6377563.396	299.3249646
Modified Airy (1849)	6377340.189	299.3249646
Australian National 1965	6378160	298.25
Bessel 1841 (Namibia)	6377483.865	299.1528128
Bessel 1841 (Ethiopia, Tokyo)	6377397.155	299.1528128
Clarke 1866	6378206.4	294.9786982139
Clarke 1880	6378249.145	293.465
Clarke 1880 (Cape)	6378249.145	293.4663077
Engelis 1985	6378136.05	298.2566
Everest (India 1830)	6377276.345	300.8017
Everest (E. Malaysia, Brunei 1967)	6377298.556	300.8017
Everest (India 1956)	6377301.243	300.8017
Everest (W. Malaysia 1969)	6377295.664	300.8017
Everest (W. Malaysia & Singapore 1948)	6377304.063	300.8017
Fischer 1960 (Mercury)	6378166	298.3
Mod. Fischer 1960 (S. Asia)	6378155	298.3
Fischer 1968 (Modified Mercury)	6378150	298.3
Helmert 1906	6378200	298.3
Hough 1960	6378270	297
IAU 1964	6378160	298.25
IAU 1976	6378140	298.257
IERS 1989	6378136	298.257
Indonesian 1974	6378160	298.247
International 1924	6378388	297
IAG 1975	6378140	298.257
Geodetic Reference System 1967	6378160	298.2471674273
Geodetic Reference System 1980	6378137	298.257222101
Krassovsky 1940	6378245	298.3
MERIT 1983	6378137	298.257
South American 1969	6378160	298.25
Soviet Geodetic System 1990	6378136	298.2578393
WGS 60	6378165	298.3
WGS 66	6378145	298.25
WGS 72	6378135	298.26
WGS 84	6378137	298.2572235630

Table 5.2 Historical geodetic datums

Datum [a]	Ellipsoid	Origin	Latitude			Longitude		
			°	′	″	°	′	″
Adindan	Clarke 1880	Station Z_V	+22	10	07.110	031	29	21.608
American Samoa 1962	Clarke 1866	Betty 13 ECC	−14	20	08.341	189	17	07.750
Arc−Cape (South Africa)	Clarke 1880	Buffelsfontein	−33	59	32.000	025	30	44.622
Argentine	International	Campo Inchauspe	−35	58	17	297	49	48
Ascension Island 1958	International	Mean of 3 stations	−07	57		345	37	
Australian Geodetic 1966	Australian National	Johnston Memorial Cairn	−25	56	54.55	133	12	30.08
Australian Geodetic 1984	Australian National	Johnston Memorial Cairn	−25	56	54.55	133	12	30.08
Geocentric Datum of Australia	GRS 80	Geocenter						
Bermuda 1957	Clarke 1866	Ft. George B 1937	+32	22	44.360	295	19	01.890
Berne 1898	Bessel	Berne Observatory	+46	57	08.660	007	26	22.335
Betio Island, 1966	International	1966 Secor Astro	+01	21	42.03	172	55	47.90
Camp Area Astro 1961–1962 USGS	International	Camp Area Astro	−77	50	52.521	166	40	13.753
Canton Astro 1966	International	1966 Canton Secor Astro	−02	46	28.99	188	16	43.47
Cape Canaveral (*)	Clarke 1866	Central	+28	29	32.364	279	25	21.230
Christmas Island Astro 1967	International	Sat.Tri.Sta. 059 RM3	+02	00	35.91	202	35	21.82
Chua Astro (Brazil-Geodetic)	International	Chua	−19	45	41.16	311	53	52.44
Corrego Alegra (Brazil-Mapping)	International	Corrego Alegre	−19	50	15.140	311	02	17.250
Easter Island 1967 Astro	International	Satrig Rm No. 1	−27	10	39.95	250	34	16.81
Efate (New Hebrides)	International	Belle Vue IGN	−17	44	17.400	168	20	33.250

Table 5.2 *(continued)*

Datum	Ellipsoid	Origin	Latitude			Longitude		
			°	′	″	°	′	″
European (Europe 50)	International	Helmertturm	+52	22	51.45	013	03	58.74
Graciosa Island (Azores)	International	Sw Base	+39	03	54.934	331	57	36.118
Gizo, Provisional DOS	International	GUX 1	−09	27	05.272	159	58	31.752
Guam	Clarke 1866	Togcha Lee No. 7	+13	22	38.49	144	45	51.56
Heard Astro 1969	International	Intsatrig 0044 Astro	−53	01	11.68	073	23	22.64
Iben Astro, Navy 1947 (Truk)	Clarke 1866	Iben Astro	+07	29	13.05	151	49	44.42
Indian 1938	Everest 1830	Kalianpur	+24	07	11.26	077	39	17.57
Isla Socorro Astro	Clarke 1866	Station 038	+18	43	44.93	249	02	39.28
Johnston Island 1961	International	Johnston Island 1961	+16	44	49.729	190	29	04.781
Kourou (French Guiana)	International	Point Fondamental	−05	15	53.699	−52	48	09.149
Kusaie, Astro 1962, 1965	International	Allen Sodano Light	+05	21	48.80	162	58	03.28
Luzon 1911 (Philippines)	Clarke 1866	Balancan	+13	33	41.000	121	52	03.000
Midway Astro 1961	International	Midway Astro 1961	+28	11	34.50	182	36	24.28
New Zealand 1949	International	Papatahi	−41	19	08.900	175	02	51.000
North American 1927	Clarke 1866	Meades Ranch	+39	13	26.686	261	27	29.494
North American 1983	GRS 80	Geocenter						
Old Bavarian	Bessel	Munich	+48	08	20.000	011	34	26.483
Old Hawaiian	Clarke 1866	Oahu West Base	+21	18	13.89	202	09	04.21
Ordnance Survey G.B. 1936	Airy 1830	Herstmonceux	+50	51	55.271	000	20	45.882
OSGB 1970 (SN)	Airy	Herstmonceux	+50	51	55.271	000	20	45.882
Palmer Astro 1969 (Antarctica)	International	ISTS 050	−64	46	35.71	295	56	39.53
Pico de las Nieves (Canaries)	International	Pico de las Nieves	+27	57	41.273	344	25	49.476

Table 5.2 *(continued)*

Datum [a]	Ellipsoid	Origin	Latitude			Longitude		
			°	′	″	°	′	″
Pitcairn Island Astro	International	Pitcairn Astro 1967	−25	04	06.97	229	53	12.17
Potsdam	Bessel 1841	Helmertturm	+52	22	53.954	013	04	01.153
Provisional S. American 1966	International	La Canoa	+08	34	17.17	296	08	25.12
Provisional S. Chile 1963	International	Hito XVIII	−53	57	07.76	291	23	28.76
Pulkovo 1942	Krassovsky 1940	Pulkovo Observatory	+59	46	18.55	030	19	42.09
Qornoq (Greenland)	International	No. 7008						
South American 1969	South American 1969	Chua	−19	45	41.653	311	53	55.936
Southeast Island (Mahe)	Clarke 1880		−04	40	39.460	055	32	00.166
South Georgia Astro	International	ISTS 061 Astro Point 1968	−54	16	38.93	323	30	43.97
Swallow Islands (Solomons)	International	1966 Secor Astro	−10	18	21.42	166	17	56.79
Tananarive	International	Tananarive Observatory	−18	55	02.10	047	33	06.75
Tokyo	Bessel 1841	Tokyo Observatory (old)	+35	39	17.51	139	44	40.50
Tristan Astro 1968	International	Intsatrig 069 RM No. 2	−37	03	26.79	347	40	53.21
Viti Levu 1916 (Fiji)	Clarke 1880	Mōnavatu (latitude only)	−17	53	28.285			
		Suva (longitude only)				178	25	35.835
Wake Island, Astronomic 1952	International	Astro 1952	+19	17	19.991	166	38	46.294
White Sands (*)	Clarke 1866	Kent 1909	+32	30	27.079	253	31	01.306
Yof Astro 1967 (Dakar)	Clarke 1880	Yof Astro 1967	+14	44	41.62	342	30	52.98

[a] Local datums marked with an ∗ were for special purposes, based on NAD 1927 values for the origin stations. Sources: Rapp (1980); Mueller et al. (1973, p. 11); Nautical Almanac Offices of UK and USA (1989, p. K13).

systems. Similar, but abbreviated versions of these tables are given in Nautical Almanac Offices of UK and USA, (1989, p. K13).

5.2.5.4 Datum Conversions

The subject of converting coordinates from one datum to another is a complex one, with a very extensive literature. Indeed, the problem almost always arises and is usually discussed whenever a new datum or reference system is formed, since there will usually be a need to transform the coordinates of points in other systems to coordinates in the new system.

Two general methods have been used in the past for datum transformations. The first is a differential method, where differential (in the partial-derivative sense) equations are formed that give the change in station coordinates $(\Delta\phi, \Delta\lambda)$ as a function of changes in datum/ellipsoid parameters (such as for changes in a, f, scale, etc.). This type of method has been most useful in the past where small differences exist between the two datums, or a minor change in an existing datum was being made. However, the derivation of the differential equations for a specific case and their application and accuracy is a complicated subject and will not be discussed further here. [Information on this type of method is available in Rapp (1980, pp. 42–74), Bomford (1971, pp. 199–207), Heiskanen and Moritz (1967, pp. 204–210), Molodenskii, Eremeev, and Yurkina (1962, pp. 13–17), Torge (1980, pp. 150–152), and DMA (1987, part 1, pp. 7-1 to 8-8).]

A second method is to do a rigorous transformation between the systems of each datum. This is often required if high accuracy is desired, or there are several or large differences between the datums. For any pair of datums, transformation parameters may have already been determined, at least for offsets and sometimes for rotation and scale. A three-step procedure is required to convert (ϕ, λ, h) from system 1 to system 2

$$(\phi, \lambda, h)_1 \Rightarrow (X, Y, Z)_1 \tag{5.54}$$

$$(X, Y, Z)_1 \Rightarrow (X, Y, Z)_2 \tag{5.55}$$

$$(X, Y, Z)_2 \Rightarrow (\phi, \lambda, h)_2. \tag{5.56}$$

The geodetic to Cartesian and Cartesian to geodetic transformations have already been described in § 5.2.4. In general, the transformation of one Cartesian system into another Cartesian system requires a translation of the origin and a rotation of the coordinate axes of the first system to align it with the second system. This takes the form of a 7-parameter similarity transformation:

$$\begin{bmatrix} X \\ Y \\ Z \end{bmatrix}_2 = \begin{bmatrix} \Delta X \\ \Delta Y \\ \Delta Z \end{bmatrix} + \begin{bmatrix} D & -R_3 & R_2 \\ R_3 & D & -R_1 \\ -R_2 & R_1 & D \end{bmatrix} \begin{bmatrix} X \\ Y \\ Z \end{bmatrix}_1 \tag{5.57}$$

where ΔX, ΔY and ΔZ are the components of the origin translation; R_1, R_2, and R_3 are the rotation angles (using small-angle formulae here); and D is the scale factor (ISO 2009, p. 343). Various forms of this 7-parameter transformation exist under various names (some not as rigorous as others). (See Kumar 1972, Rapp 1980, p. 48, NIMA 1997, Seeber 2003, pp. 27–28, and Hofmann-Wellenhof, Lichtenegger, and Collins 2001.) It is also possible that some of the parameters may not be known or can be assumed to be zero.

In some cases, the transformation parameters are not well-determined or not known at all. The user must then determine the parameters directly from observations that tie stations together between the two systems. If enough points have their coordinates determined in both systems, Eq. 5.57 or similar equations can be solved (usually in a least-squares solution) for the transformation parameters. Of course, this may not take into account any deformations of either of the datums from their idealized reference systems (due to surveying errors). Any deformations will be absorbed into the transformation parameters when they are solved for. Software for converting geographic coordinates among a wide variety of coordinate systems, map projections, and datums can be found at URL[9].

In comparing or transforming modern geocentric terrestrial reference frames, in contrast to classical datums, all the transformation parameters tend to be very small or close to zero. This is due to the adoption of common standards and conventions (e.g., IERS conventions), use of common equipment, and similar data processing techniques. The realizations of the reference frames will differ due to differences in the observing stations and the software used, among other things. There are essentially two options in satellite geodesy for computing transformations between reference frames. One can compute the orbits of the same satellites (for example, GPS) in two different reference frames and then determine 7-parameter transformations between the orbits. Alternatively, if a network of stations is available with coordinates independently determined from both reference frames, then one can compute a 7-parameter transformation between the two sets of station coordinates. As the accuracy and precision of measurements and modeling have improved, it is now common to take into account for scientific purposes the time-dependency of the 7 parameters, resulting in computation of 14-parameter transformations (see URL[3]).

To avoid transformations completely, one could measure the coordinates of all the desired points with a GPS satellite receiver—thus determining the coordinates of the points in some current reference system, bypassing any transformations entirely. This eliminates the need to use the old datums or old observations. The coordinates can be measured in an absolute sense, relative to the center of the Earth at decimeter accuracy or better if sufficient data are collected (Leandro, Santos, and Langley 2007; Bisnath and Gao 2009; Zumberge et al. 1997). Coordinates can also be determined relative to known reference points that are close by (1 km or less) or longer distances away (10s to 100s of kilometers) to accuracies of a few centimeters or even millimeters (URL[10]; Dixon 2006) by using the appropriate receiver equipment, data processing techniques and sufficient data, depending upon the application and the accuracy required. The resulting coordinates will be consistent with the geodetic reference frame and datum used for the data processing.

5.3 Gravity, Tides, and Motions of the Crust

In this section, various phenomena will be covered that affect the Earth's gravity field and coordinates of a given station. A very short summary of one method of modeling the Earth's gravity field (as a spherical harmonic series) is given, along with the IERS recommendations for a "standard" gravity field. This is followed by, almost verbatim, the *IERS Conventions (2010)* recommendations on Earth tides, ocean tides, ocean and atmospheric loading, and plate motions (IERS 2010, 2004). Finally, the effect of tides on the Earth's rotation itself is described, as given by the *IERS Conventions (2010)*.

5.3.1 Modeling the Earth's Gravity Field

The Earth's gravity can be considered as a force that is the sum of the Earth's gravitational force and the centrifugal force resulting from the Earth's rotation.

The Earth's external gravitational field can be considered a potential field whose strength V fulfills the *Laplace equation*

$$\Delta V = 0 \tag{5.58}$$

where Δ is the Laplacian operator

$$\frac{\partial^2}{\partial X^2} + \frac{\partial^2}{\partial Y^2} + \frac{\partial^2}{\partial Z^2} \tag{5.59}$$

in a cartesian X, Y, and Z coordinate system.

It is possible to develop a solution to Eq. 5.58 (Heiskanen and Moritz 1967, pp. 15–35; Torge 1980, pp. 26–29) in terms of a series of *Legendre polynomials*:

$$P_n(t) = \frac{1}{2^n \times n!} \times \frac{d^n}{dt^n}(t^2 - 1)^n \tag{5.60}$$

with

$$t = \cos\psi = \cos\theta \cos\theta' + \sin\theta \sin\theta' \cos(\lambda' - \lambda). \tag{5.61}$$

The variable ψ is the spherical distance on a unit sphere between an attracted point (at spherical coordinates r, θ, λ) and an attracting point (at r', θ', λ').

In order to express $P_n(t)$ as a function of the spherical coordinates θ and λ, it may be decomposed using *associated Legendre Functions of the first kind* of degree n and order m, obtained by differentiating $P_n(t)$ m times

$$P_{nm}(t) = (1 - t^2)^{m/2} \frac{d^m}{dt^m} P_n(t). \tag{5.62}$$

It can then be expressed by the functions

$$P_{nm}(\cos\theta) \cos m\lambda \tag{5.63}$$

$$P_{nm}(\cos\theta) \sin m\lambda \tag{5.64}$$

known as *surface spherical harmonic* functions.

A general equation for the gravitational potential then becomes

$$\begin{aligned} V = {} & \frac{G}{r} \sum_{n=0}^{\infty} \sum_{m=0}^{n} k \frac{(n-m)!}{(n+m)!} \\ & \times \frac{1}{r^n} \Bigg(P_{nm}(\cos\theta) \cos m\lambda \int\int\int_{\text{Earth}} r'^n P_{nm}(\cos\theta') \cos m\lambda \, dm \\ & + P_{nm}(\cos\theta) \sin m\lambda \int\int\int_{\text{Earth}} r'^n P_{nm}(\cos\theta') \sin m\lambda \, dm \Bigg); \end{aligned} \tag{5.65}$$

$$k = \begin{cases} 1 & \text{for } m = 0 \\ 2 & \text{for } m \neq 0 \end{cases}.$$

If the spherical component of the potential of the Earth's mass M is separated out (with $n = 0$), the ellipsoidal semimajor axis a is used to provide a scale for the unit sphere, and the integrals are replaced by *harmonic coefficients*, C_{nm} and S_{nm}, we then have

$$V = \frac{GM}{r}\left[1 + \sum_{n=1}^{\infty}\sum_{m=0}^{n}\left(\frac{a}{r}\right)^n (C_{nm}\cos m\lambda + S_{nm}\sin m\lambda) P_{nm}(\cos\theta)\right]. \quad (5.66)$$

In many cases, an alternative notation is

$$J_n = -C_n \quad (5.67)$$

$$J_{nm} = -C_{nm} \quad (5.68)$$

$$K_{nm} = -S_{nm}. \quad (5.69)$$

It may be convenient to use *fully normalized surface spherical harmonics*:

$$\overline{P}_{nm}(\cos\theta) = \sqrt{k(2n+1)\frac{(n-m)!}{(n+m)!}}\,P_{nm}(\cos\theta); \quad k = \begin{cases} 1 & \text{for } m = 0 \\ 2 & \text{for } m \neq 0 \end{cases}. \quad (5.70)$$

This results in *fully normalized coefficients*

$$\begin{Bmatrix} \overline{C}_{nm} \\ \overline{S}_{nm} \end{Bmatrix} = \sqrt{\frac{(n+m)!}{k(2n+1)(n-m)!}} \begin{Bmatrix} C_{nm} \\ S_{nm} \end{Bmatrix}; \quad k = \begin{cases} 1 & \text{for } m = 0 \\ 2 & \text{for } m \neq 0 \end{cases}. \quad (5.71)$$

It should be noted that the expansions for V converge rigorously only outside a sphere of radius a that just encloses the Earth, so that the Laplace equation may be satisfied. In practice, however, since the coefficients are normally determined empirically from measurement (e.g., from satellite observations), the series can always be considered to converge. Once a set of coefficients are determined (see § 5.3.2) the expression for V becomes valid and useful for anywhere in space.

The same expression may be used for determining the gravitational potential on the Earth's surface. However, as noted previously, it is the *gravity* potential, here denoted W (including centrifugal force) that is of primary interest on or near (i.e., moving with) the Earth's surface. We have

$$W = V + \frac{1}{2}\omega_e^2(X^2 + Y^2) \quad (5.72)$$

where ω_e is the angular velocity of the Earth, and X and Y are the coordinates of the point in question ($P(X, Y, Z)$).

It should be noted that many other representations of the Earth's gravity field exist and are widely used, depending on the application. Most commonly, W may be determined over a wide area or the Earth itself, using measured gravity-related data. Any of the standard references previously mentioned on geodesy and geodetic astronomy contain detailed information on these types of computations.

5.3.2 Representation of the Earth's Gravity Field

Gravitational models commonly used in current (2011) precision orbital analysis include, among others, the GGM series (URL[11]) of the Center for Space Research, Austin and

Table 5.3 Suggested truncation levels for use of EGM2008 at different orbits

Orbit Radius / km	Example	Truncation Level
7331	Starlette	90
12270	Lageos	20
26600	GPS	12

the EIGEN series (URL[12]) of the collaboration of GeoForschungsZentrum, Potsdam and Groupe de Recherche en Géodésie Spatiale, Toulouse. They all represent a significant improvement with respect to EGM96, the past conventional model of the *IERS Conventions (2003)* (IERS 2004), thanks to the availability of CHAMP (URL[13]) and GRACE (URL[14]) data in the 2000s.

The IERS, recognizing the recent development of new gravitational models derived from the optimal combination of GRACE data with high resolution gravitational information obtained from surface gravimetry and satellite altimetry data, recommends at this time the EGM2008 model as the conventional model.

The EGM2008 model (Pavlis et al. 2012) is complete to degree and order 2159, and contains additional spherical harmonic coefficients extending to degree 2190 and order 2159. The geocentric gravitational constant, $GM_{\oplus}$, and radius, a_e, values reported with EGM2008 (398600.4415 km^3/s^2 and 6378136.3 m) should be used as scaling parameters with its gravitational potential coefficients. They are to be considered as TT-compatible values. The recommended TCG-compatible value, $GM_{\oplus}$ = 398600.4418, should be used with the two-body term when working with Geocentric Coordinate Time (TCG) (398600.4415 or 398600.4356 should be used by those working with Terrestrial Time (TT) or Barycentric Dynamical Time (TDB), respectively). The EGM2008 model complete with error estimates is available at URL[15].

Although EGM2008 is complete to degree and order 2159, most users in space geodesy will find their needs covered by a truncated version of the model. Suggested truncation levels as a function of the orbit of interest are listed in Table 5.3. It is expected that these truncation levels provide an accuracy of 1 mm on the orbits of the indicated satellites.

The EGM2008 model was based on the ITG-GRACE03S GRACE-only gravitational model (URL[16]; see also Mayer-Gürr 2007) which is available along with its complete error covariance matrix to degree and order 180. Therefore the static gravitational field was developed assuming models complying with the *IERS Conventions (2003)* (IERS 2004) and complemented by the following:

- ocean tides: FES2004 (Lyard, Lefèvre, and Letellier 2006); see § 5.3.4;
- ocean pole tide: Desai (2002); see § 5.3.5.2;
- atmosphere and ocean de-aliasing: AOD1B RL04 (Flechtner 2007).

For some of the low-degree coefficients, the conventional geopotential model uses values which are different from the original EGM2008 values. The static field also assumes values for the secular rates of low-degree coefficients. In order to use the static field properly and

Table 5.4 Low-degree coefficients of the conventional geopotential model.

Coefficient	Value at t_0	Reference	Rate / yr^{-1}	Reference
$\bar{C}_{20}$ (zero-tide)	$-0.48416948 \times 10^{-3}$	Cheng et al. 2011	1.16×10^{-11}	Nerem et al. 1993
$\bar{C}_{30}$	0.9571612×10^{-6}	EGM2008	4.9×10^{-12}	Cheng et al. 1997
$\bar{C}_{40}$	0.5399659×10^{-6}	EGM2008	4.7×10^{-12}	Cheng et al. 1997

project it in time, the secular rates should be accounted for. The instantaneous values of coefficients $\bar{C}_{n0}$ to be used when computing orbits are given by:

$$\bar{C}_{n0}(t) = \bar{C}_{n0}(t_0) + d\bar{C}_{n0}/dt \times (t - t_0) \tag{5.73}$$

where t_0 is the epoch of J2000.0 and the values of $\bar{C}_{n0}(t_0)$ and $d\bar{C}_{n0}/dt$ are given in Table 5.4.

Note that the zero-tide C_{20} coefficient in the conventional geopotential model is obtained from the analysis of 17 years of SLR data approximately centered on year 2000 and has an uncertainty of 2×10^{-11} (Cheng, Ries and Tapley 2011). It differs significantly from the EGM2008 value obtained from 4 years of GRACE data, as it is expected that tide-like aliases will affect GRACE-based C_{20} values, depending on the averaging interval used. The tide-free value of C_{20} can be obtained as described in § 5.3.3.2.

Values for the C_{21} and S_{21} coefficients are included in the conventional geopotential model. The C_{21} and S_{21} coefficients describe the position of the Earth's figure axis. When averaged over many years, the figure axis should closely coincide with the observed position of the rotation pole averaged over the same time period. Any differences between the averaged positions of the mean figure and the mean rotation pole would be due to long-period fluid motions in the atmosphere, oceans, or Earth's fluid core (Wahr 1987, 1990). At present, there is no independent evidence that such motions are important. The conventional values for $C_{21}(t)$ and $S_{21}(t)$ are intended to give a mean figure axis that corresponds to the mean pole position consistent with the terrestrial reference frame defined in *IERS Conventions (2010)* chapter 4 (IERS 2010).

This choice for C_{21} and S_{21} is realized as follows. First, to use the gravitational potential coefficients to solve for a satellite orbit, it is necessary to rotate from the Earth-fixed frame, where the coefficients are pertinent, to an inertial frame, where the satellite motion is computed. This transformation between frames should include polar motion. We assume the polar motion parameters used are relative to the IERS Reference Pole. Then the values

$$\bar{C}_{21}(t) = \sqrt{3}\bar{x}_p(t)\bar{C}_{20} - \bar{x}_p(t)\bar{C}_{22} + \bar{y}_p(t)\bar{S}_{22}$$
$$\bar{S}_{21}(t) = -\sqrt{3}\bar{y}_p(t)\bar{C}_{20} - \bar{y}_p(t)\bar{C}_{22} - \bar{x}_p(t)\bar{S}_{22}$$

where $\bar{x}_p(t)$ and $\bar{y}_p(t)$ (in radians) represent the IERS conventional mean pole (see section 7.1.4 of *IERS Conventions (2010)* (IERS 2010)), provide a mean figure axis which coincides with the mean pole consistent with the TRF defined in *IERS Conventions (2010)* chapter 4 (*Ibid.*). Any recent value of $\bar{C}_{20}$, $\bar{C}_{22}$, and $\bar{S}_{22}$ is adequate for 10^{-14} accuracy in the

above equations, e.g., the values of the present conventional model ($-0.48416948 \times 10^{-3}$, 2.4393836×10^{-6} and $-1.4002737 \times 10^{-6}$ respectively) can be used.

The models for the low-degree terms are generally consistent with the past long-term trends, but these are not strictly linear in reality. There may be decadal variations that are not captured by the models. In addition, they may not be consistent with more recent surface mass trends due to increased ice sheet melting and other results of global climate change.

5.3.3 Solid Earth Tides

The solid Earth tide model is based on an abbreviated form of the Wahr model (Wahr 1981) using the preliminary reference Earth model (PREM) of Dziewonski and Anderson (1981) corresponding to a 1-second reference period. The Love numbers for the induced free space potential, k, and for the vertical and horizontal displacements, h and l, have been taken from Wahr's thesis, Tables 13 and 16. The long period, diurnal, and semi-diurnal terms are included. The degree 2 tides produce time dependent changes in C_{2m} and S_{2m}, through $k_{2m}^{(0)}$, which can exceed 10^{-8} in magnitude. They also produce changes exceeding 3×10^{-12} in C_{4m} and S_{4m} through $k_{2m}^{(+)}$. (The direct contributions of the degree 4 tidal potential to these coefficients are negligible.) The only other changes exceeding this cutoff amplitude are in C_{3m} and S_{3m}, produced by the degree 3 part of the tide generating potential.

5.3.3.1 Calculations of the Tide Generating Potential Coefficients

The solid-tide-induced free-space potential is most conveniently modeled as variations in the standard geopotential coefficients C_{nm} and S_{nm} (Eanes, Schutz, and Tapley 1983). The Wahr model (or any other model having frequency-dependent Love numbers) is most efficiently computed in three steps. The first step uses a frequency-independent Love number k_2 and an evaluation of the tidal potential in the time domain using a lunar and solar ephemeris. The second step corrects those arguments of a harmonic expansion of the tide-generating potential for which the error from using the k_2 of step 1 is above some cutoff amplitude (see Table 5.5).

Steps 1 and 2 can be used to compute the total tidal contribution, including the time independent (permanent) contribution to the geopotential coefficient $\bar{C}_{20}$, which is adequate for a *conventional tide free* model such as EGM2008 (see § 1.1 of the *IERS Conventions (2010)* (IERS 2010)). When using a *zero tide* model, this permanent part should not be counted twice; this is the goal of Step 3 of the computation. See § 5.3.3.2 which discusses the treatment of the permanent tide.

The changes in normalized second-degree geopotential coefficients for Step 1 are

$$\Delta\overline{C}_{20} = \frac{1}{\sqrt{5}} k_2 \frac{R_e^3}{GM_\oplus} \sum_{j=2}^{3} \frac{GM_j}{r_j^3} P_{20}(\sin\phi_j) \tag{5.74}$$

$$\Delta\overline{C}_{21} - i\Delta\overline{S}_{21} = \frac{1}{3}\sqrt{\frac{3}{5}} k_2 \frac{R_e^3}{GM_\oplus} \sum_{j=2}^{3} \frac{GM_j}{r_j^3} P_{21}(\sin\phi_j) e^{-i\lambda_j} \tag{5.75}$$

$$\Delta\overline{C}_{22} - i\Delta\overline{S}_{22} = \frac{1}{12}\sqrt{\frac{12}{5}} k_2 \frac{R_e^3}{GM_\oplus} \sum_{j=2}^{3} \frac{GM_j}{r_j^3} P_{22}(\sin\phi_j) e^{-i2\lambda_j} \tag{5.76}$$

Table 5.5 Step 2 solid tide corrections when $k_2 = 0.30$ in step 1 (using a cutoff amplitude of 9×10^{-12} for $A_m \delta k_s H_s$)

Long-Period Tides ($n = 2, m = 0$)

None except zero-frequency tide.

Diurnal Tides ($n = 2, m = 1$)

		$\overline{n}$, argument multipliers						
Doodson Number		τ	s	h	p	N'	p_1	$A_m \delta k_s H_s \times 10^{12}$
145.555	(O_1)	1	−1	0	0	0	0	−16.4
163.555	(P_1)	1	1	−2	0	0	0	−49.6
165.545		1	1	0	0	−1	0	−9.4
165.555	(K_1)	1	1	0	0	0	0	507.4
165.565		1	1	0	0	1	0	73.5
166.554	(ψ_1)	1	1	1	0	0	−1	−15.2

Semi-Diurnal Tides ($n = 2, m = 2$)

		$\overline{n}$, argument multipliers						
Doodson Number		τ	s	h	p	N'	p_1	$A_m \delta k_s H_s \times 10^{12}$
255.555	(M_2)	2	0	0	0	0	0	39.5
273.555	(S_2)	2	2	−2	0	0	0	18.4

where

k_2 = nominal second degree Love number;

R_e = equatorial radius of the Earth;

$GM_\oplus$ = gravitational parameter for the Earth;

GM_j = gravitational parameter for the Moon ($j = 2$) and Sun ($j = 3$);

r_j = distance from geocenter to Moon or Sun;

ϕ_j = body fixed geocentric latitude of Moon or Sun;

λ_j = body fixed east longitude (from Greenwich) of Moon or Sun.

One further computation to be done in Step 1 is that of the changes in the degree 4 coefficients produced by the degree 2 tides. They are given by

$$\Delta\overline{C}_{4m} - i\Delta\overline{S}_{4m} = \frac{k_{2m}^{(+)}}{5}\frac{R_e^3}{GM_\oplus}\sum_{j=2}^{3}\frac{GM_j}{r_j^3}P_{2m}(\sin\phi_j)e^{-im\lambda_j}. \tag{5.77}$$

The frequency dependence corrections to the $\Delta\bar{C}_{nm}$ and $\Delta\bar{S}_{nm}$ values obtained from Step 1 are computed in Step 2 as the sum of contributions from a number of tidal constituents belonging to the respective bands. The changes in normalized coefficients from Step 2 are:

$$\Delta\overline{C}_{nm} - i\Delta\overline{S}_{nm} = A_m \sum_{s(n,m)} \delta k_s H_s \begin{pmatrix} 1 \\ -i \end{pmatrix} \begin{matrix} n+m & \text{even} \\ n+m & \text{odd} \end{matrix} e^{i\Theta_s} \tag{5.78}$$

where

$$A_0 = \frac{1}{R_e\sqrt{4\pi}} = 4.4228 \times 10^{-8}\,\mathrm{m}^{-1} \tag{5.79}$$

$$A_\mathrm{m} = \frac{(-1)^m}{R_\mathrm{e}\sqrt{4\pi\,(2-\delta_{0m})}}, \quad \delta_{0m} = \begin{cases} 1 & \text{if } m = 0 \\ 0 & \text{if } m \neq 0 \end{cases} \tag{5.80}$$

$\delta k_s =$ difference between k at frequency s and the nominal value k_2 in the sense $k_\mathrm{s} - k_2$, plus a contribution from ocean loading;

$H_s =$ amplitude (m) of term at frequency s from the Cartwright and Tayler (1971) and Cartwright and Edden (1973) harmonic expansion of the tide-generating potential;

$\Theta_s = \overline{n} \cdot \overline{\beta} = \sum_{i=1}^{6} n_i \beta_i$;

$\bar{n} =$ six vector of multipliers of the Doodson (1921) variables;

$\bar{\beta} =$ the Doodson variables;

$\delta S_{20} = 0$.

The Doodson variables are related to the fundamental arguments (the Delaunay variables l, l', F, D, Ω) of the nutation series (see chapter 5 of *IERS Conventions (2010)* (IERS 2010)) by

$s = F + \Omega = \beta_2$ (Moon's mean longitude);

$h = s - D = \beta_3$ (Sun's mean longitude);

$p = s - l = \beta_4$ (longitude of Moon's mean perigee);

$N' = -\Omega = \beta_5$ (negative longitude of Moon's mean node);

$p_1 = s - D - l' = \beta_6$ (longitude of Sun's mean perigee);

$\tau = \theta_g + \pi - s = \beta_1$ (time angle in lunar days reckoned from lower transit);

$\theta_g =$ Greenwich Mean Sidereal Time expressed in angle units (i.e., $24^h = 360°$);

π in $(\theta_g + \pi)$ is now to be replaced by 180°.

The normalized geopotential coefficients ($\overline{C}_{nm}$, $\overline{S}_{nm}$) are related to the unnormalized coefficients (C_{nm}, S_{nm}) by

$$C_{nm} = N_{nm}\overline{C}_{nm} \tag{5.81}$$

$$S_{nm} = N_{nm}\overline{S}_{nm} \tag{5.82}$$

$$N_{nm} = \left[\frac{(n+m)!(2n+1)(2-\delta_{m0})}{(n+m)!}\right]^{1/2}. \tag{5.83}$$

Using a nominal k_2 of 0.3 and an amplitude cutoff of 9×10^{-12} change in normalized geopotential coefficients, the summation $S(n, m)$ requires six diurnal terms ($n = 2$, $m = 1$) modifying $\overline{C}_{21}$ and $\overline{S}_{21}$ and two semi-diurnal terms ($n = 2$, $m = 2$) modifying $\overline{C}_{22}$ and $\overline{S}_{22}$. With the exception of the zero-frequency tide, no long-period terms are necessary. Table 5.5 gives the required quantities for correcting the (2, 1) and (2, 2) coefficients. The correction to $\overline{C}_{20}$ is discussed in more detail in the next section (§ 5.3.3.2).

Calculation of the correction due to any tidal constituent is illustrated by the following example for K_1. Given that $A_m = A_1 = -3.1274 \times 10^{-8}$, and that $H_s = 0.36870$, $\Theta_s = (\theta_g + \pi)$, and $k_{21}^{(0)} = (0.25746 + 0.00118i)$ for this tide, one finds on subtracting the nominal value $(0.29830 - 0.00144i)$ that $\delta k_s = (-0.04084 + 0.00262i)$. Equation 5.78 then yields:

$$\begin{aligned} (\Delta\bar{C}_{21})_{K_1} &= 470.9 \times 10^{-12} \sin(\theta_g + \pi) - 30.2 \times 10^{-12} \cos(\theta_g + \pi) \\ (\Delta\bar{S}_{21})_{K_1} &= 470.9 \times 10^{-12} \cos(\theta_g + \pi) + 30.2 \times 10^{-12} \sin(\theta_g + \pi). \end{aligned} \tag{5.84}$$

The total variation in geopotential coefficients due to the solid tide is obtained by adding the results of Step 2 (Eq. 5.78) to those of Step 1 (Eqs. 5.74, 5.75, and 5.76). The sum of these steps constitutes a model of the observed instantaneous geopotential.

5.3.3.2 Treatment of the Permanent Tide

The mean value of $\Delta\overline{C}_{20}$ from Eq. 5.74 is not zero, and this permanent tide deserves special attention. Ideally, the mean value of the correction should be included in the adopted value of $\overline{C}_{20}$ and, hence, not included in the $\Delta\overline{C}_{20}$. The practical situation is not so clear, because satellite-derived values of $\overline{C}_{20}$, as in the GEM geopotentials, have been obtained using a mixture of methods, some applying the corrections and others not applying it. There is no way to ensure consistency in this regard short of re-estimating $\overline{C}_{20}$ with a consistent technique. If this is done, the inclusion of the zero-frequency term in Eq. 5.74 should be avoided, because k_2 is not the appropriate Love number to use for such a term.

The zero-frequency change in $\overline{C}_{20}$ can be removed by computing $\Delta\overline{C}_{20}$ as

$$\Delta\overline{C}^*_{20} = \Delta\overline{C}_{20} \text{ (from Eq. 5.74)} - \left\langle \Delta\overline{C}_{20} \right\rangle \tag{5.85}$$

where

$$\begin{aligned} \left\langle \Delta\overline{C}_{20} \right\rangle &= A_0 H_0 k_2 \\ &= (4.4228 \times 10^{-8})(-0.31460) k_2 \\ &= -1.39141 \times 10^{-8} k_2. \end{aligned} \tag{5.86}$$

Using $k_2 = 0.30$ then

$$\left\langle \Delta\overline{C}_{20} \right\rangle = -4.1742 \times 10^{-9} \tag{5.87}$$

or

$$\langle \Delta J_2 \rangle = -\left\langle \Delta\overline{C}_{20} \right\rangle \sqrt{5} = 9.3338 \times 10^{-9}. \tag{5.88}$$

The decision to remove or not to remove the mean from the corrections depends on whether the adopted $\overline{C}_{20}$ does or does not already contain it and on whether k_2 is a potential "solve for" parameter. If k_2 is to be estimated, then it must not multiply the zero frequency term in the correction.

In the case of EGM2008, the difference between the zero-tide and tide-free value of C_{20} is -4.1736×10^{-9}. Assuming the same values from Eq. 5.86 for A_0, H_0 and k_2, the tide-free value of C_{20} corresponding to Table 5.4 would be $-0.48416531 \times 10^{-3}$.

The use of zero-tide values and the subsequent removal of the effect of the permanent tide from the tide model is presented for consistency with the 18th IAG General Assembly Resolution 16.

5.3.3.3 Solid Tide Effect on Station Coordinates

The variations of station coordinates caused by solid Earth tides predicted using Wahr's theory are also most efficiently implemented using a two-step procedure. Only the second degree tides are necessary to retain 0.01 m precision. Third degree tides are needed for high accuracy (1 mm or better) applications. The first step uses frequency-independent Love and Shida numbers and a computation of the tidal potential in the time domain. A convenient formulation of the displacement is given in the documentation for the DEHANTTIDEINEL program (URL[17]; Mathews, Dehant, and Gipson 1997). The vector displacement of the station due to tidal deformation for step 1 can be computed from

$$\Delta\vec{r} = \sum_{j=2}^{3} \frac{GM_j R_e^4}{GM_\oplus R_j^3} \left\{ h_2\, \hat{r} \left(\frac{3(\hat{R}_j \cdot \hat{r})^2 - 1}{2} \right) + 3l_2 (\hat{R}_j \cdot \hat{r}) \left[\hat{R}_j - (\hat{R}_j \cdot \hat{r})\, \hat{r} \right] \right\} \quad (5.89)$$

where

GM_j = gravitational parameter for the Moon ($j = 2$) or the Sun ($j = 3$);

$GM_\oplus$ = gravitational parameter for the Earth;

$\hat{R}_j$, R_j = unit vector from the geocenter to Moon or Sun and the magnitude of that vector;

R_e = Earth's equatorial radius;

$\hat{r}$, r = unit vector from the geocenter to the station and the magnitude of that vector;

h_2 = nominal second-degree Love number;

l_2 = nominal Shida number.

The largest radial and transverse displacements due to the degree 2 tide are found to be 314 mm and 65 mm, respectively.

The Love numbers of the degree 3 tides may be taken as real and constant in computations to the degree of accuracy aimed at here. The displacement vector due to these tides is then given by

$$\Delta\vec{r} = \sum_{j=2}^{3} \frac{GM_j R_e^5}{GM_\oplus R_j^4} \left\{ h_3\, \hat{r} \left(\frac{5}{2}(\hat{R}_j \cdot \hat{r})^3 - \frac{3}{2}(\hat{R}_j \cdot \hat{r}) \right) + l_3 \left(\frac{15}{2}(\hat{R}_j \cdot \hat{r})^2 - \frac{3}{2} \right) \left[\hat{R}_j - (\hat{R}_j \cdot \hat{r})\hat{r} \right] \right\}. \quad (5.90)$$

Only the Moon's contribution ($j = 2$) needs to be computed because the Sun's contribution ($j = 3$) is negligible. The transverse part of the displacement (from Eq. 5.90) does not exceed 0.2 mm, but the radial displacement can reach 1.7 mm.

If nominal values for h_2 and l_2 of 0.6078 and 0.0847, respectively, are used with a cutoff of 0.0004 m of radial displacement, only one term needs to be corrected in Step 2. This is the K_1 frequency where h from Wahr's theory is 0.5203. Only the radial displacement needs

to be corrected, and to sufficient accuracy, this can be implemented as a periodic change in station height given by

$$\delta h_{STA} = \delta h_{K_1} H_{K_1} \left(-\sqrt{\frac{5}{24\pi}} \right) 3 \sin\phi \cos\phi \sin(\Theta_{K_1} + \lambda) \tag{5.91}$$

where

$\delta h_{K_1} = h_{K_1}(\text{Wahr}) - h_2(\text{Nominal}) = -0.0875;$

$H_{K_1} =$ amplitude of K_1 term (165.555) in the harmonic expansion of the tide generating potential $= 0.36878$ m;

$\phi =$ geocentric latitude of station;

$\lambda =$ east longitude of station;

$\Theta_{K_1} = K_1$ tide argument $= \tau + s = \Theta_g + \pi;$

or, simplifying,

$$\delta h_{STA} = -0.0253 \sin\phi \cos\phi \sin(\Theta_g + \lambda). \tag{5.92}$$

The effect is maximum at $\phi = 45°$ where the amplitude is 0.013 m.

There is also a zero-frequency station displacement that may or may not be included in the nominal station coordinates. The mean correction could be removed as in the discussion above. When baselines or coordinates are compared at the few-cm level, care must be taken that the correction was handled consistently. It is essential that published station coordinates identify how the zero-frequency contribution was included.

If nominal Love and Shida numbers of 0.6078 and 0.0847, respectively, along with $h^{(2)} = -0.0006$ and $l^{(2)} = 0.0002$, are used with Eq. 5.89, the permanent deformation introduced is

$$[-0.1206 + 0.0001 P_2(\sin\phi)] P_2(\sin\phi) \text{ m} \tag{5.93}$$

in the radial direction, and

$$[-0.0252 - 0.0001 P_2(\sin\phi)] \sin 2\phi \text{ m} \tag{5.94}$$

in the north direction, where $P_2(\sin\phi) = (3\sin^2\phi - 1)/2$. These are the components of the vector to be added to the *conventional tide free* computed tide-corrected position to obtain the *mean tide* position. The radial component of this restitution to obtain the *mean tide* value amounts to about −12 cm at the poles and about +6 cm at the equator.

5.3.4 Ocean Tide Model

The dynamical effect of ocean tides is most easily implemented as periodic variations in the normalized geopotential coefficients. The variations can be written as follows (Eanes, Schutz, and Tapley 1983):

$$\Delta\overline{C}_{nm} - i\,\Delta\overline{S}_{nm} = F_{nm} \sum_{s(n,m)} \sum_{+}^{-} (C^{\pm}_{snm} \mp i S^{\pm}_{snm}) e^{\pm i\Theta_s} \tag{5.95}$$

where

$$F_{nm} = \frac{4\pi G\rho_w}{g_e}\left[\frac{(n+m)!}{(n-m)!\,(2n+1)(2-\delta_{m0})}\right]^{1/2}\frac{1+k'_n}{2n+1} \tag{5.96}$$

where

$g_e = GM_\oplus/a_e^2 = 9.7803278\ \mathrm{ms}^{-2}$;

G = the universal gravitational constant $= 6.67428 \times 10^{-11}\ \mathrm{m}^3\,\mathrm{kg}^{-1}\,\mathrm{s}^{-2}$;

ρ_w = density of seawater $= 1025\ \mathrm{kg\,m}^{-3}$;

k'_n = load deformation coefficients ($k'_2 = -0.3075$, $k'_3 = -0.1954$, $k'_4 = -0.132$, $k'_5 = -0.1032$, $k'_6 = -0.0892$);

$C^{\pm}_{snm}$, $S^{\pm}_{snm}$ = ocean-tide coefficients in meters for the tide constituent s (see Table 5.6);

Θ_s = argument of the tide constituent s as defined in the solid tide model (see § 5.3.3.1).

In the current (2010) recommended ocean tide model, FES2004 (Lyard, Lefèvre, and Letellier 2006), the global ocean tides were solved from basin-scale solutions with elevation boundary conditions extracted from the Naval Surface Weapon Center (NSWC) model and from the geodetic satellite (GEOSAT) empirical model (Cartwright and Ray 1991), as well as tide gauge data in dynamically complex areas. For each constituent s in the diurnal and semi-diurnal tidal bands, both hydrodynamical modeling and data assimilation from TOPEX/Poseidon satellite altimetry data and European remote-sensing satellite (ERS) data were performed. In the long period tidal band case, no data assimilation was performed; therefore, for each constituent s, the solutions from FES2004 are purely theoretical. The digital FES2004 atlas (tidal elevation and loading/self-attraction) is available at URL[18] in the "Sea level and tides" submenu.

The summation, $\sum_{+}^{-}$, implies addition of the expression using the top signs (the prograde waves C^{+}_{snm} and S^{+}_{snm}) to that using the bottom signs (the retrograde waves C^{-}_{snm} and S^{-}_{snm}). The ocean-tide coefficients $C^{\pm}_{snm}$ and $S^{\pm}_{snm}$ as used here are related to the Schwiderski (1983) ocean-tide amplitude and phase by

$$C^{\pm}_{snm} - i\,S^{\pm}_{snm} = -i\,\hat{C}^{\pm}_{snm}e^{i(\epsilon^{\pm}_{snm}+\chi_s)} \tag{5.97}$$

where

$\hat{C}^{\pm}_{snm}$ = ocean-tide amplitude for constituent s using the Schwiderski (Schwiderski 1983) notation;

$\epsilon^{\pm}_{snm}$ = ocean-tide phase for constituents;

$$\chi_s = \begin{cases} 0 & \text{Semi-diurnal, and long period;} \\ \pi/2 & K_1\text{; (or in general for constituents with } H_s > 0\text{);} \\ -\pi/2 & O_1,\ P_1,\ Q_1\text{; (or in general for constituents with } H_s < 0\text{).} \end{cases}$$

Table 5.6 Ocean tide coefficients from the Schwiderski model

Argument Number[ab]		n	m[c]	$\hat{C}^+_{snm}$	ϵ^+_{snm}	C^+_{snm}	S^+_{snm}
				cm	deg	cm	cm
057.555	S_{sa}	2	0	.6215	221.672	−.8264	−.9284
057.555	S_{sa}	3	0	.0311	1.735	.0019	.0621
057.555	S_{sa}	4	0	.1624	92.674	.3244	−.0152
057.555	S_{sa}	5	0	.2628	251.737	−.4991	−.1647
057.555	S_{sa}	6	0	.4363	145.744	.4912	−.7213
065.455	M_m	2	0	.5313	258.900	−1.0428	−.2046
065.455	M_m	3	0	.0317	94.298	.0632	−.0047
065.455	M_m	4	0	.0998	69.054	.1863	.0713
065.455	M_m	5	0	.2279	292.291	−.4218	.1729
065.455	M_m	6	0	.0660	39.882	.0847	.1014
075.555	M_f	2	0	.8525	251.956	−1.6211	−.5281
075.555	M_f	3	0	.0951	148.236	.1001	−.1617
075.555	M_f	4	0	.2984	102.723	.5822	−.1315
075.555	M_f	5	0	.2960	223.167	−.4050	−.4318
075.555	M_f	6	0	.0880	107.916	.1675	−.0542
135.655	Q_1	2	1	.5373	313.735	−.3715	−.3882
135.655	Q_1	3	1	.3136	107.346	.0935	.2994
135.655	Q_1	4	1	.2930	288.992	−.0953	−.2770
135.655	Q_1	5	1	.2209	112.383	.0841	.2042
135.655	Q_1	6	1	.0396	287.824	−.0121	−.0377
145.555	O_1	2	1	2.4186	313.716	−1.6715	−1.7481
145.555	O_1	3	1	1.3161	83.599	−.1467	1.3079
145.555	O_1	4	1	1.4301	276.282	−.1565	−1.4215
145.555	O_1	5	1	.9505	109.128	.3115	.8980
145.555	O_1	6	1	.1870	282.623	−.0409	−.1825
163.555	P_1	2	1	.9020	313.912	−.6256	−.6498
163.555	P_1	3	1	.2976	39.958	−.2281	.1911
163.555	P_1	4	1	.6346	258.311	.1286	−.6215
163.555	P_1	5	1	.4130	104.438	.1030	.4000
163.555	P_1	6	1	.0583	276.591	−.0067	−.0579
165.555	K_1	2	1	2.8158	315.113	1.9950	1.9872
165.555	K_1	3	1	.8925	33.752	.7421	−.4959
165.555	K_1	4	1	1.9121	254.229	−.5197	1.8401
165.555	K_1	5	1	1.2111	104.672	−.3068	−1.1716
165.555	K_1	6	1	.1645	281.867	.0338	.1610
245.655	N_2	2	2	.6516	321.788	−.4030	.5120
245.655	N_2	3	2	.1084	171.923	.0152	−.1074

Table 5.6 *(continued)*

Argument[ab] Number		n	m[c]	$\hat{C}^+_{snm}$	ϵ^+_{snm}	C^+_{snm}	S^+_{snm}
				cm	deg	cm	cm
245.655	N_2	4	2	.2137	141.779	.1322	−.1679
245.655	N_2	5	2	.0836	5.034	.0073	.0832
245.655	N_2	6	2	.0674	346.544	−.0157	.0656
255.555	M_2	2	2	2.9551	310.553	−2.2453	1.9213
255.555	M_2	3	2	.3610	168.623	.0712	−.3539
255.555	M_2	4	2	1.0066	124.755	.8270	−.5738
255.555	M_2	5	2	.2751	356.561	−.0165	.2746
255.555	M_2	6	2	.4130	329.056	−.2124	.3542
273.555	S_2	2	2	.9291	314.011	−.6682	.6456
273.555	S_2	3	2	.2633	201.968	−.0985	−.2442
273.555	S_2	4	2	.3716	103.027	.3621	−.0838
273.555	S_2	5	2	.1365	3.772	.0090	.1362
273.555	S_2	6	2	.1726	280.381	−.1698	.0311
275.555	K_2	2	2	.2593	315.069	−.1832	.1836
275.555	K_2	3	2	.0943	195.007	−.0244	−.0911
275.555	K_2	4	2	.1059	103.521	.1029	−.0247
275.555	K_2	5	2	.0382	.411	.0003	.0382
275.555	K_2	6	2	.0467	281.357	−.0458	.0092

[a] The spherical harmonic decomposition of Schwiderski's models was computed by Duncan Agnew (Agnew 1996) of University of California, San Diego.
[b] The Doodson variable multipliers ($\overline{n}$) are coded into the argument number (A) after Doodson (1921) as $A = n_1(n_2+5)(n_3+5).(n_4+5)(n_5+5)(n_6+5)$.
[c] For the long-period tides ($m=0$), the value of $\hat{C}^+_{snm}$ used to compute C^+_{snm} and S^+_{snm} was twice that shown to account for the combined effect of the retrograde and prograde waves.

For clarity, Eq. 5.95 is rewritten in two forms:

$$\Delta\overline{C}_{nm} = F_{nm} \sum_{s(n,m)} [(C^+_{snm} + C^-_{snm}) \cos\Theta_s + (S^+_{snm} + S^-_{snm}) \sin\Theta_s] \tag{5.98}$$

or

$$\Delta\overline{C}_{nm} = F_{nm} \sum_{s(n,m)} [\hat{C}^+_{snm} \sin(\Theta_s + \epsilon^+_{snm} + \chi_s) + C^-_{snm} \sin(\Theta_s + \epsilon^-_{snm} + \chi_s)] \tag{5.99}$$

$$\Delta\overline{S}_{nm} = F_{nm} \sum_{s(n,m)} [(S^+_{snm} + S^-_{snm}) \cos\Theta_s - (C^+_{snm} + C^-_{snm}) \sin\Theta_s] \tag{5.100}$$

or

$$\Delta\overline{S}_{nm} = F_{nm} \sum_{s(n,m)} [\hat{C}^+_{snm} \cos(\Theta_s + \epsilon^+_{snm} + \chi_s) + C^-_{snm} \cos(\Theta_s + \epsilon^-_{snm} + \chi_s)]. \tag{5.101}$$

The summation over $s(n, m)$ should include all constituents for which Schwiderski has computed a model. Except for cases of near resonance, the retrograde terms do not produce long-period (> 1 day) orbit perturbations for the diurnal and semi-diurnal tides. For high altitude geodetic satellites like Lageos, in order to reduce the required computing time, it is recommended that out of the complete selection, only the constituents whose Cartwright and Tayler amplitudes H_s are greater than 0.5 mm be used, with their spherical harmonic expansion terminated at maximum degree and order 8.

Table 5.6 gives the values required for each of the constituents for which Schwiderski has computed a model. Note that the units in Table 5.6 are centimeters and hence must be scaled to meters for use with the constants given with Eq. 5.95.

The $(n = 2, m = 2)$ term for the S_2 argument can be modified to account for the atmospheric tide using the results of Chapman and Lindzen (1970). The modified values to be used instead of those in Table 5.6 are

$$C_{22}^{+} = -0.537 \text{ cm} \tag{5.102}$$

$$S_{22}^{+} = 0.321 \text{ cm}. \tag{5.103}$$

For the most precise applications, more than the eleven terms listed in Table 5.6 need to be modeled. This can be accomplished by assuming that the ocean tide admittance varies smoothly with frequency and by using the Schwiderski values as a guide to the interpolation to other frequencies.

5.3.5 Site Displacement Due to Ocean and Atmospheric Loading

5.3.5.1 Ocean Loading

In the past few decades, displacements due to ocean loading have been calculated by several authors [e.g., Schwiderski (1980), Eanes (1994), Egbert, Bennett, and Foreman (1994), Le Provost et al. (1994), Eanes and Bettadpur (1995), Le Provost et al. (1998), Ray (1999), Lefèvre, Lyard, and Le Provost (2000), Matsumoto, Takanezawa, and Ooe (2000), Egbert and Erofeeva (2002), Lefèvre et al. (2002), Letellier (2004), Andersen (2006), and Savcenko and Bosch (2008)]. Most of these modern models assimilate sea surface height measurements made by altimetry satellites and integrate the tide height over all ocean masses with a weighting function [Green's function, see Farrell (1972), Zschau (1983), and Scherneck (1990)].

In all these models, the locally referenced displacement vector $\mathbf{E}$ in the vertical (radial), N–S and E–W local coordinate system at time t can be computed as a sum of the contributions of n individual ocean tides

$$\mathbf{E}(t) = \sum_{i=1}^{n} \begin{cases} A_i^r \cos(\omega_i t + \phi_i - \delta_i^r) \\ A_i^{NS} \cos(\omega_i t + \phi_i - \delta_i^{NS}) \\ A_i^{EW} \cos(\omega_i t + \phi_i - \delta_i^{EW}) \end{cases} \tag{5.104}$$

where ω_i is the angular frequency of the tidal constituents and ϕ_i the corresponding astronomical argument. The astronomical argument can be computed from the subroutine ARG2.F

available at URL[19]. The amplitudes A_i^r, A_i^{NS}, A_i^{EW}, and the Greenwich phase lags δ_i^r, δ_i^{NS}, δ_i^{EW} of each tidal component are determined by the particular model assumed for the deformation of the Earth.

The site displacements resulting from the ocean tides have been compiled by D. Agnew (Agnew 1997). Tidal loading radial (height) displacement amplitude and phase values for selected laser and VLBI station locations have been computed for the semi-diurnal M_2, S_2, K_2, N_2, diurnal O_1, K_1, P_1, Q_1, and long-period M_f, M_m, and S_{sa} ocean tides using any of the leading global ocean models available from the ocean loading service website (URL[20]; Scherneck 1991) provided by M.S. Bos and H.-G. Scherneck. The implementation considers a total of 342 constituent tides whose amplitudes and phases are found by spline interpolation of the tidal admittances based on the 11 main tides.

Table 5.7 gives the amplitude and phase values for the eleven main tides at the selected SLR and VLBI stations (using ITRF2008 and ocean tide model TPXO.7.2). The phase convention of Schwiderski has been preserved. His phases for the diurnal tides differ by $\pm 90°$ from the standard Doodson definition. The height displacement, in meters, can be found for a given constituent i as follows:

$$h(i) = \text{amp}(i) \times \cos(\arg(i, t) - \text{phase}(i)) \tag{5.105}$$

where $\arg(i, t)$ is the proper angular argument to be used with the Schwiderski phases (a Fortran subroutine, HARDISP.F, for this purpose was introduced in an update to the *IERS Conventions (2003)* on November 25, 2006 provided at URL[19]). The total tidal displacement is found by summing over all 342 constituents. A negative $h(i)$ means that the surface at the predicted point has been lowered.

5.3.5.2 Ocean Pole Tide Loading

The ocean pole tide is generated by the centrifugal effect of polar motion on the oceans, characterized by the potential defined in § 6.9.2.1 of this book. Polar motion is dominated by the 14-month Chandler wobble and annual variations. At these long periods, the ocean pole tide is expected to have an equilibrium response, where the displaced ocean surface is in equilibrium with the forcing equipotential surface.

Desai (2002) provides an equilibrium model of the ocean pole tide. This model accounts for continental boundaries, mass conservation over the oceans, self-gravitation, and loading of the ocean floor. Using this model, the load of the ocean pole tide produces the following deformation vector at any point on the surface of the Earth with latitude ϕ and longitude λ. The load deformation vector is expressed here in terms of radial, north and east components, u_r, u_n, and u_e, respectively, and is a function of the wobble parameters (m_1, m_2).

$$\begin{bmatrix} u_r(\phi, \lambda) \\ u_n(\phi, \lambda) \\ u_e(\phi, \lambda) \end{bmatrix} = K \left\{ (m_1\gamma_2^R + m_2\gamma_2^I) \begin{bmatrix} u_r^R(\phi, \lambda) \\ u_n^R(\phi, \lambda) \\ u_e^R(\phi, \lambda) \end{bmatrix} + (m_2\gamma_2^R - m_1\gamma_2^I) \begin{bmatrix} u_r^I(\phi, \lambda) \\ u_n^I(\phi, \lambda) \\ u_e^I(\phi, \lambda) \end{bmatrix} \right\} \tag{5.106}$$

Table 5.7 Displacement due to ocean loading [cm in amplitude (A) and degree in phase (P)]

	M_2		S_2		K_1		O_1		N_2		P_1		K_2		Q_1		M_f		M_m		S_{sa}	
	A	*P*	*A*	*P*	*A*	*P*	*A*	*P*	*A*	*P*	*A*	*P*	*A*	*P*	*A*	*P*	*A*	*P*	*A*	*P*	*A*	*P*
Brewster	.885	82.7	.262	134.7	.863	57.1	.538	44.1	.154	54.3	.273	54.3	.068	130.5	.096	37.8	.041	6.9	.025	3.2	.021	1.2
Robled32	1.46	−89.0	.49	−62.9	.26	−69.5	.03	−115.3	.32	−106.9	.08	−74.8	.14	−65.1	.03	62.6	.03	6.8	.02	3.1	.01	0.8
Haystack	.71	−168.0	.21	−167.5	.42	−5.9	.28	−0.6	.19	175.8	.14	−5.4	.05	−169.5	.06	0.9	.02	61.0	.01	33.7	.01	8.3
Westford	.71	−168.2	.21	−167.6	.42	−5.9	.28	−0.6	.19	175.6	.14	−5.4	.05	−169.5	.06	0.9	.02	61.0	.01	33.8	.01	8.3
NRAO 140	.64	145.2	.20	173.2	.31	−1.6	.21	3.8	.13	129.0	.11	0.7	.05	166.5	.05	5.6	.01	117.5	.005	78.3	.001	53.3
Richmond	.73	159.3	.23	−178.7	.19	−3.4	.12	23.7	.16	146.7	.08	10.6	.07	−176.0	.04	36.5	.06	176.2	.03	175.0	.03	178.2
HRAS 085	.08	−168.8	.15	−128.1	.47	32.5	.32	17.1	.05	−69.3	.15	30.8	.04	−109.1	.07	10.0	.02	−167.7	.01	157.3	.01	137.3
Plattvil	.31	112.9	.14	−171.6	.50	37.2	.33	25.1	.03	87.3	.16	34.6	.04	−168.2	.06	19.0	.006	31.6	.005	9.3	.004	5.3
Vernal	.30	104.6	.13	−169.7	.62	42.1	.40	28.9	.03	66.6	.20	39.4	.04	−165.6	.07	22.2	.008	8.9	.006	−0.1	.005	2.6
Flagstaf	.10	123.4	.15	−130.4	.76	39.2	.49	25.2	.03	−84.9	.24	36.6	.05	−127.1	.09	18.0	.008	−137.9	.004	−134.3	.004	−176.5
Yuma	.06	−27.9	.18	−105.6	.99	37.3	.64	23.1	.08	−79.3	.31	34.9	.06	−104.6	.12	15.8	.02	−138.2	.008	−144.0	.008	−175.9
Ely	.28	88.4	.13	−162.6	.81	45.4	.51	31.5	.03	19.9	.25	42.7	.04	−156.8	.09	24.4	.009	−16.0	.006	−15.3	.004	−0.8
Onsala	.36	−68.2	.12	−40.4	.22	−57.0	.13	−101.9	.07	−92.5	.07	−62.6	.03	−45.4	.02	−169.4	.08	18.6	.05	11.4	.04	2.1
Reykjav	2.4	78.3	1.5	104.5	.27	−53.3	.08	−79.0	.45	78.1	.09	−53.7	.41	101.5	.01	−169.3	.08	−165.4	.04	−169.2	.04	−178.1
BlkButte	.17	−39.8	.21	−98.2	1.1	39.1	.68	24.5	.10	−74.1	.34	36.4	.07	−100.1	.12	17.1	.01	−126.3	.01	−132.9	.01	−174.6
Ocotillo	.26	−46.5	.24	−90.1	1.15	37.6	.74	23.1	.12	−75.5	.36	35.0	.08	−93.1	.13	15.7	.02	−131.0	.01	−138.7	.01	−175.0
DeadManL	.17	−31.3	.20	−99.5	1.07	40.2	.69	25.6	.09	−70.3	.34	37.4	.07	−101.3	.12	18.2	.01	−118.1	.01	−124.1	.005	−173.6
Mon Peak	.36	−46.3	.28	−85.1	1.22	37.8	.78	23.2	.15	−73.5	.38	35.1	.09	−89.1	.14	15.8	.02	−127.7	.01	−136.0	.01	−174.7
PinFlats	.27	−41.0	.23	−91.2	1.15	39.1	.73	24.5	.12	−71.8	.36	36.4	.08	−94.3	.13	17.0	.014	−122.7	.007	−130.2	.007	−174.1
Mojave12	.22	−11.3	.15	−107.5	.99	43.6	.62	28.7	.12	−55.3	.31	42.9	.05	−82.5	.12	19.8	.01	−67.2	.01	107.7	.06	73.9
PBlossom	.32	−25.7	.22	−88.7	1.22	40.9	.78	26.2	.13	−62.7	.39	38.0	.07	−92.4	.14	18.8	.012	−105.3	.006	−111.9	.005	−171.7
Pasadena	.43	−30.0	.26	−81.6	1.31	40.2	.83	25.5	.16	−62.8	.41	37.3	.08	−86.3	.15	18.0	.013	−107.7	.006	−115.6	.005	−172.1

Table 5.7 *(continued)*

	M_2		S_2		K_1		O_1		N_2		P_1		K_2		Q_1		M_f		M_m		S_{sa}	
	A	*P*	*A*	*P*	*A*	*P*	*A*	*P*	*A*	*P*	*A*	*P*	*A*	*P*	*A*	*P*	*A*	*P*	*A*	*P*	*A*	*P*
PVerdes	.77	−34.2	.38	−68.4	1.54	38.5	.98	23.7	.24	−62.1	.48	35.5	.12	−74.6	.18	16.2	.014	−112.1	.007	−121.2	.006	−172.7
MammothL	.30	50.1	.11	−139.0	1.08	46.0	.68	31.7	.10	−21.0	.34	43.3	.03	−131.3	.12	24.4	.011	−42.7	.006	−38.9	.002	−12.5
SanPaula	.53	−24.6	.27	−76.6	1.41	40.7	.89	25.9	.18	−58.3	.44	37.8	.09	−81.9	.16	18.5	.013	−100.1	.006	−108.1	.005	−170.7
Vandenbg	.89	−15.0	.31	−60.5	1.75	41.1	1.10	26.3	.25	−48.6	.55	38.2	.10	−67.8	.20	19.0	.014	−88.2	.007	−96.1	.004	−167.7
Quincy 7109	.59	60.4	.11	158.6	1.15	49.8	.72	35.7	.11	13.7	.36	47.0	.03	167.7	.13	28.7	.02	−18.2	.011	−17.0	.007	−2.7
Quincy 7221	.59	60.4	.11	158.6	1.15	49.8	.72	35.7	.11	13.7	.36	47.0	.03	167.7	.13	28.7	.02	−18.2	.011	−17.0	.007	−2.7
HatCreek	.71	62.3	.14	142.8	1.18	51.0	.73	37.0	.13	20.7	.37	48.3	.03	145.7	.13	30.1	.024	−14.0	.014	−13.4	.009	−1.9
Fort Ord 7241	.78	15.7	.10	−59.0	1.60	45.0	1.00	30.4	.20	−26.8	.50	42.2	.04	−68.2	.18	23.2	.016	−51.5	.008	−51.4	.001	−44.0
Fort Ord 7266	.78	16.6	.10	−58.7	1.60	45.0	1.00	30.5	.19	−26.0	.50	42.2	.04	−68.1	.18	23.3	.016	−50.5	.008	−50.2	.001	−38.2
SanFranc	.96	27.8	.04	5.4	1.64	46.7	1.03	32.4	.22	−12.8	.52	44.0	.02	−36.8	.18	25.4	.019	−36.2	.01	−34.4	.004	−10.4
Presidio	.96	27.8	.04	5.4	1.64	46.7	1.03	32.4	.22	−12.8	.52	44.0	.02	−36.8	.18	25.4	.019	−36.2	.01	−34.4	.004	−10.4
Pt Reyes	1.06	30.5	.06	38.2	1.70	47.3	1.06	32.9	.23	−9.2	.54	44.5	.02	−10.3	.19	25.9	.02	−33.0	.011	−31.2	.005	−8.5
Yakataga	2.72	101.9	.95	134.9	1.43	86.5	.90	74.7	.54	79.3	.46	83.5	.27	128.0	.16	68.5	.11	8.6	.06	5.3	.05	1.2
Kodiak	3.24	118.2	1.14	149.8	1.78	97.7	1.15	85.9	.64	95.4	.58	94.7	.31	143.2	.21	80.5	.12	4.9	.07	2.2	.06	.6
Kokee 1311	1.25	−121.1	.50	−116.6	1.24	60.2	.69	53.5	.24	−128.7	.40	59.0	.14	−127.5	.11	51.9	.05	−139.3	.03	−152.6	.03	−175.8
Kokee 7298	1.25	−121.1	.50	−116.6	1.24	60.2	.69	53.5	.24	−128.7	.40	59.0	.14	−127.5	.11	51.9	.05	−139.3	.03	−152.6	.03	−175.8
SndPoint	2.05	119.4	.86	152.9	1.79	113.3	1.21	101.8	.38	104.1	.58	110.0	.24	145.2	.22	96.6	.13	3.0	.07	.1	.06	.2
Kwajal26	3.16	−49.3	1.72	−31.3	1.05	−127.8	.70	−153.1	.62	−51.2	.31	−131.0	.49	−35.1	.14	−164.8	.08	−165.1	.05	−167.3	.05	−177.6
Mauna Kea	1.58	−125.7	.64	−117.6	1.30	55.4	.72	45.4	.31	−134.2	.42	54.2	.18	−126.8	.11	40.8	.06	−145.7	.04	−156.7	.03	−176.4
Hobart	.97	151.9	.15	−119.2	.71	88.3	.65	57.5	.26	121.5	.24	80.6	.02	136.5	.20	40.4	.06	14.0	.03	6.5	.03	.7
Kashima	.87	45.3	.50	69.8	1.18	−138.6	.92	−157.0	.13	55.0	.38	−143.8	.16	64.5	.18	−167.7	.03	−9.6	.01	−26.3	.004	−12.4
Wettzell 7224	.51	−70.3	.17	−40.5	.19	−64.2	.10	−95.3	.11	−89.4	.06	−67.0	.05	−43.1	.004	−161.8	.05	11.3	.03	6.2	.02	1.3
Wettzell 8834	.51	−70.3	.17	−40.5	.19	−64.2	.10	−95.3	.11	−89.4	.06	−67.0	.05	−43.1	.004	−161.8	.05	11.3	.03	6.2	.02	1.3

Table 5.7 *(continued)*

	M_2		S_2		K_1		O_1		N_2		P_1		K_2		Q_1		M_f		M_m		S_{sa}	
	A	*P*	*A*	*P*	*A*	*P*	*A*	*P*	*A*	*P*	*A*	*P*	*A*	*P*	*A*	*P*	*A*	*P*	*A*	*P*	*A*	*P*
Eflsberg	.62	−66.9	.20	−37.2	.23	−63.4	.10	−90.7	.14	−88.6	.07	−65.5	.06	−40.8	.003	175.7	.06	14.7	.04	8.2	.03	1.6
Yaragade	.35	144.8	.08	−116.1	.89	12.2	.68	7.9	.07	103.5	.28	9.5	.03	−125.2	.16	−.5	.03	−176.8	.01	−175.4	.009	−178.8
Graz	.49	−71.8	.17	−42.5	.18	−68.3	.09	−96.1	.11	−89.6	.05	−69.0	.05	−44.7	.004	−142.6	.05	8.7	.02	4.1	.02	.9
Ny Alesund	.79	179.5	.26	−132.7	.05	−35.0	.19	−115.6	.17	153.3	.02	−56.6	.08	−141.0	.05	−168.8	.18	29.3	.11	18.3	.10	3.2
Helwan	.34	−84.2	.13	−47.9	.10	179.1	.05	−153.9	.08	−96.0	.03	174.2	.04	−57.0	.01	−165.4	.01	−63.6	.006	−115.2	.006	−172.2
Metsahov 7601	.21	−65.3	.08	−31.0	.17	−62.0	.13	−103.9	.04	−88.5	.06	−69.0	.02	−35.1	.02	−150.8	.07	18.5	.04	12.1	.04	2.3
Metsahov 7805	.21	−65.2	.08	−30.9	.17	−62.0	.13	−104.0	.04	−88.5	.06	−69.0	.02	−35.0	.02	−150.8	.07	18.4	.04	12.1	.04	2.3
Grasse 7835	.70	−70.5	.24	−42.8	.22	−55.1	.09	−89.1	.16	−89.7	.06	−65.0	.07	−44.7	.005	90.2	.04	6.7	.02	1.9	.02	.8
Grasse 7605	.70	−70.5	.24	−42.8	.22	−55.1	.09	−89.1	.16	−89.7	.06	−65.0	.07	−44.7	.005	90.2	.04	6.7	.02	1.9	.02	.8
Potsdam	.45	−68.0	.15	−37.6	.20	−62.2	.11	−95.7	.10	−88.0	.07	−65.8	.04	−40.2	.007	−159.9	.06	14.6	.03	8.6	.03	1.7
Matera 7243	.54	−78.0	.20	−58.9	.15	−82.4	.08	−100.3	.12	−87.4	.04	−79.9	.06	−49.8	.004	−122.0	.03	.1	.02	−4.3	.01	−.2
Matera 7541	.54	−78.0	.20	−58.9	.15	−82.4	.08	−100.3	.12	−87.4	.04	−79.9	.06	−49.8	.004	−122.0	.03	.1	.02	−4.3	.01	−.2
Matera 7939	.54	−78.0	.20	−58.9	.15	−82.4	.08	−100.3	.12	−87.4	.04	−79.9	.06	−49.8	.004	−122.0	.03	.1	.02	−4.3	.01	−.2
Simosato	1.30	88.2	.63	97.31.17		−126.0	.89	−144.0	.25	85.8	.37	−129.5	.18	95.3	.18	−154.0	.02	−19.1	.006	−65.2	.002	−153.7
Kootwijk	.63	−58.7	.20	−28.4	.22	−67.2	.12	−78.6	.14	−82.7	.08	−66.3	.06	−31.8	.006	−113.9	.07	18.0	.04	9.8	.03	1.9
Shanghai	.74	−148.6	.22	−103.7	.67	−96.9	.53	−113.0	.15	−170.9	.19	−94.7	.05	−116.6	.10	−123.8	.002	160.4	.007	−155.5	.008	−175.1
Arequipa	.46	111.8	.19	101.8	.53	−141.9	.29	−168.2	.16	98.2	.17	−143.6	.05	114.2	.05	178.2	.05	−156.0	.03	−165.8	.03	−177.3
Borowiec	.40	−68.8	.14	−37.6	.18	−63.5	.11	−97.5	.09	−87.9	.06	−67.6	.04	−40.4	.01	−150.1	.06	13.4	.03	8.0	.03	1.6
San Fern	2.22	−109.5	.79	−85.9	.27	−84.2	.05	126.4	.48	−125.6	.08	−90.4	.22	−88.3	.05	58.8	.02	3.3	.01	.1	.01	.2
Zimmerwa	.69	−71.9	.23	−42.6	.22	−62.4	.09	−94.3	.15	−91.3	.07	−66.3	.07	−45.2	.004	106.2	.05	10.1	.03	5.0	.02	1.1

Table 5.7 *(continued)*

	M_2		S_2		K_1		O_1		N_2		P_1		K_2		Q_1		M_f		M_m		S_{sa}	
	A	P	A	P	A	P	A	P	A	P	A	P	A	P	A	P	A	P	A	P	A	P
Herstmon	.38	−155.6	.18	−99.7	.31	−61.3	.12	−105.4	.15	−133.2	.10	−60.3	.10	−78.8	.01	167.5	.07	14.9	.04	8.4	.03	1.7
Ft. Davi 7216	.15	162.1	.16	−128.9	.51	29.8	.35	17.1	.03	−125.8	.16	27.4	.05	−126.6	.07	11.0	.02	−166.3	.01	−167.7	.01	−179.0
Ft. Davi 7613	.15	162.1	.16	−128.9	.51	29.8	.35	17.1	.03	−125.8	.16	27.4	.05	−126.6	.07	11.0	.02	−166.3	.01	−167.7	.01	−179.0
Mojave 12	.14	.6	.17	−108.2	1.05	42.0	.67	27.5	.08	−61.5	.33	39.2	.06	−108.4	.12	20.1	.01	−99.7	.005	−101.8	.003	−170.6
Greenbel 7108	.81	153.8	.24	176.4	.35	−1.3	.24	3.8	.18	135.4	.12	1.3	.06	161.3	.07	7.7	.01	106.7	.01	65.1	.003	25.5
Greenbel 7920	.81	153.8	.24	176.4	.35	−1.3	.24	3.8	.18	135.4	.12	1.3	.06	161.3	.07	7.7	.01	106.7	.01	65.1	.003	25.5
Maui, HI	1.48	−126.9	.61	−120.1	1.33	56.6	.74	47.2	.29	−134.9	.43	55.3	.17	−129.5	.12	43.1	.05	−143.5	.03	−155.4	.03	−176.2
Monument Pk	.36	−46.3	.28	−85.1	1.22	37.8	.78	23.2	.15	−73.5	.38	35.1	.10	−89.1	.14	15.8	.02	−127.7	.01	−136.0	.01	−174.7
Quincy 7109	.59	60.4	.11	158.6	1.15	49.8	.72	35.7	.11	13.7	.36	47.0	.03	167.7	.13	28.7	.02	−18.2	.01	−17.0	.01	−2.7
Quincy 7221	.59	60.4	.11	158.6	1.15	49.8	.72	35.7	.11	13.7	.36	47.0	.03	167.7	.13	28.7	.02	−18.2	.01	−17.0	.01	−2.7
Simeis	.32	−70.1	.12	−37.4	.08	−102.9	.08	−112.6	.07	−85.6	.03	−101.5	.03	−41.9	.01	−139.0	.03	2.0	.02	−1.0	.01	−.6
Hartebees	1.67	−132.0	.76	−103.7	.10	120.5	.16	114.7	.03	−144.6	.03	118.5	.21	−106.5	.04	105.1	.02	−155.7	.01	−164.7	.01	−177.5
OHiggins	2.25	84.6	1.04	122.8	1.59	−117.3	1.60	−135.1	.35	61.4	.48	−121.1	.30	124.5	.37	−149.8	.16	14.0	.10	10.4	.07	2.0
Forteleza	3.55	34.2	1.15	56.8	.25	96.8	.27	31.8	.76	21.3	.08	91.7	.33	52.4	.07	−4.4	.10	−175.7	.05	−178.6	.03	−179.4
Santiago	.28	−145.2	.08	−51.8	.66	−132.3	.51	−153.6	.11	162.7	.21	−134.1	.03	−77.8	.11	−165.9	.02	−47.4	.005	−44.1	.003	−163.5

where

$$K = \frac{4\pi G a_e \rho_w H_p}{3g_e}$$

$$H_p = \left(\frac{8\pi}{15}\right)^{1/2} \frac{\omega^2 a_e^4}{GM_\oplus}$$

and

ω = nominal mean angular velocity of the Earth = 7.292115 $\times 10^{-5}$rad s^{-1};

a_e = equatorial radius of the Earth = 6378136.6 m;

$GM_\oplus$ is defined in § 5.3.3.3; g_e, G, and ρ_w are defined in § 5.3.4;

$$\gamma = (1 + k_2 - h_2) = \gamma_2^R + i\gamma_2^I = 0.6870 + 0.0036i;$$

(m_1, m_2) are the wobble parameters. Refer to § 6.9.2.1 of this book for the relationship between the wobble variables (m_1, m_2) and the polar motion variables (x_p, y_p). Functions $u_r^R(\phi, \lambda)$, $u_n^R(\phi, \lambda)$, $u_e^R(\phi, \lambda)$ are the real part of the ocean pole load tide coefficients. Functions $u_r^I(\phi, \lambda)$, $u_n^I(\phi, \lambda)$, $u_e^I(\phi, \lambda)$ are the imaginary part of the ocean pole load tide coefficients.

Maps of the required ocean pole load tide coefficients on an equally spaced 0.5 by 0.5 degree global grid are available at URL[21]. These coefficients provide the surface deformations with respect to the instantaneous center of mass of the deformed Earth including the mass of the loading ocean pole tide.

5.3.5.3 Atmospheric Loading

The procedure described below is taken from the *IERS Conventions (2003)* (IERS 2004). A time-varying atmospheric pressure distribution can induce crustal deformation. For example, pressure variations on the order of 20 hectoPascal (hPa)—and even larger—at mid-latitudes are observed in synoptic pressure systems with length scales for 1000–2000 km and periods of approximately two weeks. Seasonal pressure changes due to air mass movements between the continents and oceans can have amplitudes of up to 10 hPa in particular over the large land masses of the northern hemisphere. At the interannual periods, basin-wide air pressure signals with amplitudes of several hPa also contribute to the spectrum of the loading signal.

Other surface loads due to changes in snow and ice cover, soil moisture and groundwater, as well as ocean-bottom pressure also contribute to surface displacements. For example, at seasonal time scales, it is expected that the contribution of hydrological loads to surface displacements exceeds the one from air pressure (Blewitt et al. 2001). However, while the atmospheric load is fairly well known from global air pressure data sets, no sufficient models for ocean bottom pressure, snow and soil moisture exists at this time. Therefore, in the following, focus is on atmospheric loading although the discussion applies to any other surface loading.

Theoretical studies by Rabbel and Zschau (1985), Rabbel and Schuh (1986), vanDam and Wahr (1987), and Manabe et al. (1991) demonstrate that vertical crustal displacements of up to 25 mm are possible at mid-latitude stations due to synoptic pressure systems. Annual signals in the vertical are on the order of 1–2 mm, but maximum signals of more than 3 mm are possible over large parts of Asia, Antarctica, Australia and Greenland (Mangarotti et al. 2001; Dong et al. 2002). Pressure loading effects are larger at higher latitude sites due to the more intensive weather systems (larger in amplitude and more spatially coherent). Effects are smaller at mid-latitude sites and at locations within 500 km of the sea or ocean due to the inverted barometer response of the ocean. In all cases, horizontal crustal deformations are about one-third the amplitude of the vertical effects.

Two basic methods for computing atmospheric loading corrections to geodetic data have been applied so far: 1) using geophysical models or simple approximations derived from these models; and 2) using empirical models based on site-dependent data. The geophysical model approach is analogous to the methods described to compute ocean tidal loading effects. Both methods suffer from a number of disadvantages (see IERS 2004, § 7.1.6). In 2002 the IERS recommended that corrections for, among other surface loadings, atmospheric loading should be determined using the geophysical model approach and obtained from the Special Bureau on Loading (SBL) at URL[22].

Regression coefficients based on a geophysical model are already available for a number of VLBI sites through the SBL web page and the IERS Conventions' web page, URL[23]. The regression coefficients were computed using 18 years of the National Centers for Environmental Prediction (NCEP) Reanalysis Data (1 Jan. 1980 to 31 Dec. 1997). The data are 6–hour values of surface pressure given on a $2.5° \times 2.5°$ global grid. Vertical crustal motions at a particular site are modeled by convolving Farrell's (1972) Green's functions for a Gutenberg-Bullen A Earth model. The regression results (mm/mbar) are determined via a linear regression between the modeled crustal displacements and the local surface pressure determined from the NCEP data set. An inverted barometer model was used in determining the ocean's response to pressure.

5.3.6 Plate Motions

One of the factors that affect the definition of a terrestrial reference frame is the motion of the tectonic plates that make up the Earth's surface. As the plates move, fixed coordinates for the observing stations will become inconsistent with each other. The rates of relative motions for some regular observing sites are believed to be approximately 5 centimeters per year or larger (derived from the dating of rocks and other geophysical information). Plate motions can be measured to a precision of a few millimeters per year or better using space geodetic techniques such as VLBI, SLR, and GPS. There is considerable agreement between motions measured over a few years by space geodesy and the predictions of global plate motion models that average over the past few million years.

Work by Argus and Gordon (1991), which incorporated the plate motion model NUVEL-1 of DeMets et al. (1990), showed differences as large as 15 mm per year between their model NNR-NUVEL-1 and AM0-2 (Minster and Jordan 1978). All plates in this model move in

Table 5.8 Cartesian rotation vector for each plate using absolute plate model NNR-NUVEL-1A (no net rotation)

Plate Name	Ω_X deg/My	Ω_Y deg/My	Ω_Z deg/My
Pacific	−0.08652	0.22731	−0.57124
Cocos	−0.59731	−1.23788	0.62596
Nazca	−0.08778	−0.49143	0.55056
Caribbean	−0.01020	−0.19395	0.09585
South America	−0.05947	−0.08680	−0.04985
Antarctica	−0.04704	−0.09746	0.21234
Australia	0.44914	0.29358	0.35993
India	0.38216	0.00229	0.38904
Africa	0.05105	−0.17756	0.22471
Arabia	0.38302	−0.02985	0.38732
Eurasia	−0.05621	−0.13722	0.18065
North America	0.01478	−0.20621	−0.00877
Juan de Fuca	0.29794	0.49332	−0.33346
Philippine	0.57811	−0.41024	−0.55405
Rivera	−0.53801	−1.77388	−0.69041
Scotia	−0.02349	−0.15241	−0.07277

a right-handed sense relative to the no net rotation reference frame. This no net rotation reference frame differs substantially from the hotspot reference frame (Norton 2000) where volcanic "hotspots" are tied to the interior of the Earth.

Estimates from space geodetic measurements prompted DeMets et al. (1994) to modify NUVEL-1 angular velocities which were found to be systematically too fast. This recalibrated plate motion model is referred to as NNR-NUVEL-1A. In addition to the plate motions determined by DeMets et al. (1990), recalibrated angular velocities for the Juan de Fuca, Philippine, Rivera, and Scotia plates were provided. Although individual plate discrepancies between angular velocity measurements by space geodetic techniques and model predictions may exceed 3 mm per year (corresponding to ITRF2000 orientation rate alignment differences; see IERS (2010), chapter 4), globally averaged plate motions are very steady, within 2% to 6%, over a time scale from several years to several Myr. The cartesian rotation vector for each of the major plates is given in Table 5.8.

5.3.7 Tidal Effects in UT1

To properly compare UT1 results obtained at different epochs, the high-frequency tidal effects must be accounted for. Thus, a standard expression for the tidal variations in UT1 is required. The periodic variations in UT1 due to tidal deformation of the polar moment of inertia have been rederived (Yoder, Williams, and Parke 1981) including the tidal deformation of the Earth with a decoupled core.

This model leads to effective Love numbers that differ from the bulk value of 0.301 because of the oceans and the fluid core, which give rise to different theoretical values of the ratio k/C for the fortnightly and monthly terms. However, Yoder et al. recommend the value of 0.94 for k/C for both cases. Periodic terms in UT1 are given in Table 5.9 and Table 5.10 and are discussed in IERS Explanatory Supplement (IERS 2009) and Gross (2007). Table 5.9 includes terms due to zonal tides, with periods up to 35 days, with $k/C = 0.94$. Table 5.10 lists the remainder of the tidal terms (with periods greater than 35 days).

UT1R, ΔR, and ωR represent the regularized forms of UT1 (including periods up to 35 days), of the duration of the day, Δ, and of the angular velocity of the Earth, ω. The units are 10^{-4} s for UT, 10^{-5} s/day for Δ, and 10^{-14} rad/s for ω. To avoid confusion among possible tidal models, it is recommended that the terms δUT1, $\delta\Delta$, $\delta\omega$ be followed by the model name in parenthesis, e.g., δUT1(Yoder et al. 1981).

Oceanic tides with short periods (diurnal and sub-diurnal) cause variations in UT1 and polar motion that are only partially represented by the model given below. According to Brosche et al. (1989) and Seiler and Wünsch (1995), the contribution of the oceanic tides should be split into a part that is in phase with the solid Earth tides and an out-of-phase part. The discrepancy between the model of Yoder et al. (which already contains the general influence of the oceans) and the model of Brosche et al., amounts to a maximum of ± 0.08 msec for the fortnightly and monthly terms. The influence of the ocean tides with periods less than or equal to 24^{h} is at the level of ± 0.1 msec. Kantha, Stewart, and Desai (1998) found that both M_f and M_m tides have amplitudes of ~ 0.115 msec. Thus, the impact of these tides on length of day changes is significant.

Following the *IERS Conventions (2010)* (IERS 2010), it is recommended that a combination of the Yoder et al. (1981) elastic body tide, Wahr and Bergen (1986) anelastic body tide, and Kantha, Stewart, and Desai (1998) ocean tide models are to be used to model long-period ocean tide effects on the rotation of the Earth. The Kantha, Stewart, and Desai (1998) ocean tide model replaces the Defraigne and Smits (1999) model recommended in the *IERS Conventions (2003)* (IERS 2004). That model leaves a large signal at the fortnightly tidal period when removed from length of day observations (Gross 2009).

5.3.8 Tidal Effects in Polar Motion

As mentioned in Gross (2008), several authors have produced both dynamical and empirical models for determining the effect of ocean tides on polar motion. The *IERS Conventions (2010)* recommended model for long-period ocean tide effects on polar motion (IERS 2010, chapter 8) is the dynamical model of Dickman and Nam (1995) as reported in Dickman and Gross (2010). Dickman and Nam (1995) estimated polar motion by Fourier spectral analysis of the Space92 polar motion time series (Gross 1993). The effect on polar motion is greatest for the fortnightly M_f tide. Empirical fits to polar motion observational measurements give (prograde, retrograde) amplitudes of (69,89) μas at M_f. The modeled effect yields (prograde, retrograde) polar motion amplitudes of (66,74) μas at M_f. Table 5.11 provides corrections for the tidal variations in polar motion and polar motion excitation with periods from nine days to 18.6 years. The sum of these corrections should be subtracted from the observed polar motion and polar motion excitation values so that variations are "tide-free."

Table 5.9 Zonal tide terms with periods up to 35 days

Argument [a]					Period	δUT1		δΔ Coefficient of		δω	
l	l'	F	D	Ω	Days	sin	cos	cos	sin	cos	sin
1	0	2	2	2	5.64	−0.0235	0.0000	0.2617	0.0000	−0.2209	0.0000
2	0	2	0	1	6.85	−0.0404	0.0000	0.3706	0.0000	−0.3128	0.0000
2	0	2	0	2	6.86	−0.0987	0.0000	0.9041	0.0000	−0.7630	0.0000
0	0	2	2	1	7.09	−0.0508	0.0000	0.4499	0.0000	−0.3797	0.0000
0	0	2	2	2	7.10	−0.1231	0.0000	1.0904	0.0000	−0.9203	0.0000
1	0	2	0	0	9.11	−0.0385	0.0000	0.2659	0.0000	−0.2244	0.0000
1	0	2	0	1	9.12	−0.4108	0.0000	2.8298	0.0000	−2.3884	0.0000
1	0	2	0	2	9.13	−0.9926	0.0000	6.8291	0.0000	−5.7637	0.0000
3	0	0	0	0	9.18	−0.0179	0.0000	0.1222	0.0000	−0.1031	0.0000
−1	0	2	2	1	9.54	−0.0818	0.0000	0.5384	0.0000	−0.4544	0.0000
−1	0	2	2	2	9.56	−0.1974	0.0000	1.2978	0.0000	−1.0953	0.0000
1	0	0	2	0	9.61	−0.0761	0.0000	0.4976	0.0000	−0.4200	0.0000
2	0	2	−2	2	12.81	0.0216	0.0000	−0.1060	0.0000	0.0895	0.0000
0	1	2	0	2	13.17	0.0254	0.0000	−0.1211	0.0000	0.1022	0.0000
0	0	2	0	0	13.61	−0.2989	0.0000	1.3804	0.0000	−1.1650	0.0000
0	0	2	0	1	13.63	−3.1873	0.2010	14.6890	0.9266	−12.3974	−0.7820
0	0	2	0	2	13.66	−7.8468	0.5320	36.0910	2.4469	−30.4606	−2.0652
2	0	0	0	−1	13.75	0.0216	0.0000	−0.0988	0.0000	0.0834	0.0000
2	0	0	0	0	13.78	−0.3384	0.0000	1.5433	0.0000	−1.3025	0.0000
2	0	0	0	1	13.81	0.0179	0.0000	−0.0813	0.0000	0.0686	0.0000
0	−1	2	0	2	14.19	−0.0244	0.0000	0.1082	0.0000	−0.0913	0.0000
0	0	0	2	−1	14.73	0.0470	0.0000	−0.2004	0.0000	0.1692	0.0000
0	0	0	2	0	14.77	−0.7341	0.0000	3.1240	0.0000	−2.6367	0.0000
0	0	0	2	1	14.80	−0.0526	0.0000	0.2235	0.0000	−0.1886	0.0000
0	−1	0	2	0	15.39	−0.0508	0.0000	0.2073	0.0000	−0.1749	0.0000
1	0	2	−2	1	23.86	0.0498	0.0000	−0.1312	0.0000	0.1107	0.0000
1	0	2	−2	2	23.94	0.1006	0.0000	−0.2640	0.0000	0.2228	0.0000
1	1	0	0	0	25.62	0.0395	0.0000	−0.0968	0.0000	0.0817	0.0000
−1	0	2	0	0	26.88	0.0470	0.0000	−0.1099	0.0000	0.0927	0.0000
−1	0	2	0	1	26.98	0.1767	0.0000	−0.4115	0.0000	0.3473	0.0000
−1	0	2	0	2	27.09	0.4352	0.0000	−1.0093	0.0000	0.8519	0.0000
1	0	0	0	−1	27.44	0.5339	0.0000	−1.2224	0.0000	1.0317	0.0000
1	0	0	0	0	27.56	−8.4046	0.2500	19.1647	0.5701	−16.1749	−0.4811
1	0	0	0	1	27.67	0.5443	0.0000	−1.2360	0.0000	1.0432	0.0000
0	0	0	1	0	29.53	0.0470	0.0000	−0.1000	0.0000	0.0844	0.0000
1	−1	0	0	0	29.80	−0.0555	0.0000	0.1169	0.0000	−0.0987	0.0000
−1	0	0	2	−1	31.66	0.1175	0.0000	−0.2332	0.0000	0.1968	0.0000
−1	0	0	2	0	31.81	−1.8236	0.0000	3.6018	0.0000	−3.0399	0.0000

Table 5.9 *(continued)*

Argument[a]					Period	δUT1		δΔ Coefficient of		δω	
l	l'	F	D	Ω	Days	sin	cos	cos	sin	cos	sin
−1	0	0	2	1	31.96	0.1316	0.0000	−0.2587	0.0000	0.2183	0.0000
1	0	−2	2	−1	32.61	0.0179	0.0000	−0.0344	0.0000	0.0290	0.0000
−1	−1	0	2	0	34.85	−0.0855	0.0000	0.1542	0.0000	−0.1302	0.0000

Table 5.10 Zonal tide terms with periods greater than 35 days

Argument[a]					Period	δUT1		δΔ Coefficient of		δω	
l	l'	F	D	Ω	Days	sin	cos	cos	sin	cos	sin
0	2	2	−2	2	91.31	−0.0573	0.0000	0.0395	0.0000	−0.0333	0.0000
0	1	2	−2	1	119.61	0.0329	0.0000	−0.0173	0.0000	0.0146	0.0000
0	1	2	−2	2	121.75	−1.8847	0.0000	0.9726	0.0000	−0.8209	0.0000
0	0	2	−2	0	173.31	0.2510	0.0000	−0.0910	0.0000	0.0768	0.0000
0	0	2	−2	1	177.84	1.1703	0.0000	−0.4135	0.0000	0.3490	0.0000
0	0	2	−2	2	182.62	−49.7174	0.4330	17.1056	0.1490	−14.4370	−0.1257
0	2	0	0	0	182.63	−0.1936	0.0000	0.0666	0.0000	−0.0562	0.0000
2	0	0	−2	−1	199.84	0.0489	0.0000	−0.0154	0.0000	0.0130	0.0000
2	0	0	−2	0	205.89	−0.5471	0.0000	0.1670	0.0000	−0.1409	0.0000
2	0	0	−2	1	212.32	0.0367	0.0000	−0.0108	0.0000	0.0092	0.0000
0	−1	2	−2	1	346.60	−0.0451	0.0000	0.0082	0.0000	−0.0069	0.0000
0	1	0	0	−1	346.64	0.0921	0.0000	−0.0167	0.0000	0.0141	0.0000
0	−1	2	−2	2	365.22	0.8281	0.0000	−0.1425	0.0000	0.1202	0.0000
0	1	0	0	0	365.26	−15.8887	0.1530	2.7332	0.0263	−2.3068	−0.0222
0	1	0	0	1	386.00	−0.1382	0.0000	0.0225	0.0000	−0.0190	0.0000
1	0	0	−1	0	411.78	0.0348	0.0000	−0.0053	0.0000	0.0045	0.0000
2	0	−2	0	0	−1095.18	−0.1372	0.0000	−0.0079	0.0000	0.0066	0.0000
−2	0	2	0	1	1305.48	0.4211	0.0000	−0.0203	0.0000	0.0171	0.0000
−1	1	0	1	0	3232.86	−0.0404	0.0000	0.0008	0.0000	−0.0007	0.0000
0	0	0	0	2	−3399.19	7.8998	0.0000	0.1460	0.0000	−0.1232	0.0000
0	0	0	0	1	−6798.38	−1617.2681	0.0000	−14.9471	0.0000	12.6153	0.0000

[a] $l = 134.96° + 13.064993°(\text{MJD} - 51544.5)$ Mean anomaly of the Moon

$l' = 357.53° + 0.985600°(\text{MJD} - 51544.5)$ Mean anomaly of the Sun

$F = 93.27° + 13.229350°(\text{MJD} - 51544.5)$ L − Ω: L : Mean longitude of the Moon

$D = 297.85° + 12.190749°(\text{MJD} - 51544.5)$ Mean elongation of the Moon from the Sun

$\Omega = 125.04° - 0.052954°(\text{MJD} - 51544.5)$ Mean longitude of the ascending node of the Moon

Table 5.11 Ocean tidal variations in polar motion and polar motion excitation

Tide	Argument					Period	Polar Motion				Polar Motion Excitation			
							Prograde		Retrograde		Prograde		Retrograde	
							amp	phase	amp	phase	amp	phase	amp	phase
	l	l'	F	D	Ω	(days)	(μas)	(degrees)	(μas)	(degrees)	(μas)	(degrees)	(μas)	(degrees)
m_{tm}	1	0	2	0	1	9.12	4.43	−112.62	5.57	21.33	205.83	67.21	269.95	21.17
M_{tm}	1	0	2	0	2	9.13	10.72	−112.56	13.48	21.30	497.59	67.27	652.59	21.14
m_f	0	0	2	0	1	13.63	27.35	−91.42	30.59	13.31	841.32	88.42	1002.12	13.15
M_f	0	0	2	0	2	13.66	66.09	−91.31	73.86	13.27	2028.73	88.53	2414.94	13.11
M_{sf}	0	0	0	2	0	14.77	5.94	−87.13	6.42	11.75	168.13	92.70	194.74	11.60
M_m	1	0	0	0	0	27.56	43.74	−56.70	31.12	−0.91	643.61	123.13	520.16	−1.06
M_{sm}	−1	0	0	2	0	31.81	8.85	−51.11	5.42	−4.21	111.62	128.72	79.23	−4.36
S_{sa}	0	0	2	−2	2	182.62	86.48	−20.30	99.77	175.57	118.56	159.42	336.32	175.46
S_a	0	1	0	0	0	365.26	17.96	−17.38	152.15	170.60	3.33	161.60	332.53	170.51
M_n	0	0	0	0	1	−6798.38	208.17	166.89	186.98	166.67	221.43	166.88	175.07	166.68

5.4 Monitoring the Orientation of the Earth

Continuous monitoring of the Earth's orientation began after Seth Carlo Chandler Jr.'s discovery of the variation of latitude in 1884 (Carter and Carter 2000) and Chandler's explanation of it as polar motion (Chandler wobble). Optical astrometric methods then in use continued to be the only source of Earth orientation information up until the mid-1960s. More modern techniques then gradually took over the bulk of the activity of monitoring the orientation of the Earth, with Doppler tracking of satellites, Connected-Element Radio Interferometry (CERI), lunar laser ranging (LLR), satellite laser ranging (SLR), Very Long Baseline Interferometry (VLBI), Doppler orbitography and radiopositioning integrated by satellite (DORIS), and Global Navigation Satellite System (GNSS), such as Global Positioning System (GPS), assisting in such monitoring. Currently, the techniques of SLR, VLBI, and GPS provide most of the current high-accuracy observations for this purpose. Table 5.12 provides a listing of EOP techniques and estimated accuracies for one year.

Table 5.12 Estimated accuracies of EOP techniques in 2008 provided by IERS Rapid Service/Prediction Center (unless indicated otherwise).

Contributor Information			Estimated Accuracy			
Name, Type	x	y	UT1	LOD	$\delta\psi$ (dX)	$\delta\epsilon$ (dY)
	mas	mas	0.001s	0.001s/day	mas	mas
ILRS SLR [a]	0.17	0.23		0.047		
IAA SLR	0.19	0.23				
MCC SLR	0.18	0.20				
GSFC VLBI Intensives			0.015			
USNO VLBI Intensives			0.016			
GSFC VLBI	0.07	0.08	0.004		0.4	0.1
IAA VLBI [b]	0.09	0.12	0.004		(0.1)	(0.1)
IVS VLBI [b]	0.13	0.14	0.004		(0.1)	(0.1)
USNO VLBI	0.08	0.10	0.004		0.4	0.1
IGS Final [c]	0.01	0.02		0.02		
IGS Rapid [c]	0.04	0.05		0.03		
IGS Ultra [c]	0.05	0.06		0.03		
USNO GPS UT [d]			0.015 [d]			
EMR GPS UT [d]			0.030 [d]			
USNO AAM UT			0.015			
DORIS [e]	0.62	0.65				

[a] LOD value from http://ilrs.gsfc.nasa.gov/docs/ILRS_products_070306.pdf.
[b] IAA and IVS VLBI nutation values are in terms of dX/dY using IAU 2000A Nutation Theory.
[c] LOD value from IERS Annual Report 2007.
[d] All satellite techniques provide information on the rate of change of Universal Time contaminated by effects due to unmodeled orbit node motion. VLBI-based results have been used to correct for LOD biases and to minimize drifts in UT estimates.
[e] DORIS data are from January 1, 2009–December 12, 2009.

Before describing the observational systems and services, the basic sensitivity of the systems should be briefly explained. All the observational systems depend on observing targets whose position can be inferred in some celestial reference frame. This includes stars and solar system objects for optical astrometry, the Moon and artificial satellites for laser ranging, and radio sources for radio interferometry. The observations of these targets are then used to infer the motion of the observing instruments or, more specifically, the Earth to which they are attached. After the predicted variations from all other "defined" sources (as explained previously, including precession, nutation, the Earth's sidereal rotation, tides, etc.) have been removed, the motion that remains is attributed to polar motion and UT1−UTC variations. Systems using artificial Earth satellites depend on the sensing of a local "inertial" coordinate system, rather than an astronomically defined one.

It is also important to note that a single instrument (or single baseline for interferometric observing) can be used to determine only two components of the Earth's orientation. The components commonly determined using single-station (or single-baseline) data include *variation in latitude* ($\Delta\phi$) due to any north–south motion of the station, and UT0−UTC when there is any east–west motion of the station, attributable to Earth orientation variations. To obtain all three components of Earth orientation, it is necessary to use data from more sites.

The equations for expressing $\Delta\phi$ and UT0−UTC in terms of x_p, y_p, and UT1−UTC are

$$\Delta\phi = x_p \cos\lambda - y_p \sin\lambda \tag{5.107}$$

$$\text{UT0-UTC} = \tan\phi\,(x_p \sin\lambda + y_p \cos\lambda) + (\text{UT1-UTC}) \tag{5.108}$$

where ϕ and λ are the astronomical latitude and longitude of the station, with longitude again measured toward the east.

Sections 5.4.1–5.4.4 give brief overviews of the individual methods for Earth orientation determination. First, the current high-accuracy methods are described including VLBI, GNSS, laser ranging (both lunar and satellite) and DORIS. Second, historical methods are discussed. Third, some proposed future or alternate techniques are described. Finally, the current international service for Earth rotation is described. (A similar review also exists in Moritz and Mueller (1987), as well as in IERS Annual Reports.)

5.4.1 Very Long Baseline Interferometry

In geodetic Very Long Baseline Interferometry (VLBI), the objects being observed are a set of extragalactic radio sources. These objects, quasars and Active Galactic Nuclei (AGN), are so distant that their space motions are undetectable by current means, so theoretically they form a fixed celestial reference frame. See § 4.2 of this book for further discussion on the International Celestial Reference Frame (ICRF). Currently, more than 3400 radio source positions make up the ICRF.

The VLBI observing networks consist of two or more radio telescopes that simultaneously observe extragalactic radio sources. More than two radio telescopes are required to determine all Earth orientation parameters. Each telescope observes over several frequency bands,

typically separated by a factor of 4 to 10 in frequency, [2] to allow estimation of the ionospheric delay (Ma 2009). The signals are recorded in digital form on large data capacity discs, along with precise time signals provided by hydrogen-maser frequency standards and by incorporating GPS receivers for comparison of the local time scale with a global time scale. Typically, 60 quasars are tracked by eight observing stations several times over the course of a 24-hour observing session. Additionally, two to three stations make daily observations for 1–2 hours ("Intensive" sessions) for UT1 determination. Overlapping networks and network sessions of up to 20 stations connect the 40 global VLBI stations. The data are shipped or electronically transferred to a correlator center. The differences in arrival times of the radio source signals (*delays*), and their change with respect to time (*delay rates*) are determined between each pair of stations. Similar to the laser ranging solutions, these delays, with better than 1 cm precision, and delay rates are then used in a least-squares adjustment in order to estimate a variety of geophysical parameters and the coordinates of the radio sources.

Currently 40 radio telescopes in the world have been outfitted for making high-accuracy geodetic VLBI observations (using Mark IV/V or K5 equipment, see Schlüter and Behrend, 2007). Although many of these radio telescopes are shared between geodetic and astrophysical observations, one third are dedicated primarily to determination of Earth Orientation Parameters (EOP). Current accuracies of the data obtained include polar motion at 50–80 μas, UT1−UTC at 6–7 μs from 24^{h} sessions and at 10–15 μs from 1^{h} sessions, nutation and precession (celestial pole) corrections at 50 μas, radio source coordinates at 0.25 mas, and VLBI station coordinates at a few millimeters (Schlüter and Behrend 2007).

The International VLBI Service (IVS) for Geodesy and Astrometry (Schlüter and Behrend 2007), formerly the International VLBI Service, coordinates the acquisition and reduction of VLBI products. Information is available at the IVS website at URL[24].

5.4.2 Global Navigation Satellite System

There are four primary Global Navigation Satellite System (GNSS) systems in existence. Each of these systems, GPS, GLONASS, and the planned GALILEO and Compass, will be described. The International GNSS Service (IGS), formerly the International GPS (Global Positioning System) Service, operates a global network of more than 350 permanent, continuously operating GPS and GLONASS tracking sites. Routine operations began on January 1, 1994. The following details the current status (as of 2012) of these as well as the GALILEO navigational satellite systems. The IGS tracking network is available at URL[25] for real-time information on IGS stations. Further information about these and other navigational satellite systems can be found in Hofmann-Wellenhof, Lichtenegger, and Wasle (2008).

The Global Positioning System was designed as an all-weather, continuous, and global satellite navigation system. It was designed to be used for navigation, but it can also be used for time transfer and geodetic positioning of points on the ground. It was designed and developed by the U.S. Department of Defense (DoD). Once operated solely by the U.S. Department of

2. Up until 2010, *S* and *X* bands were at 2 and 8 GHz, respectively. After 2010, there is a broadband of frequencies at 2 and 12 GHz.

Defense, GPS is now operated jointly by a committee of civilian and DoD agencies (Joint Program Office).

The "space segment" of the system consists of 24 satellites (and spares) in orbits with a period of 11 hours 58 minutes and an altitude of 20,200 km. There is a requirement of 24 satellites for operational status; however, as many as 29–30 satellites broadcast usable tracking signals. They are equally spaced in six planes, inclined at 55° to the equator. Currently, approximately 30 satellites are operational. Each satellite broadcasts on two *L*-band frequencies, L_1 (1575.42 MHz) and L_2 (1227.60 MHz), with the two frequencies allowing the elimination of first-order ionospheric refraction effects. Modulated onto these frequencies are three codes, including: (1) "the navigation message", containing information (at 50 bits/second) on the position of the satellite and information about the satellite itself (such as diagnostics); (2) a coarse acquisition "C/A" code, a pseudorandom noise (PRN) code at a frequency of 1.022 MHz, which repeats every one millisecond (as of this writing, the limitation on the number of PRN codes restricts the number of broadcasting satellites to 32); and (3) a precise "P" code, another PRN code at a frequency of 10.23 MHz, which repeats every 38 weeks, but is reset in practice every week. Each satellite also carries a cesium or rubidium clock to provide precise time and stable frequency information.

GPS receivers "lock on" to multiple (up to 12) satellite signals, generating C/A- (or for more precision, P-) codes, shifting those codes in time to match those received from the satellites, and decoding the D-code information from the satellites. A *Standard Positioning Service* is available to all users. As one of the options available, this service allows use of the C/A code (prior to May 2, 2000, there was a degraded signal for the Block II satellites—in a process known as *Selective Availability* (SA)), for determining the receiver's position anywhere on Earth to approximately 100–200 meters. Access to the P-code (*Precise Positioning Service*) requires more specialized receivers but makes positional accuracies of 15–20 m possible. Once "locked on" to the satellites, real-time updates are available as often as every 30 seconds.

Differential techniques are a second option which allows near real-time cm-level relative positioning. In these techniques permanent ground stations continuously track GPS satellites and supply their observations over a communications link to mobile users. The observations may then be analyzed to get very high-accuracy positions for the mobile receivers. Since any change in the satellite signals will affect both receivers approximately equally (depending on the distance separating the two satellites), any degradation or coding of the signals will have little effect on the accuracy of the relative station positions. In order to increase the positional accuracy, observations can simply be made for longer periods, and with more satellites.

A third option is to use the L_1 and L_2 carrier wave signals in a differential or inference mode that is analogous to the VLBI technique. In this case, the relative positions of two sites can be established at the few mm-level on baselines of up to a few hundred km in length. Centimeter-level accuracy is available on baselines of much longer length, but uncertainties introduced by the Earth's atmosphere and the satellite positions cause increasing errors with increasing baseline length. As has already been described in Chapter 3, in addition to the positional information, the user's clock can be set relative to the GPS satellite clocks to accuracies as good as ± 0.1 nanoseconds or better, thus providing a time-transfer mechanism of extremely high accuracy.

For the purposes of Earth orientation, at least six satellite-tracking stations are in use at known locations. Carrier-phase measurements are used. It is then possible to determine the position of the satellites, as well as the orientation of the Earth with respect to the *inertial* coordinate system realized by the satellites. Operationally, such tracking is administered by IGS, the *Control Segment*, (Department of Defense tracking stations responsible for operating the satellite), and other government networks or private groups. Since July 17, 1995, when GPS became fully operational (Steigenberger et al. 2006), high-accuracy EOP values have been computed and distributed on a regular basis.

A system similar to GPS, known as the Global Navigation Satellite System (GLONASS) of Russia, will have seven satellites in each of the three orbital planes (and three spares) for a total of 21–24 satellites at full operational status. The satellites are at altitudes of 19100-km in circular orbits with periods of 11 hours 15 minutes located in three orbital planes inclined at 64.8° to the equator. Each GLONASS satellite utilizes a different frequency to broadcast its signal.

The European Space Agency (ESA) GALILEO navigational system launched its first experimental satellite on December 28, 2005. GALILEO is expected to be partially operational by 2013 and will possibly reach full operational status by 2016. The first two satellites of the GALILEO constellation were launched in October 2011. Two more satellites are expected to be launched in 2012. Thirty satellites will have altitudes of 23222-km in orbits with periods of 14 hours 22 minutes located in three orbital planes inclined at 56° to the equator. Like GPS, each GALILEO satellite will broadcast at multiple frequencies, but all satellites will use the same set of frequencies.

The first satellite of the Compass navigation satellite system (CNSS) was launched on April 14, 2007. The Beidou or Compass-M1 system will share characteristics of frequency, signal structure, and services with GPS and GALILEO (Gao et al. 2008). Compass will be comprised of 30 medium Earth orbit (MEO) satellites and 5 geostationary (GEO) satellites.

Currently, GPS provides daily polar motion accuracies of 0.1 mas or better. Additionally, daily length of day accuracies are presently 0.02–0.03 ms/day (Table 5.12). Unlike VLBI, GNSS techniques cannot determine UT1 nor precession-nutation (Gross 2007). However, a UT1-like quantity called UTGPS can be used for extrapolating UT1-UTC past the latest VLBI measurement by GPS orbit modeling (Kammeyer 2000; Tracey, Kammeyer, and Stamatakos 2008). Information regarding GNSS and associated products is available at the IGS website at URL[25].

5.4.3 Laser Ranging

Laser ranging to celestial targets was first proposed for the Moon in the late 1950s and early 1960s (Alley 1983). A laser beam is directed at a retroreflector on the Moon or artificial satellite. Half the round-trip travel time of the light multiplied by the velocity of light gives the distance to the object (subject to various corrections due to relative motion, refraction, etc.). These ranges can then be compared to their predicted values, and in subsequent analyses, corrections to the parameters involved, such as the orbital elements, the station positions, and the orientation of the Earth, may be estimated.

The most significant contribution of laser ranging today is its contribution to the development of the International Terrestrial Reference Frame (ITRF). Laser ranging is the only technique that can determine the origin of ITRF and, along with VLBI, its scale. Since the new millennium, laser ranging is also monitoring the minute offsets of the origin of the ITRF from the "instantaneous" center of mass of Earth; its accuracy is at the millimeter level (Pavlis 2002).

Today the data products of satellite and lunar laser ranging are coordinated by the International Laser Ranging Service (ILRS) which was established in September 1998. For the history and organization of the ILRS, refer to Pearlman, Degnan, and Bosworth (2002). More information can be found at the ILRS website at URL[26].

5.4.3.1 Satellite Laser Ranging

Currently there are several satellites available for laser ranging, but observations of the LAser GEOdynamics Satellites (LAGEOS)-1 and -2 currently provide the highest accuracy geodetic values. The Russian Etalon 1 and 2 satellites help to strengthen the determination of Earth orientation parameters. LAGEOS-1 itself is a composite (aluminum shell and brass core) sphere, 60 cm in diameter, with a mass of $\approx$ 407 kg, with 426 3.8 cm cube corner retroreflectors (CCRs) embedded in its surface. It is in a nearly circular orbit at a height of about 5900 km, and an inclination of 109.8°. Its relatively large mass, small surface area, and high orbit result in low atmospheric drag and insensitivity to short-wavelength components of the Earth's gravity field. More information on LAGEOS and other such geodetic satellites is available in various references listed at URL[27].

There are presently (2012) 36 SLR stations in regular operation, located on eight tectonic plates, regularly obtaining observational data by tracking approximately 30 satellites. The precision of ranges obtained from these instruments are on the order of a few millimeters (see Plag et al. 2009). These stations are operated by various governmental and university research organizations, in order to determine the satellite orbits and obtain various geophysical data relating to Earth orientation, station coordinates, changes in those values over time (thereby giving tectonic-plate motion velocities), and long-wavelength components of the Earth's gravity field. The coordinates of the stations computed by this technique have an origin which is thought to be coincident with the center of mass of the Earth to within a few millimeters. Earth-rotation results are computed at 1–day intervals (since 1993) using data less than a week old, with polar motion accurate to 0.130 milliarcseconds for recent times. As with the GNSS technique (§ 5.4.2), UT1 cannot be independently determined from SLR data. However, SLR does determine, at one-day intervals, the time rate of change of UT1, or Length-Of-Day (LOD), with an accuracy of approximately 40 μs per day (Pavlis 2010). Further information on the computational techniques involved is given in Kaula (1966, pp. 78–81), and GSFC (1976, pp. 7-11 to 7-15).

5.4.3.2 Lunar Laser Ranging

Lunar laser ranging (LLR) is identical in concept with SLR, except that the targets are arrays of cube corner reflectors placed on the Moon by the U.S. Apollo astronauts and USSR unmanned probes. However, the distance to the Moon makes it more difficult to point a laser reliably at the reflectors, and when there are return signals, they are orders of

magnitude weaker than those from the LAGEOS satellites. Currently lunar laser ranging is performed by the Centre d'Etudes et des Recherches Geodynamics et Astronomiques (CERGA) station in Grasse (near Nice), France and the McDonald Observatory, Texas (MLRS2). Additionally, since September 2007 the Apache Point Observatory Lunar Laser ranging Operation (APOLLO) in southern New Mexico delivers lunar laser ranging data, accurate at the 1 mm level, on an operational basis (see Battat et al. 2009).

Much of the same information obtained with SLR can be obtained from LLR. However, in practice, with only a limited number of stations, the primary use of the LLR systems has been for the determination of UT0−UTC (and thereby UT1−UTC), parameters of the Moon's orbit and the Moon's rotation (librations), special- and general-relativity parameter tests, and information on the tidal parameters of the Earth–Moon system. LLR also shows promise in providing quick determinations of UT0−UTC, since its computation is a simple matter as soon as the day's observations are completed at a given station. UT0−UTC is currently determined irregularly with an accuracy of ± 0.3 to ± 0.7 ms (McCarthy and Luzum, 1991). With the improved ranging accuracy at several LLR stations down to 1 cm, there is now renewed interest in LLR applications (Kopeikin et al. 2008). For the history and science of lunar laser ranging, refer to Dickey et al. (1994) and Williams and Dickey (2003).

5.4.4 Doppler Orbitography and Radiopositioning Integrated by Satellite (DORIS)

The Doppler Orbitography and Radiopositioning Integrated by Satellite (DORIS) space geodetic technique was designed and developed by the Centre National d'Etudes Spatiales (CNES) for precise altimeter orbit determinations as well as geodetic ground-station positioning (Crétaux et al. 1998; Soudarin and Crétaux 2006). DORIS is an uplink system from ground stations to spacecraft that transmits at 2036.25 MHz and 401.25 MHz. As a space geodetic technique, DORIS is unique in that it has a balanced station distribution in the northern and southern hemispheres. There are more than 50 permanent beacons broadcasting to receivers onboard seven satellites (SPOT-2, SPOT-4, SPOT-5, Jason-1, Jason-2, ENVISAT, and Cryosat-2). Station positioning by the DORIS technique has a precision of approximately 1–2 cm. Daily polar motion determinations have a precision of approximately 1–2 mas. Like GNSS and laser ranging techniques, DORIS cannot determine UT1.

The International DORIS Service (IDS) was established on July 1, 2003 to coordinate the acquisition and reduction of DORIS observations. The IDS website at URL[28] provides DORIS data products, including Earth orientation parameters, as well as more information about this technique.

5.4.5 Historical Methods

Various methods of lesser accuracy for EOP determination have been used for operational purposes in the 1960s through 1980s, with some still in operational use today for special purposes. These techniques include primarily optical astrometric methods, such as astrolabes and photographic zenith tubes (PZTs), with space techniques such as Doppler satellite tracking and Connected-Element Radio Interferometry (CERI).

5.4.5.1 Optical Astrometric Techniques

An explanation of the motion of the Earth's pole was first made by Chandler in the early 1890s (Chandler 1891a, 1891b), using transit circle observations by Küstner and others dating from the late 1880s. Chandler, and later others, also used various astrometric observations from transit circles, quadrants, and other visual optical instruments dating to the early 1700s. The 1890s saw the establishment of the International Latitude Service (ILS), which operated several stations at approximately 39° N latitude until the 1970s. The use of visual zenith tubes and the invention of photographic zenith tubes (in 1913 by Ross) brought the measurement of polar motion to accuracy levels maintained into the 1960s. The use of precise pendulum clocks in the 1930s allowed the detection of seasonal variations in the length of day. Special Moon cameras were also used from 1952 until the early 1960s in order to measure changes in the length of day against Ephemeris Time (ET) derived from the observed position of the Moon. The same equipment was also used to compare ET with atomic time and to establish the definition of the second (Markowitz et al. 1958; Markowitz 1960). The International Polar Motion Service (IPMS), following on the ILS, coordinated and reduced polar motion observations from a large number of observing sites. The Bureau International de l'Heure (BIH) did the same for UT0−UTC related observations, and also eventually began to handle polar motion data in order to provide rapid service UT1−UTC. The optical techniques continued as the only source of EOP measurements until the mid-1960s, when Doppler satellite tracking began to provide information on polar motion. More than 100 optical instruments all over the world were at one time in use for such measurements. The primary disadvantages (for improved EOP determination) of the optical astrometric techniques are their dependence on the local vertical as their primary reference and the accuracy of the star catalogs they use to define a celestial reference system. However, new solutions of EOP from optical astrometry by Vondrák et al. (1995) and Vondrák, Ron, and Štefva (2007) provide a rich database for long-term Earth orientation study. The geodetic space-based techniques that have replaced the optical astrometric techniques are little affected by variations in the local vertical and provide instead for a crust-fixed, three-dimensional reference system. Information on these instruments and the various international services involved is given in reviews (Moritz and Mueller 1987, pp. 324–337, 424–430, 456–465; Mueller 1969, pp. 80–84; Lambeck 1980, pp. 62–66; Munk and MacDonald, 1960, pp. 58–61; Bomford 1971, pp. 312, 335–338.)

5.4.5.2 Doppler Satellite Tracking

During the 1960s, Doppler tracking of the U.S. Navy Navigational Satellite System (NNSS) began to provide polar motion information on the same level of accuracy or better than the optical techniques. The polar motion data obtained via this system were used by the BIH in combination with the optically obtained values. However, this technique did suffer from the dependence of the EOP values on the particular satellites in use and from long-term drifts, and as SLR became available for polar motion monitoring in the late 1970s, began to be phased out for active EOP use. In fact, GNSS (see § 5.4.2) is the successor of these Doppler systems. An excellent review of the NNSS Doppler satellite-tracking technique is given by Kouba (1983), and a review of EOP-related use of such tracking is given by Moritz and Mueller (1987, pp. 338–344, 467–470).

5.4.5.3 Connected-Element Radio Interferometry

Connected-Element Radio Interferometry (CERI) was used to determine EOP in the late 1970s and 1980s. CERI operates in the same fashion as VLBI (and, in fact, provided the initial tests of the VLBI principle), except that the radio telescopes are physically connected by a wideband communications link, so that the observations (delays and delay rates—see § 5.4.1) are made in real time. A least-squares solution to obtain EOP, station positions, and source positions can then be made as soon as observing ends for the day. Although the speed at which results could be made available was a strong point of CERI, the small size of the arrays usually only allowed two EOP components to be determined simultaneously, such as $\Delta\phi$ and UT0−UTC. The U.S. Naval Observatory (USNO) operated such an interferometer at Green Bank, West Virginia, from October 1978 until the end of 1987. Polar motion and UT0−UTC could be determined to an accuracy of about 50 mas and 4.6 ms respectively (McCarthy et al. 1985; Matsakis et al. 1986). Another CERI operated for a short time (August-September, 1980) at Cambridge, UK (Klepczynski 1982). The eventual improvement in the turnaround time and much higher accuracy of VLBI results replaced CERI for EOP determination.

5.4.6 Alternative Techniques

Several observational methods are under development that show promise in the field of Earth orientation measurement. The use of laser-ring gyroscopes or superfluid helium interference gyroscopes may allow changes in the Earth's rotational velocity and $\Delta\phi$ to be monitored. These are of particular interest since they have no dependence on astronomical observations and may also be used as a check on current techniques. Following are more detailed accounts of these two possible alternative observational systems.

5.4.6.1 Laser-Ring Gyroscopes

A laser light beam split and sent in opposite directions around a given path on the Earth's surface can be made to interfere with itself upon meeting again, producing a beat pattern. Changes in this interference pattern will occur because of changes in the Doppler shift of the light traversing the two different paths, due to variations in the Earth's rotation. Such a device is known as a *laser-ring* or *Sagnac laser* gyroscope (Soffel et al. 1988; Stedman 1997). Theoretically, ring laser gyroscopes measure the absolute rotation of the Earth since only one measurement is required to gauge the Earth's instantaneous rotation.

The sensitivity of the ring laser depends on the area enclosed. Ring lasers with an enclosed area between 1 and 833 m^2 have been built. Sensor sensitivities range from 5×10^{-10} to 5×10^{-12} rad/s/$\sqrt{\text{Hz}}$. Currently, the most stable ring lasers experience a significant drift of 2×10^{-6} degrees per hour. Because of this stability, these sensors can detect the effect of daily and subdaily polar motion and tilt effects from solid Earth tides (Schreiber et al. 2004). Currently, ring lasers have a resolution of a magnitude worse than techniques such as VLBI and GPS; it is anticipated that within the next decade there will be both an improvement in resolution and stability of the sensor (Schreiber et al. 2004; Plag et al. 2009).

5.4.6.2 Superfluid Helium Interference Gyroscopes

The use of superfluid helium interference gyroscopes (SHIG) was proposed in 1988 for the determination of Earth rotation and polar motion (Packard 1988). It involves the use of a small

(less than 1-meter diameter) horizontal torus of superfluid helium (^{3}He or ^{4}He), in which a blockage with a pinhole is positioned. When this torus undergoes rotation (for example, because of the rotation of the Earth), it is possible to measure the phase difference or phase slips across the blockage (Schwab, Bruckner, and Packard 1997). This is proportional to the rotational velocity of the torus and, therefore, the Earth, and could be measured to 1 part in 10^9 over a few seconds. Proof of concept experiments were conducted by Schwab, Bruckner, and Packard (1997) and Simmonds et al. (2001), which clearly demonstrated that quantum interference in superfluid helium can detect small changes in the Earth's rotation. More recently, Bruckner and Packard (2003) and Sato, Joshi, and Packard (2008) demonstrated quantum mechanical phase coherence of superfluid ^{4}He over a macroscopic length scale with long-term stability. It is feasible that superfluid helium interference gyroscopes will soon be a viable alternative for the determination of Earth orientation parameters independent of astronomical observations.

5.4.7 International Services

On 1988 January 1, the International Earth Rotation Service (IERS) (URL[29]) began operation, under the auspices of the IAU and the IUGG. It replaced the Bureau International de l'Heure (BIH) and the International Polar Motion Service (IPMS) as the organization responsible for determining and predicting the orientation of the Earth. The organization changed its name on 2003 January 1 to the International Earth Rotation and Reference Systems Service, but maintained the IERS acronym. The IERS changed its structure on 2001 January 1. The following is a description of this new structure. The IERS consists of a board of directors that oversees and controls a "Central Bureau", the manager of the IERS and executive arm of the "Directing Board", and "Technique Centers" for each observational technique. An "Analysis Coordinator" ensures long-term and internal consistency of IERS products and appropriate combination of technique centers' products into one set of official IERS products. "Product Centers" are responsible for the products of the IERS. "Special Bureaus" for the geophysical components are under the Global Geophysical Fluids Center. "Combination Centers" collectively combine inputs from different techniques and develop new methods of data combination. The "Directing Board" may establish "Working Groups" to investigate topics relevant to IERS components.

The IERS publishes two different primary bulletins for the dissemination of Earth orientation data as determined from the combination of data from different observational techniques. The *IERS Bulletin A* provides information weekly on the rapid determination of the Earth's rotation, as well as predictions for future rotation. The *IERS Bulletin B* provides "final" smoothed data monthly on the rotation of the Earth. Of course, other organizations both within and outside the IERS also provide other EOP series, usually based on observational data of a given type.

The IERS is also responsible for deciding when a step in UTC is necessary in order to keep it within 0.9 s of UT1. These steps, commonly known as *leap seconds*, may be positive or negative, are of 1 second duration, are announced approximately six months ahead of time, and, according to the CCIR Recommendation (CCIR 1986), first preference is given to insertion at the end of December or June, and second preference is given at the end of March

or September. Since their introduction in 1972, leap seconds have always been positive and only dates in June and December have been used. They have been required from every six months to seven years. A table of these steps is given in *The Astronomical Almanac*, p. K9, as differences of UTC from TAI.

5.4.7.1 *IERS Bulletin A* and Other Products of IERS Rapid Service/Prediction Center

The *IERS Bulletin A* is published by the IERS Rapid Service/Prediction Center (RS/PC), at the U.S. Naval Observatory. The RS/PC acts as a "Product Center" of the IERS. The *IERS Bulletin A* is issued by 0 hours UT, Friday, of each week, and contains Earth orientation parameters determined from the combination of other recently determined EOP series, predictions of Earth orientation parameters daily up to one year in the future, and equations for predictions even further into the future. Values of TAI−UTC, DUT1, announcements of leap seconds, etc., are given. For the combined EOP series, data given include for each day: the calendar date and modified Julian date (MJD); the values of x_p, y_p, and their expected accuracies in arcseconds; and the values of UT1−UTC and their expected accuracies in seconds of time. Typically one week's worth of data are published. When available, new values from the *IERS Bulletin B* are also published. Predictions are given for each day for 365 days past the end of the combined data, consisting of the calendar date and MJD, values of x_p and y_p in arcseconds, UT1−UTC in seconds, and a table giving estimated accuracies of these values. Equations are also provided in order to extend these predictions even further. Predicted celestial pole offsets (corrections to $\Delta\psi$ and $\Delta\epsilon$) are also given. *Bulletin A* also contains celestial pole offsets with respect to the IAU 2000 resolutions (dX and dY) beginning on 1 January 2003. Units are in arcseconds.

Daily solutions of EOP are also produced at approximately 17:15 UTC each day. Each daily solution includes observed EOP values with 90 days of predictions. These solutions give near real-time EOP determination. Since September 2011, a sub-daily RS/PC EOP solution is available at http://maia.usno.navy.mil/2xdaily.

The combined series that are published weekly in the *IERS Bulletin A* is formed at the U.S. Naval Observatory by the Earth Orientation Department. The input data series used are provided by: VLBI 24–hour and 1–hour Intensives from Goddard Space Flight Center (GSFC), Institute of Applied Astronomy (IAA), and USNO; combination VLBI from the IVS; SLR data from the ILRS Series A, IAA, and Russian Mission Control Center (MCC); GPS data from the IGS (final, rapid, and ultra combined solutions); GPS "UT" solutions from USNO; and Atmospheric Angular Momentum (AAM, for UT1 prediction only) data from the National Centers for Environmental Prediction (NCEP) and the U.S. Navy Operational Global Atmospheric Prediction System (NOGAPS). Each series has systematic errors removed from each of its available components (x_p, y_p, $\delta\psi$, $\delta\epsilon$, and UT1−UTC). A weighted cubic spline curve fitted through the data is used to determine the one-day values for each component. Accuracy estimates for each input series are estimated periodically via intercomparisons of the series. The long-term biases and trends are adjusted to those of the IERS C04 series. Since 2007, the predictions for x_p and y_p are done from a least-squares, autoregressive (LS+AR) method which solves for periods fit to the last 400 days of observed x and y values. The predictions for UT1−UTC are computed using a simple differencing technique based on the last n days of data with known effects removed. A bias between the model for celestial pole

offset prediction and the last twenty days of observations is computed. This bias is tapered so that as the prediction length is extended, the bias becomes increasingly smaller. A complete description of the combination and prediction technique is given in Luzum et al. (2001), Johnson, Luzum, and Ray (2005), and Stamatakos et al. (2009).

All of the *IERS Bulletin A* information is also available on-line; for further information visit URL[30]. To be placed on the mailing list for the *IERS Bulletin A*, use the document request form at URL[31].

5.4.7.2 *IERS Bulletin B* and Other Products of IERS Earth Orientation Center

The *IERS Bulletin B* is published by the IERS Earth Orientation Center (EOC) at the Paris Observatory. The EOC acts as a "Product Center" of the IERS. The *IERS Bulletin B* is issued during the first week of each month and contains current, fixed ("final") EOP C04 values from a combination solution of a month's EOP series data, along with information on the length of day (LOD) and EOP series data used in the combined solution. The daily final values include the calendar date and MJD, smoothed values of x_p and y_p in milliarcseconds, UT1−UTC in milliseconds, and dX and dY in milliarcseconds. Daily values of celestial pole offsets $\delta\Delta\psi$ and $\delta\Delta\epsilon$ are given relatively to IAU1980 or, in the new format, IAU2000 in milliarcseconds. Smoothed values of LOD in milliseconds per day and the rotational velocity of the Earth ("Omega") in microradians/second are also given. Uncertainties of these parameters are also provided.

The input series are similar to those listed for the *IERS Bulletin A*, with, in addition, series obtained from DORIS observations also being used. The values are then smoothed using a class of robust M-Huber estimators (Bougeard, Gambis and Ray 2000). The values of UT1−UTC are also corrected for variations due to zonal Earth tides with periods up to 35 days, giving UT1R−UTC. These results are published with a sliding delay of thirty days between the publication date and the last date of the solution.

In addition to publishing the *IERS Bulletin B*, the EOC is responsible for providing long-term EOP (IERS C01) consistency, publications for time dissemination and leap second announcements. All of this information is also available on-line at URL[32]. To be placed on the mailing list for the *IERS Bulletin B*, use the document request form at URL[31].

5.4.7.3 Other Publications of the IERS

Other publications of the IERS include:

- *Special Bulletin C*—Issued irregularly to announce upcoming steps (leap seconds) in UTC.
- *Special Bulletin D*—Issued irregularly to announce upcoming changes to the value of DUT1 to be transmitted with time signals.
- *Annual Report of the IERS*—Issued annually from 1989 June on, reporting on various solutions for Earth orientation parameters and terrestrial and celestial reference systems.
- *Technical Notes of the IERS*—Issued irregularly as reports and complementary information of relevance to the work of the IERS on Earth rotation and related reference systems.

For further information, contact the Central Bureau of the IERS at the address given in § 5.4.7.2.

Acknowledgements

We gratefully acknowledge the help of Daniel Mullaney and Craig Rollins, National Geospatial-Intelligence Agency, Geoint Sciences Office.

REFERENCES

1. SIRGAS, Sistema de Referencia Geocentrico para Las Américas:
   http://www.sirgas.org.
2. EUREF, the IAG Reference Frame Sub-Commission for Europe:
   http://www.euref-iag.net/.
3. ITRF, International Terrestrial Reference Frame:
   http://itrf.ign.fr/ITRF_solutions/2008/ITRF2008.php.
4. NGA Earth Gravitational Model:
   http://earth-info.nga.mil/GandG/wgs84/gravitymod/.
5. NGA World Magnetic Model 2010:
   http://earth-info.nga.mil/GandG/wgs84/wmagmod/wmm2010.html.
6. NOAA National Geophysical Data Center, Geomagnetic Models & Software:
   http://www.ngdc.noaa.gov/geomag/WMM/DoDWMM.shtml.
7. NGS U.S. National Grid Conversion:
   http://www.ngs.noaa.gov/TOOLS/usng.shtml.
8. NGS Geodetic Tool Kit Program Descriptions:
   http://www.ngs.noaa.gov/TOOLS/program_descriptions.html.
9. NGA Software for Converting Georgraphic Coordinates between Systems:
   http://earth-info.nga.mil/GandG/geotrans/index.html.
10. JPL's Automatic Precise Positioning Service of the Global GPS Differential System:
    http://apps.gdgps.net.
11. GGM Series Gravitational Model:
    http://www.csr.utexas.edu/grace/gravity/.
12. EIGEN Series Gravitational Model:
    http://www.gfz-potsdam.de/portal/. Follow Structure > Departments > Department 1 > Global Geomonitoring . . . > Projects > GRACE > Gravity Field Results.
13. The CHAMP Mission:
    http://op.gfz-potsdam.de/champ/.
14. The Grace Mission:
    http://www.csr.utexas.edu/grace/.
15. The EGM2008 Gravity Model:
    http://earth-info.nga.mil/GandG/wgs84/gravitymod/egm2008/index.html.
16. ITG-Grace03 Gravity Field Model:
    http://www.igg.uni-bonn.de/apmg/fileadmin/itg-grace03.html.
17. DEHANTTIDEINEL Software:
    ftp://maia.usno.navy.mil/conv2010/convupdt/chapter7/dehanttideinel/DEHANTTIDEINEL.F.

18. FES2004 atlas:
http://www.aviso.oceanobs.com/index.php?id=1279.
19. ARG2.F Software:
ftp://maia.usno.navy.mil/conv2010/convupdt/chapter7/ARG2.F.
20. Ocean Tide Loading Service:
http://froste.oso.chalmers.se/loading/.
21. Ocean Pole Load Tide Coefficients Map:
ftp://tai.bipm.org/iers/convupdt/chapter7/opoleloadcoefcmcor.txt.gz.
22. Special Bureau on Loading:
http://www.sbl.statkart.no.
23. IERS Conventions Regression Coefficients:
ftp://tai.bipm.org/iers/conv2010/convupdt/chapter7/atmospheric.regr.
24. International VLBI Service for Geodesy and Astrometry (IVS):
http://ivscc.gsfc.nasa.gov/.
25. International GNSS Service (IGS):
http://igscb.jpl.nasa.gov/.
26. International Laser Ranging Service (ILRS):
http://ilrs.gsfc.nasa.gov/.
27. International Laser Ranging Service (ILRS) Satellites:
http://ilrs.gsfc.nasa.gov/satellite_missions/list_of_satellites/lag1_general.html.
28. International DORIS Service (IDS):
http://ids-doris.org/.
29. International Earth rotation and Reference systems Service (IERS):
http://www.iers.org/.
30. IERS Bulletin A:
ftp://maia.usno.navy.mil/ser7/ser7.dat.
31. IERS Bulletin A Document Request Form:
http://maia.usno.navy.mil/docrequest.html.
32. IERS Bulletin B:
http://hpiers.obspm.fr/eop-pc/.

Agnew, D. C. (1996). SPOTL: Some Programs for Ocean-Tide Loading. Reference Series 96-8, Scripps Institution of Oceanography, La Jolla, CA.

Agnew, D. C. (1997). NLOADF: A program for computing ocean-tide loading. *Journal of Geophysical Research 102*(B3), 5109–5110.

Alley, C. (1983). Laser Ranging to Retro-Reflectors on the Moon as a Test of Theories of Gravity. In *Quantum Optics, Experimental Gravity, and Measurement Theory*. New York, NY: Plenum.

Altamimi, Z., X. Collilieux, and L. Métivier (2011). ITRF2008: an improved solution of the international terrestrial reference frame. *Journal of Geodesy 85*(8), 458–473.

Andersen, O. B. (2006). See http://www.spacecenter.dk/data/global-ocean-tide-model-1/.

Argus, D. F. and R. G. Gordon (1991). No-net-rotation model of current plate velocities incorporating plate motion model Nuvel-1. *Geophysical Research Letters 18*(11), 2039–2042.

Battat, J. B. R., T. W. Murphy Jr., E. G. Adelberger, B. Gillespie, C. D. Hoyle, R. J. McMillan, E. L. Michelsen, K. Nordtvedt, A. E. Orin, C. W. Stubbs, and H. E. Swanson (2009). The Apache Point Observatory Lunar Laser Operation (APOLLO): Two Years of Millimeter-Precision Measurements of the Earth–Moon Range. *Astronomical Society of the Pacific 121*, 29–40.

BIH (1989). BIH Annual Report for 1988. Technical report, BIH, Paris Observatory, Paris.

Bisnath, S. B. and Y. Gao (2009). Innovation: Precise Point Positioning. *GPS World 20*(4), 43–50.

Blewitt, G., D. Lavallée, P. Clarke, and K. Nurutdinov (2001). A new global mode of the Earth deformation: Seasonal cycle detected. *Science 294*, 2342–2345.

Bomford, G. (1971). *Geodesy* (3 ed.). London: Oxford University Press.

Borkowski, K. M. (1989). Accurate Algorithms to Transform Geocentric to Geodetic Coordinates. *Bulletin Géodésique 63*(1), 50–56.

Boucher, C. and Z. Altamimi (1996). International Terrestrial Reference Frame. *GPS World 7*(9), 71–74.

Bougeard, M. L., D. Gambis, and R. Ray (2000). Algorithms for box constrained M-estimation: fitting large data sets with applications to Earth Orientation Parameters series. *Physics and Chemistry of the Earth 25*(9-11), 2342–2345.

Bowring, B. R. (1976). Transformations from Spatial to Geographical Coordinates. *Survey Review 23*(181), 323–327.

Brosche, P., U. Seiler, J. Suendermann, and J. Wuensch (1989). Periodic Changes in Earth's Rotation due to Oceanic Tides. *Astronomy and Astrophysics 220*, 318–320.

Bruckner, N. and R. Packard (2003). Large area multiturn superfluid slip gyroscopes. *Journal of Applied Physics 93*(3), 1798–1805.

Burkholder, E. F. (2008). *The 3-D Global Spatial Data Model: Foundation of the Spatial Data Infrastructure*. Boca Raton, Florida: CRC Press.

Carter, M. S. and W. Carter (2000). Seth Carlo Chandler Jr.: The Discovery of Variation of Latitude. In S. Dick, D. McCarthy, and B. Luzum (Eds.), *Polar Motion: Historical and Scientific Problems, ASP Conf Series Vol. 208*, San Francisco. Astronomical Society of the Pacific.

Cartwright, D. E. and A. C. Edden (1973). Corrected Tables of Tidal Harmonics. *Geophysical Journal of Royal Astronomical Society 33*, 253–264.

Cartwright, D. E. and R. D. Ray (1991). Energetics of global ocean tides from Geosat altimetry. *Journal of Geophysical Research 96*(C9), 16897–16912.

Cartwright, D. E. and R. J. Tayler (1971). New Computations of the Tide-Generating Potential. *Geophysical Journal of Royal Astronomical Society 23*, 45–74.

CCIR (1986). In *Recommendation and Reports of the CCIR*, Volume 7, Geneva, pp. 12. International Telecommunications Union. 16th Plenary Assembly, Dubrovnik.

Chandler, S. C. (1891a). On the Variation of Latitude. *The Astronomical Journal 11*, 83.

Chandler, S. C. (1891b). On the Variation of Latitude. *The Astronomical Journal 12*, 17.

Chapman, S. and R. Lindzen (1970). *Atmospheric Tides*. Dordrecht, Holland: D. Reidel.

Cheng, M. K., J. C. Ries, and B. D. Tapley (2011). Variations of the Earth's figure axis from satellite laser ranging and GRACE. *Journal of Geophysical Research 116, B1*, 1409.

Cheng, M. K., C. K. Shum, and B. D. Tapley (1997). Determination of long-term changes in the Earth's gravity field from satellite laser ranging observations. *Journal of Geophysical Research 102, B10*, 22377–22390.

Crétaux, J. F., L. Soudarin, A. Cazenave, and F. Bouille (1998). Present-day tectonic plate motions and crustal deformations from the DORIS system. *Journal of Geophysical Research 103, B12*, 30167–30181.

Defraigne, P. and I. Smits (1999). Length of day variations due to zonal tides for an elastic earth in non-hydrostatic equilibrium. *Geophysical Journal International 139*, 563–572.

DeMets, C., R. G. Gordon, D. F. Argus, and S. Stein (1990). Current Plate Motions. *Geophysical Journal International 101*, 425–478.

DeMets, C., R. G. Gordon, D. F. Argus, and S. Stein (1994). Effect of recent revisions to the geomagnetic reversal time scale on estimates of current plate motions. *Geophysical Research Letters 21*(20), 2191–2194.

Desai, S. D. (2002). Observing the pole tide with satellite altimetry. *Journal of Geophysical Research 107, C11*, 3186.

Dickey, J. O., P. L. Bender, J. E. Faller, X. X. Newhall, R. L. Ricklefs, J. G. Ries, P. J. Shelus, C. Veillet, A. L. Whipple, J. R. Wiant, J. G. Williams, and C. F. Yoder (1994). Lunar Laser Ranging: a continuing legacy of the Apollo program. *Science 265*, 482–490.

Dickman, S. R. and R. S. Gross (2010). Rotational evaluation of a long-period spherical harmonic ocean tide mode. *Journal of Geodesy 84*(4), 457–464.

Dickman, S. R. and Y. S. Nam (1995). Revised predictions of long-period ocean tidal effects on Earth's rotation rate. *Journal of Geophysical Research 100, B5*, 8233–8243.

Dixon, K. (2006). Starfire®: A Global SBAS for Sub-Decimeter Precise Point Positioning. In *Proceedings of the 19th International Technical Meeting of the Satellite Division of The Institute of Navigation (ION GNSS 2006), Ft. Worth, TX, Sept. 2006*, pp. 2286–2296.

DMA (1987). Supplement to Department of Defense World Geodetic System 1984 Technical Report. Technical Report 8350.2–A, Defense Mapping Agency, Washington, DC.

DMA (1989). The Universal Grids: Universal Transverse Mercator (UTM) and Universal Polar Stereographic (UPS). Technical Manual 8358.2, Defense Mapping Agency, Washington, DC. (http://earth-info.nga.mil/GandG/publications/tm8358.2/TM8358_2.pdf).

DMA (1990). Datums, Ellipsoids, Grids, and Grid Reference Systems. Technical Manual 8358.1, Defense Mapping Agency, Washington, DC.

Dong, D., P. Fang, Y. Bock, M. K. Cheng, and S. Miyazaki (2002). Anatomy of apparent seasonal variations from GPS-derived site position time series. *Journal of Geophysical Research 107, B4*, ETG 9–1 – ETG 9–8.

Doodson, A. T. (1921). The Harmonic Development of the Tide-Generating Potential. *Royal Society of London Proceedings Series A 100*, 305–329.

Dziewonski, A. and D. L. Anderson (1981). Preliminary reference earth model. *Physics of the Earth and Planetary Interiors 25*, 297–356.

Eanes, R. J. (1994). Diurnal and semidiurnal tides from TOPEX/POSEIDON altimetry. In *EOS Trans AGU*, Volume 75, pp. 108.

Eanes, R. J. and S. Bettadpur (1995). The CSR 3.0 global ocean tide model. Technical Memorandum CSR-TM-95-06, University of Texas, Austin, TX.

Eanes, R. J., B. Schutz, and B. Tapley (1983). Earth and Ocean Tide Effects on LAGEOS and Starlette. In *Proceedings of the Ninth International Symposium on Earth Tides*, Stuttgart. E. Schweizerbartsche Verlag Buchhandlung.

Egbert, G. D., A. F. Bennett, and M. G. G. Foreman (1994). TOPEX/POSEIDON tides estimated using a global inverse model. *Journal of Geophysical Research 99, C4*, 24821–24852.

Egbert, G. D. and S. Y. Erofeeva (2002). Efficient inverse modeling of barotropic ocean tides. *Journal of Atmospheric and Oceanic Technology 19*(2), 183–204.

Farrell, W. E. (1972). Deformation of the Earth by Surface Loads. *Reviews of Geophysics and Space Physics 10*, 761–797.

Feltens, J. (2008). Vector methods to compute azimuth, elevation, ellipsoidal normal, and the Cartesian (X, Y, Z) to geodetic (ϕ, λ, h) transformation. *Journal of Geodesy 82*(8), 493–504.

Feltens, J. (2009). Vector methods to compute azimuth the Cartesian (X, Y, Z) to geodetic (ϕ, λ, h) transformation on a triaxial ellipsoid. *Journal of Geodesy 83*(2), 129–137.

FGDC (2001). United States National Grid (USNG). Standard FGDC-STD-011-2001, Federal Geographic Data Committee, Reston, Va.

Flechtner, F. (2007). AOD1B Product Description Document. GRACE project document 327-750, Rev. 3.1.

Fukishima, T. (1999). Fast Transform from Geocentric to Geodetic Coordinates. *Journal of Geodesy 73*(11), 603–610.

Fukishima, T. (2006). Transformation from Cartesian to geodetic Coordinates Accelerated by Halley's Method. *Journal of Geodesy 79*(12), 689–693.

Gao, G. X., A. Chen, S. Lo, D. De Lorenzo, T. Walter, and P. Enge (2008). Compass M-1 Broadcast Codes and Their Application to Acquisition and Tracking. In *Proceedings of the ION National Technical Meeting 2008, San Diego, California*, pp. 133–141.

Gross, R. S. (1993). A combination of Earth orientation data: Space92. Technical memo., Jet Propulsion Laboratory, Pasadena, CA.

Gross, R. S. (2007). Earth Rotation Variations–Long Period. In T. A. Herring (Ed.), *Physical Geodesy, Treatise on Geophysics*, Volume 11, Amsterdam. Elsevier.

Gross, R. S. (2008). An improved empirical model for the effect of long-period ocean tides on polar motion. *Journal of Geodesy 83*, 635–644.

Gross, R. S. (2009). Ocean tidal effects on Earth rotation. *Journal of Geodynamics 48*(3-5), 219–225.

GSFC (1976). Mathematical Theory of the Goddard Trajectory Determination System. Technical Report X–582–76–77, Goddard Space Flight Center, Greenbelt, MD.

Heiskanen, W. and H. Moritz (1967). *Physical Geodesy*. San Francisco, CA: W. H. Freeman.

Hirt, C. (2001). Automatic Determination of Vertical Deflections in Real-Time by Combining GPS and Digital Zenith Camera for Solving the GPS-Height-Problem. In *Proceedings of the 14th International Technical Meeting of the Satellite Division of The Institute of Navigation (ION GPS 2001), Salt Lake City, UT, Sept. 2001*, pp. 2540–2551.

Hofmann-Wellenhof, B., H. Lichtenegger, and J. Collins (2001). *Global Positioning System: Theory and Practice* (6th ed.). Vienna & New York: Springer-Verlag.

Hofmann-Wellenhof, B., H. Lichtenegger, and E. Wasle (2008). *GNSS Global Navigation Satellite Systems: GPS, GLONASS, Galileo, and more*. Vienna: Springer-Verlag.

Hoyer, M., S. Arciniegas, K. Pereira, H. Fagard, R. Maturana, R. Torchetti, H. Drewes, M. Kumar, and G. Seeber (1998). The Definition and Realization of the Reference System in the SIRGAS Project. In F. K. Brunner (Ed.), *IAG Symposia 198: Advances in Positioning and Reference Frames*, Berlin-Heidelberg, pp. 167–173. Springer–Verlag.

IAU (1983). In R. M. West (Ed.), *Transactions of the International Astronomical Union*, Volume XVIII B, Dordrecht. Reidel. Proc. 18th General Assembly, Patras, 1982.

IERS (1989). Explanatory Supplement to the IERS Bulletins A and B. Technical report, U.S. Naval Observatory, Washington, DC.

IERS (1996). Conventions (1996). Technical Note 21, International Earth Rotation Service, Paris.

IERS (2004). Conventions (2003). Technical Note 32, International Earth Rotation Service, Frankfurt am Main. Verlag des Bundesamts für Kartographie und Geodäsie, D. D. McCarthy and G. Petit (Eds.).

IERS (2009). Explanatory Supplement to the IERS Bulletins A and B. Technical report, International Earth Rotation Service, Observatoire de Paris and US Naval Observatory, Paris and Washington.

IERS (2010). Conventions (2010). Technical Note 36, International Earth Rotation and Reference Systems Service, Frankfurt am Main. Verlag des Bundesamts für Kartographie und Geodäsie, G. Petit and B. Luzum (Eds.).

Iliffe, J. and R. Lott (2008). *Datums and Map Projections for Remote Sensing* (2nd ed.). Boca Raton, Florida, London, New York, Washington: CRC Press, Whittles Publishing.

ISO (2009). Information Technology—Spatial Reference Model (SRM), 2nd Edition. Standard ISO/IEC 18026:2009(E), International Organization for Standardization.

Johnson, T. J., B. J. Luzum, and J. R. Ray (2005). Improved near-term Earth rotation predictions using atmospheric angular momentum analysis and forecasts. *Journal of Geodynamics 39*, 209–221.

Kammeyer, P. (2000). A UT1-Like Quantity from Analysis of GPS Orbit Planes. *Celestial Mechanics and Dynamical Astronomy 77*, 241–272.

Kantha, L. H., J. S. Stewart, and S. D. Desai (1998). Long-period lunar fortnightly and monthly ocean tides. *Journal of Geophysical Research 103, C6*, 12639–12647.

Kaula, W. M. (1966). *Theory of Satellite Geodesy*. Waltham, MA: Blaisdell.

Klepczynski, W. J. (1982). Coordinator's Report: Connected–Elements Radio Interferometry. In G. A. Wilkins and M. Feissel (Eds.), *Project MERIT: Report on the Short Campaign*, Herstmonceux, UK. Royal Greenwich Observatory.

Kopeikin, S. M., E. Pavlis, D. Pavlis, V. A. Brumberg, A. Escapa, J. Getino, A. Gusev, J. Mueller, W. T. Ni, and N. Petrova (2008). Prospects in the orbital and rotational dynamics of the Moon with the advent of sub-centimeter lunar laser ranging. *Advances in Space Research 42*, 1378–1390.

Kouba, J. (1983). A Review of Geodetic and Geodynamic Satellite Doppler Positioning. *Reviews of Geophysics and Space Physics 21*, 27–40.

Kovalevsky, J. and I. Mueller (1981). Comments on Conventional Terrestrial and Quasi-Inertial Reference Systems. In E. Gaposchkin and B. Kolaczek (Eds.), *Reference Coordinate Systems for Earth Dynamics*, Dordrecht, Holland, pp. 375–384. Reidel.

Kovalevsky, J., I. Mueller, and B. Kolaczek (1989). *Reference Frames in Astronomy and Geophysics*. Dordrecht, Holland: Kluwer.

Kumar, M. (1972). Coordinate Transformation by Minimizing Correlations between Parameters. Report 184, Dept. of Geodetic Science, Ohio State University, Columbus, OH.

Lambeck, K. (1980). *The Earth's Variable Rotation*. Cambridge: Cambridge University Press.

Le Provost, C., M. L. Genco, F. Lyard, P. Incent, and P. Canceil (1994). Spectroscopy of the world ocean tides from a finite element hydrological model. *Journal of Geophysical Research 99, C12*, 24777–24798.

Le Provost, C., F. Lyard, J. M. Molines, M. L. Genco, and F. Rabilloud (1998). A hydrodynamic ocean tide model improved by assimilating a satellite altimeter-derived data set. *Journal of Geophysical Research 103, C3*, 5513–5529.

Leandro, R. F., M. C. Santos, and R. B. Langley (2007). GAPS: The GPS Analysis and Positioning Software—A Brief Overview. In *Proceedings of the 20th International Technical Meeting of the Satellite Division of The Institute of Navigation (ION GNSS 2007), Ft. Worth, TX, Sept. 2007*, pp. 1807–1811.

Lefèvre, F., F. Lyard, C. Le Provost, and E. J. O. Schrama (2002). FES99: A Global Tide Finite Element Solution assimilating Tide Gauge and Altimetric Information. *Journal of Atmospheric and Oceanic Technology 19*, 1345–1356.

Lefèvre, F., F. H. Lyard, and C. Le Provost (2000). FES98: A new global tide finite element solution independent of altimetry. *Geophysical Research Letters 27*(17), 2717–2720.

Letellier, T. (2004). *Etude des ondes de marée sur les plateaux continentaux*. Ph. D. thesis, Université de Toulouse III.

Lin, K.-C. and J. Wang (1995). Transformation from Geocentric to Geodetic Coordinates using Newton's Iteration. *Bulletin Geodesique 69*(4), 300–303.

Luzum, B. J., J. R. Ray, M. S. Carter, and F. J. Josties (2001). Recent improvements to IERS Bulletin A combination and prediction. *GPS Solutions 4*(3), 34–40.

Lyard, F., F. Lefèvre, and T. Letellier (2006). Modelling the global ocean tides: modern insights from FES2004. *Ocean Dynamics 56*, 394–415.

Ma, C. (2009). Present and Future Radio Reference Frames. In M. Soffel and N. Capitaine (Eds.), *Proceedings of the "Journées 2008 Systèmes de référence spatio-temporels*, Dresden and Paris, pp. 195–197. Lohrmann-Observatorium and Observatoire de Paris.

Malys, S. and J. A. Slater (1994). Maintenance and Enhancement of the World Geodetic System 1984. In *Proc. of the 7th International Technical Meeting of the Satellite Div., ION GPS-94, Salt Lake City, Utah, Sept 1994*, pp. 17–24.

Manabe, S. T., T. Sato, S. Sakai, and K. Yokoyama (1991). Atmospheric Loading Effects on VLBI Observations. Technical Report NOS 137 NGS 49, NOAA. in Proc. of the AGU Chapman Conference on Geodetic VLBI: Monitoring Global Change.

Mangiarotti, S., A. Cazenave, L. Soudarin, and J. F. Crétaux (2001). Annual vertical crustal motions predicted from surface mass redistribution and observed by space geodesy. *Journal of Geophysical Research 106, B3*, 4277–4291.

Markowitz, W. (1960). The Photographic Zenith Tube and the Dual Rate Moon Camera. In G. P. Kuiper and B. M. Middlehurst (Eds.), *Stars and Stellar Systems*, Chicago. University of Chicago Press.

Markowitz, W., R. G. Hall, L. Essen, and J. V. L. Parry (1958). Frequency of Cesium in Terms of Ephemeris Time. *Physical Review Letters I*(3).

Mathews, P. M., V. Dehant, and J. M. Gipson (1997). Tidal station displacements. *Journal of Geophysical Research 102, B9*, 20469–20477.

Matsakis, D. N., F. J. Josties, P. E. Angerhofer, D. R. Florkowski, D. D. McCarthy, X. Jiayan, and P. Yunlou (1986). The Green Bank Interferometer as a Tool for the Measurement of Earth Orientation Parameters. *The Astronomical Journal 91*(6), 1463–1473.

Matsumoto, K., T. Takanezawa, and M. Ooe (2000). Ocean Tide Models Developed by Assimilating TOPEX/POSEIDON Altimeter Data into Hydrodynamical Model: A Global Model and a Regional Model Around Japan. *Journal of Oceanography 56*, 567–581.

Maus, S. (2010). An Ellipsoidal Harmonic Representation of Earth's Lithospheric Magnetic Field to Degree and Order 720. *Geochemistry, Geophysics, Geosystems 11*(6).

Mayer-Gürr, T. (2007). ITG-Grace03s: The latest GRACE gravity field solution computed in Bonn. In *Joint International GSTM and DFG SPP Symposium Potsdam, 15-17 October 2007*.

McCarthy, D. D., P. E. Angerhofer, D. R. Florkowski, F. J. Josties, and D. N. Matsakis (1985). Connected-Element Interferometer results in project MERIT. In I. I. Mueller (Ed.), *Earth Rotation and the Terrestrial Reference Frame*, pp. 341–350.

McCarthy, D. D. and B. Luzum (1991). Combination of Precise Observations of the Orientation of the Earth. *Bulletin Géodésique 65*, 22–27.

McCarthy, D. D. and P. K. Seidelmann (2009). *Time: From Earth Rotation to Atomic Physics*. Weinheim: Wiley-VCH.

Merrigan, M., E. Swift, R. Wong, and J. Saffel (2002). A Refinement to the World Geodetic System 1984 Reference Frame. In *Proceedings of the 15th International Technical Meeting of the Satellite Division of The Institute of Navigation (ION GPS 2002), Portland, OR, Sept. 2002*, pp. 1519–1529.

Minster, J. B. and T. H. Jordan (1978). Present-Day Plate Motions. *Journal of Geophysical Research 83, B11*, 5331–5354.

Misra, P. and P. Enge (2001). *Global Positioning System, Signals, Measurements, and Performance*. Lincoln, Mass.: Ganga-Jamuna Press.

Mitchell, H. C. and L. G. Simmons (1945). The State Plane Coordinate Systems (A Manual for Surveyors). Special Publication 235, National Geodetic Survey, Rockville, MD.

Moffit, F. and H. Bouchard (1975). *Surveying* (6th ed.). New York, NY: Intext Educational Publishers.

Molodenskii, M. S., V. F. Eremeev, and M. I. Yurkina (1962). *Methods for Study of the External Gravitational Field and Figure of the Earth*. Available from the Office of Technical Services, U.S. Dept. of Commerce, Washington: Israel Program for Scientific Translations.

Moritz, H. (1980). *Advanced Physical Geodesy*. Tunbridge Wells, Kent, UK: Abacus Press.

Moritz, H. (1992). Geodetic Reference System 1980. *Bulletin Geodesique 66*(2), 187–192. The Geodesist's Handbook, C. C. Tscherning, Ed.

Moritz, H. and I. I. Mueller (1987). *Earth Rotation: Theory and Observation*. New York, NY: Ungar/Continuum.

Mueller, I. I. (1969). *Spherical and Practical Astronomy as Applied to Geodesy*. New York, NY: Ungar.

Mueller, I. I. (1988). Reference Coordinate Systems: An Update. In R. Rummel and F. Sanso (Eds.), *Theory of Satellite Geodesy and Gravity Field Determination*, Heidelberg. Springer Verlag.

Mueller, I. I., M. Kumar, J. P. Reilly, N. Saxena, and T. Soler (1973). Global Satellite Triangulation and Trilateration for the National Geodetic Satellite Program (Solutions WN 12, 14 and 16). Department of Geodetic Science Report 199, The Ohio State University, Columbus, Ohio.

Mueller, I. I. and J. D. Rockie (1966). *Gravimetric and Celestial Geodesy: A Glossary of Terms*. New York, NY: Ungar.

Munk, W. H. and G. J. F. MacDonald (1960). *The Rotation of the Earth: A Geophysical Discussion*. Cambridge: Cambridge University Press.

Nautical Almanac Offices of UK and USA (1989). *The Astronomical Almanac for the Year 1990*. Washington & London: US Government Printing Office & HM Stationery Office.

Nerem, R. S., B. F. Chao, A. Y. Au, J. C. Chan, S. M. Klosko, N. K. Pavlis, and R. G. Williamson (1993). Temporal variations of the Earth's gravitational field from satellite laser ranging to Lageos. *Geophysical Research Letters 20*(7), 595–598.

NIMA (1997). Department of Defense World Geodetic System 1984, Its Definition and Relationships with Local Geodetic Systems. Tech. Report TR8350.2, 3rd ed., National Imagery and Mapping Agency. (http://earth-info.nga.mil/GandG/publications/tr8350.2/tr8350_2.html).

NOAA (1989). North American Datum of 1983. Professional Papers NOS 2, National Oceanic and Atmospheric Administration, NGS, Rockville, MD. Charles R. Schwarz, Editor.

Norton, I. O. (2000). Global hotspot reference frames and plate motions. In M. A. Richards, R. G. Gordon, and R. D. van der Hilst (Eds.), *The History and Dynamics of Global Plate Motions: Geophysical Monograph, American Geophysical Union*, Volume 121, pp. 339–357.

Packard, R. E. (1988). Principles of a Superfluid Helium Interference Gyroscope: A New Tool to Study the Earth's Rotation. *EOS 69*(44), 1153.

Parker, W. and R. Bartholomew (1989). Issues in Automating the Military Grid Reference System. In *Proc. of the Fifth International Geodetic Symposium on Satellite Positioning, New Mexico State Univ., Las Cruces, New Mex., Mar. 13–17, 1989*, Volume 2, pp. 903–913.

Pavlis, E. C. (2002). Dynamical Determination of Origin and Scale in the Earth System from Satellite Laser Ranging. In J. Adam and K. P. Schwarz (Eds.), *Vistas for Geodesy in the New Millennium: Proceedings of the 2001 International Association of Geodesy Scientific Assembly, held in Budapest, Hungary, September 2–7, 2001*, New York, N. Y., pp. 36–41. Springer-Verlag.

Pavlis, E. C. (2010). Private communications.

Pavlis, N. K., S. A. Holmes, S. C. Kenyon, and J. K. Factor (2012). The Development and Evaluation of the Earth Gravitational Model 2008 (EGM2008). *Journal of Geophysical Research* 117, B4, B04406.

Pearlman, M. R., J. J. Degnan, and J. M. Bosworth (2002). The International Laser Ranging Service. *Advances in Space Research 30*(2), 135–143.

Plag, H.-P., Z. Altamimi, S. Bettadpur, G. Beutler, G. Beyerle, A. Cazenave, D. Crossley, A. Donnellan, R. Forsberg, R. Gross, J. Hinderer, A. Komjathy, C. Ma, A. J. Mannucci, C. Noll, A. Nothnagel, E. C. Pavlis, M. Pearlman, P. Poli, U. Schreiber, K. Senior, P. L. Woodworth, S. Zerbini, and C. Zuffada (2009). The goals, achievements, and tools of modern geodesy. In H.-P. Plag and M. Pearlman (Eds.), *Global Geodetic Observing System: Meeting the Requirements of a Global Society on a Changing Planet in 2020*, Vienna and New York, pp. Chapter 2. Springer.

Pollard, J. (2002). Iterative Vector Methods for Computing Geodetic Latitude and Height from Rectangular Coordinates. *Journal of Geodesy 76*(1), 36–40.

Rabbel, W. and H. Schuh (1986). The Influence of Atmospheric Loading on VLBI Experiments. *Journal of Geophysics Zeitschrift Geophysik 59*, 164–170.

Rabbel, W. and J. Zschau (1985). Static Deformations and Gravity Changes at the Earth's Surface due to Atmospheric Loading. *Journal of Geophysics Zeitschrift Geophysik 56*, 81–99.

Rapp, R. H. (1980). Geometric Geodesy Volume II (Advanced Techniques). Technical report, Department of Geodetic Science, The Ohio State University, Columbus, OH.

Ray, R. (1999). A Global Ocean Tide Model From TOPEX/POSEIDON Altimetry: GOT99.2. Tech. Memo. NASA/TM-1999-209478, NASA Goddard Space Flight Center, Greenbelt, MD.

Sato, Y., A. Joshi, and R. Packard (2008). Superfluid ^{4}He Quantum Interference Grating. *Physical Review Letters 101*(805302), 1–4.

Savcenko, R. and W. Bosch (2008). EOT08a, empirical ocean tide model from multi-mission satellite altimetry. Report 81, Deutsches Geodätisches Forschungsinstitut (DGFI), München.

Scherneck, H.-G. (1990). Loading Green's functions for a continental shield with a Q-structure for the mantle and density constraints from the geoid. *Bull. d'Inform. Marées Terr. 108*, 7757–7792.

Scherneck, H.-G. (1991). A Parameterized Solid Earth Tide Model and Ocean Tide Loading Effects for Global Geodetic Baseline Measurements. *Geophysical Journal International 106*, 677–694.

Schlüter, W. and D. Behrend (2007). The International VLBI Service for Geodesy and Astrometry and Its Fundamental Role in Earth-related Sciences and Applications. *Journal of Geodesy 81*(6-8), 379–387.

Schreiber, K. U., A. Velikoseltsev, M. Rothacher, T. Klügel, G. E. Stedman, and D. L. Wiltshire (2004). Direct measurement of diurnal polar motion by ring laser gyroscopes. *Journal of Geophysical Research 109*(B06405).

Schwab, K., N. Bruckner, and R. Packard (1997). Detection of the Earth's rotation using superfluid phase coherence. *Nature 386*, 585–587.

Schwiderski, E. W. (1980). On Charting Global Ocean Tides. *Reviews of Geophysics and Space Physics 18*, 243–268.

Schwiderski, E. W. (1983). Atlas of Ocean Tidal Charts and Maps, Part I: The Semidiurnal Principal Lunar Tide M_2. *Marine Geodesy 6*, 219–256.

Seeber, G. (2003). *Satellite Geodesy* (2nd ed.). Berlin–New York: Walter de Gruyter.

Seiler, U. and J. Wünsch (1995). A refined model for the influence of ocean tides on UT1 and polar motion. *Astronomische Nachrichten 316*, 419.

Simmonds, R. W., A. Marchenkov, E. Hoskinson, J. C. Davis, and R. E. Packard (2001). Quantum interference of superfluid ^{3}He. *Nature 412*, 55–58.

Slater, J. A. and S. Malys (1998). WGS 84—Past, Present and Future. In F. K. Brunner (Ed.), *Advances in Positioning and Reference Frames*. Springer-Verlag. International Assn. of Geodesy Symposia, 118.

Snay, R. A. and T. Soler (2000). Modern Terrestrial Reference Systems, Part 2: The Evolution of NAD 83. *Professional Surveyor Feb., 2000*, 16–18.

Snyder, J. P. (1983). Map Projections Used by the U.S. Geological Survey. Geological Survey Bulletin 1532, U.S. Geological Survey, U.S Government Printing Office, Washington, D.C. 2nd Edition.

Soffel, M., H. Herold, H. Ruder, and M. Schneider (1988). Reference Frames in Relativistic Space-Time. In A. K. Babcock and G. A. Wilkins (Eds.), *The Earth's Rotation and Reference Frames for Geodesy and Geodynamics: Proceedings of the 128th Symposium of the International Astronomical Union, held in Coolfont, West Virginia, U.S.A., 20-24 October 1986*, Dordrecht, Holland, pp. 99–103. Kluwer.

Soudarin, L. and J. F. Crétaux (2006). A model of present-day tectonic plate motions from 12 years of DORIS measurements. *Journal of Geodesy 80*(8-11), 609–624.

Stacey, F. D. and P. M. Davis (2008). *Physics of the Earth* (4th ed.). Cambridge, UK: Cambridge Univ. Press.

Stamatakos, N., B. Luzum, B. Stetzler, W. Wooden, and E. Schultz (2009). Recent improvements in IERS Rapid Service/Prediction Center products. In M. Soffel and N. Capitaine (Eds.), *Proceedings of the Journées 2008 Systèmes de référence spatio-temporels*, Dresden and Paris, pp. 160–163. Lohrmann-Observatorium and Observatoire de Paris.

Stedman, G. E. (1997). Ring-laser tests of funadmental physics and geophysics. *Reports on Progress in Physics 60*, 615–688.

Steigenberger, P., M. Rothacher, R. Dietrich, M. Fritsche, A. Rülke, and S. Vey (2006). Reprocessing of a global GPS network. *Journal of Geophysical Research 111*, B05402.

Stem, J. (1989). State Plane Coordinate System of 1983. NOAA Manual NOS NGS 5, National Oceanic and Atmospheric Administration.

Teisseyre, R. (Ed.) (1989). *Gravity and Low-Frequency Geodynamics*. Amsterdam: Elsevier Science Publishers.

Thomas, P. D. (1952). Conformal Projections in Geodesy and Cartography. Special Publication 251, U.S. Coast and Geodedic Survey, U.S. Government Printing Office, Washington, D.C. 5th Printing.

Torge, W. (1980). *Geodesy*. New York, NY: Walter de Gruyter. Trans. by C. Jekeli.

Torge, W. (2001). *Geodesy* (3rd ed.). Berlin–New York: Walter de Gruyter.

Tracey, J., P. Kammeyer, and N. Stamatakos (2008). Usage of the UT1-like Quantity at the USNO. In *International GNSS Service, Analysis Center Workshop, 2–6 June 2008, Miami Beach, Florida, USA*.

Turner, J. D. (2009). A non-iterative and non-singular perturbation solution for transforming Cartesian to geodetic coordinates. *Journal of Geodesy 83*(2), 139–145.

vanDam, T. M. and J. M. Wahr (1987). Displacements of the Earth's Surface due to Atmospheric Loading: Effects on Gravity and Baseline Measurements. *Journal of Geophysical Research 92*, 1281–1286.

Vondrák, J., C. Ron, I. Pešek, and A. Čepek (1995). New global solution of Earth orientation parameters from optical astrometry in 1900–1990. *Astronomy and Astrophysics 297*, 899–906.

Vondrák, J., C. Ron, and V. Štefva (2007). Solution of Earth orientation parameters in 20th century based on optical astrometry and new catalog EOC-3. In W. J. Jin, I. Platais, and M. A. C. Perryman (Eds.), *A Giant Step: from Milli- to Micro-arcsecond Astrometry, Proceedings IAU Symposium No. 248*, pp. 89–92.

Wahr, J. M. (1981). The Forced Nutations of an Elliptical, Rotating, Elastic, and Oceanless Earth. *Geophysical Journal of Royal Astronomical Society 64*, 705–727.

Wahr, J. M. (1987). The Earth's C_{21} and S_{21} gravity coefficients and the rotation of the core. *Geophysical Journal International 88*, 265–276.

Wahr, J. M. (1990). Correction and update to 'The Earth's C_{21} and S_{21} gravity coefficients and the rotation of the core'. *Geophysical Journal International 101*, 709–711.

Wahr, J. M. and Z. Bergen (1986). The effects of mantle anelasticity on nutations: Earth tides and tidal variations in rotation rate. *Geophysical Journal of Royal Astronomical Society 87*, 633–668.

Williams, J. G. and J. O. Dickey (2003). Lunar geophysics, geodesy, and dynamics. In *13th International Workshop on Laser Ranging, Proceedings From the Science Session and Full Proceedings CD-ROM*, pp. 75–86. NASA/CP-2003-212248.

Yoder, C. F., J. G. Williams, and M. E. Parke (1981). Tidal Variations of Earth Rotation. *Journal of Geophysical Research 86*, 881–891.

Zschau, J. (1983). Rheology of the Earth's mantle at tidal and Chandler Wobble periods. In J. T. Kuo (Ed.), *Proceedings of the Ninth Int. Symp. Earth Tides, New York, 1981*, Stuttgart, pp. 605–630. Schweitzerbart'sche Verlagsbuchhandlung.

Zumberge, J. F., M. B. Heflin, D. C. Jefferson, M. W. Watkins, and F. H. Webb (1997). Precise Point Positioning for the Efficient and Robust Analysis of GPS Data from Large Networks. *Journal of Geophysical Research 102*(B3), 5005–5017.

CHAPTER 6

Precession, Nutation, Polar Motion, and Earth Rotation

JAMES L. HILTON & DENNIS D. McCARTHY

6.1 Introduction

To specify positions of celestial objects it is necessary to have a reference system. An ideal reference system would provide an inertial reference frame that could be used at all frequencies of the electromagnetic spectrum, and for all magnitudes or intensities. A number of problems, unfortunately, interfere with realizing such a reference system. Among those is the fact that most observers are situated on the Earth, an observing platform that is constantly changing in orientation with respect to inertial space.

This chapter deals with those transformations necessary to determine the orientation of the Earth, the terrestrial reference system (TRS), with respect to the sky, the celestial reference system (CRS). It also describes the transformation from a reference system attached to a rotating Earth to that of a non-rotating object in the Earth's orbit about the solar system barycenter. This chapter does not include: those changes in the reference system arising from the Earth's nonlinear motion about the solar system barycenter, such as the annual aberration of light; relativistic effects, such as the deflection of light by massive objects; or changes in coordinates arising from an observer being situated on the Earth's surface rather than at the geocenter, such as horizontal parallax or diurnal aberration of light. These topics are discussed in Chapter 7. Nor does this chapter deal with those changes in position caused by the flexure of a non-rigid Earth, discussed in Chapter 5. This chapter describes how *The Astronomical Almanac* determines the orientation of the TRS with respect to the CRS. The method of transforming from the CRS to the TRS underwent major changes in 2003 and 2006. Both the old and new paradigms are discussed. The procedures for these reductions are found mainly in Section B of *The Astronomical Almanac* and Chapter 7 of this book.

At the most basic level, the transformation for a vector, $\mathbf{x}$, from the TRS, $\mathbf{x}_{TRS}$, to the CRS, $\mathbf{x}_{CRS}$, is carried out by the transformation:

$$\mathbf{x}_{CRS} = \mathbf{P}\,\mathbf{N}\,\mathbf{T}\,\mathbf{W}\,\mathbf{x}_{TRS} \tag{6.1}$$

where $\mathbf{P}$, $\mathbf{N}$, $\mathbf{T}$, and $\mathbf{W}$ are a set of rotation matrices that account for precession, nutation, Earth rotation, and polar motion, respectively. Each of these rotation matrices is the product of the three basic rotation matrices, $\mathbf{R}_1(\theta)$, $\mathbf{R}_2(\theta)$, and $\mathbf{R}_3(\theta)$

$$\mathbf{R}_1(\theta) = \begin{bmatrix} 1 & 0 & 0 \\ 0 & \cos\theta & \sin\theta \\ 0 & -\sin\theta & \cos\theta \end{bmatrix} \quad \mathbf{R}_2(\theta) = \begin{bmatrix} \cos\theta & 0 & \sin\theta \\ 0 & 1 & 0 \\ -\sin\theta & 0 & \cos\theta \end{bmatrix} \quad \text{and}$$
$$\mathbf{R}_3(\theta) = \begin{bmatrix} \cos\theta & \sin\theta & 0 \\ -\sin\theta & \cos\theta & 0 \\ 0 & 0 & 1 \end{bmatrix} \tag{6.2}$$

where θ is the rotation angle, and the subscripts refer to rotations about the x, y, and z axes, respectively, of a right-handed Cartesian reference system. Any rigid coordinate system can be mapped into any other rigid coordinate system with the same geometric origin by a series of three, non-unique, rotations (see Chapter 14).

The first two matrices on the right hand side of Eq. 6.1, **P** and **N**, represent the dynamical motion of the *Celestial Intermediate Pole* (CIP; § 6.2.3) in response to the torques arising from the gravitational attraction of the Sun, Moon, and planets of the solar system. This motion has traditionally been separated into a secular part, *precession*, and a periodic part, *nutation*. Precession, **P**, and nutation, **N**, are treated as a separate transformations. The details of these transformations are covered in § 6.6.

The third matrix on the right hand side of Eq. 6.1, **T**, is the rotation of the terrestrial reference system with respect to the celestial reference system. Thus, this matrix is

$$\mathbf{T} = \mathbf{R}_3(T) \tag{6.3}$$

where T is the angle between the Terrestrial Intermediate Origin, TIO (§ 6.9), and the origin of right ascension. In the past, the origin of right ascension was either the mean equinox of date, or the true equinox of date. Beginning in 2003, the IAU (2001d) recommends replacing the equinox and equator of date with the Celestial Intermediate Origin, CIO (§ 6.7). The name for the angle T depends on the origin of right ascension used. When the origin of right ascension is the mean equinox of date it is called the Greenwich Mean Sidereal Time, GMST (§ 6.8.5.1). When the origin of right ascension is the true equinox of date it is called the Greenwich Apparent Sidereal Time, GAST (§ 6.8.5.2). And when the origin of right ascension is the CIO it is called the Earth Rotation Angle, ERA (§ 6.8.4). The relationships between the ERA, GMST, and GAST are discussed in § 6.3 and § 6.4.

Finally, the fourth matrix on the right hand side of Eq. 6.1, **W**, is the polar motion, and gives the position of the terrestrial reference frame with respect to the TIO (§ 6.9.2). This matrix is

$$\mathbf{W} = \mathbf{R}_1(s')\mathbf{R}_2(x)\mathbf{R}_1(y) \tag{6.4}$$

where s' is the TIO locator, and the angles x and y are the angular coordinates of the CIP (§ 6.2.3) with respect to the terrestrial pole measured along the meridians at 0° and 270° (90°W), respectively.

6.2 The Celestial Reference System (CRS) and the Terrestrial Reference System (TRS)

Detailed information on the celestial reference system (CRS) itself can be found in Chapter 4, and details of the terrestrial reference system (TRS) are in Chapter 5. Both the CRS and the

TRS are rigid coordinate systems. Any such coordinate system can be described by a set of three mutually perpendicular coordinate axes. Alternatively, a direction vector, the *pole*; a plane perpendicular to that vector, the *equator*; and a fiducial point on the equator, the *origin of right ascension* [1], may describe the coordinate system.

Resolution A4 VII of the XXIst General Assembly of the International Astronomical Union (IAU 1992; URL[4]) defines the CRS. This resolution recommends the adoption of a celestial reference system based on Very Long Baseline Interferometry (VLBI) observations of extragalactic radio sources aligned as near as possible to the mean equator of J2000.0 with the origin of right ascension as near as possible to the dynamical equinox of J2000.0. This reference system is to be, ". . . computed initially for the equator and equinox J2000.0 (Julian date 2 451 545.0 TT) using the best available values of the celestial pole offset with respect to the IAU expressions for precession and nutation . . . " A reference system based on this recommendation, the International Celestial Reference System (ICRS), was adopted in 1997 in resolution B2 of the XXIIIrd General Assembly of the IAU (IAU 1997; URL[4]). The positive z-axis of the complimentary Cartesian coordinate is the north direction of the pole. The positive x-axis is the direction towards the origin of right ascension. And the positive y-axis is the direction of $z \times x$ to give a right-handed coordinate system.

The ICRS is epochless, that is, unlike prior celestial reference systems it is not tied to the orientation of the Earth at some fiducial epoch. Instead, the only way in which the ICRS will change is if the positions of the defining sources on the sky are determined more accurately. Thus, although its initial construction aligned it with the best determination of the mean equator and equinox of J2000.0, subsequent improvement of the knowledge of that equator and equinox do not alter the orientation of the ICRS. Rather, the position of the mean equator and equinox in the ICRS is altered.

It is necessary to distinguish whether the geometric origin is the solar system barycenter or the Earth's center of mass, the geocenter. If the origin is the solar system barycenter, it is referred to as the *Barycentric Celestial Reference System* (BCRS); if the origin is the geocenter, it is referred to as the *Geocentric Celestial Reference System* (GCRS). The GCRS and the BCRS are connected by a relativistic coordinate transformation (IAU 2001a). In general, the GCRS should be used when the object of interest is within several Earth diameters of the geocenter. Beyond this distance, the BCRS should be used. It is common for users to refer to the ICRS when they specifically mean the BCRS; however, the term BCRS ought to be used in these cases to prevent confusion with the more general term.

The geometric origin of the *Terrestrial Reference System* (TRS) is the geocenter. It is described by the three orthogonal reference directions with respect to the body of the Earth. The Earth rotates. Thus, the TRS is a non-inertial reference system and its orientation in space is constantly changing.

For many applications it is desirable to use a Celestial Intermediate Reference System that is related to the TRS at a particular epoch. In the past the direction of the *celestial ephemeris*

1. Unfortunately, the word origin has two different meanings when discussing reference systems. It can either be a fiducial point on the equator used as the initial point for angular measures such as longitudes and right ascensions, or it can be the initial point, or center, of the reference system. To separate these two meanings the former will always be referred to as the *origin of right ascension* or *origin of longitude* while the latter will always be referred to as the *geometric origin* in this chapter.

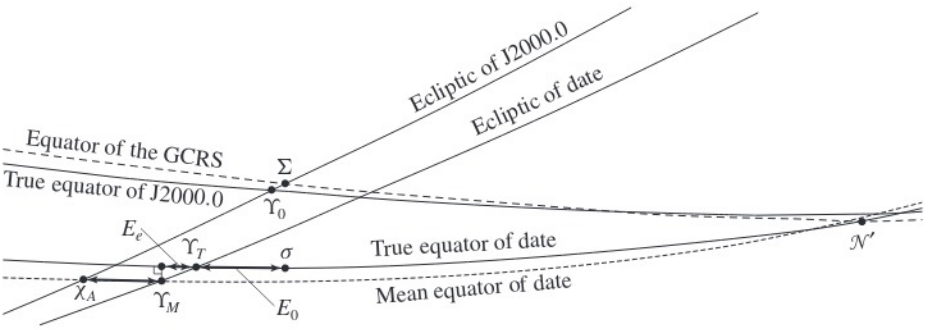


Figure 6.1 The relationship between the *Celestial Intermediate Origin* (CIO), σ, the origin of right ascension of the *Geocentric Celestial Reference System* (GCRS), Σ, the true equinox of J2000.0, Υ_0, the mean equinox of date, Υ_M, and the true equinox of date, Υ_T. The true equator of date is identical with the equator of the *Celestial Intermediate Pole* (CIP). The intersection of the equator of the GCRS and the true equator of date occurs at N'. The, GCRS is nearly aligned with the Earth's *mean* equator of J2000.0. Thus, there is a significant separation between Υ_0 and Σ.

pole defined the equator of this system. The CIP replaced the celestial ephemeris pole after 1 Jan. 2003.

6.2.1 Reference Systems in *The Astronomical Almanac*

It is useful to distinguish between a reference system and a reference frame. In the terminology that is now commonly used, a reference system is the complete specification of how a coordinate system is to be formed. It defines the origin and axes of the coordinate system. It also specifies all of the constants, models, and algorithms used to transform between observable quantities and reference data that conform to the system. A reference frame consists of a set of identifiable fiducial points along with their coordinates, which serves as the practical realization of a reference system.

In practice, there are eight reference systems that are used in *The Astronomical Almanac*. These are:

1. The *Barycentric Celestial Reference System* (BCRS): The BCRS is described by the equator, pole, and origin of right ascension (§ 6.2) as defined in IAU (1997).
2. The *Geocentric Celestial Reference System* (GCRS): The equator, pole and origin of right ascension (§ 6.2), Σ in Fig. 6.1, of the GCRS are the BCRS equator, pole, and origin of right ascension transformed relativistically from the solar system barycenter to the geocenter.
3. The *mean equator and equinox of J2000.0*: The equator and pole (§ 6.2) of J2000.0 are the CIP (§ 6.2.3) at the particular epoch J2000.0, Julian date 2 451 545.0 TT, and the plane perpendicular to it. The origin of right ascension is the position of the mean equinox of J2000.0. Except for a constant offset of about 23 milliarcseconds represented by the frame bias matrix (§ 6.5), this reference system is the same as the GCRS.

4. The *mean equator and equinox of date*: The origin of right ascension, Υ_M in Fig. 6.1, is the position of the mean equinox (§ 6.2.4) of date. The difference between the mean equator of date and the mean equator of J2000.0 is due to precession (§ 6.6.2).
5. The *true equator and equinox of date*: The equator (§ 6.2) is the equator of the CIP (§ 6.2.3). The origin of right ascension is the position of the true equinox of date (§ 6.2.4), Υ_T in Fig. 6.1,. The right ascension of this reference system may be called *apparent right ascension* to distinguish it from the right ascension used by the Intermediate Reference System below. Apparent right ascension is subtracted from Greenwich Apparent Solar Time (GAST), (§ 6.8.5.2), to give the Greenwich Hour Angle, GHA, (§ 6.8.8). The difference between the equator of the CIP and the mean equator of date is the motion arising from nutation (§ 6.6.3).
6. The *Intermediate Reference System*: Like the true equator and equinox of date, the equator (§ 6.2) of the Intermediate Reference System is the equator of the CIP (§ 6.2.3). However, the origin of right ascension (§ 6.2) is the CIO, (§ 6.7), σ in Fig. 6.1,. The right ascension for this reference system may be called *intermediate right ascension* to distinguish it from the right ascension used by the true equator and equinox of date above. The choice of the CIO as the origin of right ascension makes the relation between UT1 (§ 6.8.3) and Earth rotation a linear function. Intermediate right ascension is subtracted from the *Earth Rotation Angle*, ERA or θ, (§ 6.8.4), to give GHA.
7. The *International Terrestrial Reference System* (ITRS): The International Terrestrial Reference System was defined by the International Union of Geodesy and Geophysics in 1991. In practice, the ITRS is realized by the adopted coordinates and velocities, arising from plate tectonics and post-glacial rebound, of a large group of observing stations. These coordinates are not dependent on a reference ellipsoid, but are expressed as geocentric rectangular 3-vectors.
8. The *Terrestrial Intermediate Reference System* (TIRS): The equator and pole are the CIP equator and pole of date, and the origin of longitude is the *Terrestrial Intermediate Origin* (TIO), (§ 6.9). The difference between the ITRS and the TIRS is that the TIRS is corrected for polar motion. The z-axis of the ITRS is realized by the adopted positions of sites on the geodetic surface of the Earth while the z-axis of the TIRS is in the direction of the CIP.

6.2.2 The Conventional International Origin and the International Terrestrial Reference Frame (ITRF)

The principal axes of a body are the orthogonal directions that define a Cartesian coordinate system in which the moment of inertia tensor is a diagonal matrix, i.e., the products of inertia are zero. For an oblate rigid ellipsoid of revolution, two of the principal moments of inertia are equal, and the third principal moment is larger than the other two. In this case, the axis of the third principal moment of inertia is also the axis of figure. The Earth, however, is elastic and is not a perfect ellipsoid of revolution. Thus, its inertia tensor and the directions of the principal axes of inertia are functions of time. Nevertheless, an *instantaneous axis of figure*, F, may be defined as the line passing through the center of mass of the Earth, parallel to the eigenvector of the instantaneous inertia tensor of the Earth. The intersection of F with the surface of the Earth is the *instantaneous pole of figure*.

The position of the instantaneous axis of figure of a deformable Earth is subject to motions from distortions of the Earth, such as the body tides. The motion of this point makes it difficult to interpret the motions of F in terms of rigid-body concepts. It thus becomes useful to define the *mean surface geographic axis*, B, as an axis attached in a least-squares sense to the Earth's outer surface. Consider a network of observatories on a rigid Earth and an axis fixed with respect to the positions of the observatories. The only possible motion of that network is a time-dependent, rigid rotation; the portion of the rigid rotation that is not parallel to the axis will cause motion of the axis as the latter follows motions of the observatories defining it. On a deformable planet, other motions of the observatories may be possible, and the definition of the axis is generalized by the adopted positions of the observatories. B is this axis in the limit of an infinite number of uniformly distributed observatories. Thus, if we decompose the motion of the Earth's surface into a rigid rotation plus a residual deformation, B moves with the sense prescribed by the rigid rotation. The axis B does not respond to body tides. For a rigid Earth B and F are coincident. Crustal motions and tidal forces cause motions of those observatories with respect to B.

The *conventional international origin* [2] was defined originally by the adopted astronomical latitudes of the five observatories contributing to the International Latitude Service (ILS) (Markowitz and Guinot 1968). It roughly coincides with the mean pole F over the period from 1900 to 1905. Later, the terrestrial pole was defined by a larger number of observatories operating optical equipment (e.g., photographic zenith tubes) that reported to the International Polar Motion Service (IPMS) and the Bureau International de l'Heure (BIH). Both BIH and IPMS systems were compatible with the CIO. Satellite laser ranging (SLR) and VLBI (§ 6.2) became more accurate techniques for determining the position of the pole, and the BIH pole became strongly dependent on these data. In January 1988 the maintenance of the terrestrial reference frame was taken over by the International Earth Rotation and Reference Systems Service (IERS). The IERS maintains a pole consistent within the observational errors with those of the conventional international origin and BIH. Current higher accuracy observations require a model of plate motions in the analysis of observations. This new reference frame is called the *International Terrestrial Reference Frame* (ITRF).

6.2.3 The Celestial Intermediate Reference System and the Celestial Intermediate Pole (CIP)

Prior to the 2006 edition of *The Astronomical Almanac* the algorithms used to determine the precession and nutation of the Earth were based on the use of the Earth's rotation axis or Celestial Ephemeris Pole (CEP) rather than the CIP. The IAU (1980) defined the Celestial Ephemeris Pole as having, "no nearly-diurnal nutation with respect to a space-fixed or Earth-fixed coordinate system." Moritz and Mueller (1988) point out that this was often mistakenly assumed to be the axis of figure. However, the axis of figure does not conform to the definition of the CEP. Instead, the CEP is dynamically the same as the Tisserand mean polar axis. The Tisserand mean axes are defined, as that set of axes where the deformation field of the Earth integrated over the volume of the Earth contains no rotation (Moritz and Mueller 1988).

2. The conventional international origin is *not* the same as the celestial intermediate origin, although both can be denoted by CIO. To avoid confusion, the use of CIO in this book is reserved only for the celestial intermediate origin.

Beginning with the 2006 edition of *The Astronomical Almanac* the celestial reference system aligned with the *Celestial Intermediate Pole* (CIP) is called the *Celestial Intermediate Reference System*. Ideally, the CIP would be the projection of the line passing through the Earth's center of mass and the ITRF pole onto the sky. However, the free motion of the pole of rotation within the body of the Earth is partially stochastic and, hence, cannot be predicted with certainty.

Beginning with the 2006 edition of *The Astronomical Almanac* the algorithms used to determine the precession and nutation of the Earth use the CIP. The CIP is defined as the Tisserand mean axis of the Earth whose motion is comprised of those periodic components, observed in a celestial reference, that have periods greater than two days (IAU 2001c). For the CIP nutation is defined as the forced motions with periods greater than two days with respect to the CIP, and polar motion is defined as the free motion and the forced motions with periods less than or equal to two days. The forced motion is the solution of the Earth's equations of rotational motion accounting for all external torques (specifically the gravitational forces due to the Sun, Moon, and planets). The free motion is that motion which would exist if there were no external torques on the rotating Earth (the particular solution of the differential equations). If the Earth were rigid, the free motion wobble would have a period of about 304 days. However, for the physical, non-rigid Earth, this motion, called the Chandler wobble, has a period of about 14 months. Polar motion also includes the motions arising from changes in the distribution of the Earth's mass from the climate along with motions resulting from geophysical strains and meteorological effects.

If the two principal axes of inertia that lie in the Earth's equatorial plane were identical, then the shortest periodic motion arising from the torques of the Moon, Sun, and planets would have a period of about a month. And, the CIP would be identical to the CEP. However, these two principal axes of inertia differ by about 0.002% (Moritz and Mueller 1988). The difference in the torques about these two principal axes of inertia gives rise to small motions of the Tisserand mean axes with periods less than or approximately equal to a day. These motions have periods that are exactly equal to those of many of the tidal deformations in the Earth, and cannot be separated by observation. Thus, the requirement of dropping those terms with periods of less than two days was imposed on the CIP. One result of this definition is that the TRS is no longer fixed by the loosely defined Greenwich meridian but is moving eastward at about 0.016 mm yr^{-1}, on average (Lambert and Bizouard 2002).

In addition to the free nutation observed in all spinning bodies, there is a second free motion for the Earth. This second free motion arises from the difference in the alignment of the Earth's core and mantle, and is called the free core nutation. It is also known as the diurnal free polar motion or nearly diurnal free wobble. It produces a periodic motion of approximately 432 days of the CIP in the GCRS.

6.2.3.1 The Ecliptic

The ecliptic is generally defined as the mean plane of the Earth's orbit around the Sun. The actual plane of the Earth's orbit is constantly changing in response to the perturbations from the other planets in the solar system, making the actual determination of the ecliptic far from easy. One problem in realizing the ecliptic is a practical definition of a mean plane. To reduce the uncertainties in the definition of the ecliptic the IAU Working Group on Precession and the Ecliptic (Hilton et al. 2006) have recommended that the ecliptic be more precisely defined

as the plane perpendicular to the mean orbital angular momentum vector of the Earth-Moon barycenter passing through the Sun in the BCRS.

The "inertial" and the "rotating" ecliptics. Prior to the advent of Lunar Laser Ranging (LLR) observations, it was impossible to determine whether or not the space motions of solar system objects contained a residual global rate of rotation. Newcomb (1898) defined the "rotating" ecliptic as the plane perpendicular to the mean motion of the Earth-Moon barycenter from the point of view of an observer co-moving with the ecliptic. For such a co-moving observer, there is a component to the orientation of the ecliptic that arises from the motion of the ecliptic itself. On the other hand, Le Verrier (1855) defined the ecliptic from the point of view of an observer in inertial space. Thus, older publications used two different definitions of the ecliptic. Standish (1981) showed that the equinox based on this "rotating" definition of the mean ecliptic is 93.66 milliarcseconds (mas) to the east of the equinox based on an inertially defined ecliptic, and the obliquity of the Earth is 3.34 mas greater using the rotating definition of the ecliptic than if an inertial ecliptic is used. Thus, the ecliptic definition used can cause significant errors for applications that require accuracy better than about $0.''1$. The BCRS is oriented with respect to the inertial ecliptic while many, but not all, older reference systems, such as the FK5 and the reference system used by DE200 (Folkner et al. 1994), are oriented with respect to the rotating ecliptic. Thus, care must be used when using older data to determine if they are referring to the inertial or rotating definition of the ecliptic.

6.2.4 The Equinoxes

The classic concept of the origin of right ascension, the longitudinal coordinate of the celestial reference system, is the dynamical *vernal equinox*: The point on the celestial sphere where the celestial equator intersects the ecliptic and through which the center of the mean Sun passes as it crosses the equator going north. More specifically, it is the direction of the intersection of the projection of the Earth's equator onto the sky with the mean orbit plane of the Earth-Moon barycenter near which the Sun passes on its way north of the Earth's equator. In addition to the vernal equinox, there is also the *autumnal equinox*, which is the direction of the intersection between the Earth's equator and the ecliptic near where the center of the mean Sun passes going south. Generally, the use of the word "equinox" implies the vernal equinox

Like the ecliptic, the Earth's equator is a dynamically defined plane. Thus, neither plane is fixed in space, and the equinox is constantly changing. The change of the equinox with time requires that a date be affixed to it in order to specify a fixed direction. The reference epoch for the equinox in common use curently is J2000.0 (Julian date 2 451 545.0 TT), see § 6.7.

It is possible to refer to either the *mean equator* or the *true equator*. The mean equator is a moving equator prescribed only by secular (non-periodic) motion; that is, motion due to precession. The true equator, on the other hand, includes both secular and periodic motions; that is, motions due to both precession and nutation. Beginning with the 2006 edition of *The Astronomical Almanac*, the equator was defined as the plane perpendicular to the CIP (§ 6.2.3) that passes through the Earth's center of mass. Prior to the 2006 edition the equator was defined as the plane perpendicular to the CEP (§ 6.2.3) that passes through the Earth's center of mass. The existence of a separate mean equator and true equator implies the existence of a mean equinox and a true equinox corresponding to the directions where the mean equator intersects the ecliptic or where the true equator intersects the ecliptic. The CIO (§ 6.2.2) used in the Celestial Intermediate Reference System is independent of the dynamical equinox.

6.3 The Equation of the Equinoxes, $E_e(T)$

The *equation of the equinoxes*

$$E_e(T) = \Upsilon_T - \Upsilon_M = \text{GAST} - \text{GMST} \tag{6.5}$$

where Υ_T is the true equinox of date and Υ_M is the mean equinox of date, is the difference between the positions of the true and mean equinoxes of date. It is also equivalent to the difference between apparent and mean sidereal time,

$$\alpha_{eT} = \alpha_{eM} - E_e(T). \tag{6.6}$$

The equation of the equinoxes may be expressed in series form as

$$E_e(T) = \Delta\psi \cos\varepsilon_A + \sum_k (C'_k \sin A_k + S'_k \cos A_k) + 0.''000\,000\,87\, T \sin\Omega \tag{6.7}$$

where $\Delta\psi$ is the total nutation in longitude, ε_A is the mean obliquity of the ecliptic, Ω is the mean longitude of the ascending node of the Moon, and the coefficients C'_k and S'_k and the angular arguments A_k are used to describe the complementary terms arising from coupling between precession and nutation (Capitaine and Wallace 2006). Table 6.1 contains the values of the coefficients and angular arguments for all the complementary terms exceeding 0.5 μas (microarcseconds) between 1975 and 2025. These values are also given in Section B of *The Astronomical Almanac*. The resulting value for $E_e(T)$ is accurate to ± 30 μas.

Table 6.1 Coefficients of the series for the equation of the equinoxes, E_e, larger than 0.5 μas between 1975 and 2025

A_k [a]	C'_k (arcsec.)	S'_k [b]
Ω	−0.002 640 96	—
2Ω	−0.000 063 52	—
$2F - 2D + 3\Omega$	−0.000 011 75	—
$2F - 2D + \Omega$	−0.000 011 21	—
$2F - 2D + 2\Omega$	+0.000 004 55	—
$2F + 3\Omega$	−0.000 002 02	—
$2F + \Omega$	−0.000 001 98	—
3Ω	+0.000 001 72	—
$l' + \Omega$	+0.000 001 41	—
$l' - \Omega$	+0.000 001 26	—
$l + \Omega$	+0.000 000 63	—
$l - \Omega$	+0.000 000 63	—

[a] The definitions of the critical arguments and the formulae to compute their values are given in § 6.7.
[b] All of the amplitudes for S'_k are less than 0.5 μas. Thus, there are no entries for this column.

6.4 The Equation of the Origins, $E_o(T)$

Beginning on 1 January 2003, the IAU recommends that the azimuthal coordinate of the celestial reference system be measured from the CIO (§ 6.7) rather than the equinox. One consequence of using the CIO in place of the equinox is that there is no need to compute the equation of the equinoxes. Instead, realizing the position of the true equinox requires the *equation of the origins*, $E_o(T)$. The equation of the origins is the difference between the position of the CIO and true equinox of date. This difference is identical to the difference between the ERA (§ 6.8.4) and GAST (§ 6.8.5.2). Thus,

$$E_o(T) = \text{CIO} - \Upsilon_T = \theta - \text{GAST}. \tag{6.8}$$

Figure 6.1 illustrates the relation between the TIO (§ 6.9), the CIO, and the true equinox of date.

Any celestial object can be assigned an *equinox right ascension*, α_e, with respect to the equinox. It also can be assigned an *intermediate right ascension*, α_i, with respect to the CIO (§ 6.7). The equinox right ascension is related to the intermediate right ascension by

$$\alpha_e = \alpha_i - E_o(T). \tag{6.9}$$

Since E_o is the difference between the position of the CIO and the true equinox of date, its value is a function of the position of date of both of these points. Thus,

$$E_o(T) = s - \tan^{-1}\frac{\mathbf{NPB_1^T}\cdot\mathcal{R}_1}{\mathbf{NPB_2^T}\cdot\mathcal{R}_1} \tag{6.10}$$

where s is the CIO locator (§ 6.7), $\mathbf{NPB}_1$ and $\mathbf{NPB}_2$ are row matrices consisting of the first and second rows, respectively, of the matrix product of the frame bias, **B**, (§ 6.5); precession, **P**, (§ 6.6.2); and nutation, **N**, (§ 6.6.3) matrices with respect to the equinox, and $\mathcal{R}_1$ is a row matrix consisting of the first row of Eq. 6.51, the $\mathcal{X}$-$\mathcal{Y}$ matrix for the rotation from the intermediate reference system to the GCRS.

Alternatively, the equation of the equinoxes may be given to an accuracy of 2×10^{-6} s of time by

$$E_e(T) = \frac{1}{15}(\Delta\psi \cos\varepsilon_A + 0.''002\,64 \sin\Omega + 0.''000\,06 \sin 2\Omega) \tag{6.11}$$

provided $\Delta\psi$ and ε_A are given with sufficient accuracy.

6.5 The J2000.0 to ICRS Frame Bias Matrix

The BCRS (§ 6.2) was designed to be aligned as closely as possible to that of the mean equator and equinox of J2000.0 (IAU 1992). However, since the time of its adoption, a small, but significant offset between the mean coordinate system of J2000.0 and the BCRS has been determined to exist. Thus, when the BCRS is used as the celestial reference system, Eq. 6.1 becomes:

$$\mathbf{x}_{CRS} = \mathbf{B\,P\,N\,T\,W\,x}_{TRS} \tag{6.12}$$

where **B** is the frame bias matrix from the mean equator and equinox of J2000.0 to the BCRS. The International Earth Rotation and Reference Systems Service (McCarthy and Petit 2004) conventions have adopted a frame bias matrix in which the position of the pole of the BCRS with respect to the mean CIP of J2000.0 was determined from VLBI (§ 6.2) observations and the position of the origin of right ascension in the BCRS was determined from Lunar Laser Ranging (LLR) observations with respect to the inertial definition of the ecliptic. The value of **B** is:

$$\mathbf{B} = \begin{bmatrix} 0.999\,999\,999\,999\,994\,25 & -7.1 \times 10^{-8} & 8.056 \times 10^{-8} \\ 7.1 \times 10^{-8} & 0.999\,999\,999\,999\,996\,95 & 3.306 \times 10^{-8} \\ -8.056 \times 10^{-8} & 3.306 \times 10^{-8} & 0.999\,999\,999\,999\,996\,208 \end{bmatrix}. \tag{6.13}$$

This is the rotation from the BCRS to the mean CIP of J2000.0 used in *The Astronomical Almanac*. However, if the celestial pole offset positions were determined from LLR (Chapront, Chapront-Touzé, and Francou 2002) or the rotating definition of the ecliptic were used to determine the equinox, a significantly different rotation matrix would be obtained. For details see Hilton and Hohenkerk (2003).

6.6 Precession and Nutation

The first two matrices on the right hand side of Eq. 6.1, **P** and **N**, are the precession and nutation matrices. A coordinate system in which precession, but not nutation, has been applied to the CIP (§ 6.2.3) is described as being the *mean coordinate system of date*. If both precession and nutation have been included, the coordinate system is known as the *true coordinate system of date*. The difference between the mean and true coordinate systems depends on both the position of the equinox and the obliquity of the ecliptic. Thus, the mean coordinate system is often referred to as the *mean equinox and ecliptic of date*, while the true coordinate system is referred to as the *true equinox and ecliptic of date*.

Classically, the origin of right ascension has been the intersection of the ascending node of the ecliptic on the Earth's equator. The orientations of both of these planes are functions of time. Thus, *general precession* includes the motion of the ecliptic as well as the mean motion of Earth's equator. The motion of the poles of the ecliptic, the mean equator of date and the CIP are shown in Fig. 6.2.

The distinction between the mean system of date and the true system of date only applies to those coordinate systems where the origin of right ascension is the equinox. When the CIO (§ 6.7) is used as the origin of right ascension, the coordinate system of date always includes both precession and nutation.

6.6.1 The IAU 2000 Precession-Nutation Theory and IAU 2006/2000A

When it was adopted (IAU 2001b) the IAU 2000 precession-nutation theory was intended to replace both the previous precession (Lieske et al. 1977) and nutation (Seidelmann 1982). In addition to the full high-accuracy precession-nutation theory, IAU 2000A (Mathews, Herring, and Buffett 2002), a second lower accuracy theory, IAU 2000B (McCarthy and Luzum 2003) was formulated for lower accuracy, ≥ 1 mas, applications. Software implementing both of

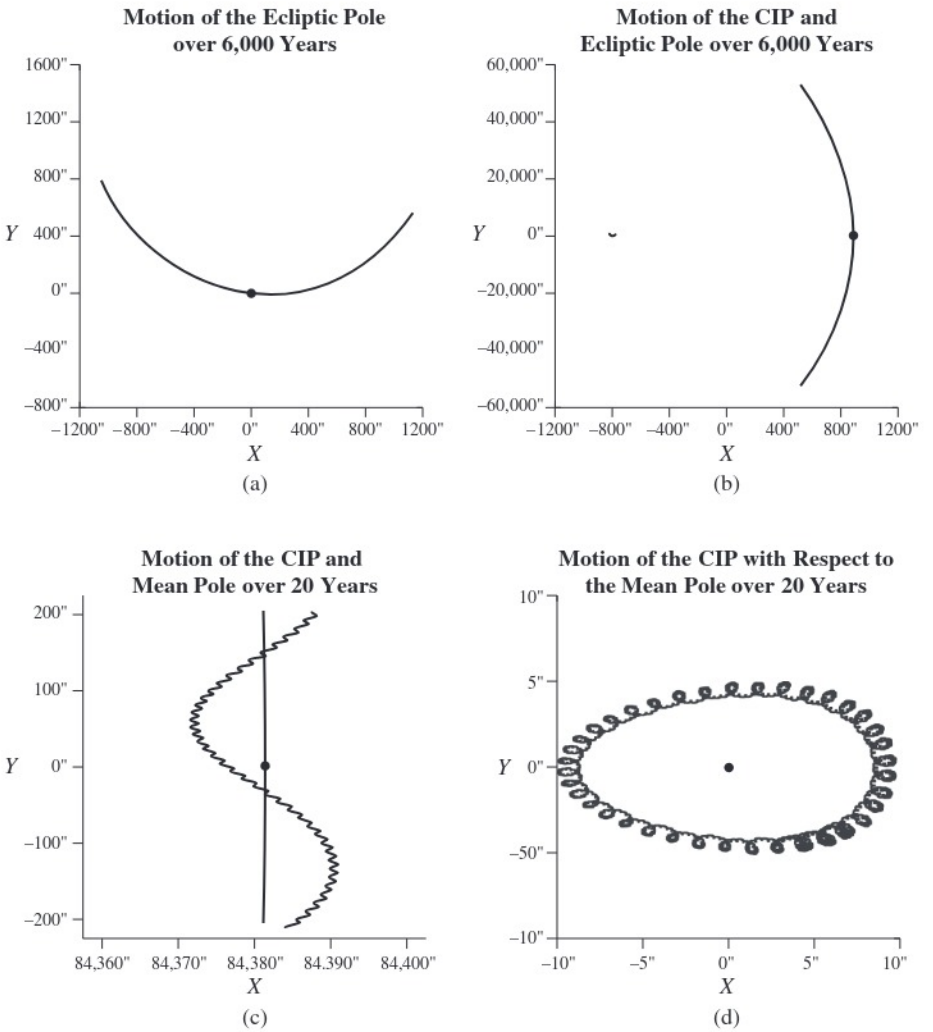


Figure 6.2 The motions of the ecliptic pole, the Earth's mean pole and the CIP on the plane of the sky. **(a)** The motion of the ecliptic over 6,000 years. The dot denotes the position of the ecliptic at J2000.0. **(b)** The motions of the ecliptic and the Earth's mean pole over 6,000 years. The dot denotes the position of the mean pole at J2000.0. **(c)** The motions if the mean pole and the CIP over 20 years. The dots denote the positions of the two poles at J2000.0. The scale in the x-direction has been stretched by a factor of ten. **(d)** The motion of the CIP with respect to the mean pole of date over 20 years. In **(a-c)**, the geometric origin is the position of the ecliptic of J2000.0 and the x-axis is the arc connecting the ecliptic of J2000.0 to the mean pole of J2000.0. In **(d)**, the geometric origin is the mean pole of date and the x-axis is the arc connecting the ecliptic of date to the mean pole of date.

these variants of the original IAU 2000 precession-nutation theory in Fortran are available from the International Earth Rotation and Reference Systems Service (IERS) at URL[1].

However, the change in precession portion of the IAU 2000 precession-nutation theory in Mathews, Herring, and Buffett (2002) only modified the Lieske et al. (1977) precession by the addition of a linear change in the rate and ignored the higher-order terms that, at that time could not be observed, but only computed from theory. Thus, the IAU Working Group on Precession and the Ecliptic (Hilton et al. 2006) recommended the use of the Capitaine, Wallace, and Chapront (2003) precession theory to modify the precession portion of the IAU precession-nutation theory. This was officially adopted by the IAU in 2006 for use beginning on 1 January 2009 (IAU 2008, Res. B1). In this book, the combined models are referred to as *IAU 2006/2000A* precession-nutation.

To be strictly correct, the adoption of the $P03$ (Capitaine, Wallace, and Chapront 2003) precession theory required small changes in the amplitudes of the nutation series arising from the difference in the position of the CIP (§ 6.2.3). The difference is only of significance for the most precise calculations. The differences between the nutation angles, $(\Delta\psi, \Delta\varepsilon)$, using the $P03$ precession and the angles, $\Delta\psi_{2000A}$, $\Delta\varepsilon_{2000A}$, in the IAU 2000A precession theory are

$$\begin{aligned} \Delta\psi - \Delta\psi_{2000A} &= (0.''4697 \times 10^{-6} - 2.''7774 \times 10^{-6} T)\Delta\psi_{2000A} \\ \Delta\varepsilon - \Delta\varepsilon_{2000A} &= -2.''7774 \times 10^{-6} T \Delta\varepsilon_{2000A}. \end{aligned} \tag{6.14}$$

Thus, the maximum adjustment in the amplitudes of the nutation after a century is only $<$ 50 μas (microarcseconds) in longitude and $<$ 30 μas in obliquity. When a distinction between the adjusted and non-adjusted models is important, this book uses the term *IAU 2006/2000A*$_R$ for the former and IAU 2006/2000A for the latter; when unimportant, the term IAU 2006/2000A is used.

Software implementing IAU 2006/2000A precession-nutation theory in Fortran and C may be found in the Naval Observatory Vector Astrometry Subroutines (NOVAS) at URL[2] and in the Standards of Fundamental Astronomy (SOFA) software URL[3].

The NOVAS software is used by the U.S. Nautical Almanac Office in the preparation of its sections of *The Astronomical Almanac*. NOVAS does *not* implement the correction to the nutation in Eqs. 6.14. In other words, it implements IAU 2006/2000A. The decision was made not to implement the correction because it was not mentioned in Hilton et al. (2006), and thus judged not to be part of the IAU standard.

Meanwhile, the SOFA software is used by Her Majesty's Nautical Almanac Office in the preparation of its sections of *The Astronomical Almanac*. SOFA, however, does implement the correction to the nutation in Eqs. 6.14. In other words, it implements IAU 2006/2000A$_R$. The reason for implementing the correction is that it is technically more correct.

In either case, the difference in the output arising from the difference between the NOVAS and the SOFA implementations are too small to be significant in the values tabulated in *The Astronomical Almanac*. The difference does not become significant unless the required accuracy is $\sim$ 60 μas or better.

6.6.2 Precession

Both the ecliptic and the plane of the equator and their intersection, the equinox, are in motion. The component of the precession due to the motion of the ecliptic (§ 6.2.3.1) is known as

precession of the ecliptic [3]. If the equator were fixed, the motion of the ecliptic alone would produce a precession of the equinox of about $12''$ per century and a decrease in the obliquity of the ecliptic of about $47''$per century.

The motion of the equator arises from the torque of the Sun, Moon, and planets on the dynamical figure of the Earth. It is separated into two parts, the *precession of the equator*, the smooth, secular motion of the mean CIP (§ 6.2) of the equator about the pole of the ecliptic, with a period of about 26,000 years, and *nutation*, the sum of the periodic motions, observed in a celestial reference frame, with periods greater than two days of the true CIP around the mean CIP with an amplitude of about $9''$. The combination of precession of the equator and precession of the ecliptic is referred to as *general precession*.

The notation used here follows Lieske et al. (1977). Lieske et al. also give a useful table containing cross-references to the notation used by previous authors. The motion of the ecliptic described by the angles π_A and Π_A, where π_A is the angle between the ecliptic at a fixed epoch and the ecliptic of date, and Π_A is the angular distance from the mean equinox, Υ_0, at the fixed epoch along the fixed ecliptic of epoch to the ascending node of the ecliptic of date (Fig. 6.3). The expressions for π_A and Π_A are given as a pair of polynomials

$$\begin{aligned} P_A &= \sin\pi_A \sin\Pi_A = s_1 t + s_2 t^2 + s_3 t^3 + \cdots \\ Q_A &= \sin\pi_A \cos\Pi_A = c_1 t + c_2 t^2 + c_3 t^3 + \cdots \end{aligned} \tag{6.15}$$

Beginning with the 2009 edition of *The Astronomical Almanac*, the Capitaine, Wallace, and Chapront (2003) expressions for π_A and Π_A derived from DE406 (Standish 1998) are used. Prior to this edition, they were obtained from Newcomb's theory of the Earth's orbital motion about the Sun with modifications to allow for improved determinations of the planetary masses. For continuity, $\pi_A > 0$ for $t >$ J2000.0 and $\pi_A < 0$ for $t <$ J2000.0. Numerical values for the current coefficients s_n and c_n are given in Table 6.2. The precessional effect due to the motion of the ecliptic is described by the angle $\mathcal{CPC}_0$ in Fig. 6.4, referred to as the accumulated precession of the ecliptic, χ_A.

The basic parameter for describing precession of the equator is ψ_A, measured along the ecliptic due to the motion of the equator at epoch t_0. This is related to Newcomb's precessional constant, which has the value P_0 at epoch t_0

$$P_0 = \left(\frac{d\psi_A}{dt} - P_g\right)\cos^{-1}\varepsilon_0 \tag{6.16}$$

where P_g is called the geodesic precession, which is a relativistic non-periodic Coriolis effect amounting to $1.''9196$ per Julian century (Fukushima 2003). The value of ψ_A and the geophysical parameters it depends on must be derived from observations.

The combined effect of precession of the ecliptic and precession of the equator is called the general precession. Lieske et al. (1977) adopted the definition of the accumulated general precession p_A, shown in Fig. 6.5, defined by Newcomb as

$$p_A = \Upsilon\mathrm{R} - \Upsilon_0\mathrm{R}. \tag{6.17}$$

3. Precession of the ecliptic was formerly called *planetary precession* and precession of the equator was formerly called *luni-solar precession* after the source of the torque for each of the components. However, modern observations are now accurate enough that torques caused by the planets make a significant contribution to the precession of the equator. Thus, Hilton et al. (2006) have recommended the older terms be replaced.

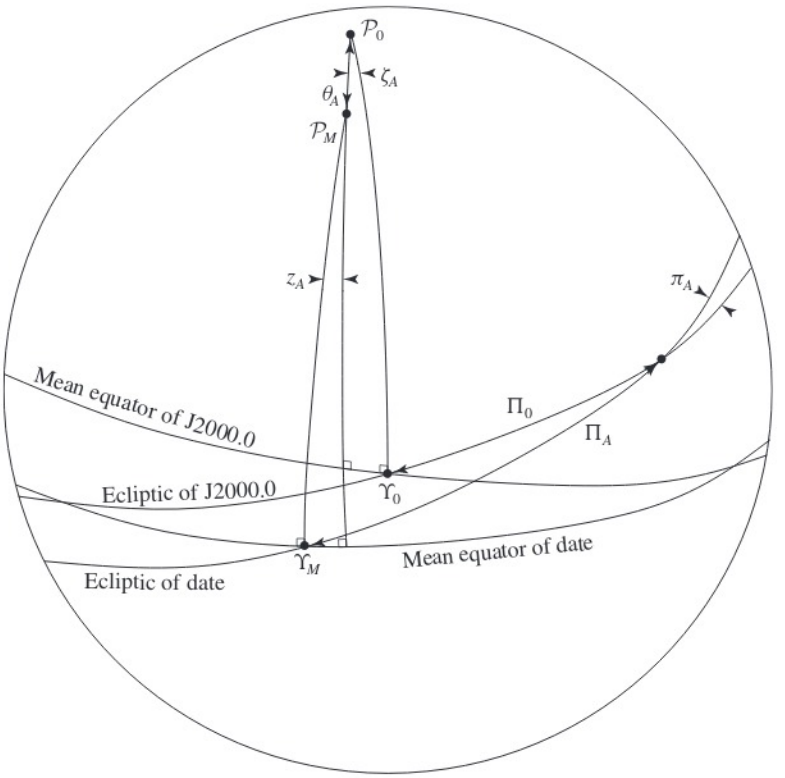


Figure 6.3 The general precession connects the mean equinox of epoch, Υ_0, to the mean equinox of date, Υ_M.

Table 6.2 Coefficients describing the position of the ecliptic of date with respect to the ecliptic of J2000.0

Quantity	($''$cy^{-1})	($''$cy^{-2})	($''$cy^{-3})	($''$cy^{-4})	($''$cy^{-5})
$\sin\pi_A \sin\Pi_A$	4.″199 094	0.″193 987 3	−0.″000 224 66	$-9.''12 \times 10^{-7}$	$1.''20 \times 10^{-8}$
$\sin\pi_A \cos\Pi_A$	−46.″811 015	0.″051 028 3	0.″000 524 13	$-6.''46 \times 10^{-7}$	$-1.''72 \times 10^{-8}$
(Prior to 2006)					
$\sin\pi_A \sin\Pi_A$	4.″197 6	0.″194 47	−0.″000 179	—	—
$\sin\pi_A \cos\Pi_A$	−46.″815 0	0.″050 59	0.″000 344	—	—

Newcomb (1895), however, adopted an expression for p_A that computed the angle Υ_0Q in Fig. 6.5, where Q is the projection of the equinox of date on the ecliptic at the fixed epoch t_0. The rates diverge by about 0.5 mas cy^{-2}. At epoch t_0, however, both procedures reduce to the same rate, p,

$$p(t_0) = p_A(t_0) = \frac{d\psi_A}{dt} - \frac{d\chi_A}{dt}\cos\varepsilon_0 = P_0\cos\varepsilon_0 - P_g - \frac{s_1}{\tan\varepsilon_0}. \tag{6.18}$$

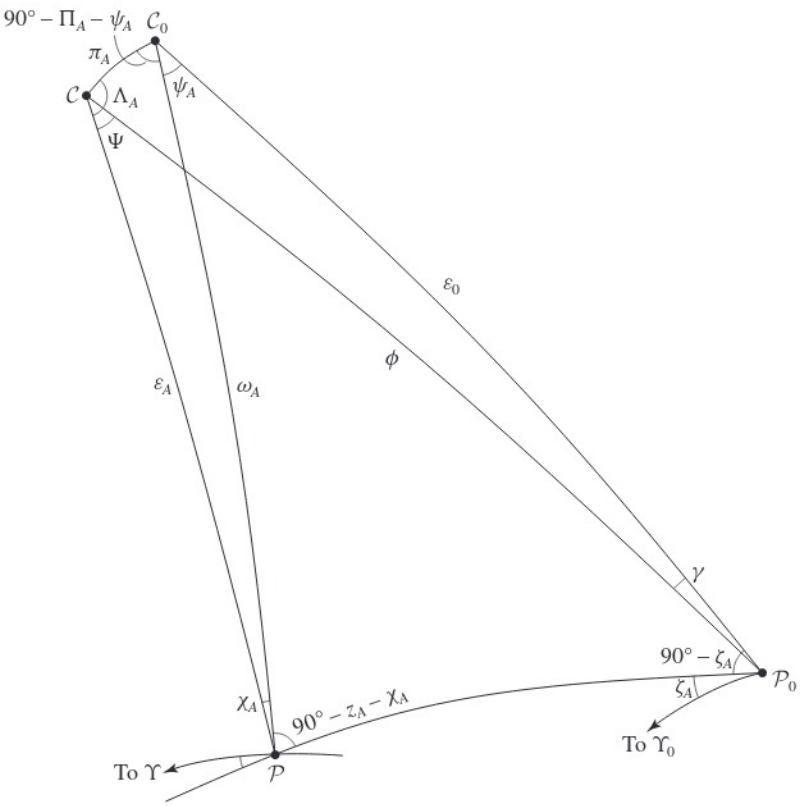


Figure 6.4 The precession angles connect the mean pole of epoch, $\mathcal{P}_0$, to the mean pole of date, $\mathcal{P}$, ecliptic pole of epoch, $\mathcal{C}_0$, and the ecliptic pole of date, $\mathcal{C}$.

The general precession, p_A, may be resolved into general precession in right ascension, m, and general precession in declination, n, where

$$\begin{aligned} p_A &= m\cos\varepsilon_0 + n\sin\varepsilon_0, \\ m &= \frac{d\psi_A}{dt}\cos\varepsilon_0 - \frac{d\chi_A}{dt} = \left(P_0\cos\varepsilon_0 - P_g\right)\cos\varepsilon_0 - \frac{s_1}{\sin\varepsilon_0}, \quad \text{and} \\ n &= \frac{d\psi_A}{dt}\sin\varepsilon_0 = \left(P_0\cos\varepsilon_0 - P_g\right)\sin\varepsilon_0. \end{aligned} \tag{6.19}$$

Prior to the adoption of the IAU 2000 resolutions, the constant of precession was derived from the analysis of the proper motions of stars. In the solar neighborhood the stars are themselves revolving about the center of the galaxy. Fricke (1977) thoroughly reviewed this method, and concluded that Newcomb's precession of the equator should be corrected by $+1\overset{''}{.}10$ per Julian century with an uncertainty of $\pm 0\overset{''}{.}15$ per Julian century. More recently, Mathews, Herring, and Buffett (2002) determined, based on VLBI (§ 6.2) observations of distant objects such as galaxies and QSOs, that Fricke overcorrected the precession of the equator by $0\overset{''}{.}29965$ per Julian century.

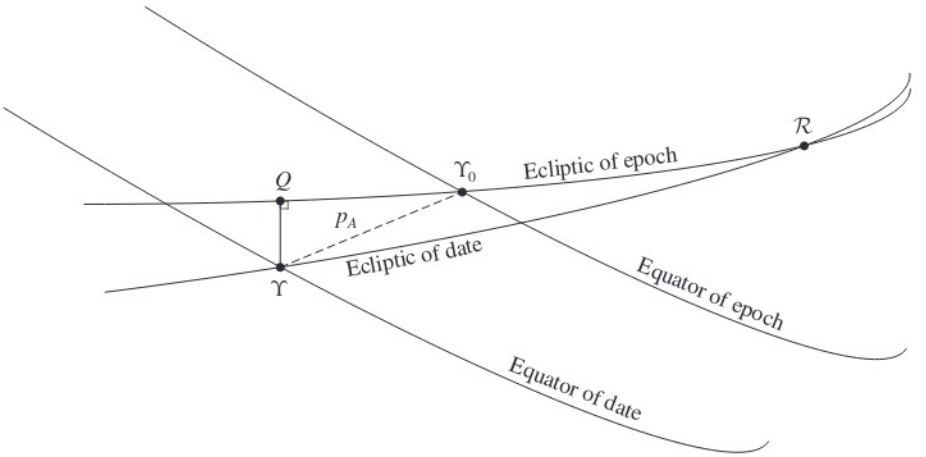


Figure 6.5 The Lieske et al. (1977) general precession in longitude is the difference between the arcs $\Upsilon\mathcal{R}$ and $\Upsilon_0\mathcal{R}$ while the Newcomb (1895) general precession in longitude is the difference between the arcs $\mathcal{Q}\mathcal{R}$ and $\Upsilon_0\mathcal{R}$.

There are several ways of parameterizing the precession. For example, the vector directions of the polar axis of the Earth and the polar axis of the ecliptic may be expressed in terms of polynomials involving time arguments (Fabri 1980; Murray 1983), which are then used to calculate the effects of precession. Williams (1994) presents four different methods in terms of various angles with respect to the ecliptic and rotational poles at a fiducial epoch. Fukushima (2003) presents a scheme for determining the positions of the ecliptic and mean rotational poles of date with respect to the pole of the ICRS rather than the mean pole of epoch. Three of these parameterizations will be discussed here.

6.6.2.1 The Lieske et al. Parameterization

The Lieske et al. (1977) method of parameterization has been the standard used since the time of Newcomb. The IAU adopted it for rigorous calculations in 1976. However, Williams (2002, private communication), Fukushima (2003) and Capitaine, Wallace, and Chapront (2003) have demonstrated that values of the angles z_A and ζ_A near the fiducial epoch are highly sensitive, in a complementary way, to the values adopted for the offset between the mean equator and equinox of epoch and the GCRS (§ 6.2) and, hence, cannot satisfactorily be represented by polynomials in t. Thus, if accuracy better than about 25 mas overall is required, either the frame bias has to be introduced as a separate rotation, as in Eq. 6.12, or a different parameterization that does not suffer from this difficulty should be adopted.

The accumulated precession angles ζ_A, z_A, and θ_A are referred to a base epoch t_0. These angles are shown with respect to the equator and ecliptic in Fig. 6.3. A detailed view of these angles with respect to the poles of the equator and ecliptic are shown in Fig. 6.4 and with respect to the mean equator and equinox of epoch and the mean equator and equinox of date in Fig. 6.4. The mean pole of the equator at t_0 is the point $\mathcal{P}_0$ and the pole of the ecliptic

Table 6.3 IAU recommended coefficients (Hilton et al. 2006) describing the position of the ecliptic of date with respect to the ecliptic of J2000.0

Quantity	($''$)	($''$cy^{-1})	($''$cy^{-2})	($''$cy^{-3})	($''$cy^{-4})	($''$cy^{-5})
ζ_A	2.650 545	2306.083 227	0.298 8499	0.018 018 28	-5.971×10^{-6}	-3.173×10^{-7}
z_A	−2.650 545	2306.077 181	1.092 7348	0.018 268 37	$-2.859\,6 \times 10^{-5}$	-2.904×10^{-7}
θ_A	—	2004.191 903	−0.429 4934	−0.041 822 64	-7.089×10^{-6}	-1.274×10^{-7}
ψ_A	—	5038.481 507	−1.079 0069	−0.0012 140 45	0.000 132 851	-9.51×10^{-8}
ω_A	84381.406 000	−0.027 754	0.051 2623	−0.007 725 03	-4.67×10^{-7}	3.337×10^{-7}
ϵ_A	84381.406 000	−46.836 769	−0.000 1831	0.002 003 40	-5.76×10^{-7}	-4.34×10^{-8}
χ_A	—	10.556 403	−2.381 4292	−001 211 97	0.000 170 663	-5.60×10^{-8}
γ_{J2000}	—	10.556 403	0.493 2044	−0.000 312 38	-2.788×10^{-6}	2.60×10^{-8}
ϕ_{J2000}	84381.406 000	−46.811 015	0.051 1269	0.000 532 89	-4.40×10^{-7}	-1.76×10^{-8}
Ψ_{J2000}	—	5038.481 507	1.558 4176	−0.000 185 22	−0.000 026 452	-1.48×10^{-8}
γ_{GCRS}	−0.052 928	10.556 378	0.493 2044	−0.000 312 38	-2.788×10^{-6}	2.60×10^{-8}
ϕ_{GCRS}	84381.412 819	−46.811 016	0.051 1268	0.000 532 89	-4.40×10^{-7}	-1.76×10^{-8}
Ψ_{GCRS}	−0.041 775	5038.481 484	1.558 4175	−0.000 185 22	−0.000 026 452	-1.48×10^{-8}

Table 6.4 Lieske et al. (1977) coefficients describing the position of the ecliptic of date with respect to the ecliptic of J2000.0. These values are *obsolete*. They are included for working with data prior to 2006. See Table 6.3 for the current recommended coefficients.

Quantity	($''$ cy^{-1})	($''$ cy^{-2})	($''$ cy^{-3})
ζ_A	2306.2181	0.301 88	0.017 998
z_A	2306.2181	1.094 68	0.018 203
θ_A	2004.3109	−0.426 65	−0.041 833

is point $\mathcal{C}_0$. At time t, $\mathcal{P}_0$ has moved to $\mathcal{P}$ and $\mathcal{C}_0$ to $\mathcal{C}$. Assume a right-handed set of three-dimensional Cartesian coordinate axes with its geometric origin at the center of the sphere, x-axis pointing to Υ_0, where the equator and ecliptic meet (the equinox) at epoch t_0. The y-axis is 90° away in an easterly direction along the equator, and the z-axis points toward the pole $\mathcal{P}_0$. Initially, precession will move $\mathcal{P}_0$ in a direction that is about $1''$ to the east of the direction toward Υ_0. Over time, the movement of the pole of the ecliptic will cause the pole of the equator to move in a somewhat different direction. The polynomial expressions for these angles are given in Table 6.3. The coefficients are from the Capitaine, Wallace, and Chapront (2003) *P*03 precession and are recommended by the IAU (Hilton et al. 2006). The coefficients used prior to the 2006 edition of *The Astronomical Almanac* are in Table 6.4. These older coefficients were derived in Lieske et al. (1977).

Implementation of the Lieske et al. parameterization begins with a rotation of $-\zeta_A$ about the z-axis. The great circle from $\mathcal{P}_0$ to the x'-axis passes through the mean pole of date, $\mathcal{P}$, as

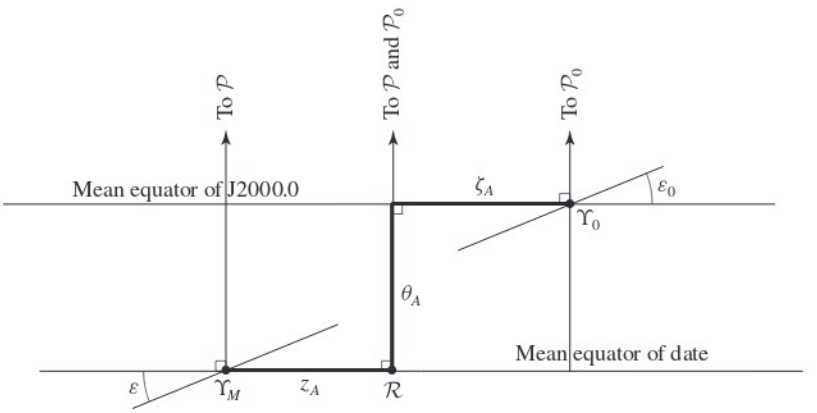


Figure 6.6 The Lieske et al. (1977) precession angles relate the mean equator and equinox of epoch, Υ_0, to the mean equator and equinox of date, Υ_M.

well (see Fig. 6.5). Thus, this great circle is perpendicular to *both* the mean equator of epoch and the mean equator of date (see Fig. 6.5). Next, a rotation of $+\theta_A$ about the y'-axis moves from the mean pole of epoch, $\mathcal{P}_0$ to the mean pole of date, $\mathcal{P}$ (Fig. 6.5). Equivalently, this rotation maps the mean equator of epoch onto the mean equator of date (Fig. 6.6). The z''-axis now points to the mean pole of date, $\mathcal{P}$ and the x''-axis points to $\mathcal{R}$ in Fig. 6.6. Finally, there is a rotation of $-z_A$ about the z''-axis so that the x'''-axis points toward Υ_M, the mean equinox of date. Thus, the precession matrix from the mean equator and equinox of epoch, t_0, to the mean equator and equinox date, t, is made up of these rotations

$$\mathbf{P} = \mathbf{R}_3(-z_A)\mathbf{R}_2(+\theta_A)\mathbf{R}_3(-\zeta_A). \tag{6.20}$$

This equation expands to

$$\mathbf{P} = \begin{bmatrix} \cos z_A \cos\theta_A \cos\zeta_A - \sin z_A \sin\zeta_A & -\cos z_A \cos\theta_A \sin\zeta_A - \sin z_A \cos\zeta_A & -\cos z_A \sin\theta_A \\ \sin z_A \cos\theta_A \cos\zeta_A + \cos z_A \sin\zeta_A & -\sin z_A \cos\theta_A \sin\zeta_A + \cos z_A \cos\zeta_A & -\sin z_A \sin\theta_A \\ \sin\theta_A \cos\zeta_A & -\sin\theta_A \sin\zeta_A & \cos\theta_A \end{bmatrix}. \tag{6.21}$$

Having calculated the precession angles for the matrix $\mathbf{P}$, the inverse matrix $\mathbf{P}^{-1}$ can be calculated in various ways. For example,

$$\begin{aligned} \mathbf{P} &= \mathbf{R}_3^{-1}(-\zeta_A)\mathbf{R}_2^{-1}(+\theta_A)\mathbf{R}_3^{-1}(-z_A) \\ &= \mathbf{R}_3^T(-\zeta_A)\mathbf{R}_2^T(+\theta_A)\mathbf{R}_3^T(-z_A) \\ &= \mathbf{R}_3(+\zeta_A)\mathbf{R}_2(-\theta_A)\mathbf{R}_3(+z_A) \end{aligned} \tag{6.22}$$

where use has been made of the property that the inverse of a rotation matrix is its transpose (i.e., it is orthogonal).

Modern precession angles and rates adopted. Beginning with the 2009 edition of *The Astronomical Almanac* the precession angles are those of the Capitaine, Wallace, and Chapront (2003) *P*03 solution. The values for the rate of precession, p [4], obliquity at epoch, ε_0, and rate of change in obliquity, $\Delta\varepsilon$ [5] at epoch J2000.0 are:

$$\begin{aligned} \mathrm{p} &= 5028.''796\,195 \text{ Julian cy}^{-1} \\ \varepsilon_0 &= 23^\circ\ 26'\ 21.''40600 \\ \Delta\varepsilon &= -0.''025\,754 \text{ Julian cy}^{-1}. \end{aligned} \tag{6.23}$$

The geodesic precession, P_g, contribution to the precession is (Fukushima 2003)

$$\mathrm{P}_g = 1.''9196 \pm 0.''0003 \text{ Julian cy}^{-1}. \tag{6.24}$$

The expressions at J2000.0 for the rates per Julian century of general precession, in longitude, p; right ascension, m; and declination, n; and π, the rate of rotation of the ecliptic, are

$$\begin{aligned} p = \frac{d}{dt}(p_A)|_{t=0} &= 5028.''796\,195 + 2.''210\,8696T + 0.''000\,238\,92T^2 \\ &\quad - 9.''5428 \times 10^{-5}T^3 - 1.''915 \times 10^{-7}T^4 \\ m = \frac{d}{dt}(\zeta_A + z_A)|_{t=0} &= 4612.''160\,408 + 2.''783\,1694T + 0.''108\,859\,95T^2 \\ &\quad - 0.''000\,138\,268T^3 - 3.''0385 \times 10^{-6}T^4 \\ n = \frac{d}{dt}(\theta_A)|_{t=0} &= 2004.''191\,903 - 0.''858\,9868T - 0.''125\,467\,92T^2 \\ &\quad - 0.''000\,028\,356T^3 - 6.''37 \times 10{-}7T^4 \\ \pi = \frac{d}{dt}(\pi_A)|_{t=0} &= 46.''998\,973 - 0.''066\,9852T - 0.''000\,376\,77T^2 \\ &\quad + 4.''52 \times 10^{-7}T^3 - 1.''1 \times 10^{-8}T^4. \end{aligned}$$

The 2006 through 2008 editions of *The Astronomical Almanac* used the precession portion of the IAU 2000A precession-nutation theory. However, the difference between the IAU 2000A precession and the *P*03 precession during that interval is insignificant either at the precision tabulated in *The Astronomical Almanac* or at the level of accuracy to which observations can currently be made. The IAU 2000A precession only corrects the linear portion of the Lieske et al. (1977) precession theory. Thus, the higher order coefficients are inconsistent with dynamical theory. Currently, the effect of the change to the higher order coefficients is too small to be observed, and hence, has to be derived from a dynamical theory as was done for *P*03.

4. With the recent improvement in the precession theory the precession of the equator, ψ_A, rather than the precession constant, p, is now considered to be the fundamental quantity.

5. Williams (1994) showed that there is a small secular change in the obliquity of the ecliptic arising from a small asymmetry in the inclination of the Moon to the ecliptic as a function of the position of its nodes on the ecliptic.

Precession angles and rates adopted by the IAU (1976). Prior to the 2006 edition of *The Astronomical Almanac* the basis for precession was Lieske et al. (1977) as modified by Lieske (1979). The following values were adopted constants at epoch J2000.0

$$\begin{aligned} \mathrm{p} &= 5029.''0966 \text{ Julian cy}^{-1} \\ \mathrm{P}_1 &= -0.''00369 \text{ Julian cy}^{-1} \\ \mathrm{P}_g &= 1.''92 \text{ Julian cy}^{-1} \\ \varepsilon_0 &= 23^\circ\ 26'\ 21.''448. \end{aligned} \tag{6.25}$$

The expressions at epoch t_0 for the rates per Julian century of general precession, in longitude, p; right ascension, m; and declination, n, and π the rate of rotation of the ecliptic, are

$$\begin{aligned} p &= \frac{d}{dt}(p_A)|_{t=0} = 5029.''0966 + 2.''222\,26T - 0.''000\,042T^2 \\ m &= \frac{d}{dt}(\zeta_A + z_A)|_{t=0} = 4612.''4362 + 2.''79312T - 0.''0002\,78T^2 \\ n &= \frac{d}{dt}(\theta_A)|_{t=0} = 2004.''3109 - 0.''853\,30T - 0.''000\,217T^2 \\ \pi &= \frac{d}{dt}(\pi_A)|_{t=0} = 47.''0029 - 0.''066\,03T + 0.''000\,598T^2. \end{aligned}$$

6.6.2.2 Other Representations of Precession

In addition to the set of angles used by Newcomb (1898) and Lieske et al. (1977) to parameterize the precession, Williams (1994) summarized four other methods of parameterizing the precession matrix using the various angles shown in Fig. 6.6.

The Fukushima-Williams parameterization.
Fukushima (2003) parameterized the precession with the angles: γ, the angle between the ecliptic pole of epoch, $\mathcal{C}_0$, and the ecliptic pole of date, $\mathcal{C}$, as viewed from the pole, $\mathcal{P}_0$, of the initial reference system [6]; ϕ, the arc from $\mathcal{P}_0$ to $\mathcal{C}$; Ψ, the angle from $\mathcal{P}_0$ to the mean pole of date, $\mathcal{P}$, as viewed from $\mathcal{C}$; and ε_A, the obliquity of the mean ecliptic of date. The precession matrix, $\mathbf{P}$, thus becomes:

$$\mathbf{P} = \mathbf{R}_1(-\varepsilon_A)\mathbf{R}_3(-\Psi)\mathbf{R}_1(\phi)\mathbf{R}_3(\gamma). \tag{6.26}$$

If the initial reference system is the mean equator and ecliptic of J2000.0, then the rotation matrices are the same as those in Eq. 37 of Williams (1994). Fukushima, however, chose the initial reference system to be the GCRS. In this case,

$$\mathbf{P}|_{T=0} = \mathbf{B} \tag{6.27}$$

where $\mathbf{B}$ is the frame bias matrix from the GCRS to the mean equator and equinox of J2000.0. Two sets of the coefficients for Ψ, ϕ, and γ as a function of time are given in Table 6.3.

6. Usually either the mean pole of J2000.0 or the pole of the BCRS.

Those with the subscript J2000 use the mean equator and equinox of J2000.0 as the initial reference frame while those coefficients with the subscript GCRS use the GCRS as the initial reference frame.

The Capitaine, Wallace, and Chapront parameterization. The Capitaine, Wallace, and Chapront (2003) parameterization separates the precession of the equator, ψ_A and ω_A (the precession in obliquity) from the precession of the ecliptic P_A and Q_A (§ 6.6.2). Capitaine et al. also recommend determining the precession matrix using Eq. 35 of Williams (1994),

$$\mathbf{P} = \mathbf{R}_3(\chi_A)\mathbf{R}_1(-\omega_A)\mathbf{R}_3(-\psi_A)\mathbf{R}_1(\varepsilon_0) \tag{6.28}$$

where χ_A is the spherical angle from the ascending node of the ecliptic of epoch along the mean equator of date to the mean equinox of date shown in Fig. 6.1, or, equivalently, the angle from the ecliptic pole of epoch to the ecliptic pole of date with its apex at the mean equatorial pole of date shown in Fig. 6.4. The angle χ_A is determined from the already known parameters for the precession using:

$$\begin{aligned} \cos\varepsilon_A &= \cos\pi_A \cos\omega_A - \sin\pi_A \sin\omega_A \cos(\Pi_A + \psi_A) \\ \sin\chi_A &= \frac{\sin\pi_A}{\sin\varepsilon_A} \sin(\Pi_A + \psi_A). \end{aligned} \tag{6.29}$$

6.6.2.3 Rigorous Reduction for Precession

The most convenient method to account for precession in transforming mean equatorial rectangular coordinates is to use the precession matrix $\mathbf{P}$ as follows:

$$\mathbf{r} = \mathbf{P}\,\mathbf{r}_0 \quad \text{or} \quad \mathbf{r}_0 = \mathbf{P}^{-1}\mathbf{r} \tag{6.30}$$

which transforms the position vector $\mathbf{r}_0$ from the mean equator and equinox of epoch t_0, to the position vector $\mathbf{r}$ with respect to the mean equator and equinox of date, and vice versa. The matrix $\mathbf{P}$ is evaluated using one of the sets of precession angles given above.

To convert quickly from the right ascension and declination of J2000.0, (α_0, δ_0), to the right ascension and declination of date, (α, δ), the precession may be rendered

$$\begin{aligned} \sin(\alpha - z_A)\cos\delta &= \sin(\alpha_0 + \zeta_A)\cos\delta_0 \\ \cos(\alpha - z_A)\cos\delta &= \cos(\alpha_0 + \zeta_A)\cos\theta_A\cos\delta_0 - \sin\theta_A\sin\delta_0 \\ \sin\delta &= \cos(\alpha_0 + \zeta_A)\sin\theta_A\cos\delta_0 + \cos\theta_A\sin\delta_0. \end{aligned} \tag{6.31}$$

The inverse of these equations are

$$\begin{aligned} \sin(\alpha_0 + \zeta_A)\cos\delta_0 &= +\sin(\alpha - z_A)\cos\delta \\ \cos(\alpha_0 + \zeta_A)\cos\delta_0 &= +\cos(\alpha - z_A)\cos\theta_A\cos\delta + \sin\theta_A\sin\delta \\ \sin\delta_0 &= -\cos(\alpha - z_A)\sin\theta_A\cos\delta + \cos\theta_A\sin\delta. \end{aligned} \tag{6.32}$$

6.6.2.4 Approximate Reduction for Precession

Approximate formulae, accurate to about 30 arcseconds, 100 years from J2000.0, for the reduction of coordinates and orbital elements referred to the mean equinox and equator or ecliptic of date, t, are:

For reduction to J2000.0	For reduction from J2000.0
$\alpha_0 = \alpha - M - N \sin\alpha_m \tan\delta_m$	$\alpha = \alpha_0 + M + N \sin\alpha_m \tan\delta_m$
$\delta_0 = \delta - N \cos\alpha_m$	$\delta = \delta_0 + N \cos\alpha_m$
$\lambda_0 = \lambda - a + b \cos(\lambda + c') \tan\beta_0$	$\lambda = \lambda_0 + a - b \cos(\lambda_0 + c) \tan\beta$
$\beta_0 = \beta - b \sin(\lambda + c')$	$\beta = \beta_0 + b \sin(\lambda_0 + c)$
$\Omega_0 = \Omega - a + b \sin(\Omega + c') \cot i_0$	$\Omega = \Omega_0 + a - b \sin(\Omega_0 + c) \cot i$
$i_0 = i - b \cos(\Omega + c')$	$i = i_0 + b \cos(\Omega_0 + c)$
$\omega_0 = \omega - b \sin(\Omega + c') \csc i_0$	$\omega = \omega_0 + b \sin(\Omega_0 + c) \csc i$

where the subscript 0 refers to epoch J2000.0, and α_m and δ_m refer to the mean epoch; with sufficient accuracy

$$\begin{aligned}
\alpha_m &= \alpha - \frac{1}{2}(M + N \sin\alpha \tan\delta) \\
\delta_m &= \delta - \frac{1}{2} N \cos\alpha_m \\
&\text{or} \\
\alpha_m &= \alpha_0 + \frac{1}{2}(M + N \sin\alpha_0 \tan\delta_0) \\
\delta_m &= \delta_0 + \frac{1}{2} N \cos\alpha_m .
\end{aligned} \tag{6.33}$$

The precession angles, to a precision of $1''$, from expressions in Table 6.3 are

$$\begin{aligned}
M = (\zeta_A + z_A) &= 1\overset{\circ}{.}281\,16T + 0\overset{\circ}{.}000\,39T^2 + 0\overset{\circ}{.}000\,01T^3 \\
N = \theta_A &= 0\overset{\circ}{.}556\,72T - 0\overset{\circ}{.}000\,12T^2 - 0\overset{\circ}{.}000\,01T^3 \\
a = p_A &= 1\overset{\circ}{.}396\,89T + 0\overset{\circ}{.}000\,31T^2 \\
b = \pi_A &= 0\overset{\circ}{.}013\,06T - 0\overset{\circ}{.}000\,01T^2 \\
c = 180^\circ - \Pi_m + \frac{1}{2}a &= 5\overset{\circ}{.}125\,89 + 0\overset{\circ}{.}939\,54T + 0\overset{\circ}{.}000\,11T^2 \\
c' = 180^\circ - \Pi_m - \frac{1}{2}a &= 5\overset{\circ}{.}125\,89 - 0\overset{\circ}{.}457\,34T - 0\overset{\circ}{.}000\,20T^2
\end{aligned} \tag{6.34}$$

where Π_m is the accumulated longitude of the node of the ecliptic of date on the mean of the ecliptic of date and the ecliptic of J2000.0. This is a different definition of Π_m than was used with the previous Lieske et al. (1977) based precession constants. In the older system $\Pi_m = \Pi_A(\tau = \frac{1}{2}t,\ T = 0)$, where τ is the time from the epoch of J2000.0 to an arbitrary intermediate epoch and T is the time from the intermediate epoch to the date of interest, in centuries. This transformation gives the longitude of the ecliptic of J2000.0 on the ecliptic of the intermediate epoch with respect to the equinox of the intermediate epoch. Unlike the Lieske et al. precession, the Capitaine, Wallace, and Chapront (2003) precession was not formulated to transform to an intermediate epoch. Thus, the older *Explanatory Supplement*

formulation for the Π_m is used (Nautical Almanac Offices of UK and USA 1961, pp. 35-38). This transformation gives the longitude of the ecliptic of J2000.0 on the ecliptic of the intermediate epoch with respect to the node of the mean equator of J2000.0. To first order, the difference in the value Π_m determined in this manner is that precession of the equator has not been included. Thus, this formulation is inherently less accurate than the one used with the Lieske et al. precession.

Formulae, valid over short periods, for the reduction from the mean equinox and equator or ecliptic of epoch t_1 (e.g., the middle of the year) to date ($t = t_1 + \tau$), where τ is a fraction of a year and $|\tau| < 1$, are

$$\begin{aligned}
\alpha &= \alpha_1 + \tau(m + n \sin\alpha_1 \tan\delta_1) & \delta &= \delta_1 + \tau\, n \cos\alpha_1 \\
\lambda &= \lambda_1 + \tau[p - \pi \cos(\lambda_1 + 6^\circ)\tan\beta] & \beta &= \beta_1 + \tau\, \pi \sin(\lambda_1 + 6^\circ) \\
\Omega &= \Omega_1 + \tau[p - \pi \sin(\Omega_1 + 6^\circ)\cot i] & i &= i_1 + \tau\, \pi \cos(\Omega_1 + 6^\circ) \\
\omega &= \omega_1 + \tau\, \pi \sin(\Omega_1 + 6^\circ)\csc i
\end{aligned} \tag{6.35}$$

where p, m, n, and π are the annual rates, evaluated at t_1.

6.6.2.5 Newcomb's Precession

Newcomb's precession angles are included as they are relevant for the transformation of some old star catalogs. Since Newcomb's value of the precession constant (Newcomb 1895) came into general use, several representations have been used for the practical realization of the accumulated precession angles denoted by ζ_0, z, and θ, to distinguish them from Lieske's precession angles ζ_A, z_A, and θ_A. Formulations are given in the *The Explanatory Supplement* (Nautical Almanac Offices of UK and USA 1961). There are also developments by: Andoyer (1911), from which the discussion by Woolard and Clemence (1966) was drawn; the introduction to the SAOC (1966); and a more recent discussion by Kinoshita (1975) repeated by Aoki et al. (1983). The formulae in Kinoshita and Aoki et al. are carried to one more significant digit than those in Andoyer.

Among the various representations, differences in the accumulated precession angles of the order of 1 mas are found in as short a time as 30 years. For example, a comparison of results from Woolard and Clemence (1966), Kinoshita (1975), and the *Explanatory Supplement* (Nautical Almanac Offices of UK and USA 1961) for the accumulated precession angles ζ_0, z, and θ between equinox and equator for the epoch B1950.0 (JD 243 3282.423 TT) and the equinox and equator of 1984 Jan $1^{\mathrm{d}}\ 0^{\mathrm{h}}$ is given in Table 6.5.

Table 6.5 Precession angles with respect to the mean equator and equinox of B1950.0 at 1984 Jan. $1^d\ 0^h$ for various precession theories

Angle	Woolard & Clemence (arcsec.)	Kinoshita (arcsec.)	Explanatory Supplement (arcsec.)	Adopted (arcsec.)
ζ_0	783.709 25	783.709 38	783.707 98	783.7092
z	783.800 93	783.801 06	783.799 42	783.8009
θ	681.388 30	681.388 49	681.387 32	681.3883

The results of the Kinoshita formulation agree with those of Woolard & Clemence at the 0.1 mas level. The Explanatory Supplement disagrees with these results at the 1 to 2 mas level. This disagreement is caused by the neglect of higher-order terms in the Explanatory Supplement (p.30). The Andoyer (Woolard and Clemence 1966) expressions for the precession angles are

$$\begin{aligned}
\zeta_0 &= (23\,035.''545 + 139.''720t + 0.''060t^2)\tau + (30.''240 - 0.''270t)\tau^2 + 17.''995\tau^3 \\
z &= (23\,035.''545 + 139.''720t + 0.''060t^2)\tau + (109.''480 + 0.''390t)\tau^2 + 18.''325\tau^3 \\
\theta &= (20\,051.''12 - 85.''29t - 0.''37t^2)\tau + (-42.''65 - 0.''37t)\tau^2 - 41.''80\tau^3
\end{aligned} \tag{6.36}$$

where t is the interval in units of 1000 tropical years of 365242.198782 days between the initial fixed epoch and B1850.0, and τ is difference between the time from the epoch of date to B1850.0 and t.

The rates of general precession in right ascension, m_0, and declination, n_0, are

$$\begin{aligned}
m_0 &= \frac{\partial}{\partial\tau}(\zeta_0 + z)|_{t=0} \\
&= 46\,071.''090 + 279.''440\,\tau + 0.''120\,\tau^2 \\
n_0 &= \frac{\partial}{\partial\tau}(\theta_0)|_{t=0} \\
&= 20\,051.''12 - 85.''29\,\tau - 0.''37\,\tau^2.
\end{aligned} \tag{6.37}$$

6.6.2.6 Differential Precession and Nutation

Differential precession and nutation may be added to the observed difference in the right ascension and declination, $\Delta\alpha$ and $\Delta\delta$, of an object relative to a comparison star to obtain the differences in the mean place for a standard epoch (e.g., J2000.0 or the beginning of the year). The differences $\Delta\alpha$ and $\Delta\delta$ are in the sense "object minus comparison star," and the corrections are in the same units as $\Delta\alpha$ and $\Delta\delta$. In the correction to right ascension the same units must be used for $\Delta\alpha$ and $\Delta\delta$.

$$\begin{aligned}
\text{correction to right ascension} &= e \tan\delta\ \Delta\alpha - f \sec^2\delta\ \Delta\delta, \\
\text{correction to declination} &= f\ \Delta\alpha, \\
\text{where } e &= -\cos\alpha(nt + \sin\varepsilon\ \Delta\psi) - \sin\alpha\ \Delta\varepsilon, \\
f &= +\sin\alpha(nt + \sin\varepsilon\ \Delta\psi) - \cos\alpha\ \Delta\varepsilon, \quad \text{and} \\
\varepsilon &= 23.^\circ44
\end{aligned} \tag{6.38}$$

where t is the time from the standard epoch to the time of observation, and n the rate of precession in declination. If t is in years, then n is in radians per year, and $\Delta\psi$ and $\Delta\varepsilon$ are the nutations in longitude and obliquity at the time of observation, in radians. The errors in arc units caused by using these formulae are of order $10^{-8}\ t^2 \sec^2\delta$ multiplied by the displacement in arc from the companion star.

6.6.3 Nutation

The non-secular motion of the Earth's rotation axis with respect to a space-fixed coordinate system is called *nutation*, and consists of both forced and free components. The forced component of the nutation arises from the torque produced by the gravitational attraction

of the Moon and, to a lesser extent, the Sun and planets on the equatorial bulge and any deformations of the Earth. It is usually modeled as a series of quasi-periodic motions whose periods and amplitudes depend on the source of the torque and the motion of the celestial bodies with respect to the rotating Earth. Setting the external force to zero in the equations of motion gives the particular integral, or free motion. This free motion depends on the constitution of the Earth including properties such as elasticity of the mantle and the size and shapes of the inner and outer cores. It is excited by internal processes, and can be determined only from observations. If the Earth were a rigid body, it would be possible to compute the coefficients of the forced nutation terms. However, like the free motion, some of the parameters of the non-rigid Earth can be determined only by observation of its motion in space.

The separation of the instantaneous axis of rotation and instantaneous axis of the principal moment of inertia gives rise to nutation components with periods that are approximately diurnal and amplitudes as large as a few milliarcseconds. In addition, the figure of the Earth is slightly tri-axial, meaning that there is a small difference between the magnitudes of the two principal moments of inertia that lie nearly in the Earth's equator as defined by the axis of rotation. This difference in the equatorial principal moments of inertia also gives rise to nearly diurnal and semidiurnal nutation components with amplitudes of no more than a few microarcseconds. Although these short-period components of the nutation are properly part of the nutation, they cannot be separated observationally from notions due to the movement of the Earth's axis within the body of the Earth. Consequently, the CIP (§ 6.2.3) is chosen to be along the axis of figure for the mean surface of a model of Earth in which the motions with periods *greater than or equal to two days* within a geocentric celestial reference frame have zero amplitude. This pole has no nearly diurnal components of motion with respect to either a space-fixed or an Earth-fixed coordinate system, and components of nutation with periods shorter than two days become part of the polar motion by definition.

The CIP is the axis about which the diurnal rotation of the Earth is applied in the transformation between celestial and terrestrial frames, so it is often referred to as the axis of rotation in general discussions. It may also be referred to as the true celestial pole of date (IAU 1976).

In the 1984 through 2006 editions of *The Astronomical Almanac*, the polar motion was measured with respect to the *celestial ephemeris pole*, chosen to be along the axis of figure for the mean surface of a model of Earth in which the free motions have zero amplitude. Prior to 1984, the ephemeris pole was chosen to be the instantaneous axis of rotation. Atkinson (1973); Atkinson (1975), however, pointed out that use of the instantaneous pole of rotation led to quasi-diurnal motions, and thus, it was not the best reference pole.

6.6.3.1 The IAU 2000A Theory of Nutation

The IAU 2000A Theory of Nutation was computed for the celestial intermediate pole by determining the nutations in longitude and obliquity of a rigid Earth (Souchay et al. 1999), and making modifications for the non-rigid Earth (Mathews, Herring, and Buffett 2002) in such a fashion that there are no nearly diurnal motions of this celestial pole with respect to either space-fixed or body-fixed (crust-fixed) coordinates. A table of the nutation amplitudes and the fundamental arguments is available in Kaplan (2005). Software implementing the data in these tables are available on the world wide web from the International Earth Rotation

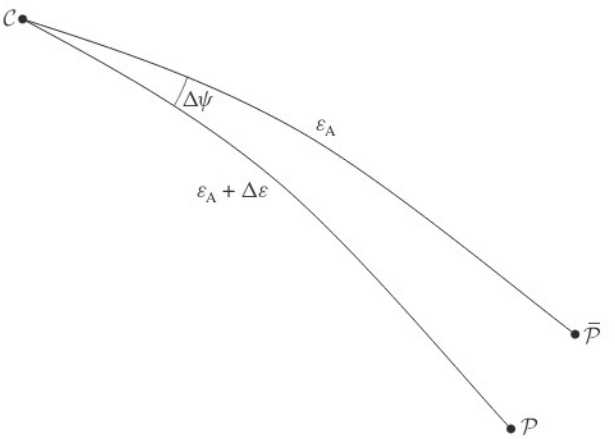


Figure 6.7 The nutations in longitude, $\Delta\psi$, and latitude, $\Delta\varepsilon$, connect the mean pole of date, $\overline{\mathcal{P}}$, to the CIP, $\mathcal{P}$, via the ecliptic pole of date, $\mathcal{C}$.

and Reference Systems Service (IERS) (URL[1]), from the USNO (URL[2]) NOVAS subroutines, and from SOFA (URL[3]).As explained in § 6.6.1 each of these software packages implements the IAU 2000 nutation in slightly different ways.

Nutation describes the motion of the CIP, $\overline{\mathcal{P}}$, relative to the mean pole, $\mathcal{P}$, and may be resolved into the components $\Delta\psi$ in longitude and $\Delta\varepsilon$ in obliquity, shown in Fig. 6.7. The nutation matrix, $\mathbf{N}$, is a sequence of three rotations which uses these angles and the mean obliquity of the ecliptic of date, ε_A, to transform equatorial coordinates referred to the Earth's mean pole of date to the CIP.

The rotations are a rotation of ε_A about the x-axis, which transforms the xy-plane from the mean equator of date to the mean ecliptic of date, followed by a rotation of $-\Delta\psi$ about the z-axis, which applies nutation in longitude and rotates the x-axis, pointing toward the mean equinox of date Υ_M, to the true equinox of date Υ_T, and lastly a rotation of $-\varepsilon$, the true obliquity of date, about the x-axis, which rotates the xy-plane to the true equator of date. The expressions for the mean and true obliquity of date are

$$\begin{aligned}\varepsilon_A &= 23^\circ\, 26'\, 21.''40600 - 46.''836\,769T - 0.''000\,1831T^2 \\ &\quad + 0.''002\,003\,40T^3 - 5.''76 \times 10^{-7}T^4 - 4.''34 \times 10^{-8}T^5 \qquad (6.39)\\ \varepsilon &= \varepsilon_A + \Delta\varepsilon \qquad (6.40)\end{aligned}$$

where $T = (\mathrm{JD} - 2\,451\,545.0) / 36525$. The nutation matrix (Emerson 1973) is

$$\begin{aligned}\mathbf{N} &= \mathbf{R}_1(-\varepsilon)\,\mathbf{R}_3(-\Delta\psi)\,\mathbf{R}_1(+\varepsilon_A)\\ &= \begin{bmatrix} \cos\Delta\psi & -\sin\Delta\psi\cos\varepsilon_A & -\sin\Delta\psi\sin\varepsilon_A \\ \sin\Delta\psi\cos\varepsilon & \cos\Delta\psi\cos\varepsilon\cos\varepsilon_A + \sin\varepsilon\sin\varepsilon_A & \cos\Delta\psi\cos\varepsilon\sin\varepsilon_A - \sin\varepsilon\cos\varepsilon_A \\ \sin\Delta\psi\sin\varepsilon & \cos\Delta\psi\sin\varepsilon\cos\varepsilon_A - \cos\varepsilon\sin\varepsilon_A & \cos\Delta\psi\sin\varepsilon\sin\varepsilon_A + \cos\varepsilon\cos\varepsilon_A \end{bmatrix}. \qquad (6.41)\end{aligned}$$

Nutation may be rigorously applied to equatorial rectangular coordinates thus:

$$\mathbf{r} = \mathbf{N}\,\mathbf{r}_0 \tag{6.42}$$

where the position vector $\mathbf{r}_0$ referred to the mean equinox of date is transformed to the position vector $\mathbf{r}$ referred to the true equinox of date.

The nutation angles $\Delta\psi$, $\Delta\varepsilon$ are evaluated using

$$\begin{aligned}\Delta\psi &= \sum_{i=1}^{n}(S_{\Delta\psi_i} + \dot{S}_{\Delta\psi_i}\,T)\sin A_i + C_{\Delta\psi\,i}\cos A_i \quad \text{and}\\ \Delta\varepsilon &= \sum_{i=1}^{n} S_{\Delta\varepsilon_i}\sin A_i + (C_{\Delta\varepsilon_i} + \dot{C}_{\Delta\varepsilon_i}\,T)\cos A_i\end{aligned} \tag{6.43}$$

where T is the time in Julian centuries and

$$\begin{aligned}A_i = {} & a_i l + b_i l' + c_i F + d_i D + e_i \Omega + f_i l_{Me} + g_i l_V\\ & + h_i l_E + j_i l_{Ma} + k_i l_J + m_i l_S + n_i l_U + o_i l_N + r_i p.\end{aligned} \tag{6.44}$$

The critical arguments in Eq. 6.44 are described in Table 6.6. The multipliers a_i through r_i, and the coefficients amplitudes in seconds of arc for $S_{\Delta\psi_i}$ through $\dot{C}_{\Delta\varepsilon_i}$ are given in the IAU 2000A Nutation Series table on pp. 88–103 of Kaplan (2005). The terms of the series are grouped according to their periods, and arranged roughly in order of magnitude of the coefficient of the nutation in longitude within each group. The values for the fundamental arguments are evaluated using Eqs. 5.17 through 5.19 of Kaplan. Values for the nutation angles and the true obliquity of the ecliptic, ε, determined using these series are tabulated at daily intervals on pages B58 through B65 of *The Astronomical Almanac*.

6.6.3.2 Approximate Nutation and Reduction

For applications that do not require an accuracy of better than one part in 10^8, the nutation matrix given in Eq. 6.41 may be simplified to

$$\mathbf{N} = \begin{bmatrix} 1 & -\Delta\psi\cos\varepsilon & -\Delta\psi\sin\varepsilon \\ +\Delta\psi\cos\varepsilon & 1 & -\Delta\varepsilon \\ +\Delta\psi\sin\varepsilon & +\Delta\varepsilon & 1 \end{bmatrix} \tag{6.45}$$

where $\Delta\psi$ and $\Delta\varepsilon$ are expressed in radians.

Equatorial rectangular coordinates referred to the mean equinox can be converted to the true equinox by application of the corrections

$$\begin{aligned}\Delta x &= -(y\cos\varepsilon + z\sin\varepsilon)\Delta\psi\\ \Delta y &= +x\cos\varepsilon\,\Delta\psi - z\Delta\varepsilon\\ \Delta z &= +x\sin\varepsilon\,\Delta\psi + y\Delta\varepsilon.\end{aligned} \tag{6.46}$$

Similarly the first-order corrections ($\Delta\alpha$, $\Delta\delta$) to right ascension or celestial ephemeris longitude and declination may be calculated directly from

$$\begin{aligned}\Delta\alpha &= (\cos\varepsilon + \sin\varepsilon\sin\alpha\tan\delta)\Delta\psi - \cos\alpha\tan\delta\Delta\varepsilon\\ \Delta\delta &= \sin\varepsilon\cos\alpha\Delta\psi + \sin\alpha\Delta\varepsilon.\end{aligned} \tag{6.47}$$

Table 6.6 Critical arguments for the IAU 2000A nutation

Symbol	Argument
l	The mean anomaly of the Moon
l'	The mean anomaly of the Sun
F	The difference $L - \Omega$ where L is the mean longitude of the Moon
D	The mean anomaly of the Moon
Ω	The longitude of the ascending node of the Moon's mean orbit on the ecliptic, measured from the mean equinox of date
l_{Me}	The mean heliocentric longitude of Mercury
l_V	The mean heliocentric longitude of Venus
l_E	The mean heliocentric longitude of the Earth
l_{Ma}	The mean heliocentric longitude of Mars
l_J	The mean heliocentric longitude of Jupiter
l_S	The mean heliocentric longitude of Saturn
l_U	The mean heliocentric longitude of Uranus
l_N	The mean heliocentric longitude of Neptune
p	An approximation of the general precession in longitude

It is also possible to calculate the nutations in longitude and obliquity to about $1''$ by considering only the dominant terms of the series Kaplan (2005, pp. 88-103), thus

$$\begin{aligned} \Delta\psi &= -0^{\circ}.0048 \sin(125^{\circ}.0 - 0^{\circ}.052\,95d) - 0^{\circ}.0004 \sin(200^{\circ}.9 + 1^{\circ}.971\,29d) \\ \Delta\varepsilon &= +0^{\circ}.0026 \cos(125^{\circ}.0 - 0^{\circ}.052\,95d) + 0^{\circ}.0002 \cos(200^{\circ}.9 + 1^{\circ}.971\,29d) \end{aligned} \tag{6.48}$$

where d is the number of days from 2 451 545.0.

6.6.3.3 Differential Nutation

For objects within a small area of sky differential nutation is always combined with differential precession; see § 6.6.2.6.

6.7 The Celestial Intermediate Origin (CIO)

Beginning on 1 January 2003, the IAU recommends the use of the Celestial Intermediate Origin (CIO) in place of the equinox as the origin of right ascension in the CRS (§ 6.2 shown in Fig. 6.1). The position of the CIO is determined kinematically and has the following properties:

1. It lies on the instantaneous celestial equator of date.
2. As it moves, there is no motion around the z-axis. That is, its motion is always perpendicular to the instantaneous equator. This has been termed a *non-rotating origin*.
3. The position of the CIO at J2000.0 (Julian date 2 451 545.0 TT) is defined to be that of the mean equinox of J2000.0.

Since its original definition it has been determined that there was a slight misalignment ($\sim$ 20 mas) between both the pole of the GCRS (§ 6.2) and the CIP (§ 6.2.3), and the CIO and the mean equinox of J2000.0. The difference between these two reference systems is constant, and the conversion from one to the other is the purpose of the frame bias matrix, **B** (§ 6.5).

The CIO is intended for use with a combined bias-precession-nutation matrix (Capitaine, Wallace, and Chapront 2003). This parameterization is in terms of the two angles, $\mathcal{X}$, in the direction toward the origin of right ascension of the GCRS (§ 6.2), and $\mathcal{Y}$, in the direction (90° to the east of x), which give the coordinates of the CIP unit vector in the GCRS. The third parameter is the CIO locator, s. Except for a tiny fixed offset, s is the difference between the length of the arcs from Σ to N' and σ to N'. The point Σ is the origin of right ascension of the GCRS, σ is the CIO, and N' is the node of the equator of the CIP on the equator of the GCRS. This matrix includes precession, nutation, coupling between precession and nutation, and frame biases. The value of s is given by

$$s = -\int_{t_0}^{t} \frac{\mathcal{X}\,\dot{\mathcal{Y}} - \mathcal{Y}\,\dot{\mathcal{X}}}{1+\mathcal{Z}}\,dt - (\Sigma N' - \sigma_0 N') \tag{6.49}$$

where σ_0 is the position of σ at JD 2 451 545.0 and

$$\mathcal{Z} = (1 - \mathcal{X}^2 - \mathcal{Y}^2)^{\frac{1}{2}}. \tag{6.50}$$

The bias-precession-nutation matrix [7] is:

$$\begin{aligned} \mathbf{NPB}_{\mathrm{CIO}} &= \mathbf{R}_3(-s)\mathbf{R} \\ &= \mathbf{R}_3(-s) \begin{bmatrix} 1 - a\,\mathcal{X}^2 & -a\,\mathcal{X}\,\mathcal{Y} & \mathcal{X} \\ -a\,\mathcal{X}\,\mathcal{Y} & 1 - a\,\mathcal{Y}^2 & \mathcal{Y} \\ -\mathcal{X} & -\mathcal{Y} & 1 - a(\mathcal{X}^2 + \mathcal{Y}^2) \end{bmatrix} \end{aligned} \tag{6.51}$$

where

$$\begin{aligned} a &\approx \frac{1}{2} + \frac{\mathcal{X}^2 + \mathcal{Y}^2}{8} \\ \mathcal{X} &= \sum_{i=1}^{5} x_i T^i + \sum_j \sum_{k=0}^{3} T^k (b_{sjk} \sin d_k + b_{cjk} \cos d_k) \\ \mathcal{Y} &= \sum_{i=1}^{5} y_i T^i + \sum_j \sum_{k=0}^{3} T^k (e_{sjk} \sin f_k + e_{cjk} \cos f_k). \end{aligned} \tag{6.52}$$

T is the time in Julian centuries from J2000.0 TT, x_i and y_i are the coefficients for the frame bias and precession in $\mathcal{X}$ and $\mathcal{Y}$, respectively, b_{sjk}, b_{cjk}, e_{sjk}, and e_{cjk} are the coefficients for the nutation and coupling between precession and nutation, and d_k and f_k are the

7. Readers should be warned that the combined matrix $\mathbf{NPB}_{\mathrm{CIO}}$ does not have a distinctive name. In *The Astronomical Almanac* and in Chapter 7 it is referred to as matrix **C**. Readers should also be warned not to confuse $\mathbf{NPB}_{\mathrm{CIO}}$ with the matrix **NPB** (without a subscript); their origins are different. In *The Astronomical Almanac* and in Chapter 7, **NPB** (without subscript) is often referred to as matrix **M**.

fundamental angular arguments for the nutation and coupling terms. The parameter s may also be represented by a series, but it is more efficient to derive s from the series for $s + \frac{1}{2}\mathcal{X}\mathcal{Y}$. The non-periodic parts of Eqs. 6.52 and the series for $s + \frac{1}{2}\mathcal{X}\mathcal{Y}$ are:

$$\begin{aligned}
\mathcal{X} &= -0.''016\,617 + 2004.''191\,898T - 0.''429\,7829T^2 \\
&\quad - 0.''198\,618\,34T^3 + 7.''578 \times 10^{-6}T^4 + 5.''9285 \times 10^{-6}T^5 \\
\mathcal{Y} &= -0.''006\,951 - 0.''025\,896T - 22.''407\,2747T^2 \\
&\quad + 0.''001\,900\,59T^3 + 0.''001\,112\,526T^4 + 0.''1358 \times 10^{-6}T^5 \qquad (6.53) \\
s &= -\frac{1}{2}\mathcal{X}\mathcal{Y} + 9.''4 \times 10^{-5} + 0.''003\,808\,65T - 0.''000\,122\,68T^2 \\
&\quad - 0.''725\,7411T^3 + 2.''798 \times 10^{-5}T^4 + 1.''562 \times 10^{-5}T^5.
\end{aligned}$$

Approximate formulae for the position of the CIP and CIO, accurate to about $0.''0001$ over the period from 1975 through 2025 are available on pages B46 and B47 of *The Astronomical Almanac*.

An explanation of the theory and the sources for machine-readable tabulations of it are in McCarthy and Petit (2004, p. 44). The elements of the matrix in Eq. 6.51 are derived from a second order expansion of cosine and sine functions, and are dimensionless. Thus, the values of $\mathcal{X}$, $\mathcal{Y}$, s, and the coefficients for the nutation and coupling between precession and nutation should be in radians. However, these values are normally given in arcseconds and must be converted.

6.8 Time and Earth Orientation

Time as measured by the Earth's rotation, may be thought of as the difference along the equator between the CRS (§ 6.2) and the projection of a terrestrial reference longitude onto the CRS. In the case of *Universal Time*, UT, the Earth's rotation is measured with respect to the mean fictitious anti-solar direction, midnight, and the terrestrial reference meridian is the origin of longitude of the TRS (§ 6.2). For local mean solar time, the Earth's rotation is measured with respect to the mean fictitious anti-solar direction (midnight), and the reference meridian is the local meridian of longitude. For sidereal time the angle is measured with respect to the mean equinox for *mean sidereal time* and the true equinox for *apparent sidereal time*. When the reference meridian for sidereal time is the TRS, the sidereal time is either *Greenwich Mean Sidereal Time*, GMST, or *Greenwich Apparent Sidereal Time*, GAST. When the reference on the CRS is the CIO (§ 6.7) and the terrestrial reference meridian is the origin of longitude of the TRS, then the angular difference is the *Earth Rotation Angle*, ERA.

Until the nineteenth century the basic unit of time, the day, was based on the assumption that the Earth's rotation rate was constant, and, the determination of time depended on astronomical observations. There are seasonal differences in the apparent motion of the Sun that have been known since at least the time of Ptolemy. These differences are *not* the result of variation in the Earth's rotation rate. They arise from the non-uniform motion of the Earth in its orbit about the Sun, and lead to the differentiation of apparent solar time and mean solar time.

The failure of successive lunar theories to represent the observed motion of the Moon eventually led to the suspicion that the rotation of the Earth was not uniform. In ephemerides calculated from gravitational theories, time is independent of the variable rotation of the Earth. Consequently, the Earth's non-uniform rotation would cause the observed hour angle of a celestial body to differ from the position tabulated in the ephemeris.

Analysis of the discrepancies between observed and computed positions revealed the difference between the Earth's rotation and a uniform timescale. These discrepancies were most evident in the mean motion of the Moon, due to the accuracy with which the position can be observed and the rapidity of its motion. Similar discrepancies in the motions of other solar system bodies, in proportion to the magnitude of their mean motions, were also observed. These discrepancies confirmed the variable rate of the Earth's rotation.

The secular retardation of the rate of rotation due to tidal interaction between the Earth and Moon was the first variation to be recognized. Adams (1853) showed that the observed secular acceleration of the mean motion of the Moon could not totally be produced by gravitational perturbations. The validity of these results was hotly contested. The issue was resolved when Ferrell (1864) and Delaunay (1865) showed from dynamical principles that the tides exert a retarding action on the rotation of the Earth, accompanied by a variation of the orbital velocity of the Moon in accordance with the conservation of angular momentum.

Newcomb (1878) considered the possibility of irregular variations of the Earth's rotation as an explanation of lunar residuals. He could not find confirmation from planetary data (Newcomb 1912), however. Some of the difficulties faced by Newcomb, and prior astronomers, arose from inadequacies in the lunar theory. This situation was rectified when Brown (1919) introduced his new tables. A number of studies offered increasing evidence of irregular variations in the Earth's rotation. Most important were papers by de Sitter (1927) and Spencer Jones (1939b), which correlated irregularities in the Moon's motion with irregularities of the inner planets.

Meanwhile, the accuracy of crystal-controlled clocks was becoming comparable with that of the rotation of the Earth. By comparing the observed rates of the clocks of national time services, Stoyko (1937) found a periodic seasonal variation in the rate of rotation.

The Earth's rotation rate was eventually found to have secular, irregular, and periodic variations. Since mean solar time was determined directly from astronomical observations of the Earth's rotation, it could no longer be considered uniform.

Thus, a uniform timescale based on the motions of the bodies of the solar system, Ephemeris Time, ET, later followed by T_{eph} (the JPL realization of Barycentric Dynamical Time, TDB) replaced the rotation of the Earth as the independent variable for planetary ephemerides. ET and T_{eph} are discussed in Chapter 3. This section will discuss time as it relates to Earth rotation that is, solar time (§ 6.8.1), Universal Time (UT) see § 6.8.3, Earth Rotation Angle (ERA) see § 6.8.4, and sidereal time (§ 6.8.5).

6.8.1 Apparent Solar Time, Mean Solar Time, and the Equation of Time

Apparent solar time is the measure of time defined by the actual diurnal motion of the Sun. If the Sun's right ascension increased at a uniform rate and the Earth's rotation were uniform, solar days would be equal in length throughout the year, and apparent solar time would then provide a uniform measure of time. However, like the Earth's rotation rate, the Sun's motion in right ascension is not uniform because the Sun moves along the ecliptic rather than the

equator, and the Sun's motion along the ecliptic is not constant due to the Earth's orbit being elliptical, not circular.

The motion of an abstract fiducial point called the *fictitious mean Sun*, defines mean solar time. This point moves uniformly in the equatorial plane at a rate that is virtually equal to the mean rate of the true Sun's motion in the ecliptic. The difference between mean solar time and apparent solar time, called the *equation of time*, is never greater than 16 minutes. The link between mean solar time and sidereal time was based on the relation

$$\text{mean solar time at Greenwich} = \text{GMST} - \text{RA}_{\odot} + 12^{\text{h}} \tag{6.54}$$

where GMST is the Greenwich Hour Angle of the mean equinox of date (i.e., Greenwich Mean Sidereal Time) and $\text{RA}_{\odot}$ is the right ascension of the fictitious mean Sun.

Underlying the concept of mean solar time was the assumption that the rotation of the Earth was uniform. In the first half of the twentieth century, the lunar ephemeris demonstrated that this assumption was incorrect (§ 6.8). Thus, mean solar time was no longer used in precise timekeeping. It was replaced by two somewhat different concepts of time: *Ephemeris Time*, ET (see Chapter 3), was introduced to satisfy the desire for a uniform measure of time, and *Universal Time*, UT, to measure the Earth's rotation. Originally UT was introduced to specify Greenwich Mean Time measured from noon instead of midnight (§ 6.8.3).

Over the centuries, the definition of mean solar time, and, hence, of the equation of time, evolved as new tables for the motion of the Sun were introduced. Thus, care must be taken in analyzing historical observations that are expressed in mean time to determine what definition was used in the reductions.

6.8.2 Greenwich Mean Time

Prior to 1925, mean solar time was reckoned from noon in astronomical practice. The mean solar day beginning at noon, 12^{h} after midnight at the beginning of the same civil date, was known as the astronomical day. Mean solar time reckoned from mean noon on the meridian of Greenwich was designated *Greenwich Mean Time*, GMT. *Local Mean Time*, LMT, was reckoned from mean noon on a local meridian. The national ephemerides for 1925, introduced a discontinuity of 12^{h} at the beginning of the year in the tabular arguments, so the instant designated December 31.5 in the volumes for 1924 was designated January 1.0 in the volumes for 1925.

In *The Nautical Almanac*, the designation Greenwich Mean Time, GMT, was still used for the new reckoning, together with local mean time where appropriate, whereas in *The American Ephemeris* the designation *Greenwich Civil Time*, GCT, was adopted, together with *local civil time*, LCT. This confusion in terminology was finally removed by dropping both designations and substituting Universal Time, UT (§ 6.8.3). Care is necessary to avoid confusion. To distinguish between the two reckonings that have both been called Greenwich Mean Time, the designation *Greenwich Mean Astronomical Time*, GMAT, should be used for the reckoning from noon. The designation UT always refers to time reckoned from Greenwich midnight, even for epochs before 1925.

In the United Kingdom, Greenwich Mean Time has been identified with the civil time or Coordinated Universal Time, UTC (§ 6.8.3.1). This connection, however, has never been formalized, so using GMT to refer to UTC should be done with care. For navigation, however,

Greenwich Mean Time has meant UT1 (§ 6.8.3). Thus, GMT has two meanings that can differ by as much as $0^{s}.9$, and the term GMT should not be used for precise purposes.

6.8.3 Universal Time (UT)

Universal Time, UT, is the de facto measure of time used as the basis for civil timekeeping. It conforms closely to the mean diurnal motion of the Sun. The apparent diurnal motion of the Sun involves both the non-uniform diurnal rotation of the Earth and the motion of the Earth in its orbit around the Sun. In practice UT is related to sidereal time by means of a numerical formula. It does not refer to the motion of the Earth and is not precisely related to the hour angle of the Sun.

UT is now derived from observations of the diurnal motion of radio sources. These observations provide the timescale designated UT1. UT0 is a local scale, which is a combination of UT and the effect of the variation of the local longitude due to polar motion.

Originally, Newcomb (1898) gave the expression for the right ascension of the fictitious mean Sun as:

$$\mathrm{RA}_{\odot} = 18^{h}\ 38^{m}\ 45^{s}.836 + 8\,640\,184^{s}.542T + 0^{s}.0929T^{2} \tag{6.55}$$

where T is measured in Julian centuries from 1900 January 0, 0^{h} Greenwich mean noon. This expression differs from that of the mean longitude of the Sun by only a slight, progressively increasing excess of $0^{s}.0203\ T^{2}$ due to the secular acceleration of the Sun and to the different rates of general precession on the ecliptic and on the equator.

Inserting Eq. 6.55 into the formula for mean solar time, Eq. 6.54, and evaluating the result at 0^{h} mean solar time on the Greenwich meridian, gives the Greenwich Mean Sidereal Time at 0^{h} mean solar time:

$$\mathrm{GMST}_{0} = 6^{h}\ 38^{m}\ 45^{s}.836 + 8\,640\,184^{s}.542T + 0^{s}.0929T^{2} \tag{6.56}$$

where T is a uniform timescale in units of Julian centuries (36525^{d}). But values calculated from this expression are not consistent with observed hour angles of stars because the rotation of the Earth is not uniform.

From the beginning of the century through 1959, these formulae were used in the British *Nautical Almanac* and in the *American Ephemeris* to define mean solar time and to relate solar time and sidereal time. As given by Newcomb, the independent variable in Eq. 6.55 is consistent with that of his solar tables.

As evidence accumulated that the Earth did not rotate uniformly, Newcomb's T was interpreted as the independent variable of the Earth's orbital revolution rather than its axial rotation. Since Newcomb's tables were the basis of the fundamental ephemerides of the inner planets, T became associated with the concept of a uniform measure of time, based on the laws of orbital dynamics.

T_E (expressed in Julian centuries of 36525 ephemeris days from 1900 January 0, 12^{h} ET) can be used in Eq. 6.55 to signify ET. Then $\mathrm{RA}_{\odot}(T_E) = R_E$ defines a uniformly moving fiducial point that is independent of the Earth's rotation.

To make Eq. 6.56 consistent with observed hour angles of the stars, Universal Time, UT, was instituted as a measure of the Earth's rotation. Then, Eq. 6.55 becomes a definition of UT, with T_U (measured in Julian centuries of 36525 days of UT from 1900 January 0, 12h

UT) serving as the independent variable: $\mathrm{RA}_{\odot}(T_U) = R_U$. The difference between R_E and R_U is given by

$$R_E - R_U = 0.002\,738\Delta T \tag{6.57}$$

where $\Delta T = \mathrm{ET} - \mathrm{UT}$.

6.8.3.1 Coordinated Universal Time

Beginning in 1962, an increasing number of broadcast time services cooperated to provide a consistent time standard. Most broadcast signals were synchronized to the redefined *Coordinated Universal Time*, UTC, in 1972. Prior to 1972, broadcast time signals were kept within 0.1 second of UT2 by introducing step adjustments, normally of 0.1 second, and occasionally by changing the duration of the UTC second. The scale UT2 resulted from applying the following formula for the seasonal variation in the rate of the Earth's rotation to UT1:

$$\mathrm{UT2} = \mathrm{UT1} + 0.022\sin 2\pi\tau - 0.012\cos 2\pi\tau - 0.006\sin 4\pi\tau + 0.007\cos 4\pi\tau \tag{6.58}$$

where τ is the fraction of the Besselian year of the observation.

The seasonal variation in the rotation of the Earth was first detected by means of crystal clocks at the Physicalisch-Technische Bundesanstalt (Scheibe and Adelsberger 1936). Stoyko (1936); Stoyko (1937); Finch (1950); Smith and Tucker (1953) confirmed these variations. Lunar tidal variations were found to be in reasonable agreement with the theory. McCarthy and Petit (2004, Chapter 8 and references therein) provide more recent reports. Originally, the research on long-term variations in the rotation of the Earth was investigated using the motion of the Moon, which was the only process available with sufficient precision (Spencer Jones 1939a; Munk and MacDonald 1960). Now atomic time is the basis for research into the Earth's rotational variations.

Since 1972, UTC differs from TAI by an integer number of seconds. It is maintained within 0.9 second of UT1 by the introduction of one-second steps (leap seconds) when necessary. Preferably a leap second is inserted at the end of June or December, but one may occur at the end of any month. DUT1, an extrapolation of the difference UT1 − UTC, accurate to approximately ± 0.1 s, is transmitted in code on some broadcast time signals.

6.8.4 Earth Rotation Angle (ERA or θ)

The relationship between a conventionally defined direction in space and a conventionally defined direction on the Earth represents the rotation of the Earth in inertial space. There are several ways to measure this relationship. In the past observations were made in a celestial reference system defined by the directions to stars. Prior to 2003 measurements were made using as a reference the equinox and its motion as realized by the IAU (1976) System of Astronomical Constants, the IAU (1980) Theory of Nutation, and the positions and proper motions of stars of the FK5 catalog. Now radio observations of quasars are used. This quasi-inertial frame was linked to the positions of quasars with the adoption of the ICRS (IAU 1997). The IAU (2001c) redefined UT1 with respect to the *Earth Rotation Angle* (ERA or θ) beginning on 2003 January 1 as

$$\begin{aligned}\theta(\mathrm{UT1}) = 2\pi[&0.779\,057\,273\,2640 + 1.002\,737\,811\,911\,354\,48\\ &\times (\text{Julian UT1 date} - 2\,451\,545.0)] \quad \text{rad.}\end{aligned} \tag{6.59}$$

6.8.5 Sidereal Time

Prior to 1960, the designation "Right Ascension of Mean Sun + 12^h" was sometimes applied to tabulations of Greenwich Sidereal Time at 0^h UT. This inexact terminology was dropped when the distinction between ET and UT was introduced in national ephemerides in 1960. Eq. 6.55, with T_U as the independent variable, was used during the period 1960–1983 to calculate tabular values of Greenwich Mean Sidereal Time at 0^h UT.

6.8.5.1 Greenwich Mean Sidereal Time (GMST)

From 1984 January 1 until 2003 January 1 Greenwich Mean Sidereal Time (GMST) was related to UT1 by:

$$\begin{aligned}\text{GMST at } 0^h \text{ UT1} = {} & 24\,110.548\,41 + 8\,640\,184.812\,866 T_U \\ & + 0.093\,104 T_U^2 - 6.2 \times 10^{-6} T_U^3 \text{ s}\end{aligned} \tag{6.60}$$

where $T_U = d_U/36525$, d_U is the integer number of days +0.5 of UT elapsed since JD 2 451 545.0 UT1 (2000 January 1, 12^h UT1) (Aoki et al. 1982). This relation conforms to the position and motion of the equinox specified in the IAU (1976) System of Astronomical Constants, the IAU (1980) Theory of Nutation, and the positions and proper motions of stars in the FK5 catalog.

When it was established, Eq. 6.60 was considered to be the definition of UT1, because at that time the observation of transits of stars with their positions and proper motions in the FK5 system was the best means to obtain UT1. As new techniques to determine UT1 became operational, the reference system modeling involved in their implementations was constrained to be consistent with this definition.

The constant term and the numerical coefficient of T_U in Eq. 6.60 were chosen so that UT1 would be continuous in value and rate through the change from the old to the new system of constants (1984 January 1). The small differences due to the change in the theory of nutation were neglected.

The variation of UT1 with respect to uniform time truly represents the irregularities of the rotation of the Earth. The average duration, Δ, of the day of UT1 in SI seconds over an n-day interval is given by

$$\Delta = 86400 - (\psi_2 - \psi_1)/n \text{ s} \tag{6.61}$$

where ψ_1 and ψ_2 are the values of UT1 − TAI in seconds at n-day intervals. The mean angular velocity of the Earth, ω, is given by

$$\omega = (86400/\Delta) \times 72.921\,151\,467 \times 10^{-6} \text{ rad s}^{-1}. \tag{6.62}$$

With the redefinition of UT1 in the IAU 2000 resolutions (IAU 2001d; URL[4]), it became necessary to provide a new definition for GMST in terms of the ERA. Beginning on 1 January 2003 the new definition of GMST has the form

$$\text{GMST} = \theta(D_U) + f(T) \tag{6.63}$$

where D_U is UT1 in days from J2000.0, f is a polynomial function, and T is the TT time in centuries from J2000.0. Using the $P03$ solution for the precession, GMST in seconds to a

precision of 0.1 μs is (Capitaine, Wallace, and Chapront 2005)

$$\begin{aligned}\mathrm{GMST}(D_U, T) = 86\,400^{\mathrm{s}}(&0.779\,057\,273\,2640 + 0.002\,737\,811\,911\,354\,48\,D_U + D_U \bmod 1)\\ &+ 0\overset{\mathrm{s}}{.}000\,967\,07 + 307\overset{\mathrm{s}}{.}477\,102\,27\,T + 0\overset{\mathrm{s}}{.}092\,772\,113\,T^2\\ &- 2\overset{\mathrm{s}}{.}93 \times 10^{-8}\,T^3 - 1\overset{\mathrm{s}}{.}997\,08 \times 10^{-5}\,T^4 - 2\overset{\mathrm{s}}{.}453 \times 10^{-9}\,T^5.\end{aligned} \tag{6.64}$$

Note that this equation for GMST now has *two* time arguments. Two time arguments are required since the angle between the TIO (§ 6.9), (that is, 0° terrestrial longitude) and the Sun depends on both the position of the Earth in its orbit about the Sun and the rotation angle of the Earth itself. Alternatively, making use of

$$\Delta\mathrm{T} = \mathrm{TT} - \mathrm{UT1} \tag{6.65}$$

Eq. 6.64 may be given in terms of UT1 and ΔT in days. To first order in ΔT Eq. 6.64 becomes

$$\begin{aligned}\mathrm{GMST}(D_U, \Delta\mathrm{T}) = (&67\,310\overset{\mathrm{s}}{.}548\,377\,08 + 86\,636\overset{\mathrm{s}}{.}555\,367\,405\,292\,D_U\\ &+ 6\overset{\mathrm{s}}{.}954\,0371 \times 10^{-11}\,D_U^2 - 6\overset{\mathrm{s}}{.}02 \times 10^{-24}\,D_U^3\\ &- 1\overset{\mathrm{s}}{.}122\,10 \times 10^{-24}\,D_U^4 - 3\overset{\mathrm{s}}{.}774 \times 10^{-32}\,D_U^5\\ &+ 0\overset{\mathrm{s}}{.}008\,418\,264\,265\,\Delta\,\mathrm{T}) \bmod 86\,400^{\mathrm{s}}.\end{aligned} \tag{6.66}$$

As of 2011 Nov. 1, the value of ΔT was 66$\overset{\mathrm{s}}{.}$54. Ignoring the linear term in ΔT decreases GMST by approximately 6.4 μs. As long as $|\Delta\mathrm{T}| \geq 12$ days the terms higher than first order are less than 0.1 μs and thus, are insignificant.

6.8.5.2 Greenwich Apparent Sidereal Time (GAST)

The expression for mean sidereal time accounts for precession but not nutation. That is, GMST defined with respect to the mean equinox of date. An additional correction called the equation of the equinoxes, E_e, (§ 6.3) can be added to GMST to obtain Greenwich Apparent Sidereal Time, GAST, the sidereal time with respect to the true equinox. Thus,

$$\mathrm{GAST} = \mathrm{GMST} + E_e. \tag{6.67}$$

The GAST may also be found by subtracting a correction, the equation of the origins, E_o, (§ 6.4), from the ERA (§ 6.8.4).

$$\mathrm{GAST} = \mathrm{ERA} - E_o. \tag{6.68}$$

6.8.6 Conversions between Universal Time and Sidereal Time

The number of seconds of sidereal time in a Julian century is obtained by differentiation of Eq. 6.64

$$\begin{aligned}s_{JC} &= \frac{\partial GMST}{\partial T} + \frac{\partial GMST}{\partial T_U}\\ &= 8\,640\,184.794\,4783 + 0.185\,544\,22T - 8.78 \times 10^{-7}T^2\\ &\quad - 0.000\,007\,9083T^3 - 1.227 \times 10^{-8}T^4\ \mathrm{s}.\end{aligned} \tag{6.69}$$

This result depends only on TT. The independence from UT1 is a direct consequence of the redefinition of sidereal time. UT1 is now strictly proportional to the Earth's rotation, so the

non-constant part of the relation comes purely from the precession of the equinox, which depends purely on TT, not UT1. Dividing s_{JC} by the number of days in a Julian century, 36525, and adding 86400 gives s_d, the number of seconds of mean sidereal time in a day of UT1:

$$\begin{aligned} s_d = {} & 86\,636.555\,3674\,05292 + 5.079\,9239 \times 10^{-6} T - 2.403 \times 10^{-11} T^2 \\ & - 2.165\,18 \times 10^{-10} T^3 - 3.359 \times 10^{-11} T^4 \text{ s} \end{aligned} \tag{6.70}$$

where T is the number of Julian centuries elapsed since JD 2 451 545.0. The quantity s represents the number of sidereal seconds in a day of Universal Time. Dividing Eq. 6.70 by 86400 gives the ratio of mean sidereal time to UT1:

$$\begin{aligned} r' = {} & 1.002\,737\,909\,344\,968\,66 + 5.879\,5415 \times 10^{-11} T - 2.782 \times 10^{-16} T^2 \\ & - 2.50500 \times 10^{-15} T^3 - 3.888 \times 10^{-18} T^4 \text{ d}. \end{aligned} \tag{6.71}$$

The inverse of this expression gives the ratio of UT1 to mean sidereal time:

$$\begin{aligned} \frac{1}{r'} = {} & 0.997\,269\,566\,334\,878\,89 - 5.847\,4780 \times 10^{-11} T + 2.766 \times 10^{-16} T^2 \\ & + 2.492\,33 \times 10^{-15} T^3 - 3.867 \times 10^{-18} T^4 \text{ d}^{-1}. \end{aligned} \tag{6.72}$$

Roughly speaking, UT1 can be regarded as solar time. Eq. 6.72 can then be thought of as giving the length of one sidereal day in units of solar days. Disregarding the secular variations, the equivalent measures of the lengths of the days are:

$$1 \text{ mean sidereal day} = 23^{\text{h}}\ 56^{\text{m}}\ 04\overset{\text{s}}{.}090\,5313 \text{ of Universal Time}$$

$$1 \text{ day of Universal Time} = 24^{\text{h}}\ 03^{\text{m}}\ 56\overset{\text{s}}{.}555\,3674 \text{ of mean sidereal time.}$$

From Eq. 6.59, the mean rotational period of the Earth is 86 164.098 903 690 3511 seconds of UT1 or $23^{\text{h}}\ 56^{\text{m}}\ 04\overset{\text{s}}{.}098\,903\,690\,3511$. The mean rate of rotation is 15.041 067 178 670 3172 seconds of arc per second of time.

6.8.6.1 Previous Conversion between Universal Time and Sidereal Time

The number of seconds of sidereal time in a Julian century used prior to the 2006 edition of *The Astronomical Almanac* was

$$s_{JC} = 8640\,184.812\,866 + 0.186\,208\,T_U - 1.86 \times 10^{-5}\,{T_U}^2 \text{ s}. \tag{6.73}$$

The number of seconds of mean sidereal time in a day of UT1 was:

$$s_d = 86\,636.555\,367\,908\,72 + 5.098\,097 \times 10^{-6}\,T_U - 5.09 \times 10^{-10}\,{T_U}^2 \text{ s}. \tag{6.74}$$

The ratio of mean sidereal time to UT1 was:

$$r' = 1.002\,737\,909\,350\,795 + 5.9006 \times 10^{-11}\,T_U - 5.9 \times 10^{-15}\,{T_U}^2 \text{ d}. \tag{6.75}$$

And the ratio of UT1 to mean sidereal time was:

$$\frac{1}{r'} = 0.997\,269\,566\,329\,084 - 5.8684 \times 10^{-11}\,T_U + 5.9 \times 10^{-15}\,{T_U}^2 \text{ d}^{-1}. \tag{6.76}$$

These older conversions use UT1 rather than TT for their time argument. The equivalent measures of the lengths of the days was:

$$1 \text{ mean sidereal day} = 23^{\text{h}}\ 56^{\text{m}}\ 04^{\text{s}}.090\ 524 \text{ of Universal Time}$$

$$1 \text{ day of Universal Time} = 24^{\text{h}}\ 03^{\text{m}}\ 56^{\text{s}}.555\ 3678 \text{ of mean sidereal time.}$$

Prior to the 2006 edition of *The Astronomical Almanac*, the mean rotational period of the Earth was assumed to be 86 164.098 903 697 32 seconds of UT1 or

$$23^{\text{h}}\ 56^{\text{m}}\ 04^{\text{s}}.098\ 903\ 697\ 32.$$

This gave a ratio of a UT1 day to the mean period of rotation of 1.002 737 811 906. The mean rate of rotation used was 15.041 067 178 669 10 seconds of arc per second of time.

6.8.7 Conversion of Local Apparent Sidereal Time to UT1

The usual procedure to express the UT1 date of an event that occurred at some instant dated in local apparent sidereal time, LAST, is:

1. Express the date in local mean sidereal time, LMST, by

$$\text{LMST} = \text{LAST} - E_e(T) \tag{6.77}$$

   where E_e is the equation of the equinoxes (§ 6.3).
2. Express the date in Greenwich Mean Sidereal Time by

$$\text{GMST} = \text{LMST} - \lambda \tag{6.78}$$

   where λ is the astronomical longitude of the event, positive toward the east. Since the pole of rotation is moving with respect to the surface of the Earth (polar motion), the local meridian is subject to small variations. The position of the rotational pole (x, y) with respect to the CIP (§ 6.2.3) can be used to correct for this effect. This correction of λ_0 (referred to the CIP) to λ is accomplished by applying the expression

$$\lambda = \lambda_0 - (x \sin \lambda_0 + y \cos \lambda_0) \tan \phi \tag{6.79}$$

   where ϕ is the astronomical latitude of the event.
3. Compute the rotational angle ϕ between 0^{h} UT1 and the event, expressed in mean sidereal time by

$$\phi = \text{GMST} - \text{GMST of } 0^{\text{h}} \text{ UT1}. \tag{6.80}$$

4. Convert ϕ, expressed as an interval of sidereal time, to an interval of UT1:

$$\text{UT1} = r'\phi \tag{6.81}$$

   where r' is the ratio of mean solar time to sidereal time intervals, given in Eq. 6.71.

For instance when the hour angle, H, of a star with apparent right ascension, α, has been measured, the corresponding UT1 value is

$$\text{UT1} = (H + \alpha - E_e - \lambda - \text{GMST of } 0^{\text{h}} \text{ UT1})r'. \tag{6.82}$$

6.8.8 Local Time and Hour Angle

The local hour angle, h, of an object is the angle between two planes. The first plane contains the geocenter, the CIP (§ 6.2.3), and the observer, and the second plane contains the geocenter, the CIP, and the object. The hour angle is positive when the object is west of the observer as viewed from the geocenter, and increases with time.

Another plane of importance is the plane containing the geocenter, the CIP, and the TIO (§ 6.9), as this defines the astronomical zero meridian [8]. An observer's longitude, λ, on the astronomical zero meridian is 0. This plane is now called the TIO meridian and is a fundamental plane of the Terrestrial Intermediate Reference System. The Greenwich Hour Angle, GHA, of an object is the difference between the angle describing the Earth's orientation and the celestial meridian containing the object. For equinox-based coordinates those angles are the apparent right ascension, α_e, and the GAST,

$$\mathrm{GHA} = \mathrm{GAST} - \alpha_e \tag{6.83}$$

and for CIO-based coordinates those angles are the intermediate right ascension, α_i, and θ

$$\mathrm{GHA} = \theta - \alpha_i. \tag{6.84}$$

The local hour angle, h, is related to the GHA by

$$\begin{aligned} h &= \mathrm{GHA} + \lambda \\ &= \mathrm{LAST} - \alpha_e \\ &= \theta - \alpha_i + \lambda \\ &= \theta - E_o(T) - \alpha_e + \lambda \end{aligned} \tag{6.85}$$

where $E_0(T)$ is the equation of the origins (§ 6.4) and λ is the observer's longitude measured positively towards east.

Alternatively, the relationship between the Greenwich Hour Angle and the TIO may be determined using a rotation matrix

$$\mathbf{r} = \mathbf{R}_3(\mathrm{LAST})\mathbf{r}_e = \mathbf{R}_3(\theta)\mathbf{r}_i \tag{6.86}$$

where $\mathbf{r}_e$ is the vector pointing to the body using the true equinox of date as the origin of right ascension and $\mathbf{r}_i$ is the same vector using the CIO as the origin of right ascension. The GHA is then

$$\mathrm{GHA} = \tan^{-1}\frac{\mathrm{r}_y}{\mathrm{r}_x} \tag{6.87}$$

where r_x and r_y are the x and y components of the vector $\mathbf{r}$. The local hour angle, h, is found by adding λ to the angle in the rotation matrix. Very precise observations require the user to apply corrections for the effect of polar motion (§ 6.9.2) and for the separation of the TIO (§ 6.9) from the ITRF origin of longitudes (§ 6.2.2).

8. The astronomical zero meridian is also known as the Greenwich meridian. This is the meridian from which the Greenwich Hour Angle is measured.

Similarly, local mean solar time, LMSoT, is related to UT by the observer's east longitude

$$\text{LMSoT} = UT + \lambda. \tag{6.88}$$

6.9 The Terrestrial Intermediate Origin (TIO)

In the past, the most commonly used reference meridian was the meridian of Greenwich. With the adoption of the IAU 2000 resolutions (IAU 2001d; URL[4]), the reference meridian is now that of the *Terrestrial Intermediate Origin* (TIO). Rather than being defined geographically, the TIO is defined kinematically such that there is no component of polar motion about the pole of rotation. This position moves over the geographic surface of the Earth. However, this motion is extremely small, about 5×10^{-7} arcseconds yr^{-1} (Lambert and Bizouard 2002), equivalent to a motion of 0.01 mm yr^{-1} at the equator.

Analogous to the CIO (§ 6.7), the TIO is defined by successive rotations through two small angles, x and y, and the TIO locator, s'. The angles x and y are the polar motion (§ 6.9.2), the angular coordinates of the CIP with respect to the terrestrial pole measured along the meridians at longitude 0° and 270° (90° W). Similar to the CIO locator, the TIO locator is determined by

$$s' = -\int_{t_0}^{t} \frac{x\dot{y} - y\dot{x}}{1+z}\, dt \tag{6.89}$$

where $t_0 = \text{JD2 451 545.0}$ and

$$z = (1 - x^2 - y^2)^{1/2}. \tag{6.90}$$

6.9.1 The Ephemeris Meridian

To facilitate practical calculations of phenomena that depend upon hour angle and geographic location, the concept of an auxiliary reference meridian, known as the *ephemeris meridian*, was introduced.

The ephemeris meridian was originally used in conjunction with ephemeris time; however, its name has been retained for use with calculations in TT. Its position is where the TIO would be if the Earth rotated uniformly at the rate implicit in the definition of TT; i.e., 1.002 737 909 350 795 ΔT east of the actual TIO on the surface of the Earth.

Calculations in terms of TT may be referred to the ephemeris meridian using the same methods as those done in UT, when referred to the TIO. Once a sufficiently accurate value of $\Delta T = \text{TT} - \text{UT}$ is known or can be predicted, the longitudes and hour angles can be referred to the TIO, and the times in TT can be expressed in UT. This procedure is followed, for example, in predictions of the general circumstances of eclipses.

For example, Eq. 6.64 gives the hour angle of the equinox at 0^{h} UT, referred to the actual TIO. However, if T is expressed in TT rather than Universal Time, Eq. 6.64 gives the hour angle of the equinox at 0^{h} TT, referred to the ephemeris meridian.

The Universal Time of transit of the Sun, Moon, or a planet across the TIO can be found by subtracting ΔT from the TT of TIO transit. To determine the TT of TIO transit, the tabulated time of transit across the ephemeris meridian must be interpolated from the geographic longitude of the ephemeris meridian (1.002 737 909 35 ΔT east) to longitude 0°.

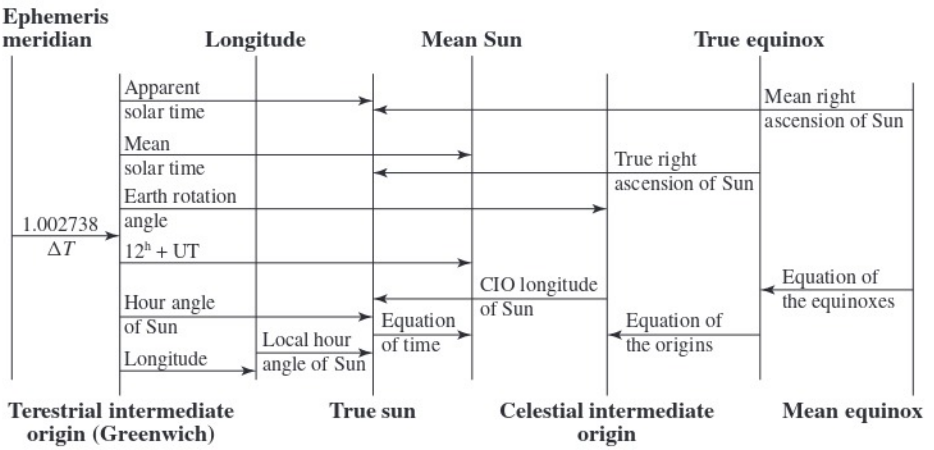


Figure 6.8 Schematic representation of the relationships between the different fiducial meridians encountered in the celestial and terrestrial coordinate systems

The Universal Time of TIO transit is given approximately by

$$\text{UT of TIO transit} = \text{TT of ephemeris transit} + \frac{\Delta T}{h}\Delta\alpha \tag{6.91}$$

where $\Delta\alpha$ is the first difference in tabular right ascension and h is the tabular interval.

Hour angles, sidereal time, and the equation of time may be defined with respect to the ephemeris meridian. But to relate such a system to observations from the surface of the Earth, the value of ΔT is required. Thus, it is more convenient and conventional to convert TT to UT by means of ΔT and to relate hour angles, longitudes, and times to the TIO.

The speed of rotation of the ephemeris meridian is such that it makes one complete revolution of 360°, relative to the mean equinox, in $23^{\mathrm{h}}\,56^{\mathrm{m}}\,04\overset{\mathrm{s}}{.}098\,903\,697\,32$ of TT. The ephemeris meridian coincided with the TIO at some date between 1900 and 1905. Figure 6.8 shows the relationship between the ephemeris meridian and the TIO. It also shows the relationships between the local meridian, the equinox, and the true and mean Sun.

6.9.2 Polar Motion

The rotation of the Earth is represented by the diurnal rotation around a reference axis whose motion with respect to the inertial reference frame is represented by the theories of precession and nutation. This reference axis, the CIP(§ 6.2.3), does not coincide with the axis of figure (maximum principal moment of inertia) of the Earth, but moves slowly (in a terrestrial reference frame) in a quasi-circular path around the axis of figure. The plane of the equator is normal to the CIP, and the motion of the terrestrial reference frame with respect to the CIP is known as polar motion. The CIP is the axis about which the diurnal rotation of the Earth is applied in the transformation between celestial and terrestrial frames, and should not be confused with the instantaneous axis of rotation. The maximum amplitude of the polar motion is typically about $0\overset{''}{.}3$, corresponding to a displacement of about 9 m on the surface of the Earth, and the principal periods are about 365 (annual wobble) and 428 (Chandler wobble) days. Figure 6.9 shows the motion of the pole of rotation with respect

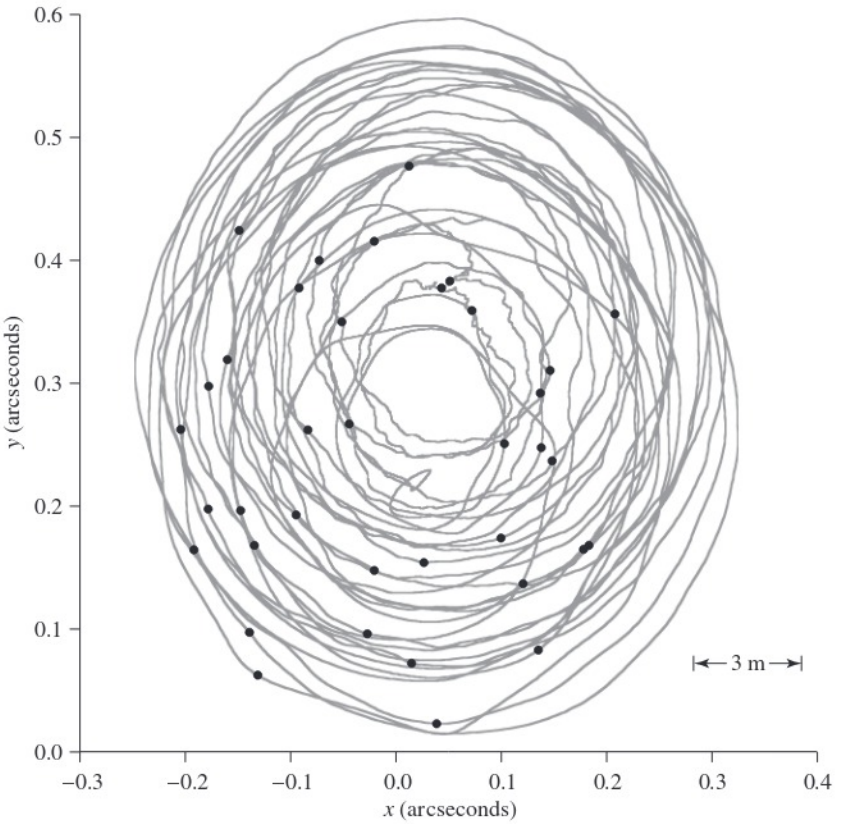


Figure 6.9 Motion of the pole with respect to the *Conventional International Origin* (the predecessor to the CIP), measured by VLBI (§ 6.2) from 1973.0 through 2009.5. The filled circles are at yearly intervals.

to the CIP for the period from 1973.5 through 2009.5 as observed from Very Long Baseline Interferometry, VLBI (§ 6.2), observations. Unpredictable geophysical forces affect the exact period and amplitude of the polar motion. Thus, the polar motion must be determined from observations.

The adoption of the set of coordinates for the instruments used to determine UT and polar motion from astronomical observations implicitly define the pole and TIO of the intermediate terrestrial reference system. The International Earth Rotation and Reference Systems Service publishes current and predicted values of x, y, and s'. Values of x and y, in seconds of arc, from 1970 January 1 onward are tabulated in Section K of *The Astronomical Almanac*. Polar motion causes variations in the zenith distance and azimuth of the CIP and hence in the values of the astronomical latitude, ϕ, and longitude, λ, that can be determined from direct astronomical observations of latitude and time.

The rigorous transformation of a vector $\mathbf{r}_0$ with respect to the frame of the true equator and equinox of date to the corresponding vector $\mathbf{r}$ with respect to the terrestrial frame is given by the formula

$$\mathbf{r} = \mathbf{R}_2(-x)\mathbf{R}_1(-y)\mathbf{R}_3(\theta)\mathbf{r}_0 \tag{6.92}$$

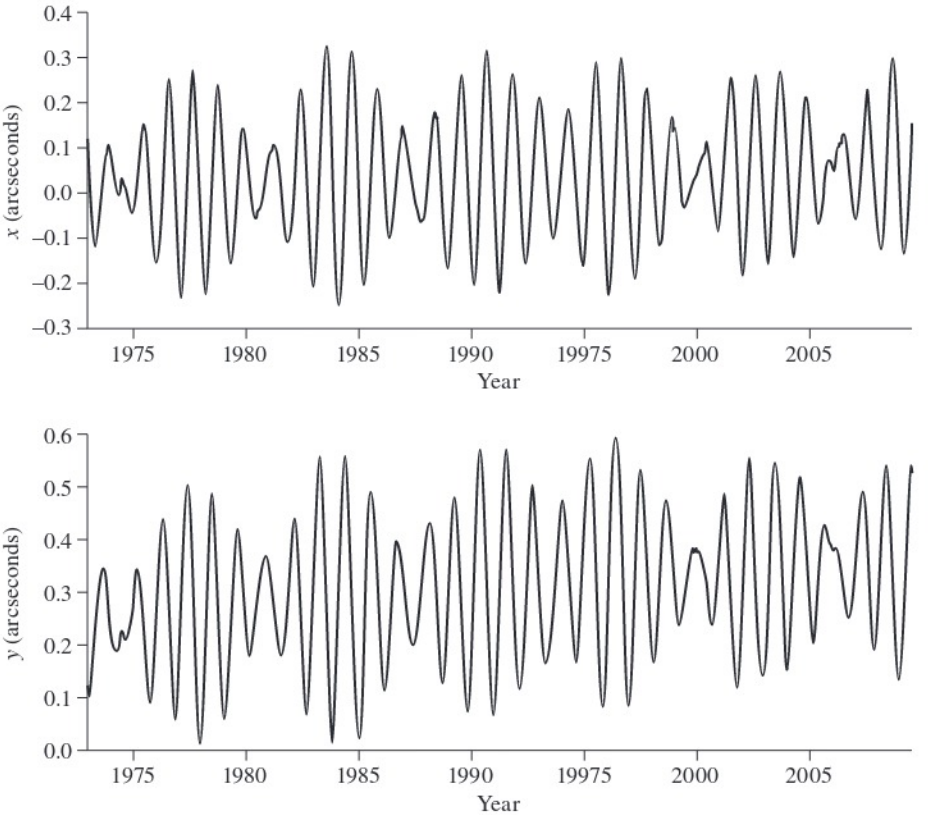


Figure 6.10 (a.) The polar motion in x measured by VLBI (§ 6.2) from 1973.0 through 2009.5. (b.) The polar motion in y measured by VLBI from 1973.0 through 2009.5.

where θ is the Earth Rotation Angle. Replacing θ with the GAST (§ 6.8.5.2) in Eq. 6.92 gives the position of this terrestrial reference frame with respect to the true equator and equinox of date. Figure 6.10 shows the observed polar motion components x and y from 1973.5 through 2009.5. The vector $\mathbf{r}$ could represent, for example, the coordinates of a point on the Earth's surface or of a satellite in orbit around the Earth.

Alternatively, the transformation can be expressed as a variation of the longitude and latitude of a point, and to first order, the departures from the mean values λ_m, ϕ_m (corresponding to vector $\mathbf{r}_0$) are given by

$$\begin{aligned} \Delta\phi &= x \cos\lambda_m - y \sin\lambda_m \\ \Delta\lambda_m &= (x \sin\lambda_m + y \cos\lambda_m) \tan\phi_m . \end{aligned} \tag{6.93}$$

The variation in longitude must be taken into account in the determination of Greenwich Mean Sidereal Time, and hence of UT, from observations.

6.9.2.1 Rotational Deformation due to Polar Motion

The variation of station coordinates caused by the polar tide should be taken into account in the highest precision, ~ 1 mas, applications. Choose a terrestrial system with reference

axes x, y, and z. The z-axis is oriented along the Earth's mean rotation axis, the x-axis is in the direction of the adopted origin of longitude, and the y-axis is oriented along the 90° E meridian.

The centrifugal potential caused by the Earth's rotation is

$$V = \frac{1}{2}[r^2|\mathbf{\Omega}|^2 - (\mathbf{r}\cdot\mathbf{\Omega})^2] \tag{6.94}$$

where $\mathbf{\Omega} = \omega[m_1\mathbf{x} + m_2\mathbf{y} + (1+m_3)\mathbf{z}]$. ω is the mean angular velocity of rotation of the Earth; m_i are small dimensionless parameters, m_1, m_2 describing polar motion, and m_3 describing variation in the rotation rate; $\mathbf{r}$ is the vector in the coordinate system rotating with the Earth from the geocenter to the station. Thus, r is the radial distance to the station.

The m_1 and m_2 terms (called *wobble parameters* in § 5.3.5.2) give a first-order perturbation in the potential V (Wahr 1985)

$$\Delta V(r, \Theta, \lambda) = -\frac{\omega^2 r^2}{2}\sin 2\Theta(m_1\cos\lambda + m_2\sin\lambda) \tag{6.95}$$

where Θ is the co-latitude, and λ is the eastward longitude. Variation in m_3 is neglected because it induces displacements that are less than a millimeter.

The radial displacement S_r and the horizontal displacements S_Θ, and S_λ are positive upward, south, and east, respectively, in a horizon system at the station due to ΔV using the formulation of tidal Love numbers (Munk and MacDonald 1960, pp. 24-25).

$$\begin{aligned} S_r &= h\frac{\Delta V}{g} \\ S_\Theta &= \frac{l}{g}\partial_\Theta \Delta V \\ S_\lambda &= \frac{l}{g\sin\Theta}\partial_\lambda \Delta V \end{aligned} \tag{6.96}$$

where g is the gravitational acceleration at the Earth's surface, and h and l are the second-order body tide displacement Love numbers.

In general, these computed displacements have a non-zero average over any given time span because m_1 and m_2, used to find ΔV, have a non-zero average. Consequently, the use of these results will lead to a change in the estimated mean station coordinates. When mean coordinates produced by different users are compared at the centimeter level, it is important to ensure that this effect has been handled consistently. It is recommended that m_1 and m_2 used in Eq. 6.95 be replaced by parameters defined to be zero for the ITRF (§ 6.2.2).

Thus, define

$$\begin{aligned} x_p &= m_1 - \overline{x} \\ y_p &= -m_2 - \overline{y} \end{aligned} \tag{6.97}$$

where $\overline{x}$ and $\overline{y}$ are the values of m_1 and $-m_2$ for the ITRF. Then, using $h = 0.6$, $l = 0.085$, and $r = a = 6.4 \times 10^6$ m,

$$\begin{aligned} S_r &= -32\sin 2\Theta(x_p\cos\lambda - y_p\sin\lambda)\ \text{mm} \\ S_\Theta &= -9\sin 2\Theta(x_p\cos\lambda - y_p\sin\lambda)\ \text{mm} \\ S_\lambda &= 9\sin\Theta(x_p\sin\lambda + y_p\cos\lambda)\ \text{mm} \end{aligned} \tag{6.98}$$

for x_p and y_p in seconds of arc. The values x_p and y_p vary by, at most, $0.''8$, so the maximum radial displacement is approximately 25 mm, and the maximum horizontal displacement is about 7 mm.

If X, Y, and Z are the Cartesian coordinates of a station in a right-hand equatorial coordinate system, the displacements of coordinates are

$$\begin{bmatrix} dX \\ dY \\ dZ \end{bmatrix} = \mathbf{R}^{\mathbf{T}} \begin{bmatrix} S_\Theta \\ S_\lambda \\ S_r \end{bmatrix} \tag{6.99}$$

where

$$\mathbf{R} = \begin{bmatrix} \cos\Theta\cos\lambda & \cos\Theta\sin\lambda & -\sin\Theta \\ -\sin\lambda & \cos\lambda & 0 \\ \sin\Theta\cos\lambda & \sin\Theta\sin\lambda & \cos\Theta \end{bmatrix}. \tag{6.100}$$

Equation 6.100 can be used to determine corrections to station coordinates due to polar tide.

The deformation caused by the polar tide also leads to time-dependent perturbations in the $C_{2,1}$ and $S_{2,1}$ geopotential coefficients. The change in the external potential caused by this deformation is $k\,\Delta V$, where Eq. 6.95 gives ΔV, and k is the degree-2 potential Love number. Using $k = 0.30$ gives

$$\begin{aligned} \overline{C}_{2,1} &= -1.3 \times 10^{-9}(x_p) \\ \overline{S}_{2,1} &= -1.3 \times 10^{-9}(-y_p) \end{aligned} \tag{6.101}$$

where x_p and y_p are in seconds of arc and are used instead of m_1 and $-m_2$ so that no mean value is introduced into $\overline{C}_{2,1}$ and $\overline{S}_{2,1}$ while making this correction.

To properly compare UT1 results obtained at different epochs, the high-frequency tidal effects should be taken into account. Thus, a standard expression for the tidal variations in UT1 is required. The IERS model is detailed in Bizouard, Eanes, and Ray (2004). However, to avoid confusion among possible tidal models, it is recommended that the terms δUT1, $\delta\Delta$, and $\delta\omega$ be followed by the model name in parentheses, e.g., δUT1(IERS 2004).

REFERENCES

1. International Earth Rotation and Reference System Service: IAU 2000 Precession-Nutation Theory ftp://maia.usno.navy.mil/conv2000/chapter5.

2. Naval Observatory Vector Astronomy Subroutines: http://aa.usno.navy.mil/software/novas/novas_info.php.

3. Standards Of Fundamental Astronomy: http://www.iausofa.org/.

4. IAU Resolutions Adopted by the General Assemblies: http://www.iau.org/administration/resolutions/general_assemblies/.

Adams, J. C. (1853). On the Secular Variation of the Moon's Mean Motion. *Philosophical Transactions CXLIII*, 397–406.

Andoyer, M. H. (1911). Les formules de la précession d'après S. Newcomb. *Bulletin Astronomique, Serie I 28*, 67–76.

Aoki, S., H. Kinoshita, B. Guinot, G. H. Kaplan, D. D. McCarthy, and P. K. Seidelmann (1982). The New Definition of Universal Time. *Astronomy and Astrophysics 105*, 359–361.

Aoki, S., M. Soma, H. Kinoshita, and K. Inoue (1983). Conversion Matrix of Epoch B1950.0 FK4–Based Positions of Stars to Epoch J2000.0 Positions in Accordance with the New IAU Resolutions. *Astronomy and Astrophysics 128*, 263–267.

Atkinson, R. d. (1973). On the 'Dynamical Variations' of Latitude and Time. *Astronomy and Astrophysics 128*, 263–267.

Atkinson, R. d. (1975). On the Earth's Axes of Rotation and Figure. *Monthly Notices of the Royal Astronomical Society 171*, 381–386.

Bizouard, C., R. Eanes, and R. Ray (2004). Tidal Variation in the Earth's Rotation. In D. D. McCarthy and G. Petit (Eds.), *IERS Technical Note No. 32: IERS Conventions (2003)*, Frankfurt am Main, pp. 92–98. Verlag des Bundesamts für Kartographie und Geodäsie.

Brown, E. W. (1919). *Tables on the Motion of the Moon*. New Haven, CT: Yale University Press.

Capitaine, N. and P. T. Wallace (2006). High Precision Methods for Locating the Celestial Intermediate Pole and Origin. *Astronomy and Astrophysics 450*, 855–872.

Capitaine, N., P. T. Wallace, and J. Chapront (2003). Expressions for IAU 2000 Precession Quantities. *Astronomy and Astrophysics 412*, 567–586.

Capitaine, N., P. T. Wallace, and J. Chapront (2005). Improvement of the IAU 2000 Precession Model. *Astronomy and Astrophysics 432*, 355–367.

Chapront, J., M. Chapront-Touzé, and G. Francou (2002). A New Determination of Lunar Orbital Parameters, Precession Constant and Tidal Acceleration from LLR Measurements. *Astronomy and Astrophysics 387*, 700–709.

de Sitter, W. (1927). On the Secular Accelerations and the Fluctuations of the Longitudes of the Moon, the Sun, Mercury, and Venus. *Bulletin of the Astronomical Institutes of the Netherlands iv*, 21–38.

Delaunay, C. E. (1865). Sur l'exitence d'une cause nouvelle ayant une action sensible sur la valeur de l'equation séculaire de la lune. *Compte Rendu des Séances de l'Académie des Sciences 61*, 1023–1032.

Emerson, B. (1973). A Method of Calculating Apparent Places of Stars. *Royal Observatory Bulletin 178*, 299–300.

Fabri, E. (1980). Advocating the Use of Vector-Matrix Notation in Precession Theory. *Astronomy and Astrophysics 82*, 123–128.

Ferrell, W. (1864). Note on the Influence of the Tides in Causing an Apparent Secular Acclereation of the Moon's Mean Motion. In *Proceedings of the American Academy of Arts and Science*, Volume VI, pp. 379–383.

Finch, H. F. (1950). On a Periodic Fluctuation in the Length of the Day. *Monthly Notices of the Royal Astronomical Society V*, 3–14.

Folkner, W. M., P. Charlot, M. H. Finger, J. G. Williams, O. J. Sovers, X. Newhall, and J. Standish, E. M. (1994). Determination of the Extragalactic-Planetary Frame Tie from Joint Analysis of Radio Interferometric and Lunar Laser Ranging Measurements. *Astronomy and Astrophysics 287*, 279–289.

Fricke, W. (1977). Basic Material for the Determination of Precession and of Galactic Rotation and a Review of Methods and Results. In *Veröffentlichungen Astron. Rechen-Inst. Heidelberg*, Volume 28, Karlsruhe. Verlag G. Braun.

Fukushima, T. (2003). A New Precession Formula. *Astronomical Journal 126*, 494–534.

Hilton, J. L., N. Capitaine, J. Chapront, J. M. Ferrandiz, A. Fienga, T. Fukushima, J. Getino, P. Mathews, J.-L. Simon, M. Soffel, J. Vondrak, P. Wallace, and J. Williams (2006). Report of the International Astronomical Union Division I Working Group on Precession and the Ecliptic. *Celestial Mechanics and Dynamical Astronomy 94*, 351–367.

Hilton, J. L. and C. Y. Hohenkerk (2003). Rotation Matrix from the Mean Dynamical Equator and Equinox at J2000.0 to the ICRS. *Astronomy and Astrophysics 413*, 765–770.

IAU (1976). Report of Joint Meeting of Commissions 4, 8, and 31 on the New System of Astronomical Constants. In *Transactions of the IAU*, Volume XVIB, Dordrecht, The Netherlands. International Astronomical Union: Reidel.

IAU (1980). Resolution 3: Recommendations of the Working Group on Nutation. In *Transactions of the IAU*, Volume XVIIB, Dordrecht, The Netherlands, pp. 40–41. International Astronomical Union: Reidel.

IAU (1992). Resolution A4: Recommendations from the Working Group on Reference Frames. In *Transactions of the IAU*, Volume XXIB, 41–52, pp. 41–52. International Astronomical Union: Kluwer.

IAU (1997). Resolution B2: On the International Celestial Reference System (ICRS). In *Transactions of the IAU*, Volume XXIIIB, Dordrecht, The Netherlands, pp. 39. International Astronomical Union: Kluwer.

IAU (2001a). Resolution B1.3 Definition of Celestial Reference System and Geocentric Celestial Reference System. In *Transactions of the IAU*, Volume XXIVB, Dordrecht, The Netherlands. International Astronomical Union: Kluwer.

IAU (2001b). Resolution B1.6: IAU 2000 Precession–Nutation Model. In *Transactions of the IAU*, Volume XXIVB, Dordrecht, The Netherlands. International Astronomical Union: Kluwer.

IAU (2001c). Resolution B1.7: Definition of Celestial Intermediate Pole. In *Transactions of the IAU*, Volume XXIVB, Dordrecht, The Netherlands. International Astronomical Union: Kluwer.

IAU (2001d). Resolution B1.8 Definition and Use of Celestial and Terrestrial Ephemeris Origins. In *Transactions of the IAU*, Volume XXIVB, Dordrecht, The Netherlands. International Astronomical Union: Kluwer.

IAU (2008). In K. A. van der Hucht (Ed.), *Transactions of the International Astronomical Union*, Volume XXVI B, Cambridge. Cambridge University Press. Proc. 26th General Assembly, Prague, 2006.

Kaplan, G. H. (2005). *The IAU Resolutions on Astronomical Reference Systems, Time Scales, and Earth Rotation Models*. Number 179 in U.S. Naval Observatory Circulars. U.S. Naval Observatory.

Kinoshita, H. (1975). *Formulas for Precession*. Number 364 in Smithsonian Astrophysical Observatory Special Report. Cambridge, MA: Smithsonian Astrophysical Observatory.

Lambert, S. and C. Bizouard (2002). Positioning the Terrestrial Ephemeris Origin in the International Terrestrial Reference Frame. *Astronomy and Astrophysics 394*, 317–321.

Le Verrier, U.-J. (1855). Recherches astronomiques: Chapitre i er. - des coordonnées astronomiques. *Annales de l'Observatoire de Paris 1*, 156–181.

Lieske, J. H. (1979). Precession Matrix Based on IAU (1976) System of Astronomical Constants. *Astronomy and Astrophysics 73*, 282–284.

Lieske, J. H., T. Lederle, W. Fricke, and B. Morando (1977). Expressions for the Precession Quantities Based upon the IAU (1976) System of Astronomical Constants. *Astronomy and Astrophysics 58*, 1–16.

Markowitz, W. and B. Guinot (Eds.) (1968). *Continental Drift, Secular Motion of the Pole and Rotation of the Earth*. Number 32 in IAU Symposium. Dordrecht, Holland: Reidel.

Mathews, P. M., T. A. Herring, and B. A. Buffett (2002). Modeling of Nutation and Precession: New Nutation Series for Nonrigid Earth and Insights into the Earth's Interior. *Journal of Geophysical Research 107*(B4), 10.1029/2001JB00390.

McCarthy, D. D. and B. J. Luzum (2003). An Abridged Model of the Precession-Nutation of the Celestial Pole. *Celestial Mechanics 85*, 37–49.

McCarthy, D. D. and G. Petit (Eds.) (2004). *IERS Conventions (2003)*. Frankfurt am Main: Verlag des Bundesamts für Kartographie und Geodäsie.

Moritz, H. and I. I. Mueller (1988). *Earth Rotation Theory and Observation*. New York: Ungar.

Munk, W. H. and G. J. F. MacDonald (1960). *The Rotation of the Earth; A Geophysical Discussion*. Cambridge, UK: Cambridge University Press.

Murray, C. A. (1983). *Vectorial Astronomy*. Bristol, UK: Hilger.

Nautical Almanac Offices of UK and USA (1961). *Explanatory Supplement to The Astronomical Ephemeris and The American Ephemeris and Nautical Almanac*. London: Her Majesty's Stationery Office. Reprinted 1974.

Newcomb, S. (1878). Researches on the Motion of the Moon. In *Washington Observations for 1875*, Washington. U.S. Government Printing Office.

Newcomb, S. (1895). The Elements of the Four Inner Planets and the Fundamental Constants. In *Supplement to the American Ephemeris and Nautical Almanac*, Washington. U.S. Government Printing Office.

Newcomb, S. (1898). *Tables of the Motion of the Earth on its Axis and Around the Sun*, Volume VI of *Astronical Papers Prepared for the Use of the American Ephemeris and Nautical Almanac*. Washington: U.S. Government Printing Office.

Newcomb, S. (1912). Researches on the Motion of the Moon, Part ii. In *Astronomical Papers Prepared for the Use of the American Ephemeris and Nautical Almanac*, Volume IX part II. Washington: U.S. Government Printing Office.

SAOC (1966). *Smithsonian Astrophysical Observatory Star Catalog, Positions and Proper Motions of 258997 Stars for the Epoch and Equinox of 1950.0*. Number 4652 in Smithsonian Publication. Washington: Smithsonian Institution.

Scheibe, A. and U. Adelsberger (1936). Schwankungen der astronomischen Tageslänge und der astronomischen Zeitbestimmung neach den quarzuhren der Physikalisch–Technischen Reichsanstalt. *Physikal. Zeitschrift 37*, 185–203.

Seidelmann, P. K. (1982). 1980 IAU Theory of Nutation: The Final Report of the IAU Working Group on Nutation. *Celestial Mechanics 27*, 79–106.

Smith, H. M. and R. H. Tucker (1953). The Annual Fluctuation in the Rate of Rotation of the Earth. *Monthly Notices of the Royal Astronomical Society 113*, 251–257.

Souchay, J., B. Loysel, H. Kinoshita, and M. Folgueria (1999). Corrections and New Developments in Rigid Earth Nutation Theory. iii. Final Tables "REN-2000". *Astronomy and Astrophysics Supplement 135*, 111–131.

Spencer Jones, H. (1939a). Non-Seasonal Changes in the Earth's Rotation. *Vistas in Astronomy 2*, 827–834.

Spencer Jones, H. (1939b). The Rotation of the Earth and the Secular Accelerations of the Sun, Moon, and Planets. *Monthly Notices of the Royal Astronomical Society 99*, 541–558.

Standish, E. M. (1998). JPL Planetary and Lunar Ephemerides, DE405/LE405. Jet Propulsion Laboratory, Interoffice Memorandum, IOM 312.F – 98 – 048.

Standish, E. M., J. (1981). Two Differing Definitions of the Dynamical Equinox and the Mean Obliquity. *Astronomy and Astrophysics 101*, L17–L18.

Stoyko, M. N. (1936). Sur la periodicité dans l'irregularité de la rotation de la terre. *Comptes-rendus 203*, 39–40.

Stoyko, M. N. (1937). Sur la periodicité dans l'irregularité de la rotation de la terre. *Comptes-rendus 205*, 79–81.

Wahr, J. M. (1985). Deformation Induced by Polar Motion. *Journal of Geophysical Research 90*, 9363–9368.

Williams, J. G. (1994). Contributions to the Earth's Obliquity Rate, Precession, and Nutation. *Astronomical Journal 108*, 711–724.

Woolard, E. W. and G. M. Clemence (1966). *Spherical Astronomy*. New York: Academic Press.

CHAPTER 7

Positions

C. Y. HOHENKERK

INTRODUCTION

This chapter provides for the reduction of celestial coordinates from one reference system to another. The coordinates are usually rectangular equatorial coordinates or equivalently right ascension, declination and hour angle. In particular the transformations from a position in the Barycentric Celestial Reference System (BCRS)—or equivalently the International Celestial Reference System (ICRS)—to a geocentric apparent or intermediate position are described, but some other systems and coordinates are discussed.

This chapter first summarizes the various reference systems, places, coordinates and notation used within the chapter. Then it describes the individual corrections of space motion, parallax, light-time, aberration and gravitational light-deflection, which are required in the transformation from the BCRS to the Geocentric Celestial Reference System (GCRS). If the requirement is for precision better than milliarcseconds (mas), when General Relativity principles are needed, then this is indicated where appropriate. Finally, vector-matrix algorithms are given for calculating various positions including, apparent, intermediate and topocentric places. Also an algorithm for calculating atmospheric refraction is included.

At the current time all these procedures conform to IAU 2006 resolutions 1 and 2 as well as IAU 2000 resolutions B1.6, B1.7 and B1.8 (IAU 2001, 2008; URL[6]).

In simple terms given a position of an object $\mathbf{u_B}$ with respect to the BCRS, then the transformation to $\mathbf{r}$, a position of date in the International Terrestrial Reference System (ITRS), may be considered thus

$$\mathbf{r} = \mathbf{W}\,\mathbf{R_3}(-\beta)\,\mathcal{R}_\Sigma\,[f\,[g\,[h\,[\mathbf{u_B}]]] \tag{7.1}$$

where, as appropriate to the object, $h[\,]$, $g[\,]$ and $f[\,]$ are schematic and represent the functions for space motion, parallax, aberration and light-deflection, producing a vector in the GCRS, and are discussed in detail in § 7.2

The transformation $\mathcal{R}_\Sigma$, which includes rotations for frame bias, precession and nutation, transforms position vectors from the GCRS to the of date system defined by the celestial intermediate pole (CIP). The origin for right ascension, and thus the paradigm, is chosen via the parameter β and is described in Capitaine and Wallace (2006). This choice will dictate whether right ascensions are measured from the equinox or from the celestial intermediate origin (CIO). Included in β, and depending on the users choice of right ascension origin, will be either, Greenwich Sidereal Time (apparent or mean) or the Earth Rotation Angle, respectively. The last transformation ($\mathbf{W}$), which includes polar motion, transforms from the Terrestrial Intermediate Reference System to the ITRS. The explanation of the theory behind

the transformations from the GCRS to the ITRS, precession, nutation, polar motion and Earth rotation are discussed in detail in Chapter 6.

Equation 7.1 expresses the process in terms of the transformation from the celestial to the terrestrial, and this ordering is followed in much of this chapter. Other explanations, for example the International Earth Rotation and Reference Systems Service (IERS) Conventions (IERS 2010), adopt the reverse process of transforming from the terrestrial to the celestial. Thus, readers are advised to ensure that the transformations they select for their purpose produces the position in the appropriate reference system.

7.1 Summary of Systems, Places, and Coordinates

In order to transform a position from one coordinate system to another it is necessary to identify the systems, the location of the observer, and the type of coordinates, which, in general terms, are all discussed in this section. Table 7.1 lists some frequently used systems, while Table 7.2 gives various place names and the implied systems. Finally, a summary of the notations used in this chapter is given.

Table 7.1 Summary of reference systems

No.	System	Equator/Pole	Origin on the Equator	Epoch
1	BCRS (ICRS)	ICRS equator and pole	ICRS (RA)	—
2	GCRS	ICRS	ICRS (RA)	—
3	J2000.0	mean equator	mean equinox (RA)	J2000.0
4	Mean	mean equator	mean equinox (RA)	of date
5	True	equator/CIP	true equinox (RA)	of date
6	Intermediate	equator/CIP	CIO (RA)	of date
7	Terrestrial	equator/CIP	TIO (GHA)	of date
8	ITRS	geodetic equator/pole	longitude (λ_{ITRS})	of date

Table 7.2 Summary of places

Place	Location of Observer	System [a]
Proper	geocentre	GCRS (2)
Local	surface of Earth	GCRS
Astrometric	geocentre	Hybrid
Mean	barycentre	mean of date (4)
Apparent	geocentre	true (or mean) of date (4 or 5)
Intermediate	geocentre	intermediate (6)
Topocentric	surface of the Earth	either (5) or (6)
Geodetic	surface of the Earth	of date (8)

[a] Numbers in parentheses refer to Table 7.1 and the numbered paragraphs within this section (§ 7.1.1).

7.1.1 Reference Systems

Table 7.1 lists some of the frequently used systems giving their designation, equator, pole and origin on the equator. This is followed by a short summary about each system. Full details about these systems can be found in other chapters.

1. Barycentric Celestial Reference System (BCRS): a system of barycentric space-time coordinates for the solar system within the framework of General Relativity. For all practical applications, the BCRS is assumed to be oriented according to the ICRS axes, the directions of which are realized by the International Celestial Reference Frame (ICRF). The ICRS is not identical to the system defined by the dynamical mean equator and equinox of J2000.0, although the difference in orientation is only about $0.''02$.
2. The Geocentric Celestial Reference System (GCRS): is a system of geocentric space-time coordinates within the framework of General Relativity. The directions of the GCRS axes are obtained from those of the BCRS (ICRS) by a relativistic transformation. Positions of stars obtained from ICRS reference data, corrected for proper motion, parallax, light-bending and aberration (for a geocentric observer) are with respect to the GCRS. The same is true for planetary positions, although the corrections are somewhat different.
3. The J2000.0 dynamical reference system; mean equator and equinox of J2000.0: a geocentric system where the origin of right ascension is the intersection of the mean ecliptic and equator of J2000.0; the system in which the IAU 2000 precession-nutation is defined. For precise applications a small rotation (frame bias, see Chapter 6, § 6.5) should be made to GCRS positions before precession and nutation are applied. The J2000.0 system may also be barycentric, for example as the reference system for catalogues.
4. The mean system of date; mean equator and equinox of date: both the origin (geocentre, heliocentre, or barycentre) and the axes should be spcified. The latter via the date (e.g., J2013.5) or via the context (J2000.0, ICRS, etc.). Nutation is ignored.
5. The true system of date; true equator and equinox of date: a geocentric system of date, the pole of which is the celestial intermediate pole (CIP), with the origin of right ascension at the equinox on the true equator of date (intermediate equator). It is a system "between" the GCRS and the Terrestrial Intermediate Reference System that separates the components labelled precession-nutation and polar motion.
6. The Celestial Intermediate Reference System; true equator and CIO of date: the IAU recommended geocentric system of date, the pole of which is the celestial intermediate pole (CIP), with the origin of right ascension at the celestial intermediate origin (CIO) which is located on the intermediate equator (true equator of date). It is a system "between" (*intermediate*) the GCRS and the Terrestrial Intermediate Reference System that separates the components labelled precession-nutation and polar motion.
7. The Terrestrial Intermediate Reference System: a rotating geocentric system of date, the pole of which is the celestial intermediate pole (CIP), with the origin of longitude the terrestrial intermediate origin (TIO), which is located on the intermediate equator

(true equator of date). The plane containing the geocentre, the CIP and TIO is the fundamental plane of this system and is called the TIO meridian and corresponds to the astronomical zero meridian.

8. The International Terrestrial Reference System (ITRS): a geodetic system realized by the International Terrestrial Reference Frame (ITRF2008), see Chapter 5. The CIP and TIO and positions in the Terrestrial Intermediate Reference System differ from positions in the ITRS, the geodetic pole and zero-longitude λ_{ITRS} on the geodetic equator by the effects of polar motion (see Chapter 6).

It is important to note that the true equator of date, the intermediate equator, the instantaneous equator are all terms for the plane orthogonal to the direction of the CIP, which in this chapter is also referred to as the "true equator of date". It is the equator of the true system of date, and the Celestial and Terrestrial Intermediate Systems.

Note the term *Greenwich meridian* is an inexact term for the zero-longitude, and thus it is important, if the precision warrants it, to establish the underlying system being used.

7.1.2 Places

There are various "names" that are used to specify different combinations of the system, the type of position and the location of the observer. These places together with the implied system and location of the observer are shown in Table 7.2.

Proper or virtual[1], local and astrometric places are all described in § 7.3, although astrometric places are considered to be in a hybrid system. The remainder are discussed in § 7.4. It is important to stress that for the highest precision it is necessary to apply the appropriate transformations and effects in the correct sequence, evaluated using the appropriate timescale.

A mean place is used to label coordinates of objects outside the solar system at a specific date. The coordinates represent the direction of the object as it would be observed from the solar system barycentre at the specified date if the masses of the Sun and other solar system bodies were negligible. Mean places are often used in star catalogues.

The terms apparent and intermediate place are used to label positions that are "geocentric of date". These positions include corrections for space motion, parallax, aberration, and light-deflection, as appropriate to the object. They also include effects of precession. An apparent place that is "mean of date" ignores nutation. The only difference between apparent and intermediate place is the location of the origin of right ascension.

A topocentric place is an apparent or an intermediate place, where the location of the observer is the surface of the Earth and **not** the geocentre. A topocentric right ascension may be measured from the equinox or the CIO. However, usually, it is GHA or LHA that is being calculated. The algorithm for calculating topocentric places is given in § 7.4.3.

The *geometric place* of an object is defined by a straight line between the centre of the Earth (or the observer) and the object at a given time, without any other correc-

1. Virtual place has exactly the same meaning as proper place. The term virtual place has been used in some U.S. Naval Observatory publications and products; it is mentioned here for completeness. To avoid confusion, this term will not be used in the future.

tions. In many cases it is used for clarity as it confirms that no corrections have been applied.

7.1.3 Coordinates

The following gives various sets of coordinates together with some relevant information about them and their use in this chapter.

Note: ensure that the units of all quantities used are compatible.

7.1.3.1 Right Ascension and Declination

Right ascension is measured in the plane of the equator from an origin on that equator. This origin of the right ascension system may be one of six different locations; ICRS origin, J2000.0 origin, GCRS origin, the mean equinox, the true equinox, or the CIO. When using the equator and equinox of date system (see item 5, § 7.1.1), right ascension is measured from the equinox and is called equinox right ascension; an apparent right ascension is always an equinox right ascension. When using the Celestial Intermediate Reference System (see item 6, § 7.1.1), right ascension is measured from the CIO and is called intermediate right ascension. Right ascension and related quantities, such as Greenwich Apparent Sidereal Time (GAST), are often expressed in time-measure ($1^{\mathrm{h}} = 15°$, etc.) unless the contrary is indicated.

Declination is measured north and south of the equator. Declinations, apparent or intermediate, derived using either equinox-based or CIO-based methods, respectively, are identical. Declination and related quantities are expressed in angular measure.

Right ascension and declination (α, δ) are transformed from an equatorial rectangular position vector $\mathbf{p} = (\xi, \eta, \zeta)$ thus

$$\alpha = \tan^{-1}\frac{\eta}{\xi} \qquad \delta = \tan^{-1}\frac{\zeta}{\sqrt{\xi^2 + \eta^2}}. \tag{7.2}$$

The quadrant of α is determined by the signs of ξ and η. Most computers have a double argument function for inverse tangent (e.g., ATAN2) which will provide the correct quadrant if the numerator and denominator are entered as separated arguments. Equation 7.2 above assumes that $\mathbf{p}$ is not necessarily a unit vector, and the distance is given by

$$|\mathbf{p}| = p = \sqrt{\xi^2 + \eta^2 + \zeta^2}. \tag{7.3}$$

7.1.3.2 Hour Angle and Right Ascension

The local hour angle of an object is the angle between two planes: the plane containing the geocentre, the CIP and the observer; and the plane containing the geocentre, the CIP and the object. Hour angle increases with time and is positive when the object is west of the observer as viewed from the geocentre.

The plane defining the astronomical zero ("Greenwich") meridian, from which Greenwich hour angles are measured, contains the geocentre, the CIP and the TIO; there, the observer's longitude λ (not λ_{ITRS}) $= 0$. This plane is called the TIO meridian and it is a fundamental plane of the Terrestrial Intermediate Reference System.

Figure 7.1 shows the relationships between the "zero-longitude" defined by the TIO, and the true equinox and the CIO, i.e., the origins of right ascension. The diagram illustrates that

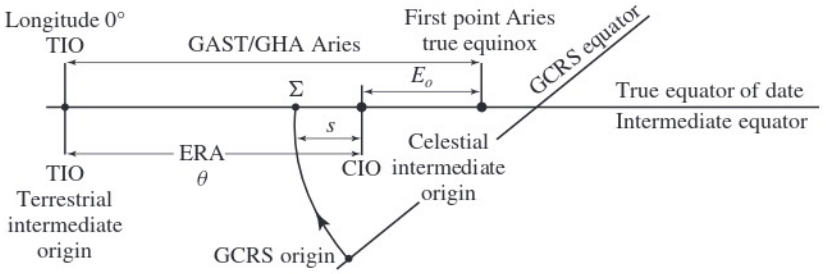


Figure 7.1 Relationships of origins

the origin of Greenwich Hour Angle, the TIO, may be obtained from either GAST or the Earth Rotation Angle (ERA, θ). The quantity s, the CIO locator, positions the GCRS origin (Σ) at the CIO. Note that the planes of the intermediate equator and the true equator of date (the pole of which is the CIP) are identical.

The following relationships are used to relate right ascensions of celestial objects to locations on the Earth and Universal Time (UT1):

Equinox-based	*CIO-based*	
$\text{GAST} = \text{GMST} + E_e$		(7.4)
$H = \text{GHA} = \text{GAST} - \alpha_e$	$H = \theta - \alpha_i$	(7.5)
$h = \text{LHA} = \text{GAST} + \lambda - \alpha_e$	$h = \theta + \lambda - \alpha_i = \theta + \lambda - (E_o + \alpha_e)$	(7.6)

where α_e and α_i are the apparent (i.e., equinox right ascension) and intermediate right ascension, respectively. E_e and E_o are the equation of the equinoxes and equation of the origins, respectively, and are described in Chapter 6, § 6.3 and § 6.4. If the equation of the equinoxes is ignored, then the right ascension, i.e., the equinox right ascension, will be with respect to the mean equinox of date (i.e., nutation has been ignored). The longitude λ is measured positive to the east.

Alternatively, use the rotation matrix $\mathbf{R}_3$ to rotate the equator and equinox of date system or the Celestial Intermediate Reference System about the z-axis (CIP) to the terrestrial system, resulting in either the TIO meridian and hour angle, or the local meridian and local hour angle.

Equinox-based	*CIO-based*	
$\mathbf{r}_e =$ position with respect to the equator and equinox of date	$\mathbf{r}_i =$ position with respect to the Celestial Intermediate Reference System	
$\mathbf{r} = \mathbf{R}_3(\text{GST})\,\mathbf{r}_e$ or	$\mathbf{r} = \mathbf{R}_3(\theta)\,\mathbf{r}_i$ or	(7.7)
$= \mathbf{R}_3(\text{GST} + \lambda)\,\mathbf{r}_e.$	$= \mathbf{R}_3(\theta + \lambda)\,\mathbf{r}_i.$	(7.8)

Then, depending on whether the Greenwich (H) or local (h) hour angle is required,

$$H \text{ or } h = \tan^{-1}\left(\frac{-\eta}{\xi}\right) \quad \text{positive to the west} \tag{7.9}$$

where $\mathbf{r} = (\xi, \eta, \zeta)$, and objects west of the meridian (setting) have positive hour angles. GST is either the Greenwich Mean (GMST) or Apparent (GAST) Sidereal Time, as appropriate, and θ is the Earth Rotation Angle. Greenwich Apparent and Mean Sidereal Times, equation of the equinoxes (E_e), ERA (θ) and equation of the origins (E_o) are tabulated daily at 0^h UT1 in *The Astronomical Almanac*.

It is important to note that when calculating hour angles it is essential that the time arguments used for the object's position and that of GAST or GMST, or ERA are for the same instant. The effect of time on the rotation of the Earth via ERA, GAST or GMST is large, while the movement of celestial objects is not as great. ERA is only a function of UT1, while GAST and GMST are functions of both UT1 and TT. The time argument of ephemerides of celestial objects is usually not UT. Timescales are discussed in Chapter 3.

The relationships above, which result in a position with respect to the Terrestrial Intermediate Reference System, require corrections for polar motion when the reduction of very precise observations are made with respect to a standard geodetic system such as the International Terrestrial Reference System (ITRS). These small corrections are (i) the alignment of the TIO onto the longitude origin ($\lambda_{\text{ITRS}} = 0$) of the ITRS, and (ii) for positioning the pole (CIP) within the ITRS see § 7.2.6.2 and Chapter 6.

Topocentric hour angle h' will be calculated similarly when the position vector $\mathbf{r}$ represents a topocentric position (see § 7.2.2.1 and § 7.4.3). At upper meridian transit $h' = 0$.

7.1.3.3 Ecliptic Longitude and Latitude

Ecliptic latitude β is measured north or south of the ecliptic. Ecliptic longitude λ is measured in the plane of the ecliptic from an origin on the ecliptic. This origin is the equinox, either the mean equinox or the true equinox. Thus equinox right ascension and declination (α_e, δ) may be converted to ecliptic coordinates (λ, β) and conversely, using the following relationships:

$$\begin{aligned}
\cos\beta\ \cos\lambda &= \cos\delta\ \cos\alpha_e \\
\cos\beta\ \sin\lambda &= \cos\delta\ \sin\alpha_e\ \cos\epsilon + \sin\delta\ \sin\epsilon \\
\sin\beta &= -\cos\delta\ \sin\alpha_e\ \sin\epsilon + \sin\delta\ \cos\epsilon
\end{aligned} \tag{7.10}$$

$$\begin{aligned}
\cos\delta\ \cos\alpha_e &= \cos\beta\ \cos\lambda \\
\cos\delta\ \sin\alpha_e &= \cos\beta\ \sin\lambda\ \cos\epsilon - \sin\beta\ \sin\epsilon \\
\sin\delta &= \cos\beta\ \sin\lambda\ \sin\epsilon + \sin\beta\ \cos\epsilon.
\end{aligned} \tag{7.11}$$

However, when given the intermediate right ascension and declination (α_i, δ), calculate the equinox right ascension from

$$\alpha_e = \alpha_i - E_o \tag{7.12}$$

where E_o is the equation of the origins. The angle ϵ in Eqs. 7.10 and 7.11 is either the mean or the true obliquity of the ecliptic. The mean obliquity, ϵ_A, is given in Eq. 7.72, while the true obliquity is $\epsilon = \epsilon_A + \Delta\epsilon$, where $\Delta\epsilon$ is the nutation in obliquity (see § 7.2.5 and Chapter 6). It is worth noting that if λ is the true longitude, then

$$\lambda = \lambda_m + \Delta\psi \tag{7.13}$$

where λ_m is the mean longitude and $\Delta\psi$ is the nutation in longitude.

Alternatively, an equatorial rectangular position vector $\mathbf{r}_i$ referred to the Celestial Intermediate Reference System, not necessarily a unit vector, may be transformed to ecliptic coordinates by first rotating the system about the CIP by the equation of the origins E_o followed by the rotation of the obliquity (ϵ) about the x-axis, thus

$$\mathbf{r}_e = \mathbf{R}_1(\epsilon)\, \mathbf{R}_3(E_o)\, \mathbf{r}_i \tag{7.14}$$

where $\epsilon = \epsilon_A$ or $\epsilon = \epsilon_A + \Delta\epsilon$ depending whether the mean or true ecliptic is required. If the initial vector (i.e., $\mathbf{r}_i$) was referred to the equator and equinox, then ignore the rotation $\mathbf{R}_3(-E_o)$. The ecliptic coordinates (λ, β) are then

$$\lambda = \tan^{-1}\frac{\eta}{\xi} \qquad \beta = \tan^{-1}\frac{\zeta}{\sqrt{\xi^2+\eta^2}} \tag{7.15}$$

where the vector is $\mathbf{r}_e = (\xi, \eta, \zeta)$, and as with right ascension, the quadrant of λ is determined by the signs of ξ and η.

7.1.3.4 Altitude and Azimuth

For an observer on the Earth at longitude λ and latitude ϕ the altitude (a) and azimuth (A_z) of a celestial object may be calculated from its local hour angle $h = H + \lambda$ (see § 7.1.3.2) and declination (δ) using the following relationships:

$$\begin{aligned} \cos a \sin A_z &= -\cos\delta \sin h \\ \cos a \cos A_z &= \sin\delta\cos\phi - \cos\delta\cos h \sin\phi \\ \sin a &= \sin\delta\sin\phi + \cos\delta\cos h\cos\phi \end{aligned} \tag{7.16}$$

where azimuth (A_z) is measured from the north through east in the plane of the horizon, altitude (a) is measured perpendicular to the horizon. The plane of the horizon is defined to be perpendicular to the apparent direction of gravity. The coordinates of the observer (λ, ϕ) are the astronomical values (see § 7.4.3.2 and § 5.2.4) and east longitude and north latitudes are positive. Zenith distance is given by $90^\circ - a$.

Alternatively, rotate the system so that the position vector $\mathbf{r}$ that is referred to the Terrestrial Intermediate Reference System is relative to the observer (λ, ϕ), *viz.*,

$$\mathbf{p} = \mathbf{R}_2(90^\circ - \phi)\, \mathbf{R}_3(\lambda)\, \mathbf{r}. \tag{7.17}$$

The first rotation is about the CIP (the z-axis) by the longitude λ, thus the rotated y-axis is then in the plane of the meridian. Then the system is rotated by $90^\circ - \phi$ about the y-axis, and the altitude and azimuth are thus given by

$$a = \tan^{-1}\frac{\zeta}{\sqrt{(\xi^2+\eta^2)}} \qquad A_z = \tan^{-1}\frac{\eta}{-\xi} \tag{7.18}$$

where the position vector $\mathbf{p} = (\xi, \eta, \zeta)$. Practically the rotation about the z-axis of λ should be included with the rotation to the TIO (zero-longitude), thus making $\mathbf{r}$ relative to the observer's meridian. The quadrant of A_z is determined by the signs of ξ and η. Most computers have a double argument function for inverse tangent (e.g., ATAN2) which will provide the correct quadrant if the numerator and denominator are entered as separated arguments.

For most purposes the values of the geodetic longitude and latitude may be used, but in some cases the effects of local gravity anomalies and polar motion must be included. For full

precision, the values of α, δ must be corrected for diurnal parallax and diurnal aberration, i.e., the topocentric coordinates should be used.

The inverse formulae are:

$$\begin{aligned} \cos\delta \sin h &= -\cos a \sin A_z \\ \cos\delta \cos h &= \sin a \cos\phi - \cos a \cos A_z \sin\phi \\ \sin\delta &= \sin a \sin\phi + \cos a \cos A_z \cos\phi. \end{aligned} \tag{7.19}$$

7.1.4 Summary of Notations

This section lists much of the matrix notation used in this chapter.

Matrices

$\mathbf{R}_1$, $\mathbf{R}_2$, $\mathbf{R}_3$. rotation matrices $\mathbf{R}_n(\phi)$, $n = 1, 2, 3$, where the original system is rotated about its x, y, or z-axis by the angle ϕ, counterclockwise as viewed from the $+x$, $+y$ or $+z$ direction, respectively (see Chapter 14 for information on matrices).

$\mathcal{R}_\Sigma$. Matrix transformation of the GCRS to the equator and GCRS origin of date. An intermediary matrix dependent on the CIP of date (see § 7.2.5.2, Eq. 7.75 and § 6.2.3).

$\mathbf{R}_3(-\beta)$. Matrix transformation about the CIP to the Terrestrial Intermediate Reference System, where the origin of right ascension (equinox or CIO) is designated by the choice of β which determines the angle of rotation and thus the paradigm used.

$\mathbf{W}$. Polar motion matrix: strictly the transformation from the Terrestrial Intermediate Reference System to the ITRS (origin $\lambda_{\text{ITRS}} = 0$).

Matrices for Equinox-Based Techniques

$\mathbf{B}$. Frame bias matrix: transformation of the GCRS to J2000.0 system, mean equator and equinox of J2000.0, see Chapter 6, § 6.5.

$\mathbf{P}$. Precession matrix: transformation of the J2000.0 system to the mean equator and equinox of date, see Chapter 6, § 6.6.

$\mathbf{N}$. Nutation matrix: transformation of the mean equator and equinox of date to the true equator and equinox of date, see Chapter 6, § 6.6.

$\mathbf{M} = \mathbf{NPB}$. CRS to equator and equinox of date matrix: transformation of the GCRS to the true equator and equinox of date, see Chapter 6.

$\mathbf{R}_3$(GAST). Earth rotation matrix: transformation of the true equator and equinox of date to the Terrestrial Intermediate Reference System (origin the TIO).

Matrices for CIO-Based Techniques

$\mathbf{C}$. CRS to Intermediate matrix: transformation of the GCRS to the Celestial Intermediate Reference System (equator and CIO of date). $\mathbf{C}$ includes frame bias and precession-nutation; see § 6.7 (but note it is referred to as $\mathbf{NPB}_{\text{CIO}}$ there).

$\mathbf{R}_3(\theta)$. Earth rotation matrix: transformation of the Celestial Intermediate Reference System to the Terrestrial Intermediate Reference System (TIO origin).

Some Symbols and Other terms

E_e. Equation of the equinoxes.

E_o. Equation of the origins.

T. an interval of time expressed in Julian centuries of 36 525 days; usually measured from J2000.0, i.e., from JD 245 1545.0 TT.

$\mathbf{r_e}$, $\mathbf{r_i}$. column position vectors (see Chapter 14), with respect to the true equinox, and intermediate system, respectively.

α, δ. right ascension and declination; in this case neither equinox (α_e) or intermediate (α_i) right ascension is specified.

μ_α, μ_δ. components of proper motion in right ascension and declination. **Check** the units carefully. Modern catalogues usually use mas/year, where the $\cos\delta$ factor has been included in μ_α.

λ, β. ecliptic longitude and latitude.

λ, ϕ. terrestrial longitude and latitude.

7.2 Components Used in the Reduction of Positions

This section describes, from a theoretical basis, the individual corrections of space motion, parallax, light-time, aberration and gravitational light-deflection, which are required for the transformation from the Barycentric Celestial Reference System (BCRS) to the Geocentric Celestial Reference System (GCRS).

This is followed by sections on the procedures for calculating the rotations for frame bias, precession and nutation, Earth rotation and polar motion that are required to transform positions referred to the GCRS to an "of date" system. Detailed information on precession, nutation and Earth rotation is given in Chapter 6, while the frame bias is discussed in § 6.5 and § 4.7. Polar motion is also discussed in detail in Chapter 6.

Lastly there is a section on astronomical refraction. Although refraction is not included in positions published in *The Astronomical Almanac*, except the standard amount included for rise and set phenomena, an accurate algorithm using numerical quadrature is given. Note, however, refraction—particularly at low altitudes—is very dependent on the atmospheric conditions at the time of the observation.

7.2.1 Space Motion

The motion in space of stellar objects as a function of time must be considered since star catalogs give the position of a star at an specified epoch and referred to a chosen reference system. Currently the chosen reference system is usually the ICRS which is aligned to the BCRS. The epoch of the star positions is usually J2000.0, but not always. For example the USNO CCD Astrographic Catalogue (UCAC2) positions are given for epoch J2000.0 and are referred to the ICRS. While Hipparcos Catalogue positions, although referred to the ICRS, are for epoch 1991.25. The FK5 and FK6 reference systems are referred to the mean equator and equinox at J2000.0.

Traditionally stellar motion has been divided into two parts: proper motion, which occurs perpendicular to the line of sight and is given as components in right ascension (μ_α) and declination (μ_δ); and radial velocity $\dot{r}$, which occurs along the line of sight. Thus the correction to position consists of the product of the star's space motion vector ($\dot{\mathbf{r}}$) with the interval between the required epoch and the epoch of the star's position in the catalog. It

should be noted that in some catalogs the secular variations of the proper motions are also included and in such cases the mean value of the proper motion during the interval must be used. In the cases of double stars the orbital motion of the components with respect to each other may also have to be included.

The position vector $\mathbf{r}$ of a star at the catalog epoch t is given by

$$\mathbf{r} = \begin{bmatrix} r\cos\delta\cos\alpha \\ r\cos\delta\sin\alpha \\ r\sin\delta \end{bmatrix} \tag{7.20}$$

where α, δ are the catalog right ascension and declination and r the barycentric distance to the star in au, which can be computed from

$$r = 1/\sin p \tag{7.21}$$

where p is the parallax of the star. If p is unknown, unavailable, or zero to within the accuracy of measurement, set it to some small but finite positive number in order to avoid mathematical indeterminacy; a choice of $1'' \times 10^{-7}$ will effectively place objects of unknown parallax at a radius of 10 Mpc.

The space motion vector $\dot{\mathbf{r}}$ of the star may be obtained by differentiating Eq. 7.20 giving

$$\dot{\mathbf{r}} = \begin{bmatrix} -\cos\delta\sin\alpha & -\sin\delta\cos\alpha & \cos\delta\cos\alpha \\ \cos\delta\cos\alpha & -\sin\delta\sin\alpha & \cos\delta\sin\alpha \\ 0 & \cos\delta & \sin\delta \end{bmatrix} \begin{bmatrix} 15srf\mu_\alpha \\ srf\mu_\delta \\ kf\dot{r} \end{bmatrix} \tag{7.22}$$

where μ_α and μ_δ are the proper motions in right ascension and declination in units of time and arc, respectively, and $\dot{r}$ is the radial velocity. The factors $15s$, s and k, convert μ_α, μ_δ and $\dot{r}$, into the required units for the space motion vector and the 15 assumes that μ_α is in units of time. The factor f is the relativistic Doppler effect. This is a simple method used by the USNO NOVAS software (Kaplan et al. 2009; URL[2]) to cater for the fact that the proper motions are observables (see below). However, in most cases f may be ignored (i.e., set $f = 1$).

If μ_α and μ_δ are in seconds of time and seconds of arc per Julian century respectively, and $\dot{r}$ is in kilometres per second, then if $\dot{\mathbf{r}}$ is required in au per day,

$$\begin{aligned} s &= 2\pi/(360 \times 3600 \times 36525) && \text{converts from } ''\text{/cy to radians/day} \\ k &= 86400/c\tau_A && \text{converts from km/s to au/day} \\ &= 86400 \times 36525/c\tau_A && \text{converts from km/s to au/cy} \end{aligned} \tag{7.23}$$

where c is the speed of light and $c\tau_A = 1.4959\,7870\,700 \times 10^8$ km is the unit distance consistent with the IAU 2009 system of constants.

However, great care needs to be taken with the proper motion in right ascension, since modern catalogues tend to tabulate $\mu_\alpha = 15\mu_\alpha \cos\delta$ and μ_δ, which are the measurements (in arc units) on the celestial sphere. In this case the relationship is

$$\dot{\mathbf{r}} = \begin{bmatrix} -\sin\alpha & -\sin\delta\cos\alpha & \cos\delta\cos\alpha \\ \cos\alpha & -\sin\delta\sin\alpha & \cos\delta\sin\alpha \\ 0 & \cos\delta & \sin\delta \end{bmatrix} \begin{bmatrix} srf\mu_\alpha \\ srf\mu_\delta \\ kf\dot{r} \end{bmatrix} \tag{7.24}$$

where the variables are defined above. Catalogues also use various units for proper motions, e.g., arcseconds per century ($''$/cy), or milliarcseconds per year (mas/yr). Use the factor 1/10 to convert from mas/yr to $''$/cy. The radial velocity ($\dot{r}$) is usually given in km/s and measured positively away from the Earth.

It is worth considering the cases in which the available data are incomplete. At present less than 20, 000 stars have known radial velocities, and of the order of about 100, 000 stars have known parallaxes, while there are tens of millions of stars with good precision proper motions.

If the proper motion components are zero, then the star has no known tangential velocity. Also, it may be the case that the proper motion components are known but not the parallax. There are millions of stars in this category and typically they have magnitudes fainter than 16th magnitude. In such a case, if a "reasonable guess" parallax value is not used, then the computed velocity components could be greater than seems physically plausible. However, this is a computational curiosity with no physical meaning or practical effect on the results of the calculation.

The radial velocity is required only for relatively nearby stars for which foreshortening effects (second-order changes in the apparent motion of the star due to the shifting aspect of its motion) are significant. However, the radial velocity is useless in this regard (and should be set to zero) if the parallax (distance) is unknown. If the star's radial velocity is zero or unknown, or has been set to zero because the parallax is not known, then the above space motion is tangent to the celestial sphere at the star's catalog position $\mathbf{r}$.

The position $\mathbf{r}_1$ of the star at epoch t_1 is then calculated from

$$\mathbf{r}_1 = \mathbf{r} + (t_1 - t)\,\dot{\mathbf{r}} \tag{7.25}$$

where $t_1 - t$ is the interval between the required epoch and the epoch of the catalog. If $\dot{\mathbf{r}}$ is in au/day, then clearly $(t_1 - t)$ must be in days. By using the space motion vector given in Eqs. 7.22 or 7.24, as appropriate, both proper motion and foreshortening effects have been included in $\mathbf{r}_1$.

The errors that are being made in this method of calculating space motion have been investigated by Stumpff (1985). Basically proper motion and radial velocity are observables which should be converted to inertial quantities. Thus catalog proper motions include the effect of aberration, whilst radial velocities include a relativistic doppler effect. NOVAS (Kaplan et al. 2009; URL[2]) multiplies each component of the space motion vector (see Eqs. 7.22 or 7.24) by the factor

$$f = (1 - \dot{r}/c)^{-1} \tag{7.26}$$

where $\dot{r}$ is the radial velocity and c is the speed of light, both in km/s. The IAU-SOFA routine (URL[3]) implements an iterative approach. Fortunately these effects are very small and are only important for a few nearby stars whose apparent motions are changing rapidly across the line of sight. Stumpff (*ibid.*) has shown that the errors in neglecting these effects can increase progressively with time so that after several decades they may become significant at the mas level.

There is no explicit correction for light-time in the stellar apparent place computation in *The Astronomical Almanac*, nor in the methods used in this chapter; it is assumed that the position and space motion vectors implicitly include the light-time and its time derivative.

A linear approximation to a star's motion in space, which ignores the changes in proper motion due to the changes in right ascension and declination, and ignores foreshortening and radial velocity may be made when the highest accuracy is not needed, or if the time interval (τ) is small such as in the Day Numbers method (see § 7.4.5.3) when τ is a fraction of a year. Corrections are made directly to the right ascension and declination, *viz.*

$$\begin{aligned} \alpha_1 &= \alpha + \tau\mu_\alpha \quad \text{or} \quad \alpha = \alpha_0 + \tau\mu_\alpha/\cos\delta \\ \delta_1 &= \delta + \tau\mu_\delta \end{aligned} \tag{7.27}$$

where $\tau = t_1 - t$ is expressed in the appropriate units.

7.2.2 Parallax

Parallax is the term used to describe the difference in the apparent direction of an object as seen from two different locations. For example, the Sun, Moon and planets are observed from the surface of the Earth, and most almanacs publish their geocentric positions. The term is usually used in connection with a shift of origin from the centre of the Earth to the surface (geocentric, a.k.a. diurnal parallax), or a shift from the barycentre or heliocentre to the geocentre (heliocentric, a.k.a. annual parallax).

The following is a simple and rigorous method of making corrections for both diurnal and annual parallax, and it is recommended that it be used in preference to approximate methods. The position vector of a body $\mathbf{u}_E$, with respect to the origin E, is given by

$$\mathbf{u}_\mathrm{E} = \mathbf{u}_\mathrm{B} - \mathbf{E}_\mathrm{B} \tag{7.28}$$

where $\mathbf{E}_B$ and $\mathbf{u}_B$ are the position vectors of the new origin and the body, respectively, with respect to the old origin and referred to the same reference frame.

Approximate methods are given for calculating diurnal and annual parallax, which are useful when the appropriate data are not available; e.g., the distance of the body is not known.

7.2.2.1 Diurnal Parallax

Diurnal parallax, also called geocentric parallax, is a shift of origin from the centre of the Earth to the surface of the Earth. Coordinates with an origin at the surface of the Earth are called topocentric coordinates, and depend on the position of the observer. Using Eq. 7.28, the topocentric rectangular equatorial coordinates of a body $\mathbf{r}'$, are given by

$$\mathbf{r}' = \mathbf{r} - \mathbf{g}(t) \tag{7.29}$$

where $\mathbf{r}$ and $\mathbf{g}(t)$ are the geocentric position vectors of the body and the observer, respectively, referred to the same reference system. In terms of the (α, δ) of the body, and ignoring polar motion gives

$$\begin{aligned} x' &= r'\cos\delta'\cos\alpha' = r\cos\delta\cos\alpha - \rho\cos\phi'\cos(\beta+\lambda) \\ y' &= r'\cos\delta'\sin\alpha' = r\cos\delta\sin\alpha - \rho\cos\phi'\sin(\beta+\lambda) \\ z' &= r'\sin\delta' \qquad\quad = r\sin\delta \qquad\quad - \rho\sin\phi' \end{aligned} \tag{7.30}$$

where the geocentric position of the observer $\mathbf{g}(t)$ is given here in terms of ρ, the distance of the observer from the centre of the Earth (in the same units as r), and the geocentric latitude ϕ' and the longitude λ (east longitudes are positive). If the origin of the right ascension system is the CIO then, $\beta = \theta$ is the Earth Rotation Angle. On the other hand, if the body is referred

to the equinox of date, then $\beta = \text{GAST}$ or $\beta = \text{GMST}$, where GAST is used with the true equinox of date and GMST with the mean equinox of date.

Section 7.4.3.2 gives the formulae for the position of the observer in the ITRS, which is an Earth-fixed (of date) reference system, while § 7.4.3.5 gives the geocentric position of the observer in the standard reference system of the ICRS.

7.2.2.2 Approximate Diurnal Parallax

Approximations to Eq. 7.30 may be made in various ways. For objects relatively close to the Earth, such as the Moon, whose parallax is significant, it can be assumed that the Earth is spherical by setting $\rho = 1$ Earth radii. For the more distant bodies such as the Sun, the planets, or comets, whose parallax amounts to only a few seconds of arc, it can be assumed that the geocentric and topocentric distance are equal, i.e., $r' = r$. Thus for such bodies the topocentric right ascension and declination, (α', δ'), may be approximated using the geocentric position (α, δ), to sufficient accuracy by the first-order approximation

$$\begin{aligned} \alpha' &= \alpha - \pi \frac{\rho}{a} \cos\phi' \sin h \sec\delta \\ \delta' &= \delta - \pi \frac{\rho}{a} (\sin\phi' \cos\delta - \cos\phi' \cos h \sin\delta) \end{aligned} \tag{7.31}$$

where π is the equatorial horizontal parallax, a the equatorial radius of the Earth, ρ the geocentric distance of the observer and h the geocentric hour angle.

The solar parallax is given by

$$\sin\pi_\odot = a/A \quad \text{and} \quad \pi_\odot = 8''.794\,143 \tag{7.32}$$

where appropriate values of a and A (the unit distance) are given in Section K of *The Astronomical Almanac*.

The equatorial horizontal parallax (horizontal parallax) of any object may be calculated from

$$\pi = \pi_\odot/\Delta \tag{7.33}$$

where Δ is the geocentric distance of the object in au.

In preliminary work on comets and minor planets, where the geocentric distance is unknown, it is convenient to calculate parallax factors p_α and p_δ for each observation; these may be used, once the geocentric distances are determined, to give the parallax corrections in the form

$$\Delta\alpha = p_\alpha/\Delta \qquad \Delta\delta = p_\delta/\Delta \tag{7.34}$$

where $\Delta\alpha = \alpha - \alpha'$ and $\Delta\delta = \delta - \delta'$. The parallax factors are calculated from

$$\begin{aligned} p_\alpha &= 8''.794\,143\ \rho\ \cos\phi' \sin h \sec\delta = 0^s.5862\,762\ \rho\ \cos\phi' \sin h \sec\delta \\ p_\delta &= 8''.794\,143\ \rho\ (\sin\phi' \cos\delta - \cos\phi' \cos h \sin\delta) \end{aligned} \tag{7.35}$$

where ρ is expressed in au.

The parallax correction for altitude, called *parallax in altitude*, is given approximately by $\pi \cos a'$, where a' is the topocentric altitude; it is added to the topocentric altitude to form the geocentric altitude to low precision (about $0'.1$); there is no correction for azimuth (Z).

This approximation does not allow for the oblateness of the Earth, which, for the Moon, can produce an error of up to $0.''2$. For an observer at latitude ϕ the oblateness of the Earth can be corrected for by adding the next term of the expansion which is

$$-\pi f \sin^2 \phi \cos a' + \pi f \sin 2\phi \cos Z \sin a' \tag{7.36}$$

where Z is the azimuth and f is the flattening (see § 7.4.3.2).

7.2.2.3 Approximate Annual Parallax

The reduction for annual parallax from the barycentric place (α, δ) to the geocentric place (α_1, δ_1) is given by

$$\begin{aligned} \alpha_1 &= \alpha + \pi(X \sin\alpha - Y \cos\alpha)/(15 \cos\delta) \\ \delta_1 &= \delta + \pi(X \cos\alpha \sin\delta + Y \sin\alpha \sin\delta - Z \cos\delta) \end{aligned} \tag{7.37}$$

where π is the parallax in arcseconds, X, Y, Z are the barycentric coordinates of the Earth in au, and the right ascension is expressed in units of time. These expressions are used in the Day Number methods (see § 7.4.5.3).

The times of reception of periodic phenomena, such as pulsar signals, may be reduced to a common origin at the barycentre by adding the light-time corresponding to the component of the Earth's position vector along the direction of the object, that is by adding to the observed times $(X \cos\alpha \cos\delta + Y \sin\alpha \cos\delta + Z \sin\delta)/c$, where $c = 173.14$ au/day, and the light-time for 1 au is $1/c = 0^{\mathrm{d}}.0057\,755$.

7.2.3 Aberration

The velocity of light is finite, and so the apparent direction of a moving celestial object from a moving observer is not the same as the geometric direction of the object from the observer at the same instant. This displacement of the apparent position from the geometric position may be attributed in part to the motion of the object, and in part to the motion of the observer, these motions being referred to an inertial frame of reference. The former part, independent of the motion of the observer, may be considered to be a correction for *light-time* and is termed *light-time displacement*; the latter part, independent of the motion or distance of the object, is referred to as *stellar aberration*, since for the stars (see § 7.2.1) the normal practice is to ignore light-time displacement. The sum of the two parts is called *planetary aberration*, since it is applicable to planets and other members of the solar system.

7.2.3.1 Light-Time

In Fig. 7.2, E is a stationary observer at time t, and P is the position of a celestial object also at time t. The dotted curve represents the orbit of P. The light which is received at E at time t was emitted by the celestial object when it was at P′ at time $(t - \tau)$ where τ is the light-time; i.e., the time taken for the light to travel from P′ to E.

Light-time is calculated iteratively, with a first approximation τ_1 calculated from the geometric distance between the object and the observer at time t, and the next approximation τ_2 calculated from the distance between P′ at $(t - \tau_1)$ and the observer at time t. No allowance has been made here for the relativistic delay caused by the Sun's gravitational field. However, the apparent and intermediate place algorithm includes this effect (see § 7.4.1.3), which is of the order of 1 microarcsecond.

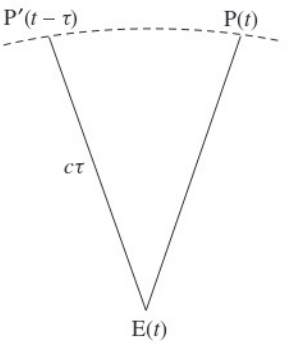


Figure 7.2 Light-time displacement

7.2.3.2 Stellar Aberration

In general, the observer at E will be moving with a velocity **V**. The apparent change in the geometric direction of the celestial object at P′ due to the motion of the observer is called *stellar aberration*. The motion of an observer on the Earth is the resultant of diurnal rotation of the Earth, the orbital motion of the Earth about the centre of mass of the solar system, and the motion of this centre of mass in space. The stellar aberration is, therefore, made up of three components, which are referred to as *diurnal aberration*, *annual aberration* and *secular aberration*. The stars and the centre of mass of the solar system may each be considered to be in uniform rectilinear motion; in this case the correction for light-time and the secular aberration are indistinguishable, and the aberrational displacement due to the relative motion is merely equal to the proper motion of the star multiplied by the light-time; it is constant for each star, and in general, is not known, and is therefore ignored (see § 7.2.1 on space motion for further discussion). The term "stellar aberration" is sometimes loosely used in contexts where "annual aberration" should strictly be used.

In Fig. 7.3, **p** is a unit vector in the geometric direction EP′, i.e., in the direction of the body at time t allowing for light-time (but ignoring the effect of light-deflection). The observer is moving with a velocity **V** relative to the stationary frame, and at time t will observe the body at P″ in the direction $\mathbf{p}_1$, where $\mathrm{P'EB} = \theta$ is the angle between the direction of motion and **p** in the stationary frame, and $\mathrm{P'EP''} = \Delta\theta$ is the displacement due to aberration in the moving frame, which is always towards the direction of motion.

The classical Newtonian expression for the direction of the source as seen by the moving observer is obtained by vector addition of velocities as follows:

$$\mathbf{p}_1 = \frac{\mathbf{p} + \mathbf{V}/c}{|\mathbf{p} + \mathbf{V}/c|}. \tag{7.38}$$

Taking the scalar part of the vector cross product of **p** with Eq. 7.38, then

$$\sin\Delta\theta = \frac{(V/c)\sin\theta}{\sqrt{(1 + 2(V/c) + (V/c)^2)}} = \frac{V}{c}\sin\theta - \frac{1}{2}\left(\frac{V}{c}\right)^2 \sin 2\theta + \cdots \tag{7.39}$$

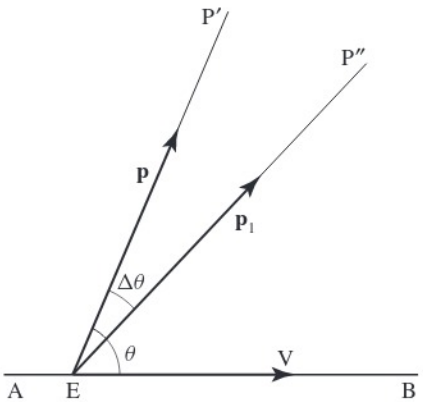


Figure 7.3 Stellar aberration

since

$$|\mathbf{p} \wedge \mathbf{p}_1| = \sin \Delta\theta, \quad |\mathbf{p} \wedge \mathbf{p}| = 0, \quad \text{and} \quad |\mathbf{p} \wedge \mathbf{V}/c| = \frac{V}{c} \sin\theta.$$

The term of order V/c is about 0.0001 or $20''$; the term $(V/c)^2$ has a maximum value of about $0''.001$.

In special relativity, the velocity of light is constant in the moving and stationary frame, and the Lorentz formula for the addition of velocities applies. Hence

$$\mathbf{p}_1 = \frac{\beta^{-1}\mathbf{p} + (\mathbf{V}/c) + (\mathbf{p} \cdot \mathbf{V}/c)(\mathbf{V}/c)/(1+\beta^{-1})}{1 + \mathbf{p} \cdot \mathbf{V}/c} \tag{7.40}$$

where $\beta^{-1} = \sqrt{1-(V/c)^2}$, again taking the modulus of the vector cross product of Eq. 7.40 with $\mathbf{p}$, then

$$\begin{aligned} \sin \Delta\theta &= \frac{(V/c)\sin\theta + \frac{1}{2}(V/c)^2 \sin 2\theta/(1+\beta^{-1})}{1+(V/c)\cos\theta} \\ &= \frac{V}{c}\sin\theta - \frac{1}{4}\left(\frac{V}{c}\right)^2 \sin 2\theta + \cdots \end{aligned} \tag{7.41}$$

which shows that special relativistic aberration and classical Newtonian aberration agree to order V/c (mas precision). However, it is recommended that special relativistic aberration (Eq. 7.40) be used, particularly when high precision is required (see also apparent and intermediate place algorithm, § 7.4.1.3 and § 7.4.1.5).

7.2.3.3 Classical Annual Aberration

In accordance with recommendations of the IAU (1952) the annual aberration is calculated as from 1960 from the actual motion of the Earth, referred to an inertial frame of reference and to the centre of mass of the solar system. The resulting aberrational displacement $\Delta\theta$ may be resolved into corrections to the directional coordinates by standard methods. If, for example $\dot{X}$, $\dot{Y}$ and $\dot{Z}$ are the components of the Earth's velocity parallel to equatorial rectangular axes,

the corrections to right ascension and declination, referred to the same equator and origin of right ascension, in the sense "apparent place minus mean place" are, to second order in V/c:

$$\begin{aligned}\cos\delta\,\Delta\alpha = &-\frac{\dot{X}}{c}\sin\alpha + \frac{\dot{Y}}{c}\cos\alpha \\ &+ \frac{1}{c^2}(\dot{X}\sin\alpha - \dot{Y}\cos\alpha)(\dot{X}\cos\alpha + \dot{Y}\sin\alpha)\sec\delta + \cdots\end{aligned} \tag{7.42}$$

and

$$\begin{aligned}\Delta\delta = &-\frac{\dot{X}}{c}\cos\alpha\sin\delta - \frac{\dot{Y}}{c}\sin\alpha\sin\delta + \frac{\dot{Z}}{c}\cos\delta \\ &- \frac{1}{2c^2}(\dot{X}\sin\alpha - \dot{Y}\cos\alpha)^2\tan\delta \\ &+ \frac{1}{c^2}(\dot{X}\cos\delta\cos\alpha + \dot{Y}\cos\delta\sin\alpha + \dot{Z}\sin\delta) \\ &\quad\times(\dot{X}\sin\delta\cos\alpha + \dot{Y}\sin\delta\sin\alpha - \dot{Z}\cos\delta) + \cdots\end{aligned} \tag{7.43}$$

These equations are usually used to first order in (V/c), and they were also used in the Day Numbers methods (see § 7.4.5.3).

To a lower precision it is possible to use the expressions

$$\dot{X} = +0.0172\sin\lambda \qquad \dot{Y} = -0.0158\cos\lambda \qquad \dot{Z} = -0.0068\cos\lambda \tag{7.44}$$

for the barycentric velocity of the Earth with respect to the mean equator and equinox of J2000.0, where λ is the apparent longitude of the Sun.

Also to first order in V/c, we obtain for the aberration in right ascension and declination due to the unperturbed elliptic component of the orbital motion of the Earth with respect to the Sun, obtained as a correction to be applied to the geometric place α, δ in order to obtain the apparent place α_1, δ_1:

$$\begin{aligned}\alpha_1 - \alpha = &-(\kappa\sin\odot + \kappa e\sin\Pi)\sin\alpha\sec\delta \\ &- (\kappa\cos\odot\cos\epsilon + \kappa e\cos\Pi\cos\epsilon)\cos\alpha\sec\delta \\ \delta_1 - \delta = &-(\kappa\sin\odot + \kappa e\sin\Pi)\cos\alpha\sin\delta \\ &- (\kappa\cos\odot\cos\epsilon + \kappa e\cos\Pi\cos\epsilon)(\tan\epsilon\cos\delta - \sin\alpha\sin\delta)\end{aligned} \tag{7.45}$$

where $\odot$ is the true geometric longitude of the Sun, e, Π are the eccentricity and longitude of perigee of the solar orbit, ϵ is the mean obliquity of the ecliptic and κ is the constant of aberration (see Eq. 7.46). The second term in each factor in Eq. 7.45 depends explicitly on the eccentricity and represents the components of the displacement due to the departure of the elliptic orbital motion from a circle. The component of the aberration that depends on e is known as elliptic aberration, and sometimes referred to as the *E-terms*.

The constant of aberration κ, is the ratio of the mean orbital speed of the Earth to the speed of light, where perturbations and the motion of the Sun relative to the barycentre are neglected, and it is derived from,

$$\kappa = na/(c\sqrt{1-e^2}) \tag{7.46}$$

Table 7.3 Coefficients (nma/c) for the planets

Venus	0.″0001	Jupiter	0.″0086	Uranus	0.″0002
Earth	0.″0001	Saturn	0.″0019	Neptune	0.″0002

where c is the speed of light, a is the mean distance of the Earth from the Sun, n is the mean motion and e is the eccentricity of the orbit.

The annual aberration due to the barycentric motion of the Sun or to the action of any particular planet may be obtained, when the ecliptic latitude of the planet is neglected, from

$$\begin{aligned}\alpha_1 - \alpha &= -\frac{nma}{c}(\sin\alpha \sin l + \cos\epsilon \cos\alpha \cos l) \sec\delta \\ \delta_1 - \delta &= -\frac{nma}{c}(\cos\alpha \sin\delta \sin l + \cos l(\sin\epsilon \cos\delta - \cos\epsilon \sin\alpha \sin\delta))\end{aligned} \tag{7.47}$$

where l is the heliocentric ecliptic longitude of the planet, m is the ratio of mass of the planet to Sun, a is the mean distance, and n is the mean motion. The coefficients to be used are given in Table 7.3.

The Sun's aberration in longitude, assuming unperturbed elliptical motion, can be given as

$$\Delta\lambda = -\kappa \sec\beta(1 + \epsilon \cos v) = \kappa a(1 - e^2)/R \tag{7.48}$$

where κ is the constant of aberration; a, e and v are the semimajor axis, eccentricity and true anomaly of the Earth's orbit; and β and R are the Sun's latitude and true distance. The e^2 term affects only the fifth significant figure; so until the constant of aberration was specified to five significant figures and the longitude of the Sun was given to three decimal figures, this term was ignored.

Measurements of radial velocity may be reduced to a common origin at the barycentre by adding the component of the Earth's velocity in the direction of the object, that is, by adding

$$\dot{X} \cos\alpha \cos\delta + \dot{Y} \sin\alpha \cos\delta + \dot{Z} \sin\delta. \tag{7.49}$$

7.2.3.4 Diurnal Aberration

The rotation of the Earth on its axis carries the observer towards the east with a velocity $\omega\rho \cos\phi'$, where ω is the equatorial angular velocity of the Earth, (the nominal mean value of ω is $7.292\,115 \times 10^{-5}$ radians per second; if a is the equatorial radius, then $a\omega = 0.465$ km/s is the equatorial rotational velocity of the surface of the Earth), and ρ and ϕ' are the geocentric distance and latitude of the observer, respectively. The corresponding constant of diurnal aberration is

$$\frac{a\omega}{c}\frac{\rho}{a} \cos\phi' = 0.''3200 \frac{\rho}{a} \cos\phi' = 0^s.02133 \frac{\rho}{a} \cos\phi'. \tag{7.50}$$

The aberrational displacement may be resolved into corrections (apparent − mean) in right ascension and declination:

$$\begin{aligned}\Delta\alpha &= 0^s.02133 \frac{\rho}{a} \cos\phi' \cos h \sec\delta \\ \Delta\delta &= 0.''3200 \frac{\rho}{a} \cos\phi' \sin h \sin\delta\end{aligned} \tag{7.51}$$

where h is the hour angle. The effect is small but is of importance in meridian observations. For a star at transit, $h = 0^\circ$ or 180°, so $\Delta\delta$ is zero, but

$$\Delta\alpha = \pm 0^{s}.02133 \frac{\rho}{a} \cos\phi' \sec\delta \tag{7.52}$$

where the plus and minus signs are used for upper and lower transits, respectively; this may be regarded as a correction to the time of transit.

Alternatively, the effect may be computed in rectangular coordinates using the following expression for the geocentric velocity ($\dot{\mathbf{g}}(t)$) vector of the observer, ignoring polar motion, with respect to the celestial equatorial reference system of date:

$$\dot{\mathbf{g}}(t) = \begin{bmatrix} -\dot{\beta}\rho \cos\phi' \sin(\beta + \lambda) \\ \dot{\beta}\rho \cos\phi' \cos(\beta + \lambda) \\ 0 \end{bmatrix} \tag{7.53}$$

where β is either the Greenwich Sidereal Time (mean or apparent) or the Earth Rotation Angle, as appropriate, and λ is the longitude (east longitudes are positive). The geocentric velocity vector of the observer is added to the barycentric velocity of the Earth's centre, to obtain the corresponding barycentric velocity vector of the observer (see § 7.4.3.3–7.4.3.5).

7.2.3.5 Planetary Aberration

Planetary aberration is the apparent displacement of the observed position of a celestial body produced by both the motion of the body and the motion of the Earth. It is often calculated by adding the correction for stellar aberration (§ 7.2.3.2) to the geometric position corrected for light-time (§ 7.2.3.1). On the other hand it may be calculated directly, either by using the barycentric positions of the body and the Earth at time $(t - \tau)$, or by using the barycentric positions and velocities of the body and the Earth at time t as described below. However, although these latter two methods are simple and widely used, the first method may be preferred since it brings out the principle that aberration depends upon the relative velocity of observer and object.

If we denote the barycentric position of the Earth at time t by $\mathbf{E}_B(t)$ and the barycentric position of the planet at time t by $\mathbf{u}_B(t)$, then the geometric geocentric position of the planet at time t, allowing for light-time, is given by

$$\mathbf{P}(t) = \mathbf{u}_B(t - \tau) - \mathbf{E}_B(t) \tag{7.54}$$

where $\tau = P/c$ is the light-time and $P = |\mathbf{P}|$. If $\mathbf{P}_1$ is the geocentric position of the planet allowing for planetary aberration, then using classical stellar aberration (Eq. 7.38), we get

$$\mathbf{P}_1 = \mathbf{P} + \tau\dot{\mathbf{E}}_B. \tag{7.55}$$

If we assume that the velocity of the Earth $\dot{\mathbf{E}}_B$ and the velocity of the planet $\dot{\mathbf{u}}_B$ are constant during the light-time, then Eq. 7.54 may be written as

$$\mathbf{P}_1 = \mathbf{u}_B(t - \tau) - \mathbf{E}_B(t - \tau) \tag{7.56}$$

or

$$\mathbf{P}_1 = \mathbf{u}_B(t) - \mathbf{E}_B(t) - \tau(\dot{\mathbf{u}}_B - \dot{\mathbf{E}}_B). \tag{7.57}$$

Since Newtonian aberration and special relativistic aberration agree to order V/c, it is only when mas precision is required that it becomes necessary to use a rigorous formula (see § 7.2.3.2).

7.2.3.6 Differential Annual Aberration

The differential coordinates of an object with respect to a "fixed" star will be affected by differential aberration; if $\Delta\alpha$, $\Delta\delta$ are the observed differences of the coordinates in the sense object minus star, then the corrections for differential annual aberration are

$$\begin{aligned}\Delta(\alpha_1 - \alpha) &= (-\dot{X}\cos\alpha - \dot{Y}\sin\alpha)\sec\delta\Delta\alpha + (-\dot{X}\sin\alpha + \dot{Y}\cos\alpha)\sec\delta\tan\delta\Delta\delta \\ \Delta(\delta_1 - \delta) &= -(-\dot{X}\sin\alpha + \dot{Y}\cos\alpha)\sin\delta\Delta\alpha + (-\dot{X}\cos\alpha - \dot{Y}\sin\alpha)\cos\delta\Delta\delta \\ &\quad - \dot{Y}\tan\epsilon_0\sin\delta\Delta\delta\end{aligned} \tag{7.58}$$

where $\dot{X}$ and $\dot{Y}$ are the Earth's barycentric velocity components with respect to the mean equinox of date and the units of each term are consistent. (Note: $+\dot{Y}$ and $-\dot{X}$ are the defunct C and D Besselian Day Numbers, respectively.) The corrections should be applied with those for differential precession and nutation to give mean positions referred to the same equator and origin of right ascension as those of the stars.

Alternatively the corrections for differential annual aberration to be added to the observed differences (in the sense moving object minus star) of right ascension and declination to give true differences are:

$$\begin{array}{lll} \text{in right ascension} & a\Delta\alpha + b\Delta\delta & \text{in units of } 0^{\mathrm{s}}.001 \\ \text{in declination} & c\Delta\alpha + d\Delta\delta & \text{in units of } 0''.01 \end{array} \tag{7.59}$$

where $\Delta\alpha$, $\Delta\delta$ are the observed differences in units of 1^{m} and $1'$ respectively, and where a, b, c, d are coefficients defined by:

$$\begin{aligned} a &= -5.701\cos(H+\alpha)\sec\delta \\ b &= -0.380\sin(H+\alpha)\sec\delta\tan\delta \\ c &= +8.552\sin(H+\alpha)\sin\delta \\ d &= -0.570\cos(H+\alpha)\cos\delta \\ H^{\mathrm{h}} &= 23.4 - \text{day of year}/15.2. \end{aligned} \tag{7.60}$$

7.2.3.7 Differential Planetary Aberration

Aberration, because of its dependence on the relative motions and distances, sometimes has complex effects where two or more bodies are involved, as, e.g., in eclipses, transits, and the phenomena of satellite systems; and on some past occasions, the determination of these effects has presented an intricate problem.

In a transit of a planet across the disk of the Sun, e.g., the external contacts occur when the observer is on the conical surface that circumscribes the Sun and the planet and has its vertex between the Sun and the planet. The internal contacts occur when the observer is on the cone circumscribing the planet and the Sun having its vertex between the planet and the Earth. The observed contacts are at the instants when the *apparent* positions of a point on the limb of the planet and a point on the limb of the Sun are the same, i.e., the ray of light from the Sun that reaches the geometric position of the observer at the instant T of contact

has grazed the planet on the way. This ray left the Sun at a previous time $T - \tau_2$ and reached the planet at time $(T - \tau_2) + \tau_1$. The circumscribing cones are formed by the grazing rays; hence, the points on the Earth and the planet that lie in the same straight line on one of the cones at the instant of a contact are the geometric position of the observer at the time T, and the geometric position of the point on the planet at time $T - \tau_2 + \tau_1$. Therefore, in the formulae of the theory of transits, for any value of the time T, all quantities depending on the time must be derived from the values of the geometric coordinates (r, l, b) of the planet at $T - \tau_2 + \tau_1$ and the geometric coordinates (r', l', b') of the Earth at T.

Similarly, in comparing observed positions of objects in the solar system with one another or with reference stars, in order to determine the coordinates of a body, great care is required in correcting the observations for aberration, according to the means of observation used, and the method of comparison.

In eclipsing binary systems, an apparent variation of the period may be produced by the variation in light-time with changing distance from the observer due to an orbital motion of the eclipsing pair with respect to a distant third component (Irwin 1959).

7.2.4 Gravitational Light-Deflection

Gravitational light-deflection was predicted by Einstein and first confirmed photographically at the eclipse of 1919 May by expeditions from Greenwich and Cambridge, England (Dyson, Eddington and Davidson 1920). It has been measured many times and most recent high precision measurements have been made with radio interferometers, which can observe sources very close to the Sun. Fomalont and Sramek (1975) have confirmed the deflection predicted by Einstein's theory with an accuracy of 1%, which is an order of magnitude more accurate than that achieved optically from eclipse observations. The deflection increases the closer the light path is to the Sun; at a heliocentric elongation of 90°, however, the deflection has decreased to $0.''004$.

The algorithm for the deflection of light is that of Yallop (1984) as given in *The Astronomical Almanac* 1984 (Nautical Almanac Offices 1983), which is an adaption of Murray's (1981) formulae. The isotropic metric has been assumed. Only the Sun's gravitational field has been included; each of the planets causes a similar effect that is smaller by a factor equal to the ratio of the planet's mass to that of the Sun (1/1047 for Jupiter). The gravitational field of the Earth, also ignored here, can deflect light by a few tenths of a milliarcsecond for ground-based observers. It may also have to be allowed for in precise astrometry with Earth satellites.

In Fig. 7.4, S is the Sun, P the body that is being observed, and E is the Earth. The unit vectors **e** and **q** represent the heliocentric directions of the Earth and the body, respectively. The heliocentric elongation of the Earth from P is ψ, where $\cos\psi = \mathbf{q} \cdot \mathbf{e}$. The geocentric direction to the body P when the light left it is given by the unit vector **p**. The dotted arc AEB represents the light-path as it passes the Earth. The tangent to the light-path at E is XEY. As the light, which was emitted at P, travels along the path AB, it is always deflected towards the Sun. At E the direction between **p** and the tangent to the light-path is $\Delta\phi$ (as shown in the figure). Einstein's general relativity theory predicts that

$$\Delta\phi = \frac{2\mu}{c^2 E} \frac{\sin\psi}{1 + \cos\psi} \tag{7.61}$$

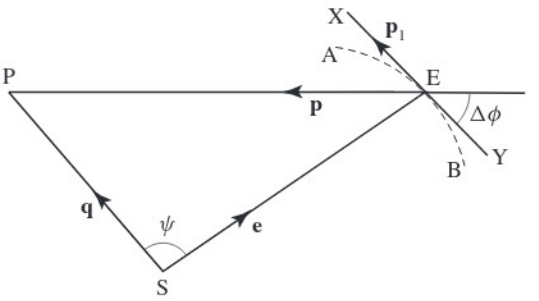


Figure 7.4 Gravitational light-deflection

where E is the distance of the Earth from the Sun, μ is the heliocentric gravitational constant, and c is the speed of light.

The apparent direction of P is along the tangent to the light-path $\mathbf{p_1}$, and by vector addition

$$\mathbf{p_1} = \mathbf{p} + \frac{(\mathbf{q} \wedge \mathbf{e}) \wedge \mathbf{p}}{\sin \psi} \Delta\phi \tag{7.62}$$

since $(\mathbf{q} \wedge \mathbf{e}) \wedge \mathbf{p}/\sin\psi$ is a unit vector in the plane PES, at right angles to $\mathbf{p}$ and pointing away from the Sun. This equation may be written in the form which is more useful for computation,

$$\mathbf{p_1} = \mathbf{p} + \frac{g_1}{g_2}\left[(\mathbf{p}\cdot\mathbf{q})\mathbf{e} - (\mathbf{e}\cdot\mathbf{p})\mathbf{q}\right]. \tag{7.63}$$

The dimensionless scalar quantities g_1 and g_2 are

$$g_1 = \frac{2\mu}{c^2 E} \quad \text{and} \quad g_2 = 1 + \mathbf{q}\cdot\mathbf{e} \tag{7.64}$$

where $\mu/c^2 = k^2\tau_A^2/86400^2$, k is the Gaussian gravitational constant, and τ_A is the light-time for unit distance (1 au) appropriate for the ephemeris being used (see § 7.4.1.3, Eq. 7.111). These constants are published in Section K of *The Astronomical Almanac*. The value of g_1 is always close to 2×10^{-8}, and g_2 varies between 0 and +2. The vector $\mathbf{p_1}$ is a unit vector to order μ/c^2.

Stars represent the asymptotic case when $\mathbf{p} = \mathbf{q}$, and Eq. 7.63 becomes

$$\mathbf{p_1} = \mathbf{p} + g_1 \frac{\mathbf{e} - (\mathbf{p}\cdot\mathbf{e})\mathbf{p}}{1 + \mathbf{p}\cdot\mathbf{e}}. \tag{7.65}$$

When one is applying the light-deflection correction in the algorithm for apparent and intermediate places (see § 7.4.1.4), using the vector $\mathbf{E_H}$ in the relativistic deflection computation introduces a minor approximation resulting from the use of the barycentric position of the Sun at the epoch of observation. The resulting error cannot exceed 0.1 mas in the worst case (object observed at the limb of the Sun with barycentric motion of the Sun orthogonal to the line of sight) and is generally much less. Furthermore, the deflection algorithm itself results from a first-order development that assumes small deviations of the photon track from

Table 7.4 Apparent deflection angles

D	0.°25	0.°5	1°	2°	5°	10°	20°	50°	90°
$\Delta\phi$	1.″866	0.″933	0.″466	0.″233	0.″093	0.″047	0.″023	0.″009	0.″004

a straight line in Euclidian space; the error in neglecting second-order effects can reach about 0.5 mas for an object observed at the Sun's limb (Kammeyer 1988, private communication).

Table 7.4 tabulates the deflection angles $\Delta\phi = g_1 \tan(\psi/2)$ (Eq. 7.61) for various values of $D = 180° - \psi$ (for stars D approximates the geocentric elongation). The body disappears behind the Sun when D is less than the limiting grazing value of about 0.°25.

Table 7.4 was produced assuming that the Earth-Sun distance $E = 1$, and thus $g_1 = 0.''00407$. The variation of the Earth-Sun distance modulates the value of g_1 by less than 2%. This simple form of the gravitational deflection formula has been noted previously by Shapiro (1967) and by Fukushima (1982, private communication). In this form, the deflection is not explicitly dependent on the distance of the emitting body from the Sun or the Earth. Therefore, to an observer on the Earth, the apparent gravitational deflection is the same for all objects that lie anywhere on a given line that extends radially outward from the Sun. This result holds regardless of the orientation of the line with respect to the Earth.

Figure 7.5 shows the magnitude of the deflection of light, as viewed from the Earth, for planets and stars as a function of the geocentric angular separation of the observed body from the centre of the Sun. Maximum deflection occurs for bodies that are about to be occulted by the Sun. Minimum deflection for Mercury and Venus occurs when they are about to transit the Sun. For the other bodies minimum deflection occurs at 180° elongation from the Sun, that is, near opposition. The figure was produced from Eq. 7.61 assuming circular orbits.

The equations for light-deflection have an indeterminacy for light-paths starting beyond the Sun on the extension of the Sun-Earth line; bodies there are hidden by the Sun's disk and unobservable in any event. For these bodies or the Sun itself, the deflection can be considered to be zero.

7.2.4.1 Approximate Light-Deflection for Stars

The increments to be added to the calculated right ascension and declination of the star may be evaluated approximately from

$$\begin{aligned} \cos D &= \sin\delta \sin\delta_s + \cos\delta \cos\delta_s \cos(\alpha - \alpha_s) \\ \Delta\alpha &= 0.^s000\,271 \frac{\cos\delta_s \sin(\alpha - \alpha_s)}{(1 - \cos D)\cos\delta} \\ \Delta\delta &= 0.''004\,07 \frac{\sin\delta \cos\delta_s \cos(\alpha - \alpha_s) - \cos\delta \sin\delta_s}{1 - \cos D} \end{aligned} \tag{7.66}$$

where $\alpha, \delta, \alpha_s, \delta_s$ are the geocentric right ascensions and declinations of the star and the Sun, respectively. For stars, D, the geocentric elongation, approximates $180° - \psi$, where ψ is the heliocentric elongation.

7.2.5 Celestial "Of Date" Positions

This section gives the rotations required to transform positions from the GCRS to a celestial "of date" system (CRS) that are used in this chapter. Simply, the of date systems are those that

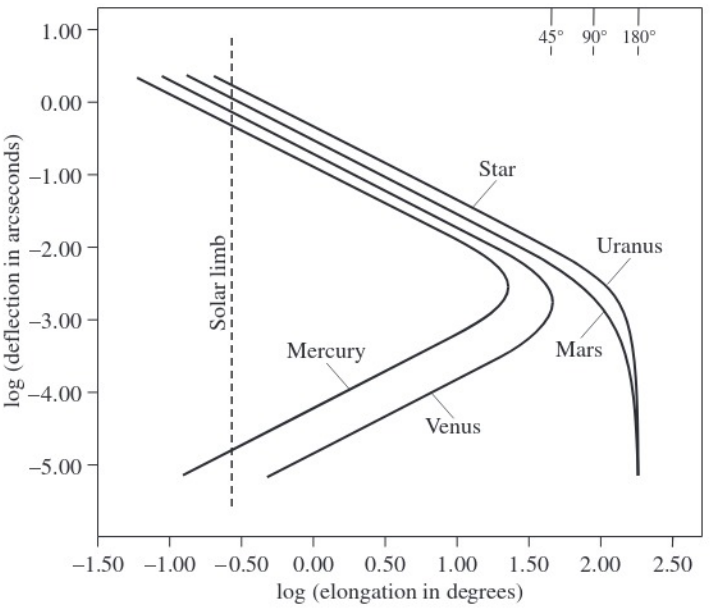


Figure 7.5 Light from the planets and stars deflected by the Sun

have precession and nutation included. Celestially they are the true equator and equinox of date or the Celestial Intermediate Reference System, which is the (true) equator and CIO of date. The transformation for the former, is designated $\mathbf{M} = \mathbf{NPB}$ where the origin of right ascension is the equinox. While the transformation matrix for the latter is designated $\mathbf{C} = \mathbf{C}(\mathcal{X}, \mathcal{Y}, s)$, where the IAU recommended origin for right ascension is the CIO (see § 7.1.1). The three concepts involved are frame bias, and precession and nutation, and practically are usually combined into a single matrix transformation.

The frame bias consist of the three offsets of the mean equator and (dynamical) mean equinox of J2000.0, provided by the current model, with respect to the GCRS; the first two offsets are the mean pole offsets at J2000.0 and the third is the offset in right ascension of the mean dynamical equinox of J2000.0. There are different offsets depending whether, for example, the object is on the FK5 or Hipparcos reference systems, which are all discussed in Chapter 4.

A practical definition of precession-nutation in the case of the Earth, consistent with the IAU 2000/2006 resolutions (IAU 2001, 2008; URL[6]), is that it is the motion of the CIP in the GCRS, including free core nutation and other corrections to the standard models: precession is the secular part of this motion plus the term of 26000-year period and nutation is that part of the CIP motion not classed as precession. Precession is discussed in Chapter 6.

Nutation is also described in Chapter 6 and Web links for the IAU 2000A series may be found via *The Astronomical Almanac Online* at URL[1]. IAU-SOFA also provides routines for calculating $\Delta\psi$ and $\Delta\epsilon$ (NUT00A and NUT06A, URL[3]). The latter routine also implements the IAU 2000A nutation but it also includes the adjustments for use with the IAU 2006 precession; the combined precession-nutation model is termed IAU 2006/2000A$_R$ in this book. Kaplan (2005) has published all the terms of the IAU 2000A nutation series, and

USNO's NOVAS subroutine package (Kaplan et al. 2009; URL[2]) also implements them (NU2000A Fortran-version; iau2000a C-version).

Detailed information on the individual matrices **B**, **P** and **N** is given in Chapter 6, § 6.5 and § 6.6. Both the combined matrices **M** and **C**, the $\mathcal{X}$, $\mathcal{Y}$ position of the CIP, the CIO locator s, the true obliquity of the ecliptic (ϵ), and the nutations in longitude and obliquity ($\Delta\psi$, $\Delta\epsilon$) are all tabulated daily at 0^{h} TT in various tables in Section B of *The Astronomical Almanac*.

The procedures described in this chapter are those used by *The Astronomical Almanac* and do not include free core nutation or any of the additional effects that are obtained by observation.

7.2.5.1 Equinox-Based Transformation

The traditional transformation combining frame bias, precession and nutation may be expressed thus

$$\mathbf{M} = \mathbf{N}\,\mathbf{P}\,\mathbf{B} = \mathbf{R}_3(-s + E_o)\,\mathcal{R}_\Sigma \tag{7.67}$$

$$= \mathbf{R}_1(-[\epsilon_\mathrm{A} + \Delta\epsilon])\,\mathbf{R}_3(-[\bar{\psi} + \Delta\psi])\,\mathbf{R}_1(\bar{\phi})\,\mathbf{R}_3(\bar{\gamma}). \tag{7.68}$$

Nutation is included via ($\Delta\psi$, $\Delta\epsilon$), the nutations in longitude and obliquity, respectively (see Chapter 6). Frame bias has been included with precession (IAU 2006, Hilton 2006) and represented by the angles $\bar{\gamma}$, $\bar{\phi}$, $\bar{\psi}$, and ϵ_A the obliquity of the ecliptic with respect to the mean equator of date, and are given by

$$\bar{\gamma} = -0.''052\,928 + 10.''556\,378\,T + 0.''493\,2044\,T^2 - 0.''000\,312\,38\,T^3 - 2.''788 \times 10^{-6}\,T^4 + 2.''60 \times 10^{-8}\,T^5 \tag{7.69}$$

$$\bar{\phi} = 84381.''412\,819 - 46.''811\,016\,T + 0.''051\,1268\,T^2 + 0.''000\,532\,89\,T^3 - 0.''440 \times 10^{-6}\,T^4 - 1.''76 \times 10^{-8}\,T^5 \tag{7.70}$$

$$\bar{\psi} = -0.''041\,775 + 5038.''481\,484\,T + 1.''558\,4175\,T^2 - 0.''000\,185\,22\,T^3 - 26.''452 \times 10^{-6}\,T^4 - 1.''48 \times 10^{-8}\,T^5 \tag{7.71}$$

$$\epsilon_\mathrm{A} = 23^\circ\,26'\,21.''406 - 46.''836\,769\,T - 0.''000\,1831\,T^2 + 0.''002\,003\,40\,T^3 - 0.''576 \times 10^{-6}\,T^4 - 4.''34 \times 10^{-8}\,T^5 \tag{7.72}$$

where T is the TT time interval in Julian centuries from J2000.0 (245 1545.0 TT). Strictly speaking precession angles should be a function of TDB, but this makes no significant difference.

The formulation of **M** in Eq. 7.67 above, in terms of $\mathcal{R}_\Sigma$ (see Eq. 7.75), s the CIO locator and E_o the equation of the origins demonstrates (Capitaine 2006) that the equinox and CIO-based (§ 7.2.5.2) paradigms are the same, except for a rotation of E_o about the CIP. This results in the different origins for measuring RA. The equation of the origins E_o is discussed in Chapter 6 (§ 6.4) and is tabulated daily at 0^{h} UT1 in Section B of *The Astronomical Almanac*. IAU-SOFA (URL[3]) provide software routines for all the quantities in this section. These concepts are discussed in full in Chapter 6.

7.2.5.2 CIO-Based Transformation

The matrix that includes frame bias, precession and nutation, and transforms positions referred to the GCRS to the Celestial Intermediate Reference System where the origin of right ascension is the CIO, may be expressed in terms of the position of the CIP $(\mathcal{X}, \mathcal{Y})$ and location of the CIO, thus

$$\mathbf{C} = \mathbf{C}(\mathcal{X}, \mathcal{Y}, s) = \mathbf{R}_3(-[E + s])\, \mathbf{R}_2(d)\, \mathbf{R}_3(E) = \mathbf{R}_3(-s)\, \mathcal{R}_\Sigma \tag{7.73}$$

where s locates the CIO (see Chapter 6) on the equator of the CIP and

$$E = \tan^{-1} \frac{\mathcal{Y}}{\mathcal{X}}, \qquad d = \tan^{-1} \sqrt{\frac{\mathcal{X}^2 + \mathcal{Y}^2}{\mathcal{Z}^2}}, \qquad \mathcal{Z}^2 = 1 - \mathcal{X}^2 - \mathcal{Y}^2. \tag{7.74}$$

The most practical way of calculating $\mathbf{C}$ is to use $\mathcal{R}_\Sigma$ (IERS 2010), which is given by

$$\mathcal{R}_\Sigma = \begin{bmatrix} 1 - a\mathcal{X}^2 & -a\mathcal{X}\mathcal{Y} & -\mathcal{X} \\ -a\mathcal{X}\mathcal{Y} & 1 - a\mathcal{Y}^2 & -\mathcal{Y} \\ \mathcal{X} & \mathcal{Y} & 1 - a(\mathcal{X}^2 + \mathcal{Y}^2) \end{bmatrix} \tag{7.75}$$

where $a = 1/(1 + \mathcal{Z})$. The $(\mathcal{X}, \mathcal{Y})$ coordinates of the CIP and s the CIO locator are given and discussed in Chapter 6[2] (§ 6.7). IAU-SOFA provides software for calculating $\mathbf{C}$ and the CIO locator s as well as the IAU 2006 series for $\mathcal{X}$, $\mathcal{Y}$ (URL[3]).

Alternatively, the $(\mathcal{X}, \mathcal{Y})$ coordinates of the CIP and $\mathcal{Z}$, may be calculated directly from the frame bias and precession-nutation angles (Capitaine 2006), and then used in Eq. 7.75. Thus

$$\begin{aligned} \mathcal{X} &= \sin\epsilon \sin\psi \cos\bar{\gamma} - (\sin\epsilon \cos\psi \cos\bar{\phi} - \cos\epsilon \sin\bar{\phi}) \sin\bar{\gamma} \\ \mathcal{Y} &= \sin\epsilon \sin\psi \sin\bar{\gamma} + (\sin\epsilon \cos\psi \cos\bar{\phi} - \cos\epsilon \sin\bar{\phi}) \cos\bar{\gamma} \\ \mathcal{Z} &= \sin\epsilon \cos\psi \cos\bar{\phi} + \cos\epsilon \cos\bar{\phi} \end{aligned} \tag{7.76}$$

where $\epsilon = \epsilon_A + \Delta\epsilon$ and $\psi = \bar{\psi} + \Delta\psi$ include the effects of nutation (see Chapter 6, § 6.6.3), while the frame bias and precession are incorporated by the angles $\bar{\gamma}$, $\bar{\phi}$, $\bar{\psi}$, and ϵ_A, and are given above in Eqs. 7.69 to 7.72.

7.2.6 Terrestrial "Of Date" Positions

This section touches on the rotations required to transform positions referred to the celestial "of date" system to one of the terrestrial systems. These systems are the Terrestrial Intermediate Reference System and the International Terrestrial Reference System (ITRS). The former system is achieved when the celestial system is rotated about the CIP so that the origin on the equator is no longer the equinox or the CIO, but is the TIO. While the latter system is the result of positioning of the TIO via the TIO locator (s') and includes the effects of polar motion. Often this is just referred to as polar motion since s' is insignificant. However, strictly, an ITRS position will need to include all the observable corrections such as free core nutation and the other parameters of the IERS (URL[5]).

2. Readers should note that matrix $\mathbf{C}$ is referred to as matrix $\mathbf{NPB}_{\mathrm{CIO}}$ in Chapter 6.

7.2.6.1 The TIO and Earth Rotation

An "of date" position in the celestial system, where the origin of right ascension is either the equinox or the CIO, may be transformed to the Terrestrial Intermediate Reference System, where the origin is the TIO. Thus GHA, or if longitude is included LHA, which are referred to the TIO ("Greenwich") meridian or the observers meridian, respectively, may be calculated. This change in origin to the TIO is achieved by a rotation of β about the z-axis, i.e., a rotation of $\mathbf{R}_3(\beta)$ about the CIP, where $\beta =$ GAST or $\beta = \theta =$ ERA and depends on the origin of right ascension and paradigm being used.

The equations for GMST, GAST and ERA are given in Chapter 6 (§ 6.8) where the topic is fully discussed (see also § 7.1.3.2). It should be remembered that GAST depends on the nutation angles (equation of the equinoxes E_e), while ERA and GMST do not. Further more, these parameters of Earth rotation, GAST(UT1,TT) and ERA(UT1), are basically functions of UT1, while precession, nutation and the solar system ephemerides are not.

7.2.6.2 Transformation to the ITRS

This section touches on the transformation ($\mathbf{W}$, see Eq. 7.1) from the Terrestrial Intermediate Reference System to the International Terrestrial Reference System (ITRS). Simply this includes the effects of polar motion. Polar motion and the TIO locator are discussed in detail in Chapter 6 (§ 6.9).

Polar motion is defined as the motion of the Earth's pole with respect to the ITRS. The main components are the Chandlerian free motion with a period of approximately 430 days, and an annual motion. It also includes sub-daily variations caused by ocean tides and periodic motions driven by gravitational torques with periods less than two days. Sub-daily variations are not included in the values distributed by the IERS (URL[5]), and are therefore to be added, after interpolation to the date of interest, using a model provided by the IERS Conventions.

Thus the transformation matrix from the Terrestrial Intermediate Reference System to the ITRS is

$$\mathbf{W} = \mathbf{R}_1(-y_p)\,\mathbf{R}_2(-x_p)\,\mathbf{R}_3(s') \tag{7.77}$$

where s', the TIO locator, is $s' = -0.''000\,047\,T$ and T is measured in Julian centuries of 36525 days from 245 1545.0 TT. The TIO locator is a measure of the secular drift of the TIO, with respect to geodetic zero longitude, that is the very slow systematic rotation of the Terrestrial Intermediate Reference System with respect to the ITRS (due to polar motion). The coordinates x_p, y_p correspond to the position of the CIP with respect to the ITRS, measured along the meridians at longitudes 0° and 270° (90° west). Current values of the coordinates, x_p, y_p, of the pole for use in the reduction of observations are published by the Central Bureau of the IERS (see *The Astronomical Almanac Online* at URL[1] for web links).

The longitude and latitude of a terrestrial observer, λ and ϕ, used in astronomical formulae (e.g., for hour angle or the determination of astronomical time), should be expressed in the Terrestrial Intermediate Reference System, that is, corrected for polar motion,

$$\lambda = \lambda_{\text{ITRS}} + \left(x_p \sin \lambda_{\text{ITRS}} + y_p \cos \lambda_{\text{ITRS}}\right) \tan \phi_{\text{ITRS}} \tag{7.78}$$

$$\phi = \phi_{\text{ITRS}} + \left(x_p \cos \lambda_{\text{ITRS}} - y_p \sin \lambda_{\text{ITRS}}\right) \tag{7.79}$$

where λ_{ITRS} and ϕ_{ITRS} are the ITRS (geodetic) longitude and latitude of the observer, and (x_p, y_p) are the ITRS coordinates of the CIP, in the same units as λ and ϕ. These formulae are approximations and should not be used for places at polar latitudes.

7.2.7 Refraction

Atmospheric refraction is included in *The Astronomical Almanac* in only a few topocentric phenomena, such as the times of rising and setting of the Sun and Moon, and in theory in the predictions of local circumstances of eclipses. However, for observational reductions the effect of refraction must be included. In this section we give several low-precision formulae, valid at the horizon, that are particularly useful for navigation as well as formulae valid for zenith distances less than 70°, which takes into account the amount of water vapour in the atmosphere. However, we start by giving an algorithm for evaluating the integral in the classical formulation using quadrature, which allows for the principal change of refraction due to variations of temperature, pressure, humidity, and even the temperature lapse rate that results in a well-defined reference value. Thus, for example, residuals of the observed values from the reference values could be used to model the local variation of refraction.

7.2.7.1 Refraction – Numerical Integration

In this section we give a precise algorithm for calculating refraction using numerical integration. The real accuracy is very dependent on the conditions, particularly for large zenith distances, and on the atmospheric model.

The atmosphere is assumed to be spherically symmetric and in hydrostatic equilibrium, and to obey the perfect gas law for the combined mixture of dry air and water vapour, and also for the dry air and water vapour separately. The two layers of the atmosphere are the troposphere and the stratosphere. The troposphere, the lowest portion, extends from the Earth to the tropopause, which is assumed to be at 11 km (h_t). In this region the temperature decreases at a constant rate ($\alpha = 0.0065$ degrees Kelvin per meter) and the relative humidity is constant and equal to its value at the observer. In the stratosphere the temperature remains constant and equal to the temperature at the tropopause (T_t) and there is no pressure due to water vapour. The upper height (h_s) of the stratosphere is taken as 80 km, since above this height refraction becomes negligible.

The total bending of a ray is given by

$$\xi = -\int_0^{z_0} \frac{r\, dn/dr}{n + r\, dn/dr}\, dz. \tag{7.80}$$

This integral is a transformation of the usual refraction integral. It has been recommended by Auer and Standish (1979, 2000) because it is more suitable for numerical integration; it is a more slowly varying function over the whole range of z and removes the problem at $z = 90°$. However, there is a discontinuity in the function dn/dr at the tropopause, and so the integral is evaluated in two parts, from $z = z_s$ to z_{ts} in the stratosphere, and from $z = z_t$ to z_0 in the troposphere.

The following procedure gives the steps required to calculate the total refraction, ξ, i.e., the sum of the refraction caused by the troposphere (ξ_t) and the stratosphere (ξ_s), from

$$\xi = \xi_t + \xi_s = \int_{z_0}^{z_t} f\, dz + \int_{z_{ts}}^{z_s} f\, dz \tag{7.81}$$

to a specified tolerance ϵ, where f is the integrand given in Eq. 7.80.

Step 1. The parameters of the Earth and the atmospheric model, which are assumed to be constant are

$$\begin{array}{llll} R = 8314.36 & M_d = 28.966 & M_w = 18.016 & \delta = 18.36 \\ r_e = 6378120 & h_t = 11\,000 & h_s = 80\,000 & \alpha = 0.0065. \end{array} \tag{7.82}$$

Step 2. The parameters of observation—the initial conditions. The observed zenith distance, z_0, of an object with wavelength of $\lambda\ \mu$m is recorded by an observer at latitude ϕ, height h_0 metres above the geoid i.e., $r_0 = r_e + h_0$ metres from the centre of the Earth. The meteorological conditions at the time of observation are the temperature T_0° Kelvin, the pressure P_0 mb and the relative humidity R_h.

Step 3. Calculate the parameters dependent on the initial conditions and the model of the atmosphere. Those denoted by C_i are needed at each step of the integration.

$$\begin{aligned} P_{w0} &= R_h(T_0/247.1)^\delta \\ \bar{g} &= 9.784(1 - 0.0026\cos 2\phi - 0.0000\,0028\,h_0) \\ A &= \left(287.604 + \frac{1.6288}{\lambda^2} + \frac{0.0136}{\lambda^4}\right)\frac{273.15}{1013.25} \times 10^{-6} \\ C_1 &= \alpha \qquad C_2 = \bar{g}M_d/R \qquad C_3 = C_2/C_1 = \gamma \\ C_4 &= \delta \qquad C_5 = P_{w0}(1 - M_w/M_d)\gamma/(\delta - \gamma) \\ C_6 &= A(P_0 + C_5)/T_0 \qquad C_7 = (AC_5 + 11.2684 \times 10^{-6}P_{w0})/T_0 \\ C_8 &= \alpha(\gamma - 1)C_6/T_0 \qquad C_9 = \alpha(\delta - 1)C_7/T_0. \end{aligned} \tag{7.83}$$

Step 4. Use the following expressions to calculate r, n and dn/dr, which depend on the atmosphere, and thus evaluate the integrand f at each step in z along the path of the ray.

The value of r corresponding to the current step in zenith distance z is found by solving Snell's law $nr\sin z = n_0 r_0 \sin z_0$ using Newton-Raphson iteration thus:

$$r_{i+1} = r_i - \left[\frac{n_i r_i - n_0 r_0 \sin z_0/\sin z}{n_i + r_i dn_i/dr_i}\right] \quad \text{for } i = 1, 2, \ldots \tag{7.84}$$

where r_i is the value of r calculated at the previous step of the integration. Convergence is rapid, so the initial estimate r_1 is not critical. Four iterations should be sufficient.

In the troposphere at distance $r \le r_t$ from the centre of the Earth, the temperature T, the refractive index n and dn/dr are calculated from

$$
\begin{aligned}
T &= T_0 - \alpha(r - r_0) \\
n &= 1 + \left[C_6 \left(\frac{T}{T_0} \right)^{\gamma-2} - C_7 \left(\frac{T}{T_0} \right)^{\delta-2} \right] \frac{T}{T_0} \\
\frac{dn}{dr} &= -C_8 \left(\frac{T}{T_0} \right)^{\gamma-2} + C_9 \left(\frac{T}{T_0} \right)^{\delta-2}.
\end{aligned} \tag{7.85}
$$

In the stratosphere at a distance r where $r_t \le r \le r_s$ and the temperature is given by $T_t = T_0 - \alpha(r_t - r_0)$ the refractive index n and dn/dr are calculated from

$$
\begin{aligned}
n &= 1 + (n_t - 1) \exp\left(-C_2 \frac{r - r_t}{T_t} \right) \\
\frac{dn}{dr} &= -\frac{C_2}{T_t} (n_t - 1) \exp\left(-C_2 \frac{r - r_t}{T_t} \right).
\end{aligned} \tag{7.86}
$$

The integrand is

$$
f\left[r, n, \frac{dn}{dr} \right] = \frac{r\, dn/dr}{n + r\, dn/dr}. \tag{7.87}
$$

Step 5. Calculate the following parameters which are required for the limits of the two integrals. At the observer, the observed zenith distance is z_0; set $r_0 = r_e + h$, and calculate $n_0, dn_0/dr_0, f_0$. At the tropopause, in the troposphere calculate $r_t = r_e + h_t$, $n_t, dn_t/dr_t, f_t$, and using Snell's law

$$
z_t = \sin^{-1} \frac{n_0 r_0 \sin z_0}{n_t r_t}. \tag{7.88}
$$

At the tropopause, in the stratosphere $r_{ts} = r_t$, and calculate $n_{ts}, dn_{ts}/dr_{ts}, f_{ts}$, and z_{ts}. At the limit of the stratosphere calculate $r_s = r_e + h_s, n_s, dn_s/dr_s, f_s$, and z_s.

Step 6. Integrate the function over the required interval using numerical quadrature, e.g., Simpson's rule, by forming the summations over equal steps of z. In the troposphere $S = (z_t - z_0)/16$ is a convenient step length to start with. Repeat the integration halving the step size each time, until there is no significance between two consecutive values and the tolerance permitted (i.e., 0.5ϵ). Repeat this step for the stratosphere. Thus, the total amount of refraction will be $\xi = \xi_t + \xi_s$.

7.2.7.2 Saastamoinen's Refraction Formula

This formula, valid for zenith distances down to 70°, was devised by Saastamoinen (1972), and it is equivalent to the refraction tables in *The Star Almanac*. Given the observed zenith distance, z_0, the temperature, pressure and the partial pressure of water vapour, (T_0, P_0, P_{w0}), the refraction for a wavelength of 0.574μm, i.e., visible light, and for an observer at sea level is

$$
\begin{aligned}
\xi = {} & 16.''271\, Q\, \tan z_0\, (1 + 0.0000\,394\, Q \tan^2 z_0) \\
& - 0.''0000\,749\, P_0 (\tan z_0 + \tan^3 z_0)
\end{aligned} \tag{7.89}
$$

where $Q = (P_0 - 0.156 P_{w0})/T_0$.

A formula to calculate P_{w0} in terms of the relative humidity is given at the start of Step 3 in § 7.2.7.1. Saastamoinen gives correction tables for other wavelengths and heights above sea level.

7.2.7.3 Low Precision Refraction

Topocentric phenomena such as the times of rising and setting, and navigational reductions require the amount of refraction accurate to $0'.5$. The following formula is dependent on the apparent altitude, H; i.e., the observed altitude corrected for the index error of the sextant and dip (see Chapter 12, § 12.3.3.1), on the temperature and pressure, and gives the amount of refraction, R, in degrees;

$$R = \left(\frac{0.28\,P}{T+273}\right)\frac{0^{\circ}.0167}{\tan(H+7.31/(H+4.4))} \tag{7.90}$$

where T, P are the temperature in degrees Celsius and the pressure in millibars. If T and P are unknown assume the term in the first bracket is unity. The effect of refraction is removed from an observation by subtracting R from the observed altitude. When only the true altitude is known, it is possible to iterate using the formula above, in order to find the observed altitude. This is necessary, particularly at low altitudes, when the refraction correction is large.

Alternatively at low altitudes, when $H < 15^{\circ}$, the following may be used

$$R = \left(\frac{P}{T+273}\right)\frac{0^{\circ}.1594 + 0.0196H + 0.00002H^2}{1 + 0.505H + 0.0845H^2}. \tag{7.91}$$

For rising and setting phenomena a constant of $34'$ is used for the horizontal refraction; thus for the centre of the Sun or Moon to be coincident with the horizon the true altitude will be $-34'$.

The observed right ascension and declination, (α, δ), of an object may be corrected, to first order, to give the true position α_1, δ_1, using the following formulae:

$$\begin{aligned} \alpha_1 &= \alpha - R\sec\delta\sin C \\ \delta_1 &= \delta - R\cos C \end{aligned} \tag{7.92}$$

where R is the refraction and C is the parallactic angle, i.e., the angle at the object in the spherical triangle pole-object-zenith. Thus when the object is on the meridian $C = 0^{\circ}$, and the amount of refraction, R, is a direct correction to declination only, but the right ascension is unaffected.

Refraction tables based on a standard temperature and pressure are printed in various publications, for example, Abalakin (1985), Pulkova (1956), together with correction tables for other temperatures and pressures. Parameters for *The Star Almanac* are $T = 7^{\circ}$C, $P =$ 1005 mb, humidity of 80%, wavelength of light 0.574μm and a mean latitude of 50° which give close agreement to the published tables. From the 2004 edition of *The Nautical Almanac* the refraction tables have been generated using this algorithm with the following parameters; temperature $T = 10^{\circ}$C, pressure $P = 1010$ mb, with 80% humidity, wavelength of light 0.50169μm, and a mean latitude of 45°. Modifying Eq. 7.90 for these specific parameters gives

$$R = \left(\frac{0.28\,P}{T+273}\right)\frac{0^{\circ}.0167}{\tan(H+7.32/(H+4.32))}. \tag{7.93}$$

7.3 Reduction of Positions from the BCRS to the GCRS

7.3.1 Proper Place

The proper or virtual place[3] represents the position of the star or planet as it would be seen from the centre of mass of the Earth at some date, in the coordinate system defined by the Earth (e.g., the GCRS), assuming that the Earth and its atmosphere were transparent and non-refracting. It can be thought of as an apparent or intermediate place expressed in the coordinate system of the reference system (e.g., GCRS).

For objects with reference data (catalogue coordinates or ephemerides) expressed in the BCRS or equivalently the ICRS, the application of corrections for space motion (for stars) and parallax, light-time (for solar system objects), light-deflection and annual aberration results in a position referred to the GCRS, and is called the *proper place*. Equation 7.1, written for planets and stars, respectively, giving the proper place are

$$\mathbf{u}_4(t') = f\,[\,g[\mathbf{u}_{\mathrm{B}}(t-\tau) - \mathbf{E}_{\mathrm{B}}(t)]] \tag{7.94}$$

$$\text{and} \quad \mathbf{u}_4(t') = f\,[\,g[\mathbf{u}_{\mathrm{B}}(t_0) + (t-t_0)\dot{\mathbf{u}}_{\mathrm{B}}(t_0) - \mathbf{E}_{\mathrm{B}}(t)]] \tag{7.95}$$

where all the symbols are defined in § 7.4.1 and § 7.4.2, respectively. The resulting proper place is computed by following § 7.4.1, Steps 1–4, or equivalently for stars § 7.4.2, Steps 1–7.

Proper places are useful for the reduction of high-precision differential astrometric observations where precession and nutation rotations need not be performed.

7.3.2 Local Place

The local place is essentially the topocentric place expressed in the coordinate system of the reference system. Local place is related to topocentric place in the same way that the proper place is related to apparent or intermediate place. Specifically, the local place represents the position of a star or planet as it would be seen from a specific location on Earth at some date and time, in the coordinate system defined by the GCRS assuming the atmosphere were non-refracting. To compute it, simply add the procedure for calculating the topocentric place (§ 7.4.3) to the procedure for computing the proper place (§ 7.3.1). (Note, the precession and nutation rotations in § 7.4.3.4 should not be omitted.) The local place has utility beyond its use in relative astrometry.

7.3.3 Astrometric Place

An astrometric place is the direction of a solar system body formed by applying the correction for the barycentric motion of this body during the light-time to the geometric geocentric position referred to the ICRS. Such a position is then directly comparable with the astrometric position of a star formed by applying the corrections for proper motion and annual parallax to the ICRS (or J2000.0) catalog direction. The gravitational deflection of light is ignored since it will generally be similar (although not identical) for the solar system body and

3. Virtual place has exactly the same meaning as proper place. The term virtual place has been used in some U.S. Naval Observatory publications and products; it is mentioned here for completeness. To avoid confusion, this term will not be used in the future.

background stars. For high accuracy applications, gravitational light-deflection effects need to be considered, and the adopted policy declared. Strictly speaking, astrometric places are not in the GCRS, but form a hybrid system.

The astrometric place of the planet or star is obtained from Eqs. 7.98 and 7.125 which reduce to

$$\mathbf{u}_4(t') = \mathbf{u}_B(t - \tau) - \mathbf{E}_B(t) \tag{7.96}$$

$$\text{and} \quad \mathbf{u}_4(t') = \mathbf{u}_B(t_0) + (t - t_0)\dot{\mathbf{u}}_B(t_0) - \mathbf{E}_B(t) \tag{7.97}$$

and is obtained by following, in § 7.4.1, Steps 1.1–2.7, or equivalently for stars in § 7.4.2, Steps 1.1–2.6.

However, it should be recognized that the gravitational deflection of light should not really be ignored in this way, since it cannot in principle be absorbed into plate constants or similar reduction parameters: the deflection is a function of position and distance. Although in any part of the sky the direction of the deflection is the same for all bodies, its magnitude is less for solar system bodies than for stars (see Fig. 7.5). Generally, this detail is of little practical importance, since only in a few special cases can it cause errors exceeding $0.''01$. Before 1984 the effects of elliptic aberration—also called E-terms—were omitted; a detailed discussion on them is given in § 3.53 of the previous edition of *The Explanatory Supplement* (Hohenkerk et al. 1992). Also, in the past the term "astrographic" place was used instead of astrometric place.

Astrometric places are simple to compute, and, therefore, have been widely used. Another attractive feature is that they can be directly plotted on an ordinary star map with negligible error in the resulting field configuration. Therefore, in *The Astronomical Almanac* astrometric places are used for the ephemerides of faint solar system bodies that are star-like in appearance, such as the ephemerides of minor planets and Pluto.

For observations of solar system bodies, it is frequently useful to compute a topocentric astrometric place. Only the correction for geocentric parallax is applied. To compute a topocentric astrometric place, simply add the procedure given in § 7.4.3 to the procedure given above for computing an astrometric place. (Again, the precession and nutation rotations in § 7.4.3.4 should not be omitted). In this case, however, the observer's velocity vector need not be computed since aberration is ignored. Topocentric astrometric places of stars are never required since the topocentric correction is vanishingly small.

In differential work it has also been customary, if not strictly correct, to neglect both the gravitational deflection of light (function $g[\ldots]$) and the aberration of light (function $f[\ldots]$). The assumption is that for sufficiently small fields these differential effects are so small that their relative positions remain unaffected. Similarly, differential refraction is often ignored, although its effect could be much larger because of the variation in colour over the same fields[4]. Any residual distortion of the field resulting from the neglect of these effects is assumed to be absorbed into plate constants or similar parameters solved for in the data reduction process.

4. One technique employed in high precision astrometry is to narrow the bandpass to minimize colour variations, and then apply differential refraction.

7.3.4 Differential Astrometry

The proper place, the local place and the astrometric place are all suitable not only for differential astrometry, but also for any kind of space astrometry where orientation of the Earth (precession and nutation) are irrelevant.

In differential work it is necessary to consider only effects which can alter the angles between the position vectors of the observed bodies, i.e., arc lengths on the celestial sphere. The orientation of the coordinate system is not considered of fundamental importance since in most cases the celestial and instrumental coordinate systems are coupled. In any event, in differential observing, the coordinate system is not established until after the fact, during the reduction of the observations.

For the reduction of high precision differential observations, the local place should be used. With available computing power it is straightforward to compute the local place of all objects within a field and use the ensemble of local places as the starting point for the reduction procedure.

7.4 Algorithms for the Reductions of Positions

This section presents a set of algorithms for calculating apparent, intermediate and topocentric places of celestial objects. These algorithms assume that the process starts from a position in the CRS, and in this chapter this is assumed to be the BCRS(ICRS). Other algorithms, such as those of the IERS (URL[5]), start with observations in the TRS, and thus great care is needed to ensure that the various transformations are implemented in the correct sense, i.e., celestial to terrestrial or terrestrial to celestial.

An apparent place is a proper place (see § 7.3.1) transformed to an "of date" position, i.e., transformed from the GCRS to a system where the origin of right ascension is the equinox on the true equator of date. If nutation is ignored, then the origin of right ascension will be the mean equinox rather than the true equinox.

An intermediate place is also a geocentric position that includes the same effects as those for an apparent place; however, the origin of right ascension is the CIO, thus the transformation from the GCRS is handled by a different transformation.

A topocentric place is an apparent or intermediate place where the origin of the system is the observer on the Earth's surface and not the geocentre.

All the above places may be reduced so that they are with respect to a terrestrial reference system, the Terrestrial Intermediate Reference System and the ITRS. Here it is essential to refer the right ascension (either mean, apparent or intermediate) to the TIO, and thus the appropriate angle, Greenwich Sidereal Time (mean or apparent), or Earth Rotation Angle, must be used. Thus, this will depend on the choice of paradigm, either equinox-based or the IAU recommenced CIO-based (see § 7.1.3.2) method.

7.4.1 Apparent and Intermediate Place Algorithm for Planets

The algorithm used to compute the apparent or intermediate place of a planet or other solar system body at an epoch of observation t', given its ephemeris with origin at the solar system

barycentre and its coordinates referred to the ICRS, can be succinctly represented as

$$\mathbf{u}_4(t') = \mathbf{R}_3(-\beta)\,\mathcal{R}_\Sigma\; f[g[\mathbf{u}_\mathrm{B}(t-\tau) - \mathbf{E}_\mathrm{B}(t)]] \tag{7.98}$$

where

t'	is the epoch of observation, in the TT timescale;
t	is the epoch of observation, in the TDB timescale;
τ	is the light-travel time from the planet to the Earth, in the TDB timescale, for light arriving at the epoch of observation t;
$\mathbf{u}_\mathrm{B}(t-\tau)$	is the barycentric position of the planet at epoch $t-\tau$, referred to the ICRS;
$\mathbf{E}_\mathrm{B}(t)$	is the barycentric position of the Earth at the epoch of observation t, referred to the ICRS;
$g[\ldots]$	is the function representing the gravitational deflection of light;
$f[\ldots]$	is the function representing the aberration of light;
$\mathcal{R}_\Sigma$	is the transformation from the GCRS to the of date system that includes frame bias, precession and nutation, and, where the origin of right ascension is the GCRS origin (Σ) on the true equator of date (see Fig. 7.1);
$\mathbf{R}_3(-\beta)$	is the rotation about the CIP that positions the origin of right ascension and determines the paradigm chosen. Earth rotation (GAST or ERA as appropriate) may be included giving coordinates referred to the Terrestrial Intermediate Reference System;
$\mathbf{u}_4(t')$	is the apparent or intermediate geocentric place of the planet at the epoch of observation t' represented as a 3-dimensional position vector (ξ, η, ζ).

This expression is schematic; the full functional forms of f and g, the elements of $\mathcal{R}_\Sigma$, the choice of β and, thus, the paradigm as well as other auxiliary calculations are not indicated.

A detailed description of the algorithm divided into numbered steps follows. In places it is divided into two columns. The first column gives the traditional *Equinox-based* method where right ascension is measured from the equinox (true or mean as required) and thus GHA must be formed using Greenwich Sidereal Time, apparent (GAST) or mean (GMST), respectively. The second column gives the CIO-based method, which is the IAU recommended paradigm, where right ascension is measured from the CIO, and ERA must be used to calculate GHA.

1. Given an instant for which the position of the planet is required, obtain the dynamical time (TDB) to use with the ephemeris. If the position is required at a given Universal Time (UT1), or the hour angle is required, then obtain a value for ΔT, which may have to be predicted.
2. Calculate the geocentric rectangular coordinates of the planet from barycentric ephemerides of the planet and the Earth at coordinate time argument TDB, allowing for light-time calculated from heliocentric coordinates.

3. Calculate the geocentric direction of the planet by allowing for light-deflection due to solar gravitation.
4. Calculate the proper direction of the planet by applying the correction for the Earth's orbital velocity about the barycentre (i.e., annual aberration). The resulting position is in the GCRS.

Equinox Method	*CIO Method*
5. Rotate from the GCRS to the system defined by the true equator and equinox of date by applying rotations for frame bias, precession and nutation.	**5.** Rotate from the GCRS to the Celestial Intermediate Reference System using the $(\mathcal{X},\mathcal{Y})$ of the CIP, and the CIO locator s to apply frame bias and precession-nutation.
6. Convert to spherical coordinates, giving the geocentric apparent right ascension and declination with respect to the true equinox and equator of date.	**6.** Convert to spherical coordinates, giving the geocentric intermediate right ascension and declination with respect to the CIO and equator of date.
7. Calculate Greenwich Apparent Sidereal Time and form the Greenwich Hour Angle for the given UT1.	**7.** Calculate the Earth Rotation Angle and form the Greenwich Hour Angle for the given UT1.

Alternatively, if right ascension is not required, combine Steps 5 and 7.

***5.** Apply frame bias, precession, nutation and Greenwich Apparent Sidereal Time to convert from the GCRS to the Terrestrial Intermediate Reference System; with origin of longitude at the TIO on the equator of date.	***5.** Rotate, using $\mathcal{X}$, $\mathcal{Y}$, s and θ to apply frame bias, precession-nutation and Earth rotation, from the GCRS to the Terrestrial Intermediate Reference System; with origin of longitude at the TIO on equator of date.

***6.** Convert to spherical coordinates, giving the Greenwich Hour Angle (H) and declination (δ) with respect to the Terrestrial Intermediate Reference System (TIO and equator of date).

Note: In Steps 7 and Steps *5 the effects of polar motion (see § 7.2.6.2 and Chapter 6) have been ignored; they are the very small difference between the ITRS zero meridian and the TIO, and the position of the CIP within the ITRS.

7.4.1.1 Relevant Time Arguments

Ascertain the instant, date and time, and timescale at which the position is required. From this time obtain the terrestrial time (TT) and the barycentric dynamical time (TDB). If the position will eventually be referred to the Earth, i.e., via the TIO and hour angle, then a UT1 time will be required.

Step 1.1. Express the instant (epoch) of observation t' as a TT Julian date. The terrestrial time is related to UT1 via the following relationship

$$t' = \mathrm{JD} + \mathrm{UT1}/24 + \Delta T/86400 \tag{7.99}$$

where JD is the Julian date at 0^{h} TT on the day, UT1 is time in hours, and $\Delta T = \mathrm{TAI} + 32^{\mathrm{s}}.184 - \mathrm{UT1}$. UT1 is affected by unpredictable irregularities in the Earth's rotation, but it is

always within $0^s.9$ of UTC, the latter defining civil time and broadcast worldwide according to international convention. These issues are discussed in detail in Chapter 3.

Step 1.2. Compute T', the number of Julian centuries in the TT timescale from J2000.0 TT (JD 245 1545.0 TT).

$$T' = (t' - 245\,1545.0)/36525. \tag{7.100}$$

Step 1.3. Compute the difference (in seconds) between the TT and TDB timescales, or equivalently T_{eph} of the JPL DE405/LE405 ephemeris, from

$$\text{TDB} - \text{TT} = 0^s.001\,657 \sin g + 0^s.000\,022 \sin(L - L_J) \tag{7.101}$$

and

$$g = 357^\circ.53 + 3.599\,905 \times 10^4\, T'$$
$$L - L_J = 246^\circ.11 + 3.296\,447 \times 10^4\, T'$$

where g is the mean anomaly of the Earth in its orbit around the Sun, and $L - L_J$ is the difference in the mean ecliptic longitudes of the Sun and Jupiter (Simon et al. 1994). Strictly the time argument in equations for g and $L - L_J$ should be TDB. The above formula for TDB − TT is accurate to about $\pm 30\mu$s over the period 1980 to 2050, when compared to the Fairhead and Bretagnon (1990) model adopted by IAU-SOFA (URL[3]). The difference between TDB and TT is often ignored, since the two timescales differ by no more than 2 milliseconds. See Moyer (1981) for a complete discussion.

Next form the TDB, or equivalently the T_{eph}, Julian date and fraction from

$$t = t' + (\text{TDB} - \text{TT})/86400 \tag{7.102}$$

and

$$T = (t - 245\,1545.0)/36525. \tag{7.103}$$

The algorithm given above is much more precise than is required for the computation of apparent or intermediate places of most solar system bodies and stars. For all solar system bodies, except the Moon and close approaching comets and asteroids, the approximation $t = t'$ will lead to errors that may approach $0''.001$ in very unfavorable circumstances. For stellar places set $t = t'$ with negligible error.

7.4.1.2 Ephemeris Data for Earth, Sun and Planet

Obtain the appropriate ephemeris data for time t and at the light-time $t - \tau$.

A standard ephemeris for the major bodies in the solar system is the Jet Propulsion Laboratory (JPL) ephemeris designated DE405/LE405 (Standish 1998a) the reference system of which is the ICRS (see Chapter 8). The positions of the Sun, Moon and planets given in *The Astronomical Almanac* and several other international almanacs are now obtained from this ephemeris. A set of analytical planetary theories fitted to DE200 has been developed by Bretagnon (1982). IAU Commission 4 website (URL[4]) lists various sources of ephemerides.

Step 2.1. Extract from the appropriate ephemeris, for the time t, the barycentric position of the planet, $\mathbf{u}_B(t)$, the barycentric position and velocity of the Earth, $\mathbf{E}_B(t)$ and $\dot{\mathbf{E}}_B(t)$, and

the barycentric position of the Sun, $\mathbf{S}_{\mathrm{B}}(t)$, all referred to the ICRS. All position vectors are assumed to be in au and velocity vectors in au/day.

The barycentric position of the Earth is used to form the geocentric position of the body (see § 7.4.1.3); the barycentric velocity of the Earth is used in the aberration computation (see § 7.4.1.5); and the heliocentric position of the Earth is used in the computation of the relativistic gravitational deflection of light (see § 7.4.1.4). Values of the components of the vectors $\mathbf{E}_{\mathrm{B}}$, $\dot{\mathbf{E}}_{\mathrm{B}}$ and $-\mathbf{E}_{\mathrm{H}}$ at 1-day intervals are tabulated in *The Astronomical Almanac*.

Step 2.2. Calculate the heliocentric position of the Earth.

$$\mathbf{E}_{\mathrm{H}}(t) = \mathbf{E}_{\mathrm{B}}(t) - \mathbf{S}_{\mathrm{B}}(t). \tag{7.104}$$

Note that the barycentric position of the Earth is that of the centre of mass of the Earth and not that of the Earth-Moon barycentre.

7.4.1.3 Geometric Position of Planet, Accounting for Light-Time

Step 2.3. Compute the geometric distance between Earth and planet, i.e., compute d, the geometric distance between the positions of the centres of mass of the planet and the Earth at time t, in au, from

$$d = |\mathbf{u}_{\mathrm{B}}(t) - \mathbf{E}_{\mathrm{B}}(t)|. \tag{7.105}$$

The geometric distance is the quantity tabulated in *The Astronomical Almanac* as the "true distance" of solar system bodies. Using d compute τ, a first approximation to the light-travel time between the planet and the Earth

$$\tau = d/c \tag{7.106}$$

where c is the speed of light expressed in au/day; its precise value may be computed from

$$c = 86400/\tau_A = 86\,400/499.004\,783\,8061 \tag{7.107}$$

where τ_A is the light-time for unit distance (1 au). The value given is that specified by the JPL DE405/LE405 ephemeris where the units are compatible with TDB.

Step 2.4. Extract from the ephemeris, for the time $t - \tau$, the barycentric position of the planet and the Sun, $\mathbf{u}_{\mathrm{B}}(t - \tau)$ and $\mathbf{S}_{\mathrm{B}}(t - \tau)$, respectively.

Step 2.5. Calculate $\mathbf{U}$ and $\mathbf{Q}$ approximations to the geocentric and heliocentric position of the centre of mass of the planet, respectively, at the epoch of observation t, from

$$\mathbf{U} = \mathbf{u}_{\mathrm{B}}(t - \tau) - \mathbf{E}_{\mathrm{B}}(t) \tag{7.108}$$

$$\mathbf{Q} = \mathbf{u}_{\mathrm{B}}(t - \tau) - \mathbf{S}_{\mathrm{B}}(t - \tau). \tag{7.109}$$

Step 2.6. Next compute τ', a better approximation to the light-travel time between the planet and the Earth from

$$c\tau' = U + (2\mu/c^2) \ln \frac{E + U + Q}{E - U + Q} \tag{7.110}$$

where τ' includes the effect of gravitational retardation due to the Sun. $U = |\mathbf{U}|$, $E = |\mathbf{E}_{\mathrm{H}}|$, $Q = |\mathbf{Q}|$. The heliocentric gravitational constant μ and the velocity of light c may be re-written as

$$\begin{aligned}\mu/c^2 &= k^2\tau_A^2/86400^2 \\ &= 0.017\,202\,098\,95^2 \times (499.004\,783\,8061/86400)^2 \\ &= 9.8706 \times 10^{-9}\end{aligned} \tag{7.111}$$

where k is the Gaussian gravitational constant and τ_A is the light-time for unit distance (Eq. 7.107 in Step 2.3) where DE405/LE405 and TDB compatible values are given.

Compare τ' with τ; if they are identical within some small tolerance continue to Step 2.7. If they are not, then replace the value of τ with the value of τ' and repeat Step 2.4 through Step 2.6 until the light-time converges to within the tolerance permitted. Since the speed of bodies in the solar system is small compared to the speed of light, this process converges rapidly.

The tolerance permitted depends on the precision desired in the final coordinates and the apparent angular speed of the body as viewed from Earth. The most rapidly moving objects in the sky are the Moon (angular rate $\approx 0''.5$ per second), Mercury (angular rate at inferior conjunction $0''.05$ per second), and the Sun (angular rate $0''.04$ per second). However, occasionally an Earth-crossing asteroid or comet may exceed these rates for short periods of time. For a computational precision of one milliarcsecond, therefore, the light-time convergence tolerance must be $0^{s}.002 = 2 \times 10^{-8}$ days or less; we suggest 1×10^{-8} days. For the Moon, *The Astronomical Almanac* uses the convergence criteria that the change in time between two iterations must not cause the distance d to change by more than 1×10^{-10} au.

Kaplan et al. (1989) ignores the second term in Eq 7.110, (order 1 micro-arcsecond), which is due to the relativistic delay caused by the Sun's gravitational field.

Step 2.7. Once τ has converged, form the geocentric and heliocentric positions of the body at time $t - \tau$, respectively from

$$\mathbf{U} = \mathbf{u}_{\mathrm{B}}(t - \tau) - \mathbf{E}_{\mathrm{B}}(t) \tag{7.112}$$

$$\text{and} \quad \mathbf{Q} = \mathbf{u}_{\mathrm{B}}(t - \tau) - \mathbf{S}_{\mathrm{B}}(t - \tau). \tag{7.113}$$

7.4.1.4 Relativistic Deflection of Light

Calculate light-deflection due to solar gravitation. A detailed explanation on light-deflection is given in § 7.2.4.

Step 3.1. First form the following unit vectors and dimensionless scalar quantities

$$\mathbf{u} = \mathbf{U}/|\mathbf{U}| \qquad \mathbf{q} = \mathbf{Q}/|\mathbf{Q}| \qquad \mathbf{e} = \mathbf{E}_{\mathrm{H}}/|\mathbf{E}_{\mathrm{H}}| \tag{7.114}$$

$$g_1 = \frac{2\mu}{c^2 E} \qquad g_2 = 1 + (\mathbf{q} \cdot \mathbf{e}) \tag{7.115}$$

where the constants μ and c are given in Step 2.6 Eq. 7.111, and $\mathbf{E}_{\mathrm{H}}$ is given in Step 2.2 Eq. 7.104.

Step 3.2. The deflected position of the body relative to the geocentric inertial frame that is instantaneously stationary in the space time reference frame of the solar system is then

$$\mathbf{u}_1 = |\mathbf{U}| \left(\mathbf{u} + \frac{g_1}{g_2} \left[(\mathbf{u} \cdot \mathbf{q})\mathbf{e} - (\mathbf{e} \cdot \mathbf{u})\mathbf{q} \right] \right). \tag{7.116}$$

The vector $\mathbf{u}_1/|\mathbf{U}|$ is a unit vector to order μ/c^2.

For the Sun or bodies lying behind the Sun on the Sun-Earth line, the light-deflection can be considered zero, so that $\mathbf{u}_1 = \mathbf{U}$.

7.4.1.5 Aberration of Light

Calculate the proper direction of the planet by applying the correction for the Earth's orbital velocity about the barycentre. A detailed explanation on aberration is given in § 7.2.3.2.

Step 4.1. Form the following quantities

$$\mathbf{u} = \mathbf{u}_1/|\mathbf{u}_1| \qquad \mathbf{V} = \dot{\mathbf{E}}_{\mathrm{B}}(t)/c \tag{7.117}$$

$$\beta^{-1} = \sqrt{1 - V^2} \qquad f_1 = (\mathbf{u} \cdot \mathbf{V}) \qquad f_2 = 1 + f_1/(1 + \beta^{-1})$$

where the velocity ($\mathbf{V}$) is expressed in units of the velocity of light and is equal to the Earth's velocity in the barycentric frame.

Step 4.2. The aberrated position of the body in the geocentric inertial frame that is moving with instantaneous velocity ($\mathbf{V}$) of the Earth relative to the natural frame is then given by the vector

$$\mathbf{u}_2 = (\beta^{-1}\mathbf{u}_1 + f_2|\mathbf{u}_1|\mathbf{V})/(1 + f_1). \tag{7.118}$$

The above algorithm includes relativistic terms (Murray 1981) (see § 7.2.3.2), which are of the order 1 milliarcsecond. Therefore, for many applications the much simpler classical formula may be used

$$\mathbf{u}_2 = \mathbf{u}_1 + |\mathbf{u}_1|\mathbf{V}. \tag{7.119}$$

7.4.1.6 Transformation to "Of Date" Positions

Rotate the resulting coordinate system, the GCRS, to the coordinate system of date by including the effects of frame bias, precession and nutation. These effects, and the various algorithms by which the matrices may be calculated are given in § 7.2.5 and described in detail in Chapter 6. The combined bias-precession-nutation matrices, $\mathbf{M}$ and $\mathbf{C}$, for equinox-based and CIO-based paradigms, respectively, are tabulated daily at 0^{h} TT in *The Astronomical Almanac* and must be interpolated to the epoch of observation.

	Equinox Method		*CIO Method*
Step 5.	The apparent position vector $\mathbf{u}_3$ is given by	**5.**	The intermediate position vector $\mathbf{u}_3$ is given by
	$\mathbf{u}_3 = \mathbf{R}_3(-s + E_o)\,\mathcal{R}_\Sigma\,\mathbf{u}_2$		$\mathbf{u}_3 = \mathbf{R}_3(-s)\,\mathcal{R}_\Sigma\,\mathbf{u}_2$
	$= \mathbf{M}\,\mathbf{u}_2 = \mathbf{NPB}\,\mathbf{u}_2$		$= \mathbf{C}\,\mathbf{u}_2$ (7.120)
	where $\mathbf{M}$ is given in § 7.2.5.1.		where $\mathbf{C}$ is given in § 7.2.5.2.

Step 6. Convert to spherical coordinates; apparent right ascension and declination α_e, δ using:

$$\alpha_e = \tan^{-1}\frac{\eta}{\xi}$$
$$\delta = \tan^{-1}\frac{\zeta}{\sqrt{\xi^2+\eta^2}}$$

6. Convert to spherical coordinates; intermediate right ascension and declination α_i, δ using:

$$\alpha_i = \tan^{-1}\frac{\eta}{\xi}$$
$$\delta = \tan^{-1}\frac{\zeta}{\sqrt{\xi^2+\eta^2}} \qquad (7.121)$$

where $\mathbf{u}_3 = (\xi, \eta, \zeta)$. The quadrant of α_e, α_i is determined by the signs of ξ and η.

7.4.1.7 Position Relative to the Earth

Relate the celestial position to the TIO so that hour angle may be calculated.

Step 7. Calculate GAST for the required UT1 and then form

$$H = \text{GAST} - \alpha_e.$$

Note: H is usually given in arc measure, while GAST and right ascension are given in units of time.

7. Calculate the ERA (θ) for the required UT1 and then form

$$H = \theta - \alpha_i. \qquad (7.122)$$

Note: H and θ are usually given in arc measure, while right ascension is given in units of time.

Alternatively combining Steps 5 and 7 before forming spherical coordinates

Step 5*. The position ($\mathbf{u}_4$) relative to the Terrestrial Intermediate Reference System is given by

$$\mathbf{u}_4 = \mathbf{R}_3(\text{GAST} - s + E_o)\mathcal{R}_\Sigma\,\mathbf{u}_2$$
$$= \mathbf{R}_3(\text{GAST})\,\mathbf{M}\,\mathbf{u}_2$$

where $\mathbf{M}$ is given in § 7.2.5.1 and § 7.2.6.1.

5*. The position ($\mathbf{u}_4$) relative to the Terrestrial Intermediate Reference System is given by

$$\mathbf{u}_4 = \mathbf{R}_3(\theta - s)\,\mathcal{R}_\Sigma\,\mathbf{u}_2$$
$$= \mathbf{R}_3(\theta)\,\mathbf{C}\,\mathbf{u}_2 \qquad (7.123)$$

where $\mathbf{C}$ is given in § 7.2.5.2 and § 7.2.6.1.

Step 6*. Convert to spherical coordinates Greenwich Hour Angle (H) and declination δ using:

$$H = \tan^{-1}\frac{-\eta}{\xi}, \qquad \delta = \tan^{-1}\frac{\zeta}{\sqrt{\xi^2+\eta^2}} \qquad (7.124)$$

where $\mathbf{u}_4 = (\xi, \eta, \zeta)$, and H is measured from the TIO meridian positive to the west, and the quadrant is determined by the signs of ξ and $-\eta$.

7.4.2 Apparent and Intermediate Place Algorithm for Stars

The algorithm used to compute the apparent or intermediate place of a star or star-like object at the instant of observation t', given its right ascension, declination and proper motion, and other data (as available) at some catalogue or reference epoch t_0 with respect to the ICRS, may be succinctly represented as:

$$\mathbf{u}_4(t') = \mathbf{R}_3(-\beta)\,\mathcal{R}_\Sigma\,f\,[\,g\,[\mathbf{u}_\text{B}(t_0) + (t - t_0)\dot{\mathbf{u}}_\text{B}(t_0) - \mathbf{E}_\text{B}(t)]] \qquad (7.125)$$

where

t'	is the epoch of observation, in the TT timescale;
t	is the epoch of observation, in the TDB timescale;
t_0	is the reference epoch of the catalogue, in the TDB timescale;
$\mathbf{u}_{\mathrm{B}}(t_0)$	is the catalog place of the star at the reference epoch t_0, represented as a 3-dimensional position vector in au; origin, solar system barycentre, and coordinates referred to the ICRS;
$\dot{\mathbf{u}}_{\mathrm{B}}(t_0)$	is the space motion vector (in au/day) of the star at the reference epoch t_0, obtained from the catalog proper motions, parallax and radial velocity;
$\mathbf{E}_{\mathrm{B}}$	is the barycentric position of the Earth at the epoch of observation t, referred to the ICRS;
$g[\ldots]$	is the function representing the gravitational deflection of light;
$f[\ldots]$	is the function representing the aberration of light;
$\mathcal{R}_{\Sigma}$	is the transformation from the GCRS to the "of date" system that includes frame bias, precession and nutation, and, where the origin of right ascension is the GCRS origin (Σ) on the true equator of date (see Fig. 7.1);
$\mathbf{R}_3(-\beta)$	is the rotation about the CIP that positions the origin of right ascension and determines the paradigm chosen. Earth rotation (GAST or ERA as appropriate) may be included giving coordinates referred to the Terrestrial Intermediate Reference System;
$\mathbf{u}_4(t')$	is the apparent or intermediate geocentric place of the star at the epoch of observation t' represented as a 3-dimensional position vector (ξ, η, ζ).

The above expression is similar to Eq. 7.98 for planets. Most of the algorithm is identical. The main modifications to the planetary reduction in the stellar case are:

(a) the distinction between TDB and TT is not significant;

(b) the more complex motion of a planet compared to that of a star. In § 7.4.1.2 and § 7.4.1.3 we had to obtain the position of the planet from an ephemeris and deal with the light-time problem explicitly; in this section we will assume uniform rectilinear motion for the star and neglect variations in light-time as the star moves, although this is discussed in § 7.2.1.

(c) the relativity term for light-deflection is modified to the asymptotic case where the star is assumed to be at infinity.

If the catalogue position of the star is not with respect to the ICRS, and the accuracy of the data warrants it, then transform it to the ICRS. See Chapter 4 for the FK5 to ICRS, and other conversions.

The steps in the stellar reduction are as follows:

7.4.2.1 Relevant Time Arguments

Step 1. Follow Steps 1.1 through 1.3 in § 7.4.1.1, or set TDB = TT, i.e., set $t = t'$, as appropriate.

7.4.2.2 Ephemeris Data for Earth, Sun and Star

Obtain at time t the appropriate ephemeris data.

Step 2.1. Extract from a planetary ephemeris, for the time t, the barycentric position and velocity of the Earth, $\mathbf{E}_B(t)$ and $\dot{\mathbf{E}}_B(t)$ and the barycentric position of the Sun, $\mathbf{S}_B(t)$, all referred to the ICRS. All position vectors are assumed to be in au and velocity vectors in au/day.

Step 2.2. Calculate the heliocentric position of the Earth ($\mathbf{E}_H$) from

$$\mathbf{E}_H(t) = \mathbf{E}_B(t) - \mathbf{S}_B(t). \tag{7.126}$$

For apparent places of stars accurate to a few milliarcseconds it is necessary only to obtain the Earth and Sun's position components to three significant digits and the Earth's velocity components to five significant digits. It is, therefore, feasible to construct relatively compact closed-form algorithms which provide the required data (Stumpff 1980b). The NOVAS software (Kaplan et al. 2009; URL[2]) of the Nautical Almanac Office of USNO contains routines that evaluates the barycentric position and velocity of the Earth, without using external files. Similarly, the IAU-SOFA routine EPV00 (URL[3]) uses a simplified solution from the VSOP planetary theory by Moisson and Bretagnon (2001) to evaluate the Earth's barycentric and heliocentric positions and velocities. However, for the highest precision, or when the apparent places of planets are being computed, more complex algorithms or external files are required.

Step 2.3. For the selected star extract from the given catalogue its position (α, δ), at some reference epoch t_0, together with μ_α and μ_δ, the corresponding proper motion components, as well as the parallax π and radial velocity $\dot{r}$ in km/s. For this particular algorithm, it is assumed that the reference system of the catalogue is the ICRS, if not, then the catalogue data must be transformed to the ICRS.

Step 2.4. Form the barycentric position vector, $\mathbf{u}_B(t_0)$ (in au), and space motion vector, $\dot{\mathbf{u}}_B(t_0)$ (au/day). In particular use Eq. 7.20 to form $\mathbf{u}_B(t_0)$ and either of Eqs. 7.22 or 7.24 to calculate the space motion vector $\dot{\mathbf{u}}_B(t_0)$ depending on the form and units of the proper motions. Detailed information on space motion is discussed in § 7.2.1.

Step 2.5. Compute the barycentric position of the star, at the epoch of observation (t), by adding the distance moved during the interval of time between the catalog epoch (t_0) and the epoch of observation

$$\mathbf{u}_B(t) = \mathbf{u}_B(t_0) + (t - t_0)\,\dot{\mathbf{u}}_B(t_0). \tag{7.127}$$

The assumption is made here and in *The Astronomical Almanac* that there is no explicit correction for light-time in these stellar computations, however this is discussed in § 7.2.1.

7.4.2.3 Geocentric Position of the Star

Step 2.6. Calculate $\mathbf{U}$, the geocentric vector of the star at the required epoch, from

$$\mathbf{U} = \mathbf{u}_B(t) - \pi\,\mathbf{E}_B(t). \tag{7.128}$$

7.4.2.4 Relativistic Deflection of Light

Calculate light-deflection due to solar gravitation. A detailed explanation on light-deflection is given in § 7.2.4.

Step 3. First form the heliocentric position of the star

$$\mathbf{Q} = \mathbf{u}_{\mathrm{B}}(t) - \mathbf{S}_{\mathrm{B}}(t) \tag{7.129}$$

which is then used in § 7.4.1.4 Steps 3.1 and 3.2 to obtain the star's geocentric position, corrected for light-deflection $\mathbf{u}_1$.

Note that Step 3.2 may be simplified (see § 7.2.4, Eq. 7.65) by substituting $\mathbf{q} = \mathbf{u}$ as stars represent the asymptotic case.

7.4.2.5 Aberration of Light

Follow Steps 4 for aberration of light in § 7.4.1.5.

7.4.2.6 The "Of Date" Positions

Follow the Steps in § 7.4.1.6 or § 7.4.1.7 as required.

7.4.3 Topocentric Place Algorithm

The topocentric place of a star or planet refers to its apparent direction as it would actually be observed from some place on Earth, neglecting atmospheric refraction. The apparent and intermediate places, developed in § 7.4.1 and § 7.4.2, can be thought of as the position of an object for a fictitious observer located at the centre of a transparent non-refracting Earth. The only difference between these places and a topocentric place is due to the slightly different position and velocity of an observer on the Earth's surface compared with those of the fictitious observer at the Earth's centre. The change in direction of the observed body due to the difference of position, is referred to as *geocentric parallax* (or diurnal parallax), and is significant only for objects in the solar system. It is typically a few arcseconds for most solar system bodies, but reaches about 1° for the Moon. The change in direction due to the difference in velocity, (due to the rotation of the Earth) is referred to as *diurnal aberration*, and is independent of the distance of the observed body, and it is always less than $0''.32$.

Atmospheric refraction also affects the apparent direction of celestial objects. In fact, refraction at all wavelengths is orders of magnitude larger than either geocentric parallax or diurnal aberration. Refraction is discussed in § 7.2.7, and as it is usually considered a correction to observations rather than an effect to be taken into account when computing a topocentric place, it is not considered here.

The simplest way of computing a topocentric place is to compute an apparent or intermediate place using the position and velocity vectors of the observer rather than the centre of mass of the Earth. That is, modify the barycentric vectors $\mathbf{E}_{\mathrm{B}}(t)$ and $\dot{\mathbf{E}}_{\mathrm{B}}(t)$ by adding the position and velocity of the observer relative to the centre of the Earth, ensuring that the latter is transformed to the reference system of the former, see Steps 5 and 6 in § 7.4.3.4 and § 7.4.3.5, respectively. This procedure is equally applicable to stars and solar system objects. The development that follows requires quantities related to precession and nutation that, in the computation of geocentric apparent or intermediate places, are not needed before Step 5 in § 7.4.1.6. These quantities should be computed, used here, and saved for later use; they are specifically noted as they arise.

7.4.3.1 Universal Time of the Observation

Step 1. Determine the Universal Time of observation, specifically, the epoch of observation in the UT1 timescale. UT1 is affected by unpredictable irregularities in the Earth's rotation, but is always within $0^s.9$ of UTC, the latter defining civil time and broadcast worldwide according to international convention. The difference $\Delta\mathrm{UT} = \mathrm{UT1} - \mathrm{UTC}$ is determined and distributed by the IERS (URL[5]). The predicted value of $\Delta\mathrm{UT}$ to within $0^s.1$ (denoted DUT1) is also coded into UTC broadcasts (see § 3.2.2, § 3.5.1, and § 3.10.1).

7.4.3.2 Terrestrial Coordinates of the Observer

There are three commonly used ways of expressing terrestrial (i.e., Earth-fixed) coordinates:

1. geocentric equatorial rectangular coordinates, x, y, z;
2. geocentric longitude, latitude and distance, λ, ϕ', ρ;
3. geodetic longitude, latitude and height, λ, ϕ, h.

Geodetic coordinates are referred to a reference spheroid (an ellipse of revolution), which is normally geocentric, and is defined by its equatorial radius (a) and flattening (f). For example, those of the 2010 Conventions (IERS 2010) are

$$a = 637\,8136.6\ \mathrm{m} \quad \text{and} \quad f = 1/298.256\,42. \tag{7.130}$$

The geodetic and geocentric longitudes of a point are the same. The following relationships hold between the geocentric and geodetic (geographic) coordinates:

$$\mathbf{r} = \begin{bmatrix} x \\ y \\ z \end{bmatrix} = \begin{bmatrix} \rho\cos\phi'\cos\lambda \\ \rho\cos\phi'\sin\lambda \\ \rho\sin\phi' \end{bmatrix} = \begin{bmatrix} (aC+h)\cos\phi\cos\lambda \\ (aC+h)\cos\phi\sin\lambda \\ (aS+h)\sin\phi \end{bmatrix} \tag{7.131}$$

where a is the equatorial radius of the spheroid and C and S are auxiliary functions that depend on the geodetic latitude and the flattening f of the reference spheroid (see Eqs. 7.130). It follows from the properties of the ellipse that

$$C = (\cos^2\phi + (1-f)^2\sin^2\phi)^{-1/2} \qquad S = (1-f)^2 C. \tag{7.132}$$

Geocentric coordinates may be calculated directly from geodetic coordinates and conversely. It is easier to use an iterative procedure for the inverse calculation (see Chapter 5, § 5.2.4). Series expansions, which contain terms up to f^3, for S, C, ρ and $\phi - \phi'$ are:

$$\begin{aligned} S = 1 &- \frac{3}{2}f + \frac{5}{16}f^2 + \frac{3}{32}f^3 - \left(\frac{1}{2}f - \frac{1}{2}f^2 - \frac{5}{64}f^3\right)\cos 2\phi \\ &+ \left(\frac{3}{16}f^2 - \frac{3}{32}f^3\right)\cos 4\phi - \frac{5}{64}f^3\cos 6\phi \end{aligned} \tag{7.133}$$

$$\begin{aligned} C = 1 &+ \frac{1}{2}f + \frac{5}{16}f^2 + \frac{7}{32}f^3 - \left(\frac{1}{2}f + \frac{1}{2}f^2 + \frac{27}{64}f^3\right)\cos 2\phi \\ &+ \left(\frac{3}{16}f^2 + \frac{9}{32}f^3\right)\cos 4\phi - \frac{5}{64}f^3\cos 6\phi \end{aligned} \tag{7.134}$$

$$\rho = 1 - \frac{1}{2}f + \frac{5}{16}f^2 + \frac{5}{32}f^3 + \left(\frac{1}{2}f - \frac{13}{64}f^3\right)\cos 2\phi$$
$$- \left(\frac{5}{16}f^2 + \frac{5}{32}f^3\right)\cos 4\phi + \frac{13}{64}f^3 \cos 6\phi \tag{7.135}$$

$$\phi - \phi' = \left(f + \frac{1}{2}f^2\right)\sin 2\phi - \left(\frac{1}{2}f^2 + \frac{1}{2}f^3\right)\sin 4\phi + \frac{1}{3}f^3 \sin 6\phi. \tag{7.136}$$

The expressions for ρ and $\phi - \phi'$ are for points on the spheroid ($h = 0$), and the latter quantity is sometimes known as the "reduction in latitude" or "the angle of the vertical", and it is of order $10'$ in mid-latitudes. To a first approximation when h is small, the geocentric radius is increased by h/a and the angle of the vertical is unchanged. The height h refers to a height above the reference spheroid and differs from the height above mean sea level (i.e., above the geoid) by the "undulation of the geoid" at the point.

Step 2. Obtain $\mathbf{r}$ (in meters) the position vector of the observer in an Earth-fixed, geocentric, right-handed coordinate system, with the xy-plane the Earth's equator, the xz-plane the ITRS meridian, and the z-axis pointed towards the north terrestrial pole. In terms of the observer's geodetic latitude ϕ, longitude λ (east longitudes positive) and height h above the Earth's reference ellipsoid, [for most purposes the height above mean sea level (the regional geoid) can be used], $\mathbf{r}$ is given by Eq. 7.131 and the latest values for a and f may be found in Section K of *The Astronomical Almanac*.

7.4.3.3 Geocentric Position and Velocity of the Observer

Step 3. Compute the geocentric position and velocity of the observer, with respect to the celestial of date reference system, in meters, and meters/second, respectively, from

$$\mathbf{g}(t) = \mathbf{R}_3(-\beta)\mathbf{W}^{-1}\,\mathbf{r} \tag{7.137}$$
$$= \mathbf{R}_3(-\beta)\,\mathbf{R}_3(-s')\,\mathbf{R}_2(x_p)\,\mathbf{R}_1(y_p)\,\mathbf{r} \tag{7.138}$$

$$\dot{\mathbf{g}}(t) = \dot{\beta}\,\hat{\mathbf{k}} \wedge \mathbf{g}(t) \tag{7.139}$$
$$= \dot{\beta}\begin{bmatrix} -\sin\beta & -\cos\beta & 0 \\ \cos\beta & -\sin\beta & 0 \\ 0 & 0 & 0 \end{bmatrix}\mathbf{W}^{-1}\,\mathbf{r}. \tag{7.140}$$

Polar motion ($\mathbf{W}^{-1}$, see § 7.2.6.2) involving (x_p, y_p) the coordinates of the CIP in the ITRS, and s' the TIO locator (see Chapter 6), transforms from the ITRS to the Terrestrial Intermediate Reference System. Note that here the transformation starts from the TRS, as in the IERS Conventions. The rotation $\mathbf{R}_3(-\beta)$ rotates the Terrestrial Intermediate Reference System about the CIP to the celestial system. The choice of β determines the celestial system and the paradigm; for equinox-based positions set $\beta =$ GAST; for CIO-based positions set $\beta = \theta$, the Earth Rotation Angle. This choice will determine choices in Step 5 below, and the origin of right ascension will either be the true equinox or the CIO, respectively. GAST and θ (the ERA), are determined at the time of observation and are given in Chapter 6 (see § 6.8.4 and § 6.8.5). Note, that ERA and GAST are basically functions of UT1, while precession and nutation are not.

Strictly speaking in the velocity equation (Eq. 7.139) $\dot{\beta}$ will be either $\dot{\text{GAST}}$ or $\dot{\theta}$, respectively, depending on the choice of paradigm. However, the difference between the rates in the two paradigms is very small, and noting that the velocity of the observer on the surface of the Earth is then added to the velocity of the Earth (see Step 6, § 7.4.3.5) as part of the aberration correction, it is sufficient to replace $\dot{\beta}$ with the standard value of the nominal mean angular velocity of the Earth $\omega = 7.292\,115 \times 10^{-5}$ radians/second. The unit vector $\hat{\mathbf{k}}$ points towards the north CIP of date.

Polar motion, which affects the components of the observer's geocentric position vector at the 10-meter (0.″3) level, and may be neglected if desired by replacing $\mathbf{R}_1(y_p)$ and $\mathbf{R}_2(x_p)$ by unit matrices. The drift of the TIO within the ITRS is less than 50 microarcseconds after a century (see § 7.2.6.2), which is insignificant, thus $\mathbf{R}_3(-s')$ may also be replaced by a unit matrix. Neglecting polar motion affects the computed topocentric place of the Moon by several milliarcseconds, with a much smaller effect, inversely proportional to distance, for other bodies. If effects at this level are important, corrections are also required to refer the regional geoid (the coordinate system for the observer's geodetic latitude, longitude and height) to the Earth's reference ellipsoid. In forming the velocity of the observer a standard value for the rotation rate of the Earth has been used, and the small effects due to the variation in rate from this value and due to the change of the polar motion components have been ignored.

More information on the computation of an observer's geocentric coordinates are given in Section K of *The Astronomical Almanac*, Mueller (1969), Taff (1981), as well as Chapter 5.

Step 4. Convert the geocentric position and velocity vectors to units of au and au/day, respectively, by multiplying $\mathbf{g}(t)$ by $1/A$ and $\dot{\mathbf{g}}(t)$ by $86400/A$, where $A = 1.495\,978\,706\,91 \times 10^{11}$ is the number of metres in 1 au and is the value from the JPL DE405/LE405 ephemeris.

7.4.3.4 Position and Velocity of the Observer in the ICRS

Transform the vectors $\mathbf{g}(t)$ and $\dot{\mathbf{g}}(t)$ from the of date system to the ICRS, which is a space-fixed coordinate system and the coordinate system in which the position and velocity of the Earth are expressed.

Step 5.

	Equinox Method		*CIO Method*
5.	$\mathbf{G}(t) = \mathbf{M}^{-1}\,\mathbf{g}(t)$		$\mathbf{G}(t) = \mathbf{C}^{-1}\,\mathbf{g}(t)$
	$\dot{\mathbf{G}}(t) = \mathbf{M}^{-1}\,\dot{\mathbf{g}}(t)$		$\dot{\mathbf{G}}(t) = \mathbf{C}^{-1}\,\dot{\mathbf{g}}(t)$ (7.141)
	where the inverse $\mathbf{M}^{-1} = \mathbf{M}^{\mathrm{T}}$ the transpose of $\mathbf{M}$ (see § 7.2.5.1)		where the inverse $\mathbf{C}^{-1} = \mathbf{C}^{\mathrm{T}}$ the transpose of $\mathbf{C}$ (see § 7.2.5.2).

The most efficient procedure would be to evaluate the elements of the matrix at this point and save them for later use in Step 5 of § 7.4.1.6, noting that here the inverse matrix is used.

Strictly, the frame bias, precession, and nutation matrices define a transformation between a space-fixed system and a slowly rotating system. The slow rotation is the changing orientation of the Earth's axis due to external torques that the precession and nutation theories describe. Therefore, the conversion of the observers velocity given in Eq. 7.141 is missing a Coriolis term. However, the equivalent linear velocity of this rotation is of order 10^{-5}

m/second for an observer on the surface of the Earth, comparable to the tracking velocity of large telescopes and completely negligible.

7.4.3.5 Barycentric Position and Velocity of the Observer

Step 6. Calculate the barycentric position and velocity of the observer $\mathbf{O}_{\mathrm{B}}(t)$ and $\dot{\mathbf{O}}_{\mathrm{B}}(t)$, by adding the geocentric position and velocity of the observer, $\mathbf{G}(t)$ and $\dot{\mathbf{G}}(t)$, obtained above, to the barycentric position and velocity of the Earth $\mathbf{E}_{\mathrm{B}}(t)$ and $\dot{\mathbf{E}}_{\mathrm{B}}(t)$ obtained in Step 2.1 of § 7.4.1.2, thus

$$\begin{aligned} \mathbf{O}_{\mathrm{B}} &= \mathbf{E}_{\mathrm{B}}(t) + \mathbf{G}(t) \\ \dot{\mathbf{O}}_{\mathrm{B}} &= \dot{\mathbf{E}}_{\mathrm{B}}(t) + \dot{\mathbf{G}}(t). \end{aligned} \tag{7.142}$$

Then redefine the vectors $\mathbf{E}_{\mathrm{B}}(t)$ and $\dot{\mathbf{E}}_{\mathrm{B}}(t)$ to be identical to $\mathbf{O}_{\mathrm{B}}(t)$ and $\dot{\mathbf{O}}_{\mathrm{B}}$.

7.4.3.6 Topocentric Place

Step 7. Continuing at Step 2.1 in § 7.4.1.2, the other steps follow as before, except that the transformation matrix (see Step 5 above) from the GCRS need not be re-computed in the steps in § 7.4.1.6.

The right ascension α and declination δ obtained at Step 6 represent the topocentric place of the object at the epoch of observation. The topocentric hour angle of the object may be calculated by replacing Steps 5 and 6 by Steps 5* and 6*. Alternatively see § 7.1.3.2, where hour angle is given in terms of right ascension.

In many cases the above procedure may be simplified but most care is needed for objects in the inner solar system when the highest precision is required. For objects beyond the inner solar system, to milliarcsecond precision, when using the equinox method nutation may be ignored throughout. That is, mean sidereal time can be used instead of apparent sidereal time (the equation of the equinoxes can be considered zero) and nutation may be neglected. Additionally, the difference between UT1 and UTC timescales can be ignored. However, these simplifications may not result in any real computational saving. The nutation parameters would have to be calculated anyway in a later step. Furthermore, these simplifications affect the computed sidereal time at the 1^{s} level, and will therefore cause errors in the computed topocentric hour angle of this magnitude. Therefore, in many cases, carrying out the full procedure, and saving the values of the relevant nutation and time variables for later use, may be the most prudent course.

7.4.4 Summary of the Algorithms

The development of the apparent and intermediate place algorithms using matrix/vector notation is rigorous and allows the planet and star algorithms to use those parts which are common to both. It also allows users to tailor their program to their own needs, as well as the testing of alternative, or simplified, algorithms for special purposes.

In this unified approach for planets and stars, position vectors have been used throughout. Many other algorithms use unit vectors (see *The Astronomical Almanac*). There are penalties either way, and if the procedures are carefully implemented the results will be identical.

The method given here involves a series of steps. However, if the observation time remains the same, quantities such as the time arguments, the ephemeris data for the Earth, the precession and nutation matrices can be saved and re-used. For example, when there

are a large number of "of date" places to be computed, it is more efficient to compute the places of all bodies at a given observing epoch before moving to a new observing epoch. The major computational burden in the algorithm involves the retrieval of data from the planetary ephemeris in § 7.4.1.2 Steps 2.1 through 2.6 and the evaluation of the two nutation angles $\Delta\psi$ and $\Delta\epsilon$ or equivalently the $(\mathcal{X}, \mathcal{Y})$ coordinates of the CIP, that are involved in the calculation of the transformation from the GCRS to "of date" position see, § 7.4.1.6, § 7.2.5) and Chapter 6.

If computational time becomes critical (such as within telescope control systems or in micro-computer implementations), the method of obtaining the ephemeris and nutation data must be considered. Self-contained algorithms can often be simplified by truncating small terms from the series, if high precision in the final place is not required. Consideration should also be given to pre-computing the required data for fixed intervals and storing the data in an external file which can be efficiently accessed and interpolated. Planetary ephemeris data are frequently distributed in this form anyway. Pre-computing and storing the elements of the combined bias-precession-nutation matrix $\mathbf{M}$ or $\mathbf{C}$ (see § 7.2.5) is also feasible. The convenience of self-contained algorithms must be weighed against the number of calculations required, the accuracy of the algorithm, and the accuracy needed for the final result.

7.4.5 Approximate Algorithms

This section summarizes mean places and the method of Day Numbers. Together these techniques were a useful procedure for calculating apparent places of stars accurately ($\pm 0\overset{''}{.}01$) where most of the information was pre-computed. First, however, we give an algorithm for calculating the intermediate place, accurate to about $\pm 1''$ over a century and the resulting altitude and azimuth.

7.4.5.1 Approximate CIO-based Method

The following is an approximate procedure based on the CIO method for calculating the intermediate position of a star for a specified UT1 instant. During the process the intermediate right ascension and declination (α_i, δ_i), the GHA, LHA, and the altitude and azimuth (a, A_Z) are all calculated. The procedure given is accurate to about $\pm 1''$ between 1925 and 2100, however, between 1900 and 1925 the errors may reach $1\overset{''}{.}7$ due to the approximation of the Earth's velocity. This analysis assumed that the ERA was calculated accurately.

Strictly, all the parameters, except the ERA (θ), should be evaluated for the equivalent TT (UT1 + ΔT) instant.

Step 1. Given the observer's position (λ, ϕ) and a given UT1 instant, (i.e., a specified date and UT1 time), calculate the UT1 Julian date and fraction (JD). Also form the intervals D_U in days and T in Julian centuries, respectively, from J2000.0 = 245 1545.0 UT1.

$$D_U = \text{JD} - 245\,1545.0 \quad \text{and} \quad T = D_U/36525. \tag{7.143}$$

Step 2. Evaluate the position $(\mathbf{q})$ and space motion $(\mathbf{m})$ vectors of the star with respect to the ICRS (see § 7.2.1, Eqs. 7.20 and 7.22 or 7.24).

Step 3. Apply space motion and ignore parallax to give the approximate geocentric position of the star at the epoch of date,

$$\mathbf{p} = \mathbf{q} + T\mathbf{m}. \tag{7.144}$$

Step 4. Apply aberration and precession-nutation, resulting in an of date position

$$\mathbf{r} = \mathbf{V} + \mathbf{C}(\mathcal{X}, \mathcal{Y}, s)\,\mathbf{p} \tag{7.145}$$

where $\mathbf{V} = (V_x, V_y, V_z)$ in au/day is the approximate barycentric velocity of the Earth (see Eqs. 7.44). The more accurate the approximation of $\mathbf{V}$ the better the result. The precession-nutation matrix $\mathbf{C}$ is approximated by ignoring the tiny rotation s, and simplifying Eq 7.75. Expanding the matrix equation gives

$$\begin{bmatrix} x_i \\ y_i \\ z_i \end{bmatrix} = \frac{1}{c} \begin{bmatrix} +0.0172 \sin L \\ -0.0158 \cos L \\ -0.0068 \cos L \end{bmatrix} + \begin{bmatrix} 1 - \mathcal{X}^2/2 & 0 & -\mathcal{X} \\ 0 & 1 & -\mathcal{Y} \\ \mathcal{X} & \mathcal{Y} & 1 - \mathcal{X}^2/2 \end{bmatrix} \begin{bmatrix} p_x \\ p_y \\ p_z \end{bmatrix}. \tag{7.146}$$

Thus, first calculate the following quantities

$$L = 280\overset{\circ}{.}5 + 36000\overset{\circ}{.}8\,T \tag{7.147}$$

$$\Omega = 125\overset{\circ}{.}0 - 1934\overset{\circ}{.}1\,T \tag{7.148}$$

$$\mathcal{X} = +2004\overset{''}{.}19\,T - 0\overset{''}{.}43\,T^2 - 6\overset{''}{.}84\,\sin\Omega - 0.52\,\sin 2L \tag{7.149}$$

$$\mathcal{Y} = -0\overset{''}{.}03\,T - 22\overset{''}{.}41\,T^2 + 9\overset{''}{.}21\,\cos\Omega + 0.57\,\cos 2L. \tag{7.150}$$

These simple formulae for $\mathcal{X}$ and $\mathcal{Y}$ are accurate to $\pm 0\overset{''}{.}6$ between 1900 and 2100, thus keeping this part of the approximation well below the target accuracy of $1''$. The ecliptic longitude of the Sun, L, is used in both the position of the CIP and approximating the barycentric velocity of the Earth. The speed of light is given by $c = 173.14$ au/d.

Multiplying out the matrix and rewriting in terms of coordinates, the position of the star with respect to the Celestial Intermediate Reference System is given by

$$x_i = V_x + p_x\,(1 - \mathcal{X}^2/2) - p_z\,\mathcal{X} \tag{7.151}$$

$$y_i = V_y + p_y - p_z\mathcal{Y} \tag{7.152}$$

$$z_i = V_z + p_x\,\mathcal{X} + p_y\,\mathcal{Y} + p_z\,(1 - \mathcal{X}^2/2) \tag{7.153}$$

where $\mathcal{X}$ and $\mathcal{Y}$ must be expressed in radians. Use Eq. 7.2 replacing (ξ, η, ζ) with (x_i, y_i, z_i) to give (α_i, δ) the approximate intermediate place.

Step 5. Next transform to the observers local system, by rotations of $\theta + \lambda$ about the CIP, followed by a rotation of $90° - \phi$ about the y-axis in the plane of the observer's local meridian, giving

$$x = -[x_i\,\cos(\theta + \lambda) + y_i\,\sin(\theta + \lambda)]\,\sin\phi + z_i\,\cos\phi \tag{7.154}$$

$$y = -x_i\,\sin(\theta + \lambda) + y_i\,\cos(\theta + \lambda) \tag{7.155}$$

$$z = +[x_i\,\cos(\theta + \lambda) + y_i\,\sin(\theta + \lambda)]\,\cos\phi + z_i\,\sin\phi \tag{7.156}$$

where the Earth Rotation Angle is given by

$$\begin{aligned} \theta &= 2\pi(0.7790\,5727\,32640 + 1.0027\,3781\,1911\,35448\,D_{\mathrm{U}}) \text{ radians} \\ &= 360°(0.7790\,5727\,32640 + 0.0027\,3781\,1911\,35448\,D_{\mathrm{U}} + D_{\mathrm{U}} \bmod 1). \end{aligned} \tag{7.157}$$

$D_{\mathrm{U}} \bmod 1$ is the fraction of the UT1 day remaining after removing all the whole days. At this stage the quantities GHA $= \theta - \alpha_i$ and LHA $= \theta - \alpha_i + \lambda$, may also be formed (see § 7.1.3.2). It should be noted that there are no approximations in this or the next step.

Step 6. Finally convert from x, y, z coordinates to altitude (a) and azimuth (A_z)

$$a = \tan^{-1} \frac{z}{\sqrt{(x^2 + y^2)}} \quad \text{and} \quad A_z = \tan^{-1} \frac{y}{x} \tag{7.158}$$

where azimuth is measured from north through east in the plane of the horizon and altitude is measured perpendicular to the horizon (see § 7.1.3.4). To approximate the topocentric altitude (to about 0.′1) add the parallax in altitude (see § 7.2.2.2) and refraction (see § 7.2.7.3).

7.4.5.2 Mean Places

Mean places are a concept that is particularly used for positions of stars and other objects outside the solar system. The mean place represents the direction of the object as it would hypothetically be observed from the solar system barycentre at the specified date. The coordinate system must be specified; positions could be referred to a standard coordinate system (ICRS, J2000.0, etc.) or one "of date".

Section H of *The Astronomical Almanac* includes lists of the mean places of different types of stars and stellar objects. These are barycentric positions that are tabulated with respect to the mean equinox of the middle of the year, e.g., J2013.5. To calculate such a mean place at a given date, take the ICRS (barycentric) catalogue position (**r**) (as found in most star catalogues), apply space motion (see § 7.2.1 and Eq. 7.25) from the epoch of the catalogue position (t) to the required date (t_1) and then transform from the ICRS to the mean equinox of date (**PB**), thus

$$\mathbf{r_2} = \mathbf{P\,B}\,(\mathbf{r} + (t_1 - t)\,\dot{\mathbf{r}})$$

An apparent place (see § 7.4.2) with nutation ignored, i.e., place with respect to the mean equinox of date, is useful when calculating hour angles since the lengthy calculation of nutation angles is not required. Hour angles are discussed in § 7.1.3.2. This concept does not apply to the IAU recommended Celestial Intermediate Reference System which may be referred to as the equator and CIO of date.

7.4.5.3 Methods Using Day Numbers

Historically there are two Day Numbers techniques, Besselian Day Numbers and Independent Day Numbers. These techniques are described in the § 3.34 of the previous edition of the *Explanatory Supplement* (Hohenkerk et al. 1992) and the Besselian Day Numbers were last tabulated in *The Astronomical Almanac* for 2003.

In summary, the apparent (equinox) right ascension and declination (α_1, δ_1), of a star at an epoch $t + \tau$, which includes the effects of precession, nutation, annual aberration, proper motion, annual parallax, and includes the second-order day numbers (J and J'), may be calculated either using the Besselian Day Numbers A, B, C, D, E, and star constants, from

$$\begin{aligned} \alpha_1 &= \alpha + Aa + Bb + Cc + Dd + E + J \tan^2 \delta + \tau\mu_\alpha + \pi\,(dX - cY) \\ \delta_1 &= \delta + Aa' + Bb' + Cc' + Dd' + J' \tan \delta + \tau\mu_\delta + \pi\,(d'X - c'Y) \end{aligned} \tag{7.159}$$

or using the Independent Day Numbers f, g, G, h, H, from

$$\begin{aligned} \alpha_1 &= \alpha + f + g \sin\,(G + \alpha) \tan \delta + h \sin\,(H + \alpha) \sec \delta + J \tan^2 \delta \\ &\quad + \tau\mu_\alpha + \pi(dX - cY) \\ \delta_1 &= \delta + g \cos\,(G + \alpha) + h \cos\,(H + \alpha) \sin \delta + i \cos \delta + J' \tan \delta \\ &\quad + \tau\mu_\delta + \pi(d'X - c'Y) \end{aligned} \tag{7.160}$$

where α, δ are the right ascension and declination of the star for the mean equinox and epoch of t, and μ_α and μ_δ are the annual proper motions in right ascension and declination, respectively and π is the parallax. X and Y are the barycentric coordinates of the Earth. For stars, the corrections for the deflection of light was not included.

Acknowledgements. Acknowledgements are due to the original authors and others as much of the material in this chapter—particular on the effects space motion, parallax, aberration, light deflection and refraction—is taken from Chapter 3 of the previous edition (Hohenkerk et al. 1992) which was collaborative effort between the Nautical Almanac Offices of the U.S. and UK.

REFERENCES

1. The Astronomical Almanac Online:
http://asa.usno.navy.mil or http://asa.hmnao.com.
2. Naval Observatory Vector Astrometry Software (NOVAS):
http://aa.usno.navy.mil/software/novas/novas_info.php.
3. IAU Standards of Fundamental Astronomy (SOFA) Software Collection:
http://www.iausofa.org/.
4. IAU Commission 4 (Ephemerides):
http://www.iaucom4.org/.
5. International Earth Rotation and Reference Systems Service:
http://www.iers.org/.
6. IAU Resolutions Adopted by the General Assemblies:
http://www.iau.org/administration/resolutions/general_assemblies/.

Abalakin, V. K. (1985). *Refraction Tables of Pulkovo Observatory* (5th ed.). Leningrad: Academy of Sciences of the USSR. Nauka Publishing House.

Auer, L. H. and E. M. Standish (1979). Astronomical Refraction: Computational Method for All Zenith Angles. Technical note, Yale University Astronomy Department, New Haven, CT.

Auer, L. H. and E. M. Standish (2000). Astronomical Refraction: Computational Method for All Zenith Angles. *Astronomical Journal 119*, 2472–2474.

Capitaine, N. and P. T. Wallace (2006). High Precision Methods for Locating the Celestial Intermediate Pole and Origin. *Astronomy and Astrophysics 450*, 855–872.

Dyson, F. W., A. S. Eddington, and C. Davidson (1920). A Determination of the Deflection of Light by the Sun's Gravitational Field, from Observations Made at the Total Eclipse of May 29, 1919. *Royal Society of London Philosophical Transactions Series A 220*, 291–333.

Einstein, A. (1956). *The Meaning of Relativity* (5th ed.). Princeton and London: Princeton University Press.

Fairhead, L. and P. Bretagnon (1990). An analytical formula for the time transformation TD−TT. *Astronomy and Astrophysics 229*, 240–247.

Fomalont, E. B. and R. A. Sramek (1975). A confirmation of Einstein's general theory of relativity by measuring the bending of microwave radiation in the gravitational field of the Sun. *Astrophysical Journal 199*, 749–755.

Hilton, J. L., N. Capitaine, J. Chapront, J. M. Ferrandiz, A. Fienga, T. Fukushima, J. Getino, P. Mathews, J.-L. Simon, M. Soffel, J. Vondrak, P. Wallace, and J. Williams (2006). Report of the International

Astronomical Union Division I Working Group on Precession and the Ecliptic. *Celestial Mechanics and Dynamical Astronomy 94*, 351–367.

Hohenkerk, C. Y. and A. T. Sinclair (1985). The computation of angular atmospheric refraction at large zenith angles. Technical Note 63, HM Nautical Almanac Office, Greenwich.

Hohenkerk, C. Y., B. Yallop, C. A. Smith, and A. T. Sinclair (1992). Celestial Reference Systems. In P. K. Seidelmann (Ed.), *Explanatory Supplement to The Astronomical Almanac*, Chapter 3, pp. 95–198. Mill Valley, CA: University Science Books.

IAU (2001). In H. Rickman (Ed.), *Transactions of the International Astronomical Union*, Volume XXIV B, San Francisco. Astronomical Society of the Pacific. Proc. 24th General Assembly, Manchester, 2000.

IAU (2008). In K. A. van der Hucht (Ed.), *Transactions of the International Astronomical Union*, Volume XXVI B, Cambridge. Cambridge University Press. Proc. 26th General Assembly, Prague, 2006.

IERS (2010). Conventions (2010). Technical Note 36, International Earth Rotation and Reference Systems Service, Frankfurt am Main. Verlag des Bundesamts für Kartographie und Geodäsie, G. Petit and B. Luzum (Eds.).

Kaplan, G. H. (2005). The IAU Resolutions on Astronomical Reference Systems, Time Scales, and Earth Rotation Models. Circular 179, U.S. Naval Observatory, Washington, DC.

Kaplan, G. H., J. A. Bangert, J. L. Bartlett, W. K. Puatua, and A. K. B. Monet (2009). User's Guide to NOVAS 3.0. Circular 180, U.S. Naval Observatory, Washington, DC.

Kaplan, G. H., J. A. Hughes, P. K. Seidelmann, C. A. Smith, and B. D. Yallop (1989). Mean and apparent place computations in the new IAU system. III. Apparent, topocentric, and astrometric places of planets and stars. *Astronomical Journal 97*, 1197–1210.

Moisson, X. and P. Bretagnon (2001). Analytical Planetary solution VSOP2000. *Celestial Mechanics and Dynamical Astronomy 80*, 205–213.

Murray, C. A. (1981). Relativistic astrometry. *Monthly Notices of the Royal Astronomical Society 195*, 639–648.

Murray, C. A. (1985). *Vectorial Astrometry* (5th ed.). Bristol: Hilger.

Nautical Almanac Offices of UK and USA (1983). *The Astronomical Almanac for the Year 1984*. Washington & London: US Government Printing Office & HM Stationery Office.

Pulkova Obs. (1956). *Refraction tables of Pulkova Observatory* (4th ed.). Moscow and Leningrad: Academy of Sciences Press.

Saastamoinen, J. (1972). Introduction to practical computation of astronomical refraction. *Bulletin of Geodesy 106*, 383–397.

Seidelmann, P. K. (Ed.) (1992). *Explanatory Supplement to The Astronomical Almanac*. Mill Valley, CA: University Science Books.

Shapiro, I. I. (1967). New method for the detection of light deflection by solar gravity. *Science 157*, 806–808.

Simon, J. L., P. Bretagnon, J. Chapront, M. Chapront-Touzé, G. Francou, and J. Laskar (1994). Numerical expressions for precession formulae and mean elements for the Moon and planets. *Astronomy and Astrophysics 282*, 663–683.

Standish, E. M. (1998a). JPL Planetary and Lunar Ephemerides, DE405/LE405. IOM 312.F-98-048, Jet Propulsion Laboratory.

Standish, E. M. (1998b). Time scales in JPL and CfA ephemerides. *Astronomy and Astrophysics 336*, 381–384.

Stumpff, P. (1979). The rigorous treatment of stellar aberration and doppler shift, and the barycentric motion of the Earth. *Astronomy and Astrophysics 78*, 229–238.

Stumpff, P. (1980a). On the relationship between classical and relativistic theory of stellar aberration. *Astronomy and Astrophysics 84*, 257–259.

Stumpff, P. (1980b). Two self-consistent Fortran subroutines for the computation of the Earth's motion. *Astronomy and Astrophysics Supplement Series 41*, 1–8.

Stumpff, P. (1985). Rigorous treatment of the heliocentric motion of stars. *Astronomy and Astrophysics 144*, 232–240.

Taff, L. G. (1981). *Computational Spherical Astronomy*. New York: Wiley.

Wallace, P. T. and N. Capitaine (2006). Precession-nutation procedures consistent with IAU 2006 resolutions. *Astronomy and Astrophysics 459*, 981–985.

Yallop, B. D. (1983). *The Astronomical Almanac for the Year 1984*. Washington & London: US Government Printing Office & HM Stationery Office. Pages B16-B41.

FURTHER READING

Atkinson, R. d. (1972). Modem Aberration for Observations of any Date. *Astronomical Journal 77*, 512–517.

Capitaine, N., J. Chapront, S. Lambert, and P. T. Wallace (2003). Expressions for the celestial intermediate pole and celestial ephemeris origin consistent with the IAU 2000A precession-nutation model. *Astronomy and Astrophysics 400*, 1145–1154.

Capitaine, N. and A. Gontier (1993). Accurate procedure for deriving UTI at a submilliarcsecond accuracy from Greenwich Sidereal Time or from the stellar angle. *Astronomy and Astrophysics 275*, 645–650.

Capitaine, N., B. Guinot, and D. D. McCarthy (2000). Definition of the Celestial Ephemeris Origin and of UT1 in the International Celestial Reference Frame. *Astronomy and Astrophysics 355*, 398–405.

Capitaine, N., P. T. Wallace, and J. Chapront (2003). Expressions for IAU 2000 Precession Quantities (IAU 2006 P03 model). *Astronomy and Astrophysics 412*, 567–586.

Capitaine, N., P. T. Wallace, and J. Chapront (2005). Improvement of the IAU 2000 precession model. *Astronomy and Astrophysics 432*, 355–367.

Capitaine, N., P. T. Wallace, and D. D. McCarthy (2003). Expressions to Implement the IAU 2000 Definition of UT1. *Astronomy and Astrophysics 406*, 1135–1149.

Chapront, J., M. Chapront-Touzé, and G. Francou (2002). A new determination of lunar orbital parameters, precession constant and tidal acceleration from LLR measurements. *Astronomy and Astrophysics 387*, 700–709.

Chauvenet, W. (1960). *A Manual of spherical and practical astronomy - Vol.1: Spherical astronomy; Vol.2: Theory and use of astronomical instruments. Method of least squares* (revised and corr., 5th ed.). New York: Dover Publication.

Duncombe, R. L., W. Fricke, P. K. Seidelmann, and G. A. Wilkins (1977). Joint report of the working groups of the IAU Commission 4 on precession, planetary ephemerides, units and time-scales. In E. A. Müller and A. Jappel (Eds.), *Transactions of the International Astronomical Union*, Volume XVI B, Dordrecht, pp. 56. Reidel. Proc. 16th General Assembly, Grenoble, 1976.

Duncombe, R. L., P. K. Seidelmann, and T. C. van Flandern (1975). Celestial reference systems derivable from solar system dynamics. In B. Kolaczek and G. Weiffenbach (Eds.), *IAU Colloq. 26: On Reference Coordinate Systems for Earth Dynamics*, pp. 223–233.

Eichelberger, W. S. (1904). Reduction tables for transit circle observations. In *Publications of the United States Naval Observatory, 2nd Series*, Volume 4, part 4, appendix 2. Washington: US Government Printing Office.

Emerson, B. (1973). A method of calculating apparent places of stars. *Royal Greenwich Observatory Bulletin 178*, 299–300.

Garfinkel, B. (1944). An investigation in the theory of astronomical refraction. *Astronomical Journal 50*, 169–179.

Garfinkel, B. (1967). Astronomical refraction in a polytropic atmosphere. *Astronomical Journal 72*, 235–254.

Green, R. M. (1985). *Spherical Astronomy* (5th ed.). Cambridge and New York: Cambridge University Press.

Harzer, P. (1924a). Berechnung der Ablenkung der Lichtstrahlen in der Atmosphäre der Erde auf rein meteorologisch-physikalischer Grundlage. *Publikation der Sternwarte in Kiel* (13).

Harzer, P. (1924b). Gebrauchstabellen zur Berechnung der Ablenkungen der Lichtstrahlen in der Atmosphäre der Erde für die Beobachtungen am grossen Kieler Meridiankreise. *Publikation der Sternwarte in Kiel* (14).

IERS (2004). Conventions (2003). Technical Note 32, International Earth Rotation Service, Frankfurt am Main. Verlag des Bundesamts für Kartographie und Geodäsie, D. D. McCarthy and G. Petit (Eds.).

Kaplan, G. H. (1981). The IAU resolutions on astronomical constants, time scales, and the fundamental reference frame. Circular 163, U.S. Naval Observatory, Washington, DC.

Kovalevsky, J. and P. K. Seidelmann (2004). *Fundamentals of Astrometry*. Cambridge and New York: Cambridge University Press.

Lederle, T. and H. Schwan (1984). Procedure for computing the apparent places of fundamental stars (APFS) from 1984 onwards. *Astronomy and Astrophysics 134*, 1–6.

Mathews, P. M., T. A. Herring, and B. A. Buffet (2002). Modeling of nutation and precession New nutation series for nonrigid Earth and insights into the Earth's interior. *Journal of Geophysical Research 107*, 2068–2093.

Moyer, T. D. (1981). Transformation from proper time on earth to coordinate time in solar system barycentric space-time frame of reference. I. II. *Celestial Mechanics 23*, 33–56.

Nautical Almanac Offices of UK and USA (1961). *Explanatory Supplement to The Astronomical Ephemeris and The American Ephemeris and Nautical Almanac*. London: Her Majesty's Stationery Office. Reprinted 1974.

Porter, J. G. and D. H. Sadler (1953). The accurate calculation of apparent places of stars. *Monthly Notices of the Royal Astronomical Society 113*, 455–467.

Smart, W. M. (1944). *Text-book in Spherical Astronomy*. Cambridge: Cambridge University Press.

Standish, E. M. (1982). Orientation of the JPL ephemerides, DE200/LE200, to the dynamical equinox of J2000. *Astronomy and Astrophysics 114*, 297–302.

Stumpff, P. (1986). Relativistic and perspective effects in proper motions and radial velocities of stars. In J. Kovalesky and V. A. Brumberg (Eds.), *Relativity in Celestial Mechanics and Astronomy, IAU Symposium 114*, pp. 193–198. Dordrecht: Reidel.

Willis, J. E. (1941). A determination of astronomical refraction from physical data. *Transactions of the American Geophysical Union*, 324.

Woolard, E. W. and G. M. Clemence (1981). *Spherical Astronomy*. New York & London: Academic Press.

CHAPTER 8

Orbital Ephemerides of the Sun, Moon, and Planets

E. MYLES STANDISH & JAMES G. WILLIAMS

8.1 Fundamental Ephemerides

The fundamental planetary and lunar ephemerides of *The Astronomical Almanac*, starting in the year 2003, are DE405/LE405 of Caltech's Jet Propulsion Laboratory (JPL). They replace JPL's DE200 which have been used in the almanac since 1984. Previous to 1984, the fundamental ephemerides were based upon analytical *theories*; these are described in § 8.2. DE405/LE405 result from a least-squares adjustment of a previously existing ephemeris to a variety of observational data (measurements), followed by a numerical integration of the dynamical equations of motion which describe the gravitational physics of the solar system. These fundamental ephemerides are the bases for computing the planetary and lunar positions and other related phenomena that are listed in the almanac.

For the final (integration) phase of the ephemeris creation process, there are three main ingredients, each of which constitutes a major phase itself:

- the equations of motion describing the gravitational physics which govern the dynamical motions of the bodies,
- a method for integrating the equations of motion, and
- the initial conditions and dynamical constants; i.e., the starting positions and velocities of the bodies at some initial epoch along with the values for various constants which affect the motion (e.g., planetary masses).

It is mainly the accuracy of the third component, the initial conditions and dynamical constants, which determines the accuracy of modern-day ephemerides, since the other two components (the physics and the integration method) are both believed to be sufficiently complete and accurate. The values of the initial conditions and constants are determined by the least-squares adjustment of them to the observational data (measurements), and the accuracy of this adjustment, and thus of the ephemerides themselves, depends primarily upon the distribution, variety, and accuracy of the observational data. This crucial part of the ephemeris creation process is given in § 8.5.

It is assumed that the equations of motion accurately describe the basic physics which govern the motion of the major bodies of the solar system - at least to the presently observable accuracy. For the motion of the Moon, the fitting of the lunar ephemeris to the lunar laser ranging observations is used to estimate the constants involved and to help distinguish various models of the lunar interior, Earth-raised tides, etc. The equations of motion are given in § 8.3.

Numerical integration of the equations of motion is the only known method capable of computing fundamental ephemerides at an accuracy which is comparable to that of the modern-day observations; analytical theories have not been able to attain such high accuracy. The computer program which was used to integrate the equations of motion for DE405/LE405 has been demonstrated to be sufficiently accurate (Newhall, Standish, and Williams 1983).

The reference frame for the ephemerides is the International Celestial Reference Frame (ICRF: Ma et al. 1998). The advantages for using the frame are many; they are discussed in § 8.6.

The independent variable of the equations of motion, and, thus, of the fundamental ephemerides themselves, may be termed, "T_{eph}". It is a fully rigorous relativistic coordinate time, implicitly defined by the equations of motion themselves. T_{eph} may be considered *similar* to previously-defined "ET" or to "TDB", since their average rates are the same, even though there are basic differences in the definitions. The time recently defined by the IAU, "TCB", is mathematically equivalent to T_{eph}; TCB and T_{eph} differ by only a constant rate. (For a discussion, see Standish (1998)).

This chapter describes the previous ephemerides used in *The Astronomical Almanac* (§ 8.2); presents the equations of motion used in computing the present ephemeris, DE405 (§ 8.3); gives some detail about the numerical integration program (§ 8.4); describes the observational data to which DE405 was adjusted (§ 8.5); discusses the reference frame of the ephemerides (§ 8.6); gives some of the formulae used in reducing the observational data (§ 8.7); presents the values of the initial conditions and constants of DE405 (§ 8.8); estimates the accuracy of the ephemerides (§ 8.9); gives sets of Keplerian elements useful for producing approximate planetary coordinates (§ 8.10); and shows the sources where DE405/LE405 may be found on CDrom and over the internet (§ 8.11).

8.2 Previous Ephemerides Used in *The Astronomical Almanac*

8.2.1 Ephemerides Prior to 1984

Before 1984, the ephemerides for the Sun, Mercury, Venus, and Mars were based on the theories and tables of Newcomb (1898a,b,c,d). Computerized evaluations of the tables were used from 1960 through 1980. From 1981 to 1983, the ephemerides were based on the evaluations of the theories themselves. The ephemerides of the Sun were derived from the algorithm given by S. Newcomb in *Tables of the Sun* (Newcomb 1898d). Newcomb's theories of the inner planets (1895–1898) served as the basis for the heliocentric ephemerides of Mercury, Venus, and Mars. In the case of Mars, the corrections derived by F.E. Ross (1917) were applied.

Ephemerides of the outer planets, Jupiter, Saturn, Uranus, Neptune, and Pluto, were computed from the heliocentric rectangular coordinates obtained by numerical integration (Eckert, Brouwer, and Clemence 1951). Although perturbations by the inner planets (Clemence 1954) were included in the printed geocentric ephemerides of the outer planets, they were omitted from the printed heliocentric ephemerides and orbital elements.

The lunar ephemeris, designated by the serial number $j = 2$, was calculated directly from E.W. Brown's algorithm instead of from his *Tables of Motion of the Moon* (1919). This was specified in the *Improved Lunar Ephemeris* (Eckert, Jones, and Clark 1954).

To obtain a strictly gravitational ephemeris expressed in the measure of time defined by Newcomb's *Tables of the Sun*, the fundamental arguments of Brown's tables were amended by removing the empirical term and by applying to the Moon's mean longitude the correction, $-8.''72 - 26.''74\ T - 11.''22\ T^2$, where T is measured in Julian centuries from 1900 January 0.5 (JED 2415020.0. In addition, this ephemeris was based on the IAU (1964) System of Astronomical Constants, and was further improved in its precision by transformation corrections (Eckert, Walker, and Eckert 1966, Eckert, Van Flandern, and Wilkins 1969). The expressions for the mean longitude of the Moon and its perigee were adjusted to remove the implicit partial correction for aberration (Clemence, Porter, and Sadler 1952).

8.2.2 Ephemerides from 1984 through 2002

During the years 1984–2003, the JPL ephemerides, DE200/LE200, were the bases of the ephemerides in *The Astronomical Almanac*. The equations of motion were essentially those used in JPL's DE102 (Newhall, Standish, and William 1983); they are also described in the previous *Explanatory Supplement* (Standish et al. 1992). The observations to which these ephemerides were fit is documented in Standish (1990). The reference frame of DE200 is the mean equator and dynamical equinox of J2000.0, as determined and described in Standish (1982).

8.2.3 Ephemerides Starting in 2003

Starting in 2003, the fundamental planetary and lunar ephemerides of *The Astronomical Almanac* are DE405/LE405, referenced, as noted above, to the International Celestial Reference Frame (ICRF). The remainder of this chapter describes the creation of DE405.

8.3 Equations of Motion

Equations of motion describe the forces upon the planets, Sun and Moon which affect their motions and the torques upon the Moon which affect its orientation. It is believed that the equations described here are correct and complete to the level of accuracy of the observational data. I.e., given the accuracy of the observations, there is nothing to suggest that other forces or different forces are present in the solar system. The uncertainties existing in the planets' and Moon's motions are certainly explainable, considering the uncertainties in the observations and in the fitted initial conditions and dynamical constants.

The major elements of this section were developed at JPL over the past few decades. Just the formulae are given here; also included are references to their descriptions, previously published by those responsible for their development.

The equations of motion used for the creation of DE405/LE405 included contributions from: (a) point-mass interactions among the Moon, planets, and Sun; (b) general relativity (isotropic, parametrized post-Newtonian); (c) Newtonian perturbations of selected asteroids; (d) action upon the figure of the Earth from the Moon and Sun; (e) action upon the figure of the Moon from the Earth and Sun; (f) physical libration of the Moon, modeled as a solid body with tidal and rotational distortion, including both elastic and dissipational effects, (g) the effect upon the Moon's motion caused by tides raised upon the Earth by the Moon and Sun, and (h) the perturbations of 300 asteroids upon the motions of Mars, the Earth, and the Moon.

8.3.1 Point-Mass Interactions

The principal gravitational force on the nine planets, the Sun, and the Moon is modeled by considering those bodies to be point masses in the isotropic, parametrized post-Newtonian (PPN) n-body metric (Will 1974). The n-body equations were derived by Estabrook (1971b) from the variation of a time-independent Lagrangian action integral formulated in a non-rotating solar-system-barycentric Cartesian coordinate frame. Also included are Newtonian gravitational perturbations from 300 asteroids, chosen because they have the most pronounced effect on the Earth–Mars range over the time span covered by the accurate spacecraft ranging observations.

For each body i, the point-mass acceleration is given by

$$\begin{aligned}\ddot{\mathbf{r}}_{i_{\text{point mass}}} = \sum_{j\neq i} \frac{\mu_j(\mathbf{r}_j-\mathbf{r}_i)}{r_{ij}^3}\Bigg\{1 &- \frac{2(\beta+\gamma)}{c^2}\sum_{k\neq i}\frac{\mu_k}{r_{ik}} - \frac{2\beta-1}{c^2}\sum_{k\neq j}\frac{\mu_k}{r_{jk}} \\ &+ \gamma\left(\frac{v_i}{c}\right)^2 + (1+\gamma)\left(\frac{v_j}{c}\right)^2 - \frac{2(1+\gamma)}{c^2}\dot{\mathbf{r}}_i\cdot\dot{\mathbf{r}}_j \\ &- \frac{3}{2c^2}\left[\frac{(\mathbf{r}_i-\mathbf{r}_j)\cdot\dot{\mathbf{r}}_j}{r_{ij}}\right]^2 + \frac{1}{2c^2}(\mathbf{r}_j-\mathbf{r}_i)\cdot\ddot{\mathbf{r}}_j\Bigg\} \\ &+ \frac{1}{c^2}\sum_{j\neq i}\frac{\mu_j}{r_{ij}^3}\{[\mathbf{r}_i-\mathbf{r}_j]\cdot[(2+2\gamma)\dot{\mathbf{r}}_i-(1+2\gamma)\dot{\mathbf{r}}_j]\}(\dot{\mathbf{r}}_i-\dot{\mathbf{r}}_j) \\ &+ \frac{(3+4\gamma)}{2c^2}\sum_{j\neq i}\frac{\mu_j\ddot{\mathbf{r}}_j}{r_{ij}} + \sum_{m=1}^{3}\frac{\mu_m(\mathbf{r}_m-\mathbf{r}_i)}{r_{im}^3} + \sum_{c,s,m}\mathbf{F}\end{aligned} \tag{8.1}$$

where $\mathbf{r}_i$, $\dot{\mathbf{r}}_i$, and $\ddot{\mathbf{r}}_i$ are the solar-system-barycentric position, velocity, and acceleration vectors of body i;$\mu_j = Gm_j$, where G is the gravitational constant and m_j is the mass of body j; $r_{ij} = |\mathbf{r}_j - \mathbf{r}_i|$; β is the PPN parameter measuring the nonlinearity in superposition of gravity; γ is the PPN parameter measuring space curvature produced by unit rest mass (in this integration, as in general relativity, $\beta = \gamma = 1$); $v_i = |\dot{\mathbf{r}}_i|$; and c is the velocity of light.

The quantity $\ddot{\mathbf{r}}_j$ appearing in two terms on the right-hand side of Eq. 8.1 denotes the barycentric acceleration of each body j due to Newtonian effects of the remaining bodies and the asteroids. Thus, the right-hand side of the equation is dependent upon the left-hand side, and so, rigorously, the computation should be iterated. However, use of Newtonian accelerations for these terms is sufficiently accurate.

In the next-to-last term on the right-hand side of Eq. 8.1, quantities employing the index m refer to the "Big 3" asteroids, Ceres, Pallas, and Vesta. The last term represents forces upon the Earth, Moon, and Mars, only, from 297 other asteroids, grouped according to three taxonomic classes (C, S, M). The asteroid forces were computed in the following way:

- The orbits of the Big 3 asteroids were integrated under the forces of themselves, the nine planets, the Sun, and the Moon, using initial conditions from the *dastcom* file maintained by JPL's Solar System Dynamics Group. These orbits were fit with Chebychev polynomials and used in the succeeding integration of the 297 non-Big 3

asteroids. For the eventual integration of DE405, periodic mean orbits were used for the Big 3 asteroids which had been fit to their integrated orbits.

- The 297 individual orbits were integrated under the gravitational forces of the Sun, planets, and the Big 3 asteroids. At each step, the force vectors of these non-Big 3 asteroids upon the Earth, Moon and Mars were computed, summed, and stored in 3 temporary files, one for the sums of the 218 C-class asteroids, one for the sums of the 58 S-type asteroids, and one for the sums of the 21 M-type asteroids. Also stored in the same temporary files were the contributions from these non-Big 3 asteroids to the solar system's center of mass. The vectors from these temporary files were fit with Chebychev polynomials and stored in a final file to be used in the main planetary and lunar integration.
- The radii, masses, and taxonomic classes of the 297 asteroids used in DE405/LE405 are listed in § 8.8.

8.3.2 Solar System Barycenter

In the n-body metric, all dynamical quantities are expressed with respect to a center of mass whose definition is modified from the usual Newtonian formulation. The solar system barycenter is given by Estabrook (1971a) as

$$\sum_i \mu_i^* \mathbf{r}_i = 0 \tag{8.2}$$

where

$$\mu_i^* = \mu_i \left\{ 1 + \frac{1}{2c^2} v_i^2 - \frac{1}{2c^2} \sum_{j \neq i} \frac{\mu_j}{r_{ij}} \right\}$$

and where μ_i is the gravitational constant times the mass of the i^{th} body; v_i is the barycentric speed of the i^{th} body.

During the process of numerical integration the equations of motion for only the Moon and planets were actually evaluated and integrated. The barycentric position and velocity of the Sun were obtained from the equations of the barycenter. It should be noted that each of the two barycenter equations depends upon the other, requiring an iteration during the evaluation of the solar position and velocity.

8.3.3 Figure Effects

Long-term accuracy of the integrated lunar orbit requires the inclusion of the figures of the Earth, Moon, and Sun in the mathematical model. In DE405 the gravitational effects due to figures include:

1. The force of attraction between the zonal harmonics (through fourth degree) of the Earth and the point-mass Moon, Sun, Venus, and Jupiter;
2. the force of attraction between the zonal harmonics (through fourth degree) and the second- through fourth-degree tesseral harmonics of the Moon and the point-mass Earth, Sun, Venus, and Jupiter;

3. The dynamical form-factor of the Sun (J_2).

The contribution to the inertial acceleration of an extended body arising from the interaction of its own figure with an external point mass is expressed in the $\xi\eta\zeta$ coordinate system, where the ξ-axis is directed outward from the extended body to the point mass; the $\xi\zeta$-plane contains the figure (rotational) pole of the extended body, and the η-axis completes the right-handed system.

In that system (see, e.g., Moyer 1971),

$$\begin{bmatrix} \ddot{\xi} \\ \ddot{\eta} \\ \ddot{\zeta} \end{bmatrix} = -\frac{\mu}{r^2}\left\{ \sum_{n=2}^{n_1} J_n \left(\frac{\mathcal{R}}{r}\right)^n \begin{bmatrix} (n+1)\,P_n(\sin\phi) \\ 0 \\ -\cos\phi\, P_n'(\sin\phi) \end{bmatrix} \right. \tag{8.3}$$

$$\left. + \sum_{n=2}^{n_2} \left(\frac{\mathcal{R}}{r}\right)^n \sum_{m=1}^{n} \begin{bmatrix} -(n+1)\;P_n^m(\sin\phi)\;[+C_{nm}\cos m\lambda + S_{nm}\sin m\lambda] \\ m\sec\phi\;P_n^m(\sin\phi)\;[-C_{nm}\sin m\lambda + S_{nm}\cos m\lambda] \\ \cos\phi\;P_n^{m\prime}(\sin\phi)\;[+C_{nm}\cos m\lambda + S_{nm}\sin m\lambda] \end{bmatrix} \right\}$$

where μ is the gravitational constant G times the mass of the point body; r is the center-of-mass separation between the two bodies; n_1, and n_2 are the maximum degrees of the zonal and tesseral expansions, respectively; $P_n(\sin\phi)$ is the Legendre polynomial of degree n; $P_n^m(\sin\phi)$ is the associated Legendre function of degree n and order m; J_n is the zonal harmonic for the extended body; C_{nm}, S_{nm} are the tesseral harmonics for the extended body; $\mathcal{R}$ is the equatorial radius of the extended body; ϕ is the latitude of the point mass relative to the body-fixed coordinate system in which the harmonics are expressed; and λ is the east longitude of the point mass in the same body-fixed coordinate system.

The primes denote differentiation with respect to the argument $\sin\phi$. The accelerations are transformed into the solar-system-barycentric Cartesian system by application of the appropriate rotation matrix.

The interaction between the figure of an extended body and a point mass also induces an inertial acceleration of the point mass. If $\ddot{\mathbf{r}}_{fig}$ denotes the acceleration given in Eq. 8.3 when expressed in solar-system-barycentric coordinates, then the corresponding acceleration of the point mass, $\ddot{\mathbf{r}}_{pm}$, is

$$\ddot{\mathbf{r}}_{pm} = -\frac{m_{fig}}{m_{pm}}\ddot{\mathbf{r}}_{fig} \tag{8.4}$$

where m_{fig} and m_{pm} are the masses of the extended body and point mass, respectively.

The orientation of the Earth includes precession, obliquity change (Lieske et al. 1977), and 18.6-year nutation. The correction for precession, $d\Phi_Y/dt$, was set to -0.″1193/cy ($\Delta p = -0.''3$/cy), and the obliquity rate correction, -$d\Phi_X/dt$, was taken from (Williams 1994). In addition, offsets to the Earth's orientation at J2000.0, Φ_X and Φ_Y, were determined through the strength of the lunar laser ranging data. The values for all four parameters are given in Table 8.4.

8.3.4 Lunar Gravity Coefficients

For the Moon, the 2nd degree gravity field is time-varying, and the harmonic gravity coefficients are computed from the moment-of-inertia tensor, where the time dependence has been accounted for. For near principal axis alignment, the 1st order relations for the coefficients

are given by

$$\begin{aligned} J_2^m(t) &= \frac{I_{33}(t) - \frac{1}{2}[I_{11}(t) + I_{22}(t)]}{m\mathcal{R}^2} \\ C_{22}^m(t) &= \frac{I_{22}(t) - I_{11}(t)}{4m\mathcal{R}^2} \\ C_{21}(t) &= -I_{13}(t)/m\mathcal{R}^2 \\ S_{21}(t) &= -I_{32}(t)/m\mathcal{R}^2 \\ S_{22}(t) &= -I_{21}(t)/2m\mathcal{R}^2 \end{aligned} \tag{8.5}$$

where the I_{ij} are the components of the moment-of-inertia tensor, to be described later; m is the lunar mass and $\mathcal{R}$, the lunar radius.

8.3.5 Lunar Physical Libration: Coordinates

The orientation of the Moon is given by a set of Euler angles, ϕ, θ, and ψ, which relate the Moon-centered, rotating lunar system to the reference frame of the ephemerides (nominally, the ICRF). The elastic Moon is distorted by tides and rotation, but the mean principal axes are well-defined. This Moon-centered mean-principal-axis frame is here called the selenographic frame. The angles are ϕ, the angle from the x-axis of the ephemeris reference frame along the xy-plane to the intersection of the lunar equator; θ, the inclination of the lunar equator upon the xy-plane; and ψ, the longitude from that intersection along the lunar equator to the prime meridian.

Instead of integrating the second derivatives of the Euler angles, their first derivatives are expressed in terms of the selenocentric, body-fixed angular velocity vector, $\boldsymbol{\omega}$:

$$\begin{aligned} \dot{\phi} &= (\omega_x \sin\psi + \omega_y \cos\psi)/\sin\theta \\ \dot{\theta} &= \omega_x \cos\psi - \omega_y \sin\psi \\ \dot{\psi} &= \omega_z - \dot{\phi}\cos\theta. \end{aligned} \tag{8.6}$$

The first derivatives of the Euler angles and the first derivatives of $\boldsymbol{\omega}$ are integrated, as seen in the following subsection.

8.3.6 Physical Libration Differential Equations

The moment of inertia tensor, $\mathbf{I}$, has a rigid-body contribution plus two variable contributions due to tidal and rotational distortions. The distortions are functions of the lunar position and rotational velocities, computed at time, $t - \tau_m$, where τ_m is a time-lag of about 4 hours in DE405, as determined from the fits to the lunar laser ranging data. The time delay allows for dissipation when flexing the Moon (Williams et al. 2001).

The angular momentum vector can be expressed in inertial or body-fixed coordinates; it is the product of the moment of inertia tensor (given in § 8.3.7) and the angular velocity vector: $\mathbf{L} = \mathbf{I}\,\boldsymbol{\omega}$. The time derivative of the angular momentum vector is equal to the torque. In an inertial coordinate system: $\mathbf{N} = d\mathbf{L}/dt$, but in a rotating system,

$$\mathbf{N} = \frac{d}{dt}(\mathbf{I}\,\boldsymbol{\omega}) + \boldsymbol{\omega} \times \mathbf{I}\,\boldsymbol{\omega} \tag{8.7}$$

where the second term on the right side puts the time derivative into the body-fixed system.

The complete equation of motion for the lunar librations is then given by

$$\dot{\boldsymbol{\omega}} = \mathbf{I}^{-1}\{\Sigma_i \mathbf{N}_{fig-pm} + \mathbf{N}_{fig-fig} - \dot{\mathbf{I}}\,\boldsymbol{\omega} - \boldsymbol{\omega} \times \mathbf{I}\,\boldsymbol{\omega}\} \tag{8.8}$$

where the torques have been separated into the sums of the torques upon the lunar figure from external point masses, i, and from the Earth's extended figure. These are discussed later in the section.

8.3.7 The Moment of Inertia Tensor

The three parts of the moment of inertia tensor represent the rigid body, the tidal distortion, and the spin distortion, where the latter two include both elasticity and dissipation. The body-fixed selenographic reference frame uses the rigid body principal axes. In this frame, the tensor is

$$\begin{aligned}\mathbf{I} = &\begin{bmatrix} A & 0 & 0 \\ 0 & B & 0 \\ 0 & 0 & C \end{bmatrix} \\ &- \frac{k_{2m} m_e R_m^5}{r^5} \begin{bmatrix} x^2 - \frac{1}{3}r^2 & xy & xz \\ xy & y^2 - \frac{1}{3}r^2 & yz \\ xz & yz & z^2 - \frac{1}{3}r^2 \end{bmatrix} \\ &+ \frac{k_{2m} R_m^5}{3G} \begin{bmatrix} \omega_x^2 - \frac{1}{3}(\omega^2 - n^2) & \omega_x\omega_y & \omega_x\omega_z \\ \omega_x\omega_y & \omega_y^2 - \frac{1}{3}(\omega^2 - n^2) & \omega_y\omega_z \\ \omega_x\omega_z & \omega_y\omega_z & \omega_z^2 - \frac{1}{3}(\omega^2 + 2n^2) \end{bmatrix}\end{aligned} \tag{8.9}$$

where the coordinates and rotational velocities, $\mathbf{r}$ and $\boldsymbol{\omega}$, are evaluated at time $t - \tau_m$, and where k_{2m} is the lunar potential Love number; m_e is the mass of the Earth; R_m is the equatorial radius of the Moon; r is the Earth-Moon distance; x, y, z are the components of the Earth-Moon vector aligned with the rigid body principal axes; ω_x, ω_y, ω_z are the components of $\boldsymbol{\omega}$ in the selenographic system; and n is the average lunar mean motion.

8.3.8 Time Derivative of the Inertia Tensor

$$\begin{aligned}\dot{\mathbf{I}} = &\frac{5k_{2m} m_e R_m^5 \mathbf{r}\cdot\dot{\mathbf{r}}}{r^7} \begin{bmatrix} x^2 - \frac{1}{3}r^2 & xy & xz \\ xy & y^2 - \frac{1}{3}r^2 & yz \\ xz & yz & z^2 - \frac{1}{3}r^2 \end{bmatrix} \\ &- \frac{k_{2m} m_e R_m^5}{r^5} \begin{bmatrix} 2(x\dot{x} - \frac{1}{3}\mathbf{r}\cdot\dot{\mathbf{r}}) & x\dot{y} + \dot{x}y & x\dot{z} + \dot{x}z \\ x\dot{y} + \dot{x}y & 2(y\dot{y} - \frac{1}{3}\mathbf{r}\cdot\dot{\mathbf{r}}) & y\dot{z} + \dot{y}z \\ x\dot{z} + \dot{x}z & y\dot{z} + \dot{y}z & 2(z\dot{z} - \frac{1}{3}\mathbf{r}\cdot\dot{\mathbf{r}}) \end{bmatrix} \\ &+ \frac{k_{2m} R_m^5}{3\,G} \begin{bmatrix} 2(\omega_x\dot{\omega}_x - \frac{1}{3}\boldsymbol{\omega}\cdot\dot{\boldsymbol{\omega}}) & \omega_x\dot{\omega}_y + \dot{\omega}_x\omega_y & \omega_x\dot{\omega}_z + \dot{\omega}_x\omega_z \\ \omega_x\dot{\omega}_y + \dot{\omega}_x\omega_y & 2(\omega_y\dot{\omega}_y - \frac{1}{3}\boldsymbol{\omega}\cdot\dot{\boldsymbol{\omega}}) & \omega_y\dot{\omega}_z + \dot{\omega}_y\omega_z \\ \omega_x\dot{\omega}_z + \dot{\omega}_x\omega_z & \omega_y\dot{\omega}_z + \dot{\omega}_y\omega_z & 2(\omega_z\dot{\omega}_z - \frac{1}{3}\boldsymbol{\omega}\cdot\dot{\boldsymbol{\omega}}) \end{bmatrix}\end{aligned} \tag{8.10}$$

8.3.9 Principal Moments

The rigid-body principal moments are A, B, and C, with the C axis aligned toward the pole.

$$\begin{aligned} A &= \frac{2(1-\beta_L\gamma_L)}{(2\beta_L-\gamma_L+\beta_L\gamma_L)} M_m \mathcal{R}_m^2 J_2^{\text{rigid}} \\ B &= \frac{2(1+\gamma_L)}{(2\beta_L-\gamma_L+\beta_L\gamma_L)} M_m \mathcal{R}_m^2 J_2^{\text{rigid}} \\ C &= \frac{2(1+\beta_L)}{(2\beta_L-\gamma_L+\beta_L\gamma_L)} M_m \mathcal{R}_m^2 J_2^{\text{rigid}} \end{aligned} \tag{8.11}$$

where β_L and γ_L are defined by the relations, $\beta_L = (C-A)/B$ and $\gamma_L = (B-A)/C$; a_m is the semimajor axis of the lunar orbit; and $J_2^{\text{rigid}} = J_2^{\text{input}} + k_{2m}\frac{M_e}{M_m}\left(\frac{\mathcal{R}_m}{a_m}\right)^3$. Note that J_2^{input} does not have physical significance. The quantities, J_2^{input}, β_L, γ_L, μ_m, the 3^{rd} degree harmonics, k_{2m}, and τ_m are quantities which are solved for in the least-squares data fits and then input into the integration program; $\mathcal{R}_m$ and the 4^{th} degree harmonics are input, but not solved for; A, B, C, and J_2^{rigid} are derived from the preceding relations. For further discussion, see Newhall and Williams (1997).

8.3.10 Figure–Point Mass Torques upon the Moon

From a single point-mass (body) acting upon the figure of the Moon, the lunar torque is given by

$$\mathbf{N}_{fig-pm} = M_m \mathbf{r}_{pm} \times \ddot{\mathbf{r}}_{fig} \tag{8.12}$$

where $\mathbf{r}_{pm}$ is the selenocentric position of the point mass and $\ddot{\mathbf{r}}_{fig}$ is the inertial acceleration due to the point-mass. Torques are computed for the figure of the Moon interacting with the Earth, Sun, Venus, and Jupiter.

8.3.11 Figure–Figure Torque upon the Moon

Yoder (1979) and Eckhardt (1981) showed that figure–figure torques are important for the Moon. Three significant terms of the torque upon the figure of the Moon from the Earth's figure (J_{2e}) are

$$\begin{aligned} \mathbf{N}_{fig-fig} = \frac{15\,\mu_e \mathcal{R}_e^2 J_{2e}}{2\,r_e^5} \{\, &(1-7\sin^2\phi)[\hat{\mathbf{r}}_\mathbf{e} \times \mathbf{I}\hat{\mathbf{r}}_\mathbf{e}] \\ &+ 2\sin\phi\,[\hat{\mathbf{r}}_\mathbf{e} \times \mathbf{I}\hat{\mathbf{P}}_\mathbf{e} + \hat{\mathbf{P}}_\mathbf{e} \times \mathbf{I}\hat{\mathbf{r}}_\mathbf{e}] \\ &- \frac{2}{5}[\hat{\mathbf{P}}_\mathbf{e} \times \mathbf{I}\hat{\mathbf{P}}_\mathbf{e}]\,\} \end{aligned} \tag{8.13}$$

where $\hat{\mathbf{P}}_\mathbf{e}$ is the direction vector of the Earth's pole and $\hat{\mathbf{r}}_\mathbf{e}$ is the direction vector of the Earth from the Moon, both expressed in the selenographic reference frame; $\mathbf{I}$ is the lunar moment of inertia tensor; $\mathcal{R}_e$ is the equatorial radius of the Earth in au's; and for this equation, ϕ is defined by $\sin\phi = \hat{\mathbf{r}}_\mathbf{e} \cdot \hat{\mathbf{P}}_\mathbf{e}$. Figure–figure acceleration of the lunar orbit is not considered.

8.3.12 Acceleration of the Moon from Earth Tides

The tides raised upon the Earth by the Sun and Moon affect, in turn, the motion of the Moon. For this, let

G = gravitational constant

for the distorted body (in this case, the Earth),

M = mass
R = radius
$\dot{\theta}$ = sidereal rotation rate
k_{2j} = frequency dependent Love numbers ($j = 0, 1, 2 \Rightarrow$ slow zonal, diurnal, semidiurnal tides)
τ_j = frequency dependent time delays ($j = 0, 1, 2 \Rightarrow$ slow zonal, diurnal, semidiurnal tidal dissipation)

for the perturbed body (in this case, the Moon),

m = mass
$\mathbf{r}$ = position (centered on mass M)

for the tide-raising body (in this case, the Moon and Sun),

m' = mass
$\mathbf{r}'$ = position (centered on mass M)

For each frequency band, back-date the position of the tide-raising body by the time-delay, τ_j, and rotate that vector, about the distorted body's rotational pole, through the lag angle, $\dot{\theta}\tau_j$, giving

$$\mathbf{r}_j^* = \mathcal{R}_3(\dot{\theta}\tau_j)\mathbf{r}'(t - \tau_j). \tag{8.14}$$

For the acceleration of the perturbed body with respect to the distorted body (Moon with respect to Earth), break $\mathbf{r}$ and $\mathbf{r}^*$ into equatorial and polar components (with respect to the distorted body): $\mathbf{r} = \boldsymbol{\rho} + \mathbf{z}$ and $\mathbf{r}^* = \boldsymbol{\rho}^* + \mathbf{z}^*$.

$$\begin{aligned}\ddot{\mathbf{r}}(\text{tide}) = \frac{3}{2}\frac{Gm'(1+\frac{m}{M})\mathcal{R}^5}{r^5}\Bigg\{ &\frac{k_{20}}{r_0^{*5}}\left([2z_0^{*2}\mathbf{z} + \rho_0^{*2}\boldsymbol{\rho}] - \frac{5[(zz_0^*)^2 + \frac{1}{2}(\rho\rho_0^*)^2]\mathbf{r}}{r^2} + r_0^{*2}\mathbf{r}\right) \\ &+ \frac{k_{21}}{r_1^{*5}}\left(2[(\boldsymbol{\rho}\cdot\boldsymbol{\rho}_1^*)\mathbf{z}_1^* + zz_1^*\boldsymbol{\rho}_1^*] - \frac{10zz_1^*(\boldsymbol{\rho}\cdot\boldsymbol{\rho}_1^*)\mathbf{r}}{r^2}\right) \\ &+ \frac{k_{22}}{r_2^{*5}}\left([2(\boldsymbol{\rho}\cdot\boldsymbol{\rho}_2^*)\boldsymbol{\rho}_2^* - \rho_2^{*2}\boldsymbol{\rho}] - \frac{5[(\boldsymbol{\rho}\cdot\boldsymbol{\rho}_2^*)^2 - \frac{1}{2}(\rho\rho_2^*)^2]\mathbf{r}}{r^2}\right)\Bigg\}\end{aligned} \tag{8.15}$$

Note that $\rho\rho_i^* = |\rho||\rho_i^*|$; it is *not* $\rho \cdot \rho_i^*$. The acceleration from both Sun- and Moon-raised tides is computed. Tides raised on the Earth by the Moon do not influence the mutual barycentric motion, and the effect of Sun-raised tides on the barycentric motion is not considered. The tidal acceleration due to tidal dissipation is implicit in the above acceleration. The explicit conversion of the three Love numbers and time delays to tidal $\dot{n}$ requires a separate theory.

8.4 The Numerical Integration of DE405/LE405

The numerical integration of Eqs. 8.1, 8.6, and 8.8 was carried out using a variable-step-size, variable-order Adams method (Krogh 1972). The actual order of the 33 equations at any instant is determined by a specified error bound and by the behavior of backward differences of accelerations.

It has proved numerically more suitable to integrate the lunar ephemeris relative to the Earth rather than to the solar system barycenter. The solar-system-barycentric Earth and Moon states are replaced by the quantities $\mathbf{r_{em}}$ and $\mathbf{r_B}$, given by

$$\mathbf{r_{em}} = \mathbf{r_m} - \mathbf{r_e} \tag{8.16}$$

and

$$\mathbf{r_B} = \frac{\mu_e \mathbf{r_e} + \mu_m \mathbf{r_m}}{\mu_e + \mu_m} \tag{8.17}$$

where the subscripts e and m denote the Earth and Moon, respectively. Note that $\mathbf{r_{em}}$ is the difference of solar-system-barycentric vectors and is distinguished from a geocentric vector by the relativistic transformation from the barycenter to geocenter. (The vector $\mathbf{r_B}$ can be interpreted as representing the coordinates of the Newtonian Earth–Moon barycenter relative to the solar system barycenter. It has no physical significance and does not appear in force calculations; it is solely a vehicle for improving the numerical behavior of the differential equations.)

8.4.1 Estimated Integration Error

The method of error control used in the integration puts a limit on the absolute value of the estimated error in velocity of each equation at the end of every integration step. Step size and integration orders were adjusted on the basis of estimated error. The limits selected for DE405 were 2×10^{-17} au/day in each component of the equations of motion for the planets and Moon, and 2×10^{-15} rad d^{-1} for each component of the libration equations.

Integrations prior to DE405 were performed on a Univac mainframe computer in double precision, with a 60-bit mantissa; DE405 was integrated on a VAX Alpha in quadruple precision. In all cases, the integration error has been significantly less than the estimated error resulting from the uncertainties in the adjustment of the initial conditions and constants to the observational data. These latter errors are discussed later in § 8.9.

8.4.2 Adopted Constants

The integration requires the input of numerical values for a number of parameters. Some of these parameters, such as the initial positions and velocities of the planets and Moon, result from the least-squares fits and are different in each fit. Other parameters, such as some of the masses and the Earth's zonal harmonics, come from outside sources and are only rarely changed for these present purposes. Some parameters, such as the mass of the Earth–Moon system, can be derived from the data, but for convenience are changed only when statistically significant improvements can be made over the standard values. The lists of initial conditions and constants are given in § 8.8.

The list of the initial conditions and dynamical constants used in the integration of the equations of motion used for the creation of DE405 is given in § 8.8. Also given in § 8.8 is a list of constants used in the reduction of the observational data which were determined in the least-squares solution.

8.5 Observational Data Fit by the Planetary and Lunar Ephemerides

In creating modern ephemerides, the majority of the effort is directed toward the set of observational data (measurements) to which the ephemerides are fit and to the fitting process itself. This section describes the observational data used in the creation of DE405/LE405. These observational data and their references are available over the internet at URL[1].

Table 8.1 presents the different types of observational data fit by DE405, along with the time-span, the bodies observed, the coordinates measured, the inherent accuracy, and the number of observations. These different sets of observations are discussed briefly here, with some of the unique features of their reductions presented in § 8.7. References to the data can be found at URL[1].

8.5.1 Optical Data

Classical ephemerides over the past centuries have been based entirely upon optical observations: almost exclusively, meridian circle transit timings. With the advent of planetary radar, spacecraft missions, VLBI, etc., the situation for the four inner planets has changed dramatically.

All of the optical observations for the Sun, Mercury, Venus, and Mars were omitted from the least-squares adjustment leading to DE405. The newer and more accurate data types determine these orbits far more accurately (by orders of magnitude) than do the optical data. Since relatively large systematic errors are known to remain in the optical observations, even after the many corrections described in Standish (1990), and since at that time there was a large uncertainty connected with the frame-tie between the FK5 and ICRF reference frames, inclusion of the optical observations for the inner planets could have been detrimental for their ephemerides. Thus, the initial conditions for the inner four planets were adjusted to ranging data primarily, with the VLBI observations serving to orient the whole inner planetary system onto the ICRF.

For Jupiter, the initial conditions were fit to a number of different types of observations, not all of which seemed to be fully consistent with each other. Since that time, however, subsequent analyses of the Jupiter ephemeris, using more recent measurements from the Galileo spacecraft, indicate that the errors are no larger than about 150 km ($0.''05$).

For the outermost four planets, the optical observations are effectively the only observations and are expected to remain so for a number of years.

8.5.2 Meridian Transits

Transit observations are differential in nature—the planetary observations undergo the same processing as those of the observed stars, both being related to the standard catalog of the

epoch. The observations are published as geocentric apparent right ascensions and declinations, taken at the time of meridian passage. For comparison, then, one obtains a computed position from the ephemerides by iterating to find the time at which the local apparent hour angle of the planet is zero. The formulation for computing apparent places is essentially identical to that described in Chapter 7.

8.5.3 Photographic and CCD Astrometry

Photographic and CCD astrometric observations are handled in the same way. The observations based upon the 1950 reference frame (those of Pluto) were transformed onto the J2000.0 frame using the precession and equinox corrections of Fricke (1971, 1982). Those based upon the (J2000.0) FK5 were then transformed onto the ICRF using preliminary corrections supplied by Morrison (1996).

8.5.4 Occultation Timings

The timings were supplied in *normal point* form — corrections to the specific ephemeris used in the reductions. The reductions were made by those modeling the Uranian rings and the Neptunian disk and transmitted to the author by Nicholson (1992).

8.5.5 Astrolabe

Astrolabe observations are effectively timings of an object when its apparent altitude above the horizon attains a certain pre-determined value. These observations are described in Debarbat and Guinot (1970).

8.5.6 Radiometric Emission Measurements

The radiometric emission from the Jovian and Saturnian satellites and from the disks of Uranus and Neptune were measured differentially against the then-existing radio reference catalogue, a precursor to the IERS (International Earth Rotation and Reference system Service) Radio Catalogue, which is itself the precursor of the ICRF. The observations were taken at the Very Large Array (VLA) in Soccoro, New Mexico by Muhleman et al. (1985), Muhleman, Berge, and Rudy (1986) Muhleman, Berge, and Jones (1988) and by Berge, Muhleman, and Linfield (1988). They are presented in *normal point* form — corrections to the specific ephemeris used in the reductions.

8.5.7 Ranging Data

A *range* measurement is the actual round-trip time of the electromagnetic signal from when it leaves the transmitter until the time it arrives at the receiver. The signal is returned from a spacecraft transponder or from a planet, having bounced off of a spot on the surface where the normal to the surface points toward the Earth. The timing is done at the antennae by atomic clocks in what may be considered UTC.

The ranging observations reflected from the surface of Mercury, Venus, or Mars, are accurate to a level of about 100 meters. However, for ephemeris purposes, variations in the topography of a planet's surface introduce a noise-like uncertainty. This enters directly into the process of deducing the distance from the spot on the surface to the center of mass of the planet. Methods to reduce these uncertainties are described in § 8.7.

Table 8.1 Observational data fit by DE405. The columns contain the observatory/source, the time coverage, the bodies measured, the components measured, the *a priori* uncertainties of a measurement, the number of observations and the group totals.

Observatory	years	bodies	coords.	*a priori* sigmas	#	group totals
Optical Meridian Transits						
Washington	1911–1994	Sun, . . . , Nep	r.a., dec.	1.″0 / 0.″5	14242	
Herstmonceux	1957–1982	Sun, . . . , Nep	r.a., dec.	1.″0 / 0.″5	2851	17093
Photoelectric Meridian Transits						
La Palma	1984–1993	Mar, . . . , Plu	r.a., dec.	0.″25	6410	
Bordeaux	1985–1996	Sat, Ura, Nep	r.a., dec.	0.″25	854	
Tokyo	1986–1988	Mar, . . . , Nep	r.a., dec.	0.″5	498	
Flagstaff - USNO	1995	Plu	r.a., dec.	0.″1	20	7782
Photographic Astrometry of Pluto						
(Pre-disc)	1914–1927	Pluto	r.a., dec.	0.″5	28	
Lowell	1930–1951				620	
Yerkes-McD	1930–1953				310	
(Nrml pts.)	1930–1958				66	
MacDonald	1949–1953				56	
Yerkes	1962–1963				42	
Palomar	1963–1965				8	
Dyer	1964–1981				44	
Bordeaux	1967				24	
Asiago	1969–1978				350	
Torino	1973–1982				74	
Copenhagen	1975–1978				150	
Flagstaff	1980–1994				16	
Lick	1980–1985				56	
La Silla	1988–1989				58	1902
CCD Astrometry of Uranus, Neptune and Pluto						
Flagstaff - USNO	1995–1996	Ura, Nep	r.a., dec.	0.″20	313	
Flagstaff - USNO	1995–1996	Plu	r.a., dec.	0.″20	63	
Bordeaux	1995–1996	Plu	r.a., dec.	0.″20	13	389
Occultation Timings						
Uranus rings	1977–1983	Ura	r.a., dec.	0.″14	14	
Neptune disk	1968–1985	Nep	r.a., dec.	0.″27	18	32
Astrolabe						
Quito	1969	Sat	r.a., dec.	0.″3–1.″6	1	
Algiers	1969–1973	Mar,Sat			48	
San Fernando	1970–1978	Mar,Jup,Sat			338	
Besançon	1971–1973	Sat			44	
Paris	1971–1978	Mar,Sat			146	
OCA	1972–1981	Mar,Jup,Sat			202	
Santiago	1975–1985	Ura			284	1063

Table 8.1 *(continued)*

Observatory	years	bodies	coords.	*a priori* sigmas	#	group totals
Radar Ranging						
Arecibo	1967–1982	Mer,Ven	range	10 km	284	
Haystack	1966–1971	Mer,Ven		1.5	188	
Goldstone13	1964–1970	Ven		1.5	9	
Gldstn 13–14	1970–1977	Mer,Ven		1.5	23	
Goldstone14	1970–1993	Mer,Ven		1.5	376	880
Mars Radar–Ranging Closure Points						
Goldstone14	1971–1993	Mars	diff. range	1.5	65	65
Radio Astrometry of Thermal Emission						
VLA	1987	Jup, . . . , Nep	r.a., dec.	0.″03–0.″1	10	10
Spacecraft Measurements						
Mariner 9	1971–1972	Mars	range	35–120 m	629	
Pioneer 10	1973	Jupiter	range	3 km	1	
Pioneer 11	1974			12 km	1	
Viking Lander	1976–1980	Mars	range	7 m	1018	
	1980–1981			12 m	264	
Voyager 1 OD	1979	Jupiter	r.a., dec.	0.″01, 0.″05	2	
			range	3 km	1	
Voyager 2 OD	1979		range	3 km	1	
Phobos OD	1989	Mars	range	0.5 km	1	
Phobos VLBI	1989	Mars	r.a., dec.	0.″01–0.″1	2	
Ulysses VLBI & OD	1992	Jupiter	r.a., dec.	0.″003, 0.″006	2	
			range	3 km	1	
Magellan VLBI	1990–1994	Venus	r.a., dec.	0.″003–0.″01	18	
Galileo OD	1995	Jupiter	r.a., dec.	0.″05, 0.″2	2	
			range	20 km	1	1956
Frame-Tie Determination						
ICRF frame-tie	1988	Earth	$\hat{\mathbf{r}}_\oplus$, $\hat{\mathbf{h}}_\oplus$	0.″003	6	6
Lunar Laser Ranging						
	1969–1996	Moon	range	2–30 cm	11218	11218
Nominal Values						
					1	1
Total						42410

Ranging observations to spacecraft can be accurate to a level of only a couple of meters, though these observations are also affected by a number of factors, including the delay of the signal through the solar corona, delays in the electronic circuitry, and uncertainties in the spacecraft's position—either from orbital uncertainties or from a lander's position on a planet's rotating surface.

In any case, the computations of all ranging measurements are very similar. The formulation is given in § 8.7.

8.5.8 Orbiter Range Points

Orbiter range points are received in the form of *normal points*, a representation of modified distance measurements. The original round-trip range and Doppler measurements are reduced using the JPL Orbit Determination Program (Moyer 1971). This reduction is an adjustment for all relevant parameters, except for those of the planetary ephemeris, including the spacecraft orbit, the planet's mass and gravity field, etc. As such, the resultant range residuals represent derived corrections to the nominal planetary ephemeris used in the reduction. These residuals are then added to the geometric (instantaneous Earth–planet) range in order to give a pseudo "observed" range point.

References for the sources of the normal points are given in the website URL[1].

8.5.9 Lander Range Data

Lander range data are two-way ranging measurements taken of landed spacecraft on the surface of a planet. These data are reduced using the formulae given in § 8.7 with the reflection point on the planet's surface being represented by the location of the lander on the planet. For this, one needs the surface coordinates of the landers and the orientation of the planet in order to orient the lander into the ephemeris reference frame.

8.5.10 VLBI Data

VLBI measurements of a spacecraft with respect to background sources from a radio source catalogue may be combined with the planetocentric spacecraft trajectory in order to yield a positional determination of the planet with respect to the reference frame of the radio source catalogue. For DE405, there were two such points from the Phobos spacecraft nearing its encounter with Mars and 18 from the Magellan spacecraft in its orbit around Venus. Venus is relatively free from the asteroid perturbations that introduce uncertainties into the ephemeris of Mars, so that its ephemeris can be more accurately projected in time. Therefore, the Venus orbit, (which connects Venus into the inner planetary system), in conjunction with the VLBI observations of Venus, is important in orienting the inner planet system onto the radio frame.

8.5.11 Lunar Laser Range Data

The Lunar Laser Range (LLR) data consist of time-of-flight measurements of the laser pulses from McDonald Observatory, Haleakala, or L'Observatoire de la Côte d'Azur (OCA) to any one of four retroreflectors on the Moon and back again. The retroreflectors are at the Apollo

11, 14, and 15 landing sites and on the Lunokhod 2 vehicle. In the solutions for DE405, there were 11218 range points, distributed from 1969 to 1996.

The LLR data are deposited in the National Space Science Data Center and the International Laser Ranging Service. During the least-squares fit the ranges have been weighted according to the instrumental errors that accompany each point. The simple post-fit rms residual in one-way range was about 30 cm in 1970 and improved to about 3 cm throughout the 1990's.

8.6 The Orientation of DE405/LE405

In the past, the 1950-based ephemerides of JPL have been aligned onto the (1950) FK4 reference frame (Fricke and Kopff 1963). Starting with DE200, the ephemerides were aligned onto their own mean equator and dynamical equinox of J2000.0 (see Standish 1982).

The JPL planetary and lunar ephemerides starting with DE400 have been aligned onto the International Celestial Reference Frame (ICRF)—formerly, the *IERS frame*. This choice of the ICRF is advantageous for a number of reasons:

1. The ICRF is now the standard reference frame in astronomy.
2. The timing and polar motion data used for the orientation of the Earth, distributed by the IERS, are now referred to the ICRF.
3. The ephemerides are now fit to a number of VLBI observations which were referenced to the ICRF. Among all of the ephemeris observations which are explicitly given in a celestial reference system, these ICRF-based ones are the most accurate.
4. The ICRF is stable; it is accessible; it will not show any net rotation when the coordinates are improved in the future.

8.6.1 Adjustment of DE405 onto the ICRF Reference Frame

DE405 was adjusted to fit the ICRF-based VLBI observations of the Magellan Spacecraft orbiting Venus (18 points, 1990–94) and of the Phobos Spacecraft as it approached Mars (2 points, 1989) as described in the previous section. These data serve to align the ephemerides automatically onto the ICRF during the least-squares adjustment. The inherent accuracy of each of these data points is about 3–10 milliarcseconds.

Ephemerides of the outer planets rely almost entirely upon optical observations. These were initially referenced to various stellar catalogues, then transformed onto the FK4 using the formulae of Schwan (1983), then onto the FK5 system by applying the equinox offset and motion parameters of Fricke (1982), and finally onto the ICRF using a tentative set of transformation tables supplied by Morrison (1996).

8.7 Various Formulae Used in the Reduction of the Observational Data

In the course of reducing various types of observations, coming from many different sources, it is necessary to apply a number of modeling formulae and corrections to the initially received measurements. This section presents some of the details.

8.7.1 Phase Corrections

For the planetary disk observations, the planet is usually not fully illuminated and therefore shows a crescent or gibbous disk. For the outer planets where the phase angle, i, is always small, the following formula, chosen simply from empirical considerations, was applied to the published transit observations:

$$\left| \begin{array}{c} \Delta\alpha \\ \Delta\delta \end{array} \right| = \left| \begin{array}{c} \sin\Theta \\ \cos\Theta \end{array} \right| B_k \sin 2i \tag{8.18}$$

where i is the angle between the Earth and the Sun as seen from the planet; Θ is the position angle of the mid-point of the illuminated edge, measured clockwise from north. Phase corrections were of prime importance for the inner planets when their optical observations were included in earlier ephemerides. For the outer planets, the phase corrections for only Jupiter are of much significance.

8.7.2 Corrections to Precession and Equinox Drift

The optical residuals in right ascension and declination were reduced using the 1976 IAU (Fricke 1971, 1982) values for precession and equinox drift. More recent estimates for precession had indicated a further correction to the IAU value of $\Delta p = -0.''3/\text{cy}$. Also, any existing secular-like trends, such as equinox drift, were modeled by the quantity, Δk, using the standard formulae,

$$\begin{aligned} \Delta\alpha &= (\Delta k + \Delta n \sin\alpha \tan\delta) T_{2000} \\ \Delta\delta &= (\Delta n \cos\alpha) T_{2000} \end{aligned} \tag{8.19}$$

where T_{2000} is the time in centuries past J2000.0, $\Delta n = \Delta p \sin\varepsilon$, and ε is the obliquity.

In DE405, the value of Δp was set to $-0.''3/\text{cy}$; that for Δk was determined to be $-0.''062/\text{cy}$ in the solution.

8.7.3 Computation of Ranges

A range measurement is the actual round-trip time of the electromagnetic signal from when it leaves the transmitter until the time it arrives at the receiver. The timing is done by the (UTC) clock at the antenna; thus, the observation is essentially the UTC times of transmission and of reception.

For an observation received at the time t_R (expressed in units of $\mathrm{T_{eph}}$, the time which is the independent variable of the equations of motion), the round-trip light-time is given by the difference $UTC(t_R) - UTC(t_R - \tau_d - \tau_u)$, where

$$\tau_u = |\mathbf{r}_\mathrm{B}(t_R - \tau_d) - \mathbf{r}_\mathrm{A}(t_R - \tau_d - \tau_u)|/c + \Delta\tau_u[rel] + \Delta\tau_u[cor] + \Delta\tau_u[tropo] \tag{8.20}$$

and

$$\tau_d = |\mathbf{r}_\mathrm{A}(t_R) - \mathbf{r}_\mathrm{B}(t_R - \tau_d)|/c + \Delta\tau_d[rel] + \Delta\tau_d[cor] + \Delta\tau_d[tropo] \tag{8.21}$$

and where τ_u and τ_d are the light-times (in $\mathrm{T_{eph}}$ units) of the upleg and the downleg, respectively; $\mathbf{r}_\mathrm{A}$ is the solar-system-barycentric position of the antenna on the Earth's surface;

$\mathbf{r}_B$ is the solar-system-barycentric position of the *bounce point*, either a responding spacecraft or the reflection point on the planet's surface; c is the velocity of light; and the three $\Delta\tau'$s are the corrections to the light-times due to relativity, the electron content of the solar corona, and the Earth's troposphere, respectively. The two formulae are each solved iteratively, first for τ_d then for τ_u.

8.7.4 Antenna Location

The location of the antenna is computed in a straightforward manner using the proper formulae (precession, nutation, UT1, and polar motion) with which one orients the Earth, and in particular the observing station, onto the ICRF, the reference frame of the ephemerides. The formulation was the same as that given by the IERS standards document of 2003 (URL[2]). though the geological drifts of the stations were being omitted during the time of DE405's creation.

8.7.5 Time Delay for Relativity

The time-delay due to relativity, given by Shapiro (1964), is obtained by integrating along the signal path over the value of the potential. For each leg of the signal path, the delay is given by the formula

$$\Delta\tau_{rel} = \frac{(1+\gamma)GM}{c^3} \ln\left|\frac{e+p+q}{e+p-q}\right| \tag{8.22}$$

where γ is the PPN parameter of general relativity and where e, p, and q are the heliocentric distance of the Earth, the heliocentric distance of the planet, and the geocentric distance of the planet, respectively. These distances are evaluated at $t-\tau_d$ for the planet, at $t-\tau_d-\tau_u$ for the Earth during the upleg, and at t for the Earth during the downleg. This formula has been augmented since the creation of DE405 (see Moyer (2000)) in order to allow for the increased length of the signal path due to the path's bending. Further, it is now necessary to apply this correction for not only the Sun's potential but also for that of Jupiter, since the latter alters Earth–Mars ranging by a meter or so.

8.7.6 Time Delay for the Solar Corona

The delay from the solar corona (see Muhleman and Anderson 1981) is obtained by integrating along the signal path from point P_1 to point P_2 over the density of ionized electrons, N_e (cm^{-3}),

$$\Delta\tau_{cor} = \frac{40.3}{cf^2}\int_{P_1}^{P_2} N_e\, ds \tag{8.23}$$

where c is the speed of light (cm/sec), f is the frequency (Hz), and s is the linear distance (cm). The density is given by

$$N_e = \frac{A}{r^6} + \frac{ab/\sqrt{a^2\sin^2\beta + b^2\cos^2\beta}}{r^2} \tag{8.24}$$

where r is the heliocentric distance expressed in units of the solar radius and β is the solar latitude. The values for the constants, A, a, and b are included in Table 8.5. When near conjunction the major uncertainties of ranging observations are due to uncertainty in N_e, a number which is highly time-dependent. Since the delay is frequency dependent, the total delay may be calibrated using dual-frequency ranging; otherwise, the parameters in the preceding formula must represent some sort of mean values.

For some ranging, measurements were taken in two separate frequencies, so that one can remove the effect entirely since it is frequency-dependent and may therefore be solved-for.

8.7.7 Time Delay for the Troposphere

The delay from the Earth's troposphere for radio frequencies is discussed by Chao (1970). For each leg, it is

$$\Delta\tau_{tropo} = 7 \text{ nsec}/(\cos z + 0.0014/(0.045 + \cot z)) \tag{8.25}$$

where z is the zenith distance at the antenna.

8.7.8 Modeling the Surface of Mercury

For radar observations, the point of reflection on the surface of Mercury was approximated by a triaxial ellipsoid. Following Anderson et al. (1996), a set of fully normalized Legendre functions to the second degree was adjusted to fit the surface:

$$\begin{aligned} R_0 = {} & + c_{10}\sqrt{3}\sin\phi + (c_{11}\cos\lambda + s_{11}\sin\lambda)\sqrt{3}\cos\phi + c_{20}\frac{\sqrt{5}}{2}(3\sin^2\phi - 1) \\ & + (c_{21}\cos\lambda + s_{21}\sin\lambda)\sqrt{15}\sin\phi\cos\phi + (c_{22}\cos 2\lambda + s_{22}\sin 2\lambda)\frac{\sqrt{15}}{2}\cos^2\phi \end{aligned} \tag{8.26}$$

where λ is the longitude and ϕ is the latitude of the echo point on the surface. The least-squares adjustment for DE405 yielded:

$R_0 \equiv 2,439,760$ m	$c_{10} = +920 \pm 523$ m	$c_{11} = +186 \pm 38$ m	$s_{11} = -245 \pm 38$ m
$c_{21} = +79 \pm 157$ m	$s_{21} = +744 \pm 166$ m	$c_{22} = +292 \pm 32$ m	$s_{22} = +345 \pm 34$ m

Since the latitude, ϕ, of the radar echo point on Mercury is always within 12 degrees of the equator, c_{20} is highly correlated ($\gg 0.99$) with R_0 and was therefore omitted from the solution. For the other parameters, they serve merely as a smoothing function for determining the Mercury ephemeris. For more definitive values in regard to the shape of Mercury, see Anderson et al. (1996).

8.7.9 Modeling the Surface of Venus

The surface of Venus was modeled using a topographical map fit to measurements from the Pioneer Venus Orbiter spacecraft (Pettengill et al. 1980). The map is referenced to a sphere whose radius was determined to be 6052.26 ± 0.03 km in the least-squares adjustment. With such modeling, the radar residuals of Venus are reduced from over 2 km to less than 1 km.

8.7.10 Modeling the Surface of Mars—Closure Points

The severe topography on the surface of Mars shows variations of many kilometers. These introduce scatter into the observations which is not entirely random, thus presenting the danger of systematic errors.

Therefore, the radar ranging to Mars was used only in the *closure point* mode. Closure points are pairs of days during which the observed points on the surface of Mars are nearly identical with respect to their longitudes and latitudes on Mars. Since the same topographical features are observed during each of the two days, the uncertainty introduced by the topography may be eliminated by subtracting the residuals of one day from the corresponding ones of the other day. The remaining difference is then due to only the ephemeris drift between the two days. The closure points for Mars have *a priori* uncertainties of about 100 m or less when the points are within 0.2 degrees of each other on the martian surface.

8.7.11 Viking Lander Computations

The range data from the Viking Landers on the surface of Mars were reduced using the formulae given above with the reflection point on the planet's surface being represented by the location of the lander on Mars. For this, one needs the Martian coordinates of the landers as well as a set of angles used to express the orientation of Mars within the ephemeris reference frame. The position of the lander, expressed in the frame of the ephemeris, is given by

$$\mathbf{r} = \mathbf{r}_x(-\varepsilon)\mathbf{r}_z(-\Omega)\mathbf{r}_x(-I)\mathbf{r}_z(-\Omega'_q)\mathbf{r}_x(-I'_q)\mathbf{r}_z(-V')\mathbf{r}_0 \tag{8.27}$$

where ε is the obliquity of the ecliptic; Ω and I are the node and inclination of the mean Martian orbit upon the (J2000.0) ecliptic; Ω_q and I_q are the mean node and inclination of the Martian equator upon the mean orbit; V is the longitude of the Martian prime meridian measured along the equator from the intersection of the orbit; and $\mathbf{r}_0$, the Mars-fixed coordinates of the lander, and where

$$\Omega'_q = \Omega_q - \Delta\psi, \qquad I'_q = I_q + \Delta\varepsilon \quad \text{and} \quad V' = V + \Delta\psi \cos I'_q \tag{8.28}$$

where $\Delta\psi$ and $\Delta\varepsilon$ express the nutation of Mars, computed from the formulation of Lyttleton, Cain, and Liu (1979). The Mars-fixed coordinates of the lander are computed from the cylindrical coordinates,

$$\mathbf{r}_0^T = [u\cos\lambda,\ u\sin\lambda,\ v]^T. \tag{8.29}$$

The values for the parameters used in the reductions are given in § 8.8. The values for ε, Ω, and I were adopted: those for Ω_q, I_q, and V, as well as the coordinates of the landers, were estimated in the least-squares adjustments. For a more extensive treatment including parameter values, see Folkner et al. (1998).

8.8 Initial Conditions and Constants of DE405/LE405

The starting conditions for DE405/LE405 were the result of two successive least-squares adjustments. The first adjustment was a solution for all of the relevant parameters whose values were best determined from the ephemeris data. Then, some of the parameters were rounded off (at a negligible level) for the sake of appearance and ease of use. These rounded

values were then forced as known constants into the second solution which produced a minor adjustment to the other parameters.

This chapter gives the numerical values of all of the parameters that were used in the final integration of DE405/LE405. The starting epoch was Julian Ephemeris Date 2440400.5 (June 28, 1969)—chosen as being the last "0400" date before the start of the Lunar Laser Ranging observations. Table 8.2 gives the cartesian coordinates of the heliocentric planets, the solar system barycentric Sun and the geocentric Moon. The orientation parameters of the Moon are given in Table 8.3, the dynamical constants (those in the equations of motion) are presented in Table 8.4, a number of parameters used in the reduction of the observational data (but not in the equations of motion) are shown in Table 8.5, and Table 8.6 gives the radii and taxonomic classes of the 297 non-Big 3 asteroids used in DE405.

Table 8.2 Initial conditions at JED (T_{eph}) 2440400.5 (June 28, 1969). J2000.0 equatorial coordinates and velocities of the heliocentric planet-system barycenters, the solar system barycentric Sun, and the geocentric Moon [au, au/day].

Mercury	0.3572602064472754D+00	−0.9154904243051842D-01	−0.8598103998694038D-01
	0.3367845662193786D-02	0.2488934284224929D-01	0.1294407158679597D-01
Venus	0.6082494331856041D+00	−0.3491324431959006D+00	−0.1955443457854069D+00
	0.1095242010990884D-01	0.1561250673986247D-01	0.6328876451746666D-02
EM Bary	0.1160149091391665D+00	−0.9266055536403853D+00	−0.4018062776069881D+00
	0.1681162005220229D-01	0.1743131687982032D-02	0.7559737671361461D-03
Mars	−0.1146885824390927D+00	−0.1328366530833488D+01	−0.6061551894193808D+00
	0.1448200480794475D-01	0.2372854923607114D-03	−0.2837498361023970D-03
Jupiter	−0.5384209406992146D+01	−0.8312476561610838D+00	−0.2250947570335499D+00
	0.1092363291218498D-02	−0.6523294191192267D-02	−0.2823012267219439D-02
Saturn	0.7889889933822818D+01	0.4595710726926013D+01	0.1558431516725090D+01
	−0.3217203491093664D-02	0.4330632233555692D-02	0.1926417463799453D-02
Uranus	−0.1826990081497826D+02	−0.1162711580219047D+01	−0.2503695407425549D+00
	0.2215401656274106D-03	−0.3767653558246162D-02	−0.1653243804922394D-02
Neptune	−0.1605954509192446D+02	−0.2394294829087950D+02	−0.9400422780354008D+01
	0.2643122791576562D-02	−0.1503492080758795D-02	−0.6812710048723478D-03
Pluto	−0.3048782211215555D+02	−0.8732454301967293D+00	0.8911296984184755D+01
	0.3225621959332332D-03	−0.3148747927551605D-02	−0.1080177931593696D-02
Moon	−0.8081773279114842D-03	−0.1994630001620399D-02	−0.1087262660838102D-02
	0.6010848166591298D-03	−0.1674454606151515D-03	−0.8556214497398617D-04
Sun	0.4502508156233894D-02	0.7670747009323788D-03	0.2660568051770271D-03
	−0.3517482096451887D-06	0.5177625399584830D-05	0.2229101854391665D-05

Table 8.3 J2000.0 angular coordinates of the lunar physical librations [rad, rad/day]

ϕ_M, θ_M, ψ_M	0.00512995970515812456	0.38239065587686011507	1.29414222411027863099
ω_{xM}, ω_{yM}, ω_{zM}	0.00004524704499022800	−0.00000223092763198743	0.22994485870136698411

Table 8.4 Dynamical constants used in the integration of DE405/LE405

Defining Constants, Scale Factor		
k^2	0.01720209895^2	Gauss' (gravitational) constant
c	299792.458 [km/sec]	speed of light
au	149597870.691 [km/au]	scale factor
Planetary Masses		
GM_s/GM_1	6023600.	$mass^{-1}$ for Mercury
GM_s/GM_2	408523.71	$mass^{-1}$ for Venus
GM_s/GM_B	328900.5614	$mass^{-1}$ for EM-Bary
GM_s/GM_4	3098708.	$mass^{-1}$ for Mars
GM_s/GM_5	1047.3486	$mass^{-1}$ for Jupiter
GM_s/GM_6	3497.898	$mass^{-1}$ for Saturn
GM_s/GM_7	22902.98	$mass^{-1}$ for Uranus
GM_s/GM_8	19412.24	$mass^{-1}$ for Neptune
GM_s/GM_9	135200000.	$mass^{-1}$ for Pluto
GM_e/GM_m	81.30056	Earth-Moon mass ratio
Asteroid Masses and Densities		
m_{Ceres}	4.7×10^{-10} GM_s	Mass of Ceres
m_{Pallas}	1.0×10^{-10} GM_s	Mass of Pallas
m_{Vesta}	1.3×10^{-10} GM_s	Mass of Vesta
ρ_C	1.8	Mean density of C-type asteroids
ρ_S	2.4	Mean density of S-type asteroids
ρ_M	5.0	Mean density of M-type asteroids
Relativity, $\dot{G}$, $J_2(Sun)$		
β	1.0	PPN parameter
γ	1.0	PPN parameter
$\dot{G}$	0.0	rate of change of the gravitational constant
J_{2s}	2×10^{-7}	dynamical form-factor of the Sun
Earth Parameters		
$\mathcal{R}_e$	6378.137 [km]	radius of the Earth
J_{2e}	0.001082626	zonal harmonics of the Earth
J_{3e}	−0.000002533	
J_{4e}	−0.000001616	
k_{2e0}	0.34	potential Love number for zonal Earth tides
k_{2e1}	0.30	for diurnal Earth tides
k_{2e2}	0.30	for semidiurnal Earth tides
τ_{e0}	0.0	time-lag for the zonal Earth tides
τ_{e1}	0.01290895939 [days]	for diurnal Earth tides
τ_{e2}	0.00694178558 [days]	for semidiurnal Earth tides

Table 8.4 *(continued)*

Φ_X	0.0	X-axis rotation at J2000.0
Φ_Y	0.0	Y-axis rotation at J2000.0
$d\Phi_X/dt$	0.000244 [″/yr]	negative obliquity rate correction: $-\Delta\dot{\varepsilon}$
$d\Phi_Y/dt$	−0.001193 [″/yr]	precession correction: $+\Delta p \sin\varepsilon$
Moon Parameters		
$\mathcal{R}_m$	1738.0 [km]	radius of the Moon
β_L	0.0006316121	lunar moment parameters
γ_L	0.0002278583	
k_{2m}	0.0299221167	potential love number of the Moon
τ_m	0.1667165558 [days]	time-lag for the lunar solid-body tide
J_{2m} [a]	0.000204312007	*input* zonal harmonics of the Moon
J_{3m}	0.000008785470	
J_{4m}	−0.000000145383	
$C_{3,1m}$	0.000030803810	*input* tesseral harmonics of the Moon
$C_{3,2m}$	0.000004879807	
$C_{3,3m}$	0.000001770176	
$S_{3,1m}$	0.000004259329	
$S_{3,2m}$	0.000001695516	
$S_{3,3m}$	−0.000000270970	
$C_{4,1m}$	−0.000007177801	
$C_{4,2m}$	−0.000001439518	
$C_{4,3m}$	−0.000000085479	
$C_{4,4m}$	−0.000000154904	
$S_{4,1m}$	0.000002947434	
$S_{4,2m}$	−0.000002884372	
$S_{4,3m}$	−0.000000788967	
$S_{4,4m}$	0.000000056404	

[a] Note, as described in § 8.3, the values used for J_{2m}, $C_{2,2m}$, $C_{2,1m}$, $S_{2,1m}$, and $S_{2,2m}$ are computed from the (time-varying) lunar moment-of-inertia tensor. The J_{2m} listed here is input; the rigid value, used in the force and torque equations, is derived from this input value and from the potential Love number, k_{2m}. The rigid value of $C_{2,2m}$ is computed from J_{2m}, β_L, and γ_L.

Table 8.5 Auxiliary constants used in the observational reductions for DE405/LE405

Mars Orientation Parameters		
ε	23.4392811 [°]	Mean obliquity of the ecliptic
$\dot{\varepsilon}$	0.0 [°/day]	
Ω	49.6167 [°]	Node of Mars' mean orbit upon ecliptic
$\dot{\Omega}$	0.0 [°/day]	
I	1.85137 [°]	Inclination of Mars' mean orbit upon ecliptic
$\dot{I}$	0.0 [°/day]	
Ω_q	35.4371 [°]	Node of Mars' equator upon Mars' orbit
$\dot{\Omega}_q$	-5.76×10^{-6} [°/day]	
I_q	25.1886 [°]	Inclination of Mars' equator upon Mars' orbit
$\dot{I}_q$	-0.1094×10^{-6} [°/day]	
V	1.3361259 [°]	Longitude of Mars' prime meridian
$\dot{V}$	350.89198512444 [°/day]	
Viking Spacecraft Coordinates		
λ_1	311.82160 [°]	longitude of Viking Lander # 1
u_1	3136.520 [km]	axial distance
v_1	1284.469 [km]	z-height
λ_1	134.05322 [°]	longitude of Viking Lander # 2
u_1	2277.366 [km]	axial distance
v_1	2500.054 [km]	z-height
Solar Corona Parameters (see Eq. 8.24)		
A	1.06×10^{8} [cm^{-3}]	
a	4.89×10^{5} [cm^{-3}]	
b	3.91×10^{5} [cm^{-3}]	

Table 8.6 The 297 non-Big 3 individual asteroids used in the integration of DE405. The taxonomic class and the radius in km are given.

0010	Hygiea	C	214.5	0109	Felicitas	C	45.8	0238	Hypatia	C	78.0
0013	Egeria	C	107.5	0111	Ate	C	69.5	0240	Vanadis	C	54.0
0019	Fortuna	C	100.0	0112	Iphigenia	C	37.8	0241	Germania	C	84.5
0024	Themis	C	99.0	0114	Kassandra	C	51.5	0247	Eukrate	C	68.5
0031	Euphrosyne	C	124.0	0117	Lomia	C	77.0	0259	Aletheia	C	92.5
0034	Circe	C	59.0	0120	Lachesis	C	89.0	0266	Aline	C	56.5
0035	Leukothea	C	54.0	0121	Hermione	C	108.5	0268	Adorea	C	71.0
0036	Atalante	C	54.5	0127	Johanna	C	61.0	0275	Sapientia	C	57.5
0038	Leda	C	60.0	0128	Nemesis	C	97.0	0276	Adelheid	C	63.5
0041	Daphne	C	91.0	0130	Elektra	C	94.5	0283	Emma	C	75.0
0045	Eugenia	C	107.0	0134	Sophrosyne	C	53.5	0303	Josephina	C	51.5
0046	Hestia	C	65.5	0137	Meliboea	C	75.0	0304	Olga	C	34.2
0047	Aglaja	C	68.5	0139	Juewa	C	81.0	0308	Polyxo	C	74.0
0048	Doris	C	112.5	0140	Siwa	C	57.0	0313	Chaldaea	C	50.5
0049	Pales	C	77.0	0141	Lumen	C	67.5	0324	Bamberga	C	114.0
0050	Virginia	C	44.0	0143	Adria	C	46.4	0326	Tamara	C	50.0
0051	Nemausa	C	76.5	0144	Vibilia	C	73.0	0329	Svea	C	40.2
0052	Europa	C	156.0	0145	Adeona	C	77.5	0334	Chicago	C	85.0
0053	Kalypso	C	59.5	0146	Lucina	C	68.5	0335	Roberta	C	46.8
0054	Alexandra	C	85.5	0147	Protogeneia	C	68.5	0336	Lacadiera	C	36.0
0056	Melete	C	58.5	0150	Nuwa	C	78.5	0344	Desiderata	C	69.0
0058	Concordia	C	48.9	0154	Bertha	C	96.0	0345	Tercidina	C	50.0
0059	Elpis	C	86.5	0156	Xanthippe	C	63.0	0350	Ornamenta	C	61.5
0062	Erato	C	49.6	0159	Aemilia	C	65.5	0356	Liguria	C	67.5
0065	Cybele	C	120.0	0160	Una	C	42.5	0357	Ninina	C	55.0
0070	Panopaea	C	63.5	0162	Laurentia	C	52.5	0358	Apollonia	C	45.9
0072	Feronia	C	44.6	0163	Erigone	C	38.2	0360	Carlova	C	60.5
0074	Galatea	C	61.5	0164	Eva	C	55.0	0362	Havnia	C	49.0
0076	Freia	C	95.0	0165	Loreley	C	80.0	0363	Padua	C	48.5
0078	Diana	C	62.5	0168	Sibylla	C	77.0	0365	Corduba	C	55.0
0081	Terpsichore	C	62.0	0171	Ophelia	C	60.5	0366	Vincentina	C	49.0
0083	Beatrix	C	42.1	0173	Ino	C	79.5	0372	Palma	C	97.5
0084	Klio	C	41.5	0175	Andromache	C	53.5	0373	Melusina	C	49.8
0085	Io	C	78.5	0176	Iduna	C	62.5	0375	Ursula	C	108.0
0086	Semele	C	63.5	0185	Eunike	C	82.5	0377	Campania	C	47.2
0087	Sylvia	C	135.5	0187	Lamberta	C	67.5	0381	Myrrha	C	62.0
0088	Thisbe	C	116.0	0191	Kolga	C	52.5	0386	Siegena	C	86.5
0090	Antiope	C	62.5	0194	Prokne	C	87.0	0388	Charybdis	C	60.0
0091	Aegina	C	57.0	0195	Eurykleia	C	44.9	0393	Lampetia	C	53.0
0093	Minerva	C	85.5	0200	Dynamene	C	66.0	0404	Arsinoe	C	50.5
0094	Aurora	C	106.0	0203	Pompeja	C	60.0	0405	Thia	C	64.5
0095	Arethusa	C	72.5	0205	Martha	C	41.8	0407	Arachne	C	48.8
0096	Aegle	C	87.0	0206	Hersilia	C	56.5	0409	Aspasia	C	84.0
0098	Ianthe	C	54.5	0209	Dido	C	74.5	0410	Chloris	C	64.0
0099	Dike	C	39.5	0210	Isabella	C	45.0	0412	Elisabetha	C	46.6
0102	Miriam	C	43.0	0211	Isolda	C	74.0	0419	Aurelia	C	66.5
0104	Klymene	C	63.5	0212	Medea	C	70.0	0420	Bertholda	C	73.0
0105	Artemis	C	61.5	0213	Lilaea	C	42.3	0423	Diotima	C	108.5
0106	Dione	C	73.5	0225	Henrietta	C	62.0	0424	Gratia	C	45.2
0107	Camilla	C	118.5	0233	Asterope	C	54.0	0426	Hippo	C	67.0

Table 8.6 *(continued)*

0431	Nephele	C	48.9	0751	Faina	C	57.5	0071	Niobe	S	43.6
0442	Eichsfeldia	C	33.8	0762	Pulcova	C	71.0	0080	Sappho	S	40.9
0444	Gyptis	C	85.0	0769	Tatjana	C	51.0	0089	Julia	S	79.5
0449	Hamburga	C	44.3	0772	Tanete	C	61.5	0103	Hera	S	47.6
0451	Patientia	C	115.0	0773	Irmintraud	C	49.5	0115	Thyra	S	41.8
0454	Mathesis	C	42.2	0776	Berbericia	C	88.5	0124	Alkeste	S	39.8
0455	Bruchsalia	C	43.8	0780	Armenia	C	48.5	0148	Gallia	S	52.0
0466	Tisiphone	C	60.5	0788	Hohensteina	C	54.5	0181	Eucharis	S	53.5
0469	Argentina	C	64.5	0790	Pretoria	C	88.0	0192	Nausikaa	S	53.5
0476	Hedwig	C	60.5	0791	Ani	C	53.5	0196	Philomela	S	73.0
0481	Emita	C	58.0	0804	Hispania	C	80.5	0221	Eos	S	55.0
0488	Kreusa	C	79.0	0814	Tauris	C	58.0	0230	Athamantis	S	57.5
0489	Comacina	C	72.0	0895	Helio	C	73.5	0236	Honoria	S	45.2
0490	Veritas	C	60.5	0909	Ulla	C	60.0	0287	Nephthys	S	35.0
0491	Carina	C	50.5	0914	Palisana	C	39.5	0328	Gudrun	S	23.5
0498	Tokio	C	42.4	1015	Christa	C	50.5	0346	Hermentaria	S	55.0
0505	Cava	C	57.5	1021	Flammario	C	51.5	0349	Dembowska	S	71.5
0506	Marion	C	54.5	1093	Freda	C	60.0	0354	Eleonora	S	81.0
0508	Princetonia	C	73.5	1467	Mashona	C	56.0	0385	Ilmatar	S	47.0
0511	Davida	C	168.5	0003	Juno	S	133.5	0387	Aquitania	S	53.0
0514	Armida	C	55.0	0005	Astraea	S	62.5	0389	Industria	S	40.8
0521	Brixia	C	60.5	0006	Hebe	S	96.0	0416	Vaticana	S	44.8
0535	Montague	C	38.5	0007	Iris	S	101.5	0433	Eros	S	10.0
0536	Merapi	C	79.0	0008	Flora	S	70.5	0471	Papagena	S	67.5
0545	Messalina	C	57.5	0009	Metis	S	85.0	0532	Herculina	S	112.5
0554	Peraga	C	49.2	0011	Parthenope	S	81.0	0674	Rachele	S	50.5
0566	Stereoskopia	C	87.5	0012	Victoria	S	58.5	0980	Anacostia	S	44.5
0568	Cheruskia	C	44.9	0014	Irene	S	83.5	1036	Ganymed	S	20.5
0595	Polyxena	C	57.0	0015	Eunomia	S	136.0	0016	Psyche	M	132.0
0596	Scheila	C	58.5	0017	Thetis	S	46.6	0021	Lutetia	M	49.8
0602	Marianna	C	65.0	0018	Melpomene	S	74.0	0022	Kalliope	M	93.5
0618	Elfriede	C	62.0	0020	Massalia	S	75.5	0069	Hesperia	M	71.5
0626	Notburga	C	52.0	0023	Thalia	S	55.5	0075	Eurydike	M	29.1
0635	Vundtia	C	50.0	0025	Phocaea	S	39.1	0077	Frigga	M	35.5
0654	Zelinda	C	66.0	0026	Proserpina	S	49.4	0092	Undina	M	66.0
0663	Gerlinde	C	52.0	0027	Euterpe	S	65.5	0097	Klotho	M	43.5
0683	Lanzia	C	58.0	0028	Bellona	S	63.0	0110	Lydia	M	44.5
0690	Wratislavia	C	72.5	0029	Amphitrite	S	109.5	0129	Antigone	M	62.5
0691	Lehigh	C	46.3	0030	Urania	S	52.0	0135	Hertha	M	41.0
0694	Ekard	C	46.4	0032	Pomona	S	41.3	0201	Penelope	M	35.2
0702	Alauda	C	101.0	0037	Fides	S	56.0	0216	Kleopatra	M	70.0
0704	Interamnia	C	166.5	0039	Laetitia	S	79.5	0224	Oceana	M	35.0
0705	Erminia	C	69.5	0040	Harmonia	S	55.5	0250	Bettina	M	42.8
0709	Fringilla	C	49.8	0042	Isis	S	53.5	0322	Phaeo	M	36.9
0712	Boliviana	C	66.0	0043	Ariadne	S	32.6	0337	Devosa	M	31.6
0713	Luscinia	C	54.5	0044	Nysa	S	36.6	0338	Budrosa	M	31.1
0739	Mandeville	C	55.0	0057	Mnemosyne	S	58.0	0347	Pariana	M	27.1
0740	Cantabia	C	47.2	0063	Ausonia	S	54.0	0369	Aeria	M	31.1
0747	Winchester	C	89.0	0068	Leto	S	63.5	0849	Ara	M	49.0

8.8.1 Asteroids

The initial conditions for all 300 asteroids came from a file maintained by the Solar System Dynamics Group at JPL. The radii from the same file were used to compute the masses of each of the 297 *non*-Big3 individual asteroids from the formula, $GM = 6.27 \times 10^{-22} \mathrm{R}^3 \rho_k$, where R is the radius of the asteroid in kilometers and where ρ_k is the density of the k^{th} taxonomic class of asteroids (S, C, or M), given in Table 8.6.

8.9 Positional Errors of the Planetary and Lunar Ephemerides

Estimates of ephemeris errors are based upon a number of factors, including the accuracies of the observational data, the stability to various parameter and data combinations tested in the least-squares adjustments, the observed abilities to predict positions into the future, knowledge of the uncertainties associated with various relevant factors, etc. However, one may get a more definitive assessment comparing two ephemerides, assuming that the differences are due mainly to the older ephemeris, the newer one having benefitted from refined modeling and enhanced data sets.

This section first discusses the accuracies of the ephemerides, showing how the different data types contribute to the various ephemeris parameters; it then presents comparisons of DE200 and of DE405 with a recent ephemeris, DE409.

8.9.1 Inner Four Planets: Ephemerides from Ranging and VLBI

The ephemerides of the four innermost planets along with the Moon and the Sun are all well-known with respect to each other (intra-planet distances and angles) because of the accurate ranging observations to which the ephemerides are adjusted. Furthermore, the mean motion of this whole inner-body system is also well-determined by fitting to the ranging observations. For explanations of this latter fact, see Williams and Standish (1989) or Standish and Williams (1990).

The orientation of the inner planet system is provided by VLBI observations of the Magellan Spacecraft orbiting Venus and the Phobos Spacecraft on its approach to Mars. These observations link the spacecraft to the ICRF (International Celestial Reference System), and thus the planet to the ICRF, given that the planetocentric spacecraft orbit is sufficiently well-determined. An additional frame-tie (Folkner et al. 1993) was determined using the well-established Earth-based positions of the VLBI antennae, linked to the LLR (lunar laser ranging) telescopes by means of ground surveys. The positions of these telescopes, in turn, are connected to the Moon's orbit using the LLR data, and since the Moon's orbit is sensitive to the position of the strongly perturbing Sun, it is tied to the heliocentric Earth orbit.

Radar ranging observations have inherent accuracies of less than 100 meters, though the unmodeled uncertainties introduced by the surface topographies are a few hundred meters and more. Spacecraft orbits, on the other hand, have shown accuracies of 10 meters or less. The VLBI observations have uncertainties of a few milliarcseconds; with about 20 of them, the uncertainty of the orientation of the whole inner planet ephemeris system of DE405 is

0.″001–0.″002 which is the equivalent of a kilometer or so at the typical distances between the inner planets.

Thus, during the present decade or so, relative distances between two of the inner-solar-system bodies are accurate to 100–200 meters; relative angles between the inner bodies (e.g., Earth-Sun-planet angle) are accurate to less than 0.″001. The orientation is accurate to 0.″001–0.″002. Away from the present epoch of accurate ranging and VLBI, the accuracies deteriorate due to the uncertainties in the mean motions caused by the perturbative effects of the asteroids.

8.9.2 Uncertainties from Asteroid Perturbations

The masses of the asteroids are not well-known, and therefore it has not been possible to model their perturbations with full accuracy. Williams (1984) estimated that due to the asteroids, the mean motions of the inner planets have uncertainties on the order of 0.″02/century—a couple of kilometers per decade.

8.9.3 Outer Planets: Reliance on the Classical Optical Observations

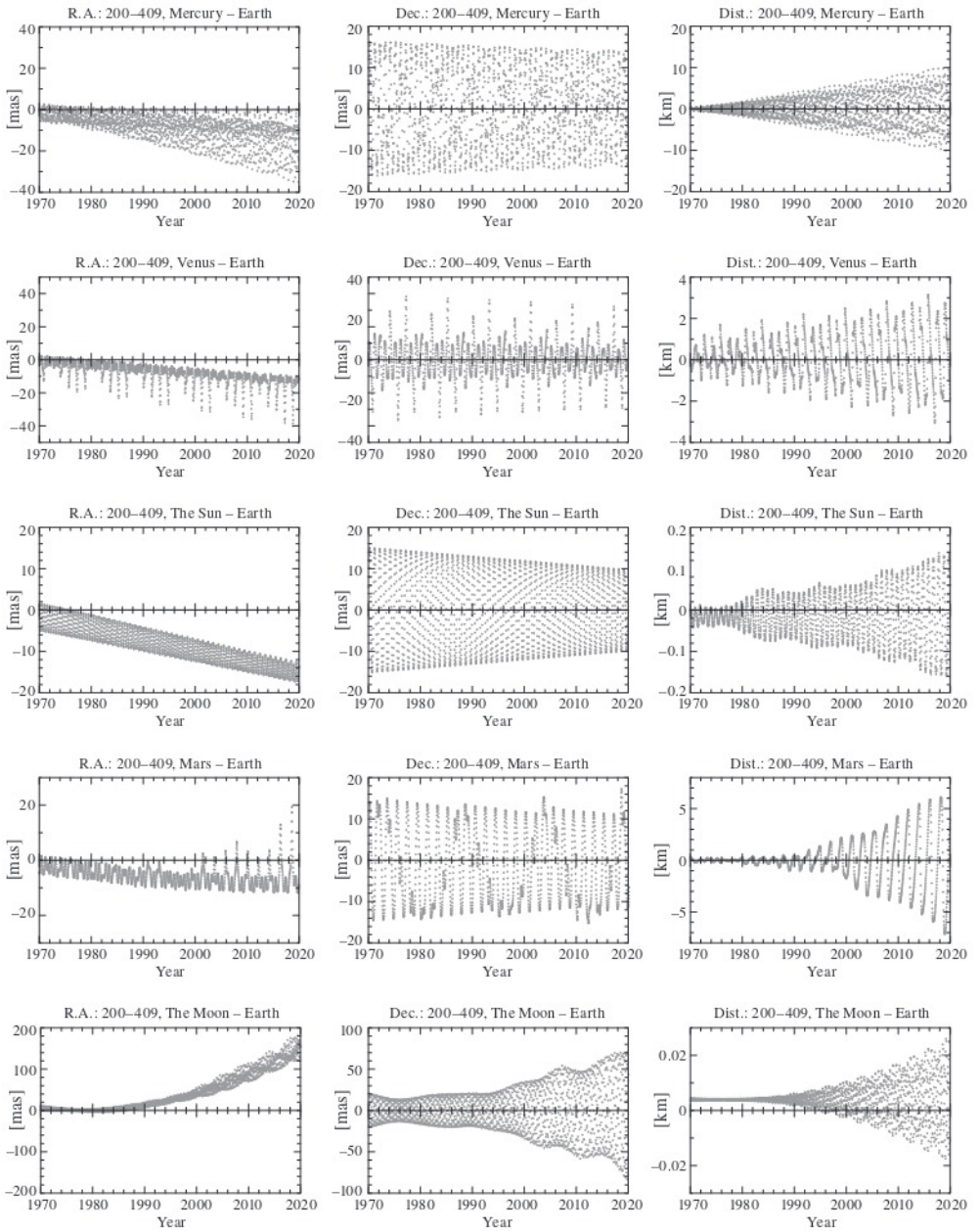
In contrast to those of the inner planets, the ephemerides of the outer planets rely almost entirely upon optical observations in which *systematic* errors over the past have been at the level of 0.″1 or so. As a result, the outer planet ephemerides are much less accurate than those of the planets observed with ranging. Modern CCD measurements now show single (presumably *random*) observation measurement errors of about 0.″1 so that present-day plane-of-sky positions (directions) are determined to a few hundredths of an arcsecond. For times away from the present, the accuracy deteriorates significantly, especially with the outermost planets.

8.9.4 Planetary Positional Errors in the Almanacs, 1984–2002

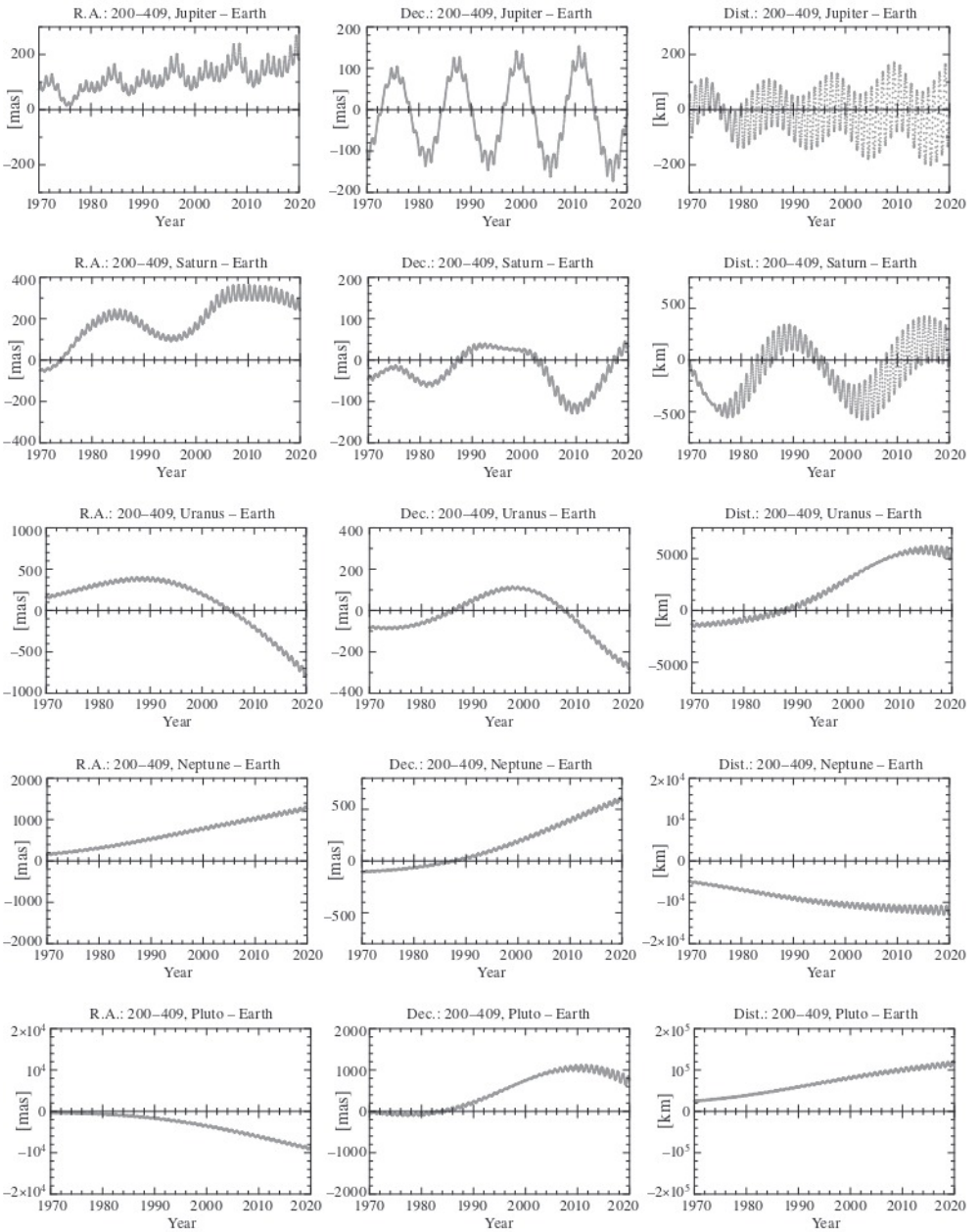
A comparison between DE200, created before 1980, and DE409, created in 2003, shows differences which must, for the most part, be attributed to the errors in DE200; thus, these differences give good estimates of the errors in the positions of *The Astronomical Almanac* for the years, 1984–2002. Plots of the differences are given in Figs. 8.1 through 8.10.

8.9.5 Planetary Position Uncertainties in 2003

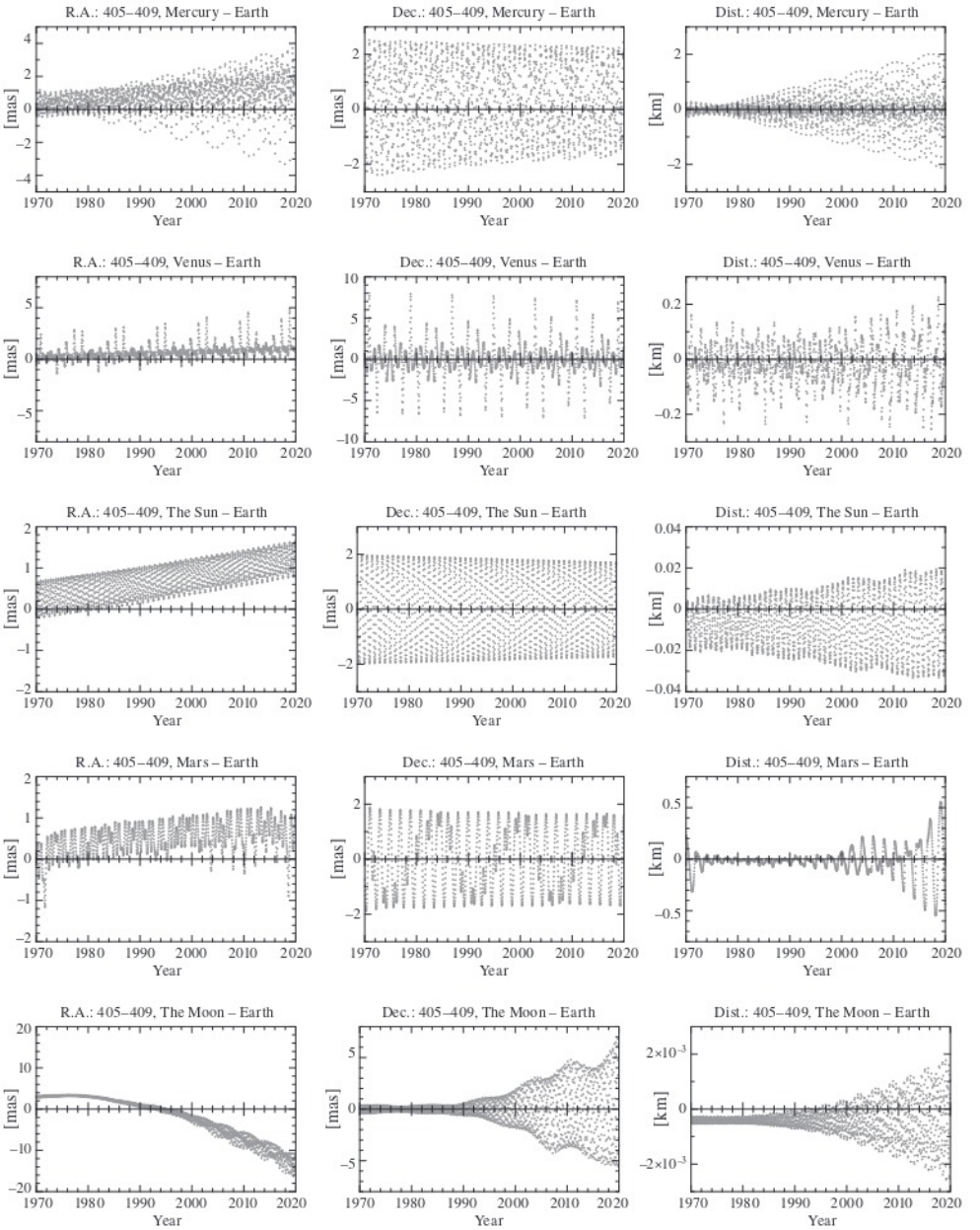
One can also compare DE405 with DE409. Importantly, this more recent ephemeris includes both ranging and VLBI measurements of the MGS (1999–) and the Odyssey (2002–) spacecraft in orbit around Mars (Konopliv 2002, 2003; Border 2002, 2003), and also the continuing CCD measurements of the outer planets and their satellites (Stone 1998; Stone and Harris 2000). As such, DE409 is believed to be more accurate than DE405, and the differences certainly represent the sizes of the uncertainties in DE405, if not estimates of the actual errors themselves. The differences, DE405−DE409, are shown in Figs. 8.11 through 8.20.



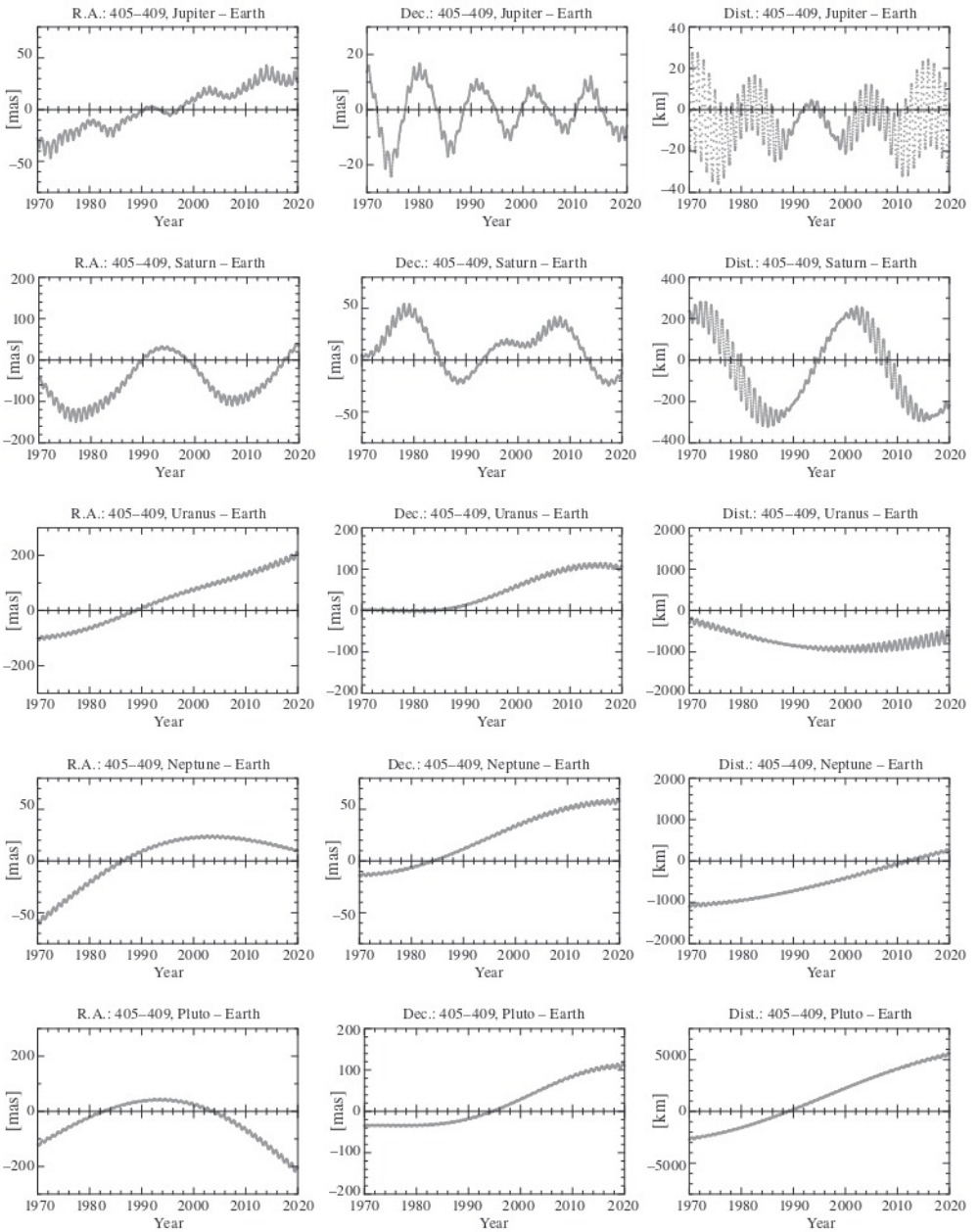
Figures 8.1–8.5 Differences in right ascension, declination and distance between DE200−DE409



Figures 8.6–8.10 Differences in right ascension, declination and distance between DE200−DE409



Figures 8.11–8.15 Differences in right ascension, declination and distance between DE405−DE409



Figures 8.16–8.20 Differences in right ascension, declination and distance between DE405−DE409

It may be immediately noticed that the later differences, DE405−DE409, are significantly smaller than those of DE200−DE405. As the observational data accumulate, the convergence of the ephemerides becomes a good indicator of the inherent errors and uncertainties.

The comparisons of both DE200 and DE405 with DE409 are discussed in further detail in Standish (2004).

8.10 Keplerian Elements for Approximate Positions of the Major Planets

Lower accuracy formulae for planetary positions have a number of important applications when one doesn't need the full accuracy of an integrated ephemeris. They are often used in observation scheduling, telescope pointing, and prediction of certain phenomena as well as in the planning and design of spacecraft missions.

Approximate positions of the nine major planets may be found by using Keplerian formulae with their associated elements and rates. Such elements are not intended to represent any sort of mean; they are simply the result of being adjusted for a best fit. As such, it must be noted that the elements are not valid outside the given time-interval over which they were fit.

The elements are given in Table 8.7 or in Tables 8.8 and 8.9, depending upon the time-interval over which they were fit and within which they are to be used.

Formulae for using them are given in § 8.10.1.

Table 8.7 Keplerian elements and their rates, with respect to the mean ecliptic and equinox of J2000.0, valid for the time-interval A.D. 1800–A.D. 2050

	a [au,au/cy]	e [rad,rad/cy]	I [deg,deg/cy]	L [deg,deg/cy]	ϖ [deg,deg/cy]	Ω [deg,deg/cy]
Mercury	0.38709927	0.20563593	7.00497902	252.25032350	77.45779628	48.33076593
	0.00000037	0.00001906	−0.00594749	149472.67411175	0.16047689	−0.12534081
Venus	0.72333566	0.00677672	3.39467605	181.97909950	131.60246718	76.67984255
	0.00000390	−0.00004107	−0.00078890	58517.81538729	0.00268329	−0.27769418
EM Bary	1.00000261	0.01671123	−0.00001531	100.46457166	102.93768193	0.0
	0.00000562	−0.00004392	−0.01294668	35999.37244981	0.32327364	0.0
Mars	1.52371034	0.09339410	1.84969142	−4.55343205	−23.94362959	49.55953891
	0.00001847	0.00007882	−0.00813131	19140.30268499	0.44441088	−0.29257343
Jupiter	5.20288700	0.04838624	1.30439695	34.39644051	14.72847983	100.47390909
	−0.00011607	−0.00013253	−0.00183714	3034.74612775	0.21252668	0.20469106
Saturn	9.53667594	0.05386179	2.48599187	49.95424423	92.59887831	113.66242448
	−0.00125060	−0.00050991	0.00193609	1222.49362201	−0.41897216	−0.28867794
Uranus	19.18916464	0.04725744	0.77263783	313.23810451	170.95427630	74.01692503
	−0.00196176	−0.00004397	−0.00242939	428.48202785	0.40805281	0.04240589
Neptune	30.06992276	0.00859048	1.77004347	−55.12002969	44.96476227	131.78422574
	0.00026291	0.00005105	0.00035372	218.45945325	−0.32241464	−0.00508664
Pluto	39.48211675	0.24882730	17.14001206	238.92903833	224.06891629	110.30393684
	−0.00031596	0.00005170	0.00004818	145.20780515	−0.04062942	−0.01183482

Table 8.8 Keplerian elements and their rates, with respect to the mean ecliptic and equinox of J2000.0, valid for the time-interval 3000 B.C.–A.D. 3000. Further, the computation of M for Jupiter through Pluto *must* be augmented by the additional terms described in Eq. 8.30 and given in Table 8.9.

	a [au,au/cy]	e [rad,rad/cy]	I [deg,deg/cy]	L [deg,deg/cy]	ϖ [deg,deg/cy]	Ω [deg,deg/cy]
Mercury	0.38709843	0.20563661	7.00559432	252.25166724	77.45771895	48.33961819
	0.00000000	0.00002123	−0.00590158	149472.67486623	0.15940013	−0.12214182
Venus	0.72332102	0.00676399	3.39777545	181.97970850	131.76755713	76.67261496
	−0.00000026	−0.00005107	0.00043494	58517.81560260	0.05679648	−0.27274174
EM Bary	1.00000018	0.01673163	−0.00054346	100.46691572	102.93005885	−5.11260389
	−0.00000003	−0.00003661	−0.01337178	35999.37306329	0.31795260	−0.24123856
Mars	1.52371243	0.09336511	1.85181869	−4.56813164	−23.91744784	49.71320984
	0.00000097	0.00009149	−0.00724757	19140.29934243	0.45223625	−0.26852431
Jupiter	5.20248019	0.04853590	1.29861416	34.33479152	14.27495244	100.29282654
	−0.00002864	0.00018026	−0.00322699	3034.90371757	0.18199196	0.13024619
Saturn	9.54149883	0.05550825	2.49424102	50.07571329	92.86136063	113.63998702
	−0.00003065	−0.00032044	0.00451969	1222.11494724	0.54179478	−0.25015002
Uranus	19.18797948	0.04685740	0.77298127	314.20276625	172.43404441	73.96250215
	−0.00020455	−0.00001550	−0.00180155	428.49512595	0.09266985	0.05739699
Neptune	30.06952752	0.00895439	1.77005520	304.22289287	46.68158724	131.78635853
	0.00006447	0.00000818	0.00022400	218.46515314	0.01009938	−0.00606302
Pluto	39.48686035	0.24885238	17.14104260	238.96535011	224.09702598	110.30167986
	0.00449751	0.00006016	0.00000501	145.18042903	−0.00968827	−0.00809981

Table 8.9 Additional terms which must be added to the computation of M for Jupiter through Pluto, 3000 B.C.to A.D. 3000, as described in Eq. 8.30

	b	c	s	f
Jupiter	−0.00012452	0.06064060	−0.35635438	38.35125000
Saturn	0.00025899	−0.13434469	0.87320147	38.35125000
Uranus	0.00058331	−0.97731848	0.17689245	7.67025000
Neptune	−0.00041348	0.68346318	−0.10162547	7.67025000
Pluto	−0.01262724			

8.10.1 Formulae for Using the Keplerian Elements

Keplerian elements given in the Tables 8.7–8.9 are

a_o, $\dot{a}$	semimajor axis [au, au/century]
e_o, $\dot{e}$	eccentricity [radians, radians/century]
I_o, $\dot{I}$	inclination [degrees, degrees/century]
L_o, $\dot{L}$	mean longitude [degrees, degrees/century]
ϖ_o, $\dot{\varpi}$	longitude of perihelion [degrees, degrees/century] ($\varpi = \omega + \Omega$)

Ω_o, $\dot{\Omega}$ longitude of the ascending node [degrees, degrees/century]

In order to obtain the coordinates of one of the planets at a given Julian Ephemeris Date, T_{eph},

1. Compute the value of each of that planet's six elements: $a = a_o + \dot{a}T$, etc., where T, the number of centuries past J2000.0, is T=(T_{eph}-2451545.0)/36525.
2. Compute the argument of perihelion, ω, and the mean anomaly, M:

$$\omega = \varpi - \Omega \quad ; \quad M = L - \varpi + bT^2 + c\cos(fT) + s\sin(fT) \tag{8.30}$$

   where the last three terms must be added to M for Jupiter through Pluto when using the formulae for 3000 B.C.to A.D. 3000.
3. Modulus the mean anomaly so that $-180° \le M \le +180°$ and then obtain the eccentric anomaly, E, from the solution of Kepler's equation (see § 8.10.2):

$$M = E - e^* \sin E \tag{8.31}$$

   where $e^* = 180/\pi \times e = 57.29578\, e$.
4. Compute the planet's heliocentric coordinates in its orbital plane, $\mathbf{r}'$, with the x'-axis aligned from the focus to the perihelion:

$$x' = a(\cos E - e) \quad ; \quad y' = a\sqrt{1-e^2}\,\sin E \quad ; \quad z' = 0. \tag{8.32}$$

5. Compute the coordinates, $\mathbf{r}_{ecl}$, in the J2000.0 ecliptic plane, with the x-axis aligned toward the equinox:

$$\mathbf{r}_{ecl} = \mathcal{M}\mathbf{r}' \equiv \mathcal{R}_z(-\Omega)\mathcal{R}_x(-I)\mathcal{R}_z(-\omega)\mathbf{r}' \tag{8.33}$$

   so that

$$\begin{aligned} x_{ecl} = {} & (\cos\omega\cos\Omega - \sin\omega\sin\Omega\cos I)\; x' + (-\sin\omega\cos\Omega - \cos\omega\sin\Omega\cos I)\; y' \\ y_{ecl} = {} & (\cos\omega\sin\Omega + \sin\omega\cos\Omega\cos I)\; x' + (-\sin\omega\sin\Omega + \cos\omega\cos\Omega\cos I)\; y' \\ z_{ecl} = {} & (\sin\omega\sin I)\; x' + (\cos\omega\sin I)\; y' \end{aligned} \tag{8.34}$$

6. If desired, obtain the equatorial coordinates in the "ICRF", or "J2000.0 frame", $\mathbf{r}_{eq}$:

$$\begin{aligned} x_{eq} &= x_{ecl} \\ y_{eq} &= +\cos\varepsilon\; y_{ecl} - \sin\varepsilon\; z_{ecl} \\ z_{eq} &= +\sin\varepsilon\; y_{ecl} + \cos\varepsilon\; z_{ecl} \end{aligned} \tag{8.35}$$

   where the obliquity at J2000.0 is $\varepsilon = 23.^\circ 43928$.

8.10.2 Solution of Kepler's Equation, $M = E - e\sin E$

Given the mean anomaly, M, and the eccentricity, e, both in radians, start with

$$E_0 = M + e\sin M \tag{8.36}$$

and iterate the following three equations, with $n = 0, 1, 2, \ldots$, until $|\Delta E| \le tol$:

$$\Delta M = M - (E_n - e\sin E_n) \;;\; \Delta E = \Delta M/(1 - e\cos E_n) \;;\; E_{n+1} = E_n + \Delta E. \tag{8.37}$$

For the approximate formulae in this present context, $tol = 10^{-7}$ radians is sufficient.

Table 8.10 Approximate errors in right ascension, α, declination, δ, and distance, ρ, from the Keplerian formulation of § 8.10.3

	1800–2050			3000 B.C.to A.D. 3000		
	α [″]	δ [″]	ρ [1000 km]	α [″]	δ [″]	ρ [1000 km]
Mercury	15	1	1	20	15	1
Venus	20	1	4	40	30	8
EM Bary	20	8	6	40	15	15
Mars	40	2	25	100	40	30
Jupiter	400	10	600	600	100	1000
Saturn	600	25	1500	1000	100	4000
Uranus	50	2	1000	2000	30	8000
Neptune	10	1	200	400	15	4000
Pluto	5	2	300	400	100	2500

8.10.3 Approximate Accuracies of the Keplerian Formulae

Table 8.10 gives the accuracies that one can expect from the Keplerian formulation given in this section.

8.11 The Availability of Ephemerides

The fundamental ephemerides used in *The Astronomical Almanac* since 1984, DE200 (1984–2002) and DE405(2003–), are both available on a CD-ROM from the publisher, Willmann-Bell, see URL[3]. The package allows a professional user to obtain the rectangular coordinates of the Sun, Moon, and nine major planets by means of a simple subroutine written in standard Fortran:

Willmann-Bell, Inc.
PO Box 35025
Richmond, VA 23235
804-320-7016
804-272-5920 (Fax)

The ephemerides are also available as described in URL[4]; see links within that website. Also described there are references to other packages and toolkits for the use of the ephemerides, as well as to the software being available in other programming languages.

The README on URL[4] also contains a few modifications to the software from the CD-ROM. However, it should be easier for the user to retrieve the software from the website, even when using the data files from the CD-ROM.

One may also use the interactive website, *Horizons*, URL[5], which uses the JPL ephemerides, giving positional data (in 2011) for over 70 astronomical quantities for the 8 planets and Pluto, more than 170 natural satellites and over 500 000 asteroids and comets; Horizons uses the full precision of the JPL ephemerides.

There are certainly other sources of ephemerides, though not all use DE200 or DE405, the fundamental ephemerides of *The Astronomical Almanac*. Further, there do exist a number of packages which provide less accurate positions for the solar system bodies.

A description of a number of options may be found at URL[6].

Acknowledgements

The research described in this chapter was carried out at the Jet Propulsion Laboratory, California Institute of Technology, under a contract with the National Aeronautics and Space Administration. Government sponsorship is acknowledged.

REFERENCES

1. Observational Data Used for Ephemeris Production: http://ssd.jpl.nasa.gov/plan-eph-data/index.html.
2. IERS Conventions 2003 (Technical Note 32): http://www.usno.navy.mil/USNO/earth-orientation/eo-info/general/conv2003/.
3. Commercially Available JPL Planetary and Lunar Ephemerides: http://www.willbell.com/software/jpl.htm.
4. JPL Ephemerides Export Information: http://iau-comm4.jpl.nasa.gov/README.
5. JPL Horizons System: http://ssd.jpl.nasa.gov/?horizons.
6. Ephemerides via IAU Commission 4: http://iaucom4.org/ephemerides.html.

Anderson, J. D., R. F. Jurgens, E. L. Lau, and M. A. Slade (1996). Shape and Orientation of Mercury from Radar Ranging Data. *Icarus 124*, 690–697.

Berge, G. L., D. O. Muhleman, and R. P. Linfield (1988). Very Large Array Observations of Uranus at 2.0 cm. *Astronomical Journal 96*, 388–395.

Border, J. S. (2002, 2003). Private communications.

Brown, E. W. (1919). *Tables of the Motion of the Moon*. New Haven, CT: Yale University Press.

Chao, C. C. (1970). A Preliminary Estimation of Tropospheric Influence on the Range and Range Rate Data During the Closest Approach of the MM71 Mars Mission. Technical Memo 391-129, Jet Propulsion Laboratory.

Clemence, G. M. (1954). Perturbations of the Five Outer Planets by the Four Inner Ones. In *Astronomical Papers of the American Ephemeris and Nautical Almanac*, Volume XIII, part V. Washington, DC: U.S. Government Printing Office.

Clemence, G. M., J. G. Porter, and D. H. Sadler (1952). Aberration in the Lunar Ephemeris. *Astronomical Journal 57*, 46–47.

Debarbat, S. and B. Guinot (1970). *La Methode des Hauteurs Egales en Astronomie*. Paris: Gordon & Breach.

Eckert, W., D. Brouwer, and G. M. Clemence (1951). Coordinates of the Five Outer Planets 1953–2060. In *Astronomical Papers of the American Ephemeris and Nautical Almanac*, Volume XII. Washington, DC: U.S. Government Printing Office.

Eckert, W. J., R. Jones, and H. K. Clark (1954). *Improved Lunar Ephemeris 1952–1959*. Washington, D.C.: U.S. Naval Observatory, Nautical Almanac Office.

Eckert, W. J., T. C. Van Flandern, and G. A. Wilkins (1969). A Note on the Evaluation of the Latitude of the Moon. *Monthly Notices of the Royal Astronomical Society 146*, 473–478.

Eckert, W. J., M. J. Walker, and D. D. Eckert (1966). Transformation of the Lunar Coordinates and Orbital Parameters. *Astronomical Journal 71*, 314–332.

Eckhardt, D. H. (1981). Theory of the libration of the Moon. *Moon and the Planets 25*, 3–49.

Estabrook, F. B. (1971a). Private communications.

Estabrook, F. B. (1971b). Derivation of Relativistic Lagrangian for n-Body Equations containing Relativity Parameters β and γ. IOM 14 June 1971, Jet Propulsion Laboratory. Section 328.

Folkner, W. F., C. F. Yoder, D. N. Yuan, E. M. Standish, and R. A. Preston (1998). Interior Structure and Seasonal Mass Redistribution of Mars from Radio Tracking of Mars Pathfinder. *Science 278*, 1749–1752.

Folkner, W. M., P. Charlot, M. H. Finger, J. G. Williams, O. J. Sovers, X. X. Newhall, and E. M. Standish (1993). Determination of the extragalactic frame tie from joint analysis of radio interferometric and lunar laser ranging measurements. *Astronomy and Astrophysics 287*, 279–289.

Fricke, W. (1971). A Rediscussion of Newcomb's Determination of Precession. *Astronomy and Astrophysics 13*, 298–308.

Fricke, W. (1982). Determination of the Equinox and Equator of the FK5. *Astronomy and Astrophysics 107*, L13–L16.

Fricke, W. and A. Kopff (1963). *Fourth Fundamental Catalogue (FK4)*. Heidelberg: Astronomisches Rechen-Institut. Veroffentlichungen #10.

Konopliv, A. S. (2002, 2003). Private communications.

Krogh, F. T. (1972). *Lecture Notes in Mathematics, 362*. New York: Springer-Verlag. p. 22.

Lieske, J. H., T. Lederle, W. Fricke, and B. Morando (1977). Expressions for the Precession Quantities Based upon the IAU (1976) System of Astronomical Constants. *Astronomy and Astrophysics 58*, 1–16.

Lyttleton, R. A., D. L. Cain, and A. S. Liu (1979). Nutation of Mars. JPL Publication 79-85, Jet Propulsion Laboratory.

Ma, C., E. F. Arias, T. M. Eubanks, A. L. Fey, A.-M. Gontier, C. S. Jacobs, O. J. Sovers, B. A. Archinal, and P. Charlot (1998). The International Celestial Reference Frame as Realized by Very Long Baseline Interferometry. *Astronomical Journal 116*, 516–546.

Morrison, L. V. (1996). Private communications.

Moyer, T. D. (1971). Mathematical Formulation of the Double-Precision Orbit Determination Program (DPODP). Technical Report 32-1527, Jet Propulsion Laboratory.

Moyer, T. D. (2000). Formulation for Observed and Computed Values of Deep Space Network Data Types for Navigation. JPL Publication 00-7, Jet Propulsion Laboratory.

Muhleman, D. O. and J. D. Anderson (1981). Solar Wind Electron Densities from Viking Dual-Frequency Radio Measurements. *Astrophysical Journal 247*, 1093–1101.

Muhleman, D. O., G. L. Berge, and D. Jones (1988). VLA Observations of Neptune and the Mass of Triton. Informal report, CalTech.

Muhleman, D. O., G. L. Berge, and D. J. Rudy (1986). Precise VLA Positions and Flux-Density Measurements of the Jupiter System. *Astronomical Journal 92*, 1428–1435.

Muhleman, D. O., G. L. Berge, D. J. Rudy, A. E. Niell, R. P. Linfield, and E. M. Standish (1985). Precise Position Measurements of Jupiter, Saturn and Uranus Systems with the Very Large Array. *Celestial Mechanics 37*, 329–337.

Newcomb, S. (1898a). Tables of the Heliocentric Motion of Mars. In *Astronomical Papers of the American Ephemeris and Nautical Almanac*, Volume VI, part IV. Washington, DC: U.S. Government Printing Office.

Newcomb, S. (1898b). Tables of the Heliocentric Motion of Mercury. In *Astronomical Papers of the American Ephemeris and Nautical Almanac*, Volume VI, part II. Washington, DC: U.S. Government Printing Office.

Newcomb, S. (1898c). Tables of the Heliocentric Motion of Venus. In *Astronomical Papers of the American Ephemeris and Nautical Almanac*, Volume VI, part III. Washington, DC: U.S. Government Printing Office.

Newcomb, S. (1898d). Tables of the Motion of the Earth on its Axis and Around the Sun. In *Astronomical Papers of the American Ephemeris and Nautical Almanac*, Volume VI, part I. Washington, DC: U.S. Government Printing Office.

Newhall, X. X., E. M. Standish, and J. G. Williams (1983). DE102: a numerically integrated ephemeris of the Moon and planets spanning forty-four centuries. *Astronomy and Astrophysics 125*, 150–167.

Newhall, X. X. and J. G. Williams (1997). Estimation of the Lunar Physical Librations. *Celestial Mechanics and Dynamical Astronomy 66*, 21–30.

Nicholson, P. D. (1992). Private communications.

Pettengill, G. H., E. Eliason, P. G. Ford, G. B. Loriot, H. Masursky, and G. E. McGill (1980). Pioneer Venus Radar Results: Altimetry and Surface Properties. *Journal of Geophysical Research 85, A13*, 8261–8270.

Ross, F. E. (1917). New Elements of Mars. In *Astronomical Papers of the American Ephemeris and Nautical Almanac*, Volume IX, part II. Washington, DC: U.S. Government Printing Office.

Schwan, H. (1983). *A Method for the Determination of a System of Positions and Proper Motions of Stars with an Application to the Washington 6 Inch TC Observations*. Heidelberg: Astronomisches Rechen-Institut. Veroffentlichungen #30.

Shapiro, I. I. (1964). Fourth Test of General Relativity. *Physical Review Letters 13*, 789.

Standish, E. M. (1982). Orientation of the JPL Ephemerides, DE200/LE200, to the Dynamical Equinox of J2000. *Astronomy and Astrophysics 114*, 297–302.

Standish, E. M. (1990). The observational basis for JPL's DE200, the planetary ephemerides of the Astronomical Almanac. *Astronomy and Astrophysics 233*, 252–271.

Standish, E. M. (1998). Time Scales in the JPL and CfA Ephemerides. *Astronomy and Astrophysics 336*, 381–384.

Standish, E. M. (2004). An approximation to the errors in the planetary ephemerides of the Astronomical Almanac. *Astronomy and Astrophysics 417*, 1165–1171.

Standish, E. M., X. X. Newhall, J. G. Williams, and D. K. Yoemans (1992). Orbital Ephemerides of the Sun, Moon, and Planets. In P. K. Seidelmann (Ed.), *Explanatory Supplement to The Astronomical Almanac*, Chapter 5, pp. 279–323. Mill Valley, CA: University Science Books.

Standish, E. M. and J. G. Williams (1990). Dynamical Reference Frames in the Planetary and Earth–Moon Systems. In J. H. Lieske and V. K. Abalakin (Eds.), *Inertial Coordinate System on the Sky*, Dordrecht, pp. 173–181. Kluwer.

Stone, R. C. (1998). CCD Positions for the Outer Planets in 1996-97 Determined in the Extragalactic Reference Frame. *Astronomical Journal 116*, 1461–1469.

Stone, R. C. and F. H. Harris (2000). CCD Positions Determined in the International Celestial Reference Frame (ICRF) for the Outer Planets and Many of their Satellites in 1995-99. *Astronomical Journal 119*, 1985–1998.

Will, C. M. (1974). The theoretical tools of experimental gravitation. In B. Bertotti (Ed.), *Experimental Gravitation*, New York. Academic Press. Proceedings of the International School of Physics "Enrico Fermi"; course 56.

Williams, J. G. (1984). Determining Asteroid Masses from Perturbations on Mars. *Icarus 57*, 1–13.

Williams, J. G. (1994). Contributions to the Earth's obliquity rate, precession, and nutation. *Astronomical Journal 108*, 711–724.

Williams, J. G., D. H. Boggs, C. F. Yoder, J. T. Ratcliff, and J. O. Dickey (2001). Lunar rotational dissipation in solid body and molten core. *Journal of Geophysical Research 106 E11*, 27933–27968.

Williams, J. G. and E. M. Standish (1989). Dynamical Reference Frames in the Planetary and Earth–Moon Systems. In J. Kovalevsky, I. I. Mueller, and B. Kolaczek (Eds.), *Reference Frames*, Dordrecht. Kluwer.

Yoder, C. F. (1979). Effects of the Spin–Spin Interaction and the Inelastic Tidal Deformation on the Lunar Physical Librations. In P. E. Nacozy and S. Ferraz-Mello (Eds.), *Natural and Artificial Satellite Motion*, University of Texas Press. Austin.

CHAPTER 9

Planetary Satellites and Rings

JAMES R. ROHDE AND MARK STOLLBERG

9.1 Introduction

The ephemerides of most satellites in *The Astronomical Almanac* are calculated from a set of analytical expressions, termed a *theory*, for the motion of the satellite in an orbit that is basically an ellipse, but subject to various perturbing forces, such as the oblateness of the planet and the attractions of other satellites and the Sun. The orbits of the outer satellites of Jupiter are highly perturbed and representations by theories are not sufficiently accurate. In these cases numerical integrations of the equations of motion of the satellites are used.

The objective of this chapter is to describe the theory of the motion of each of the principal satellites in enough detail for search and identification purposes. In many cases, a description of the complete theory that can be used for the precise analysis of observations is given, but in cases where the theories contain large numbers of periodic terms, only an outline of the theory is given, together with references to where the complete theory can be found.

There has been a recent proliferation of known satellites associated with the gas giant planets. A set of criteria has been developed for which satellites are included in *The Astronomical Almanac*; see § 9.6 for details. A more complete listing of the satellites is given in *The Astronomical Almanac Online* at URL[1].

9.2 Orbital Elements and Perturbations

9.2.1 Orbital Elements

In this section we use a fairly common notation to define the *osculating elements*, formulae, and transformations. The orientation of the orbital plane relative to a reference plane and origin are described by three elements, which are shown in Figs. 9.1 and 9.2. These elements are

$$\omega = \text{argument of the pericenter}$$
$$\Omega = \text{longitude of the ascending node}$$
$$i = \text{inclination.}$$

In addition, the size and shape of the orbit are described by the semimajor axis a and eccentricity e. The position of the satellite along the orbit, measured from the pericenter, is described by the *mean anomaly* M or the *true anomaly* f. The difference $f - M$ is known

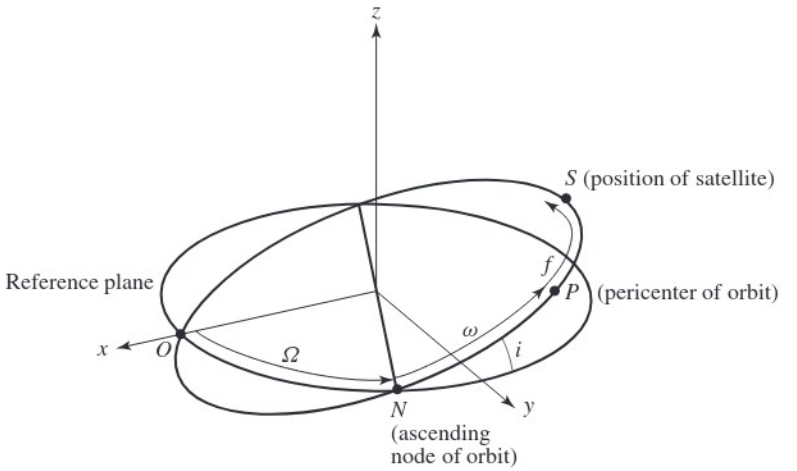


Figure 9.1 The orbital elements used to describe the orbital plane relative to a reference plane and an origin of longitude O

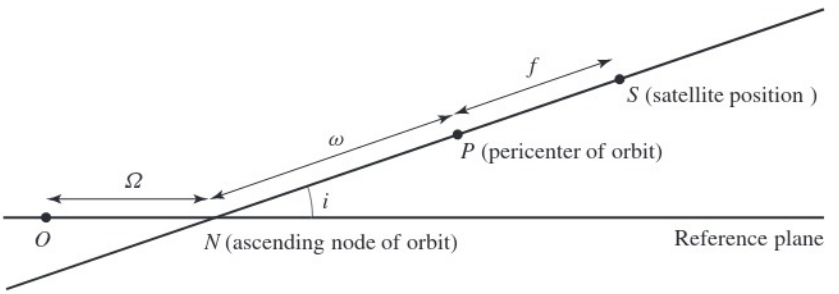


Figure 9.2 An equivalent form of the orbital elements. The end-on view of a great circle on the celestial sphere is represented as a straight line. Triangles formed by such lines are spherical triangles, and the formulae of spherical trigonometry apply.

as the *equation of center*. The equation of center can be approximated to sufficient accuracy for the satellites by

$$f - M = \left(2e - \frac{1}{4}e^3\right)\sin M + \frac{5}{4}e^2 \sin 2M + \frac{13}{12}e^3 \sin 3M. \tag{9.1}$$

For many satellites the pericenter is ill-defined since e is small, or the node is ill-defined since i is small. In the former case it is usual to use the quantity λ, rather than M, and in the latter case the quantity ϖ, rather than ω, where

$$\begin{aligned} \lambda &= M + \omega + \Omega \qquad \text{(the mean longitude)} \\ \varpi &= \omega + \Omega \qquad \text{(the longitude of pericenter)}. \end{aligned} \tag{9.2}$$

9.2.2 Secular Perturbations of the Orbit

If the orbit were unperturbed, then all the elements would remain constant except the mean anomaly M, which would increase at a constant rate n, the mean motion of the satellite. For a perturbed orbit the same elliptical model can be used, but the orbital elements, now called osculating elements, are functions of time, typically of the form of a constant plus periodic terms. In addition, the angular elements can have a linear (or secular) variation with time. The form of the expressions for the osculating elements depends on the reference plane chosen. The oblateness of the planet causes the pole of the orbital plane to precess around the pole of the planet, and solar perturbations cause it to precess around the pole of the planet's orbit. Perturbations by other satellites cause precession around the poles of their orbital planes, but usually this effect is smaller than the other two effects. Because the satellites' orbital poles are usually close to the pole of the planet, their effect is primarily an addition to the oblateness effect. The *Laplacian plane* is the reference plane about whose axis the satellite's orbit precesses as a result of these two major effects. The axis of the Laplacian plane is coplanar with and between the polar and orbital axes of the planet. Hence, the node of the orbit regresses around a plane that lies between the equatorial and orbital planes of the planet, and has a common line of intersection with the planes. The orbit maintains a constant inclination to the Laplacian plane (apart from other, usually smaller perturbing effects). The Laplacian plane is also known as the *invariable plane* through the planet.

The location of the Laplacian plane is shown in Fig. 9.3. It divides the angle between the equatorial and orbital planes into parts i_1 and i_2, where

$$2n^2 J_2 r_0^2 \sin 2i_2 = a^2 n'^2 (1 - e'^2)^{-1/2} \sin 2i_1 \tag{9.3}$$

where J_2 is the oblateness coefficient of the planet; r_0 is the equatorial radius of the planet; n' is the orbital mean motion of the planet; e' is the orbital eccentricity of the planet; and n is the mean motion of the satellite.

Apart from small short-period perturbations, the motion of the satellite's orbit relative to the Laplacian plane is such that

$$\begin{aligned} \gamma &= \text{constant} \\ \theta &= \theta_0 - K(t - t_0) \end{aligned} \tag{9.4}$$

where γ is the inclination of the satellite's orbit to the Laplacian plane, and θ is the arc reckoned from the intersection of the planet's equatorial and orbital planes along the Laplacian plane to the node of the satellite's orbit on the Laplacian plane. However, it is usually more convenient to take a plane other than the Laplacian plane as the reference plane, as it eases the calculation of perturbations by other objects, and also eases the transformation of the calculated position to a reference frame based on the Earth's equator (which is needed for comparison with observations). If, for example, the orbital plane of the planet in Fig. 9.3 is taken as the reference plane, then the osculating inclination and longitude of the node will be the angles i and Ω. The formulae of spherical trigonometry give

$$\begin{aligned} \sin i \sin(\Omega - \Omega_1) &= \sin \gamma \sin \theta \\ \sin i \cos(\Omega - \Omega_1) &= \cos \gamma \sin i_1 + \sin \gamma \cos i_1 \cos \theta \end{aligned} \tag{9.5}$$

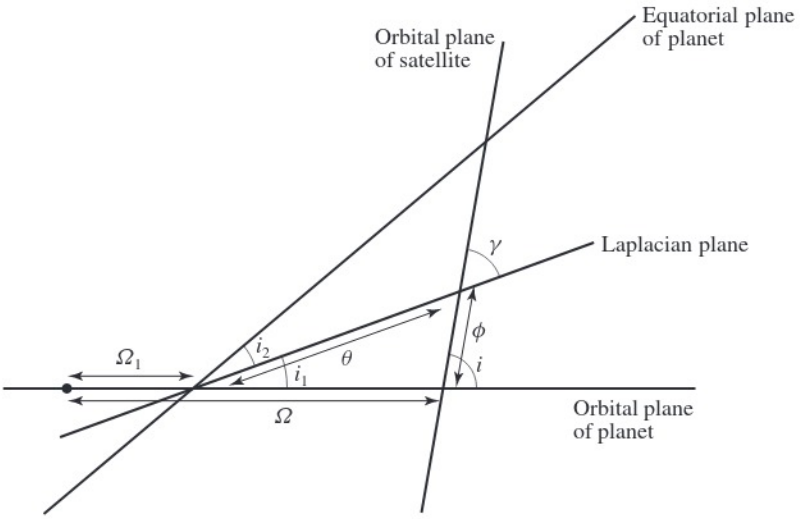


Figure 9.3 The Laplacian plane

where i_1, Ω_1 are the inclination and longitude of the node of the Laplacian plane relative to the adopted reference plane; and γ and θ are defined above. In most cases γ is small, and so $(\Omega - \Omega_1)$ is small as well. Thus, the following approximate formulae are obtained:

$$\begin{aligned} i &= i_1 + \gamma \cos\theta \\ \Omega &= \Omega_1 + \gamma \sin\theta / \sin i. \end{aligned} \tag{9.6}$$

Hence, the use of a reference plane other than the Laplacian plane introduces a periodic oscillation into the osculating inclination and longitude of the node. Note that i_1 and Ω_1 are quantities whose values are determined by the physical properties of the system. The arbitrary constants associated with the inclination and node are the quantities γ and the phase of θ. This choice of reference plane also introduces a periodic variation, equal to the angular difference $\phi + \Omega - \Omega_1 - \theta$, into the longitude of the pericenter and the mean longitude. This periodic variation is given approximately by

$$\Delta\varpi, \ \ \Delta\lambda = \gamma \tan \frac{1}{2} i_1 \sin\theta. \tag{9.7}$$

For most satellites the oblateness effect on the orbital plane is much larger than the solar perturbations, and so the Laplacian plane is very close to the equatorial plane. For a more distant satellite, such as Iapetus, the effects are comparable, so the Laplacian plane lies about midway between the equatorial and orbital planes. For the Moon, the solar perturbations dominate, and the Laplacian plane virtually coincides with the Earth's mean orbital plane—the ecliptic.

The oblateness, solar, and other perturbations also cause secular variations of the longitude of pericenter (in most cases the pericenter advances around the orbit) and of the mean longitude of the satellite, so that the mean motion in longitude is different from (generally greater than) the value derived from Kepler's law for an unperturbed orbit. It is this overall

rate of motion that is quoted as the satellite's mean motion, and it is thus an observed mean motion. Hence, when using the mean motion to determine the mass of the planet from Kepler's law, one must allow for the part of it due to secular perturbations.

It is useful to note in this context that the semimajor axis of the orbit is affected in a similar way. The various perturbing forces cause perturbations of the eccentricity and the longitude of the pericenter of the form

$$\begin{aligned} \Delta e &= A \cos M \\ e\Delta\varpi &= A \sin M. \end{aligned} \tag{9.8}$$

The effect of these terms on the true longitude is zero to first-order. The perturbation of the distance r arising from Δe and $\Delta\varpi$ is obtained from

$$r = a(1 - e \cos M) \tag{9.9}$$

with $M = \lambda - \varpi$.

Differentiating Eq. 9.9, we have

$$\begin{aligned} \Delta r &= -a \cos M \Delta e - ae \sin M \Delta\varpi \\ &= -aA. \end{aligned} \tag{9.10}$$

It is the normal practice to ignore these terms in e and ϖ, and to determine the value of the semimajor axis from observations that will absorb the constant term. This must be allowed for when computing the mass of the planet from Kepler's law.

9.2.3 Perturbations due to Commensurabilities

There are many instances of pairs of satellites with mean motions, n and n', having a relationship of the form

$$pn \simeq qn' \tag{9.11}$$

where p and q are two small integers. Such a situation is called a commensurability of mean motions or, more simply, an *orbital resonance*, because it causes increased mutual perturbations. This resonance effect is caused by a repeated geometric relationship of the positions of the two satellites (their longitudes) relative to a particular point in their orbits. This point is usually the pericenter of one of the satellites, but for Mimas-Tethys it is the midpoint of their nodes on the equator of Saturn. We shall take as an example the case where the commensurability is

$$2n' - n - \dot{\varpi} \simeq 0. \tag{9.12}$$

The prime refers to the outer satellite, and $\dot{\varpi}$ is the secular rate of change of the longitude of the pericenter of the inner satellite, caused by the oblateness of the planet, other perturbations, and by the resonance itself. As a result the angular argument

$$\theta = 2\lambda' - \lambda - \varpi \tag{9.13}$$

varies very slowly. If θ either increases or decreases continually, then the motion is termed *circulation*, because the position of conjunctions of the satellites circulates around their orbits, and in this case the mutual perturbations are not particularly large. In many cases, however,

the average rate of change of θ is zero, and the value of θ oscillates about either 0° or 180°, depending on the type of commensurability. This type of motion is termed *libration*. In this example, the libration is about 0°, and we can write θ as

$$\theta = (\lambda - \varpi) - 2(\lambda - \lambda') = 0^\circ + \text{oscillation}\,. \tag{9.14}$$

At a conjunction of the satellites, $\lambda - \lambda' = 0$, and so $\lambda - \varpi$ will be close to zero also, and hence all conjunctions occur near the pericenter of the inner satellite orbit. As might be expected, this particular type of resonance has a significant perturbing effect on the longitudes of the two satellites, and on the longitude of pericenter and eccentricity of the inner satellite. If the libration amplitude is small, then the libration can be represented adequately by a single periodic term; e.g.,

$$\theta = 0^\circ + B\,\sin(\beta t + \varepsilon). \tag{9.15}$$

If the amplitude is large, e.g., for the Titan-Hyperion and Mimas-Tethys resonances, then a Fourier series is needed to represent the libration. The amplitude B and phase ε of the libration are the arbitrary constants associated with e and ϖ. The libration frequency β is a function of the masses of the satellites, the closeness of the commensurability, and the libration amplitude, if it is large.

The principal effects of this resonance on the orbit are to cause perturbations of the longitudes of the satellites with the period of the libration, and to cause a forced component of the eccentricity, whose magnitude depends on the mass of the perturbing satellite and the closeness of the commensurability. This forced component is usually the largest component of the eccentricity.

The commensurabilities that are of most significance in the satellite systems are listed in Table 9.1. In addition many of the features of the rings of Saturn are associated with commensurabilities with satellites. Some of the small satellites of Saturn are in 1:1 commensurabilities with the major satellites. These commensurabilities cause the small satellites to follow or precede the major satellites by 60° in their orbits. The 2:1 commensurabilities among the Galilean satellites Io, Europa, and Ganymede are closely associated with the Laplace commensurability that affects all three satellites; as a result, the long-term mean value of $(n_1 - 3n_2 + 2n_3)$ is exactly zero, and the angular argument $(\lambda_1 - 3\lambda_2 + 2\lambda_3)$ has a mean value of 180°, and oscillates about this value with amplitude 0°.066 and period 2070 days.

9.2.4 Long-Period Perturbations by Other Satellites

The pericenters and nodes of satellite orbits move slowly compared with the orbital speed, and so the relative motion of the pericenters or nodes of a pair of satellites is slow, and significant perturbations can arise from the arguments $\varpi - \varpi'$ or $\Omega - \Omega'$. In the planetary system these are called *secular perturbations*, but they are in fact of very long period—25,000 years and longer. In the satellite systems the periods are much shorter, and the perturbations are usually represented by periodic terms. The magnitude of this effect depends on the mass of the perturbing satellite and the size of its eccentricity or inclination. Hence, for example, in the Saturn system only the effects of Titan are significant. Its effect on the osculating

Table 9.1 Principal commensurabilities among satellites

Argument [a]	Satellites	Libration Amplitude [b]
$2\lambda' - \lambda - \varpi$	Enceladus-Dione	1°.5
$''$	Io-Europa	1°
$''$	Europa-Ganymede	3°
$2\lambda' - \lambda - \varpi'$	Enceladus-Dione	C
$''$	Io-Europa	3°
$''$	Europa-Ganymede	C
$4\lambda' - 2\lambda - \Omega - \Omega'$	Mimas-Tethys	97°
$4\lambda' - 3\lambda - \varpi'$	Titan-Hyperion	36°
$2\lambda'' - 3\lambda' + \lambda$	Io-Europa-Ganymede	0°.07
$2\lambda'' - 3\lambda' + \lambda$	Miranda-Ariel-Umbriel	C

[a] A prime refers to the outer satellite of a pair or to the middle satellite of a triplet. Double-primes refer to the outer satellite of triple commensurabilities.
[b] Circulation motion is denoted by C.

eccentricity e and longitude of pericenter ϖ of Rhea are of the form

$$\begin{aligned} e\cos\varpi &= e_{\mathrm{p}}\cos\varpi_{\mathrm{p}} + e_{\mathrm{f}}\cos\varpi_{\mathrm{T}} \\ e\sin\varpi &= e_{\mathrm{p}}\sin\varpi_{\mathrm{p}} + e_{\mathrm{f}}\sin\varpi_{\mathrm{T}} \end{aligned} \tag{9.16}$$

where ϖ_{T} is the longitude of the pericenter of Titan, e_{f} is a forced component of the eccentricity caused by its resonance with Titan, and e_{p}, ϖ_{p} are the proper eccentricity and longitude of pericenter of Rhea, so that e_{p} and the phase of ϖ_{p} are arbitrary constants, and the rate of ϖ_{p} is due principally to the oblateness of Saturn.

This effect is particularly noticeable for Rhea, as the forced eccentricity e_{f} is much larger than the proper eccentricity e_{p}. In this particular case ϖ_{T} is the proper longitude of pericenter of Titan, and e_{f} is related to the proper eccentricity and mass of Titan.

In the satellite systems of Jupiter and Saturn there are several satellites of large mass compared to that of the other satellites, and so they are liable to cause sizable forced eccentricities or inclinations on each other's orbits. These forced components can themselves cause significant forced components on other satellites, and the resulting terms can have frequencies quite different from the natural frequencies of the system due to the oblateness, etc. To compute these perturbations the eigenvalue theory used for the secular perturbation theory of the planets must be used (see Brouwer and Clemence 1961).

9.3 Planetocentric Rectangular Coordinates

The theory of the motion of a satellite gives expressions for the osculating elements as functions of time. In many cases it is more convenient to represent the position of a satellite in its orbit in rectangular coordinates rather than osculating elements. Let the osculating elements of the satellite be a, e, i, λ, ϖ, and Ω. Then,

1. calculate the mean anomaly M from

$$M = \lambda - \varpi. \tag{9.17}$$

2. Determine the eccentric anomaly E from Kepler's equation

$$E - e \sin E = M. \tag{9.18}$$

3. Calculate the coordinates x, y in the orbital plane (where the x-axis is toward the pericenter) from

$$\begin{aligned} x &= a(\cos E - e) \\ y &= a(1 - e^2)^{1/2} \sin E. \end{aligned} \tag{9.19}$$

Methods for solving Kepler's equation can be found in standard celestial mechanics texts.

4. Next calculate the coordinates x_1, y_1, z_1 relative to the reference plane and x-axis direction used for a particular satellite. If, as in Fig. 9.1, the orbit is related directly to the reference plane by the orbital elements, then x_1, y_1, z_1 are given by

$$\begin{bmatrix} x_1 \\ y_1 \\ z_1 \end{bmatrix} = \mathbf{R}_3(-\Omega)\mathbf{R}_1(-i)\mathbf{R}_3(-\omega) \begin{bmatrix} x \\ y \\ 0 \end{bmatrix} \tag{9.20}$$

where $\omega = \varpi - \Omega$, and $\mathbf{R}_i(a)$ for $i = 1, 2, 3$ is a rotation through an angle a about the current x-, y-, or z-axis respectively (see § 14.4 for expressions for these rotation matrices). This particular transformation is given explicitly as

$$\begin{aligned} x_1 &= (x \cos\omega - y \sin\omega) \cos\Omega - (x \sin\omega + y \cos\omega) \sin\Omega \cos i \\ y_1 &= (x \cos\omega - y \sin\omega) \sin\Omega + (x \sin\omega + y \cos\omega) \cos\Omega \cos i \\ z_1 &= (x \sin\omega + y \cos\omega) \sin i. \end{aligned} \tag{9.21}$$

A more complicated case is shown in Fig. 9.4, where the orbit is referred to an intermediate plane (e.g., the equator of the planet) which is itself referred to the reference plane and x-axis direction. The coordinates x_1, y_1, z_1 are given by

$$\begin{bmatrix} x_1 \\ y_1 \\ z_1 \end{bmatrix} = \mathbf{R}_3(-\Omega_e)\mathbf{R}_1(-i_e)\mathbf{R}_3(-N + \Omega_e)\mathbf{R}_1(-\gamma)\mathbf{R}_3(-\omega) \begin{bmatrix} x \\ y \\ 0 \end{bmatrix} \tag{9.22}$$

where i_e and Ω_e are the inclination and node of the intermediate plane, and γ and N are the inclination and node of the orbital plane, as shown in Fig. 9.4.

If the coordinates x_1, y_1, z_1 are referred to the ecliptic and equinox of B1950.0, then the coordinates x_2, y_2, z_2 of the satellite relative to the center of mass of the planet, in the frame of the Earth's equator and equinox of B1950.0, are

$$\begin{bmatrix} x_2 \\ y_2 \\ z_2 \end{bmatrix} = \mathbf{R}_1(-\varepsilon) \begin{bmatrix} x_1 \\ y_1 \\ z_1 \end{bmatrix} \tag{9.23}$$

where $\varepsilon = 23^\circ.44578787$ is the obliquity of the ecliptic at B1950.0.

If the coordinates must be referred to the equator and equinox of some epoch other than B1950.0 (e.g., "of date" or of J2000.0), then precession should be applied to x_2, y_2, z_2. The precession matrix from B1950.0 to J2000.0 is given in § 3.591 of Hohenkerk et al. (1992).

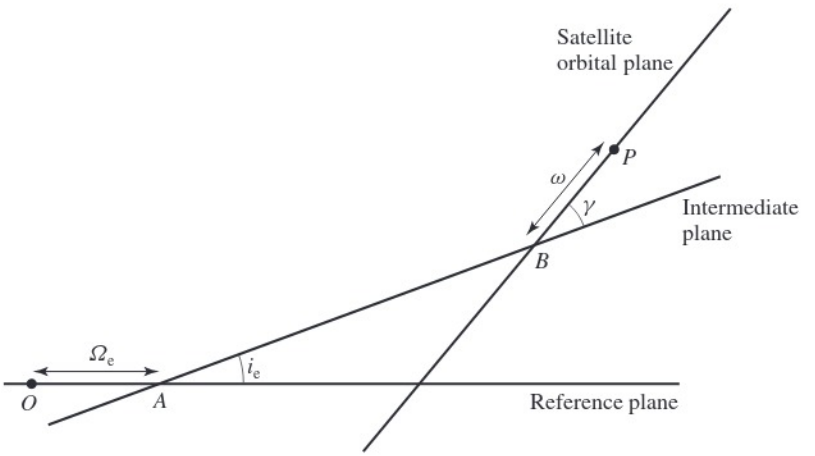


Figure 9.4 The satellite orbit referred to an intermediate plane, where P is the pericenter of the satellite orbit and $N = \Omega_e + A\,B$

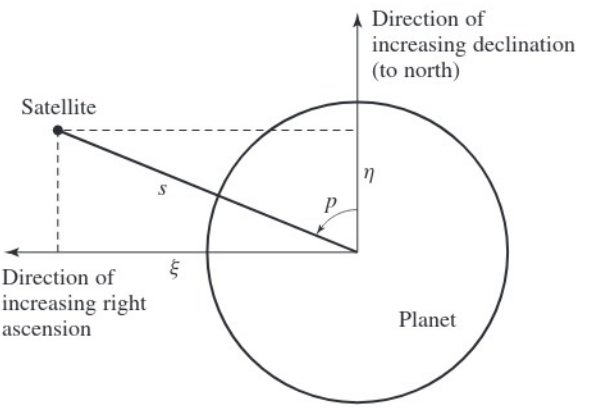


Figure 9.5 Coordinates of the satellite relative to the planet: p = position angle, s = angular distance, $\xi = \Delta\alpha \cos\delta$, and $\eta = \Delta\delta$. $\Delta\alpha$ = difference in right ascension (satellite minus planet), $\Delta\delta$ = difference in declination (satellite minus planet), and δ = declination of planet.

We now consider the apparent position of the satellite as seen by an observer on the Earth. Let $\xi = \Delta\alpha \cos\delta$ and $\eta = \Delta\delta$ be the differential coordinates of the satellite in right ascension and declination respectively (see Fig. 9.5). The differences are in the sense satellite minus center of planet. Then, to first order,

$$\begin{aligned} \xi &= (y_2 \cos\alpha - x_2 \sin\alpha)/r \\ \eta &= (z_2 \cos\delta - x_2 \sin\delta \cos\alpha - y_2 \sin\delta \sin\alpha)/r \end{aligned} \tag{9.24}$$

where α and δ are the right ascension and declination of the planet; r is the distance of the planet from the Earth, in the same units as x_2, y_2, z_2 (usually au); and ξ and η are in radians.

The position angle p and angular distance s of the satellite relative to the planet are given by

$$\tan p = \xi/\eta$$
$$s = (\xi^2 + \eta^2)^{1/2}. \tag{9.25}$$

9.4 Traditional Method

9.4.1 The Apparent Orbit

The apparent orbit of a satellite on the geocentric celestial sphere is an ellipse that is the orthogonal projection, in the direction of the line of sight, of the actual orbit in space. In a circular orbit, the orbital diameter that is perpendicular to the line of sight is projected into the major axis of the apparent ellipse. At its extremities, the satellite is at its greatest elongations from the primary. In planning observations of satellites with short-period orbits, times of greatest elongations are more useful than differential coordinates.

At times of greatest elongation the satellite and planet center are separated by an apparent angular distance a/Δ, where a is the apparent semimajor axis in arcseconds at a distance of one astronomical unit and Δ is the geocentric distance of the primary. The orbital diameter that lies in the plane formed by the line of sight and the normal to the orbital plane, projects into the minor axis. At the further extremity of this diameter, the satellite is in superior geocentric conjunction with the primary, and at the nearer extremity it is at inferior conjunction. The ratio of the semiminor axis to the semimajor axis is the absolute value of sin B, where B is the angle between the line of sight and the plane of the orbit.

On the planetocentric celestial sphere of the primary, the path of the satellite is a great circle, and the positions of the satellite on the planetocentric sphere at any time are obtained from the orbital elements. To represent these positions, the same coordinate systems are adopted as those defined on the geocentric celestial sphere by the equator and the ecliptic. Because of the mathematically infinite radius of the celestial sphere, these reference circles are in identically the same positions on the planetocentric sphere as on the geocentric sphere. The Earth on the planetocentric sphere is diametrically opposite the geocentric position of the planet, and, therefore, at right ascension $\alpha \pm 180°$ and declination $-\delta$, where α and δ are the geocentric coordinates of the planet.

Referred to the celestial equator, the position of the great circle that the satellite describes on the planetocentric sphere is represented by its inclination (J) and the right ascension (N) of its ascending node, or by the right ascension ($N - 90°$) and declination ($90° - J$) of the pole of the orbit. The major axis of the apparent elliptic orbit that the satellite describes on the geocentric sphere is parallel to the plane of this great circle.

In Fig. 9.6 the following angles are indicated:

P: The position angle of the minor axis of the apparent orbit, measured from North. The axis selected is the one pointing toward the pole of the orbit relative to which the satellite motion is direct.

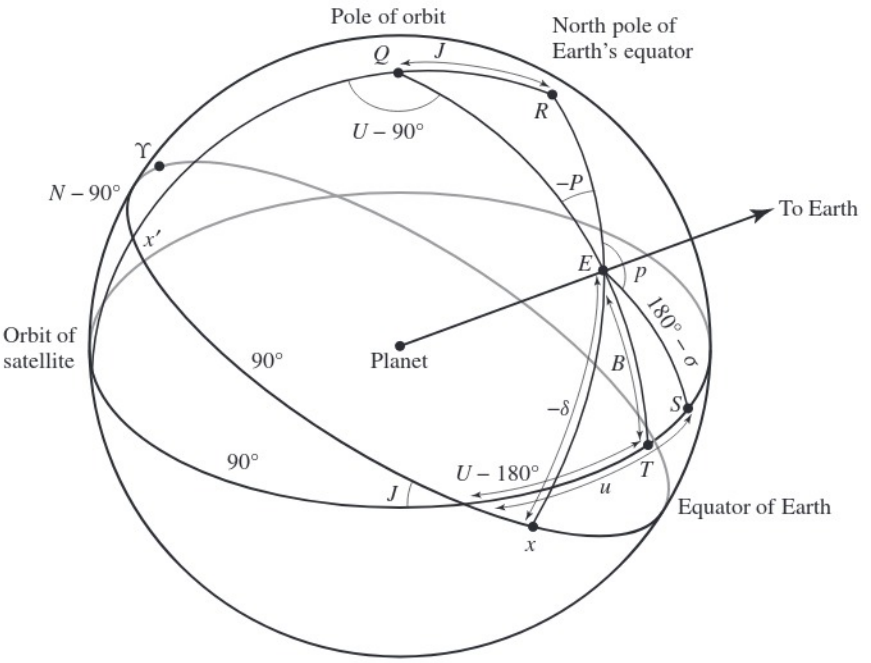


Figure 9.6 Planetocentric celestial sphere. The Earth has right ascension, $180^\circ + \alpha$, and declination, $-\delta$. $\Upsilon x = 180^\circ + \alpha$ and $x'x = 180^\circ + \alpha - (N - 90^\circ) = \alpha - N - 90^\circ$.

B: the planetocentric latitude of the Earth relative to the orbital plane of the satellite; positive toward the pole of the orbit for which motion is direct.

U: the geocentric longitude of the planet measured around the orbit of the satellite, from the ascending node on the Earth's equator. Hence, the planetocentric longitude of the Earth, measured from the same point, is $U - 180^\circ$.

From spherical triangle QRE shown in Fig. 9.7 we obtain

$$\begin{aligned}
\cos B \sin U &= +\cos J \cos\delta \sin(\alpha - N) + \sin J \sin\delta \\
\cos B \cos U &= +\cos\delta \cos(\alpha - N) \\
\sin B &= +\sin J \cos\delta \sin(\alpha - N) - \cos J \sin\delta \\
\cos B \sin P &= -\sin J \cos(\alpha - N) \\
\cos B \cos P &= +\sin J \sin\delta \sin(\alpha - N) + \cos J \cos\delta .
\end{aligned} \tag{9.26}$$

The position of the satellite is described by u—the planetocentric longitude of the satellite measured in the same way as U—and σ—the planetocentric angular displacement of the satellite from the anti-Earth direction; σ takes the value 0° to 180°, and has the value 180° when the satellite lies between the planet and the Earth.

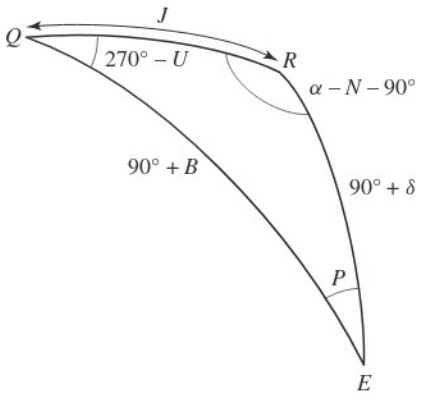


Figure 9.7 Spherical triangle used to compute U, B, and P

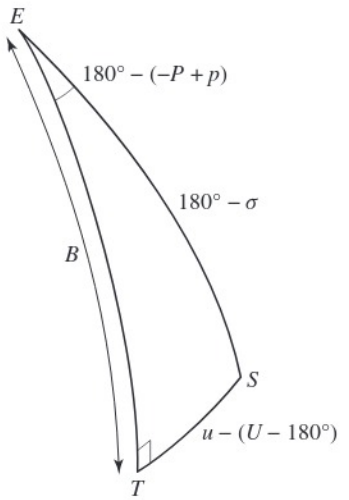


Figure 9.8 Spherical triangle used to compute σ and $p - P$

From spherical triangle ETS shown in Fig. 9.8 we obtain

$$\begin{aligned} \sin\sigma \sin(p - P) &= \sin(u - U) \\ \sin\sigma \cos(p - P) &= \sin B \cos(u - U) \\ \cos\sigma &= \cos B \cos(u - U). \end{aligned} \tag{9.27}$$

Let r be the distance of the satellite from the planet, Δ be the distance of the planet from the Earth, Δ_s be the distance of the satellite from the Earth, and s be the geocentric distance of the satellite from the planet. r, Δ, and Δ_s are measured in units of length, and s is measured in units of arc.

Then, from the plane triangle formed by the Earth, the planet, and the satellite,

$$\begin{aligned} \Delta_s \sin s &= r \sin\sigma \\ \Delta_s \cos s &= r \cos\sigma + \Delta. \end{aligned} \tag{9.28}$$

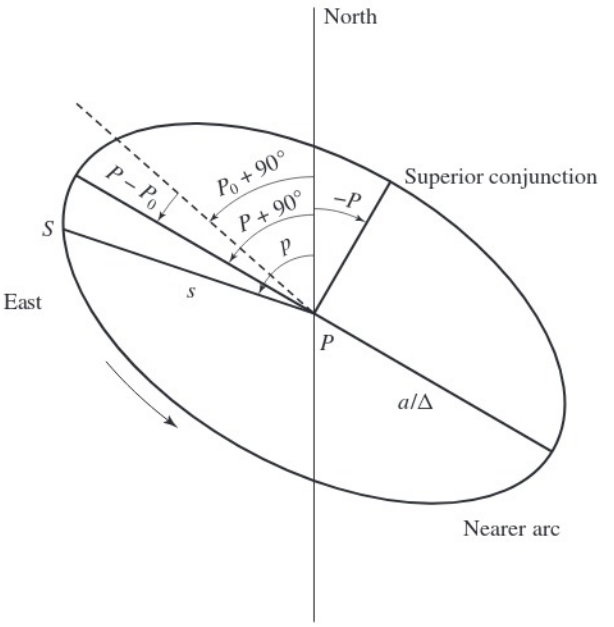


Figure 9.9 Apparent orbit of a satellite of the primary P as projected on the geocentric sphere. This figure shows the situation when the Earth is north of the orbital plane of the satellite.

With sufficient accuracy we may write:

$$s = \frac{r}{\Delta \sin 1''} \sin\sigma = \frac{a}{\Delta} \sin\sigma \tag{9.29}$$

where a is the apparent semimajor axis in arcseconds at a distance of one astronomical unit. Rigorous formulae for p and s in terms of the differential coordinates of the satellite, and also in terms of the planetocentric coordinates, are given later.

At greatest elongation, $u - U = \pm 90°$, $\sigma = 90°$, and $s = a/\Delta$ where the position angle $p = P \pm 90°$. At the extremities of the minor axis of the apparent orbit, the satellite is at inferior or superior conjunction; $u - U$ is $0°$ or $180°$, $\sigma = B$, and the position angle is P or $P + 180°$. Evidently, when the Earth is north of the orbital plane, the satellite is at inferior conjunction at the southern extremity of the minor axis, and is at superior conjunction at the northern extremity (see Fig. 9.9); B is then positive if the motion is direct, negative if retrograde. When the Earth is south of the orbital plane, superior conjunction is at the southern extremity of the minor axis, and B is negative in direct motion, positive in retrograde motion. Irrespective, therefore, of whether the motion is direct or retrograde, the position angle at superior conjunction, when B is positive, is $p = P$; when B is negative, it is $p = P + 180°$.

The apparent orbit becomes increasingly elliptical as the Earth approaches the orbital plane, and reduces to a straight line when the Earth is in this plane. As the Earth passes through the plane and B changes sign, each superior and inferior conjunction occurs at the opposite extremity of the minor axis from that at which it previously took place. Similarly,

when the Earth is in the plane that is perpendicular to the orbital plane and contains the celestial pole, the minor axis is exactly in the north-south direction, and the major axis is exactly east-west. As the Earth passes through this plane, the extremity of the major axis that formerly was the more northerly becomes the more southerly.

Only when J is not too greatly different from 0° or 180° is the direction of the minor axis necessarily nearly enough north and south for the elongations to be strictly and unambiguously described as eastern and western. When J is in the neighborhood of 90°, as in the case of the satellites of Uranus and Pluto, the direction of the minor axis on the celestial sphere ranges from north-south to east-west. This introduces confusion in the terminology for the elongations, but in general they are more appropriately regarded as northern and southern than as eastern and western.

In the ephemerides for finding the apparent distance s and position angle p, the factor $\sin\sigma$ giving the ratio of s to the apparent distance at greatest elongation is denoted by F, and therefore the apparent distance of the satellite from the primary is given by

$$s = Fa/\Delta. \tag{9.30}$$

With P_0 denoting an arbitrary fixed integral number of degrees near the value of P at opposition, the value of p at any time is expressed in the form $p_1 + p_2$. p_1 is the sum of the approximate position angle at elongation and the amount of motion in position angle since elongation. p_2, depending on the date, denotes the correction $P - P_0$. In calculating F and p_1, the value of the eccentricity of the apparent orbit at opposition is used; consequently, in the values of s and p that are derived from them, the effect of the variation of the eccentricity of the apparent orbit is neglected.

Many of the values described in this section are tabulated and presented on *The Astronomical Almanac Online* .

9.4.2 Calculating Tabulated Values

The apparent positions of the satellites are represented by their positions relative to the primary, expressed either by the apparent angular distance and position angle, or by the differential spherical (or rectangular) coordinates in right ascension and declination. The tabular values are corrected for light-time, and are directly comparable with observations at the tabular times. It is usually sufficiently accurate to use the light-time from the planet to the Earth. The timescale of the theories of the satellites is TDB. The timescale of the ephemerides in *The Astronomical Almanac* is usually UT. The value of ΔT, where

$$\Delta T = \mathrm{TT} - \mathrm{UT}, \quad \text{and } \mathrm{TT} \approx \mathrm{TDB} \tag{9.31}$$

is approximated at the time of production of the book and used in the computations.

9.4.2.1 Times of Greatest Elongation

The method for calculating the inclination, orbital longitude, and longitude of the ascending node with respect to the Earth's equator, J, u, and N, respectively, can vary from satellite to satellite. The descriptions for these calculations are contained in § 9.7 through § 9.12. Given that J, u, and N have been computed for 0^{h} on a given date, and that the right ascension and declination of the primary, α and δ, are known, U, B, and P are calculated from Eqs. 9.26.

The angle to the nearest elongation is given by

$$du = 90^\circ - (u - U). \tag{9.32}$$

The time for the satellite to transit this angle is

$$dt = du/n. \tag{9.33}$$

If dt is greater than one day, J, u and N, and then U, B, and P are redetermined for 0^h on the next day. A new dt is then computed. The light-time correction $0^h.13861\Delta$ is then applied to give the time of elongation. Δ is the Earth–planet distance.

9.4.2.2 Apparent Distance and Position Angle

Given J, u, and N on the date of opposition, P is determined from Eqs. 9.26. P_0 is the integral part of P. Now from J, u, and N at 0^h on any date, U, B and P are computed from Eqs. 9.26. $p - P$ and $\sin\sigma = F$ are found from Eqs. 9.27. p_1 is the sum of $p - P$ and P_0. p_2 is the difference $P - P_0$, where P is the value for 0^h on the date in question, not the value at opposition. The determination of a/Δ is a straightforward computation from the semimajor axis, a, and the Earth–planet distance, Δ.

9.4.2.3 Differential Coordinates

To first order, the differential right ascension and declination in the sense satellite minus planet are

$$\begin{aligned} \Delta\alpha &= s \sin p \sec(\delta + \Delta\delta) \\ \Delta\delta &= s \cos p \end{aligned} \tag{9.34}$$

where s is calculated from Eq. 9.29 and $p = p_1 + p_2$.

9.5 Modern Method

9.5.1 The Apparent Orbit

9.5.1.1 Differential Tangent Plane Coordinates

For the computation of satellite positions it is necessary to have available either a set of subroutines that evaluate satellite positions from their orbital elements and perturbations at any specified time, or use the mixed function data (§ 9.5.1.2). The satellite positions (x_2, y_2, z_2) from Eq. 9.23 are precessed to the equator and equinox of J2000.0, which is more convenient for modern observations. Let α and δ be the right ascension and declination of the planet. Then the differential coordinates X, Y of the satellite relative to the planet, referred to axes lying in the tangent plane (see Fig. 9.10) are

$$X = k(y_2 \cos\alpha - x_2 \sin\alpha) \tag{9.35}$$

$$Y = k(z_2 \cos\delta - x_2 \cos\alpha \sin\delta - y_2 \sin\alpha \sin\delta) \tag{9.36}$$

where

$$k = \Delta/(\Delta + z_2 \sin\delta + y_2 \cos\delta \sin\alpha + x_2 \cos\delta \cos\alpha) \tag{9.37}$$

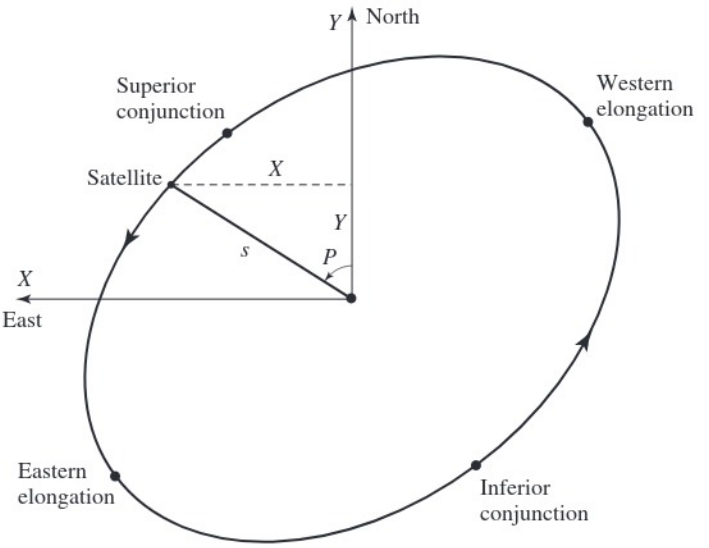


Figure 9.10 Apparent orbit of the satellite projected on to the tangent plane, and the coordinate system used

and Δ is the current distance of the planet from the Earth. X and Y will be in astronomical units but can be converted to angular quantities (arcseconds) as seen from the Earth by multiplying by $3600 \times 180/(\pi \times \Delta)$. These are the X and Y referred to in the following discussion.

9.5.1.2 Mixed Functions Approximation

The variations of the tangent plane coordinates are quasi-periodic in character. Using a novel approach formulated by Chapront and Vu (1984), these coordinates can be represented compactly by a mixture of periodic and secular functions (mixed functions). For satellite ephemerides represented by these mixed functions astronomers require to compute the observables $\Delta\alpha \cos\delta$ and $\Delta\delta$ where $\Delta\alpha$ and $\Delta\delta$ are the differences in right ascension and declination of the satellite from the planet respectively. Since $\Delta\alpha$ and $\Delta\delta$ are small, to the first order in small quantities

$$\Delta\alpha \cos\delta = X \tag{9.38}$$

$$\Delta\delta = Y \tag{9.39}$$

and to the second order

$$\Delta\alpha \cos\delta = X + \sin 1'' XY \tan\delta \tag{9.40}$$

$$\Delta\delta = Y - \sin 1'' \frac{X^2}{2} \tan\delta. \tag{9.41}$$

The formulae correct to the second order are needed for satellites with large elongation, such as Iapetus.

This approach to represent satellite ephemerides has been used by Arlot et al. (1986). The satellite ephemerides for the major satellites of Mars, Jupiter, Saturn, and Uranus produced

at The Institut de Mécanique Céleste et de Calcul des Éphémérides (IMCCE) use this form. Taylor (1995) has followed the same approach producing ephemerides of the eight major satellites of Saturn using the mixed functions approximation but with different original theories. This work was later extended to produce ephemerides for the major satellites of Mars, Jupiter, Uranus, and Triton of Neptune's system. These ephemerides have been used in the computation of phenomena and approximate ephemerides, following the methods described in § 9.5.2.1 and § 9.5.2.2 respectively. In producing the mixed functions the complete satellite theories were used. The mixed functions approximation allows a satellite ephemeris to be represented compactly while still retaining the precision of the original theory. It is particularly suited to fast-moving satellites where the chosen interval for fitting can be equal to several orbital periods.

Briefly, this method represents the differential tangent plane coordinates by a linear combination of a set of basis functions to model the quasi-periodic character of the coordinates on a chosen time interval mapped to the interval [-1, 1] by a linear transformation of the time. From fitting the mixed functions approximation of the coordinate to the coordinate over this chosen time interval using the quadratic mean and seeking the minimum of it, one obtains the coefficients of the basis functions. In fact, the interval for the fitting was taken slightly longer than the original chosen interval, as a maximum error at the ends of the interval is a common feature of the fitting process.

If we let $f(t)$ be a coordinate, then for a chosen interval, one can represent this by

$$f(t) \simeq a_0 + a_1 t + b_1 \sin(\nu t + \phi_1) + b_2 \sin(2\nu t + \phi_2) + b_3 t \sin(\nu t + \phi_3) + b_4 t^2 \sin(\nu t + \phi_4) \tag{9.42}$$

where a_0, a_1; b_i, $i = 1, \ldots, 4$; ϕ_i, $i = 1, \ldots, 4$ are functions of the solved-for coefficients, interval size, and amount the limits of the original interval for fitting was extended. ν is the main frequency of the motion of the satellite.

Taylor (1995), and the extension of this work to other satellite systems, used the same fitting parameters, namely the length of interval to fit over and number of coefficients solved for, as are used in the ephemerides produced at IMCCE. For Triton, the form as given above was used (i.e., no coefficients in the fitting process were taken as zero) and the intervals for which the mixed functions were valid was 66 days. For all satellites, the production of a mixed function ephemeris for the time interval over which the approximation is valid, the absolute differences from the original coordinates are about $0''.01$ or less.

9.5.2 Calculating Tabulated Values

9.5.2.1 Times of Elongation and Conjunction

The phenomena for the satellites are computed using the method described in Taylor and Sinclair (2003), except for the Galilean satellites where a different scheme is used. This is due to the fact that their orbits are always seen virtually edge-on from the Earth; see § 9.8.1.

The times of elongation and conjunction are tabulated in *The Astronomical Almanac* to a precision of 0.1 hour. The simple method of computing these times is to start at the beginning of the required year and take a time step of 0.1 hour throughout the whole year. At each step

calculate the tangent plane coordinates as described in § 9.5.1.1. Then, the apparent angular distance s and position angle P are computed from

$$s = \sqrt{(X^2 + Y^2)} \tag{9.43}$$

$$\tan P = X/Y. \tag{9.44}$$

Times when s reaches a maximum or minimum are singled out. The times when s is a maximum are times of elongation, with eastern elongations being those for which X is positive and the northern elongations being those for which Y is positive. The times when s is a minimum are times of conjunction. For a direct satellite, the conjunction following eastern elongation is inferior conjunction and the conjunction following northern elongation is superior conjunction.

Using the IAU numbering system, the phenomena listed in *The Astronomical Almanac* for satellites Mars I, II, Saturn I to VIII, Uranus I to V, and Neptune I are all computed using this method. In Taylor and Sinclair (2003) a comparison was made of this method with the traditional method as previously used to compute satellite phenomena. The new method was preferred since the times of phenomena were considered better, as they refer to the actual orbit rather than a projection of an idealized circular orbit.

9.5.2.2 Approximate Apparent Distance and Position Angle

The method given in Taylor and Sinclair (2003) is used to compute tables to calculate approximate apparent distance and position angle. It was shown in this paper that it gives similar results to the traditional method previously used to compute these tabular values.

Once all times of greatest eastern (or northern) elongation have been computed for a particular satellite, the times are compared to the time of opposition for that satellite's planet. The first eastern elongation time after opposition is chosen as the start time for computing the table of apparent distances and position angles for one satellite orbit. In the case of Mars, where opposition occurs every other year, in years when no opposition is expected the first eastern elongation time after either January 1 or December 31 of the edition year is chosen for the computations. The choice of date depends on which yields the better view of the satellites.

For the chosen orbit using the same time step for a satellite that was used previously in the traditional method, X and Y offsets as described in § 9.5.1.1 are computed. Equations 9.43 and 9.44 are then used to calculate the angular distance and position angle. Denoting s_0 (in radians) and Δ_0 to be the angular distance and current distance of the planet from the Earth respectively at these times and a the semimajor axis of the satellite orbit, we can form the scaled distance

$$F = \frac{s_0 \Delta_0}{a}. \tag{9.45}$$

A table of scaled distances for the chosen orbit can then be computed.

A separate table gives the multiplying factors, which are values of the quantity a/Δ throughout the year, at intervals as used in the traditional method. These values are multiplied by the conversion factor from radians to seconds of arc.

To compute the approximate apparent distance and position angle at any time t in the year we find firstly the time interval from the last greatest eastern (or northern) elongation. Then, using this time interval as the time argument, extract from the table of scaled distances and position angles F and P. P will be the approximate position angle required. Enter with time argument t the table giving the multiplying factors and find the value of a/Δ. The approximate apparent distance in seconds of arc will be

$$s = \frac{Fa}{\Delta}. \tag{9.46}$$

9.6 Satellite Data in *The Astronomical Almanac* and Notation

9.6.1 Presented Data

Data tables for the satellites are found in Section F of *The Astronomical Almanac* and in *The Astronomical Almanac Online* URL[1]. Due to the recent proliferation of known satellites associated with the gas giant planets, a set of selection criteria has been established under which satellites will be included in the printed data tables in the *The Astronomical Almanac*. These criteria are the following: The visual magnitude of the satellite must not be fainter than 23.0 and the satellite must be sanctioned by the IAU with a roman numeral and a name designation. Satellites that have yet to receive IAU approval are designated as works-in-progress and shall be included at a later time should such approval be granted, provided their visual magnitudes are not fainter than 23.0. A more complete version of the tables, including satellites with visual magnitudes fainter than 23.0, is found at *The Astronomical Almanac Online*.

Positional data presented for the brighter satellites generally fall in two broad categories—elongations or differential coordinates. Elongations are typically given for satellites with orbits less than 90 days, and differential coordinates are provided for the longer period ones. Table 9.2 summarizes the positional information in *The Astronomical Almanac*.

Computations requiring poles of rotation and prime meridian data utilize the latest published report from IAU/IAG Working Group on Cartographic Coordinates and Rotational Elements (Archinal et al. 2011). See URL[2] for additional details.

9.6.2 Notation

Many different notations have been used in the literature for the orbital elements of the satellites. The notations for the angular elements used in the balance of this chapter are described below.

For those satellites for which the orbit is referred directly to the ecliptic and equinox of B1950.0 or J2000.0 the notation is

λ = mean longitude

ϖ = longitude of the pericenter

Ω = longitude of the ascending node

i = inclination.

Table 9.2 Summary of satellite positional data in *The Astronomical Almanac*

Planet		Satellite	Elongations	Diff. Coordinates
Mars	I	Phobos	yes	no
	II	Deimos	yes	no
Jupiter	I	Io	*	*
	II	Europa	*	*
	III	Ganymede	*	*
	IV	Callisto	*	*
	V	Amalthea	yes	no
	VI	Himalia	no	yes
	VII	Elara	no	yes
	VIII	Pasiphae	no	yes
	IX	Sinope	no	yes
	X	Lysithea	no	yes
	XI	Carme	no	yes
	XII	Ananke	no	yes
	XIII	Leda	no	yes
Saturn	I	Mimas	yes	no
	II	Enceladus	yes	no
	III	Tethys	yes	no
	IV	Dione	yes	no
	V	Rhea	yes	no
	VI	Titan	yes	no
	VII	Hyperion	yes	yes
	VIII	Iapetus	yes	yes
	IX	Phoebe	no	yes
Uranus	I	Ariel	yes	no
	II	Umbriel	yes	no
	III	Titania	yes	no
	IV	Oberon	yes	no
	V	Miranda	yes	no
Neptune	I	Triton	yes	no
	II	Nereid	no	yes
Pluto	I	Charon	yes	no

Where an intermediate reference plane is used (usually the equatorial plane of the planet or the Laplacian plane) the notation used for the angular elements is

$$L = \text{mean longitude}$$
$$P = \text{longitude of the pericenter}$$
$$\theta = \text{longitude of the ascending node}$$
$$\gamma = \text{inclination}.$$

When the orbital elements are referred to the Earth equator and equinox of B1950.0 or J2000.0, the notation used for the angular elements is

$$l = \text{mean longitude}$$
$$\pi = \text{longitude of the pericenter}$$
$$N = \text{longitude of the ascending node}$$
$$J = \text{inclination}.$$

The reason for using the ecliptic as the reference plane for the orbits is for convenience rather than any good dynamical or observational reason. The planes of dynamical significance are the equatorial and orbital planes of the planet. The plane of observational significance is the Earth's equatorial plane. The orbital elements of the planets are, however, referred to the ecliptic, and so it was probably a convenient frame in which to calculate solar and planetary perturbations.

9.7 The Satellites of Mars

Ephemerides of the greatest eastern elongations are given for the satellites of Mars in *The Astronomical Almanac*. The ephemerides of the satellites are computed from elements given by Sinclair (1989).

Phobos

$$a = 6.269\,74 \times 10^{-5}\ \text{au}$$
$$n = 1128^{\circ}.844\,556/\text{day}$$
$$e = 0.0150$$
$$\gamma = 1^{\circ}.10$$
$$\theta = 327^{\circ}.90 - 0^{\circ}.435\,33\,d$$
$$L = 232^{\circ}.41 + nd + 0^{\circ}.001\,24y^2$$
$$P = 278^{\circ}.96 + 0^{\circ}.435\,26\,d$$
$$N_a = 47^{\circ}.39 - 0^{\circ}.0014\,y$$
$$J_a = 37^{\circ}.27 + 0^{\circ}.0008\,y.$$

Deimos

$$a = 1.568\,28 \times 10^{-4}\ \text{au}$$
$$n = 285^{\circ}.161\,888/\text{day}$$
$$e = 0.0004$$

$$\gamma = 1.^{\circ}79$$
$$\theta = 240.^{\circ}38 - 0.^{\circ}01801\, d$$
$$L = 28.^{\circ}96 + nd - 0.27 \sin h$$
$$P = 111.^{\circ}7 + 0.^{\circ}01798\, d$$
$$h = 196.^{\circ}55 - 0.^{\circ}01801\, d$$
$$N_a = 46.^{\circ}37 - 0.^{\circ}0014\, y$$
$$J_a = 36.^{\circ}62 + 0.^{\circ}0008\, y$$

where

$$d = \text{JD} - 2\,441\,266.5$$
$$y = d/365.25.$$

These elements are referred to the fixed Laplacian planes of the satellites. The angular elements are shown in Fig. 9.11. The orbital elements are defined as follows: the semimajor axis a; the mean daily motion n; the eccentricity e; the inclination γ; the longitude of the ascending node, θ, measured from the ascending node of the Laplacian plane on the Earth's equator along the Laplacian plane to the node of the orbit; L, the mean longitude reckoned from the vernal equinox along the Earth's equator to the ascending node of the Laplacian plane, then along the Laplacian plane to the ascending node of the orbit, and then along the orbit to the mean position of the satellite; P, the longitude of the pericenter, measured in the same manner as L from the vernal equinox to the pericenter; N_a, the longitude of the ascending node of the Laplacian plane reckoned from the vernal equinox along the Earth's equator; J_a, the inclination of the Laplacian plane to the Earth's equator; h, reckoned along the Laplacian plane from its ascending node on the orbital plane of Mars to the ascending node of the satellite orbit.

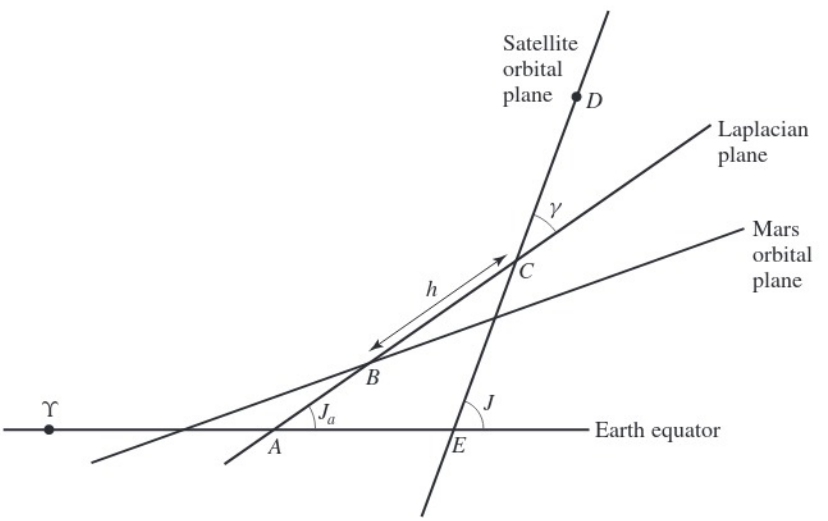


Figure 9.11 Reference system for Phobos and Deimos. D = position of satellite pericenter, $\theta = AC$, $L = \Upsilon A + AB + BC + CD$ + mean anomaly, $P = \Upsilon A + AB + BC + CD$, $N_a = \Upsilon A$, and $N = \Upsilon E$.

Though the theories for the motion of the satellites contain several periodic terms, the only periodic perturbation of importance for Earth-based observations is $L = -0.27 \sin h$ for Deimos.

J and N, the inclination and ascending node of the satellite orbit on the Earth's equator can be found by considering the spherical triangle AEC in Fig. 9.11. From spherical trigonometry we have

$$\begin{aligned} \sin J \sin(N - N_a) &= \sin \gamma \sin \theta \\ \sin J \cos(N - N_a) &= \cos \gamma \sin J_a + \sin \gamma \cos J_a \cos \theta. \end{aligned} \tag{9.47}$$

Now find the arc length EC of triangle AEC from

$$\begin{aligned} \sin J \sin EC &= \sin J_a \sin \theta \\ \sin J \cos EC &= \cos J_a \sin \gamma + \sin J_a \cos \gamma \cos \theta. \end{aligned} \tag{9.48}$$

u follows from

$$u = EC + L - N_a - \theta + (f - M) \tag{9.49}$$

where $(f - M)$ is the equation of center that is computed via Eq. 9.1, where

$$M = L - P. \tag{9.50}$$

The computation of the tabulated values follows as described in § 9.4.2.

9.8 The Satellites of Jupiter

9.8.1 The Galilean Satellites

The ephemerides and phenomena of Satellites I–IV given in *The Astronomical Almanac* are based on the theory of Lieske (1977), with constants due to Arlot (1982). Lieske's theory is a revision of the theory by Sampson (1921). A shortened version of Lieske's theory is presented below, which will give the positions of the satellites to about 500 km. The constants used below are from Lieske (1987):

$$\begin{aligned} 10^7 \xi_1 = & -41279 \cos(2L_1 - 2L_2); \\ 10^7 \nu_1 = & -5596 \sin(P_3 - P_4) - 2198 \sin(P_1 + P_3 - 2\Pi_J - 2G) \\ & + 1321 \sin(\phi_l) - 1157 \sin(L_1 - 2L_2 + P_4) \\ & - 1940 \sin(L_1 - 2L_2 + P_3) - 791 \sin(L_1 - 2L_2 + P_2) \\ & + 791 \sin(L_1 - 2L_2 - P_2) + 82363 \sin(2L_1 - 2L_2); \\ 10^7 \zeta_1 = & +7038 \sin(L_1 - \theta_1) + 1835 \sin(L_1 - \theta_2); \\ 10^7 \xi_2 = & -3187 \cos(L_2 - P_3) - 1738 \cos(L_2 - P_4) \\ & + 93748 \cos(L_1 - L_2); \end{aligned}$$

$$
\begin{aligned}
10^7\nu_2 = & -1158\sin(-2\Pi_J + 2\Psi) + 1715\sin(-2\Pi_J + \theta_3 + \Psi - 2G) \\
& - 1846\sin(G) + 2397\sin(P_3 - P_4) - 3172\sin(\phi_l) \\
& - 1993\sin(L_2 - L_3) + 1844\sin(L_2 - P_2) \\
& + 6394\sin(L_2 - P_3) + 3451\sin(L_2 - P_4) \\
& + 4159\sin(L_1 - 2L_2 + P_4) + 7571\sin(L_1 - 2L_2 + P_3) \\
& - 1491\sin(L_1 - 2L_2 + P_2) - 185640\sin(L_1 - L_2) \\
& - 803\sin(L_1 - L_3) + 915\sin(2L_1 - 2L_2); \\
10^7\zeta_2 = & +81575\sin(L_2 - \theta_2) + 4512\sin(L_2 - \theta_3) \\
& - 3286\sin(L_2 - \Psi); \\
10^7\xi_3 = & -14691\cos(L_3 - P_3) - 1758\cos(2L_3 - 2L_4) \\
& + 6333\cos(L_2 - L_3) - 7894\sin(L_3 - P_4); \\
10^7\nu_3 = & -1488\sin(-2\Pi_J + 2\Psi) + 411\sin(-\theta_3 + \Psi) \\
& + 346\sin(-\theta_4 + \Psi) - 2338\sin(G) \\
& + 6558\sin(P_3 - P_4) + 523\sin(P_1 + P_3 - 2\Pi_J - 2G) \\
& + 314\sin(\phi_l) - 943\sin(L_3 - L_4) \\
& + 29387\sin(L_3 - P_3) + 15800\sin(L_3 - P_4) \\
& + 3218\sin(2L_3 - 2L_4) + 226\sin(3L_3 - 2L_4) \\
& - 12038\sin(L_2 - L_3) - 662\sin(L_1 - 2L_2 + P_4) \\
& - 1246\sin(L_1 - 2L_2 + P_3) + 699\sin(L_1 - 2L_2 + P_2) \\
& + 217\sin(L_1 - L_3); \\
10^7\zeta_3 = & -2793\sin(L_3 - \theta_2) + 32387\sin(L_3 - \theta_3) \\
& + 6871\sin(L_3 - \theta_4) - 16876\sin(L_3 - \Psi); \\
10^7\xi_4 = & +1656\cos(L_4 - P_3) - 73328\cos(L_4 - P_4) \\
& + 182\cos(L_4 - \Pi_J) - 541\cos(L_4 + P_4 - 2\Pi_J - 2G) \\
& - 269\cos(2L_4 - 2P_4) + 974\cos(L_3 - L_4); \qquad (9.51) \\
10^7\nu_4 = & -407\sin(-2P_4 + 2\Psi) + 309\sin(-2P_4 + \theta_4 + \Psi) \\
& - 4840\sin(-2\Pi_J + 2\Psi) + 2074\sin(-\theta_4 + \Psi) \\
& - 5605\sin(G) - 204\sin(2G) \\
& - 495\sin(5G' - 2G + \phi_2) + 234\sin(P_4 - \Pi_J) \\
& - 6112\sin(P_3 - P_4) - 3318\sin(L_4 - P_3) \\
& + 146673\sin(L_4 - P_4) + 178\sin(L_4 - \Pi_J - G) \\
& - 363\sin(L_4 - \Pi_J) + 1085\sin(L_4 + P_4 - 2\Pi_J - 2G) \\
& + 672\sin(2L_4 - 2P_4) + 218\sin(2L_4 - 2\Pi_J - 2G)
\end{aligned}
$$

$$
\begin{aligned}
&+ 167 \sin(2L_4 - \theta_4 - \Psi) - 142 \sin(2L_4 - 2\Psi) \\
&+ 148 \sin(L_3 - 2L_4 + P_4) - 390 \sin(L_3 - L_4) \\
&- 195 \sin(2L_3 - 2L_4) + 185 \sin(3L_3 - 7L_4 + 4P_4); \\
10^7 \zeta_4 = &+ 773 \sin(L_4 - 2\Pi_J + \Psi - 2G) \\
&- 5075 \sin(L_4 - \theta_3) + 44300 \sin(L_4 - \theta_4) \\
&- 76493 \sin(L_4 - \Psi);
\end{aligned}
$$

where

$$
\begin{aligned}
L_1 &= 106.^\circ 078\,590\,000 + 203.^\circ 488\,955\,363\,0643\, t \\
L_2 &= 175.^\circ 733\,787\,000 + 101.^\circ 374\,724\,556\,6245\, t \\
L_3 &= 120.^\circ 561\,385\,500 + 50.^\circ 317\,609\,153\,404\,62\, t \\
L_4 &= 84.^\circ 455\,823\,000 + 21.^\circ 571\,070\,875\,179\,61\, t \\
\phi_l &= 184.^\circ 415\,351\,000 + 0.^\circ 173\,569\,02\, t \\
P_1 &= 82.^\circ 380\,231\,000 + 0.^\circ 161\,022\,75\, t \\
P_2 &= 128.^\circ 960\,393\,000 + 0.^\circ 046\,456\,44\, t \\
P_3 &= 187.^\circ 550\,171\,000 + 0.^\circ 007\,124\,08\, t \\
P_4 &= 335.^\circ 309\,254\,000 + 0.^\circ 001\,839\,39\, t \\
\Pi_J &= 13.^\circ 470\,395\,000 \\
\theta_1 &= 308.^\circ 365\,749\,000 - 0.^\circ 132\,806\,10\, t \\
\theta_2 &= 100.^\circ 438\,938\,000 - 0.^\circ 032\,615\,35\, t \\
\theta_3 &= 118.^\circ 908\,928\,000 - 0.^\circ 007\,176\,78\, t \\
\theta_4 &= 322.^\circ 746\,564\,000 - 0.^\circ 001\,760\,18\, t \\
\Psi &= 316.^\circ 500\,101\,000 - 0.^\circ 000\,002\,48\, t \\
G' &= 31.^\circ 978\,528\,0244 + 0.^\circ 033\,459\,733\,896\, t \\
G &= 30.^\circ 238\,021\,0168 + 0.^\circ 083\,092\,561\,789\,694\,53\, t \\
\phi_2 &= 52.^\circ 144\,596\,6929 \\
t &= \text{JD} - 2\,443\,000.5.
\end{aligned}
\tag{9.52}
$$

L_i, P_i, and θ_i are the mean longitude, proper periapse, and proper node of satellite i. ϕ_l is the libration phase angle; Π_J is the longitude of perihelion of Jupiter; Ψ is the longitude of the origin of the coordinates (Jupiter's pole); G' and G are the mean anomalies of Saturn and Jupiter; ϕ_2 is the phase angle in solar $(A/R)^3$ with angle $5G' - 2G$.

To convert ξ, ν, and ζ to rectangular coordinates $\bar{x}$, $\bar{y}$, and $\bar{z}$ in the moving Jovian equatorial frame, Eqs. 9.53 and 9.54 can be used. Satellite subscripts have been omitted for clarity.

$$
\begin{aligned}
\bar{x} &= a(1 + \xi) \cos(L - \Psi + \nu) \\
\bar{y} &= a(1 + \xi) \sin(L - \Psi + \nu) \\
\bar{z} &= a\zeta.
\end{aligned}
\tag{9.53}
$$

The coefficients a are

$$a_1 = 0.002\,819\,347 \text{ au}$$
$$a_2 = 0.004\,485\,872 \text{ au}$$
$$a_3 = 0.007\,155\,352 \text{ au}$$
$$a_4 = 0.012\,585\,436 \text{ au}.$$

The formula for finding the coordinates in the Earth equatorial frame of 1950.0 is

$$\mathbf{r} = \mathbf{R}_1(-\varepsilon)\mathbf{R}_3(-\Omega)\mathbf{R}_1(-J)\mathbf{R}_3(-\Phi)\mathbf{R}_1(-I)\bar{\mathbf{r}} \tag{9.54}$$

where

$$\bar{\mathbf{r}} = (\bar{x}, \bar{y}, \bar{z})^{\mathrm{T}}$$
$$\mathbf{r} = (x, y, z)^{\mathrm{T}}$$
$$\varepsilon = 23^\circ\ 26'\ 44\overset{''}{.}84$$
$$\Omega = 99\overset{\circ}{.}997\,54$$
$$J = 1\overset{\circ}{.}306\,91$$
$$\Phi = \Psi - \Omega$$
$$I = 3\overset{\circ}{.}104\,01.$$

ε is the obliquity of the ecliptic; Ω is the longitude of the ascending node of Jupiter; J is the inclination of Jupiter's orbit to the ecliptic; I is the inclination of Jupiter's orbit to Jupiter's equator. The rotation matrices $\mathbf{R}_i$ are defined in § 9.1.5 and described in Chapter 14.

The data tabulated in *The Astronomical Almanac* consist of: the approximate times of superior geocentric conjunction; the times of the geocentric phenomena; and the approximate configurations, in graphical form, of the satellites relative to the disk of Jupiter.

The Terrestrial Time of each superior geocentric conjunction is given for each satellite to the nearest minute. The phenomena for which times are given are eclipses, occultations, transits, and shadow transits. The TT of the beginning and end of each phenomenon (disappearance and reappearance for eclipses and occultations, ingress and egress for transits and shadow transits) are given to the nearest minute for all phenomena that are observable. When Jupiter is in opposition, the shadow may be hidden by the disk and no eclipses can be observed. In general, eclipses may be observed on the western side of Jupiter before opposition and on the eastern side after opposition. Before opposition the disappearance only of Satellite I into the shadow may be observed since it is occulted before it emerges from the shadow; after opposition only the reappearances from the shadow are visible. The same is true in general of Satellite II, although occasionally both phenomena can be seen. In the case of Satellites III and IV, both phases of the eclipses are usually visible except near certain oppositions. Similarly the occultation disappearances and reappearances of a satellite cannot be observed if, at the time concerned, the satellite is eclipsed. For Satellites I and II there are, in general, cycles of six phenomena consisting of both phases of both transit and shadow transit, one phase of the eclipse, and the other phase of the occultation.

For Satellite IV, none of the phenomena occur when the plane of the orbit of the satellite—essentially the same as that of Jupiter's equator—is inclined at more than about 2° to the line from Jupiter to the Earth (for occultations and transits) or to the Sun (for eclipses and shadow transits).

Owing to the finite disks of the satellites, the phenomena do not take place instantaneously —the times refer to the center of the disk. When the Earth is near the satellites' orbital planes, one satellite may be eclipsed by the shadow of another, or may occult another. This so-called *mutual event season* happens about every six years for the Galilean satellites. Typically predictions are made by collaborators and printed in *The Astronomical Almanac*. A description of a method of prediction is given by Levin (1934).

The configurations of the four satellites relative to the disk of Jupiter are shown in *The Astronomical Almanac* in graphical form, on the pages facing the tabular ephemerides of the times of the eclipses and other phenomena. These are generally provided by colleagues at Institut de Mécanique Céleste et de Calcul des Éphémérides (IMCCE) under a long-standing data exchange agreement.

9.8.2 Jupiter's Fifth Satellite, Amalthea

The data given in *The Astronomical Almanac* consist of the Universal Times of every 20th eastern elongation. The elongations are computed from the following circular orbital elements, referred to the equator of Jupiter, given by van Woerkom (1950):

$$\begin{aligned} t_0 &= 1903 \text{ September } 1.5 \text{ UT} = \text{JD } 2\,416\,359.0; \\ a &= 249.''55; \\ \gamma &= 24.'1; \\ \theta &= 82.^\circ5 - 914.^\circ62\, t; \\ n &= 722.^\circ63175/\text{day}; \\ L_0 &= 194.^\circ98; \\ \delta L_0 &= -0.^\circ113 - 0.^\circ0076\, t + 0.^\circ000\,35\, t^2; \\ t &= (\text{JD} - t_0)/365.25. \end{aligned} \tag{9.55}$$

a is the apparent semimajor axis at a distance of one astronomical unit; γ, the inclination to the equator of Jupiter; θ, the longitude of the ascending node; n, the mean motion per solar day; L_0, the mean longitude at epoch t_0; and δL_0, the correction to mean longitude. $t - t_0$ is reckoned in Julian years. The longitudes are measured in the plane of the equator of Jupiter, from the ascending node of the mean orbital plane of Jupiter on the plane of the equator of Jupiter as shown in Fig. 9.12. From these orbital elements:

$$\begin{aligned} \text{sidereal period} \quad & 0.^\text{d}499\,910\,83 = 11.^\text{h}997\,860 \\ \text{mean synodic period} \quad & 0.^\text{d}499\,968\,51 = 11.^\text{h}999\,244. \end{aligned}$$

In determining these elements, van Woerkom adopted Souillart's elements of the equator of Jupiter, but for the calculation of the elongations in *The Astronomical Almanac* the right ascension and declination of Jupiter's pole of Davies et al. (1989) are used:

$$\begin{aligned} \alpha_0 &= 268.^\circ05 - 0.^\circ009\, T \\ \delta_0 &= 64.^\circ49 + 0.^\circ003\, T \end{aligned} \tag{9.56}$$

where α_0 and δ_0 are referred to the equator and equinox of J2000.0

$$T = (\text{JD} - 2\,451\,545.0)/36525.$$

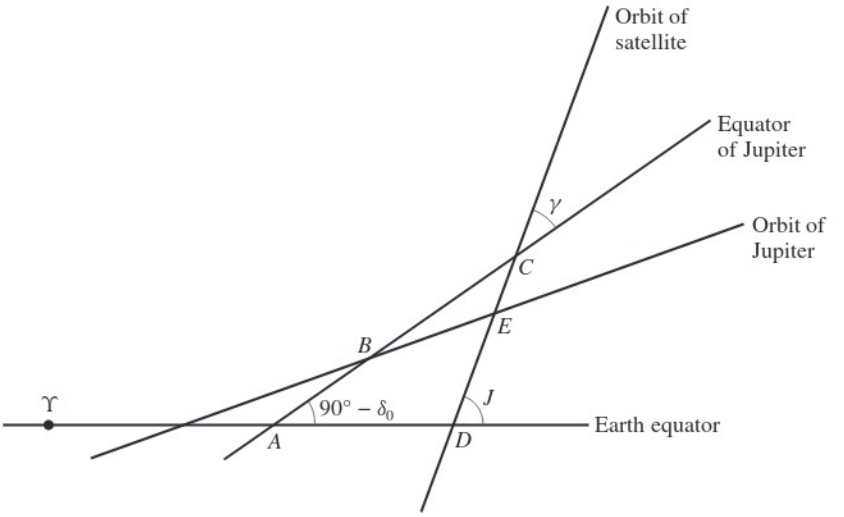


Figure 9.12 Reference system for Amalthea and Thebe. $\Delta = 180^\circ - AB, \theta = 180^\circ + BC$, $\theta - \Delta = AC$, $\psi = DC$, $N = \Upsilon D$, and $\alpha_0 = \Upsilon A - 90^\circ$

The right ascension, N, of the node of the orbit on the Earth's equator; the inclination, J, of the orbit to the Earth's equator; and the arc, ψ, along the orbit from the node on the Earth's equator to the node on Jupiter's equator are given by

$$\begin{aligned}
\sin J \sin(N - \alpha_0) &= +\cos\delta_0 \cos\gamma + \sin\delta_0 \sin\gamma \cos(\theta - \Delta) \\
\sin J \cos(N - \alpha_0) &= -\sin\gamma \sin(\theta - \Delta) \\
\cos J &= +\sin\delta_0 \cos\gamma - \cos\delta_0 \sin\gamma \cos(\theta - \Delta) \\
\sin J \sin\psi &= +\cos\delta_0 \sin(\theta - \Delta) \\
\sin J \cos\psi &= +\sin\delta_0 \sin\gamma + \cos\delta_0 \cos\gamma \cos(\theta - \Delta)
\end{aligned} \tag{9.57}$$

in which $\theta - \Delta$ (the arc along Jupiter's equator from its node on the Earth's equator to the node of the satellite's orbit) is given by

$$\begin{aligned}
\theta - \Delta &= 219.^\circ 8 - 2.^r 540\,574\,87(t - t_0); \quad (2.^r 54 \ldots = \text{rev per year}) \\
&= 219.^\circ 8 - 2.^\circ 504\,057\,37d
\end{aligned} \tag{9.58}$$

where d is the number of days from the epoch (JD 2416359.0).

The quantities N, J, and ψ are calculated from the preceding equations at 0^h at any date, and are then used to form U (B and P are not required) from Eqs. 9.26. The orbital longitude, u, measured from the node on the Earth's equator, at 0^h on that date is derived from

$$\begin{aligned}
u &= L_0 + nd - \theta + \psi + \delta L_0 \\
&= \psi + 112.^\circ 37 + 2.^r 014\,2662\,d.
\end{aligned} \tag{9.59}$$

Then the times of the elongations on that date are

$$\begin{aligned} &\text{eastern elongation} \quad 0^{\text{h}}.033\,327(U + 90^\circ - u) + 0^{\text{h}}.138\,61\Delta \\ &\text{western elongation} \quad 0^{\text{h}}.033\,327(U + 270^\circ - u) + 0^{\text{h}}.138\,61\Delta \end{aligned}$$

in which Δ is the geocentric distance of Jupiter. The terms in Δ are the corrections for light-time; for strict accuracy they should be interpolated to the times of geometric elongation which the first terms represent.

The calculation of elongation time need be made for only a few of the ephemeris dates, the others being obtained by means of multiples of the period. For strict accuracy, the calculation should be repeated with the values of the quantities at the calculated times instead of at 0^{h}; but for the tabular accuracy of $0^{\text{h}}.1$, this is unnecessary.

9.8.3 Jupiter's Sixth through Thirteenth Satellites

Differential right ascensions and declinations of Satellites VI–XIII are presented in *The Astronomical Almanac*. The coordinates are referred to the equator and equinox of J2000.0. They are computed with a variable-order, variable-step-size numerical integrator developed by Shampine and Gordon (1975). The equations of motion in x, y and z are:

$$\begin{aligned} \frac{d^2x}{dt^2} &= -\frac{M_{\text{J}}x}{r_{\text{js}}^3}\left[1 - \frac{3J_2r_{\text{J}}^2}{2r_{\text{js}}^2}(5\mu^2 - 1)\right] + \sum_{i=1}^{9} M_i\frac{x_i - x}{r_{\text{ij}}^3} - \frac{x_i}{r_{\text{is}}^3} \\ \frac{d^2y}{dt^2} &= -\frac{M_{\text{J}}y}{r_{\text{js}}^3}\left[1 - \frac{3J_2r_{\text{J}}^2}{2r_{\text{js}}^2}(5\mu^2 - 1)\right] + \sum_{i=1}^{9} M_i\frac{y_i - y}{r_{\text{ij}}^3} - \frac{y_i}{r_{\text{is}}^3} \\ \frac{d^2z}{dt^2} &= -\frac{M_{\text{J}}z}{r_{\text{js}}^3}\left[1 - \frac{3J_2r_{\text{J}}^2}{2r_{\text{js}}^2}(5\mu^2 - 3)\right] + \sum_{i=1}^{9} M_i\frac{z_i - z}{r_{\text{ij}}^3} - \frac{z_i}{r_{\text{is}}^3} \\ \mu &= \frac{z}{r} \end{aligned} \tag{9.60}$$

where the perturbing bodies are the Sun and planets. M_{J} is the mass of Jupiter; the M_i's are the masses of the perturbing bodies; r_{J} is the radius of Jupiter; r_{js} is Jupiter-satellite distance; x_i, y_i, and z_i are the rectangular components of the satellite-perturbing body distance; r_{is} is the satellite-perturbing body distance; r_{ij} is the Jupiter-perturbing body distance. Planetary coordinates are taken from the DE405/LE405 (see Chapter 8). The reciprocal masses, in solar mass units, and the J_2 for Jupiter used in integrations are as follows:

Sun	1.0	Mercury	6023600.0
Venus	408523.5	Earth	332946.038
Mars	3 098710.0	Jupiter	1047.35
Saturn	3498.0	Uranus	22960.0
Neptune	19314.0	Pluto	130000000.0
J_2 of Jupiter	0.01475		

The starting planetocentric coordinates and velocities from Rohde (1990) are given in Table 9.3. The differential coordinates are computed from Eqs. 9.24.

Table 9.3 The starting planetocentric coordinates and velocities of some Jovian satellites (Rohde 1990). Epoch JD 2447890.5 = 1989 December 30

Satellite			r (au)	v (au/day)
VI	Himalia	x	−0.0394627736618	+0.0013683275790
		y	−0.0722678670569	−0.0002593437765
		z	−0.0170810682702	−0.0010464833518
VII	Elara	x	−0.0619697457552	+0.0004392130964
		y	−0.0044124460879	−0.0020946808809
		z	+0.0265446659756	−0.0003974001515
VIII	Pasiphae	x	−0.0474722144088	−0.0010182557362
		y	−0.1000885430216	+0.0011925451174
		z	−0.0009486933348	+0.0009171895371
IX	Sinope	x	−0.0579232252532	+0.0011014867506
		y	+0.1464131750776	+0.0002877970106
		z	+0.0885266909368	−0.0003615702389
X	Lysithea	x	+0.0683709404212	+0.0006111658968
		y	−0.0114622412925	+0.0012863404782
		z	−0.0304090473403	+0.0013466750538
XI	Carme	x	−0.1221787634075	−0.0007075200606
		y	−0.1048136497855	+0.0009285971336
		z	−0.0685824702747	+0.0001468741809
XII	Ananke	x	+0.1246479748900	−0.0006562509816
		y	−0.0256709692336	−0.0013514562258
		z	−0.0203855454615	+0.0002939680931
XIII	Leda	x	+0.0356054434403	+0.0013645601641
		y	−0.0810815597479	+0.0006286869081
		z	+0.0052592795262	+0.0005799993600

9.9 The Rings and Satellites of Saturn

9.9.1 The Rings of Saturn

The rings of Saturn lie in its equatorial plane. The inclination and ascending node of this plane on the Earth's equator are determined from the north pole of Saturn as defined by Davies et al. (1989). The outer, inner, and dusky rings in this publication correspond to the A, B, and C rings, respectively. The Cassini division lies between the inner and outer rings. The dimensions of the outer ring and the factors for calculating the relative dimensions of the rings are from Esposito et al. (1984).

The ephemeris of the rings contains the following quantities that determine the Saturnicentric positions of the Earth and Sun referred to the plane of the rings, upon which the appearance of the rings depends:

U = the geocentric longitude of Saturn, measured in the plane of the rings eastward from its ascending node on the mean equator of the Earth; the Saturnicentric longitude of the Earth, measured in the same way, is $U + 180°$.

B = the Saturnicentric latitude of the Earth referred to the plane of the rings, positive toward the north; when B is positive, the visible surface of the rings is the northern surface.

P = the geocentric position angle of the northern semiminor axis of the apparent ellipse of the rings, measured from the north toward the east.

U' = the heliocentric longitude of Saturn, measured in the plane of the rings eastward from its ascending node on the ecliptic; the Saturnicentric longitude of the Sun, measured in the same way, is $U' + 180°$.

B' = the Saturnicentric latitude of the Sun referred to the plane of the rings, positive toward the north; when B' is positive, the northern surface of the rings is the illuminated surface.

P' = the heliocentric position angle of the northern semiminor axis of the rings on the heliocentric celestial sphere, measured eastward from the circle of latitude through Saturn.

The right ascension and declination of the north pole of Saturn are according to Davies et al. (1989),

$$\begin{aligned} \alpha_S &= 40.^\circ 58 - 0.^\circ 036\, T \\ \delta_S &= 83.^\circ 54 - 0.^\circ 004\, T \end{aligned} \tag{9.61}$$

where α_S and δ_S are referred to the equator and equinox of J2000.0 and (T = (JD − 2 451 545.0)/365 25).

Adding the variations due to precession, calculated by the formulae in § 6.6.2, gives the elements referred to the ecliptic and mean equinox of date; from them, the inclination, J, to the mean equator of date and the right ascension, N, of the ascending node measured from the mean equinox of date are obtained from

$$\begin{aligned} J &= 90^\circ - \delta_0 \\ N &= \alpha_0 + 90^\circ. \end{aligned} \tag{9.62}$$

The arc ϕ from the ascending node of the ring plane on the Earth's equator along the ring plane to its ascending node on the ecliptic is obtained from

$$\sin N \cot \phi = \cot \varepsilon \sin J - \cos J \cos N \tag{9.63}$$

where ε is the mean obliquity of date. From the elements referred to the equator of the Earth, and from the geocentric equatorial coordinates of Saturn, the ephemeris of U, B, and P is calculated by Eqs. 9.26. These quantities are defined with reference to the ring plane in the same way as with reference to the orbital plane of a satellite; but the effect of nutation must

first be removed from the apparent right ascension and declination of Saturn, to refer the position of the planet to the same equinox as the elements of the reference plane.

U', B', and P' may be obtained by formulae exactly analogous to Eqs. 9.26 from the ecliptic elements of the plane of the rings and the heliocentric longitude, l, and latitude, b, of Saturn, referred to the mean equinox of date:

$$\begin{aligned}
\cos B' \sin P' &= -\sin i \cos(l - \Omega) \\
\cos B' \cos P' &= +\cos i \cos b + \sin i \sin b \sin(l - \Omega) \\
\sin B' &= -\cos i \sin b + \sin i \cos b \sin(l - \Omega) \\
\cos B' \sin U' &= +\sin i \sin b + \cos i \cos b \sin(l - \Omega) \\
\cos B' \cos U' &= +\cos b \cos(l - \Omega).
\end{aligned} \tag{9.64}$$

The rings become invisible when

1. The ring-plane passes through the Sun, since neither side of the rings is then illuminated.
2. The ring-plane passes between the Sun and the Earth, since the unilluminated side of the rings is facing the Earth.
3. The ring-plane passes through the Earth, since the rings are too thin to be visible edge on.

Twice during each revolution of Saturn around the Sun—near the times when the ring-plane passes through the Sun—the Earth usually crosses the ring-plane three times, though occasionally it crosses only once. The last occasion on which only one passage of the Earth through the ring-plane occurred was in 1950.

9.9.2 The Satellites of Saturn

The Astronomical Almanac presents times of greatest eastern elongation for Satellites I–V, times of elongations (eastern and western) and conjunctions for Satellites VI–VIII, and differential right ascensions and declinations for Satellites VII–IX.

Eclipses, occultations, transits, and shadow-transits of the satellites occur during a limited period each time the Earth passes through the plane of the rings. Methods for calculating these phenomena are described by Comrie (1934). See also Taylor (1951).

Ephemerides are not provided for Satellites X–LII although orbital, physical, and photometric data are listed for a number of these satellites on pages F2–F5 of *The Astronomical Almanac* and for all of these satelllites at *The Astronomical Almanac Online* website. Janus was discovered in 1967. Epimetheus, Helene, Telesto, and Calypso satellites were discovered by ground-based observations during 1980. Atlas, Prometheus, and Pandora were discovered by Voyager. Many of the satellites are co-orbital. Janus and Epimetheus follow horseshoe paths in a reference frame rotating at their mean orbital speed. Telesto and Calypso orbit at the L_4 and L_5 Lagrangian points of Tethys. Helene is near the L_4 Lagrangian point of Dione. Pandora and Prometheus are the shepherd satellites of the F-ring.

9.9.2.1 Mimas, Enceladus, Tethys, and Dione

The orbital theories for Mimas, Enceladus, Tethys, and Dione are based on Kozai (1957). The values of the elements for Mimas, Enceladus, Tethys, and Dione are from Taylor and

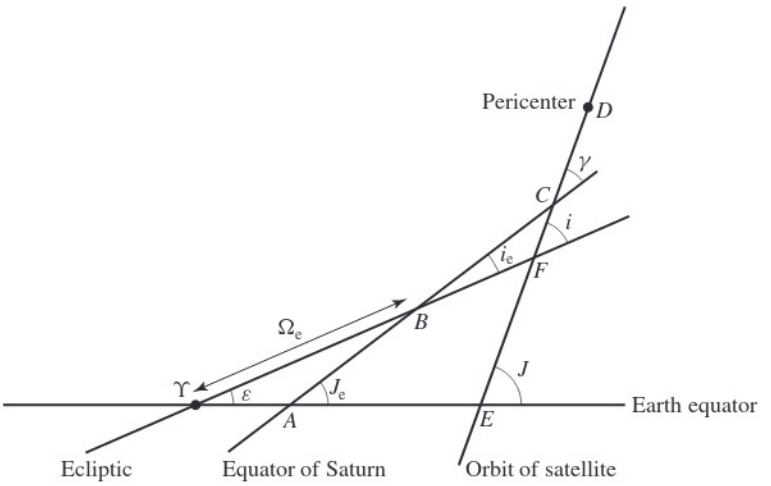


Figure 9.13 Reference plane for Mimas, Enceladus, Tethys and Dione. $\theta_1 = \Upsilon B + BC$, $P = \Upsilon B + BC + CD$, $N = \Upsilon E$, and $L_1 = \Upsilon B + BC + CD +$ mean anomaly. Ω_e and e_e are the ascending node and inclination of Saturn's equator relative to the Earth's equator and equinox of B1950.0, respectively. Values used are $\Omega_e = 168.^\circ 8387$ and $i_e = 28.^\circ 0653$.

Shen (1988), with mean motion and secular rates for Mimas and Enceladus from Kozai and corresponding quantities for Tethys and Dione from Garcia (1972). The elements of Mimas, Enceladus, Tethys, and Dione are referred to the B1950.0 equator of Saturn (see Fig. 9.13). The only significant periodic perturbations on these satellites are the mutual perturbations of Mimas and Tethys, and those of Enceladus and Dione. In each case, they are caused by a close 2:1 commensurability of mean motions. These perturbations affect the longitude and are denoted by ΔL.

The orbital elements of Mimas are as follows:

$$
\begin{aligned}
d &= \text{JD} - 2\,411\,093.0 \\
t &= d/365.25 \\
T &= 5.^\circ 0616[((\text{JD} - 2\,433\,282.423)/365.25) + 1950.0 - 1866.06] \\
a &= 0.001\,241\,71 \text{ au} \\
n &= 381.^\circ 994\,516/\text{day} \\
e &= 0.019\,86 \\
\gamma &= 1.^\circ 570 \\
\theta_1 &= 49.^\circ 4 - 365.^\circ 025\, t \\
L_1 &= 128.^\circ 839 + nd - 43.^\circ 415 \sin T - 0.^\circ 714 \sin 3T \\
&\quad - 0.^\circ 020 \sin 5T \\
P &= 107.^\circ 0 + 365.^\circ 560\, t
\end{aligned}
\tag{9.65}
$$

where a is the semimajor axis; n the daily mean motion; e the eccentricity; γ the inclination of the orbital plane to Saturn's equator; θ_1 the longitude of the ascending node; L_1 the mean longitude; and P the longitude of the pericenter.

The orbital elements of Enceladus are given by:

$$
\begin{aligned}
d &= \text{JD} - 2\,411\,093.0 \\
t &= d/365.25 \\
a &= 0.001\,589\,35 \text{ au} \\
n &= 262.^{\circ}731\,9052/\text{day} \\
e &= 0.005\,32 \\
\gamma &= 0.^{\circ}036 \\
\theta_1 &= 145^{\circ} - 152.^{\circ}7\,t \\
L_1 &= 200.^{\circ}155 + nd + 15.'38 \sin(59.^{\circ}4 + 32.^{\circ}73\,t) \\
&\quad + 13.'04 \sin(119.^{\circ}2 + 93.^{\circ}18\,t) \\
P &= 312.^{\circ}7 + 123.^{\circ}42\,t
\end{aligned}
\tag{9.66}
$$

where the variables are defined in the same manner as for Mimas.

The orbital elements of Tethys are as follows:

$$
\begin{aligned}
d &= \text{JD} - 2\,411\,093.0 \\
t &= d/365.25 \\
T &= 5.^{\circ}0616[((\text{JD} - 2\,433\,282.423)/365.25) + 1950.0 - 1866.06] \\
a &= 0.001\,970\,69 \text{ au} \\
n &= 190.^{\circ}697\,920\,278/\text{day} \\
e &= 0.000\,212 \\
\gamma &= 1.^{\circ}1121 \\
\theta_1 &= 111.^{\circ}41 - 72.^{\circ}247\,54\,t \\
L_1 &= 284.^{\circ}9982 + nd + 2.^{\circ}0751 \sin T + 0.^{\circ}0341 \sin 3\,T \\
&\quad + 0.^{\circ}0010 \sin 5\,T \\
P &= 97^{\circ} + 72.^{\circ}29\,t
\end{aligned}
\tag{9.67}
$$

where the variables are defined in the same manner as for Mimas.

The orbital elements of Dione are given by:

$$
\begin{aligned}
d &= \text{JD} - 2\,411\,093.0 \\
t &= d/365.25 \\
a &= 0.002\,524\,13 \text{ au} \\
n &= 131.^{\circ}534\,920\,026/\text{day} \\
e &= 0.001\,715 \\
\gamma &= 0.^{\circ}0289 \\
\theta_1 &= 228^{\circ} - 30.^{\circ}6197\,t \\
L_1 &= 255.^{\circ}1183 + nd - 0.'88 \sin(59.^{\circ}4 + 32.^{\circ}73\,t) \\
&\quad - 0.'75 \sin(119.^{\circ}2 + 93.^{\circ}18\,t) \\
P &= 173.^{\circ}6 + 30.^{\circ}8381\,t
\end{aligned}
\tag{9.68}
$$

where the variables are defined in the same manner as for Mimas.

To determine the times of greatest eastern elongation we must first find the orbital longitude, u; the longitude of the ascending node N of the orbit on the Earth's equator; and the inclination of the orbit to the Earth's equator, J. From spherical trigonometry we have from triangle BFC in Fig. 9.13,

$$\begin{aligned} \sin i \sin BF &= \sin\gamma \sin(\theta_1 - \Omega_e) \\ \sin i \cos BF &= \cos\gamma \sin i_e + \sin\gamma \cos i_e \cos(\theta_1 - \Omega_e) \end{aligned} \tag{9.69}$$

which can be solved for BF and i. The arc length FC and its quadrant can be found from the equations

$$\begin{aligned} \sin i \sin FC &= \sin(\theta_1 - \Omega_e) \sin i_e \\ \sin i \cos FC &= \cos i_e \sin\gamma + \sin i_e \cos\gamma \cos(\theta_1 - \Omega_e). \end{aligned} \tag{9.70}$$

Similarly, from the triangle ΥEF we have

$$\begin{aligned} \sin J \sin N &= \sin i \sin(\Omega_e + BF) \\ \sin J \cos N &= \cos i \sin\varepsilon + \sin i \cos\varepsilon \cos(\Omega_e + BF) \end{aligned} \tag{9.71}$$

which can be solved for J and N. Then the arc EF and its quadrant can be found from

$$\begin{aligned} \sin J \sin EF &= \sin(\Omega_e + BF) \sin\varepsilon \\ \sin J \cos EF &= \cos\varepsilon \sin i + \sin\varepsilon \cos i \cos(\Omega_e + BF) \end{aligned} \tag{9.72}$$

u then follows from

$$u = P - \theta_1 + EF + FC + \text{true anomaly}. \tag{9.73}$$

The tabulated orbital elements γ, a, and e are listed above. The remaining elements must be computed. From the spherical triangle ΥAB in Fig. 9.13 we have

$$\begin{aligned} \sin J_e \sin AB &= \sin\varepsilon \sin\Omega_e \\ \sin J_e \cos AB &= \cos\varepsilon \sin i_e + \sin\varepsilon \cos i_e \cos\Omega_e \end{aligned} \tag{9.74}$$

which can be solved for AB.

Then

$$\begin{aligned} \theta &= \theta_1 - \Omega_e + AB \\ L &= L_1 - \Omega_e + AB \\ M &= L_1 - P. \end{aligned} \tag{9.75}$$

9.9.2.2 Rhea, Titan, Hyperion, and Iapetus

The orbital theories for Rhea and Titan are from Sinclair (1977). The orbital elements are from Taylor and Shen (1988) with the mean motions and secular rates used from Garcia (1972). The theory and orbital elements for Hyperion are from Taylor (1984). The theory for the motion of Iapetus is taken from Sinclair (1974) with some additional periodic terms from Harper et al. (1988). The orbital elements for Iapetus are from Taylor and Shen (1988).

Because of the oblateness of Saturn and solar perturbations, the orbit plane of Rhea precesses at a constant inclination around the Laplacian plane of Rhea. Because we are using

the ecliptic as the reference plane, this motion around the Laplacian plane appears as periodic variations in λ, ϖ, Ω, and i. The osculating elements are given by:

$$\begin{aligned}
a &= 0.003\,524\,00\text{au} \\
n &= 79\overset{\circ}{.}690\,040\,0700/\text{day} \\
\gamma_0 &= 0\overset{\circ}{.}3305 \\
e\sin\varpi &= 0.000\,210\sin\pi + 0.001\,00\sin\varpi_{\mathrm{T}} \\
e\cos\varpi &= 0.000\,210\cos\pi + 0.001\,00\cos\varpi_{\mathrm{T}} \\
\lambda &= 359\overset{\circ}{.}4727 + nd \\
&\quad + \kappa\sin\gamma_0\tan\frac{1}{2}i_{\mathrm{e}}\sin(356\overset{\circ}{.}87 - 10\overset{\circ}{.}2077\,t) \\
i &= i_{\mathrm{e}} - 0\overset{\circ}{.}0455 \\
&\quad + \kappa\sin\gamma_0\cos(356\overset{\circ}{.}87 - 10\overset{\circ}{.}2077\,t) + 0\overset{\circ}{.}0201\cos N_{\mathrm{T}} \\
\Omega &= \Omega_{\mathrm{e}} - 0\overset{\circ}{.}0078 + [\kappa\sin\gamma_0\sin(356\overset{\circ}{.}87 - 10\overset{\circ}{.}2077\,t) \\
&\quad + 0\overset{\circ}{.}0201\sin N_{\mathrm{T}}]/\sin i_{\mathrm{e}}
\end{aligned} \tag{9.76}$$

where

$$\begin{aligned}
\pi &= 305^\circ + 10\overset{\circ}{.}2077\,t \\
\varpi_{\mathrm{T}} &= 276\overset{\circ}{.}49 + 0\overset{\circ}{.}5219(\mathrm{JD} - 2\,411\,368.0)/365.25 \\
N_{\mathrm{T}} &= 44\overset{\circ}{.}5 - 0\overset{\circ}{.}5219(\mathrm{JD} - 2\,411\,368.0)/365.25 \\
\kappa &= 57\overset{\circ}{.}295\,78 \\
d &= \mathrm{JD} - 2\,411\,093.0 \\
t &= d/365.25.
\end{aligned} \tag{9.77}$$

Here a is the semimajor axis; n is the daily mean motion; e is the eccentricity; ϖ and λ are the longitude of pericenter and the mean longitude, respectively, reckoned from the vernal equinox along the ecliptic to the ascending node and thence along the orbit; i and Ω are the inclination and ascending node of the orbit with respect to the ecliptic of 1950.0. The angular elements are shown in Fig. 9.14.

The coefficient 0.00100 in the expressions for $e\sin\varpi$ and $e\cos\varpi$ is a forced eccentricity due to Titan. The algebraic expression for this is given in Sinclair (1977). The inclination and node of Rhea's Laplacian plane relative to the ecliptic (1950.0) are $i = i_{\mathrm{e}} - 0\overset{\circ}{.}0455$ and $\Omega = \Omega_{\mathrm{e}} - 0\overset{\circ}{.}0078$.

There are a number of significant solar perturbations on Titan's orbit and, as for Rhea, λ, Ω, and i are affected by periodic variations due to the reference plane not being the Laplacian plane. The solar perturbations are functions of the mean elements of the apparent orbit of the Sun about Saturn. The solar elements needed are λ_{s}, Ω_{s}, and i_{s} (which are defined in Fig. 9.15), and l_{s}, the mean anomaly. Approximate values of i, Ω, and ϖ are also needed, and these are denoted by i_{a}, Ω_{a}, and ϖ_{a}. These quantities are given by the following expressions:

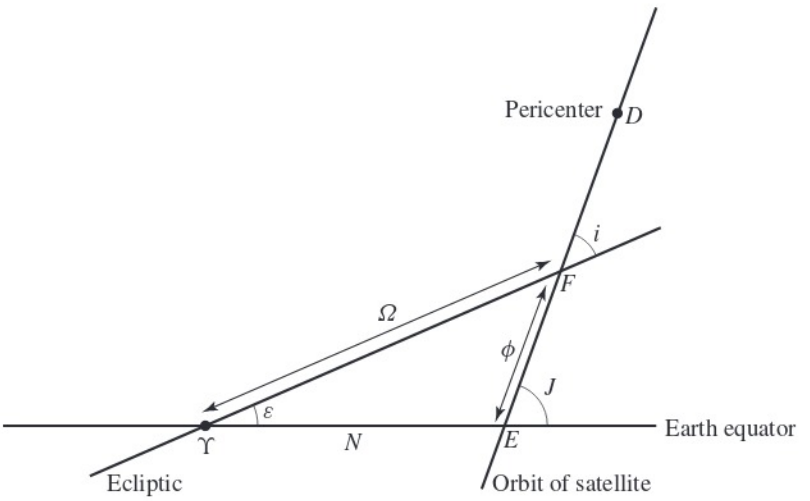


Figure 9.14 Reference system for Rhea, Titan, Hyperion, Iapetus, and Phoebe. $\varpi = \Upsilon F + FD$ and $\lambda = \Upsilon F + FD +$ mean anomaly.

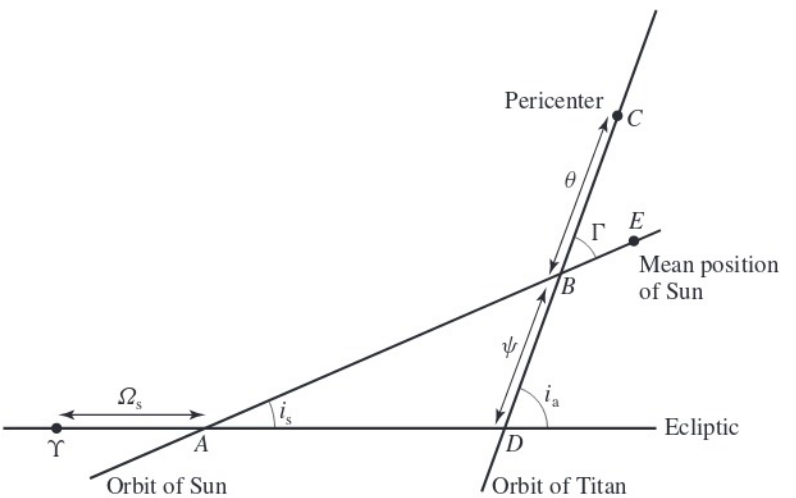


Figure 9.15 Angles needed to evaluate solar perturbations on Titan. $\Omega_a = \Upsilon D$, $\theta = \Upsilon A + AB$, $\varpi_a = \Upsilon D + DC$, and $\lambda_s = \Upsilon A + AE$.

$$
\begin{aligned}
T &= (\mathrm{JD} - 2\,415\,020.0)/36525 \\
l_\mathrm{s} &= 175^\circ\!.4762 + 1221^\circ\!.5515\,T \\
i_\mathrm{s} &= 2^\circ\!.4891 + 0^\circ\!.002\,435\,T \\
\Omega_\mathrm{s} &= 113^\circ\!.350 - 0^\circ\!.2597\,T \\
\lambda_\mathrm{s} &= 267^\circ\!.2635 + 1222^\circ\!.1136\,T \\
t &= (\mathrm{JD} - 2\,411\,368.0)/365.25 \\
\kappa &= 57^\circ\!.295\,78 \\
\gamma_0 &= 0^\circ\!.2990 \\
i_\mathrm{a} &= i_\mathrm{e} - 0^\circ\!.6204 + \kappa \sin\gamma_0 \cos(41^\circ\!.28 - 0^\circ\!.5219\,t) \\
\Omega_\mathrm{a} &= \Omega_\mathrm{e} - 0^\circ\!.1418 + \kappa \sin\gamma_0 \sin(41^\circ\!.28 - 0^\circ\!.5219\,t)/\sin i_\mathrm{e} \\
\varpi_\mathrm{a} &= 275^\circ\!.837 + 0^\circ\!.5219\,t.
\end{aligned}
\tag{9.78}
$$

The quantities $(i_\mathrm{e} - 0^\circ\!.6204)$ and $(\Omega_\mathrm{e} - 0^\circ\!.1418)$ define the inclination and node of the Laplacian plane of Titan. The auxiliary angles—θ, Γ, Ψ, g, and L_s—are given by:

$$
\begin{aligned}
\cos\Gamma &= \cos i_\mathrm{s}\cos i_\mathrm{a} + \sin i_\mathrm{s}\sin i_\mathrm{a}\cos(\Omega_\mathrm{a} - \Omega_\mathrm{s}) \\
\sin\Gamma\sin\Psi &= \sin i_\mathrm{s}\sin(\Omega_\mathrm{a} - \Omega_\mathrm{s}) \\
\sin\Gamma\cos\Psi &= \cos i_\mathrm{s}\sin i_\mathrm{a} - \sin i_\mathrm{s}\cos i_\mathrm{a}\cos(\Omega_\mathrm{a} - \Omega_\mathrm{s}) \\
\sin\Gamma\sin(\theta - \Omega_\mathrm{s}) &= \sin i_\mathrm{a}\sin(\Omega_\mathrm{a} - \Omega_\mathrm{s}) \\
\sin\Gamma\cos(\theta - \Omega_\mathrm{s}) &= -\sin i_\mathrm{s}\cos i_\mathrm{a} \\
&\quad + \cos i_\mathrm{s}\sin i_\mathrm{a}\cos(\Omega_\mathrm{a} - \Omega_\mathrm{s}) \\
L_\mathrm{s} &= \lambda_\mathrm{s} - (\theta - \Omega_\mathrm{s}) - \Omega_\mathrm{s} \\
g &= \varpi_\mathrm{a} - \Omega_\mathrm{a} - \Psi.
\end{aligned}
\tag{9.79}
$$

The osculating elements of Titan are given by:

$$
\begin{aligned}
a &= 0.008\,167\,65\ \mathrm{au} \\
n &= 22^\circ\!.576\,973\,85/\mathrm{day} \\
e &= 0.028\,815 - 0.000\,184\cos 2g + 0.000\,073\cos 2(L_\mathrm{s} - g) \\
\varpi &= \varpi_\mathrm{a} + \kappa[0.006\,30\sin 2g + 0.002\,50\sin 2(L_\mathrm{s} - g)] \\
\lambda &= 261^\circ\!.3121 + nd + \kappa[\sin\gamma_0 \tan\frac{1}{2}i_\mathrm{e}\sin(41^\circ\!.28 \\
&\quad - 0^\circ\!.5219\,t) - 0.000\,176\sin l_\mathrm{s} - 0.000\,215\sin 2L_\mathrm{s} \\
&\quad + 0.000\,057\sin(2L_\mathrm{s} + \Psi)] \\
i &= i_\mathrm{a} + 0.000\,232\kappa\cos(2L_\mathrm{s} + \Psi) \\
\Omega &= \Omega_\mathrm{a} + 0.000\,503\kappa\sin(2L_\mathrm{s} + \Psi)
\end{aligned}
\tag{9.80}
$$

where $d = \mathrm{JD} - 2\,411\,368.0$; $t = d/365.25$; and $\kappa = 57^\circ\!.295\,78$.

The algebraic expressions for the coefficients of these periodic terms are given in Sinclair (1977).

The osculating elements of Hyperion's orbit are given by:

$$
\begin{aligned}
a &= 0.009\,9040 - 0.000\,034\,22\cos\tau \text{ au}\\
n &= 16^\circ.919\,9514/\text{day}\\
e &= 0.104\,41 - 0.004\,01\cos\tau + 0.000\,09\cos(\zeta-\tau)\\
&\quad + 0.023\,21\cos\zeta - 0.000\,09\cos(\zeta+\tau) - 0.001\,10\cos 2\zeta\\
&\quad + 0.000\,13\cos(31^\circ.9 + 61^\circ.7524\,T)\\
i &= i_e - 0^\circ.747 + 0^\circ.6200\cos(105^\circ.31 - 2^\circ.392\,T)\\
&\quad + 0^\circ.315\cos(38^\circ.73 - 0^\circ.5353\,T)\\
&\quad - 0^\circ.018\cos(13^\circ + 24^\circ.44\,T)\\
\Omega &= \Omega_e + ((-0^\circ.061 + 0^\circ.6200\sin(105^\circ.31 - 2^\circ.392\,T)\\
&\quad + 0^\circ.315\sin(38^\circ.73 - 0^\circ.5353\,T)\\
&\quad - 0^\circ.018\sin(13^\circ + 24^\circ.44\,T))/\sin(i_e - 0.747)\\
\lambda &= 176^\circ.7481 + nd + 0^\circ.1507\sin(105^\circ.31 - 2^\circ.392\,T)\\
&\quad + 9^\circ.089\sin\tau + 0^\circ.007\sin 2\tau - 0^\circ.014\sin 3\tau\\
&\quad + 0^\circ.192\sin(\zeta-\tau) - 0^\circ.091\sin\zeta + 0^\circ.211\sin(\zeta+\tau)\\
&\quad - 0^\circ.013\sin(176^\circ + 12^\circ.22\,T) + 0^\circ.017\sin(8^\circ + 24^\circ.44\,T)\\
\varpi &= 69^\circ.993 - 18^\circ.6702\,T + 0^\circ.1507\sin(105^\circ.31 - 2^\circ.392\,T)\\
&\quad - 0^\circ.47\sin\tau - 13^\circ.36\sin\zeta + 2^\circ.16\sin 2\zeta\\
&\quad + 0^\circ.07\sin(31^\circ.9 + 61^\circ.7524\,T)
\end{aligned}
\tag{9.81}
$$

where

$$
\begin{aligned}
d &= \text{JD} - 2\,415\,020.0\\
T &= \text{JD} - 2\,433\,282.423\,459\,05)/365.2422 + 50.0\\
\tau &= 93^\circ.13 + 0^\circ.562\,039\,d\\
\zeta &= 148^\circ.72 - 19^\circ.184\,T.
\end{aligned}
$$

Here again the elements are reckoned in the same way as for Rhea.

The orbital plane of Iapetus is inclined at about 8° to its Laplacian plane, which is itself inclined at about 15° to the equatorial plane of Saturn, and 12° to the orbital plane of Saturn. As a result, the motion of the orbital plane of Iapetus is quite complicated, and is described by cubic polynomials in time for i and Ω. The osculating elements are computed as follows:

$$
\begin{aligned}
t &= \text{JD} - 2\,409\,786.0\\
t_c &= t/36525\\
T &= (\text{JD} - 2\,415\,020.0)/36525.
\end{aligned}
$$

The elements computed from constant and secular terms are:

$$\begin{aligned}
a &= 0.023\,809\,84 \text{ au} \\
n &= 4^\circ.537\,957\,11/\text{day} \\
e &= 0.028\,8184 + 0.000\,575\,t_\mathrm{c} \\
i &= 18^\circ.459\,59 - 0^\circ.9555\,t_\mathrm{c} - 0^\circ.0720\,t_\mathrm{c}^2 + 0^\circ.0054\,t_\mathrm{c}^3 \\
\lambda &= 76^\circ.198\,54 + nt \\
\varpi &= 352^\circ.905 + 11^\circ.65\,t_\mathrm{c} \\
\Omega &= 143^\circ.1294 - 3^\circ.797\,t_\mathrm{c} + 0^\circ.116\,t_\mathrm{c}^2 + 0^\circ.008\,t_\mathrm{c}^3.
\end{aligned} \tag{9.82}$$

The auxiliary angles needed to compute periodic terms are calculated as follows:

$$\begin{aligned}
\theta &= 4^\circ.367 - 0^\circ.195\,T \\
\Theta &= 146^\circ.819 - 3^\circ.918\,T \\
\lambda_\mathrm{s} &= 267^\circ.263 + 1222^\circ.114\,T \\
\varpi_\mathrm{s} &= 91^\circ.796 + 0^\circ.562\,T \\
\lambda_\mathrm{T} &= 261^\circ.319 + 22^\circ.576\,974(\mathrm{JD} - 2\,411\,368.0) \\
\varpi_\mathrm{T} &= 277^\circ.102 + 0^\circ.001\,389(\mathrm{JD} - 2\,411\,368.0) \\
\phi &= 60^\circ.470 + 1^\circ.521\,T \\
\Phi &= 205^\circ.055 - 2^\circ.091\,T.
\end{aligned} \tag{9.83}$$

From these we compute the following:

$$\begin{aligned}
l &= \lambda - \varpi \\
l_\mathrm{s} &= \lambda_\mathrm{s} - \varpi_\mathrm{s} \\
l_\mathrm{T} &= \lambda_\mathrm{T} - \varpi_\mathrm{T} \\
g &= \varpi - \Omega - \theta \\
g_\mathrm{s} &= \varpi_\mathrm{s} - \Theta \\
g_\mathrm{T} &= \varpi_\mathrm{T} - \Phi \\
g_\mathrm{l} &= \varpi - \Omega - \phi.
\end{aligned} \tag{9.84}$$

Some of the expressions for the perturbations involve e and i. For these the following expressions are used.

$$\begin{aligned}
e &= 0.028\,8184 + 0.000\,575\,t_\mathrm{c} \\
i &= 18^\circ.459\,59 - 0^\circ.9555\,t_\mathrm{c} - 0^\circ.0720\,t_\mathrm{c}^2 + 0^\circ.0054\,t_\mathrm{c}^3.
\end{aligned} \tag{9.85}$$

The following perturbations are to be added to the elements

$$\begin{aligned}
\Delta a &= 10^{-5}a[7.87\cos(2l + 2g - 2l_\mathrm{s} - 2g_\mathrm{s}) + 98.79\cos(l + g_\mathrm{l} - l_\mathrm{T} - g_\mathrm{T})] \\
\Delta e &= 10^{-5}[-140.97\cos(g_\mathrm{l} - g_\mathrm{T}) + 37.33\cos(2l_\mathrm{s} + 2g_\mathrm{s} - 2g) \\
&\quad + 11.80\cos(l + 2g - 2l_\mathrm{s} - 2g_\mathrm{s}) + 24.08\cos l + 28.49\cos(2l + g_\mathrm{l} - l_\mathrm{T} - g_\mathrm{T}) \\
&\quad + 61.90\cos(l_\mathrm{T} + g_\mathrm{T} - g_\mathrm{l}) + 0.496\cos(3l_\mathrm{s} + 2g_\mathrm{s} - 2g)]
\end{aligned}$$

$$
\begin{aligned}
\Delta i = {} & 0\overset{\circ}{.}042\,04\cos(2l_s + 2g_s + \theta) + 0\overset{\circ}{.}002\,35\cos(l + g_l + l_T + g_T + \phi) \\
& + 0\overset{\circ}{.}003\,60\cos(l + g_l - l_T - g_T + \phi) + 0\overset{\circ}{.}0005\cos(4l_s + 2g_s) \\
& + 0\overset{\circ}{.}0058\cos(3l_s + 2g_s) - 0\overset{\circ}{.}0024\cos(l_s + 2g_s) \\
\Delta\lambda = {} & -0\overset{\circ}{.}042\,99\sin(l + g_l - l_T - g_T) - 0\overset{\circ}{.}007\,89\sin(2l + 2g - 2l_s - 2g_s) \\
& - 0\overset{\circ}{.}063\,12\sin ls - 0\overset{\circ}{.}002\,95\sin 2l_s - 0\overset{\circ}{.}022\,31\sin(2l_s + 2g_s) \\
& + 0\overset{\circ}{.}006\,50\sin(2l_s + 2g_s + \theta) \\
\Delta\varpi = {} & [0\overset{\circ}{.}080\,77\sin(g_l - g_T) + 0\overset{\circ}{.}021\,39\sin(2l_s + 2g_s - 2g) \\
& - 0\overset{\circ}{.}006\,76\sin(l + 2g - 2l_s - 2g_s) + 0\overset{\circ}{.}013\,80\sin l \\
& + 0\overset{\circ}{.}016\,32\sin(2l + g_l - l_T - g_T) + 0\overset{\circ}{.}035\,47\sin(l_T + g_T - g_l) \\
& + 0\overset{\circ}{.}000\,28\sin(3l_s + 2g_s - 2g)]/e \\
\Delta\Omega = {} & [0\overset{\circ}{.}042\,04\sin(2l_s + 2g_s + \theta) + 0\overset{\circ}{.}002\,35\sin(l + g_l + l_T + g_T + \phi) \\
& + 0\overset{\circ}{.}003\,58\sin(l + g_l - l_T - g_T + \phi) - 0\overset{\circ}{.}0006\sin 2l_s \\
& + 0\overset{\circ}{.}0003\sin(4l_s + 2g_s) + 0\overset{\circ}{.}0028\sin(3l_s + 2g_s) \\
& - 0\overset{\circ}{.}0012\sin(l_s + 2g_s) - 0\overset{\circ}{.}0142\sin l_s]/\sin i\,.
\end{aligned}
\tag{9.86}
$$

To determine J, u, and N, we can use the spherical triangle ΥEF in Fig. 9.14 to obtain

$$
\begin{aligned}
\sin J\sin N &= \sin i\sin\Omega \\
\sin J\cos N &= \cos i\sin\varepsilon + \sin i\cos\varepsilon\cos\Omega
\end{aligned}
\tag{9.87}
$$

which can be solved for N and J. The arc ϕ can be found from the equation

$$
\sin J\sin\phi = \sin\Omega\sin\varepsilon. \tag{9.88}
$$

u then follows from

$$
u = \varpi - \Omega + \phi + \text{true anomaly}\,. \tag{9.89}
$$

The tabulated orbital elements a and e were shown previously. The remaining elements are computed as follows. To calculate θ we first find the arc AC in Fig. 9.13. From spherical trigonometry we have for the triangle AEC:

$$
\sin(N - N_e)\cot\theta = \cos(N - N_e)\cos J_e - \sin J_e\cot J \tag{9.90}
$$

which can be solved for θ. M is given by

$$
M = \lambda - \varpi. \tag{9.91}
$$

γ can be determined by the formula

$$
\sin\gamma\sin\theta = \sin J\sin(N - N_e). \tag{9.92}
$$

L is found by first finding the arc length FC from

$$
\sin FC\sin\gamma = \sin(\Omega - \Omega_e)\sin i_e. \tag{9.93}
$$

L is then given by

$$
L = \lambda - \Omega - FC + \theta. \tag{9.94}
$$

The differential coordinates of Hyperion and Iapetus are computed as follows: the rectangular coordinates x and y of the satellite in the orbital plane are found from Eqs. 9.19. These coordinates are then transformed to the Earth equator and equinox by Eqs. 9.20 and 9.21. The differential coordinates ξ and η are then computed through Eqs. 9.24.

9.9.2.3 Phoebe

The orbital elements used in *The Astronomical Almanac* are those determined by Zadunaisky (1954). The ephemerides consist of differential right ascensions and declinations given at 2-day intervals. The elements are referred to the ecliptic and equinox of 1950.0. The values of the elements are as follows:

$$\begin{aligned} a &= 0.086\,5752 \text{ au} \\ n &= 0\overset{\circ}{.}653\,97/\text{day} \\ \lambda &= 277\overset{\circ}{.}872 - 0\overset{\circ}{.}654\,1068\,t \\ e &= 0.163\,26 \\ \varpi &= 280\overset{\circ}{.}165 - 0\overset{\circ}{.}195\,86\,T \\ i &= 173\overset{\circ}{.}949 - 0\overset{\circ}{.}020\,T \\ \Omega &= 245\overset{\circ}{.}998 + 0\overset{\circ}{.}413\,53\,T \end{aligned} \tag{9.95}$$

where

$$\begin{aligned} t &= \text{JD} - 2\,433\,282.5 \\ T &= t/365.25. \end{aligned}$$

a is the semimajor axis; λ, the mean longitude measured from the equinox along the ecliptic to the ascending node then along the orbit; e, the eccentricity; ϖ, the longitude of the pericenter reckoned from the equinox along the ecliptic to the ascending node then along the orbit to the pericenter; i, the inclination of the orbit to the ecliptic; and Ω, the longitude of the ascending node of the orbit on the ecliptic reckoned from the equinox.

To compute the differential right ascension and declination, the x and y coordinates in the orbital plane are found using Eq 9.19, where

$$M = \lambda - \varpi. \tag{9.96}$$

The coordinates are transformed to the Earth equator and equinox using Eqs. 9.20 and 9.21. Finally, $\Delta\alpha$ and $\Delta\delta$ are computed from ξ and η using Eq. 9.24.

9.10 The Rings and Satellites of Uranus

Orbital elements are given for the rings of Uranus as determined by Elliot et al. (1981). Times of greatest northern elongations are given for Satellites I through V; Ariel, Umbriel, Titania, Oberon, and Miranda. The orbital elements of these satellites are from Laskar and Jacobson (1987). The theory is developed in elliptical elements. Leading secular and periodic perturbations in the elements are quoted below.

Miranda

$$
\begin{aligned}
m/M_{\mathrm{U}} &= 0.075 \times 10^{-5} \\
n &= 4.443\,522\,67 - 0.000\,136\,65 \cos(0.621 \times 2\pi T + 5.89) \text{ radians/day} \\
L &= -0.238\,051\,58 + 4.445\,190\,55\,T \\
&\quad + 0.025\,472\,17 \sin(-2.181\,67 \times 10^{-4} \times 2\pi T + 1.32) \\
&\quad - 0.003\,088\,31 \sin(-4.363\,36 \times 10^{-4} \times 2\pi T + 2.64) \\
&\quad - 3.181 \times 10^{-4} \sin(-6.545\,02 \times 10^{-4} \times 2\pi T + 3.97) \text{ radians} \\
z &= 1.312\,38 \times 10^{-3} \exp i\,(1.5273 \times 10^{-4} \times 2\pi T + 0.61) \\
&\quad - 1.2331 \times 10^{-4} \exp i\,(0.086\,06 \times 2\pi T + 0.15) \\
&\quad + 1.9410 \times 10^{-4} \exp i\,(0.707 \times 2\pi T + 6.05) \\
\zeta &= 0.037\,871\,71 \exp i\,(-1.544\,49 \times 10^{-4} \times 2\pi T + 5.70).
\end{aligned}
\tag{9.97}
$$

Ariel

$$
\begin{aligned}
m/M_{\mathrm{U}} &= 1.49 \times 10^{-5} \\
n &= 2.492\,542\,57 \text{ radians/day} \\
L &= 3.098\,046\,41 + 2.492\,952\,52\,T \\
&\quad - 1.860\,50 \times 10^{-3} \sin(-2.181\,67 \times 10^{-4} \times 2\pi T + 1.32) \\
&\quad + 2.1999 \times 10^{-4} \sin(-4.363\,36 \times 10^{-4} \times 2\pi T + 2.64) \text{ radians} \\
z &= 1.187\,63 \times 10^{-3} \exp i\,(4.727\,824 \times 10^{-5} \times 2\pi T + 2.41) \\
&\quad + 8.6159 \times 10^{-4} \exp i\,(2.179\,316 \times 10^{-5} \times 2\pi T + 2.07) \\
\zeta &= 3.5825 \times 10^{-4} \exp i\,(-4.782\,474 \times 10^{-5} \times 2\pi T + 0.40) \\
&\quad + 2.9008 \times 10^{-4} \exp i\,(-2.156\,628 \times 10^{-5} \times 2\pi T + 0.59).
\end{aligned}
\tag{9.98}
$$

Umbriel

$$
\begin{aligned}
m/M_{\mathrm{U}} &= 1.45 \times 10^{-5} \\
n &= 1.515\,954\,90 \text{ radians/day} \\
L &= 2.285\,401\,69 + 1.516\,148\,11\,T \\
&\quad + 6.6057 \times 10^{-4} \sin(-2.181\,67 \times 10^{-4} \times 2\pi T + 1.32) \text{ radians} \\
z &= -2.2795 \times 10^{-4} \exp i\,(4.727\,824 \times 10^{-5} \times 2\pi T + 2.41) \\
&\quad + 3.904\,69 \times 10^{-3} \exp i\,(2.179\,132 \times 10^{-5} \times 2\pi T + 2.07) \\
&\quad + 3.0917 \times 10^{-4} \exp i\,(1.580\,524 \times 10^{-5} \times 2\pi T + 0.74) \\
&\quad + 2.2192 \times 10^{-4} \exp i\,(2.936\,3068 \times 10^{-6} \times 2\pi T + 0.43) \\
&\quad + 5.4923 \times 10^{-4} \exp i\,(-0.011\,57 \times 2\pi T + 5.71) \\
\zeta &= 1.113\,36 \times 10^{-3} \exp i\,(-2.156\,628 \times 2\pi T + 0.59) \\
&\quad + 3.5014 \times 10^{-4} \exp i\,(-1.401\,373 \times 10^{-5} \times 2\pi T + 1.75).
\end{aligned}
\tag{9.99}
$$

Titania

$$
\begin{aligned}
m/M_{\mathrm{U}} &= 3.97 \times 10^{-5} \\
n &= 0.721\,663\,16 \text{ radians/day} \\
L &= 0.856\,358\,79 + 0.721\,718\,51\,T \text{ radians} \\
z &= 9.3281 \times 10^{-4} \exp i\,(1.580\,524 \times 10^{-5} \times 2\pi T + 0.74) \\
&\quad + 1.120\,89 \times 10^{-3} \exp i\,(2.936\,3068 \times 10^{-6} \times 2\pi T + 0.43) \\
&\quad + 7.9343 \times 10^{-4} \exp i\,(-6.9008 \times 10^{-3} \times 2\pi T + 1.82) \\
\zeta &= 6.8572 \times 10^{-4} \exp i\,(-1.401\,373 \times 10^{-5} \times 2\pi T + 1.75) \\
&\quad + 3.7832 \times 10^{-4} \exp i\,(-1.971\,3918 \times 10^{-6} \times 2\pi T + 4.21).
\end{aligned}
\tag{9.100}
$$

Oberon

$$
\begin{aligned}
m/M_{\mathrm{U}} &= 3.45 \times 10^{-5} \\
n &= 0.466\,580\,54 \text{ radians/day} \\
L &= -0.915\,591\,80 + 0.466\,692\,12\,T \text{ radians} \\
z &= -7.5868 \times 10^{-4} \exp i\,(1.580\,524 \times 10^{-5} \times 2\pi T + 0.74) \\
&\quad + 1.397\,34 \times 10^{-3} \exp i\,(2.936\,3068 \times 10^{-6} \times 2\pi T + 0.43) \\
&\quad - 9.8726 \times 10^{-4} \exp i\,(-6.9008 \times 10^{-3} \times 2\pi T + 1.82) \\
\zeta &= -5.9633 \times 10^{-4} \exp i\,(-1.401\,373 \times 10^{-5} \times 2\pi T + 1.75) \\
&\quad + 4.5169 \times 10^{-4} \exp i\,(-1.971\,3918 \times 10^{-6} \times 2\pi T + 4.21)
\end{aligned}
\tag{9.101}
$$

with $T = \mathrm{JD} - 2\,444\,239.5$ and $i = \sqrt{-1}$.

Here m/M_{U} is the ratio of the mass of the satellite to the mass of Uranus; n is the daily mean motion; L is the mean longitude measured from the ascending node of Uranus' equator on the Earth's equator to the ascending node of the satellite orbit on Uranus' equator along the orbit to the mean position of the satellite. z and ζ are converted to classical elements with the following formulae

$$
\begin{aligned}
z &= e \exp(i\,P) \\
\zeta &= \sin\frac{\gamma}{2} \exp(i\theta)
\end{aligned}
\tag{9.102}
$$

where e is the eccentricity; P is the longitude of the pericenter reckoned from the ascending node of Uranus' equator on the Earth's equator of 1950.0, along Uranus' equator to the ascending node of the orbit on Uranus' equator, and then along the orbit to the pericenter; γ is the inclination of the orbital plane to Uranus' equator; θ is the longitude of the ascending node of the orbit on Uranus' equator measured from the ascending node of Uranus' equator on the Earth's equator.

Referred to the Earth's equator the motions of the satellites are direct. However, referred to the ecliptic they are retrograde, having an angle of inclination of roughly 98°. The orbital plane is inclined at such a large angle to the Earth's equator that the semimajor axis of the apparent orbit usually lies nearly north and south. Consequently, the greatest elongations are designated as northern and southern elongations instead of eastern or western. Only when the Earth is near the plane through the celestial pole perpendicular to the orbital plane, as during

1986–1987, is the minor axis of the apparent orbit directed approximately north and south. Even then, the north pole of the orbital plane may lie to the south of the geocentric position of Uranus. The north pole of the orbital plane is that from which the satellites' motion appears to be counterclockwise. This pole corresponds to the physical ephemeris south pole of Uranus, which is defined as lying south of the invariable plane of the solar system.

During the course of one revolution of Uranus, the Earth passes twice through the plane perpendicular to the orbital plane when the apparent orbits of the satellites are almost circular; and likewise, it passes twice through the orbital plane when the apparent orbits become straight lines. The Earth passed through the orbital plane from south to north in 1966, and the sequence of geometric relations during the interval from then until 2050 exemplifies the cycle during the 84-year period of Uranus.

1966–2008:	Earth north of orbital plane; B positive.
	Superior conjunction at position angle P.
1966–1986:	Northern elongation at $P + 90°$, when $u - U = 90°$.
1986:	Earth passed through plane perpendicular to
	orbital plane, at $U = 270°$.
1986–2008:	Northern elongation at $P - 90°$, when $u - U = 270°$.
2008:	Earth passed through orbital plane, north to
	south; $B = 0°$.
2008–2050:	Earth south of orbital plane; B negative.
	Superior conjunction at position angle $P + 180°$.
2008–2030:	Northern elongation at $P - 90°$, when $u - U = 270°$.
2030:	Earth passes through plane perpendicular to
	orbital plane, at $U = 90°$.
2030–2050:	Northern elongation at $P + 90°$, when $u - U = 90°$.

At the passage of the Earth through the plane perpendicular to the orbital plane, the position angle of the northern elongation changes by 180°, because the more northerly and more southerly extremities of the major axis are interchanged. The angle P is the position angle of the pole of the orbital plane that lies north of the celestial equator; but either the eastern or western extremity of the minor axis may be directed toward this pole, according to circumstances. Northern elongation may be to either the east or west of north. The elongations cannot be unambiguously designated as eastern and western.

To calculate the values of J, u, and N, consider spherical triangle ABD in Fig. 9.16. Spherical trigonometry gives us:

$$\begin{aligned} \sin J \sin(N - N_e) &= \sin\gamma \sin\theta \\ \sin J \cos(N - N_e) &= \cos\gamma \sin J_e + \sin\gamma \cos J_e \cos\theta \end{aligned} \tag{9.103}$$

which can be solved for J and N. The values of N_e and J_e, the longitude of the ascending node of Uranus' equator and its inclination to the Earth's equator, are found from the coordinates of Uranus' south pole: $\alpha_0 = 77^h.43$ and $\delta_0 = +15^\circ.10$ (Davies et al. 1989):

$$\begin{aligned} N_e &= \alpha_0 + 90° \\ J_e &= 90° - \delta_0. \end{aligned} \tag{9.104}$$

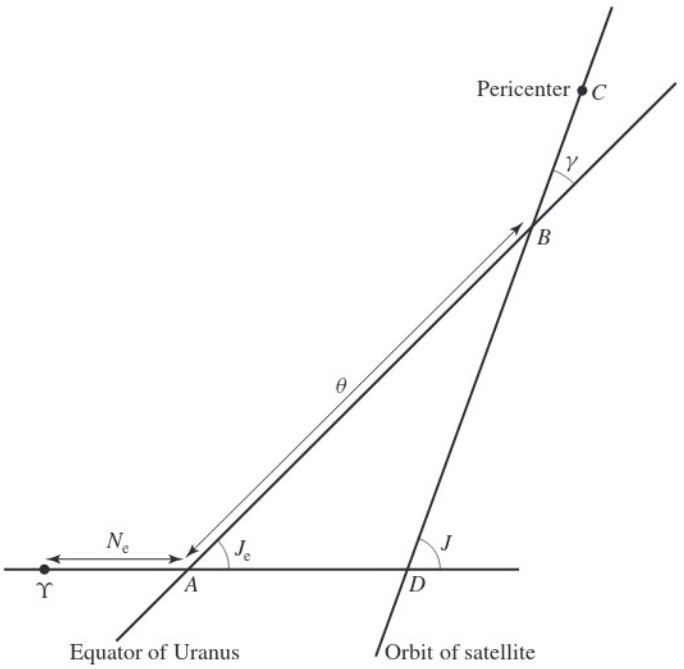


Figure 9.16 Reference system for the Uranian satellites. $N = \Upsilon D$, $P = AB + BC$, and $L = AB + BC +$ mean anomaly.

The arc length DB is found from

$$\sin DB \sin \gamma = \sin(N - N_e) \sin J_e. \tag{9.105}$$

Then

$$u = L - \theta + DB + (f - M) \tag{9.106}$$

where $(f - M)$ is the equation of center which can be found from Eq. 9.1, and

$$M = L - P. \tag{9.107}$$

Orbital, physical, and photometric data are presented on pages F2–F5 of *The Astronomical Almanac* for 7 of the 10 small satellites discovered by Voyager. Data for all 10 satellites are presented at *The Astronomical Almanac Online*. The orbits of these satellites all lie inside the orbit of Miranda. Cordelia and Ophelia are shepherd satellites for the ε-ring. It has also been proposed that Cordelia is the outer shepherd for the δ-ring, and that Ophelia is the outer shepherd of the γ-ring. Since Voyager, 3 more satellites have been discovered within the orbit of Miranda. A total of 9 irregular satellites with orbital periods in the range 500–3000 days, most of them in retrograde orbits, have also been discovered recently. Orbital, physical, and photometric data for these 12 satellites are presented at *The Astronomical Almanac Online*.

9.11 The Satellites of Neptune

Ephemerides are given for the greatest eastern elongations of Triton, calculated from the orbital elements determined by Harris (1984). Differential right ascensions and declinations are given for Nereid from orbital elements computed by Jacobson (1990).

9.11.1 Triton

The orbit of Triton is retrograde. The orbit, as far as it has been determined from observations, is circular. The orbital plane is defined with respect to a fixed reference plane. This reference plane is defined such that the projections of spin angular momentum of Neptune and the orbital angular momentum of Triton on the plane are equal and opposite. The pole of this fixed plane with respect to the Earth's equator and equinox of J2000.0 are

$$\begin{aligned} \alpha_{\rm p} &= 298\overset{\circ}{.}72 + 2\overset{\circ}{.}58 \sin N - 0\overset{\circ}{.}04 \sin 2N \\ \delta_{\rm p} &= 42\overset{\circ}{.}63 - 1\overset{\circ}{.}90 \cos N + 0\overset{\circ}{.}01 \cos 2N \\ N &= 359\overset{\circ}{.}28 + 54\overset{\circ}{.}308\, T \\ T &= ({\rm JD} - 2\,451\,545.0)/36525. \end{aligned} \tag{9.108}$$

The orbital elements of Triton referred to the fixed plane (see Fig. 9.17) are

$$\begin{aligned} t_0 &= {\rm JD}\ 2\,433\,282.5 \\ a &= 488\overset{''}{.}49 \\ e &= 0 \\ n &= 61\overset{\circ}{.}258\,8532/{\rm day} \\ L_0 &= 200\overset{\circ}{.}913 \\ \gamma &= 158\overset{\circ}{.}996 = 21\overset{\circ}{.}004\ {\rm retrograde} \\ \theta &= 151\overset{\circ}{.}401 + 0\overset{\circ}{.}578\,06({\rm JD} - t_0)/365.25 \end{aligned} \tag{9.109}$$

where a is the greatest elongation at unit distance; e is the eccentricity; n is the daily mean motion; L_0 is the mean longitude reckoned from the ascending node through the invariable plane at epoch; γ is the inclination of the orbital plane to the invariable plane; and θ is the angle from the intersection of invariable plane with the Earth's equatorial plane of 1950.0 to the ascending node of the orbit through the invariable plane.

Because the retrograde direction of the motion is represented by an orbital inclination greater than 90°, the ascending node of the orbit is the point at which the satellite crosses the equator from south to north. The pole of the orbit from which the motion appears counterclockwise is the south pole, at position angle P. Elongation is at position angle $P - 90°$, when $u - U = 270°$.

Twice during the course of one revolution of Neptune, about 165 years, the Earth passes through the orbital plane of Triton, when the apparent orbit becomes a straight line. The Earth crossed the orbital plane from north to south near the end of 1952; for an interval during 1950–1954, Triton transited the disk of Neptune and was occulted by the disk during each revolution. Before 1953, B was negative, and inferior conjunction was on the southern arc of the apparent orbit at position angle P. Since the passage through the orbital plane, B has been positive, and inferior conjunction is on the northern arc at $P + 180°$. The Earth will pass through the orbital plane again in 2035.

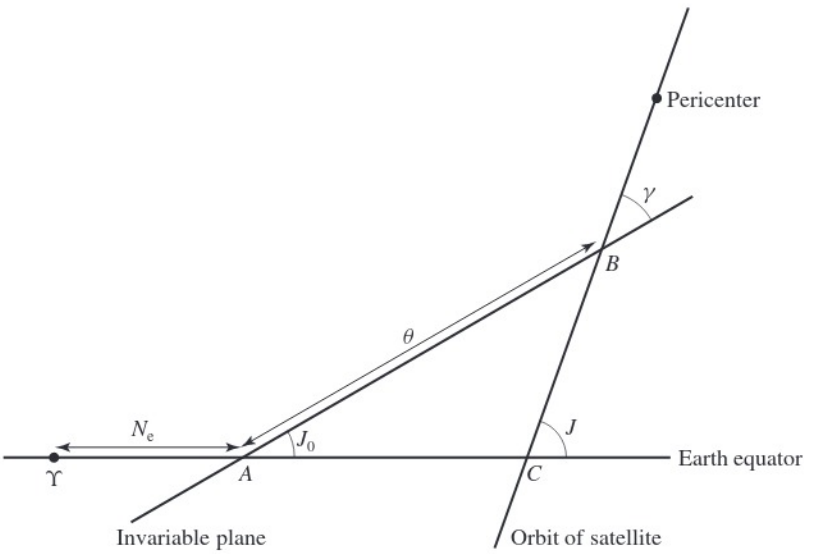


Figure 9.17 Reference system for Triton. $N = \Upsilon C$.

When the numerical value of B reaches a maximum as the Earth passes through the plane perpendicular to the orbital plane, as in 1987, the minor axis of the apparent orbit lies exactly north and south, the major axis lies east and west, and the position angle of the more northerly elongation changes by 180°. Before 1987, the western elongation was the more northerly; since then, the eastern elongation has been the more northerly.

The computation of J, u, and N is as follows. From the spherical triangle in Fig. 9.17 we have

$$\begin{aligned} \sin J \sin(N - N_e) &= \sin\gamma \sin\theta \\ \sin J \cos(N - N_e) &= \cos\gamma \sin J_e + \sin\gamma \cos J_e \cos\theta \end{aligned} \tag{9.110}$$

which can be solved for J and N. N_e and J_e, the longitude of the node and the inclination of the invariable plane to the Earth's equator, are found from

$$\begin{aligned} N_e &= \alpha_p + 90^\circ \\ J_e &= 90^\circ - \delta_p \end{aligned} \tag{9.111}$$

where α_p and δ_p are, respectively, the right ascension and declination of Neptune's pole. The arc length CB can be computed from

$$\sin CB \sin\gamma = \sin(N - N_e) \sin J_e. \tag{9.112}$$

u follows from

$$u = L_0 + CB + n(\mathrm{JD} - t_0) \tag{9.113}$$

where JD is the Julian date of interest.

9.11.2 Nereid

The orbit of Nereid is unique among the satellites in the solar system, because of its extreme eccentricity and the great difference in its inclination from that of Triton. Jacobson (1990)

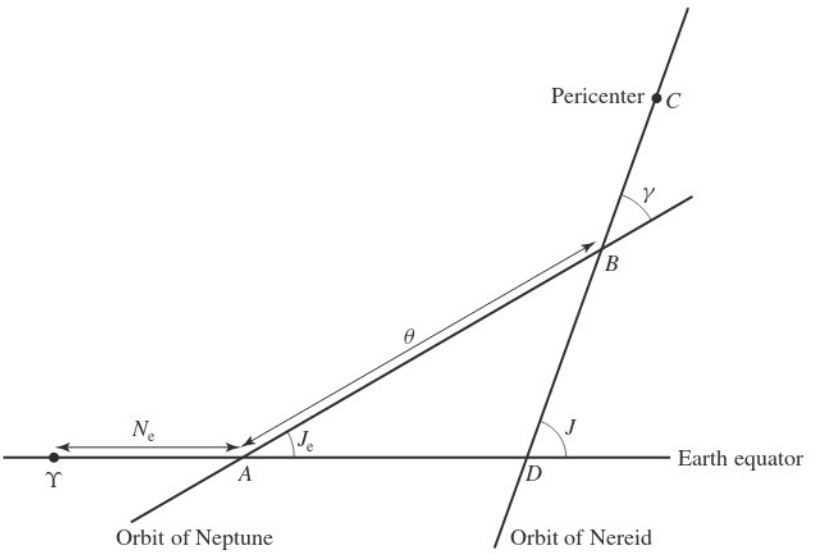


Figure 9.18 Reference system for Nereid. $N = \Upsilon D$ and $P = AB + BC$.

improved on the previous orbital theory of Mignard (1981) by accounting for the perturbations to Nereid's orbit due to Triton. The orbital elements of Nereid referred to the mean orbital plane of Neptune are (see Fig. 9.18):

$$\begin{aligned}
\Omega &= 315.^{\circ}995\,8928 - 3.^{\circ}650\,272\,562\,T \\
\gamma &= 6.^{\circ}748\,231\,850 \\
e &= 0.750\,876\,291 \\
\theta &= 251.^{\circ}724\,2240 + 0.^{\circ}869\,604\,8083\,T \\
a &= 0.036\,840 \text{ au} \\
n &= 0.^{\circ}999\,622\,7244 \text{ /day} \\
M &= 251.^{\circ}149\,846\,88 + 0.^{\circ}999\,646\,5329\,t - \theta
\end{aligned} \tag{9.114}$$

where θ is the longitude of the node, n is the mean daily motion, M is the mean anomaly of date, T is reckoned in Julian centuries, and t is the number of days elapsed from JD 2433680.5. The inclination, γ, is referred to Neptune's orbital plane. The longitude of the node is measured in Neptune's orbital plane from its intersection with the 1950.0 celestial equator. The orbit of Neptune is taken to have inclination, $J_e = 22.^{\circ}313$, and longitude of ascending node, $N_e = 3.^{\circ}522$ with respect to the 1950.0 celestial equator.

The differential right ascension and declination x and y coordinates in the orbital plane are computed from the Eqs. 9.19. These coordinates are transformed to the orbital plane using

$$\begin{bmatrix} x_1 \\ y_1 \\ z_1 \end{bmatrix} = \mathbf{R}_3(-\theta)\mathbf{R}_1(-\gamma)\mathbf{R}_3(-P) \begin{bmatrix} x \\ y \\ 0 \end{bmatrix} \tag{9.115}$$

where $P = \theta - \Omega$. These coordinates are then transformed to the Earth equator and equinox of 1950.0 using

$$\begin{bmatrix} x_2 \\ y_2 \\ z_2 \end{bmatrix} = \mathbf{R}_3(-N_e)\mathbf{R}_1(-J_e) \begin{bmatrix} x_1 \\ y_1 \\ z_1 \end{bmatrix}. \tag{9.116}$$

The coordinates x_2, y_2, z_2 are then used to compute $\Delta\alpha$ and $\Delta\delta$ from ξ and η using Eq. 9.24.

9.12 The Satellites of Pluto

Times of greatest northern elongation are presented in *The Astronomical Almanac* for Charon; neither Hydra nor Nix are presented, as they fall outside of the selection criterion of being magnitude 23.0 or brighter. The orbital elements from which the Charon data are calculated are taken from Tholen (1985). The elements, referred to the Earth's equator and equinox of 1950.0, are

$$\begin{aligned} a &= 0.000\,127\,88 \text{ au} \\ n &= 56\overset{\circ}{.}3625/\text{day} \\ J &= 94\overset{\circ}{.}3 \\ N &= 223\overset{\circ}{.}7 \\ l_0 &= 78\overset{\circ}{.}6 \\ t_0 &= \text{JD } 2\,445\,000.5 \end{aligned} \tag{9.117}$$

where a is the semimajor axis; n, the mean daily motion; J, the inclination of the orbital plane to the Earth equator of 1950.0; N, the longitude of the ascending node reckoned from the vernal equinox; l_0, the mean longitude at epoch reckoned from the ascending node along the orbit; and t_0, the date of epoch.

The orbit of Charon is retrograde. The pole of the orbit from which the motion appears counterclockwise is the south pole, at position angle P. Elongation is at position angle $P - 90°$, when $u - U = 270°$.

Twice during the course of one revolution of Pluto, about 248 years, the Earth passes through the orbital plane of Charon, when the apparent orbit becomes a straight line. The Earth crossed the orbital plane three times during 1987–1988, the end result being a crossing from north to south. In the interval 1985–1990, Charon transited the disk of Pluto and was occulted by the disk during each revolution. Before 1987, B was negative, and inferior conjunction was on the southern arc of the apparent orbit at position angle P. Since the passage through the orbital plane, B has been positive, and inferior conjunction is on the northern arc at $P + 180°$.

When the numerical value of B reaches a maximum as the Earth passes through the plane perpendicular to the orbital plane, as in 2050, the minor axis of the apparent orbit lies exactly north and south, the major axis lies east and west, and the position angle of the more northerly elongation changes by 180°. Before 2050, the western elongation is the more northerly; after 2050, the eastern elongation will be the more northerly.

Since the orbit is referred to the Earth equator and equinox of 1950.0, J and N are already known. u is found simply from

$$u = l_0 + n(\text{JD} - t_0) \tag{9.118}$$

where JD is the Julian date of interest.

Acknowledgments

Acknowledgments are due to Andrew Sinclair because much of this chapter is taken *verbatim* from Chapter 6 of the previous edition (Rohde and Sinclair 1992).

REFERENCES

1. The Astronomical Almanac Online: http://asa.usno.navy.mil or http://asa.hmnao.com.

2. IAU/IAG Working Group on Cartographic Coordinates and Rotational Elements: http://astrogeology.usgs.gov/Page/groups/name/IAU-WGCCRE.

Archinal, B. A., M. F. A'Hearn, E. Bowell, A. Conrad, G. J. Consolmagno, G. E. Hunt, R. Courtin, T. Fukushima, D. Hesteroffer, J. L. Hilton, G. A. Krasinsky, G. Neumann, J. Oberst, P. K. Seidelmann, P. Stooke, D. J. Tholen, P. C. Thomas, and I. P. Williams (2011). Report of the IAU Working Group on Cartographic Coordinates and Rotational Elements: 2009. *Celestial Mechanics and Dynamical Astronomy 109*(2), 101–135.

Arlot, J. E. (1982). New Constants for Sampson-Lieske Theory of the Galilean Satellites of Jupiter. *Astronomy and Astrophysics 107*, 305–310.

Arlot, J. E., J. Chapront, C. Ruatti, and D. T. Vu (1986). Compact ephemerides of the main satellites of Jupiter, Saturn and Uranus. *Astronomy and Astrophysics Supp. Series 65*(2), 383–403.

Brouwer, M. and G. M. Clemence (1961). *Methods of Celestial Mechanics*. London: Academic Press.

Chapront, J. and D. T. Vu (1984). A new compact representation of ephemerides - Application to the motion of Pluto, the sun and the Galilean satellites of Jupiter. *Astronomy and Astrophysics 141*, 131–143.

Comrie, L. J. (1934). Phenomena of Saturn's Satellites. *Memoirs of the British Astronomical Association 30*, 97–106.

Davies, M. E., V. K. Abalakin, M. Bursa, G. E. Hunt, J. H. Lieske, B. Morando, R. H. Rapp, P. K. Seidelmann, A. T. Sinclair, and Y. S. Tjuflin (1989). Report of the IAU/IAG/Cospar Working Group on Cartographic Coordinates and Rotational Elements of the Planets and Satellites: 1988. *Celestial Mechanics 46*, 187–204.

Elliot, J. L., R. G. French, J. A. Frogel, J. H. Elias, D. J. Mink, and W. Liller (1981). Orbits of Nine Uranian Rings. *Astronomical Journal 86*, 444–455.

Esposito, L. W., J. N. Cuzzi, J. H. Holberg, E. A. Marouf, G. L. Tyler, and C. C. Porco (1984). Saturn's Rings: Structure, Dynamics, and Particle Properties. In T. Gerhels and M. S. Matthews (Eds.), *Saturn*, pp. 463–545. Tucson, AZ: University of Arizona Press.

Garcia, H. A. (1972). The Mass and Figure of Saturn by Photographic Astrometry of Its Satellites. *Astronomical Journal 77*, 684–691.

Harper, D., D. B. Taylor, A. T. Sinclair, and S. Kaixian (1988). The Theory of the Motion of Iapetus. *Astronomy and Astrophysics 191*, 381–384.

Harris, A. W. (1984). Physical Properties of Neptune and Triton Inferred from the Orbit of Triton. In J. T. Bergstralh (Ed.), *Uranus and Neptune*, NASA Conference Publication 2330, Washington, DC, pp. 357–373. NASA.

Hohenkerk, C. Y., B. Yallop, C. A. Smith, and A. T. Sinclair (1992). Celestial Reference Systems. In P. K. Seidelmann (Ed.), *Explanatory Supplement to The Astronomical Almanac*, Chapter 3, pp. 184–185. Mill Valley, CA: University Science Books.

Jacobson, R. A. (1990). The orbits of the satellites of Neptune. *Astronomy and Astrophysics 231*, 241–250.

Kozai, Y. (1957). On the Astronomical Constants of Saturnian Satellites System. *Annals of the Tokyo Observatory, Series 2 5*, 73–106.

Laskar, J. and R. A. Jacobson (1987). An Analytical Ephemeris of the Uranian Satellites. *Astronomy and Astrophysics 188*, 212–224.

Levin, A. E. (1934). Mutual Eclipses and Occultations of Jupiter's Satellites. *Memoirs of the British Astronomical Association 30*, 149–183.

Lieske, J. H. (1977). Theory of Motion of Jupiter's Galilean Satellites. *Astronomy and Astrophysics 56*, 333–352.

Lieske, J. H. (1987). Galilean Satellite Evolution: Observational Evidence for Secular Changes in Mean Motions. *Astronomy and Astrophysics 176*, 146–158.

Mignard, F. (1981). The Mean Elements of Nereid. *Astronomical Journal 86*, 1728–1729.

Rohde, J. R. (1990). Unpublished.

Rohde, J. R. and A. T. Sinclair (1992). Orbital Ephemerides of Rings and Satellites. In P. K. Seidelmann (Ed.), *Explanatory Supplement to The Astronomical Almanac*, Chapter 6, pp. 325–381. Mill Valley, CA: University Science Books.

Sampson, R. A. (1921). Theory of the Four Great Satellites of Jupiter. *Memoirs of the Royal Astronomical Society 63*, 1–270.

Shampine, L. F. and M. K. Gordon (1975). *Computer Solutions of Ordinary Differential Equations*. San Francisco: W. H. Freeman and Company.

Sinclair, A. T. (1974). A Theory of the Motion of Iapetus. *Monthly Notices of the Royal Astronomical Society 169*, 591–605.

Sinclair, A. T. (1977). The Orbits of Tethys, Dione, Rhea, Titan and Iapetus. *Monthly Notices of the Royal Astronomical Society 180*, 447–459.

Sinclair, A. T. (1989). The Orbits of the Satellites of Mars Determined from Earth-based and Spacecraft Observations. *Astronomy and Astrophysics 220*, 321–328.

Taylor, D. B. (1984). A Comparison of the Theory of the Motion of Hyperion with Observations Made During 1967-1982. *Astronomy and Astrophysics 141*, 151–158.

Taylor, D. B. (1995). Compact ephemerides for differential tangent plane coordinates of planetary satellites. Technical Note 68, HM Nautical Almanac Office, UKHO, Taunton, UK.

Taylor, D. B. and K. X. Shen (1988). Analysis of Astrometric Observations from 1967 to 1983 of the Major Satellites of Saturn. *Astronomy and Astrophysics 200*, 269–278.

Taylor, D. B. and A. T. Sinclair (2003). Approximate ephemerides and phenomena of natural satellites. Technical Note 73, HM Nautical Almanac Office, UKHO, Taunton, UK.

Taylor, S. W. (1951). On the Shadow of Saturn on Its Rings. *Astronomical Journal 55*, 229–230.

Tholen, D. J. (1985). The Orbit of Pluto's Satellite. *Astronomical Journal 90*, 2353–2359.

van Woerkom, A. J. J. (1950). The Motion of Jupiter's Fifth Satellite, 1892-1949. In *Astronomical Papers of the American Ephemeris and Nautical Almanac*, Volume XIII. Washington, DC: U.S. Government Printing Office.

Zadunaisky, P. E. (1954). A Determination of New Elements of the Orbit of Phoebe, Ninth Satellite of Saturn. *Astronomical Journal 59*, 1–6.

CHAPTER 10

Physical Ephemerides of Solar System Bodies

JAMES L. HILTON

10.1 Introduction

The physical ephemerides of solar system bodies give information on the appearance of the apparent disks of those objects. Physical ephemerides are used for making and reducing observations of the surface markings of an object, determining the exact center of an object's disk from observations of the limbs of the object, and estimating the object's apparent brightness.

In general, the physical ephemerides can be broken into two groups:

1. information depending on the rotational elements and cartographic coordinates, and
2. the phase and apparent brightness of the object, which depend on the position of the Earth and Sun relative to the object and the object's physical appearance.

Unless otherwise stated, all coordinates given in this chapter refer to the Barycentric Celestial Reference System (BCRS). The quantity T is the time in Julian centuries of 36525 days from J2000.0, and t is the time in days (86400 SI seconds) from J2000.0. All values tabulated in *The Astronomical Almanac* are geocentric and have been corrected for the effects of aberration.

10.2 Rotational Elements and Cartographic Coordinates

The cartographic coordinates of an object consist of the orientation of the north pole for a planet or planetary satellite or the positive pole for a dwarf planet or other small solar system object[1], and the position of the prime meridian of the object with respect to an inertial reference frame. These elements are given by the three quantities: α, δ, and W as a function of time, shown in Fig. 10.1.

The angles α and δ are the right ascension and declination of date of the planet's north pole or dwarf planet's positive pole. The International Astronomical Union (IAU) definition of the north pole of a planet (Archinal et al. 2011a) is the rotation axis that lies on the north side of the invariable plane of the solar system. The positive pole is pole around which the object rotates in a counterclockwise direction. The angles α and δ may vary slowly with time due to the precession of the object about its polar axis. In the absence of other information,

1. Henceforth, a *planet* will refer to a planet or planetary satellite and a *dwarf planet* will refer to a dwarf planet or other small solar system body, unless otherwise specified.

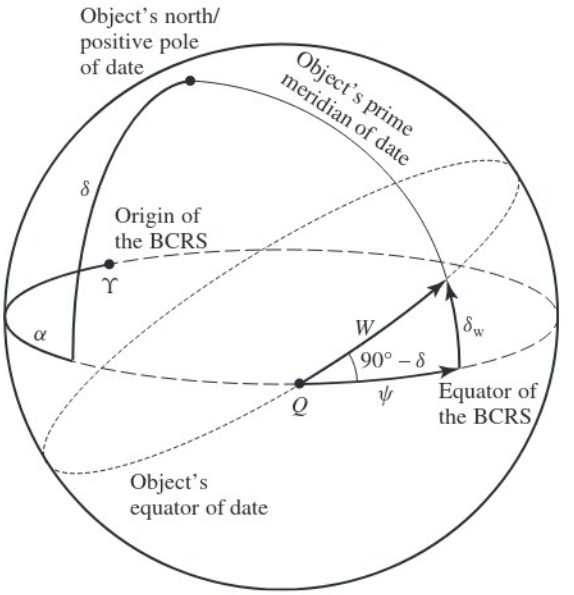


Figure 10.1 The position of the north pole and prime meridian of a solar system body in Earth equatorial coordinates

the axis of rotation is assumed to be normal to the mean orbital plane. This assumption is currently made for most of the satellites.

The angle W is measured along the object's equator, in a counterclockwise direction when viewed from the north pole for a planet or positive pole for a dwarf planet[2], from the ascending node of the object's equator on the BCRS (§ 6.2) to the point where the prime meridian of the object crosses its equator. The right ascension of the node, Q, is at $6^{\mathrm{h}} + \alpha$, and the inclination of the object's equator to the Earth's equator is $90° - \delta$. The object and its prime meridian are generally assumed to rotate uniformly; hence W varies linearly with time. If a cartographic position for the prime meridian is assigned to an object, that is, if a suitable observable surface feature defines the position of the prime meridian, the expression for W is chosen so that the ephemeris position follows the motion of the cartographic position. There may be errors in the rotational elements of the object that will cause the cartographic position to drift away from the ephemeris position by a small amount ΔW. The angle ΔW is measured positively counterclockwise from the ephemeris position of W as viewed from above the north pole. For a prime meridian that has a cartographic definition, the ephemeris definition of W may change as more accurate information on the motion of the cartographic prime meridian is obtained.

The IAU definition for the north pole requires the rotation about that pole to be classified as either direct or retrograde. Direct rotation is counterclockwise as viewed from above the

2. This definition means that the parameter W is not purely the rotation of the planet. It includes a small contribution resulting from the precession of the planet with respect to the plane of the BCRS (§ 6.2). However, except for Mercury, the Earth, and Mars, the contribution from planetary precession and nutation is much smaller than the uncertainty in their rotation rates.

body's north pole, while retrograde rotation is clockwise. For a body with direct rotation, W increases with time. For most of the satellites it is assumed that the rotation period is identical to the mean orbital period. For dwarf planets, the rotation is always direct; however, the obliquity of the pole may be greater than 90°.

The definitions for the solar prime meridian and pole in § 10.5 are derived from Carrington (1863). The definitions for the prime meridian and pole of each of the planets, satellites, and minor planets for which the IAU has accepted a cartographic coordinate system are found in Archinal et al. (2011a); Archinal et al. (2011b). The values for poles and prime meridians of the planets and the dwarf planets (1) Ceres and (134340) Pluto used in *The Astronomical Almanac* are in Table 10.1. In general, the expressions giving α_{J2000}, δ_{J2000}, and W should be accurate to one tenth of a degree. Two decimal places, however, are given to assure consistency when changing coordinate systems. The added zero digits to the rate values of W are for computational consistency and are not an indication of greater accuracy. Three significant digits beyond the decimal point are given in the expressions for Mars, reflecting the greater confidence in its accuracy.

10.2.1 Planetocentric and Planetographic Coordinate Systems

Both planetocentric and planetographic systems of coordinates are used in the study of the planets and satellites. Both systems are based on the same fundamental axis of rotation, but differ, as described below, in their definitions of latitude, longitude, and range. Planetocentric coordinates are used for general purposes and are based on a right-handed system of axes with its origin at the center of mass of the object. Planetographic coordinates are used for cartographic purposes and depend on the adoption of a reference surface, usually a spheroid, which approximates an equipotential surface of the object. The latitude and ranges for both of these coordinate systems are shown in Fig. 10.2.

The planetographic reference surfaces for most of the planets are spheroids for which the equatorial radius, a, is larger than the polar radius, b (Fig. 10.2). Since the equipotential surface is usually a spheroid, the shape of the spheroid is related to that of a sphere by its geometric flattening, f,

$$f = \frac{a - b}{a}. \tag{10.1}$$

For some of the planets and most of the satellites the reference surface is a sphere. For some satellites, such as Phobos, Deimos, and Hyperion, the reference surface should be triaxial. However, triaxial ellipsoids would make many computations more complicated, especially those related to map projections. Therefore, spherical or spheroidal reference surfaces are usually used in mapping programs. The polar axis for each reference surface is assumed to be the mean axis of rotation as defined by the adopted rotational elements. For most of the planets the present accuracy of measurement does not reveal a deviation between the axis of rotation and the axis of figure. The equatorial radii and flattenings of the planets and Pluto are found on page E6 (E88 prior to 2005) of *The Astronomical Almanac* and in Table 10.2. The radii (spherical, spheroidal, or triaxial as applicable) of the natural satellites of the planets, with minimum apparent magnitudes less than or equal to 23.0, are found on pages F3 and F5 of *The Astronomical Almanac* and in Table 10.3. A more complete list of satellites, including those with minimum apparent magnitudes greater than 23.0 and ones with

Table 10.1 The positions of the poles and prime meridians of the planets and Pluto

Planet	Parameter and Value
Mercury	$\alpha_0 = 281.^\circ0097 - 0.^\circ0328\,T$
	$\delta_0 = 61.^\circ4143 - 0.^\circ0049\,T$
	$W = 329.^\circ5469 + 6.^\circ138\,5205\,t + 0.^\circ009\,938\,22 \sin M_1 - 0.^\circ001\,045\,81 \sin M_2$
	$\quad - 0.^\circ000\,102\,80 \sin M_3 - 0.^\circ000\,023\,64 \sin M_4 - 0.^\circ000\,005\,32 \sin M_5$
Venus	$\alpha_0 = 272.^\circ76$
	$\delta_0 = 67.^\circ16$
	$W = 160.^\circ20 - 1.^\circ481\,3688\,t$
Earth	$\alpha_0 = 0.^\circ00 - 0.^\circ641\,T$
	$\delta_0 = 90.^\circ00 - 0.^\circ557\,T$
	$W = 190.^\circ147 + 360.^\circ985\,6235\,t$
Mars	$\alpha_0 = 317.^\circ681\,43 - 0.^\circ1061\,T$
	$\delta_0 = 52.^\circ886\,50 - 0.^\circ0609\,T$
	$W = 176.^\circ630 + 350.^\circ891\,982\,26\,t$
Jupiter	$\alpha_0 = 268.^\circ056\,595 - 0.^\circ006\,499\,T + 0.^\circ000\,117 \sin J_1 + 0.^\circ000\,938 \sin J_2$
	$\quad + 0.^\circ001\,432 \sin J_3 + 0.^\circ000\,030 \sin J_4 + 0.^\circ002\,150 \sin J_5$
	$\delta_0 = 64.^\circ495\,303 + 0.^\circ002\,413\,T + 0.^\circ000\,050 \cos J_1 + 0.^\circ000\,404 \cos J_2$
	$\quad + 0.^\circ000\,617 \cos J_3 - 0.^\circ000\,013 \cos J_4 + 0.^\circ000\,926 \cos J_5$
	$W = 284.^\circ95 + 870.^\circ536\,0000\,t$
Saturn	$\alpha_0 = 40.^\circ589 - 0.^\circ036\,T$
	$\delta_0 = 83.^\circ537 - 0.^\circ004\,T$
	$W = 38.^\circ90 + 810.^\circ793\,9024\,t$
Uranus	$\alpha_0 = 257.^\circ311$
	$\delta_0 = -15.^\circ175$
	$W = 203.^\circ81 - 501.^\circ160\,0928\,t$
Neptune	$\alpha_0 = 299.^\circ36 + 0.^\circ70 \sin N$
	$\delta_0 = 43.^\circ46 - 0.^\circ51 \cos N$
	$W = 253.^\circ18 + 536.^\circ312\,8492\,t - 0.^\circ48 \sin N$
Ceres	$\alpha_0 = 291.^\circ$
	$\delta_0 = 59.^\circ$
	$W = 170.^\circ90 + 952.^\circ1532\,t$
Pluto	$\alpha_0 = 132.^\circ993$
	$\delta_0 = -6.^\circ163$
	$W = 302.^\circ695 + 56.^\circ362\,5225\,t$

The values for M_n, J_n, and N are:

$M_1 = 174.^\circ791\,086 + 4.^\circ092\,335\,t$
$M_2 = 349.^\circ582\,171 + 8.^\circ184\,670\,t$
$M_3 = 164.^\circ373\,257 + 12.^\circ277\,005\,t$
$M_4 = 339.^\circ164\,343 + 16.^\circ369\,340\,t$
$M_5 = 153.^\circ955\,429 + 20.^\circ461\,675\,t$
$J_1 = 99.^\circ360\,714 + 4850.^\circ4046\,T$
$J_2 = 175.^\circ895\,369 + 1191.^\circ9605\,T$
$J_3 = 300.^\circ323\,162 + 262.^\circ5475\,T$
$J_4 = 114.^\circ012\,305 + 6070.^\circ2476\,T$
$J_5 = 49.^\circ511\,251 + 64.^\circ3000\,T$
$N = 357.^\circ85 + 52.^\circ316\,T$

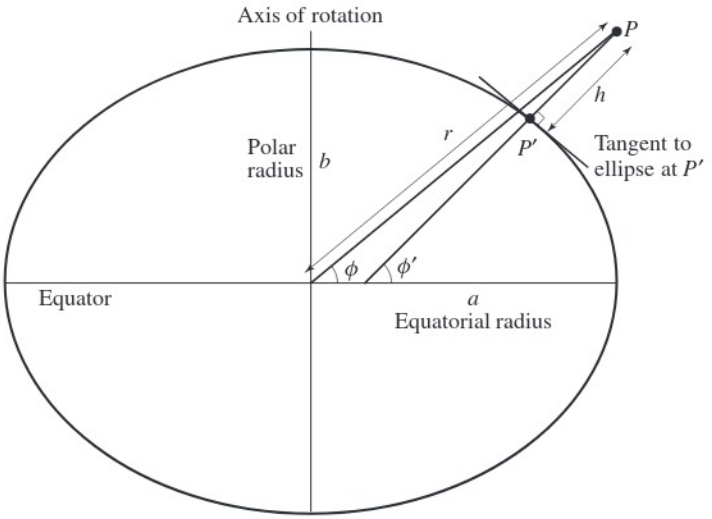


Figure 10.2 Planetocentric and planetographic coordinates systems

Table 10.2 The equatorial radii and flattenings of the planets and Pluto

Planet	Equatorial Radius (km)	Flattenning
Mercury	2439.7	0.0
Venus	6051.8	0.0
Earth	6378.14	0.003 353 64
Mars[a]	3396.2	0.006 772
		0.005 000
Jupiter	71492.	0.064 874
Saturn	60268.	0.097 962
Uranus	25559.	0.022 927
Neptune	24764.	0.017 081
Pluto	1195.	0.

[a] Two flattening values are given for Mars. The first value is determined using the north polar radius and the second using the south polar radius (Smith et al. 1999).

provisional IAU designations, are given in *The Astronomical Almanac Online* at http://asa.usno.navy.mil or http://asa.hmnao.com.The equatorial diameters and geometric albedos of the dwarf planets, Ceres, Pluto, (136108) Haumea, (136199) Eris, and (136472) Makemake are found on page G3.

Different methods were used to derive the values for the equatorial radii and geometric flattening of the different planets and satellites. Thus, they do not always refer to common definitions. Some radii are derived from star or spacecraft occultation measurement, some limb fitting, and some control-network computations. The spheroid for the Earth, for example,

Table 10.3 The radii of planetary satellites

Planet	Satellite		Radii (km)
Earth		Moon	1737.4
Mars	I	Phobos	13.4 × 11.2 × 9.2
	II	Deimos	7.5 × 6.1 × 5.2
Jupiter	I	Io	1830 × 1819 × 1815
	II	Europa	1565
	III	Ganymede	2634
	IV	Callisto	2403
	V	Amalthea	131 × 73 × 61
	VI	Himalia	85
	VII	Elara	43
	VIII	Pasiphae	30
	IX	Sinope	19
	X	Lysithea	18
	XI	Carme	23
	XII	Ananke	14
	XIII	Leda	10
	XIV	Thebe	55 × 45
	XV	Adrastea	13 ×10 × 8
	XVI	Metis	20
	XVII	Callirrhoe	4
	XVIII	Themisto	4
	XIX	Megaclite	2.7
	XX	Taygete	2.5
	XXI	Chaldene	1.9
	XXII	Harpalyke	2.2
	XXIII	Kalyke	2.6
	XXIV	Iocaste	2.6
	XXV	Erinome	1.6
	XXVI	Isonoe	1.9
	XXVII	Praxidike	3.4
	XXVIII	Autonoe	2
	XXIX	Thyone	2
	XXX	Hermippe	2
	XXXI	Aitne	1.5
	XXXII	Eurydome	1.5
	XXXIII	Euanthe	1.5
	XXXVI	Sponde	1
	XXXVII	Kale	1
Saturn	I	Mimas	209 × 196 × 191
	II	Enceladus	256 × 247 × 245
	III	Tethys	536 × 528 × 526
	IV	Dione	560
	V	Rhea	764

Table 10.3 *(continued)*

Planet	Satellite	Radii (km)
Saturn	VI Titan	2575
	VII Hyperion	180 × 140 × 113
	VIII Iapetus	718
	IX Phoebe	110
	X Janus	97 × 95 × 77
	XI Epimetheus	69 × 55 × 55
	XII Helene	18 × 16 × 15
	XIII Telesto	15 × 12.5 × 7.5
	XIV Calypso	15 × 8 × 8
	XV Atlas	18.5 × 17.2 × 13.5
	XVI Prometheus	74 × 50 × 34
	XVII Pandora	55 × 44 × 31
	XVIII Pan	10
	XIX Ymir	8
	XX Paaliaq	9.5
	XXI Tarvos	6.5
	XXII Ijiraq	5
	XXIV Kiviuq	7
	XXVI Albiorix	13
	XXVIII Erriapo	4.3
	XXIX Siarnaq	16
Uranus	I Ariel	581 × 578 × 578
	II Umbriel	585
	III Titania	789
	IV Oberon	761
	V Miranda	240 × 234 × 233
	IX Cressida	39.8
	X Desdemona	32
	XI Juliet	46.8
	XII Portia	67.6
	XIII Rosalind	36
	XIV Belinda	40.3
	XV Puck	81
	XVI Caliban	49
	XVII Sycorax	95
Neptune	I Triton	1353
	II Nereid	170
	V Despina	75
	VI Galatea	88
	VII Larissa	104 × 89
	VIII Proteus	218 × 208 × 201
Pluto	I Charon	593

refers to mean sea level, a definition that can be used only for the Earth. The radii and axes of the large gaseous planets, Jupiter, Saturn, Uranus, and Neptune refer to a one-bar pressure surface. The radii in the tables are not necessarily the appropriate values for use in dynamical studies. Instead, the radius actually used to derive a dynamical parameter such as the value of J_2 should always be used in conjunction with that value.

In both the planetocentric and planetographic systems, the fundamental reference z-axis is the mean axis of rotation with the positive direction being toward the north pole. The equator is the plane passing through the center of mass of the planet, perpendicular to the z-axis. The x-axis is defined by the intersection of the plane of the equator and the plane containing the prime meridian. The choice of the prime meridian is arbitrary. The y-axis is then orthogonal to the other two axes and makes a right-handed coordinate system. The angular coordinates used in these two systems are latitude and longitude. The range for a planetocentric coordinate system is the distance from the center of mass, while the range for a planetographic system is the height above or below a reference surface.

Latitude (Fig. 10.2) is measured north and south of the equator with the northern latitudes designated as positive. The *planetocentric* latitude of a point on the surface of a planet is the angle ϕ between the equatorial plane and the line segment connecting the point to the center of mass. The *planetographic* latitude of a point is the angle ϕ' between the line segment normal to the equipotential surface from that point to the equatorial plane. For a spherical object, the planetocentric and planetographic latitudes are identical.

Longitude is measured along the equator from the prime meridian. *Planetocentric* longitudes, λ, are measured positively in the counterclockwise direction when viewed from the north pole. *Planetographic* longitudes, λ', on the other hand, are measured positively in the direction opposite to the object's rotation. The planetographic longitude increases in the clockwise direction when viewed from above the north pole for an object with direct rotation. Planetocentric longitudes are measured from the ephemeris position of the prime meridian as defined by the rotational elements, while planetographic longitudes are measured from the cartographic position of the prime meridian as defined by the adopted longitude of some clearly observable surface feature. For the Earth, the Sun, and the Moon, longitudes are measured from 0° to 180° east and west. East longitude (counterclockwise when viewed from above the north pole) is commonly considered to be positive.

In the planetographic system, a point P not on the reference surface is specified by the planetographic longitude and latitude of the point P' on the reference surface at which the normal line segment connecting P to the equatorial plane passes through the reference surface and the height, h, of P above or below the reference surface.

10.2.2 Coordinate Systems of Small Bodies

A spherical or ellipsoidal model shape has traditionally been used to define large bodies. For small, irregularly shaped bodies, however, an ellipsoid model is obviously inappropriate, except perhaps for dynamical studies. For very irregular bodies, the concept of a reference ellipsoid ceases to be useful for most purposes. For these bodies, topographic shapes are usually represented by a grid of radii to the surface as a function of planetocentric latitude and longitude.

Another difficulty for small bodies is that two coordinates (i.e., spherical angular measures) may not uniquely identify a point on the surface of the body. In other words it is possible

to have a line from the center of the object intersect the surface more than once. This phenomenon can also happen on large and mostly ellipsoidal objects such as the Earth, where features such as overhanging cliffs and natural bridges and arches may occur. On large bodies such features are very small relative to the body size and often ignored at the scale of most topographic maps. For small bodies these features may be fairly large relative to the body size. However, even on small bodies this problem is usually restricted to small areas. But it still may make a planetocentric coordinate system difficult to use. Examples are on Eros (at a small patch west of Psyche), on Kleopatra (Ostro et al. 2000), possibly on Toutatis near its 'neck', and possibly near the south pole of Ida, where some radii may intersect the surface more than once. Cartographers have ad hoc tricks for a specific map, such as interpolating across the problem area from areas that are uniquely defined, or by showing overlapping contours. A Cartesian or other coordinate geometry may be preferable for arbitrarily complex shapes, such as a toroidal comet nucleus, where an active region has eaten its way through the nucleus. Such coordinate geometries may also be useful for irregular bodies imaged only on one side, such as 19P/Borrelly and 81P/Wild 2.

Digital cartography has become increasingly popular with the introduction of large mass storage to computer systems. Cartographic databases are important when considering irregularly shaped bodies and other bodies, where a file containing the coordinates for each pixel can describe the surface. In this case, the reference sphere has shrunk to a point. If known, other parameters such as brightness and gravity can be associated with each pixel. With proper programming, pictorial and projected views of the body can then be displayed.

The IAU Working Group on Cartographic Coordinates and Rotational Elements (Seidelmann et al. 2002) recommends that longitudes on minor planets and comets should be measured, if possible, from 0 to 360 degrees in a right-hand system from a designated prime meridian with the origin at the center of mass. For irregular bodies where orthographic digital projections are adopted to preserve the irregular appearance of the body without artificial distortion, these projections should follow the right-hand rule.

Table 10.4 contains data on the size and shape of selected minor planets and comets from Archinal et al. (2011a); Archinal et al. (2011b). The first column gives the *effective radius* of the body and an estimate of the accuracy of this measurement. The effective radius is the radius of a sphere with a volume equivalent to the body's volume. The next three columns are estimates of the radii measured along the three principal axes. The uncertainties in the values for the radii of different bodies in Table 10.4 may have different meanings. Sometimes they are standard errors of a particular data set, sometimes simply an estimate or expression of confidence.

Section G of *The Astronomical Almanac* includes the estimated mean diameters of 95 asteroids. Table 10.5 and *The Astronomical Almanac Online* (URL[1]) give the estimated diameter(s) and references for those same 95 asteroids. If more than a mean diameter is available for a particular asteroid the mean diameter, d_m, is

$$d_m = \sqrt[3]{a\ b^2} \tag{10.2}$$

when a polar, a, and equatorial, b, diameter are available and

$$d_m = \sqrt[3]{a\ b\ c} \tag{10.3}$$

when a tri-axial, $a \times b \times c$, figure is available.

Table 10.4 The radii and effective radius of selected asteroids and comets

Body	Effective Radius (km)	Principal axes (km)	(km)	(km)
216 Kleopatra	—	108.5	47	40.5
243 Ida	15.65 ± 0.6	26.8	12	7.6
433 Eros	8.45 ± 0.02	—	—	—
951 Gaspra	6.1 ± 0.4	9.1	5.2	4.4
3908 Nyx	0.500 ± 0.075	—	—	—
6489 Golevka	0.265 ± 0.015	—	—	—
$1998JM_8$	3.5	—	—	—
$1998ML_{14}$	0.05	—	—	—
19P/ Borrelly	—	4.22 ± 0.05	3.5 ± 0.2	—

Table 10.5 The diameters of the asteroids

Asteroid Name	Diameters (km)	σ (km)	Reference
1 Ceres	974.6×909.4	3.6×3.2	Thomas et al. (2005)
2 Pallas	$570 \times 525 \times 482$	$22 \times 4 \times 15$	Drummond and Christou (1994)
3 Juno	290.2×245.6	1.6×3.8	Millis et al. (1981)
4 Vesta	$571 \times 544 \times 434$	$2 \times 2 \times 4$	Drummond, Fugate, and Christou (1998)
5 Astrea	120	14	Magri et al. (1999)
6 Hebe	190.4	7.1	Dunham and Mallen (1979)
7 Iris	211	22	Magri et al. (1999)
8 Flora	138	9	Magri et al. (1999)
9 Metis	235×165	10	Storrs et al. (1999)
10 Hygiea	444	35	Ragazzoni et al. (2000)
11 Parthenope	153.3	3.1	Tedesco et al. (2002)
12 Victoria	112.8	3.1	Tedesco et al. (2002)
13 Egeria	207.6	8.3	Tedesco et al. (2002)
14 Irene	180	7	[a]
15 Eunomia	370×240	39×20	Ragazzoni et al. (2000)
16 Psyche	$304 \times 303 \times 197$	$5 \times 3 \times 4$	Drummond and Christou (2008)
17 Thetis	90.0	3.7	Tedesco et al. (2002)
18 Melpomene	138	18	Magri et al. (1999)
19 Fortuna	225	13	Storrs et al. (1999)
20 Massalia	145	17	Magri et al. (1999)
21 Lutetia	116	17	Magri et al. (1999)
22 Kalliope	181	5	Tedesco et al. (2002)
23 Thalia	107.5	2.2	Tedesco et al. (2002)
24 Themis	175	24	[a]

Table 10.5 *(continued)*

	Asteroid Name	Diameters (km)	σ (km)	Reference
25	Phocaea	75.1	3.6	Tedesco et al. (2002)
26	Prosperina	94.8	1.7	Tedesco et al. (2002)
27	Euterpe	118	21	Magri et al. (1999)
28	Bellona	120.9	3.4	Tedesco et al. (2002)
29	Amphitrite	212.2	6.8	Tedesco et al. (2002)
30	Urania	100.2	2.4	Tedesco et al. (2002)
31	Euphrosyne	256	12	Tedesco et al. (2002)
32	Pomona	80.8	1.6	Tedesco et al. (2002)
37	Fides	108.4	1.9	Tedesco et al. (2002)
39	Laetitia	149.5	8.6	Tedesco et al. (2002)
40	Harmonia	107.6	6.2	Tedesco et al. (2002)
41	Daphne	187	21	Magri et al. (1999)
42	Isis	100.2	3.4	Tedesco et al. (2002)
43	Ariadne	65.9	2.5	Tedesco et al. (2002)
44	Nysa	71	4	Tedesco et al. (2002)
45	Eugenia	214.6	4.2	Tedesco et al. (2002)
48	Doris	221.8	7.5	Tedesco et al. (2002)
51	Nemausa	170×136	4×9	Dunham et al. (1984)
52	Europa	302.5	5.4	Tedesco et al. (2002)
54	Alexandra	165.8	3.4	Tedesco et al. (2002)
60	Echo	60.2	1.8	Tedesco et al. (2002)
63	Ausonia	103.1	2.4	Tedesco et al. (2002)
64	Angelina	56.2	0.3	[a]
65	Cybele	230	16	Taylor (1981)
67	Asia	58.1	1.4	Tedesco et al. (2002)
68	Leto	122.6	5.3	Tedesco et al. (2002)
69	Hesperia	138.1	4.7	Tedesco et al. (2002)
71	Niobe	83.4	1.7	Tedesco et al. (2002)
79	Eurynome	66.5	1.6	Tedesco et al. (2002)
80	Sappho	79	10	Magri et al. (1999)
85	Io	164	10	Erikson et al. (1999)
87	Sylvia	$350 \times 264 \times 227$	$19 \times 14 \times 33$	Drummond and Christou (2008)
88	Thisbe	232	12	Millis et al. (1983)
89	Julia	151.5	3.1	Tedesco et al. (2002)
92	Undina	126.4	3.4	Tedesco et al. (2002)
94	Aurora	204.9	3.6	Tedesco et al. (2002)
97	Klotho	83	10	Magri et al. (1999)
103	Hera	91.2	5.6	Tedesco et al. (2002)
107	Camilla	223	17	Tedesco et al. (2002)
115	Thyra	79.8	1.4	Tedesco et al. (2002)

Table 10.5 *(continued)*

Asteroid Name	Diameters (km)	σ (km)	Reference
121 Hermione	209	5	Tedesco et al. (2002)
128 Nemesis	188	4	Tedesco et al. (2002)
129 Antigone	138	12	[a]
135 Hertha	79	2	Tedesco et al. (2002)
185 Eunike	157.5	2.6	Tedesco et al. (2002)
192 Nausikaa	95	13	Magri et al. (1999)
194 Prokne	169	20	Magri et al. (1999)
196 Philomela	136.4	6.3	Tedesco et al. (2002)
216 Kleopatra	$217 \times 94 \times 81$	$54 \times 23 \times 20$	Ostro et al. (2000)
230 Athamantis	109	2	Tedesco et al. (2002)
270 Anahita	51	2	Tedesco et al. (2002)
287 Nephthys	67.6	1.4	Tedesco et al. (2002)
324 Bamberga	$215 \times 199 \times 199$	$15 \times 7 \times 7$	Drummond and Christou (2008)
346 Hermentaria	106.5	2.2	Tedesco et al. (2002)
349 Dembowska	139.7	4.3	Tedesco et al. (2002)
354 Eleonora	155.2	8.5	Tedesco et al. (2002)
372 Palma	188.6	3.2	Tedesco et al. (2002)
387 Aquitania	100.5	2.9	Tedesco et al. (2002)
389 Industria	79.2	2.4	Tedesco et al. (2002)
409 Aspasia	161.6	6.8	Tedesco et al. (2002)
423 Diotima	208.8	4.9	Tedesco et al. (2002)
433 Eros	$34.2 \times 11.2 \times 11.2$	$0.2 \times 0.2 \times 0.2$	Veverka et al. (2000)
451 Patientia	225.0	4.4	Tedesco et al. (2002)
471 Papagena	134.2	5.2	Tedesco et al. (2002)
511 Davida	326.1	5.3	Tedesco et al. (2002)
532 Herculina	207	25	Magri et al. (1999)
654 Zelinda	127.4	3.9	Tedesco et al. (2002)
702 Alauda	194.7	3.2	Tedesco et al. (2002)
704 Interamnia	329	10	Drummond and Christou (2008)

[a] Diameter calculated from equation D (in km) $= 1329\, p^{-0.5} 10^{-H/5}$ (V. Shor 2003, private communication) where the albedo, p, is taken from the polarimetry albedos in Davis and Neese (2002) and the absolute visual magnitude, H, is taken from Tholen (2009).

10.3 Phases and Magnitudes

10.3.1 Absolute and Apparent Magnitudes

Neglecting variations from rotation or other intrinsic causes, the observed visual magnitude, V, for a solar system body is

$$V = V(1, 0) + 5 \log_{10}(d\, r) + \Delta m(i) \tag{10.4}$$

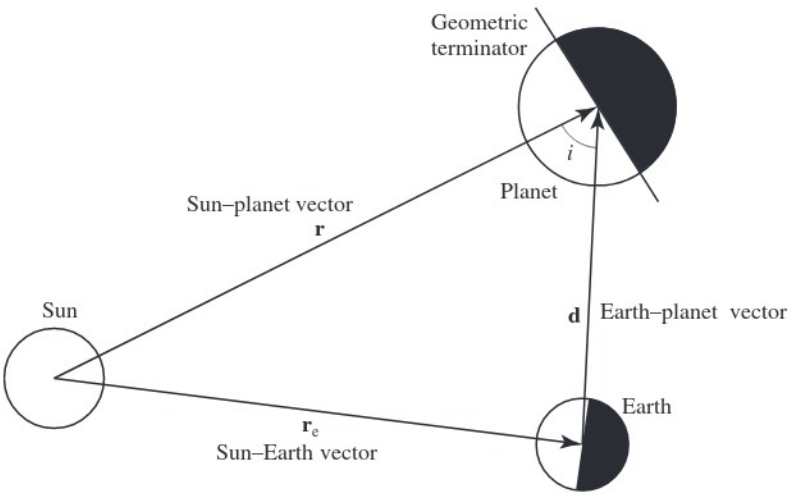


Figure 10.3 The basic vectors and angle of illumination, i, in the Earth–Sun–planet plane

where d, r, and i, shown in Fig. 10.3, are, respectively, the Earth–planet distance in au, the planet's distance from the Sun in au, and the phase angle. $\Delta m(i)$ is the correction for the variation in brilliancy of the planet with phase angle, i. $V(1, 0)$[3] is the magnitude of the body at 1 au from the Sun, seen at a distance of 1 au, with a phase angle of 0°.

The quantity $\Delta m(i)$ is determined empirically. It is the result of two effects. The first source of variation arises from the fraction of the illuminated disk visible from the Earth as it varies with i. The second effect is due to the properties of diffuse reflection from the object's surface and/or atmosphere. The parameter $\Delta m(i)$ for planets and satellites is expressed as a power series in i, retaining as many terms as necessary to represent the observations.[4] For the outer planets a single term is usually sufficient, hence $\Delta m(i)$ for the planets is usually referred to as the phase coefficient.

The tabulated magnitude of an object is the integrated total visual magnitude. The magnitudes for Mercury and Venus are from Hilton (2005). Those of the other planets and Pluto[5] are based on Harris (1961) with values for $V(1, 0)$ from de Vaucouleurs (1970) for all but Jupiter, whose $V(1, 0)$ value is from Irvine et al. (1968). The solar phase angle, i, is the apparent angular distance at the object between the Sun and the Earth. For Mercury, Venus, the Moon, and many Near Earth Objects (NEOs), such as the Apollos, the Amors, and the Atens, which cross the orbits of the Earth and/or Mars, i may become very large or even go through the entire range of phase angle. For Mars and its satellites i can be as large as 47°, and for Jupiter and its satellites i can be as large as 12°. Thus, for the main belt minor planets, i may be substantial. For the rest of the planets, satellites, and Kuiper belt objects the maximum value of i is only a few degrees.

3. For minor planets $V(1, 0)$ is referred to as H (§ 10.4.3).

4. See Eq. 10.38 in § 10.4.3 for the $\Delta m(i)$ function used for minor planets.

5. Due to its previous status as a planet, Pluto's apparent magnitude is determined in the same manner as those of the planets. The apparent magnitudes of the other dwarf planets are detemined using the algorithm described in § 10.4.3.

Many objects show an opposition surge in their luminosities at small phase angles (5° or less). The exact cause of the opposition surge is not completely understood; however, the size of the surge depends on both the composition and size of the constituent particles of the body's regolith. The literature contains many studies (e.g., Nelson et al. 2000) attempting to both understand and quantify this phenomenon.

If the intrinsic properties of a planet cause its brightness to vary, the problem of predicting the apparent magnitude at a given time is considerably more complicated. The causes of intrinsic variability are the existence of surface markings on the planet, and changes in the planet's atmosphere, such as clouds, or volatile surface markings, such as the Martian ice caps. Surface markings on an object give rise to brightness variations that depend on the rotation of the object. Atmosphere changes or volatile surface markings give rise to variations of an irregular nature. Atmospheric variations may be short-lived, such as sand storms on Mars, or persist for long periods of time, such as the Great Red Spot on Jupiter. Because the atmospheric variations and volatile markings are erratic, their effects on a planet's albedo cannot be predicted with accuracy, although some, such as the Martian ice caps, generally follow a regular cycle. None of these erratic or atmospheric variations are currently taken into account in *The Astronomical Almanac*.

For some purposes, it is convenient to use the mean opposition magnitude, V_0, which is related to $V(1, 0)$ by

$$V_0 = V(1, 0) + 5 \log_{10} [a(a - 1)] \tag{10.5}$$

where a is the semimajor axis of the planet's orbit in au.

The values for $V(1, 0)$, V_0, and the phase series or phase coefficients for the planets, the Galilean satellites, and Pluto are tabulated in Table 10.6. The values for $V(1, 0)$, V_0, and the phase series or phase coefficients for the planets and Pluto are tabulated on page E6 (E88 prior to 2005) of *The Astronomical Almanac*. Since both Mercury and Venus are interior to the orbit of the Earth, they do not come into opposition with the Earth and, hence, have no value for V_0. The values for $V(1, 0)$, V_0, and Johnson color indices, $B - V$ and $U - B$, for the satellites are given, if known, in Table 10.7 and on pages F3 and F5 of *The Astronomical Almanac*.

10.3.2 Surface Brightness

The surface brightness, SB, of an object is the average brightness value for the illuminated portion of the apparent disk. The units for the surface brightness are visual magnitudes per square arcsecond. Assuming the body is an oblate spheroid, the apparent geometric area, A, of the apparent disk is

$$A = \pi a b' \tag{10.6}$$

where a is the equatorial radius of the object, b' is the apparent polar radius of the object. Then, assuming the fraction of light forward scattered by the atmosphere is insignificant, the surface brightness is

$$SB = V + 2.5 \log_{10}(kA) \tag{10.7}$$

where k is the geometric fraction of the object illuminated (Eq. 10.33). If a significant amount of light is forward scattered, as can happen with Venus near inferior conjunction (e.g., Hilton 2005), the total area of the planet seen by the observer may be significantly greater than the apparent geometric area.

Table 10.6 The visual magnitudes and phase coefficients for the planets, Pluto, and the Galilean satellites of Jupiter

Body	$V(1, 0)$ (mag)	V_0 (mag)	$\Delta m(i)^a$ (mag)
Mercury	−0.60	—	$0.0498\,i - 0.000488\,i^2 + 3.02 \times 10^{-6}\,i^3$
Venus[b]	−5.18	—	$0.0103\,i + 0.000057\,i^2 + 0.13 \times 10^{-6}\,i^3$
Venus[c]	0.17	—	$-0.0096\,i$
Earth	−3.86	—	—
Mars	−1.52	−2.01	$0.016\,i$
Jupiter	−9.40	−2.70	$0.005\,i$
Saturn	−8.88	+0.67	$0.044\,i$
Uranus	−7.19	+5.52	$0.0028\,i$
Neptune	−6.87	+7.84	$0.041\,i$
Pluto	−1.0	+15.12	$0.041\,i$
Io	−1.68	+5.02	$0.46\,i - 0.0010\,i^2$
Europa	−1.41	+5.29	$0.0312\,i - 0.00125\,i^2$
Ganymede	−2.09	+4.61	$0.323\,i - 0.00066\,i^2$
Callisto	−1.05	+5.65	$0.078\,i - 0.00274\,i^2$

[a] The coefficient i is the phase angle in degrees.
[b] $2.^\circ 7 < i < 163.^\circ 6$
[c] $163.^\circ 6 < i < 170.^\circ 2$

Table 10.7 The visual magnitudes and Johnson colors of the satellites

Planet	Satellite	Geometric Albedo	$V(1, 0)(mag)$	V_0 (mag)	B−V	U−B
Earth	Moon	0.12	+0.21	−12.74	0.92	0.46
Mars	I Phobos	0.07	+11.8	11.4	0.6	
	II Deimos	0.08	+12.89	12.5	0.65	0.18
Jupiter	I Io	0.63	−1.68	5.02	1.17	1.30
	II Europa	0.67	−1.41	5.29	0.87	0.52
	III Ganymede	0.43	−2.09	4.61	0.83	0.50
	IV Callisto	0.17	−1.05	5.6	0.86	0.55
	V Amalthea	0.09	+7.4	14.1	1.50	
	VI Himalia	0.04	+8.14	14.6	0.67	0.30
	VII Elara	0.04	+10.0	16.3	0.69	0.28
	VIII Pasiphae	0.04	+10.33	17.03	0.63	0.34
	IX Sinope	0.04	+11.6	18.1	0.7	
	X Lysithea	0.04	+11.7	18.3	0.7	
	XI Carme	0.04	+11.3	17.6	0.7	
	XII Ananke	0.04	+12.2	18.8	0.7	
	XIII Leda	0.04	+13.5	19.5	0.7	
	XIV Thebe	0.047	+9.0	16.0	1.3	
	XV Adrastea	0.1	+12.4	18.7		

Table 10.7 *(continued)*

Planet	Satellite	Geometric Albedo	$V(1, 0)(mag)$	V_0 (mag)	B−V	U−B
Jupiter	XVI Metis	0.061	+10.8	17.5		
	XVII Callirrhoe	0.04	+14.2	20.7		
	XVIII Themisto	0.04	+14.4	21.0		
	XIX Megaclite	0.04	+15.0	21.7		
	XX Taygete	0.04	+15.4	21.9		
	XXI Chaldene	0.04	+15.7	22.5		
	XXII Harpalyke	0.04	+15.2	22.2		
	XXIII Kalyke	0.04	+15.3	21.8		
	XXIV Iocaste	0.04	+14.5	21.8		
	XXV Erinome	0.04	+16.0	22.8		
	XXVI Isonoe	0.04	+15.9	22.5		
	XXVII Praxidike	0.04	+15.0	21.2		
	XXVIII Autonoe	0.04	+15.4	22.0		
	XXIX Thyone	0.04	+15.7	22.3		
	XXX Hermippe	0.04	+15.5	22.1		
	XXXI Aitne	0.04	+16.1	22.7		
	XXXII Eurydome	0.04	+16.1	22.7		
	XXXIII Euanthe	0.04	+16.2	22.8		
	XXXVI Sponde	0.04	+16.4	23.0		
	XXXVII Kale	0.04	+16.4	23.0		
Saturn	I Mimas	0.5	+3.3	12.8		
	II Enceladus	1.0	+2.1	11.8	0.70	0.28
	III Tethys	0.8	+0.6	10.3	0.73	0.30
	IV Dione	0.6	+0.8	10.4	0.71	0.31
	V Rhea	0.6	+0.1	9.7	0.78	0.38
	VI Titan	0.2	−1.28	8.4	1.28	0.75
	VII Hyperion	0.3	+4.63	14.4	0.78	0.33
	VIII Iapetus	0.2^a	+1.5	11.0	0.72	0.30
	IX Phoebe	0.081	+6.89	16.5	0.70	0.34
	X Janus	0.6	+4.4	14.4		
	XI Epimetheus	0.5	+5.4	15.6		
	XII Helene	0.6	+8.4	18.4		
	XIII Telesto	1.0	+8.9	18.5		
	XIV Calypso	0.7	+9.1	18.7		
	XV Atlas	0.4	+8.4	19.0		
	XVI Prometheus	0.6	+6.4	15.8		
	XVII Pandora	0.5	+6.4	16.4		
	XVIII Pan	0.5		19.4		

Table 10.7 *(continued)*

Planet	Satellite	Geometric Albedo	$V(1, 0)(mag)$	V_0 (mag)	B−V	U−B
Saturn	XIX Ymir	0.06		21.6		
	XX Paaliaq	0.06	+12.2	21.2		
	XXI Tarvos	0.06	+13.2	22.0		
	XXII Ijiraq	0.06	+13.6	22.5		
	XXIV Kiviuq	0.06	+13.1	21.9		
	XXVI Albiorix	0.06		20.4		
	XXVIII Erriapo	0.06	+14.0	22.9		
	XXIX Siarnaq	0.06		20.0		
Uranus	I Ariel	0.39	+1.45	13.7	0.65	
	II Umbriel	0.21	+2.10	14.5	0.68	
	III Titania	0.27	+1.02	13.5	0.70	0.28
	IV Oberon	0.23	+1.23	13.7	0.68	0.20
	V Miranda	0.32	+3.6	15.8		
	IX Cressida	0.07	+9.5	22.3		
	X Desdemona	0.07	+9.8	22.5		
	XI Juliet	0.07	+8.8	21.7		
	XII Portia	0.07	+8.3	21.1		
	XIII Rosalind	0.07	+9.8	22.5		
	XIV Belinda	0.07	+9.4	22.1		
	XV Puck	0.07	+7.5	20.4		
	XVI Caliban	0.07	+9.7	22.4		
	XVII Sycorax	0.07	+8.2	20.8		
Neptune	I Triton	0.756	−1.24	13.5	0.72	0.29
	II Nereid	0.155	+4.0	19.7	0.65	
	V Despina	0.090	+7.9	22.5		
	VI Galatea	0.079	+7.6	22.4		
	VII Larissa	0.091	+7.3	22.0		
	VIII Proteus	0.096	+5.6	20.3		
Pluto	I Charon	0.372	+0.9	17.3		

10.4 The Apparent Disk of a Solar System Body

Most bodies with diameters $\gtrsim 500$ km, such as a planet, dwarf planet, or large satellite, are essentially oblate spheroids in shape with a semimajor axis, a, and a semiminor axis, b. The apparent disk of such a body is an ellipse with an apparent flattening, f', dependent on the apparent tilt of the object's axis. The apparent flattening of the object is always less than or

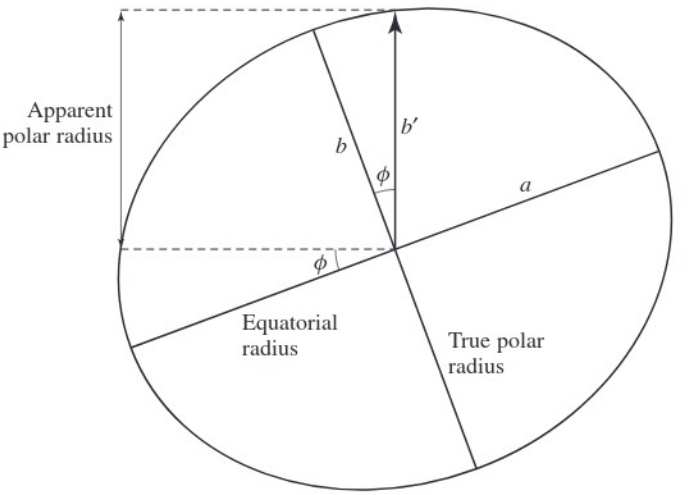


Figure 10.4 The geometric appearance of the apparent polar radius, b'

equal to its true flattening. The apparent polar radius and the apparent flattening of an object are derived from the parametric equation for an ellipse:

$$\begin{aligned} r &= \sqrt{x^2 + y^2} \\ x &= a\cos\phi \\ y &= b\sin\phi \end{aligned} \tag{10.8}$$

where x is the length of the projection of the point along the major axis from the center of the ellipse, y is the length of the projection of the point along the minor axis from the center, and ϕ is the planetocentric latitude of the sub-Earth point, the angle between the line segment connecting the point with the center of the ellipse and the semimajor axis (Fig. 10.4). The apparent polar semiminor axis for a geocentric observer is the length of the line segment, b'. Using Eqs. 10.8 the apparent semiminor axis, b', is

$$b' = \sqrt{a^2\cos^2\phi + b^2\sin^2\phi}. \tag{10.9}$$

Rearranging Eq. 10.1, gives

$$b = a(1-f) \tag{10.10}$$

Thus,

$$\begin{aligned} b' &= \sqrt{a^2\cos^2\phi + a^2(1-f)^2\sin^2\phi} \\ &= a\sqrt{1+(f^2-2f)\sin^2\phi} \\ &= a\sqrt{1+(f^2-2f)\left(\frac{\mathbf{b}'\cdot\mathbf{b}}{|\mathbf{b}'||\mathbf{b}|}\right)^2} \end{aligned} \tag{10.11}$$

where $\mathbf{b}'$ is the vector from the planetocenter to the apparent polar axis and $\mathbf{b}$ is the vector from the planetocenter to the true polar axis. The apparent semiminor axis, b' is, to first order in f

$$b' = a\left[1 - f\left(\frac{\mathbf{b}' \cdot \mathbf{b}}{|\mathbf{b}'||\mathbf{b}|}\right)^2\right]. \tag{10.12}$$

Thus, to first order, the apparent flattening, f', of the body is

$$f' = \frac{a - b'}{a}. \tag{10.13}$$

The maximum error arising from using a first order expansion is 0.13% or $0.''014$ for Saturn. For more accurate applications

$$f' = f\,\sin^2\phi + \frac{f^2}{2}\left(\sin^4\phi - \sin^2\phi\right) \tag{10.14}$$

to second order in f.

10.4.1 Sub-Earth Points and Sub-Solar Points

The tabulated quantities for the sub-Earth point, sub-solar point, and the greatest *defect of illumination* on the apparent disk of an object as it is seen from an observer on the Earth are illustrated in Fig. 10.5. At the center of the apparent disk is the sub-Earth point, e. The two other points of reference are the sub-solar point, s, and the north pole of the body, n. The apparent position of s with respect to e is designated by the apparent distance d_s and position angle, PA_s, of s. Similarly, the apparent position of n is designated by d_n and PA_n. The position angles are measured eastward from north, N, on the celestial sphere. The direction north is defined by the great circle on the celestial sphere passing through the center of the object's apparent disk and the Celestial Intermediate Pole (§ 6.2.3) of date. The apparent distance of a tabulated point is listed as positive if the point lies on the visible hemisphere of the object and negative if the point is on the far side of the object. Thus, as point n or s passes from the visible hemisphere to the far side, or vice versa, the sign of the distance changes abruptly, but the position angle varies continuously. On the other hand, when the point passes close to the center of the disk, the sign of the distance remains unchanged, but both the distance and position angle may vary rapidly and may appear to be discontinuous in a fixed interval tabulation.

The planetographic coordinates of the sub-Earth and sub-solar points are determined as follows: First, the position ephemerides are used to calculate the heliocentric equatorial rectangular coordinates for the body, $\mathbf{r}$, and the Earth, $\mathbf{r}_e$ at a given Julian Date in TT [JD(TT)]. The distance vector, $\Delta\mathbf{r}$, from the Earth to the object is

$$\Delta\mathbf{r} = \mathbf{r} - \mathbf{r}_e. \tag{10.15}$$

The light-time correction, δt, is found from $\Delta\mathbf{r}$ by dividing by the speed of light, c

$$\delta t = \frac{|\Delta\mathbf{r}|}{c}. \tag{10.16}$$

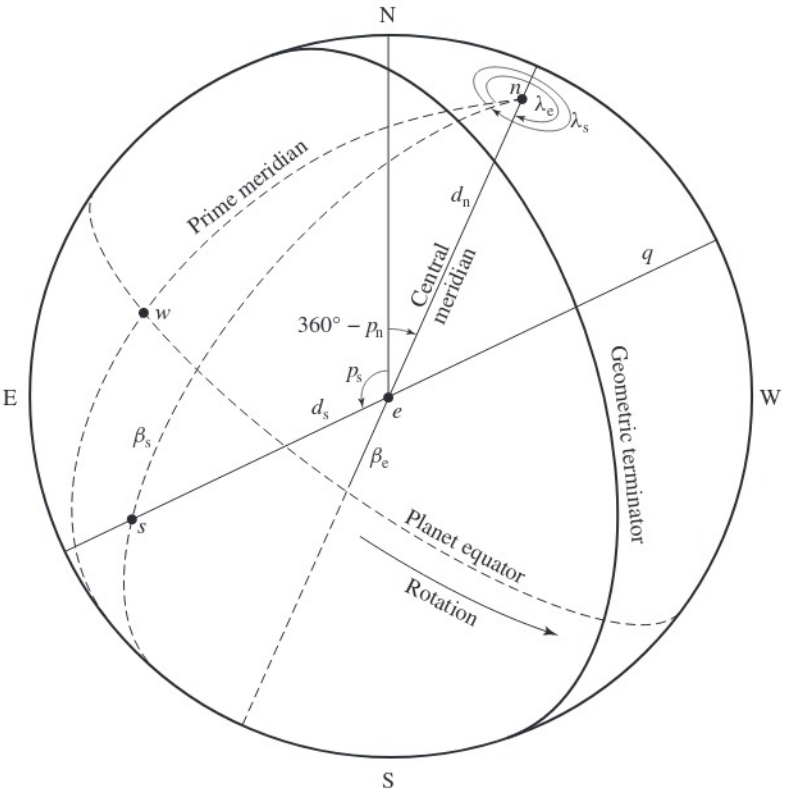


Figure 10.5 The disk of a planet as seen from an observer on the Earth

The difference JD(TT) $- \delta t$ is calculated to approximate the time at which the image of the body, as observed at the Earth at JD(TT), left the body. Thus, $\mathbf{r}_{\mathrm{JD(TT)}-\delta t}$, is the approximate position of the body as observed from the Earth at time JD(TT). This process may be iterated, if desired, to produce a more accurate body position; however, body motions are slow enough that to the precision of *The Astronomical Almanac* no more than a single iteration is ever required. The position of the Earth, $\mathbf{r}_e$, and the apparent position of the body, $\mathbf{r}_{\mathrm{JD(TT)}-t}$, are then transformed from the mean equator and ecliptic of J2000.0 to the true equator and ecliptic of date using the frame bias, precession and nutation routines described in § 6.5 and § 6.6. The transformed position vectors are designated $\mathbf{r}_{ed}$ for the Earth and $\mathbf{r}_d$ for the body. The distance vector, $\Delta\mathbf{r}$, is recomputed by using $\mathbf{r}_{ed}$ and $\mathbf{r}_d$ as in Eq. 10.15 and then corrected for aberration in position as described in § 7.2.3. The unit vector along the body-Sun line,

$$\mathbf{s} = \frac{-\mathbf{r}_d}{|\mathbf{r}_d|} \tag{10.17}$$

is the planetocentric unit vector denoting the direction of the Sun from the body. Prior to the 2013 edition the position vector from the body to the Sun did not correct for the aberration of light. However, the difference between the directions of the aberrated and the unaberatted

vector is always less than 0.°01 for all tabulated bodies. Similarly, the planetocentric unit vector, including aberration, pointing from the body to the Earth is

$$\mathbf{e} = \frac{-\Delta\mathbf{r}}{|\Delta\mathbf{r}|}. \tag{10.18}$$

The position of the north pole of date of the body in the coordinates of the mean equator and equinox of J2000.0, (α_0, δ_0), is found using the appropriate expression from Table 10.1. These coordinates are transformed to the equator and equinox of date, (α_d, δ_d). The unit vector $\mathbf{n}$ is the planetocentric unit vector of the body's north pole. In terms of the right ascension and declination $\mathbf{n}$ is

$$\begin{aligned} \mathbf{n} &= (\cos\delta_d \cos\alpha_d, \cos\delta_d \sin\alpha_d, \sin\delta_d) \\ &= \mathbf{N}\,\mathbf{P}\,\mathbf{B}\,(\cos\delta_0 \cos\alpha_0, \cos\delta_0 \sin\alpha_0, \sin\delta_0) \end{aligned} \tag{10.19}$$

where $\mathbf{P}$, $\mathbf{N}$, and $\mathbf{B}$ are the precession, nutation, and frame bias matrices, respectively (see § 6.5 and § 6.6). The planetocentric unit vector for the intersection of the planet's prime meridian and equator, $\mathbf{w}_d$, is also required. Its declination, δ_w, is

$$\sin\delta_w = \sin W \cos\delta_0 \tag{10.20}$$

where W is the rotation angle of the body's prime meridian; refer to Fig. 10.1. The current values of W for the planets, Ceres, and Pluto (Archinal et al. 2011a; Archinal et al. 2011b) are given in Table 10.1. The angle δ_w lies between $+90°$ and $-90°$, so there is no loss of generality.

Let the arc, ψ, run from the node of the planet's equator of date along the equator of the BCRS to the arc representing δ_w as shown in Fig. 10.1. Then

$$\sin\psi = \frac{\sin W \sin\delta_0}{\cos\delta_w} \quad \text{and} \quad \cos\psi = \frac{\cos W}{\cos\delta_w}. \tag{10.21}$$

The right ascension of the planet's north pole of date is 6^{h} $(90°)$ less than the position of its node. Thus, the right ascension of $\mathbf{w}$ is

$$\alpha_w = \alpha_0 + 90° + \psi. \tag{10.22}$$

The vector $\mathbf{w}$ is thus

$$\mathbf{w} = \mathbf{N}\,\mathbf{P}\,\mathbf{B}\,(\cos\delta_w \cos\alpha_w, \cos\delta_w \sin\alpha_w, \sin\delta_w). \tag{10.23}$$

The coordinates for the sub-Earth and sub-solar points are computed using the planetary polar vector, $\mathbf{n}$, and $\mathbf{w}$ to determine the rotation from the equatorial coordinate system to determine the *planetocentric* latitude and the *planetographic* longitude (from the definition of W). The flattening of the planet, f, is used to convert the planetocentric latitude to the planetographic latitude. The process of determining the sub-Earth and sub-solar points by setting up a coordinate system where the planetary polar vector, $\mathbf{n}$, is the z-axis, $\mathbf{w}$ is the x-axis, and the y-axis of the coordinate system completes a *left-handed* coordinate system, that is

$$\mathbf{y} = \mathbf{w} \times \mathbf{n}. \tag{10.24}$$

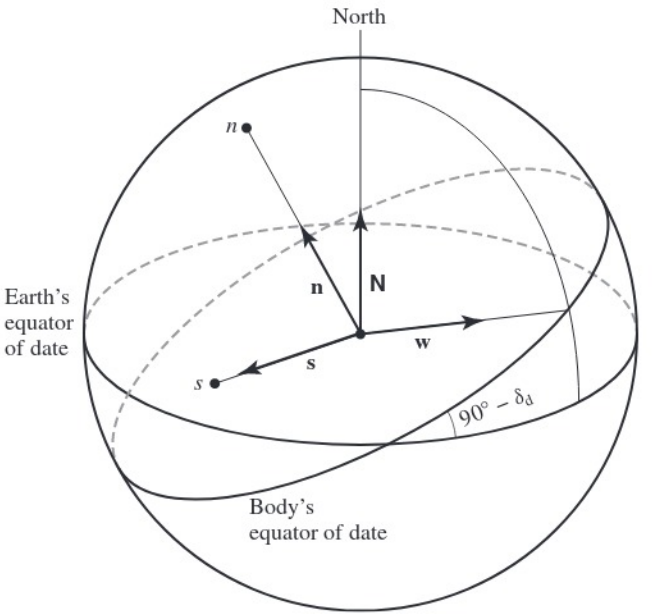


Figure 10.6 Planetocentric unit vectors for points of interest on the disk of a planet, and the angles giving the position of the pole and sub-solar point with respect to the Earth's mean equator and pole of date

The components of the unit vector for the sub-Earth point, **e**, are

$$\mathbf{e} = (\mathbf{e} \cdot \mathbf{w}, \mathbf{e} \cdot \mathbf{y}, \mathbf{e} \cdot \mathbf{n}). \tag{10.25}$$

The planetocentric and planetographic latitudes and planetographic longitude of the sub-Earth point are

$$\begin{aligned} \phi_e &= \sin^{-1} \mathbf{e}_z \\ \phi'_e &= \tan^{-1} \frac{\tan \phi_e}{1 - f^2} \\ \lambda'_e &= \tan^{-1} \frac{\mathbf{e}_y}{\mathbf{e}_x}. \end{aligned} \tag{10.26}$$

For retrograde rotation, $\lambda'_e = 360° - \lambda'_e$ as found in Eq. 10.26.

The planetographic latitude and longitude of the sub-solar point are found by replacing the position for the Sun, (α_s, δ_s), in place of the sub-Earth point (α_d, δ_d) in Eqs. 10.19 through 10.26.

Determining the apparent distance and position angle of the body's north pole starts by specifying a coordinate system in which the yz-plane is the plane of the sky, the y-axis points toward the west as seen on the plane of the sky, and the x-axis points toward the Earth. In the equatorial coordinates of date, the direction for the north pole of the Earth is $\mathbf{N} = (0, 0, 1)$. Thus, the directions for axes,$(\mathbf{u}_i, \mathbf{u}_j, \mathbf{u}_k)$, of the coordinate system in the

equatorial coordinates of date are

$$\begin{aligned} \mathbf{u}_i &= \mathbf{e} \\ \mathbf{u}_j &= \mathbf{e} \times \mathbf{N} \\ \mathbf{u}_k &= \mathbf{N}. \end{aligned} \tag{10.27}$$

The coordinates for the north pole vector in this coordinate system are

$$P(\mathbf{n} \cdot \mathbf{u}_i, \mathbf{n} \cdot \mathbf{u}_j, \mathbf{n} \cdot \mathbf{u}_k) \tag{10.28}$$

where P is the apparent polar diameter of the body. The position angle, p_n of the north pole is

$$p_n = \tan^{-1} \frac{\mathbf{n}_y}{\mathbf{n}_z}. \tag{10.29}$$

The length of the projection from the center of mass to the north pole on the body is

$$r = \sqrt{\mathbf{n}_x^2 + \mathbf{n}_z^2}. \tag{10.30}$$

The apparent distance, d_n, in arcseconds, is

$$d_n = 206264.8062 \frac{r}{|\Delta \mathbf{r}| - \mathbf{n}_x}. \tag{10.31}$$

The position angle, p_s, and apparent distance, d_s, of the sub-solar point are calculated similarly using the unit vector for the Sun, **s**, and the apparent radius of the body at the latitude of the sub-solar point rather than **n** and the apparent polar radius. The apparent radius of the body at the sub-solar point is derived using Eq. 10.8 and substituting the planetocentric latitude of the sub-solar point, ϕ_s for ϕ.

The phase angle,

$$i = \cos \mathbf{s} \cdot \mathbf{e} \tag{10.32}$$

of a body is the planetocentric elongation of the Earth from the Sun. The phase, k, is the ratio of the illuminated area of the disk to the total area of the disk as seen from the Earth. Assuming that the apparent disk of the body is circular,

$$k = 0.5(1 + \cos i). \tag{10.33}$$

The planetographic longitude and latitude of the sub-Earth point and the planetographic longitude of the sub-solar point along with the distance and position angle of s for Mercury are tabulated in Section E of *The Astronomical Almanac*. The pole of rotation of Mercury is nearly perpendicular to the plane of its orbit (Margot et al. 2007). Thus, the planetographic latitude of the sub-solar point does not differ significantly from 0°, and is not tabulated.

The planetographic longitudes and latitudes of the sub-Earth and sub-solar points along with the distance and position angle of s are tabulated for Venus, Mars, Jupiter, and Saturn in Section E of *The Astronomical Almanac*.

The planetographic latitudes of the sub-Earth point for Uranus and Neptune are tabulated in Section E. For Uranus and Neptune the difference in position between the sub-Earth and sub-solar points is never greater than 0.″1. Thus, values for the sub-solar point are not tabulated for these bodies.

The planetographic longitude and latitude of the sub-Earth point for Ceres and Pluto are tabulated on in Section G. Like Uranus and Neptune the difference in position between the sub-Earth and sub-solar points is never greater than $0''.1$. Thus, values for the sub-solar point are not tabulated for these bodies either.

The position angles and apparent distances of the north poles of Mercury, Venus, Mars, Jupiter and Saturn are tabulated in Section E of *The Astronomical Almanac*. The position angle and apparent distance of the north pole of Uranus and Neptune are tabulated as well.

10.4.2 The Greatest Defect of Illumination

The geometric terminator, the plane orthogonal to the direction of the Sun passing through the center of mass of the object (Fig. 10.5), is used to compute the phase and the maximum geometric defect of illumination. The maximum geometric defect of illumination, q, is the length of the portion of the line segment across the face of the body passing through the sub-Earth and sub-solar points, s and e, that is not illuminated (Fig. 10.6). The defect of illumination does not include non-geometric effects such as the refraction of light through the body's atmosphere.

The apparent equatorial semidiameter, r_{eq} of the body, in seconds of arc, is

$$r_{eq} = 206264.8062 \frac{a}{|\Delta \mathbf{r}|}. \tag{10.34}$$

The ratio of the apparent polar diameter to the equatorial diameter depends on the planetocentric latitude, ϕ, of the sub-Earth point (Fig. 10.5), and is found by rearranging Eq. 10.11

$$\frac{b'}{a} = \sqrt{1 + (f^2 - 2f)\sin^2 \phi}. \tag{10.35}$$

The maximum geometric defect of illumination is

$$q = 2r_{eq}\left[1 - \left(1 - \frac{b'}{a}\right)\sin^2\left(p_s - p_n + 90^\circ\right)\right](1 - k). \tag{10.36}$$

Its position angle, p_q, measured from celestial north, is:

$$p_q = \begin{cases} p_s + 180^\circ & p_s < 180^\circ \\ p_s - 180^\circ & p_s \geq 180^\circ. \end{cases} \tag{10.37}$$

The greatest defects of illumination for Mercury, Venus, Mars, Jupiter, and Saturn are tabulated on the even numbered pages of E54 through E76 of *The Astronomical Almanac*. Owing to both the small phase angles and small apparent diameters, the greatest defects of illumination of Uranus and Neptune are always less than $0''.01$, and, hence, not tabulated.

10.4.3 The Apparent Magnitudes of the Minor Planets

In Section G *The Astronomical Almanac* tabulates the apparent magnitude for 92 minor planets (90 asteroids and the probable dwarf planets (2) Pallas and (4) Vesta) at opposition. These comprise the set of minor planets for which the apparent magnitude is ≤ 11 (≤ 12 if the minor planet's mean diameter ≥ 200 km.) at mean opposition. In addition, *The Astronomical*

Almanac tabulates the apparent magnitudes daily for 60 days either side of opposition for the fourteen minor planets (2) Pallas, (3) Juno, (4) Vesta, (6) Hebe, (7) Iris, (8) Flora, (9) Metis, (10) Hygiea, (15) Eunomia, (16) Psyche, (52) Europa, (65) Cybele, (511) Davida, and (704) Interamnia.

Commission 20 of the IAU adopted the apparent magnitude system for minor planets termed the H-G magnitude system in 1985 (Marsden 1986). This system is based on Bowell et al. (1989). The mean visual magnitude, $V(i)$, of a minor planet as a function of phase, i, is calculated using the relation.

$$V(i) = H - 2.5\log[(1-G)\Phi_1(i) + G\Phi_2(i)] \tag{10.38}$$

where

$$H \equiv V(1, 0) \tag{10.39}$$

is the visual magnitude of the minor planet at 1 au from the Earth, 1 au from the Sun, and a phase angle of 0°, G is the slope parameter, and $\Phi_1(i)$ and $\Phi_2(i)$ are empirically determined phase functions. Thus, the second term on the right hand side of Eq. 10.38 constitutes the phase function, $\Delta m(i)$.

The slope parameter, G, is a measure of the gradient of the phase curve. It has been scaled so that $G \approx 0$ for low-albedo bodies and $G \approx 1$ for high-albedo bodies. However, it is possible for G to have values less than 0 or greater than 1. The values for G for each of the 93 selected minor planets along with the values for H are given in Table 10.8 and on pages G2 and G3 of *The Astronomical Almanac* for those minor planets tabulated.

The phase functions, $\Phi_1(i)$ and $\Phi_2(i)$, are normalized to unity at i = 0. The relations used for these functions are:

$$\Phi_1(i) = \exp\left[-3.33\left(\tan\frac{i}{2}\right)^{0.63}\right] \quad \text{and} \quad \Phi_2(i) = \exp\left[-1.87\left(\tan\frac{i}{2}\right)^{1.22}\right]. \tag{10.40}$$

These equations are valid for phase angles of $0° \le i \le 120°$. Equation A4 of Bowell et al. (1989) gives a somewhat more accurate set of expressions for $\Phi_1(i)$ and $\Phi_2(i)$.

The apparent visual magnitude, V, of the minor planet is then

$$V = V(i) + 5\log rd \tag{10.41}$$

where r is the heliocentric distance of the minor planet and d is its geocentric distance in au's.

In addition to the apparent magnitude at opposition, *The Astronomical Almanac* tabulates the mean diameters, d_m, for each of the 93 minor planets listed on pages G2 and G3. The mean diameter is specifically the one that would produce the same volume as an ellipsoidal body with diameters, a, b, and c, that is

$$d_m = \sqrt[3]{a\,b\,c}. \tag{10.42}$$

The diameters used for the minor planets come from several sources and are available from *The Astronomical Almanac Online* at URL[1].

Table 10.8 The H and G parameters for the minor planets

Minor Planet	H (mag)	G (mag)
1 Ceres	3.34	0.12
2 Pallas	4.13	0.11
3 Juno	5.33	0.32
4 Vesta	3.20	0.32
5 Astrea	6.85	0.15
6 Hebe	5.71	0.24
7 Iris	5.15	0.15
8 Flora	6.49	0.28
9 Metis	6.28	0.17
10 Hygiea	5.43	0.15
11 Parthenope	6.55	0.15
12 Victoria	7.24	0.22
13 Egeria	6.74	0.15
14 Irene	6.30	0.15
15 Eunomia	5.28	0.23
16 Psyche	5.90	0.20
17 Thetis	7.76	0.15
18 Melpomene	6.51	0.25
19 Fortuna	7.13	0.10
20 Massalia	6.50	0.25
21 Lutetia	7.35	0.11
22 Kalliope	6.45	0.21
23 Thalia	6.95	0.15
24 Themis	7.08	0.19
25 Phocaea	7.83	0.15
26 Prosperina	7.50	0.15
27 Euterpe	7.00	0.15
28 Bellona	7.09	0.15
29 Amphitrite	5.85	0.20
30 Urania	7.57	0.15
31 Euphrosyne	6.74	0.15
32 Pomona	7.56	0.15
37 Fides	7.29	0.24
39 Laetitia	6.10	0.15
40 Harmonia	7.00	0.15
41 Daphne	7.12	0.10
42 Isis	7.53	0.15
43 Ariadne	7.93	0.11
44 Nysa	7.03	0.46
45 Eugenia	7.46	0.07
48 Doris	6.90	0.15
51 Nemausa	7.35	0.08
52 Europa	6.31	0.18
54 Alexandra	7.66	0.15
60 Echo	8.21	0.27
63 Ausonia	7.55	0.25

Table 10.8 *(continued)*

Minor Planet	H (mag)	G (mag)
64 Angelina	7.67	0.48
65 Cybele	6.62	0.01
67 Asia	8.28	0.15
68 Leto	6.78	0.05
69 Hesperia	7.05	0.19
71 Niobe	7.30	0.40
79 Eurynome	7.96	0.25
80 Sappho	7.98	0.15
85 Io	7.61	0.15
87 Sylvia	6.94	0.15
88 Thisbe	7.04	0.14
89 Julia	6.60	0.15
92 Undina	6.61	0.15
94 Aurora	7.57	0.15
97 Klotho	7.63	0.15
103 Hera	7.66	0.15
107 Camilla	7.08	0.08
115 Thyra	7.51	0.12
121 Hermione	7.31	0.15
128 Nemesis	7.49	0.15
129 Antigone	7.07	0.33
135 Hertha	8.23	0.15
185 Eunike	7.62	0.15
192 Nausikaa	7.13	0.03
194 Prokne	7.68	0.15
196 Philomela	6.54	0.15
216 Kleopatra	7.30	0.29
230 Athamantis	7.35	0.27
270 Anahita	8.75	0.15
287 Nephthys	8.30	0.22
324 Bamberga	6.82	0.09
346 Hermentaria	7.13	0.15
349 Dembowska	5.93	0.37
354 Eleonora	6.44	0.37
372 Palma	7.20	0.15
387 Aquitania	7.41	0.15
389 Industria	7.88	0.15
409 Aspasia	7.62	0.29
423 Diotima	7.24	0.15
433 Eros	11.16	0.46
451 Patientia	6.65	0.19
471 Papagena	6.73	0.37
511 Davida	6.22	0.16
532 Herculina	5.81	0.26
654 Zelinda	8.52	0.15
702 Alauda	7.25	0.15
704 Interamnia	5.94	−0.02

10.5 Physical Ephemeris of the Sun

The physical ephemeris of the Sun tabulated in *The Astronomical Almanac* consists of the position angle of the solar axis, the heliographic sub-Earth latitude and longitude, the horizontal parallax, and the apparent semidiameter of the Sun. These quantities along with the ephemeris transit time are tabulated on the odd numbered pages C7 though C21.

For the sake of continuity as requested by Commission 10 of the IAU (IAU 1986), the elements used to calculate the physical ephemeris of the Sun are from Carrington (1863). The values of the physical constants for the ephemeris are:

1. adopted mean sidereal rotation rate at 14° latitude, $851'\ \text{day}^{-1}$;
2. inclination of solar equator to the ecliptic, $I = 7\overset{\circ}{.}25$;
3. longitude of the ascending node of the solar equator on the ecliptic, $\Omega = 75\overset{\circ}{.}76 + 0\overset{\circ}{.}01397\,T$, where T is the time, in years, from J2000.0 (JD245 1545.0); and
4. the equatorial semidiameter of the Sun, $d_S = 696,\,000$ km.

Carrington's elements do not include the motion of the ecliptic. That is, the rotation of the Sun is given with respect to the ecliptic of 1850. However, Carrington's elements do include precession, represented by the linear term in the relation for Ω, which is the rate of precession since 1850 as determined by Carrington. The uncertainty in both the inclination of the solar equator to the ecliptic, $\pm 0\overset{\circ}{.}002$, and the position of the node, $\pm 0\overset{\circ}{.}01$ (Beck and Giles 2005), are large enough that any error introduced arising from neglecting the motion of the ecliptic, differences between Carrington's rate of precession and the currently accepted value, or higher order terms in the precession is insignificant. The flattening of the Sun is assumed to be extremely small ($f \approx 0$). Because the Sun is a gaseous body, it does not rotate rigidly. The sidereal period given is for the mean rotation rate of the Sun at a latitude of 14° on either side of its equator.

The position of the north pole of the Sun derived from the inclination of the Sun and the longitude of the ascending node with respect to the mean equator and equinox of J2000.0 is:

$$\alpha_0 = 286\overset{\circ}{.}1300 \quad \text{and} \quad \delta_0 = 63\overset{\circ}{.}8700. \tag{10.43}$$

The position of the prime meridian derived from the mean sidereal period of the Sun is[6]:

$$W = 84\overset{\circ}{.}10 + 14\overset{\circ}{.}1844\,000\,t \tag{10.44}$$

where t is the time, in days, from J2000.0 (JD 245 1545.0).

Unlike other solar system bodies, the position for the prime meridian of the Sun has traditionally included both the light-time correction and aberration. This situation is a relic of Carrington's method for reducing his observations. However, both these quantities are nearly constant for the Sun. Thus, prior to the advent of fast computers these corrections were simply included in the position of the prime meridian to reduce the number of calculations needed to

6. The rotation rate of $14\overset{\circ}{.}184\,4000\ \text{day}^{-1}$ is the value officially adopted by the IAU Working Group on Cartographic Coordinates. Carrington states that the adopted rotation period is 25.380 days, which is equivalent to a rotation rate of $14\overset{\circ}{.}184\,3972\ \text{day}^{-1}$. However, in his reductions the actual rotation rate Carrington used was $851'\ \text{day}^{-1}$, which is equivalent to $14\overset{\circ}{.}183\,3333\ \text{day}^{-1}$.

determine the physical ephemeris of the Sun. Archinal et al. (2011a) have removed the light-time correction and aberration from the position of the prime meridian. Thus, beginning with the 2009 edition of *The Astronomical Almanac* the relation for the prime meridian of the Sun, adjusted for light-time and aberration becomes

$$W = 84.^{\circ}176 + 14.^{\circ}1844\,000\,t. \tag{10.45}$$

An additional digit in W is included so that the physical ephemeris of the Sun may be treated in the same manner as the other planets and ensures consistency with previous calculations. The additional digit does not represent an increase in the accuracy of the position of the prime meridian at J2000.0. Henceforward, the Sun will be treated like every other solar system body in regard to the position of its prime meridian.

The horizontal parallax of an object is the difference in direction between the topocentric coordinates of an object when the center of the object is on the astronomical horizon and its geocentric coordinates. Thus, the horizontal parallax, HP, of the Sun is

$$HP = \sin^{-1}\frac{R_e}{|\mathbf{r}_e|}. \tag{10.46}$$

where $R_e = 6378.14$ km, the IAU equatorial radius of the Earth (Archinal et al. 2011a) and $\mathbf{r}_e$ is the Earth–Sun distance.

Similarly, the semidiameter, SD, of the Sun, in arcseconds, is

$$SD = 206\,264.8062\,\frac{d_S}{2|\mathbf{r}_e|}. \tag{10.47}$$

The tabulated semidiameter is then converted to arcminutes and seconds.

10.6 Physical Ephemeris of the Moon

In *The Astronomical Almanac* data for the physical ephemeris of the Moon, the sub-Earth longitude, latitude, the physical libration, and the position angle of the lunar pole are tabulated to an accuracy of $0.^{\circ}001$. The Sun's selenographic latitude and co-longitude and the position angle of the bright limb are tabulated to an accuracy of $0.^{\circ}01$. The data tabulated for the Moon consist of the apparent position, the true distance, horizontal parallax, and semidiameter tabulated on even numbered pages D6 through D20. The Earth's selenographic longitude and latitude; physical librations in longitude, latitude, and position angle; the Sun's selenographic co-longitude and latitude, the position angles of the axis and bright limb, and the fraction illuminated are tabulated on the odd pages D7 through D21. Beginning with the 2013 edition, the physical librations will not be tabulated.

The coordinate system used for the physical ephemeris of the Moon is the mean Earth-mean polar axis coordinate system. In this coordinate system, the z-axis is the mean lunar pole of rotation and the x-axis is the mean direction from the center of the Moon to the geocenter. Another commonly used coordinate system is that of the lunar principal moments of inertia.

On the average, the same hemisphere of the Moon is always turned toward the Earth, but there are periodic oscillations, or *librations*, of the apparent position of the lunar surface that allows about 59% of the surface to be seen from the Earth. The librations are due partly to *physical librations*—oscillations of the actual rate of rotation of the Moon with respect to its mean rotation rate. A second, much larger component of the librations are the *geocentric*

optical librations, which are the result of the nonuniform motion of revolution of the Moon on its elliptical path about the Earth–Moon barycenter. Both of these effects are taken into account in the computation of the Earth's selenographic longitude, λ_e, and latitude, β_e, and of the position angle, C, of the axis of rotation. The contributions from the physical librations were tabulated separately in *The Astronomical Almanac* through the 2012 edition. A third component to the librations, the *topocentric optical librations*, is the result of the difference between the viewpoints of an observer on the surface of the Earth and a hypothetical observer at the geocenter. The topocentric optical librations may be as large as 1° and have important effects on the apparent contour of the limb. The topocentric optical librations are not tabulated in *The Astronomical Almanac* because the values depend on the observer's position. Instead, a method for estimating the topocentric optical librations is given on page D5 of *The Astronomical Almanac* and at the end of this section. MICA, the *Multiyear Interactive Computer Almanac*, computes the topocentric optical librations from rigorous formulae. The difference between MICA and the method given for estimating the topocentric optical librations is, at most, 1″ (0.0003).

The selenographic coordinates of the Earth and Sun specify the point on the lunar surface where the Earth and Sun, respectively, are in the selenographic zenith. The tabulated selenographic longitude and latitude of the Earth include the total geocentric (both optical and physical) librations in longitude and latitude, respectively. When the libration in selenographic longitude of the Earth is positive, the mean center of the lunar disk is displaced eastward on the celestial sphere, exposing to view a region of the western limb. When the libration in selenographic latitude of the Earth is positive, the mean center of the lunar disk is displaced toward the south, and a region of the north limb is exposed to view.

The offset matrix, $\mathbf{U}$, from the principal moment of inertia of the Moon coordinates to the mean direction of the Earth–mean rotation axes LE403 is

$$\mathbf{U} = \mathbf{R}_1(-0.''146)\mathbf{R}_2(-79.''077)\mathbf{R}_3(-63.''899) \tag{10.48}$$

where $\mathbf{R}_1$, $\mathbf{R}_2$, and $\mathbf{R}_3$ are the Eulerian rotation matrices around the first, second, and third axes, respectively, i.e.,

$$\mathbf{R}_1 = \begin{bmatrix} 1 & 0 & 0 \\ 0 & \cos\theta & \sin\theta \\ 0 & -\sin\theta & \cos\theta \end{bmatrix}, \quad \mathbf{R}_2 = \begin{bmatrix} \cos\theta & 0 & \sin\theta \\ 0 & 1 & 0 \\ -\sin\theta & 0 & \cos\theta \end{bmatrix},$$
$$\text{and} \quad \mathbf{R}_3 = \begin{bmatrix} \cos\theta & \sin\theta & 0 \\ -\sin\theta & \cos\theta & 0 \\ 0 & 0 & 1 \end{bmatrix}. \tag{10.49}$$

Let $\mathbf{M}$ be the selenocentric unit vector for the selenocentric longitude, λ_M, and latitude, β_M, reckoned from the mean Earth direction-mean pole of rotation, i.e.,

$$\mathbf{M} = \begin{bmatrix} \cos\lambda_M \sin\beta_M \\ \sin\lambda_M \sin\beta_M \\ \cos\beta_M \end{bmatrix} \tag{10.50}$$

and $\mathbf{P}$ is the selenocentric unit vector for the selenocentric longitude, λ_M, and latitude, β_M, reckoned from the principal moments of inertia. The flattening of the Moon is assumed to

be zero (Archinal et al. 2011a), so the selenographic latitude is identical to the selenocentric latitude. The selenographic co-longitude of the Sun tabulated in *The Astronomical Almanac* is the east selenographic longitude of the morning geometric terminator. It is determined by subtracting the selenographic longitude of the Sun from 90° and, if the result is negative, adding 360°. Co-longitudes of 270°, 0°, 90°, and 180° correspond, approximately, to New Moon, First Quarter, Full Moon, and Last Quarter, respectively. The age of the Moon is computed as the time elapsed, in days, since the most recent moment at which the selenographic co-longitude of the Sun was 270°.

The position angle of the midpoint of the bright limb is the same as the position angle of the sub-solar point, and is computed in the manner described for the sub-solar point in § 10.4.1. Like the other position angles, the position angle of the midpoint of the bright limb is measured eastward around the disk from north. The fraction of the Moon illuminated, k, is the same as the phase. This quantity is computed as described in § 10.4.1.

10.6.1 Calculating Librations

10.6.1.1 Calculating Physical Librations

The physical libration of the Moon is determined from the lunar rotation angles included in LE403 (Standish et al. 1995). These angles, described in Newhall and Williams (2000), are with respect to the mean equator and equinox of J2000.0. Thus, they must first be rotated into the reference frame of the mean equinox and ecliptic of date.

The rotation angles stored in the JPL lunar ephemerides, Fig. 10.7, are: ϕ, the angle along the Earth's mean equator of J2000.0 from the mean equinox of J2000.0[7] to the ascending node of the true lunar equator of date on the Earth's mean equator of J2000.0; θ, the inclination of the lunar true equator of date on the Earth's mean equator of J2000.0; and ψ, the angle along the lunar true equator of date from the node with the Earth's mean equator of J2000.0 to the selenographic origin. These three angles are quite different from the traditional angles ϕ_C, the angle along the Earth's true equator of date from the true equinox of date to the descending node of the true lunar equator of date on the Earth's true equator of date; θ_C, the inclination of the true lunar equator of date to the Earth's equator of date; and $\psi_C = \tau - \sigma + F + 180°$, the angle along the lunar true equator of date from the ecliptic of date to the selenographic prime meridian (see Fig. 10.7). F is the difference $L - \Omega$, where L is the mean longitude of the Moon on the ecliptic of date. Thus, the JPL rotation angles need to be transformed from angles on the mean equator and equinox of J2000.0 to angles on the mean ecliptic and equinox of date.

The rotation matrix, $\mathbf{A}$, from the selenographic coordinate system to the mean equator and equinox of J2000.0 is:

$$\mathbf{A} = \mathbf{R}_3(\phi)\, \mathbf{R}_1(\theta)\, \mathbf{R}_3(\psi). \tag{10.51}$$

7. In actuality, neither LE403 (Standish et al. 1995) nor LE405 (Standish 1998) are aligned to the mean equator and equinox of J2000.0, but to the ICRS (Ma et al. 1998). However, Capitaine, Wallace, and Chapront (2003) show that there is a slight rotation between the JPL ephemerides and the ICRS proper. Thus, the description of using the mean equator and equinox of J2000.0 will be used to describe the orientation of the JPL ephemerides.

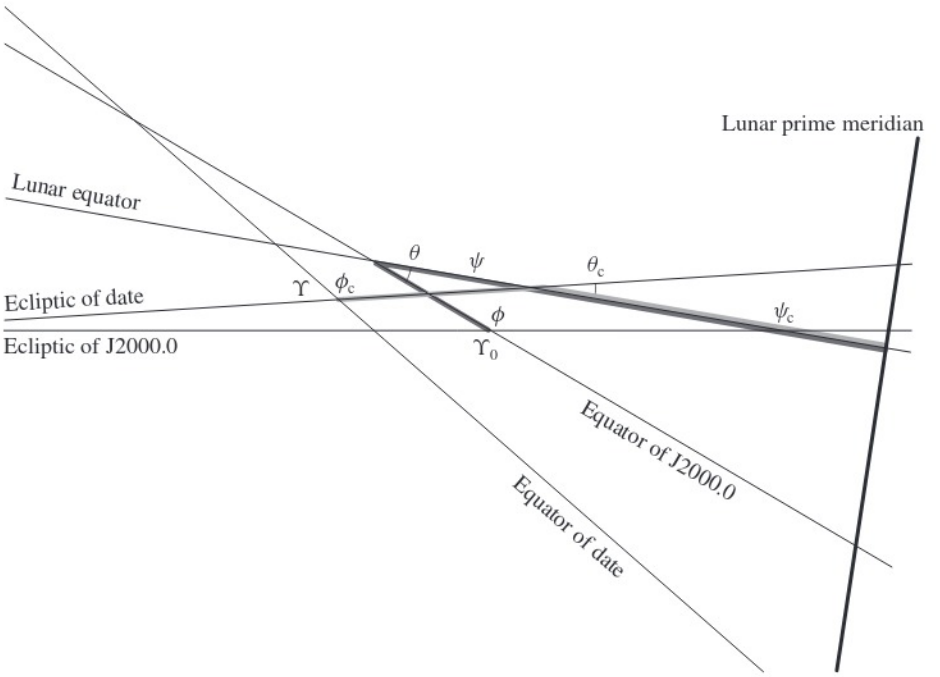


Figure 10.7 The angles for the position of the lunar prime meridian and equator with respect to the equator and equinox of J2000.0 as given in the JPL ephemerides and the traditional angles given with respect to the ecliptic and equinox of date

The complete rotation matrix is

$$\mathbf{A} = \begin{bmatrix} \cos\phi\cos\psi - \sin\phi\cos\theta\sin\psi & -\cos\phi\sin\psi - \sin\phi\cos\theta\cos\psi & \sin\psi\sin\theta \\ \sin\phi\cos\psi + \cos\phi\cos\theta\sin\psi & -\sin\phi\sin\psi + \cos\phi\cos\theta\cos\psi & -\cos\psi\sin\theta \\ \sin\theta\sin\psi & \sin\theta\cos\psi & \cos\theta \end{bmatrix}. \quad (10.52)$$

Let the vector **x** point toward the intersection of the lunar equator and selenographic prime meridian, and the vector **z** point toward the lunar pole. In the principal moments of inertia, selenographic reference frame, these vectors are

$$\mathbf{x}^{sel} = \begin{bmatrix} 1 \\ 0 \\ 0 \end{bmatrix} \quad \text{and} \quad \mathbf{z}^{sel} = \begin{bmatrix} 0 \\ 0 \\ 1 \end{bmatrix}. \quad (10.53)$$

These vectors in the reference frame of the mean equator and equinox of J2000.0 are

$$\mathbf{x}^{J2000} = \mathbf{A}\,\mathbf{U}\,\mathbf{x}^{PMI} \quad \text{and} \quad \mathbf{z}^{J2000} = \mathbf{A}\,\mathbf{U}\,\mathbf{z}^{PMI}. \quad (10.54)$$

The vectors are then precessed and nutated to the system of date:

$$\mathbf{x}^{date} = \mathbf{N}\,\mathbf{P}\,\mathbf{x}^{J2000} \quad \text{and} \quad \mathbf{z}^{date} = \mathbf{N}\,\mathbf{P}\,\mathbf{z}^{J2000}. \quad (10.55)$$

where **N** is the nutation matrix and **P** is the precession matrix.

The inclination of the lunar equator on the ecliptic of date, θ_c, is the dot product between the lunar pole and the pole of the ecliptic of date, $\mathbf{z}^{eclip}$,

$$\cos\theta_c = \mathbf{z}^{date} \cdot \mathbf{z}^{eclip} = z_3^{date} \tag{10.56}$$

where

$$\mathbf{z}^{eclip} = \begin{bmatrix} 0 \\ 0 \\ 1 \end{bmatrix}. \tag{10.57}$$

The quantities z_1^{date}, z_2^{date}, and z_3^{date} are the rectangular components of $\mathbf{z}^{date}$, the selenographic pole, along the axes of the ecliptic reference system of date. Thus, z_1^{date} points towards the equinox of date, z_3^{date} points towards the ecliptic pole of date, and z_2^{date} points along the third coordinate of the right handed rectangular coordinate system defined by the other two coordinate directions.

The angle from the mean equinox of date to the node of the lunar equator on the ecliptic is ϕ_c. The node, $\mathbf{\Omega}$, is the unit vector of the cross product of the lunar pole with the ecliptic pole,

$$\mathbf{\Omega} = \frac{\mathbf{z}^{date} \times \mathbf{z}^{eclip}}{|\mathbf{z}^{date} \times \mathbf{z}^{eclip}|} = \frac{z_2^{date}\mathbf{i} - z_1^{date}\mathbf{j}}{\sqrt{(z_1^{date})^2 + (z_2^{date})^2}} \tag{10.58}$$

where $\mathbf{i}$ and $\mathbf{j}$ are the unit vectors in the ecliptic reference system of date and point towards the equinox of date and the direction at right angles to the equinox in the plane of the ecliptic, respectively. The quantity $\cos\phi_c$ is the dot product of the node with the unit vector pointing to the equinox,

$$\cos\phi_c = \mathbf{\Omega} \cdot \mathbf{x}^{eq} = \Omega_1 = \frac{z_2^{date}}{\sqrt{(z_1^{date})^2 + (z_2^{date})^2}} \tag{10.59}$$

and $\sin\phi_c$ is the magnitude of the cross product,

$$\sin\phi_c = \det\left(\mathbf{\Omega} \times \mathbf{x}^{eq}\right) = \Omega_2 = \frac{-z_1^{date}}{\sqrt{(z_1^{date})^2 + (z_2^{date})^2}} \tag{10.60}$$

where

$$\mathbf{x}^{eq} = \begin{bmatrix} 1 \\ 0 \\ 0 \end{bmatrix}. \tag{10.61}$$

Finally, ψ_c, the angular distance along the lunar equator from the node of the lunar equator on the ecliptic of date to the lunar prime meridian, is determined from

$$\cos\psi_c = \mathbf{\Omega} \cdot \mathbf{x}^{date} \quad \text{and} \quad \sin\psi_c = (\mathbf{z}^{date} \times \mathbf{\Omega}) \cdot \mathbf{x}^{date}. \tag{10.62}$$

The apparent positions of the Sun and Moon are used in the calculations to determining the physical librations of the Moon. Thus, except for the inappreciable difference between

the light-time from the Sun to the Moon and from the Sun to the Earth, aberration is already included.

Prior to *The Astronomical Almanac* for 2011, the analytic theory for the libration of the Moon used was that of Eckhardt (1981); Eckhardt (1982) for the physical libration of the Moon; however, the IAU value for the inclination of the mean lunar equator to the ecliptic, 1° 32′ 32.″7, is used instead of Eckhardt's value. In addition, there are printing errors in Eckhardt's published values, so any attempt to use that theory must be done with care. Although the values of Eckhardt's constants differ slightly from those of the IAU, the difference is of no consequence for the precision of the tabulation, except for the inclination of the lunar equator. Included in the calculations were perturbations for all terms greater than 0.″0001.

10.6.1.2 Calculating Geocentric Optical Librations

The optical librations are determined assuming that the Moon is in a Cassini state, that is:

1. It is rotating at a uniform rate,
2. Its mean axis of rotation is perpendicular to the mean plane of its orbit, and
3. The mean axis pointing towards the Earth is perpendicular to both the mean plane of its orbit and the ecliptic.

Thus, given the ecliptic longitude and latitude of the Moon, $(\lambda_{ME}, \beta_{ME})$, the position angle, P_N, (Fig. 10.8) of the Moon with respect to its mean node, Ω_O, (Simon et al. 1994) is

$$P_N = \lambda_{ME} - \Omega_O - \Delta\psi \tag{10.63}$$

where $\Delta\psi$ is the Earth's nutation in longitude (§ 6.6.3); that is, P_N is measured from the node of the Moon's orbit on the ecliptic. Rotating the unit vector denoted by (P_N, β_{ME}) about the node of the mean plane of the lunar orbit on the ecliptic by the mean inclination of the lunar

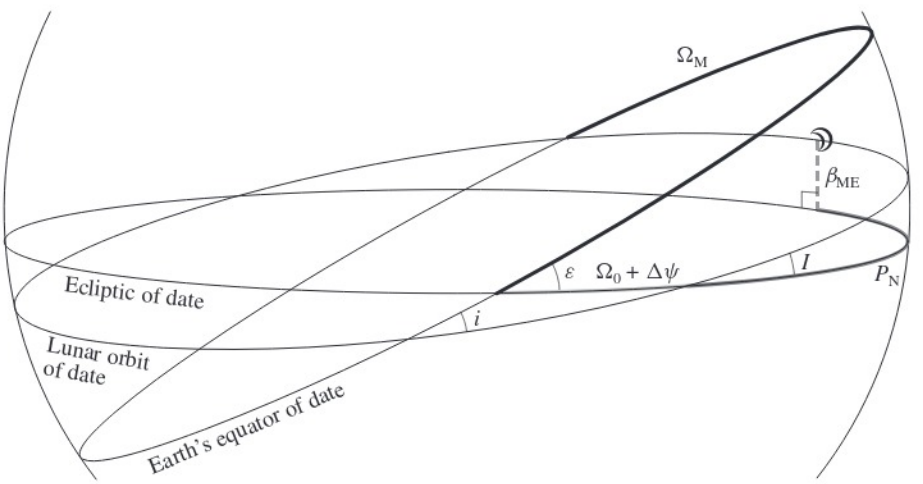


Figure 10.8 The angles of the lunar orbit used in the determination of the apparent librations of the Moon

orbit gives $(\lambda_{MM}, \beta_{MM})$, the longitude and latitude of the Moon in the coordinate system of the mean plane of the lunar orbit where the origin of longitude is the node of the mean plane of the lunar orbit on the ecliptic,

$$\begin{bmatrix} \cos\beta_{MM}\cos\lambda_{MM} \\ \cos\beta_{MM}\sin\lambda_{MM} \\ \sin\beta_{MM} \end{bmatrix} = \mathbf{R}_1(-I) \begin{bmatrix} \cos\beta_{ME}\cos P_N \\ \cos\beta_{ME}\sin P_N \\ \sin\beta_{ME} \end{bmatrix}. \tag{10.64}$$

The mean selenographic longitude and latitude (λ_O, β_O) of the sub-Earth point are then

$$\lambda_O = \lambda_{MM} + \Omega_O - \lambda_M \quad \text{and} \quad \beta_O = -\beta_{MM} \tag{10.65}$$

where λ_M is the mean orbital longitude of the Moon (Simon et al. 1994).

The inclination, i, and longitude of the descending node, Ω_M, of the lunar orbit on the true equator of date are:

$$\cos i = \cos I \cos\epsilon + \sin I \sin\epsilon \cos(\Omega + \Delta\psi) \tag{10.66}$$

$$\tan\Omega_M = \frac{-\sin I \sin(\Omega + \Delta\psi)}{\cos I \sin\epsilon + \sin I \cos\epsilon \cos(\Omega + \Delta\psi)} \tag{10.67}$$

where $I = 1°32'33''.6$, the mean inclination of the lunar orbit on the ecliptic (Newhall and Williams 2000), and ϵ is the true obliquity of date.

The latitude of the lunar pole, β_P, as seen by an observer at the Earth's geocenter is

$$\sin\beta_P = -\sin P_N \cos\beta_M \sin I - \sin\beta_M \cos I \tag{10.68}$$

where β_M is the lunar ecliptic latitude in the coordinates of the true equinox and ecliptic of date.

The mean position angle, PA_O, of the lunar pole as seen by an observer at the Earth's geocenter is

$$\sin PA_O = \frac{-\sin i \cos(\alpha - \Omega_M)}{\cos\beta_P} \tag{10.69}$$

where α is the Moon's right ascension with respect to the true equator and equinox of date.

The angles λ_O, β_O, and PA_O constitute the optical librations of the Moon. Repeating Eqs. 10.64 through 10.69 and substituting ϕ_c for λ_{ME}, θ_c for β_{ME},

$$\Omega_T = (\phi_c + \psi)c - 180° \tag{10.70}$$

for Ω_O, and

$$\lambda_T = 180° - \psi_c \tag{10.71}$$

for λ_M gives the true librations, λ_T, β_T, and PA_T.

The physical librations, λ_P, β_P, and PA_P, are then

$$\begin{aligned} \lambda_P &= \lambda_T - \lambda_O \\ \beta_P &= \beta_T - \beta_O \\ PA_P &= PA_T - PA_O. \end{aligned} \tag{10.72}$$

λ_P, β_P, and PA_P will not be tabulated after the 2012 edition.

10.6.1.3 Calculating Topocentric Optical Librations

The differential corrections to be applied to the tabular geocentric librations to form the topocentric librations are derived in Atkinson (1951). The formulae for the topocentric corrections are

$$\begin{aligned}\Delta\lambda_m &= -HP'\frac{\sin(Q_m - C_m)}{\cos b}\\ \Delta\beta_m &= +HP'\cos(Q_m - C_m)\\ \Delta C_m &= +\sin(\beta_m - \Delta\beta_m)l - HP'\sin Q\tan b\end{aligned} \tag{10.73}$$

where λ_m is the selenographic longitude, β_m is the selenographic latitude, C_m is the position angle of the axis of rotation, Q_m is the geocentric parallactic angle subtended by the Moon, and HP' is the parallax between the point of observation on the Earth's surface and the geocenter, commonly called the diurnal parallax.

The horizontal parallax, HP, occasionally called the geocentric horizontal parallax, is found from the Earth–Moon distance, $|\mathbf{r}_m|$, and the equatorial radius of the Earth, $R_e = 6378.137$ km.

$$\sin HP = \frac{R_e}{|\mathbf{r}_m|}. \tag{10.74}$$

The geocentric (a.k.a. diurnal) parallax, HP', is computed from the horizontal parallax using

$$\sin HP' = \frac{\sin z \sin HP}{1 - \sin z \sin HP} \tag{10.75}$$

where z is the geocentric zenith angle of the Moon. The values of Q and z are calculated from the geocentric right ascension, α_m, and declination, δ_m, of the Moon:

$$\begin{aligned}\sin z \sin Q &= \cos\Phi \sin h\\ \sin z \cos Q &= \cos\delta_m \sin\Phi - \sin\delta_m \cos\Phi \cos h\\ \cos z &= \sin\delta_m \sin\Phi + \cos\delta_m \cos\Phi \cos h\end{aligned} \tag{10.76}$$

where Φ is the geocentric latitude of the observer and h is the local hour angle of the Moon,

$$h = \mathrm{LST} - \alpha_m \tag{10.77}$$

where LST is the apparent local sidereal time.

In the interpolation of the tabular geocentric librations to the time of observation, second differences must be taken into account. The semidiameter, SD, of the Moon, in radians, is

$$SD = \tan^{-1}\frac{R_m}{|\mathbf{r}_m|} \tag{10.78}$$

where $R_m = 1737.4$ km is the radius of the Moon and $|\mathbf{r}_m|$ is the Earth–Moon distance.

10.7 Physical Ephemerides of the Planets

In addition to the quantities described in § 10.3 and 10.4, the planetocentric orbital longitude of the Sun, L_S, is tabulated for Mars, Jupiter, Saturn, Uranus, and Neptune in *The Astronomical Almanac,* and for all of the planets and Pluto in MICA. This angle is measured eastward

in the body's orbital plane from its instantaneous vernal equinox. The planet's vernal equinox is the point where the ascending node of the planet's equator crosses the plane of its orbit about the Sun. Thus,

$$L_S = \cos^{-1} \frac{\mathbf{r}_p \cdot \mathbf{r}_{ve}}{|\mathbf{r}_p||\mathbf{r}_{ve}|} \tag{10.79}$$

where $\mathbf{r}_p$ is the vector in ecliptic rectangular coordinates of the planet and $\mathbf{r}_{ve}$ is the vector in ecliptic rectangular coordinates of the planet's instantaneous vernal equinox. The correct quadrant is determined from the sign of the third component of

$$\mathbf{r}_p \times \mathbf{r}_{ve}. \tag{10.80}$$

Values for L_S of 0°, 90°, 180°, and 270° correspond to the beginning of spring, summer, autumn, and winter, respectively, in the body's northern hemisphere.

Unless otherwise noted, the positions of the planetary poles and the prime meridians and the planetary radii and flattenings are those in Archinal et al. (2011a). The values for $V(1, 0)$, the magnitude of the planets at a distance of 1 au and at a phase angle of 0°, are from de Vaucouleurs (1970), and the values for the phase coefficient, $\Delta m(i)$, are from Harris (1961).

10.7.1 Mercury

Since Mercury's orbit about the Sun is interior to the orbit of the Earth, Mercury is seen to go through the entire range of phase angles. Prior to the edition for 2005, the values for $V(1, 0)$ and $\Delta m(i)$ are from de Vaucouleurs (1970) and Harris (1961), respectively. For the 2005 and 2006 editions of *The Astronomical Almanac* the phase coefficient was replaced by a quadratic expression determined by fitting the photometric observations of Danjon (1949); Danjon (1954) using the de Vaucouleurs (1970) correction from m to V for Mercury (Hilton 2005, private communication). The expression for $\Delta m(i)$ is valid for phase angles in the range $3° < i < 123°$. For $i < 3°$ and $i > 123°$, Mercury was too close to the Sun to be observed by Danjon. The uncertainty in the predicted visual magnitude is about 0.12 mag. Beginning with the edition for 2007, the values for $V(1, 0)$ and $\Delta m(i)$ are determined from an analysis of the Mallama et al. (2003) LASCO/SOHO and ground-based observations of Mercury (Hilton 2005). For these data the valid range in phase for $\Delta m(i)$ is 2° to 170°, and the uncertainty in the predicted visual magnitude is about 0.10 mag. Magnitudes are not printed in *The Astronomical Almanac* when Mercury's phase is outside the valid range. The cartographic prime meridian of Mercury is defined so that the 20° meridian passes through the center of the crater Hun Kal.

10.7.2 Venus

Venus rotates in a retrograde fashion, thus the sign for the motion of the prime meridian is negative. Like Mercury, the flattening of Venus is negligible; so the equatorial and polar radii of Venus are identical.

Also like Mercury, Venus' orbit is interior to the Earth's orbit, so it has a phase angle that varies from 0° to 180°. Prior to the edition for 2005, the values for $V(1, 0)$ and $\Delta m(i)$ are from de Vaucouleurs (1970) and Harris (1961), respectively. For the 2005 and 2006 editions of *The*

Astronomical Almanac the phase coefficient was replaced by a quadratic expression determined by fitting the photometric observations of Danjon (1949) using the de Vaucouleurs (1970) correction from m to V for Venus (Hilton 2005, private communication). The expression for $\Delta m(i)$ is valid for phase angles in the range $0\overset{\circ}{.}9 < i < 170\overset{\circ}{.}7$. For $i < 0\overset{\circ}{.}9$ and $i > 170\overset{\circ}{.}7$, Venus is too close to the Sun to be observed photometrically. The uncertainty in the predicted visual magnitude is about 0.05 mag. Beginning with the edition for 2007, the values for $V(1, 0)$ and $\Delta m(i)$ are determined from an analysis of the Mallama (2005) ground-based observations of Venus (Hilton 2005). For these data the valid range in phase for $\Delta m(i)$ is $2\overset{\circ}{.}2 < i < 163\overset{\circ}{.}6$. The uncertainty in the predicted visual magnitude is about 0.05 mag. Magnitudes are not printed in *The Astronomical Almanac* when Venus's phase is outside the valid range.

10.7.3 Mars

Although the phase angle of Mars can be as large as 47°, the current phase relation for its magnitude contains only a single linear term. Mars' surface contains a large number of visible markings. These markings cause the brilliancy of Mars to vary about 0.15 mag. over its period of rotation. The amplitude of the variation is not fixed, however, and is modified by other factors such as the transparency of the atmosphere due to planet-wide sandstorms. There appears to be a variation over the Martian year as well. All these additional factors can cause variations in the visual magnitude of up to 0.1 mag. These are not accounted for in the tabulated magnitudes. The cartographic prime meridian of Mars is defined so that it passes through the center of the crater Airy-O.

10.7.4 Jupiter

Multiple longitude systems are defined for Jupiter. Each system corresponds to a different apparent rate of motion. System III, which applies to the origin of radio emissions on Jupiter, is the preferred system. System I applies to the mean atmospheric equatorial rotation of the planet. System II applies to the mean atmospheric rotation north of the south component of the north equatorial belt and south of the north component of the south equatorial belt of Jupiter. The rotation rates for both System I and System II are uncertain and subject to change. The sub-Earth and sub-solar longitudes tabulated in *The Astronomical Almanac* are based on System III.

Jupiter is the most luminous of the planets. The value used for $V(1, 0)$ is taken from Irvine et al. (1968). Variations in its brilliancy with rotation are small, ~ 0.01 mag. and irregular. Also, there are long-period variations correlated with changes in the surface features of the planet.

10.7.5 Saturn

For Saturn only System III [observed rotation of radio emissions; Desch and Kaiser (1981)] rotations are defined. Galopeau and Lecacheux (2000) noted that the apparent period of Saturn's radio emissions vary on the order of a percent over periods of years. The angular momentum of the planet is orders of magnitude too large to allow for such large changes in the rotation period over such a short period of time. Gurnett et al. (2007) conclude that there is a slippage between the System III rotation rate arising in Saturn's plasma disk, and that its

internal rotation is the source for this discrepancy. Thus, the use of Saturn's radio emissions as an indicator for its rotation rate is in question.

Like Jupiter, the mean rotation rate of the atmosphere is uncertain. The previously defined System I rotation system has been found to be of little use since the Voyager encounters with Saturn, and is no longer supported by the IAU.

Because of the high brilliance of Saturn's rings, the brilliance of the planet alone is not well known. Thus, the combined planet-ring magnitude and surface brightness are tabulated. The phase coefficient for Saturn includes the rings. The visual magnitude in Table 10.6 is the extrapolated value for the planet alone at 1 au and 0° phase angle. There is, however, an additional term for variation in the brightness of the planet with the aspect of the rings:

$$V_r = -2.60|\sin e| + 1.25\sin^2 e \tag{10.81}$$

where V_r is the visual magnitude of the rings and e is the Saturnocentric sub-Earth latitude. There is little evidence for variations of the magnitude in the brightness of Saturn with rotation or over extended periods of time.

10.7.6 Uranus

Like Venus, Uranus' rotation is retrograde. The latitude of Uranus' north pole with respect to the invariable plane is 6.°92, but its declination with respect to the equator is -15.°18. Thus, Uranus' north pole is in the south celestial hemisphere. There is evidence for variation of the brightness of Uranus with rotation, but it has not been confirmed. A small term with a period of 84 years is expected in Uranus' magnitude due to the flattening of the planet and the high inclination of its equator to its orbital path. It is also possible that there are changes in Uranus' albedo with time. For example, Rages, Hammel, and Freidson (2004) document changes in the appearance of Uranus' south pole over the period from 1994 to 2002. Just as for Saturn, only the rotation rate for radio emissions (System III) is defined for Uranus.

10.7.7 Neptune

The phase angle of Neptune at greatest elongation is only 1.°9, so the variation in brightness of the planet from its phase angle is insignificant. There is some evidence of variation in the brightness of Neptune with its rotation. There is no evidence of long-period variations in its brightness. Only the System III rotation system for radio sources is defined for Neptune.

10.8 Physical Ephemerides of the Dwarf Planets

The apparent visual magnitudes of Ceres, Pluto, and Eris are found along with their geocentric astrometric positions beginning on page G5 on years when there is an opposition. In addition, physical ephemerides for Ceres and Pluto at ten day intervals throughout the year are found in Section G immediately after the positional ephemerides of the dwarf planets. These ephemerides tabulate the apparent visual magnitude, phase angle, planetocentric orbital longitude of the Sun, L_S, sub-Earth longitude and latitude and position angle of the positive pole.

The positions for the positive pole and the prime meridian of Ceres and Pluto are derived from Archinal et al. (2011a); Archinal et al. (2011b). The motion of the prime meridian and the position of the pole for Pluto are based on the assumptions that Charon's orbital

plane is coincidental with Pluto's equatorial plane and that the orbital motion of Charon is synchronous with Pluto's rotation. Pluto's flattening is unknown due to its great distance from the Sun and small size, but is presumed to be small because of its slow rotation rate.

The apparent magnitudes of Ceres and Eris are determined using the Tholen (2009) H and G parameters in the algorithm described in § 10.4.3. The values of H and G are tabulated on page G3. The apparent magnitudes of Pluto are determined using the algorithm described in § 10.3.1. The values of V_0 and Δm are tabulated in Table 10.6.

The given brilliancy at a distance of 1 au and a phase angle of 0° is the combined magnitude of Pluto and its satellite, Charon. The brilliancy in Harris (1961) is that of the combined Pluto-Charon system. In actuality, it has changed over time as different albedo features of the planet become visible (see Marcialis 1988). Binzel and Mulholland (1984) determined the phase coefficient. The combined magnitude of the Pluto-Charon system changes with rotation due to the differing albedos and surface markings of the two bodies. The rotational change in magnitude, like the mean magnitude, has also been changing with time as different albedo features of the planet and satellite are exposed to the Earth in Pluto's orbit around the Sun. The rotational difference between the minimum and maximum brilliancy was 0.11 mag. in 1954 (Harris 1961) and 0.291 mag. in 1981 (Marcialis 1988). The period of the rotational variations is 6.3867 days. During the eclipse season the Pluto-Charon mutual events changes in the magnitude as much as 0.50 mag. (Tholen, Buie, and Swift 1987) were observed. The prime meridian of Pluto is defined to fall along the mean vector connecting Pluto to Charon.

10.9 Physical Ephemerides of the Satellites

Aside from the Moon, the disks of all of the satellites have apparent diameters of less than $2''$ when viewed from the Earth or nearby space. They are so small that they are difficult to observed directly, except from interplanetary probes. Thus, the amount of information tabulated for the physical ephemerides is less than that for the planets. These data are limited to the satellite's dimensions, geometric albedo, $V(1, 0)$, and the $B - V$ and $U - B$ colors, if available. These data are found on pages F3 and F5 of *The Astronomical Almanac* and in Tables 10.3 and 10.7 here. Unless otherwise stated, the values for the sidereal period of the satellites are from Archinal et al. (2011a), and the value for the phase coefficients are from Harris (1961).

The recent proliferation of known satellites associated with the gas giant planets has lead to the development of selection criteria to determine which satellites are to be included in the data tables presented on pages F2–F5. The mean apparent visual magnitude of the tabulated satellites must not be fainter than 23.0, and the satellite must have an IAU approved Roman numeral and name. Satellites that have not received IAU approval are considered "works in progress." A satellite may be included at a later time, provided its mean apparent visual magnitude is not fainter than 23.0. A more complete version of these tables is found at *The Astronomical Almanac Online* at URL[1].

10.9.1 Satellites of Mars

Mars' two natural satellites, Phobos and Deimos, are both triaxial ellipsoids, with their longest axis pointed toward the planet. The source for the reference surfaces of these satellites is Pollack et al. (1973) who used Mariner 9 measurements.

Table 10.9 The rotation parameters for Mars' satellites

Satellite	Parameter and Value
I Phobos	$\alpha_0 = 317.^\circ68 - 0.^\circ108\,T + 1.^\circ79 \sin M_1$
	$\delta_0 = 52.^\circ90 - 0.^\circ061\,T - 1.^\circ08 \cos M_1$
	$W = 35.^\circ06 + 1128.^\circ844\,5850\,t + 8.^\circ864\,T^2 - 1.^\circ42 \sin M_1 - 0.^\circ78 \sin M_2$
II Deimos	$\alpha_0 = 316.^\circ65 - 0.^\circ108\,T + 2.^\circ98 \sin M_3$
	$\delta_0 = 53.^\circ52 - 0.^\circ061\,T - 1.^\circ78 \cos M_3$
	$W = 79.^\circ41 + 285.^\circ161\,8970\,t - 0.^\circ520\,T^2 - 2.^\circ58 \sin M_3 + 0.^\circ19 \cos M_3$
The values for M_n are:	
	$M_1 = 169.^\circ51 - 0.^\circ435\,7640\,t$
	$M_2 = 192.^\circ93 + 1128.^\circ409\,6700\,t + 8.^\circ864\,T^2$
	$M_3 = 53.^\circ47 - 0.^\circ018\,1510\,t$

Both satellites have rotation periods that are synchronous with their orbital periods. Both also have secular accelerations in their rotation rates, which appear as quadratic terms in the motion of their prime meridians. These acceleration terms arise from secular changes in the semimajor axes of their orbits. The differing signs for the acceleration terms in the motion of the satellites' prime meridians indicate that Phobos' orbit is contracting with time while Deimos' orbit is expanding. The rotation parameters for the Martian satellites are given in Table 10.9.

The masses of Phobos and Deimos were determination by Sjogren (1983) from the perturbations of the Viking Orbiters during their close flybys of the satellites. Information on the magnitudes of Phobos and Deimos, their albedos, and their colors are derived from Viking photometry of the satellites that has been analyzed by Klaasen, Duxbury, and Veverka (1979). Because the satellites are very near Mars, information on the phase coefficients for both satellites and the $(U - B)$ color for Phobos are useless for ground-based observations and are not given.

10.9.2 Satellites of Jupiter

The rotation parameters for the Galilean satellites [Io (JI), Europa (JII), Ganymede (JIII), and Callisto (JIV)], along with Amalthea (JV), Thebe (JXIV), Adrastea (JXV), and Metis (JXVI)] are given in Table 10.10. All these satellites have mean periods of rotation that are synchronous with their orbital periods.

The values for the visual magnitude at 1 au and 0° phase angle, the albedos, and the colors of the Jovian satellites are from Morrison (1982). The Galilean satellites have been observed well enough that well determined phase relations, in Table 10.6, have been derived for them.

The reference surfaces for Amalthea (Smith et al. 1979); the Galilean satellites (Davies et al. 1979); and JXIV, JXV, and JXVI; Burns (1986) were derived from measurements of the Voyager spacecraft pictures of the satellites. Estimates of the sizes of the outer Jovian satellites are from Tholen and Zellner (1984) and are based on the albedos of JVI and JVII (Himalia and Elara).

Table 10.10 The rotation parameters for Jupiter's satellites

Satellite	Parameter and Value
I Io	$\alpha_0 = 268.^\circ05 - 0.^\circ009\,T + 0.^\circ094 \sin J_3 + 0.^\circ024 \sin J_4$
	$\delta_0 = 64.^\circ50 + 0.^\circ003\,T + 0.^\circ040 \cos J_3 + 0.^\circ011 \cos J_4$
	$W = 200.^\circ39 + 203.^\circ488\,9538\,t - 0.^\circ085 \sin J_3 - 0.^\circ022 \sin J_4$
II Europa	$\alpha_0 = 268.^\circ08 - 0.^\circ009\,T + 1.^\circ086 \sin J_4 + 0.^\circ060 \sin J_5 + 0.^\circ015 \sin J_6$ $+0.^\circ009 \sin J_7$
	$\delta_0 = 64.^\circ51 + 0.^\circ003\,T + 0.^\circ468 \cos J_4 + 0.^\circ026 \cos J_5 + 0.^\circ007 \cos J_6$ $+0.^\circ002 \cos J_7$
	$W = 36.^\circ022 + 101.^\circ374\,7235\,t - 0.^\circ980 \sin J_4 - 0.^\circ054 \sin J_5 - 0.^\circ014 \sin J_6$ $-0.^\circ008 \sin J_7$
III Ganymede	$\alpha_0 = 268.^\circ20 - 0.^\circ009\,T - 0.^\circ037 \sin J_4 + 0.^\circ431 \sin J_5 + 0.^\circ091 \sin J_6$
	$\delta_0 = 64.^\circ57 + 0.^\circ003\,T - 0.^\circ016 \cos J_4 + 0.^\circ186 \cos J_5 + 0.^\circ039 \cos J_6$
	$W = 44.^\circ064 + 50.^\circ317\,6081\,t + 0.^\circ033 \sin J_4 - 0.^\circ389 \sin J_5 - 0.^\circ082 \sin J_6$
IV Callisto	$\alpha_0 = 268.^\circ72 - 0.^\circ009\,T - 0.^\circ068 \sin J_5 + 0.^\circ590 \sin J_6 + 0.^\circ010 \sin J_8$
	$\delta_0 = 64.^\circ83 + 0.^\circ003\,T - 0.^\circ029 \cos J_5 + 0.^\circ254 \cos J_6 - 0.^\circ004 \cos J_8$
	$W = 259.^\circ51 + 21.^\circ571\,0715\,t + 0.^\circ061 \sin J_5 - 0.^\circ533 \sin J_6 - 0.^\circ009 \sin J_8$
V Amalthea	$\alpha_0 = 268.^\circ05 - 0.^\circ009\,T - 0.^\circ84 \sin J_1 + 0.^\circ01 \sin 2J_1$
	$\delta_0 = 64.^\circ49 + 0.^\circ003\,T - 0.^\circ36 \cos J_1$
	$W = 231.^\circ67 + 722.^\circ631\,4560\,t + 0.^\circ76 \sin J_1 - 0.^\circ01 \sin 2J_1$
XIV Thebe	$\alpha_0 = 268.^\circ05 - 0.^\circ009\,T - 2.^\circ11 \sin J_2 + 0.^\circ04 \sin 2J_2$
	$\delta_0 = 64.^\circ49 + 0.^\circ003\,T - 0.^\circ91 \cos J_2 + 0.^\circ01 \cos 2J_2$
	$W = 8.^\circ56 + 533.^\circ700\,4100\,t + 1.^\circ91 \sin J_2 - 0.^\circ04 \sin 2J_2$
XV Adrastea	$\alpha_0 = 268.^\circ05 - 0.^\circ009\,T$
	$\delta_0 = 64.^\circ49 + 0.^\circ003\,T$
	$W = 33.^\circ29 + 1206.^\circ998\,6602\,t$
XVI Metis	$\alpha_0 = 268.^\circ05 - 0.^\circ009\,T$
	$\delta_0 = 64.^\circ49 + 0.^\circ003\,T$
	$W = 346.^\circ09 + 1221.^\circ254\,7301\,t$

The values for J_n are:

$J_1 = 73.^\circ32 + 91,472.^\circ9\,T$
$J_2 = 24.^\circ62 + 45,137.^\circ2\,T$
$J_3 = 283.^\circ90 + 4850.^\circ7\,T$
$J_4 = 355.^\circ80 + 1191.^\circ3\,T$
$J_5 = 119.^\circ90 + 262.^\circ1\,T$
$J_6 = 229.^\circ80 + 64.^\circ3\,T$
$J_7 = 352.^\circ25 + 2382.^\circ6\,T$
$J_8 = 113.^\circ35 + 6070.^\circ0\,T$

Table 10.11 Standard cartographic longitudes for Jupiter's satellites

Satellite	Crater	Longitude (deg.)
II Europa	Cilix	182
III Ganymede	Anat	128
IV Callisto	Saga	326

Galilean satellite masses are calculated from the perturbation in the paths of the Pioneer and Voyager spacecraft flybys (Campbell and Synott 1985). The masses of the rest of the satellites are based upon their individual sizes and the mean density of the compositions inferred from their albedos.

Three of the Galilean satellites have cartographic coordinates defined by surface craters. The cartographic definitions are given in Table 10.11.

10.9.3 Satellites of Saturn

Rotation parameters for Saturn's major satellites are given in Table 10.12.

Wisdom et al. (1984) have shown that one of the major Saturnian satellites, Hyperion, may be tumbling chaotically rather than being in synchronous rotation. This tumbling is a result of Hyperion's triaxial shape and its rather elliptical orbit with a semimajor axis near the 4:3 resonance with Titan.

The reference surfaces for the larger satellites are derived from Smith et al. (1982). The sizes of the smaller satellites are derived from their geometric albedos (Thomas et al. 1983).

Morrison, Owen, and Sonderblom (1986) determined the magnitudes, albedos, and colors of Saturn's satellites. Iapetus is especially interesting, because the leading hemisphere is over two magnitudes dimmer than its trailing hemisphere. Windorn (1950) gives a parametric equation for the brightness (not the magnitude) of the satellite of

$$B = 0.571 - 0.429 \sin k \tag{10.82}$$

where k is its orbital longitude, with the maximum occurring at greatest western elongation. More recent papers (e.g., Morrison et al. 1975) have shown that this expression is a good first order expression of Iapetus' brightness.

Tyler et al. (1981); Tyler et al. (1982) determined the tabulated masses for Mimas, Enceladus, Tethys, Dione, Rhea, Titan, and Iapetus from the deflections of the Voyager trajectories. The masses of Enceladus and Mimas are of lower accuracy and are contradicted by resonance theories (e.g., Greenberg 1984). Six of the major Saturnian satellites have cartographic coordinates defined by surface craters. The cartographic definitions are given in Table 10.13.

10.9.4 Satellites of Uranus

The rotation parameters for 15 of the known satellites of Uranus are given in Table 10.14.

The radii for the Uranian satellites (Smith et al. 1986) are derived from measurements of Voyager photographs. The masses for the five large satellites, Viellet (1983) are derived from mutual orbital perturbations. Smith et al. (1986) also determined the magnitudes, albedos, and colors for the large Uranian satellites from Voyager 2 photometry.

Table 10.12 Rotation parameters for Saturn's satellites

Satellite	Parameter and Value
I Mimas	$\alpha_0 = 40.^\circ66 - 0.^\circ036\,T + 13.^\circ56 \sin S_3$
	$\delta_0 = 83.^\circ52 - 0.^\circ004\,T - 1.^\circ53 \cos S_3$
	$W = 333.^\circ46 + 381.^\circ994\,5550\,t - 13.^\circ48 \sin S_3 - 44.^\circ85 \sin S_5$
II Enceladus	$\alpha_0 = 40.^\circ66 - 0.^\circ036\,T$
	$\delta_0 = 83.^\circ52 - 0.^\circ004\,T$
	$W = 6.^\circ32 + 262.^\circ731\,8996\,t$
III Tethys	$\alpha_0 = 40.^\circ66 - 0.^\circ036\,T + 9.^\circ66 \sin S_4$
	$\delta_0 = 83.^\circ52 - 0.^\circ004\,T - 1.^\circ09 \cos S_4$
	$W = 8.^\circ95 + 190.^\circ697\,9085t - 9.^\circ60 \sin S_4 + 2.^\circ23 \sin S_5$
IV Dione	$\alpha_0 = 40.^\circ66 - 0.^\circ036\,T$
	$\delta_0 = 83.^\circ52 - 0.^\circ004\,T$
	$W = 357.^\circ6 + 131.^\circ534\,9316\,t$
V Rhea	$\alpha_0 = 40.^\circ38 - 0.^\circ036\,T + 3.^\circ10 \sin S_6$
	$\delta_0 = 83.^\circ55 - 0.^\circ004\,T - 0.^\circ35 \cos S_6$
	$W = 235.^\circ16 + 79.^\circ690\,0478\,t - 3.^\circ08 sin S_6$
VI Titan	$\alpha_0 = 39.^\circ4827$
	$\delta_0 = 83.^\circ4279$
	$W = 186.^\circ5855 + 22.^\circ576\,9768\,t$
VIII Iapetus	$\alpha_0 = 318.^\circ16 - 3.^\circ949\,T$
	$\delta_0 = 75.^\circ03 - 1.^\circ143\,T$
	$W = 355.^\circ2 + 4.^\circ537\,9572\,t$
IX Phoebe	$\alpha_0 = 356.^\circ90$
	$\delta_0 77.^\circ80$
	$W = 178.^\circ58 + 931.^\circ639\,t$
X Janus	$\alpha_0 = 40.^\circ58 - 0.^\circ036\,T - 1.^\circ623 \sin S_2 + 0.^\circ023 \sin 2S_2$
	$\delta_0 = 83.^\circ52 - 0.^\circ004\,T - 0.^\circ183 \cos S_2 + 0.^\circ001 \cos 2S_2$
	$W = 58.^\circ83 + 518.^\circ235\,9876\,t + 1.^\circ613 \sin S_2 - 0.^\circ023 \sin 2S_2$
XI Epimetheus	$\alpha_0 = 40.^\circ58 - 0.^\circ036\,T - 3.^\circ153 \sin S_1 + 0.^\circ086 \sin 2S_1$
	$\delta_0 = 83.^\circ52 - 0.^\circ004\,T - 0.^\circ356 \cos S_1 + 0.^\circ005 \cos 2S_1$
	$W = 293.^\circ87 + 518.^\circ490\,7239\,t + 3.^\circ133 \sin S_1 - 0.^\circ086 \sin 2S_1$
XII Helene	$\alpha_0 = 40.^\circ85 - 0.^\circ036\,T$
	$\delta_0 = 83.^\circ34 - 0.^\circ004\,T$
	$W = 245.^\circ12 + 131.^\circ617\,4056\,t$
XIII Telesto	$\alpha_0 = 50.^\circ51 - 0.^\circ036\,T$
	$\delta_0 = 84.^\circ06 - 0.^\circ004\,T$
	$W = 56.^\circ88 + 190.^\circ697\,9332\,t$

Table 10.12 *(continued)*

Satellite	Parameter and Value
XIV Calypso	$\alpha_0 = 36.^\circ41 - 0.^\circ036\ T$
	$\delta_0 = 85.^\circ04 - 0.^\circ004\ T$
	$W = 153.^\circ51 + 190.^\circ674\ 2373\ t$
XV Atlas	$\alpha_0 = 40.^\circ58 - 0.^\circ036\ T$
	$\delta_0 = 83.^\circ53 - 0.^\circ004\ T$
	$W = 137.^\circ88 + 598.^\circ306\ 0000\ t$
XVI Prometheus	$\alpha_0 = 40.^\circ58 - 0.^\circ036\ T$
	$\delta_0 = 83.^\circ53 - 0.^\circ004\ T$
	$W = 296.^\circ14 + 587.^\circ289\ 0000\ t$
XVII Pandora	$\alpha_0 = 40.^\circ58 - 0.^\circ036\ T$
	$\delta_0 = 83.^\circ53 - 0.^\circ004\ T$
	$W = 162.^\circ92 + 572.^\circ789\ 1000\ t$
XVIII Pan	$\alpha_0 = 40.^\circ6 - 0.^\circ036\ T$
	$\delta_0 = 83.^\circ53 - 0.^\circ004\ T$
	$W = 48.^\circ8 + 626.^\circ044\ 0000\ t$
The values for S_n are:	
	$S_1 = 353.^\circ32 + 75,\ 706.^\circ7\ T$
	$S_2 = 28.^\circ72 + 75,\ 706.^\circ7\ T$
	$S_3 = 177.^\circ40 - 36,\ 505.^\circ5\ T$
	$S_4 = 300.^\circ00 - 7225.^\circ9\ T$
	$S_5 = 316.^\circ45 + 506.^\circ2\ T$
	$S_6 = 345.^\circ20 - 1016.^\circ3\ T$

Table 10.13 Standard cartographic longitudes for Saturn's satellites

Satellite	Crater	Longitude (deg.)
I Mimas	Palomides	162
II Enceladus	Salih	5
III Tethys	Arete	299
IV Dione	Palinurus	63
V Rhea	Tore	340
VIII Iapetus	Almeric	276

10.9.5 Satellites of Neptune

The physical ephemerides of six of the known satellites of Neptune are included in *The Astronomical Almanac*. The rotation parameters for those satellites are given in Table 10.15.

The mass, radius, and colors of Triton are determined from Voyager 2 data. Little is known of Nereid except its magnitude at 1 au and 0° phase angle (Morrison and Cruikshank 1974).

Table 10.14 Rotation parameters for Uranus' satellites

Satellite	Parameter and Value
I Ariel	$\alpha_0 = 257.^\circ 43 + 0.^\circ 29 \sin U_{13}$ $\delta_0 = -15.^\circ 10 + 0.^\circ 28 \cos U_{13}$ $W = 156.^\circ 22 - 142.^\circ 835\,6681\, t + 0.^\circ 05 \sin U_{12} + 0.^\circ 08 \sin U_{13}$
II Umbriel	$\alpha_0 = 257.^\circ 43 + 0.^\circ 21 \sin U_{14}$ $\delta_0 = -15.^\circ 10 + 0.^\circ 20 \cos U_{14}$ $W = 108.^\circ 05 - 86.^\circ 868\,8923\, t - 0.^\circ 09 \sin U_{12} + 0.^\circ 06 \sin U_{14}$
III Titania	$\alpha_0 = 257.^\circ 43 + 0.^\circ 29 \sin U_{15}$ $\delta_0 = -15.^\circ 10 + 0.^\circ 28 \cos U_{15}$ $W = 77.^\circ 74 - 41.^\circ 351\,4316\, t + 0.^\circ 08 \sin U_{15}$
IV Oberon	$\alpha_0 = 257.^\circ 43 + 0.^\circ 16 \sin U_{16}$ $\delta_0 = -15.^\circ 10 + 0.^\circ 16 \cos U_{16}$ $W = 6.^\circ 77 - 26.^\circ 739\,4932\, t + 0.^\circ 04 \sin U_{16}$
V Miranda	$\alpha_0 = 257.^\circ 43 + 4.^\circ 41 \sin U_{11} - 0.^\circ 04 \sin 2U_{11}$ $\delta_0 = -15.^\circ 08 + 4.^\circ 25 \cos U_{11} - 0.^\circ 02 \cos 2U_{11}$ $W = 30.^\circ 70 - 254.^\circ 690\,6892\, t - 1.^\circ 27 \sin U_{12} + 0.^\circ 15 \sin 2U_{12} + 1.^\circ 15 \sin U_{11}$ $-0.^\circ 09 \sin 2U_{11}$
VI Cordelia	$\alpha_0 = 257.^\circ 31 - 0.^\circ 15 \sin U_1$ $\delta_0 = -15.^\circ 18 + 0.^\circ 14 \cos U_1$ $W = 127.^\circ 69 - 1074.^\circ 520\,5730\, t - 0.^\circ 04 \sin U_1$
VII Ophelia	$\alpha_0 = 257.^\circ 31 - 0.^\circ 09 \sin U_2$ $\delta_0 = -15.^\circ 18 + 0.^\circ 09 \cos U_2$ $W = 130.^\circ 35 - 956.^\circ 406\,8150\, t - 0.^\circ 03 \sin U_2$
VIII Bianca	$\alpha_0 = 257.^\circ 31 - 0.^\circ 16 \sin U_3$ $\delta_0 = -15.^\circ 18 + 0.^\circ 16 \cos U_3$ $W = 105.^\circ 46 - 828.^\circ 391\,4760\, t - 0.^\circ 04 \sin U_3$
IX Cressida	$\alpha_0 = 257.^\circ 31 - 0.^\circ 04 \sin U_4$ $\delta_0 = -15.^\circ 18 + 0.^\circ 04 \cos U_4$ $W = 59.^\circ 16 - 776.^\circ 581\,6320\, t - 0.^\circ 01 \sin U_4$
X Desdemona	$\alpha_0 = 257.^\circ 31 - 0.^\circ 17 \sin U_5$ $\delta_0 = -15.^\circ 18 + 0.^\circ 16 \cos U_5$ $W = 95.^\circ 08 - 760.^\circ 0531\,690\, t - 0.^\circ 04 \sin U_5$
XI Juliet	$\alpha_0 = 257.^\circ 31 - 0.^\circ 06 \sin U_6$ $\delta_0 = -15.^\circ 18 + 0.^\circ 06 \cos U_6$ $W = 302.^\circ 56 - 730.^\circ 125\,3660\, t - 0.^\circ 02 \sin U_6$

Table 10.14 *(continued)*

	Satellite	Parameter and Value
XII	Portia	$\alpha_0 = 257^\circ.31 - 0^\circ.09 \sin U_7$
		$\delta_0 = -15^\circ.18 + 0^\circ.09 \cos U_7$
		$W = 25^\circ.03 - 701^\circ.486\,5870\, t - 0^\circ.02 \sin U_7$
XIII	Rosalind	$\alpha_0 = 257^\circ.31 - 0^\circ.29 \sin U_8$
		$\delta_0 = -15^\circ.18 + 0^\circ.28 \cos U_8$
		$W = 314^\circ.90 - 644^\circ.631\,1260\, t - 0^\circ.08 \sin U_8$
XIV	Belinda	$\alpha_0 = 257^\circ.31 - 0^\circ.03 \sin U_9$
		$\delta_0 = -15^\circ.18 + 0^\circ.03 \cos U_9$
		$W = 297^\circ.46 - 577^\circ.362\,8170\, t - 0^\circ.01 \sin U_9$
XV	Puck	$\alpha_0 = 257^\circ.31 - 0^\circ.33 \sin U_{10}$
		$\delta_0 = -15^\circ.18 + 0^\circ.31 \cos U_{10}$
		$W = 91^\circ.24 - 472^\circ.545\,0690\, t - 0^\circ.09 \sin U_{10}$

The values for U_n are:

$U_1 = 115^\circ.75 + 54,\, 991^\circ.87\, T$
$U_2 = 141^\circ.69 + 41,\, 887^\circ.66\, T$
$U_3 = 135^\circ.03 + 29,\, 927^\circ.35\, T$
$U_4 = 61^\circ.77 + 25,\, 733^\circ.59\, T$
$U_5 = 249^\circ.32 + 24,\, 471^\circ.46\, T$
$U_6 = 43^\circ.86 + 22,\, 278^\circ.41\, T$
$U_7 = 77^\circ.66 + 20,\, 289^\circ.42\, T$
$U_8 = 157^\circ.36 + 16,\, 652^\circ.76\, T$
$U_9 = 101^\circ.81 + 12,\, 872^\circ.63\, T$
$U_{10} = 138^\circ.64 + 8061^\circ.81\, T$
$U_{11} = 102^\circ.23 - 2024^\circ.22\, T$
$U_{12} = 316^\circ.41 + 2863^\circ.96\, T$
$U_{13} = 304^\circ.01 - 51^\circ.94\, T$
$U_{14} = 308^\circ.71 - 93^\circ.17\, T$
$U_{15} = 340^\circ.82 - 75^\circ.32\, T$
$U_{16} = 259^\circ.14 - 504^\circ.81\, T$

Table 10.15 Rotation parameters for Neptune's satellites

Satellite	Parameter and Value
I Triton	$\alpha_0 = 299.^\circ36 - 32.^\circ35 \sin N_7 - 6.^\circ28 \sin 2N_7 - 2.^\circ08 \sin 3N_7 - 0.^\circ74 \sin 4N_7$
	$-0.^\circ28 \sin 5N_7 - 0.^\circ11 \sin 6N_7 - 0.^\circ07 \sin 7N_7 - 0.^\circ02 \sin 8N_7$
	$-0.^\circ01 \sin 9N_7$
	$\delta_0 = 41.^\circ17 + 22.^\circ55 \cos N_7 + 2.^\circ10 \cos 2N_7 + 0.^\circ55 \cos 3N_7 + 0.^\circ16 \cos 4N_7$
	$+0.^\circ05 \cos 5N_7 + 0.^\circ02 \cos 6N_7 + 0.^\circ01 \cos 7N_7$
	$W = 296.^\circ53 - 61.^\circ257\,2637\,t + 22.^\circ25 \sin N_7 + 6.^\circ73 \sin 2N_7 + 2.^\circ05 \sin 3N_7$
	$+0.^\circ74 \sin 4N_7 + 0.^\circ28 \sin 5N_7 + 0.^\circ11 \sin 6N_7 + 0.^\circ05 \sin 7N_7$
	$+0.^\circ02 \sin 8N_7 + 0.^\circ01 \sin 9N_7$
III Naiad	$\alpha_0 = 299.^\circ36 + 0.^\circ70 \sin N - 6.^\circ49 \sin N_1 + 0.^\circ25 \sin 2N_1$
	$\delta_0 = 43.^\circ36 - 0.^\circ51 \cos N - 4.^\circ75 \cos N_1 + 0.^\circ09 \cos 2N_1$
	$W = 254.^\circ06 + 1222.^\circ844\,1209\,t - 0.^\circ48 \sin N + 4.^\circ40 \sin N_1 - 0.^\circ27 \sin 2N_1$
IV Thalassa	$\alpha_0 = 299.^\circ36 + 0.^\circ70 \sin N - 0.^\circ28 \sin N_2$
	$\delta_0 = 43.^\circ45 - 0.^\circ51 \cos N - 0.^\circ21 \cos N_2$
	$W = 102.^\circ06 + 1155.^\circ755\,5612\,t - 0.^\circ48 \sin N + 0.^\circ19 \sin N_2$
V Despina	$\alpha_0 = 299.^\circ36 + 0.^\circ70 \sin N - 0.^\circ09 \sin N_3$
	$\delta_0 = 43.^\circ45 - 0.^\circ51 \cos N - 0.^\circ07 \cos N_3$
	$W = 306.^\circ51 + 1075.^\circ734\,1562\,t - 0.^\circ49 \sin N + 0.^\circ06 \sin N_3$
VI Galatea	$\alpha_0 = 299.^\circ36 + 0.^\circ70 \sin N - 0.^\circ07 \sin N_4$
	$\delta_0 = 43.^\circ43 - 0.^\circ51 \cos N - 0.^\circ05 \cos N_4$
	$W = 258.^\circ09 + 839.^\circ659\,7686\,t - 0.^\circ48 \sin N + 0.^\circ05 \sin N_4$
VII Larissa	$\alpha_0 = 299.^\circ36 + 0.^\circ70 \sin N - 0.^\circ27 \sin N_5$
	$\delta_0 = 43.^\circ41 - 0.^\circ51 \cos N - 0.^\circ20 \cos N_5$
	$W = 179.^\circ41 + 649.^\circ053\,4470\,t - 0.^\circ48 \sin N + 0.^\circ19 \sin N_5$
VIII Proteus	$\alpha_0 = 299.^\circ27 + 0.^\circ70 \sin N - 0.^\circ05 \sin N_6$
	$\delta_0 = 42.^\circ91 - 0.^\circ51 \cos N - 0.^\circ04 \cos N_6$
	$W = 93.^\circ38 + 320.^\circ765\,4228\,t - 0.^\circ48 \sin N + 0.^\circ04 \sin N_6$

The values for N_n are:

$$N = 357.^\circ85 + 52.^\circ316\,T$$
$$N_1 = 323.^\circ92 + 62,606.^\circ6\,T$$
$$N_2 = 220.^\circ51 + 55,064.^\circ2\,T$$
$$N_3 = 354.^\circ27 + 46,564.^\circ5\,T$$
$$N_4 = 75.^\circ31 + 26,109.^\circ4\,T$$
$$N_5 = 35.^\circ36 + 14,325.^\circ4\,T$$
$$N_6 = 142.^\circ61 + 2824.^\circ6\,T$$
$$N_7 = 177.^\circ85 + 52.^\circ316\,T$$

Table 10.16 Rotation parameters for Pluto's satellite, I Charon

$\alpha_0 = 312.^\circ 993$
$\delta_0 = -6.^\circ 163$
$W = 122.^\circ 695 - 56.^\circ 362\,5225\,t$

The diameter is based on an assumed albedo of 0.4. Recent studies by Williams et al. (1991) of Nereid indicate that it may have a non-synchronous rotation.

10.9.6 Satellites of Pluto

Charon, Pluto's only large satellite, is assumed to orbit in the plane of Pluto's equator and is in synchronous rotation. The position of its north pole and prime meridian are given in Table 10.16.

The mass, diameter, and magnitude of Charon are based on observations of Charon-Pluto eclipses (Dunbar and Tedesco 1986).

REFERENCES

1. The Astronomical Almanac Online: http://asa.usno.navy.mil or http://asa.hmnao.com.

Archinal, B. A., M. F. A'Hearn, E. Bowell, A. Conrad, G. J. Consolmagno, R. Courtin, T. Fukushima, D. Hestroffer, J. L. Hilton, G. A. Krasinsky, G. Neumann, J. Oberst, P. K. Seidelmann, P. Stooke, D. J. Tholen, P. C. Thomas, and I. P. Williams (2011a). Report of the IAU/IAG Working Group on Cartographic Coordinates and Rotational Elements: 2009. *Celestial Mechanics and Dynamical Astronomy 109*, 101–135.

Archinal, B. A., M. F. A'Hearn, A. Conrad, G. J. Consolmagno, R. Courtin, T. Fukushima, D. Hestroffer, J. L. Hilton, G. A. Krasinsky, G. Neumann, J. Oberst, P. K. Seidelmann, P. Stooke, D. J. Tholen, P. C. Thomas, and I. P. Williams (2011b). Errata: Report of the IAU/IAG Working Group on Cartographic Coordinates and Rotational Elements: 2006 & 2009. *Celestial Mechanics and Dynamical Astronomy 110*, 401–403.

Atkinson, R. D. (1951). The Computation of Topocentric Librations. *Monthly Notices of the Royal Astronomical Society 111*, 448–454.

Beck, J. G. and P. Giles (2005). Helioseismic Determination of the Solar Rotation Axis. *Astrophysical Journal 621*, L153–L156.

Binzel, R. P. and J. D. Mulholland (1984). Photometry of Pluto During the 1983 Opposition: A New Determination of the Phase Coefficient. *Astronomical Journal 89*, 1759–1761.

Bowell, E., B. Hapke, D. Domingue, K. Lumme, J. Peltoniemi, and A. W. Harris (1989). Application of Photometric Models to Asteroids. In R. P. Binzel, T. Gehrels, and M. S. Matthews (Eds.), *Asteroids II*, Tucson, AZ, pp. 524–556. U. of Arizona Press.

Burns, J. (1986). Some Background About Satellites. In J. A. Burns and M. S. Matthews (Eds.), *Satellites*, Tucson. AZ, pp. 1–38. U. of Arizona Press.

Campbell, J. K. and S. P. Synott (1985). Gravity Field of the Jovian System from Pioneer and Voyager Tracking Data. *Astronomical Journal 90*, 364–372.

Capitaine, N., P. T. Wallace, and J. Chapront (2003). Expressions for IAU 2000 Precession Quantities. *Astronomy and Astrophysics 412*, 567–586.

Carrington, R. C. (1863). *Observations of Spots on the Sun*. London: Williams and Norgate.

Danjon, A. (1949). Photométrie et colorimétrie des planètes Mercure et Vénus. *Bulletin Astronomique, 2e Serie 14*, 315–345.

Danjon, A. (1954). Magnitude et albedo visuels de la planète Mercure. *Bulletin Astronomique, 2e Serie 17*, 363.

Davies, M. E., T. A. Hauge, F. Y. Katayama, and J. A. Roth (1979). Control networks for the galilean satellites: November 1979. The Rand Corporation, R-2532-JPL/NASA.

Davis, D. R. and C. Neese (2002). Asteroid Albedos EAR-A-5-DDR-ALBEDOS-V1.1. available at the Small Bodies Data Archives (http://www.psi.edu/pds/resource/albedo.html).

de Vaucouleurs, G. (1970). Photométrie de surfaces planètaires. In A. Dollfus (Ed.), *Interiors of Planets and Satellites*, London, pp. 226–316. Academic.

Desch, M. D. and M. L. Kaiser (1981). Voyager Measurement of the Rotation Period of Saturn's Magnetic Field. *Geophysics Research Letters 8*, 253–256.

Drummond, J. and J. Christou (2008). Triaxial Ellipsoid Dimensions and Rotational Poles of Seven Asteroids from Lick Observatory Adaptive Optics Images, and of Ceres. *Icarus 197*, 480–496.

Drummond, J. and J. C. Christou (1994). Images of Asteroids 1 Ceres, 2 Pallas, and 4 Vesta with Adaptive Optics at the Starfire Optical Range. In M. A. Ealy and F. Merkle (Eds.), *Interiors of Planets and Satellites*, London, pp. 468–471. SPIE.

Drummond, J. D., R. O. Fugate, and J. C. Christou (1998). Full Adaptive Optics Images of Asteroids Ceres and Vesta; Rotational Poles and Triaxial Ellipsoid Dimensions. *Icarus 132*, 80–99.

Dunbar, R. S. and E. F. Tedesco (1986). Modeling Pluto-Charon Mutual Eclipse Events: I. First-Order Models. *Astronomical Journal 92*, 1201–1209.

Dunham, D. W. and G. Mallen (1979). The Dimensions of (6) Hebe as a Result of Occultation Observations. *Revista Mexicana de Astronomia y Astrofisica 4*, 205–208.

Dunham, E. W., R. L. Baron, S. Conner, D. W. Dunham, J. B. Dunham, G. Schneider, H. L. Cohen, I. Helms, V. T., M. Croom, and J. Safko (1984). Results from the Occultation of 14 Pscium by (51) Nemausa. *Astronomical Journal 89*, 1755–1758.

Eckhardt, D. H. (1981). Theory of the Libration of the Moon. *The Moon and the Planets 25*, 3–49.

Eckhardt, D. H. (1982). Planetary and Earth Figure Perturbations in the Libration of the Moon. In O. Calame (Ed.), *High-Precision Earth Rotation and Earth–Moon Dynamics*, Dordrecht, Holland, pp. 193–198. Reidel.

Erikson, A., J. Berthier, P. V. Denchev, A. W. Harris, Z. Ioannou, A. Kryszczynska, C.-I. Langerkvist, P. Magnusson, T. Michalowski, A. Nathues, J. Piironen, P. Pravec, L. Sarounova, and F. Velichko (1999). Photometric Observations and Modeling of the Asteroid 85 Io in Conjunction with Data from an Occultation Event During the 1995-96 Apparition. *Planetary and Space Sciences 47*, 327–330.

Galopeau, P. H. M. and A. Lecacheux (2000). Variations of Saturn's Radio Rotation Period Measured at Kilometer Wavelengths. *Journal of Geophysical Research 105*, 13089–13101.

Greenberg, R. (1984). Orbital Resonances among Saturn's Satellites. In T. Gerhels and M. S. Matthews (Eds.), *Saturn*, Tucson, AZ, pp. 593–608. University of Arizona Press.

Gurnett, D. A., A. M. Persoon, W. S. Kurth, J. B. Groene, T. F. Averkamp, M. K. Dougherty, and D. J. Southwood (2007). The Variable Rotation Period of the Inner Region of Saturn's Plasma Disk. *Science 316*, 442–445.

Harris, D. L. (1961). Photometry and Colorimetry of Planets and Satellites. In G. P. Kuiper and B. A. Middlehurst (Eds.), *Planets and Satellites*, Chicago, pp. 272–342. University of Chicago Press.

Hilton, J. L. (2005). Improving the Visual Magnitudes of the Planets in The Astronomical Almanac. I. Mercury and Venus. *Astronomical Journal 129*, 2902–2906.

IAU (1986). Resolution C6: Carrington Reference System. In J.-P. Swings (Ed.), *Transactions of the International Astronomical Union*, Volume XIX B, Dordrecht, pp. 45–46. Reidel. Proc. 19th General Assembly, Delhi, 1985.

Irvine, W. M., T. Simon, D. H. Menzel, C. Pikoos, and A. T. Young (1968). Multicolor Photoelectric Photometry of the Brighter Planets. III. Observations from Boyden Observatory. *Astronomical Journal 73*, 807.

Klaasen, K. P., T. C. Duxbury, and J. Veverka (1979). Photometry of Phobos and Deimos from Viking Orbiter Images. *Journal of Geophysical Research 84*, 8478–8486.

Ma, C., E. F. Arias, T. M. Eubanks, A. L. Fey, A.-M. Gontier, C. S. Jacobs, O. J. Sovers, B. A. Archinal, and P. Charlot (1998). The International Celestial Reference Frame as Realized by Very Long Baseline Interferometry. *Astronomical Journal 116*, 516–546.

Magri, C., S. J. Ostro, K. D. Rosema, M. D. Thomas, D. L. Mitchell, D. B. Campbell, J. F. Chandler, I. I. Shapiro, J. D. Giorgini, and D. K. Yeomans (1999). Mainbelt Asteroids: Results of Arecibo and Goldstone Radar Observations of 37 Objects During 1980–1995. *Icarus 140*, 379–407.

Mallama, A. (2005). The Phase Curve of Venus. *Bulletin of the American Astronomical Society 37*, 484.

Mallama, A., D. Wang, and R. A. Howard (2003). Photometry of Mercury from SOHO/LASCO and Earth. The Phase Function from 2 to 170°. *Icarus 155*, 253–264.

Marcialis, R. L. (1988). A Two Spot Albedo Model for the Surface of Pluto. *Astronomical Journal 95*, 941–947.

Margot, J.-L., S. J. Peale, R. F. Jurgens, M. A. Slade, and I. V. Holin (2007). Large Longitude Libration of Mercury Reveals a Molten Core. *Science 316*, 710–714.

Marsden, B. G. (1986). Notes from the IAU General Assembly. Minor Planet Circulars Nos. 10193 and 10194.

Millis, R. L., L. H. Wasserman, E. Bowell, O. G. Franz, N. M. White, G. W. Lockwood, R. Nye, R. Bertram, A. Klemola, E. Dunham, R. L. Baron, J. L. Elliot, A. Harris, J. W. Young, J. Faulkner, R. Stanton, H. J. Reitsema, W. B. Hubbard, B. Zellner, L. Lebofsky, D. P. Cruikshank, L. S. Macknik, E. E. Becklin, D. Morrison, C. J. Lonsdale, T. D. Kunkle, T. Lee, I. Gatley, M. F. A'Hearn, D. L. DuPuy, R. Nolthenius, H. Ford, D. McKenna, Z. Placova, K. Horne, W. H. Sandman, G. E. Taylor, and R. Tucker (1981). The Diameter of Juno from Its Occultation of AG+0 1022. *Astronomical Journal 86*, 306–313.

Millis, R. L., L. H. Wasserman, O. G. Franz, E. Bowell, A. Klemola, R. C. Elliot, W. G. Smethells, P. M. Price, C. P. McKay, D. I. Steel, E. Everhart, and E. M. Everhart (1983). The Diameter of 88 Thisbe from Its Occultation of SAO 187124. *Astronomical Journal 88*, 229–235.

Morrison, D. (1982). Introduction to the Satellites of Jupiter. In D. Morrison (Ed.), *Satellites of Jupiter*, Tucson, AZ, pp. 3–43. University of Arizona Press.

Morrison, D. and D. P. Cruikshank (1974). Physical Properties of the Natural Satellites. *Space Science Review 15*, 641–739.

Morrison, D., T. J. Jones, D. P. Cruikshank, and R. E. Murphy (1975). The Two Faces of Iapetus. *Icarus 24*, 157–171.

Morrison, D., T. Owen, and L. A. Sonderblom (1986). The Satellites of Saturn. In J. A. Burns and M. S. Matthews (Eds.), *Satellites*, Tucson, AZ, pp. 764–801. University of Arizona Press.

Nelson, R. M., B. W. Hapke, W. D. Smythe, and L. J. Spilker (2000). The Opposition Effect in Simulated Planetary Regoliths. Reflectance and Circular Polarization Ratio Change at Small Phase Angle. *Icarus 147*, 545–558.

Newhall, X. X. and J. G. Williams (2000). Estimation of the Lunar Physical Librations. *Celestial Mechanics 66*, 21–30.

Ostro, S. J., R. S. Hudson, M. C. Nolan, J.-L. Margot, D. J. Scheeres, D. B. Campbell, C. Magri, J. D. Giosini, and D. K. Yeomans (2000). Radar Observations of Asteroid 216 Kleopatra. *Science 288*, 836–839.

Pollack, J. B., J. Veverka, M. Noland, C. Sagan, T. C. Duxbury, J. Acton, C. H., G. H. Born, W. K. Hartmann, and B. A. Smith (1973). Mariner 9 Television Observations of Phobos and Deimos, 2. *Journal of Geophysical Research 78*, 4313–4326.

Ragazzoni, R., A. Baruffolo, E. Marchetti, A. Ghedina, J. Farinato, and T. Niero (2000). Speckle Interferometry Measurements of the Asteroids 10-Hygiea and 15-Eunomia. *Astronomy and Astrophysics 354*, 315–320.

Rages, K. A., H. B. Hammel, and A. J. Freidson (2004). Evidence for Temporal Changes at Uranus' South Pole. *Icarus 171*, 548–554.

Seidelmann, P. K., V. K. Abalakin, M. Bursa, C. de Bergh, J. H. Lieske, J. Oberst, J. L. Simon, E. M. Standish, P. Stooke, and P. C. Thomas (2002). Report of the IAU/IAG/COSPAR Working Group on Cartographic Coordinates and Rotational Elements of the Planets and Satellites: 2000. *Celestial Mechanics 82*, 83–111.

Simon, J. L., P. Bretagnon, J. Chapront, M. Chapront-Touzé, G. Francou, and J. Laskar (1994). Numerical Expressions for Precession Formulae and Mean Elements for the Moon and the Planets. *Astronomy and Astrophysics 282*, 663–683.

Sjogren, W. L. (1983). Planetary Geodesy. *Reviews of Geophysics and Space Physics 21*, 528–537.

Smith, B. A., L. A. Sonderblom, R. Batson, P. Bridges, J. Inge, H. Masursky, E. Shoemaker, R. Beebe, J. Boyce, G. Briggs, A. Bunker, S. A. Collins, C. V. Hansen, T. V. Johnson, J. L. Mitchell, R. J. Terrile, I. Cook, A. F., J. Cuzzi, J. B. Pollack, G. E. Danielson, D. Morrison, T. Owen, C. Sagan, J. Ververka, R. Strom, and V. E. Suomi (1982). A New Look at the Saturn System: The Voyager 2 Images. *Science 215*, 504–537.

Smith, B. A., L. A. Sonderblom, R. Beebe, D. Bliss, J. M. Boyce, A. Brahic, G. A. Briggs, R. H. Brown, S. A. Collins, I. Cook, A. F., S. K. Croft, J. N. Cuzzi, G. E. Danielson, M. E. Davies, T. E. Dowling, D. Godfry, C. J. Hansen, C. Harris, G. E. Hunt, A. P. Ingersoll, T. V. Johnson, R. J. Krauss, H. Masursky, D. Morrison, T. Owen, J. Plescia, J. B. Pollack, C. P. Porco, K. Rages, C. Sagan, E. M. Shoemaker, L. A. Sromovsky, C. Stoker, R. G. Strom, V. E. Suomi, S. P. Synott, R. J. Terrile, P. Thomas, W. R. Thompson, and J. Veverka (1986). Voyager 2 in the Uranian System: Imaging Science Results. *Science 233*, 43–64.

Smith, B. A., L. A. Sonderblom, R. Beebe, J. Boyce, G. Briggs, M. Carr, S. A. Collins, I. Cook, A. F., G. E. Danielson, M. E. Davies, G. E. Hunt, E. Ingersoll, T. V. Johnson, H. Masursky, J. McCauley, D. Morrison, T. Owen, C. Sagan, E. M. Shoemaker, R. Strom, V. E. Suomi, and J. Veverka (1979). The Galilean Satellites and Jupiter: Voyager 2 Imaging Science Results. *Science 206*, 927–950.

Smith, D. E., M. T. Zuber, S. C. Solomon, R. J. Phillips, J. W. Head, J. B. Garvin, W. B. Banerdt, D. O. Muhleman, G. H. Pettingill, G. A. Neumann, F. G. Lemoine, J. B. Abshire, O. Aharonson, C. D. Brown, S. A. Hauck, A. B. Ivanov, P. J. McGovern, H. J. Zwally, and T. C. Duxbury (1999). The Global Topography of Mars and Implications for Surface Evolution. *Science 284*, 1495–1503.

Standish, E. M. (1998). JPL Planetary and Lunar Ephemerides, DE405/LE405. Jet Propulsion Laboratory, Interoffice Memorandum, IOM 312.F – 98 – 048.

Standish, E. M., X. X. Newhall, J. G. Williams, and W. M. Folkner (1995). JPL Planetary and Lunar Ephemerides, DE403/LE403. Jet Propulsion Laboratory, Interoffice Memorandum, IOM 312.10 127.

Storrs, A., B. Weiss, B. Zellner, W. Burleson, R. Sichitiu, E. Wells, C. Kowal, and D. Tholen (1999). Imaging Observations of Asteroids with Hubble Space Telescope. *Icarus 137*, 260–268.

Taylor, G. E. (1981). The Size of the Minor Planet 65-Cybele. *Journal of the British Astronomical Association 92*, 13–15.

Tedesco, E. F., Noah, P. V., M. Noah, and S. D. Price (2002). The Supplemental IRAS Minor Planet Survey. *Astronomical Journal 123*, 1056–1085.

Tholen, D. J. (2009). Asteroid Absolute Magnitudes V12.0. EAR-A-5-DDR-ASTERMAG-V12.0. available at the Small Bodies Data Archives (http://www.psi.edu/pds/resource/astermag.html).

Tholen, D. J., M. W. Buie, and C. E. Swift (1987). Circumstances for Pluto-Charon Mutual Events in 1988. *Astronomical Journal 94*, 1681–1685.

Tholen, D. J. and B. Zellner (1984). Multi-color Photometry of the Outer Jovian Satellites. *Icarus 53*, 341–347.

Thomas, P. C., J. W. Parker, L. A. McFadden, C. T. Russell, S. A. Stern, M. V. Sykes, and E. F. Young (2005). Differentiation of the Asteroid Ceres as Revealed by Its Shape. *Nature 437*, 224–226.

Thomas, P. C., J. Veverka, D. Morrison, M. Davies, and T. V. Johnson (1983). Saturn's Small Satellites: Voyager Imaging Results. *Journal of Geophysical Research 88*, 8743–8754.

Tyler, G. L., V. R. Eshleman, J. D. Anderson, G. S. Levy, G. F. Lindal, G. E. Wood, and T. A. Croft (1981). Radio Science Investigations of the Saturnian System: Voyager 1 Preliminary Results. *Science 212*, 201–206.

Tyler, G. L., V. R. Eshleman, J. D. Anderson, G. S. Levy, G. F. Lindal, G. E. Wood, and T. A. Croft (1982). Radio Science with Voyager 2 at Saturn: Atmosphere and Ionosphere and Masses of Mimas, Tethys, and Iapetus. *Science 215*, 553–558.

Veverka, J., M. Robinson, P. Thomas, S. Murchie, I. Bell, J. F., N. Izenberg, C. Chapman, A. Harch, M. Bell, B. Carcich, A. Cheng, B. Clark, D. Domingue, D. Dunham, R. Farquhar, M. J. Gaffey, E. Hawkins, J. Joseph, R. Kirk, H. Li, P. Lucey, M. Malin, P. Martin, L. McFadden, W. J. Merline, J. K. Miller, J. Owen, W. M., C. Peterson, L. Prockter, J. Warren, D. Wellnitz, B. G. Williams, and D. K. Yeomans (2000). NEAR at Eros: Imaging and Spectral Results. *Science 2000*, 2088–2097.

Viellet, C. (1983). *De l'observation et du mouvement des satellites d'Uranus*. Ph. D. thesis, Université de Paris, Paris.

Williams, I. P., D. H. P. Jones, and D. P. Taylor (1991). The Rotation of Nereid. *Monthly Notices of the Royal Astronomical Society 250*, 1p–2p.

Windorn, T. (1950). Der Lichtwechsel de Saturn Satelliten Iapetus im Jahre 1949. In *Mitt. Univ.-Sternw.*, Volume 5, Wein, pp. 19–29.

Wisdom, J., S. J. Peale, and F. Mignard (1984). The Chaotic Rotation of Hyperion. *Icarus 58*, 137–152.

CHAPTER 11

Eclipses of the Sun and Moon

ALAN D. FIALA, JOHN A. BANGERT & STEVEN A. BELL

11.1 Introduction

All bodies orbiting in the solar system cast a shadow away from the Sun. In the most general terms, an *eclipse* occurs when the shadow of one body falls upon another and temporarily blocks out a portion of the solar illumination. An eclipse is distinct from an *occultation*, which is a block in the line of sight. Before this distinction was understood, however, a long history of observation from Earth created different names for the phenomena, depending on what objects were involved. The shadow of the Moon falling upon the Earth was called a *solar eclipse*; the shadow of the Earth falling upon the Moon was called a *lunar eclipse*; and the shadow of a planet falling upon the Earth was called a *transit* (across the Sun). By strict application of these definitions, a solar eclipse is really an occultation.

The basic methods by which eclipses of the Sun and Moon and transits of Venus and Mercury are predicted and described were introduced by Bessel and extensively developed by Chauvenet (1891). The discussion here will be limited to describing the calculation of data that are necessary to observe any of these phenomena from the Earth.

Bessel's method of calculating eclipse predictions is based on the following concept: A body casts a shadow, the axis of which is a line extended from the center of the Sun through the center of the body. Observations, by necessity, are constrained to the topocentric coordinate system. However, the geometry and kinematics are easier to describe in a system oriented to the cone of the shadow—that is, one in which the z-axis is either parallel to, or coincident with, the shadow axis, and the xy-plane passes through the center of the body on which the shadow falls. This plane is also known as the *Besselian plane*. A description of the progress of the eclipse is calculated in this coordinate system, and then is transformed to a topocentric system as necessary. *Elements* describe the geometry of the configuration as a function of time; *circumstances* describe distinct, observable events by time and place.

Diagrams in treatises on eclipses by necessity are exaggerated to illustrate points. Hence, the diagrams tend to disguise the fact that, in reality, the bodies involved are very small, far apart, and moving relatively slowly. Thus, the shadows cast are long and slender, there are many small angles, and the relative short-term motions are very nearly linear. These qualities were used to advantage by people equipped only with tables and a calculator, as it was necessary and adequate to use approximations and intermediate trigonometric constructs. In the era of computers, the use of approximations and simplifying constructs is reduced but not eliminated. Also, it is helpful to newer generations of astronomers to discuss spherical trigonometry by incorporating more vector and matrix notation instead of direction cosines.

11.1.1 Eclipse Data Available from the Nautical Almanac Offices

11.1.1.1 International Agreements

Ever since astronomical ephemerides and almanacs have been published, eclipse information has been included. This was a natural action because the extensive calculations required are based on predicted ephemerides. In modern times, the situation is much eased, but the Nautical Almanac Offices of the U.S. Naval Observatory and the United Kingdom continue to provide information on every eclipse of each year. The information conforms to International Astronomical Union (IAU) standards and is not changed without adequate notice to the IAU. This may cause some misunderstandings (e.g., in the value of k, described in § 11.1.2), or occasional difficulties when a convention changes (for instance, longitude is now considered positive to the east of Greenwich). Some changes that improve production without changing the information are adopted by decisions within the Nautical Almanac Offices. Other special publications for individual eclipses are designed to assist the scientific observer as much as possible. Since 1949, at the request of the appropriate Commissions of the IAU, the principal circumstances of all solar eclipses have been routinely calculated and made available several years in advance of the publication of the annual almanac. In the spirit of this agreement, a web site, *Eclipses Online* found at URL[2], has been created to provide eclipse information covering the period A.D. 1501–2100. Further information can be found in § 11.5.

11.1.1.2 Data Provided in *The Astronomical Almanac*

Elements and general circumstances are given in *The Astronomical Almanac* for all solar and lunar eclipses, including the penumbral lunar eclipses that occur during the year. For the solar eclipses, maps are given from which approximate local circumstances may be obtained for any particular place, and the Besselian elements are presented in polynomial form for the calculation of accurate local circumstances for any point on or above the surface of the Earth. For total and annular solar eclipses, the latitudes and longitudes of points on the central line and on the northern and southern limits, the duration of the total or annular phase, and the altitude and azimuth of the Sun on the central line are tabulated. These are presented in longitude order at intervals of one degree. For lunar eclipses, times of the major circumstances are presented on a diagram showing the Moon's path with respect to the Earth's penumbral and umbral shadows. Additionally, a map showing the eclipse's visibility on the surface of the Earth is given. Since the circumstances and their times are the same for all parts of the Earth, any particular phase is visible from any point at which the Moon is above the horizon. Further details are described in § 11.5.2.

For years in which a transit of Mercury or Venus occurs, general circumstances and a map are given, by which approximate local circumstances may easily be estimated. Formulae are also provided for the computation of more accurate local circumstances. The presented data are more fully described in § 11.6.

The information that appears in *The Astronomical Almanac* is prepared approximately three years before the event. A provisional value of ΔT to the nearest whole second is assigned, so that the time argument is provisional Universal Time (UT) or, more precisely, provisional UT1 (see § 3.2.2). More details are given in § 11.1.2 and § 11.3.6.3.

The predictions given in *The Astronomical Almanac* take no account of the effects of refraction, although refraction may be significant for the reduction of observations intended

Table 11.1 Selected USNO eclipse circulars

Cir. No.	Date	Title
1	1949 July 18	Tracks of total solar eclipses in 1952, 1953, 1954
2	1949 September 19	Tracks of total solar eclipses in 1955, 1956, 1957
16	1950 May 4	Tracks of total solar eclipses in 1958, 1959, 1960
40	1952 December 8	Annular and partial solar eclipses in 1955, 1956, and 1957. Non-central total eclipses of 1957
53	1954 August 20	Annular eclipses in 1958, 1959
59	1955 June 28	Solar eclipses, 1960–1963
85	1958 April 16	Solar eclipses, 1963–1967
89	1960 June 15	Solar eclipses, 1968–1970
101	1964 July 29	Solar eclipses, 1971–1975
113	1966 December 15	Solar eclipses, 1976–1980
142	1973 April 20	Solar eclipses, 1981–1990
170	1986 November 7	Solar eclipses, 1991–2000

to give precise positions. The Besselian elements, however, are rigorously independent of refraction.

11.1.1.3 Data Provided in Other Publications

Material from the section of *The Astronomical Almanac* on solar and lunar eclipses and transits is also published, in advance of publication of *The Astronomical Almanac* itself, in the small booklet *Astronomical Phenomena*. Descriptions of eclipses and solar eclipse maps are also published in *The Nautical Almanac*. Both publications are issued annually by the U.S. Naval Observatory and Her Majesty's Nautical Almanac Office.

In 1949, the U.S. Naval Observatory began a publication series called the U.S. Naval Observatory Circulars. The series transmited astronomical data resulting from continuing programs but not available in any other publications. Two of the continuing programs that contributed many issues to this series are solar eclipse predictions and sunspot counts. There were two kinds of solar eclipse circulars. First, there were circulars issued well in advance that gave just the principal circumstances of all solar eclipses in a multiple-year period. These are listed in Table 11.1.

Second, the Observatory issued circulars for specific solar eclipses; these circulars contained extensive information for observers to choose a site and calculate accurate local circumstances. Before the circulars began in 1949, this information was issued in Supplements to the annual *American Ephemeris*. Until 1991, it was the policy of the U.S. Naval Observatory to issue a circular for each total solar eclipse, with very few exceptions, and for selected annular solar eclipses that had some observationally interesting features. Typically these circulars contained general information and circumstances, Besselian elements, a discussion of anticipated meteorological conditions along the eclipse path, local circumstances for selected locations, the lunar limb profile and limb corrections, the path of the central phase tabulated by time and longitude at sea level and at flying altitudes, and detailed maps of the portion

of the path over land. The U.S. Naval Observatory planned to release each circular 12 to 18 months in advance of a particular eclipse and to incorporate the best value of ΔT available at the time of preparation. However, the lead time and contents were subject to regular review with respect to meeting the reported needs of the scientific community. In 1992, the USNO eclipse circulars were discontinued. NASA has produced a series of *Eclipse Bulletins* covering eclipses from 1994 to 2010 containing predictions and meteorological information for the professional and lay community. Material is also available at URL[2] and URL[3], the former using techniques based on those used in *The Astronomical Almanac*.

11.1.2 Corrections to the Ephemerides

The basic quantities for calculations of solar and lunar eclipses are: the apparent right ascension (α_s), declination (δ_s), and distance (R_s) of the Sun, and the apparent right ascension (α_m), declination (δ_m), and distance (R_m) of the Moon, for every hour of Terrestrial Time (TT) during the eclipse; and the ephemeris sidereal time at 0^h TT for the day of the eclipse and for the following day. The apparent places of the Sun and the Moon are computed rigorously using the same ephemerides for the Sun and the Moon as are used for *The Astronomical Almanac*, and using the reduction methods described elsewhere in this book (see Chapter 7). At the time of this writing, the ephemerides are based upon the DE405/LE405 produced by the Jet Propulsion Laboratory (see Chapter 8). The ephemeris sidereal time at 0^h TT, which is the local apparent sidereal time on the ephemeris meridian, is virtually the same numerically as the (Greenwich) apparent sidereal time at 0^h UT, as tabulated in *The Astronomical Almanac*.

Gravitational ephemerides refer to the positions of the centers of mass of the bodies concerned. Eclipses, however, are governed by the positions of the centers of figures of the Sun and the Moon. The center of figure of the Moon does not coincide with its center of mass; to allow for this difference, empirical corrections are made to the mean equatorial coordinates of the Moon, referred to the center of mass of the Earth. Unpublished investigations have shown that the corrections depend upon the lunar librations at the time of an eclipse. The range of the corrections is less than $0''.5$, and for the calculations in *The Astronomical Almanac*, only the minimum corrections are applied. These are $\Delta\lambda = +0''.50$ and $\Delta\beta = -0''.25$ for the LE405 lunar ephemeris. The corrections are made during the apparent place computation by rotating the mean equatorial geocentric coordinates of the Moon into the ecliptic system, applying the corrections in the ecliptic system, and rotating back into the equatorial system. The corrections are applied as constants for each eclipse.

The semidiameters of the Sun and the Moon used in the calculation of eclipses do not include irradiation. The adopted semidiameter of the Sun (s_s) is computed directly from the ephemeris of the Sun, thereby using the ephemeris constants. However, the apparent semidiameter of the Moon is calculated by putting its sine equal to $k \sin \pi_m$, where π_m is the horizontal parallax and k, the ratio of the Moon's radius to the equatorial radius of the Earth, is an adopted constant. The IAU adopted a value of k ($k = 0.272\,5076$) in August 1982. Before that time, two different values of k were used in computing a solar eclipse. The value taken for the lunar ephemeris was used for the most part, but in practice it was too large for the total phase in total solar eclipses because of the effects of the rough lunar limb. As an approximate correction for this effect, a smaller value of k was adopted solely for calculating the duration on the central line of total solar eclipses. This smaller value caused numerical inconsistencies

as well as misunderstandings on the part of users of the information. Therefore, when the new value was adopted in 1982 to conform to the value used in occultation predictions, it was agreed implicitly that limb effects are no longer accounted for, but are averaged, and if an observer considers them to be important, then corrections must be calculated and applied separately. It is possible for these effects to advance or retard predicted second- or third-contact times on the central line by as much as two seconds apiece. The same limb corrections can be applied in the case of annular solar eclipses, or even lunar eclipses, but the effects will not be observable. It is only in the case of a total solar eclipse that the presence or absence of any light from the solar disk is easily detected and is hence critical to delicate observations.

The calculation of the occurrence of eclipses does not depend upon the timescale for the portions restricted to the spatial relationships of the Earth, Moon, and Sun. However, for calculation of phenomena as they are related to the surface of the Earth for time and place of visibility, it is necessary to use Universal Time (UT1) in the best approximation possible. This approximation is achieved by adjusting the ephemerides at the start of the calculations. The predictions in *The Astronomical Almanac* were given in ephemeris time (ET) until 1981, when ΔT had become large enough that it was deemed more useful to publish the predictions in provisional Universal Time (see § 11.3.6.3 for details).

11.2 The Occurrence of Lunar and Solar Eclipses

11.2.1 Overview

The purpose of this section is to develop conditions that can be used to determine whether an eclipse will occur at a particular conjunction or opposition of the Sun and Moon. The approach is, first, to develop a general expression for the geocentric least angular separation of the Moon and either the Sun or the antisolar point, when one of the latter is in the vicinity of one of the nodes of the Moon's orbit. Second, expressions for the apparent sizes of the shadows are found. Finally, discrimination tests are established. Specifically, to develop the conditions for a lunar eclipse, the apparent sizes of the umbral and penumbral shadows of the Earth are compared to the geocentric least angular separation of the Moon and the antisolar point. To develop the conditions for a solar eclipse, expressions for the geocentric least angular separation of the Sun and the Moon are derived from the geometry of each particular type of solar eclipse and are compared with the geocentric apparent angular semidiameters.

11.2.2 Geocentric Least Angular Separation

Consider the Sun and the Moon at a time of conjunction or opposition in longitude. In order for an eclipse to occur, the Sun (or the antisolar point) and the Moon must each be near the same one of the nodes of the Moon's orbit. Thus, the ecliptic latitude of the Moon (β_m) will be small, and plane geometry may be used.

This situation is illustrated in Fig. 11.1. This is a general representation; β_m may be positive (above the ecliptic) or negative (below the ecliptic). Correspondingly, N may be either the ascending or descending node of the lunar orbit. For a lunar eclipse, S represents the antisolar point at opposition. For a solar eclipse, S represents the center of the Sun at conjunction. For either case, M represents the center of the Moon. Take the absolute value of β_m, which is the latitude of the Moon at opposition for a lunar eclipse, or at conjunction

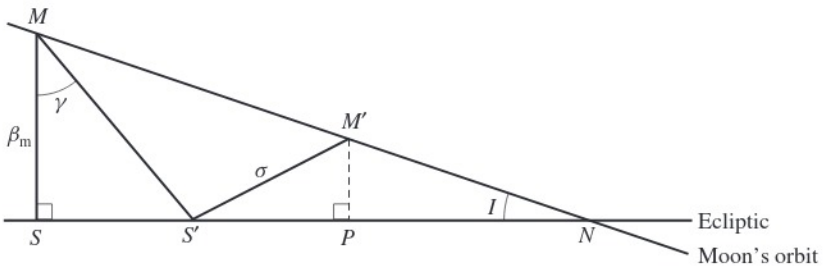


Figure 11.1 Geometric construct for determining whether any kind of eclipse will occur when the Moon is near one of the nodes of its orbit on the ecliptic. In this figure, N is the descending node as seen from outside the orbit, looking toward Earth. Let S represent the Sun or its antisolar point, and M the Moon, at conjunction or opposition, respectively, when the separation is the lunar latitude $\beta_{\rm m}$. At some later time when the two points have moved to S', M', then the instantaneous separation is σ.

for a solar eclipse. The primed values, M' and S', represent positions at a time when angle $SMS' = \gamma$, and the angular separation of M' and S' is σ. I is the inclination of the Moon's orbit to the ecliptic.

We wish now to derive an expression for σ in terms of known quantities. Define a quantity λ, a ratio of the longitudinal motions:

$$\lambda = \frac{SP}{SS'} = \frac{\text{Moon's motion in longitude}}{\text{Sun's motion in longitude}}. \tag{11.1}$$

From the geometry:

$$\sigma^2 = (S'P)^2 + (M'P)^2 \tag{11.2}$$

where

$$S'P = SP - SS' = (\lambda - 1)\beta_{\rm m} \tan\gamma. \tag{11.3}$$

$$M'P = NP \tan I = (SN - SP) \tan I = \beta_{\rm m}(1 - \lambda \tan\gamma \tan I). \tag{11.4}$$

Thus,

$$\sigma^2 = \beta_{\rm m}^2[(\lambda - 1)^2 \tan^2\gamma + (1 - \lambda \tan I \tan\gamma)^2]. \tag{11.5}$$

In order to find the value of γ at which σ^2 is a minimum, take the derivative of Eq. 11.5 with respect to γ and set it equal to zero. After some algebra, the result is:

$$\tan\gamma = \frac{\lambda \tan I}{(\lambda - 1)^2 + \lambda^2 \tan^2 I}. \tag{11.6}$$

Substitute Eq. 11.6 into Eq. 11.5 to obtain:

$$\sigma = \beta_{\rm m}(\lambda - 1)[(\lambda - 1)^2 + \lambda^2 \tan^2 I]^{-1/2}. \tag{11.7}$$

This equation may be simplified by the following change of variables. Let

$$\tan I' \equiv \frac{\lambda}{\lambda - 1} \tan I. \tag{11.8}$$

I' is the angle at which the moving Moon would appear to intersect the ecliptic from the point of view of an observer on the moving point S. Then

$$\sigma = \beta_{\mathrm{m}} \cos I'. \tag{11.9}$$

Equations 11.7 and 11.9 give expressions for the geocentric least angular separation between the Moon and the Sun at conjunction, or the geocentric least angular separation of the Moon and the antisolar point at opposition of the Sun and Moon.

11.2.3 Occurrence of Lunar Eclipses

Now that we have an expression for the least angular separation of the Moon and the antisolar point near opposition, let us examine how to use it to test for the occurrence of a lunar eclipse. From the geometry of the shadow cone, we shall find a relationship between the size of the cone and other well-known quantities.

11.2.3.1 Apparent Semidiameters of the Shadow Cones

The penumbral shadow cone of the Earth is defined by the interior tangents between the Sun and the Earth. Figure 11.2 illustrates the geometry. In the diagram, S is the center of the Sun, E is the center of the Earth, and M is a point on the penumbral cone at the distance of the Moon. The line LM is the semidiameter of the cone at the distance of the Moon. The known quantities are angle GME, which is the lunar horizontal parallax (π_{m}) based on the mean radius of the Earth; angle SET, which is the apparent semidiameter of the Sun (s_{s}); and angle ETG, which is the parallax of the Sun (π_{s}). We wish to find LM as the angular quantity LEM seen from the Earth, designated f_1. Angle EVM is an intermediate angle, so that angle EVM = angle ETG + angle SET. We want f_1 = angle LEM = angle GME + angle EVM. Thus,

$$f_1 = \pi_{\mathrm{m}} + \pi_{\mathrm{s}} + s_{\mathrm{s}}. \tag{11.10}$$

The cross-section of the shadow is not a true circle, because the Earth is not a true sphere. To compensate, a mean radius for the Earth is substituted, which is equivalent to substituting for π_{m} a parallax π_1 reduced to latitude 45°, so that $\pi_1 = 0.998\,340\pi_{\mathrm{m}}$. Moreover, observation has shown that the atmosphere of the Earth increases the apparent semidiameter of the shadow by approximately one-fiftieth. Hence,

$$f_1 = 1.02(\pi_1 + \pi_{\mathrm{s}} + s_{\mathrm{s}}). \tag{11.11}$$

The umbral shadow cone of the Earth is defined by the exterior tangents between the Sun and the Earth. The vertex falls beyond the Earth and beyond the Moon's distance as well. Figure 11.3 illustrates the geometry. In this diagram, S and E represent the centers of the Sun and the Earth, respectively, and M is a point on the umbral cone at the distance of the Moon. All angles are as described in the previous section, except that angle VEM,

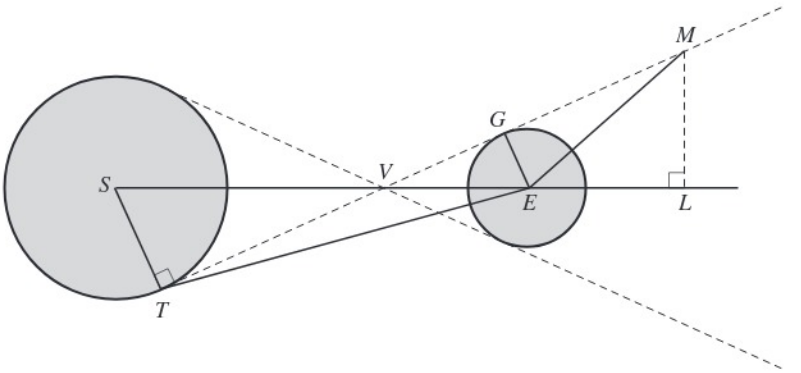


Figure 11.2 Geometric parameters of the Earth's penumbral shadow, relating its angular size to observed quantities. In this diagram, $\angle GME = \pi_m$, $\angle ETG = \pi_s$, $\angle SET = s_s$, and $\angle LEM = f_1$.

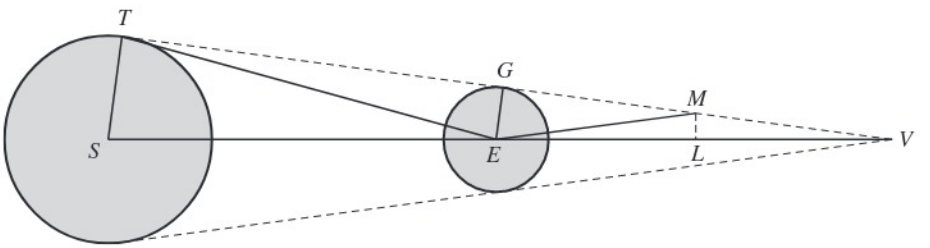


Figure 11.3 Geometric parameters of the Earth's umbral shadow, relating its angular size to observed quantities. In this diagram, $\angle GME = \pi_m$, $\angle ETG = \pi_s$, $\angle SET = s_s$, and $\angle VEM = f_2$.

the apparent semidiameter of the umbral cone (f_2), replaces angle f_1. From triangle VEM, $f_2 =$ angle $GME -$ angle EVM, and from triangle TEV, angle $EVT =$ angle $EVM =$ angle $SET -$ angle ETG. Thus,

$$f_2 = 1.02(\pi_1 + \pi_s - s_s) \tag{11.12}$$

after compensation for the effect of the Earth's atmosphere on the semidiameter of the shadow.

11.2.3.2 Conditions for a Lunar Eclipse

There are several types of lunar eclipse, depending upon what portion of the Earth's shadow the Moon passes through. We will consider the conditions for each. All conditions should be tested to find the maximum possible eclipse.

Conditions for a penumbral lunar eclipse. A *penumbral lunar eclipse* occurs when the Moon enters partially or completely into the penumbral cone, but not the umbral cone. The right side of Fig. 11.4 illustrates the limiting case for a penumbral lunar eclipse, where $f = f_1$. In this diagram, S represents the antisolar point and M' represents the center of the Moon. Let SM' be the geocentric least angular separation (σ) given by Eq. 11.9; $M'T'$ is s_m. A penumbral eclipse will occur if σ is less than $f_1 + s_m$. Thus, the condition for a penumbral lunar eclipse is

$$\sigma < 1.02(\pi_1 + \pi_s + s_s) + s_m. \tag{11.13}$$

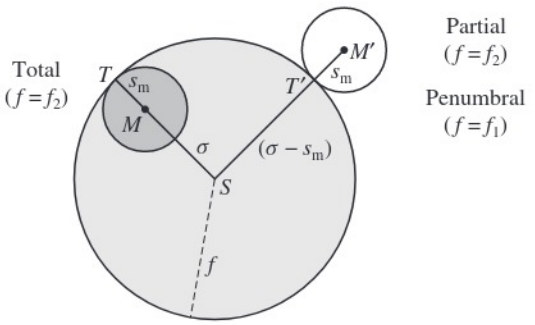


Figure 11.4 Composite diagram showing limiting conditions for different types of lunar eclipses, not to scale. Limiting conditions that separate types of eclipses occur when the separation of the center of the Moon and the shadow axis is equal to the sum or difference of the apparent radius of the Moon and the radius of the cross-section of one of the shadow cones at the distance of the Moon. Let the small circle represent the Moon, with radius s_m, the shaded circle represent either the umbra, with radius f_2, or the penumbra, with radius f_1, and σ represent the distance between centers S and M or M'. On the left side, if $\sigma \leq f - s_m$, the Moon is *totally* immersed in the shadow. On the right side, if $\sigma \geq f + s_m$, the Moon is just out of the shadow. If the Moon lies between these two limits, it is *partially* eclipsed in the shadow. The type of eclipse is named for its maximum phase—total (umbral), partial (umbral), total penumbral, or partial penumbral.

Conditions for a partial lunar eclipse. A *partial lunar eclipse* occurs when the Moon passes through the penumbral cone and partly, but not completely, into and through the umbra. The right side of Fig. 11.4 also illustrates the limiting case for a partial (umbral) lunar eclipse, except this time, $f = f_2$. A partial eclipse will occur if σ is less than $f_2 + s_m$. Thus, the condition for a partial lunar eclipse is

$$\sigma < 1.02(\pi_1 + \pi_s - s_s) + s_m. \tag{11.14}$$

Conditions for a total lunar eclipse. A *total lunar eclipse* occurs when the Moon passes through the penumbral cone and completely into and through the umbral cone. The left side of Fig. 11.4 illustrates the limiting case for a total (umbral) lunar eclipse, where $f = f_2$. In this diagram, S represents the antisolar point and M represents the center of the Moon. Let SM be the geocentric least angular separation (σ) given by Eq. 11.9; MT is s_m. A total eclipse will occur if σ is less than $f_2 - s_m$. Thus, the condition for a total lunar eclipse is

$$\sigma < 1.02(\pi_1 + \pi_s - s_s) - s_m. \tag{11.15}$$

11.2.4 Occurrence of Solar Eclipses

The geometry to test for the occurrence of a solar eclipse is similar to that for a lunar eclipse. In this situation, we are examining the shadow of the Moon instead of that of the Earth. The shadow is, of course, smaller and shorter, the vertex being at about the same distance from the Moon as the Earth. Moreover, the Earth is much larger, so that it can never be completely within the Moon's shadow. In searching for the occurrence of a solar eclipse, we use the center of the Earth as the reference point of observation. The expression for least angular separation of the centers of the Sun and Moon still applies.

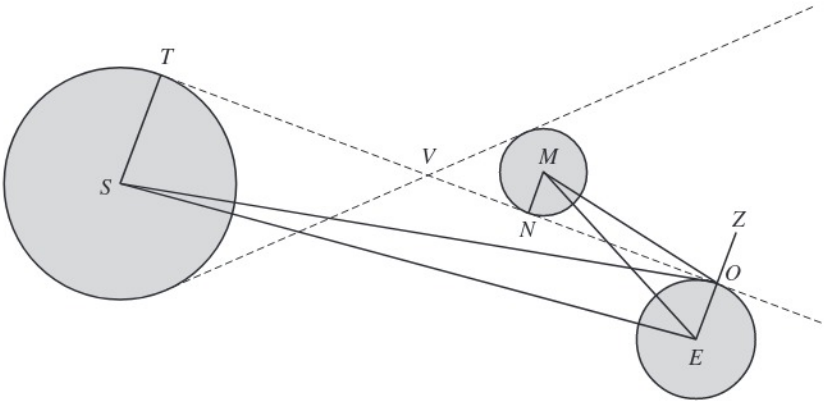


Figure 11.5 Known geometric parameters in the limiting configuration for a partial solar eclipse, when the Moon is externally tangent. As seen by an observer at O, the apparent disks of the Sun and the Moon are externally tangent along the line OT. In this diagram, $\angle ZOM = z'_{\rm m}$, $\angle ZEM = z_{\rm m}$, $\angle ZOS = z'_{\rm s}$, $\angle ZES = z_{\rm s}$, $\angle MON = s'_{\rm m}$, and $\angle SOT = s'_{\rm s}$.

11.2.4.1 Conditions for a Solar Eclipse

There are also several types of solar eclipse, depending upon what portion of the shadow reaches the Earth's surface. We will examine the conditions for each. It is not necessary to correct for atmospheric augmentation of the Moon's shadow; the Moon has no atmosphere. It is also not necessary to correct the parallax for shape; this is done by limb corrections, if needed (Herald 1983).

Conditions for a partial solar eclipse. A *partial solar eclipse* occurs when the Earth passes through the penumbra of the Moon's shadow, but not the umbra. (Also, *partial phase* is seen by an observer in the penumbra during any type of solar eclipse.) Figure 11.5 illustrates the limiting case for a partial solar eclipse. In this figure, S represents the center of the Sun, M the center of the Moon, and E the center of the Earth. Point O, on the Earth, lies on the edge of the penumbral cone, depicted by line segment OT, which also serves as the horizon at O; point Z is at the zenith for an observer at O. The topocentric zenith distances of the Moon and the Sun at O are:

$$\begin{aligned} z'_{\rm m} &= 90^\circ - \angle MON = 90^\circ - s'_{\rm m} \\ z'_{\rm s} &= 90^\circ - \angle TOS = 90^\circ + s'_{\rm s}. \end{aligned} \tag{11.16}$$

where $s'_{\rm m}$ and $s'_{\rm s}$ are the topocentric semidiameters of the Moon and the Sun, respectively. The geocentric angular separation between the Moon and the Sun is angle MES, which is equal to the difference between the geocentric zenith distances of the Sun and the Moon, $z_{\rm s} - z_{\rm m}$. The geocentric zenith distances (z) are related to their corresponding topocentric values (z') by

$$z = z' - \pi' \tag{11.17}$$

where π' is the geocentric parallax. Assuming a spherical Earth, π' is given in terms of the horizontal parallax (π) by

$$\pi' = \sin^{-1}(\sin\pi \sin z'). \tag{11.18}$$

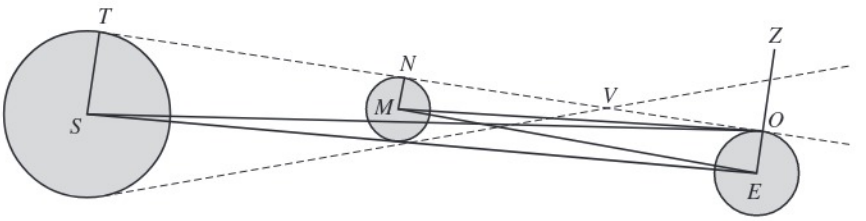


Figure 11.6 Known geometric parameters in the limiting configuration for a partial solar eclipse, when the Moon is internally tangent. As seen by an observer at O, the apparent disks of the Sun and the Moon are internally tangent along the line OT. In this diagram, $\angle ZOM = z'_{\mathrm{m}}$, $\angle ZEM = z_{\mathrm{m}}$, $\angle ZOS = z'_{\mathrm{s}}$, $\angle ZES = z_{\mathrm{s}}$, $\angle MON = s'_{\mathrm{m}}$, and $\angle SOT = s'_{\mathrm{s}}$.

Substituting Eqs. 11.16 and 11.18 into Eq. 11.17, neglecting the augmentation of the semidiameters, and setting $\cos s'$ equal to unity yields

$$\begin{aligned} z_{\mathrm{m}} &= 90^\circ - s_{\mathrm{m}} - \pi_{\mathrm{m}} \\ z_{\mathrm{s}} &= 90^\circ + s_{\mathrm{s}} - \pi_{\mathrm{s}}. \end{aligned} \tag{11.19}$$

Setting angle MES equal to the geocentric least angular separation (σ) yields

$$\sigma = z_{\mathrm{s}} - z_{\mathrm{m}} = s_{\mathrm{s}} + s_{\mathrm{m}} + \pi_{\mathrm{m}} - \pi_{\mathrm{s}}. \tag{11.20}$$

A solar eclipse will occur when the apparent least angular separation of the centers of the Sun and the Moon is less than the sum of their apparent semidiameters. Thus, the condition for a partial solar eclipse as seen from the geocenter is

$$\sigma < s_{\mathrm{s}} + s_{\mathrm{m}} + \pi_{\mathrm{m}} - \pi_{\mathrm{s}}. \tag{11.21}$$

Conditions for a central solar eclipse. If the observer on Earth passes through the penumbra of the Moon's shadow and into the umbra, he or she experiences a *central solar eclipse*. If the reference observing point is in the umbra on the inside of the vertex, the eclipse is *total*. If the reference point is in the umbra on the outside of the vertex, the eclipse is *annular*. If the reference point is in the umbra and passes through the vertex, it is an *annular-total eclipse*, also called a *hybrid eclipse*. In the rare event that an observer near a pole sees a total eclipse, but the shadow axis does not pass through the surface of the Earth, the eclipse is a *noncentral total eclipse*. A central solar eclipse will occur when the apparent separation of the centers of the Sun and the Moon is less than the absolute value of the difference of the apparent semidiameters. The condition for the occurrence of an annular solar eclipse is specifically derived in this section, but the same condition may be used to differentiate between the occurrence of any type of central solar eclipse (total, annular, or annular-total) and the occurrence of a partial solar eclipse. Figure 11.6 illustrates the geometry. The definitions in this figure are identical to the definitions of Fig. 11.5, except that point O now lies on the edge of the umbral cone. The topocentric zenith distances at O are

$$\begin{aligned} z'_{\mathrm{m}} &= 90^\circ + \angle MON = 90^\circ + s'_{\mathrm{m}} \\ z'_{\mathrm{s}} &= 90^\circ + \angle TOS \;\; = 90^\circ + s'_{\mathrm{s}}. \end{aligned} \tag{11.22}$$

Just as in the preceding section, the geocentric angular separation between the Moon and the Sun is angle MES, which is equal to $|z_s - z_m|$, the difference between the geocentric zenith distances of the Sun and the Moon. Employing the same procedure and approximations as in the preceding section, the condition for an annular solar eclipse is

$$\sigma < |s_s - s_m + \pi_m - \pi_s| \tag{11.23}$$

which, as stated before, may be used as a general condition for any central solar eclipse. If $s_m > s_s$, the eclipse is total; if $s_m < s_s$, it is annular. If σ is near zero, the eclipse may be annular-total, but that determination requires further calculation.

11.3 Solar Eclipses

Section 11.1 described considerations for ephemerides to use in calculating eclipses. Section 11.2 described how to find approximately when an eclipse of any kind may occur. This section describes how to calculate the details of a solar eclipse.

11.3.1 Fundamental Equations: Introduction

Bessel developed the method used to calculate and describe precisely any eclipse, based on using a coordinate system oriented to the shadow axis. The basic steps are: elements are calculated in the Besselian system to describe geometrical quantities; the observer's position is transformed to Bessel's coordinate system; equations of condition are formed; circumstances are derived that describe the time and place of observable events or conditions in the Besselian system; the circumstances are transformed back to topocentric or geocentric coordinates.

11.3.2 Besselian Elements

11.3.2.1 The Fundamental Coordinate System: Overview

To use Bessel's method for solar eclipses, the geometric position of the shadow of the Moon with respect to the Earth is described in a coordinate system (Fig. 11.7) wherein the origin of coordinates is the geocenter, the z-axis is parallel to the axis of the shadow and positive toward the Moon, the x-axis passes through the equator and is positive toward the east, and the y-axis is positive toward the north. This is the *fundamental coordinate system*, and the xy-plane is the *fundamental plane*. The intersection of the shadow with the fundamental plane is two circles concentric about the axis. The surface of the Earth moves with respect to this plane, because the Earth is rotating on its axis and moving in orbit.

11.3.2.2 Calculation of the Besselian Elements: Transformation to the Fundamental Coordinate System

In the geocentric equatorial coordinate system, let $\mathbf{R}_s$ be the position vector of the Sun, and $\mathbf{R}_m$ that of the Moon. Let $\mathbf{G} = \mathbf{R}_s - \mathbf{R}_m$ be a vector collinear with the shadow axis. In astronomical units,

$$\left|\hat{\mathbf{R}}_s\right| = r_s = 1$$

$$r_m = \frac{R_m}{R_s} = \frac{\sin \pi_0}{R_s \sin \pi_m}$$

$$g = \frac{G}{R_s}$$

$\pi_0 =$ horizontal parallax of the Sun at mean distance

$$\mathbf{r}_s = \begin{bmatrix} \cos \alpha_s \cos \delta_s \\ \sin \alpha_s \cos \delta_s \\ \sin \delta_s \end{bmatrix}$$

$$\mathbf{r}_m = \frac{\sin \pi_0}{R_s \sin \pi_m} \begin{bmatrix} \cos \alpha_m \cos \delta_m \\ \sin \alpha_m \cos \delta_m \\ \sin \delta_m \end{bmatrix}. \tag{11.24}$$

By definition,

$$\mathbf{g} = \mathbf{r}_s - \mathbf{r}_m = g \begin{bmatrix} \cos d \cos a \\ \cos d \sin a \\ \sin d \end{bmatrix} \tag{11.25}$$

where (a, d) is the geocentric equatorial right ascension and declination of the intersection of the shadow's axis with the celestial sphere (point Z).

Recall from § 11.3.2.1 the fundamental coordinate system (x, y, z) whose z-axis is parallel to the shadow axis, or to $\mathbf{g}$. The plane $z = 0$ is the fundamental plane, the x-axis

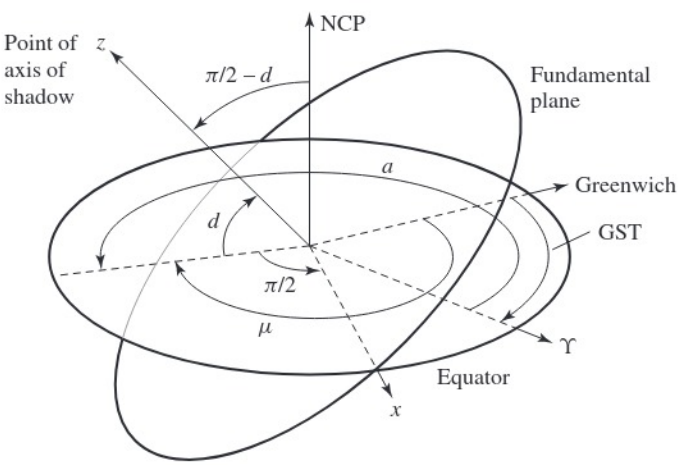


Figure 11.7 Transformation of geocentric equatorial coordinates to the fundamental plane. Take the x-axis pointed at Υ and rotate it around the z-axis (toward NCP) to $a + \pi/2$; then rotate around the new x-axis by $\pi/2 - d$ to make the new z-axis parallel to the shadow axis.

is the intersection of the fundamental plane with the equator (positive to the east), and the y-axis completes the triad (positive to the north).

Hence,

$$\mathbf{r}_{\text{mFund.}} = \frac{1}{\sin \pi_{\text{m}}} \mathbf{R}_1 \left(\frac{\pi}{2} - d \right) \mathbf{R}_3 \left(a + \frac{\pi}{2} \right) \mathbf{r}_{\text{mGeoc.}} \tag{11.26}$$

in units of Earth radii. ($\mathbf{R}_1$ and $\mathbf{R}_3$ are standard rotation matrices, positive direction, about the x-axis and z-axis, respectively. See § 14.4 for further details.)

In the (x, y, z) system, let the unit vectors be $\mathbf{i}$, $\mathbf{j}$, and $\mathbf{k}$. Then

$$\begin{aligned} \mathbf{g} \times \mathbf{k} &= 0 \\ \mathbf{g} \cdot \mathbf{i} &= 0 \\ \mathbf{g} \cdot \mathbf{j} &= 0 \\ \mathbf{k} &= \frac{\mathbf{g}}{g} \begin{bmatrix} \cos d \cos a \\ \cos d \sin a \\ \sin d \end{bmatrix} \end{aligned} \tag{11.27}$$

and the orthogonal unit vectors are

$$\mathbf{i} = \begin{bmatrix} -\sin a \\ \cos a \\ 0 \end{bmatrix}, \qquad \mathbf{j} = \begin{bmatrix} -\cos a \sin d \\ -\sin a \sin d \\ \cos d \end{bmatrix}. \tag{11.28}$$

By working out Eq. 11.26 or by resolving the lunar position vector into components using Eq. 11.28,

$$\mathbf{r}_{\text{mFund}} = \frac{1}{\sin \pi_{\text{m}}} \begin{bmatrix} \cos \delta_{\text{m}} \sin(\alpha_{\text{m}} - a) \\ \sin \delta_{\text{m}} \cos d - \cos \delta_{\text{m}} \sin d \cos(\alpha_{\text{m}} - a) \\ \sin \delta_{\text{m}} \sin d + \cos \delta_{\text{m}} \cos d \cos(\alpha_{\text{m}} - a) \end{bmatrix}. \tag{11.29}$$

(x, y) are the coordinates of the intersection of the axis of the shadow with the fundamental plane.

In presenting Besselian elements of eclipses for practical use, the right ascension a of the point Z is conventionally replaced by the Greenwich Hour Angle μ of that point, given by

$$\mu = \text{Greenwich Apparent Sidereal Time} - a.$$

In practical calculation, the Greenwich Sidereal Time is evaluated according to the precepts given in Chapter 3 (see § 3.2.1).

11.3.2.3 Parameters of the Shadow Cone

The radii of the umbra and penumbra on the fundamental plane can be easily calculated given the generating angle of each cone, and the perpendicular distance of each vertex from the fundamental plane. Refer to Figs. 11.8 and 11.9 for the plane geometry of a cross-section of the cone. This geometry relates the desired quantities to the known size and separation of the bodies.

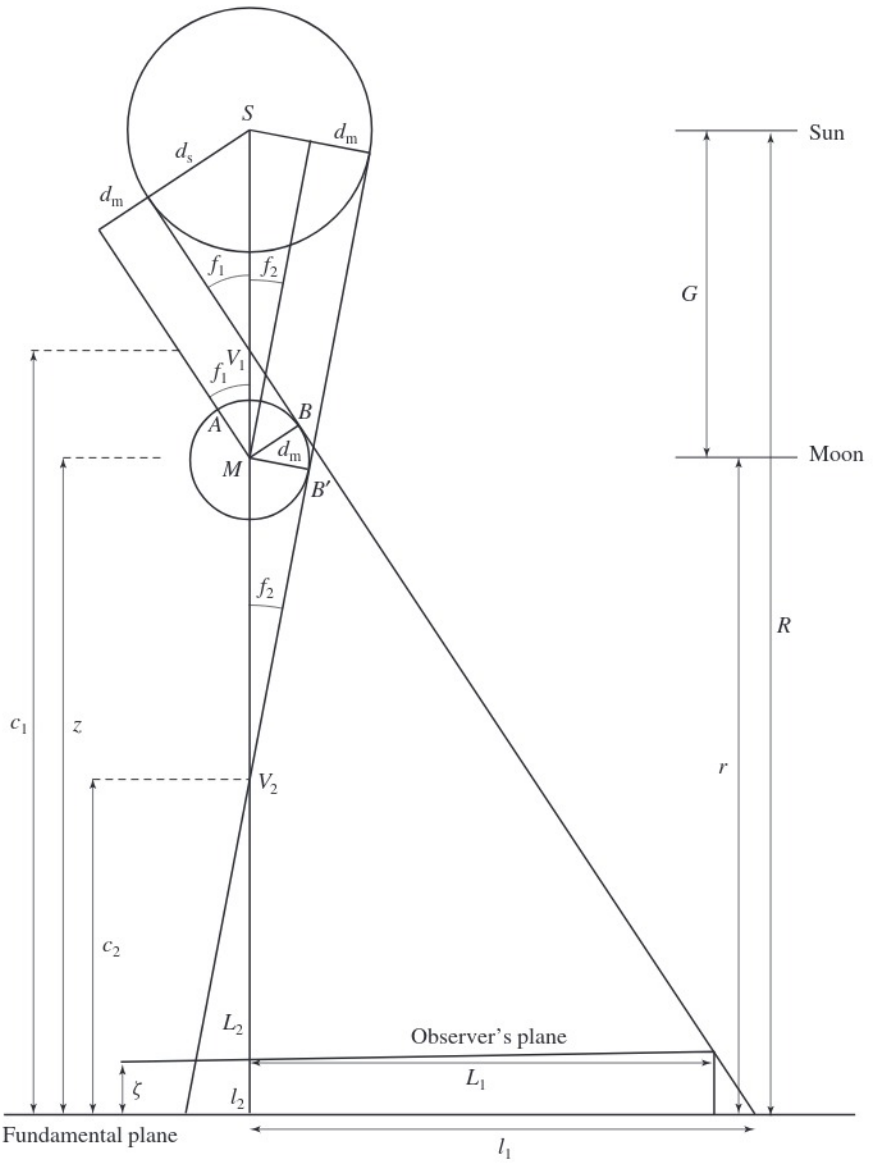


Figure 11.8 Components of shadow cones in the Besselian fundamental reference system. The Sun is centered at S, with apparent semidiameter d_s, at height R above the fundamental plane. The Moon is centered at M, with semidiameter d_m, at height $r = z$ above the fundamental plane. The fundamental plane, through the Earth's center, and the observer's plane are perpendicular to the axis through SM, the separation being ζ. The penumbra has its vertex V_1 at height c_1 above the fundamental plane, radius l_1 in the fundamental plane, L_1 in the observer's plane, vertex angle f_1. Similarly for the umbra. (Subscript 1 refers to penumbra, 2 to umbra.)

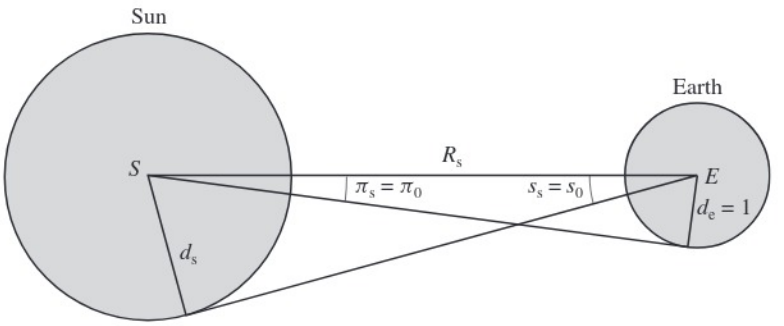


Figure 11.9 Relationships among angular semidiameter s, apparent semidiameter d, and parallax π. R_s is expressed in Earth radii.

From Fig. 11.8,

$$\begin{aligned} \sin f_1 &= \frac{d_s + d_m}{g R_s} \\ \sin f_2 &= \frac{d_s - d_m}{g R_s}. \end{aligned} \tag{11.30}$$

To transform to units of Earth equatorial radii (see Fig. 11.9),

$$\begin{aligned} d_e \equiv 1 &= R_s \sin \pi_s \\ d_s \quad &= R_s \sin s_s = \frac{\sin s_s}{\sin \pi_s} = \frac{\sin s_0}{\sin \pi_0} \end{aligned} \tag{11.31}$$

where $\pi_s = \pi_0 / R_s$, $s_s = s_0 / R_s$. For the Moon, set

$$d_m = k \text{ Earth radii}, \quad \text{where } k = d_m / d_e. \tag{11.32}$$

Then

$$\begin{aligned} d_e \equiv 1 &= R_m \sin \pi_m \\ d_m = k &= R_m \sin s_m = \frac{\sin s_m}{\sin \pi_m}. \end{aligned} \tag{11.33}$$

Let $R = R_s \sin \pi_0$ be the distance to the Sun in astronomical units. Substituting Eqs. 11.31 through 11.33 into Eq. 11.30 and reducing yields

$$\begin{aligned} \sin f_1 &= (\sin s_0 + k \sin \pi_0)/gR \\ \sin f_2 &= (\sin s_0 - k \sin \pi_0)/gR. \end{aligned} \tag{11.34}$$

The numerators are evaluated using adopted values for k, s_0, and π_0. Equations 11.24 and 11.25 give g, and R is from the solar ephemeris.

The distances c_1, c_2, of the vertices of the penumbral and umbral cones above the fundamental plane are shown in Fig. 11.8. Figures 11.10 and 11.11 show that

$$\begin{aligned} c_1 &= z + k \operatorname{cosec} f_1 \\ c_2 &= z - k \operatorname{cosec} f_2 \end{aligned} \tag{11.35}$$

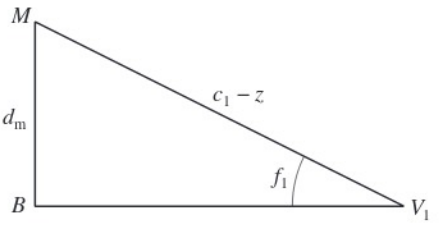


Figure 11.10 Vertex angle of the penumbra, detail from Fig. 11.8. $\sin f_1 = d_m/(c_1 - z)$.

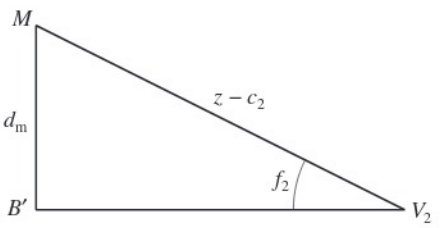


Figure 11.11 Vertex angle of the umbra, detail from Fig. 11.8. $\sin f_2 = d_m/(z - c_2)$.

and hence the radii l_1, l_2 of the penumbra and umbra on the fundamental plane are obtained from

$$l_1 = c_1 \tan f_1$$
$$l_2 = c_2 \tan f_2. \tag{11.36}$$

The quantities z, k, c_1, c_2, l_1, and l_2 are in units of Earth radii. The convention of signs introduced in Eq. 11.35 makes l_2 negative for total eclipses—i.e., the vertex is below the fundamental plane. For annular eclipses, l_2 is positive, and of course l_1 is always positive.

11.3.2.4 Summary of Besselian Elements

The quantities $x, y, \sin d, \cos d, \mu, l_1, l_2, \tan f_1, \tan f_2, \dot{\mu}$, and $\dot{d}$ are conventionally designated as Besselian elements. (N.B. It is conventional in almanacs to use the notation μ', d' for the derivatives with respect to time.) In the publications, the first seven quantities are presented as low-order polynomials as functions of time. The remaining four quantities, to the precision required, are constant for the entire eclipse and are given at the conjunction value. Using all these quantities, the size and orientation of the shadow cone with respect to the surface of the Earth and the fundamental plane may be calculated for any instant during the eclipse.

11.3.2.5 A Note on Practical Calculation

In practice, using a computer, one begins the computation by constructing short ephemerides of the Sun and the Moon from the desired source, at a convenient interval, say, one hour, and then subtabulates to smaller intervals as desired. However, it is possible with some ephemerides stored in polynomial form to take the beginning ephemeris directly at the desired interval. This directness is especially helpful in calculating points of curves near the beginning and end of a central solar eclipse.

Initially, for each eclipse, calculations are carried out using a ten-minute time interval, but for some instances additional calculations at an interval of 30 seconds or less are necessary. In

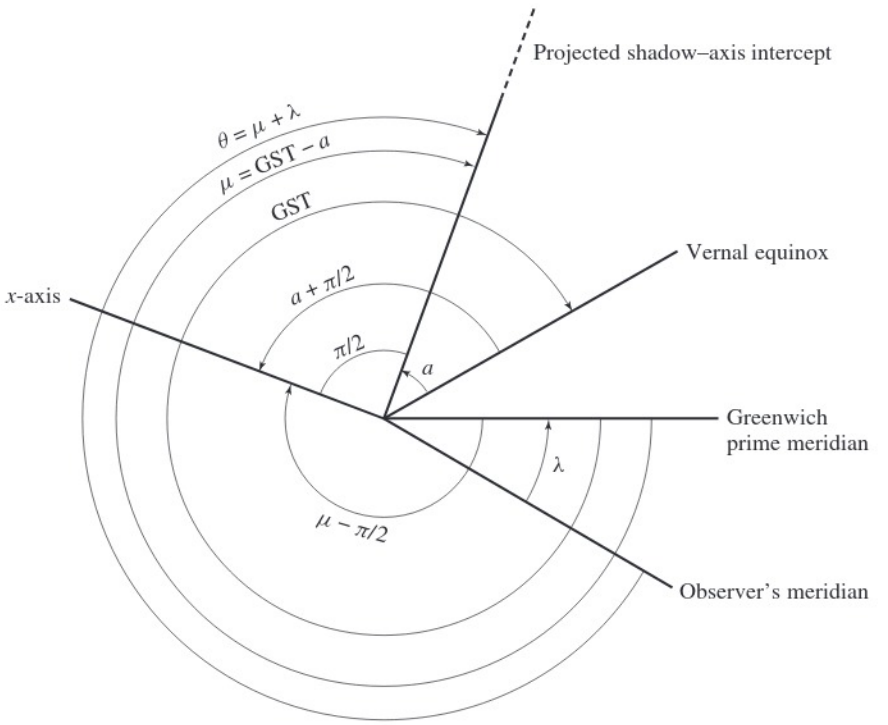


Figure 11.12 Angular quantities in the geocentric equatorial plane

all instances, the Besselian elements, derivatives, and auxiliary quantities are calculated from the ephemeris entries and carried as an array; none is assumed to be constant. Derivatives are taken numerically. Most quantities change so slowly that only a low-order scheme is required.

11.3.3 Coordinates of the Observer

11.3.3.1 Geocentric Position

Consider an observer located on the surface of the Earth in longitude λ, at geocentric latitude ϕ', and at a distance ρ from the center of the terrestrial spheroid. The longitude is not now corrected for ΔT and is considered positive east (right-handed system). Careful attention must be paid to algebraic signs (see Fig. 11.12). In the x-, y-, z-axes of the fundamental plane system, in units of the Earth's equatorial radius, let the observer's position vector be

$$\boldsymbol{\rho}_{\mathrm{F}} = \begin{bmatrix} \xi \\ \eta \\ \zeta \end{bmatrix}. \tag{11.37}$$

In the geocentric equatorial system, let the observer's position be

$$\boldsymbol{\rho}_{\mathrm{G}} = \rho \begin{bmatrix} \cos\phi' \cos\lambda \\ \cos\phi' \sin\lambda \\ \sin\phi' \end{bmatrix}. \tag{11.38}$$

The transformation to the fundamental system is very similar to that of Eq. 11.26:

$$\boldsymbol{\rho}_{\mathrm{F}} = \mathbf{R}_1\left(\frac{\pi}{2} - d\right)\mathbf{R}_3\left(-\left(\mu - \frac{\pi}{2}\right)\right)\boldsymbol{\rho}_{\mathrm{G}}. \tag{11.39}$$

It is convenient to use the local hour angle in further calculations. Because by current convention the Greenwich Hour Angle (μ) and longitude (λ) are measured in opposite directions, the local hour angle (θ) is

$$\theta = \mu + \lambda. \tag{11.40}$$

Applying Eq. 11.39 to Eq. 11.38, combining terms by multiple-angle formulae, substituting Eq. 11.40, and resolving the components along the unit vectors gives

$$\begin{aligned}
\xi &= \rho \cos\phi' \sin\theta \\
\eta &= \rho \sin\phi' \cos d - \rho \cos\phi' \sin d \cos\theta \\
\zeta &= \rho \sin\phi' \sin d + \rho \cos\phi' \cos d \cos\theta.
\end{aligned} \tag{11.41}$$

11.3.3.2 Geocentric Velocity

It will also be necessary to know how the observer is moving with respect to the fundamental plane. The components of the motion are rotations about the same two axes used in the coordinate transformation: rotation about the polar axis of the Earth because of both the rotation of the Earth and the motion of the Moon, and about the axis pointing to the equinox because of the motion of the Moon. In the geocentric rectangular equatorial system, the rotation vector is

$$\boldsymbol{\omega}_{\mathrm{G}} = \begin{bmatrix} \dot{d} \\ 0 \\ \dot{\mu} \end{bmatrix}. \tag{11.42}$$

Transforming to the fundamental plane,

$$\boldsymbol{\omega}_{\mathrm{F}} = \mathbf{R}_1\left(\frac{\pi}{2} - d\right)\boldsymbol{\omega}_{\mathrm{G}} = \begin{bmatrix} \dot{d} \\ \dot{\mu}\cos d \\ \dot{\mu}\sin d \end{bmatrix}. \tag{11.43}$$

The velocity of the observer with respect to the fundamental plane is

$$\dot{\boldsymbol{\rho}}_{\mathrm{F}} = \boldsymbol{\omega}_{\mathrm{F}} \times \boldsymbol{\rho}_{\mathrm{F}} = \mathbf{R}_1\left(\frac{\pi}{2} - d\right)\boldsymbol{\omega}_{\mathrm{G}} \times \boldsymbol{\rho}_{\mathrm{F}}. \tag{11.44}$$

The operation $\boldsymbol{\omega}_{\mathrm{F}}\times$ may be expressed as a matrix premultiplier:

$$\boldsymbol{\Omega} = [\boldsymbol{\omega}_x, \boldsymbol{\omega}_y, \boldsymbol{\omega}_z] = \begin{bmatrix} 0 & -\dot{\mu}\sin d & \dot{\mu}\cos d \\ \dot{\mu}\sin d & 0 & -\dot{d} \\ -\dot{\mu}\cos d & \dot{d} & 0 \end{bmatrix}. \tag{11.45}$$

Substitution of Eq. 11.45 into Eq. 11.44 yields

$$\dot{\boldsymbol{\rho}}_{\mathrm{F}} = \boldsymbol{\Omega}\boldsymbol{\rho}_{\mathrm{F}} = \begin{bmatrix} \dot{\mu}(-\eta\sin d + \zeta\cos d) \\ \dot{\mu}\xi\sin d - \dot{d}\zeta \\ -\dot{\mu}\xi\cos d + \dot{d}\eta \end{bmatrix}. \tag{11.46}$$

11.3.3.3 Coordinates of Observer with Respect to the Fundamental Plane, Corrected for Flattening

Consider a spheroid of ellipticity e. Geodetic positions are specified on the surface. Calculations of eclipse tracks in the fundamental plane are no problem, nor are local circumstances for a given point. However, in translating any point from the fundamental plane to the surface of the spheroid, evaluation of ζ requires knowing ρ, the distance of any point from the center of the Earth. This distance is a function only of latitude, so that ζ could be determined by successive approximation.

However, Bessel devised a procedure to provide a direct computation of ζ from ξ, η. This procedure requires a set of auxiliary Besselian elements, based on the Besselian element d and the ellipticity e of the spheroid.

Let a and b be the equatorial and polar radius, respectively, of the spheroid. Then

$$\begin{aligned} &\text{flattening, } f = \frac{a-b}{a}, \quad \text{and} \\ &\text{ellipticity, } e = (1 - b^2/a^2)^{1/2}. \end{aligned} \tag{11.47}$$

Define

$$C = (1 - e^2 \sin^2 \phi)^{-1/2}, \qquad S = (1 - e^2)C;$$

or

$$C = (\cos^2 \phi + (1 - f)^2 \sin^2 \phi)^{-1/2}, \qquad S = (1 - f)^2 C. \tag{11.48}$$

The relations between geocentric latitude ϕ' and geocentric distance of observer ρ and geodetic latitude ϕ are

$$\begin{aligned} \rho \sin \phi' &= S \sin \phi \\ \rho \cos \phi' &= C \cos \phi. \end{aligned} \tag{11.49}$$

To eliminate ρ and ϕ', transform to a parametric latitude ϕ_1, defined by:

$$\cos \phi_1 = \rho \cos \phi' = \frac{\cos \phi}{(1 - e^2 \sin^2 \phi)^{1/2}} \equiv C \cos \phi. \tag{11.50}$$

Then, from Eqs. 11.48, 11.49, and 11.50,

$$\sin \phi_1 = (1 - \cos^2 \phi_1)^{1/2} = \frac{\rho \sin \phi'}{(1 - e^2)^{1/2}}. \tag{11.51}$$

Inversely,

$$\begin{aligned} \rho \cos \phi' &= \cos \phi_1 &&\equiv C \cos \phi \\ \rho \sin \phi' &= (1 - e^2)^{1/2} \sin \phi_1 &&\equiv S \sin \phi. \end{aligned} \tag{11.52}$$

Substituting into Eq. 11.41,

$$\begin{aligned} \xi &= \cos \phi_1 \sin \theta \\ \eta &= \sin \phi_1 (1 - e^2)^{1/2} \cos d - \cos \phi_1 \sin d \cos \theta \\ \zeta &= \sin \phi_1 (1 - e^2)^{1/2} \sin d + \cos \phi_1 \cos d \sin \theta. \end{aligned} \tag{11.53}$$

Now to eliminate the terms in d and e, define

$$\begin{aligned} \text{in } \eta: \qquad \sin d &= \rho_1 \sin d_1 \\ (1-e^2)^{1/2} \cos d &= \rho_1 \cos d_1 \\ \text{in } \zeta: \qquad (1-e^2)^{1/2} \sin d &= \rho_2 \sin d_2 \\ \cos d &= \rho_2 \cos d_2. \end{aligned} \tag{11.54}$$

Then

$$\begin{aligned} \xi &= \cos\phi_1 \sin\theta \\ \eta_1 = \eta/\rho_1 &= \sin\phi_1 \cos d_1 - \cos\phi_1 \sin d_1 \cos\theta \\ \zeta &= \rho_2(\sin\phi_1 \sin d_2 + \cos\phi_1 \cos d_2 \cos\theta). \end{aligned} \tag{11.55}$$

Define

$$\zeta_1^2 = 1 - \xi^2 - \eta_1^2. \tag{11.56}$$

After extensive algebraic manipulation and reduction, this becomes

$$\zeta_1 = \sin\phi_1 \sin d_1 + \cos\phi_1 \cos d_1 \cos\theta. \tag{11.57}$$

It is desirable to eliminate ϕ_1 and θ. Then Eq. 11.55 combined with Eq. 11.57 may be written

$$\begin{bmatrix} \xi \\ \eta_1 \\ \zeta_1 \end{bmatrix} = \mathbf{R}_1(-d_1) \begin{bmatrix} \cos\phi_1 \sin\theta \\ \sin\phi_1 \\ \cos\phi_1 \cos\theta \end{bmatrix}. \tag{11.58}$$

Hence,

$$\begin{bmatrix} \cos\phi_1 \sin\theta \\ \sin\phi_1 \\ \cos\phi_1 \cos\theta \end{bmatrix} = \mathbf{R}_1(d_1) \begin{bmatrix} \xi \\ \eta_1 \\ \zeta_1 \end{bmatrix}. \tag{11.59}$$

Apply components of Eq. 11.59 to the expression for ζ in Eq. 11.55 and reduce to obtain

$$\zeta = \rho_2 \left[\zeta_1 \cos(d_1 - d_2) - \eta_1 \sin(d_1 - d_2)\right]. \tag{11.60}$$

11.3.3.4 Auxiliary Besselian Elements and Summary

The following defined quantities are part of a set known as *auxiliary elements*; more are defined in § 11.3.4.2. These elements are used to introduce the flattening of the Earth into the eclipse calculations. All quantities are in units of Earth's equatorial radius.

$$\begin{aligned} \rho_1 &= (1 - e^2 \cos^2 d)^{1/2} \\ \rho_2 &= (1 - e^2 \sin^2 d)^{1/2} \\ \sin d_1 &= \sin d/\rho_1 \\ \cos d_1 &= (1-e^2)^{1/2} \cos d/\rho_1 \\ \sin(d_1 - d_2) &= e^2 \sin d \cos d/\rho_1\rho_2 \\ \cos(d_1 - d_2) &= (1-e^2)^{1/2}/\rho_1\rho_2. \end{aligned} \tag{11.61}$$

(The subscripts *do not* refer to the umbra and penumbra.) In computation, all these quantities are carried with the regular elements at the same interval, even though ρ_1, ρ_2, and $(d_1 - d_2)$ are nearly constant for the duration of the eclipse. Once the elements are available and a point $(\zeta, \eta, 0)$ is given in the fundamental plane, then ϕ and ζ are obtained as follows: point (ξ, η_1, ζ_1) is calculated from the definitions of η_1 and ζ_1 in Eqs. 11.55 and 11.56. Next, Eq. 11.59 gives ϕ_1 and θ; Eq. 11.52 gives ϕ; and Eq. 11.60 or 11.53 gives ζ.

11.3.4 Conditional and Variational Equations

11.3.4.1 Introduction

This section establishes conditions by which eclipse phenomena may be distinguished and calculated.

11.3.4.2 Conditions Defining General Circumstances and Curves

Consider now the relation between observer and shadow. We have, in the fundamental plane reference system, the geocentric position of the observer $\boldsymbol{\rho} = (\xi, \eta, \zeta)$. The geocentric position of the intersection of the shadow axis with a plane through the observer parallel to the fundamental plane is

$$\mathbf{r} = \begin{bmatrix} x \\ y \\ \zeta \end{bmatrix}. \tag{11.62}$$

Now define the vector in the observer's plane from observer to shadow axis as

$$\boldsymbol{\Delta} = \mathbf{r} - \boldsymbol{\rho}. \tag{11.63}$$

In the plane through the observer, let Q be the position angle of the axis, measured from north through east, so that the unit vector

$$\hat{\boldsymbol{\Delta}} = \begin{bmatrix} \sin Q \\ \cos Q \\ 0 \end{bmatrix}. \tag{11.64}$$

The radius (L) of the shadow at height ζ above the fundamental plane is

$$L = l - \zeta \tan f \tag{11.65}$$

subscripted for umbra or penumbra, and L may be positive or negative.

Equations of condition. We may now impose geometric and dynamic conditions in order to calculate eclipse phenomena. We know $\mathbf{r}$. We may consider two cases from Eq. 11.63: one, in which $\boldsymbol{\rho}$ is not known but we wish to find the locus of all points satisfying a condition as a function of time (curve); the other, in which $\boldsymbol{\rho}$ is fixed and we want the times of significant configurations (circumstances).

Much of the following discussion applies to either case, the difference being the choice of knowns and unknowns. First, consider the more general cases, in which $\boldsymbol{\rho}$ is not known. The discussion applies to both umbra and penumbra, so the subscripts are omitted.

If the observer is on the edge of the shadow (penumbra or umbra) or, more generally, the surface of the shadow cone, the eclipse is either beginning or ending. This surface location may be defined by imposing the geometric condition

$$|\boldsymbol{\Delta}| = |L|, \quad \text{or} \quad \boldsymbol{\Delta} \cdot \boldsymbol{\Delta} - L^2 = 0. \tag{11.66}$$

Consider Eq. 11.66 now as a general expression that can be evaluated at any instant. The equation has two roots. If they are imaginary, then the observer is outside the shadow. If they are equal, then the eclipse is simultaneously beginning and ending—i.e., *grazing*—and the observer is on either the northern or southern limit of the shadow. This limit may be defined by imposing the dynamic condition

$$\frac{d}{dt}(\boldsymbol{\Delta} \cdot \boldsymbol{\Delta} - L^2) = 0$$

or

$$\boldsymbol{\Delta} \cdot \dot{\boldsymbol{\Delta}} - L\dot{L} = 0. \tag{11.67}$$

Since

$$|\boldsymbol{\Delta}| = |L|, \quad \text{this reduces to } \hat{\boldsymbol{\Delta}} \cdot \dot{\boldsymbol{\Delta}} - \dot{L} = 0. \tag{11.68}$$

It is always the case that $df/dt \approx 0$ for f_1 and f_2, so it is sufficiently accurate to use

$$\begin{aligned} \dot{L} &= \dot{l} - \dot{\zeta} \tan f \\ \dot{\zeta} &= \boldsymbol{\omega}_z \cdot \boldsymbol{\rho}. \end{aligned} \tag{11.69}$$

In Eq. 11.68, substitute

$$\begin{aligned} \dot{\boldsymbol{\Delta}} &= \dot{\mathbf{r}} - \dot{\boldsymbol{\rho}} \\ \dot{\boldsymbol{\rho}} &= \boldsymbol{\omega}_{\mathrm{F}} \times \boldsymbol{\rho}_{\mathrm{F}} = \boldsymbol{\omega}_{\mathrm{F}} \times (\mathbf{r} - \boldsymbol{\Delta}) \end{aligned}$$

to get

$$\hat{\boldsymbol{\Delta}} \cdot \dot{\mathbf{r}} - \hat{\boldsymbol{\Delta}} \cdot (\boldsymbol{\omega}_{\mathrm{F}} \times (\mathbf{r} - \boldsymbol{\Delta})) + \tan f \boldsymbol{\omega}_z \cdot (\mathbf{r} \cdot \boldsymbol{\Delta}) - \dot{l} = 0. \tag{11.70}$$

In the second term,

$$\hat{\boldsymbol{\Delta}} \cdot (\boldsymbol{\omega}_{\mathrm{F}} \times (\mathbf{r} - \boldsymbol{\Delta})) = \hat{\boldsymbol{\Delta}} \cdot (\boldsymbol{\omega}_{\mathrm{F}} \times \mathbf{r}). \tag{11.71}$$

From Eq. 11.45:

$$\begin{aligned} \boldsymbol{\omega} \times \mathbf{r} &= \begin{bmatrix} 0 & -\dot{\mu}\sin d & \dot{\mu}\cos d \\ \dot{\mu}\sin d & 0 & -\dot{d} \\ -\dot{\mu}\cos d & \dot{d} & 0 \end{bmatrix} \begin{bmatrix} x \\ y \\ \zeta \end{bmatrix} \\ &= \dot{\mu} \begin{bmatrix} -y\sin d + \zeta\cos d \\ x\sin d - \zeta\dot{d}/\dot{\mu} \\ -x\cos d + y\dot{d}/\dot{\mu} \end{bmatrix} \\ &= \dot{\mu} \begin{bmatrix} -y\sin d \\ x\sin d \\ -x\cos d \end{bmatrix} - \zeta \begin{bmatrix} -\dot{\mu}\cos d \\ \dot{d} \\ -y\dot{d}/\zeta \end{bmatrix}. \end{aligned} \tag{11.72}$$

From Eqs. 11.43, 11.45, and 11.66:

$$\boldsymbol{\omega}_{\mathrm{F}} = \begin{bmatrix} \dot{d} \\ \dot{\mu}\cos d \\ \dot{\mu}\sin d \end{bmatrix}, \qquad \boldsymbol{\omega}_z = \begin{bmatrix} -\dot{\mu}\cos d \\ 0 \\ 0 \end{bmatrix}, \qquad \boldsymbol{\Delta} = \hat{\boldsymbol{\Delta}}(l - \zeta \tan f). \tag{11.73}$$

Substitute these and Eqs. 11.66, 11.71, 11.72 into Eq. 11.70 and, through algebraic manipulation, collect terms as factors of $\boldsymbol{\Delta}\cdot$ and ζ to obtain

$$\boldsymbol{\Delta}\cdot\left\{\dot{\mathbf{r}} - \dot{\mu}\begin{bmatrix} -y\sin d \\ x\sin d \\ -x\cos d \end{bmatrix} - l\tan f\,\boldsymbol{\omega}_z\right\} + \zeta\{\sec^2 f\,\hat{\boldsymbol{\Delta}}\cdot\boldsymbol{\omega}_z\}$$
$$-\dot{l} + \tan f\,\boldsymbol{\omega}_z\cdot\mathbf{r} = 0. \tag{11.74}$$

Equation 11.74 may be written in component form as:

$$\begin{bmatrix} \sin Q \\ \cos Q \\ 0 \end{bmatrix}^T \left\{\begin{bmatrix} \dot{x} \\ \dot{y} \\ \dot{\zeta} \end{bmatrix} + \dot{\mu}\begin{bmatrix} y\sin d \\ -x\sin d \\ x\cos d \end{bmatrix} - l\tan f\begin{bmatrix} -\dot{\mu}\cos d \\ \dot{d} \\ 0 \end{bmatrix}\right\}$$
$$+\zeta\sec^2 f\begin{bmatrix} \sin Q \\ \cos Q \\ 0 \end{bmatrix}^T\begin{bmatrix} -\dot{\mu}\cos d \\ \dot{d} \\ 0 \end{bmatrix} - \dot{l} + \tan f\begin{bmatrix} -\dot{\mu}\cos d \\ \dot{d} \\ 0 \end{bmatrix}^T\begin{bmatrix} x \\ y \\ \zeta \end{bmatrix} = 0. \tag{11.75}$$

Additional auxiliary elements. Using a computer, Eq. 11.75 may be used in this form to find combinations of ζ, Q that satisfy it, and hence the limiting curves. For efficiency, however, it is conventional to define auxiliary quantities a, b, c with derivatives $\dot{a}, \dot{b}, \dot{c}$, there being a separate set for umbra and penumbra as distinguished by subscripting and use of the corresponding angle f, such that

$$\begin{bmatrix} \sin Q \\ \cos Q \\ 0 \end{bmatrix}^T\begin{bmatrix} \dot{c} \\ -\dot{b} \\ 0 \end{bmatrix} + \zeta\sec^2 f\begin{bmatrix} \sin Q \\ \cos Q \\ 0 \end{bmatrix}^T\begin{bmatrix} -\dot{\mu}\cos d \\ \dot{d} \\ 0 \end{bmatrix} + \dot{a} = 0. \tag{11.76}$$

Thus, to make Eq. 11.75 identical to Eq. 11.76,

$$\begin{aligned} \dot{a} &= -\dot{l} && - \dot{\mu}x\cos d\tan f && + y\dot{d}\tan f \\ \dot{b} &= -\dot{y} && + \dot{\mu}x\sin d && + l\dot{d}\tan f \\ \dot{c} &= \dot{x} && + \dot{\mu}y\sin d && + l\dot{\mu}\tan f\cos d. \end{aligned} \tag{11.77}$$

In older references, the approximations $\dot{d}\tan f_i = 0$, $\sec^2 f_i = 1$ are used, which are reasonable and adequate for limited computer resources.

Now collect terms in $\sin Q$, $\cos Q$:

$$\dot{a} + \sin Q(\dot{c} - \dot{\mu}\zeta\cos d\sec^2 f) + \cos Q(-\dot{b} + \zeta\dot{d}\sec^2 f) = 0. \tag{11.78}$$

Multiply by $\sec Q$ to obtain

$$\tan Q = \frac{\dot{b} - \dot{d}\,\zeta\sec^2 f - \dot{a}\sec Q}{\dot{c} - \dot{\mu}\,\zeta\sec^2 f\cos d}. \tag{11.79}$$

The application of this fundamental equation to calculate limits of the shadows will be described in § 11.3.5.5. In calculations for *The Astronomical Almanac*, the auxiliary quantities are calculated along with the Besselian elements and carried in an array as a function of time.

11.3.4.3 A Note on Practical Calculation

The Besselian elements, both regular and auxiliary, are nearly linear in behavior during an eclipse, such that integration or numerical differentiation seldom requires more than a third-order Lagrangian scheme, and linear interpolation is often adequate. In preparing computer programs and carrying elements in an array, however, it is always necessary to be sure that angular quantities change monotonically, especially when passing through 360°. It is also necessary to carry enough entries at the beginning and end of the eclipse to allow interpolation, but not so many that the behavior of the tabulated elements accelerates or reverses and potentially creates specious extrema.

Even though in calculations for *The Astronomical Almanac* all quantities are carried in double precision (15–16 digits), the published data should be considered accurate only to the number of significant figures presented.

11.3.5 Calculation of General Solar Eclipse Phenomena

11.3.5.1 Introduction

The Besselian and auxiliary elements are the basis of calculating all further phenomena associated with each eclipse, utilizing, of course, the necessary ephemeris data given in the eclipse section or elsewhere in *The Astronomical Almanac*. The eclipse section also gives positions on the surface of the Earth as a function of time, where well-defined phases or phenomena occur according to certain geometric or dynamical conditions—e.g., geocentric beginning and end of each phase. These data are given in tabular and graphical form, and are known as *general circumstances, elements* of the eclipse, and curves of several kinds. The independent variable, unless stated otherwise, is Universal Time. Conversely, for a given imposed condition, a time may be either deduced or assumed, and the coordinates $(\xi, \eta, 0)$ determined. Using the auxiliary elements ρ_1, ρ_2, d_1, d_2, the quantities ζ and (ξ, η_1, ζ_1) may be calculated and then transformed to $\lambda, \theta, \phi_1, \phi$. General circumstances are usually calculated before the curves, but for purposes of exposition, calculation of the curves is described first.

Eclipse curves are the loci of points on the spheroid of the Earth at some specified radius, usually the surface. These curves delineate set boundary conditions, and, hence, define areas within which certain eclipse phenomena are visible; they also show times of occurrence. They are produced by going through a table of Besselian elements as a function of time, calculating a table of derived discriminants, and evaluating whether imposed criteria are satisfied.

General circumstances (as opposed to local circumstances) are individual points and times at which extrema of the curves occur on the spheroid of reference.

11.3.5.2 Basic Geometry

In general, eclipse phenomena are treated and calculated using the fundamental triangle in the fundamental plane shown in Fig. 11.13.

By imposing various conditions and finding corresponding points in the fundamental plane, it is then but a relatively easy step to project the point to the surface and convert to latitude and longitude as described in § 11.3.3.

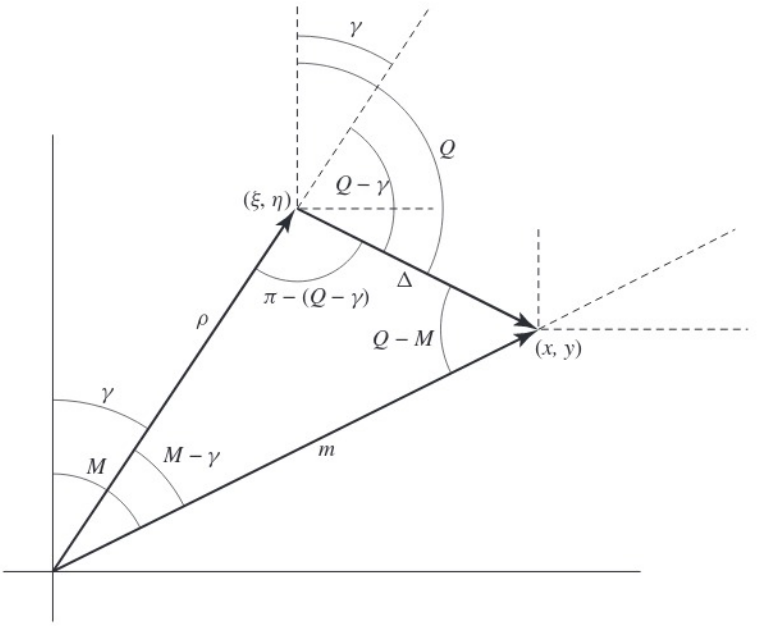


Figure 11.13 Relationship between rectangular and polar reference systems with the origins at the geocenter or the observer's projected point, in the fundamental reference plane. Angles are measured from the north, or y-axis. In the geocentric system, the observer's projected point may be specified as (ξ, η) or (ρ, γ); the shadow axis intercept may be specified as (x, y) or (m, M). In the reference system centered at the observer's projected point, the position of the shadow axis intercept is $(x - \xi, y - \eta)$ or (Δ, Q).

11.3.5.3 Relationships

The fundamental relationship of the geocenter $(0, 0)$, the projected axis of the shadow (x, y), and the projected position of the observer (ξ, η) is:

$$\boldsymbol{\rho} = \mathbf{m} - \boldsymbol{\Delta}. \tag{11.80}$$

As derived in § 11.3.4.2, if the point of the observer is "tangent" to the path of the shadow, such that the eclipse is beginning and ending simultaneously, then the second fundamental relation, which is a condition on Q, is (from Eq. 11.78)

$$a_i - b_i \cos Q + c_i \sin Q + \zeta(1 + \tan^2 f_i)(\dot{d} \cos Q - \dot{\mu} \cos d \sin Q) = 0, \quad i = 1 \text{ or } 2. \tag{11.81}$$

ρ is usually not unity; it contains flattening and height above the geoid.

These relationships are also used:

$$\begin{bmatrix} \xi \\ \eta \end{bmatrix} = \begin{bmatrix} x - \Delta \sin Q \\ y - \Delta \cos Q \end{bmatrix} = \begin{bmatrix} \rho \sin \gamma \\ \rho \cos \gamma \end{bmatrix}. \tag{11.82}$$

Furthermore, the cosine law for plane triangles (dot-product) gives

$$\begin{aligned}
\boldsymbol{\Delta}\cdot\boldsymbol{\Delta} = (\mathbf{m}-\boldsymbol{\rho})\cdot(\mathbf{m}-\boldsymbol{\rho}) \quad &\Leftrightarrow \cos(\gamma - M) = \frac{m^2+\rho^2-\Delta^2}{2m\rho} \\
\boldsymbol{\rho}\cdot\boldsymbol{\rho} = (\mathbf{m}-\boldsymbol{\Delta})\cdot(\mathbf{m}-\boldsymbol{\Delta}) &\Leftrightarrow \cos(Q - M) = \frac{m^2+\Delta^2-\rho^2}{2m\Delta} \\
\mathbf{m}\cdot\mathbf{m} = (\boldsymbol{\rho}+\boldsymbol{\Delta})\cdot(\boldsymbol{\rho}+\boldsymbol{\Delta}) \quad &\Leftrightarrow \sin(\gamma - Q) = \frac{\Delta^2+\rho^2-m^2}{2\Delta\rho}.
\end{aligned} \tag{11.83}$$

The sine law for planar trigonometry (cross-product) gives

$$\begin{aligned}
\mathbf{m}\times\boldsymbol{\Delta} &= \hat{\mathbf{k}}\Delta(x\cos Q - y\sin Q) \\
&= \hat{\mathbf{k}}\Delta m\sin(Q-M) \quad \text{and} \\
\boldsymbol{\rho}\times\boldsymbol{\Delta} &= (\mathbf{m}-\boldsymbol{\Delta})\times\boldsymbol{\Delta} = \mathbf{m}\times\boldsymbol{\Delta} \\
&= \hat{\mathbf{k}}\rho\Delta\sin(\gamma - Q).
\end{aligned} \tag{11.84}$$

Another useful relation is

$$2\sin^2\frac{1}{2}(\gamma - M) = 1 - \cos(\gamma - M) = \frac{(l-m+\rho)(l+m-\rho)}{2m\rho}. \tag{11.85}$$

11.3.5.4 Flattening

Flattening is taken into account by altering ρ and γ slightly to $r\rho$ and γ'. Assume that $\xi^2+\eta_1^2+\zeta_1^2 = r^2$. Now if $\zeta_1 = 0$, then $\xi^2+\eta_1^2 = r^2$. Let

$$\begin{aligned}
\xi &= r\rho\sin\gamma &&= r\sin\gamma' \\
\eta &= r\rho\cos\gamma &&= r\rho_1\cos\gamma' \\
\eta_1 &= \eta/\rho_1 &&= r\cos\gamma'.
\end{aligned} \tag{11.86}$$

Then

$$\tan\gamma' = \xi/\eta_1 = \rho_1\xi/\eta = \rho_1\tan\gamma \tag{11.87}$$

and

$$\frac{\sin\gamma'}{\sin\gamma} = \rho = \rho_1\frac{\cos\gamma'}{\cos\gamma}. \tag{11.88}$$

The following iterative procedure accounts for flattening. Ordinarily, three iterations are sufficient, for each of $\pm(\gamma - m)$.

To start, assume $|\boldsymbol{\rho}| = 1$, where $\boldsymbol{\rho} = |\xi, \eta|$ from Eq. 11.82 and Fig. 11.13

$$\begin{aligned}
&\text{(a)} \quad \sin\gamma = \xi/\rho, \quad \cos\gamma = \eta/\rho \\
&\text{(b)} \quad \tan\gamma' = \rho_1\sin\gamma/\cos\gamma \\
&\text{(c)} \quad \gamma' = \tan^{-1}(\tan\gamma') \\
&\text{(d)} \quad \rho = \sin\gamma'/\sin\gamma.
\end{aligned} \tag{11.89}$$

Repeat the steps of Eq. 11.89 three or more times, until convergence. Then $\xi = \sin\gamma'$, $\eta_1 = \cos\gamma'$ (and $\zeta_1 = 0$).

11.3.5.5 Curves

The order in which curves are computed is not important; computations are all done independently from the tabulated elements. However, it helps to leave computation of the outline curves until last.

Rising and setting curves. An observer who is at a point of intersection of the penumbral cone with the fundamental plane is also on the sunrise/sunset terminator and may, weather permitting, see a partial eclipse beginning or ending at sunrise or sunset. The locus of all such points on the Earth's surface, known as the rising and setting curve, is shown graphically on eclipse maps in *The Astronomical Almanac* with the label *Eclipse begins at sunrise*, *Eclipse ends at sunset*, and so on.

The rising and setting curve is the locus of end points of the outline curves for the penumbra as it intersects the terminator. At a selected instant, there are two points on the curve or no points. If there are two points, each belongs to one of two series. For a succession of instants, the two series of points trace different branches of the same curve and are joined at first contact (penumbra emerges from the terminator and intersects the Earth's surface) and last contact (penumbra merges completely into the terminator and leaves the Earth's surface). The track of the penumbra always generates at least one limit curve (see subtopic "Central line, duration of central eclipse, and width of path," below), either northern or southern, but if both the northern and southern limits exist for an interval of time (i.e., the central path is in equatorial regions), then during that interval the rising and setting curve does not exist—the penumbral shadow is completely emerged from the terminator. The result is that the rising and setting curve forms two separate loops like elongated teardrops, each loop being generated in two segments. Otherwise, if there is only one limiting curve, then the loops are joined, and the curve of rising and setting forms a distorted figure-eight. In either case, one loop or lobe is for rising, the other for setting. In a series of similar eclipses, both forms occur. When the first separation of the loops occurs in the series, the break into separate loops does not occur at the apparent node, but near it.

In the fundamental plane, the circle of the penumbral cone, at any instant, intersects the surface of the Earth in no points or in two points (which may occasionally be coincident). In the fundamental triangle,

$$\zeta = 0, \qquad \Delta = l_1 \qquad \text{are imposed conditions.} \tag{11.90}$$

If $\mathbf{R}_3$ is the matrix for positive rotation about the z-axis, then

$$\boldsymbol{\rho} \equiv \frac{\rho}{m}\mathbf{R}_3[\pm(\gamma - M)]\mathbf{m}. \tag{11.91}$$

i.e.,

$$\mathbf{R}_3 = \begin{bmatrix} \cos[\pm(\gamma - M)] & \pm\sin[\pm(\gamma - M)] & 0 \\ \mp\sin[\pm(\gamma - M)] & \cos[\pm(\gamma - M)] & 0 \\ 0 & 0 & 1 \end{bmatrix} \tag{11.92}$$

where one uses all top signs or all bottom signs.

If, by the cosine law (Eq. 11.83), $\cos(\gamma - M) < 0$, then there are no points on the curve for the selected instant.

Curves of maximum eclipse in the horizon. Any locus of points that satisfies the fundamental relation given in Eq. 11.81 (a dynamic constraint) is a curve of maximum eclipse. If the geometric conditions are also imposed that $\zeta = 0$, $\Delta = l_1$, then we have the curve of maximum eclipse at sunrise or sunset, or maximum eclipse in the horizon. On the map this curve approximately bisects the lobes of the rising and setting curves. It is continuous if the rising and setting curves are joined, otherwise not. It is also generated in two branches, as are the rising and setting curves.

From Eq. 11.81,

$$\begin{aligned} \zeta &= 0 \\ a_1 - b_1 \cos Q + c_1 \sin Q &= 0 \end{aligned} \tag{11.93}$$

and from Eq. 11.84,

$$\boldsymbol{\rho} \times \boldsymbol{\Delta} = \mathbf{m} \times \boldsymbol{\Delta} \Rightarrow \rho \sin(\gamma - Q) = x \cos Q - y \sin Q. \tag{11.94}$$

From Eq. 11.93 find two values of Q, then for each find a value of γ, then γ' as before (Eq. 11.89).

Points exist on these curves only if both these conditions are satisfied:

$$\sin(\gamma - Q) \leq 1 \quad \text{and} \tag{11.95}$$

$$(x - \xi)^2 + (y - \eta_1 \rho_1)^2 \leq l_1^2. \tag{11.96}$$

Central line, duration of central eclipse, and width of path. The central line is the locus of the points of intersection of the axis of the shadow with the surface of the Earth. The following conditions must be satisfied:

$$\begin{aligned} \boldsymbol{\rho} \cdot \mathbf{m} &= \rho m \\ \boldsymbol{\rho} \times \mathbf{m} &= 0 \\ \xi = x, \quad \eta = y, \quad \eta_1 &= y/\rho_1 \\ \xi^2 + \eta^2 + \zeta^2 &= r^2 \rho^2 \\ \xi^2 + \eta_1^2 + \zeta_1^2 &= r^2. \end{aligned} \tag{11.97}$$

From Eqs. 11.97 and 11.60:

$$\begin{aligned} \zeta_1 &= +(r^2 - \xi^2 - \eta_1^2)^{1/2} \\ \zeta &= \rho_2 [\zeta_1 \cos(d_1 - d_2) - \eta_1 \sin(d_1 - d_2)]. \end{aligned} \tag{11.98}$$

Points on the opposite side of the spheroid may be found by taking the negative values of ζ_1.

The duration of central eclipse may be estimated by disregarding vertical motion and considering only the instantaneous size and velocity of the intersection of the shadow with the plane through the observing point and parallel to the fundamental plane.

From the section on conditional and variational equations (Eq. 11.70):

$$\dot{\boldsymbol{\rho}}_{\mathrm{F}} = \boldsymbol{\omega}_{\mathrm{F}} \times \boldsymbol{\rho}_{\mathrm{F}}$$

has components

$$\begin{aligned} \dot{\xi} &= \dot{\mu}(-y \sin d + \zeta \cos d) \\ \dot{\eta} &= \dot{\mu} x \sin d - \dot{d} \zeta. \end{aligned} \tag{11.99}$$

Using the definitions

$$n^2 = (\dot{x} - \dot{\xi})^2 + (\dot{y} - \dot{\eta})^2$$
$$L_2 = l_2 - \zeta \tan f_2$$

the duration is

$$2L_2/n \qquad \text{(with appropriate sign).} \tag{11.100}$$

The units must be converted as necessary. Normally the conversion is from hours to seconds of time. Before 1982, L_2 had to be adjusted for different values of k.

In local circumstances, however, the accurate duration is the difference between appropriate pairs of contact times.

The width of the path, perpendicular to the direction of motion, may be estimated by a formula derived by Mikhailov (1931):

$$\text{width} = 2L_2 \left\{ \zeta^2 + \left[\frac{\xi}{n}(\dot{x} - \dot{\xi}) + \frac{\eta}{n}(\dot{y} - \dot{\eta}) \right]^2 \right\}^{-1/2}. \tag{11.101}$$

Northern and southern limits of umbra or penumbra. Each curve limiting a shadow path is the locus of points on the surface of the Earth's spheroid tangent to the path of the shadow, such that first and last contacts are simultaneous, or else maximum occurs in the horizon. The umbra nearly always has both limits on the surface because it is so small, but the penumbra often has only one. The northern and southern limits of the umbral track define the central path; the northern and/or southern limits of the penumbral track, plus the curve of rise and set, define the limits of the eclipse.

Impose the condition that Eq. 11.81 must be satisfied. Choose a value of ζ. If a complete set of limits is being generated, it is usual to begin with $\zeta = 0$. Then the coefficients of $\sin Q$ and $\cos Q$ are evaluated and the left-hand side of Eq. 11.81 is used as a discriminant. This discriminant is evaluated for a run of Q, starting from a first guess obtained by setting $\dot{a}_i = 0$, and proceeding a degree at a time until two zero points are found (by inverse interpolation when the discriminant changes sign). Then for each Q, iterate on ζ as follows, using Besselian elements:

$$L_i = l_i - \zeta \tan f_i$$
$$\xi = x - L_i \sin Q$$
$$\eta_1 = (y - L_i \sin Q)/\rho_1$$
$$\zeta_1^2 = r^2 - \xi^2 - \eta_1^2 \qquad \text{(If } \zeta_1^2 < 0\text{, there exists no point.)}$$

Normally choose $\zeta_1 \geq 0$ to continue. $\zeta_1 < 0$ may be used to continue the curve below the horizon.

$$\zeta = \rho_2[\zeta_1 \cos(d_1 - d_2) - \eta_1 \sin(d_1 - d_2)] \tag{11.102}$$
$$i = \text{umbra or penumbra.}$$

Put this value of ζ into Eq. 11.81, and repeat until it converges to the required tolerance. In *The Astronomical Almanac*, that is 10^{-5} Earth radii. In extremes of these curves, the iteration may begin oscillating about some mean value, in which case the mean is taken to continue the iteration.

When the iteration converges, then the point is assigned to a limit by the discriminant:

$$L_i \cos Q < 0 \text{ for northern limit}$$
$$L_i \cos Q > 0 \text{ for southern limit.} \tag{11.103}$$

The coordinates (ξ, η_1, ζ_1) are then easily converted to (ϕ, λ).

Outline curves. An outline curve of the shadow (umbra or penumbra) on the spheroid is the locus of all points at which the corresponding central or partial eclipse is beginning or ending at a given time. Outline curves for the penumbra, showing the places where the partial phase is beginning or ending at stated times, are plotted on the maps presented in *The Astronomical Almanac* and other publications. (See also § 11.3.6.1.) Outline curves of the umbra are not published. For all practical purposes, it is acceptable to neglect the flattening of the Earth in these calculations, but for the maps in *The Astronomical Almanac*, it is not neglected.

The angle Q becomes the independent variable. At the instant for which the curve is calculated, if both the northern and southern limits of the penumbra exist, then Q has the complete range of 0° to 360°. If not, the extreme values must be found; they are two points on the curve for which $\zeta = 0$. Because these points are on the limiting curves, in the computer program an initial test is made for the availability of points already computed for the limiting curves.

Those points are then verified from the equations

$$\begin{aligned} \xi &= x - L_i \sin Q \\ \eta_1 \rho_1 &= y - L_i \cos Q \\ \xi^2 + \eta_1^2 + \zeta_1^2 &= 1 \end{aligned} \tag{11.104}$$

in which $\zeta_1 = 0$. Once the end points are found and the correct portion of the arc which intersects the illuminated surface is established, points are calculated at one-degree steps of Q, iterating as described for the northern/southern limit curves and requiring $\zeta_1 > 0$. If desired for special purposes, points below the horizon may be found by using the solutions for $\zeta_1 < 0$.

Other curves. For 1960–1980, maps in the *American Ephemeris and Nautical Almanac* showed curves of equal middle and equal semiduration of eclipse. These curves were constructed graphically from the intersections of a network of outline curves, as there is no way to calculate them directly.

Curves of maximum eclipse are not prepared for regular publications, but may be readily calculated. Such calculations are an extension of the procedure for the curve of maximum eclipse in the horizon, in which the condition $\zeta = 0$ is removed, and ζ becomes the independent variable—i.e.,

Choose ζ;
Find Q (two values) from Eq. 11.81;
Find γ from $\sin(\gamma - Q) = (x \cos Q - y \sin Q)/r\rho$ (fundamental cross-product).

If neither value of Q gave an imaginary result, only one may be an eclipsed point in most cases. It is also required that

$$|\Delta| \le |L|, \quad \text{or} \quad (x - \xi)^2 + (y - \eta)^2 > L_i^2. \tag{11.105}$$

If this test is met, iteration may proceed as usual.

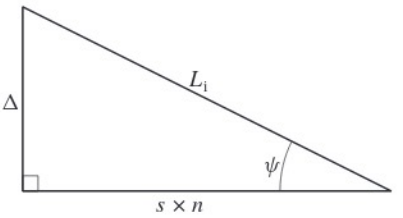


Figure 11.14 Definition of auxiliary quantity ψ. L is radius of the shadow in the plane of the observer, Δ is distance of observer from the axis, n is speed of separation, s is semiduration.

From maximum eclipse, semiduration of the partial phase may be estimated as follows. Define ψ in Fig. 11.14, where s is the semiduration and n is the speed of the shadow. The respective units are hours and equatorial radii per hour. Then

$$s = (L_i \cos \psi)/n,$$

where

$$\begin{aligned} \sin \psi &= \Delta / L_i \\ n^2 &= (\dot{x} - \dot{\xi})^2 + (\dot{y} - \dot{\eta})^2 \\ \dot{\xi} &= \dot{\mu} \cos \psi \cos \theta \\ \dot{\eta} &= \dot{\mu} \xi \sin d. \end{aligned} \tag{11.106}$$

The exact duration is found from the difference in times of first and last contacts, as described in § 11.3.6.2.

The magnitude of the eclipse is found from

$$\frac{L_1 - \Delta}{L_1 + L_2}. \tag{11.107}$$

If L_2 is not available, the approximation $L_2 = L_1 - 0.5459$ is used. (Subscript 1 for penumbra, 2 for umbra.)

Curves of equal semiduration or equal magnitude must be found by inverse interpolation on curves of maximum eclipse. (See § 11.3.6 on local circumstances for further discussion of magnitude.)

11.3.5.6 General Circumstances

A collection of event points known as *the general circumstances* are the important extrema of the curves of the eclipse. They define the bounds of the eclipse on the spheroidal surface and in time. They also join together the various curves and are essential in preparing the eclipse map. General circumstances are computed from the Besselian elements through a set of discriminants. For each discriminant, a table of values is calculated for a sequence of times, and used as described in the subtopics within this (§ 11.3.5.6) section. In practice, general circumstances are calculated before the complete curves are generated. If circumstances are required for high altitudes, the calculations are repeated for a larger spheroid.

The first and last contacts of the penumbra occur for every solar eclipse. They are the points where the shadow cone of the Moon first and last encounters the spheroidal surface. These points are shown on the eclipse maps as *First Contact* and *Last Contact*, and always lie on the rising and setting curve. The times at which they occur define the date(s) of the eclipse.

If the eclipse is central, then there are first and last contacts of the umbra. These are the extreme end points of the central line, and fall on the curve of maximum eclipse in the horizon.

For a central eclipse, there are also extreme points of the northern and southern limits of the central track. It is a rare occurrence when only one limit exists. These points also fall on the curve of maximum eclipse in the horizon.

The extreme points of the northern and southern limits of the penumbra fall on both the rising and setting curve and the curve of maximum eclipse in the horizon and, thus, mark the joining points. The extremes need not be known accurately; they are the points at which an observer theoretically could "see" the limb of the Moon brush the limb of the Sun for an instant. If the eclipse curves have been calculated taking flattening of the spheroid into account, the same must be done for these points or the curves will not link.

The point of central eclipse at local apparent noon or midnight is self-explanatory, i.e., maximum occurs on the meridian. Meridian passage at midnight may occur in the polar regions.

The point of greatest eclipse is calculated only for partial eclipses and shown on the eclipse map. It is the point on the spheroidal surface that comes closest to the axis of the shadow, and it lies on the curve of maximum eclipse in the horizon.

First and last contacts of the penumbra. First and last contacts of the penumbra occur when the shadow cone is tangential to the spheroid. Thus at two instants,

$$x^2 + y^2 = (l_1 + \rho)^2. \tag{11.108}$$

Taking the flattening of the Earth into account, let

$$\begin{aligned} m^2 &= x^2 + y^2 \\ m_1^2 &= x^2 + y_1^2 \\ y_1 &= y/\rho_1 \\ \rho &= m/m_1. \end{aligned} \tag{11.109}$$

Then $x^2 + y_1^2 = (l_1 + m/m_1)^2$ is the condition; the discriminant is

$$D_1 \equiv x^2 + y_1^2 - (l_1 + m/m_1)^2. \tag{11.110}$$

In the table of discriminants, the times of the contacts are calculated by inverse interpolation when $D_1 = 0$. These times are used to obtain x, y, and ρ_1. At the times of contact,

$$\begin{aligned} \xi &= x/m_1 \\ \eta_1 &= y_1/m_1 = y/\rho_1 m_1 \\ \zeta_1 &= 0 \end{aligned} \tag{11.111}$$

gives the data to compute latitude and longitude by successive approximation.

Beginning and end of central eclipse. Central eclipse begins and ends when the shadow axis is tangential to the Earth's surface—i.e.,

$$\begin{aligned} x^2 + y_1^2 &= 1 \\ \xi &= x \\ \eta_1 &= y_1 \\ \zeta_1 &= 0. \end{aligned} \tag{11.112}$$

The discriminant is

$$D_2 \equiv x^2 + y_1^2 - 1 \tag{11.113}$$

and the procedure is the same as for the penumbra.

Extreme points of umbral and penumbral limits. The extreme points of the limits of umbra and penumbra are found by setting $\zeta_1 = 0$ and then calculating tan Q from Eq. 11.79.

$$\begin{aligned} \cos Q &= \pm(1 + \tan^2 Q)^{-1/2} \\ \sin Q &= \cos Q \tan Q \\ \xi &= x - l_i \sin Q, \quad i = 1, 2, \\ \eta_1 &= (y \mp l_i \cos Q)/\rho_1, \quad i = 1, 2, \\ \xi^2 + \eta_1^2 &= 1. \end{aligned} \tag{11.114}$$

Note that the sign of cos Q determines whether the point is on the northern or southern limit. Note also that there are two cones and, therefore, four discriminants of the form

$$D_i \equiv (x - l \sin Q)^2 + \left(\frac{y - l \cos Q}{\rho_1}\right)^2 - 1, \quad i = 3, \ldots, 6. \tag{11.115}$$

Again, the times are found by inverse interpolation, and the coordinates, with flattening taken into account, by the usual procedure.

Central eclipse on the meridian. Central eclipse on the meridian—noon or midnight—is the point on the central line at conjunction of the Sun and the Moon in right ascension. The discriminant is x, and the condition is $x = 0$. Test the signs carefully in polar regions, to distinguish noon from midnight.

Greatest eclipse. In partial eclipses, the maximum magnitude, or greatest eclipse, occurs at the point on the surface of the spheroid that comes closest to the axis of the shadow. The magnitude changes very slowly, so high precision is not required. The eclipse will occur in the horizon at this point, and it is sufficient to find the time when the shadow axis is closest to the center of the Earth or when the rate of change of separation goes to zero. Hence, the discriminant is

$$D_7 \equiv x\dot{x} + y\dot{y}. \tag{11.116}$$

When the time is known, position is found as before. The distance of the observer from the axis is

$$\Delta = m - \rho. \tag{11.117}$$

The magnitude of the greatest eclipse for this case is

$$\frac{l_1 - \Delta}{l_1 + l_2}. \tag{11.118}$$

11.3.6 Local Circumstances

Before proceeding, the reader should review § 11.3.4 on conditional and variational equations. Local circumstances provide a description of eclipse phenomena relative to a fixed reference position, which is equivalent to fixing ρ as constant.

11.3.6.1 Eclipse Maps

The eclipse maps currently given in *The Astronomical Almanac* show the region over which various phases of each solar eclipse may be seen and the times at which phases occur. Each map is a plot of the curves described in § 11.3.5.5, except that outline curves are limited to those of the penumbra every hour.

The outline curves are divided into leading edge (in short dash) and trailing edge (in long dash). Except for certain extreme cases, the shadow outline moves generally from west to east. For a given location, first contact (the beginning of partial eclipse) occurs when the leading edge of the shadow arrives; similarly, last contact (the end of partial eclipse) occurs when the trailing edge arrives. First or last contact may be estimated from the map to within a few minutes.

11.3.6.2 Precise Calculations

There are many refinements to be considered in performing precise calculations: choosing a consistent ephemeris, corrections for Earth's rate of rotation, and, for the Moon, offset of center of figure from center of mass; correcting for irregularities of the lunar limb; and effects of the Earth's atmosphere (refraction in solar eclipses and the effect on the shadow in lunar eclipses).

Some elements (e.g., the radius of the shadow cone) used to describe an eclipse remain nearly constant for the duration. Elements that change do so very nearly linearly. In effect, an observer sees an eclipse as two disks of fixed size, one crossing the other in a straight line at constant speed.

In conventional notation, define u, v such that:

$$\mathbf{r} - \boldsymbol{\rho} = \begin{bmatrix} x - \xi \\ y - \eta \\ 0 \end{bmatrix} \equiv \begin{bmatrix} u \\ v \\ 0 \end{bmatrix} = \mathbf{m}. \tag{11.119}$$

The distance from the observer to the nearest point of the shadow axis is $|\mathbf{m}| \equiv m$. Let the relative velocity be $\mathbf{n} = \dot{\mathbf{m}}$, and then the relative speed is $|\mathbf{n}| \equiv n$. The rate of separation is $\mathbf{m} \cdot \mathbf{n}$, and maximum eclipse occurs when the shadow axis is closest to the observer, or $\mathbf{m} \cdot \mathbf{n} = 0$.

Contact times and duration. At the beginning or end of penumbral, or partial, phase, the condition is $m = L_1$. Similarly, if the chosen point is in the central path, then at the beginning or end of umbral phase $m = L_2$.

There are methods for finding the times of these phenomena by successive iteration, using approximations and auxiliary angles. However, it is simpler to tabulate u, v, L (where L is either radius) as a function of time, and also the discriminant $u^2 + v^2 - L^2$. When the discriminant goes to zero, inverse interpolation gives the time of the local contact. Duration is the difference between the two contact times for the umbra.

Position angles. The projected shadow is a reflection of what the observer sees in the sky, so the position angle of contact, Q, may be found from

$$\mathbf{m} = \begin{bmatrix} L \sin Q \\ L \cos Q \\ 0 \end{bmatrix}. \tag{11.120}$$

The angle Q is measured eastward from the north, on the solar limb as the observer sees it, or the projected shadow circle on the imaginary plane of reference. From the observer's point of view, however, the vertex (up) is not usually north. The parallactic angle C, defined by $\tan C = \xi/\eta$, is the measure of the difference. The position angle V of the contact point from the vertex is

$$V = Q - C. \tag{11.121}$$

Magnitude and obscuration. Magnitude is commonly confused with obscuration. Magnitude is defined as the fraction of the solar diameter covered by the Moon at the time of greatest phase and is expressed in units of the solar diameter. Obscuration is the fraction of the surface of the solar disk obscured by the Moon.

In the case of a total eclipse, the magnitude can be greater than 1.0. To derive the expression, however, consider the annular case shown in Fig. 11.15. An observer at point B in the penumbra sees part $S'B'$ of the solar diameter blocked off, whereas an observer at point E in the umbra sees the Moon's entire disk projected in DD' on the Sun, SS'.

The known quantities are

$$\begin{aligned} P'O &= PO = L_1 \\ fA'O &= AO = L_2 \\ BO &= m. \end{aligned} \tag{11.122}$$

$$\begin{aligned} \text{At B, magnitude } M_1 &= S'B'/SS' \\ &= PB/PA' \text{ by simple proportion} \\ &= (PO - BO)/(PO + OA') \\ &= (L_1 - m)/(L_1 + L_2). \end{aligned} \tag{11.123}$$

$$\begin{aligned} \text{At E, magnitude } M_2 &= DD'/S'S \\ &= (S'D - S'D')/S'S \\ &= PE/PA' - AE/PA' \\ &= PA/PA' \\ &= (L_1 - L_2)/(L_1 + L_2). \end{aligned} \tag{11.124}$$

For a total eclipse, in which the plane is on the other side of the vertex, A and A' are reversed, so that $OA = -L_2$, and the expression is identical. Note also that this is the diameter of the lunar disk in units of the diameter of the solar disk.

The degree of obscuration is now calculated using L_1, L_2, and m. In Fig. 11.16, A is the center of the lunar disk, B is the center of the solar disk. The disks overlap, with intersections at C, C'. The line AB joins the centers and intersects the circumferences and the chord CC' at

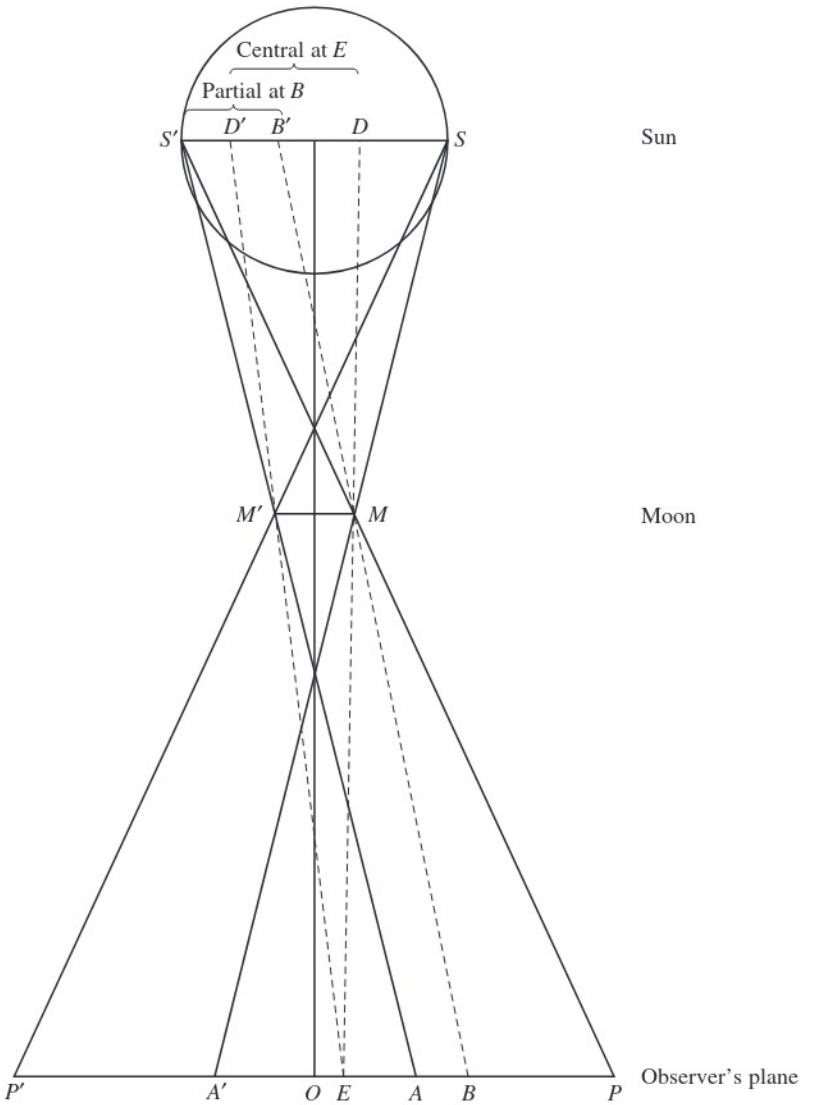


Figure 11.15 Magnitude is the fraction of the linear diameter of the Sun covered by the Moon. In this schematic of an annular eclipse, in the observer's plane, $A'A$ is the zone of annularity. To an observer within that zone at point E, the Moon's cross-section MM' projects onto SS' as DD'. Hence the magnitude is $D'D/S'S$. To an observer at point B in the zone of partial eclipse, $S'B'$ is obscured, hence the magnitude is $S'B'/S'S$.

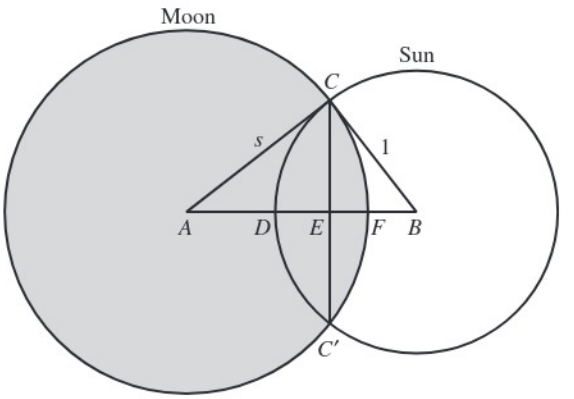


Figure 11.16 Obscuration is the fraction of the area of the solar disk obscured by the Moon. Here it is the ratio of the area of segment $CDC'F$ to the area of the solar disk.

the indicated points. Let the lunar radius be $s = AC$. The solar radius is taken as unity; hence $BC = 1$ and $AC = M_2 \equiv s$. By definition also, and in units of solar radius, $M_1 = DF/2$, or $DF = 2M_1$. Finally,

$$AB = 1 + s - DF. \tag{11.125}$$

In terms of known quantities, then

$$\begin{aligned} BC &= 1 \\ AC = M_2 &= \frac{L_1 - L_2}{L_1 + L_2} \equiv s \\ DF &= 2\frac{L_1 - m}{L_1 + L_2} \\ AB &= 1 + \frac{L_1 - L_2}{L_1 + L_2} - \frac{2(L_1 - m)}{L_1 + L_2} = \frac{2m}{L_1 + L_2}. \end{aligned} \tag{11.126}$$

The area of the solar disk covered by the Moon is given by

$$S = \text{segment } CFC' + \text{segment } CDC', \tag{11.127}$$

$$\begin{aligned} \text{segment } CFC' &= 2(\text{sector } ACF - \text{triangle } ACE) \\ \text{segment } CDC' &= 2(\text{sector } BCD - \text{triangle } BCE). \end{aligned} \tag{11.128}$$

Using angles in radians:

$$\begin{aligned} \text{Area of sector } ACF &= sA \\ \text{Area of sector } BCD &= B \\ CE &= s \sin A = \sin B \\ AE &= s \cos A \\ EB &= \cos B. \end{aligned} \tag{11.129}$$

Substituting into Eqs. 11.128 and then Eq. 11.127:

$$\text{segment } CFC' = 2\left(\frac{1}{2}s^2A - \frac{1}{2}s^2 \sin A \cos A\right)$$

$$\text{segment } CDC' = 2\left(\frac{1}{2}B - \frac{1}{2}\sin B \cos B\right)$$

$$\begin{aligned} S &= (s^2A + B) - (s^2 \sin A \cos A + \sin B \cos B) \\ &= (s^2A + B) - s \sin C. \end{aligned} \tag{11.130}$$

The area of the solar disk is π; hence the obscuration as a fraction of the disk is $S' = S/\pi$.

The angles A, B, and C may be evaluated from fundamental rules of trigonometry. The working relations are:

$$\begin{aligned} \cos C &= (L_1^2 + L_2^2 - 2m^2)/(L_1^2 - L_2^2), \quad 0 \le C \le \pi \\ \cos B &= (L_1L_2 + m^2)/m(L_1 + L_2), \qquad 0 \le B \le \pi \\ A &= \pi - (B + C). \end{aligned} \tag{11.131}$$

If an observer wishes to construct a diagram showing the exact relationships of the disks during the course of an eclipse, it is useful to have calculated these quantities at a convenient tabular interval. Note that during central phase, all intersections cease to exist and the quantities are undefined. During that phase, for an annular eclipse $S' = s^2$; for a total eclipse, $S' = 1$.

11.3.6.3 Differential Corrections in Space and Time

Differential corrections were in times past used to adjust precisely calculated local circumstances to nearby locations. However, computing equipment has reached such a stage of advancement that differentials have fallen into disuse in favor of repeating the whole calculation for the new site.

Calculations are normally provided in provisional Universal Time (UT) or, more precisely, UT1 (see § 3.2.2) using a predicted value of ΔT. For record purposes this is not necessarily the best practice, but for the convenience of users it was deemed significant enough to be necessary. If a later value of ΔT is adopted—such that the offset becomes $\Delta T + \delta T$—then tabular quantities may be corrected quite easily by applying

$$\delta\lambda = -1.002738\,\delta T \quad \text{(longitude measured eastward)} \tag{11.132}$$

to all longitudes in the tabulated phenomena, and subtracting δT algebraically from all tabulated times expressed in UT. Finally, interpolate the table back to the original arguments.

For calculation of circumstances at elevations above the spheroid, the assumed radius of the Earth is increased accordingly and the calculations repeated.

11.4 Lunar Eclipses

11.4.1 Introduction

The calculation of lunar eclipses follows the same principles as that of solar eclipses. The fundamental plane is perpendicular to the axis of the shadow, and the origin of coordinates

is the shadow's axis. The z-coordinate is not used. Since the observer is on the body that is casting the shadow, the circumstances are the same for all parts of the Earth from which the Moon is visible.

The criteria for the occurrence of a lunar eclipse, and the definitions of the types that may occur, are given in § 11.2.3.

11.4.2 Computations

Equations 11.13 and 11.14 define specific values of the separation of centers at which contacts occur (see Fig. 11.4). By conventional notation deriving from solar eclipses, the angular distance between the centers of the Moon and the shadow is designated L and at times of contact has values as follows:

$$\begin{aligned} &\text{at beginning and end of the penumbral eclipse,} && L_1 = f_1 + s_\mathrm{m};\\ &\text{at beginning and end of the umbral eclipse,} && L_2 = f_2 + s_\mathrm{m};\\ &\text{at beginning and end of the total eclipse,} && L_3 = f_2 - s_\mathrm{m}. \end{aligned} \tag{11.133}$$

As is the case for solar eclipses, for dates when a lunar eclipse is to be calculated, apparent ephemerides of the Sun and the Moon are generated at a suitable interval, by subtabulation if necessary. The usual interval is 10 minutes. The ephemeris is corrected for the offset of the center of figure from the center of mass, as appropriate for the chosen ephemeris, and the argument is changed to UT by applying ΔT.

11.4.2.1 Besselian Elements

As in § 11.3.2.2 and Eq. 11.24, the geocentric unit vector to the Sun, in an equatorial system, is

$$\mathbf{r}_\mathrm{sG} = \begin{bmatrix} \cos\alpha_\mathrm{s}\cos\delta_\mathrm{s} \\ \sin\alpha_\mathrm{s}\cos\delta_\mathrm{s} \\ \sin\delta_\mathrm{s} \end{bmatrix}. \tag{11.134}$$

It follows that the vector of the antisolar point, along the axis, is $\mathbf{r}_\mathrm{aG} = -\mathbf{r}_\mathrm{sG}$. This vector corresponds to $\mathbf{g}$ in Eq. 11.25, with $a = \alpha_\mathrm{s} + 12^\mathrm{h}$, $d = -\delta_\mathrm{s}$, for a geocentric system and eliminates the step of solving for (a, d). To transform the Moon's position to a geocentric system in which the z-axis is parallel to the axis of the shadow, apply the same rotations as given in Eq. 11.26, but for units use seconds of arc. This calculation gives Eqs. 11.29, without the unit conversion factor, and from which only (x, y) in the fundamental plane are used.

To summarize:

$$\mathbf{r}_\mathrm{aG} = \begin{bmatrix} \cos a\cos d \\ \sin a\cos d \\ \sin d \end{bmatrix} = -\mathbf{r}_\mathrm{sG} = \begin{bmatrix} -\cos\alpha_\mathrm{s}\cos\delta_\mathrm{s} \\ \sin\alpha_\mathrm{s}\cos\delta_\mathrm{s} \\ -\sin\delta_\mathrm{s} \end{bmatrix}. \tag{11.135}$$

$$\begin{aligned} \mathbf{r}_\mathrm{mF} = \mathbf{R}_1\left(\frac{\pi}{2} - d\right)\mathbf{R}_3\left(a + \frac{\pi}{2}\right)\mathbf{r}_\mathrm{mG} &= \begin{bmatrix} \cos\delta_\mathrm{m}\sin(\alpha_\mathrm{m} - a) \\ \sin\delta_\mathrm{m}\cos d - \cos\delta_\mathrm{m}\sin d\cos(\alpha_\mathrm{m} - a) \\ \sin\delta_\mathrm{m}\sin d + \cos\delta_\mathrm{m}\cos d\cos(\alpha_\mathrm{m} - a) \end{bmatrix} \\ &= [\,x \quad y \quad z\,]^T \end{aligned} \tag{11.136}$$

where

$$d = -\delta_s$$
$$a = \alpha_s + \pi.$$

In the fundamental plane—i.e., where $z = 0$—the separation is

$$m = (x^2 + y^2)^{\frac{1}{2}}. \tag{11.137}$$

Call the vector form $\mathbf{m}$. The hourly variation, $\dot{\mathbf{m}}$, is found by numerical differentiation or, if a polynomial representation is used, by differentiating the polynomial.

The Besselian elements for a lunar eclipse are x, y, $\dot{x}$, $\dot{y}$, m, L_1, L_2, L_3, f_1, f_2. There is no widely accepted convention, however, and the elements are not published in *The Astronomical Almanac*.

11.4.2.2 Contact Times

The contact times can now be found by either of two methods.

One method is to choose a time T_0 near opposition, with corresponding $\mathbf{m}_0$, $\dot{\mathbf{m}}_0$. For a contact at time $T = T_0 + t$, in which t is positive or negative and L is chosen from Eq. 11.133,

$$(\mathbf{m}_0 + \dot{\mathbf{m}}_0\, t) \cdot (\mathbf{m}_0 + \dot{\mathbf{m}}_0\, t) = \mathbf{L} \cdot \mathbf{L}. \tag{11.138}$$

Equation 11.138 may be solved as a quadratic equation in t; use the two roots to estimate the two contacts. The two times may then be used to start a second iteration, and convergence is very rapid.

Alternatively, the following discriminants may be tabulated as a function of time:

$$L_1 - m$$
$$L_2 - m$$
$$L_3 - m \tag{11.139}$$

for a timespan starting before opposition such that initially $m \approx 1.5L_1$, and continuing until the first discriminant has passed through zero twice.

No approximations or manipulations are necessary. At each time step, the discriminants are examined for a change of sign from the preceding step; when a change occurs, find the time of the zero by inverse interpolation. The cases that may occur appear in Table 11.2, and must occur in the sequence indicated.

In special cases where examination indicates that one phase might have begun and ended within a single tabular interval, subtabulation or the alternative method of polynomial iteration may be necessary.

11.4.2.3 Time of Greatest Obscuration

The time of greatest obscuration occurs when the axis of the shadow is closest to the center of the Moon, or when $\mathbf{m}$ is a minimum:

$$\frac{d}{dt}(\mathbf{m} \cdot \mathbf{m}) = 0 \quad \text{or} \quad \mathbf{m} \cdot \dot{\mathbf{m}} = 0. \tag{11.140}$$

The quantity

$$\mathbf{m} \cdot \dot{\mathbf{m}} = x\dot{x} + y\dot{y} \tag{11.141}$$

may also be tabulated as a discriminant and the zero found by inverse interpolation.

Table 11.2 Sequences and conditions for contact times

Start[a]	Condition	End
No eclipse	$L_1 - m < 0$	No eclipse
Penumbral eclipse begins	$L_1 - m = 0$	Penumbral eclipse ends
Penumbral eclipse	$L_1 - m > 0$ and $L_2 - m < 0$	Penumbral eclipse
Partial eclipse begins	$L_2 - m = 0$ and $L_3 - m < 0$	Partial eclipse ends
Partial eclipse	$L_3 - m < 0$	Partial eclipse
Total eclipse begins	$L_3 - m = 0$	Total eclipse ends
Total eclipse	$L_3 - m > 0$	Total eclipse

[a] Note: The events in the leftmost column of the table occur in sequence from the top down, and in the rightmost column of the table, from the bottom up.

11.4.2.4 Magnitude

The magnitude is the fraction of the Moon's diameter covered by shadow, in units of the lunar diameter. As published, magnitude corresponds only to the maximum obscuration, but for use in special calculations, it may be calculated as a function of time for both umbra and penumbra.

The expression is

$$\frac{L_i - m}{2s_{\mathrm{m}}}, \quad i = 1,\ 2 \tag{11.142}$$

in which L_1 is used for penumbral magnitude and L_2 for umbral magnitude. Magnitude may be greater than unity, but not negative.

11.4.2.5 Position Angles

The position angle of contact P on the limb of the Moon is the position angle M of **m** at the instant of contact, measured eastward (clockwise) from the north; i.e.,

$$\begin{aligned} \tan M &= x/y \\ P &= M \qquad\quad \text{for interior contacts} \\ &= M + 180^\circ \quad \text{for exterior contacts.} \end{aligned} \tag{11.143}$$

11.4.2.6 Sub-lunar Points

The latitudes (ϕ) and longitudes (λ) of places that have the Moon in the zenith at given times are given by

$$\begin{aligned} \phi &= \delta_{\mathrm{m}} \\ \lambda &= \text{Greenwich Apparent Sidereal Time} - \alpha_{\mathrm{m}}. \end{aligned} \tag{11.144}$$

For a given position (ϕ_0, λ_0) found from this, the horizon circle is the locus of points on a great circle that satisfy the condition:

$$\tan\phi = -\cot\phi_0 \cos(\lambda_0 - \lambda). \tag{11.145}$$

Values of λ may be assumed and coordinate pairs calculated. The hemisphere defined by this central point and horizon circle is where the Moon is above the horizon at the instant.

11.5 Eclipses Online

Eclipses Online, found at URL[2], is a canon of solar and lunar eclipse information for phenomena in the period A.D. 1501 to A.D. 2100. Currently, it provides information on a total of 2881 eclipses composed of 1421 solar eclipses and 1460 lunar eclipses.

It was originally designed to provide both local and general circumstances for solar eclipses and general circumstances for lunar eclipses. These web pages can be seen as a partial replacement for the eclipse information formerly provided in the circulars produced by the U.S. Naval Observatory (see § 11.1.1.3). Having selected a particular year, the eclipses occurring during that year are listed. This in turn provides the necessary links to the individual eclipse pages themselves. The software underpinning the general information on the site is that used in *The Astronomical Almanac*. Consequently, predictions make use of the fractional radius of the Moon, k, adopted by the IAU although values of quantities such as ΔT may be different than those used in *The Astronomical Almanac* for the appropriate year.

11.5.1 Solar Eclipses

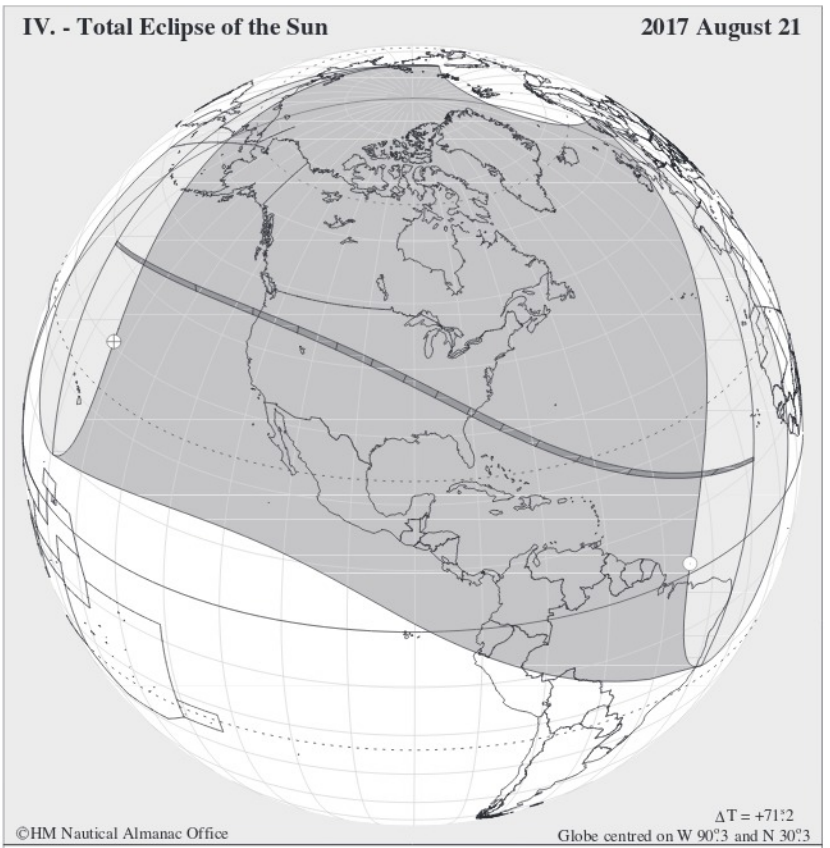
Typical solar eclipse information starts with a global view of the eclipse showing an orthographic projection of the eclipse "footprint" and, where appropriate, the areas of the globe from which partial, annular or total eclipses can be seen denoted by different types of shading. Light shading indicates which parts of the eclipse footprint take place at sunrise and sunset and medium shading denotes the parts of the footprint where the whole eclipse can be viewed. The darkest shading indicates the path of totality, annularity or a combination of both for total, annular and hybrid eclipses, respectively.

A number of curves are plotted on the diagram indicating the northern and southern limits of the penumbral shadow where appropriate, the start and end of the eclipse at both sunrise and sunset and maximum eclipse at sunrise and sunset. Where appropriate, the northern and southern limits of totality or annularity are also given. For all eclipses, the point at which the shadow first contacts the Earth's surface is denoted by ($\oplus$) and similarly where the shadow leaves the Earth's surface by ($\odot$). In the case of a partial eclipse, the point of greatest eclipse is denoted by ($\otimes$).

The title of the diagram includes the type of eclipse, its place in the sequence of eclipses of the year and the Greenwich calendar date of the eclipse. At the foot of the diagram, the adopted ΔT value is given as well as the point on the Earth's surface at which the projection is centered.

A summary of the general circumstances is given below the plot. This includes the time and location of the first and last contact of the shadow with the Earth's surface, greatest eclipse in the case of a partial eclipse including the maximum magnitude of the eclipse, the beginning and end of the northern and southern penumbral limits where appropriate, the beginning and end of the northern and southern umbral limits and the central line limits where appropriate in the case of annular, total and hybrid eclipses, and also central eclipse at local noon. The symbols described above are repeated with this information. An example of a solar eclipse diagram for the 2017 August 21 total eclipse of the Sun can be found in Fig. 11.17.

An animation of the eclipse is provided using software developed by Dr. Andrew Sinclair, a former head of HM Nautical Almanac Office. This combines the umbral and penumbral shadows of the eclipse and the motion of the day/night terminator depicted at five-minute



Circumstances	Time (UT) h m	Longitude ° ′	Latitude ° ′
⊕ Eclipse begins; first contact with Earth	15 46.8	W153 04.5	N30 32.5
Beginning of southern limit of penumbra	16 32.9	W159 18.4	N 8 38.7
Beginning of southern limit of umbra	16 48.8	W171 24.4	N39 27.7
Beginning of centre line; central eclipse begins	16 49.0	W171 34.3	N39 43.9
Beginning of northern limit of umbra	16 49.3	W171 44.3	N40 00.2
Beginning of northern limit of penumbra	18 06.2	E 71 40.1	N77 34.4
Central eclipse at local apparent noon	18 13.2	W 92 32.5	N38 55.3
End of northern limit of penumbra	18 45.1	E 12 38.4	N61 55.3
End of northern limit of umbra	20 01.8	W 27 18.7	N11 16.1
End of centre line; central eclipse ends	20 02.1	W 27 25.7	N11 00.9
End of southern limit of umbra	20 02.3	W 27 32.7	N10 45.8
End of southern limit of penumbra	20 18.0	W 38 11.4	S20 17.2
⊙ Eclipse ends; last contact with Earth	21 04.3	W 44 59.0	N 1 42.2

Figure 11.17 Example of solar eclipse diagrams found on *Eclipses Online* site.

intervals. It also shows the Greenwich date of the start of the eclipse, the current UT time and the duration of annularity or totality appropriate to the eclipse being displayed.

Local circumstances are provided based on a gazetteer of some 1500 locations around the world made up of major population centers, capitals of countries and a number of places providing a good distribution of locations around the world. Those locations falling in the footprint of the eclipse are listed. The exceptions are those locations within the region delimited by the "maximum eclipse at sunrise" curve and "eclipse ends at sunrise" curve, and its counterpart, the region delimited by the "maximum eclipse at sunset" curve and "eclipse begins at sunset" curve. These exceptions will be removed in a future revision of the site.

The table of locations lying within the footprint meeting the condition mentioned previously provides access to both a local circumstances diagram and an animation of the eclipse as seen from that location. Those locations in the path of annularity or totality are highlighted. Each location also provides a link to the eclipse history of that location between A.D. 1501 and A.D. 2100.

The local circumstances plot shows the orientation of the Sun and Moon (denoted by a dashed circular outline) at first and last contact with either (1) in the outline to denote first contact or (4) to denote last contact. The Sun is shown as it appears at maximum eclipse. This may be a yellow, partially-obscured Sun denoting the maximum partial eclipse, a black disk surrounded by a white serrated edge denoting a total eclipse or a black circle with a yellow ring around it denoting an annular eclipse. The title of the plot includes the location and country for which the diagram has been constructed, the latitude and longitude of the location, the Greenwich date and the maximum obscuration of the eclipse expressed as a percentage. The times of the principal phases of the eclipse from the selected location are given below the plot in UT.

The animation itself is an animated Graphics Interchange Format (GIF) file showing the progress of the eclipse. The Moon is displayed as a dashed circular outline and the Sun as a yellow disk. The relative orientation of the Sun and Moon is displayed at one-minute intervals during the partial phase of the eclipse dropping to ten-second intervals for totality or annularity as appropriate. The eclipsed part of the Sun is shown as a black area. Totality is denoted in the same manner as the local circumstance plot. The title of the animation includes the chosen location and country and the current Greenwich date. The lower part of the animation shows the current azimuth, altitude and obscuration of the Sun, the UT time and the status of the eclipse. The horizon is also depicted as a brown region when the eclipse occurs at around sunrise or sunset.

At the foot of the page is the eclipse listing for the year and, in a handful of cases, additional information connected with the eclipse is give such as historical information or some significant event connected with the eclipse.

11.5.2 Lunar Eclipses

In the case of lunar eclipses, the eclipse information is provided in the same way as it is in *The Astronomical Almanac* since the 2005 edition. A full description of the plot can be found below and an example of a lunar eclipse diagram for 2014 April 15 can be found in Fig. 11.18.

Information on lunar eclipses is presented in the form of a diagram consisting of two parts. The upper panel shows the path of the Moon relative to the penumbral and umbral shadows

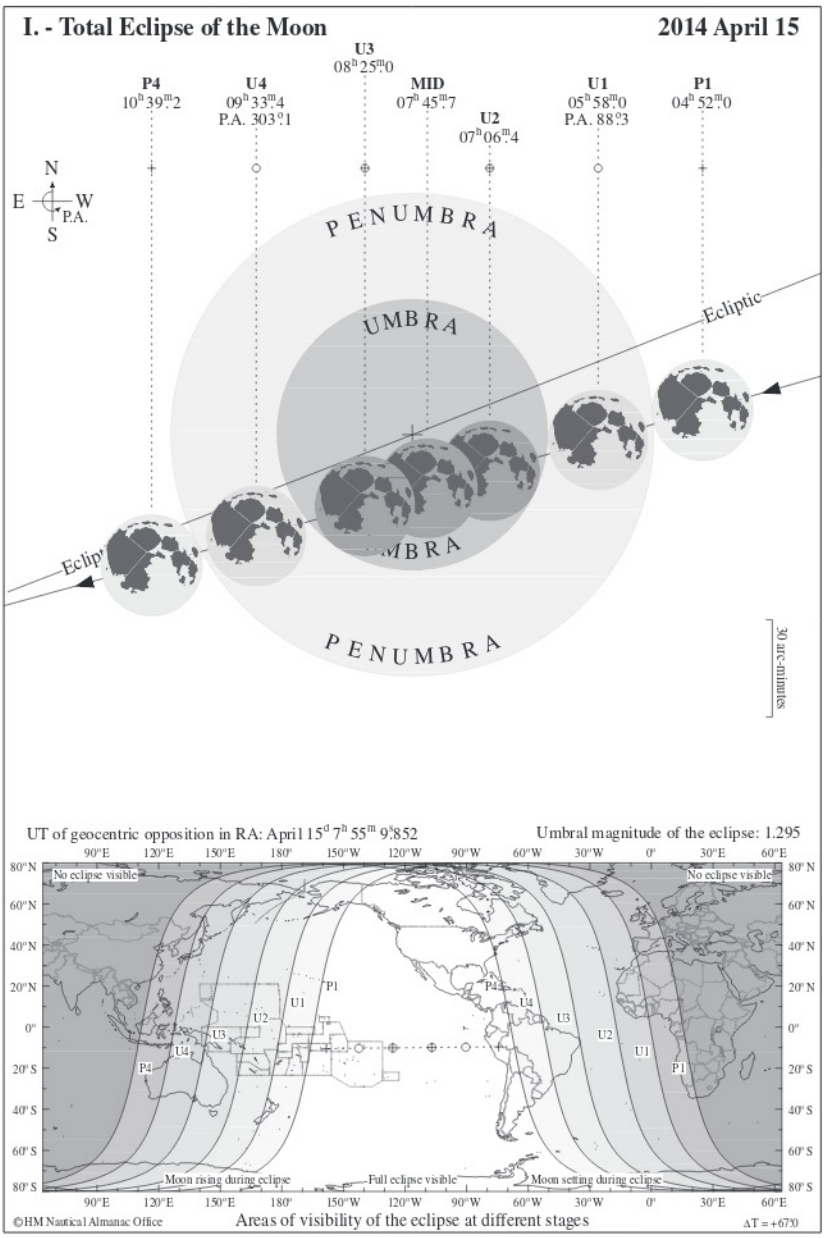


Figure 11.18 Example of lunar eclipse diagrams found on *Eclipses Online* site.

of the Earth. The lower panel shows the visibility of the eclipse from the surface of the Earth. The title of the upper panel includes the type of eclipse, its place in the sequence of eclipses of the year and the Greenwich calendar date of the eclipse. The inner darker circle is the umbral shadow of the Earth and the outer lighter circle is that of the penumbra. The axis of the shadow of the Earth is denoted by (+) with the eclipse shown for reference purposes. A 30-arcminute scale bar is provided on the right-hand side of the diagram and the orientation is given by the cardinal points displayed on the small graphic on the left-hand side of the diagram. The position angle (PA), printed for the first and fourth umbral contacts, is measured from the North point of the lunar disk through East along the limb of the Moon to the point of contact. For convenience, the general direction of this measurement is shown on the graphic by the use of an arc extending anti-clockwise (eastwards) from North terminated with an arrow head.

Moon symbols are plotted at the principal phases of the eclipse to show its position relative to the umbral and penumbral shadows. The UT times of the different phases of the eclipse to the nearest tenth of a minute are printed above or below the Moon symbols as appropriate. P1 and P4 are the first and last external contacts of the penumbra, respectively, and denote the beginning and end of the penumbral eclipse, respectively. U1 and U4 are the first and last external contacts of the umbra denoting the beginning and end of the partial eclipse, respectively. U2 and U3 are the first and last internal contacts of the umbra and denote the beginning and end of the total phase, respectively. MID is the middle of the eclipse. The position angle is given for P1 and P4 for penumbral eclipses and U1 and U4 for partial and total eclipses. The UT time of the geocentric opposition in right ascension of the Sun and Moon and the magnitude of the eclipse are given above or below the Moon symbols as appropriate.

The lower panel is a cylindrical equidistant map projection showing the Earth centered on the longitude at which the Moon is in the zenith at the middle of the eclipse. The visibility of the eclipse is displayed by plotting the Moon rise/set terminator for the principal phases of the eclipse for which timing information is provided in the upper panel of the diagram. The terminator for the middle of the eclipse is not plotted for the sake of clarity.

The unshaded area indicates the region of the Earth from which all of the eclipse is visible, whereas the darkest shading indicates the area from which the eclipse is invisible. The different shades of gray indicate regions where the Moon is either rising or setting during the principal phases of the eclipse. The Moon is rising on the left hand side of the diagram after the eclipse has started, and is setting on the right-hand side of the diagram before the eclipse ends. Labels are provided to this effect.

Symbols are plotted showing the locations for which the Moon is in the zenith at the principal phases of the eclipse. The points at which the Moon is in the zenith at P1 and P4 are denoted by (+), at U1 and U4 by ($\odot$), and at U2 and U3 by ($\oplus$). These symbols are also plotted on the upper panel where appropriate. The value of ΔT used for the calculation of the eclipse circumstances is given below the diagram. Country boundaries are also provided to assist the user in determining the visibility of the eclipse at a particular location.

11.6 Transits

General information about transits of Mercury and Venus can be found in Meeus (1989). Information concerning specific transits of Mercury and Venus is tabulated in *The Astronomical Almanac*. This information consists of the geocentric phases of the transit, a world map

Table 11.3 Transits of Mercury for 112 years

Transit Month	33-year cycle	13-year cycle
November	1907-1940-1973-2006	1914-1927-1940-1953
	1927-1960-1993	1960-1973-1986-1999
	1953-1986-2019	1993-2006-2019
May	1924-1957	1924-1937
	1937-1970-2003	1957-1970
		2003-2016

(Mercator projection) which indicates the beginning and ending curves of the transit from which a user can determine the regions of visibility, and a table of local circumstances for locations worldwide. All circumstances are provided in Universal Time (UT) with a provisional value of ΔT. If, closer to the time of the transit, a better value of ΔT is obtained, the data may be corrected using the new value.

Before computation of the general circumstances of the transit is performed, the exact time of conjunction in right ascension between the Sun and the transiting planet is determined. An approximate time for the middle of the transit, determined beforehand, serves as the center point for a ten-hour span of time over which the apparent places of the Sun and the transiting planet are determined (see § 7.4.1). Using the DE405/LE405 ephemeris (see Chapter 8) and the NOVAS software (URL[4]), differences in apparent right ascension between the transiting planet and the Sun are determined at consecutive 15-minute intervals. Once a minimum is reached, a precise time of conjunction is found using a Lagrangian inverse interpolation scheme during the 15-minute interval in which the conjunction occurs.

After the time of conjunction has been determined, the geocentric phases are computed. Starting at the beginning of the ten-hour ephemeris span, a search is made at one minute intervals for four contact points: ingress, exterior contact; ingress, interior contact; egress, interior contact; and egress, exterior contact. The four contact points are illustrated in Fig. 11.19. The transit ends at the time of the last contact.

At the times of first and fourth contact points, the apparent separation between the center of the Sun and the center of the transiting planet is equal to the sum of their semidiameters; that is, when

$$\sigma = s_s + s_p \tag{11.146}$$

where s_p is the apparent semidiameter of the transiting planet, s_s is the apparent semidiameter of the Sun, and σ is the apparent angular separation between the centers of the two. At the times of second and third contact points, the apparent separation between the center of the two bodies is equal to the difference of their semidiameters; that is, when

$$\sigma = s_s - s_p. \tag{11.147}$$

For each one-minute interval the apparent places, semidiameters, apparent separation between centers, and the time rate of change of the separation for the Sun and the planet are computed. The apparent separation between the two bodies and the sum of the semidiameters

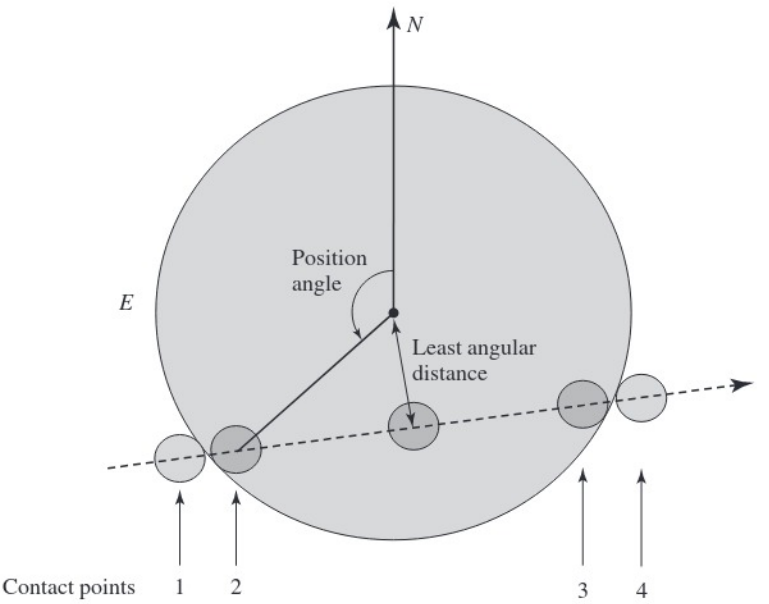


Figure 11.19 Example showing the four contact points and least angular distance for a transit across the Sun's disk. Contact point 1 is ingress, exterior contact; contact point 2 is ingress, interior contact; contact point 3 is egress, interior contact; and contact point 4 is egress, exterior contact. The position angle for contact point 2 is also illustrated.

are computed, and then evaluated against the criterion of Eq. 11.146. When the test indicates that the first contact point has been reached, a Lagrangian interpolation scheme is employed to determine the first contact time precisely. From this point on, the computation of apparent places, semidiameters, apparent separation between centers, and the time rate of change of the separation for the two bodies continues, but now the criterion of Eq. 11.147 is used. When the test indicates that the second contact point has been reached, the Lagrangian interpolation scheme is again employed to determine the second contact time precisely. Contact points three and four are found in a similar manner. Associated with each contact point is a position angle (P), measured from the apparent north pole of the Sun towards the east to the contact point; see Fig. 11.19.

The time of least angular distance lies between the second and third contact times. After the second contact time has been determined, the apparent distance between the center of the Sun and the center of the transiting planet is tested to determine the minimum value. The checks continue until the minimum value is reached. At that point, the same Lagrangian interpolation scheme employed to determine the contact times is used to determine the time of the least angular distance; the value of the least angular distance is also computed.

The transit diagram printed in *The Astronomical Almanac* is a Mercator projection map of the Earth with two curves plotted. The curve labeled "Transit begins at Sunrise/Sunset" is the great circle having for its pole the sub-planet point for the transiting planet at the time of exterior ingress. (The sub-planet point being the point on Earth where the planet is at the

zenith). Similarly, the curve labeled "Transit ends at Sunrise/Sunset" is the great circle with its pole at the sub-planet point at the time of exterior egress. These two sub-planet points are determined via the technique shown in Eq. 11.144, but substituting the α, δ of the planet instead of the Moon. Points on the great circle are found using Eq. 11.145 and plotted. Other labels on the diagram indicate where the entire transit is visible as well as where the transit is in progress at sunrise or sunset.

The table of local (topocentric) circumstances for locations across the Earth is assembled by using an extensive list of geographic locations.

For each location, the process of finding the four contact points and computing the associated data is performed as described above, except that instead of apparent (geocentric) places of the Sun and planet, topocentric places are used (see § 7.4.3). The table published in *The Astronomical Almanac* presents selected locations where at least two of the five phases (i.e., four contact points and the least angular distance) are above the horizon. Due to space considerations, only a limited number of locations can be presented in the book. Beginning with the 2012 transit of Venus, *The Astronomical Almanac Online* will present a more complete table of locations.

Acknowledgements

Acknowledgements are due to Mark Stollberg (U.S. Naval Observatory), who wrote § 11.6, Transits.

REFERENCES

1. The Astronomical Almanac Online:
http://asa.usno.navy.mil or http://asa.hmnao.com.

2. Eclipses Online:
http://astro.ukho.gov.uk/eclipse/.

3. NASA Eclipse Website:
http://eclipse.gsfc.nasa.gov/.

4. Naval Observatory Vector Astrometry Software (NOVAS):
http://aa.usno.navy.mil/software/novas/novas_info.php.

Chauvenet, W. (1891, Reprint 1960). *A Manual of spherical and practical astronomy - Vol.1: Spherical astronomy* (revised and corr., 5th ed.). New York: Dover Publication.

Herald, D. (1983). Correcting Predictions of Solar Eclipse Contact Times for the Effects of Lunar Limb Irregularities. *Journal of the British Astronomical Association 93*, 241–246.

Meeus, J. (1989). *Transits*. Richmond, Va.: Willmann-Bell.

Mikhailov, A. (1931). Über die Berechnung der Breite der Totalitätszone bei Sonnenfinsternissen. *Astronomisches Nachrichten 243*, 51.

Nautical Almanac Offices of UK and USA (1961). *Explanatory Supplement to The Astronomical Ephemeris and The American Ephemeris and Nautical Almanac*. London: Her Majesty's Stationery Office. Reprinted 1974.

FURTHER READING

Green, R. (1985). *Spherical Astronomy*. Cambridge: Cambridge University Press.

Link, F. (1969). *Eclipse Phenomena in Astronomy*. New York: Springer-Verlag.

Liu, B.-L. (1983). Canon of Lunar Eclipses from 1000 B.C. to A.D. 3000. *Publications of the Purple Mountain Observatory 2*, 1.

Meeus, J., C. Grosjean, and W. Vanderleen (1966). *Canon of Solar Eclipses*. Oxford: Pergamon Press.

Meeus, J. and H. Mucke (1983). *Canon of Lunar Eclipses, −2002 to 2526* (2nd ed.). Vienna: Astronomical Office.

Mitchell, S. A. (1951). *Eclipses of the Sun* (5th ed.). New York: Columbia University Press.

Mucke, H. and J. Meeus (1983). *Canon of Solar Eclipses −2003 to +2526*. Vienna: Astronomical Office.

Murray, C. A. (1985). *Vectorial Astrometry* (5th ed.). Bristol: Hilger.

Newcomb, S. (1882). Discussion and results of observations on transits of Mercury, from 1677 to 1881. In *Astronomical Papers of the American Ephemeris and Nautical Almanac*, Volume I, part VI. Washington, DC: U.S. Government Printing Office.

Oppolzer, T. R. v. (1887). *Canon der Finsternisse*. Vienna and New York: Imperial Academy of Science and Dover Publications. Reprinted 1962 w/ English translation.

Smart, W. M. (1977). *Text-book in Spherical Astronomy* (6th ed.). Cambridge: Cambridge University Press.

Williams, W. J. (1971). Prediction and analysis of solar eclipse circumstances. Technical Report NTIS No. AD726626, National Technical Information Service, Springfield, Virginia.

CHAPTER 12

Astronomical Phenomena

B.D. YALLOP, C.Y. HOHENKERK, & S.A. BELL

12.1 General Aspects of the Night Sky

The configurations and phenomena of the Sun, Moon, and planets as seen from the Earth arise from their apparent movement in the sky. Most of the phenomena published in the "Diary of Phenomena" for example, are geocentric; the remainder are heliocentric.

The Earth rotates about its polar axis once a day and produces an apparent motion of the night sky about the celestial poles. In the Northern Hemisphere the north celestial pole is elevated above the horizon. Facing away from the elevated celestial pole, an observer sees the Sun, Moon, planets, and stars rise in the east and set in the west. They reach their highest altitude as they cross the local meridian. When the observer turns to face the elevated celestial pole, stars nearest the pole neither rise nor set. They become circumpolar and cross the meridian each day once above the pole at their highest altitude and once below the pole at their lowest altitude. In the Northern Hemisphere, circumpolar stars appear to rotate about the north celestial pole anticlockwise. In the Southern Hemisphere the effect is reversed and they appear to rotate clockwise.

Superimposed on the diurnal rotation is an annual rotation caused by the Earth's orbiting the Sun. Since the stars are seen by the naked eye after sunset, the constellations appear to move from east to west, and to return to the same position after a year. Relative to the Sun, the stars rise and set roughly four minutes earlier each day. In the course of a month, the night sky appears to move two hours in right ascension to the west. Also because of this orbital motion of the Earth, the circumpolar stars in the Northern Hemisphere appear to rotate once a year in an anticlockwise direction around the north celestial pole and in a clockwise direction about the south celestial pole.

The Moon moves in an orbit inclined to the ecliptic by 5°.16; the Moon makes one revolution about the sky from west to east in about a month. During this period the phases of the Moon complete a cycle from new to full and back to new. The orbit of the Moon is moving around the ecliptic, so that other aspects of the Moon's position in the sky, such as its maximum and minimum declination, change from one month to the next.

It is important to know when the planets are in the most favourable position for observation. The outer planets, for example, are best seen around opposition. They are in their most unfavourable position around conjunction. The inner planets are different—they are in their most favourable position near greatest elongation, even though they are not at full phase. At superior conjunction the phase is around full, but the planets are difficult to see because they are furthest from the Earth and usually too close to the Sun. At inferior conjunction the inner

planets are nearest to the Earth, but again they are difficult to see because their phase is small, and they are too close to the Sun as viewed from Earth.

Often the times of phenomena need not have any great precision; sometimes the nearest hour or even the nearest day are sufficient for observational purposes. The dates and times, however, usually depend on the coordinate system. For historical reasons the conjunctions and oppositions of planets have been calculated in geocentric ecliptic coordinates, e.g., time of conjunction is when the ecliptic longitudes are equal. On the other hand, the conjunctions of planets with other planets, bright stars, or the Moon have always been calculated using equatorial coordinates; the phenomena are then observed more easily with an equatorially mounted telescope. In some cases the times of phenomena have been defined as the maxima or minima of the distances from the Sun or the Earth or the elongation from another body. In such cases, the phenomena are independent of the coordinate system.

12.2 Configurations of the Sun, Moon, and Planets

The *Universal Times* (UT) of the principal astronomical phenomena involving configurations of the Sun, Moon, and planets are given in *The Astronomical Almanac* pp. A1–A11 under the heading "Phenomena". These data are also available for planning purposes in *Astronomical Phenomena*, published up to two years in advance of *The Astronomical Almanac*. In most cases the times are given to the nearest hour, but for certain heliocentric phenomena of the planets, only the date appears. The times of the phenomena of greatest general interest—the beginning of the seasons and the phases of the Moon—are to the nearest minute, although the accuracy is of no significance.

Times may be calculated using a daily tabular ephemeris. For quantities that vary slowly with time, such as planetary apsides, a tabular interval of five days gives better results. On the other hand, quantities such as the phases of the Moon vary rapidly, and a shorter interval of a half or quarter day is more appropriate. If the ephemeris is in *Terrestrial Time* (TT), then, to convert to UT, subtract the correction $\Delta T = \mathrm{TT} - \mathrm{UT}$ to the time obtained at the end of the calculation.

The time t of the phenomenon derives from a functional expression involving the parameters associated with the phenomenon. The time of the phenomenon is calculated from the equation $f(t) = 0$ or $f'(t) = 0$, where $f'(t) = df(t)/dt$.

12.2.1 Interesting Phenomena of the Sun, Earth, and Moon

12.2.1.1 Equinoxes and Solstices

The times of the equinoxes and solstices are defined to be when the Sun's apparent ecliptic longitude λ_S is a multiple of 90°; i.e., it is calculated from $f(t) = 0$, where $f(t) = \lambda_S - 0°$, 90°, 180°, or 270°. Thus in the northern hemisphere, for the spring equinox $f(t) = \lambda_S$, for the summer solstice $f(t) = \lambda_S - 90°$, for the autumn equinox $f(t) = \lambda_S - 180°$ and for the winter solstice $f(t) = \lambda_S - 270°$. At the equinoxes the Sun crosses the equator. At that time the lengths of the day and night are approximately equal everywhere, however the length of the day exceeds the length of the night slightly due to refraction, semidiameter, and parallax of the Sun.

Table 12.1 Time of commencement of the seasons during the 21st century.
Note: The total range in times is about 54 hours in each case.

		Spring	Summer	Autumn	Winter
		d h	d h	d h	d h
Latest	2003	March 21 01	June 21 19	Sept. 23 11	Dec. 22 07
Earliest	2096	19 14	20 07	21 23	20 21

The time of the commencement of the seasons changes progressively during the leap-year cycle. Because the period of revolution of the Earth about the Sun is not commensurate with the Gregorian calendar year, it is only after a complete cycle of four centuries that the seasons again commence at approximately the same times. In the present century the latest dates for the seasons occurred in 2003, and the earliest will be in 2096 (see Table 12.1).

12.2.1.2 Perihelion and Aphelion of the Earth

In the "Diary of Phenomena," the times when the Earth is at perihelion (the Sun is at perigee) are defined to be those for which the Sun's geometric distance R is a minimum. Likewise, the times when the Earth is at aphelion (the Sun is at apogee) are defined to be when R is a maximum. Thus, if t is the time of perihelion, it is calculated from the equation $f'(t) = 0$ where $f(t) = R$. The times do not always agree with those calculated from the times when the Sun is at perigee or apogee in its mean elliptical orbit (i.e., the time t when the mean longitude of perigee $\Gamma = 0$, or apogee $\Gamma - 180^\circ = 0$) because of perturbations by the planets.

It is worth noting that the times of Earth at perihelion and aphelion vary in date more than other annually-occuring phenomena such as the start of the seasons. This is due to the presence of the Moon. Because perihelion and aphelion are defined by the distance between the center of the Sun and the center of the Earth, the Earth's position in its monthly motion around the Earth-Moon barycenter greatly affects the time of perihelion and aphelion. Due to the fact that the position of the Moon doesn't repeat from year to year on the same date, neither does the position of the Earth with respect to the Earth-Moon barycenter. This produces what appears to be a quasi-random variation in the dates of perihelion and aphelion. In the 21st century, time of the earliest perihelion is January 2 at 1^h (2005) and the latest is January 5 at 22^h (2096). Earliest and latest aphelion are July 3 at 16^h (2044) and July 7 at 15^h (2083). Times are TT, but at this precision the difference between TT and UT is negligible.

12.2.1.3 Phases of the Moon

The times of the phases of the Moon are tabulated to the nearest minute of UT in *The Astronomical Almanac* pp. A1 and D1 and are given to the nearest hour of UT in the "Diary" on pp. A9–A11. They are the times when the excess of the Moon's apparent geocentric ecliptic longitude λ_M over the Sun's apparent geocentric ecliptic longitude is 0°, 90°, 180°, or 270°—i.e., the times when $f(t) = 0$ where $f(t) = \lambda_M - \lambda_S$ for new Moon, $f(t) = \lambda_M - \lambda_S - 90^\circ$ for first quarter, $f(t) = \lambda_M - \lambda_S - 180^\circ$ for full Moon and $f(t) = \lambda_M - \lambda_S - 270^\circ$ for last quarter. Because the times are determined from geocentric coordinates, they are independent of location on the Earth.

Owing to the rapid variations in the distance and velocity of the Moon, the intervals between successive phases are not constant, and it is not possible to check these times by differencing. Moreover, there is no simple prediction formula with which to make a comparison. Examination of the higher differences of the successive times of the same phenomenon provides a check.

The phases of the Moon do not recur on exactly the same dates in any regular cycle, but the approximate dates of the phases in any year can be found from the dates on which the phase occurred 19 years previously. Thus in the Metonic cycle, in which 19 tropical years are nearly equal to 235 synodic months (new moon to new moon), the phases recur on dates that are the same or differ by one or occasionally two days, depending on the number of intervening leap years and on the perturbations of the Moon. For example, during 2000 the dates are the same as in 1981 on thirty occasions, and differ by one day for the remaining nineteen.

Another relevant cycle is the Saros, which consists of 233 synodic months and equals nearly 19 passages of the Sun through the node of the Moon's orbit; not only will the moon phases recur but eclipses as well. Moreover in this cycle the Moon's apse makes 239 revolutions and returns to nearly the same position, so the durations of solar eclipses are similar as well.

12.2.2 Geocentric Phenomena

The times of geocentric phenomena are calculated from the expressions for $f(t)$ listed below. Table 12.2 contains the phenomena for which the time is obtained from the equation $f(t) = 0$. Table 12.3 contains phenomena for which the time is obtained from the equation $f'(t) = 0$. In this table, except for the stationary points in right ascension, the phenomena are independent of the coordinate system.

The notation λ, α, δ refers to the apparent geocentric ecliptic longitude, right ascension, and declination; and the subscripts S, M, p, b refer to the Sun, Moon, planet, or bright star, respectively. The distances r, R, Δ, and ρ refer to the geometric distances of the Sun–planet, Earth–Sun, Earth–planet, and Earth–Moon, respectively; π is the horizontal parallax of the Moon and s is the semidiameter of the planet at 1 au. The five bright stars used in the "Diary" are *Aldebaran*, *Pollux*, *Regulus*, *Spica*, and *Antares*. It should be noted that, at current epochs, planetary and lunar occultations of *Pollux* are not possible.

The following formulae are useful for calculating elongation and longitude:

$$\cos E = \sin \delta_p \sin \delta_s + \cos \delta_p \cos \delta_s \cos(\alpha_p - \alpha_s) \tag{12.1}$$

$$\tan \lambda = \frac{\sin \epsilon \sin \delta + \cos \epsilon \cos \delta \sin \alpha}{\cos \delta \cos \alpha} \tag{12.2}$$

where ϵ is the true obliquity of the ecliptic.

12.2.2.1 Visibility of Planets

Table 12.4 shows the criteria adopted for the "Diary" for the minimum elongations from the Sun at which Mercury, the bodies used in navigation, and the minor planets can be seen with the naked eye.

Table 12.2 Geocentric phenomena for which $f(t) = 0$

Phenomenon	$f(t)$	Remarks
Seasons:		
Vernal Equinox	λ_S	March equinox, First Point of Aries
Summer Solstice	$\lambda_S - 90°$	June solstice
Autumnal Equinox	$\lambda_S - 180°$	September equinox
Winter Solstice	$\lambda_S - 270°$	December solstice
Conjunctions of the planets with the Sun:		
Inferior planets:		
inferior conjunction	$\lambda_p - \lambda_S$	$\lambda_p - \lambda_S$ changes from plus to minus
superior conjunction	$\lambda_p - \lambda_S$	$\lambda_p - \lambda_S$ changes from minus to plus
Superior planets:		
conjunction	$\lambda_p - \lambda_S$	
opposition	$\lambda_p - \lambda_S - 180°$	
Phases of the Moon:		
New Moon	$\lambda_M - \lambda_S$	
First Quarter	$\lambda_M - \lambda_S - 90°$	
Full Moon	$\lambda_M - \lambda_S - 180°$	
Last Quarter	$\lambda_M - \lambda_S - 270°$	
Conjunctions of other bodies:		
planet with planet	$\alpha_{p_1} - \alpha_{p_2}$	separation $= \delta_{p_1} - \delta_{p_2}$
planet with bright star	$\alpha_p - \alpha_b$	separation $= \delta_p - \delta_b$
Moon with planet	$\alpha_M - \alpha_p$	separation $= \delta_M - \delta_p$
Moon with bright star	$\alpha_M - \alpha_b$	separation $= \delta_M - \delta_b$

12.2.2.2 Synodic Periods

Once the date and time of a geocentric phenomenon are known, the approximate time of the next similar phenomenon may be estimated by adding the synodic period T of the body concerned. The eccentricities of the orbits of the Earth and the body, and the perturbations by other bodies, will introduce errors in this estimate. Table 12.5 gives synodic periods of the planets, Pluto, Ceres and the three brightest minor planets. The periods may be used for a systematic search for geocentric phenomena.

The synodic period T is calculated from the mean motion of the planet, n_{p}, and the mean motion of the Earth, n_{e}. Thus,

$$T = \frac{360°}{n_p - n_e} \text{ for inner planets, and } T = \frac{360°}{n_e - n_p} \text{ for outer planets.} \quad (12.3)$$

For the slowly moving objects, the error in using these values is small, but for Mercury, Venus, and Mars, the mean synodic period is less useful. Much more accurate estimates of

Table 12.3 Geocentric phenomena for which $f'(t) = 0$

Body	Phenomenon	$f(t)$	Remarks
Mercury	Greatest elongation	E	$-28° \le E \le +28°$
Venus			$-47° \le E \le +47°$
Venus	Greatest brilliancy	$\dfrac{(r+\Delta+R)(r+\Delta-R)}{(r\ \Delta)^3}$	$0.39\text{ au} < \Delta < 0.47\text{ au}$
Venus	Greatest illuminated extent	$\dfrac{\pi s^2(r+\Delta+R)(r+\Delta-R)}{4r\Delta^3}$	where $\pi = 3.14159\ldots$
Earth	Apsides	$r = R$	At perihelion r is a minimum At aphelion r is a maximum
Moon	Apsides	$\rho = 1/\sin\pi$	At perigee ρ is a minimum At apogee ρ is a maximum
		π	At perigee π is a maximum At apogee π is a minimum
Mars	Closest approach	Δ	
Planet	Stationary in right ascension	α_p	

Table 12.4 Visibility criteria for geocentric phenomena

Body	Minimum Elongation
Moon, Mars, Saturn	15°
Minor planets	15°
Venus, Jupiter	10°
Mercury	10° + visual magnitude of Mercury

Table 12.5 Synodic periods of selected solar system objects

Object	Days	Object	Days	Object	Days
Mercury	116	Saturn	378	Ceres	467
Venus	584	Uranus	370	Pallas	466
Mars	780	Neptune	367	Juno	474
Jupiter	399	Pluto	367	Vesta	504

when these planets may be seen again in the same part of the sky may be made by using long-period cycles that contain, with varying degrees of accuracy, integral numbers of revolutions of the Earth and the planet. (See Table 12.6.)

Any particular phenomenon of a planet repeats itself after each cycle at the same time of year and in the same part of the sky. However, repetition does not occur after a single synodic period. For Venus a useful and accurate form of the relation is

$$5 \text{ mean synodic periods} = 8 \text{ calendar years} - 2^{\text{d}}.4 \tag{12.4}$$

unless the interval includes a century year that is not a leap year.

Table 12.6 Long-period cycles of Mercury, Venus, and Mars

For Mercury	54 sidereal periods =	13 years +	2 days
	137 sidereal periods =	33 years −	1 day
For Venus	13 sidereal periods =	8 years −	1 day
	359 sidereal periods =	243 years −	$\frac{1}{2}$ day
For Mars	8 sidereal periods =	15 years +	17 days
	17 sidereal periods =	32 years −	9 days
	25 sidereal periods =	47 years +	8 days
	42 sidereal periods =	79 years −	1 day

Table 12.7 Heliocentric phenomena

Phenomenon	$f(t)$	Type	Remarks
Nodes	b	$f(t) = 0$	At the descending node, b is decreasing.
			At the ascending node, b is increasing.
Apsides	r	$f'(t) = 0$	At aphelion, r is a maximum.
			At perihelion, r is a minimum.
Greatest latitudes	b	$f'(t) = 0$	At greatest latitude North, b is positive.
			At greatest latitude South, b is negative.

12.2.3 Heliocentric Phenomena

Certain heliocentric phenomena of the planets are given in *The Astronomical Almanac*, p. A3. The dates of perihelion and aphelion are those on which the geometric distance of the planet from the Sun is a minimum and maximum respectively; the dates are thus the times when the first derivative of the distance is zero—i.e., $f'(t) = dr/dt = 0$. Owing to the presence of perturbations in the planetary motion, these dates may differ from those obtained from the angular elements of the mean orbits. The actual disturbed motion of the planets is also used to determine the dates when they pass through the nodes on the ecliptic, and when they reach greatest latitudes north or south. At the nodes, the heliocentric latitude is zero; i.e., $f(t) = b = 0$. The value of $f(t)$ changes from negative to positive at the ascending node, and from positive to negative at the descending node. These dates are given each year for Mercury, Venus, and Mars, but they occur less frequently for the other planets, and in these cases are given as additional notes when necessary. The dates on which a planet has its greatest latitude north or south is determined as the times at which the first derivative of the latitude is zero—i.e., $f'(t) = db/dt = 0$. Table 12.7 shows $f(t)$ for the various phenomena.

12.3 Risings, Settings, and Twilight

The astronomer is concerned with the phenomena of rising, setting, and twilight primarily in regard to the planning of observations. Precision of better than a minute of time is not

required for this purpose, and extensive tables of these phenomena are in *The Astronomical Almanac*, pp. A14–A77.

The tabulated times of the phenomena refer to sea level with a clear horizon and an adopted correction for refraction under normal meteorological conditions. The actual times of rising and setting may differ considerably, especially near extreme conditions when the altitude is changing slowly. This difference can reach half a minute of time at mid-latitudes and more at high latitudes. The illumination at the beginning or end of twilight also varies greatly with meteorological conditions. Precise times have little real significance, except in special circumstances, such as navigation at sea.

No data are given for the times of rising and setting of planets. Data may be obtained fairly simply from navigation tables such as the *Rapid Sight Reduction Tables for Navigation*. Within their range of declination (0°–29°), these tables may also be used to find the times of rising and setting of stars.

Section 12.3.3 gives algorithms that may easily be programmed into a computer to calculate the times of the phenomena.

12.3.1 Sunrise, Sunset, and Twilight

The data given in *The Astronomical Almanac* enable the times of sunrise, sunset, and the beginning and end of civil, nautical, and astronomical twilight to be found for any position between latitudes 66° north and 55° south. The times, tabulated for every fourth day, are the local mean times of the phenomena on the meridian of Greenwich and in the specified latitude; interpolation is necessary to obtain the local mean times for intermediate latitudes, for intermediate days, and for longitude. To an accuracy of about five minutes this interpolation can generally be done by sight; near limiting conditions, when interpolation becomes difficult, large changes of time correspond to only small changes in depression and accurate times have little real meaning.

Interpolation for latitude is nonlinear. Interpolation for longitude, which is rarely justified, can be combined with the interpolation for date by increasing for west longitudes, or decreasing for east longitudes, the Greenwich date by the appropriate fraction (longitude in degrees/360); for sunrise and sunset, the error due to neglecting the variation with longitude amounts to a maximum of two minutes in latitudes up to 60°. The times so obtained are local mean times, which can be converted to universal time by applying longitude in time—adding if west and subtracting if east. Standard times are obtained by adding (subtracting) to the local time four minutes for every degree of longitude west (east) of the standard meridian.

At the tabulated times of sunrise and sunset, the geocentric zenith distance of the center of the Sun is 90° 50′; i.e., a geocentric altitude of −50′, of which 34′ is allowed for horizontal refraction and 16′ for semidiameter; the Sun's apparent upper limb is thus on the horizon. Corrections are necessary if some other value of the altitude is required, (such as for the conventional meteorological value of −34′) or to allow for the height of the observer and the elevation of the actual horizon. In such cases use Eq. 12.5.

At the times given for civil, nautical, and astronomical twilight, the altitude of the center of the Sun is −6°, −12° and −18° respectively. These tabulations will produce times for any desired altitude between −50′ and −18°.

The Nautical Almanac, *The US Air Almanac* and *The UK Air Almanac* tabulate the times of sunrise, sunset, and the beginning and end of civil twilight (altitude −6°) every three days

for latitudes between 72° north and 60° south; times of the beginning and end of nautical twilight (altitude −12°) are also in *The Nautical Almanac*. *The US Air Almanac* and *The UK Air Almanac* provide graphs that enable corrections to the time of sunrise or sunset. These corrections give the times at which the Sun has altitudes between 0° and −12° (that is, depressions to 12°).

Sunrise or sunset at a height H meters above the level of the horizon occurs when the Sun's altitude is approximately

$$-50' - 2.'12\sqrt{H} \quad (1.'17 \text{ for } H \text{ in feet}) \tag{12.5}$$

so that the same table can be used to give corrections for height to the times of sunrise and sunset. In *The US Air Almanac* and *The UK Air Almanac* the corrections can be obtained from graphs. The constant 2.12 is really a slowly decreasing function of H, but below a height of about 5000 m it is constant; it decreases to a value of 2.00 at 100000 m.

Times of rising and setting and associated phenomena change rapidly from day to day in polar regions or may not occur for long periods, the Sun being continuously above or below the horizon; accurate times are therefore difficult to tabulate. Diagrams are given in *The US Air Almanac* and *The UK Air Almanac* that enable approximate times that are sufficiently accurate for all practical purposes to be obtained.

12.3.1.1 A Low Precision Ephemeris for the Sun

The following algorithm gives the equation of time (E), the Greenwich Hour Angle (GHA), declination (δ), and semidiameter (SD) of the Sun, in degrees, to a precision of better than $1.'0$, which can be used with the algorithm for rising and setting (see § 12.3.3). The equation of time is also useful for erecting sundials and determining the transit time of the Sun.

1. Using the Julian date, JD, and the universal time, UT, in hours, calculate T, the number of centuries from J2000.0:

$$T = (\text{JD} + \text{UT}/24 - 2451545.0)/36525. \tag{12.6}$$

2. Calculate the solar arguments; the mean longitude corrected for aberration, L; the mean anomaly, G; the ecliptic longitude, λ; and the obliquity of the ecliptic, ϵ:

$$\begin{aligned} L &= 280.^\circ460 + 36000.^\circ770\, T \quad \text{(remove multiples of } 360^\circ\text{)} \\ G &= 357.^\circ528 + 35999.^\circ050\, T \\ \lambda &= L + 1.^\circ915 \sin G + 0.^\circ020 \sin 2G \\ \epsilon &= 23.^\circ4393 - 0.^\circ01300\, T. \end{aligned} \tag{12.7}$$

3. The equation of time E, the GHA, δ, and SD are given by

$$\begin{aligned} E &= -1.^\circ915 \sin G - 0.^\circ020 \sin 2G + 2.^\circ466 \sin 2\lambda - 0.^\circ053 \sin 4\lambda \\ \text{GHA} &= 15\,\text{UT} - 180^\circ + E \\ \delta &= \sin^{-1}(\sin\epsilon \sin\lambda) \\ SD &= 0.^\circ267/(1 - 0.017\cos G). \end{aligned} \tag{12.8}$$

Plotting the position of the apparent Sun relative to the mean Sun (which moves uniformly along the equator) produces the analemmic curve, see Fig. 12.1. The displacement of the

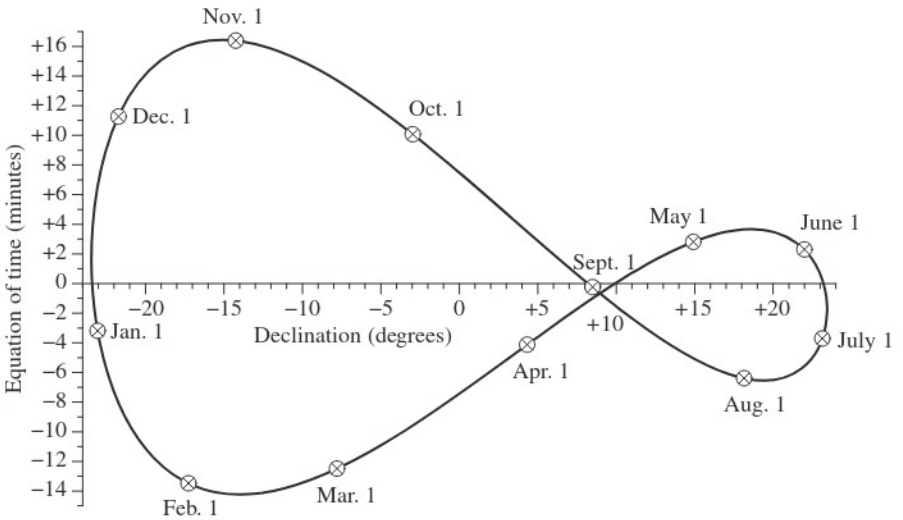


Figure 12.1 The analemmic curve

apparent Sun in longitude is given by the equation of time (E) and the displacement in latitude is given by the declination (δ). The progress of the apparent Sun throughout the year is indicated at the beginning of each month on the closed curve. The analemmic curve plays an important role in certain types of sundial.

12.3.2 Moonrise and Moonset

The tables in *The Astronomical Almanac* give, for every day and for a range of latitudes from 66° north to 55° south, the local mean times of moonrise and moonset for the meridian of Greenwich. Interpolation for latitude and longitude is necessary to obtain local times for other places. In practice, times are rarely required more accurately than to within about five minutes, and interpolation can be done mentally. Formal interpolation, using tables such as those given in *The Nautical Almanac* and *The US Air Almanac*, yields times accurate to about two minutes. The times so obtained may be converted to universal time or standard time by applying longitude in time—adding if west and subtracting if east. Times for latitudes between 72° north and 60° south are given in *The Nautical Almanac* and *The US Air Almanac*. In *The US Air Almanac* and *The UK Air Almanac* times appear in graphical form above 72° north, right up to the North Pole.

In calculating the times of moonrise and moonset, the true altitude h of the center of the Moon is

$$h = -34' - \text{semidiameter} + \text{horizontal parallax} \tag{12.9}$$

where $34'$ is allowed for horizontal refraction; depending upon the distance of the Moon, h lies in the range $5'$ to $11'$. At these times, the upper limb of the Moon is on the horizon; no allowance is made for phase. At a height of H meters above the horizon, the altitude of the Moon when its upper limb is on the horizon is decreased by $2.'12\sqrt{H}$ (see § 12.3.3.1).

The Moon revolves around the Earth and makes one complete revolution relative to the Sun in a synodic month of mean length 29.53 days; in that time the Moon, therefore, appears to lose one transit across any meridian and, in general, one rising and one setting. During each month there is, therefore, no moonrise on one local day (near last quarter) and no moonset on one local day (near first quarter). In high latitudes the times of the phenomena change rapidly from day to day and may not occur for long periods, the Moon being continuously above or below the horizon; in these extreme conditions the times of moonrise and moonset sometimes decrease from day to day, instead of the usual increase in lower latitudes, and it is possible to have two moonrises or two moonsets during the same local day.

12.3.3 Formulae Associated with Rising and Setting

Consider first an algorithm for calculating the times of rising or setting of a body at true altitude h.

The GHA and declination (δ) of the body are required to about one minute of arc as a function of UT. For the Moon, the horizontal parallax π is also required. To speed up the calculation, which is iterative, it is convenient to express GHA, δ, and π as daily polynomials. For the Moon second-order polynomials are required for GHA and δ, and first order for π. For other bodies like the Sun and the inner planets, first-order polynomials are sufficient. For stars and outer planets, a constant daily value for declination may be adopted. Alternatively low-precision formulae for the ephemeris of the Sun (§ 12.3.1.1) may be used. For the Moon, the low-precision formulae on p. D22 of *The Astronomical Almanac* may be used.

At sunrise and sunset the apparent altitude of the upper limb on the horizon is zero and hence the adopted true altitude in degrees is $h = -50/60 - 0.0353\sqrt{H}$ where H is the height, in meters, of the observer above the horizon.

Similarly at moonrise and moonset the apparent altitude of the upper limb on the horizon is zero and the adopted true altitude $h = -34/60 + 0.7275\pi - 0.0353\sqrt{H}$. At rise and set of a star or a planet, the apparent altitude of the body is zero; hence, $h = -34/60 - 0.0353\sqrt{H}$.

Other important cases to consider are twilights: civil twilight $h = -6°$, nautical twilight $h = -12°$, and astronomical twilight $h = -18°$.

The time of rise or set, UT, in hours, is found by solving iteratively the equation

$$\mathrm{UT} = \mathrm{UT}_0 - (\mathrm{GHA} + \lambda \pm t)/15 \tag{12.10}$$

where the plus sign is used for rise and the minus sign for set, and t is the hour angle of the body at UT_0, which is given by

$$\cos t = \frac{\sin h - \sin\phi \ \sin\delta}{\cos\phi \ \cos\delta} \tag{12.11}$$

and ϕ is the latitude and λ the longitude (positive to the east).

$$\begin{aligned} &\text{If } \cos t > +1, \quad \text{set } t = 0°; \\ &\text{If } \cos t < -1, \quad \text{set } t = 180°. \end{aligned} \tag{12.12}$$

As an initial guess, set $\mathrm{UT}_0 = 12^{\mathrm{h}}$, although any value in the range 0^{h} to 24^{h} will do. After each iteration, add multiples of 24^{h} to set UT in the range 0^{h} to 24^{h}. Replace UT_0 by UT until the difference between them is less than $0^{\mathrm{h}}.008$. If for several iterations $\cos t > 1$, it is likely

that there is no phenomenon and the body remains below the true altitude h all day. On the other hand, if $\cos t < -1$, the body remains above the true altitude all day. In each lunation, around first quarter, there is always a day when the Moon does not set, and another, around last quarter, when the Moon does not rise.

At latitudes above 60° the algorithm may fail, and it is necessary to use a more systematic approach. If h_0 is the adopted true altitude, the times when $h = h_0$ where

$$\sin h = \sin\phi \ \sin\delta + \cos\phi \ \cos\delta \ \cos(\text{GHA} + \lambda) \tag{12.13}$$

are the times of rising or setting.

These roots, if they exist, will lie between the true altitude at 0^{h} and 24^{h} and the maximum and minimum altitudes during the day. The maximum and minimum altitudes occur at or very near upper and lower transit. These times are found by setting $t = 0°$ and $t = 180°$ in Eq. 12.10 and iterating.

Only for the Moon at high latitudes is it necessary to calculate the maximum and minimum altitudes more precisely. This calculation is done by fitting a second-order polynomial to the true altitude at points around upper or lower transit and differentiating with respect to time to find the turning point.

12.3.3.1 Effects of Dip and Refraction

Dip is required for reducing sights made with a marine sextant and for calculating the true altitude of a body at rise and set. Dip is the apparent angle between the geometric horizon (at right angles to the vertical) and the visible horizon. For an observer at height H above the surface of the Earth, dip $D(H) = 1.'75\sqrt{H}$, where H is in meters ($0.'97\sqrt{H}$ if H is in feet) (see Woolard and Clemence 1966, p. 215).

A navigator using a marine sextant sets on the apparent horizon and wants to know how much the horizon appears to be below the horizontal and therefore only needs to know the dip. On the other hand, when computing the times of rise or set of a body, we need to know the true altitude when the body appears to be on the horizon, which involves dip and the refraction between the horizon and the observer $R(H)$, where $R(H) = 0.'37\sqrt{H}$ and H is in meters (or $0.'20\sqrt{H}$ if H is in feet).

In Fig. 12.2, O is the observer at height H above the surface of the Earth, S is the body at rise or set, and A is the observer's horizon. The true altitude of S from the vantage point A is $-34'$ due to refraction. The true altitude of S from O is the true altitude at $A - D(H) - R(H) = -34' - 1.'75\sqrt{H} - 0.'37\sqrt{H} = -34' - 2.'12\sqrt{H}$.

Refraction, the bending of light as it passes through the atmosphere, is illustrated in Fig. 12.2 for the rising or setting of a celestial object. The following approximate formulae (Bennett 1982) are valid for all altitudes and standard meteorological conditions. A more precise algorithm is given in § 7.2.7. The amount of refraction, R, is given by

$$R(h_a) = \frac{0.^{\circ}0167}{\tan\left(h_a + 7.31/(h_a + 4.4)\right)} \tag{12.14}$$

where h_a is the apparent altitude. Alternatively, if h is the true altitude, then

$$R(h) = \frac{0.^{\circ}0167}{\tan\left(h + 8.6/(h + 4.4)\right)}. \tag{12.15}$$

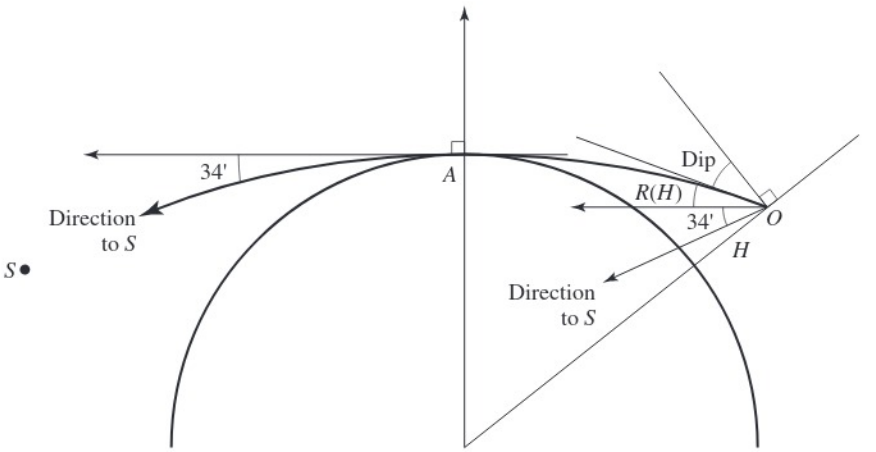


Figure 12.2 The horizon at rising or setting

12.3.3.2 Time for a Specified Shadow Length

The lengths of shadows depend upon the apparent altitude of the Sun, h_a. The true altitude h of the Sun is needed to find the required time where

$$h = h_a - R(h_a) \tag{12.16}$$

and R is the refraction at apparent altitude h_a which may be calculated approximately using Eq. 12.14. Alternatively, if h is known and h_a is required use Eq. 12.15 for calculating the refraction at true altitude h and set

$$h_a = h + R(h). \tag{12.17}$$

12.3.3.3 Rates of Change

The rate of change of hour angle with altitude may be obtained by differentiating the altitude as shown in Eq. 12.13. Assuming that λ, ϕ, and δ do not change with time, then the change in time, (Δt), in hours, for a given change in altitude (Δh), in degrees, can be calculated from the simple expression

$$\Delta t = \frac{1}{\Delta\text{LHA}\ \cos\phi\ \sin Z}\,\Delta h \tag{12.18}$$

where ΔLHA is the rate of change of hour angle per hour and Z is the azimuth. For the Sun, $\Delta\text{LHA} = 15°$ per hour and for the Moon, $\Delta\text{LHA} = 14°.493$ per hour.

Near rise and set when $h \approx 0°$, this expression can be further simplified to

$$\begin{aligned} \Delta t &= A\,\Delta h \\ \text{where } A &= 60/\left(\Delta\text{LHA}\sqrt{\cos^2\phi - \sin^2\delta}\right) \end{aligned} \tag{12.19}$$

and Δt is now in minutes of time. This correction is accurate to within a few minutes provided A does not exceed 20 and Δh does not exceed a few degrees.

12.3.3.4 Time for a Specified Azimuth

Another interesting problem is to calculate the time when the azimuth Z of a body takes a particular value. The time UT is calculated iteratively from

$$\mathrm{UT} = \mathrm{UT}_0 - (\mathrm{GHA} + \lambda \pm t)/15 \tag{12.20}$$

where the plus sign is used if $Z < 180^\circ$ and the minus sign is used otherwise. t is calculated from

$$\cos t = \frac{-ab \pm \sqrt{1 + a^2 - b^2}}{1 + a^2} \tag{12.21}$$

where $a = \tan Z \sin \phi$, $b = -\cos \phi \tan \delta \tan Z$, and the plus sign is used if $90^\circ < Z < 270^\circ$; otherwise use the minus sign. In the special cases $Z = 90^\circ$ and $Z = 270^\circ$ or if $1 + a^2 - b^2 < 0$, then

$$\begin{aligned} \cos t &= -b/a = \tan \delta / \tan \phi; \\ \text{If } \cos t &> +1, \text{ set } \cos t = +1; \\ \text{If } \cos t &< -1, \text{ set } \cos t = -1. \end{aligned} \tag{12.22}$$

Iterate Eq. 12.20 until UT differs from UT_0 by less than $0^{\mathrm{h}}.008$.

12.3.3.5 Times of Transit

Times of transit are required to low precision for planning observations, and for setting instruments. The times for a particular place may be calculated for any body by iterating Eq. 12.10 and setting $t = 0^\circ$. For the Sun, the transit time may be determined from $12^{\mathrm{h}} - E/15$, where E is the equation of time given in § 12.3.1.1.

12.3.4 Illumination

The ground illumination (i.e., the illuminance on a horizontal surface) from natural sources varies considerably during the day. The variation of the illumination on a horizontal surface, in clear conditions, on the surface of the Earth is shown diagrammatically in Fig. 12.3 as a function of altitude.

This section contains a simple method of calculating ground illuminance from sunlight, twilight, and moonlight based on data published by the Radio Corporation of America (RCA 1974). A more precise method is available in Janiczek and DeYoung (1987). This method is based on the extensive Natural Illumination Charts produced by Brown.

Data from the handbook have been represented by sets of cubic polynomials for the Sun and the full Moon at mean distance, for various ranges of altitudes, in Table 12.8. The illuminance is measured in lux or lumens per square meter; however, the logarithm of the illuminance has been used because large ranges are involved, and also the sensitivity of the human eye varies in proportion to the logarithm of intensity. Thus the illuminance I in lux is given by

$$\log_{10} I = l_0 + l_1 x + l_2 x^2 + l_3 x^3 \tag{12.23}$$

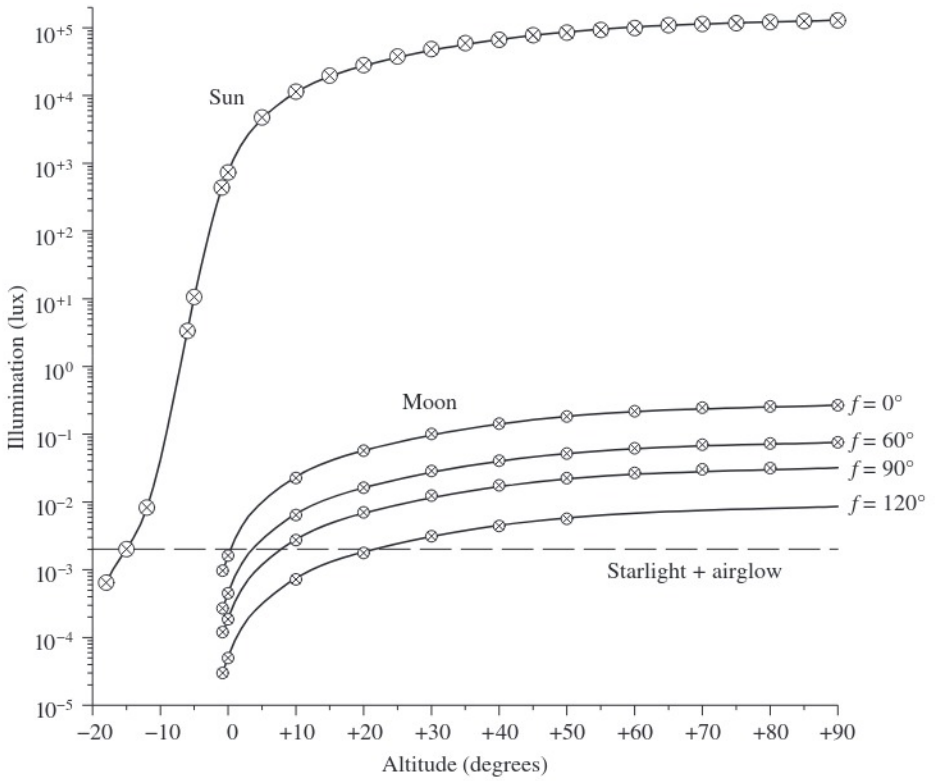


Figure 12.3 Ground illumination from various sources. f = 0° corresponds to approximately the full moon, f = 90° to the first or third quarter, etc.

Table 12.8 Coefficients for calculating ground illumination

Altitude range		From the Sun				Maximum error
		l_0	l_1	l_2	l_3	
20°	90°	3.74	3.97	−4.07	1.47	0.02
5	20	3.05	13.28	−45.98	64.33	0.02
−0.8	5	2.88	22.26	−207.64	1034.30	0.02
−5	−0.8	2.88	21.81	−258.11	−858.36	0.02
−12	−5	2.70	12.17	−431.69	−1899.83	0.01
−18	−12	13.84	262.72	1447.42	2797.93	0.01
		From the Full Moon at Mean Distance				
20°	90°	−1.95	4.06	−4.24	1.56	0.02
5	20	−2.58	12.58	−42.58	59.06	0.03
−0.8	5	−2.79	24.27	−252.95	1321.29	0.03

where $x = h/90$, h is the altitude, and l_0, l_1, l_2, l_3 are the appropriate set of coefficients given in Table 12.8 for various ranges of altitude. To obtain the total ground illumination from the Moon, corrections for phase and parallax must also be added (see § 12.3.4.2).

The values for the Sun in daylight give the illuminance from direct and indirect sunlight in a cloudless sky. The values for indirect sunlight are about a factor of 10 smaller. If the sky is overcast, the values for indirect sunlight should be reduced by about a factor of 10, and if the sky is very dark by about a factor of 100. A correction of $2 \log_{10}(S/S_0)$, where S is the semidiameter of the Sun and S_0 is the semidiameter at mean distance, should be added to the daylight illuminance to allow for the variable distance of the Sun from the Earth.

When the Sun is below the horizon, the sky is illuminated from the sources discussed in the following sections.

12.3.4.1 Twilight

This is caused by the scattering of sunlight from the upper layers of the Earth's atmosphere. It begins at sunset (ends at sunrise) and is conventionally taken to end (or begin) when the center of the Sun reaches an altitude of $-18°$; this is also referred to as *astronomical twilight*. At an altitude of $-18°$, the indirect illumination from the Sun on a horizontal surface is about 6×10^{-4} lux, rather less than the contribution from starlight and airglow. The actual brightness of the sky depends on where the observer looks and where the illumination is coming from, as well as on meteorological conditions.

In navigational practice and for certain civil purposes, two intermediate steps in the twilight period are recognized and tabulated: *civil twilight* ends (or begins) when the Sun reaches an altitude of $-6°$ and *nautical twilight* ends (or begins) when the Sun reaches an altitude of $-12°$. Before morning and after evening civil twilight, outdoor activities that depend on natural lighting require artificial illumination. The degree of illumination at the beginning and end of civil twilight (in good conditions and in the absence of other illumination) is usually described for navigational purposes as illumination such that the brightest stars are visible and the sea horizon is clearly defined; for the beginning and end of nautical twilight, the corresponding statement is that the sea horizon is in general not visible and it is too dark for the observation of altitudes with reference to the horizon.

12.3.4.2 Moonlight

The illumination received from the Moon varies according to phase, altitude, and atmospheric extinction. From full Moon in the zenith, the intensity of illumination on a horizontal surface is approximately 0.27 lux, equivalent to that from the Sun at an altitude of about $-8°$. The amount of ground illumination at night from moonlight—$\log_{10} M$, where M is the illuminance in lux—may be calculated from L_1, the ground illumination from a Full Moon at altitude h, at a mean distance that has been corrected for phase (L_2) and parallax (L_3) as follows:

$$\log_{10} M = L_1 + L_2 + L_3. \tag{12.24}$$

Extracting the appropriate set of l's from the table and setting $x = h/90$, where h is the altitude of the Moon, then

$$
\begin{aligned}
L_1 &= l_0 + l_1 x + l_2 x^2 + l_3 x^3 \\
L_2 &= -8.68 \times 10^{-3}\, f - 2.2 \times 10^{-9}\, f^4 \\
L_3 &= 2 \log_{10}(\pi/0.951); \qquad (12.25) \\
\text{where } f &= 180^\circ - E \\
\text{and } \cos E &= \sin \delta_S \ \sin \delta_M + \cos \delta_S \cos \delta_M \ \cos(\alpha_M - \alpha_S).
\end{aligned}
$$

Figure 12.3 also shows the ground illumination on a horizontal surface from the standard phases of the Moon at mean distance and at various altitudes. The half Moon gives only one-ninth as much light as the full Moon. For astronomical observations, the position of the Moon in the sky, rather than the general illumination, is the most important factor.

12.3.4.3 Starlight, Airglow, Aurora, Zodiacal Light, and Gegenschein

The total illumination from the stars contributes about 2.2×10^{-4} lux, rather less than the Sun at the beginning and end of astronomical twilight. The illumination from the stars together with airglow contributes about 2×10^{-3} lux. The illumination from the aurora (which depends upon solar activity) may in rare cases be comparable with moonlight. The other sources are very faint and never give an illumination greatly exceeding that from starlight. As with moonlight, the position of the source is the most important factor for astronomical observations.

12.4 Occultations

Only dates and general areas of visibility for the occultations of planets and bright stars by the Moon are published in *The Astronomical Almanac*. As the International Lunar Occultation Centre ceased operations in March 2009, coordination of occultation observations by the Moon is now handled by The International Occultation Timing Association (IOTA) at URL[2].

12.4.1 Occultations of Stars

Whenever a star is within an angular distance from the Moon that is less than the sum of the Moon's horizontal parallax and semidiameter, it will be occulted from some point on the Earth. The large number of occultations makes it impossible to publish maps of each occultation in *The Astronomical Almanac*. However, global visibility maps are available on *The Astronomical Almanac Online* website (URL[1]). It is possible, however, to calculate and display these maps on a personal computer. The calculations require the Besselian elements, which are defined in a similar way to those for eclipses (see § 11.3.2). In occultations, the fundamental plane passes through the center of the Earth and is perpendicular to the line joining the star and the center of the Moon—i.e., to the axis of shadow. The origin of the coordinates is the center of the Earth; the x-axis is the intersection of the Earth's equator with the fundamental plane and is taken as positive toward the east; the y-axis is perpendicular to that of x and is taken as positive toward the north in the fundamental plane. The great distance of the star implies that the fundamental plane is perpendicular to the line joining the center of the Earth to the star, and that the Moon's shadow is essentially a cylinder whose intersection with the fundamental plane is a circle of invariable size, its diameter being equal to that of

the Moon. The coordinates of the center of this circle—i.e., the axis of shadow—are denoted by x and y. The adopted unit of linear measurement is the Earth's equatorial radius.

The Besselian elements are given for one instant only—namely, the time of conjunction of the star and Moon in right ascension, when x is zero. They are:

$$\begin{aligned} T_0 &= \text{the UT of conjunction in right ascension;} \\ H &= \text{the Greenwich Hour Angle of the star at } T_0; \\ Y &= y \text{ at } T_0; \\ x',\ y' &= \text{the hourly rates of change in } x \text{ and } y; \\ \alpha_s,\ \delta_s &= \text{the right ascension and declination of the star.} \end{aligned}$$

The formulae for x and y, the coordinates of the center of the shadow in the fundamental plane, are

$$\begin{aligned} x \sin\pi &= \cos\delta\ \sin(\alpha - \alpha_s) \\ y \sin\pi &= \sin\delta\ \cos\delta_s - \cos\delta\ \sin\delta_s\ \cos(\alpha - \alpha_s) \end{aligned} \tag{12.26}$$

where α and δ are the right ascension and declination of the Moon at a particular Universal Time and π is the parallax.

For prediction purposes these reduce to

$$x = \frac{\alpha - \alpha_s}{\pi}\ \cos\delta; \qquad y = \frac{\delta - \delta_s}{\pi} + 0.0087\, x(\alpha - \alpha_s)\ \sin\delta_s \tag{12.27}$$

where α, δ, and π are in degrees.

At conjunction

$$\begin{aligned} x &= 0; \qquad y = Y = \frac{\delta - \delta_s}{\pi} \\ x' &= \frac{\alpha' \cos\delta}{\pi}; \qquad y' = \frac{\delta'}{\pi} - Y\frac{\pi'}{\pi}. \end{aligned} \tag{12.28}$$

Here the primed quantities are hourly variations that arise from differentiating the Moon's daily polynomial coefficients for α, δ, and π.

The rectangular coordinates of the center of the shadow on the surface of the Earth at Universal Time t from conjunction are given by

$$\begin{aligned} x &= x't \\ y &= y't + Y \\ z &= \sqrt{(1 - x^2 - y^2)} \end{aligned} \tag{12.29}$$

where z is measured along the shadow axis from the fundamental plane toward the Moon. The longitude and latitude (λ, ϕ) of this point on the surface of the Earth are calculated from

$$\begin{aligned} \phi &= \sin^{-1}(y\cos\delta + z\sin\delta) \\ h &= \tan^{-1}\frac{x}{-y\sin\delta + z\cos\delta} \\ \lambda &= h - (H + 15 \times 1.002738\, t). \end{aligned} \tag{12.30}$$

The rectangular coordinates of the edge of the shadow on the surface of the Earth,a (ξ, η, ζ), are given by

$$\begin{aligned} \xi &= x - k \ \sin Q \\ \eta &= y - k \ \cos Q \\ \zeta &= \sqrt{(1 - \xi^2 - \eta^2)} \end{aligned} \tag{12.31}$$

where $k = 0.2725$ is the radius of the Moon in Earth radii and Q cycles through the range 0° to 360°. The longitude and latitude (λ, ϕ) of a point on the edge of the shadow is obtained from Eq. 12.30 by replacing (x, y, z), with (ξ, η, ζ).

The remainder of this section describes how to plot a map of the area of visibility of an occultation. Project the longitudes and latitudes of the continents, islands, and places of interest onto the plane that passes through the center of the Earth and is perpendicular to the direction defined by a vector from the center of the Earth to the place λ_c, ϕ_c. Here (λ_c, ϕ_c) is the longitude and latitude of the center of the shadow at the time of conjunction. This plane rotates with the Earth and coincides with the fundamental plane at conjunction. The rectangular coordinates of a place at longitude and latitude (λ, ϕ) are given by

$$\begin{aligned} u &= \cos\phi \ \sin(\lambda - \lambda_c) \\ v &= \sin\phi \ \cos\phi_c - \cos\phi \ \sin\phi_c \cos(\lambda - \lambda_c) \\ w &= \sin\phi \ \sin\phi_c + \cos\phi \ \cos\phi_c \cos(\lambda - \lambda_c) \end{aligned} \tag{12.32}$$

where u and v are in the plane (with the origin at the center of the Earth), u is to the east, v is to the north, and w is the height of the place above the plane; $w \geq 0$ for all places to be plotted.

To plot the edge of the shadow at any time during the occultation, calculate the rectangular coordinates of the center of the shadow x_0, y_0, from Eq. 12.29. Then calculate the coordinates ξ, η, ζ of the edge of the shadow from Eq. 12.31 and obtain the corresponding (λ, ϕ) from Eq. 12.30. Finally project the (λ, ϕ) of the shadow outline onto the same plane as the continents, etc., using the coordinates (u, v) in Eq. 12.32.

When $\xi^2 + \eta^2 > 1$, the shadow is only partially on the Earth. To find the values Q_1 and Q_2 where the edge of the shadow cuts the surface of the Earth, see Fig. 12.4, where O is the center of the Earth and S is the center of the shadow.

The great circle arc AB between the polar angle θ_1 and θ_2 is then plotted by setting $x = \cos\theta$, $y = \sin\theta$, and $z = 0$, and using Eqs. 12.30 and 12.32. The polar angles are found as follows: Calculate Q_1 and Q_2 from

$$\sin(Q_1 + S) = \frac{k^2 + D^2 - 1}{2kD} \quad \text{and} \quad Q_2 = 180° - Q_1 - 2S \tag{12.33}$$

$$\text{where } D = \sqrt{(x_0^2 + y_0^2)} \quad \text{and} \quad S = \tan^{-1}(y_0/x_0).$$

Then for $i = 1$ and 2

$$\begin{aligned} \xi_i &= x_0 - k \sin Q_i \\ \eta_i &= y_0 - k \cos Q_i \\ \text{and} \quad \theta_i &= \tan^{-1}(\eta_i/\xi_i), \ 0° \leq \theta_i \leq 360°. \end{aligned} \tag{12.34}$$

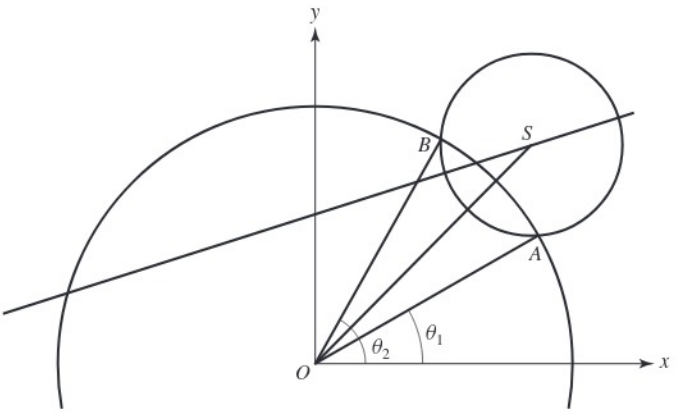


Figure 12.4 Fundamental plane showing path of occultation

The total area of visibility of the occultation may also be plotted by repeating the calculation for a series of times between the start and the end of the occultation on the same diagram.

A similar procedure may be applied for predicting the areas of visibility of occultations of planets by the Moon.

12.4.2 Occultations of Planets

The prediction of occultation of stars (or minor planets) by planets (or by minor planets) largely centers on the search for conjunction in right ascension within the limits of difference of declination that make an occultation possible. These limits are very small, being approximately the sum of the horizontal parallax and the semidiameter of the planet.

The observations themselves yield useful information on the diameters of planets and about the shape of minor planets.

The actual prediction follows the basic principles underlying those for eclipses, occultations, and transits; but more direct and less formal methods are used because the angles involved are much smaller and the prediction much less precise.

An occultation will take place as seen from some point on the Earth's surface, provided the difference $\delta - \delta_s$ in apparent declination at the time of conjunction in right ascension satisfies the condition

$$\left|\delta - \delta_s\right| < (\pi + s)/\left|\sin \rho\right| \tag{12.35}$$

where π and s are respectively the equatorial horizontal parallax and semidiameter of the planet and ρ is the position angle of its direction of motion. Note must be taken of the position of the Sun, as for lunar occultation, because it is generally useless to predict occultations of stars in daylight.

Methods of prediction are described by Taylor (1955); the paper also described the determination of the actual limits of occultation. The IOTA (see § 12.4) provides predictions of planetary occultations (URL[2]) that are also published in *Sky and Telescope*. Predictions

of planetary occultations are also published in *The Handbook of the British Astronomical Association* and the *Observer's Handbook* of the Royal Astronomical Society of Canada.

12.5 Pole Star Tables

The proximity of the second-magnitude star α Ursæ Minoris, (Polaris or the Pole Star), to the north pole of the sky has given it a special significance for the convenient determination of direction and latitude. This is particularly so in the fields of navigation and surveying, for which the Pole Star's constant availability for observations (in northern latitudes) and the simple methods that can be used for the reduction of observations are invaluable. For the more precise requirements of astronomy, the Pole Star's distance from the true pole is sufficiently large that the special methods of reduction no longer confer an advantage over standard methods. Thus Pole-Star tables are restricted to the precision required in navigation and surveying. The principal table with the precision required by surveyors is included in *The Astronomical Almanac*, pp. B88–B91.

An alternative to the Polaris table is to use expressions involving coefficients for the GHA and the polar distance p (see § 12.5.1). These coefficients are provided on p. B92 and include the 5.5 magnitude star σ Octantis, which lies close to the south celestial pole.

If the polar distance of Polaris is denoted by p (of the order of one degree) and its local hour angle by t, then its altitude h and azimuth Z, as seen from an observer in latitude ϕ, are given by solving the spherical triangle (see Fig. 12.5) formed by the North Pole, the zenith, and Polaris, S.

Because p is small, the solution may be expanded as

$$h = \phi + p\cos t - \frac{1}{2}p\sin p\ \sin^2 t\ \tan\phi + \cdots,$$
$$-Z\ \cos\phi = p\sin t + p\sin p\ \sin t\ \cos t\ \tan\phi + \cdots. \tag{12.36}$$

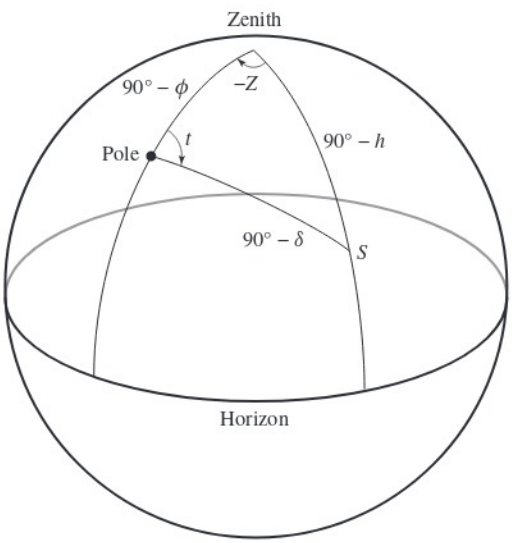


Figure 12.5 *P Z S* triangle for Polaris

In each case, the next term of the expansion is of order $p \sin^2 p \tan^2 \phi$ and cannot, for many years, exceed 0.′1 for latitudes up to 70°.

For convenience of tabulation, these expressions are rewritten in the form

$$\begin{aligned}
\phi - h = & -(p_0 \cos t_0 - \frac{1}{2} p_0 \sin p_0 \sin^2 t_0 \tan \phi_0) \\
& + \frac{1}{2} p_0 \sin p_0 \sin^2 t_0 (\tan \phi - \tan \phi_0) \\
& - (p \cos t - p_0 \cos t_0) = a_0 + a_1 + a_2 \\
Z \cos \phi = & -(p_0 \sin t_0 + p_0 \sin p_0 \sin t_0 \cos t_0 \tan \phi_0) \\
& - p_0 \sin p_0 \sin t_0 \cos t_0 (\tan \phi - \tan \phi_0) \\
& - (p \sin t - p_0 \sin t_0) = b_0 + b_1 + b_2
\end{aligned} \tag{12.37}$$

in which p_0 and t_0 are the polar distance and hour angle of a convenient point close to the mean position of Polaris throughout the year, and ϕ_0 is a mean latitude, usually chosen to be 50°. The mean position of Polaris (which must not be confused with its mean place) is usually chosen to have convenient exact values for its right ascension α_0 and polar distance p_0.

The first terms (a_0, b_0) in the modified expressions are functions of a single variable, local sidereal time, LST, because

$$t_0 = \text{LST} - \alpha_0 \tag{12.38}$$

and may be tabulated at a suitable interval of LST.

The second terms (a_1, b_1) are functions of t_0 (i.e., of LST) and of latitude and must thus be tabulated in a double-entry table with arguments LST and latitude. By incorporating a mean value (corresponding to latitude ϕ_0) in the first term, the magnitude of these terms can be kept down to about 0.′5; terms may thus be tabulated at wide intervals of latitude and LST.

Similarly, the third terms (a_2, b_2) are functions of t_0 and of the apparent position of Polaris (i.e., "of date"). By proper choice of p_0 and α_0, the magnitude of these terms can be kept down, during the year, to about 0.′5; and they can also be tabulated at wide intervals of date and LST.

As will be seen from the Polaris table in *The Astronomical Almanac*, the single-entry table of a_0 and b_0 is arranged in twenty four columns, each containing values for one hour of LST; this arrangement enables separate tables of a_1 and b_1, and of a_2 and b_2, to be given for each hour of LST. In the column corresponding to the hour of LST all these terms are taken from single-entry tables—the first with argument minutes and seconds of LST, the second with argument latitude, and the third with argument date. The error in using the tables for the hour, without interpolation for LST, is greatest for the second term b_1 (owing to its dependence on sin 2 t_0) and may reach 0.′15 for extreme latitudes; otherwise the error is small.

The complications of these tabulations are unnecessary for astronomical use, but valuable for navigational use, in which simplicity of tabular entry and of interpolation are of foremost importance. The Polaris table in *The Nautical Almanac* is essentially the same as the table in *The Astronomical Almanac*, except for the intervals of tabulation (1° in LST or LHA of the first point of Aries) and from a further simplification for the user by adding constants (whose sum is one degree) to a_0, a_1, a_2 to make them always positive. Since lower precision is required in azimuth the b coefficients have been replaced by a simpler table of azimuth as a function of LHA Aries and latitude.

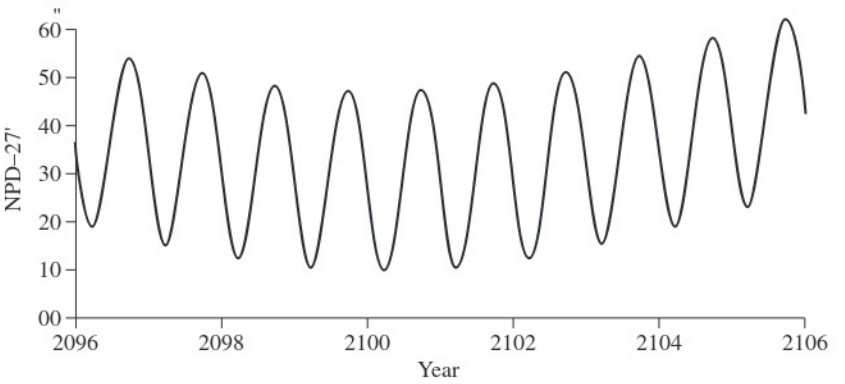


Figure 12.6 Polaris north polar distance 2096–2105

12.5.1 Derivation of the Pole Star Coefficients

The Greenwich Hour Angle (GHA) and polar distance (p) are expressed as series of polynomial terms that allow for precession and proper motion, and also as series of trigonometric terms that contain the leading terms in aberration and nutation. Thus

$$\begin{aligned} \text{GHA} &= a_0 + a_1 L + a_2 \sin L + a_3 \cos L + a_4 \sin M + a_5 \cos M \\ &\quad + a_6 \sin 2L + a_7 \cos 2L + 15\text{UT} \\ p &= a_0 + a_1 L + a_2 \sin L + a_3 \cos L + a_4 \sin M + a_5 \cos M \\ &\quad + a_6 \sin 2L + a_7 \cos 2L \end{aligned} \tag{12.39}$$

where $a_0, a_1, \ldots, a_7$ are two sets of constants in degrees, UT is the Universal Time in hours, $L = L'n$, $M = \Omega' n$ (where L' and Ω' are the rates of change of the mean aberrated longitude of the Sun and the mean longitude of the ascending node of the Moon), and n is the interval from the beginning of the period to the time required.

The coefficients are determined by the method of least-squares. Annual coefficients are derived by taking daily values. Using all eight coefficients, the annual fit gives maximum errors of $\pm 0''.2$. If only the first four terms are used in the least-squares approximation then the maximum errors increase to $\pm 1''.0$. Pole Star coefficients have been calculated for the ten-year period 2096 to 2105, based on its FK4 position and proper motion to demonstrate the principle of the method. The north polar distance is found to decrease from its present value of about $48'$ to $27'\ 10''$ on 2100 March 20 and will then increase. The distance will reach 1° by about 2250 and 2° by about 2450. (See Fig. 12.6.)

The Pole-Star coefficients may be used to calculate the UT of upper culmination of Polaris (UC) at the observer's longitude, the UT of the elongation west (EW), and the elongation east (EE) at the observer's longitude and latitude.

Calculate GHA_0, and p_0 at 0^h UT. Then calculate the local hour angle $\text{LHA}_0 = \text{GHA}_0 + \lambda$, where λ is the observer's longitude. Upper culmination occurs at time

$$t^\text{h} = \frac{360 - \text{LHA}_0}{15.041069} \tag{12.40}$$

and also at time $t^{\mathrm{h}} - 23.934$ on the previous day. Elongation east and elongation west occur at times

$$t^{\mathrm{h}} \pm \frac{\cos^{-1}(\tan\phi \tan p_0)}{15.041069} \tag{12.41}$$

where the plus sign is used for EW, and the minus sign for EE, and ϕ is the observer's latitude. If necessary add or subtract $23^{\mathrm{h}}.934$ to the time of the phenomenon to obtain a time nearer the time of observation.

REFERENCES

1. The Astronomical Almanac Online:
http://asa.usno.navy.mil or http://asa.hmnao.com.

2. The International Occultation Timing Association (IOTA):
http://lunar-occultations.com/iota/lunarreport.htm.

Bennett, G. (1982). The Calculation of Astronomical Refraction in Marine Navigation. *Journal of the Institute of Navigation 35*, 255.

Janiczek, P. and J. DeYoung (1987). Computer Programs for Sun and Moon Illuminance with Contingent Tables and Diagrams. Circular 171, USNO, Washington, DC.

Radio Corporation of America (1974). *Sources of Radiation*. RCA. Section 6, p. 61.

Taylor, G. (1955). The prediction of occultation of stars by minor planets. *Journal of the British Astronomical Association 65*, 84.

Woolard, E. and G. Clemence (1966). *Spherical Astronomy*. New York and London: Academic Press. p. 215.

CHAPTER 13

Stars and Stellar Systems

SUSAN G. STEWART

13.1 Introduction

The Stars and Stellar Systems section of *The Astronomical Almanac* is a collection of tables containing coordinates and associated data for a wide variety of sources. The sources span the entire wavelength regime from radio, visible, X-ray and gamma ray and types from single stars to stellar groupings. The tables are representative of the wide variety of astronomical research and aim to present a comprehensive sample of sources for each. Tables are selected based on their usefulness and the availability of reliable data. We work closely with the International Astronomical Union (IAU) and its working groups to ensure that the data presented in the tables are the most reliable and currently relevant available.

Sources are often chosen to serve as finding lists and, hence, are distributed isotropically where possible. This is especially the case of the stellar tables where there are seemingly an unlimited number of sources to choose from. Other selection criteria, such as magnitude, may limit the selection further. Some of the tables serve a specific purpose such as standards for calibration. Selection criteria for each table is listed in the Notes and References section of *The Astronomical Almanac* and discussed in further detail below.

Several of the more popular lists are provided in downloadable form on *The Astronomical Almanac Online* website in the form of ASCII and PDF tables. Searchable databases of bright stars and *UBVRI* Landolt photometric standard stars, selected on position and magnitude, are also available on the website.

13.1.1 Data Presentation

The tables are a combination of commonly used designations, coordinates, data and notes. The data and associated properties such as magnitudes, spectral types, velocities, fluxes, etc. are chosen on the advice of experts in their respective fields and aim to be the most useful to the observer. These data are generally static, while a new set of coordinates, obtained for the current edition via a precession routine, are generated annually. Positions for sources are accurate to the precision listed in tables and, in general, are given to be sufficient for identification using a telescope.

The tables of ICRF2 radio source positions, radio flux calibrators, pulsars and gamma ray sources do not have their positions updated annually, instead, the ICRS J2000.0 positions are given. Given that the ICRF radio sources actually define the ICRF whose axes are fixed in time (see Chapter 4), the table is naturally fixed as well. The decision to present the radio flux

calibrators and pulsars in a similar manner was based on the fact that both the flux calibrators and pulsars are often observed similarly and simultaneously with the ICRF objects.

Data going into each table are checked annually for updates. In addition to the positional data, some tables are revised more frequently than others for a few reasons, typically due to data changing quickly or to newly published data. For example, the double star orbital parameters are generated annually due to their changing orientation, whereas the table of open clusters, pulsars and exoplanets are updated frequently due to on-going research which is readily available.

13.1.2 Sources of Data

Given the wide array of data provided in the Stars and Stellar Systems section of *The Astronomical Almanac*, there are various sources from which they originate. The tables are either compiled by USNO astronomers from recommended catalogs or provided entirely by a person or group in the astronomical community. The stellar data tend to be compiled from catalogs with recommended selection criteria, while the shorter wavelength data come from a compilation of published results augmented by personal research. The tables of photometric and radial velocity standards are selected and prepared by the IAU Committees responsible for maintaining them. The specific sources for data in each table are discussed below as well as listed in the Notes and References section of *The Astronomical Almanac*.

13.1.3 Sources of Position

Positional data are included in each table in this section of *The Astronomical Almanac*. Often the original data sources for a table contain imprecise or inaccurate positions. In these cases, the positions have likely been updated using an astrometric quality catalog. Specifics for each table are given in the Notes and Reference section of *The Astronomical Almanac*. For many of the tables, the U.S. Naval Observatory Merged Astrometric Database, NOMAD, was used.

13.1.3.1 NOMAD

Quite often users of star catalogs want the best astrometry available. Although existing data services provide a wealth of astrometry—the best example being the Centre de Donnees astronomiques de Strasbourg (CDS; URL[2])—yet none give users the single most accurate result for any particular object. During the 1990s the U.S. Naval Observatory undertook a project to provide this information. The result of this project, named Naval Observatory Merged Astrometric Database, or NOMAD, became publicly available in 2004 (Zacharias et al. 2004a); see URL[3].

NOMAD is a database containing information on over 1 billion stars, including all the bright stars. The faint limiting magnitude is about $V = 20$. It provides the best astrometry (and often the best photometry) for any set of stars. For each star, only one high-quality position and proper motion is listed, regardless of the number of catalogs in which the star is listed. Several photometric bands are given, including 2MASS near IR photometry. Additionally, there are cross references to other catalogs. The database is accessed through a Graphical User Interface.

Astrometry in NOMAD is taken from six input catalogs: *The Hipparcos Catalogue* (Perryman and ESA 1997); *Tycho-2* (Høg et al. 2000), UCAC2 (Zacharias et al. 2004b), YB6 (an unpublished re-measurement of the Lick and Yale proper motion plates, Monet 2004), 2MASS point source catalog (Cutri et al. 2003; URL[4]), and USNO-B (Monet et al. 2003). Due to varying magnitude-dependent accuracies of the input catalogs, the following precedence is used for the astrometry found in NOMAD. For stars brighter than $V = 8.0$: *Hipparcos*, *Tycho-2*, then UCAC2. For $V = 8.0$ and fainter, the order of precedence is *Hipparcos*, UCAC2, *Tycho-2*, USNO-B, YB6, then 2MASS. As for photometry, the optical data are taken in the following order: *Tycho-2*, YB6, USNO-B, then UCAC2. For near IR photometry, only 2MASS was used.

Since NOMAD provides high quality astrometry for any star regardless of magnitude, it has been used as the basis of positions and motions in many tables found in *The Astronomical Almanac*.

13.2 Stellar Data

13.2.1 Bright Stars

One of the most used parts of *The Astronomical Almanac* is the table of Bright Stars. It is used for a wide array of purposes, most notably to set telescope coordinates, focus cameras, and calibrate optics. For this reason, you will often find a copy of the book in a telescope dome. It is useful in preparing finding charts for observing runs or for training students in observational techniques. The list is also used for nautical, air, and land navigation. Due to its popularity to a wide range of users, the list is constructed to be an isotropic, dense group of stars to the visual magnitude limit of 5.5.

The original selection was taken from the *Basic Fifth Fundamental Catalogue* (FK5, Fricke et al. 1988) and the fifth edition of the *Yale Bright Star Catalog* (BSC5, Hoffleit and Warren 1991). All stars brighter than visual magnitude 5.5 in the FK5 and 4.5 in the BSC were included. Also integrated into the table was a list of MK Atlas standards and anchor points for the MK spectral classification system (Morgan, Abt, and Tapschott 1978; Keenan and McNeil 1976). Since many of these standard stars overlap with stars already included in the above selection, a separate table in *The Astronomical Almanac* was not necessary. When the coordinates of the bright stars were updated to the International Celestial Reference System (ICRS), it was decided to keep the selection of stars the same as in previous years since it was complete. Thus, the criteria for inclusion in the list of Bright Stars are those mentioned above, plus being listed in the *Hipparcos Catalogue*. Only 14 stars from the original FK5/BSC selected list were excluded due to this final criterion.

Positions for the list of Bright Stars are taken from the *Hipparcos Catalog*. The proper motion, parallax and radial velocity, when available, are included in the routines which produce geocentric stellar positions for the mean equator and equinox of the middle of the edition year. From the 2003 edition through the 2008 edition, the Bright Star list typically used *Hipparcos* positions with *Tycho-2 Catalogue* proper motions. In the preparation of the 2009 edition, *Tycho-2* proper motions were replaced, so that all stars now use *Hipparcos* astrometry; the effects were minimal. If a star is listed in the *Hipparcos Double and Multiple*

System annex (DMS), then the astrometry in the DMS takes precedence. An exception is for stars marked with an "o" flag in the table. These are wide orbit stars: positions of each star are calculated using center-of-light FK5 astrometry and orbital data from the *Sixth Catalog of Orbits of Visual Binary Stars* at URL[5].

The apparent visual magnitudes and colors are taken from the BSC5, since these have been carefully scrutinized over the years. For several stars with large variability, a magnitude range is determined on a case by case basis. Spectral types originate from W. P. Bidelman who maintained a card catalog of stellar spectral types, compiled by a lifetime of personal research. He graciously provided types for the stars listed here, and since then, they have been updated by R.F. Garrison. The MK standards define the spectral classification system and types are taken from the MK atlas. The anchor points are a subset of standard stars which have survived through the years with no change, and which, therefore, represent the most stable points in the system. A note is given in the table when either the magnitudes or spectral types are from more than one stellar source (i.e., a blended image).

13.2.2 Double Stars

Double star systems permit the determination of the stellar mass, hence their importance in astrophysics, given that the structure and evolution of a star are basically dependent on two parameters: (1) the initial chemical content, and (2) the initial mass. While most of the main sequence is well determined, the two ends are still poorly characterized, as are stars off the main sequence. Even for stellar types which are well known, additional mass determinations can probe more subtle differences in chemical properties as well as intra- and inter-cluster variations. The numbers and distribution of binary stars also provide insights into the process of star formation.

Double and multiple stars constitute an important fraction of the stellar population. The term double star includes optical pairs formed by chance juxtaposition of unrelated stars, as well as true binaries that are physically related. For many double stars there is not enough information to determine whether the pair is physical; therefore, catalogs also include optical doubles. Historically, double stars have also been differentiated by the observational means used to discover and study them. Thus, there are not only visual doubles, but also spectroscopic, astrometric, photometric, interferometric, and occultation pairs. With the development of modern observing techniques, however, these distinctions are increasingly blurred.

Multiple systems, containing more than two components, generally are classed as either *hierarchical* or *nonhierarchical*. In the first instance, a typical triple will contain a close pair and a third component, located at a distance many times the separation of the close pair. These hierarchical multiples, despite being quite small, are usually virialized. In the second instance, the separations of all the components are roughly the same. Examples of these classes are Epsilon Hydrae (hierarchical) and the Trapezium (nonhierarchical).

Nomenclature for double stars is extremely mixed. Visual pairs are usually designated by the discoverer's abbreviation and serial number, although some observers have neglected to number all or a portion of their pairs. Eclipsing pairs are designated by the variable star nomenclature. Spectroscopic binaries are usually designated by their Bayer/Flamsteed designation or HD number. Occultation binaries are often denoted by their SAO or ZC num-

ber, although this is by no means universal. There appears to be no standard nomenclature whatsoever for astrometric or other more exotic binaries, which are given a multitude of designations taken from various catalogs. An effort is underway to unify the various nomenclature schemes. For further details on this effort, see the Washington Multiplicity Catalog (WMC) webpage at URL[6].

With a few exceptions, the primary (A component) of a visual double is the brighter star; the secondary (B component) is fainter. There are systems of very small magnitude difference, however, where this distinction is arbitrary. Further, there are cases where the distinction of which component is brighter depends on the observed wavelength. Additional components in a multiple system are designated C, D, and so on, in order of discovery; simultaneous discoveries are ordered by increasing separation. It sometimes happens that a new, close, companion is discovered in an already defined system. The convention is then to designate it with lower case letters. For example, if the A component of a wide pair is split into a close pair, then star A is redesignated as the system Aa,Ab. However, these rules of component designation have not always been historically followed. The WMC is striving to correct all these errors.

The table of Selected Double Stars in *The Astronomical Almanac* gives orbital data for double stars in the table of Bright Stars. Positions are of the primary star and taken from the Bright Star table. As indicated by the epoch, the orbital data are either the most recent measure (a date in the past) or calculated for the epoch of the edition. The criteria for inclusion in the table is that the pair (1) is listed in the table of Bright Stars; (2) includes the primary; (3) has a separation greater than 3 arcseconds; and (4) has a magnitude difference of less than 3 magnitudes. A few other systems of recent interest are also present. Therefore, the systems that are included are those that would be seen by most observers with a moderate-sized telescope.

The data listed in this table are taken from the *Washington Double Star Catalog* (WDS; URL[7]), also issued in CD form. It is an update of earlier editions of the WDS (1984, 1996 and 2001) and is the replacement for the *Index Catalog of Visual Double Stars*, 1961.0, issued by the Lick Observatory, and commonly called the IDS. While the format of the WDS was initially the same as the IDS, the catalog has evolved to include other parameters such as precise (arcsecond) coordinates of the primary, proper motion of the secondary, and codes to indicate the object is in one of the other USNO double star catalogs. As of this writing (2012), the WDS contains orbital data and other information for components of 108,628 systems. The "current" version of the WDS is regenerated each day and made available on the website. This site also includes lists of "neglected" doubles (those needing observation or confirmation), verified single stars (for calibration purposes), cross-references to historical double star catalogs and modern astrometric catalogs, as well as various statistical and historical files. The companion catalog to the WDS is the *Photometric Magnitude Difference Catalog* at URL[8]. This catalog contains the differential measures of each pair.

13.2.2.1 Other Double Star Data

The U.S. Naval Observatory also maintains the *Visual Orbit Catalog* (currently in its 6th version; URL[5]), which contains orbital elements, ephemerides, notes, orbit plots, and objective grades for 2,236 orbits of 2,127 systems (as of January 2011) as well as an additional subset of orbits considered of sufficient quality to be used for scale calibration. A list of 1,165

systems whose motion can be characterized as rectilinear is available from USNO at URL[9]. These optical systems can also be quite effective for scale calibration purposes as well as differential proper motion determinations.

The USNO also maintains the *Magnitude Difference Catalog* (54,436 systems, 165,058 measures as of November 2011) of this quantity and the *Interferometric Measures Catalog*, which contains many of the same measures of this type common to the WDS, but provides additional information such as the wavelength of observation.

Eclipsing and cataclysmic binaries are listed by Downes et al. (2001), Ritter and Kolb (1998), van Paradijs (1995), and Svechnikov and Bessonova (1984). These catalogs contain a variety of parameters whose enumeration is not appropriate for this discussion.

The venerable catalog of orbits of spectroscopic binaries by Batten, Fletcher, and McCarthy (1989) is in the process of being updated by IAU Commission 30 (Radial Velocities) under the guidance of D. Pourbaix. For further information see URL[10]. Unfortunately, there is no modern catalog for known or suspected spectroscopic binaries that have no calculated orbit.

13.2.3 Photometric Standards

Photometric systems are defined by the filters used to measure flux of objects in different wavelength passbands. The various photometric systems in use are summarized in Table 15.5 of *Allen's Astrophysical Quantities* (Allen and Cox 2000). Widely used at this time is the *UBVRI* Johnson-Kron-Cousins system which is a combination of the Johnson-Morgan *UBV* system (Johnson and Morgan 1953) and the Kron-Cousins *RI* (Kron, White, and Gascoigne 1953; Cousins 1976). This system has broad passbands 700–1000 Å wide, with effective wavelengths of 3600 Å, 4400 Å, 5500 Å, 6400 Å and 7900 Å, respectively.

Standard stars are used to define photometric systems. They are needed to calibrate telescopes and reduce raw observations to produce stellar magnitudes. The standards provided by Landolt are widely used to define the *UBVRI* system. These standards are located in a narrow band surrounding the celestial equator and, therefore, are convenient to astronomers worldwide. At their inception, they served to fill the need for a fainter list of standard stars given the improvement of telescope optics. Landolt's first list was of 642 faint *UBV* standard stars $10.5 < V < 12.5$ within a 1 degree band of the celestial equator (Landolt 1973), followed by a list of 223 faint *UBVRI* standards stars $7 < V < 12.5$ and $-0.3 < (B - V) < +2.0$ within a 2 degree band of the celestial equator (Landolt 1983). The second list had stars calibrated in the *UBV* by the first list and *RI* of Cousins (1976). The observations are made in what is termed *selected areas* with finding charts listed in the publication.

Beginning with the 2013 edition of *The Astronomical Almanac*, the printed list is based on Landolt (2009) which provides new *UBVRI* observations of 202 stars centered on the celestial equator, augmenting the 526 stars from Landolt (1992) which had been the source in earlier editions. The almanac list is comprised of the combined list given in Table 2 of Landolt (2009) and provides standard star observations in the magnitude range $8.90 < V < 16.30$ and color range $-0.35 < (B - V) < +2.30$. The list serves to provide standards for intermediate and large size telescopes in both hemispheres.

For the list in *The Astronomical Almanac*, many of the positions of the stars given in Table 2 of Landolt (2009) were replaced with those from the Naval Observatory Merged

Astrometric Database (NOMAD; URL[3]), which provides the best positions on the ICRF from the following sources in the order given: *Hipparcos Catalogue*, *Tycho-2*, UCAC2, or USNO-B (see § 13.1.3.1). Proper motions are also included in the calculation of the positions when provided in the database. However, for positions of stars new to the 2013 edition from years prior, their positions are taken from Landolt (2009); their accuracy has yet to be verified and may be off by several arcseconds.

The Landolt standards replaced the bright *UBVRI* standards from Johnson beginning with the 2003 edition of *The Astronomical Almanac*. Given that the Johnson standards are stars about V magnitude 6.0 and brighter, it was deemed that they were too bright for much of the work being done at the time—especially observations using CCD photometers—and probably only useful to small telescope users. There are also known variables on the list and rather large known random errors, given that for many stars there are less than 10 observations. The Johnson standards are now provided on *The Astronomical Almanac Online* for epoch J2000.0. The list was selected by H.L. Johnson from those given in Johnson et al. (1966), who selected an evenly distributed group of 107 stars, with 45 stars being primary standards of the *UBV* or *UBVRI* systems, and the rest of the stars were those that were observed many times (those stars with more than 9 observations). The star names, positions, and spectral types are taken from the Bright Star list.

Also included in *The Astronomical Almanac* are standards for the Strömgren *uvby* intermediate-band photometric system and the Hβ narrow-band system, providing an excellent tool for supplementing the wide-band photometric systems. Wide-band systems give only a few parameters that can be used to get information on stellar (and other) characteristics, such as surface temperatures, absolute magnitudes, and interstellar reddening (and absorption). The intermediate and narrow-band photometric indices offer more potential and are designed also to be able to separate parameters. For example, indices are responsive not only to temperature, but to a variety of other parameters, such as heavy element abundance and surface gravity. Because they are seen in most stars—they are strongest in stars with a surface temperatures of about 10,000 kelvin (stellar spectral type A)—the hydrogen Balmer series are often used to determine stellar radial velocities by analyzing the Doppler shift of these lines. Photometric standards for these systems are, therefore, important tools in insuring both accurate and precise photometry that can be used for these purposes.

The Strömgren photometric system was pioneered by Strömgren (1956) and upgraded by Crawford (1958), hence it is sometimes referred to as the Strömgrem-Crawford photometric system. The passbands are 180–300 Å wide centered at 3500 Å, 4110 Å, 4670 Å, and 5470 Å, with a pair of passbands at 4680 Å associated with the hydrogen Balmer lines.

The *uvby* and Hβ standards widely used by photometric observers and listed in *The Astronomical Almanac* are those of Perry, Olsen, and Crawford (1987). Only the 319 stars which have four-color data are included. Star names and numbers in the list are taken from the BSC; spectral types are those from the Bright Star list (pp. H2–H31). Visual magnitudes are taken from the original reference and, therefore, may disagree with those given elsewhere in this section.

The third set of photometric standards included in *The Astronomical Almanac* are suitable for the reduction of astronomical spectroscopic observations in the optical and ultraviolet wavelengths. Spectroscopy pertains to the dispersion of an object's light into its component colors (i.e., energies) and probes the interaction between radiation and matter as a function of

wavelength. Spectroscopy is possible by appropriate techniques in all wavelength regimes; spectrophotometry refers to spectroscopy with visible, near-ultraviolet, and near-infrared light. Applications of spectroscopy are the backbone of astrophysics, probing both the conditions of emission of radiation and its modification en route to the observer. By dispersing and analyzing an object's light, astronomers can infer the physical properties of that object (such as temperature, mass, luminosity and composition). The standards provide absolute spectral energy distributions with which to calibrate observations using these techniques.

The data for the spectrophotometric standard stars listed in *The Astronomical Almanac* were recommended by the IAU Standard Stars Working Group and taken from the European Southern Observatory's (ESO) site at URL[11] except for the positions which are taken from the NOMAD database as described in § 13.1.3.1 (URL[3]). Finding charts for the sources and plots of the magnitude and flux against wavelength are found on the website.

The standards on the ESO list are from four sources. The ultraviolet standards are from the Hubble Space Telescope (HST) ultraviolet spectrophotometric standards which are based on International Ultraviolet Explorer (IUE) and optical spectra and calibrated by the primary white dwarf standards (Turnshek et al. 1990; Bohlin et al. 1990). The optical standards are based on Hale 5m observations in the 7 to 16 magnitude range (Oke 1990) and CTIO observations of southern hemisphere secondary and tertiary standard stars (Hamuy et al. 1992, 1994). Data for four white dwarf primary spectrophotometric standards in the 11–13 magnitude range based on model atmospheres and HST Faint Object Spectrograph (FOS) observations in 10 Å to 3 microns are also included (Bohlin, Colina, and Finley 1995).

13.2.4 Radial Velocity Standards

The motion of an object along the line of sight from an observer can be obtained directly from spectroscopic measurements. Radial velocity observations are used for a wide range of applications (cluster dynamics, galaxy dynamics, stellar pulsations, mass and orbital element determinations in spectroscopic binary systems, etc.), but the instrumentation used, reduction of data, and standardization of the results are roughly similar. A reliable set of radial velocity standards are crucial in monitoring instrument stability and zero-points. The difficulty with creating a list of standards has been that they must be non-variable sources in magnitude with a sufficient history of observations.

In the late 1980s, IAU Commission 30 on Radial Velocities established a Working Group on Standard Stars, tasked to create a system of standards. Since this time, the list of standards in *The Astronomical Almanac* has been mirroring the recommendations which have resulted from their efforts in establishing a system of standards. The list was initially based on two reports from Commission 30 (IAU 1957, 1973) which combined represented the IAU radial velocity stars with late spectral types at that time. At the IAU General Assemblies in both Kyoto (1997) and Manchester (2000) it was the policy of the reestablished Working Group to remove stars from this provisional list that showed velocity variations greater than about 1 km/s, while continuing the work of three observatories developing an officially sanctioned list of standards. Geneva Observatory, Dominion Astrophysical Observatory (DAO), and the Center for Astrophysics (CfA) have each been working on establishing the list. The work of the three observatories is summarized in a report of IAU Commission 30 (IAU 1992).

Geneva Observatory has observed potential radial velocity standard stars for over 20 years using the CORAVEL instrument. These include many giants known to possess an intrinsic

velocity variability at the level of a few hundreds of m/s or less. This list is useful for low- and medium-precision work. Using the high-precision velocities from the Elodie spectrometer, it is possible to correct the small systematic color terms in the CORAVEL velocities. A set of 350 dwarf stars is being followed with this instrument with a precision of 10 m/s and a zero-point stability of a few m/s, to form in the future a new set of high-precision standards. Both lists are found at URL[12]; see also Udry et al. (1999).

The results of photographic standard star measurements at DAO have a precision of 150 m/s over a time span of almost 20 years, with an absolute zero-point linked to asteroids with a precision of 100 m/s or better. The comparison with Elodie velocities shows an absence of any color terms.

In the past, the comparison of the Geneva velocities and the combined DAO and CfA velocities showed a color term, the source of which is still not clear. Work continues on understanding this issue. Until it is resolved, Commission 30 cannot recommend a revised list. There has not been a great amount of resolution on this issue since the Manchester IAU General Assembly. The emergence of the higher precision radial velocity requirements associated with the study of exoplanets certainly has reinforced the need to continue work to this end.

In the 2002 edition of *The Astronomical Almanac*, a list of faint stars with radial velocity data (Evans 1968) was added to extend the list to the Southern Hemisphere. There was some trepidation from Commission 30 as to adding these 14 stars, but it was decided they were suitable, since they had been observed for more than 20 years.

The three lists provided by the IAU references were upgraded for the almanac by adding positions and proper motions from the *Hipparcos Catalogue*; V magnitudes from the BSC, the *Hipparcos Catalogue*, or SIMBAD; and spectral types from the list of Bright Stars (pp. H2–H31), the BSC, the *Hipparcos Catalogue*, or the original IAU list.

13.2.5 Variable Stars

Stars with variable light output are classified based on the type of variability exhibited and are divided in two main categories, intrinsic and extrinsic. The intrinsic variables are stars undergoing internal physical changes due to pulsations or eruptions. Intrinsic variable stars include pulsating stars (Cepheid variables, RR Lyrae stars, RV Tauri Stars, and long period variables such as Mira type stars) and erupting stars (supernovae, novae, recurrent novae, and dwarf novae, symbiotic stars, and R Coronae Borealis stars). Extrinsic variables are due to external factors and include stars such as eclipsing binaries and rotating variables. Variable star data can provide a wealth of information about stellar properties that can be used to understand other stars such as mass, radius, luminosity, and temperature. Cepheid variables allow for determining distances to far away galaxies and the age of the universe.

The variability of magnitude in stars can range from periods of a fraction of a second to years, depending upon the type. Therefore, variable stars need a long history of observations to be correctly classified and understood. The American Association of Variable Star Observers (AAVSO; URL[13]) is an established organization of professional and amateur astronomers which serves to coordinate, collect, evaluate, analyze, publish, and archive variable star observations.

The list in *The Astronomical Almanac* was selected and updated by astronomers at the AAVSO. It is based on data provided by the AAVSO and, since the 2000 edition, information

contained within the fourth edition of the *General Catalogue of Variable Stars* (GCVS, Kholopov et al. 1996), the *Sky Catalogue 2000.0, Volume 2* (Hirshfeld and Sinnott 1997), and *A Catalogue and Atlas of Cataclysmic Variables, 2nd Edition* (Downes, Webbink, and Shara 1997). The selection of these sources is based on having the brightest stars from each classification represented. Specific criteria for inclusion are given in the Notes and References section of *The Astronomical Almanac*. Positions and proper motions were updated for the list in *The Astronomical Almanac*, starting with the 2006 edition, using the NOMAD database which is consistent with the ICRS (see § 13.1.3.1 and URL[3]).

The nomenclature used for variable stars was developed by F.W.A. Argelander in the mid-1800s. According to this method, the first star discovered in a constellation is given the letter R, followed by the genitive form of the Latin name of the constellation. Subsequent variables in the same constellation are named S, T, and so on to Z, followed by RR to RZ; then SS to SZ, and so on to ZZ, after which follow AA to AZ, and so on to QZ, the 334th variable in a constellation. The next variable found in a constellation is named V335 plus the genitive. Stars which have been assigned Greek letters prior to the start of this system, such as Omicron Ceti, or small Roman letters, such as g Herculis, continue to keep those names.

13.2.6 Exoplanets and Host Stars

An extrasolar planet, or exoplanet for short, is a planet that orbits a star other than the Sun and that is beyond the solar system. Most have been detected through radial velocity observations—the Doppler method—and other indirect methods rather than actual imaging. Given the increased interest and research in exoplanets, adding them to *The Astronomical Almanac*, starting with the 2011 version, was considered to be valuable to the observing community.

The table of exoplanets and their host stars is based upon updated versions of the *Catalog of Nearby Exoplanets* (Butler 2006). The almanac draws from the most currently available version at the time of publication which can be found at URL[14] where a table of host star characteristics is also available. It contains all the known exoplanets with masses and orbits established by Doppler measurements of stars within 200 parsecs. Given the number of exoplanets continues to grow rapidly, selection criteria must be applied to keep the table in the almanac to a manageable size. For example, for the 2013 edition of *The Astronomical Almanac*, a subset from the data set was chosen using a host star magnitude limit of $V < 8$. Also incorporated into the table are all transiting exoplanets, which pushes the limiting magnitude of the table in the almanac to about $V = 10$. The catalog's author and exoplanet pioneer, P. Butler, suggested that useful properties of the exoplanets and host stars from the catalog would fall into two categories. For those most interested in the properties of the planets, orbital period, eccentricity, and time of periastron are the most helpful. This for instance is what is needed to calculate time of transit for the transiting planets. Those most interested in the host stars of exoplanets would want $B - V$ magnitude, parallax, and metallicity. The V magnitude of the star would be useful in both instances. These data are taken from the online catalog and included in *The Astronomical Almanac* table.

Positions, proper motions and parallaxes (where available) for the host stars were taken independently from the NOMAD database (§ 13.1.3.1; URL[3]). The mid-year positions for the host stars given in *The Astronomical Almanac* table are improved from those positions

listed in the original version of the catalog as they are both more accurate and precise; several inconsistencies in the catalog were corrected.

13.2.7 Pulsars

Radio pulsars are rapidly rotating neutron stars having strong magnetic fields. Because of their small physical size, pulsars are unresolved by even the largest radio interferometers, and are valuable as astrometric reference sources. Because of their large moments of inertia, the rotation period of pulsars is extremely regular, in most cases showing only a linear increase in the period with time as the pulsar loses energy. The oldest, coolest pulsars have long-term spin stabilities comparable to the best terrestrial clocks and are being studied for use as navigational beacons, similar to GPS. The discovery of pulsars twice resulted in the award of the Nobel Prize in Physics: in 1974 to Antony Hewish for the discovery of the first pulsars, and in 1993 to Joseph Taylor and Russell Hulse for the discovery of the first binary pulsar, B1913+16.

The list of pulsars in *The Astronomical Almanac* dates from the 2007 edition. It is derived from Manchester et al. (2005; URL[15]) and updated annually. The positions are, in nearly all cases, timing positions which are measures of arrival times on various dates spread over a time period. These are accurate well under an arcsecond for "normal" pulsars and under the milliarcsecond level for millisecond pulsars. Positions are in the coordinate system defined by the JPL planetary ephemeris. (The particular ephemeris used may vary from source to source, depending on how recently the analysis was done.) In a few cases, interferometric positions with comparable accuracy have been obtained.

13.3 Clusters and Galaxies

13.3.1 Open Star Clusters

Open clusters are irregularly shaped groups of stars moving together with roughly the same space motion. They generally lie in the galactic plane and contain prominent young stars or star forming regions. Unlike associations which are often dynamically unbound groups of stars less than 1 million years old, open clusters are dynamically bound groups of stars ranging in ages from less than 1 million years to more than 1 billion years. It is theorized that open clusters are those dynamically bound associations which survived being dispersed into smaller groups of stars. Open clusters are distinctly different from globular clusters, which are several billion years old and found in the galactic halo.

Open clusters are a crucial element in understanding the structure and history of our Galaxy, given that distances and ages of open clusters can be determined with better accuracy than for isolated field stars. Open cluster systems are key to understanding galactic dynamics, because they span a relatively wide range of ages which can be determined with more precision than any other spiral arm tracer. They are used to better understand the motion of spiral arms to derive the galactic rotation curve. They also provide a means to map the chemical composition in our Galaxy. In addition, open clusters provide a set of coeval stars with different masses that can be used to derive and test theories of star formation, such as the initial mass function, rate of matter transferred into stars, the rate of density of cloud, and rate of binary stars.

The table of open clusters was selected by Gosta Lyngå based upon the 5th (1987) edition of the Lund-Strasbourg catalog (original edition described by G. Lyngå 1981). The clusters were selected on the basis of the availability of data at the time and, therefore, comprise the most observed open clusters. The selection of the clusters remained while the data were updated over the years. For the 2005 edition of *The Astronomical Almanac*, cluster data were updated using the *New Catalog of Optically Visible Open Clusters and Candidates* (Dias et al. 2002). The online version of the catalog is available at URL[16], where additional data parameters are given and updated annually. *The Astronomical Almanac* for 2013 uses version 3.1 of this catalog. Another useful resource for open cluster data is John-Claude Mermilliod's WEBDA open cluster database at URL[17].

Listed in the table of open clusters are a number of associations that might not develop into physically bound clusters. These are the Trapezium cluster and some of the Collinder objects. The Blanco and Upgren clusters are considered physical entities, because their members have similar motions and physical properties, although they are only a small part of the total stellar population inside the volume they occupy. Clusters that are only the apparent result of the distribution of obscuring clouds have been excluded from the list.

Two identifications are given for each cluster. The first is the designation adopted by the IAU, while the second is the traditional name (Alter et al. 1970). The International Astronomical Union decided in 1979 on a nomenclature consisting of a "C" for cluster, four digits for hours and minutes of right ascension (1950.0) and a plus or minus sign plus three digits for degrees and tenths of degrees of declination (1950.0).

All data parameters for the open clusters are taken from the *New Catalog of Optically Visible Open Clusters and Candidates* (Dias et al. 2002) including positions and proper motions. Positions are consistent with the ICRS and referred to the mean equator and equinox of the middle of the Julian year.

The tabulated angular diameter of a cluster refers to the cluster's nucleus. The published values of angular diameters of clusters sometimes differ by a large factor due to different limiting magnitudes for different studies and to different opinions about the extent of each cluster.

Distances refer to the open cluster's distance from the Sun. Its determination depends on the chemical composition which is not known for many clusters. Assuming a solar composition, as is usually done, introduces some uncertainty. The most reliable way to determine the distance of an open cluster is to observe its color-magnitude diagram and fit the diagram to the main sequence of nearby stars. When a cluster includes a number of main sequence stars, this method of determining distances is superior to other methods used for distant stars or star systems. For the distance of a nearby cluster with a long main sequence, a precision as low as 10% can be achieved.

Trumpler classification is defined by R.S. Trumpler (1930). The classification scheme contains the following classes:

- Concentration of cluster stars
  - I detached, strong central concentration
  - II detached, little central concentration
  - III detached, no noticeable concentration
  - IV not well detached, appearing like a star-field concentration

- Range of stellar brightness
  - 1 most stars of nearly the same brightness
  - 2 medium range in brightness
  - 3 bright and faint stars in the cluster
- Richness of cluster (number of stars in the cluster)
  - p poor (< 50 stars)
  - m moderately rich (50–100 stars)
  - r rich (> 100 stars)
- Nebulosity
  - n cluster is involved in nebulosity

The definition of the metallicity ratio is the logarithmic ratio of the abundances of iron and hydrogen divided by the corresponding ratio for the solar spectrum. Log (Fe/H) is mostly determined from photometric narrow band or intermediate band studies. In practice, metal lines other than those of iron influence the parameter.

The logarithm to the base 10 of the cluster age in years is determined from the turnoff point on the main sequence. To have a homogeneous set of cluster ranges, Janes, Tilley, and Lyngå derived a calibration of the logarithm of age as a function of the turn-off color. The listed values of around 6.0 (one million years) can be considered as rough upper limits in most cases. Clusters of that age group might still be in the process of star formation and thus have a large spread in age between member stars. Clusters with logarithmic ages higher than 7.0 may be in error of up to a few tenths of a unit.

Interstellar extinction in front of the cluster in the visual band is tabulated using the assumption that $A_V = 3E_{(B-V)}$. The color excess $E_{(B-V)}$ is derived from some of the brightest cluster members.

An expected update to the open clusters in coming editions will include the distance from the galactic plane. By knowing the galactic latitude and the distance, one can easily compute the distance from the galactic plane, usually noted z.

13.3.2 Globular Star Clusters

For more than a century, globular clusters have provided astronomers with testbed laboratories for all kinds of astrophysical processes. First noticed for their variable star populations (RR Lyrae stars, Population II Cepheids, red-giant variables, novae), they later became essential proving grounds for the development of the theory of stellar structure and stellar evolution, and they remain the single most important way to measure the age of our Galaxy. Globular clusters are very tightly bound, giving them spherical shapes and relatively high stellar densities toward their centers, and contain more stars than the less dense open clusters. Found in the halo of a galaxy, globular clusters are fairly common. It is thought that globular clusters contain some of the oldest and first stars to be produced in a galaxy and formed with the parent galaxy rather than as distinctly separate objects. The 1970s and 1980s saw the discoveries of new high-energy sources within globular clusters (X-ray binaries and millisecond pulsars), and computer modeling of the internal dynamical evolution of clusters all the way through to core collapse. Newer observations are concentrating on tracing the faintest stars within the

clusters (the bottom ends of the ancient white-dwarf sequence), and on the characteristics of globular clusters in other galaxies.

The list of globular clusters in *The Astronomical Almanac* is provided by William E. Harris, who maintains a database of Milky Way globular clusters at URL[18]. The online list is updated regularly and provides data on distances, velocities, metallicities, luminosities, colors, and dynamical parameters.

13.3.3 Bright Galaxies

The bright galaxies are used by many groups doing high-resolution work on giant and supergiant stars, star formation and stellar populations, star clusters and associations, HII regions, novae and other bright variables, planetary nebulae, gas and dust distribution, spiral arm modeling, dark matter searches, dwarf companions, the nearby velocity field, and as fundamental or secondary calibrators for the extragalactic distance scale. The two hundred or so galaxies in *The Astronomical Almanac* form the backbone for all of these studies, so they constitute a finding list of the most important galaxies in the nearby universe. These are generally the most photogenic extragalactic objects as well, so they appear often in popular publications. Therefore, the list is also useful for the non-specialist as a handy reference to the basic properties of the galaxies.

The 198 galaxies selected for inclusion in *The Astronomical Almanac* are generally brighter than B-band magnitude 11.5 and larger than 5.0 arcminutes. These galaxies were extracted from an updated version of the *Third Reference Catalogue of Bright Galaxies* (RC3, de Vaucouleurs et al. 1991) or, in the case of two dwarf spheroidal galaxies (in Sextans and Sagittarius) not included in RC3, from the literature (see Irwin and Hatzidimitriou 1995; Ibata et al. 1997).

In most cases, the RC3 equatorial position has been replaced with a more accurate weighted mean position based on measurements from many different sources, some unpublished. Nominally, all positions are on the ICRS, explained elsewhere in this volume. Where positions for unresolved nuclear radio sources from high-resolution interferometry (usually at 6- or 20-cm) are known to coincide with the position of the optical nucleus, we have adopted the radio positions. Similarly, we have adopted positions from the 2-Micron All-Sky Survey (2MASS, see e.g., Jarrett et al. 2003) where these coincide with the optical nucleus. Positions for magellanic irregular galaxies without nuclei (e.g., LMC, NGC 6822, IC 1613) are for the centers of the bars in these galaxies. Positions for the dwarf spheroidal galaxies (e.g., Fornax, Sculptor, Carina) refer to the peaks of the optical luminosity distributions. The precision with which the position is listed reflects the accuracy with which it is known. The mean errors in the listed positions are 2–3 digits in the last place given.

A galaxy's morphological type is based on the revised Hubble system described by de Vaucouleurs (1959a, 1963). The system includes four classes: Ellipticals (E), Lenticulars (L), Spirals (S), and Irregulars (I). In the L and S classes (disk galaxies), two families, ordinary (A) and barred (B), are distinguished, with transition types denoted AB. Each family can exist in two varieties, depending on the absence (s) or presence (r) of an inner ring structure, with transition types denoted (rs). In the L class, the relative importance of the two major components of a galaxy—the spheroid (or bulge) and the disk—is denoted by the superscript "-" (early, i.e., most similar to E), "0" (intermediate), and "+" (late, i.e., more similar to S).

The stage along the Hubble sequence of spirals is denoted by a, b, c, and d in order of decreasing bulge-to-disk ratio and increasing development of the arms. The transition type between L and S is denoted S0/a; between S and magellanic irregulars (Im), by Sm. Thus, the Large Magellanic Cloud is the prototype of SB(s)m, and the Andromeda galaxy (M31) of SA(s)b. An outer ring structure is designated by the symbol (R) preceding the Hubble-stage designation. The puzzling nonmagellanic irregulars, of which M82 is the prototype, are designated I0. Edge-on systems are signaled by the suffix "sp" (for "spindle"). Peculiarities are noted by the suffix "pec." For more detailed discussions of galaxy morphology, see Sandage (1975) and Buta (1989).

Because physical properties, such as color index, hydrogen index, bulge-to-disk ratio, and so on, are closely correlated with stage along the Hubble sequence, it is convenient to attach to the stage a numerical scale, T, from −5 at E, through 0 at S0/a, to 10 at Im. The luminosity class, L, introduced by van den Bergh (1960 a, b)—or better, the luminosity index Λ =(T + L)/10 (de Vaucouleurs 1979)—is correlated with absolute magnitude. The *L* scale, listed in *The Astronomical Almanac*, corresponds to van den Bergh luminosity class. At its inception, L ran from 1 for a bright giant galaxy, to 9 for a faint dwarf system (luminosity classes I–V). In the RC3, the system was extended to include 10 and 11 on the numerical scale (classes V–VI and VI). For details, see Buta et al. (1994).

The isophotal apparent major diameter of galaxies, denoted Log D_{25}, is given in the table for the isophote level 25.0 B-magnitude per square arcsecond (B-m/ss). The level corresponds roughly to the visible size of the galaxy image seen on the Palomar Observatory Sky Survey paper prints (blue light), and to the diameters listed in the Uppsala General Catalog (Nilson 1973) for northern galaxies. Note that *isophotal* diameters are not *metric* diameters. The former depend on the surface brightness (specific intensity) of the galaxy image. The latter do not depend on surface brightness, and while they are better indications of the true size of galaxies, they are more difficult to measure and are not yet available for many galaxies. Note that to avoid negative logarithms, it is given in the table in units of 0.1 arcminute.

The ratio of the major and minor axes at the isotope level 25.0 blue mag/arcsec^2 (R_{25} = D_{25}/d_{25}) is also listed in logarithmic form. The precision is usually better than 0.1. The isophotal axis ratios given in the table are corrected for the systematic errors that affect visual measurements of photographic plates (de Vaucouleurs 1959b). (For more details on systematic and random errors in diameter and axis ratios, see Paturel et al. 1987 and Paturel et al. 1991.)

The total apparent B-band magnitudes, B_T^w are generally derived from photoelectric measurements or detailed photographic surface photometry in the Johnson B system. These magnitudes are weighted means of the best available magnitudes extrapolated to infinity to allow for the generally small fraction of the luminosity contributed by the outermost regions of a galaxy, as explained in the *Introduction to RC3*. The precision is generally 0.1 mag or better. (For details, see Buta et al. 1995.) For some applications, the observed magnitudes need to be corrected for galactic and internal extinction, which are both controversial and uncertain by 0.1 to 0.2 mag or more in extreme cases (e.g., an edge-on spiral galaxy near the galactic plane). The total color indices, $(B-V)_T$ and $(U-B)_T$, in the Johnson *UBV* systems are as observed; i.e., uncorrected for galactic and internal extinction. The range is roughly from $+3.0 > (B-V)_T > +0.1$ and $-0.3 > (U-B)_T > +0.6$ as one moves along the Hubble sequence from E (yellow-orange) to Im (whitish) through L and S types. By an

oversimplification, the extreme types are often described as "red" and "blue" galaxies. The colors give crude indications of the energy distribution in the continuum and, hence, of the stellar composition of a galaxy. However, the colors are often modified by line emission from HII regions (which decreases the color index, or increases the blueness) and internal dust extinction (which increases the color index, or increases the redness).

The heliocentric radial velocity, derived from optical observations and 21-cm neutral hydrogen radio emission, is given in km/s and calculated with the optical convention that $\Delta\lambda = v/c$. For the small redshifts involved, this convention is entirely adequate. For a discussion of systematic and accidental errors in radial velocities, see the *Introduction to RC3*. For cosmological applications, it is better to replace the conventional solar motion of 300 km/s toward $l = 90°$, $b = 0°$ (see IAU 1977), with the total velocity vector of 371.0 km/s toward $l = 264.14°$, $b = +48.26°$ relative to the cosmic background radiation (see Fixsen et al. 1996).

Data for other galaxies can be found in two online databases: NED, the NASA/IPAC Extragalactic Database at URL[19]; and LEDA, the Lyon-Meudon Extragalactic Database at URL[20].

13.3.4 Quasi-Stellar Objects

A quasar (the name is actually a contraction of "quasi-stellar radio source") is an extremely bright and distant active galactic nucleus. There was a great deal of initial controversy over the nature of quasars, but there is now a general consensus that they are a compact halo of matter surrounding a supermassive black hole. They are observed as high redshift sources in the infarared, optical, ultraviolet, radio, X-Ray and gamma ray frequencies. They seem rather stellar (point-like), rather than extended sources similar to galaxies. They display rapid changes in luminosity and are believed to be powered by the accretion of material into their nuclei, making these luminous versions of active galaxies. No other currently known mechanism appears able to explain the vast energy output and rapid variability.

At present, more than 100,000 quasars are known, all with redshifts ranging from $0.06 > z > 6.4$; redshift is defined as $z = (\lambda - \lambda_0) / \lambda_0$, where λ_0 is the laboratory wavelength for the spectral line being observed. Quasar redshifts are almost always measured with the broad-emission lines of hydrogen, helium, and other heavy elements that are characteristic of quasars. Most quasars are brightest in their rest-frame near-ultraviolet (near the 1216 Å (Lyman-alpha line of hydrogen), but due to the tremendous redshifts of these sources, that peak luminosity has been observed as far as 9000 Å in the near infrared. The redshifts correspond to distances between 780 million and 28 billion light-years. Due to these great distances, quasars offer a glimpse into the very early universe. At this time, the Sloan Digital Sky Survey is in the process of measuring quasar properties; once complete, it will provide redshift values for approximately 100,000 quasars.

The list of quasars is originally from *A Catalogue of Quasars and Active Galactic Nuclei, 1st ed.* (Véron-Cetty and Véron 1984) using selection parameters suggested by Tim Heckman. These selection parameters did not have any physical significance other than allowing a list of quasars with a variety of characteristics. Since this catalog has been updated many times, *The Astronomical Almanac* for 2009 used the 12th edition of the catalog (Véron-Cetty and Véron 2006; URL[21]). When updated, the aim for the list was to be a subsample of those types that are popular in current research interests: the optically brightest, strongest in radio

and X-ray, highest known redshifts, gravitational lenses, brightest quasars with interesting absorption systems (e.g., PHL 5200), high redshift quasars suitable for He II Gunn-Peterson observations (e.g., H1700+64, QSO 0302–003).

13.4 Wavelength Specific Sources

13.4.1 Radio-Source Positional Calibrators

The International Celestial Reference Frame (ICRF) sources are used for calibration of many radio observations made using the VLBA and the European VLBI Network. However, all astronomers use the ICRF indirectly, as the Hipparcos Celestial Reference Frame (HCRF) is linked directly to the ICRF. The ICRF is the IAU recommended fundamental astronomical reference frame and the positions in the ICRF form the underlying basis for all astrometry. Basically, the ICRF is the frame to which all other reference frames, at all wavelengths, are referred (see Chapter 4).

The ICRF is a space-fixed frame based on high accuracy radio positions measured by VLBI. They are accurate for pointing and calibration of radio telescopes. The list of radio source positions which originally defined the ICRF was introduced in the 1999 edition of *The Astronomical Almanac* following its adoption by the IAU as the fundamental reference frame in January 1998 (Ma et al. 1998); only the 212 defining sources of the ICRF were included due to space considerations. The ICRF defining sources were the best and most stable positions based on the knowledge of the sources at the time the ICRF was defined.

An update to the ICRF occured in August of 2009 in conjunction with the XXVII IAU General Assembly (IAU 2010, Res. B3; IERS 2009). This second realization of the ICRF, termed the ICRF2, contains precise positions of 3414 compact radio sources. Maintenance of ICRF2 is made using a set of 295 new defining sources selected on the basis of positional stability, lack of extensive intrinsic source structure, and spatial distribution. These 295 defining sources are presented in *The Astronomical Almanac*. Positions of all ICRF2 sources are available at URL[22].

Information on the known physical characteristics of the ICRF2 radio sources includes, where known, the object type, 8.4 Ghz and 2.3 Ghz flux, spectral index, V magnitude, redshift, and a classification of spectrum. Notes for many ICRF2 defining sources are also presented.

This table is compiled by A.-M. Gontier and is derived by sequentially assembling the data from the following primary sources:

1. *Large Quasar Astrometric Catalog* (LQAC), a compilation of 12 largest quasar catalogues containing 113666 quasars, which provided information when available on photometry, redshift, and radio fluxes (Souchay et al. 2009, available at URL[2] as catalogue J/A+A/494/799). This source was used to provide information on flux at 8.4 GHz and 2.3 GHz and initial information for the redshift and the magnitude.
2. *Optical Characteristics of Astrometric Radio Sources* which includes 4261 radio sources with J2000.0 coordinates, redshift, V magnitude, object type and comments (Malkin and Titov 2008; URL[23]).
3. *Catalogue of Quasars and Active Galactic Nuclei, 12th Edition* which includes 85221 quasars, 1122 BL Lac objects and 21737 active galaxies together with known lensed

quasars and double quasars (Véron-Cetty and Véron 2006, available at URL[2] as catalogue VII/248, also used for the table of quasars in § 13.3.4).

4. *An All-Sky Survey of Flat-Spectrum Radio Sources* providing precise positions, subarcsecond structures, and spectral indices for some 11000 sources (Healey et al. 2007, available at URL[2] as catalogue J/ApJS/171/61).
5. *The Optical Spectroscopy of 1Jy, S4 and S5 Radio Source Identifications* which gives position, magnitude, type of the optical identification, flux at 5GHz and two-point spectral index between 2.7 GHz and 5 GHz (Stickel and Kuehr 1994; Stickel, Fried, and Kuehr 1989, available at URL[2] as catalogue III/175).

13.4.2 Radio-Flux Calibrators

Calibration is a necessary step in the reduction of radio flux observations for research purposes. Absolute calibration of radio flux data is required to delete systematic effects such as those from the receiver, the antenna, or the atmosphere. An accurate calibration of the observations enables comparison of data observed at different telescopes and at different times. All fields of radio astronomy require accurate absolute calibration, especially variability studies of radio sources. Calibration of measurements also allows the means to determine the telescope efficiency, offering the possibility to study the properties (e.g., surface RMS) of the antenna.

Using sources, like the ones given in *The Astronomical Almanac*, are the easiest way to calibrate a radio telescope. A direct, absolute calibration is very difficult especially for large telescopes (if possible at all). The three primary standards—the strongest three radio sources (Cas A, Cyg A, and Tau A)—are unsuitable for the calibration of large antennas. Absolute calibration of these three primary standards requires the use of small antennas given these sources, particularly at high frequencies, have finite sizes and are all partially resolved using large antennas. It is necessary to have a list of secondary calibrators, the flux densities of which are determined with reference to these primary standards. Many, if not all, centimeter wavelength radio telescopes use the secondary flux density standards provided in this table.

The data in the table were originally taken from Baars et al. (1977) and updated nearly every year by Kraus, Krichbaum, Pauliny-Toth and Witzel with new measurements. The original data are derived as follows:

1. The absolute spectrum of Cas A, with its secular rate of decrease taken into account, was derived for epoch 1980.0 between frequencies of 300 MHz and 30 GHz.
2. The absolute spectra of Cyg A and Tau A were derived from direct measurements and from measurements of the ratios of their flux density to that of Cas A.
3. An accurate spectrum for the somewhat weaker source Vir A was established from direct, accurate ratios of its flux density to those of Cas A and Cyg A.
4. This Vir A spectrum was used as a basis for obtaining accurate relative spectra of the secondary sources provided in the table.

For flux calibration of interferometers and synthesis telescopes, only three sources are suitable: 3C48, 3C147, and 3C286. Positions for 3C48 and 3C147 are taken from Elsmore and Ryle (1976). The position of 3C 286 is taken from the list of astrometric radio sources. Other

sources may need a correction for angular size when used with the largest single antennas at high frequencies.

There are two important notes of caution in using these standards. Extrapolation of flux densities beyond the given frequency range printed is not advisable. Also, some sources contain compact, opaque components that may be variable. For example, 3C48 shows some variability around 1.6 GHz and 20 GHz (Perley and Crane 1985). The flux density of 3C147 is variable (Simon et al. 1983; Andrew, MacLeod, and Feldman 1981) as is its structure (Preuss et al. 1984). For accurate calibrations of flux density measurements, several sources from the table should be utilized in order to account for such effects.

A table with polarization data for the most prominent sources is also provided by A. Kraus which gives the polarization degree and angle for a number of frequencies.

13.4.3 X-Ray and Gamma Ray Sources

In the broadest terms, an X-ray or gamma ray source can be defined as any source emitting X-rays or gamma rays. Since most X-rays and gamma rays are emitted when an abrupt change occurs in a charged particle's trajectory near the source, sources are required to have a strong gravitational/magnetic field. The types of X-ray and gamma ray sources have increased over the years as instruments became better able to detect such sources. It has long been known that our Sun is both an X-ray and gamma ray source (many X-ray sources turn out to be gamma ray sources, but not all), and it has also been known for a while that black holes and neutron stars (both isolated ones and those in binary systems, whether a pulsar or not) are both X-ray and gamma ray sources. Other sources are active galactic nuclei (AGNs), quasars, many galaxies, and supernovae. More recently, it has been discovered that the intergalactic medium in some parts of the sky emits copious amounts of X-rays. Gamma ray bursts (GRBs) are the most energetic of gamma ray sources, but they have also been found to produce X-rays after the initial burst of gamma rays. Even the source of so-called "cosmic rays" has been recently discovered to be many very faint X-ray and gamma ray sources, that mix their emissions with those from more easily identified sources to produce the cosmic ray background that has been known for many years.

To detect X-ray sources, instruments must be placed outside the Earth's atmosphere, since it does a good job of blocking most X-rays from getting to the Earth's surface. Most gamma rays are blocked by the atmosphere so many gamma ray instruments are put into orbit also. However, the most energetic gamma rays (those in the GeV–TeV energy range) can get through the Earth's atmosphere and so there are some gamma ray instruments on the ground that seek to detect these very energetic particles.

These sources are of interest to optical astronomers for multiple reasons. It is of interest to know, for example in the case of X-ray binaries, what kind of star is supplying the matter that feeds the black hole or neutron star. By knowing its magnitude (whether visual or infrared) an educated guess can be made about the size and age of the companion star. This is useful for determining the orbit of the X-ray or gamma ray source and its mass and age. It is also interesting to know how the X-ray/gamma ray source affects its companion star. The loss of mass from the companion to the X-ray/gamma ray source can change how the star evolves. In some cases, it has been speculated that the known X-ray binary was initially two non X-Ray emitting stars in a binary system, and their interaction caused a supernova that gave

birth to the X-ray source that we now detect. In the case of isolated pulsars, many of which are first observed at radio wavelengths, it is interesting to know if these pulsars emit energy at other wavelengths. Many do; the Crab pulsar and the Vela pulsar being two well-known examples. Even more recently, once GRBs were shown to have an X-ray afterglow, further optical observations revealed an optical afterglow as well. And of course, since the source of GRBs was (and still is) unknown, these optical observations often showed a galaxy at or near the supposed location of the GRB. The current understanding of GRB sources is that they occur in galaxies and might be even more energetic than Supernovae (one theory calls these sources "Hypernovae"). Optical observations of galaxies, AGN, and Quasars can again give some insight to these X-ray/gamma ray sources by determining their age, what kind of stars they are composed of, and other possible mechanisms that might help the high-energy astronomer understand the X-ray/Gamma ray emission process from these sources.

The X-Ray and gamma ray sources listed in *The Astronomical Almanac* are well-studied and historically important sources drawn from published results, selected by individuals in this particular field of research. The X-Ray binary sources are from the catalogs of van Paradijs (1995) and Liu, van Paradijs and van den Heuvel (2000, 2001). Other sources are selected from the *Fourth Uhuru Catalog* (Forman et al. 1978). Positions for X-ray sources are taken from NOMAD as described in § 13.1.3.1 (URL[3]). The gamma ray sources are selected from three catalogs to cover their broad energy range: low-energy gamma rays (photon energies < 100 keV) are taken from *The Fourth IBIS/ISGRI Soft Gamma-Ray Survey Catalog* (Bird et al. 2010); high-energy gamma rays (photon energies between 100 MeV and 100 GeV) are taken from *Fermi Large Area Telescope Second Source Catalog* (Fermi-LAT Collaboration 2011); and very-high-energy gamma rays (photon energies above 100 GeV) are taken from *TeVCat Online Catalog for TeV Astronomy* available at URL[24]. Some sources are bright in two or all three energy ranges.

Acknowledgements

The author would like to recognize the following individuals who contributed material for this chapter: Brian Mason (§ 13.2.2, Double Stars), Janet Mattei (§ 13.2.5, Variable Stars), Stephen Thorsett (§ 13.2.6, Pulsars), Harold Corwin (§ 13.3.3, Bright Galaxies), Anne-Marie Gontier (§ 13.4.1, Radio-Source Positional Calibrators) and Mark Stollberg (§ 13.4.3, X-Ray and Gamma Ray Sources).

REFERENCES

1. The Astronomical Almanac Online:
http://asa.usno.navy.mil or http://asa.hmnao.com.
2. Centre de Donnees astronomiques de Strasbourg (CDS):
http://cdsweb.u-strasbg.fr/.
3. Naval Observatory Merged Astrometric Database (NOMAD):
http://www.usno.navy.mil/USNO/astrometry/optical-IR-prod/nomad/.
4. 2 Micron All Sky Survey point source catalog:
http://irsa.ipac.caltech.edu/applications/Gator/.
5. Sixth Catalog of Orbits of Visual Binary Stars:
http://www.usno.navy.mil/USNO/astrometry/optical-IR-prod/wds/orb6/.

6. Washington Multiplicity Catalog (WMC):
http://www.usno.navy.mil/USNO/astrometry/optical-IR-prod/wds/wmc/.

7. Washington Double Star Catalog (WDS):
http://www.usno.navy.mil/USNO/astrometry/optical-IR-prod/wds/WDS/wds/.

8. Photometric Magnitude Difference Catalog:
http://www.usno.navy.mil/USNO/astrometry/optical-IR-prod/wds/dm3.

9. Catalog of Rectilinear Elements:
http://www.usno.navy.mil/USNO/astrometry/optical-IR-prod/wds/lin1.

10. The 9th Catalogue of Spectroscopic Binary Orbits:
http://sb9.astro.ulb.ac.be/.

11. ESO's Optical and UV Spectrophotometric Standard Stars:
http://www.eso.org/sci/observing/tools/standards/spectra/.

12. Geneva Radial-Velocity Standard Stars:
http://obswww.unige.ch/~udry/std/std.html.

13. American Association of Variable Star Observers (AAVSO):
http://www.aavso.org/aavso/.

14. Exoplanets.org:
http://exoplanets.org/.

15. Australia Telescope National Facility Pulsar Catalogue:
http://www.atnf.csiro.au/research/pulsar/psrcat.

16. New Catalog of Optically Visible Open Clusters and Candidates:
http://www.astro.iag.usp.br/~wilton/.

17. WEBDA open cluster database:
http://www.univie.ac.at/webda/.

18. Milky Way globular clusters:
http://www.physics.mcmaster.ca/~harris/mwgc.dat.

19. NASA/IPAC Extragalactic Database:
http://nedwww.ipac.caltech.edu/.

20. Lyon-Meudon Extragalactic Database:
http://leda.univ-lyon1.fr/.

21. Veron Catalog of Quasars and AGN:
http://heasarc.nasa.gov/W3Browse/all/veroncat.html.

22. ICRS Product Center:
http://hpiers.obspm.fr/icrs-pc/.

23. Optical Characteristics of Astrometric Radio Sources:
http://www.gao.spb.ru/english/as/ac_vlbi/sou_car.dat.

24. TeVCat online catalog for TeV Astronomy
http://tevcat.uchicago.edu/.

Allen, C. W. and A. N. Cox (2000). *Allen's Astrophysical Quantities (4th edition)*. New York: AIP Press; Springer.

Alter, G., B. Balazs, J. Ruprecht, and J. Vanysek (1970). *Catalogue of Star Clusters and Associations (2nd ed.)*. Budapest: Akademiai Kiado.

Andrew, B. H., J. M. MacLeod, and P. A. Feldman (1981). Standard sources at 10.6 GHz and variability in 3C147. *Astronomy and Astrophysics 99*, 36–38.

Baars, J. W. M., R. Genzel, I. I. K. Pauliny-Toth, and A. Witzel (1977). The absolute spectrum of CAS A - an accurate flux density scale and a set of secondary calibrators. *Astronomy and Astrophysics 61*, 99–106.

Batten, A. H., J. M. Fletcher, and D. G. McCarthy (1989). Eighth Catalog of the Orbital Elements of Spectroscopic Binary Systems. *Publications of the Dominion Astrophysical Observatory 17*, 1.

Bird, A. J., A. Bazzano, L. Bassani, F. Capitanio, M. Fiocchi, A. B. Hill, A. Malizia, V. A. McBride, S. Scaringi, V. Sguera, J. B. Stephen, P. Ubertini, A. J. Dean, F. Lebrun, R. Terrier, M. Renaud, F. Mattana, D. Götz, J. Rodriguez, G. Belanger, R. Walter, and C. Winkler (2010). The Fourth IBIS/ISGRI Soft Gamma-ray Survey Catalog. *Astrophysical Journal Supplement Series 186*, 1–9.

Bohlin, R. C., L. Colina, and D. S. Finley (1995). White Dwarf Standard Stars: G191-B2B, GD 71, GD 153, HZ 43. *Astronomical Journal 110*, 1316.

Bohlin, R. C., A. W. Harris, A. V. Holm, and C. Gry (1990). The Ultraviolet Calibration of the Hubble Space Telescope. IV - Absolute IUE Fluxes of Hubble Space Telescope Standard Stars. *Astrophysical Journal Supplement Series 73*, 413–439.

Buta, R. J. (1989). Galaxy Morphology and Classification. In H. G. Corwin and L. L. Bottinelli (Eds.), *The World of Galaxies*, pp. 29–47. Springer-Verlag.

Buta, R. J., H. G. Corwin, G. de Vaucouleurs, A. de Vaucouleurs, and G. Longo (1995). Integrated photoelectric magnitudes and color indices of bright galaxies in the Johnson UBV system. *Astronomical Journal 109*, 517–542.

Buta, R. J., S. Mitra, G. de Vaucouleurs, and H. G. Corwin, Jr. (1994). Mean morphological types of bright galaxies. *Astronomical Journal 107*, 118–134.

Butler, R. P., J. T. Wright, G. W. Marcy, D. A. Fischer, S. S. Vogt, C. G. Tinney, H. R. A. Jones, B. D. Carter, J. A. Johnson, C. McCarthy, and A. J. Penny (2006). Catalog of Nearby Exoplanets. *Astrophysical Journal 646*, 505–522.

Cousins, A. W. J. (1976). VRI standards in the E regions. *Memoirs of the Royal Astronomical Society 81*, 25.

Crawford, D. L. (1958). Two-Dimensional Spectral Classification by Narrow-Band Photometry for B Stats in Clusters and Associations. *Astrophysical Journal 128*, 185.

Cutri, R. M., M. F. Skrutskie, S. van Dyk, et al. (2003). The IRSA 2MASS All-Sky Point Source Catalog. Technical report, NASA/IPAC Infrared Science Archive.

de Vaucouleurs, G. (1959a). Classification and Morphology of External Galaxies. *Handbuch der Physik 53*, 275.

de Vaucouleurs, G. (1959b). Photographic dimensions of the brighter galaxies. *Astronomical Journal 64*, 397.

de Vaucouleurs, G. (1963). Revised Classification of 1500 Bright Galaxies. *Astrophysical Journal Supplement 8*, 31.

de Vaucouleurs, G. (1979). The extragalactic distance scale. V - Tertiary distance indicators. *Astrophysical Journal 227*, 380–390.

de Vaucouleurs, G., A. de Vaucouleurs, H. Corwin, R. J. Buta, G. Paturel, and P. Fouque (1991). *Third Reference Catalogue of Bright Galaxies (RC3)*. New York: Springer-Verlag.

Dias, W. S., B. S. Alessi, A. Moitinho, and J. R. D. Lepine (2002). New Catalog of Optically Visible Open Clusters and Candidates. *Astronomy and Astrophysics 389*, 871–873.

Downes, R., R. F. Webbink, and M. M. Shara (1997). A Catalog and Atlas of Cataclysmic Variables-Second Edition. *Publications of the Astronomy Society of the Pacific 109*, 345–440.

Downes, R. A., R. F. Webbink, M. M. Shara, H. Ritter, U. Kolb, and H. W. Duerbeck (2001). A Catalog and Atlas of Cataclysmic Variables - On-line Version. *Publications of the Astronomy Society of the Pacific 113*, 764–768.

Elsmore, B. and M. Ryle (1976). Further astrometric observations with the 5-km radio telescope. *Monthly Notices of the Royal Astronomical Society 174*, 411–424.

Evans, D. S. (1968). Vitesses Radiales (Radial Velocities). *Transactions of the International Astronomical Union XIII B*, 168.

Fermi-LAT Collaboration (2011). Fermi Large Area Telescope First Source Catalog. *ArXiv e-prints*, 1108.1435.

Fixsen, D. J., E. S. Cheng, J. M. Gales, J. C. Mather, R. A. Shafer, and E. L. Wright (1996). The Cosmic Microwave Background Spectrum from the Full COBE FIRAS Data Set. *Astrophysical Journal 473*, 576.

Forman, W., C. Jones, L. Cominsky, P. Julien, S. Murray, G. Peters, H. Tananbaum, and R. Giacconi (1978). The Fourth Uhuru Catalog of X-ray Sources. *Astrophysical Journal Supplement Series 38*, 357–412.

Fricke, W., H. Schwan, T. Lederle, et al. (1988). *Fifth Fundamental Catalogue Part I*. Heidelberg: Veroeff. Astron. Rechen-Institut.

Hamuy, M., N. B. Suntzeff, S. R. Heathcote, A. R. Walker, P. Gigoux, and M. M. Phillips (1994). Southern Spectrophotometric Standards, 2. *Publications of the Astronomical Society of the Pacific 106*, 566–589.

Hamuy, M., A. R. Walker, N. B. Suntzeff, P. Gigoux, S. R. Heathcote, and M. M. Phillips (1992). Southern Spectrophotometric Standards. *Publications of the Astronomical Society of the Pacific 104*, 533–552.

Healey, S. E., R. W. Romani, G. B. Taylor, E. M. Sadler, R. Ricci, T. Murphy, J. S. Ulvestad, and J. N. Winn (2007). CRATES: An All-Sky Survey of Flat-Spectrum Radio Sources. *Astrophysical Journal Supplement Series 171*, 61–71.

Hirshfeld, A. and R. W. Sinnott (1997). *Sky catalogue 2000.0. Volume 2: Double stars, variable stars and nonstellar objects*. Cambridge, UK and Cambridge, MA: Cambridge University Press and Sky Publishing Corp.

Hoffleit, D. and C. Jaschek (1991). *The Bright Star Catalogue* (5th ed.). New Haven, CT.: Yale University Observatory.

Høg, E., C. Fabricius, V. V. Makarov, S. Urban, T. Corbin, G. Wycoff, U. Bastian, P. Schwekendiek, and A. Wicenec (2000). The Tycho-2 catalogue of the 2.5 million brightest stars. *Astronomy and Astrophysics 355*, L27–L30.

IAU (1957). In P. T. Oosterhoff (Ed.), *Transactions of the International Astronomical Union*, Volume IX, Cambridge, pp. 442. Cambridge University Press. Proc. 9th General Assembly, Dublin, 1955.

IAU (1973). In C. de Jager (Ed.), *Transactions of the International Astronomical Union*, Volume XV A, Boston, pp. 409. Reidel. Reports on Astronomy.

IAU (1977). In E. A. Müller and A. Jappel (Eds.), *Transactions of the International Astronomical Union*, Volume XVI B, Dordrecht, pp. 201. Reidel. Proc. 16th General Assembly, Grenoble, 1976.

IAU (1992). In J. Bergeron (Ed.), *Transactions of the International Astronomical Union*, Volume XXI B, Dordrecht. Kluwer. Proc. 21st General Assembly, Beunos Aires, 1991.

IAU (2010). In *Transactions of the International Astronomical Union*, Volume XXVII B. Proc. 27th General Assembly, Rio de Janeiro, 2009, in preparation.

Ibata, R. A., R. F. G. Wyse, G. Gilmore, M. J. Irwin, and N. B. Suntzeff (1997). The Kinematics, Orbit, and Survival of the Sagittarius Dwarf Spheroidal Galaxy. *Astrophysical Journal 113*, 634.

IERS (2009). The Second Realization of the International Celestial Reference Frame By Very Long Baseline Interferometry. Technical Note 35, International Earth Rotation Service, Frankfurt am Main. Verlag des Bundsesamts fur Kartographie und Geodesie, A. Fey and D. Gordon (Eds.).

Irwin, M. and D. Hatzidimitriou (1995). Structural parameters for the Galactic dwarf spheroidals. *Monthly Notices of the Royal Astronomical Society 277*, 1354.

Jarrett, T. H., T. Chester, R. Cutri, S. E. Schneider, and J. P. Huchra (2003). The 2MASS Large Galaxy Atlas. *Astrophysical Journal 125*, 525–554.

Johnson, H. L., B. Iriarte, R. I. Mitchell, and W. Z. Wisniewskj (1966). UBVRIJKL Photometry of the Bright Stars. *Communications of the Lunar Planetary Lab 4*, 99. Table 2.

Johnson, H. L. and W. W. Morgan (1953). Fundamental Stellar Photometry for Standards of Spectral Type on the Revised System of the Yerkes Spectral Atlas. *Astrophysical Journal 117*, 313.

Keenan, P. C. and R. C. McNeil (1976). *Atlas of Spectra of the Cooler Stars: Types G, K, M, S, and C*. Ohio: Ohio State University Press.

Kholopov, P. N. (1985). *General Catalogue of Variable Stars (fourth edition)*. Moscow: Nauka Publ. House.

Kholopov, P. N., N. N. Samus', M. S. Frolov, V. P. Goranskij, N. A. Gorynya, N. N. Kireeva, N. P. Kukarkina, N. E. Kurochkin, G. I. Medvedeva, and N. B. Perova (1996). General Catalog of Variable Stars, 4th Ed. *VizieR Online Data Catalog 2139*.

Kron, G. E., H. S. White, and S. C. B. Gascoigne (1953). Red and Infrared Magnitudes for 138 Stars Observed as Photometric Standards. *Astrophysical Journal 118*, 502.

Landolt, A. U. (1973). UBV Photoelectric Sequences in the Celestial Equatorial Selected Areas 92-115. *Astronomical Journal 78*, 959.

Landolt, A. U. (1983). UBVRI Photometric Standard Stars Around the Celestial Equator. *Astronomical Journal 88*, 439–460.

Landolt, A. U. (1992). UBVRI Photometric Standard Stars in the Magnitude Range 11.5-16.0 Around the Celestial Equator. *Astronomical Journal 104*, 340–371.

Landolt, A. U. (2009). UBVRI Photometric Standard Stars Around the Celestial Equator: Updates and Additions. *Astronomical Journal 137*, 4186–4269.

Liu, Q. Z., J. van Paradijs, and E. P. J. van den Heuvel (2000). A Catalogue of High-Mass X-ray Binaries. *Astronomy and Astrophysics Supplement 147*, 25–49.

Liu, Q. Z., J. van Paradijs, and E. P. J. van den Heuvel (2001). A Catalogue of Low-Mass X-ray Binaries. *Astronomy and Astrophysics 368*, 1021–1054.

Lynga, G. (1981). Astronomical Data Center Bulletin. Circular 2, NASA/GSFC, Greenbelt, MD.

Ma, C., E. F. Arias, T. M. Eubanks, A. L. Fey, A. M. Gontier, C. S. Jacobs, O. J. Sovers, B. A. Archinal, and P. Charlot (1998). The International Celestial Reference Frame as Realized by Very Long Baseline Interferometry. *Astronomical Journal 116*, 516–546.

Malkin, Z. and O. Titov (2008). Optical Characteristics of Astrometric Radio Sources. In *Measuring the Future, Proc. Fifth IVS General Meeting, A. Finkelstein, D. Behrend (Eds.), 2008, p. 183-187*, pp. 183–187.

Manchester, R. N., G. B. Hobbs, A. Teoh, and M. Hobbs (2005). The Australia Telescope National Facility Pulsar Catalogue. *Astronomical Journal 129*, 1993–2006.

Monet, D. G. (2004). Private Communication.

Monet, D. G., S. E. Levine, B. Canzian, et al. (2003). The USNO-B Catalog. *Astronomical Journal 125*, 984–993.

Morgan, W. W., H. A. Abt, and J. W. Tapschott (1978). *Revised MK Spectral Atlas for Stars Earlier than the Sun*. Williams Bay, WI and Tucson, AZ: Yerkes Obs. and Kitt Peak Nat. Obs.

Nilson, P. (1973). *Uppsala General Catalogue of Galaxies*. Uppsala: Roy. Soc. Sci. Uppsala.

Oke, J. B. (1990). Faint Spectrophotometric Standard Stars. *Astronomical Journal 99*, 1621–1631.

Paturel, G., P. Fouque, A. Lauberts, E. A. Valentijn, H. G. Corwin, and de Vaucouleurs (1987). Standard Photometric Diameters of Galaxies. III - Reduction of the Diameters in the ESO-B and SGC Catalogues to the Standard Diameter System at the 25 mag/sq Arcsec Brightness Level. *Astronomy and Astrophysics 184*, 86.

Paturel, G., A. M. Garcia, P. Fouque, and R. Buta (1991). An Extragalactic Database. III—Diameter Reduction. *Astronomy and Astrophysics 243*, 319–327.

Perley, R. A. and P. C. Crane (1985). 3C48 Variability. *NRAO Newsletter 25*, 1.

Perry, C. L., E. H. Olsen, and D. L. Crawford (1987). A Catalog of Bright UVBY Beta Standard Stars. *Publications of the Astronomy Society of the Pacific 99*, 1184–1200.

Perryman, M. A. C. and ESA (Eds.) (1997). *The HIPPARCOS and TYCHO catalogues. Astrometric and photometric star catalogues derived from the ESA HIPPARCOS Space Astrometry Mission*, Volume 1200 of *ESA Special Publication*.

Preuss, E., W. Alef, N. Whyborn, P. N. Wilkinson, and K. I. Kellermann (1984). The Milliarcsecond Core of 3C147 at 6-cm. In R. Fanti, K. Kellermann, and G. Setti (Eds.), *VLBI and Compact Radio Sources*, pp. 29. Dordrecht, Holland: Reidel. IAU Symp. No. 110.

Ritter, H. and U. Kolb (1998). Catalogue of Cataclysmic Binaries, Low-mass X-ray Binaries and Related Objects (Sixth edition). *Astronomy and Astrophysics Supplement 129*, 83.

Sandage, A. (1975). Classification and Stellar Content of Galaxies Obtained from Direct Photography. In A. Sandage, M. Sandage, and J. Kristian (Eds.), *Galaxies and the Universe*, pp. 1–35. Chicago: University of Chicago Press. Volume IX of Stars and Stellar Systems.

Simon, R. S., A. C. S. Readhead, A. T. Moffet, P. N. Wilkinson, B. Allen, and B. F. Burke (1983). Low Frequency Variability and Predicted Superluminal Motion in 3C147. *Nature 302*, 487–490.

Souchay, J., A. H. Andrei, C. Barache, S. Bouquillon, A.-M. Gontier, S. B. Lambert, C. Le Poncin-Lafitte, F. Taris, E. F. Arias, D. Suchet, and M. Baudin (2009). Large Quasar Astrometric Catalog. *Astronomy and Astrophysics 494*, 799.

Stickel, M., J. W. Fried, and H. Kuehr (1989). Optical Spectroscopy of 1 Jy BL Lacertae Objects and Flat Spectrum Radio Sources. *Astronomy and Astrophysics Supplement Series 80*, 103–114.

Stickel, M. and H. Kuehr (1994). An Update of the Optical Identification Status of the S4 Radio Source Catalogue. *Astronomy and Astrophysics Supplement Series 103*, 349–363.

Strömgren, B. (1956). Two-dimensional Spectral Classification of F stars through Photoelectric Photometry with Interference Filters. *Vistas in Astronomy 2*, 1336–1346.

Svechnikov, M. A. and L. A. Bessonova (1984). Catalog of Orbital Elements, Masses and Luminosities of Close Double Stars. *Bull. Inform. CDS 26*, 99.

Trumpler, R. J. (1930). Preliminary Results on the Distances, Dimensions and Space Distribution of Open Star Clusters. *Lick Observatory Bulletin XIV*, 154.

Turnshek, D. A., R. C. Bohlin, R. L. Williamson, O. L. Lupie, J. Koornneef, and D. H. Morgan (1990). An Atlas of Hubble Space Telescope Photometric, Spectrophotometric, and Polarimetric Calibration Objects. *Astronomical Journal 99*, 1243–1261.

Udry, S. Mayor, M., E. Maurice, J. Andersen, M. Imbert, H. Lindgren, J. C. Mermilliod, B. Nordström, and L. Prévot (1999). 20 years of CORAVEL Monitoring of Radial-Velocity Standard Stars. In J. Hearnshaw and C. Scarfe (Eds.), *Precise Stellar Radial Velocities, Victoria, IAU Coll. 170*, pp. 383.

van den Bergh, S. (1960a). A Preliminary Liminosity Classification for Galaxies of Type Sb. *Astrophysical Journal 131*, 558.

van den Bergh, S. (1960b). A Preliminary Luminosity Clssification of Late-Type Galaxies. *Astrophysical Journal 131*, 215.

van Paradijs, J. (1995). A Catalogue of X-Ray Binaries. In W. H. G. Lewin, J. van Paradijis, and E. P. J. van den Heuvel (Eds.), *X-ray Binaries*, pp. 536. University of Chicago Press. Volume IX of Stars and Stellar Systems.

Véron-Cetty, M. P. and P. Véron (1984). A Catalogue of Quasars and Active Nuclei. *ESO Scientific Report 1.*

Véron-Cetty, M. P. and P. Véron (2006). A Catalogue of Quasars and Active Nuclei: 12th edition. *Astronomy and Astrophysics 455*, 773–777.

Zacharias, N., D. G. Monet, S. E. Levine, S. E. Urban, R. Gaume, and G. L. Wycoff (2004a). The Naval Observatory Merged Astrometric Dataset (NOMAD). *Bulletin of the American Astronomical Society 36*, 1418.

Zacharias, N., S. E. Urban, M. I. Zacharias, G. L. Wycoff, D. M. Hall, D. G. Monet, and T. J. Rafferty (2004b). The Second US Naval Observatory CCD Astrograph Catalog (UCAC2). *Astronomical Journal 127*, 3043–3059.

CHAPTER 14

Computational Techniques

R. L. DUNCOMBE

14.1 Introduction to Computing Techniques

In this section we will examine several computing techniques of special relevance to astronomical calculation. For a more general treatment, see textbooks on computing methods and numerical analysis. A short note on elementary computing principles is also included in *Interpolation and Allied Tables* (H.M. Nautical Almanac Office 1956), which covers the sources of mistakes, the nature of checks, and the nature and effect of the inevitable errors due to rounding-off and other causes. These topics, although of fundamental importance, are not discussed here.

An important principle of computation is that the data used determine the maximum precision of a calculation. This precision can be reduced by poor computing—for example, by a poor choice of formula or by the failure to retain an adequate number of figures in the intermediate stages—but it can never be increased. Generally no simple relation exists between the errors (absolute or relative) of the final result and of the data, though a relation can readily be seen numerically by following through the calculation step by step, and often geometrically. It is misleading to quote a result to more figures than is justified by the data on which it is based, and it is erroneous to do so if an inadequate number of figures have been retained in the intermediate stages.

Retaining more figures than necessary is a waste of effort if it significantly increases the work involved. In some operations, however, especially in those done on a computer, extra figures involve very little additional work; but in other operations, an extra figure may require a more elaborate formula or extra word length, resulting in much more additional work. A suitable number of figures is that which offers the greatest convenience consistent with the building-up error, due to accumulation of rounding-offs, not exceeding the error of the data; this must be judged in relation to each calculation.

Mathematical formulae, if correct, adequately give a desired precision in the result; but they may be inefficient, inconvenient, and misleading. One example is the inefficiency of determining a small angle from its cosine; for a stated precision of angular measurement the number of decimals in the cosine is inversely proportional to the angle; and for a fixed number of decimals in the cosine (the usual and convenient case) the precision obtainable decreases as the angle decreases. Consider, for example, the formula for the third side of a spherical triangle, (Fig. 14.1) given two sides and the included angle,

$$\cos a = \cos b \cos c + \sin b \sin c \cos A = z \tag{14.1}$$

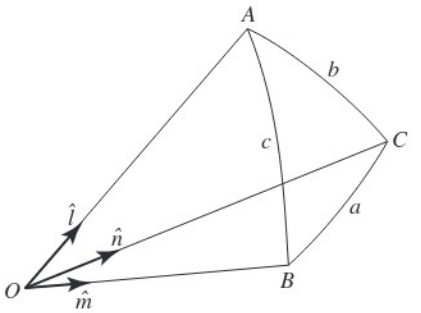


Figure 14.1 Spherical triangle

in which a is to be determined from measured values of b, c, and A. When a is small, it can be found to the same precision as the data only by the apparently incorrect procedure of retaining more decimals in each trigonometric function on the right-hand side (z) of the equation than the data appear to justify. This is legitimate because both $b - c$ and A must be small so that their cosines are known to extra figures. There are circumstances, however, in which the inconvenience of such a procedure is outweighted by other factors.

The apparent failure of a mathematical formula should not be confused with real geometrical limitations of precision. In the spherical triangle ABC,

$$\begin{aligned} &\sin a \sin B = \sin b \sin A = x \\ &\sin a \cos B = \cos b \sin c - \sin b \cos c \cos A = y; \end{aligned} \tag{14.2}$$

both x and y are small (y by the cancellation of two nearly equal components) if a is small. It is not legitimate here to use extra figures in the trigonometric functions in x and y, and B can be found with a precision only proportional to csc a; this precision is, however, clearly adequate to fix the point C (from BA). Similar arguments hold for the angle C. Neither B nor C can individually be determined as precisely as b, c, or A; but the sum $B + C$ can be so determined, as may be seen from geometric considerations and from the equation

$$\cot \frac{1}{2}(B + C) = \frac{\cos \frac{1}{2}(b + c)}{\cos \frac{1}{2}(b - c)} \tan \frac{1}{2}A. \tag{14.3}$$

Important problems in astronomy may require the sum (or difference) of two angles to be known more precisely than is possible with either (for example, the elements of a planetary orbit); therefore, great care is required in handling them. The recommended method is to determine one of the angles and then treat it as exact in finding the other, which must not be found independently.

Although there may be some uncertainty of precision in determining an angle, there should be no uncertainty of quadrant. This can always be achieved by adequate choice of formulae. For example, the following formulae for the solution of a spherical triangle, in which two sides and the included angle are given, are always adequate if the sides are less than 180°.

$$\begin{aligned}
\sin a \sin B &= \sin b \sin A && = x \\
\sin a \cos B &= \cos b \sin c - \sin b \cos c \cos A && = y \\
\cos a &= \cos b \cos c + \sin b \sin c \cos A && = z \\
\sin a \cos C &= \sin b \cos c - \cos b \sin c \cos A \\
\sin a \sin C &= \sin c \sin A .
\end{aligned} \tag{14.4}$$

The check $x^2 + y^2 + z^2 - 1 = 0$ is useful. The sign of z determines the quadrant of a, and the signs of x and y that of B; similarly with C.

In astronomical problems, the sides and angles of triangles on the celestial sphere may be of any magnitude, and it is undesirable to solve them by methods that restrict the sides to arcs less than 180°. The preceding general formulae are all valid for triangles with sides of any length, and may be applied immediately to the general triangles of spherical astronomy without any restriction to values less than 180°. Furthermore, to make the solution determinate, it is only necessary to find the algebraic sign of both the sine and the cosine of each arc or angle that may exceed 180° to fix the quadrants in which they lie. Any of the cases of the general triangle is determinate when, in addition to the three given parts, the algebraic sign of the cosine of one of the required parts is also given. In most practical problems the conditions of the problem supply this sign. In general triangles the utmost care should be taken to specify unambiguously the direction of measurement of angles and arcs.

Collectively, the preceding formulae are sufficient for the solution of the general triangle without restriction on the magnitudes of the parts, but, in practice, the additional formulae

$$\begin{aligned}
\cos A &= -\cos B \cos C + \sin B \sin C \cos a \\
\sin A \cos b &= \cos B \sin C + \sin B \cos C \cos a \\
\sin A \cos c &= \sin B \cos C + \cos B \sin C \cos a \\
\sin A \cot B &= \sin c \cot b - \cos c \cos A \\
\sin A \cot C &= \sin b \cot c - \cos b \cos A
\end{aligned} \tag{14.5}$$

are very useful. (Collected formulae are given in Table 14.5.)

In practice, the trigonometric functions of b, c, and A are taken out with a number of decimals depending on the precision of the data, and the capacity of the computer to be used. Table 14.1 gives corresponding precisions of angle and number of decimals.

If no additional work is involved, it is clearly advantageous to use more decimals than the precision warrants, since the effect of rounding-off errors is then much reduced. For instance, seven decimals give just sufficient coverage for data known to about 0.″02 and for results to

Table 14.1 Precision of angle and number of decimals for trigonometric functions

$1'$	$= 0.00029$	1^s	$= 0.00007$	0.0001	$= 0.'34 = 1^s.4$
$1''$	$= 0.0000048$	$0^s.1$	$= 7 \times 10^{-6}$	1×10^{-6}	$= 0.''2 = 0^s.014$
$0.''1$	$= 5 \times 10^{-7}$	$0^s.01$	$= 7 \times 10^{-7}$	1×10^{-7}	$= 0.''02 = 0^s.0014$
$0.''01$	$= 5 \times 10^{-8}$	$0^s.001$	$= 7 \times 10^{-8}$	1×10^{-8}	$= 0.''002 = 0^s.00014$

Table 14.2 The method of inverse use

	0°	45°	90°	135°	180°	225°	270°	315°	360°
x	+	+	+	+	−	−	−	−	−
y	+	+	−	−	−	−	+	+	+
tan or cot	tan	cot	cot	tan	tan	cot	cot	tan	cot
D or C arg	D	C	D	C	D	C	D	C	D

Table 14.3 Range of precision of the inverse determination of an angle

Errors corresponding to 1×10^{-6} in function	0° 180°	45° 225°	90° 270°	135° 315°	180° 360°
Use function	sin	cos	cos	sin	
Error in angle	0.″2	0.″29	0.″2	0.″29	0.″2
Use function	tan	cot	cot	tan	
Error in angle	0.ˢ014	0.ˢ007	0.ˢ014	0.ˢ007	0.ˢ014

be rounded off to 0.″1; but interpolation in eight-figure tables at interval 1″ offers little, if any, more difficulty than interpolation in seven-figure tables at interval 10″, and eight decimals can be used with little extra work.

In the solution of Eqs. 14.4 and 14.5, a is found either from $\cos a = z$ or from $\sin a = (x^2 + y^2)^{1/2}$, whichever is the smaller. Assuming a is less than 180°, the ambiguity of the second formula is resolved according to the sign of z. B is found from

$$\tan B = \frac{x}{y} \quad \text{or} \quad \cot B = \frac{y}{x}, \tag{14.6}$$

according to which ratio is less than unity. The quadrant is determined by the signs of x and y, since, if a is less than 180°, $\sin a$ is positive.

Most trigonometric tables are arranged semi-quadrantally, with direct (D) and complementary (C) arguments. Table 14.2 shows the method of inverse use in finding B. There is no difficulty in systematic computation.

The range of precision of the inverse determination of an angle from its sine (or cosine) and tangent (or cotangent) is indicated in Table 14.3. The table is arranged to show the range of angle for which the alternative trigonometric function should be used, and gives the error in the angle corresponding to an error of 1×10^{-6} in the function.

The technique of inverse interpolation, referred to briefly in § 14.2.3, is a powerful tool in the solution of transcendental equations and of equations in which the algebraic solution is complicated. The fundamental principle of such methods lies in the tabulation of a discriminant, defined so that it attains a predetermined value (usually zero) when the original equation is satisfied, and the calculation of the unknown argument corresponding to the predetermined value of the discriminant by the process of inverse interpolation. Although these methods may involve more calculation than direct methods, they have two

considerable advantages. First, they are usually independent of theoretical developments, of any approximations that may be necessary in such developments, and of extrapolations. Second, the correctness of the calculations and of the required answer, and the precision of that answer, are directly under the control of the computer. Illustrations of the use of these methods are to be found in the preceding sections, particularly in the calculation of the local circumstances of eclipses (§ 11.3.6) and the derivation of the times of moonrise and moonset (§ 12.3.2).

The availability of high-speed computers has changed the relative importance to be attached to the various factors entering into a computation. It is no longer desirable to restrict the amount of calculation to a minimum: many repetitions of a simple iteration are often preferable to a more sophisticated direct calculation. In particular, many of the transformations of coordinates arising in astronomy can be efficiently handled by the direct use of the accurate formulae, instead of by approximate series expressions. These often involve multiplying a column matrix representing the direction cosines by a transformation matrix, as is done, for example, in the application of precession and nutation. Close attention to the precision of computation is generally unnecessary, since many extra figures can be kept without any extra work.

Computing techniques adapted to computers are given in most modern texts on computing (see Hildebrand 1987 and Press et al. 1986).

14.2 Interpolation and Subtabulation

14.2.1 Introduction and Notation

The interpolation methods described in this section, together with the accompanying tables, are usually sufficient to interpolate to full precision the ephemerides in *The Astronomical Almanac*. Additional notes, formulae and tables are given in the booklets *Interpolation and Allied Tables* (H.M. Nautical Almanac Office 1956) and *Subtabulation* (H.M. Nautical Almanac Office 1958) and in many textbooks on numerical analysis. It is recommended that interpolated values of the Moon's right ascension, declination, and horizontal parallax be derived from the daily polynomial coefficients that are provided for this purpose in *The Astronomical Almanac Online* at URL[1].

The term f_p denotes the value of the function $f(t)$ at the time $t = t_0 + ph$, where h is the interval of tabulation, t_0 is a tabular argument, and $p = (t - t_0)/h$ is known as the interpolating factor. The notation for the differences of the tabular values is shown in Table 14.4; it is derived from the use of the central-difference operator δ, which is defined by:

$$\delta f_p = f_{p+1/2} - f_{p-1/2}. \tag{14.7}$$

The symbol for the function is usually omitted in the notation for the differences. Tables are given for use with Bessel's interpolation formula for p in the range 0 to +1. The differences may be expressed in terms of function values for convenience in the use of computers.

$$p = \text{the interpolating factor} = (t - t_0)/(t_1 - t_0) = (t - t_0)/h \tag{14.8}$$

Table 14.4 Differences in tabular arguments

Argument	Function	Difference 1st	2nd	3rd	4th	
t_{-2}	f_{-2}		δ^2_{-2}			$\delta_{1/2} = f_1 - f_0$
		$\delta_{-3/2}$		$\delta^3_{-3/2}$		$\delta^2_0 = \delta_{1/2} - \delta_{-1/2}$
t_{-1}	f_{-1}		δ^2_{-1}		δ^4_{-1}	$= f_1 - 2f_0 + f_{-1}$
		$\delta_{-1/2}$		$\delta^3_{-1/2}$		$\delta^2_0 + \delta^2_1 = f_2 - f_1 - f_0 + f_{-1}$
t_0	f_0		δ^2_0		δ^4_0	$\delta^3_{1/2} = \delta^2_1 - \delta^2_0$
		$\delta_{1/2}$		$\delta^3_{1/2}$		$= f_2 - 3f_1 + 3f_0 - f_{-1}$
t_{+1}	f_{+1}		δ^2_1		δ^4_1	$\delta^4_0 = \delta^3_{1/2} - \delta^3_{-1/2}$
		$\delta_{3/2}$		$\delta^3_{3/2}$		$= f_2 - 4f_1 + 6f_0 - 4f_{-1} + f_{-2}$
t_{+2}	f_{+2}		δ^2_2			$\delta^4_0 + \delta^4_1 = f_3 - 3f_2 + 2f_1 + 2f_0 - 3f_{-1} + f_{-2}$

14.2.2 Interpolation Formulae

Bessel's interpolation formula in this notation is

$$f_p = f_0 + p\delta_{1/2} + B_2(\delta^2_0 + \delta^2_1) + B_3\delta^3_{1/2} + B_4(\delta^4_0 + \delta^4_1) + \cdots \tag{14.9}$$

where

$$\begin{aligned} B_2 &= p(p-1)/4 \\ B_3 &= p(p-1)(p-\tfrac{1}{2})/6 \\ B_4 &= (p+1)p(p-1)(p-2)/48. \end{aligned} \tag{14.10}$$

The maximum contribution to the truncation error of f_p, for $0 < p < 1$, from neglecting each order of difference is less than 0.5 in the unit of the end figure of the tabular function if $\delta^2 < 4$, $\delta^3 < 60$, $\delta^4 < 20$, and $\delta^5 < 500$. Everett's interpolation formula in this notation is

$$f_p = f_0 + p\delta_{1/2} + E^2_0\delta^2_0 + E^2_1\delta^2_1 + E^4_0\delta^4_0 + E^4_1\delta^4_1 + \cdots \tag{14.11}$$

where

$$\begin{aligned} E^2_0 &= -p(p-1)(p-2)/6 \\ E^2_1 &= (p+1)p(p-1)/6 \\ E^4_0 &= -(p+1)p(p-1)(p-2)(p-3)/120 \\ E^4_1 &= (p+2)(p+1)p(p-1)(p-2)/120. \end{aligned} \tag{14.12}$$

LaGrange's interpolation formula to second order in this notation is

$$f_p = f_{-1}\left(\frac{1}{2}p^2 - \frac{1}{2}p\right) + f_0(1-p^2) + f_1\left(\frac{1}{2}p^2 + \frac{1}{2}p\right). \tag{14.13}$$

This formula has the advantage that the interpolation can be done entirely in terms of the functional values. The disadvantages are that the coefficients are required to the same number of significant figures as the function, and that the number of values of the function to use in any particular case is not easily determined without knowing the size of the differences.

14.2.3 Inverse Interpolation

Inverse interpolation to derive the interpolating factor p, and hence the time, for which the function takes a specified value f_p is carried out by successive approximations. The first estimate p_1 is obtained from

$$p_1 = (f_p - f_0)/\delta_{1/2}. \tag{14.14}$$

This value of p is used to obtain an estimate of B_2, from the critical table or otherwise, and hence an improved estimate of p from

$$p = p_1 - B_2(\delta_0^2 + \delta_1^2)/\delta_{1/2}. \tag{14.15}$$

This last step is repeated until there is no further change in B_2 or p; the effects of higher-order differences may be taken into account in this step.

14.2.4 Polynomial Representations

It is sometimes convenient to construct a simple polynomial representation in the form

$$f_p = a_0 + a_1 p + a_2 p^2 + a_3 p^3 + a_4 p^4 + \cdots \tag{14.16}$$

which may be evaluated in the nested form

$$f_p = (((a_4 p + a_3)\, p + a_2)\, p + a_1)p + a_0. \tag{14.17}$$

Expressions for the coefficients a_0, a_1, etc., may be obtained from Stirling's interpolation formula, neglecting fifth-order differences:

$$\begin{aligned} a_0 &= f_0 \\ a_1 &= (\delta_{1/2} + \delta_{-1/2})/2 - a_3 \\ a_2 &= \delta_0^2/2 - a_4 \\ a_3 &= (\delta_{1/2}^3 + \delta_{-1/2}^3)/12 \\ a_4 &= \delta_0^4/24. \end{aligned} \tag{14.18}$$

This is suitable for use in the range $-1/2 \le p \le +1/2$, and it may be adequate in the range $-2 \le p \le 2$, but it should not normally be used outside this range. Techniques are available in the literature for obtaining polynomial representation that give smaller errors over similar or larger intervals. The coefficients may be expressed in terms of function values rather than differences.

14.2.5 Chebyshev Polynomials

Polynomials of different types can be generated for fitting data. Historically Fourier Series have been used for planetary, lunar, and nutation theories. Carpenter (1966) provided the first application of Chebyshev polynomials for the representation of planetary theories over a specified time period. Now the JPL Development Ephemerides are given in Chebyshev polynomials (see Chapter 8). They provide a compact means of providing the data and an accurate method of interpolation at the same time. While Fourier series give accurate representation at the middle of an interval of time and reduced accuracy with distance from the middle, Chebyshev polynomials are weighted for increased accuracy at the ends. However, the Chebyshev polynomials lose accuracy rapidly outside the specified interval.

Economized polynomials, such as Chebyshev, provide efficient and accurate expressions that may be easily evaluated with a computer. The coefficients a_i of the Chebyshev expansion

$$f_x = \frac{a_0}{2} + \sum_{i=1}^{n} a_i T_i(x) \tag{14.19}$$

are computed for prescribed time spans, where f_x is the function represented, $T_i(x)$ is the Chebyshev polynomial of the i-th degree, and x is the normalized time variable. To evaluate a Chebyshev expansion, it is necessary to normalize the time variable on the interval for which the series is valid. Attempts to use these series beyond the specified time intervals for which they are valid will produce erroneous results.

The Chebyshev polynomials of the first kind are defined by the recurrence relation

$$\begin{aligned} T_0(x) &= 1 \\ T_1(x) &= x \\ T_{n+1}(x) &= 2x\,T_n(x) - T_{n-1}(x). \end{aligned} \tag{14.20}$$

The Chebyshev polynomials of the first kind can be defined by the trigonometric identity

$$T_n(x) = \cos(n \arccos x) = \cosh(n \ \operatorname{arccosh} x) \tag{14.21}$$

where

$$T_n(\cos(\theta)) = \cos(n\theta). \tag{14.22}$$

Evaluating the first two Chebyshev polynomials,

$$T_0(x) = \cos(0x) = 1 \tag{14.23}$$

$$T_1(\cos(x)) = \cos(x) \tag{14.24}$$

one can straightforwardly determine that

$$\begin{aligned} \cos(2\theta) &= 2\cos\theta\cos\theta - \cos(0\theta) = 2\cos^2\theta - 1 \\ \cos(3\theta) &= 2\cos\theta\cos(2\theta) - \cos\theta = 4\cos^3\theta - 3\cos\theta \end{aligned} \tag{14.25}$$

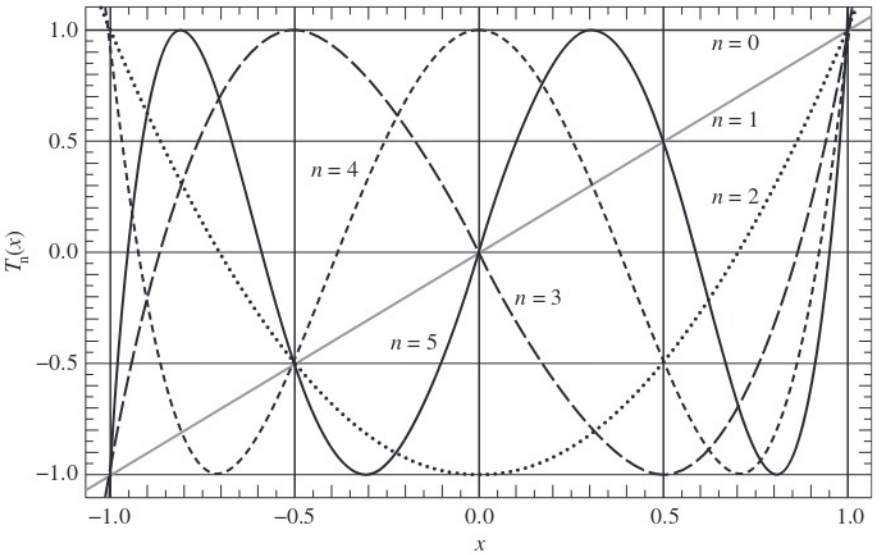


Figure 14.2 The first few Chebyshev polynomials of the first kind in the domain $-1 < x < 1$: The flat T_0, T_1, T_2, T_3, T_4 and T_5

and so forth. The Chebyshev polynomials are illustrated in Fig. 14.2. Further information is given in Lanczos (1956) and Fox and Parker (1972).

14.3 Plane and Spherical Trigonometry

In astronomical problems, the sides and angles of triangles on the celestial sphere may be of any magnitude, and it is undesirable to solve them by methods that restrict the sides to arcs less than 180°. The general formulae given in Table 14.5 are valid for triangles with sides of any length, and may be applied immediately to the general triangles of spherical astronomy without any restriction to values less than 180°. Furthermore, to make the solution determinate, it is only necessary to find the algebraic sign of both the sine and the cosine of each arc or angle that may exceed 180°, to fix the quadrants in which they lie. Any of the cases of the general triangle is determinate when, in addition to the three given parts, the algebraic sign of the sine or the cosine of one of the required parts is also given. In most practical problems it happens that the conditions of the problem supply this sign. In general triangles the utmost care should be taken to specify unambiguously the direction of measurement of angles and arcs.

In Fig. 14.3 the arc $P'P$ subtends the small angle b, measured in radians, r is the radius and $P'R$ is perpendicular to OP at R. The radius of the circle times the angle subtended in radians equals the arc length, hence $r \times b = P'P$.

When b is small enough that $P'R$ approximates $P'P$ then $\sin b = P'R/r$ and $b = P'P/r$. Thus, $\sin b = b$ and $\tan b = b$. If in the small angle of b radians there are q minutes of arc (q'), then $\sin q' = q \sin 1'$.

Table 14.5 Formulae for plane and spherical triangles
(The angles of the triangle are denoted by A, B, C; the opposite sides, by a, b, c. Other formulae may be obtained by cyclic changes of A, B, C and a, b, c.)

Plane Triangle	Spherical Triangle
$a \sin B = b \sin A$	$\sin a \sin B = \sin b \sin A$
$a \cos B = c - b \cos A$	$\sin a \cos B = \cos b \sin c - \sin b \cos c \cos A$
$a^2 = b^2 + c^2 - 2bc \cos A$	$\cos a = \cos b \cos c + \sin b \sin c \cos A$
$a \cos C = b - c \cos A$	$\sin a \cos C = \sin b \cos c - \cos b \sin c \cos A$
$a \sin C = c \sin A$	$\sin a \sin C = \sin c \sin A$
$\sin \frac{1}{2}(B + C) = \cos \frac{1}{2}A$	$\cos \frac{1}{2}a \sin \frac{1}{2}(B + C) = \cos \frac{1}{2}A \cos \frac{1}{2}(b - c)$
$\cos \frac{1}{2}(B + C) = \sin \frac{1}{2}A$	$\cos \frac{1}{2}a \cos \frac{1}{2}(B + C) = \sin \frac{1}{2}A \cos \frac{1}{2}(b + c)$
$a \sin \frac{1}{2}(B - C) = (b - c) \cos \frac{1}{2}A$	$\sin \frac{1}{2}a \sin \frac{1}{2}(B - C) = \cos \frac{1}{2}A \sin \frac{1}{2}(b - c)$
$a \cos \frac{1}{2}(B - C) = (b + c) \sin \frac{1}{2}A$	$\sin \frac{1}{2}a \cos \frac{1}{2}(B - C) = \sin \frac{1}{2}A \sin \frac{1}{2}(b + c)$
$s = (a + b + c)$	$s = \frac{1}{2}(a + b + c)$
$r^2 = (s - a)(-b)(s - c)/s$	$m^2 = \sin(s - a) \sin(s - b) \sin(s - c) \sin s$
Area $= sr = \frac{1}{2}bc \sin A$	Area $= A + B + C - 180°$
$bc \sin^2 \frac{1}{2}A = (s - b)(s - c)$	$\sin b \sin c \sin^2 \frac{1}{2}A = \sin(s - b) \sin(s - c)$
$bc \cos^2 \frac{1}{2}A = s(s - a)$	$\sin b \sin c \cos^2 \frac{1}{2}A = \sin s \sin(s - a)4$
$\tan \frac{1}{2}A = r/(s - a)$	$\tan \frac{1}{2}A = m/\sin(s - a)$

Additional Formulae	Right-angled Triangle $A = 90°$
$\sin A \sin b = \sin B \sin a$	$\sin a \sin B = \sin b$
	$\sin a \cos B = \cos b \sin c$
	$\cos a = \cos b \cos c$
	$\sin a \cos C = \sin b \cos c$
$\sin A \sin c = \sin C \sin a$	$\sin a \sin C = \sin c$
$\cos a \cos B = \sin a \cot c - \sin B \cot C$	$\sin B \cos a = \cos b \cos C$
$\cos a \cos C = \sin a \cot b - \sin C \cot B$	$\cos B = \cos b \sin C$
$\cos b \cos A = \sin b \cot c - \sin A \cot C$	$\sin B \cos c = \cos C$
$\cos c \cos A = \sin c \cot b - \sin A \cot B$	$\sin B \sin c = \sin b \sin C$
$S = \frac{1}{2}(A + B + C)$	$\tan a = \tan b \sec C$
$M^2 = -\cos(S - A) \cos(S - B) \cos(S - C)/\cos S$	$\tan a = \tan c \sec B$
$\sin B \sin C \sin^2 \frac{1}{2}a = -\cos S \cos(S - A)$	$\cos a = \cot B \cot C$
$\sin B \sin c \cos^2 \frac{1}{2}a = \cos(S - B) \cos(S - C)$	$\tan b = \sin c \tan B$
$\tan \frac{1}{2}a = \cos(S - A)/M$	$\tan c = \sin b \tan C$

Table 14.5 *(continued)*

Quadrantal Triangle: $a = 90^\circ$		
$\sin A \sin b = \sin B$	$\sin b \sin A = \sin B$	$\tan A = -\tan B \sec c$
$\sin A \cos b = \cos B \sin C$	$\sin b \cos A = -\cos B \cos c$	$\tan A = -\tan C \sec b$
$\cos A = -\cos B \cos C$	$\cos b = \cos B \sin c$	$\cos A = -\cot b \cot c$
$\sin A \cos c = \sin B \cos C$	$\sin b \cos C = \cos c$	$\tan B = \sin C \tan b$
$\sin A \sin c = \sin C$	$\sin b \sin C = \sin B \sin c$	$\tan c = \sin B \tan c$

Spherical Triangle in Which b is Small
$a - c = -b \cos A + \frac{1}{2} b^2 \cot c \sin^2 A + \cdots$
$B \sin C = +bA + \frac{1}{2} b^2 \cot c \sin 2A + \cdots$
$180^\circ - C - A = +b \cot c \sin A + \frac{1}{4} b^2 (1 + 2\cot^2 c) \sin 2A + \cdots$

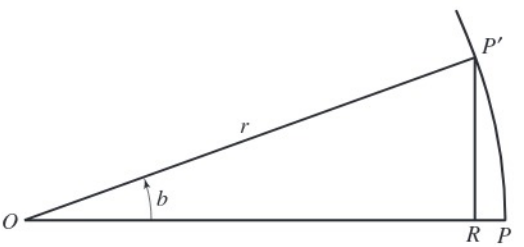


Figure 14.3 Arc of circle

14.4 Matrix and Vector Techniques

14.4.1 Matrix Multiplication

Two matrices **A** and **B** form the product **AB**, where the superscript indicates the row and the subscript indicates the column,

$$\mathbf{A} = \begin{bmatrix} a_1^1 & a_2^1 & a_3^1 \\ a_1^2 & a_2^2 & a_3^2 \\ a_1^3 & a_2^3 & a_3^3 \end{bmatrix}, \qquad \mathbf{B} = \begin{bmatrix} b_1^1 & b_2^1 & b_3^1 \\ b_1^2 & b_2^2 & b_3^2 \\ b_1^3 & b_2^3 & b_3^3 \end{bmatrix} \tag{14.26}$$

$$\mathbf{AB} = \begin{bmatrix} a_1^1 b_1^1 + a_2^1 b_1^2 + a_3^1 b_1^3 & a_1^1 b_2^1 + a_2^1 b_2^2 + a_3^1 b_2^3 & a_1^1 b_3^1 + a_2^1 b_3^2 + a_3^1 b_3^3 \\ a_1^2 b_1^1 + a_2^2 b_1^2 + a_3^2 b_1^3 & a_1^2 b_2^1 + a_2^2 b_2^2 + a_3^2 b_2^3 & a_1^2 b_3^1 + a_2^2 b_3^2 + a_3^2 b_3^3 \\ a_1^3 b_1^1 + a_2^3 b_1^2 + a_3^3 b_1^3 & a_1^3 b_2^1 + a_2^3 b_2^2 + a_3^3 b_2^3 & a_1^3 b_3^1 + a_2^3 b_3^2 + a_3^3 b_3^3 \end{bmatrix}. \tag{14.27}$$

14.4.2 Rotation of Axes Using Matrices

In practical computations it is often necessary to change the orientation of reference frames. This is frequently done by performing three rotations, one each about the x, y, and z axes.

In *The Astronomical Almanac*, these matrices are designated $\mathbf{R}_1$, $\mathbf{R}_2$, and $\mathbf{R}_3$ respectively. Given a right-handed system of rectangular coordinates x, y, z, and rotating the system positively through the angle ϕ_1 about the x-axis (i.e., counterclockwise as viewed from the $+x$ direction), the new coordinates x', y', z' are related to the original coordinates by

$$\begin{aligned} x' &= x \\ y' &= y\cos\phi_1 + z\sin\phi_1 \\ z' &= -y\sin\phi_1 + z\cos\phi_1. \end{aligned} \tag{14.28}$$

In matrix notation, this becomes

$$\begin{bmatrix} x' \\ y' \\ z' \end{bmatrix} = \mathbf{R}_1(\phi_1)\begin{bmatrix} x \\ y \\ z \end{bmatrix}, \quad \text{where } \mathbf{R}_1(\phi_1) = \begin{bmatrix} 1 & 0 & 0 \\ 0 & \cos\phi_1 & \sin\phi_1 \\ 0 & -\sin\phi_1 & \cos\phi_1 \end{bmatrix}. \tag{14.29}$$

Similarly, for a positive rotation ϕ_2 about the y-axis,

$$\begin{bmatrix} x' \\ y' \\ z' \end{bmatrix} = \mathbf{R}_2(\phi_2)\begin{bmatrix} x \\ y \\ z \end{bmatrix}, \quad \text{where } \mathbf{R}_2(\phi_2) = \begin{bmatrix} \cos\phi_2 & 0 & -\sin\phi_2 \\ 0 & 1 & 0 \\ \sin\phi_2 & 0 & \cos\phi_2 \end{bmatrix}. \tag{14.30}$$

Again, for a positive rotation ϕ_3 about the z-axis,

$$\begin{bmatrix} x' \\ y' \\ z' \end{bmatrix} = \mathbf{R}_3(\phi_3)\begin{bmatrix} x \\ y \\ z \end{bmatrix}, \quad \text{where } \mathbf{R}_3(\phi_3) = \begin{bmatrix} \cos\phi_3 & \sin\phi_3 & 0 \\ -\sin\phi_3 & \cos\phi_3 & 0 \\ 0 & 0 & 1 \end{bmatrix}. \tag{14.31}$$

The equation for two positive rotations may be written as

$$\begin{bmatrix} x' \\ y' \\ z' \end{bmatrix} = \mathbf{R}_1(\phi_1)\mathbf{R}_2(\phi_2)\begin{bmatrix} x \\ y \\ z \end{bmatrix} \tag{14.32}$$

where the matrix product $\mathbf{R}_1(\phi_1)\mathbf{R}_2(\phi_2)$ is

$$\begin{bmatrix} \cos\phi_2 & 0 & -\sin\phi_2 \\ \sin\phi_1\sin\phi_2 & \cos\phi_1 & \sin\phi_1\cos\phi_2 \\ \cos\phi_1\sin\phi_2 & -\sin\phi_1 & \cos\phi_1\cos\phi_2 \end{bmatrix}. \tag{14.33}$$

For three successive positive rotations (ϕ_1), (ϕ_2), (ϕ_3) about the x-, y-, and z-axes, respectively

$$\begin{bmatrix} x' \\ y' \\ z' \end{bmatrix} = \mathbf{R}_1(\phi_1)\mathbf{R}_2(\phi_2)\mathbf{R}_3(\phi_3)\begin{bmatrix} x \\ y \\ z \end{bmatrix} \tag{14.34}$$

where the matrix product of $\mathbf{R}_1(\phi_1)\mathbf{R}_2(\phi_2)\mathbf{R}_3(\phi_3)$ is

$$\begin{bmatrix} \cos\phi_2\cos\phi_3 & \cos\phi_2\sin\phi_3 & -\sin\phi_2 \\ \sin\phi_1\sin\phi_2\cos\phi_3 - \cos\phi_1\sin\phi_3 & \sin\phi_1\sin\phi_2\sin\phi_3 + \cos\phi_1\cos\phi_3 & \sin\phi_1\cos\phi_2 \\ \cos\phi_1\sin\phi_2\cos\phi_3 + \sin\phi_1\sin\phi_3 & \cos\phi_1\sin\phi_2\sin\phi_3 - \sin\phi_1\cos\phi_3 & \cos\phi_1\cos\phi_2 \end{bmatrix}. \tag{14.35}$$

This case comprises a rotation (ϕ_1) about the x-axis, a rotation (ϕ_2) around the new position of the y-axis, and a rotation (ϕ_3) around the final position of the z-axis.

The matrix denoting any number of rotations can be derived by multiplication following the precepts below.

14.4.3 Spherical Coordinates Using Vectors

Consider a triangle ABC (Fig. 14.1) scribed on the surface of a sphere of unit radius whose center is denoted by O. Each side abc is a portion of a great circle defined by $BOC = a$, $AOC = b$, and $AOB = c$.

A is the angle between the planes BOA and COA, B is the angle between the planes AOB and COB, and C is the angle between planes AOC and BOC.

Take $\mathbf{l}$, $\mathbf{m}$, $\mathbf{n}$, as nonorthogonal unit vectors along OA, OB, and OC respectively. The cross product $\mathbf{l} \times \mathbf{m}$ is a vector of magnitude $\sin c$ directed orthogonally to the plane AOB. In the same manner, the cross product $\mathbf{l} \times \mathbf{n}$ is a vector of magnitude $\sin b$ orthogonal to AOC. A is the angle between these two vectors.

The dot product of these two vectors is

$$\begin{aligned} (\mathbf{l}\times\mathbf{m})\cdot(\mathbf{l}\times\mathbf{n}) &= \sin c \sin b \cos A \\ &= \mathbf{l}\cdot[\mathbf{m}\times(\mathbf{l}\times\mathbf{n})] \\ &= \mathbf{l}\cdot[\mathbf{l}(\mathbf{m}\cdot\mathbf{n}) - \mathbf{n}(\mathbf{l}\cdot\mathbf{m})] \\ &= (\mathbf{m}\cdot\mathbf{n}) - (\mathbf{l}\cdot\mathbf{n})(\mathbf{l}\cdot\mathbf{m}) \\ &= \cos a - \cos b\cos c \end{aligned} \tag{14.36}$$

which gives

$$\cos a = \cos b\cos c + \sin b\sin c\cos A. \tag{14.37}$$

Similar equations for $\cos b$ and $\cos c$ are easily obtained.

From the definition of the vector product, we find

$$\begin{aligned} \sin A &= \frac{|(\mathbf{l}\times\mathbf{m})\times(\mathbf{l}\times\mathbf{n})|}{|\mathbf{l}\times\mathbf{m}|\,|\mathbf{l}\times\mathbf{n}|} \\ &= \frac{|-\mathbf{l}[\mathbf{m},\mathbf{l},\mathbf{n}] + \mathbf{m}[\mathbf{l},\mathbf{l},\mathbf{n}]|}{\sin b\sin c} \\ &= \frac{[\mathbf{l},\mathbf{m},\mathbf{n}]}{\sin b\sin c}. \end{aligned} \tag{14.38}$$

Thus,

$$\frac{\sin A}{\sin a} = \frac{\sin B}{\sin b} = \frac{\sin C}{\sin c}. \tag{14.39}$$

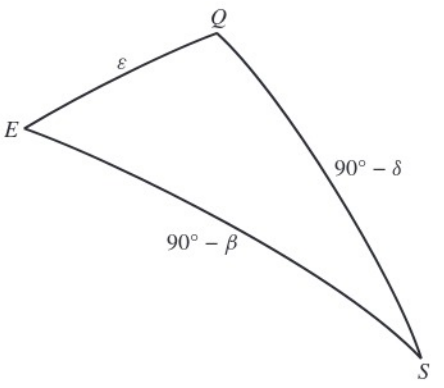


Figure 14.4 Triangle on unit sphere

Other formulae of spherical trigonometry (see Table 14.5) may be obtained from Eqs. 14.38 and 14.39.

An example of the application of vectors to the solution of a problem in spherical trigonometry concerns transforming the coordinates of a star from right ascension (α) and declination (δ) to ecliptic longitude (λ) and latitude (β).

Given the triangle EQS (Fig. 14.4) on a sphere of unit radius with center at O, Q is the pole of the celestial equator, E is the pole of the ecliptic, and S is the star.

The side EQ is the obliquity of the ecliptic (ϵ), the side QS is $90^\circ - \delta$, and the side ES is $90^\circ - \beta$. Two great circles passing through E and Q, each being orthogonal to side ES, intersect the equator and ecliptic planes at the vernal equinox. Then the angle $EQS = 90^\circ + \alpha$, and the angle $SEQ = 90^\circ - \lambda$.

Using these quantities the problem is easily solved by the equations previously derived:

$$\begin{aligned} \sin\beta &= \sin\delta\cos\epsilon - \cos\delta\sin\alpha\sin\epsilon \\ \cos\beta\cos\lambda &= \cos\delta\cos\alpha \\ \cos\beta\sin\lambda &= \sin\delta\sin\epsilon + \cos\delta\sin\alpha\cos\epsilon. \end{aligned} \tag{14.40}$$

The problem can also be solved by the use of vectors. Assume axes $\mathbf{l}$, $\mathbf{m}$, $\mathbf{n}$ (forming the conventional right-handed triad) with $\mathbf{l}$ pointing to the vernal equinox and $\mathbf{n}$ directed toward the north pole of the equator (Q). Also assume the right-handed triad $\mathbf{u}$, $\mathbf{v}$, $\mathbf{w}$ with $\mathbf{u}$ directed to the vernal equinox and $\mathbf{w}$ toward the pole of the ecliptic (E).

Then

$$\begin{aligned} \mathbf{u} &= \mathbf{l} \\ \mathbf{v} &= \mathbf{m}\cos\epsilon - \mathbf{n}\sin\epsilon \\ \mathbf{w} &= \mathbf{m}\sin\epsilon + \mathbf{n}\cos\epsilon. \end{aligned} \tag{14.41}$$

The components of OS projected onto the equatorial and ecliptic axes are

$$\begin{aligned} &\cos\delta\cos\alpha, \quad \cos\delta\sin\alpha, \quad \sin\delta, \\ &\cos\beta\cos\lambda, \quad \cos\beta\sin\lambda, \quad \sin\beta, \end{aligned}$$

leading to the original trigonometric equations.

14.4.4 Specific Coordinate Transformations

14.4.4.1 Geocentric Coordinate Transformations

For geocentric spherical coordinates there are the four practical reference systems of:

1. Azimuth/Altitude System: Azimuth (A) is measured from the north through east in the plane of the horizon, and altitude (a) measured perpendicular to the horizon. In astronomy, the zenith distance ($z = 90° - a$) is more generally used, but the altitude is retained in the formulae for reasons of symmetry.
2. Hour Angle/Declination System: Hour angle (h) is measured westward in the plane of the equator from the meridian, and declination (δ) is measured perpendicular to the equator, positive to the north.
3. Right Ascension/Declination System: Right ascension (a) is measured from the equinox or CIO eastward in the plane of the equator, and declination (δ) is measured perpendicular to the equator, positive to the north.
4. Longitude/Latitude System: Longitude (λ) is measured from the equinox eastward in the plane of the ecliptic, and latitude (β) is measured perpendicular to the ecliptic, positive to the north.

Formulae for transforming equatorial right ascension and declination to ecliptic longitude and latitude may be written using direction cosines (unit vectors) and (rotation matrices) as follows:

$$\begin{bmatrix} \cos\beta\cos\lambda \\ \cos\beta\sin\lambda \\ \sin\beta \end{bmatrix} = \begin{bmatrix} 1 & 0 & 0 \\ 0 & \cos\epsilon & \sin\epsilon \\ 0 & -\sin\epsilon & \cos\epsilon \end{bmatrix} \begin{bmatrix} \cos\delta\cos\alpha \\ \cos\delta\sin\alpha \\ \sin\delta \end{bmatrix}. \tag{14.42}$$

The inverse transformation, using $[R_\epsilon]$ to denote the rotation matrix, is

$$\begin{bmatrix} \cos\delta\cos\alpha \\ \cos\delta\sin\alpha \\ \sin\delta \end{bmatrix} = [R_\epsilon]^{-1} \begin{bmatrix} \cos\beta\cos\lambda \\ \cos\beta\sin\lambda \\ \sin\beta \end{bmatrix}. \tag{14.43}$$

The transformations correspond to simple rotations about the x-axis through ϵ, which is the obliquity of the ecliptic corresponding to the particular equator and ecliptic used.

Transformation from right ascension/declination to local hour angle/declination may be carried out by substitution of

$$h = \text{local sidereal time} - \alpha.$$

The two systems are identical apart from the origin and direction angular measurement. The transformation may also be considered as a rotation about the axis perpendicular to the equatorial plane and positive in the direction of the North Pole. Thus,

$$\begin{bmatrix} \cos\delta\cos h \\ \cos\delta\sin h \\ \sin\delta \end{bmatrix} = \begin{bmatrix} \cos t_s & \sin t_s & 0 \\ -\sin t_s & \cos t_s & 0 \\ 0 & 0 & 1 \end{bmatrix} \begin{bmatrix} \cos\delta\cos\alpha \\ \cos\delta\sin\alpha \\ \sin\delta \end{bmatrix} \tag{14.44}$$

where t_s is the local sidereal time.

Transformation of local hour angle/declination to azimuth/altitude involves a rotation of the reference frame through an angle $90° - \phi$ in the plane of the meridian, where ϕ is the geocentric latitude, followed by a rotation about the new vertical by 180°. Thus,

$$\begin{bmatrix} \cos a \cos A \\ \cos a \sin A \\ \sin a \end{bmatrix} = \begin{bmatrix} -1 & 0 & 0 \\ 0 & -1 & 0 \\ 0 & 0 & 1 \end{bmatrix} \begin{bmatrix} \sin\phi & 0 & -\cos\phi \\ 0 & 1 & 0 \\ \cos\phi & 0 & \sin\phi \end{bmatrix} \begin{bmatrix} \cos\delta\cos h \\ \cos\delta\sin h \\ \sin\delta \end{bmatrix} \quad (14.45)$$

In this transformation the diagonal matrix is its own inverse and, if $[R_\phi]$ denotes the rotation in the meridian plane with inverse, then

$$[R_\phi]^{-1} = \begin{bmatrix} \sin\phi & 0 & \cos\phi \\ 0 & 1 & 0 \\ -\cos\phi & 0 & \sin\phi \end{bmatrix} \quad (14.46)$$

and

$$\begin{bmatrix} \cos\delta\cos h \\ \cos\delta\sin h \\ \sin\delta \end{bmatrix} = [R_\phi]^{-1} \begin{bmatrix} -1 & 0 & 0 \\ 0 & -1 & 0 \\ 0 & 0 & 1 \end{bmatrix} \begin{bmatrix} \cos a \cos A \\ \cos a \sin A \\ \sin a \end{bmatrix}. \quad (14.47)$$

The corresponding equatorial rectangular coordinates and distance are denoted by X, Y, Z, and R for the Sun and by ξ, η, ζ, and Δ for the planets; they are derived from the spherical coordinates by the formulae:

$$\begin{aligned} \frac{X}{R} \text{ or } \frac{\xi}{\Delta} &= \cos\delta\cos\alpha \\ \frac{Y}{R} \text{ or } \frac{\eta}{\Delta} &= \cos\delta\sin\alpha \\ \frac{Z}{R} \text{ or } \frac{\zeta}{\Delta} &= \sin\delta. \end{aligned} \quad (14.48)$$

Geocentric ecliptic rectangular coordinates are rarely (if ever) used.

14.4.4.2 Heliocentric Coordinate Transformations

For heliocentric coordinates there are only the two practical reference systems—the equatorial and the ecliptic. In the equatorial system only rectangular coordinates are used. The relationships between the ecliptic rectangular coordinates (x_c, y_c, z_c), the ecliptic longitude, latitude, and distance (l, b, r), and the equatorial rectangular coordinates (x, y, z) are

$$\begin{bmatrix} x_c &= r\cos b\cos l \\ y_c &= r\cos b\sin l \\ z_c &= r\sin b \end{bmatrix} = [R_\epsilon] \begin{bmatrix} x \\ y \\ z \end{bmatrix} \quad (14.49)$$

$$\begin{bmatrix} x \\ y \\ z \end{bmatrix} = [R_\epsilon]^{-1} \begin{bmatrix} x_c \\ y_c \\ z_c \end{bmatrix}. \quad (14.50)$$

The conversion from heliocentric to geocentric coordinates is performed in terms of equatorial rectangular coordinates using

$$\begin{aligned} \xi &= x + X \\ \eta &= y + Y \\ \zeta &= z + Z \end{aligned} \tag{14.51}$$

where X, Y, Z are the geocentric coordinates of the Sun.

The calculation of the spherical coordinates from the rectangular coordinates, or from the known direction cosines, typified by

$$\begin{aligned} \Delta \cos\delta \cos\alpha &= \xi \\ \Delta \cos\delta \sin\alpha &= \eta \\ \Delta \sin\delta &= \zeta \end{aligned} \tag{14.52}$$

is performed by

$$\begin{aligned} \tan\alpha &= \eta/\xi \\ \Delta &= \sqrt{\xi^2 + \eta^2 + \zeta^2} \\ \cot\alpha &= \xi/\eta \\ \sin\delta &= \zeta/\Delta. \end{aligned} \tag{14.53}$$

The quadrant of α is determined by the signs of ξ and η, and that of δ by the sign of ζ. Δ and $\Delta\cos\delta$ are always positive. The formulae for α and δ may be written as

$$\begin{aligned} \alpha &= \tan^{-1}\eta/\xi, \quad \text{or } \arctan\eta/\xi, \\ &= \cot^{-1}\xi/\eta, \quad \text{or } \operatorname{arccot}\xi/\eta, \\ \delta &= \sin^{-1}\zeta/\Delta, \quad \text{or } \arcsin\zeta/\Delta, \end{aligned} \tag{14.54}$$

provided that the appropriate values, and not necessarily the principal values, of the multi-valued functions are taken.

Many of the conversions above correspond to a simple rotation of the frame of reference about one of its axes. These are special cases of the general conversion from a set of axes designated by x, y, z to a set designated by x', y', z'. The two systems are connected by the formulae

$$\begin{aligned} x &= l_1x' + l_2y' + l_3z' & x' &= l_1x + m_1y + n_1z \\ y &= m_1x' + m_2y' + m_3z' & y' &= l_2x + m_2y + n_2z \\ z &= n_1x' + n_2y' + n_3z' & z' &= l_3x + m_3y + n_3z \end{aligned} \tag{14.55}$$

where l_1, m_1, n_1; l_2, m_2, n_2; and l_3, m_3, n_3 are the direction cosines of x', y', z' referred to the system x, y, z. The direction cosines satisfy the relations typified by

$$\begin{aligned} l_1^2 + m_1^2 + n_1^2 &= 1 \\ l_2l_3 + m_2m_3 + n_2n_3 &= 0 \\ l_1^2 + l_2^2 + l_3^2 &= 1 \\ m_1n_1 + m_2n_2 + m_3n_3 &= 0. \end{aligned} \tag{14.56}$$

These nine quantities can be expressed in terms of the Eulerian angles θ, ϕ, ψ as

$$\begin{aligned} l_1 &= +\cos\phi\cos\theta\cos\psi - \sin\phi\sin\psi \\ l_2 &= -\cos\phi\cos\theta\sin\psi - \sin\phi\cos\psi \\ l_3 &= +\cos\phi\sin\theta \\ m_1 &= +\sin\phi\cos\theta\cos\psi + \cos\phi\sin\psi \\ m_2 &= -\sin\phi\cos\theta\sin\psi + \cos\phi\cos\psi \\ m_3 &= +\sin\phi\sin\theta \\ n_1 &= -\sin\theta\cos\psi \\ n_2 &= +\sin\theta\sin\psi \\ n_3 &= +\cos\theta. \end{aligned} \tag{14.57}$$

In this case the conversion corresponds to a rotation ϕ about the z-axis, θ about the new position of the y-axis, and ψ about the new (and final) position of the z-axis. The transformation is equivalent to a single rotation about some line not in general coincident with one of the axes; but such single rotations are not frequently encountered in astronomical practice.

14.5 Numerical Calculus

14.5.1 Numerical Differentiation

Successive derivatives of a function are closely related to the successive orders of differences. Thus to obtain the exact expression for the derivatives in terms of differences it is necessary merely to differentiate any of the interpolation formulae (see § 14.2) as many times as required.

Differentiation of Bessel's interpolation formula leads to

$$hf'_p = \delta_{1/2} + \frac{1}{2}\left(p - \frac{1}{2}\right)(\delta_0^2 + \delta_1^2) + \frac{1}{12}(1 - 6p + 6p^2)\delta_{1/2}^3 + \cdots \tag{14.58}$$

where f'_p denotes the value of df/dt at the point $t = t_0 + ph$.

This formula is intended for use in the range $0 \le p \le 1$; the maximum value of the third-difference coefficient is $1/12$ and occurs at $p = 0$ and 1. At $p = 1/2$ the formula reduces to

$$hf'_{1/2} = \delta_{1/2} - \frac{1}{24}\delta_{1/2}^3 + \frac{3}{640}\delta_{1/2}^5 - \cdots. \tag{14.59}$$

Differentiation of Stirling's interpolation formula leads to

$$hf'_p = \mu\delta_0 + p\delta_0^2 - \frac{1}{6}(1 - 3p^2)\mu\delta_0^3 + \cdots \tag{14.60}$$

where, for example, $\mu\delta_0^3 = \frac{1}{2}(\delta_{-1/2}^3 + \delta_{1/2}^3)$. This formula is intended for use in the range $-1/2 \le p \le 1/2$; the maximum value of the coefficient of the mean third difference is 1/6 and occurs at $p = 0$. At $p = 0$ the formula reduces to

$$hf_0' = \mu\delta_0 - \frac{1}{6}\mu\delta_0^3 + \frac{1}{30}\mu\delta_0^5 - \cdots. \tag{14.61}$$

The condition for a maximum or minimum is that $f_p' = 0$. For Stirling's formula this condition may be expressed as:

$$p = \frac{-\mu\delta_0 + \frac{1}{6}(1 - 3p^2)\mu\delta_0^3 - \cdots}{\delta_0^2}. \tag{14.62}$$

This equation must normally be solved by successive approximations. The maximum contribution from the third difference is $1/6\ \mu\delta_0^3/\delta_0^2$, and, if this is Negligible, p may be evaluated directly from

$$p = -\mu\delta_0/\delta_0^2 = -\frac{1}{2} - \delta_{-1/2}/\delta_0^2. \tag{14.63}$$

In astronomical usage, the terms *variation* and *motion* are synonymous with "derivative with respect to time," when qualified by an adjective defining the unit of time, and are usually evaluated for the tabular points. The term *secular variation* usually implies a second derivative with respect to time.

The second derivative f_p'' is obtained by differentiating the formulae for f_p' for Stirling's formula this leads to

$$h^2 f_p' = \delta_0^2 + p\mu\delta_0^3 + \cdots \tag{14.64}$$

and, when $p = 0$, to

$$h^2 f_p'' = \delta_0^2 - \frac{1}{12}\delta_0^4 + \frac{1}{90}\delta_0^6 - \cdots. \tag{14.65}$$

In terms of central differences, the derivatives to order 10 at the tabular point and at the half-way point are listed in Table 14.6. Primes are used to denote differentiation with respect to x. For example,

$$h^2 f_p'' = h^2 \frac{d^2}{dx^2} f(x_0 + ph) = \frac{d^2}{dp^2} f_p. \tag{14.66}$$

For higher derivatives the primes are replaced by italicized roman numerals. In general formulae, $f_p^{(n)}$ is used to denote the nth derivative of f with respect to x at the point $x_0 + ph$.

The formulae in Table 14.6 may also be written by substituting for the differences their values in terms of the function. Additional expressions for derivatives in terms of the functional values are as follows:

$$
\begin{aligned}
hf_0' &= \frac{1}{2}(f_1 - f_{-1}) - \frac{1}{6}\mu\delta^3 f_0 + \cdots \\
&= \frac{1}{12}(-f_2 + 8f_1 - 8f_{-1} + f_{-2}) + \frac{1}{30}\mu\delta^5 f_0 - \cdots \\
&= \frac{1}{60}(f_3 - 9f_2 + 45f_1 - 45f_{-1} + 9f_{-2} - f_{-3}) - \frac{1}{140}\mu\delta^7 f_0 + \cdots \\
h^2 f_0'' &= (f_1 - 2f_0 + f_{-1}) - \frac{1}{12}\delta^4 f_0 + \cdots \\
&= \frac{1}{12}(-f_2 + 16f_1 - 30f_0 + 16f_{-1} - f_{-2}) + \frac{1}{90}\delta^6 f_0 - \cdots \\
&= \frac{1}{180}(2f_3 - 27f_2 + 270f_1 - 490f_0 + 270f_{-1} - 27f_{-2} + 2f_{-3}) - \frac{1}{560}\delta^8 f_0 + \cdots \\
hf_{1/2}' &= (f_1 - f_0) - \frac{1}{24}\delta^3 f_{1/2} + \cdots \\
&= \frac{1}{24}(-f_2 + 27f_1 - 27f_0 + f_{-1}) + \frac{3}{640}\delta^5 f_{1/2} - \cdots \\
&= \frac{1}{1920}(9f_3 - 125f_2 + 2250f_1 - 2250f_0 + 125f_{-1} - 9f_{-2}) - \frac{5}{7168}\delta^7 f_{1/2} + \cdots \\
h^2 f_{1/2}'' &= \frac{1}{2}(f_2 - f_1 - f_0 + f_{-1}) - \frac{5}{24}\mu\delta^4 f_{1/2} + \cdots \\
&= \frac{1}{48}(-5f_3 + 39f_2 - 34f_1 - 34f_0 + 39f_{-1} - 5f_{-2}) + \frac{259}{5760}\mu\delta^6 f_{1/2} - \cdots .
\end{aligned}
\tag{14.67}
$$

For further formulae see the *Interpolation and Allied Tables* (H.M. Nautical Almanac Office 1956) and the *Handbook of Mathematical Functions* (Abramowitz and Stegun 1973).

14.5.2 Numerical Integration

When studying motions within the solar system it is necessary to use the solution of ordinary differential equations of the second order. This normally involves the simultaneous integration of three second-order differential equations to produce an ephemeris in rectangular coordinates of a planet, comet, or satellite with time as the independent argument.

In numerical differentiation, the derivatives of a function are expressed in terms of the differences. In numerical integration, the opposite method is used. Derivatives of some function are computed and checked by differencing, to form a table of $f, \delta, \delta^2, \delta^3, \delta^4$, and so on. In the simplest case, where the values of the function to be integrated can be calculated in advance, it is possible to compute a starting value of the first summation f' and to extend the table in either direction by applying successive values of f. For a double integration, a starting value for f'' must be evaluated and successive values of f' applied. Expressions to evaluate the first and second integrals are derived by integrating an interpolation formula, for example,

Table 14.6 Derivatives to an order of 10

Derivatives at a Tabular Point	Derivatives at a Halfway Point
$hf'_0 = \mu\delta_0 - \frac{1}{6}\mu\delta_0^3 + \frac{1}{30}\mu\delta_0^5 - \cdots$	$hf'_{1/2} = \delta_{1/2} - \frac{1}{24}\delta_{1/2}^3 + \frac{3}{640}\delta_{1/2}^5 - \cdots$
$h^2 f''_0 = \delta_0^2 - \frac{1}{12}\delta_0^4 + \frac{1}{90}\delta_0^6 - \cdots$	$h^2 f''_{1/2} = \mu\delta_{1/2}^2 - \frac{5}{24}\mu\delta_{1/2}^4 + \frac{259}{5760}\mu\delta_{1/2}^6 - \cdots$
$h^3 f'''_0 = \mu\delta_0^3 - \frac{1}{4}\mu\delta_0^5 + \frac{7}{120}\mu\delta_0^7 - \cdots$	$h^3 f'''_{1/2} = \delta_{1/2}^3 - \frac{1}{8}\delta_{1/2}^5 + \frac{37}{1920}\delta_{1/2}^7 - \cdots$
$h^4 f_0^{iv} = \delta_0^4 - \frac{1}{6}\delta_0^6 + \frac{7}{240}\delta_0^8 - \cdots$	$h^4 f_{1/2}^{iv} = \mu\delta_{1/2}^4 - \frac{7}{24}\mu\delta_{1/2}^6 + \frac{47}{640}\mu\delta_{1/2}^8 - \cdots$
$h^5 f_0^{v} = \mu\delta_0^5 - \frac{1}{3}\mu\delta_0^7 + \frac{13}{144}\mu\delta_0^9 - \cdots$	$h^5 f_{1/2}^{v} = \delta_{1/2}^5 - \frac{5}{24}\delta_{1/2}^7 + \frac{47}{1152}\delta_{1/2}^9 - \cdots$
$h^6 f_0^{vi} = \delta_0^6 - \frac{1}{4}\delta_0^8 + \frac{13}{240}\delta_0^{10} - \cdots$	$h^6 f_{1/2}^{vi} = \mu\delta_{1/2}^6 - \frac{3}{8}\mu\delta_{1/2}^8 + \frac{209}{1920}\mu\delta_{1/2}^{10} - \cdots$
$h^7 f_0^{vii} = \mu\delta_0^7 - \frac{5}{12}\mu\delta_0^9 + \frac{31}{240}\mu\delta_0^{11} - \cdots$	$h^7 f_{1/2}^{vii} = \delta_{1/2}^7 - \frac{7}{24}\delta_{1/2}^9 + \frac{133}{1920}\delta_{1/2}^{11} - \cdots$
$h^8 f_0^{viii} = \delta_0^8 - \frac{1}{3}\delta_0^{10} + \frac{31}{360}\delta_0^{12} - \cdots$	$h^8 f_{1/2}^{viii} = \mu\delta_{1/2}^8 - \frac{11}{24}\mu\delta_{1/2}^{10} + \frac{871}{5760}\mu\delta_{1/2}^{12} - \cdots$
$h^9 f_0^{ix} = \mu\delta_0^9 - \frac{1}{2}\mu\delta_0^{11} + \cdots$	$h^9 f_{1/2}^{ix} = \delta_{1/2}^9 - \frac{3}{8}\delta_{1/2}^{11} + \cdots$
$h^{10} f_0^{x} = \delta_0^{10} - \frac{5}{12}\delta_0^{12} + \cdots$	$h^{10} f_{1/2}^{x} = \mu\delta_0^{10} - \frac{13}{24}\mu\delta_{1/2}^{12} + \cdots$

$$\int^{1/2} f(x)\,dx = \omega\left[f'_{1/2} + \frac{1}{24}\delta_{1/2} - \frac{17}{5760}\delta_{1/2}^3 + \frac{367}{967680}\delta_{1/2}^5 - \cdots\right]$$

$$\iint^{0} f(x)\,dx^2 = \omega^2\left[f''_0 + \frac{1}{12}f_0 - \frac{1}{240}\delta_0^2 + \frac{31}{60480}\delta_0^4 - \cdots\right]. \tag{14.68}$$

Additional formulae are given in H.M. Nautical Almanac Office (1956) and in Abramowitz and Stegun (1973).

In the integration of orbits the problem is more complicated because the function that is to be integrated is undetermined until the integral becomes known. Thus it is necessary to proceed stepwise using extrapolation and approximation at each step. Because of the availability of computers, as well as the rectangular coordinates of the principal planets, two methods for the numerical integration of the orbits have proved useful, Cowell's and Encke's.

When one is utilizing Cowell's approach, the equations of motion are integrated to give directly the positions of the perturbed body in rectangular coordinates. For a planet or comet, the origin usually is the Sun and at each step the attractions of the perturbing bodies would be added to that of the Sun.

With Cowell's method, however, the origin may be any perturbing body, or even a double star, since no use is made of a conic section as the first approximation. The single condition is that the motions of all perturbing bodies relative to the selected origin should be known. A disadvantage of Cowell's method is that the integrals comprise numerous significant figures that vary extensively with time. Thus, the integration tables are prone to converge rather slowly, which may require the use of a short step interval. The basic equations in the Cowell approach are

$$\ddot{x} = -k^2(1+m)\frac{x}{r^3} + \sum_j k^2 m_j\left(\frac{x_j - x}{\rho_j^3} - \frac{x_j}{r_j^3}\right) \tag{14.69}$$

with similar equations in y and z. The masses are expressed in terms of the mass of the Sun, k equals the Gaussian constant, m is the mass of the perturbed body, and m_j the masses of the perturbing bodies. The first term is the attraction of the Sun on m, and the first term in parentheses is the attraction of m_j on m. The last term in parentheses is the action of the perturbing bodies on the Sun.

In Encke's method the unperturbed orbit of the mass m about the Sun is assumed known. Hence only the difference between the unperturbed position and the perturbed position needs to be determined. The equations may be written

$$\ddot{x} - \ddot{x}_0 = \ddot{\xi} = k^2(1+m)\left(\frac{x_0}{r_0^3} - \frac{x}{r^3}\right) + \sum_j k^2 m_j \left(\frac{x_j - x}{\rho_j^3} - \frac{x_j}{r_j^3}\right) \tag{14.70}$$

with similar equations for $\ddot{\eta}$ and $\ddot{\zeta}$. These equations could be integrated directly, but since ξ is small, many figures would have to be carried in the term $(x_0/r_0^3 - x/r^3)$ to retain significance in the difference. On the assumption that ξ, η and ζ are so small compared to x, y, z that their squares can be neglected, the equation can be transformed by the use of auxiliary quantities q and f where

$$q = \frac{x_0\xi + y_0\eta + z_0\zeta}{r_0^2}$$
$$f = \frac{1 - (1+2q)^{-3/2}}{q}. \tag{14.71}$$

The final Encke equations become

$$\omega^2\ddot{\xi} = \omega^2 k^2(1+m)\frac{1}{r_0^3}(fqx - \xi) + \sum_j \omega^2 k^2 m_j \left(\frac{x_j - x}{\rho_j^3} - \frac{x_j}{r_j^3}\right). \tag{14.72}$$

Where ω represents the interval of integration. Similar equations hold for $\ddot{\eta}$ and $\ddot{\zeta}$.

Encke's procedure normally allows a larger step size than Cowell's but when close approaches happen, the Encke perturbations tend to grow rapidly in size, requiring a smaller step interval.

Other approaches to the numerical solution of differential equations are provided by Runge-Kutta methods. These are single-step methods with each step being independent of those preceding.

Given:

$$\frac{dx}{dt} = f(t, x); \quad x(t_0) = x_0. \tag{14.73}$$

A widely used Runge-Kutta method (to the fourth order) involves the following operations for one step. Here h is the step interval.

$$
\begin{aligned}
f_0 &= f(t_0, x) \\
f_1 &= f\left(t_0 + \frac{1}{2}h, x_0 + \frac{1}{2}hf_0\right) \\
f_2 &= f\left(t_0 + \frac{1}{2}h, x_0 + \frac{1}{2}hf_1\right) \\
f_3 &= f\left(t_0 + h, x_0 + hf_2\right) \\
&\cdots .
\end{aligned} \tag{14.74}
$$

Then

$$
x(t_0 + h) \approx x_1 = x_0 + \frac{1}{6}(f_0 + 2f_1 + 2f_2 + f_3). \tag{14.75}
$$

Similar equations exist in y and z.

Equations to the fourth order are not sufficiently accurately for most orbital calculations but this serves as an example of the method. For modifications of the method refer to Danby (1988).

In all the step-by-step methods for numerical solution of differential equations some precautions apply:

1. The interval of tabulation must be monitored in cases of close approach, since the approximations used in the iterative process may prove to be of insufficient accuracy. Automatic methods to vary the step size are now in use with some methods.
2. The accumulation of round-off errors must be monitored. The probable error after n steps can be estimated.
3. If the method of solution adopted makes use of truncated formulae either corrections must be applied subsequently or the number of figures in the solution must be reduced accordingly.

Examples of numerical integrations may be found in Brouwer and Clemence (1961) and in Danby (1988).

An example of a multistep scheme is the Adams-Bashforth method. The order of this method is limited by the number of terms the user is willing to compute. The formulae for this method are

$$
x_{n+1} = x_n + h \sum_{k=0}^{N} \alpha_k \nabla^k f_n \tag{14.76}
$$

where

$$
\begin{aligned}
N &= \text{the number of terms} \\
\alpha &= 1, \frac{1}{2}, \frac{5}{12}, \frac{3}{8}, \frac{251}{720}, \frac{95}{288}, \ldots \\
\nabla^k f_n &= \nabla^{k-1} f_n - \nabla^{k-1} f_{n-1} \\
\nabla^0 f_n &= f_n \\
f_n &= f(x_n, t_n).
\end{aligned}
$$

This method can be started using a single step method such as the Runge-Kutta.

To differentially correct the initial conditions of the motion, one integrates seven orbits simultaneously. The first orbit uses unaltered initial conditions. Each of the rest of the orbits uses initial conditions for which one coordinate or velocity has been incremented by a small amount. Earth-based observations are right ascensions and declinations of the satellite. The residuals for these observations can be expressed as

$$\Delta\alpha_i = \frac{\partial\alpha_i}{\partial X_0}\Delta X_0 + \frac{\partial\alpha_i}{\partial Y_0}\Delta Y_0 + \frac{\partial\alpha_i}{\partial Z_0}\Delta Z_0 + \frac{\partial\alpha_i}{\partial \dot{X}_0}\Delta \dot{X}_0 + \frac{\partial\alpha_i}{\partial \dot{Y}_0}\Delta \dot{Y}_0 + \frac{\partial\alpha_i}{\partial \dot{Z}_0}\Delta \dot{Z}_0$$
$$\Delta\delta i = \frac{\partial\delta_i}{\partial X_0}\Delta X_0 + \frac{\partial\delta_i}{\partial Y_0}\Delta Y_0 + \frac{\partial\delta_i}{\partial Z_0}\Delta Z_0 + \frac{\partial\delta_i}{\partial \dot{X}_0}\Delta \dot{X}_0 + \frac{\partial\delta_i}{\partial \dot{Y}_0}\Delta \dot{Y}_0 + \frac{\partial\delta_i}{\partial \dot{Z}_0}\Delta \dot{Z}_0 \tag{14.77}$$

where α and δ are the right ascension and declination respectively; X_0, Y_0, Z_0, $\dot{X}_0$, $\dot{Y}_0$, and $\dot{Z}_0$ are the initial coordinates and velocities; the subscript i refers to the number of the observation. The partial derivatives are evaluated numerically, and can be written in the form

$$\frac{\partial\alpha_i}{\partial X_0} = \frac{\alpha_i(X_0 + \Delta X_0, Y_0, Z_0, \dot{X}_0, \dot{Y}_0, \dot{Z}_0) - \alpha_i(X_0, Y_0, Z_0, \dot{X}_0, \dot{Y}_0, \dot{Z}_0)}{\Delta X_0}. \tag{14.78}$$

The differential corrections can be written as

$$\Delta\mathbf{R} = (\mathbf{A}^T\mathbf{A})^{-1}\mathbf{A}^T\Delta\mathbf{r}. \tag{14.79}$$

where $\Delta\mathbf{R}$ is the matrix of corrections to the initial conditions, $\mathbf{A}$ is the matrix of the partial derivatives, and $\Delta\mathbf{r}$ is the matrix of residuals.

14.6 Statistics

14.6.1 Accumulation of Error

The formulae listed in Table 14.7 indicate the way in which errors accumulate in simple arithmetical operations. The distribution of accumulated error is usually nearly normal, whatever the distributions of the original errors, so the standard deviation of the error, calculated from the formulae, is of value in the examination of the differences of tabulated functions. The notation used and assumptions made in the table are:

- a_i is the absolute error of A_i, in the sense of given value minus true value. These errors are assumed to be unbiased and independent.
- α_i is the variance, or mean square value, of the error of A_i. The standard deviation of the error is the square root of variance.
- i, m, and n are integers. k is a known constant. r is equally likely to take any value between $-1/2$ and $+1/2$. p is equally likely to take any value between 0 and 1.
- k, r, and p are considered to be free from error, that is, they are exact or are known to more significant figures than the quantities A_i.
- e is the error arising from the rounding of the final result; it is assumed that a guarding figure is kept in intermediate results. e is equally likely to take any value between $\pm 1/2$ so that its variance is $1/12$, equal to the integral of e^2 between $\pm 1/2$, in units

Table 14.7 Accumulation of error in arithmetical operations

Operation	Absolute Error	Variance of Error (unit 1/12)
$\sum_{i=1}^{n} A_i$	$\sum_{i=1}^{n} a_i$	$\sum_{i=1}^{n} \alpha_i$
$mA \sum_{i=1}^{n} m_i A_i$	$ma \sum_{i=1}^{n} m_i A_i$	$m^2\alpha \sum_{i=1}^{n} m_i \alpha_i$
$\sum_{i=1}^{n} i A_i$ (n large)	$\sum_{i=1}^{n} i a_i$	$\frac{1}{3}n^3\alpha$ if $\alpha_i = \alpha$ for all i
$kA \sum_{i=1}^{n} k_i A_i$	$ka + e \sum_{i=1}^{n} k_i a_i + e$	$k^2\alpha + 1 \sum_{i=1}^{n} k_i^2 \alpha_i + 1$
krA	$kra + e$	$\frac{1}{12}k^2\alpha + 1$
$g(p)A$	$g(p)a + e$	$\int_0^1 \{g(p)\}^2 dp.\alpha + 1$
$\sum_{i=1}^{n} p^i A_i$ (for $\alpha_i = \alpha$)	$\sum_{i=1}^{n} p^i a_i + e$	$(1 + \frac{1}{3} + \frac{1}{5} + \cdots + \frac{1}{2n+1})\alpha + 1$
$A_1 A_2$	$A_2 a_1 + A_1 a_2 + e$	$A_2^2 \alpha_1 + A_1^2 \alpha_2 + 1$
A^n	$nA^{n-1}a + e$	$n^2 A^{2n-2}\alpha + 1$
$\frac{1}{A}$	$(-\frac{1}{A^2})a + e$	$(1/A^4)\alpha + 1$
$A^{1/2}$	$(\frac{1}{2}A^{1/2})a + e$	$(\frac{1}{4}A)\alpha + 1$
$\frac{A_1}{A_2}$	$(\frac{1}{A_2})a_1 - (\frac{A_1}{A_2^2})a_2 + e$	$(\frac{1}{A_2^2})\alpha_1 + (\frac{A_1^2}{A_2^4})\alpha_2 + 1$
n^{th} difference of $A(x)$	$\sum_{i=1}^{n} (-1)^i (i^n) a_i$	$\frac{\alpha(2n!)}{(n!)^2}$ if α is constant
$f(A_1, A_2, \ldots)$	$\frac{\partial f}{\partial A_1}a_1 + \frac{\partial f}{\partial A_2}a_2 + \cdots + e$	$\left(\frac{\partial f}{\partial A_1}\right)^2 \alpha_1 + \left(\frac{\partial f}{\partial A_2}\right)^2 \alpha_2 + \cdots + 1$
$f(A)$ by direct interpolation	$af'(A) + e_r + e_i + e$	$\{f'(A)\}^2\alpha + v_r + v_t + 1$
$f(A)$ by inverse interpolation	$(a - e_r - e_t) f'(A) + e$	$\{f'(A)\}^2(\alpha + v_r + v_t) + 1$

of the last place retained. For convenience all variances are expressed in this unit of 1/12.

In addition, e_r is the error due to the rounding-off errors in the tabular values, including their effects on the differences; e_t is the truncation error, and v_r, v_t are the variances of e_r and e_t. If all values of the interpolating factor p are equally likely, v_r varies from 0.67 for linear interpolation to 0.81 for interpolation with fifth differences. If $f(A)$ is determined from a critical table, its error is that of a simple rounding-off error unless the number of figures in the argument is small or unless the interval in the respondent is greater than unity.

14.6.2 The Method of Least-Squares

14.6.2.1 Introduction

When one is measuring the physical universe, certain constants must be determined from observation, such as the orbital elements of a satellite about its primary or the rotational elements about its axis. Methods for *ab initio* determination of orbital elements from three or more observations are well-documented in the literature (Herget 1948). The more typical case

assumes that approximate values of the constants are available on which a provisional theory can be based. This theory is then used to construct positions against which the observations can be compared. Thus, each observation minus the computed place forms a difference, referred to as an $O - C$. The errors in these differences can arise from three sources: errors in the observations; errors in the constants on which the computed positions are based; and errors in the theory itself. Only the first two error sources will be treated in the following discussion, which concerns the analysis of $O - C$'s to improve the initial approximation to the constants.

14.6.2.2 Errors of Observation: Frequency Distribution

Errors of observation may arise from many sources. The size of these errors vary and, in general, follow the normal distribution curve or probability distribution curve wherein small errors occur more frequently than large errors, and positive errors occur with the same frequency as negative errors. In most problems, the frequency distribution of the errors is not known in advance. However, if each observation is assumed to be affected by the sum of several simultaneous, independent errors, we may assume the distribution of the errors to be accidental rather than systematic, the latter being the case where all the errors have a common origin. As there is no satisfactory mathematical theory of systematic errors, we must proceed initially on the assumption that the errors are accidental. In this case if a set of random variables x are independent of each other, the theory of probability postulates that the frequency distribution of the sum of such variables, each with its own frequency distribution, will slowly approach the function

$$Y = \frac{h}{\sqrt{\pi}} \exp(-h^2 x^2) \tag{14.80}$$

where h is defined as the index of precision. This is related to the standard deviation σ, or the root-mean-square error by $h^2 = 1/2\sigma^2$.

The best fit to a series of n observations, according to the principle of least-squares, is the one that reduces the sum of the squares of the errors to a minimum. Assuming that the index of precision is constant in this set of observations and letting the errors associated with each observation, O_i, be x_i, the probability, P_i, of occurrence of error x_i becomes

$$P_i = \frac{h}{\sqrt{\pi}} \exp(-h^2 x_i^2)\, dx_i. \tag{14.81}$$

Assuming that P is independent, the probability that each error will occur in turn is

$$P = \left(\frac{h}{\sqrt{\pi}}\right)^n \exp\left(-h^2 \sum_{i=0}^{n} x_i^2\right) dx_1\, dx_2 \ldots dx_n. \tag{14.82}$$

Thus, it can be stated that the set of errors that maximize P in Eq. 14.82 will produce the best fit to the observations because at that point $\sum_{i=1}^{n} x_i^2$ is a minimum.

If the index of precision varies with each observation, the introduction of the factor h_i requires knowing the correspondence between the h_i and the arbitrary weight of an observation, based on unit weight. If the precision index corresponding to weight 1 is h, and the precision index corresponding to weight w_1 is h_1, the probability that an error of size

x will occur in an observation of weight 1 is

$$P = \frac{h}{\sqrt{\pi}} \exp(-h^2 x^2)\, dx. \tag{14.83}$$

Also the probability of an error of size x occurring in an observation of weight w_1 is

$$P = \frac{h_i}{\sqrt{\pi}} \exp(-h_i^2 x^2)\, dx. \tag{14.84}$$

Assuming that $P = P_1$, that is that an error of size x has an equal probability of occurring in both Eqs. 14.83 and 14.84, leads to

$$\begin{aligned} w_1 &= (h_1/h)^2 \\ w_i &= (h_i/h)^2 \end{aligned} \tag{14.85}$$

which shows that the weights are proportional to the precision indices. In terms of the precision index h and the weights w_i,

$$P = \left(\frac{w_1 \cdot w_2 \cdots w_n}{\pi}\right)^{n/2} h^n \exp\left[-h \sum_{i=1}^{n} w_i x_i^2\right] dx_1\, dx_2 \ldots dx_n. \tag{14.86}$$

showing that for P to be a maximum, the $\sum_{i=1}^{n} w_i\, x_i^2$ must be a minimum.

Assume O_i (where $i = 1, 2, 3, \ldots, n$) to be observations of a quantity for which τ is the true value. The error x_i of each observation is $x_i = O_i - \tau$. Using the standard deviation σ instead of the precision index h, the best estimate γ of the true value τ is that which reduces

$$1/2\sigma^2 \sum (O_1 - \gamma)^2$$

to a minimum. To do this requires that $\partial \sum / \partial \gamma = 0$; i.e., $2 \sum (O_i - \gamma) = 0$, from which $\gamma = 1/n \sum O_i$, or the best estimate is the arithmetic mean.

Given n observations O_i, having normally distributed errors x_i, the error of the arithmetic mean is

$$x = \frac{1}{n} \sum x_i \tag{14.87}$$

which is a linear combination of n random variables. If the mean error of one observation is σ, then it can be shown that the mean error of the arithmetic mean is the σ of one observation divided by the $\sqrt{n}$.

Once the estimate γ of the true value τ of the measured quantity is obtained, a residual r can be formed by $O_i - \gamma = r_i$. Also $O_i - \tau = x_i$, where the x_i are the true errors of the observations. Then

$$\begin{aligned} \sum x_i = \sum O_i - n\tau &= n\gamma - n\tau \\ \gamma &= \tau + \sum x_i/n \\ r_i &= x_i - \sum x_i/n. \end{aligned} \tag{14.88}$$

Let σ_r be the mean error of the residuals and σ_x be the mean error of the errors x_i, then

$$\sigma_r^2 = ((n-1)/n)^2 \sigma_x^2 + (n - 1/n^2)\sigma_x^2 = (n - 1/n)\sigma_x^2. \tag{14.89}$$

Since $\sigma_r^2 = \sum r^2/n$, then $\sigma_x^2 = \sum r^2/n - 1$ and the mean-square error of the arithmetic mean in terms of the residuals is

$$\Gamma = \sqrt{\sum r^2/n(n-1)}. \tag{14.90}$$

14.6.2.3 The Method of Least-Squares

In many problems the quantity measured is not the one that we wish to correct. A simple case involves one unknown, η, to be determined from measurements ζ_i, where $i = 1, 2, 3, \ldots, n$. Thus $\zeta = f(\eta)$. Let η_c be the provisionally known value of η, and η_0 be the value to be determined from the measurements, then the difference $\eta_0 - \eta_c = \Delta\eta$. Calculating from η_c for each measurement i, gives $\Delta_i\zeta = \zeta_i - \zeta_c$. Using a Taylor's series expansion, $\Delta\zeta$ may be written as a function of $\Delta\eta$,

$$\Delta\zeta = \frac{\partial f}{\partial \eta}\Delta\eta + \frac{1}{2}\frac{\partial^2 f}{\partial \eta^2}(\Delta\eta)^2 + \frac{1}{6}\frac{\partial^3 f}{\partial \eta^3}(\Delta\eta)^3 + \cdots. \tag{14.91}$$

Assuming $\Delta\eta$ is small enough that its square and higher powers can be ignored, then

$$\left(\frac{\partial f}{\partial \eta}\right)_i \Delta\eta = \Delta\zeta_i \tag{14.92}$$

and we have n equations where in each case the $(\partial f/\partial\eta)$ is a known numerical coefficient. Denoting the coefficients by A, the equations of condition can be written $A\Delta\eta = \Delta\zeta$. The preferred value of the unknown is that for which

$$\frac{\partial}{\partial \Delta\eta} = \sum (A_i\Delta\eta - \Delta_i\zeta)^2 = 0. \tag{14.93}$$

Differentiating gives $\sum A^2\Delta\eta = \sum A\Delta\zeta$, thus $\Delta\eta = \sum A\Delta\zeta \Big/ \sum A^2$ and $\Delta\eta + \eta_c = \eta_0$.

In a more general problem it may be necessary to determine more unknowns than one from a series of measurements. The constants of a planetary orbit C_i (where $i = 1, 2, 3, \ldots, n$) may already be approximately known and can be used to compute the η_c corresponding to each observation η_0, then $\eta_0 - \eta_c = \Delta\eta$. Let the corrections to the approximate values of the orbital constants be E_i, so that the corrected constants are $C_i + E_i$. The equations of condition can then be written

$$\frac{\partial \eta}{\partial C_1}E_i + \frac{\partial \eta}{\partial C_2}E_2 + \cdots + \frac{\partial \eta}{\partial C_n}E_n = \Delta\eta. \tag{14.94}$$

Setting $\partial\eta/\partial C_1 = A$, $\partial\eta/\partial C_2 = B$, $\partial\eta/\partial C_3 = C$, and so on, the conditional equation can be written

$$AE_1 + BE_2 + CE_3 + \cdots + NE_n = \Delta\eta. \tag{14.95}$$

Supposing there are no errors in the $\Delta\eta$, i.e., that the theory used is adequate, and that the observations contain no errors, then the only source of error in the solution comes from the approximate values of the constants. The theory of linear equations states that n independent equations of condition are necessary and sufficient to determine the E_i. With the above restrictions as to the source of errors, the solution will yield values of E that will exactly satisfy the n equations. Normally, however, accidental errors in the values of $\Delta\eta$

prevent the derivation of the exact values of E_i. Increasing the number m of observations and thus the number of conditional equations will decrease the effect of the accidental errors. In some problems in dynamical astronomy it is not unusual to have m exceed n by a factor of 1000. Since values of E_i are derived that do not exactly satisfy the conditional equations, the procedure is to evaluate the left-hand side of the equations and subtract from the corresponding $\Delta\eta$ to produce residuals r. The best values of the E_i are those that reduce the sum of the squares of the residuals (r) to a minimum as discussed earlier.

In the instance where there are m equations of condition, with $m > n$, the procedure is to form n normal equations for solution. The normals are formed as follows. Given the conditional equations,

$$\begin{aligned} A_1E_1 + B_1E_2 + C_1E_3 + \cdots + N_1E_n &= \Delta\eta_1 \\ A_2E_1 + B_2E_2 + C_2E_3 + \cdots + N_2E_n &= \Delta\eta_2 \\ A_3E_1 + B_3E_2 + C_3E_3 + \cdots + N_3E_n &= \Delta\eta_3 \text{ etc.}, \end{aligned} \tag{14.96}$$

multiply through each conditional equation by the coefficient A_i and sum to form the first normal equation in the array in Eq. 14.97, where the brackets represent summation. Then multiply through each conditional equation by B_i and sum to form the second line of the array. Repeat with C_i to form the third line of the array. The procedure is repeated through the coefficient of E_n and the symmetry of the resulting array of n equations in n unknowns reduces the complexity of the solution.

$$\begin{aligned} [A_i^2]E_1 + [A_iB_i]E_2 + [A_iC_i]E_3 + \cdots + [A_iN_i]E_n &= [A_i\Delta\eta_i] \\ [B_iA_i]E_1 + [B_i^2]E_2 + [B_iC_i]E_3 + \cdots + [B_iN_i]E_n &= [B_i\Delta\eta_i] \\ [C_iA_i]E_1 + [C_iB_i]E_2 + [C_i^2]E_3 + \cdots + [C_iN_i]E_n &= [C_i\Delta\eta_i]. \end{aligned} \tag{14.97}$$

When the m equations of condition are not all of equal weight, each equation may be multiplied through by the square root of its weight before forming the normals.

Methods of solution of the normal equations are numerous and are detailed in the references given at the end of this chapter.

REFERENCES

1. The Astronomical Almanac Online: http://asa.usno.navy.mil or http://asa.hmnao.com.

Abramowitz, M. and I. Stegun (1973). *Handbook of Mathematical Functions* (9th ed.). New York: Dover Press.

Brouwer, D. and G. Clemence (1961). *Methods of Celestial Mechanics*. New York and London: Academic Press.

Carpenter, L. (1966, June). Solutions to planetary perturbation motion equations by Chebyshev series. Techinical Note D-3168, NASA.

Danby, J. (1988). *Fundamentals of Celestial Mechanics* (2nd ed.). Richmond, VA: Willmann-Bell, Inc.

Fox, L. and I. Parker (1972). *Chebyshev Polynomials in Numerical Analysis*. Oxford, England: Oxford University Press.

Herget, P. (1948). *Computation of Orbits*. Willmann-Bell, Inc., Richmond, VA: Published privately by the author.

Hildebrand, F. (1987). *Introduction to Numerical Analysis*. New York: Dover Press.

H.M. Nautical Almanac Office (1956). *Interpolation and Allied Tables*. London: H.M. Stationery Office.

H.M. Nautical Almanac Office (1958). *Subtabulation: A Companion Booklet to Interpolation and Allied Tables*. London: H.M. Stationery Office.

Lanczos, C. (1956). *Applied Analysis*. Englewood Cliff, NJ: Prentice-Hall.

Press, W., B. Flannery, S. Teukolsky, and W. Vetterling (1986). *Numerical Recipes, The Art of Scientific Computing*. Cambridge, England: Cambridge University Press.

CHAPTER 15

Calendars

E. G. RICHARDS

15.1 Introduction

15.1.1 Overview

A calendar is a system for assigning a unique name, its date, to every day so that the order of the dates is apparent and the interval in days between two dates can be readily calculated. A date is generally specified by three numbers: a *day* of the month, D, a *month*, M and a *year*, Y; in most calendars, the months also have names.

Most calendars are based on astronomical cycles so that the days of the month cycle in approximate synchrony with the lunations (the cycle of the phases of the Moon) and the months cycle in approximate synchrony with the seasons of the year.

Since the number of lunations in a year and the number of days in a lunation are not integral (and also slowly change with time), extra intercalary days or months may be inserted into occasional years to maintain a long-term average synchrony with the astronomical cycles. Years in which a day or month is intercalated are sometime called *leap years*. The Romans called years with an extra day *bissextile years*.

Solar calendars, such as the current *Gregorian calendar*, maintain accurate synchrony with the astronomical year while abandoning any attempt to keep the months in synchrony with the lunations of the Moon. *Lunar calendars*, such as the Islamic calendar, maintain synchrony of the months and abandon synchrony with the Sun. *Luni-solar calendars*, such as the Jewish, Chinese and Christian Ecclesiastic calendars, attempt to maintain synchrony with both.

According to a recent estimate (Fraser 1987), there are about forty calendars in use in the world today and more that have been abandoned. This chapter is concerned with only a few of these. We discuss here nine. The first of these is the Gregorian calendar, which is now used throughout the world for secular purposes. It is the official calendar of the United Kingdom (since 1752), but not of the United States (which has no official calendar). We discuss a further six (the Julian, Jewish, Islamic, Indian, Chinese and Bahá'i calendars), which are in current use to determine the proper dates of religious or cultural activities. We discuss two more (The Ancient Egyptian and the French Republican calendars), which are of historical interest. Brief historical summaries and the details of the operation are given for each of these nine calendars, but we do not discuss their usage. Algorithms are given for arithmetic calendars (see § 15.1.4) for converting dates in one to those in others.

Despite a vast literature on calendars, truly authoritative references, particularly in English, are difficult to find. One such is Reingold and Dershowitz (1997, 2001). Richards (1998)

surveys a broad variety of calendars and Aveni (1990) stresses their cultural contexts rather than their operational details. Fotheringham (1935), Doggett (1992) and the *Encyclopaedia of Religion and Ethics* (Hastings 1910), in its section on "Calendars," offer basic information on historical calendars. Blackburn and Holford-Stevens (1999) give detailed information about customs appertaining to each day of the year and on a variety of calendars. The sections on "Calendars" and "Chronology" in all editions of the *Encyclopaedia Britannica* provide useful historical surveys. Ginzel (1906,1911) remains an authoritative, if dated, standard of calendrical scholarship. References on individual calendars are given in the relevant sections. See also URL[1], URL[2], URL[3], URL[4], and URL[5].

15.1.2 Uses of Calendars

Calendars have been used from the earliest times to regulate hunting, agricultural practices and other economic activities. Later they were important in regulating religious rituals, fasts and feasts. Most major religions use a special calendar and most calendars are associated with a religion. From the beginnings of civilization calendars have been used to date receipts, contracts and other documents and to order social life and to define holidays.

Details of their uses in religious practices are discussed in the *Encyclopaedia of Religion and Ethics* (Hastings 1910) and in Blackburn and Holford-Stevens (1999).

15.1.3 Astronomical Bases of Calendars

The principal astronomical cycles are the year (based on the revolution of the Earth around the Sun), the month (based on the revolution of the Moon around the Earth) and the day (based on the rotation of the Earth on its axis). The complexity of calendars arises because the month and the year do not comprise an integral number of days, and because they are neither constant nor perfectly commensurable with each other (see Doggett 1992).

The *tropical year* is today defined as the time needed for the Sun's mean longitude to increase by 360° (Danjon 1959; Meeus and Savoie 1992). This varies from year to year by several minutes, but it may be averaged over several years to give the mean tropical year. It may be noted that this definition differs from the traditional definition, which is the mean period between two vernal equinoxes.

The intervals between any particular pair of *equinoxes* or *solstices* are not equal to one another or to the tropical year; they are also subject to variations from year to year but may be averaged over a number of years. The arithmetic mean of the four average intervals based on the two equinoxes and the two solstices is equivalent to the value of the mean tropical year. These matters are discussed by Steel (2000).

It is sometimes assumed that the tropical year represents the period of the cycle of the seasons. It may be noted, however, that the Gregorian calendar is tied to the vernal equinox year and the Chinese calendar to the winter solstice.

The following approximate expression, based on the *orbital elements* of Laskar (1986), may be used to calculate the length of the mean tropical year in the distant past. Note, however, that *The Astronomical Almanac* has not used these equations, nor does it use the orbital elements from Laskar, but starting from the 2004 edition, it uses the orbital elements of Simon et al. (1994):

$$365\overset{\mathrm{d}}{.}242\,189\,6698 - 0.000\,006\,153\,59\,T - 7.29 \times 10^{-10}\,T^2 + 2.64 \times 10^{-10}\,T^3. \quad (15.1)$$

Table 15.1 Approximate lengths of the astronomical cycles

Year [a]	Days in Year [b]	Days in lunation [c]	Length of day	Days [d]/year	Days [e]/lunation
	1 day = 86400 seconds (SI)				
2000	365.24219	29.53059	86400.003	365.24217	29.53059
1500	365.24222	29.53059	86399.995	365.24224	29.53059
1000	365.24225	29.53059	86399.886	365.24231	29.53059
500	365.24228	29.53059	86399.878	365.24237	29.53059
0	365.24231	29.53058	86399.969	365.24244	29.53059
−500	365.24234	29.53058	86399.961	365.24250	29.53060
rate of change [f] (ppb)	−17	73	20	-37	53

[a] Astronomical year; i.e., the year Y B.C. is designated astronomical year 1−Y.
[b] The mean tropical year as given by Eq. 15.1.
[c] Mean Synodic period as given by Eq. 15.2
[d] Days of a length in seconds (SI) as given in column 4
[e] Days of a length in seconds (SI) as given in column 4
[f] The rates of change of these periods themselves change over the centuries, but the proportional rates of increase, expressed as parts per billion (10^9) per century, are given for the year 2000

The synodic month, or lunation, the mean interval between conjunctions of the Moon and Sun, corresponds to the cycle of lunar phases. The following expression for the synodic month is based on the lunar theory of Chapront-Touzé and Chapront (1988):

$$29^{\mathrm{d}}.530\,588\,8531 + 0.000\,000\,216\,21\,T - 3.64 \times 10^{-10}\,T^2 \qquad (15.2)$$

but any particular cycle may vary from the mean by up to seven hours.

In these expressions, T is the number of *Julian centuries* (of 36525 days) measured from 2000 January 1 in *Terrestrial Time* (TT). It is given by $T = (J - 245\,1545.0)/36525$ where J is the *Julian date* (see § 15.1.10).

The lengths of the tropical year and *synodic month* are given by these formulae in days of 86400 seconds (SI) of *International Atomic Time* (TAI). See Chapter 3 for further information on timescales.

Historians (Stephenson 1997) have also found that the length of the mean solar day expressed in TAI is not constant. It appears to be increasing by about 0.0017 seconds per century because of tidal and other effects. It also suffers from both periodic and small random changes.

The lengths of the cycles change slowly with time and expressions 15.1 and 15.2 only represent approximations and are included in this chapter only for illustrative reasons. The lengths of these cycles calculated from them for representative years are shown in. Table 15.1.

15.1.4 Astronomical, Observational and Arithmetic Calendars

Some calendars, termed observational calendars, rely on actual sightings of a new moon, solstice, equinox; or some other natural phenomenon to determine the start of the months and the years or when to intercalate a day or a month. The times of the sightings are subject

to error on account of the weather and such calendars cannot be constructed in advance. Examples are the ancient Jewish calendar and the Islamic calendar as it is generally used to determine important religious dates (such as the start of Ramadan); both of these depend on sightings of the crescent of the new moon. The heliacal rising of Sopdet (Sirius) may, at one time, have signalled the start of the ancient Egyptian year. It is likely that many calendars now lost were observational. Note that the local time at which an observation is made may fall in different days according to the locality of the observer.

Astronomical calendars depend on a model to predict the times of such events. These models have changed over the centuries as astronomical knowledge improved. Examples of astronomical calendars include the Chinese and Indian luni-solar calendars, the original form of the French Republican calendar and one form of the Bahá'i calendar. Astronomical calendars usually specify that the events be observed or calculated for a particular meridian. Thus events used in the Chinese calendar are observed at a meridian at 120° East (but before 1929 at the meridian of Beijing). The French Republican calendar specified the meridian of Paris.

Arithmetic calendars abandon any explicit references to astronomical events and are regulated by fixed rules, though they may have been designed in an attempt to keep their years or months in step with the astronomical periods. Examples include the current Gregorian calendar and its predecessor, the Julian calendar, as well as the ancient Egyptian calendar, the modern Jewish calendar and the civil Islamic calendar (used by historians of Islamic culture).

15.1.5 Visibility of the Crescent Moon

Several observational calendars rely on the first sighting of new moons. Under optimal conditions, the crescent Moon has been sighted about 15.4 hours after the astronomical new moon (i.e., the *conjunction*) (Schaefer 1988). Usually, however, it is not seen until it is more than twenty-four hours old. Babylonian astronomers were the first to develop methods for calculating first visibility, though no surviving tables are explicitly concerned with this (Neugebauer 1975, pp. 533–540). The earliest known visibility tables are by al-Khwarizmi, a ninth-century astronomer of Baghdad (King 1987). These tables, and many subsequent tables, were based on the Indian criterion that the Moon will be visible if the local hour angle of the Moon at sunset is equal to or less than 78°. With the development of Islamic astronomy more complex criteria were developed.

Modern models for predicting first visibility incorporate celestial mechanics, spherical astronomy, selenology, atmospheric physics, and ophthalmology. Bruin (1977) was the first to prepare such a model. Ilyas (1984), recognising that the Islamic calendar is used around the world, introduced the concept of an *International Lunar Dateline*, west of which the Moon should be visible under good observing conditions. Schaefer (1988) has further investigated the theory of this. Extensive observing programs were once organised by Doggett, Seidelmann, and Schaefer (1988) and Doggett and Schaefer (1989); see also URL[7].

15.1.6 Non-astronomical Cycles and the Week

The calendars of many societies have incorporated cycles with no astronomical basis. Cycles of days include the eight-day cycle (*Nundinae*) of the Romans, the 13 and 20 day cycles of Central America and the market weeks, of various lengths, of Africa. The Ancient Egyptian

calendar and the French Republican calendar used a 10-day cycle, and the Bolsheviks in Russia experimented with a four-day "week." Most of the world today recognises the seven-day week which has religious significance for Christians, Jews and Muslims.

The seven-day week probably originated in Babylon as a useful, if inexact, division of the lunar month and was probably adopted by the Jewish people at the time of the Babylonian exile in the sixth century B.C.. It is likely that it has run continuously and without interruption since these times to the present day (but see Zerubavel E. (1989). The seven-day cycle was widely used in the Roman Empire from the first century B.C.. According to Cassius Deo each of the seven "wandering stars," the Sun, the Moon and the five naked-eye planets known to the ancients, was assigned cyclically to each of the 24 hours of each day in the order of their apparent speed in the heavens. The star assigned to the first hour was the regent of the day. The names of the regents gave each day its name and the order of the days in this astrological week. These names, or their equivalents in other languages and pantheons, are still used today. Saturn's day coincided with the Jewish Sabbath, though the Jews never used the Roman names.

Colson (1926) and Zerubavel (1989) are standard references on the week. Richards (1998) gives a comprehensive list of the names of the days of the week. Zerubavel (1989) also considers other week-like numerical cycles used by past and present cultures.

Cycles of years have also had significance for various cultures. The Romans used a 15-year cycle of indiction for taxation purposes. The Chinese have a cycle of 60 years comprised of two simultaneous cycles of 10 and 12 years (60 is the lowest common multiple of 10 and 12). The years in both of these Chinese cycles carried names. The cultures of Central America and of India used several cycles of years; some are exceedingly long.

15.1.7 Historical Eras and Chronology

Astronomical cycles with a period greater than a year have rarely been used in calendars. Instead, years have generally been numbered from some important event, secular or religious. Thus, regnal dates count the years from the accession of a ruler and the numbering starts afresh with each new ruler. Other calendars count years from an important event, maybe in the remote past, which initiates an era. Thus, the Islamic calendar counts the years from the date of the flight of the Prophet from Mecca to Medina and the Christians count from the presumed birth of Christ. In other calendars, Chinese, Indian, Mayan, years were sometimes counted in cycles of various lengths; the cycles themselves may also be counted.

The first day of the first month of the year numbered 1 is sometimes called the epoch of the calendar. Table 15.2 shows the starting year of a few of the eras of historical importance.

15.1.8 The Christian Era

The epoch of the Christian calendar is usually, but wrongly, taken to be the birth of Christ. This epoch was established by the sixth-century scholar Dionysius Exiguus who was compiling a table of dates of Easter. An existing table covered the nineteen-year period denoted 228–247, where years were counted from the beginning of the reign of the Roman emperor Diocletian. Dionysius continued the table for a nineteen-year period, which he designated Anno Domini Nostri Jesu Christi 532–550. Thus, Dionysius' Anno Domini 532 is equivalent to Anno Diocletiani 248. In this way a correspondence was established between the new Christian

Table 15.2 Some eras

Name of era	Year of epoch	Used by	Event commemorated
Byzantine Era[a]	−5508	Byzantium	Creation of the world
Anno Mundi (A.M.)[a]	−3760	Judaism	Creation of the world
Kali-yuga	−3101	India	Mean conjunction of planets
[b]	−2636	Chinese	Traditional start of 60 year cycles
Ab Urbe Condita (A.U.C.)[a]	−752	Roman Empire	Legendary foundation of Rome
The Era of Nabonassar[a]	−746	Alexandria, Early astronomers	Accession of Babylonian King Nabonassar
Jimmu Tenno[a]	−659	Japan	Accession of Emperor Jimmu Tenno; adoption of Chinese calendar
Seleucid Era[a]	−312	Selucid Empire	Foundation of Empire by Seleucis
Anno Domini (A.D. or C.E)	1	Christianity	Approximate date of Birth of Christ
Saka Era[a]	78	India	Uncertain; possible accession of King Salivahana
Era of Diocletian[a]	283	Coptic & Ethiopian churches; Roman Empire	Accession of Roman Emperor Diocletian
Era of the Hegira (A.H.)[a]	622	Islam	Prophet's flight from Mecca
Republican Era (E.R.)	1792	France	Foundation of the Republic
Badi Era (B.E.)	1844	Bahá'i	Declaration of the Bab

[a] The dates of the start of the year in these eras are currently given in *The Astronomical Almanac*.
[b] The Chinese used no era as such but counted years in cycles of 60. The cycles were sometimes counted with the first starting in −2636.

era and an existing system associated with historical records. However, Dionysius did not use an accurate date for the birth of Christ and scholars generally believe that Christ was born some years before A.D. 1, but the historical evidence is not adequate to allow a definitive dating.

Years after the epoch of the Christian calendar are traditionally labeled: A.D. (Anno Domini) but the label C.E. (Common Era) is preferred by some. Likewise the traditional label of years before A.D. 1 has been B.C. (Before Christ) but some prefer B.C.E. (Before Common Era).

It is often possible to assign a date in a calendar to days preceding the epoch or the date on which it was first used. Such dates are termed *proleptic* dates. Bede, the eighth-century English historian, began the practice of counting years backward from A.D. 1 (see

Colgrave and Mynors 1969). In this system, the year A.D. 1 is preceded by the year 1 B.C., with no intervening year 0. Because of this numerical discontinuity, this "historical" system is cumbersome for comparing ancient and modern dates. I have used +1 (etc.) to designate A.D. 1 (etc.). The year +1 is naturally preceded by year 0, which is preceded by year −1. Since the use of negative numbers developed slowly in Europe, this system of dating was delayed until the eighteenth century, when it was introduced by the astronomer Jacques Cassini (Cassini 1740).

15.1.9 Dates

The date of any day is specified by giving the year and the month in which it falls and its day of the month and maybe the day of the week. There are many conventions concerning the order in which these are presented. We shall specify here dates by giving the day of the week, the year number, the name of the month and the day of the month in that order.

Note that in nearly all calendars, the first day of a month is day 1—rather than day 0; likewise, the first month of a year is month 1—rather than month 0. This is in contradistinction to other systems for specifying time; thus the first hour of a day is hour 0—rather than hour 1.

We shall use, following the practice of historians, the Julian calendar (see § 15.3.4) for dates before 1582 and the Gregorian for dates after, but it is usual to specify the calendar used for dates between 1582 and 1800. We shall not always label the years with either A.D./B.C. or C.E./B.C.E. Instead a positive year number should be read to imply a year in the Common Era (A.D.), whilst a negative year implies a year before that (B.C.). Thus, a year 2000 means A.D. 2000 whilst −1000 implies 1001 B.C.. In general negative year, −Y is equivalent to 1 − Y B.C.. We will, however, use the terms A.D. or B.C. when referring to centuries.

The time of day of the start of a day varies in different Calendars. Thus, the Gregorian day runs from midnight to midnight, but the Islamic and Jewish days start some six hours earlier and run from dusk (at a nominal 6 p.m.) to dusk. This raises the point as to which, for example, Gregorian day or date corresponds to a given Islamic or Jewish date. The usual convention, which we follow here and in *The Astronomical Almanac*, is that dates in different calendars correspond when they contain the same noon. Thus the Islamic and Jewish days start some six hours before the corresponding Gregorian day. In some Indian calendars the day starts at dawn, some six hours later.

15.1.10 Julian Day Numbers and Julian Dates

Dating systems in medieval Europe caused considerable confusion. Some states used regnal dating (with a plethora of local rulers); others used the Anno Domini system. Moreover different states used different days to start their years. Although the Romans had used January 1 to start their years, Christendom often used March 25th, though other days were sometimes used.

In the sixteenth century, Joseph Justus Scaliger (1540–1609) tried to resolve the patchwork of historical eras by dating every event according to a single system (Scaliger 1583). Instead of introducing negative year counts, he sought an initial epoch before any historical record. His approach utilised three calendrical cycles: the 28-year solar cycle (the period after which weekdays and calendar dates repeat in the Julian calendar), the nineteen-year cycle of

golden numbers (the period after which the Moon's phases approximately repeat on the same calendar dates), and the fifteen-year indiction cycle (the Roman tax cycle).

Scaliger could, therefore, characterise a year by a triplet of numbers (**S, G, I**); **S**, the number of the year in the solar cycle, runs from 1 to 28; **G**, the golden number of the year, runs from 1 to 19; **I**, the number of the year in the Indiction cycle runs from 1 to 15. He noted that a given combination would recur after 7980 ($= 28 \times 19 \times 15$) years. This he called a *Julian Period*, because it was based on the Julian calendar year. For his initial epoch, Scaliger chose the year in which **S**, **G** and **I** were all equal to 1. He knew that the year 1 (A.D. 1) had **S** = 10, **G** = 2 and **I** = 4 and worked out that the combination (1,1,1) occurred in the year −4712 (4713 B.C.) which was year 1 of Scaliger's Julian period.

Although Scaliger's original idea was to introduce a count of years, nineteenth-century astronomers adapted this system to create a count of days elapsed since the beginning of the Julian period. John Herschel (1849) gave a thorough explanation of the system and provided a table of "Intervals in Days between the Commencement of the Julian Period, and that of some other remarkable chronological and astronomical Eras."

Astronomers have extended this idea by appending to the day number, the time of day expressed as a decimal fraction of a day. The resulting numbers called Julian dates define any instant of time. Thus 2 451 545.0 corresponds to noon on 2000 January 1 as observed at a meridian of 0° (Greenwich) in the Gregorian calendar. At a meridian of 0°, the day 2000 January 1 began 12 hours earlier at 2 451 544.5. Further east, the day begins earlier and further west, later.

It is important to note these Julian dates specify an instant in *Universal Time* (UT), not local time. A day in the Gregorian calendar begins at midnight, the world over, at an instant that varies with longitude, and hence is specified by different Julian dates. This is inconvenient when considering calendars. It is, therefore, useful to define a Julian Day Number, **J**, (to be distinguished from a Julian date) which is a whole number, and which may be used to label each of the days. The Julian Day Number of Saturday 2000 January 1 is then 2 451 545 and of Tuesday −4712 January 1 it is 1. URL[7] provides a useful program for interconverting dates and Julian dates.

15.1.11 Luni-solar Calendars

It may be noted that 19 astronomical years and 235 lunations both contain about 6939 days. This was realised in Babylon in about the 5th century B.C., and gave rise to a calendar usually ascribed to Meton of Athens (5th century B.C.). In this, each year of a 19-year cycle contains 12 months of alternately 29 and 30 days, but 7 of the 19 years contain a 13th intercalated month of 30 days. Thus the 19 years contain 235 months or 6936 days. The average number of days per year is about 365.05 ($= 6936/19$) and the average number of days per month is about 29.51. In the short term, such a calendar keeps, on average, in rough synchrony with both the Sun and the Moon. The accuracy of this Metonic calendar can be improved by judicious intercalations of extra days, and a variant of it is used in both the Jewish and the Christian Ecclesiastical calendars.

The luni-solar calendars of China and India similarly interpolate leap months, but use astronomical considerations to decide when to intercalate and when to begin a year or a month. The months themselves may begin on the day of a conjunction of the Moon (new

moon) and are thus synchronised with the lunations, but these calendars also make use of solar months. These are defined by dividing the ecliptic into twelve sections, analogous to the sign of the Zodiac, and separated by 30° of solar longitude. The temporal lengths of both the lunar months and of the solar months vary throughout the year. Thus, although the starting dates of the solar and lunar months generally alternate, so that each lunar month contains the start of just one solar month, there are years in which a lunar month contains the start of two solar months (i.e., the solar month is entirely contained in a lunar month) or of no solar month (i.e., the lunar month is entirely contained in a solar month). The points at which extra months are intercalated are determined by such months. This results in the intercalation of about 7 extra months in 19 years and achieves a result similar to that of the Metonic calendar.

15.1.12 Accuracy of Calendars

The question of accuracy for observational calendars does not arise. The accuracy of an astronomical calendar depends on the adequacy of the underlying astronomical theory and the precision of the celestial observations on which it is based. Although arithmetic calendars do not explicitly refer to astronomical cycles, they are usually founded on an attempt to maintain their years in synchrony with the tropical year or their months in synchrony with the lunar cycle. These attempts can never be wholly accurate if only because the astronomical periods change with time, albeit slowly. To assess their accuracy, the synodic period may be compared to the average length of the calendar month and the mean tropical year (or the vernal equinox or winter solstices year) may be compared to the average length of the calendar year. A useful parameter is the number of years required for a calendar cycle to become one day out of phase with the corresponding astronomical cycle in some particular year. Bear in mind that the lengths of these astronomical cycles are themselves slowly changing (see Table 15.1).

High precision in the average lengths of the months was achieved quite early on account of the ease with which the mean synodic period can be measured. The precise measurement of the length of the year (solstice to solstice or equinox to equinox) seems to have presented a greater challenge. The most accurate solar calendar in general use is the Gregorian calendar in which there are 146 097 days in 400 years or 365.2425 days/year. Today, in A.D. 2000, the Gregorian calendar year is slightly longer than the mean vernal equinox year (365.24237 days) and, neglecting its change with time, would be one day out relative to the vernal equinox year after about another 8000 years. Various proposals have been made (Delambre 1821; Herschel 1849) to improve this accuracy but none take count of the slowly changing length of the year and day.

At the other extreme, the ancient Egyptian civil calendar contained 365 days. This lagged a further day behind the tropical year every four years or by 365 days in about 1500 years.

15.2 The Ancient Egyptian Calendar

15.2.1 History of the Egyptian Calendars

Ancient Egyptian civilisation, from the start of the Old Kingdom to the annexation of Egypt by Augustus, lasted some 2500 years. It employed several calendars for religious and for civil purposes, but it is not known when these were first instituted. The year of the civil calendar contained a constant 365 days divided into 12 months of 30 days each, followed by

Table 15.3 Months in the ancient Egyptian calendar

Month	Month
1. Thoth	7. Phanemoth
2. Paophi	8. Pharmouti
3. Athyr	9. Pachons
4. Cohiac	10. Payni
5. Tybi	11. Epiphi
6. Mesir	12. Mesori

The five epagomenal days followed Mesori.

5 *epagomenal* days belonging to no month. The names of the months are shown in Table 15.3. The year began on Thoth 1. Since 365 is a poor approximation to the number of days in the year, the start of the year cycled slowly through the seasons with a period of about 1500 years. There was no Egyptian Era, instead the years were counted from the accession of each Pharaoh in regnal fashion, but Ptolemy used the era of Nabonassar (E.N.) (see § 15.1.7).

The Roman writer Censorinus noted that the Julian calendar date 139 July 20 (Julian Day Number 1 772 028)) was Thoth 1 in the Egyptian calendar. This day started year 887 E.N.

The Egyptian calendar was reformed by the Roman Emperor Augustus in 23 B.C.. He decreed that a sixth epagomenal day should be inserted once every four years to keep it in synchrony with the Julian calendar. This modified calendar is sometimes called the Alexandrian calendar.

This Alexandrian calendar is not extinct even today. Calendars closely similar to it are used by the Coptic Church in modern Egypt and in Ethiopia. It was also used by a variety of cultures and religions including The Zoroastrian Parsees, the Armenian Church and the French Republicans after their revolution.

15.2.2 Rules of the Egyptian Calendar

The Egyptian calendar has 12 months of 30 days in each; the five epagomenal days may be considered to form a thirteenth month of five days. Thus, each year has exactly 365 days. The day Thoth 1, 1 E.N. was Wednesday, February 26, −746 in the proleptic Julian Calendar and had a Julian Day Number 1 448 638.

The Alexandrian version has an extra leap day, a sixth epagomenal day, intercalated at the end of the thirteenth month once every four years.

15.3 The Roman and Julian Calendars

15.3.1 Introduction

The Roman calendar was probably originally lunar and relied on intercalations, which were applied haphazardly. It underwent several alterations in which the names and lengths of the months were changed, although some of the details are lost. By −45, there were 12 months

mostly with names similar to those in the current Gregorian calendar, though the numbers of days in several were different. The year started on Januarius 1.

At one time the years were indicated by a regnal system that mentioned the names of the current Consuls. Later, in the first century B.C., the years were numbered from the presumed date of the foundation of Rome, −752; these are termed *ab urbe condita* (A.U.C). Later still the Emperor Diocletian instituted an era which started with his accession in 283.

15.3.2 Divisions of the Roman Months

The Roman months were divided into three unequal sections, which may, when the Roman calendar was lunar, have marked the phases of the Moon. The last days of each section, which we may call the division points, were called the Kalends (*Kalendae*), the Nones (*Nonae*) and the Ides (*Idus*). The Kalends was the first day of the month; the Ides, the thirteenth of the month, except in March, May, July, and October, when it was the fifteenth day. The Nones was always eight days before the Ides (see Table 15.4). The days preceding the division points were termed Prid. Kal. (*pridie* = day before), Prid. Non. and Prid. Id. respectively. The remaining days were numbered backwards from the division days as indicated in Table 15.4 and labelled with the month in which the division point fell. For example, January 4 was termed Prid. Non. Jan. and January 11 was III Id. Jan. Confusingly, but logically, the days preceding the Kalends which fell in the previous month were labelled by the month in which the division point fell, rather than the month to which they belonged; thus December 30 was called III Kal. Jan. This Roman system is occasionally used, even to this day.

15.3.3 Caesar's Reform

By −46, the Roman calendar had gone badly awry; the months no longer followed the lunations and the year had lost step with the cycle of seasons (see Michels 1978; Bickerman 1980). This state of affairs was reformed by Julius Caesar (107–44 B.C.), who took the advice of the Alexandrian astronomer, Sosigenes.

Caesar first inserted 90 days into the year −45 to bring the months of the Roman calendar back to their traditional places with respect to the seasons. This year has been called "the last year of confusion." He next changed the length of some of the old months. Finally he made provision for an intercalary day to be inserted every four years. This intercalary day (see § 15.3.5) was inserted before VI Kal. Mar. and termed Bis VI Kal. Mar.; it fell between VI I Kal. Mar. (February 23) and VI Kal. Mar. (February 25th). Years in which this was done were termed *bissextile years*.

This new Roman calendar, the Julian calendar, was thus a solar calendar. The average length of the calendar year was 365.25 days so that the vernal equinox fell back from March 21 by one day in about 130 years. Nevertheless it served as a standard for European civilisation until the Gregorian Reform of 1582.

Following Caesar's death, the Roman calendrical authorities misapplied the leap-year rule, with the result that the intercalary day was inserted every third, rather than every fourth, year. This error was rectified by Augustus in −8. The details of this correction are uncertain but it is likely that he decreed that there should be no intercalation in the years −7 to +6 and that there should be intercalary days (leap days) inserted every fourth year from then on (i.e., in years 8, 12, 16 . . .).

Table 15.4 Roman dating in the Julian calendar

	Januarius Augustus December	Februarius	Martius Maius Julius October	Aprilis Junius September November
1	Kalendae	Kalendae	Kalendae	Kalendae
2	IV Non.	IV Non.	VI Non.	IV Non.
3	III Non.	III Non.	V Non.	III Non.
4	Prid. Non.	Prid. Non.	IV Id.	Prid. Non.
5	Nonae	Nonae	III Non.	Nonae
6	VIII Id.	VIII Id.	Prid. Non.	VIII Id.
7	VII Id.	VII Id.	Nonae	VII Id.
8	VI Id.	VI Id.	VIII Id.	VI Id.
9	V Id.	V Id.	VII Id.	V Id.
10	IV Id.	IV Id.	VI Id.	IV Id.
11	III Id.	III Id.	V Id.	III Id.
12	Prid. Id.	Prid. Id.	IV Id.	Prid. Id.
13	Idus	Idus	III Id.	Idus
14	XIX Kal.	XVI Kal.	Prid. Ides	XVIII Kal.
15	XVIII Kal.	XV Kal.	Ides	XVII Kal.
16	XVII Kal.	XIV Kal.	XVII Kal.	XVI Kal.
17	XVI Kal.	XIII Kal.	XVI Kal.	XV Kal.
18	XV Kal.	XII Kal.	XV Kal.	XIV Kal.
19	XIV Kal.	XI Kal.	XIV Kal.	XIII Kal.
20	XIII Kal.	X Kal.	XIII Kal.	XII Kal.
21	XII Kal.	IX Kal.	XII Kal.	XI Kal.
22	XI Kal.	VIII Kal.	XI Kal.	X Kal.
23	X Kal.	VII Kal.	X Kal.	IX Kal.
24	IX Kal.	VI Kal.	IX Kal.	VIII Kal.
25	VIII Kal.	V Kal.	VIII Kal.	VII Kal.
26	VII Kal.	IV Kal.	VII Kal.	VI Kal.
27	VI Kal.	III Kal.	VI Kal.	V Kal.
28	V Kal.	Prid. Kal.	V Kal.	IV Kal.
29	IV Kal.		IV Kal.	III Kal.
30	III Kal.		III Kal.	Prid. Kal.
31	Prid. Kal.		Prid. Kal	

15.3.4 The Julian Calendar in Medieval Europe

Through the Middle Ages the use of the Julian calendar evolved and acquired local peculiarities that continue to snare the unwary historian. There were variations in the initial epoch for counting years, the date for beginning the year, and the method of specifying the day of the month. Not only did these vary with time and place, but also with purpose. Different conventions were sometimes used for dating ecclesiastical records, fiscal transactions, and personal correspondence.

Caesar designated January 1 as the beginning of the year. However, other conventions flourished at different times and places. The most popular alternatives were March 1, March 25, and December 25. This continues to cause problems for historians, since, for example, 998 February 28 as recorded in a city that began its year on March 1, would be the same day as 999 February 28 of a city that began the year on January 1.

By the eleventh century, consecutive counting of days from the beginning of the month came into use, displacing the Roman system of divisions. Local variations continued, however, including counts of days from dates that commemorate local saints. A uniform standard for recording dates was instituted only after the inauguration and spread of the Gregorian calendar. The leap day became February 29 instead of the day after February 23.

Cappelli (1930), Grotefend and Grotefend (1941), and Cheney (1981) offer guidance through the maze of medieval dating.

Today the Julian calendar continues to be used by chronologists. The Julian proleptic calendar is formed by applying the rules of the Julian calendar to times before Caesar's reform. This provides a simple chronological system for correlating other calendars and serves as the basis for the Julian Day Numbers (see § 15.1.10).

15.3.5 Rules for the Julian Calendar

The month names and the number of days in each are listed in Table 15.5 for the Julian calendar. The months in the Gregorian calendar are identical.

Table 15.5 Months and days therein of the Julian and Gregorian calendars

Month			Month[a]		
1.	January (Januarius)	31	7.	July (Julius[b])	31
2.	February (Februarius)	28[c]	8.	August (Augustus[d])	31
3.	March (Martius)	31	9.	September (September)	30
4.	April (Aprilis)	30	10.	October (October)	31
5.	May (Maius)	31	11.	November (November)	30
6.	June (Junius)	30	12.	December (December)	31

[a] These months were at one time the 5th, 6th 7th, 8th, 9th and 10th aptly named months of the Roman year.
[b] Originally called Quintilis but renamed in honour of Julius Caesar.
[c] In a leap year, February has 29 days
[d] Originally called Sextilis but renamed in honour of the emperor Augustus.

A Julian calendar year thus contains 365 days or 366 in a leap year. Years are, today, counted from the initial epoch defined by Dionysius Exiguus (see § 15.1.8). A leap day, February 29, is intercalated after February 28 in leap years. Leap years are divisible by 4, e.g., +2000 was a leap year but +2001 was not. For this purpose, year 0 (or 1 B.C., see § 15.1.9) is considered to be divisible by 4.

The epoch of the calendar (Saturday, 1 January 1) had a Julian Day Number 1 721 424

15.4 The Gregorian Calendar

15.4.1 History of the Gregorian Reform

The early Christians church adopted the Julian calendar and used it as the basis for calculating the date of Easter following the recommendation of the Council of Nicea held in 325. March 21 was assumed to be the date of the equinox and the Metonic cycle was used as the basis for calculating the lunar phases.

By the thirteenth century it was realised that the true vernal equinox had regressed from March 21 to an earlier day in March. Over the next four centuries, scholars debated the "correct" time for celebrating Easter and the need for a reform of the calendar. The Church made intermittent attempts to remedy the matter, without taking action.

By the sixteenth century the equinox had shifted to March 11, and astronomical new moons were occurring four days before the dates assumed in the calculation of the date of Easter. At the behest of the Council of Trent, Pope Pius V introduced a new Breviary in 1568 and Missal in 1570, both of which included adjustments to the lunar tables and the leap-year system. Pope Gregory XIII, who succeeded Pope Pius in 1572, convened a commission to consider reform of the calendar, since he considered his predecessor's measures inadequate.

This commission adopted a proposal suggested by Aloysius Lilius (1510–1576) and issued a report written by Christopher Clavius (1537–1612) which resulted in a papal bull, "inter Gravissimas" signed by Gregory XIII on 1582 February 24.

Ten days were deleted from the calendar, so that 1582 October 4 was followed by 1582 October 15, thereby causing the vernal equinox of 1583 and subsequent years to return to about March 21. The rules for intercalating a leap day were changed, and a new method of calculating the dates of Easter was introduced. The new method of intercalation meant that a period of 400 years contained 146 097 days. Since 146 097 is divisible by 7, the Gregorian civil calendar exactly repeats after 400 years. The average number of days in a year is 365.2425. (see Table 15.1). It would be one day out of synchrony with the vernal equinox year after about another 3000 years (if the year were to remain unchanged in length).

This Gregorian calendar today serves as an international standard for civil use. In addition, it regulates the ecclesiastical calendar of the Catholic and Protestant churches but was rejected by the Orthodox churches. It was first promulgated and adopted throughout the Roman Catholic world; the Protestant states initially rejected it, but one by one they accepted it over the coming centuries. England (and her then American colonies) finally accepted the change in 1752 when 11 days were lost; contrary to popular belief there is no evidence for riots in protest at this (Poole 1998). The Eastern Orthodox churches continue to use the Julian calendar with the traditional lunar tables for calculating Easter. Because the purpose of the Gregorian calendar was to regulate the cycle of Christian holidays, its acceptance in the non-Christian world was initially not at issue.

Detailed information about the Gregorian reform may be found in the collection of papers resulting from a conference sponsored by the Vatican to commemorate its four-hundredth anniversary (Coyne, Hoskin and Pedersen 1983).

15.4.2 Rules for the Civil Use of the Gregorian Calendar

The Gregorian calendar uses the same months with the numbers of days as it predecessor, the Julian calendar (see Table 15.5). Days are counted from the first day of each month.

Years are counted from the initial epoch defined by Dionysius Exiguus (see § 15.1.8), and each begins on January 1. A common year has 365 days but a leap year has 366, with an intercalary day, designated February 29, preceding March 1. Leap years are determined according to the following rule:

> Every year that is exactly divisible by 4 is a leap year, except for years that are exactly divisible by 100, but these centurial years are leap years if they are exactly divisible by 400.

As a result, the year 2000 was a leap year, whereas 1900 and 2100 are not.

The epoch of the Gregorian calendar, (1 January 1) was Monday, 1 January 3 in the Julian calendar or Julian Day Number 1 721 426.

15.4.3 Rules for the Ecclesiastical Calendar

The ecclesiastical calendars of Christian churches are based on cycles of movable and immovable feasts. Christmas is the principal immovable feast, with its date set at December 25. Easter is the principal movable feast, and dates of most other movable feasts are determined with respect to Easter. However, the movable feasts of the Advent and Epiphany seasons are Sundays reckoned from Christmas and the Feast of the Epiphany, respectively.

In both the Julian and Gregorian calendars, the date of Easter is defined to occur on the Sunday following the ecclesiastical full moon that falls on or next after March 21. This should not be confused with the popular notion that Easter is the first Sunday after the first full moon following the vernal equinox. In the first place, the vernal equinox does not necessarily occur on March 21. Secondly, the ecclesiastical full moon is not the astronomical full moon. It is based on tables that do not take into account the full complexity of lunar motion. As a result, the date of an ecclesiastical full moon may differ from that of the true full moon. However, the Gregorian system of leap years and lunar tables prevents any progressive departure of the tabulated date from the astronomical phenomena.

The ecclesiastical full moon is defined as day 14 of a lunation, where the day of the ecclesiastical new moon is counted as day 1. The tables are based on the Metonic cycle, in which 235 mean synodic months contain 6939.688 days. Since nineteen Gregorian years contain 6939.6075 days, the dates of Moon's phases in a given year will recur on nearly the same dates nineteen years later. To prevent the 0.08-day difference between the cycles from accumulating, the tables incorporate adjustments to synchronise the system over longer periods of time. Additional complications arise because the ecclesiastical lunations are of 29 or 30 integral days. The entire calendar involves a cycle 5 700 000 years containing 2 081 882 250 days, which are equated to 70 499 175 lunations. After this period, the dates of Easter repeat themselves.

The date of Easter as calculated in the Gregorian calendar is used by the Catholic and most Protestant churches. However, the Eastern Orthodox churches still calculate the date of Easter in the Julian calendar, though some such churches have, in this century, modified the original method of calculation.

15.4.4 Calculation of the Date of Easter Sunday

The date of Easter was calculated using three parameters.

The first of these is the Dominical (or Sunday) Letter. This defines the positions in a year of the Sundays. It is obtained by labelling the days of the year consecutively with the seven letters A to G. And for the next 7, again A–G and so on. The Dominical Letter is the letter so assigned to the first Sunday (and every other). It changes from year to year.

Equating A with 1, B with 2 etc., the Dominical Letter for year Y is given by the equivalent to the number, N, in:

$$N = 7 - \text{mod}(Y + Y/4 + 4, 7) \quad \text{in the Julian calendar} \tag{15.3}$$

or

$$N = 7 - \text{mod}(Y + Y/4 - Y/100 + Y/400 - 1, 7) \quad \text{in the Gregorian calendar.} \tag{15.4}$$

The second, the Golden number, is the position (1 to 19) of a year in the 19 year Metonic cycle. If Y is the year in either the Julian or Gregorian calendar, the golden number, G, is given by:

$$G = 1 + \text{mod}(Y, 19). \tag{15.5}$$

The third is the Epact of a year. It is the age in days (0 to 29) of the ecclesiastical moon on the first day of the year (January 1).

For the Dionysian canon (tied to the Julian calendar), the epact, E, of a year with a Golden number G is given by:

$$E = \text{mod}(11 * G - 3, 30). \tag{15.6}$$

In the Gregorian canon, the calculation of the epact is more complicated. First the basic formula for the epact is changed to:

$$E = \text{mod}(11 * G - 10, 30). \tag{15.7}$$

But this must be modified by the addition of the so called solar (SOL) and lunar (LUN) equations.

The solar equation firstly makes an adjustment needed to return the date of the vernal equinox to its traditional date close to March 21. Secondly it makes an adjustment of the decreased length of the Gregorian year. It is given by:

$$\text{SOL} = H - H/4 - 12. \tag{15.8}$$

The lunar equation likewise gives an adjustment to correct the average length of a lunation to value more close to that of the real Moon. It is given by:

$$\text{LUN} = (H - 15 - (H - 17)/25)/3. \tag{15.9}$$

In both these expressions, $H = Y/100$ where Y is the year.

A further adjustment of 1 day is required of the Golden number if $E = 25$ and $G \geq 12$ or $E = 24$. This is to maintain a traditional requirement that no two new moons fell on the same day of the year in a Metonic cycle of 19 years. It may be calculated as V in

$$V = E/24 - E25 + (G/12) * (E/25 - E - 26) \tag{15.10}$$

so that the adjusted Epact is

$$E = \text{mod}(11 * G - 10, 30) - \text{mod}(\text{SOL} - \text{LUN}, 30) + V. \tag{15.11}$$

The day of Easter Sunday is then given as a Day of March, S, (i.e., counting from March 1 as day 1) in terms of this modified epact E by:

$$S = R + \text{mod}(7 + N - C, 7) \tag{15.12}$$

where

$$C = 1 + \text{mod}(R + 2, 7) \tag{15.13}$$

and

$$R = 45 - E \quad \text{if } E < 24 \tag{15.14}$$

$$\text{or } R = 75 - E \quad \text{if } E \geq 24 \tag{15.15}$$

See § 15.11.1 for a full explanation of the mathematical notation used here. Details of the calculation are discussed at length by Butcher (1877), Oudin (1940) and Richards (1998).

15.5 The Jewish Calendar

15.5.1 History of the Jewish Calendar

The codified Jewish calendar as we know it today is generally considered to date from about 359, though the exact date is uncertain.

Jewish calendrical practices before that are uncertain. The earliest evidence indicates a calendar based on observations of the phases of the new moon at Jerusalem. Since the Bible mentions seasonal festivals, there were probably intercalations. There was probably an evolution of conflicting calendrical practices.

The Babylonian exile, in the first half of the sixth century B.C., greatly influenced the Jewish calendar. The names of the months are very similar to those in the Babylonian calendar and the practice of intercalating months may have been learnt from the Babylonians.

During the period of the Sanhedrin the calendar was observational; months began with sightings of the crescent of the new moon. A committee of the Sanhedrin met to evaluate reports of sightings. If sightings were not possible, the new month was begun 30 days after the beginning of the previous month. Decisions on intercalation were influenced, if not determined entirely, by the state of vegetation and animal life. Although eight-year, nineteen-year, and longer-period intercalation cycles may have been instituted at various times prior to Hillel II, there is little evidence that they were employed consistently over long periods. The Sanhedrin was entrusted to run the calendar and only its members knew how to do it.

After the Diaspora, this arrangement became unworkable; by the time news of sightings at Jerusalem reach outlying Jewish communities, the start of the months was well past. The patriarch Hillel II is credited with reforming this state of affairs by disseminating codified rules, which anybody, anywhere, could follow.

The exact details of Hillel's calendar have not survived, but it is generally considered to include rules for intercalation over nineteen-year cycles. Up to the tenth century A.D., however, there was disagreement about the proper years for intercalation and the initial epoch for reckoning years.

The modern Jewish calendar is the official calendar of Israel and is the liturgical calendar of the Jewish faith.

15.5.2 Rules for the Modern Jewish Calendar

The day of the Jewish calendar is divided into 24 hours and each hour into 1080 *halakim (hk).* Thus, there are 10 seconds in 3 halakim. The day begins at 18.00 P.M., that is six hours in advance of our current calendrical day and this is counted as 0 hr 0 hk in Jewish timekeeping. The days of the week are numbered from Sunday (1) to Saturday, the Sabbath (7).

As it exists today, the Jewish calendar is a luni-solar calendar that is based on calculation rather than observation and is based on the Metonic calendar. Its regulation depends on three levels of abstraction. First, there is the real astronomical moon; secondly, a highly regular but fictitious moon whose behaviour is close to the average behaviour of the real Moon and which defines the astronomical calendar. Each month and year of the latter starts at the instant of conjunction of the fictitious moon; this is termed a *Molad*. Thirdly, there is the civil calendar; the months and years of this start on, or up to two days after, the *molad*. Thus, the start of a civil year may be postponed from the date of its *molad* by the application of four rules *(dehiyyot).*

The epoch of the calendar is taken to occur in the same year, −3760, as the Creation as described in Genesis. This year was calculated in about the 10th century by Maimonedes from data in the Bible, which gives the generation times of the Patriarchs from Adam, and important historical dates culminating in the sack of Jerusalem by the Romans which can be dated historically. The results of such calculations are controversial but Maimonedes' value is accepted by the Jewish religion.

Years counted from this epoch define the Mundane Era (Anno Mundi, A.M.) and it may be noted that the Jewish year, Y, currently begins in the autumn of the Gregorian or Julian year: $Y - 3761$. The epoch of the calendar, the first day of Tishri is 1 A.M. is on Monday, −3760 October 7 in the proleptic Julian calendar with a Julian Day Number of 347 998. This epoch is not the date of the creation itself; this is taken to have occurred in the next September.

The years are counted in cycles of 19 years, and in this period there are 12 common years of 12 months apiece and 7 leap years each containing 13 months; thus there are 235 months in the 19-year cycle. The leap years are now fixed as the 3rd, 6th, 8th, 11th, 14th, 17th and 19th year of each cycle

The total period of this 19-year cycle is 6939 days, 16 hours, 595 halakim (=6939.689 590 days) so that the average number of days in a year is 365.24682. Thus, the average start of the Jewish year is currently falling behind the mean tropical year by about 1 day in 200 years.

Each civil year is deemed to start with the first day of the first month, Tishri. The first (fictitious) *molad*, which initiates year 1, and which is the first year of a 19 year cycle, is

Table 15.6 Number of days in the six categories of the Jewish year

	Common year	Leap year
Deficient	353	383
Regular	354	384
Abundant	355	385

Table 15.7 Months and days therein of the Jewish calendar

	Month			Month	
1.	Tishri	30	7.	Nisan	30
2.	Heshvan	29 [a]	8.	Iyar	29
3.	Kislev	30 [b]	9.	Sivan	30
4.	Tebet	29	10.	Tammuz	29
5.	Shebat	30	11.	Ab	30
6.	Addar	29 [c]	12.	Elul	29

[a] In an abundant year, Heshvan has 30 days.
[b] In a deficient year, Kislev has 29 days.
[c] In a leap year, Addar has 30 days; it is followed by Addar II with 29 days.

deemed to have taken place on the Monday, October 7, −3760 at 11:20 P.M. or Tishri 1, A.M. 1 at 5 hr, 204 hk; it is a simple matter to calculate the *molad* of Tishri of any succeeding year by adding an appropriate multiple of the interval between successive *moladot* to the time of this first *molad*.

Successive *moladot* occur at fixed intervals of 29 days 12 hr and 793 hk (= 29.530 594 days). They do not coincide with the phases of the real astronomical Moon, but they should remain in average synchrony for a very long time. Calendrical dates are worked out, independent of longitude using local times.

The rules of postponement and the insertion of leap month imply that the number of days in a year varies. There are six types of calendar year, according to the number of days in them. Firstly, a year may be common or leap; common years contain 12 months and leap years contain 13. Furthermore any year may be deficient, regular or abundant. The numbers of days in the six types of year are shown in Table 15.6. The names of the months and the number of days therein are shown in Table 15.7 Generally the number of days in the month alternate between 30 and 29.

15.5.3 Rules for Postponement (Dehiyyot)

Below are the four rules that determine whether Tishri 1 should be postponed until after its *molad*. The first three are sometimes termed astronomical rules while the fourth is termed a political rule. We also give below the reason underlying each rule. Only one of the astronomical postponements should be applied. Rule (4) is applied last but its application may be required after the application of one of the other three to give a second postponement.

1. If the Molad of Tishri falls at or after 18 hr 0 hk (i.e., noon), Tishri 1 is postponed by one day. If this causes Tishri 1 to fall on day 1, 4, or 6, (Sunday, Wednesday or Friday) then Tishri 1 is postponed an additional day to satisfy Rule (4).

Before the introduction of the new calendar, the Molad of Tishri was determined by the first sighting of the new moon; this would always be close to the Sun. If the *molad* occurred before dusk (nominally 6:00 P.M.), it might not be visible and would be taken to fall on the next day. Rule (1) preserves this traditional feature.

2. If the Molad of Tishri of a common year (i.e., of twelve months) falls on a Tuesday (day 3) at or after 9 hr, 204 hk, then Tishri 1 is postponed one day to the Wednesday (day 4). Rule (4) would then require a further postponement to the Thursday.

Should this rule apply to year Y, it may be calculated that the *Molad* of the succeeding year, Y+1, would fall twelve months later on a Saturday on or after 18 hr, 0 hk. Year Y+1 would then be postponed one day by Rule (1) and a further day by Rule (4). This would then mean that year Y would have an unacceptable 356 days. This is avoided by postponing the start of year Y by one day so that it would have 355 days.

3. If the Molad of Tishri of a common year following a leap year falls on a Monday (day 2) at or after 15 hr, 589 hk, then Tishri 1 is postponed one day to the Tuesday (day 3).

Should this rule apply to the common year Y, it may be calculated that the *Molad* of the previous leap year, Y−1, would occur (thirteen months earlier) on a Tuesday on or after 18 hr, 0 hk. Year Y−1 would thus have been postponed by one day by Rule (1) and then a further day by Rule (4). This would then mean that year Y−1 had an unacceptable 382 days. This is avoided by postponing the start of year Y by one day so that year Y−1 would have 383 days.

4. If the Molad of Tishri falls on a Sunday, Wednesday or Friday (days 1, 4 or 6), then Tishri 1 is postponed by one day.

This (political) rule prevents Hoshanna Rabba (Tishri 21) from occurring on the Sabbath and Yom Kippur (Tishri 10) from occurring on the day before or after the Sabbath. Work (including the preparation of food and the burial of the dead,) is forbidden on Yom Kippur and the Sabbath; this rule prevents there being two consecutive days on which work is forbidden. Work is necessary on Hoshanna Rabba and Rule (4) eliminates any conflict.

A thorough discussion of both the functional and religious aspects of the *dehiyyot* is provided by Cohen (1981).

15.5.4 Determining Tishri 1

The calendar year begins with the first day of Rosh Hashanah (Tishri 1). This is determined by the day of the Molad of Tishri and the four rules of postponements (*dehiyyot*). The *dehiyyot* can postpone Tishri 1 to one or two days after the *molad*.

It is traditional to denote the Molad of Tishri by four numbers: the number of weeks elapsed since the creation, the day of the week (Sunday is day 1), the hour of the day (from 6 P.M.) and the number of halakim after the start of that hour. The useful periods of time in this convention are shown in Table 15.8. The number of weeks can usually be ignored.

Table 15.8 Periods corresponding to different numbers of lunations

Lunations	Weeks-Days-Hours-Halakim
1	4-1-12-0793
12	50-4-08-0876
13	54-5-21-0589
235	991-2-16-0595

The day and time of the Molad of Tishri of any given year can be found by adding the time of the first epochal *molad* to the times of all the lunations that precede it. The number of weeks in these calculations may be ignored, and if the number of days exceeds 7, it may be reduced by 7.

Example 1. Find the weekday and time of the Molad of Tishri of Anno Mundi (A.M.) 2.

A.M. 1 is a common year with 12 lunations. Thus the time of the *Molad* of 2 A.M is found by adding the time for these 12 lunations to the time of the first epochal *Molad*.

	Days-Hours-Halakim
epochal *molad*	2-05-0204
+12 lunations	4-08-0876
Molad of Tishri, A.M. 2	6-14-0000

The molad of A.M. 2 fell on day 6 at 14 hr 0 hk; this corresponds to Friday at A.M. 8

Example 2. Find the day Tishri 1, A.M. 5760.

The Molad of Tishri of A.M. 5760 is preceded by 5759 complete years since the initial epoch; these comprise 303 complete nineteen-year cycles plus two common years. The lunation constants given previously may be added to the epochal *molad* to give the time and weekday of the *molad*.

		Days-Hours-Halakim
Epochal molad		2-05-0204
19-year cycles	303 × 2-16-0595	2-22-1005
Ordinary years	2 × 4-08-0876	1-17-0672
Leap years	0 × 5-21-0589	0-00-0000
Molad of Tishri A.M. 5760		6-21-0801

Since the *molad* occurs on day 6, *dehiyyah* (4) causes Tishri 1 to be postponed to day 7. Tishri 1 of A.M. 5760 fell on day 7 (Saturday).

15.5.5 Determining the Length of the Year

The number of days in a year, Y, may be found by calculating the dates of its *molad* and that of the succeeding year, Y+1. After application of the rules of postponement, the number of

days in Y may be calculated. This should fall within the limits given in Table 15.6. It is then a simple matter to ascertain the date of the start of each month given the data in Table 15.7 or Table 15.15.

15.5.6 Terminology of the Jewish Calendar

The following are terms used in the Jewish calendar:

Deficient (*hasher*) month: a month comprising 29 days.

Full (*male*) month: a month comprising 30 days.

Common year: a year comprising 12 months, with a total of 353, 354, or 355 days.

Leap year: a year comprising 13 months, with a total of 383, 384, or 385 days.

Abundant year (*shelemah*): a year in which the months of Heshvan and Kislev both contain 30 days.

Deficient year (*haser*): a year in which the months of Heshvan and Kislev both contain 29 days.

Regular year (*kesidrah*): a year in which Heshvan has 29 days and Kislev has 30 days.

Halakim (singular, *helek*): "parts" of an hour; there are 1080 hk in an hour.

Molad (plural, *moladot*): "birth" of the Moon, taken to mean the time of the Sun of the notional calendrical moon.

Dehiyyah (plural, *dehiyyot*): "postponement"; a rule delaying 1 Tishri until after the *molad*

15.6 The Islamic Calendar

15.6.1 Introduction

The Islamic calendar is a purely lunar calendar in which months correspond to the lunar phases. As a result, the cycle of twelve lunar months regresses through the seasons over a period of about 33 years. For religious purposes, Muslims begin the months with the first visibility of the lunar crescent of the new moon.

An arithmetic calendar, sometimes called the civil Islamic calendar that approximates the lunar phase cycle is often used. This is used by chronologists in studying Islamic history and as a civil calendar in some Muslim countries.

The seven-day week is observed with each day beginning at sunset. Weekdays are specified by number, with day 1 corresponding to Sunday (see § 15.1.9). Day 6, which is called *Jum'a*, is the day for congregational prayers, but unlike the Sabbath days of the Christians and Jews, it is not a day of rest. It begins at sunset on Thursday and ends at sunset on Friday.

For religious purposes, each month begins, in principle, with the first sighting of the lunar crescent after the new moon. This is particularly important for establishing the beginning and end of Ramadan. If the weather causes uncertainties, a new month may be declared thirty days after the beginning of the preceding month. Although various predictive procedures have been used for determining first visibility (see § 15.1.5), they have always had an equivocal status. In practice, there is disagreement among countries, religious leaders, and scientists about whether to rely on observations, which are subject to error, or to use calculations, which may

Table 15.9 Months and days therein of the formal Islamic calendar

	Month [a]			Month	
1.	Muharram	30	7.	Rajab	30
2.	Safar	29	8.	Shaabán	29
3.	Rabi' I	30	9.	Ramadân [b]	30
4.	Rabi' II	29	10.	Shawwál	29
5.	Jumada I	30	11.	Dhú'l-Qa'da	30
6.	Jumada II	29	12.	Dhú'l-Hijjab	29 [c]

[a] Muharram, Rajab, Dhú'l-Qa'da, and Dhú'l-Hijjab are holy months
[b] Month of fasting
[c] In a leap year, Dhúl-Hijjab has 30 days.

be based on poor models. It may be noted that the instant of observation of a new moon may fall in different days in different parts of the world. See URL[10] for details of the ongoing Moon watch project.

The years are reckoned from the Era of the Hijra, commemorating the migration of the Prophet and his followers from Mecca to Medina.

The history and construction of the Islamic calendar are discussed by Burnaby (1901), Mayr and Spuler (1961), and by Freeman-Grenville (1963).

15.6.2 History of the Islamic Calendar

The form of the Islamic calendar, as a lunar calendar without intercalation, was laid down by the Prophet in the Qur'an (Sura IX, verse 36–37) and in his sermon at the Farewell Pilgrimage. This was a departure from the luni-solar calendar commonly used in the Arab world, in which an intercalary month was added as deemed necessary.

Caliph 'Umar I is credited with establishing the Hijra Era in A.H. (Anno Hegira) 17, but it is not known how the initial date was determined. Calculations show that the astronomical new moon (i.e., the conjunction of the Sun and Moon) occurred on +622 July 14 at 0444 UT.

15.6.3 Rules for the Arithmetic Islamic Calendar

Each year has twelve months; odd-numbered months have thirty days and even-numbered months have twenty-nine days as indicated in Table 15.9. In leap years, the twelfth month, Dhú'l-Hijjab, receives an extra day. The first day of the year is Muharram 1.

There are eleven leap years in a cycle of thirty years. These are years 2, 5, 7, 10, 13, 16, 18, 21, 24, 26, and 29 of the cycle (though a different set is sometimes used). The year 1 A.H. was the first of a cycle.

The epoch, 1/1/1 A.H. of the formal calendar is generally taken to correspond to Friday, 622 July 16 in the Julian calendar or Julian Day Number 1 948 440 but it started at sunset on the previous Thursday. Some authors take the epoch to correspond to this Thursday.

The mean length of a month in the thirty-year cycle is about 29.530 56 days; the calendar months will remain on average in synchrony with the lunations of the Moon to within a day for about 3000 years.

15.7 The Indian Calendars

15.7.1 History of Indian Calendars

Owing to the continuity of Indian civilisation and the diversity of cultural influences, the history of calendars in India is complex. In the mid-1950s, the Calendar Reform Committee (1955), set up by the Indian Government after independence, reported that there were about 30 calendars in use for regulating Hindu, Buddhist, and Jain religious festivals. Some of these were also used for civil dating. These calendars fall into two main types: the, so-called solar calendars (see § 15.7.2) and the luni-solar calendars (see § 15.7.3). Each has local variations which follow long-established customs and the astronomical practices of local calendar makers. In addition, Muslims in India used the Islamic calendar, and the Indian government uses the Gregorian calendar for administrative purposes.

Early allusions to a luni-solar calendar with intercalated months are found in the hymns from the Rig Veda, dating from the second millennium B.C.. Literature from 1300 B.C. to A.D. 300 provides information of a more specific nature. They describe a five-year luni-solar calendar coordinating solar years with synodic and sidereal lunar months.

Indian astronomy developed considerably during the first few centuries A.D., as advances in Babylonian and Greek astronomy reached India. Traditional calendric practices were adapted to new astronomical constants and models for the motion of the Moon and Sun. These were described in astronomical treatises of this period known as *Siddhantas* but some of these have not survived. The *Surya Siddhanta*, originated in the fourth century but was revised over the following centuries. It influenced Indian calendrics up to, and even after, the calendar reform of A.D. 1957.

The Calendar Reform Committee (1955) inaugurated, for civil use, an arithmetic solar calendar, the Reformed Saka calendar (see § 15.7.4). As well as this, it also attempted to reconcile traditional calendrical practices with modern astronomical concepts. According to their proposals, precession is accounted for and calculations of solar and lunar position are based on accurate modern methods. All astronomical calculations are performed with respect to a Central Station at longitude $82^\circ\ 30'$ East, latitude $23^\circ\ 11'$ North. For religious purposes solar days are reckoned from sunrise to sunrise.

The Committee thus set guidelines for religious calendars, which require calculations of the motions of the Sun and Moon. Tabulations of the religious holidays are prepared by the India Meteorological Department and published annually in *The Indian Astronomical Ephemeris*. Despite the attempt to establish a unified calendar for all of India, many local variations still exist and many local calendar makers continue to use traditional astronomical concepts and formulae, some of which date back 1500 years.

The day begins at sunrise, but the Indian calendars are perhaps unique in using a unit of time that may be shorter than a day: the *tithi*. Most holidays occur on specified *tithis*. Lunations are divided into 30 lunar days called *tithis*. A *tithi* is defined as the time required for the longitude of the Moon to increase by 12° over the longitude of the Sun. Thus, the length of a *tithis* may vary from about 20 hours to nearly 27 hours. During the waxing phases, *tithis* are counted from 1 to 15 with the designation *Sukla*. *Tithis* for the waning phases are designated *Krsna* and are again counted from 1 to 15. Each day is assigned the number of the *tithis* current at sunrise. Occasionally a short *tithi* will begin after sunrise and be completed before the next sunrise. Similarly a long *tithis* may span two sunrises. In the former case, a

Table 15.10 Months of the Indian solar calendar

	Sankrânti name	Zodiacal name	Length in days		*Sankrânti* name	Zodiacal name	Length in days
1.	Mesha	Aries	30.9	7.	Tula	Libra	29.9
2.	Vrishabha	Taurus	31.4	8.	Vrischika	Scorpio	29.5
3.	Mithuna	Gemini	31.6	9.	Dhanu	Sagittarius	29.4
4.	Karka	Cancer	31.5	10.	Makara	Capricorn	29.5
5.	Simha	Leo	31.0	11.	Kumbha	Aquarius	29.8
6.	Kanya	Virgo	30.5	12.	Mina	Pisces	30.3

number is omitted from the day count. In the latter, a day number is repeated. The logic of Days and *tithis* is analogous to that of lunar and solar months (see § 15.7.3).

The seven-day week has been used in India since at least 484 and the names of the days are derived from planetary Gods as in the Roman astrological week.

Different modes of counting the years have been used. Some initialise the count at the start of a dynasty of rulers. One such is the Saka era commencing in the year 78. Other counts are astronomically based such as the Kali-yoga whose epoch in −3101 is the date of the most recent mean conjunction of the seven planets or wandering stars (which includes the Sun and the Moon) known to the ancients.

Pingree (1978) provides a survey of the development of mathematical astronomy in India. Although he does not deal explicitly with calendars, this material is necessary for a full understanding of the history of India's calendars. Sewell (1912, 1989) and Sewell and Dikshit (1911) provide a comprehensive account of the traditional calendars. They are also discussed by Chatterjee (1987).

15.7.2 The Traditional Indian Solar Calendar

The starts of the solar months are determined by the arrival of the Sun at twelve longitudinal positions in the ecliptic measured from Aries and spaced at equal angles of 30°; these are called *sankrântis* and are analogous to the signs of the Zodiac; they carry Sanskrit names mostly similar in meaning to the Western names as shown in Table 15.10. Since the velocity of the Sun around the ecliptic is not constant, the lengths of these months vary by several days.

Originally, the times at which the Sun reached each *sankrânti* were calculated on the basis of a mean Sun. More recent calendars are based on the true longitudes of the Sun.

15.7.3 The Traditional Indian Luni-solar Calendar

The luni-solar calendars operate in the manner described in § 15.1.11. The start of a month is determined by a new moon (or full moon, according to local custom); this feature maintains synchrony between the months and the lunations. The names of the months are similar to those given in Table 15.11.

The first month of the year is Chaitra (or in some regions, another month). The starts of the solar months are defined by the *sankrântis* (see Table 15.10). If two lunations commence

Table 15.11 Months in the Indian luni-solar calendar

Month		Month [a]	
1.	Chaitra	7.	Asvina
2.	Vaisakha	8.	Kartika
3.	Jyaistha	9.	Margasira
4.	Ashadha	10.	Pausha
5.	Sravana	11.	Magha
6.	Bhadrapada	12.	Phalguna

[a] The months in the Reformed Saka calendar have similar names but month 6 is named Bhada and month 9 is named Agrahayuna.

in the same solar month, the two bear the same name but the first is described with the prefix *adhika*, or intercalary. Years containing such a year have thirteen lunar months. This is equivalent to the intercalation of a month.

More rarely, a short solar month will occur without containing the start of a lunation. In that case, the name of the lunar month is omitted; this is equivalent to an extracalation. Such a (*ksaya*) month can occur only in the months near the Earth's perihelion passage. In compensation, a month in the first half of the year will have had two new moons, so the year will still have twelve lunar months. *Ksaya* months are separated by as few as nineteen years and as many as 141 years.

15.7.4 Rules of the Reformed Saka Calendar

The names of the 12 months and the number of days in each are indicated in Table 15.11. There are 365 days in each common year and 366 in a leap year.

Years are counted from the year 78 which initiates the Saka Era (E.S.), a traditional epoch in Indian calendars. The epoch of the calendar is Wednesday, 79 March 24, in the Julian calendar or Julian Day Number 1 749 995.

Leap years coincide with those of the Gregorian calendar. To determine leap years, first add 78 to the Saka year. If this sum is evenly divisible by 4, the year is a leap year, unless the sum is a multiple of 100. In the latter case, the year is not a leap year unless the sum is also a multiple of 400.

Each date in this calendar corresponds, in common years, to a corresponding date in the Gregorian calendar; thus Chaitra 1 corresponds to March 22. In leap years from Phalunga 10 to Vaisakha 21, the corresponding Gregorian date must be advanced by one day.

15.8 The Chinese Calendar

15.8.1 History of the Chinese Calendar

In China the astronomical luni-solar calendar, was a sacred document, sponsored and promulgated by the reigning monarch. For more than two millennia, a Bureau of Astronomy made astronomical observations, calculated astronomical events such as eclipses, prepared astrological predictions, and maintained the calendar (Needham 1959). A successful calendar

not only served practical needs, but also confirmed the consonance between Heaven and the imperial court.

Like the luni-solar Indian calendar (see § 15.7.2), the months of the Chinese calendar start on the day of a new moon. Solar months, analogous to the signs of the Zodiac and the Indian *sankrântis*, are used to define intercalary months, which occur every two or three years.

Analysis of surviving astronomical records inscribed on oracle bones reveals a Chinese luni-solar calendar, with intercalation of lunar months, dating back to the Shang dynasty of the fourteenth century B.C. Since then, there have been more than 50 changes in the details.

From the earliest records, the beginning of the year occurred at a new moon near the winter solstice but the choice of the month to begin the civil year varied with time and place. In the late second century B.C., a reform established the practice, which continues today, of requiring the winter solstice to occur in month 11. This reform also introduced the intercalation system in which dates of new moons are compared with the 24 solar terms (see § 15.8.3). However, calculations were based on the mean motions resulting from the cyclic relationships. Inequalities in the Moon's motions were incorporated as early as the seventh century A.D. (Sivin 1969), but the Sun's mean longitude was used for calculating the solar terms until 1644. Since 1645, the calendar is based on the true positions of the Sun and Moon and its accuracy depends on the accuracy of the astronomical theories and calculations. Before 1929, the calculation referred to observations at Beijing (116° 25′ East), but since then to the 120° East meridian.

Years were counted from a succession of eras established by reigning emperors (but see § 15.8.2). Although the accession of an emperor would mark a new era, an emperor might also declare a new era at various times within his reign in an attempt to re-establish a broken connection between Heaven and Earth (as personified by the emperor). The break might be revealed by the death of an emperor, the occurrence of a natural disaster, or the failure of astronomers to predict a celestial event such as an eclipse. In the latter case, a new era might mark the introduction of new astronomical or calendrical models.

Western (pre-Copernican) astronomical theories were introduced to China by Jesuit missionaries in the seventeenth century and more modern Western concepts gradually became known. Following the revolution of 1911, the traditional practice of counting years from the accession of an emperor was abolished.

Published calendrical tables are often in disagreement about the Chinese calendar. Some of the tables are based on mean, or at least simplified, motions of the Sun and Moon. Some are calculated for other meridians than 120° East. Some incorporate a rule that the eleventh, twelfth, and first months are never followed by an intercalary month. This is sometimes not stated as a rule, but as a consequence of the rapid change in the Sun's longitude when the Earth is near perihelion. However, it is incorrect when the motions of the Sun and Moon are accurately calculated.

Reference works give a variety of rules for establishing New Year's Day and for intercalation in the luni-solar calendar. Since the calendar was originally based on the assumption that the Sun's motion was uniform through the seasons, the published rules are frequently inadequate to handle special cases.

Although the Gregorian calendar is used in the Peoples' Republic of China for administrative purposes, the traditional Chinese calendar is used for setting traditional festivals and for timing agricultural activities in the countryside. The Chinese calendar is also used by Chinese communities around the world.

Table 15.12 Celestial Stems and the Earthly Branches of the sexagenary cycle

Celestial Stems		Early Branches		
1.	jia	1.	zi	rat
2.	yi	2.	chou	ox
3.	bing	3.	yin	tiger
4.	ding	4.	mao	hare
5.	wu	5.	chen	dragon
6.	ji	6.	si	snake
7.	geng	7.	wu	horse
8.	xin	8.	wei	sheep
9.	ren	9.	shen	monkey
10.	gui	10.	you	fowl
		11.	xu	dog
		12.	hai	pig

15.8.2 Sexagenary Cycle

Sexagenary cycles were used to count months, days, and fractions of a day. The use of the sixty-day cycle is seen in the earliest astronomical records and, although it has fallen into disuse in everyday life, it is still tabulated in calendars. By contrast the sixty-year cycle was introduced in the first century A.D. or possibly a century earlier (Tung 1960; Needham 1959) and is still used today.

The sexagenary cycle is a list of 60 names, each being a combination of one of ten Celestial Stem names and one of twelve Earthly Branch names each taken in cyclic order. After six repetitions of the set of stems and five repetitions of the branches, a complete cycle of pairs is completed and a new cycle begins. The Earthly Branch names are usually translated as the names of animals, but the Celestial Stem names are said to be untranslatable. These names are shown in Table 15.12.

It is customary to number the sexagenary cycles of years so that the first cycle began in −2636.

The initial year (*jia-zi*) of the current cycle began on 1984 February 2. *jia* is the first Celestial Stem name and *zi* is the first Earthly Branch. The numbers of the Celestial Stem (C) and of the Earthly Branch (E) of the Chinese year starting in the Gregorian year Y are given by:

$$\mathrm{C} = 1 + \mathrm{mod}(Y - 4,\ 10) \qquad E = 1 + mod(Y - 4,\ 12) \tag{15.16}$$

mod(A,B) denotes the remainder when A is divided by B. It follows that the year starting in 2000 is *geng-chen*, a year of the Dragon.

15.8.3 Major and Minor Terms

The tropical year is divided into 24 solar terms, in 15° segments of solar longitude. These divisions are paired into twelve minor terms (*Jieqi*) and twelve major terms (*Zhonggi*) as

Table 15.13 Chinese solar terms

	Term [a]	Name	Sun's Longitude	Approximate Gregorian Date	Approximate Duration in days
J1	Lichun	Beginning of Spring	315	Feb. 4	
Z1	Yushui	Rain Water	330	Feb. 19	29.8
J2	Jingzhe	Waking of Insects	345	Mar. 6	
Z2	Chunfen	Spring Equinox	0	Mar. 21	30.2
J3	Qingming	Pure Brightness	15	Apr. 5	
Z3	Guyu	Grain Rain	30	Apr. 20	30.7
J4	Lixia	Beginning of Summer	45	May 6	
Z4	Xiaoman	Grain Full	60	May 21	31.2
J5	Mangzhong	Grain in Ear	75	June 6	
Z5	Xiazhi	Summer Solstice	90	June 22	31.4
J6	Xiaoshu	Slight Heat	105	July 7	
Z6	Dashu	Great Heat	120	July 23	31.4
J7	Liqiu	Beginning of Autumn	135	Aug. 8	
Z7	Chushu	Limit of Heat	150	Aug. 23	31.1
J8	Bailu	White Dew	165	Sept. 8	
Z8	Qiufen	Autumnal Equinox	180	Sept. 23	30.7
J9	Hanlu	Cold Dew	195	Oct. 8	
Z9	Shuangjiang	Descent of Frost	210	Oct. 24	30.1
J10	Lidong	Beginning of Winter	225	Nov. 8	
Z10	Xiaoxue	Slight Snow	240	Nov. 22	29.7
J11	Daxue	Great Snow	255	Dec. 7	
Z11	Dongzhi	Winter Solstice	270	Dec. 22	29.5
J12	Xiaohan	Slight Cold	285	Jan. 6	
Z12	Dahan	Great Cold	300	Jan. 20	29.5

[a] Terms are classified as minor (*Jieqi*), J, or major (*Zhonggi*), Z, followed by the number of the term.

shown in Table 15.13. These terms are numbered and assigned names that are seasonal or meteorological in meaning. For convenience the minor and major terms are denoted by J and Z, respectively, followed by the number. The major terms define the starts of solar months. Because of the ellipticity of the Earth's orbit, the lengths of the solar months vary with the season as with the Indian *Sankrântis* (see § 15.7.2).

15.8.4 Rules for the Modern Chinese Calendar

Here, we give the rules based on those that are currently used for calendars prepared by the Purple Mountain Observatory (1984) and discussed by Reingold and Dershowitz (2001) and by Aslaksen in URL[4].

The Chinese term *sui* is the period from one winter solstice (Z11) to the next.

1. The instants of conjunctions and major solar terms are calculated for meridians of 120° East.

2. The days are measured from midnight to midnight.
3. The first day of a month is the day in which a conjunction of the Moon (new moon) falls.
4. If a *sui* contains 13 complete months, one of them is a leap month.
5. This leap month is the first in the *sui* that contains no major solar term.
6. Months are assigned numbers 1 to 12 (but not names); a leap month is assigned the same number as its predecessor.
7. The winter solstice (Z11) always falls in month 11.
8. Years are counted in sexagenary year cycles.

The current sexagenary year cycle started in 1984 which is named *jia-zi*, a year of the Rat and the first day of the first month of this year was 1984 February 2 or Julian Day Number 2 445 733. Cycles are sometimes counted with the first starting in −2636.

A corollary of rule 4 is that a *sui* with only 12 complete months contains no leap month even though one of its months may contain no major solar term.

The application of these rules results in there being about 7 leap months every 19 years. A common year of twelve months contains 353, 354, or 355 days; a leap year of thirteen months contains 383, 384, or 385.

If a month contains no solar term, the two solar terms immediately preceding its conjunction and the one following it are the same. It is convenient, here, to refer to such a month as an empty month. The number of the latest solar term preceding any event can be found by calculating the longitude of the Sun at the time of the event and rounding it down to a multiple of 30°.

The calculation of the details of the Chinese calendar for a year requires access to tables or formulae for ascertaining the instants, in local time, of the winter solstice and the lunar conjunctions at a meridian of 120° East.

15.8.5 Finding the First Day of a Chinese Year

To determine the first day of the Chinese year that starts in the Gregorian year Y:

1. Calculate the dates, W_{Y-1} and W_Y, in which the winter solstices of years $Y-1$ and Y occur.
2. Calculate the day, M_a, of the conjunction of the Moon that falls first after W_{Y-1} and the date M_d of the conjunction that falls last on or before W_Y.
3. Calculate the number of complete lunations in the period M_a to M_d; this is the integer, L, nearest to $(M_d - M_a)/29.53$.
4. Calculate the date of the next conjunction, M_b, after M_a.
5. If $L = 11$, there is no leap month in the *sui* W_{Y-1} to W_Y. W_{Y-1} falls in month 11 of $Y-1$ and month 12 starts on M_a, so that the Chinese year starts with the next conjunction, M_b. Note that the Chinese year may yet contain a leap month after W_Y.
6. If $L = 12$, there is a leap month in the *sui*. This leap month is the first lunation in the *sui* that contains no major solar term. Calculate the date, M_c, of the next lunation after M_b. If the month initiated by M_a is empty, it is a leap month; likewise M_b is a leap

month if it is empty. In either case, the Chinese New Year starts on M_c, but if neither M_a nor M_b are empty, the year starts on M_b.

Example 1. Find the first day of the Chinese year starting in Gregorian year 2000.

From Eq. 15.16, we find that 2000 is *geng-chen*, a year of the Dragon.

We find the following dates:

W_{Y-1}	The winter solstice in 1999	Dec 22
W_Y	The winter solstice in 2000	Dec 21
M_a	The first conjunction after W_{Y-1}	2000 Jan 7
M_b	The next conjunction after M_a	2000 Feb 5
M_d	The last conjunction on or before W_Y	2000 Nov 25

Thus, $L = 11$, there is no leap month in the *sui* and the year begins on M_b, 2000 Feb 5.

Example 2.. Find the first day of the Chinese year in 2033 and the first day of its leap month. 2033 is an anomalous year whose details are sometimes in error in published Chinese almanacs.

We find that 2033 is *gui-chou*, a year of the Ox.

We find the following dates:

W_{Y-1}	The winter solstice in 2032	Dec 21
W_Y	The winter solstice in 2033	Dec 21
M_a	The first conjunction after W_{Y-1}	2033 Jan 1
M_b	The next conjunction after M_a	2033 Jan 31
M_c	The next conjunction after M_b	2033 Mar 1
M_d	The last conjunction on or before W_Y	2033 Dec 21

Thus, $L = 12$ and there is a leap month in the *sui*, but we find that neither M_a nor M_b are empty, so that the year begins on M_b, 2033 Jan 31.

15.8.6 Finding the First Day of Each Month in a Chinese Year

To determine which month, if any, is the leap month and to number the months of a year:

1. Determine the dates, N_Y and N_{Y+1} of the starts of the years Y and $Y + 1$ as described in § 15.8.5.
2. Also note from the calculation of N_{Y+1} which of the last two lunations of year Y that started on M_a or M_b, are empty, if either are.
3. Calculate the number of lunations, K, in the period N_Y and N_{Y+1}; this is given by the integer nearest to $(N_{Y+1}$ and $N_Y)/29.53$.
   If $K = 12$, the year starting on N_Y has no leap months and its months are numbered 1 to 12.
   If $K = 13$, one of these 13 months is a leap month. This is the month starting on M_a

or M_b if either was empty.
If neither of these is empty, find the first empty month in the first 10 months. This is the leap month.

4. Number the months from N_Y consecutively except that the leap month is assigned the same number as its predecessor.

Example 1. Find the months in the Chinese year starting in Gregorian year 2000.

We find the following:

N_Y	First day of 2000	2000 Feb 5
N_{Y+1}	First day of 2001	2001 Jan 24

Thus $K = 12$; there is no leap month and the months are numbered consecutively 1 to 12.

Example 2. Find the months in the Chinese year starting in Gregorian year 2033.

We find the following:

N_Y	First day of 2033	2033 Jan 31
N_{Y+1}	First day of 2034	2034 Feb 19
M_a	First conjunction after W_Y	2033 Dec 22
M_b	Next conjunction after M_a	2034 Jan 20

Thus $K = 13$; there is a leap month. We find that the month starting on M_a is empty so that the month starting on 2033 Dec 22 is a leap month. This leap month comes after month 11 (which contains the winter solstice) so that it is also assigned the number 11. The leap month is followed by month 12 and preceded by month 1 to 11.

15.9 The French Republican Calendar

After the French revolution, a new astronomical calendar was inaugurated in 1792. This was modelled after the Alexandrian calendar (see § 15.2.1). The year began on the day of the autumnal equinox as observed at Paris. There were 12 months in the year, each having 30 days and a meteorological name. These were followed by 5 epagomenal days with a sixth in leap years. There were three "weeks" of 10 days in each month. Each of the days of the year was given a name.

Initially there was a leap day (a *franciade*) every four years, the first in year 4 E.R. Later, modifications of this leap year rule were discussed but never ratified. The years, in the Republican Era (E.R.) were counted from the epoch on Saturday, 1792 September 22 in the Gregorian calendar or Julian Day Number 2 375 840. The calendar was not popular and was abolished by Napoleon who reinstated the Gregorian calendar in 1806.

15.10 The Bahá'i Calendar

The Bahá'i faith arose in the 19th century and its adherents use the Bahá'i or Badi calendar to determine their religious celebrations. The number 19 has special significance in this faith.

The calendar is an astronomical calendar whose year begins on the day of the vernal equinox, but commonly an arithmetic variation is used in which the year begins on March 21 in the Gregorian calendar. There are 19 months, each having 19 days, in the year followed by four epagomenal days with a fifth in leap years; these are inserted at the end of the 18th month. Each of the days of the year is given a name. The years, in the Bahá'i Era (E.B.) are counted from the epoch on Thursday, 1844 March 21 in the Gregorian calendar or Julian Day Number 2 394 647.

15.11 Calendar Conversion Algorithms

15.11.1 Introduction

The conversion of dates in one calendar to the corresponding date in another is best done by converting the date in the first calendar to a Julian Day Number and then converting that to a date in the second. In this section we provide algorithms for converting a variety of arithmetic calendars to Julian Day Numbers and vice versa. These use the method described by Hatcher (1985) and elaborated by Parisot (1986) and by Richards (1998). The calendars and the parameters that are required for each conversion are listed in Table 15.14. Conversions involving the Jewish calendar are treated in § 15.11.4. We also give algorithms for determining the day of the week and of the date of Easter Sunday.

In the algorithms given below, all variables are integers. The solidus (/) denotes integer division in which any remainder is ignored. The symbol * denotes multiplication. mod(A,B) represents the remainder when A is divided by B (i.e., A modulo B). For example:

0/12 = 0	9/12 = 0	15/12 = 1
0*12 = 0	9*12 = 108	15*12 = 180
mod(0,12) = 0	mod(9,12) = 9	mod(15,12) = 3

Table 15.14 Selected arithmetic calendars, with parameters for algorithms

	Calendar[a]	y	j	m	n	r	p	q	v	u	s	t	w	A	B	C
1	Egyptian	3968	47	0	13	1	365	0	0	1	30	0	0			
2	Ethiopian	4720	124	0	13	4	1461	0	3	1	30	0	0			
3	Coptic	4996	124	0	13	4	1461	0	3	1	30	0	0			
4	Republican[b]	6504	111	0	13	4	1461	0	3	1	30	0	0	396	578797	−51
5	Julian	4716	1401	2	12	4	1461	0	3	5	153	2	2			
6	Gregorian	4716	1401	2	12	4	1461	0	3	5	153	2	2	184	274277	−38
7	Civil Islamic	5519	7664	0	12	30	10631	14	15	100	2951	51	10			
8	Bahá'i[c]	6560	1412	19	20	4	1461	0	3	1	19	0	0	184	274273	−50
9	Saka	4794	1348	1	12	4	1461	0	3	1	31	0	0	184	274073	−36

[a] Where #4, 6, 8, and 9 are calendars that intercalate leap days with the same frequency as the in the Gregorian calendar.

[b] Although the French Republican calendar was originally an astronomical calendar, it was abolished in 1806 before the intercalations differed from that of the Gregorian calendar. Discussions were held to amend it with a different rule of intercalation, but the proposals were never put into effect.

[c] Although the Bahá'i calendar was defined as an astronomical calendar, it is generally operated as an arithmetic calendar with a Gregorian frequency of intercalation.

Table 15.15 Number of days, A(**K**,**M**), in the Jewish calendar that precede the first day of the month **M** for a year characterised by **K**

K	M = 1	2	3	4	5	6	7	8	9	10	11	12	13
1	0	30	59	88	117	147	176	206	235	265	294	324	—
2	0	30	59	89	118	148	177	207	236	266	295	325	—
3	0	30	60	90	119	149	178	208	237	267	296	326	—
4	0	30	59	88	117	147	177	206	236	265	295	324	354
5	0	30	59	89	118	148	178	207	237	266	296	325	355
6	0	30	60	90	119	149	179	208	238	267	297	326	356

We also use the notation "$A \geq B$" to mean "A is greater than or equal to B"; "$A > B$" to mean "A is greater than B"; and "$A < B$" to mean "A is less than B."

In several of the algorithms we use Table 15.15. The entry in this table in row K and in the column headed by M gives the number of days in a Jewish year which precede month M, in a year of character K. We refer to this as A(K,M).

A date is represented by the year, **Y**, in the appropriate era; a month number, **M** (epagomenal days are presumed to fall in an extra, short month), and the day of the month, **D**. Julian Day Numbers are represented by **J**. A number **W** is used to represent the day of the week with **W** = 1 for Sunday, . . . , **W** = 7 for Saturday.

15.11.2 Calculating the Day of the Week

Algorithm 1. The day of the week number, **W**, of Julian Day Number **J** is given by:

$$\mathbf{W} = 1 + \text{mod}(J + 1, 7)$$

Algorithm 2. The day of the week number, **W**, of the date **D/M/Y** in the Gregorian calendar is given by:

1. $a = \text{mod}(9 + \mathbf{M}, 12)$
2. $b = \mathbf{Y} - a/10$
3. $\mathbf{W} = 1 + \text{mod}(2 + \mathbf{D} + (13 * a + 2)/5 + b + b/4 - b/100 + b/400, 7)$

15.11.3 Interconverting Dates and Julian Day Numbers

Algorithm 3. To convert a date **D/M/Y** in one of the calendars listed in Table 15.14 to a Julian Day Number, **J**:

1. $h = \mathbf{M} - m$
2. $g = \mathbf{Y} + y - (n - h)/n$
3. $f = \text{mod}(h - 1 + n, n)$
4. $e = (p * g + q)/r + \mathbf{D} - 1 - j$
5. $\mathbf{J} = e + (s * f + t)/u$

For the Saka calendar (10), replace step 5 by:

5a. $Z = f/6$

5b. $\mathbf{J}e + ((31 - Z) * f + 5 * Z)/u$

For Gregorian type calendars (4, 6, 8, and 9) finish with:

6. $\mathbf{J} = \mathbf{J} - (3 * ((g + A)/100))/4 - C$

Algorithm 4. To convert a Julian Day Number, **J**, to a date in one of the calendars listed in Table 15.14:

1. $f = \mathbf{J} + j$
2. $e = r * f + v$
3. $g = \text{mod}(e, p)/r$
4. $h = u * g + w$
5. $\mathbf{D} = (\text{mod}(h, s))/u + 1$
6. $\mathbf{M} = \text{mod}(h/s + m, n) + 1$
7. $\mathbf{Y} = e/p - y + (n + m - \mathbf{M})/n$

For Gregorian type calendars (4, 6, 8, and 9) insert between steps 1 and 2:

1a. $f = f + (((4 * \mathbf{J} + B)/146\,097) * 3)/4 + C$

For the Saka calendar (9), replace steps 4 and 5 with:

a. $X = g/365$

b. $Z = g/185 - X$

c. $s = 31 - Z$

d. $w = -5 * Z$

4a. $h = u * g + w$

5a. $\mathbf{D} = (6 * X + \text{mod}(h, s))/u + 1$

15.11.4 Converting Dates in the Jewish Calendar

Algorithm 5. To calculate the Julian Day Number, **J**, of the 1st day of Tishri in the Jewish year **Y** A.M.:

1. $b = 31\,524 + 765\,433 * ((235 * \mathbf{Y} - 234)/19)$
2. $d = b/259\,20$
3. $e = \text{mod}(b, 259\,20)$
4. $f = 1 + \text{mod}(d, 7)$
5. $g = \text{mod}(7 * \mathbf{Y} + 13, 19)/12$
6. $h = \text{mod}(7 * \mathbf{Y} + 6, 19)/12$

7. If $e \geq 19440$
   or $e \geq 9924$ and $f = 3$ and $g = 0$
   or $e \geq 16\,788$ and $f = 2$ and $g = 0$ and $h = 1$
   then $d = d + 1$
8. $\mathbf{J} = d + \text{mod}(\text{mod}(d + 5, 7), 2) + 347\,997$

N.B. If integers requiring more than 15 bits are not acceptable, steps 1 to 3 may be replaced by:

1a. $a = (235 * \mathbf{Y} - 234)/19$

1b. $b = 204 + 793 * a$

1c. $c = 5 + 12 * a + b/1080$

2a. $d = 1 + 29 * a + c/24$

3a. $e = \text{mod}(b, 1080) + 1080 * \text{mod}(c, 24)$

Algorithm 6. To calculate the Jewish year, Y, in which Julian Day Number J falls:

1. $\mathbf{M} = (25\,920 * (\mathbf{J} - 347\,996))/765\,433$
   N.B. The ratio $25\,820/765\,433 = 0.033\,863\,18$;
   M may be set to the integral part of $0.033\,863\,18 * (\mathbf{J} - 347\,996)$.
2. $Y = 19 * (M/235) + (19 * \text{mod}(M, 235) - 2)/235 + 1$
3. Calculate, using algorithm 5, the Julian Day Number, **K**, of 1 Tishri
   for the year **Y** A.M.
4. If $\mathbf{K} > \mathbf{J} : \mathbf{Y} = \mathbf{Y} - 1$

Algorithm 7. To calculate the date in the Jewish calendar, **D/M/Y** which corresponds to Julian Day Number **J**.

1. Calculate the Jewish year, Y A.M., in which J falls using algorithm 6.
2. Calculate, using algorithm 5, the Julian Day Number,
   a, of 1 Tishri 1 in the year Y A.M.
3. Calculate, using algorithm 5, the Julian Day Number,
   b, of 1 Tishri 1 in the year Y+1 A.M.
4. $\mathbf{K} = b - a - 352 - 27 * (\text{mod}(7 * \mathbf{Y} + 13, 19)/12)$
   N.B. **K** characterizes the year **Y**
5. $c = \mathbf{J} - a + 1$
6. From Table 15.15, find the highest **M** such that A(**K**,**M**) < c
7. $\mathbf{D} = c - A(\mathbf{M}, \mathbf{K})$

Algorithm 8. To calculate the Julian Day Number, **J**, which corresponds to a Jewish date **D/M/Y**:

1. Calculate, using algorithm 5, the Julian Day Number,
   a, of 1 Tishri 1 in the year **Y** A.M.
2. Calculate, using algorithm 15.11.4.1, the Julian Day Number,
   b, of 1 Tishri 1 in the year **Y**+1 A.M.

3. $K = b - a - 352 - 27 * (\text{mod}(7 * \mathbf{Y} + 13, 19)/12)$
4. $\mathbf{J} = a + A(\mathbf{M} - 1, K) + \mathbf{D} - 1$

15.11.5 Calculating the Date of Easter

Easter Sunday in the Christian ecclesiastical calendar falls in March (month 3) or April (month 4).

Algorithm 9. To calculate the month $\mathbf{M}$ and day of the month $\mathbf{D}$ of Easter Sunday in the year $\mathbf{Y}$ in the Julian calendar:

1. $a = 22 + \text{mod}(225 - 11 * \text{mod}(\mathbf{Y}, 19), 30)$
2. $g = a + \text{mod}(56 + 6 * \mathbf{Y} - \mathbf{Y}/4 - a, 7)$
3. $\mathbf{M} = 3 + g/32$
4. $\mathbf{D} = 1 + \text{mod}(g - 1, 31)$

Algorithm 10. To calculate the month $\mathbf{M}$ and day of the month $\mathbf{D}$ of Easter Sunday for the year $\mathbf{Y}$ in the Gregorian calendar:

1. $a = \mathbf{Y}/100$
2. $b = a - a/4$
3. $c = \text{mod}(\mathbf{Y}, 19)$
4. $e = \text{mod}(15 + 19 * c + b - (a - (a - 17)/25)/3, 30)$
5. $f = e - (c + 11 * e)/319$
6. $g = 22 + f + \text{mod}(140004 - Y - Y/4 + b - f, 7)$
7. $\mathbf{M} = 3 + g/32$
8. $\mathbf{D} = 1 + \text{mod}(g - 1, 31)$

An online calculator for calculating the date of Easter is available in URL[7].

15.12 Calendar Conversion Programs

The following programs and internet sites may be useful to the reader. The appearance of these does not constitute endorsement by the United States Department of Defense (DoD), the United States Department of the Navy, or the U.S. Naval Observatory of the linked web sites, or the information, products or services contained therein. The above-mentioned parties do not exercise any editorial control over the information you may find at these locations nor do they accept responsibility for loss or damage arising from the use of the information on these site.

1. CALENDRICA
   This interconverts between dates in 25 calendars. It is supplied with Calendrical Calculations Millennium Edition: (Reingold and Dershowitz 2001)

2. CALENDAR
   This interconverts between dates in 15 calendars; it may be downloaded from URL[6]: http://www.ricswal.plus.com
3. CALISTO
   This interconverts dates, particularly English regnal and ecclesiastical dates. It may be downloaded from URL[9].

Acknowledgments

Acknowledgments are due to LeRoy Doggett as some of the material in this chapter is taken from Chapter 12 of the previous edition (Doggett 1992).

REFERENCES

1. Calendopaedia, an encyclopaedia of calendrical information, by Michael Astbury: http://calendopedia.com/.
2. The home page of Dr. J.R. Stockton. It provides information with a mathematical emphasis on various aspects of calendars and astronomy: http://www.merlyn.demon.co.uk.
3. A commercial site sponsoring Project Pluto, providing information on calendars: http://www.projectpluto.com.
4. The home page of Professor H. Aslaksen providing information concerning several calendars including the mathematics of the Chinese calendar: http://www.math.nus.edu.sg/aslaksen/calendar/chinese.shtml.
5. The Web Exhibits Project, an educational site sponsored by various educational organisations providing information on a variety of calendar: http://webexhibits.org.
6. The home page of E.G. Richards containing a detailed mathematical treatment of D.A. Hatcher's method of interconverting dates. It also contains algorithms for interconverting calendars and a calendar conversion program which may be downloaded: http://www.ricswal.plus.com.
7. The website of the Astronomical Applications Department of the U.S. Naval Observatory containing information on various calendars and a converter to get the Julian date to calendar date and vice versa: http://aa.usno.navy.mil/.
8. A commercial site which provides links and information a variety of calendrical topics: http://calendarzone.com.
9. A useful glossary of special days and calendrical terms. You can also download a calendar conversion program: http://freespace.virgin.net/guy.etchells/Cal.htm.
10. An invitation to participate in the Moon Watch project and report your sightings: http://astro.ukho.gov.uk/moonwatch/.

Aveni, A. F. (1990). *Empires of Time*. London: I.B. Tauris & Co. Ltd.

Bickerman, E. J. (1980). *Chronology of the Ancient World*. London: Thames and Hudson.

Blackburn, B. and L. Holford-Stevens (1999). *The Oxford Companion to the Year*. Oxford: Oxford University Press.

Bruin, F. (1981). The First Visibility of the Lunar Crescent. *Vistas in Astronomy 21*, 331–358.

Burnaby, S. B. (1901). *The Elements of the Jewish and Muhammadan Calendars*. London: George Bell & Sons.

Butcher, S. (1877). *The Ecclesiastical Calendar: Its Theory and Construction*. London: Macmillan.

Calendar Reform Committee (1955). Report of the Calendar Reform Committee. Technical report, Council for Scientific and Industrial Research, New Delhi.

Cappelli, A. (1930). *Cronologia Cronografia e Calendario perpetuo*. Milan.

Cassini, J. (1740). *Tables astronomiques du Soleil et de la Lune*. Paris.

Chapront-Touzé, M. and J. Chapront (1988). ELP 2000–85: a Semi-Analytical Lunar Ephemeris Adequate for Historical Times. *Astronomy and Astrophysics 190*, 342–352.

Chatterjee, S. K. (1987). Indian Calendars. In G. Swarup et al. (Eds.), *History of Oriental Astronomy*, Cambridge. Cambridge University Press.

Cheney, C. R. (1981). *A Handbook of Dates for Students of English History*. London: Royal Historical Society.

Colgrave, B. and R. A. B. Mynors (1969). *Bede's Ecclesiastical History of the English People*. Oxford.

Colson, F. (1926). *The Week*. Cambridge: Cambridge University Press.

Coyne, G. V., M. A. Hoskin, and O. Pedersen (Eds.) (1983). *Gregorian Reform of the Calendar*, Vatican City. Pontifica Academia Scientiarum.

Danjon, A. (1959). *Astronomie Génerale*. Paris.

Delambre, J. B. J. (1821). *Histoire de l'astronomie Moderne*. Paris.

Doggett, L. E. (1992). Calendars. In *Explanatory Supplement to The Astronomical Almanac*, Chapter 12. Mill Valley, CA: University Science Books.

Doggett, L. E. and B. E. Schaefer (1989). Results of the July Moonwatch. *Sky & Telescope 77*, 373–375.

Doggett, L. E., P. K. Seidelmann, and B. E. Schaefer (1988). Moonwatch—July 14, 1988. *Sky & Telescope 76*, 34–35.

Fotheringham, J. K. (1935). The Calendar. In *The Nautical Almanac*, pp. 755–771. London.

Fraser, J. T. (1987). *Time; the Familiar Stranger*. Amherst: University of Massachusetts Press.

Freeman-Grenville, G. S. P. (1963). *The Muslim and Christian Calendars*. London.

Ginzel, F. K. (1906, 1911). *Handbuch der Mathematischen und Technischen Chronologie*. Leipzig.

Grotefend, H. and O. Grotefend (1941). *Taschenbuch der Zeitrechnung des deutschen Mittelalters und der Neuzeit*. Hannover.

Hastings, J. (Ed.) (1910). *Encyclopaedia of Religion and Ethics*, Edinburgh. Clark.

Hatcher, D. A. (1985). Generalised Equations for Julian Day Numbers and Calendar Dates. *Journal of the Royal Astronomical Society 26*, 151–155.

Herschel, J. F. W. (1849). *Outlines of Astronomy*. London.

Ilyas, M. (1984). *A Modern Guide to Astronomical Calculations of Islamic Calendar Times and Qibla*. Kuala Lumpur.

King, D. A. (1987). Some Early Islamic Tables for Determining Lunar Crescent Visibility. In D. King and G. Saliba (Eds.), *From Deferent to Equant: A Volume of Studies in the History of Science in the Ancient and Medieval Near East in Honour of E. S. Kennedy*, Volume 500 of *Annals of the New York Academy of Sciences*. New York.

Laskar, J. (1986). Secular Terms of Classical Planetary Theories Using the Results of General Relativity. *Astronomy and Astrophysics 157*, 59–70.

Mayr, J. and B. Spuler (1961). *Wüstenfeld-Maler'sche Vergleichungs-Tabellen*. Wiesbaden.

Meeus, J. and D. Savoie (1992). The History of the Tropical Year. *Journal of the British Astronomical Association 102*, 40–42.

Michels, A. K. (1978). *The Calendar of the Roman Republic*. Princeton: Princeton University Press.

Needham, J. (1959). *Science and Civilisation in China*. Cambridge: Cambridge University Press.

Neugebauer, O. (1975). *A History of Ancient Mathematical Astronomy, Part III*. New York.

Oudin, J. M. (1940). Étude sur la Date de Pâques. *Bull. Astronomique (2) 12*, 391–410.

Parise, F. (1982). *The Book of Calendars*. New York.

Parisot, J. P. (1986). Additif to the Paper of D.A. Hatcher: 'Generalised Equations for Julian Day Numbers and Calendar Dates'. *Quarterly Journal of the Royal Astronomical Society 27*, 506–507.

Pingree, D. (1978). History of Mathematical Astronomy in India. In *Dictionary of Scientific Biography*, Volume XV, pp. 533–633. New York.

Poole, R. (1998). *Time's alteration: Calendar Reform in Early Modern England*. London: University College London Press.

Purple Mountain Observatory (1984). *The Newly Compiled Perpetual Chinese Calendar (1840–2050)*. Beijing: Popular Science Publishing House.

Reingold, E. M. and N. Dershowitz (1997). *Calendrical Calculations*. Cambridge: Cambridge University Press.

Reingold, E. M. and N. Dershowitz (2001). *Calendrical Calculations Millennium Edition*. Cambridge: Cambridge University Press.

Reingold, E. M. and N. Dershowitz (2002). *Calendrical Tabulations*. Cambridge: Cambridge University Press.

Resnikoff, L. A. (1943). Jewish Calendar Calculations. *Scripta Mathematica 9*, 274–277.

Richards, E. G. (1998). *Mapping Time: The Calendar and its History*. Oxford: Oxford University Press.

Scalinger, J. J. (1583). *De emendatione temporum*. Paris.

Schaefer, B. E. (1988). Visibility of the Lunar Crescent. *Quarterly Journal of the Royal Astronomical Society 29*, 511–523.

Sewell, R. (1912). *Indian Chronology*. London: George Allen.

Sewell, R. (1989). *The Siddhantas and the Indian Calendar*. New Delhi: Asian Educational Services. reprinted.

Sewell, R. and S. B. Dikshit (1911). *The Indian Calendar*. London: George Allen.

Simon, J. L., P. Bretagnon, J. Chapront, M. Chapront-Touzé, G. Francou, and J. Laskar (1994). Numerical expressions for precession formulae and mean elements for the Moon and the planets. *Astronomy and Astrophysics 282*, 663–683.

Sivin, N. (1969). *Cosmos and Computation in Early Chinese Mathematical Astronomy*. Leiden.

Spier, A. (1952). *The Comprehensive Hebrew Calendar*. New York.

Steel, D. (2000). *Marking Time*. New York: Wiley.

Stephenson, F. R. (1997). *Historical Eclipses and Earth's Rotation*. Cambridge: Cambridge University Press.

Tung Tso-Pin (1960). *Chronological Tables of Chinese History*. Hong Kong.

Zerubavel, E. (1989). *The Seven Day Circle*. Chicago and London: University of Chicago Press.

APPENDIX A

Bases and Constants

A.1 Bases

Each year, the data presented in the *The Astronomical Almanac* and the underlying bases used to generate them are reviewed. Typically modifications are made in every edition. Section L (Notes and References) documents the scientific bases underlying that year's publication. This includes such items as the fundamental celestial and terrestrial reference systems, precession and nutation models, timescales, ephemerides, and sources of stellar data. Readers interested in such material should refer to the individual editions of *The Astronomical Almanac*. Additionally, Section K (Tables and Data) and *The Astronomical Almanac Online* (URL[1]) provide tables of selected astronomical constants.

A.2 Astronomical Constants

At its 2009 General Assembly in Rio de Janeiro, the International Astronomical Union adopted Resolution B2 on astronomical constants (URL[2]). The IAU (2009) System of Astronomical Constants is given at URL[3]. This list replaces the IAU (1976) System of Astronomical Constants. The 1976 values have long been recognized as obsolete, and for many years an IAU working group maintained a list of the "current best estimates" of the values of important quantities. Over the years, various revisions of the International Earth Rotation and Reference Systems Service (IERS) Conventions (formerly called the IERS Standards) have also listed numerical standards that were widely used within the astronomical, geodetic, and geophysical communities. Constant values are always tied to specific theories, and because the dynamical theories (including those of precession and nutation and the planetary ephemerides) evolved rapidly in the 1980s and 1990s, there was a reluctance to officially endorse a new set of constants that would be superseded in a few years.

However, with the adoption of new theories of nutation (in 2000) and precession (in 2006), a consensus emerged within Division I of the IAU in 2006 that the time had come to officially recommend a new set of constant values. The IAU Working Group on Numerical Standards of Fundamental Astronomy was established to provide a list of recommended values (IAU 2009; Luzum et al. 2011) and, as mentioned above, the working group's list was adopted at the 2009 IAU General Assembly.

The latest edition of the IERS Conventions (IERS 2010) has incorporated the IAU (2009) System of Astronomical Constants into its recommended list of numerical standards, so there is now uniformity in the recommended constant values across related fields.

A.2.1 CODATA

On a broader scope, in 1966 the International Council of Science (ICSU) established the Committee on Data for Science and Technology, CODATA (URL[4]). CODATA's major objective is to help foster and advance science and technology through developing and sharing knowledge about data and the activities that work with data. CODATA maintains lists of internationally recognized values of the fundamental physical constants. Users are encouraged to use the links at URL[4] for further details.

A.2.2 Future of the Astronomical Unit

As this book goes to press (2012), there have been discussions about "freezing" the value of the astronomical unit at its 2009 value ($1.495\,978\,707\,00 \times 10^{11}$ m in TDB-compatible units), and a proposal to that effect will be presented at the IAU General Assembly in 2012. If adopted, the astronomical unit would cease to be a measurable value and would become a defining constant. Such a change would have implications for the computation of planetary ephemerides, the most important of which would be to make the heliocentric gravitational constant (essentially, the mass of the Sun) an adjustable parameter in the construction of the ephemerides. See the discussions by Capitaine and Guinot (2009) and Klioner (2008, Section 10).

REFERENCES

1. The Astronomical Almanac Online:
http://asa.usno.navy.mil or http://asa.hmnao.com.

2. IAU Resolutions Adopted by the General Assemblies:
http://www.iau.org/administration/resolutions/general_assemblies/.

3. IAU Numerical Standards for Fundamental Astronomy:
http://maia.usno.navy.mil/NSFA/.

4. Committee on Data for Science and Technology, CODATA:
http://www.codata.org/.

Capitaine, N. and B. Guinot (2009). The Astronomical Units. In M. Soffel and N. Capitaine (Eds.), *Proceedings of the Journées 2008 Systèmes de Référence Spatio-Temporels*, Lohrmann-Observatorium and Observatoire de Paris, pp. 73–74. at http://syrte.obspm.fr/jsr/journees2008/Capitaine2.pdf and http://arxiv.org/abs/0812.2970.

IAU (2008). Division I / Working Group on Numerical Standards of Fundamental Astronomy Triennial Report 2006-2009. In K. A. van der Hucht (Ed.), *Transactions of the International Astronomical Union*, Volume XXVI B, Cambridge, pp. 60–62. Cambridge University Press. Proc. 26th General Assembly, Prague, 2006.

IERS (2010). Conventions (2010). Technical Note 36, International Earth Rotation and Reference Systems Service, Frankfurt am Main. Verlag des Bundsesamts für Kartographie und Geodäsie, G. Petit and B. Luzum (Eds.).

Klioner, S. A. (2008). Relativistic Scaling of Astronomical Quantities and the System of Astronomical Units. *Astronomy and Astrophysics 478*, 951–958.

Luzum, B., N. Capitaine, A. Fienga, W. Folkner, T. Fukushima, J. Hilton, C. Hohenkerk, G. Krasinsky, G. Petit, E. Pitjeva, M. Soffel, and P. Wallace (2011). The IAU 2009 system of astronomical constants: the report of the IAU working group on numerical standards for Fundamental Astronomy. *Celestial Mechanics and Dynamical Astronomy 110*, 293–304.

APPENDIX B

Acronyms

ΔT	TT − UT1
ΔUT1	UT1 − UTC, to ± 0.1 second
μas	microarcsecond
2MASS	Two Micron All Sky Survey
AAM	Atmospheric angular momentum
AAVSO	American Association of Variable Star Observers
AC	Astrographic Catalogue
ACES	Atomic Clock Ensemble in Space
ACT	Astrographic Catalog Tycho
AD	Anno Domini (Common Era)
AGN	Active Galactic Nuclei
AGU	American Geophysical Union
A.H.	Anno Hegira (Islamic Calendar)
A.M.	Anno Mundi (Jewish Calendar)
APOLLO	Apache Point Observatory Lunar Laser ranging Operation
AsA	The Astronomical Almanac
AsAO	The Astronomical Almanac Online
A.U.C.	Ab Urbe Condita (Roman Calendar)
BC	Before Christ (Before Common Era)
BCE	Before Common Era
BCRS	Barycentric Celestial Reference System
B.E.	Badi Era (Baha'i calendar)
BIH	Bureau Internationale de l Heure
BIPM	Bureau International des Poids et Mesures
BSC5	Yale Bright Star Catalog
BTS	BIH Terrestrial System
c	speed of light
C/A	coarse acquisition code, GPS
CCD	Charge coupled device
CCDS	Comite Consultatif pour la Definition de la Seconde
CCIR	International Radio Consultative Committee

CCRs	corner cube retroreflectors
CDS	Centre de Donnees stellaires in Strasbourg
CE	Common Era (Anno Domini)
CERGA	Centre d'Etudes et de Recherches Geodynamics et Astronomiques
CERI	Connected Element Radio Interferometry
CEP	Celeatial Ephemeris Pole
CfA	Center for Astrophysics
CGPM	Conference General des Poids et Mesures
CIF	Celestial Intermediate Frame
CIO	Conventional International Origin (obsolete)
CIO	Celestial Intermediate Origin
CIP	Celestial Intermediate Pole
CIPM	Comite International des Poids et Mesures
CMP	conventional mean pole
CNES	Centre National d'Etudes Spatiales
CRS	Celestial Reference System
CTRF	Conventional Terrestrial Reference Frame
CTRS	Conventional Terrestrial Reference System
cy	century
DAO	Dominion Astrophysical Observatory
DE	Development Ephemeris
DE405/LE405	JPL's Development & Lunar Ephemeris, number 405
DMA	Defense Mapping Agency (then NIMA, now NGA)
DMS	Hipparcos Double Star and Multiple System annex
DoD	Department of Defense
DORIS	Doppler Orbitography and Radio positioning Integrated by Satellite
EAL	Echelle Atomique Libre
EB	Bahai Era
EGM	Earth Gravitational Model
EN	Era of Nabonassar
EOC	Earth Orientation Center
EOP	Earth Orientation Parameters
E.R.	Republican Era (French Republican Calendar)
ERA	Earth Rotation Angle
ERP	Earth Rotation Parameters
ERS	European remote-sensing satellite
ESA	European Space Agency
ET	Ephemeris Time
ETRF	European Terrestrial Reference Frame
FCN	Free Core Nutation
FK3	Fundamental Katalog 3

FK4	Fundamental Catalogue 4
FK5	Fundamental Catalogue 5
GAST	Greenwich Apparent Sidereal Angle
GC	General Catalogue
GCRF	Geocentric Celestial Reference Frame
GCRS	Geocentric Celestial Reference System
GCT	Greenwich Civil Time
GCVS	General Catalog of Variable Stars
GEM	Goddard Earth Model
GGM	GRACE Gravity Model
GHA	Greenwich Hour Angle
GLONASS	GLObal NAvigation Satellite System
GMAT	Greenwich Mean Astronomical Time
GMST	Greenwich Mean Sidereal Time
GMT	Greenwich Mean Time
GNSS	Global Navigation Satellite System
GPS	Global Positioning System
GRACE	Gravity Recovery and Climate Experiment
GRBs	Gamma Ray Bursts
GRS	Geocentric Reference System or Geodetic Reference System
GRT	General Relativity Theory
GSD	Greenwich sidereal date
GSFC	Goddard Space Flight Center
GST	Greenwich Sidereal Time
GTRF	Geocentric True Reference Frame
GTRS	Geocentric True Reference System
HCRS	Hipparcos Catalog Reference System
HCRF	Hipparcos Catalog Reference Frame
HMNAO	Her Majesty's Nautical Almanac Office
HST	Hubble Space Telescope
IAA	Institute of Applied Astronomy
IAG	International Association for Geodesy
IAU	International Astronomical Union
IAU 2000A	IAU precession-nutation model of 2000 (use between 2003–2008)
IAU 2006/2000A	IAU precession-nutation model of 2006 (use after 2009)
ICRF	International Celestial Reference Frame
ICRF1	International Celestial Reference Frame (1st version)
ICRF2	International Celestial Reference Frame (2nd version)
ICRS	International Celestial Reference System
IDS	International DORIS Service
IDS	Index Catalog of Visual Double Stars

IERS	International Earth Rotation and Reference Systems Service
IGS	International GPS Service, International GNSS Service
ILRS	International Laser Ranging Service
ILS	International Latitude Service
IPMS	International Polar Motion Service
IRP	IERS Reference Pole
IRS	International Reference Star catalog
ITRF	International Terrestrial Reference Frame
ITRF2	2nd ITRF
ITRS	International Terrestrial Reference System
ITU-R	International Telecommunications Union-Radio communications
IUGG	International Union of Geodesy and Geophysics
IVS	International VLBI Service for Geodesy and Astronomy
JD	Julian Date
JDN	Julian Day Number
JGM	Joint Gravity Model
JPL	Jet Propulsion Laboratory
K	degrees Kelvin
LAGEOS	LAser GEOdynamics Satellites
LAST	Local Apparent Sidereal Time
LAT	Local Apparent Solar Time
LCC	Lambert conformal conic
LCT	Local Civil Time
LE	Lunar Ephemeris
LEDA	Lyon-Meudon Extragalactic Database
LHA	Local hour angle
LLR	Lunar Laser Ranging
LMST	Local Mean Sidereal Time
LMSoT	Local Mean Solar Time
LMT	Local Mean Time
LOD	Length of Day
LORAN-C	Long Range Aid to Navigation
LQAC	Large Quasar Astrometric Catalog
LQRF	Large Quasar Reference Frame
LS+AR	least-squares, autoregressive
LST	Local Sidereal Time
mas	milliarcsecond
MCC	Russian Mission Control Center
MJD	Modified Julian Day
MK	Morgan-Keenan system
MLRS2	McDonald Laser Ranging Station 2

mm	millimeter
MSL	mean sea level
NAD	North American Datum
nas	nanoarcsecond
NASA	National Aeronautical and Space Agency
NAVD	North American Vertical Datum
NCEP	National Centers for Environmental Prediction
NEA	near Earth asteroids
NED	NASA/IPAC Extragalactic Database
NGA	National Geospatial-intelligence Agency (formerly DMA and NIMA)
NGS	National Geodetic Survey
NIMA	National Imaging and Mapping Agency (formerly DMA, now NGA)
NIST	National Institute of Standards and Technology
nm	nanometer
NNSS	Navy Navigational Satellite System
NOAA	National Oceanic and Atmospheric Administration
NOGAPS	Navy Operational Global Atmospheric Prediction System
NOMAD	Naval Observatory Merged Astrometric Database
NOVAS	Naval Observatory Vector Astrometry Software
NRCAN	Natural resources CANada
ns	nanosecond
NSWC	Naval Surface Weapons Center
NTP	Network Time Protocol
OAM	ocean angular momentum
ppb	parts per billion
PPN	parameterized post-Newtonian
PREM	preliminary reference Earth model
PRN	pseudorandom noise
PZT	Photographic Zenith Tube
RC3	Third Reference Catalogue of Bright Galaxies
RGO	Royal Greenwich Observatory
rms	root mean square
RS/PC	Rapid Service/Prediction Center
s	second
SA	selective availability
SAO	Smithsonian Astrophysical Observatory
SBL	Special Bureau on Loading
SHIG	superfluid helium interference gyroscopes
SI	Systeme International
SIMBAD	main database of the CDS
SIRGAS	Sistema de Referencia Geocentrico para Las Américas

SLR	Satellite Laser Ranging
SOFA	Standards of Fundamental Astronomy
SRT	Special Relativity Theory
ST	Sidereal Time
STScI	Space Telescope Science Institute
TAI	International Atomic Time
TCB	Barycentric Coordinate Time
TCG	Geocentric Coordinate Time
TDB	Barycentric Dynamical Time
TDT	Terrestrial Dynamical Time
T_{eph}	Barycentric Ephemeris Time
TIO	Terrestrial Intermediate Origin
TIRS	Terrestrial Intermediate Reference System
TRS	Terrestrial Reference System
TT	Terrestrial Time
TWSTT	Two Way Satellite Time Transfer
UBVRI	ultraviolet blue visual red infrared
UCAC	USNO CCD Astrographic Catalog
UPS	Universal Polar Stereographic
USNAO	U.S. Nautical Almanac Office
USNG	U.S. National Grid
USNO	U.S. Naval Observatory
USNO-B	USNO all-sky catalog of $\approx 10^8$ stars
UT	Universal Time
UTC	Universal Time Coordinated
UTM	Universal Transverse Mercator
UT0	Universal Time 0
UT1	Universal Time 1
UT1R	UT1 regularized
UT2	Universal Time 2
VLA	Very Large Array
VLBA	Very Large Baseline Array
VLBI	Very Long Baseline Interferometer
WDS	Washington Double Star Catalog
WGD	World Geodetic Datum
WGD2000	World Geodetic Datum 2000
WGS	World Geodetic System
WMC	Washington Multiplicity Catalog
WMM	World Magnetic Model
YB6	Lick Yale proper motion plates

APPENDIX C

Glossary

aberration (of light): the relativistic apparent angular displacement of the observed position of a celestial object from its *geometric position*, caused by the motion of the observer in the *reference system* in which the trajectories of the observed object and the observer are described. (See *aberration, planetary.*)

aberration, annual: the component of *stellar aberration* resulting from the motion of the Earth about the Sun.

aberration, diurnal: the component of *stellar aberration* resulting from the observer's *diurnal motion* about the center of the Earth due to Earth's rotation.

aberration, E-terms of: the terms of *annual aberration* which depend on the *eccentricity* and longitude of *perihelion* of the Earth. (See *Keplerian elements.*)

aberration, elliptic: see *aberration, E-terms of.*

aberration, planetary: the apparent angular displacement of the observed position of a solar system body from its instantaneous geometric direction as would be seen by an observer at the geocenter. This displacement is produced by the combination of *aberration of light* and *light-time displacement*.

aberration, secular: the component of *stellar aberration* resulting from the essentially uniform and almost rectilinear motion of the entire solar system in space. Secular *aberration* is usually disregarded.

aberration, special relativistic: In special relativity the velocity of light is constant in all inertial frames, and the Lorentz formula for addition of velocities applies. To first order Newtonian and relativistic aberration agree.

aberration, stellar: the apparent angular displacement of the observed position of a celestial body resulting from the motion of the observer. Stellar aberration is divided into diurnal, annual, and secular components. (See *aberration, annual; aberration, diurnal; aberration, secular.*)

Absolute time: conceptually a unique uniform time that can be measured by any ideal clock irrespective of its position and state of motion in the whole universe; used in Newtonian physics and mechanics.

altitude: the angular distance of a celestial body above or below the *horizon*, measured along the great circle passing through the body and the *zenith*. Altitude is 90° minus the *zenith distance.*

analemma: a curve showing the angular offset, as a function of time, of a celestial body (usually the Sun) from its mean position on the *celestial sphere* as viewed from another celestial body (usually the Earth). In the case of the Sun as seen from the Earth this is a curve resembling a figure eight that is commonly printed on globes.

angle of the vertical: see *reduction in latitude.*

angular momentum: the measure of the extent to which an object will continue to rotate or revolve about a reference point unless acted upon by an external torque.

angular momentum vector: a vectorial integral of motion of a body. In an *inertial frame of reference*, the time-derivative of the angular momentum vector is equal to the vectorial sum of the external torques. The angular momentum can be decomposed into a sum of the orbital angular momentum vector (associated with the orbital motion of the body as a whole) and the spin angular momentum vector (associated with the rotation of the body about its center of mass). The orbital angular-momentum vector is equal to the mass of the body multiplied by the cross-product of the position and the velocity of the center of mass. The spin angular-momentum vector is equal to the product of the inertia *tensor* by the angular velocity vector.

annual parallax: see *parallax, heliocentric.*

anomaly: the angular separation of a body in its *orbit* from its *pericenter*.

anomaly, eccentric: in undisturbed elliptic motion, the angle measured at the center of the *orbit* ellipse from *pericenter* to the point on the circumscribing auxiliary circle from which a perpendicular to the major axis would intersect the orbiting body. (See *anomaly, mean; anomaly, true.*)

anomaly, mean: the product of the *mean motion* of an orbiting body and the interval of time since the body passed the *pericenter*. Thus, the mean anomaly is the angle from the pericenter of a hypothetical body moving with a constant angular speed that is equal to the mean motion. In realistic computations, with disturbances taken into account, the mean anomaly is equal to its initial value at an *epoch* plus an integral of the mean motion over the time elapsed since the epoch. (See *anomaly, eccentric; anomaly, mean at epoch; anomaly, true.*)

anomaly, mean at epoch: the value of the *mean anomaly* at a specific *epoch*, i.e., at some fiducial moment of time. It is one of the six *Keplerian elements* that specify an *orbit*. (See *orbital elements.*)

anomaly, true: the angle, measured at the focus nearest the *pericenter* of an *elliptical orbit*, between the pericenter and the *radius vector* from the focus to the orbiting body; one of the standard *orbital elements*. (See *anomaly, eccentric; anomaly, mean.*)

aphelion: the point in an *orbit* that is the most distant from the Sun.

apocenter: the point in an *orbit* that is farthest from the origin of the *reference system*. (See *aphelion; apogee.*)

apogee: the point in an *orbit* that is the most distant from the Earth. Apogee is sometimes used with reference to the apparent orbit of the Sun around the Earth.

apparent place (or position): the *proper place* of an object expressed with respect to the *true (intermediate) equator and equinox of date*.

apparent solar time: see *solar time, apparent.*

appulse: the least apparent distance between one celestial object and another, as viewed from a third body. For objects moving along the *ecliptic* and viewed from the Earth, the time of appulse is close to that of *conjunction* in *ecliptic longitude*.

Aries, First point of: another name for the *vernal equinox*.

aspect: the position of any of the *planets* or the Moon relative to the Sun, as seen from the Earth.

astrographic place: same as *astrometric place*. Obsolete.

astrometric ephemeris: an *ephemeris* of a solar system body in which the tabulated positions are *astrometric places*. Values in an astrometric ephemeris are essentially comparable to catalog *mean places* of stars after the star positions have been updated for *proper motion* and *parallax*.

astrometric place (or position): the direction of a solar system body formed by applying the correction for *light-time displacement* to the *geometric position*. Such a position is directly comparable with the catalog positions of background stars in the same area of the sky, after the star positions have been updated for *proper motion* and *parallax*. There is no correction for *aberration* or *deflection of light* since it is assumed that these are almost identical for the solar system body and background stars. An astrometric place is expressed in the *reference system* of a star catalog; in *The Astronomical Almanac*, the reference system is the *International Celestial Reference System (ICRS).*

astronomical coordinates: the longitude and latitude of the point on Earth relative to the *geoid*. These coordinates are influenced by local gravity anomalies. (See *latitude, terrestrial; longitude, terrestrial; zenith.*)

astronomical refraction: see *refraction, astronomical.*

astronomical unit (au): the radius of a circular *orbit* in which a body of negligible mass, and free of *perturbations*, would revolve around the Sun in $2\pi/k$ *days*, k being the *Gaussian gravitational constant*. This is slightly less than the *semimajor axis* of the Earth's orbit.

astronomical zenith: see *zenith, astronomical.*

atmospheric loading: the crustal deformation caused by changes in the weight of a column of air.

atomic second: see *second, Système International (SI).*

augmentation: the amount by which the apparent *semidiameter* of a celestial body, as observed from the surface of the Earth, is greater than the semidiameter that would be observed from the center of the Earth.

autumnal equinox: see *equinox, autumnal.*

axis of inertia: any the three axes constituting an orthogonal right-handed Cartesian coordinate system wherein the inertia *tensor* of a body assumes a diagonal form. The three diagonal elements are termed the principal moments of inertia. If both the shape and mass density of a celestial body are symmetrical under rotation about a given axis, this axis (the symmetry axis) is a principal axis. It is also referred to as the axis of figure.

azimuth: the angular distance measured eastward along the *horizon* from a specified reference point (usually north). Azimuth is measured to the point where the great circle determining the *altitude* of an object meets the horizon.

barycenter: the center of mass of a system of bodies; e.g., the center of mass of the solar system or the Earth-Moon system.

barycentric: with reference to, or pertaining to, the *barycenter* (usually of the solar system).

Barycentric Celestial Reference System (BCRS): a system of *barycentric* spacetime coordinates for the solar system within the framework of general relativity. The *metric tensor* to be used in the system is specified by the *IAU* 2000 resolution B1.3. For all practical applications, unless otherwise stated, the BCRS is assumed to be oriented according to the *ICRS* axes. (See *Barycentric Coordinate Time (TCB).*)

Barycentric Coordinate Time (TCB): the coordinate time of the *Barycentric Celestial* Reference System *(BCRS)*, which advances by *SI seconds* within that system. TCB is related to *Geocentric Coordinate Time (TCG)* and *Terrestrial Time (TT)* by relativistic transformations that include a secular term. (See *second, Système International (SI).*)

Barycentric Dynamical Time (TDB): the timescale defined by the *IAU* (originally in 1976; named in 1979; revised in 2006) for use as an independent argument of *barycentric ephemerides* and equations of motion. TDB is a linear function of *Barycentric Coordinate Time (TCB)* that on average tracks *TT* over long *periods* of time; differences between TDB and TT evaluated at the Earth's surface remain under 2 ms for several thousand *years* around the current *epoch*. TDB is functionally equivalent to $T_{\mathbf{eph}}$, the independent argument of the JPL planetary and lunar ephemerides DE405/LE405. (See *second, Système International (SI).*)

Barycentric Ephemeris Time (T_{eph}): the timescale of the Jet Propulsion Laboratory development *ephemerides* (the DE nnn series for solar system bodies) that has been scaled to *Terrestrial Time (TT).* It is equivalent to the redefined *Barycentric Dynamical Time (TDB)* as redefined by the *IAU* in 2006. (See *Barycentric Coordinate Time (TCB).*)

Besselian elements: the quantities tabulated for the calculation of accurate predictions of an *eclipse* or *occultation* for any point on or above the surface of the Earth.

calendar: a system of reckoning time in units of solar *days*. The days are enumerated according to their position in cyclic patterns usually involving the motions of the Sun and/or the Moon.

- **calendar, Gregorian**: the *calendar* introduced by Pope Gregory XIII in 1582 to replace the *Julian calendar*. This calendar is now used as the civil calendar in most countries. In the Gregorian calendar, every *year* that is exactly divisible by four is a leap year, except for centurial years, which must be exactly divisible by 400 to be leap years. Thus 2000 was a leap year, but 1900 and 2100 are not leap years.
- **calendar, Julian**: the *calendar* introduced by Julius Caesar in 46 B.C. to replace the Roman calendar. In the Julian calendar a common *year* is defined to comprise 365 *days*, and every fourth year is a leap year comprising 366 days. The Julian calendar was superseded by the *Gregorian calendar*.
- **calendar, proleptic**: the extrapolation of a *calendar* prior to its date of introduction.

catalog equinox: see *equinox, catalog.*

Celestial Ephemeris Origin (CEO): the original name for the *Celestial Intermediate Origin (CIO)* given in the *IAU* 2000 resolutions. Obsolete.

celestial equator: the plane perpendicular to the *Celestial Intermediate Pole (CIP)*. Colloquially, the projection onto the *celestial sphere* of the Earth's *equator*. (See *mean equator and equinox; true equator and equinox.*)

Celestial Intermediate Origin (CIO): the *non-rotating origin* of the *Celestial Intermediate Reference System*. Formerly referred to as the *Celestial Ephemeris Origin (CEO).*

Celestial Intermediate Origin locator (CIO locator): denoted by s, is the difference between the *Geocentric Celestial Reference System (GCRS) right ascension* and the intermediate right ascension of the intersection of the *GCRS* and intermediate *equators*.

Celestial Intermediate Pole (CIP): the reference pole of the *IAU 2006/2000A precession-nutation* model. The motions of the CIP are those of the Tisserand mean axis of the Earth with *periods* greater than two *days*. (See *nutation; precession.*)

Celestial Intermediate Reference System: a *geocentric reference system* related to the *Geocentric Celestial Reference System (GCRS)* by a time-dependent rotation taking into account *precession-nutation*. It is defined by the intermediate *equator* of the *Celestial Intermediate Pole (CIP)* and the *Celestial Intermediate Origin (CIO)* on a specific date.

celestial pole: see *pole, celestial.*

celestial pole offsets: the time-dependent corrections to the *precession-nutation* model, determined by observations. The IERS provides the *celestial pole* offsets in the form of the differences, dX and dY, of the *CIP* coordinates in the *GCRS* with respect to the *IAU* recommended precession-nutation model, *IAU 2006/2000A*. That is, the CIP is realized by IAU 2006/2000A plus these celestial pole offsets. In parallel, the IERS also provides the offsets, $d\psi$ and $d\epsilon$, in longitude and *obliquity* with respect to the IAU 1976/1980 precession-nutation model. (See *Earth orientation.*)

celestial pole offsets at J2000.0: the offsets of the direction of the mean pole at *J2000.0*, provided by the current *IAU precession* model, with respect to the *GCRS*. These offsets are part of what is often called *frame bias*, which is the matrix that expresses the small difference in orientation between the GCRS and the *mean equator and equinox* of J2000.0.

celestial sphere: an imaginary sphere of arbitrary radius upon which celestial bodies may be considered to be located. As circumstances require, the celestial sphere may be centered at the observer, at the Earth's center, or at any other location.

center of figure: the point so situated relative to the apparent figure of a body that any line drawn through it divides the figure into two parts having equal apparent areas. If the body is oddly shaped, the center of figure may lie outside the figure itself.

center of light: same as *center of figure* except referring only to the illuminated portion.

cesium fountain: a precise time and *frequency standard* that realizes the SI definition of the *second* by vertically launching supercooled cesium atoms through a microwave cavity and allowing gravity to bring the atoms back down through the cavity. (See *second, Système International (SI).*)

Chandler wobble: the approximately 435-*day* quasi-periodic motion of the *CIP* in the *ITRF* corresponding, in the *non-rigid Earth*, to the free Eulerian motion of a rigid oblate spheroid rotating about its principal axis of symmetry.

coeval stars: stars that are the same age.

conjunction: the phenomenon in which two bodies have the same apparent *ecliptic longitude* or *right ascension* as viewed from a third body. Conjunctions are usually tabulated as *geocentric* phenomena. For Mercury and Venus, geocentric inferior conjunctions occur when the planet is between the Earth and Sun, and superior conjunctions occur when the Sun is between the planet and Earth. (See *longitude, ecliptic.*)

constellation: **1.** A grouping of stars, usually with pictorial or mythical associations, that serves to identify an area of the *celestial sphere*. **2.** One of the precisely defined areas of the celestial sphere, associated with a grouping of stars, that the *International Astronomical Union (IAU)* has designated as a constellation.

Coordinated Universal Time (UTC): the timescale available from broadcast time signals. UTC differs from *International Atomic Time (TAI)* by an integral number of *seconds*; it is maintained within $\pm 0^{s}.9$ seconds of *UT1* by the introduction of *leap seconds*. (See *International Atomic Time (TAI); leap second; Universal Time (UT).*)

Coriolis effect: a dynamical effect caused by a fictitious Coriolis force, which appears in the equation of motion of an object in a rotating frame of reference.

culmination: the passage of a celestial object across the observer's *meridian*; also called "meridian passage."

culmination, lower: (also called "culmination below pole" for circumpolar stars and the Moon) the crossing farther from the observer's *zenith*.

culmination, upper: (also called "culmination above pole" for circumpolar stars and the Moon) or *transit* is the crossing closer to the observer's *zenith*.

datum: in geodesy, a *reference frame* in which positional measurements are made or expressed.

day: an interval of 86 400 *SI seconds*, unless otherwise indicated. (See *second, Système International (SI).*)

declination: the angular distance on the *celestial sphere* north or south of the *celestial equator*. It is measured along the *hour circle* passing through the celestial object. Declination is usually given in combination with *right ascension* or *hour angle*.

deep ocean dissipation: a process that disperses the ocean tidal energy in the deep oceans. (See *tides, ocean.*)

defect of illumination: (sometimes, greatest defect of illumination): the maximum angular width of the unilluminated portion of the apparent disk of a solar system body measured along a radius.

deflection of light: the angle by which the direction of a light ray is altered from a straight line by the gravitational field of the Sun or other massive object. As seen from the Earth, objects appear to be deflected radially away from the Sun by up to $1\farcs75$ at the Sun's *limb*. Correction for this effect, which is independent of wavelength, is included in the transformation from *mean place* to *apparent place.*

deflection of the vertical: the angle between the astronomical *vertical* and the geodetic vertical. (See *astronomical coordinates; geodetic coordinates; zenith.*)

delta T: see ΔT (found at the end of the glossary).

delta UT1: see ΔUT1 (or ΔUT) (found at the end of the glossary).

depression of the horizon: same as *dip of the horizon*.

dip of the horizon: the apparent angle between the astrometric *horizon* and the visible horizon assuming a level region on the Earth's surface. The effect is largely due to the *height* of the observer and atmospheric *refraction*.

direct motion: for orbital motion in the solar system, motion that is counterclockwise in the *orbit* as seen from the north pole of the *ecliptic*; for an object observed on the *celestial sphere*, motion that is from west to east, resulting from the relative motion of the object and the Earth.

diurnal motion: the apparent daily motion, caused by the Earth's rotation, of celestial bodies across the sky from east to west.

diurnal parallax: see *parallax, geocentric.*

Doodson arguments: a set of six basic angular arguments multiplied by small integers (Doodson numbers) and summed to specify each tidal *frequency*.

Doppler effect: the change in frequency of a received signal due to the relative radial motion of an observer with respect to the source of the signal.

Doppler effect, in general relativity: an extension of the Doppler effect, to the realm of general relativity. While in *Newtonian mechanics* and special relativity the Doppler effect remains

purely kinematic, in general relativity it becomes a dynamical effect, as the gravitational field contributes to the effect.

Doppler effect, in special relativity: an extension from the non-relativistic Doppler effect as the equations include the *time dilation* effect of special relativity. They describe the total difference in observed frequencies and possess the required Lorentz symmetry.

dwarf planet: a celestial body that is in *orbit* around the Sun, has sufficient mass for its self-gravity to overcome rigid body forces so that it assumes a hydrostatic equilibrium (nearly round) shape, has not cleared the neighbourhood around its orbit, and is not a satellite. (See *planet.*)

dynamical equinox: the ascending *node* of the Earth's mean *orbit* on the Earth's *true equator*; i.e., the intersection of the *ecliptic* with the *celestial equator* at which the Sun's *declination* changes from south to north. (See *catalog equinox; equinox; true equator and equinox.*)

dynamical time: the family of timescales introduced in 1984 to replace *ephemeris time (ET)* as the independent argument of dynamical theories and *ephemerides*. (See *Barycentric Dynamical Time (TDB); Terrestrial Time (TT).*)

Earth orientation: the information specifying the relationship of terrestrial and celestial *reference frames*. Typically specified by four small angles and one time difference; two coordinates of the *CIP* in the *ITRS* (accounting for *polar motion*), two *celestial pole offsets* (corrections to the *precession-nutation* model), and the quantity $UT1-UTC$ (specifying the accumulated difference in *length of day*).

Earth Rotation Angle (ERA): the angle, θ, measured along the *equator* of the *Celestial Intermediate Pole (CIP)* between the direction of he *Celestial Intermediate Origin (CIO)* and the *Terrestrial Intermediate Origin (TIO)*. It is a linear function of $UT1$; its time derivative is the Earth's angular velocity.

eccentricity: **1.** A parameter that specifies the shape of a conic secton. **2.** One of the standard *elements* used to describe an elliptic or *hyperbolic orbit*. For an *elliptical orbit*, the quantity $e = \sqrt{1-(b^2/a^2)}$, where a and b are the lengths of the *semimajor* and semiminor axes, respectively. (See *orbital elements.*)

eclipse: the obscuration of a celestial body caused by its passage through the shadow cast by another body.

eclipse, annular: a *solar eclipse* in which the solar disk is not completely covered but is seen as an annulus or ring at maximum eclipse. An annular eclipse occurs when the apparent disk of the Moon is smaller than that of the Sun. (See *eclipse, solar.*)

eclipse, lunar: an *eclipse* in which the Moon passes through the shadow cast by the Earth. The eclipse may be total (the Moon passing completely through the Earth's *umbra*), partial (the Moon passing partially through the Earth's umbra at maximum eclipse), or penumbral (the Moon passing only through the Earth's *penumbra*).

eclipse, solar: actually an *occultation* of the Sun by the Moon in which the Earth passes through the shadow cast by the Moon. It may be total (observer in the Moon's *umbra*), partial (observer in the Moon's *penumbra*), annular, or annular-total. (See *eclipse, annular.*)

ecliptic: **1.** The mean plane of the *orbit* of the Earth-Moon *barycenter* around the solar system barycenter. **2.** The apparent path of the Sun around the *celestial sphere*.

ecliptic latitude: see *latitude, ecliptic.*

ecliptic longitude: see *longitude, ecliptic.*

Einstein's relativity principle, in general relativity: the outcome of any local non-gravitational experiment in a freely falling laboratory is independent of the velocity of the laboratory and its location in spacetime.

Einstein's relativity principle, in special relativity: two inertial frames are completely indistinguishable with respect to all non-gravitational interactions. Thus, non-gravitational physical experiments cannot determine in which inertial system an observer is located. More rigorously, in special relativity, all equations of motion stay form-invariant under transformations interconnecting coordinates and time measured in different inertial frames of reference. (When two such frames are parameterized with Cartesian coordinates, the transformations are those of Lorentz.) In general relativity, the relativity principle gives way to a more general statement, called the *Equivalence principle*.

elements: a set of parameters used to describe the position and/or motion of an astronomical object.

elements, Besselian: see *Besselian elements.*

elements, Keplerian: see *Keplerian elements.*

elements, mean: see *mean elements.*

elements, orbital: see *orbital elements.*

elements, osculating: see *osculating elements.*

ellipsoidal height: in geodesy, the *height* above the adopted *reference ellipsoid*.

elongation: the *geocentric* angle between two celestial objects.

elongation, greatest: the maximum value of a *planetary elongation* for a solar system body that remains interior to the Earth's *orbit*, or the maximum value of a *satellite elongation*.

elongation, planetary: the *geocentric* angle between a *planet* and the Sun. Planetary *elongations* are measured from 0° to 180°, east or west of the Sun.

elongation, satellite: the *geocentric* angle between a satellite and its primary. Satellite *elongations* are measured from 0° east or west of the *planet*.

epact: **1.** The age of the Moon. **2.** The number of *days* since new moon, diminished by one day, on January 1 in the Gregorian ecclesiastical lunar cycle. (See *calendar, Gregorian; lunar phases.*)

epagomenal days: the additional *days*, not included in a lunar *month*, to complete a solar *year*.

ephemeris: a tabulation of the positions of a celestial object in an orderly sequence for a number of dates.

ephemeris hour angle: an *hour angle* referred to the *ephemeris meridian*.

ephemeris longitude: the longitude measured eastward from the *ephemeris meridian*. (See *longitude, terrestrial.*)

ephemeris meridian: see *meridian, ephemeris.*

ephemeris second: the *second* (defined in 1960) as 1/31556925.9747 of the *tropical year* at 1900 January 0 12 hours *Ephemeris Time*. It was superseded by the *SI second*, the length of which was calibrated to the ephemeris second. Obsolete.

ephemeris time (ET): the timescale used prior to 1984 as the independent variable in gravitational theories of the solar system. In 1984, ET was replaced by *dynamical time*.

Ephemeris Time Revised (ET_R): the timescale used for *epochs* prior to 1955, whose measurement unit is the *SI (atomic) second* which had the value of 0h 0m 32.184 s on 1958 January 0, 0h 0m 0s *TAI*, continuous with *Terrestrial Time* prior to 1955. Determined prior to 1956 from the comparison of observations and theories of the motions of the Sun, Moon, and *planets*.

ephemeris transit: the passage of a celestial body or point across the *ephemeris meridian*.

epoch: an arbitrary fixed instant of time or date used as a chronological reference datum for *calendars*, celestial *reference systems*, star catalogs, or orbital motions. (See *calendar; orbit.*)

equation of the equinoxes: the difference apparent *sidereal time* minus mean sidereal time, due to the effect of *nutation* in longitude on the location of the *equinox*. Equivalently, the difference between the *right ascensions* of the *true* and *mean equinoxes*, expressed in time units. (See *sidereal time.*)

equation of the origins: the arc length, measured positively eastward, from the *Celestial Intermediate Origin (CIO)* to the *equinox* along the intermediate *equator*; alternatively the difference between the *Earth Rotation Angle (ERA)* and *Greenwich Apparent Sidereal Time* ($ERA - GAST$).

equation of time: the difference *apparent solar time* minus *mean solar time*.

equator: the great circle on the surface of a body formed by the intersection of the surface with the plane passing through the center of the body perpendicular to the axis of rotation. (See *celestial equator.*)

equinox: **1.** Either of the two points on the *celestial sphere* at which the *ecliptic* intersects the *celestial equator*. **2.** The time at which the Sun passes through either of these intersection points; i.e., when the apparent *ecliptic longitude* of the Sun is 0° or 180°. **3.** The *vernal equinox*. (See *mean equator and equinox; true equator and equinox.*)

- **equinox, autumnal**: **1.** The decending *node* of the *ecliptic* on the *celestial sphere*. **2.** The time which the apparent *ecliptic longitude* of the Sun is 180°.
- **equinox, catalog**: the intersection of the *hour angle* of zero *right ascension* of a star catalog with the *celestial equator*. Obsolete.
- **equinox, dynamical**: the ascending *node* of the *ecliptic* on the Earth's *true equator*.
- **equinox, vernal**: **1.** The ascending *node* of the *ecliptic* on the *celestial equator*. **2.** The time at which the apparent *ecliptic longitude* of the Sun is 0°.

Equivalence principle: A group of postulates from general relativity (the weak equivalence principle, the strong equivalence principle, and the Einstein equivalence principle) that restrict the information content of physical experiments, that is, the capacity of experiments to distinguish between physical scenarios. For example, these postulates address whether an experiment can distinguish between gravity and acceleration, or between a freely falling frame of reference and one that is unaccelerated but free of any external gravitational field.

era: a system of chronological notation reckoned from a specific event.

ERA: see *Earth Rotation Angle (ERA).*

Euclidian geometry: the set of Euclid's definitions and axioms pertaining to a space and structures therein. This is the study of flat spaces.

FCN: see *free core nutation (FCN).*

flattening: a parameter that specifies the degree by which a *planet*'s figure differs from that of a sphere; the ratio $f = (a - b)/a$, where a is the equatorial radius and b is the polar radius.

foreshortening effect: (or foreshortening terms) the second-order changes in the apparent angular motion of a star due to the changing viewing geometry over long periods of time. The effect is important only for nearby stars with high *proper motion* and high *radial velocity*. Also called perspective acceleration. (See *proper motion.*)

frame bias: the orientation of the *mean* equator *and equinox* of *J2000.0* with respect to the *Geocentric Celestial Reference System (GCRS)*. It is defined by three small and constant angles, two of which

describe the offset of the mean pole at J2000.0 and the other is the *GCRS right ascension* of the mean inertial *equinox* of J2000.0.

free core nutation (FCN): a free retrograde diurnal mode in the motion of the Earth's rotation axis with respect to the Earth, due to the non-alignment of the rotation axis of the core and of the mantle; it also appears as a long *period* (of 432 *days*) free *nutation* of the *CIP* in the *GCRS*.

free falling frame: a local frame which falls freely in external gravitational fields and which is sufficiently small that inhomogeneities in external gravitational fields can be ignored.

frequency: the number of *periods* of a regular, cyclic phenomenon in a given measure of time, such as a *second* or a *year*. (See *period; second, Système International (SI); year.*)

frequency standard: a generator whose output is used as a precise *frequency* reference; a primary frequency standard is one whose frequency corresponds to the adopted definition of the *second*, with its specified accuracy achieved without calibration of the device. (See *second, Système International (SI).*)

Galileo: a European satellite navigation system. (Formerly a NASA interplanetary spacecraft that orbited Jupiter from 1995 to 2003.)

GAST: see *Greenwich Apparent Sidereal Time (GAST).*

Gaussian gravitational constant: (k = 0.017 202 098 95): the constant defining the astronomical system of units of length (*astronomical unit (au)*), mass (solar mass) and time (*day*), by means of Kepler's third law. The dimensions of k^2 are those of Newton's constant of gravitation: $L^3M^{-1}T^{-2}$.

geocentric: with reference to, or pertaining to, the center of the Earth.

Geocentric Celestial Reference System (GCRS): a system of *geocentric* spacetime coordinates within the framework of general relativity. The *metric tensor* used in the system is specified by the *IAU* 2000 resolutions. The GCRS is defined such that its spatial coordinates are kinematically non-rotating with respect to those of the *Barycentric Celestial Reference System (BCRS)*. (See *Geocentric Coordinate Time (TCG).*)

Geocentric Coordinate Time (TCG): the coordinate time of the *Geocentric Celestial Reference System (GCRS)*, which advances by *SI seconds* within that system. TCG is related to *Barycentric Coordinate Time (TCB)* and *Terrestrial Time (TT)*, by relativistic transformations that include a secular term. (See *second, Système International (SI).*)

geocentric coordinates: **1.** The latitude and longitude of a point on the Earth's surface relative to the center of the Earth. **2.** Celestial coordinates given with respect to the center of the Earth. (See *latitude, terrestrial; longitude, terrestrial; zenith.*)

geocentric zenith: see *zenith, geocentric.*

geodesic precession and nutation: an effect from relativistic theory in the transformations of the fixed directions in the *BCRS* into a dynamically non-rotating *geocentric reference system*. The largest components of the relativistic rotation of the *GCRS* with respect to a dynamically non-rotating geocentric reference system in the framework of general relativity. Geodesic precession is the secular part of the rotation and geodesic nutation is the periodic part. Because the *IAU* reference systems are defined as kinematically non-rotating, geodesic precession and nutation appear as *Coriolis*-like motions in the IAU 2000 precession-nutation model, rather than in the BCRS-GCRS transformation.

geodetic coordinates: the latitude and longitude of a point on the Earth's surface determined from the geodetic *vertical* (normal to the *reference ellipsoid*). (See *latitude, terrestrial; longitude, terrestrial; zenith.*)

geodetic zenith: see *zenith, geodetic.*

geoid: an equipotential surface that coincides with mean sea level in the open ocean. On land it is the level surface that would be assumed by water in an imaginary network of frictionless channels connected to the ocean.

geometric position: the position of an object defined by a straight line (vector) between the center of the Earth (or the observer) and the object at a given time, without any corrections for *light-time*, *aberration*, etc.

geop: a surface of constant geopotential.

GHA: see *Greenwich Hour Angle (GHA).*

Global Positioning System (GPS): a U.S. satellite navigation system. Also known as NAVSTAR or NAVSTAR/GPS.

GLONASS: a Russian satellite navigation system.

GMST: see *Greenwich Mean Sidereal Time (GMST).*

GPS: see *Global Positioning System (GPS).*

GPS time: the timescale based on received time signals from *GPS* satellites that is maintained within better than 1 microsecond of *UTC*, or *TAI*, modulo one *second*. It is ahead of TAI by 19s and differs from UTC depending on the number of *leap seconds*, since GPS Time is not adjusted for leap seconds.

greatest defect of illumination: see *defect of illumination.*

Greenwich Apparent Sidereal Time (GAST): the *Greenwich Hour Angle* of the *true equinox of date*.

Greenwich Hour Angle (GHA): the angular distance on the *celestial sphere* measured westward along the *celestial equator* from the *Greenwich meridian* to the *hour circle* that passes through a celestial object or point.

Greenwich Mean Sidereal Time (GMST): the *Greenwich Hour Angle* of the *mean equinox of date*.

Greenwich meridian: see *meridian, Greenwich.*

Greenwich sidereal date (GSD): the number of *sidereal days* elapsed at Greenwich since the beginning of the Greenwich sidereal *day* that was in progress at the *Julian date (JD)* 0.0.

Greenwich sidereal day number: the integral part of the *Greenwich sidereal date (GSD).*

Gregorian calendar: see *calendar, Gregorian.*

grid coordinate systems: the coordinate systems from conformal projection of spherical or ellipsoidal planetary surfaces onto a plane surface.

height: the distance above or below a reference surface such as mean sea level on the Earth or a planetographic reference surface on another solar system *planet*.

heliocentric: with reference to, or pertaining to, the center of the Sun.

heliocentric parallax: see *parallax, heliocentric.*

horizon: **1.** A plane perpendicular to the line from an observer through the *zenith*. **2.** The observed border between Earth and the sky.

- **horizon, astronomical**: the plane perpendicular to the line from an observer to the *astronomical zenith* that passes through the point of observation.
- **horizon, geocentric**: the plane perpendicular to the line from an observer to the *geocentric zenith* that passes through the center of the Earth.
- **horizon, natural**: the border between the sky and the Earth as seen from an observation point.

horizontal parallax: see *parallax, horizontal.*

horizontal refraction: see *refraction, horizontal.*

hour angle: the angular distance on the *celestial sphere* measured westward along the *celestial equator* from the *meridian* to the *hour circle* that passes through a celestial object.

hour circle: a great circle on the *celestial sphere* that passes through the *celestial poles* and is therefore perpendicular to the *celestial equator*.

hydrogen maser: a precise time and *frequency standard* that produces coherent electromagnetic waves through stimulated emission of hydrogen atoms.

hyperfine levels: the energy levels in the structure of individual atoms and molecules that originate from the interaction of the spin of the nucleus (or nuclei, in molecules) with internally generated electric and magnetic fields. These levels constitute the hyperfine structure of the atom of a molecule.

IAU: see *International Astronomical Union (IAU).*

IAU 2000A nutation model: the *nutation* portion of the *IAU 2000A precession-nutation model* which is still in use in *IAU 2006/2000A*. This represents the nutation of the *CIP* in the *GCRS* for those who need a model at 0.2 mas level of accuracy. An abridged model, designated IAU 2000B, is available for those who only require a model at the 1 mas level.

IAU 2000A precession-nutation model: the *IAU* recommended *precession-nutation* model for use between 1 Jan. 2003 and 1 Jan. 2009. When it was adopted, it was intended to replace both the previous *precession* and *nutation*. However, the precession portion did not correct for the higher order terms. A new precession theory was adopted by the IAU in 2006. Obsolete. (See *IAU 2006/2000A*.)

IAU 2006/2000A: the *IAU*-sanctioned *precession-nutation* model for use after 1 Jan. 2009. The precession theory is the P03 development from Capitaine, Wallace and Chapront (2003, A&A 412 586) and was officially adopted in 2006 (IAU 2008, resolution B1). The nutation theory is that of Mathews, Herring, and Buffett (2002, JGR, 107, 2068) and was adopted in 2000 (IAU 2001, resolution B1.6). Some implementations of IAU 2006/2000A—most notably SOFA—incorporate supplemental adjustments to nutation to make the two theories compatible. These adjustments are from Wallace and Capitaine (2006 A&A, 459 981) and currently total a few 10s of microarcseconds. The precession-nutation model with adjustments is named *IAU 2006/2000A*$_{\mathrm{R}}$ within this book when a distinction is needed.

IAU 2006/2000A$_{\mathrm{R}}$: the IAU 2006/2000A *precession-nutation* model with supplemental adjustments to nutation; the adjustments are from Wallace and Capitaine (2006 A&A, 459 981). Also referred to as *IAU 2006/2000A*$_{\mathrm{R06}}$ and *IAU* 2006/2000A(R06) in some publications.

illuminated extent: the illuminated area of an apparent planetary disk, expressed as a solid angle.

inclination: **1.** The angle between two planes or their poles. **2.** Usually, the angle between an orbital plane and a reference plane. **3.** One of the standard *orbital elements* that specifies the orientation of the *orbit*.

inertial coordinate system: a coordinate system that is capable of parameterising an *inertial reference system*. While a *reference system* is a frame constituted by physical bodies, a coordinate system is a chart. Each reference system can be parameterised with a continuous multitude of coordinate systems.

inertial coordinates: a special class of coordinate systems in special relativity or Newtonian physics (i.e., in flat spacetimes) in which the laws of physics are substantially simpler than in non-inertial ones. Inertial coordinates are in constant, uniform motion with respect to each other, while non-inertial coordinates are accelerating with respect to all inertial coordinates.

inertial reference frame: a frame wherein a body subject to no external influences moves uniformly along a straight line, as postulated by Newton's First Law. The existence of inertial frames is accepted within the Newtonian physics as well as in special and general relativity. In general relativity, inertial frames are implemented by non-rotating freely falling frames. In these frames, *inertial coordinates* can be introduced only locally.

inertial reference system: see *inertial reference frame.*

instantaneous orbit: see *orbit, instantaneous.*

intercalate: to insert an interval of time (e.g., a *day* or a *month*) within a *calendar*, usually so that it is synchronized with some natural phenomenon such as the seasons or *lunar phases*.

intermediate place (or position): the *proper place* of an object expressed with respect to the true (intermediate) *equator* and *CIO of date*.

International Astronomical Union (IAU): an international non-governmental organization that promotes the science of astronomy. The IAU is composed of both national and individual members. In the field of positional astronomy, the IAU, among other activities, recommends standards for data analysis and modeling, usually in the form of resolutions passed at General Assemblies held every three years.

International Atomic Time (TAI): the continuous timescale resulting from analysis by the Bureau International des Poids et Mesures of atomic time standards in many countries. The fundamental unit of TAI is the *SI second* on the *geoid*, and the *epoch* is 1958 January 1. (See *second, Système International (SI).*)

International Celestial Reference Frame (ICRF): **1.** A set of extragalactic objects whose adopted positions and uncertainties realize the *International Celestial* Reference System *(ICRS)* axes and give the uncertainties of those axes. **2.** The name of the radio catalog whose 212 defining sources serve as fiducial points to fix the axes of the *ICRS*, recommended by the *International Astronomical Union (IAU)* in 1997.

International Celestial Reference System (ICRS): a time-independent, kinematically non-rotating *barycentric reference system* recommended by the *International Astronomical Union (IAU)* in 1997. Its axes are those of the *International Celestial Reference Frame (ICRF).*

international meridian: see *meridian, Greenwich.*

International Terrestrial Reference Frame (ITRF): a realization of *ITRS* by a set of instantaneous coordinates (and velocities) of reference points distributed on the topographic surface of the Earth (mainly space geodetic observing stations and related markers). Currently the ITRF provides a model for estimating, to high accuracy, the instantaneous positions of these points, which is the sum of conventional corrections provided by the IERS Convention center (*solid Earth tides*, pole tides) and of a regularized position. At present, the latter is modeled by a piecewise linear function, the linear part accounting for such effects as tectonic plate motion, postglacial rebound, and the piecewise aspect representing discontinuities such as seismic displacements. The initial orientation of the ITRF is that of the BIH Terrestrial System (its predecessor) at *epoch* 1984.0. (See *meridian, Greenwich; Terrestrial Intermediate Origin (TIO).*)

International Terrestrial Reference System (ITRS): a time-dependent, non-*inertial reference system* co-moving with the geocenter and rotating with the Earth. The ITRS is the recommended system in which to express positions on the Earth.

International Terrestrial Reference System zero-meridian: see *meridian, Greenwich.*

invariable plane: the plane through the center of mass of the solar system perpendicular to the *angular momentum vector* of the solar system.

irradiation: an optical effect of contrast that makes bright objects viewed against a dark background appear to be larger than they really are.

J2000.0: defined in the framework of general relativity by the *IAU* as being the event (*epoch*) at the geocenter and at the date 2000 January 1.5 *TT* = *Julian Date* 245 1545.0 TT. Note that this event has different dates in different timescales.

Julian calendar: see *calendar, Julian.*

Julian date (JD): the interval of time in *days* and fractions of a day, since 4713 B.C. January 1, Greenwich noon, Julian *proleptic calendar*. In precise work, the timescale, e.g., *Terrestrial Time (TT)* or *Universal Time (UT)*, should be specified.

Julian date, modified (MJD): the *Julian date (JD)* minus 2400000.5.

Julian day number: the integral part of the *Julian date (JD)*.

Julian year: see *year, Julian.*

Keplerian elements: a certain set of six *orbital elements*, sometimes referred to as the Keplerian set. Historically, this set included the *mean anomaly* at the *epoch*, the *semimajor axis*, the *eccentricity* and three Euler angles: the *longitude of the ascending node*, the *inclination*, and the *argument of pericenter*. The time of *pericenter* passage is often used as part of the Keplerian set instead of the mean *anomaly* at the epoch. Sometimes the longitude of pericenter (which is the sum of the longitude of the ascending *node* and the argument of pericenter) is used instead of either the longitude of the ascending node or the argument of pericenter.

Laplacian plane: **1.** For *planets* see *invariable plane*. **2.** For a system of satellites, the fixed plane relative to which the vector sum of the disturbing forces has no orthogonal component.

latitude, celestial: see *latitude, ecliptic.*

latitude, ecliptic: the angular distance on the *celestial sphere* measured north or south of the *ecliptic* along the great circle passing through the poles of the ecliptic and the celestial object. Also referred to as *celestial latitude*.

latitude, terrestrial: the angular distance on the Earth measured north or south of the *equator* along the *meridian* of a geographic location.

leap second: a *second* inserted as the 61^{st} second of a minute at announced times to keep *UTC* within $0^s.9$ of *UT1*. Generally, leap seconds are added at the end of June or December as necessary, but may be inserted at the end of any *month*. Although it has never been utilized, it is possible to have a negative leap second in which case the 60^{th} second of a minute would be removed. (See *Coordinated Universal Time (UTC); second, Système International (SI); Universal Time (UT).*)

length of day: strictly the number of fixed length *seconds* in the *day* determined from the rotation of the Earth, but most often used to refer to the excess length of day or the difference between the length of day and 86,400 *SI seconds*.

Lense-Thirring effect: also referred to as frame dragging. It originates in the general theory of relativity and is caused by a gravitomagnetic field induced by rotation of a massive body, which drags a local inertial frame in the direction of rotation of the body. As a consequence, the spin of a gyroscope, and/or the orbital plane of a test particle, orbiting the central body, undergo the *precession* around the *angular momentum* of the central body. Lense-Thirring precession is a smaller part of *geodesic precession and nutation*.

librations: the real or apparent oscillations of a body around a reference point. When referring to the Moon, librations are variations in the orientation of the Moon's surface with respect to an observer on the Earth. Physical librations are due to variations in the orientation of the Moon's rotational axis in inertial space. The much larger optical librations are due to variations in the rate of the Moon's orbital motion, the *obliquity* of the Moon's *equator* to its orbital plane, and the diurnal changes of geometric perspective of an observer on the Earth's surface.

light-time: the interval of time required for light to travel from a celestial body to the Earth.

light-time displacement: the difference between the *geometric* and *astrometric place* of a solar system body. It is caused by the motion of the body during the interval it takes light to travel from the body to Earth.

light-year: the distance that light traverses in a vacuum during one *year*. Since there are various ways to define a year, there is an ambiguity in the exact distance; the *IAU* recommends using the *Julian year* as the time basis. A light-year is approximately 9.46×10^{12} km, 5.88×10^{12} statute miles, 6.32×10^{4} *au*, and 3.07×10^{-1} *parsecs*. Often distances beyond the solar system are given in parsecs.

light, deflection of: see *deflection of light.*

limb: the apparent edge of the Sun, Moon, or a *planet* or any other celestial body with a detectable disk.

limb correction: generally, a small angle (positive or negative) that is added to the tabulated apparent *semidiameter* of a body to compensate for local topography at a specific point along the *limb*. Specifically for the Moon, the angle taken from the Watts lunar limb data (Watts, C. B., APAE XVII, 1963) that is used to correct the semidiameter of the Watts mean limb. The correction is a function of position along the limb and the apparent *librations*. The Watts mean limb is a circle whose center is offset by about $0\farcs6$ from the direction of the Moon's center of mass and whose radius is about $0\farcs4$ greater than the semidiameter of the Moon that is computed based on its *IAU* adopted radius in kilometers.

Liouville equation: a generalized Eulerian equation of motion, which allows for internal motions, i.e., mass redistribution inside the rotating system.

local sidereal time: the *hour angle* of the *vernal equinox* with respect to the local *meridian*.

longitude of the ascending node: given an *orbit* and a reference plane through the primary body (or center of mass): the angle, Ω, at the primary, between a fiducial direction in the reference plane and the point at which the orbit crosses the reference plane from south to north. Equivalently, Ω is one of the angles in the reference plane between the fiducial direction and the line of *nodes*. It is one of the six *Keplerian elements* that specify an orbit. For planetary orbits, the primary is the Sun, the reference plane is usually the *ecliptic*, and the fiducial direction is usually toward the *equinox*.

longitude, celestial: see *longitude, ecliptic.*

longitude, ecliptic: the angular distance on the *celestial sphere* measured eastward along the *ecliptic* from the *dynamical equinox* to the great circle passing through the poles of the ecliptic and the celestial object. Also referred to as *celestial longitude*.

longitude, terrestrial: the angular distance measured along the Earth's *equator* from the *Greenwich meridian* to the *meridian* of a geographic location.

Lorentz transformation: In special and general relativity, a linear, four-dimensional transformation between the time and Cartesian space coordinates parameterizing two inertial frames moving uniformly with constant velocity with respect to each other.

Love numbers: the coefficients relating the observed amplitudes of displacements of the Earth's surface and variations in the Earth's gravity field due to the solid Earth tide generating potential.

luminosity class: the distinctions in intrinsic brightness among stars of the same *spectral type*, typically given as a Roman numeral. It denotes if a star is a supergiant (Ia or Ib), giant (II or III), subgiant (IV), or main sequence—also called dwarf (V). Sometimes subdwarfs (VI) and white dwarfs (VII) are regarded as luminosity classes. (See *spectral types or classes.*)

lunar phases: the cyclically recurring apparent forms of the Moon. New moon, first quarter, full moon and last quarter are defined as the times at which the excess of the apparent *ecliptic longitude* of the Moon over that of the Sun is 0°, 90°, 180° and 270°, respectively. (See *longitude, ecliptic.*)

lunation: the *period* of time between two consecutive new moons.

lunisolar tidal deceleration: the deceleration of the rotation of the Earth due to tidal interactions, mainly with the Moon and Sun. Conservation of *angular momentum* is maintained by the acceleration of the Moon's orbital motion.

magnitude of a lunar eclipse: the fraction of the lunar diameter obscured by the shadow of the Earth at the greatest *phase* of a *lunar eclipse*, measured along the common diameter. (See *eclipse, lunar.*)

magnitude of a solar eclipse: the fraction of the solar diameter obscured by the Moon at the greatest *phase* of a *solar eclipse*, measured along the common diameter. (See *eclipse, solar.*)

magnitude, stellar: a measure on a logarithmic scale of the brightness of a celestial object. Since brightness varies with wavelength, often a wavelength band is specified. A factor of 100 in brightness is equivalent to a change of 5 in stellar magnitude, and brighter sources have lower magnitudes. For example, the bright star Sirius has a visual-band magnitude of -1.46 whereas the faintest stars detectable with an unaided eye under ideal conditions have visual-band magnitudes of about 6.0.

mass monopole: a body whose gravitational field is spherically symmetric in its local frame. In a relativistic framework all higher Blanchet-Damour mass and spin multipole moments (quadrupole and higher mass moments, spin and higher spin moments) of the body vanish in that frame.

mean distance: an average distance between the primary and the secondary gravitating body. The meaning of the mean distance depends upon the chosen method of averaging (i.e., averaging over the time, or over the *true anomaly*, or the *mean anomaly*. It is also important what power of the distance is subject to averaging.) In this volume the mean distance is defined as the inverse of the time-averaged reciprocal distance: $(\int r^{-1}\,dt)^{-1}$. In the two body setting, when the disturbances are neglected and the *orbit* is elliptic, this formula yields the *semimajor axis*, a, which plays the role of mean distance.

mean elements: the average values of the *orbital elements* over some section of the *orbit* or over some interval of time. They are interpreted as the *elements* of some reference (mean) orbit that approximates the actual one and, thus, may serve as the basis for calculating orbit *perturbations*. The values of mean elements depend upon the chosen method of averaging and upon the length of time over which the averaging is made.

mean equator and equinox: the celestial coordinate system defined by the orientation of the Earth's equatorial plane on some specified date together with the direction of the *dynamical equinox* on that date, neglecting *nutation*. Thus, the mean *equator* and *equinox* moves in response only to *precession*. Positions in a star catalog have traditionally been referred to a catalog equator and equinox that approximate the mean equator and equinox of a *standard epoch*. (See *catalog equinox; true equator and equinox.*)

mean motion: in undisturbed elliptic motion, the constant angular speed required for a body to complete one revolution in an *orbit* of a specified *semimajor axis*.

mean place: the coordinates of a star or other celestial object (outside the solar system) at a specific date, in the *Barycentric Celestial Reference System (BCRS)*. Conceptually, the coordinates represent the direction of the object as it would hypothetically be observed from the solar system *barycenter* at the specified date, with respect to a fixed coordinate system (e.g., the axes of the *International Celestial Reference Frame (ICRF)*), if the masses of the Sun and other solar system bodies were negligible.

mean solar time: see *solar time, mean.*

meridian: a great circle passing through the *celestial poles* and through the *zenith* of any location on Earth. For planetary observations a meridian is half the great circle passing through the *planet*'s poles and through any location on the planet.

meridian, ephemeris: a fictitious *meridian* that rotates independently of the Earth at the uniform rate implicitly defined by *Terrestrial Time (TT)*. The ephemeris meridian is 1.002 738 ΔT east of the *Greenwich meridian*, where $\Delta\mathrm{T} = \mathrm{TT} - \mathrm{UT1}$.

meridian, Greenwich: (also called *international* or *prime meridian*) is a generic reference to one of several origins of the Earth's longitude coordinate (zero-longitude). In *The Astronomical Almanac*, it is the plane defining the astronomical zero-meridian, also called the *TIO meridian*; it contains the geocenter, the *Celestial Intermediate Pole* and the *Terrestrial Intermediate Origin*. Other definitions are: the x-z plane of the *International Terrestrial* Reference System *(ITRS)*; the zero-longitude meridian of the World Geodetic System 1984 (*WGS-84*); and the meridian that passes through the transit circle at the Royal Observatory, Greenwich. Note that the latter meridian is about 100 m west of the others.

meridian, international: see *meridian, Greenwich.*

meridian, prime: on Earth, same as *Greenwich meridian*. On other solar system objects, the zero-longitude *meridian*, typically defined via international convention by an observable surface feature or rotational *elements*.

Metonic cycle: a 6940-*day* cycle closely approximating 19 *tropical years* or 235 *synodic months*.

metric space: generally, a region of space wherein the notion of distance between elements is defined. In relativity, a linear space where a dot-product (and, via the dot-product, also a distance) is defined with aid of a *metric tensor*.

metric tensor: a mathematical object, expressed by a four-dimensional matrix (symmetrical, in Einstein's relativity), that is used to calculate distances and angles in spacetime. While in special relativity the metric tensor defines only the geometric properties of the spacetime, in general relativity it also describes the potentials of the gravitational field, which are found by solving the Einstein-Hilbert equations.

moment of inertia: an integral parameter that measures an object's resistance to changes in its angular-velocity vector. The moment of inertia is equal to one of the diagonal elements of the inertia *tensor* in the coordinate system where the inertia tensor is diagonalized.

month: a calendrical unit that approximates the *period* of revolution of the Moon. Also, the period of time between the same dates in successive *calendar* months.

month, sidereal: the *period* of revolution of the Moon about the Earth (or Earth-Moon *barycenter*) in a fixed *reference frame*. It is the mean period of revolution with respect to the background stars. The mean length of the sidereal *month* is approximately 27.322 *days*.

month, synodic: the *period* between successive new moons (as seen from the geocenter). The mean length of the synodic *month* is approximately 29.531 *days*.

moonrise, moonset: the times at which the apparent upper *limb* of the Moon is on the *astronomical horizon*. In *The Astronomical Almanac*, they are computed as the times when the true *zenith distance*, referred to the center of the Earth, of the central point of the Moon's disk is $90^\circ\,34' + s - \pi$, where s is the Moon's *semidiameter*, π is the *horizontal parallax*, and $34'$ is the adopted value of *horizontal refraction*.

nadir: the point on the *celestial sphere* diametrically opposite to the *zenith*.

NAVSTAR: see *Global Positioning System (GPS)*.

Newcomb's theory of the Sun: formally, *Tables of the Motion of the Earth on its Axis and Around the Sun*, developed by Simon Newcomb and published in "The Astronomical Papers Prepared for the Use of the American Ephemeris and Nautical Almanac, Volume VI, Part I" in 1895. It was the basis of the *geocentric* ephemeris of the Sun, timescales, and astronomical constants for about 80 *years*.

Newtonian mechanics: a description of motions, based on the laws of Newton acting in a Newtonian spacetime. The latter is a *tensor* product of a three-dimensional Euclidean space and a one-dimensional time. The time is assumed to be absolute—i.e., to flow uniformly at all points of the Euclidean space, and not to depend upon the motion of the observer.

node: either of the points on the *celestial sphere* at which the plane of an *orbit* intersects a reference plane. The position of one of the nodes (the *longitude of the ascending node*) is traditionally used as one of the standard *orbital elements*.

non-rigid Earth: a model of the Earth used in geophysical studies that includes the effects of an elastic mantle and liquid outer core. Modern models also often include the effects of oceans on the surface.

non-rotating origin: in the context of the *GCRS* or the *ITRS*, a point on the intermediate (instantaneous) *equator* that serves as an azimuthal origin. Its instantaneous motion with respect to the system (GCRS or ITRS as appropriate) has no component along the intermediate equator (i.e., its instantaneous motion is perpendicular to it). It is called the *Celestial Intermediate Origin (CIO)* in the GCRS and the *Terrestrial Intermediate Origin (TIO)* in the ITRS. The *geocentric* angle between the *CIO* and the *TIO* is the *Earth Rotation Angle (ERA)*.

numerical integration: the process of calculating the motion of a body by integrating the equations of motion.

nutation: the oscillations in the motion of the rotation pole of a freely rotating body that is undergoing torque from external gravitational forces. Nutation of the Earth's pole is specified in terms of components in *obliquity* and longitude.

obliquity: in general, the angle between the equatorial and orbital planes of a body or, equivalently, between the rotational and orbital poles. For the Earth the obliquity of the *ecliptic* is the angle between the planes of the *equator* and the ecliptic; its value is approximately 23º44.

occultation: the obscuration of one celestial body by another of greater apparent diameter; especially the passage of the Moon in front of a star or *planet*, or the disappearance of a satellite behind the disk of its primary. If the primary source of illumination of a reflecting body is cut off by the occultation, the phenomenon is also called an *eclipse*. The occultation of the Sun by the Moon is a *solar eclipse*. (See *eclipse, solar.*)

ocean loading: the crustal deformation caused by changes in the weight of a column of water.

of date: the term applied to *reference frames* or directions to celestial bodies indicating that the effects of *precession* (mean) and *nutation* (true) have been applied.

opposition: the phenomenon whereby two bodies have apparent *ecliptic longitudes* or *right ascensions* that differ by 180° as viewed by a third body. Oppositions are usually tabulated as *geocentric* phenomena.

orbit: the path in space followed by a celestial body as a function of time. (See *orbital elements.*)

orbit, elliptical: a closed *orbit* with an *eccentricity* less than 1.

orbit, hyperbolic: an open *orbit* with an *eccentricity* greater than 1.

orbit, instantaneous: the unperturbed two-body *orbit* that a body would follow if *perturbations* were to cease instantaneously. Each orbit in the solar system (and, more generally, in any perturbed two-body setting) can be represented as a sequence of instantaneous ellipses or hyperbolae whose parameters are called *orbital elements*. If these *elements* are chosen to be osculating, each instantaneous orbit is tangential to the physical orbit. (See *orbital elements; osculating elements.*)

orbit, parabolic: an open *orbit* with an *eccentricity* of 1.

orbital elements: a set of six independent parameters that specifies an *instantaneous orbit*. Every real *orbit* can be represented as a sequence of instantaneous ellipses or hyperbolae sharing one of their foci. At each instant of time, the position and velocity of the body is characterised by its place on one such instantaneous curve. The evolution of this representation is mathematically described by evolution of the values of orbital elements. Different sets of geometric parameters may be chosen to play the role of orbital elements. The set of *Keplerian elements* is one of many such sets. When the Lagrange constraint (the requirement that the instantaneous orbit is tangential to the actual orbit) is imposed upon the orbital elements, they are called *osculating elements*.

orthometric height: the *height* measured along the curved plumbline above the *geoid*.

osculating elements: a set of parameters that specifies the instantaneous position and velocity of a celestial body in its perturbed *orbit*. Osculating elements describe the unperturbed (two-body) orbit that the body would follow if *perturbations* were to cease instantaneously. (See *orbit, instantaneous; orbital elements.*)

parallax: the difference in apparent direction of an object as seen from two different locations; conversely, the angle at the object that is subtended by the line joining two designated points.

parallax, annual: see *parallax, heliocentric.*

parallax, diurnal: see *parallax, geocentric.*

parallax, geocentric: the angular difference between the *topocentric* and *geocentric* directions toward an object. Also called *diurnal parallax*.

parallax, heliocentric: the angular difference between the *geocentric* and *heliocentric* directions toward an object; it is the angle subtended at the observed object. Also called *annual parallax*.

parallax, horizontal: the angular difference between the *topocentric* and a *geocentric* direction toward an object when the object is on the *astronomical horizon*.

parallax, solar: the angular width subtended by the Earth's equatorial radius when the Earth is at a distance of 1 *astronomical unit (au)*. The value for the solar *parallax* is 8.794143 arcseconds.

parallax in altitude: the angular difference between the *topocentric* and *geocentric* direction toward an object when the object is at a given *altitude*.

parsec: the distance at which one *astronomical unit (au)* subtends an angle of one arcsecond; equivalently the distance to an object having an *annual parallax* of one arcsecond. One parsec is $1/\sin(1'') = 206264.806$ *au*, or about 3.26 *light-years*.

penumbra: **1.** The portion of a shadow in which light from an extended source is partially but not completely cut off by an intervening body. **2.** The area of partial shadow surrounding the *umbra*.

pericenter: the point in an *orbit* that is nearest to the origin of the *reference system*. (See *perigee; perihelion.*)

pericenter, argument of: one of the *Keplerian elements*. It is the angle measured in the *orbit* plane from the ascending *node* of a reference plane (usually the *ecliptic*) to the *pericenter*.

perigee: the point in an *orbit* that is nearest to the Earth. Perigee is sometimes used with reference to the apparent orbit of the Sun around the Earth.

perihelion: the point in an *orbit* that is nearest to the Sun.

period: the interval of time required to complete one revolution in an *orbit* or one cycle of a periodic phenomenon, such as a cycle of *phases*.

perturbations: **1.** The deviations between the actual *orbit* of a celestial body and an assumed reference orbit. **2.** The forces that cause deviations between the actual and reference orbits. Perturbations, according to the first meaning, are usually calculated as quantities to be added to the coordinates of the reference orbit to obtain the precise coordinates.

phase: **1.** The name applied to the apparent degree of illumination of the disk of the Moon or a *planet* as seen from Earth (crescent, gibbous, full, etc.). **2.** The ratio of the illuminated area of the apparent disk of a celestial body to the entire area of the apparent disk; i.e., the fraction illuminated. **3.** Used loosely to refer to one aspect of an *eclipse* (partial phase, annular phase, etc.). (See *lunar phases.*)

phase angle: the angle measured at the center of an illuminated body between the light source and the observer.

photometry: a measurement of the intensity of light, usually specified for a specific wavelength range.

piezoelectric effect: the ability of some materials (e.g., quartz crystals) to generate an electric potential in response to applied mechanical stress or to deform mechanically when an electric field is applied.

Planck's constant: (denoted by $\hbar$) a fundamental physical constant equal to the quantum of action in quantum physics. It is the proportionality constant between the energy of a photon and its electromagnetic *frequency*. It is also the proportionality coefficient between the momentum of a photon and the frequency of its associated electromagnetic wave.

planet: a celestial body that is in *orbit* around the Sun, has sufficient mass for its self-gravity to overcome rigid body forces so that it assumes a hydrostatic equilibrium (nearly round) shape, and has cleared the neighbourhood around its orbit. (See *dwarf planet.*)

planetocentric coordinates: coordinates for general use, where the z-axis is the mean axis of rotation, the x-axis is the intersection of the planetary *equator* (normal to the z-axis through the center of mass) and an arbitrary *prime meridian*, and the y-axis completes a right-hand coordinate system. Longitude of a point is measured positive to the prime *meridian* as defined by rotational *elements*. Latitude of a point is the angle between the planetary equator and a line to the center of mass. The radius is measured from the center of mass to the surface point.

planetographic coordinates: coordinates for cartographic purposes dependent on an equipotential surface as a reference surface. Longitude of a point is measured in the direction opposite to the rotation (positive to the west for direct rotation) from the cartographic position of the *prime meridian*

defined by a clearly observable surface feature. Latitude of a point is the angle between the planetary *equator* (normal to the z-axis and through the center of mass) and normal to the reference surface at the point. The *height* of a point is specified as the distance above a point with the same longitude and latitude on the reference surface.

plate motions: the movements of the large-scale portions of the Earth's crust called tectonic plates. Colloquially, continental drift.

polar motion: the quasi-periodic motion of the Earth's pole of rotation with respect to the Earth's solid body. More precisely, the angular excursion of the *CIP* from the *ITRS* z-axis. (See *Celestial Intermediate Pole (CIP); International Terrestrial Reference System (ITRS).*)

polar motion, secular: a non-periodic motion of the Earth's pole toward the direction of approximately 75° west longitude.

polar wobble: see *wobble, polar.*

pole, celestial: either of the two points projected onto the *celestial sphere* by the Earth's axis. Usually, this is the axis of the *Celestial Intermediate Pole (CIP)*, but it may also refer to the instantaneous axis of rotation, or the *angular momentum vector*. All of these axes are within $0.''1$ of each other. If greater accuracy is desired, the specific axis should be designated.

pole, Tisserand mean: the *angular momentum* pole for the Earth about which the total internal angular momentum of the Earth is zero. The motions of the *Celestial Intermediate Pole (CIP)* (described by the conventional theories of *precession* and *nutation*) are those of the Tisserand mean pole with *periods* greater than two *days* in a celestial *reference system* (specifically, the *Geocentric Celestial Reference System (GCRS)*).

post-glacial rebound: the rise of land masses that were depressed by the weight of ice sheets during the last glacial period. Also called continental rebound, isostatic rebound, post-ice age isostatic recovery.

precession: the smoothly changing orientation (secular motion) of an orbital plane or the *equator* of a rotating body. Applied to rotational dynamics, precession may be excited by a singular event, such as a collision, a progenitor's disruption, or a tidal interaction at a close approach (free precession); or caused by continuous torques from other solar system bodies, or jetting, in the case of comets (forced precession). For the Earth's rotation, the main sources of forced precession are the torques caused by the attraction of the Sun and Moon on the Earth's equatorial bulge, called precession of the equator (formerly known as lunisolar precession). The slow change in the orientation of the Earth's orbital plane is called *precession of the ecliptic* (formerly known as planetary precession). The combination of both motions—that is, the motion of the equator with respect to the *ecliptic*—is called general precession.

precession of the ecliptic: see *precession.*

precession of the equator (and CIP): see *precession.*

prime meridian: see *meridian, prime.*

proleptic calendar: see *calendar, proleptic.*

proper motion: the projection onto the *celestial sphere* of the space motion of a star relative to the solar system; thus the transverse component of the space motion of a star with respect to the solar system. Proper motion is usually tabulated in star catalogs as changes in *right ascension* and *declination* per *year* or century.

proper place: the direction of an object in the *GCRS* that takes into account orbital or space motion and *light-time* (as applicable), light-deflection, and *annual aberration*. Thus, the position (*geocentric*

right ascension and *declination*) at which the object would actually be seen from the center of the Earth if the Earth were transparent, non-refracting, and massless. Unless otherwise stated, the coordinates are expressed with respect to the GCRS axes, which are derived from those of the *ICRS*.

proper time: in relativistic theory, the time measured by an ideal clock moving together with an observer. Proper time is directly observable and, therefore, independent of any coordinates.

quadrature: a configuration in which two celestial bodies have apparent longitudes that differ by 90° as viewed from a third body. Quadratures are usually tabulated with respect to the Sun as viewed from the center of the Earth. (See *longitude, ecliptic.*)

radial velocity: the rate of change of the distance to an object, usually corrected for the Earth's motion with respect to the solar system *barycenter*.

radius vector: an imaginary line from the center of one body to another, often from the heliocenter. Sometimes only the length of the vector is given.

reduction in latitude: the difference between the *geocentric* latitude and the geodetic latitude. It is determined by the direction perpendicular to the tangent to the *reference ellipsoid* at the site. Also called angle of the *vertical*.

reference ellipsoid: an oblate spheroid (ellipsoid of revolution) that approximates the *geoid* over the entire Earth. A reference ellipsoid is specified by its equatorial radius and polar *flattening*.

reference frame: the realization of a *reference system* through adopted directions or spatial coordinates.

reference system: conceptual description of a four dimensional structure required to specify the location of, or directions to, physical objects and their rates of change.

refraction: the change in direction of travel (bending) of a light ray as it passes obliquely from a medium of lesser/greater density to a medium of greater/lesser density.

- **refraction, astronomical**: the change in direction of travel (bending) of a light ray as it passes obliquely through the atmosphere. As a result of *refraction* the observed *altitude* of a celestial object is greater than its geometric altitude. The amount of refraction depends on the altitude of the object and on atmospheric conditions.
- **refraction, horizontal**: the *astronomical refraction* at the *astronomical horizon*; often, an adopted value of $34'$ is used in computations for sea level observations.

relativistic light-deflection: the bending of the path of light in a gravitational field of a massive body towards that body.

retrograde motion: for orbital motion in the solar system, motion that is clockwise in the *orbit* as seen from the north pole of the *ecliptic*; for an object observed on the *celestial sphere*, motion that is from east to west, resulting from the relative motion of the object and the Earth. (See *direct motion.*)

right ascension: the angular distance on the *celestial sphere* measured eastward along the *celestial equator* from the *equinox* to the *hour circle* passing through the celestial object. Right ascension is usually given in combination with *declination*.

Saros: a cycle of 233 *synodic months* (approximately 6585.3213 *days*, or nearly 18 *years* 11 days) used to predict *eclipses* of the Sun and Moon.

second, ephemeris: see *ephemeris second.*

second, Système International (SI): the duration of 9 192 631 770 cycles of radiation corresponding to the transition between two *hyperfine levels* of the ground state of cesium 133.

selenocentric: with reference to, or pertaining to, the center of the Moon.

semidiameter: the angle at the observer subtended by the equatorial radius of the Sun, Moon or a *planet*.

semimajor axis: **1.** Half the length of the major axis of an ellipse. **2.** A standard element used to describe an *elliptical orbit*. (See *orbital elements.*)

Shida number: the coefficients relating the observed amplitudes of the horizontal displacements of the Earth's surface and the horizontal component of the corresponding static solid Earth tide.

SI second: see *second, Système International (SI).*

sidereal day: the *period* between successive *transits* of the *equinox*. The mean sidereal *day* is approximately 23 hours, 56 minutes, 4 *seconds*. (See *sidereal time.*)

sidereal hour angle: the angular distance on the *celestial sphere* measured westward along the *celestial equator* from the *equinox* to the *hour circle* passing through the celestial object. It is equal to 360° minus *right ascension* in degrees.

sidereal month: see *month, sidereal.*

sidereal time: the *hour angle* of the *equinox*. If the *mean equinox* is used, the result is mean sidereal time; if the *true equinox* is used, the result is apparent sidereal time. The hour angle can be measured with respect to the local *meridian* or the *Greenwich meridian*, yielding, respectively, local or Greenwich (mean or apparent) sidereal times.

solar parallax: see *parallax, solar.*

solar time: the measure of time based on the *diurnal motion* of the Sun.

- **solar time, apparent**: the measure of time based on the *diurnal motion* of the true Sun. The rate of diurnal motion undergoes seasonal variation caused by the *obliquity* of the *ecliptic* and by the *eccentricity* of the Earth's *orbit*. Additional small variations result from irregularities in the rotation of the Earth on its axis.
- **solar time, mean**: a measure of time based conceptually on the *diurnal motion* of a fiducial point, called the fictitious mean Sun, with uniform motion along the *celestial equator*.

solstice: either of the two points on the *ecliptic* at which the apparent longitude of the Sun is 90° or 270°; also the time at which the Sun is at either point. (See *longitude, ecliptic.*)

spacetime metric: see *metric tensor.*

spectral types or classes: the categorization of stars according to their spectra, primarily due to differing temperatures of the stellar atmosphere. From hottest to coolest, the commonly used Morgan-Keenan spectral types are O, B, A, F, G, K and M. Some other extended spectral types include W, L, T, S, D and C. (See *luminosity class.*)

standard epoch: a date and time that specifies the *reference system* to which celestial coordinates are referred. (See *mean equator and equinox.*)

stationary point: the time or position at which the rate of change of the apparent *right ascension* of a *planet* is momentarily zero. (See *apparent place (or position).*)

stratosphere: the layer of Earth's atmosphere above the *troposphere* between approximately 10 km and 50 km above the surface, where temperatures rise with *height* in contrast with the troposphere where temperatures decrease with height.

sunrise, sunset: the times at which the apparent upper *limb* of the Sun is on the *astronomical horizon*. In *The Astronomical Almanac* they are computed as the times when the true *zenith distance*, referred to the center of the Earth, of the central point of the disk is 90° 50′, based on adopted values of 34′ for *horizontal refraction* and 16′ for the Sun's *semidiameter*.

surface brightness: the visual *magnitude* of an average square arcsecond area of the illuminated portion of the apparent disk of the Moon or a *planet*.

survey foot: a non-SI unit of length used in past land surveys whose length can vary from country to country.

synodic month: see *month, synodic.*

synodic period: the mean interval of time between successive *conjunctions* of a pair of *planets*, as observed from the Sun; or the mean interval between successive conjunctions of a satellite with the Sun, as observed from the satellite's primary.

synodic time: pertaining to successive *conjunctions*; successive returns of a *planet* to the same *aspect* as determined by Earth.

syzygy: **1.** A configuration where three or more celestial bodies are positioned approximately in a straight line in space. Often the bodies involved are the Earth, Sun and either the Moon or a *planet*. **2.** The times of the new moon and full moon.

T_{eph}: see *Barycentric Ephemeris Time (T_{eph}).*

TAI: see *International Atomic Time (TAI).*

TCB: see *Barycentric Coordinate Time (TCB).*

TCG: see *Geocentric Coordinate Time (TCG).*

TDB: see *Barycentric Dynamical Time (TDB).*

TDT: see *Terrestrial Dynamical Time (TDT).*

tensor: see *metric tensor.*

terminator: the boundary between the illuminated and dark areas of a celestial body.

Terrestrial Dynamical Time (TDT): the timescale for apparent *geocentric ephemerides* defined by a 1979 *IAU* resolution. In 1991, it was replaced by *Terrestrial Time (TT)*. Obsolete.

Terrestrial Ephemeris Origin (TEO): the original name for the *Terrestrial Intermediate Origin (TIO)*. Obsolete.

Terrestrial Intermediate Origin (TIO): the *non-rotating origin* of the *Terrestrial Intermediate Reference System (TIRS)*, established by the *International Astronomical Union (IAU)* in 2000. The TIO was originally set at the *International Terrestrial Reference Frame (ITRF)* origin of longitude and throughout 1900–2100 stays within 0.1 mas of the *ITRF* zero-*meridian*. Formerly referred to as the *Terrestrial Ephemeris Origin (TEO).*

Terrestrial Intermediate Origin locator (TIO locator): (denoted by s) an arc used in locating the *TIO*. Considering the *node* of the *ITRS equator* on the instantaneous equator (orthogonal to the *CIO*), $s\prime$ is the difference in the longitudes of that node measured from (1) the ITRS origin and (2) the TIO. The TIO was originally set at the *ITRF* origin of longitude and remains very close to it. As a consequence of *polar motion*, the TIO moves, and $s\prime$ changes, by approximately 50 μas (1.5 mm) per century.

Terrestrial Intermediate Origin meridian (TIO meridian): the moving plane passing through the geocenter, the *CIP*, and the *TIO*. (See *meridian, Greenwich.*)

Terrestrial Intermediate Reference System (TIRS): a *geocentric reference system* defined by the intermediate *equator* of the *Celestial Intermediate Pole (CIP)* and the *Terrestrial Intermediate Origin (TIO)* on a specific date. It is related to the *Celestial Intermediate Reference System* by a rotation of the *Earth Rotation Angle*, θ, around the *Celestial Intermediate Pole*.

Terrestrial Time (TT): an idealized form of *International Atomic Time (TAI)* with an *epoch* offset; in practice TT = TAI + $32^{s}.184$. TT thus advances by *SI seconds* on the *geoid*. Used as an independent argument for apparent *geocentric ephemerides*. (See *second, Système International (SI).*)

tidal acceleration: see *lunisolar tidal deceleration.*

tidal deceleration: see *lunisolar tidal deceleration.*

tidal friction: the frictional force caused by the interaction between the tides and the Earth's surface. (See *lunisolar tidal deceleration.*)

tides, ocean: the periodic rise and fall of ocean waters due to the attraction of the Moon and Sun.

tides, solid Earth: the periodic rise and fall of areas of the Earth crust due to the attraction of the Moon and Sun.

time dilation: the observed difference of elapsed time between two observers which are moving relative to each other, or being differently situated with respect to nearby gravitational masses.

topocentric: with reference to, or pertaining to, a point on the surface of the Earth.

topocentric place (or position): the *proper place* of an object computed for a specific location on or near the surface of the Earth (ignoring atmospheric *refraction*) and expressed with respect to either the *true (intermediate) equator and equinox of date* or the *true equator* and *CIO* of date. In other words, it is similar to an *apparent* or *intermediate place*, but with corrections for *geocentric parallax* and *diurnal aberration*. (See *aberration, diurnal; parallax, geocentric.*)

transit: **1.** The passage of the apparent center of the disk of a celestial object across a *meridian*. **2.** The passage of one celestial body in front of another of greater apparent diameter (e.g., the passage of Mercury or Venus across the Sun or Jupiter's satellites across its disk); however, the passage of the Moon in front of the larger apparent Sun is called an *annular eclipse*. (See *eclipse, annular; eclipse, solar.*)

- **transit, shadow**: the passage of a body's shadow across another body; however, the passage of the Moon's shadow across the Earth is called a *solar eclipse*.

troposphere: the lowest portion of Earth's atmosphere up to approximately 10 km above the surface. It contains approximately 75% of the atmosphere's mass and 99% of its water vapor and aerosols. (See *stratosphere.*)

true equator and equinox: the celestial coordinate system defined by the orientation of the Earth's equatorial plane on some specified date together with the direction of the *dynamical equinox* on that date. The true equator and equinox are affected by both *precession* and *nutation*. (See *mean equator and equinox; nutation; precession.*)

TT: see *Terrestrial Time (TT).*

twilight: the interval before *sunrise* and after *sunset* during which the scattering of sunlight by the Earth's atmosphere provides significant illumination. The qualitative descriptions of *astronomical*, *civil* and *nautical twilight* will match the computed beginning and ending times for an observer near sea level, with good weather conditions, and a level *horizon*. (See *sunrise, sunset.*)

- **twilight, astronomical**: the illumination level at which scattered light from the Sun exceeds that from starlight and other natural sources before *sunrise* and after *sunset*. Astronomical twilight is defined to begin or end when the geometric *zenith distance* of the central point of the Sun, referred to the center of the Earth, is 108°.
- **twilight, civil**: the illumination level sufficient that most ordinary outdoor activities can be done without artificial lighting before *sunrise* or after *sunset*. Civil twilight is defined to begin or

end when the geometric *zenith distance* of the central point of the Sun, referred to the center of the Earth, is 96°.

twilight, nautical: the illumination level at which the *horizon* is still visible even on a Moonless night allowing mariners to take reliable star sights for navigational purposes before *sunrise* or after *sunset*. Nautical twilight is defined to begin or end when the geometric *zenith distance* of the central point of the Sun, referred to the center of the Earth, is 102°.

umbra: the portion of a shadow cone in which none of the light from an extended light source (ignoring *refraction*) can be observed.

undulation of the geoid: for a given location on the surface of the Earth, the difference in *height* between the *geoid* and the *reference ellipsoid*.

Universal Time (UT): a generic reference to one of several timescales that approximate the mean *diurnal motion* of the Sun; loosely, *mean solar time* on the *Greenwich meridian* (previously referred to as Greenwich Mean Time). In current usage, UT refers either to a timescale called UT1 or to *Coordinated Universal Time (UTC)*; in this volume, UT always refers to UT1. UT1 is formally defined by a mathematical expression that relates it to *sidereal time*. Thus, UT1 is observationally determined by the apparent diurnal motions of celestial bodies, and is affected by irregularities in the Earth's rate of rotation. *UTC* is an atomic timescale but is maintained within $0^{s}.9$ of UT1 by the introduction of 1-*second* steps when necessary. (See *leap second.*)

UT1: see *Universal Time (UT).*

UT1R: UT1 corrected for the effects of short-period zonal tides (periods less that 15 days) specified by the defining table of coefficients.

UTC: see *Coordinated Universal Time (UTC).*

vernal equinox: see *equinox, vernal.*

vertical: the apparent direction of gravity at the point of observation (normal to the plane of a free level surface).

virtual place: see *proper place.*

week: an arbitrary *period* of *days*, usually seven days; approximately equal to the number of days counted between the four *phases of the Moon*. (See *lunar phases.*)

WGS-84: the World Geodetic System 1984 *reference ellipsoid*, with an equatorial radius of 6378137 meters and a polar *flattening* of 1/298.257223563. The WGS-84 ellipsoid is the reference for *GPS* coordinates. Latitude, longitude, and *height* measured relative to the WGS-84 ellipsoid, converted to *geocentric* Cartesian form, are consistent with the *ITRS* to within a few centimeters.

wobble, polar: **1.** In current practice including the phraseology used in *The Astronomical Almanac*, it is identical to *polar motion*. **2.** In certain contexts it can refer to specific components of polar motion, e.g., *Chandler wobble* or annual wobble. (See *polar motion.*)

wobble, Chandler: see *Chandler wobble.*

world lines: the path of an object as it travels through four-dimensional spacetime.

year: a *period* of time based on the revolution of the Earth around the Sun, or the period of the Sun's apparent motion around the *celestial sphere*. The length of a given year depends on the choice of the reference point used to measure this motion.

year, anomalistic: the *period* between successive passages of the Earth through *perihelion*. The anomalistic *year* is approximately 25 minutes longer than the *tropical year*.

year, Besselian: the *period* of one complete revolution in *right ascension* of the fictitious mean Sun, as defined by Newcomb. Its length is shorter than a *tropical year* by $0.148 \times \mathrm{T}$ *seconds*, where T is centuries since 1900.0. The beginning of the Besselian year occurs when the fictitious mean Sun is at *ecliptic longitude* 280°. Obsolete.

year, calendar: the *period* between two dates with the same name in a *calendar*, either 365 or 366 *days*. The *Gregorian calendar*, now universally used for civil purposes, is based on the *tropical year*.

year, eclipse: the *period* between successive passages of the Sun (as seen from the geocenter) through the same lunar *node* (one of two points where the Moon's *orbit* intersects the *ecliptic*). It is approximately 346.62 *days*.

year, Julian: a *period* of 365.25 *days*. It served as the basis for the *Julian calendar*.

year, sidereal: the *period* of revolution of the Earth around the Sun in a fixed *reference frame*. It is the mean period of the Earth's revolution with respect to the background stars. The sidereal *year* is approximately 20 minutes longer than the *tropical year*.

year, tropical: the *period* of time for the *ecliptic longitude* of the Sun to increase 360 degrees. Since the Sun's *ecliptic* longitude is measure with respect to the *equinox*, the tropical *year* comprises a complete cycle of seasons, and its length is approximated in the long term by the civil *(Gregorian) calendar*. The mean tropical year is approximately 365 *days*, 5 hours, 48 minutes, 45 *seconds*.

zenith: in general, the point directly overhead on the *celestial sphere*.

zenith, astronomical: the extension to infinity of a plumb line from an observer's location.

zenith, geocentric: the point projected onto the *celestial sphere* by a line that passes through the geocenter and an observer.

zenith, geodetic: the point projected onto the *celestial sphere* by the line normal to the Earth's geodetic ellipsoid at an observer's location.

zenith distance: the angular distance on the *celestial sphere* measured along the great circle from the *zenith* to the celestial object. Zenith distance is 90° minus *altitude*.

ΔT: the difference between *Terrestrial Time (TT)* and *Universal Time (UT)*: $\Delta \mathrm{T} = \mathrm{TT} - \mathrm{UT1}$.

ΔUT1 (or ΔUT): the value of the difference between *Universal Time (UT)* and *Coordinated Universal Time (UTC)*: $\Delta \mathrm{UT1} = \mathrm{UT1} - \mathrm{UTC}$.

3C 273B, 115

aberration, 28, 249, 263, 289
  annual, 29, 264, 265, 267
    differential, 269
  constant of, 266
  diurnal, 29, 264, 267, 293
  elliptic (E-terms), 266, 282
  planetary, 28, 263, 268
    differential, 269
  secular, 264
  special relativistic, 265, 269
  stellar, 28, 263, 264, 265
absolute time. *See* time
Adams-Bashforth method. *See* numerical integration
Adrastea, 439. *See also* Jupiter
airglow, 521
algorithms
  calendars, 617, 618, 619, 621
  conversion of coordinates, 238, 281, 283, 289, 290, 293, 297, 298, 300. *See also* coordinate transformations
  conversion of timescales, 68, 92, 93, 236, 237
  datum conversions, 147
  ICRS to other systems, 117
  rising, 515
  setting, 515
α (alpha) Ursæ Minoris. *See* Polaris
altitude, 20, 24, 135, 256, 569
Amalthea, 373, 374, 439. *See also* Jupiter
analemmic curve, 513, 514
analytical theory, 34
angle of the vertical, 295
Anno Domini (AD), 590, 591
Anno Hegira (A.H.), 607
Anno Mundi (A.M.), 602
aphelion, 508, 511
  Earth, 507
  planets, 511
apogee, 507, 508
apparent *topic*. *See* specific topic
Ariel, 388, 389, 441. *See also* Uranus
asteroids, 37
  in DE405/LE405, 308, 330, 331, 332
  diameters, 407, 408, 409, 410
    mean, 423
  magnitude parameters (H and G), 423, 424, 425
  magnitudes
    apparent, 422, 423
    mean, 423
  perturbations, 333
  phase function, 423
  radii, effective, 407, 408
  synodic period, 509
astrometric observables, 54, 55
astrometry, 182
  differential, 283
  space-based, 283
Astronomical Almanac Online, 8, 67, 273, 276, 347, 360, 365, 378, 392, 403, 407, 423, 438, 502, 521, 529, 535, 559, 625
astronomical constants, 3, 8, 9, 69, 111, 219, 233, 234, 271, 307, 625, 626
astronomical unit (au), 27, 30, 626
atmospheric loading, 168
atomic time. *See* time
aurora, 521
axis of figure, 20, 203
azimuth, 20, 135, 256, 569
  time for a specified azimuth, 518

Barycentric Celestial Reference System (BCRS), 4, 46, 56, 59, 106, 201, 202, 208, 249, 250, 251
Barycentric Coordinate Time (TCB). *See* timescales
Barycentric Dynamical Time (TDB). *See* timescales
Before Christ (BC), 590, 591
Before Common Era (BCE), 590, 591
Besselian elements. *See* eclipses and occultations
bias. *See* frame bias
BIH Terrestrial System (BTS), 125, 126, 184
binary stars. *See* stars, double and multiple
bissextile years, 585, 595
Bureau International de l'Heure (BIH), 84, 85, 125, 182, 204
Bureau International des Poids et Mesures (BIPM), 84, 85, 86, 95, 96

calendar, 9, 14, 585
  accuracy, 593
  Alexandrian, 594, 616
  arithmetic, 588
  astronomical, 588
  Bahá'i, 616
  Chinese, 610, 611, 612, 613
    history, 610
    rules, 613, 614
    sexagenary cycle, 612
  Christian, 589. *See also* calendar, Gregorian
  civil, 14, 598, 599
  conversion algorithms, 617, 618, 619, 621
  day
    beginning, 591
  day of week calculation, 618
  ecclesiastical, 599
    rules, 599
  ecclesiastical full Moon, 599
  Egyptian (ancient), 588, 589, 593
    history, 593
    months, 594
    rules, 594
  eras. *See* eras
  French Republican, 589, 616
  Gregorian, 14, 591, 598, 619
    history, 598
    months, 597
    rules, 599
  Indian, 608
    history, 608
    luni-solar, 609
    months, 609, 610
    Saka, 610, 619
    solar, 609
  internet sites, 621
  Islamic, 606
    history, 607
    months, 607
    rules, 607
  Jewish, 601, 603, 604, 605, 618, 619
    history, 601
    months, 603
    rules, 602
  Julian, 14, 91, 591, 594, 595, 596, 597
    history, 595
    months, 597
    rules, 597
  lunar, 585
  luni-solar, 585, 592, 608, 611
  Metonic, 592, 602
  observational, 587
  proleptic, 14, 590, 597
  Roman, 594
  Saka. *See* calendar, Indian
  solar, 585
  solar cycle, 591
  year
    beginning, 597
Callisto, 369, 439. *See also* Jupiter
Calypso, 378. *See also* Saturn
Carrington's elements, 426
Cartesian inertial coordinate systems, 46
cartographic coordinates, 399. *See also* coordinate systems
cartography, digital, 407
catalog
  All-Sky Survey of Flat-Spectrum Radio Sources, 546
  Catalog of Nearby Exoplanets, 538
  Catalogue of Quasars and Active Galactic Nuclei, 545
  FK5, 3, 105, 106, 111, 112, 114, 115, 118, 234, 531
  Hipparcos Catalogue, 3, 105, 106, 112, 113, 114, 115, 530, 531, 537
  Index Catalog of Visual Double Stars, 533
  Interferometric Measures Catalog, 534

International Celestial Reference Frame (ICRF, ICRF2). *See* International Celestial Reference Frame
Large Quasar Astrometric Catalog (LQAC), 545
Large Quasar Reference Frame (LQRF), 116
Magnitude Difference Catalog, 534
New Catalog of Optically Visible Open Clusters and Candidates, 540
NOMAD, 530, 531, 534, 536, 538, 548
Optical Characteristics of Astrometric Radio Sources, 545
Optical Spectroscopy of 1Jy, S4 and S5 Radio Source Identifications, 546
Photometric Magnitude Difference Catalog, 533
Third Reference Catalogue of Bright Galaxies (RC3), 542
Two Micron All Sky Survey (2MASS), 116, 530, 542
Tycho-2, 3, 116, 530, 531
UCAC, 116, 530
USNO-B, 530
Visual Orbit Catalog, 533
VLBA Calibrator Survey, 116
Washington Double Star Catalog (WDS), 533
Washington Multiplicity Catalog (WMC), 533
Yale Bright Star Catalog (BSC5), 531
Celestial Ephemeris Pole (CEP), 224
Celestial Intermediate Frame (CIF), 6
Celestial Intermediate Origin (CIO), 6, 76, 80, 125, 200, 202, 203, 204, 206, 208, 209, 227, 228, 229, 238, 249, 250, 251, 253, 254, 273
Celestial Intermediate Pole (CIP), 5, 8, 200, 202, 203, 204, 205, 206, 209, 210, 212, 224, 225, 229, 240, 249, 250, 251, 273, 274, 275, 276, 277, 284, 291, 298
Celestial Intermediate Reference System, 78, 201, 204, 206, 251, 253, 273, 275, 300
celestial reference system. *See* reference system
Centre de Donnees astronomiques de Strasbourg (CDS), 530
Ceres, 37, 403. *See also* planets, dwarf
Chandlerian free motion, 276
Chandler wobble, 24, 163, 175, 276
Charon, 396, 447. *See also* Pluto
Chebyshev polynomials, 562, 563
Christmas, 599
CIO-based system. *See* reference system
CIO locator, 208, 228, 254, 274, 275
circulation, 351
clock, 93. *See also* frequency standards
portable, 99
quartz-crystal, 93, 95
relativistic effects on, 45
stable, 45
vapor cell, 94
clock standards. *See* frequency standards
clusters. *See* star clusters
comets, 38
radii, effective, 407, 408
commensurabilities. *See* orbital resonance
Common Era (CE), 590, 591
COMPASS, 177, 179
conic sections, 30, 31, 575
conjunction, 40, 41, 42, 68, 288, 351, 356, 359, 363, 364, 372, 391, 393, 396, 458, 459, 500, 505, 506, 509, 522, 524, 587, 588, 590, 607, 609, 614, 615, 616
Connected-Element Radio Interferometry (CERI), 183
constants. *See* astronomical constants and ephemeris, DE405
conventional international origin, 125, 203, 204, 241
conversion algorithms. *See* algorithms
coordinate clock comparison, 99
Coordinated Universal Time. *See* timescales, Universal Time
coordinate frames, 15. *See also* coordinate systems, reference frame, and reference system
barycentric, 17
geocentric, 17
heliocentric, 17
planetocentric, 17, 357
selenocentric, 17
selenographic, 311
topocentric, 17, 23
coordinates, 252, 253. *See also* positions and place
astronomical, 22, 130, 131
Cartesian, 133, 134
cartographic, 399
geocentric, xxi, 21, 130, 131, 134, 294

coordinates *(continued)*
geodetic, xxi, 21, 22, 130, 131, 250, 294
geographic, 22, 133, 134, 142, 148, 294
planetocentric, 38, 43, 353, 401, 403, 406, 419
planetographic, 38, 43, 401, 403, 406, 417, 419
rectangular, 2, 16, 17, 21, 109, 117, 249, 261, 268, 294, 341, 353, 371, 388, 417, 431, 435, 522, 523, 566, 570
spherical, 16, 21, 285, 290, 570
using vectors, 567
terrestrial, 22, 294
topocentric, 20, 25, 257, 261, 427
coordinate synchronization, 99
coordinate systems, 15. *See also* coordinate frames, reference frame, and reference system
Cartesian, 46, 132
cartographic, 399
celestial, 18
geocentric geographical, 132
grid, 136
local, 134
local horizon, 135
selenographic, 429
small bodies, 406
state plane, 142
terrestrial, 20, 125
topocentric, 23
coordinate time. *See* time
coordinate transformations. *See also* algorithms
between celestial and terrestrial, 25
Cartesian, 134
geocentric, 569, 570
geographic, 142, 148
heliocentric, 570
state plane, 142
Cordelia, 392. *See also* Uranus
Cowell's method. *See* numerical integration
crescent moon
visibility, 588

datum
conversions, 147
geocentric, 131
geodetic, 128, 142, 144
horizontal, 129
North American, 129
North American Vertical, 131
vertical, 129
day
beginning of calendar. *See* calendar, day
mean solar, 81, 587
day numbers, 300. *See also* Greenwich sidereal and Julian
day of week calculation, 618
DE200/LE200. *See* ephemeris
DE403/LE403. *See* ephemeris
DE405/LE405. *See* ephemeris
declination, 18, 20, 108, 253, 569. *See also* coordinates
defect of illumination, 417, 422
deflection of light. *See* light-deflection
deflection of the vertical, 23, 129, 132, 133
dehiyyot, 602, 603
Deimos, 367, 438, 439. *See also* Mars
ΔAT, 87, 92
ΔT, 82, 92, 284, 285, 360, 454, 456, 457, 491, 492, 495, 499, 500, 506
ΔUT, 294
Dione, 378, 379, 441. *See also* Saturn
Dionysian cycle, 600
Dionysius Exiguus, 589
dip of horizon, 280, 516
disk of planet
apparent, 415, 418
flattening, 415
dissipation
deep ocean, 77
Dominical letter, 600
Doppler effect, 28, 54
relativistic, 259
DORIS, 125, 175, 181
double stars. *See* stars, double and multiple
DUT1, 97, 233, 294
dwarf planets. *See* planets, dwarf
dynamical time. *See* time

Earth. *See also* planets
angular velocity, 234, 267
aphelion, 507
gravity field, 148
modeling, 149
representation, 150
non-rigid, 205
oblateness, 20, 27, 263
perihelion, 507

rotation. *See* Earth rotation
tides. *See* Earth tides
Earth Gravitational Model (EGM2008), 126, 131, 151, 152, 153
Earth Orientation
monitoring, 175
alternative techniques, 183
historical, 181
international services, 184
Earth Orientation Parameters (EOP), 175, 177
Earth rotation, 25, 76
matrix, 257
rate, 25, 230
variation, 25, 77
Earth Rotation Angle (ERA), 6, 11, 78, 80, 229, 233, 249
Earth tides, 314. *See also* tide
permanent, 148, 156
solid, 148, 153, 154
Easter, 598, 599
calculation, 600, 621
Échelle Atomique Libre (EAL), 84
eclipses (lunar), 41, 453, 491
Besselian elements, 492
Besselian plane, 453
Bessel's method, 453
conditions, 457, 459, 461, 494
contact times, 493, 494
greatest obscuration, 493
magnitude, 494, 499
online information, 497, 498
partial, 461
penumbral, 460
penumbral shadow cone, 459
position angles, 494
sub-lunar points, 494
total, 461
umbral shadow cone, 459
Eclipses Online (website), 495
lunar eclipses, 497
solar eclipses, 495
eclipses (solar), 40, 41, 453, 464
annular, 463
annular-total, 463
Besselian elements, 464, 469, 472, 473
Besselian plane, 453
Bessel's method, 453, 464
central, 463
beginning, 485
end, 485
central on the meridian, 486
conditions, 457, 458, 461, 462, 463
contact times, 487
curves, 474, 480
central line, 481
duration of central eclipse, 481
general circumstances, 484
maximum eclipse in the horizon, 481
outline, 483
rising and setting, 480
width of path, 481
duration, 487
first contact, 485
flattening, 479
fundamental coordinate system, 464
general circumstances, 474, 477
grazing, 475
greatest, 486
hybrid, 463
last contact, 485
limb effects, 457
limits, 482, 486
magnitude, 484, 486, 488, 489, 495
maps, 487
noncentral total, 463
obscuration, 488, 490
online information, 495, 496
partial, 462
phenomena, 477
position angles, 488
shadow cone, 466
total, 463
ecliptic, 18, 108, 205
coefficients, 213, 216
inertial, 5, 206
precession of. *See* precession
rotating, 5, 206
ecliptic latitude. *See* latitude
Einstein's equations, 51
Einstein's relativity principle, 49. *See also* general relativity and special relativity
Electromagnetic Signal Transfer, 101
elevation angle, 135
ellipsoid, 128, 130, 143
flattening, 129
height, 128, 132
reference. *See* reference ellipsoid
semimajor axis, 129

ellipsoid *(continued)*
surface, 127
elongation, 40, 42, 172, 173, 270, 272, 356, 360, 361, 421, 508, 510, 528
Enceladus, 378, 379, 441. *See also* Saturn
Encke's method. *See* numerical integration
Epact, 600
epagomenal days, 593
ephemeris, 33, 109
apparent, 29
astrometric, 29
DE200/LE200, 307
DE403/LE403, 428, 429
DE405/LE405, 7, 116, 286, 305, 307
approximate positions, 338
asteroids, 308, 330, 331, 332, 333
availablility, 341
constants, 325, 327, 328, 329
data reduction, 321, 322, 323, 324, 325
error estimates, 332, 333
initial conditions, 325, 326, 332
observations, 316, 317, 318, 319, 320
orientation, 321
starting epoch, 326
error estimates, 332, 334, 335, 336, 337, 338, 339, 341
fundamental, 286, 305
initial conditions, 305
inner planets, 332
integration error, 315
low precision for Sun, 513
lunar, 306
outer planets, 333
physical. *See* physical ephemeris
representative, 35
ephemeris meridian, 239
Ephemeris Time (ET). *See* timescales
Epimetheus, 378. *See also* Saturn
equation of center, 348
equation of the equinoxes, 11, 78, 207, 235, 254
equation of the origins, 7, 78, 208, 235, 254
equation of time, 13, 81, 231, 513
equations of condition, 582
equations of motion, 30, 307
equator
celestial, 17
of date, 108, 117, 203, 252
galactic, 18
intermediate, 252
of J2000.0, 105, 106, 107, 113, 117, 201, 202, 208, 250, 273
mean, 117, 201, 202, 203, 206, 209, 250, 251, 420
precession of. *See* precession
true, 203, 206, 241, 252
equinox, 18, 108, 206, 506, 509
autumnal, 509
catalog, 109
of date, 108, 117, 203, 241
dynamical, 115
of J2000.0, 107, 113, 117, 202
mean, 202, 203
precession of. *See* precession
true, 203, 253
vernal, 509
equinox-based system. *See* reference system
equinox drift, 322
equipotential surface, 401
equivalence principle, 50
eras (calendar), 590
Christian, 589
Hijra, 607
Mundane, 602
Saka, 610
Eris, 403. *See also* planets, dwarf
errors
accumulation, 578
observation, 580
root-mean-square, 580
E-terms. *See* aberration, elliptic (E-terms)
Euler angles, 311
Europa, 369, 439. *See also* Jupiter
European Terrestrial Reference Frame (ETRF), 124
exoplanets, 538
host stars, 538
extended bodies, 35

figure effects, 309
FK5. *See* catalog
flattening. *See* disk of planet, ellipsoid, planets, and satellites
foot (length)
International, 142
survey, 142
foreshortening effects, 260

frame bias, 249, 251, 273
  matrix, 117, 202, 208, 228
frame bias-precession-nutation matrix, 228
frequency standards, 9, 96
  atomic beam, 94
  atomic fountain, 95
  caesium beam, 94
  trapped ion, 95

galaxies
  bright, 542
  Hubble sequence, 543
  morphological type, 542
Galilean satellites, 369, 439. *See also* Jupiter, satellites
  phase coefficients, 413
  visual magnitudes, 413
GALILEO (spacecraft), 98, 177, 179
gamma parameter (γ), 45, 323, 327
gamma ray bursts (GRBs), 547
gamma ray sources, 547
Ganymede, 369, 439. *See also* Jupiter
gauge, 51
  harmonic, 57
general relativity, 45, 57, 64, 75, 99, 249, 270, 323
Geocentric Celestial Reference System (GCRS), 4, 46, 56, 99, 201, 202, 250, 251
Geocentric Coordinate Time (TCG). *See* timescales
geodesics, 136
  null, 54
geodetic datums. *See* datum
Geodetic Reference System 1980 (GRS 80), 129, 131
geoid, 23, 127, 128, 131
  undulation, 23, 128, 129, 295
geometric area
  apparent, 412
geopotential coefficients, 151, 153, 244
geopotential surface (geop), 127, 128
  reference (geoid), 127, 128, 129, 131
Global Navigation Satellite System (GNSS), 175, 177, 179, 182
Global Positioning System (GPS), 98, 126, 177
globular clusters. *See* star clusters
GLONASS, 98, 177, 179
golden number, 91, 591, 600
GPS Time. *See* timescales
gravitational potential
  geocentric ($GM_\oplus$), 151
  Newtonian, 47
gravity vector
  local, 128
Greenwich Civil Time, 14, 231
Greenwich Hour Angle (GHA), 80, 203, 231, 238, 250, 254, 276, 284, 298, 466, 471, 513, 527
Greenwich Mean Astronomical Time (GMAT), 231
Greenwich Mean Time (GMT), 14, 231
Greenwich meridian. *See* meridian
Greenwich sidereal date, 79
Greenwich sidereal day number, 79
Greenwich Sidereal Time (GST), 12, 78, 79, 249
  apparent, 6, 79, 229, 235
  mean, 79, 229, 231, 232, 234, 237
Gregorian calendar. *See* calendar
Gregorian canon, 600
gyroscopes
  laser-ring, 183
  superfluid helium interference, 183

halakim, 602
Haumea, 403. *See also* planets, dwarf
Helene, 378. *See also* Saturn
Hipparcos. *See* catalog
Hipparcos Celestial Reference Frame (HCRF), 105, 106, 113, 545
horizon, 135, 256, 517
  astronomical, 17, 427
  geometric, 516
  local, 135
horizon system. *See* coordinate systems, local horizon
horizontal parallax. *See* parallax
hour angle
  local, 20, 80, 238, 253
  rate of change, 517
  sidereal, 18
Hubble sequence. *See* galaxies
Hydra, 396. *See also* Pluto
hydrogen maser, 94
Hyperion, 381, 383, 441. *See also* Saturn

Iapetus, 381, 383, 441. *See also* Saturn

IAU 2000. *See* precession-nutation
IAU 2000A. *See* precession-nutation
IAU 2000B. *See* precession-nutation
IAU 2006. *See* precession-nutation
IAU 2006/2000A. *See* precession-nutation
IAU 2006/2000A$_R$. *See* precession-nutation
ICRF. *See* International Celestial Reference Frame (ICRF, ICRF2)
ICRS. *See* International Celestial Reference Systems (ICRS)
Ides, 595
IERS Bulletin A, 185
IERS Bulletin B, 186
IERS publications, 185, 186
IERS Reference Pole (IRP), 125
illumination
  ground, 518, 519
  from starlight, 521
indiction cycle, 91, 589, 591
intercalate, 585, 592, 617
Intermediate Reference System, 203, 250
International Atomic Time (TAI). *See* timescales
International Celestial Reference Frame (ICRF, ICRF2), 4, 18, 105, 106, 107, 112, 113, 115, 251, 321, 545
International Celestial Reference System (ICRS), 4, 18, 59, 105, 107, 112, 114, 115, 117, 201, 250
  axes, 107
  data in, 115
  origin, 115
  pole, 115
International Earth Rotation and Reference Systems Service (IERS), 95, 113, 184. *See also* IERS
International Latitude Service (ILS), 125, 182
International Polar Motion Service (IPMS), 125, 182, 184, 204
International Terrestrial Reference Frame (ITRF), 6, 22, 124, 125, 180, 203, 204. *See also* ITRF2008
International Terrestrial Reference System (ITRS), 6, 46, 99, 124, 125, 131, 203, 249, 250, 252, 275, 276
interpolation methods, 559
  Bessel, 560
  Everett, 560
  inverse, 561
  LaGrange, 560
invariable plane, 18, 349, 399
Io, 369, 439. *See also* Jupiter
ITRF2008, 126, 252
ITU-R, 85, 86, 96

Janus, 378. *See also* Saturn
Johnson UBVRI, 9, 534
Julian calendar. *See* calendar
Julian date, 15, 91, 592
  modified, 15, 91
Julian day, 91
Julian day number, 15, 91, 592, 618
Julian period, 592
Julian year. *See* year
Jupiter, 421, 436. *See also* planets
  satellites, 369, 373, 375, 376, 439
    cartographic longitudes, 441
    phase coefficients, 413
    rotation parameters, 440
    visual magnitudes, 413

Kalends, 595
Keplerian elements. *See* orbital elements
Kuiper belt, 37

Lambert conformal conic (LCC), 136, 141
Landolt standards, 535
Laplacian plane, 18, 349, 350
latitude, 20, 21, 22, 24, 127, 130, 131, 136, 294, 406, 477. *See also* coordinates
  astronomical, 129, 132, 241
  ecliptic, 18, 255
  footpoint, 139
  geocentric, 569
  geodetic, 132, 296, 472
laws of motion, 29
L_C, 89
leap seconds, 14, 86, 95, 96, 98, 184, 185, 186, 233
leap year, 585, 597, 599, 603, 607. *See also* calendar
least-squares method, 579, 582
length of day, 25, 77, 179, 186, 587
  seasonal variation, 77, 182
librations, 352, 427, 432. *See also* Moon
light-deflection, 29, 45, 249, 272, 273
  approximate, 272
  gravitational, 270, 271, 282

relativistic, 288, 292
light-time, 260, 263, 287, 322
light-time displacement, 28, 263, 264, 417
local *topic*. *See* specific topic
longitude, 21, 22, 127, 130, 131, 136, 294, 406, 477. *See also* coordinates and nutation in
astronomical, 129, 132, 241
ecliptic, 255
geocentric, 132, 569
geodetic, 132, 296
origin, 253
LORAN-C, 97
Love numbers, 36, 153, 157, 243
lunar calendar. *See* calendar
lunar gravity coefficients, 310
lunar laser ranging (LLR), 52, 53, 179, 180
data, 320
lunar polynomials, 9, 559
luni-solar calendar. *See* calendar

magnitudes. *See also* asteroids, eclipses, satellites, and planets
of solar system bodies
mean opposition, 412
visual, 410
Makemake, 403. *See also* planets, dwarf
map projections, 136
Mars, 421, 436, 511. *See also* planets
closest approach, 508
prime meridian, 436
satellites, 367, 368, 438
rotation parameters, 439
surface, 325
mass monopole, 48
matrix
CRS to intermediate, 257
CRS to of date, 257
Earth rotation, 257
frame bias, 117, 202, 208, 228, 257
frame bias-precession-nutation, 228
nutation, 225, 257
precession, 217, 257
matrix arithmetic, 565
multiplication, 565
rotations using, 257, 565
mean *topic*. *See* specific topic
Mercury, 421, 435, 511. *See also* planets
greatest elongation, 508
inferior conjunction, 288
prime meridian, 435
surface, 324
meridian, 135
astronomical origin, 253
Greenwich, 239, 252, 253
local, 17
prime, 400
reference, 125
TIO, 238
transit. *See* meridian transit
meridian transit, 39, 255, 316
meter
definition, 49
Metis, 439. *See also* Jupiter, asteroids
Metonic cycle, 508, 600
metric tensor, 57
Military Grid Reference System, 136
Mimas, 378, 379, 441. *See also* Saturn
minor planets. *See* asteroids
Miranda, 388, 392, 441. *See also* Uranus
mixed functions approximation, 363
Molad, 602, 603, 604
month. *See* calendars and synodic
Moon, 37, 505. *See also* lunar
age, 429
apogee, 508
center of figure, 456
center of mass, 456
crescent visibility. *See* crescent moon
ecclesiastical full. *See* calendar, ecclesiastical full Moon
figure-figure torque, 313
figure-point mass torques, 313
fraction illuminated, 429
limb effects, 457
offset matrix, 428
optical librations, 428, 432
perigee, 508
phases, 507, 509
physical ephemeris, 427
physical libration, 311, 326, 427, 429
prime meridian, 430
rise. *See* moonrise
secular acceleration, 230
semidiameter, 434, 456
set. *See* moonset
topocentric librations, 434
Moon camera, 182

moonlight, 520
moonrise, 514
  algorithms. *See* algorithms, rising
moonset, 514
  algorithms. *See* algorithms, setting
multiple stars. *See* stars, double and multiple
mutual events, 373

National Geospatial-Intelligence Agency (NGA), 126
Naval Observatory Vector Astrometry Software. *See* NOVAS
Navy Navigational Satellite System (NNSS), 182
Near Earth Asteroids (NEA), 37
Neptune, 421, 437. *See also* planets
  satellites, 393, 443
    rotation parameters, 446
Nereid, 394, 395, 443. *See also* Neptune
Network Time Protocol (NTP), 99
Newton's theory of gravity, 46
Nix, 396. *See also* Pluto
NOMAD. *See* catalog
Nones, 595
non-rotating origin, 6, 76, 80
normal equations, 583
North American Datum, 129
North American Vertical Datum, 131
NOVAS, 8, 211, 225, 259, 274, 292, 500
numerical differentiation, 572
numerical integration, 34, 315, 574
  Adams-Bashforth method, 577
  Cowell's method, 34, 575
  differential corrections, 35
  Encke's method, 576
  Runga-Kutta method, 576
nutation, 19, 209, 212, 223, 225, 249, 273. *See also* precession-nutation
  differential, 223, 227
  forced component, 223
  free component, 223
  free core, 205
  geodesic, 4
  in longitude, 26, 79, 207, 211, 223, 224, 225, 226, 227, 255, 274, 432
  matrix, 225, 257
  in obliquity, 211, 223, 224, 225, 227, 255, 274
  reduction
    approximate, 226
    rigorous, 226

Oberon, 388, 390, 441. *See also* Uranus
obliquity. *See also* nutation in
  of the ecliptic, 18, 19, 79, 206, 207, 212, 226, 255, 274, 329, 340, 568, 569
occultations, 40, 453, 521, 524
  Besselian elements, 521, 522
  planets, 524
  stars, 521
ocean loading, 162
  displacement, 164, 165, 166, 167
ocean pole tide loading, 163
ocean tide. *See also* Earth tides and tide
  coefficients, 160
  model, 158
Oort's cloud, 38
open clusters. *See* star clusters
Ophelia, 392. *See also* Uranus
opposition, 40, 272, 364, 372, 412, 458, 459, 499, 509
opposition surge, 411
orbital elements, 32, 33, 347, 348
  Keplerian, 338
  osculating, 9, 347
  perturbations, 349, 351, 352
orbital motion, 29. *See also* orbital elements
orbital resonance, 162, 351, 352, 353, 441
orthometric height, 128
osculating elements. *See* orbital elements

P03. *See* precession
Pandora, 378. *See also* Saturn
parallax, 27, 249, 259, 261
  in altitude, 262
  annual. *See* parallax, heliocentric
  diurnal. *See* parallax, geocentric
  factors, 262
  geocentric (a.k.a. diurnal), 27, 261, 262, 293, 434
  heliocentric (a.k.a. annual), 27, 261, 263
  horizontal, 27, 262, 427, 434
    Sun, 427
  solar, 28, 262
parametrized post-Newtonian (PPN), 33, 45, 64, 308, 323, 327

perigee, 507, 508
perihelion, 508, 511
  Earth, 507
  planets, 511
phase, 42, 421. *See also* Moon
phase angle, 42, 421
  solar, 411
phase coefficients, 411, 413. *See also* planets
phase corrections, 322
phase function. *See* asteroids
phenomena, 506
  geocentric, 508, 509, 510
  heliocentric, 511
Phobos, 367, 438, 439. *See also* Mars
Phoebe, 383, 388. *See also* Saturn
photographic zenith tubes, 182
photometric standards. *See* stars, standards
physical ephemeris, 42, 399. *See also* planets, satellites, Sun, and Moon
place, 252. *See also* positions and coordinates
  apparent, 283
    algorithm, 283, 290
  astrographic, 282
  astrometric, 250, 281
  of date, 250, 283, 289
  geocentric, 252, 283, 292
  intermediate, 250, 283
    algorithm, 283, 290
  local, 250, 281
  mean, 250, 300
  proper, 281
  topocentric, 250, 252, 283, 293, 297
  topocentric astrometric, 282
  virtual, 281
planetocentric. *See* coordinates
planetographic. *See* coordinates
planets, 37. *See also* Mercury, Venus, etc.
  aphelion, 511
  dwarf, 37, 399, 400. *See also* Pluto, Ceres, Haumea, Eris, and Makemake
    magnitudes, 411
    physical ephemeris, 437
    rotation, 401
  equatorial radius, 403
  flattening, 403, 419
  gaseous, 37
  giant, 37
  inner, 332, 505
  minor. *See* asteroids
  outer, 333, 505
  perihelion, 511
  phase coefficients, 413
  physical ephemeris, 434
  pole, 402
  prime meridian, 402
  stationary, 508
  synodic period, 509
  terrestrial, 37
  variability, 412
  visibility, 508
  visual magnitudes, 413
plate motions, 169
Pluto, 37, 403, 422, 437. *See also* planets, dwarf
  equatorial radius, 403
  flattening, 403
  phase coefficients, 413
  physical ephemeris, 437
  pole, 402
  prime meridian, 402, 438
  satellites, 396, 447
    rotation parameters, 447
  visual magnitudes, 413
Polaris, 525, 526, 527. *See also* Pole star
polar motion, 21, 24, 224, 240, 242, 249, 276
  excitation, 174
  ocean tidal variations, 174
  tidal effects, 171
pole of figure, 203
Pole star
  coefficients, 527
  tables, 525
positional uncertainties, 333
positions, 252. *See also* place and coordinates
  apparent, 252
  barycentric, 297
  of date, 272
  geocentric, 295
  geocentric of date, 252
  geometric, 287
  ICRS, 296
  intermediate, 252, 298
  mean, 252
  of planets, 287
  terrestrial of date, 275
post-glacial rebound, 77

post-Newtonian theory, 56
precession, 209, 211, 249, 273, 322. *See also* precession-nutation
  angles, 214, 217, 222
  constant of, 112
  differential, 223
  of the ecliptic, 5, 19, 211
  of the equator, 5, 19
  of the equinox, 212
  general, 212, 213, 215, 218
  geodesic, 4, 212, 218
  luni-solar, 19, 212
  matrix, 217, 257
  Newcomb's, 222
  P03, 211, 216, 218, 235
  parameterization, 214
    Capitaine et al., 220
    Fukushima-Williams, 219
    Lieske, 215
  planetary, 19, 212
  reduction
    approximate, 220
    rigorous, 220
precession-nutation, 19, 209. *See also* nutation and precession
  geodesic, 46
  IAU 2000, 209, 251
  IAU 2000A, 5, 78, 209, 218, 224, 227
  IAU 2000B, 209
  IAU 2006, 5, 78
  IAU 2006/2000A, 5, 78, 114, 209, 211
  IAU 2006/2000A$_R$, 211, 273
preliminary reference Earth model (PREM), 153
prime meridian. *See* meridian, Sun, Mercury, Venus, etc.
  planets. *See* planets
  solar. *See* Sun
prime vertical. *See* vertical
principal moments, 313
Prometheus, 378. *See also* Saturn
proper motion, 28, 109, 110, 111, 258
proper time. *See* time
pulsars, 539

quasars, 112, 115, 544

radial velocity, 28, 258, 267
radial velocity standards, 536
radio-flux calibrators, 546
radio-source positional calibrators, 545
radio time signals, 97
radius. *See* asteroids, comets, satellites, and flattening
redshift, 544
reduction in latitude, 295
reference ellipsoid, 127, 143
  GRS 80, 131
  WGS 84, 131
reference frame, 108, 202. *See also* Celestial Intermediate, European Terrestrial, International Celestial, Hipparcos Celestial, International Terrestrial, and Large Quasar
  dynamical, 109
  errors, 109
  hotspot, 170
  inertial, 100, 101
  local, 100, 101
  moving, 6
  no net rotation, 170
  non-rotating, 101
  rotating, 99, 101
reference system, 108, 202, 251. *See also* Barycentric Celestial, Celestial Intermediate, Geocentric Celestial, Geodetic, Intermediate, International, International Terrestrial, Military Grid, and Terrestrial Intermediate
  celestial (CRS), 76, 200, 240
  CIO-based, 7, 77, 80, 251
    transformation, 275, 298
  conventional, 123
  equinox-based, 7, 80
    of date, 202, 251
    J2000.0, 202, 251
    transformation, 274
  geodetic, 124
  geodetic 1980 (GRS 80), 129, 131
  relationship between, 202, 569
  terrestrial (general), 123, 124
  terrestrial (TRS), 76, 200, 201, 240
  terrestrial (WGS 84), 124, 126, 131
refraction, 29, 277, 293, 516
  low precision, 280
  numerical integration, 277
  Saastamoinen's formula, 279
  tables, 280

relativity. *See* general relativity and special relativity
Revised Ephemeris Time, 10
Rhea, 381, 383, 441. *See also* Saturn
right ascension, 7, 18, 108, 253, 569. *See also* coordinates
  apparent, 203, 253
  CIO, 7
  equinox, 7, 208, 253, 254
  intermediate, 203, 208, 253
  origin, 201, 202, 249, 253, 254
rising, 511, 517
  algorithms, 515
rotational deformation, 242
rotational elements. *See* rotational parameters
rotational parameters, 399. *See also* planets and Sun
rotations
  using matrices, 257, 565
Runga-Kutta method. *See* numerical integration

sankrânti, 609
Saros, 41, 508
satellite laser ranging, 53, 180
satellites, 37, 353, 366, 401. *See also* Mars, Jupiter, etc.
  apparent distance, 361, 364
  apparent orbit, 356, 359, 361, 362
  differential coordinates, 361
  flattening, 403
  greatest elongation, 356, 360, 363
  Johnson colors, 413, 414, 415
  mean motion, 351
  orbital elements
    notations, 365
  phenomena, 363
  physical ephemeris, 438
  position angle, 355, 361, 364
  radii, 404, 405, 406
  visual magnitudes, 413, 414, 415
satellite tracking
  Doppler, 182
Saturn, 421, 436. *See also* planets
  rings, 376
  satellites, 378, 381, 388, 441
    cartographic longitudes, 441, 443
    rotation parameters, 442, 443
Scaliger, Joseph Justus, 591
sea level
  mean, 127, 129
seasons
  beginning of, 507
second
  atomic, 83
  of ephemeris time, 82
  SI, 9, 75, 83, 84, 96
  of sidereal time, 235
  TAI, 96
secular variation, 573
semidiameter. *See also* Sun and Moon
  apparent, 422
setting, 511, 517
  algorithms, 515
sexagenary cycle. *See* calendar, Chinese
shadow length, 517
Shapiro delay, 323
Shida number, 157
sidereal day, 78
sidereal time, 11, 12, 77, 231, 234
  apparent, 11, 77, 80, 229, 237
  local, 11, 80, 237
  mean, 11, 78, 81, 229, 237
  seconds of, 235
σ Octantis, 525. *See also* Pole star
simultaneity, 56
Sistema de Referencia Geocentrico para Las Américas (SIRGAS), 124
SOFA, 8, 211, 225, 260, 273, 275, 286, 292
solar. *See also* Sun
solar calendar. *See* calendar
solar corona delay, 323
solar cycle (calendar), 591
solar day. *See* day
solar system barycenter, 309, 326
solar time, 12, 229
  apparent, 13, 81, 230
  local, 13, 229, 238
  mean, 10, 229, 231, 238
solstice, 506, 509
space motion, 249, 258
spacetime metric, 49, 50
special relativity theory (SRT), 48, 51
spectroscopic observables, 52, 53
spin distortion, 312
standard deviation, 580
Standards of Fundamental Astronomy. *See* SOFA

star clusters
  globular, 539, 541
  open, 539
  Trumpler classification, 540
starlight
  illumination from, 521
stars
  bright, 531
  clusters. *See* star clusters
  coeval, 539
  data sources, 530. *See also* catalog
  double and multiple, 110, 111, 532
    astrometric, 532
    cataclysmic, 534
    eclipsing, 270, 532, 534
    exotic, 532
    hierarchical, 532
    nonhierarchical, 532
    occultations, 532
    spectroscopic, 532, 534
    visual pairs, 532
  light. *See* starlight
  standards
    Johnson UBVRI, 9, 534
    Landolt, 535
    photometric, 534
    radial velocity, 536
    spectrophotometric, 535
    Strömgren *uvby*, 535
  variable, 537
    extrinsic, 537
    intrinsic, 537
station coordinates
  solid tide effects, 157
statistics, 578
stellar motion. *See* proper motion, radial velocity, and space motion
stratosphere, 277
Strömgren *uvby*, 535
sub-Earth point, 417, 421
sub-solar point, 417, 421
sui, 613
Sun, 36. *See also* solar
  fictitious mean, 81, 231, 232
  horizontal parallax, 427
  inclination, 426
  longitude of ascending node, 426
  north pole, 426
  physical ephemeris, 426
  prime meridian, 401, 426
  rise. *See* sunrise
  selenographic co-longitude, 429
  semidiameter, 426, 427
  set. *See* sunset
  sidereal rotation rate
    mean, 426
sunrise, 39, 512
  algorithm. *See* algorithms, rising
sunset, 39, 512
  algorithms. *See* algorithms, setting
surface brightness, 412
surveys. *See* catalog
synodic month, 587
synodic period
  of planets, 509

T_{eph}. *See* timescales
Telesto, 378. *See also* Saturn
tensor. *See also* metric tensor
  energy-momentum, 57
  moment of inertia, 312
terminator, 42, 480
Terrestrial Dynamical Time (TDT). *See* timescales
Terrestrial Intermediate Origin (TIO), 6, 76, 80, 238, 239, 250, 251, 253, 254, 275, 276
Terrestrial Intermediate Reference System (TIRS), 203, 249, 251, 276
Terrestrial Reference Systems. *See* reference system (terrestrial)
Terrestrial Time (TT). *See* timescales
Tethys, 378, 379, 441. *See also* Saturn
Thebe, 374, 439. *See also* Jupiter
tidal distortion, 312
tidal effects
  on polar motion, 171
  on station coordinates, 157
  in UT1, 170
tidal friction, 36
tidal potential, 153
  Newtonian, 48
tidal terms
  zonal, 172, 173
tide. *See also* Earth tides, ocean tide, and tidal
  permanent, 148, 156
  solid Earth, 148, 153, 154
time. *See also* timescales
  absolute, 75

atomic, 83
civil, 85, 231
coordinate, 50, 56, 76, 100, 101
dynamical, 10, 81
Earth rotation, 76
local, 13, 231
mean, 13, 231
proper, 50, 56, 75, 99
time arguments, 285
time dissemination, 85, 96, 97, 98, 99, 186
by internet, 99
time domain, 45
timekeeping, 93
agencies, 95
devices, 93. *See also* clock and frequency standards
timescales, 92
atomic, 9
Barycentric Coordinate Time (TCB), 4, 7, 10, 56, 88
Barycentric Dynamical Time (TDB), 7, 10, 11, 83, 88, 89
conversions. *See* algorithms
Ephemeris Time (ET), 10, 82, 84, 230, 231
Geocentric Coordinate Time (TCG), 4, 7, 10, 56, 88, 89
GPS Time, 98
International Atomic Time (TAI), 9, 84, 87, 233
relationship between, 92, 93
relativistic, 68
scaled coordinate, 69
T_{eph}, 7, 11, 88, 89
Terrestrial Dynamical Time (TDT), 10, 83, 88, 89
Terrestrial Time (TT), 7, 10, 84, 88, 239
units, 70
Universal Time, 11, 12, 14, 77, 229, 231, 232, 294
Coordinated (UTC), 14, 85, 87, 233
UT0, 81, 232
UT0−UTC, 176, 181
UT1, 6, 80, 81, 170, 232, 233
UT2, 81, 233
time zones, 14, 86, 88
TIO locator, 239, 275, 276
TIO meridian. *See* meridian
Tishri, 602, 604
Titan, 381, 383, 441. *See also* Saturn
Titania, 388, 389, 441. *See also* Uranus
tithi, 608
topography, 128
transit
across the disk of the Sun, 40, 269, 453, 499
contact points, 500, 501
diagram, 501
general circumstances, 500
local circumstances, 502
Mercury, 499, 500
time of conjunction, 500
Venus, 499
meridian, 39, 255, 316
shadow, 40
times of, 518
triangles
plane, 563, 565
spherical, 556, 563, 565
trigonometry, 563
functions, 556
Triton, 393, 394, 443. *See also* Neptune
troposhere, 277
troposphere delay, 324
Trumpler classification, 540
twilight, 39, 511, 520
astronomical, 39, 512, 520, 521
civil, 39, 512, 520
nautical, 39, 512, 520
Two Micron All Sky Survey (2MASS). *See* catalog
two-way satellite time transfer (TWSTT), 99
Tycho-2. *See* catalog

U.S. National Grid System (USNG), 136
U.S. Naval Observatory Circulars, 455
UBVRI system, 9, 534
UCAC. *See* catalog
Umbriel, 388, 389, 441. *See also* Uranus
undulation of the geoid. *See* geoid
Universal Polar Stereographic (UPS), 136, 138, 139
Universal Time. *See* timescales
Universal Transverse Mercator (UTM), 136, 137, 138
Uranus, 421, 437. *See also* planets
rings, 388
satellites, 388, 389, 390, 392, 441
rotation parameters, 444, 445

UT0, UT1, UT2, etc.. *See* timescales, Universal Time
UTC. *See* timescales, Universal Time

variable stars. *See* stars
variation in latitude, 176
velocity of light, 48
Venus, 421, 435, 511. *See also* planets
  greatest brilliance, 508
  greatest elongation, 508
  greatest illuminated extent, 508
  surface, 324
vertical
  local, 128
  prime, 132
    radius of curvature, 134
Very Long Baseline Interferometry (VLBI), 112, 176
  data, 320
Viking landers, 325
VLBI. *See* Very Long Baseline Interferometry

Washington Double Star Catalog. *See* catalog
week, 588. *See also* calendar
World Geodetic System (WGS 84), 124, 126, 131. *See also* geoid, reference ellipsoid, and reference system (terrestrial)
world lines, 50
World Magnetic Model (WMM 2010), 126

X-ray sources, 547

year. *See also* calendar
  beginning of calendar. *See* calendar, year
  Besselian, 15
  Julian, 15
  length, 587, 593
  tropical, 586

zenith distance, 135, 256

Summary of Reference Systems

Reference System	Fundamental Plane and Pole	Origin on the Fundamental Plane	Epoch	Notes
BCRS (ICRS)	ICRS X-Y plane/Z-axis	ICRS X-axis (RA)	none	1, 3, B
GCRS	ICRS X-Y plane/Z-axis	ICRS X-axis (RA)	none	2, 3, G
J2000.0	mean equator/mean pole	mean equinox (RA)	J2000.0	3, B
mean equatorial	mean equator/mean pole	mean equinox (RA)	of date	4, U
true equatorial	true equator/CIP	true equinox (RA)	of date	4, G
mean ecliptic	ecliptic/ecliptic pole	mean equinox (λ, l)	of date	4, 5, U
true ecliptic	ecliptic/ecliptic pole	true equinox (λ, l)	of date	4, 5, U
Celestial Intermediate	true equator/CIP	CIO (RA)	of date	4, G
Terrestrial Intermediate	true equator/CIP	TIO (GHA)	of date	6, G
ITRS	ITRS X-Y plane/Z-axis	ITRS X-axis (λ)	none	6, 7, G

[1] The ICRS defines the spatial orientation of the BCRS. For all practical purposes, the designations are interchangeable.

[2] The GCRS axes are not exactly those of the ICRS; they are obtained from the BCRS (ICRS) by a relativistic transformation.

[3] The BCRS, ICRS, GCRS, and J2000.0 axes are oriented to within 100 mas of each other.

[4] The difference between "mean" and "true" is that the latter takes into account nutation. Caution: do not confuse a mean system with a mean place, which has a different definition.

[5] The mean ecliptic is always implied. Ecliptic coordinates are usually expressed in degrees longitude and latitude. By convention, the symbols λ and l are used for geocentric and heliocentric longitudes, respectively.

[6] The difference between the ITRS and the Terrestrial Intermediate Reference System is that the latter takes into account polar motion. The differences can be a few tens of meters.

[7] The ITRS is consistent with WGS 84 within about one cm. WGS 84 forms the basis for spatial coordinates obtained by GPS (i.e., geodetic latitude and longitude).

[B] Barycentric. The location of the origin is the solar system barycenter.

[G] Geocentric. The location of the origin is the geocenter.

[U] Undefined. The location of the origin must be determined by context or explicitly stated.

Summary of Astronomical Places

Place	Location of Observer	Axes
mean	barycenter	mean of date or ICRS
geometric	barycenter	ICRS
proper	geocenter	GCRS
apparent	geocenter	true of date
intermediate	geocenter	intermediate
astrometric	geocenter	ICRS
topocentric	Earth's surface	true of date or intermediate
local	Earth's surface	GCRS

Mean place: typically what is found in most star catalogs. It is the barycentric direction of a non-solar system object that takes into account its orbital and space motions (as applicable). Conceptually, it is the direction of the object as it would be observed from the solar system barycenter at a specified date, with respect to specified coordinate axes (usually the mean equator and equinox of a specified date or the ICRS), if the masses of the Sun and other solar system bodies were negligible. Do not confuse this with a "mean" reference system.

Geometric place: typically the output of solar system ephemerides. It is the position of a solar system object defined by a straight line (vector) between the origin (the solar system barycenter unless otherwise stated) and the object at a given time, without any corrections for light-time, aberration, light deflection, etc.

Proper place: the geocentric direction of an object that takes into account orbital motion, space motion, and light-time (as applicable), light deflection, and annual aberration. Unless otherwise stated, it is expressed with respect to the GCRS axes. Conceptually, it is the direction of the object as it would be observed from the center of the Earth if the Earth were transparent, non-refracting, and massless.

Apparent place: the proper place of an object expressed with respect to the true equator and equinox of date.

Intermediate place: the proper place of an object expressed with respect to the true equator and CIO of date.

Astrometric place: the geocentric direction of a solar system object computed by applying the correction for light-time displacement to the geometric position. Such a position is directly comparable with the catalog positions of background stars in the same area of the sky, after the star positions have been updated for proper motion and parallax. An astrometric place is expressed with respect to the axes of the reference system of a star catalog, e.g., the ICRS axes.

Topocentric place: the proper place of an object transformed to a specific location on or near the surface of the Earth. Atmospheric refraction is ignored. It is expressed with respect to the true equator and either the true equinox of date or CIO of date. It is similar to an apparent or intermediate place, but includes corrections for geocentric parallax and diurnal aberration.

Local place: a topocentric place of an object expressed with respect to the GCRS axes.

Useful Time Relationships

$$
\begin{aligned}
\mathrm{UT1} &= \mathrm{UTC} + (\mathrm{UT1} - \mathrm{UTC}) && \text{UT1-UTC available from IERS} \\
\mathrm{TAI} &= \mathrm{UTC} + \Delta\mathrm{AT} && \text{[Table 3.1]} \\
\mathrm{TT} &\equiv \mathrm{TDT} \approx \mathrm{ET} \approx \mathrm{TAI} + 32.184\mathrm{s} && \text{[Eq. 3.23]} \\
\Delta\mathrm{T} &= \mathrm{TT} - \mathrm{UT1} = 32.184s + \Delta\mathrm{AT} - (\mathrm{UT1} - \mathrm{UTC}) &&
\end{aligned}
$$

$$
\begin{aligned}
\mathrm{GMST}(t_U, t) &= \theta(t_U) - E_{\mathrm{prec}}(t) && \text{[Eq. 3.7]} \\
t &= (\mathrm{TT} - 2\,451\,545.0\ \mathrm{TT})\ \text{in days}/36525 && \\
\theta(t_U) &= 2\pi(0.779\,057\,273\,2640 + 1.002\,737\,811\,911\,354\,48\,t_U) && \text{[Eq. 3.3]} \\
t_U &= \text{UT1 Julian date} - 2\,451\,545.0 && \\
E_{\mathrm{prec}}(t) &= -0.''014\,506 - 4612.''156\,533\,53\,t - 1.''391\,581\,65\,t^2 && \text{[Eq. 3.4]} \\
&\quad + 0.''000\,000\,44\,t^3 + 0.''000\,029\,956\,t^4 &&
\end{aligned}
$$

$$
\begin{aligned}
\mathrm{TCG} - \mathrm{TT} &= \mathrm{L_G} \times (\text{TAI Julian date} - 2\,443\,144.5) \times 86\,400\mathrm{s} && \text{[Eq. 3.27]} \\
\mathrm{L_G} &= 6.969\,290\,134 \times 10^{-10} && \\
\mathrm{TCB} &= \mathrm{TCG} + \frac{\mathrm{L_c} \times (\mathrm{TT} - \mathrm{TT_0}) + P(\mathrm{TT}) - P(\mathrm{TT_0})}{1 - \mathrm{L_B}} + \mathrm{c}^{-2}\mathbf{v_e} \cdot (\mathbf{x} - \mathbf{x_e}) && \text{[Eq. 3.26]} \\
\mathrm{L_C} &= 1.480\,826\,8674 \times 10^{-8} && \\
\mathrm{L_B} &= 1.550\,519\,7678 \times 10^{-8} && \\
\mathrm{TDB} &= \mathrm{TCB} - \mathrm{L_B} \times (\mathrm{JD_{TCB}} - 2\,443\,144.500\,3725) \times 86\,400\mathrm{s} + \mathrm{TDB_0} && \text{[Eq. 3.24]} \\
\mathrm{TDB_0} &= -6.55 \times 10^{-5}\mathrm{s} && \\
\mathrm{TDB} &\cong \mathrm{T_{eph}} &&
\end{aligned}
$$

UT1 is subject to irregularities in the Earth's rotation.

UTC is an atomic timescale but is maintained within 0.9 s of UT1 by the introduction of 1-second steps (leap seconds) when necessary.

ΔAT is an integral number of seconds that increases by 1 s whenever a positive leap second is introduced into UTC; the current value can be found at the beginning of each issue of IERS Bulletin A.

TT is considered a continuation of Terrestrial Dynamical Time (TDT) and Ephemeris Time (ET).

When computing GMST, ensure that the Earth Rotation Angle, θ, and the precession of the equinox in right ascension, E_{prec}, are in the same units.

$\mathrm{TT_0}$ corresponds to TAI JD 2 443 144.5 (1977 January 1, 0h).

Periodic terms denoted by $P(\mathrm{TT})$ have a maximum amplitude of around 1.7 ms.

$\mathbf{x_e}$ and $\mathbf{v_e}$ are the barycentric position and velocity of the Earth; $\mathbf{x}$ is the barycentric position of the observer.